L. Santiago Medina Kimberly E. Applegate
C. Craig Blackmore *Editors*

Evidence-Based Imaging in Pediatrics

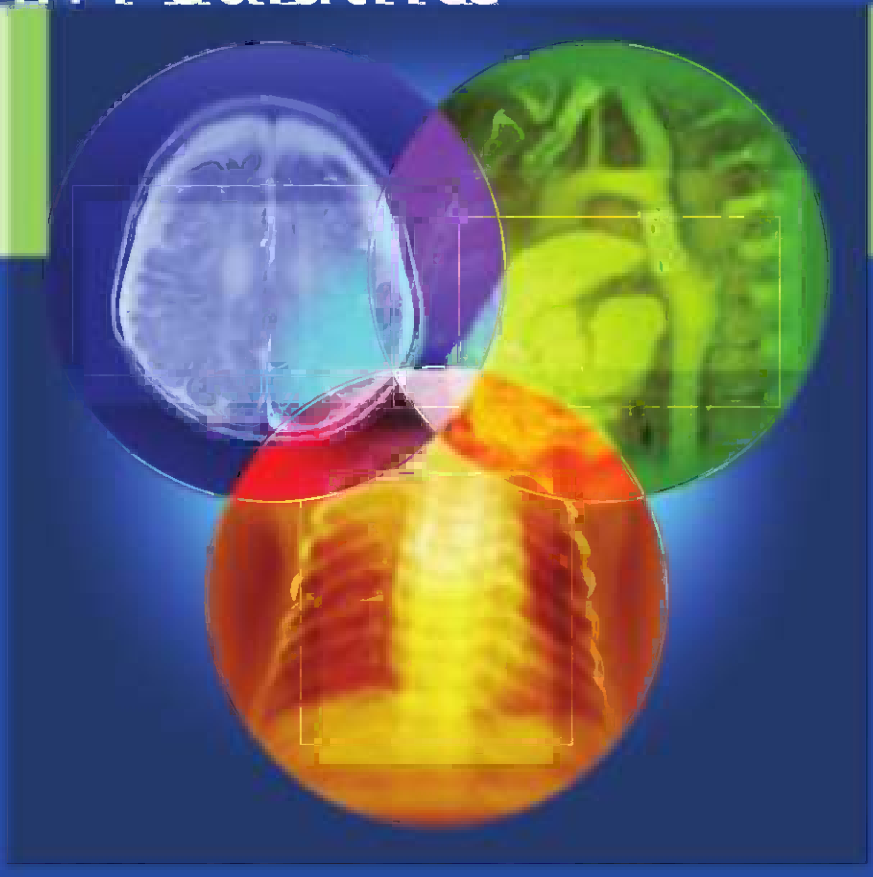

Optimizing Imaging in Pediatric Patient Care

Springer

Evidence-Based lmaging in Pediatrics

L. Santiago Medina, MD, MPH
Co-Director Division of Neuroradiology and Brain Imaging, Director of the Health Outcomes, Policy, and Economics (HOPE) Center, Department of Radiology, Miami Children's Hospital, Miami, FL 33155, USA
santiago.medina@mch.com
Former Lecturer in Radiology, Harvard Medical School, Boston, MA 02114
smedina@post.harvard.edu

Kimberly E. Applegate, MD, MS, FACR
Vice Chair of Quality and Safety, Department of Radiology Emory University School of Medicine, 1364 Clifton Rd NE, Suite D112, Atlanta, GA 30322
keapple@emory.edu

C. Craig Blackmore, MD, MPH
Scientific Director, Center for Health Care Solutions, Department of Radiology, Virginia Mason Medical Center, Seattle, Washington
craig.blackmore@vmmc.org

Evidence-Based lmaging in Pediatrics

Optimizing Imaging in Pediatric Patient Care

With 146 Illustrations, 11 in Full Color

Foreword by Jay E. Berkelhamer, MD, FAAP
Foreword by Bruce J. Hillman, MD

Springer

Editors
L. Santiago Medina, MD, MPH
Co-Director Division of Neuroradiology and Brain Imaging
Director of the Health Outcomes, Policy, and Economics (HOPE) Center
Department of Radiology
Miami Children's Hospital
Miami, FL 33155, USA
santiago.medina@mch.com
Former Lecturer in Radiology
Harvard Medical School
Boston, MA 02114
smedina@post.harvard.edu

C. Craig Blackmore, MD, MPH
Scientific Director, Center for Health Care Solutions
Department of Radiology
Virginia Mason Medical Center
Seattle, WA 98111, USA
craig.blackmore@vmmc.org

Kimberly E. Applegate, MD, MS, FACR
Vice Chair of Quality and Safety
Department of Radiology
Emory University School of Medicine
Atlanta, Georgia 30322, USA
keapple@emory.edu

ISBN 978-1-4419-0921-3 e-ISBN 978-1-4419-0922-0
DOI 10.1007/978-1-4419-0922-0
Springer New York Dordrecht Heidelberg London

Library of Congress Control Number: 2009938480

Printed on acid-free paper

Springer is part of Springer Science+Business Media (www.springer.com)

To our patients who are our best teachers
and to the researchers, who made this book possible.
To our families, friends, and mentors.

Foreword

Medical imaging has revolutionized how we care for children and is the fastest growing area of health care today. Every clinician, from generalist to sub-specialist, will order imaging tests on children as he or she determines the course of action in caring for sick children. Given the high cost of health care and the large number of uninsured children who lack access to care, we must optimize how we use imaging to be more sophisticated and more prudent health care providers. Current worldwide economic conditions will cause physicians everywhere to confront more limited resources and weigh the costs and benefits of health care spending: "Medical technology (including radiology) itself is not the problem. It is why, how and how often it is used and by whom which creates the problem."* This book is an important step forward toward optimizing the use of imaging in children.

Most books and resources on imaging focus on how to interpret imaging and on the potential benefits of the newest imaging technologies. Less attention has been given to determining when it is appropriate to image, with what modality, and how to apply the results of imaging to clinical care. This book fills that gap, by defining how imaging can most optimally be used to diagnose or exclude the common conditions in children. Critically, the authors also provide a summary of the supporting evidence and the limitations of today's evidence-based literature.

Chapters 1 and 2 introduce the health care provider to the language, methods, and applications of evidence-based medical care. These chapters describe the common research methods used to study the role of imaging in medicine and reporting. From there, the chapters cover the most prevalent conditions and diseases affecting children in the developed nations, providing an evidence-based summary of the role of imaging in infection, inflammation, congenital disorders, trauma, neoplasm, in utero fetal assessment, and cardiovascular anomalies. Recognized leaders in radiology who understand and use the evidence-based care approach have collaborated to make the book both state of the art and readable for all physicians who care for children. Most of the individual chapters have been written by pediatric radiologists in partnership with pediatricians and other specialist physicians, providing both radiology and clinical perspectives.

Designed as a practical guide for use at the clinic or bedside rather than as a reference tome, the book eloquently captures the nuances of medical practice today and empowers the reader to use the current evidence behind medical imaging. It is a valuable book for all health care providers who care for children, from pediatricians to emergency physicians to family practice clinicians and radiologists.

*Chisholm R. Guidelines for radiological investigations [editorial]. BMJ 1991; 303:797–780.

As can be gathered from the above statements, I have decided to include this book on my "must haves" list and expect that readers will improve their skills as diagnosticians by incorporating the approaches promoted by the authors.

Jay E. Berkelhamer, MD, FAAP
Past President, American Academy of Pediatrics

Foreword

I am honored to write this foreword on several counts. First, the idea of evidence-based imaging is one in which I passionately believe. Our usual acceptance of anecdote and habit as a rationale for clinical imaging decision making is fraught with hazard for both patients and our society. Second, the editors and chapter authors have done an amazing job of putting forth an approach that is philosophically sound—one in which I can believe. Third is the focus of the book. Because of our somewhat belated concern over the long-term effects of increasingly prevalent diagnostic radiation, children and adolescents have become a lightning rod for the potential hazards of marginal and inappropriate imaging care. Finally, a book like this has even greater importance in the context of our current times. As I write this foreword, the world is plunging deep into recession. People are losing their jobs, and, with this, they are losing their health insurance. The new US President, Barack Obama, ran on a platform of instituting universal health care in the United States. What he has proposed is a very expensive plan. Where is the funding to come from? A major target, according to the new administration, is to reduce the amount of care that does not contribute to improving health. As we know, sometimes it can be difficult to distinguish beneficial from unnecessary or harmful imaging care. In this regard, this book provides us with a framework for more cost-effective decision making and direction for determining the most appropriate imaging for specific clinical presentations.

Such direction provides a "just in time" remedy for the ills that regulators and payers believe to be rife in imaging. Relatively few radiologists seem consciously aware of why we are such targets for payment reform, but perceptions that we are doing too little to reduce inappropriate imaging are a major contributor. At the root of our problem is a lack of critical reading and thinking skills. Because of how medical students and trainees are educated—with an emphasis on remembering vast amounts of minutia—too few radiologists have learned to consider critically what they read or hear in the lectures of our field's eminences. Even in our most esteemed journals, literature reviews tend to be exhaustive regurgitations of everything that has been written, without providing much insight into which studies were performed more rigorously. Few take the time to consider what information is unique to the institution generating the data and which is more generalizable to all of our practices. The emphasis remains on reading shadows rather than on what might well be our role in care coordination.

The aim of *Evidence-Based Imaging in Pediatrics* is nothing less than to begin to reverse these conditions. The editors and chapter authors are well positioned to accomplish this end. They are the anomalies in our field who have seen modern imaging practice and think we could do better. Reading *Evidence-Based Imaging in Pediatrics* provides a window into how they think as they evaluate the literature and arrive at their conclusions, which we can use as models for our own improvement. Importantly, the editors have designed a uniform approach for each chapter and held the

authors' feet to the fire to adhere to it. As a result, we do not have to adapt to a different framework as we move from gastrointestinal disease to musculoskeletal conditions to abnormalities of the vascular system. The literature reviews that follow are selective and critical, rating the strength of the literature to provide insight into the degree of confidence the reader might have in reviewing the conclusions. At the end of each chapter, the authors present the imaging approaches best supported by the evidence and what gaps exist that should give us pause for further consideration.

The outcome is a highly approachable text that suits the needs of both the busy practitioner who wants a quick consultation on a patient with whom he or she is actively engaged and of the radiologist who wishes a comprehensive, in-depth view of an important topic. Most importantly, from my perspective, the book goes counter to the current trend of "dumbing down" radiology, a trend so abhorrent in many modern textbooks. To the contrary, *Evidence-Based Imaging in Pediatrics* is an intelligent effort that respects the reader's potential to think for one's self.

Bruce J. Hillman, MD
Theodore E. Keats Professor
Department of Radiology
The University of Virginia
Charlottesville, VA

Preface

"All is flux, nothing stays still.
Nothing endures but change."
Heraclitus, 540–480 B.C.

Certainly, Heraclitus' philosophy is apparent to those who care for children: we watch them grow and change continually, and yet each child does so at different rates and in different ways. Medical imaging has grown exponentially in the last three decades with the development of many promising and often non-invasive diagnostic studies and therapeutic modalities. The corresponding medical literature has also exploded in volume, leading to information overload for health care providers. In addition, the literature varies in scientific rigor and clinical applicability, and publications on the same topic may contradict each other. The purpose of this book is to employ stringent evidence-based medical criteria in order to systematically review the evidence defining the appropriate use of medical imaging in infants and children and to present to the reader a concise summary of the best medical imaging choices for the care of infants and children.

The 41 chapters cover the most prevalent conditions and diseases that affect children in developed countries. Most of the chapters have been written by pediatric radiologists in close collaboration with pediatric clinical physicians and surgeons in order to provide a balanced analysis of the different medical topics and the role of imaging. We cannot answer all the questions we face in the clinical care of children today—medical imaging is a delicate balance of science and art, often without data for guidance—but we can empower the reader with the current evidence behind medical imaging.

To make the book user friendly and to enable fast access to pertinent information, we have organized all of the chapters in the same format. The chapters are framed around important and provocative clinical questions relevant to the daily physician's practice. A short listing of issues at the beginning of each chapter helps three different tiers of users: (1) the busy physician searching for a quick guidance, (2) the meticulous physician seeking deeper understanding, and (3) the medical-imaging researcher requiring a comprehensive resource. Key points and summarized answers to the important clinical issues are at the beginnings of the chapters, so the busy clinician can understand the most important evidence-based imaging data in seconds. This fast bottom-line information is also available in an electronic fully searchable format so that an expeditious search can be done using a handheld device on the run or a computer at the medical office, hospital, or at home. Each important question and summary is followed by a detailed discussion of the supporting evidence so that the meticulous physician can have a clear understanding of the science behind the evidence.

In each chapter, the evidence discussed in the chapter is presented in Take Home Tables and Figures, which provide an easy review in the form of summary tables and flow charts. The Imaging Case Studies highlight the strengths and limitations of the different imaging studies with vivid examples. Toward the ends of the chapters, the best imaging protocols are described to assure that the imaging studies are well standardized and done with the highest available quality. The final sections of the chapters are called Future Research; here, provocative questions are raised for physicians and non-physicians interested in advancing medical imaging.

Not all research and not all evidences are created equal. Accordingly, throughout the book, we use a four-level classification detailing the strength of the evidence and based on the Oxford Criteria: Level I (strong evidence), Level II (moderate evidence), Level III (limited evidence), and Level IV (insufficient evidence). The strength of the evidence is presented in parenthesis throughout the chapters so the reader gets immediate feedback on the weight of the evidence behind each topic.

Finally, we had the privilege of working with a group of outstanding contributors from major medical centers and universities in North America and Europe. We believe that the authors' expertise, breadth of knowledge, and thoroughness in writing different chapters provide a valuable source of information and can guide decision making for physicians and patients. In addition to guiding practice, the evidence summarized in the chapters may have policy-making and public health implications. Finally, we hope that the book highlights key points and generates discussion, promoting new ideas for future research.

L. Santiago Medina, MD, MPH
Kimberly E. Applegate, MD, MS
C. Craig Blackmore, MD, MPH

Contents

Contributors

Nolan Altman, MD
Chief, Department of Radiology, Miami Children's Hospital, Miami, FL 33155, USA

Sudha Anupindi, MD
Assistant Professor of Radiology, Department of Radiology, at the Children's Hospital of University of Pennsylvania School of Medicine, Philadelphia, PA 19104, USA

Yoshimi Anzai, MD, MPH
Professor, Department of Radiology, University of Washington Medical Center, Seattle, WA 98195, USA

Kimberly E. Applegate, MD, MS, FACR
Vice Chair of Quality and Safety, Department of Radiology, Emory University School of Medicine, Atlanta, Georgia 30322, USA

Stephen Ashwal, MD
Chief, Division of Pediatric Neurology, Department of Pediatrics, Loma Linda University, Loma Linda, CA 92350, USA

Rama Ayyala, MD
Department of Internal Medicine, Mount Sinai Medical Center, New York, NY 10029, USA

Martha C. Ballesteros, MD
Pediatric Radiologist, Department of Radiology, Miami Children's Hospital, Miami, FL 33155, USA

Carol E. Barnewolt, MD
Assistant Professor, Department of Radiology, Harvard Medical School, Co-Director, Division of Ultrasound, Department of Radiology, Children's Hospital Boston, Boston, MA 02115, USA

D. Gregory Bates, MD
Clinical Assistant Professor of Radiology, Department of Radiology, The Ohio State University College of Medicine and Public Health, Nationwide Children's Hospital, Columbus, OH 43205, USA

Barry R. Berch, MD
Department of Pediatric Surgery, Vanderbilt University School of Medicine, Nashville, TN 37232, USA

Byron Bernal, MD, CCTI
Neuroscientist, Department of Radiology, Miami Children's Hospital, Miami, FL 33155, USA

Rob A.C. Bilo, MD
Department of Forensic Pathology, Netherlands Forensic Institute, 2497GB, The Hague, The Netherlands

G. Brian Black, MD, FRCS(C), FACS
Professor of Surgery, Paediatric Orthopedic Surgeon, Department of Surgery (Orthopedics), Winnipeg Children's Hospital, University of Manitoba, Winnipeg, MB R3A 1S1, Canada

C. Craig Blackmore, MD, MPH
Scientific Director, Center for Health Care Solutions, Department of Radiology, Virginia Mason Medical Center, Seattle, WA 98111, USA

Dorothy I. Bulas, MD
Professor of Radiology and Pediatrics, Department of Diagnostic Imaging and Radiology, George Washington University School of Medicine and Health Sciences, Children's National Medical Center, Washington DC 20010, USA

Luisa F. Cervantes, MD
Pediatric Radiologist, Department of Radiology, Miami Children's Hospital, Miami, FL 33155, USA

Soonmee Cha, MD
Associate Professor, Department of Radiology and Biomedical Imaging, University of California San Francisco, San Francisco, CA 94143, USA

Pranav Chitkara, BS, MD
Department of Internal Medicine, Baylor College of Medicine, Houston, TX 77030, USA

Garry Choy, MD, MS
Department of Radiology, Massachusetts General Hospital, Boston, MA 02114, USA

Leonard P. Connolly, MD
Assistant Professor of Radiology, Associate Radiologist, Department of Nuclear Medicine/ Radiology, Harvard Medical School, Massachusetts General Hospital, Boston, MA 02114, USA

Erin A. Cooke, MD
Department of Radiology, Virginia Mason Medical Center, Seattle, WA 98101, USA

Andrea Doria, MD, PhD, MSc
Clinician Scientist/General Radiologist, Department of Diagnostic Imaging, The Hospital for Sick Children, Toronto, ON 5MG 1X8, Canada

Carlos R. Estrada, MD
Instructor in Surgery (Urology), Department of Urology, Harvard Medical School, Children's Hospital Boston, Boston, MA 02115, USA

Lynn Ansley Fordham, MD
Associate Professor and Chief of Pediatric Imaging, Department of Radiology, University of North Carolina School of Medicine, North Carolina Children's Hospital, Chapel Hill, NC 27599, USA

Donald P. Frush, MD
Professor of Radiology and Pediatrics, Division of Pediatric Radiology, Department of Radiology, Duke Medical Center, Durham, NC 27710, USA

Debbie S. Gipson, MD, MS
Associate Professor, Division of Nephrology and Hypertension, University of North Carolina at Chapel Hill, Chapel Hill, NC 27599, USA

Joel A. Gross, MD, MS
Associate Professor, Chief, and Fellowship Director, Emergency Radiology, Department of Radiology, Harborview Medical Center, University of Washington School of Medicine, Seattle, WA 98104, USA

Brian E. Grottkau, MD
Chief of Pediatric Orthopaedics, Department of Orthopaedic Surgery, Massachusetts General Hospital for Children/Harvard Medical School, Boston, MA 02114, USA

Jeffrey C. Hellinger, MD
Assistant Professor of Radiology, Department of Radiology, Children's Hospital of Philadelphia, University of Pennsylvania School of Medicine, Philadelphia, PA 19104, USA

Marta Hernanz-Schulman, MD
Professor, Radiology and Pediatrics, Radiology Vice-Chair in Pediatrics, Radiologist-in-Chief and Medical Director, Department of Diagnostic Imaging, Vanderbilt Children's Hospital, Monroe Carell Jr Children's Hospital at Vanderbilt, Nashville, TN 37232, USA

Barbara A. Holshouser, PhD
Associate Professor, Department of Radiology, Loma Linda University Medical Center, Loma Linda, CA 92354, USA

Diego Jaramillo, MD, MPH
Radiologist-in-Chief, Department of Radiology, The Children's Hospital of Philadelphia, Professor of Radiology, Department of Radiology, University of Pennsylvania School of Medicine, Philadelphia, PA 19104, USA

Boaz Karmazyn, MD
Department of Pediatric Radiology, Assistant Professor of Radiology, Indiana University School of Medicine, Riley Hospital for Children, Indianapolis, IN 46202, USA

Marc S. Keller, MD
Professor of Clinical Radiology, Department of Radiology, Children's Hospital of Philadelphia, Philadelphia, PA 19104, USA

Judith Kelsen, MD
Department of Pediatrics, Children's Hospital of Philadelphia, Philadelphia, PA 19104, USA

Geetika Khanna, MD, MS
Assistant Professor, Washington University School of Medicine, 510 S. Kings highway, Campus Box 8131-MIR, St Louis, MO 63110

John Y. Kim, MD
Chairman, Department of Radiology, Texas Health Presbyterian Hospital of Plano, Plano, TX 75093, USA

Jaroslaw Krejza, MD, PhD
Associate Professor of Radiology, Department of Radiology, Division of Neuroradiology, University of Pennsylvania, Philadelphia, PA 19104, USA; Department of Nuclear Medicine, University of Gdansk, Gdansk, Poland

Rajesh Krishnamurthy, MB, BS
Assistant Professor of Radiology, EB Singleton Department of Diagnostic Imaging, Texas Children's Hospital, Baylor College of Medicine, Houston, TX 77030, USA

Edward Y. Lee, MD, MPH
Assistant Professor of Radiology, Department of Radiology, Children's Hospital Boston, Harvard Medical School, Boston, MA 02115, USA

Petar Mamula, MD
Director of Kohl's Endoscopy Suite, Assistant Professor of Pediatrics, Department of Pediatrics, University of Pennsylvania School of Medicine, Children's Hospital of Philadelphia, Philadelphia, PA 19104, USA

F.A. Mann, MD
Department of Medical Imaging, Seattle Radiologists, Swedish Medical Center, Seattle, WA 98104, USA

Amit M. Mathur, MBBS, MD
Associate Professor of Pediatrics, Department of Pediatrics/Newborn Medicine, Washington University School of Medicine, St. Louis Children's Hospital, St. Louis, MO 63110, USA

Robert C. McKinstry, MD, PhD
Associate Professor, Department of Pediatric Radiology, St. Louis Children's Hospital, Washington University, St. Louis, MO 63017, USA

L. Santiago Medina, MD, MPH
Co-Director Division of Neuroradiology and Brain Imaging, Director of the Health Outcomes, Policy, and Economics (HOPE) Center, Department of Radiology, Miami Children's Hospital, Miami, FL 33155, USA; Former Lecturer in Radiology, Harvard Medical School, Boston, MA 02114

Elias R. Melhem, MD, PhD
Professor of Radiology, Department of Radiology, Division of Neuroradiology, University of Pennsylvania, Philadelphia, PA 19104, USA

Elka Miller, MD
Pediatric Radiologist, Department of Radiology, The Hospital for Sick Children, Toronto, ON M5G 1X8, Canada

Toshio Moritani, MD, PhD
Assistant Professor, Department of Radiology, University of Iowa Hospitals and Clinics, Iowa City, IA 52242, USA

Wallace W. Neblett III, MD
Professor of Pediatric Surgery and Pediatrics, Chairman, Department of Surgery; Department of Pediatric Surgery, Vanderbilt University School of Medicine, Nashville, TN 37232, USA

Els L.F. Nijs, MD
Assistant Professor of Radiology, Department of Radiology, Children's Hospital of Philadelphia, Philadephia, PA 19104, USA

Huub G.T. Nijs, MD, PhD
Department of Forensic Pathology, Netherlands Forensic Institute, Lann Van Ypenburg 6, 2497GB, The Hague, The Netherlands

Natan Noviski, MD
Chief, Pediatric Critical Care Medicine, Massachusetts General Hospital, Associate Professor of Pediatrics, Harvard Medical School, Department of Pediatric Critical Care Medicine, Boston, MA 02114, USA

Udochukwu E. Oyoyo, MPH
Department of Radiology, Loma Linda University Medical Center, Loma Linda, CA 92354, USA

Esperanza Pacheco-Jacome, MD
Co-Director of Neuroradiology and Brain Imaging, Department of Radiology, Miami Children's Hospital, Miami, FL 33155, USA

Angelisa Paladin, MD, MS
Associate Professor, Department of Radiology, University of Washington, Seattle, WA 98195, USA

Andres H. Peña, MD
Department of Radiology, Children's Hospital of Philadelphia, Philadelphia, PA 19104, USA

Michelle Perez, BS, LPN
Health Outcomes, Policy and Economics (HOPE) Center, Department of Radiology, Miami Children's Hospital, Miami, FL 33155, USA

Tina Young Poussaint, MD
Associate Professor of Radiology, Department of Radiology, Harvard Medical School, Attending Neuroradiologist, Department of Radiology, Children's Hospital Boston, Boston, MA 02115, USA

Stefan Puig, MD MSc
Associate Professor, Head of Department, Research Programm on Evidence-Based Medical Diagnostics, Institute of Public Health, Paracelsus Private Medical University, Salzburg A-5020, Austria

James G. Ravenel, MD
Chief of Thoracic Imaging, Department of Radiology, The Medical University of South Carolina, Charleston, SC 29425, USA

Martin H. Reed, MD, FRCP(C)
Head, Section of Pediatric Radiology, Department of Diagnostic Imaging, University of Manitoba Health Sciences Centre/Children's Hospital, Winnipeg, MB R3A 1S1, Canada

Ricardo Restrepo, MD
Pediatric Radiologist, Fellowship Director, Department of Radiology, Miami Children's Hospital, Miami, FL 33155, USA

Yutaka Sato, MD
Professor of Radiology, Department of Radiology, University of Iowa, Iowa City, IA 52242, USA

Christopher Schettino, MD
Department of Radiology, Miami Children's Hospital, Miami, FL 33155, USA

Marilyn J. Siegel, MD
Professor of Radiology and Pediatrics, Mallinckrodt Institute of Radiology, Washington University Medical School, St. Louis, MO 63110, USA

Gerard A. Silvestri MD, MS
Professor of Medicine, Department of Medicine, Medical University of South Carolina, Charleston, SC 29425, USA

Richard W. Sutherland, MD
Associate Professor, Department of Surgery, Division of Urology, University of North Carolina Children's Hospital, Chapel Hill, NC 27599, USA

Maciej Swiat, MD, PhD
Department of Neurology, Aging, Degenerative and Cerebrovascular Diseases, Medical University of Silesia/Central University Hospital, Katowice, Poland; Department of Radiology, Division of Neuroradiology, University of Pennsylvania, Philadelphia, PA 19104, USA

Maciej Tomaszewski, MD, PhD
Department of Radiology, Division of Neuroradiology, University of Pennsylvania, Philadelphia, PA 19104, USA

Karen A. Tong, BSc, MD
Associate Professor, Department of Radiology, Loma Linda University, Loma Linda, CA 92354, USA

Neil Vachhani, MD
Department of Radiology, Children's Hospital of Philadelphia, Philadelphia, PA 19104, USA

Rick R. van Rijn, MD, PhD
Pediatric Radiologist, Department of Radiology, Emma Children's Hospital/Academic Medical Centre Amsterdam, Meibergdreef 9, Amsterdam 1105 AZ, The Netherlands

Elza Vasconcellos, MD
Director, Headache Disorders Clinic, Department of Neurology, Miami Children's Hospital, Miami, FL 33155

Daniel N. Vinocur, MD
Department of Radiology, Children's Hospital Boston. Harvard Medical School. Boston, Massachusetts

Sjirk J. Westra, MD
Associate Professor, Department of Radiology, Harvard Medical School, Massachusetts General Hospital, Boston, MA 02114, USA

Phoebe H. Yager, MD
Pediatric Intensivist, Massachusetts General Hospital, Assistant in Pediatrics, Harvard Medical School, Department of Pediatric Critical Care Medicine, Boston, MA 02114, USA

Part I

Principles, Methodology, and Radiation Risk

1

Principles of Evidence-Based Imaging

L. Santiago Medina, C. Craig Blackmore, and Kimberly E. Applegate

Medicine is a science of uncertainty and an art of probability.

Sir William Osler

Issues

I. What is evidence-based imaging?
II. The evidence-based imaging process
  a. Formulating the clinical question
  b. Identifying the medical literature
  c. Assessing the literature
    1. What are the types of clinical studies?
    2. What is the diagnostic performance of a test: sensitivity, specificity, and receiver operating characteristic (ROC) curve?
    3. What are cost-effectiveness and cost-utility studies?
  d. Types of economic analyses in medicine
  e. Summarizing the data
  f. Applying the evidence
III. How to use this book

I. What Is Evidence-Based Imaging?

The standard medical education in Western medicine has emphasized skills and knowledge learned from experts, particularly those encountered in the course of postgraduate medical education, and through national publications and meetings. This reliance on experts, referred to by Dr. Paul Gerber of Dartmouth Medical School as "eminence-based medicine"

L.S. Medina (✉)
Co-Director Division of Neuroradiology and Brain Imaging, Director of the Health Outcomes, Policy, and Economics (HOPE) Center, Department of Radiology, Miami Children's Hospital, Miami, FL 33155, USA
e-mail: santiago.medina@mch.com

This chapter is based on a previous chapter titled "Principles of Evidence-Based Imaging" by LS Medina and CC Blackmore that appeared in *Evidence-Based Imaging: Optimizing Imaging in Patient Care* edited by LS Medina and CC Blackmore. New York: Springer Science+Business Media, 2006.

L.S. Medina et al. (eds.), *Evidence-Based Imaging in Pediatrics*,
DOI 10.1007/978-1-4419-0922-0_1, © Springer Science+Business Media, LLC 2010

(1), is based on the construct that the individual practitioner, particularly a specialist devoting extensive time to a given discipline, can arrive at the best approach to a problem through his or her experience. The practitioner builds up an experience base over years and digests information from national experts who have a greater base of experience due to their focus in a particular area. The evidence-based imaging (EBI) paradigm, in contradistinction, is based on the precept that a single practitioner cannot through experience alone arrive at an unbiased assessment of the best course of action. Assessment of appropriate medical care should instead be derived through evidence-based process. The role of the practitioner, then, is not simply to accept information from an expert, but rather to assimilate and critically assess the research evidence that exists in the literature to guide a clinical decision (2–4).

Fundamental to the adoption of the principles of EBI is the understanding that medical care is not optimal. The life expectancy at birth in the United States for males and females in 2005 was 75 and 80 years, respectively (Table 1.1). This is slightly lower than the life expectancies in other industrialized nations such as the United Kingdom and Australia (Table 1.1). The United States spends at least 15.2% of the gross domestic product in order to achieve this life expectancy. This is significantly more than the United Kingdom and Australia, which spend about half that (Table 1.1). In addition, the U.S. per capita health expenditure is $6096, which is twice the expenditures in the United Kingdom or Australia. In conclusion, the United States spends significantly more money and resources than other industrialized countries to achieve a similar outcome in life expectancy. This implies that a significant amount of resources is wasted in the U.S. health care system. The United States in 2007 spent $2.3 trillion in health care. By 2016, the U.S. health percent of the gross domestic product is expected to grow to 20% or $4.2 trillion (5). Recent estimates prepared by the Commonwealth Fund Commission (USA) on a High Performance Health System indicate that $1.5 trillion could be saved over a 10-year period if a combination of options, including evidence-based medicine and universal health insurance, was adopted (6).

Simultaneous with the increase in health care costs has been an explosion in available medical information. The National Library of Medicine PubMed search engine now lists over 18 million citations. Practitioners cannot maintain familiarity with even a minute subset of this literature without a method of filtering out publications that lack appropriate methodological quality. Evidence-based imaging is a promising method of identifying appropriate information to guide practice and to improve the efficiency and effectiveness of imaging.

Evidence-based imaging is defined as medical decision making based on clinical integration of the best medical imaging research evidence with the physician's expertise and with patient's expectations (2–4). The best medical imaging research evidence often comes from the basic sciences of medicine. In EBI, however, the basic science knowledge has been translated into patient-centered clinical research, which determines the accuracy and role of diagnostic and therapeutic imaging in patient care (3). New evidence may make current diagnostic tests obsolete and new ones more accurate, less invasive, safer, and less costly (3).

Table 1.1. Life expectancy and health care spending in three developed countries

	Life expectancy at birth (2005)		Percentage of GDP in health care (2003) (%)	Per capita health expenditure (2007)
	Male	Female		
United States	**753**	**803**	**15.2**	**$6,096**
United Kingdom	**774**	**814**	**7.8**	**$2,560**
Australia	**795**	**845**	**9.2**	**$3,123**

GDP, gross domestic product.

Sources: Organization for Economic Cooperation and Development Health Data File 2002, www.oecd.org/els/health; United Kingdom Office of National Statistics; Australian Bureau of Statistics; Per capita expenditures: *Human Development Report, 2007,* United Nations, hdr.undp.org; Life expectancy: Kaiser Family Foundation web site with stated source: WHO, World Health Statistics 2007, available at: http://www.who.int/whosis/en/.

The physician's expertise entails the ability to use the referring physician's clinical skills and past experience to rapidly identify high-risk individuals who will benefit from the diagnostic information of an imaging test (4). Patient's expectations are important because each individual has values and preferences that should be integrated into the clinical decision making in order to serve our patients' best interests (3). When these three components of medicine come together, clinicians and imagers form a diagnostic team, which will optimize clinical outcomes and quality of life for our patients.

II. The Evidence-Based Imaging Process

The evidence-based imaging process involves a series of steps: (A) formulation of the clinical question, (B) identification of the medical literature, (C) assessment of the literature, (D) summary of the evidence, and (E) application of the evidence to derive an appropriate clinical action. This book is designed to bring the EBI process to the clinician and imager in a user-friendly way. This introductory chapter details each of the steps in the EBI process. Chapter 2 discusses how to critically assess the literature. The rest of the book makes available to practitioners the EBI approach to numerous key medical imaging issues. Each chapter addresses common pediatric disorders ranging from congenital anomalies to asthma to appendicitis. Relevant clinical questions are delineated, and then each chapter discusses the results of the critical analysis of the identified literature. The results of this analysis are presented with meta-analyses where appropriate. Finally, we provide simple recommendations for the various clinical questions, including the strength of the evidence that supports these recommendations.

A. Formulating the Clinical Question

The first step in the EBI process is formulation of the clinical question. The entire process of evidence-based imaging arises from a question that is asked in the context of clinical practice. However, often formulating a question for the EBI approach can be more challenging than one would believe intuitively. To be approachable by the EBI format, a question must be specific to a clinical situation, a patient group, and an outcome or action. For example, it would not be appropriate to simply ask which imaging technique is better—computed tomography (CT) or radiography. The question must be refined to include the particular patient population and the action that the imaging will be used to direct. One can refine the question to include a particular population (which imaging technique is better in pediatric victims of high-energy blunt trauma) and to guide a particular action or decision (to exclude the presence of unstable cervical spine fracture). The full EBI question then becomes, In pediatric victims of high-energy blunt trauma, which imaging modality is preferred, CT or radiography, to exclude the presence of unstable cervical spine fracture? This book addresses questions that commonly arise when employing an EBI approach for the care of children and adolescents. These questions and issues are detailed at the start of each chapter.

B. Identifying the Medical Literature

The process of EBI requires timely access to the relevant medical literature to answer the question. Fortunately, massive on-line bibliographical references such as PubMed are available. In general, titles, indexing terms, abstracts, and often the complete text of much of the world's medical literature are available through these on-line sources. Also, medical librarians are a potential resource to aid identification of the relevant imaging literature. A limitation of today's literature data sources is that often too much information is available and too many potential resources are identified in a literature search. There are currently over 50 radiology journals, and imaging research is also frequently published in journals from other medical subspecialties. We are often confronted with more literature and information than we can process. The greater challenge is to sift through the literature that is identified to select that which is appropriate.

C. Assessing the Literature

To incorporate evidence into practice, the clinician must be able to understand the published literature and to critically evaluate the strength of the evidence. In this introductory chapter on the process of EBI, we focus on discussing types of research studies. Chapter 2 is a detailed discussion of the issues in determining the validity and reliability of the reported results.

1. What Are the Types of Clinical Studies?

An initial assessment of the literature begins with determination of the type of clinical study: descriptive, analytical, or experimental (7). *Descriptive* studies are the most rudimentary, as they only summarize disease processes as seen by imaging, or discuss how an imaging modality can be used to create images. Descriptive studies include case reports and case series. Although they may provide important information that leads to further investigation, descriptive studies are not usually the basis for EBI.

Analytic or *observational* studies include cohort, case–control, and cross-sectional studies (Table 1.2). Cohort studies are defined by risk factor status, and case–control studies consist of groups defined by disease status (8). Both case–control and cohort studies may be used to define the association between an intervention, such as an imaging test, and patient outcome (9). In a cross-sectional (prevalence) study, the researcher makes all of his measurements on a single occasion. The investigator draws a sample from the population (i.e., asthma in 5- to 15-year-olds) and determines distribution of variables within that sample (7). The structure of a cross-sectional study is similar to that of a cohort study except that all pertinent measurements (i.e., PFTs) are made at once, without a follow-up period. Cross-sectional studies can be used as a major source for health and habits of different populations and countries, providing estimates of such parameters as the prevalence of asthma, obesity, and congenital anomalies (7, 10).

Table 1.2. Study design

	Prospective follow-up	Randomization of subjects	Controls
Case report or series	No	No	No
Cross-sectional study	No	No	Yes
Case–control study	No	No	Yes
Cohort study	Yes/no	No	Yes
Randomized controlled trial	Yes	Yes	Yes

Reprinted with the kind permission of Springer Science+Business Media from by Medina and Blackmore (40).

In *experimental studies* or *clinical trials*, a specific intervention is performed and the effect of the intervention is measured by using a control group (Table 1.2). The control group may be tested with a different diagnostic test and treated with a placebo or an alternative mode of therapy (7, 11). Clinical trials are epidemiologic designs that can provide data of high quality that resemble the controlled experiments done by basic science investigators (8). For example, clinical trials may be used to assess new diagnostic tests (e.g., high-resolution CT for cystic fibrosis) or new interventional procedures (e.g., stenting for coronary artery anomalies).

Studies are also traditionally divided into retrospective and prospective (Table 1.2) (7, 11). These terms refer more to the way the data are gathered than to the specific type of study design. In *retrospective studies*, the events of interest have occurred before study onset. Retrospective studies are usually done to assess rare disorders, for pilot studies, and when prospective investigations are not possible. If the disease process is considered rare, retrospective studies facilitate the collection of enough subjects to have meaningful data. For a pilot project, retrospective studies facilitate the collection of preliminary data that can be used to improve the study design in future prospective studies. The major drawback of a retrospective study is incomplete data acquisition (10). Case–control studies are usually retrospective. For example, in a case–control study, subjects in the case group (patients with perforated appendicitis) are compared with subjects in a control group (nonperforated appendicitis) to determine factors associated with perforation (e.g., duration of symptoms, presence of appendicolith, size of appendix) (10).

In *prospective studies*, the event of interest transpires after study onset. Prospective stud-

ies, therefore, are the preferred mode of study design, as they facilitate better control of the design and the quality of the data acquired (7). Prospective studies, even large studies, can be performed efficiently and in a timely fashion if done on common diseases at major institutions, as multicenter trials with adequate study populations (12). The major drawback of a prospective study is the need to make sure that the institution and personnel comply with strict rules concerning consents, protocols, and data acquisition (11). Persistence, to the point of irritation, is crucial to completing a prospective study. Cohort studies and clinical trials are usually prospective. For example, a cohort study could be performed in children with splenic injury in which the risk factor of presence of arterial blush is correlated with the outcome of failure of nonmedical management, as the patients are followed prospectively over time (10).

The strongest study design is the prospective randomized, blinded clinical trial (Table 1.2) (7). The randomization process helps to distribute known and unknown confounding factors, and blinding helps to prevent observer bias from affecting the results (7, 8). However, there are often circumstances in which it is not ethical or practical to randomize and follow patients prospectively. This is particularly true in rare conditions, and in studies to determine causes or predictors of a particular condition (9). Finally, randomized clinical trials are expensive and may require many years of follow-up. Not surprisingly, randomized clinical trials are uncommon in radiology. The evidence that supports much of radiology practice is derived from cohort and other observational studies. More randomized clinical trials are necessary in radiology to provide sound data to use for EBI practice (3).

2. *What Is the Diagnostic Performance of a Test: Sensitivity, Specificity, and Receiver Operating Characteristic (ROC) Curve?*

Defining the presence or absence of an outcome (i.e., disease and nondisease) is based on a standard of reference (Table 1.3). While a perfect standard of reference or so-called gold standard can never be obtained, careful attention should be paid to the selection of the standard that should be widely believed to offer the best approximation to the truth (13).

Table 1.3. Two-way table of diagnostic testing

	Disease (gold standard)	
Test result	**Present**	**Absent**
Positive	**a (TP)**	**b (FP)**
Negative	**c (FN)**	**d (TN)**

FN, false negative; FP, false positive; TN, true negative; TP, true positive.

Reprinted with the kind permission of Springer Science+Business Media from by Medina and Blackmore (40).

In evaluating diagnostic tests, we rely on the statistical calculations of sensitivity and specificity (see Appendix 1). Sensitivity and specificity of a diagnostic test are based on the two-way (2 × 2) table (Table 1.3). Sensitivity refers to the proportion of subjects with the disease who have a positive test and is referred to as the true positive rate (Fig. 1.1). Sensitivity, therefore, indicates how well a test identifies the subjects with disease (7, 14).

Specificity is defined as the proportion of subjects without the disease who have a negative index test (Fig. 1.1) and is referred to as the true negative rate. Specificity, therefore, indicates how well a test identifies the subjects with no disease (7, 11). It is important to note that the sensitivity and specificity are characteristics of the test being evaluated and are therefore usually independent of the prevalence (proportion of individuals in a population who have disease at a specific instant) because the sensitivity only deals with the diseased subjects, whereas the specificity only deals with the nondiseased subjects. However, sensitivity and specificity both depend on a threshold point for considering a test positive and hence may change according to which threshold is selected in the study (11, 14, 15) (Fig. 1.1A). Excellent diagnostic tests have high values (close to 1.0) for both sensitivity and specificity. Given exactly the same diagnostic test, and exactly the same subjects confirmed with the same reference test, the sensitivity with a low threshold is greater than the sensitivity with a high threshold. Conversely, the specificity with a low threshold is less than the specificity with a high threshold (Fig. 1.1B) (14, 15).

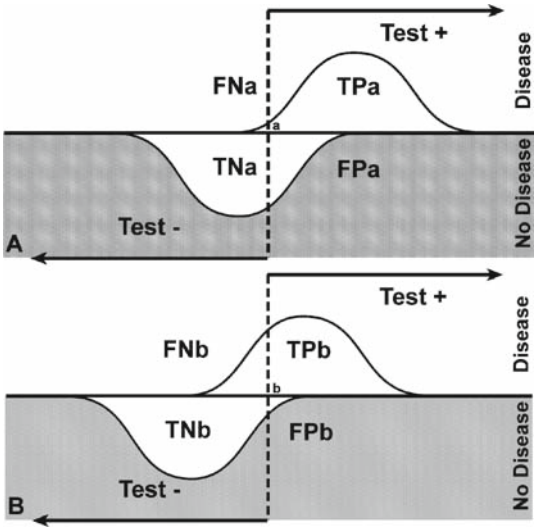

Figure 1.1. Test with a low (A) and high (B) threshold. The sensitivity and specificity of a test change according to the threshold selected; hence, these diagnostic performance parameters are threshold dependent. Sensitivity with low threshold (TPa/diseased patients) is greater than sensitivity with a higher threshold (TPb/dis-eased patients). Specificity with a low threshold (TNa/nondiseased patients) is less than specificity with a high threshold (TNb/nondiseased patients). FN, false negative; FP, false positive; TN, true negative; TP, true positive. (Reprinted with permission of the American Society of Neuroradiology from Medina (11).)

The effect of threshold on the ability of a test to discriminate between disease and nondisease can be measured by a receiver operating characteristic (ROC) curve (11, 15). The ROC curve is used to indicate the trade-offs between sensitivity and specificity for a particular diagnostic test and hence describes the discrimination capacity of that test. An ROC graph shows the relationship between sensitivity (*y*-axis) and 1–specificity (*x*-axis) plotted for various cutoff points. If the threshold for sensitivity and specificity are varied, an ROC curve can be generated. The diagnostic performance of a test can be estimated by the area under the ROC curve. The steeper the ROC curve, the greater the area and the better the discrimination of the test (Fig. 1.2). A test with perfect discrimination has an area of 1.0, whereas a test with only random discrimination has an area of 0.5 (Fig. 1.2). The area under the

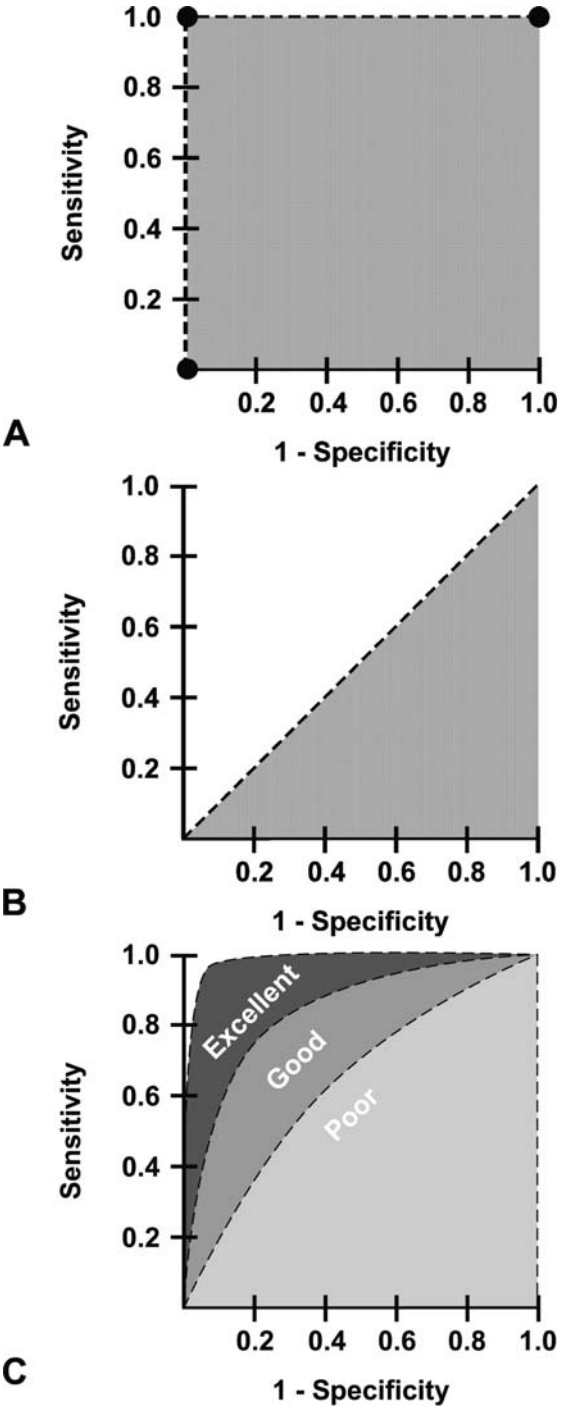

Figure 1.2. The perfect test (A) has an area under the curve (AUC) of 1. The useless test (B) has an AUC of 0.5. The typical test (C) has an AUC between 0.5 and 1. The greater the AUC (i.e., excellent > good > poor), the better the diagnostic performance. (Reprinted with permission of the American Society of Neuroradiology from Medina (11).)

ROC curve usually determines the overall diagnostic performance of the test independent of the threshold selected (11, 15). The ROC curve is threshold independent because it is generated by using varied thresholds of sensitivity and specificity. Therefore, when evaluating a new imaging test, in addition to the sensitivity and specificity, an ROC curve analysis should be done so that the threshold-dependent and threshold-independent diagnostic performance can be fully determined (10).

3. What Are Cost-Effectiveness and Cost-Utility Studies?

Cost-effectiveness analysis (CEA) is an objective scientific technique used to assess alternative health care strategies on both cost and effectiveness (16–18). It can be used to develop clinical and imaging practice guidelines and to set health policy (19). However, it is not designed to be the final answer to the decision-making process; rather, it provides a detailed analysis of the cost and outcome variables and how they are affected by competing medical and diagnostic choices.

Health dollars are limited regardless of the country's economic status. Hence, medical decision makers must weigh the benefits of a diagnostic test (or any intervention) in relation to its cost. Health care resources should be allocated so the maximum health care benefit for the entire population is achieved (10). Cost-effectiveness analysis is an important tool to address health cost-outcome issues in a cost-conscious society. Countries such as Australia usually require robust CEA before drugs are approved for national use (10).

Unfortunately, the term *cost-effectiveness* is often misused in the medical literature (20). To say that a diagnostic test is truly cost-effective, a comprehensive analysis of the entire short- and long-term outcomes and costs needs to be considered. Cost-effectiveness analysis is an objective technique used to determine which of the available tests or treatments are worth the additional costs (21).

There are established guidelines for conducting robust CEA. The U.S. Public Health Service formed a panel of experts on cost-effectiveness in health and medicine to create detailed standards for cost-effectiveness analysis. The panel's recommendations were published as a book in 1996 (21).

D. Types of Economic Analyses in Medicine

There are four well-defined types of economic evaluations in medicine: cost-minimization studies, cost–benefit analyses, cost-effectiveness analyses, and cost-utility analyses. They are all commonly lumped under the term *cost-effectiveness analysis*. However, significant differences exist among these different studies.

Cost-minimization analysis is a comparison of the cost of different health care strategies that are assumed to have identical or similar effectiveness (16). In medical practice, few diagnostic tests or treatments have identical or similar effectiveness. Therefore, relatively few articles have been published in the literature with this type of study design (22). For example, a recent study demonstrated that functional magnetic resonance imaging (MRI) and the Wada test have similar effectiveness for language lateralization, but the later is 3.7 times more costly than the former (23).

Cost–benefit analysis (CBA) uses monetary units such as dollars or euros to compare the costs of a health intervention with its health benefits (16). It converts all benefits to a cost equivalent and is commonly used in the financial world where the cost and benefits of multiple industries can be changed to only monetary values. One method of converting health outcomes into dollars is through a contingent valuation or willingness-to-pay approach. Using this technique, subjects are asked how much money they would be willing to spend to obtain, or avoid, a health outcome. For example, a study by Appel et al. (24) found that individuals would be willing to pay $50 for low osmolar contrast agents to decrease the probability of side effects from intravenous contrast. However, in general, health outcomes and benefits are difficult to transform to monetary units; hence, CBA has had limited acceptance and use in medicine and diagnostic imaging (16, 25).

Cost-effectiveness analysis (CEA) refers to analyses that study both the effectiveness and cost of competing diagnostic or treatment strategies, where effectiveness is an objective measure (e.g., intermediate outcome: number of strokes detected; or long-term outcome: life-

years saved). Radiology CEAs often use intermediate outcomes, such as lesion identified, length of stay, and number of avoidable surgeries (16, 18). However, ideally, long-term outcomes such as life-years saved (LYS) should be used (21). By using LYS, different health care fields or interventions can be compared.

Cost-utility analysis is similar to CEA except that the effectiveness also accounts for quality of life issues. Quality of life is measured as utilities that are based on patient preferences (16). The most commonly used utility measurement is the quality-adjusted life year (QALY). The rationale behind this concept is that the QALY of excellent health is more desirable than the same 1 year with substantial morbidity. The QALY model uses preferences with weight for each health state on a scale from 0 to 1, where 0 is death and 1 is perfect health. The utility score for each health state is multiplied by the length of time the patient spends in that specific health state (16, 26). For example, let us assume that a patient with a congenital heart anomaly has a utility of 0.8 and he spends 1 year in this health state. The patient with the cardiac anomaly would have a 0.8 QALY in comparison with his neighbor who has a perfect health and hence a 1 QALY.

Cost-utility analysis incorporates the patient's subjective value of the risk, discomfort, and pain into the effectiveness measurements of the different diagnostic or therapeutic alternatives. In the end, all medical decisions should reflect the patient's values and priorities (26). That is the explanation of why cost-utility analysis is becoming the preferred method for evaluation of economic issues in health (19, 21). For example, in low-risk newborns with intergluteal dimple suspected of having occult spinal dysraphism, ultrasound was the most effective strategy with an incremented cost-effectiveness ratio of $55,100 per QALY. In intermediate-risk newborns with low anorectal malformation, however, MRI was more effective than ultrasound at an incremental cost-effectiveness of $1000 per QALY (27).

Assessment of Outcomes: The major challenge to cost-utility analysis is the quantification of health or quality of life. One way to quantify health is descriptively. By assessing what patients can and cannot do, how they feel, their mental state, their functional independence, their freedom from pain, and any number of other facets of health and well-being that are referred to as domains, one can summarize their overall health status. Instruments designed to measure these domains are called health status instruments. A large number of health status instruments exist, both general instruments, such as the SF-36 (28), and instruments that are specific to particular disease states, such as the Roland scale for back pain. These various scales enable the quantification of health benefit. For example, Jarvik et al. (29) found no significant difference in the Roland score between patients randomized to MRI versus radiography for low back pain, suggesting that MRI was not worth the additional cost. There are additional issues in applying such tools to children, as they may be too young to understand the questions being asked. Parents can sometimes be used as surrogates, but parents may have different values and may not understand the health condition from the perspective of the child.

Assessment of Cost: All forms of economic analysis require assessment of cost. However, assessment of cost in medical care can be confusing, as the term *cost* is used to refer to many different things. The use of charges for any sort of cost estimation, however, is inappropriate. Charges are arbitrary and have no meaningful use. Reimbursements, derived from Medicare and other fee schedules, are useful as an estimation of the amounts society pays for particular health care interventions. For an analysis taken from the societal perspective, such reimbursements may be most appropriate. For analyses from the institutional perspective or in situations where there are no meaningful Medicare reimbursements, assessment of actual direct and overhead costs may be appropriate (30).

Direct cost assessment centers on the determination of the resources that are consumed in the process of performing a given imaging study, including *fixed costs* such as equipment and *variable costs* such as labor and supplies. Cost analysis often utilizes activity-based costing and time motion studies to determine the resources consumed for a single intervention in the context of the complex health care delivery system. *Overhead*, or *indirect cost*, assessment includes the

costs of buildings, overall administration, taxes, and maintenance that cannot be easily assigned to one particular imaging study. Institutional cost accounting systems may be used to determine both the direct costs of an imaging study and the amount of institutional overhead costs that should be apportioned to that particular test. For example, Medina et al. (31) in a vesicoureteral reflux imaging study in children with urinary tract infection found a significant difference (p <0.0001) between the mean total direct cost of voiding cystourethrography ($112.7 ± $10.33) and radionuclide cystography ($64.58 ± $1.91).

E. Summarizing the Data

The results of the EBI process are a summary of the literature on the topic, both quantitative and qualitative. *Quantitative analysis* involves, at minimum, a descriptive summary of the data and may include formal *meta-analysis* where there is sufficient reliably acquired data. *Qualitative analysis* requires an understanding of error, bias, and the subtleties of experimental design that can affect the reliability of study results. Qualitative assessment of the literature is covered in detail in Chapter 2; this section focuses on meta-analysis and the quantitative summary of data.

The goal of the EBI process is to produce a single summary of all of the data on a particular clinically relevant question. However, the underlying investigations on a particular topic may be too dissimilar in methods or study populations to allow for a simple summary. In such cases, the user of the EBI approach may have to rely on the single study that most closely resembles the clinical subjects upon whom the results are to be applied or may be able only to reliably estimate a range of possible values for the data.

Often, there is abundant information available to answer an EBI question. Multiple studies may be identified that provide methodologically sound data. Therefore, some method must be used to combine the results of these studies in a summary statement. *Meta-analysis* is the method of combining results of multiple studies in a statistically valid manner to determine a summary measure of accuracy or effectiveness (32, 33). For diagnostic studies, the summary estimate is generally a summary sensitivity and specificity, or a summary ROC curve.

The process of performing meta-analysis parallels that of performing primary research. However, instead of individual subjects, the meta-analysis is based on individual studies of a particular question. The process of selecting the studies for a meta-analysis is as important as unbiased selection of subjects for a primary investigation. Identification of studies for meta-analysis employs the same type of process as that for EBI described above, employing Medline and other literature search engines. Critical information from each of the selected studies is then abstracted usually by more than one investigator. For a meta-analysis of a diagnostic accuracy study, the numbers of true positives, false positives, true negatives, and false negatives would be determined for each of the eligible research publications. The results of a meta-analysis are derived not just by simply pooling the results of the individual studies, but instead by considering each individual study as a data point and determining a summary estimate for accuracy based on each of these individual investigations. There are sophisticated statistical methods of combining such results (34).

Like all research, the value of a meta-analysis is directly dependent on the validity of each of the data points. In other words, the quality of the meta-analysis can only be as good as the quality of the research studies that the meta-analysis summarizes. In general, meta-analysis cannot compensate for selection and other biases in primary data. If the studies included in a meta-analysis are different in some way, or are subject to some bias, then the results may be too heterogeneous to combine in a single summary measure. Exploration for such heterogeneity is an important component of meta-analysis.

The ideal for EBI is that all practice be based on the information from one or more well-performed meta-analyses. However, there is often too little data or too much heterogeneity to support formal meta-analysis.

F. Applying the Evidence

The final step in the EBI process is to apply the summary results of the medical literature to

the EBI question. Sometimes the answer to an EBI question is a simple yes or no, as for this question: Does a normal clinical exam exclude unstable cervical spine fracture in patients with minor trauma? Commonly, the answers to EBI questions are expressed as some measure of accuracy. For example, how good is CT for detecting appendicitis? The answer is that CT has an approximate sensitivity of 94% and specificity of 95% (35). However, to guide practice, EBI must be able to answer questions that go beyond simple accuracy, for example, Should CT scan then be used for appendicitis? To answer this question it is useful to divide the types of literature studies into a *hierarchical framework* (36) (Table 1.4). At the foundation in this hierarchy is assessment of *technical efficacy*: studies that are designed to determine if a particular proposed imaging method or application has the underlying ability to produce an image that contains useful information. Information for technical efficacy would include signal-to-noise ratios, image resolution, and freedom from artifacts. The second step in this hierarchy is to determine if the image predicts the truth. This is the *accuracy* of an imaging study and is generally studied by comparing the test results to a reference standard and defining the sensitivity and the specificity of the imaging test. The third step is to incorporate the physician into the evaluation of the imaging intervention by evaluating the effect of the use of the particular imaging intervention on physician certainty of a given diagnosis (physician decision making) and on the actual management of the patient (*therapeutic efficacy*). Finally, to be of value to the patient, an imaging procedure must not only affect management but also improve outcome. *Patient outcome efficacy* is the determination of the effect of a given imaging intervention on the length and quality of life of a patient. A final efficacy level is that of society, which examines the question of not simply the health of a single patient, but that of the health of society as a whole, encompassing the effect of a given intervention on all patients and including the concepts of *cost* and *cost-effectiveness* (36).

Some additional research studies in imaging, such as clinical prediction rules, do not fit readily into this hierarchy. *Clinical prediction rules* are used to define a population in whom imaging is appropriate or can safely be avoided. Clinical prediction rules can also be used in combination with CEA as a way of deciding between competing imaging strategies (37).

Ideally, information would be available to address the effectiveness of a diagnostic test on all levels of the hierarchy. Commonly in imaging, however, the only reliable information that is available is that of diagnostic accuracy. It is incumbent upon the user of the imaging literature to determine if a test with a given sensitivity and specificity is appropriate for use in a given clinical situation. To address this issue, the concept of Bayes' theorem is critical. Bayes' theorem is based on the concept that the value of the diagnostic tests depends not only on the characteristics of the test (sensitivity and specificity) but also on the prevalence (pretest probability) of the disease in the test population. As the prevalence of a specific disease decreases, it becomes less likely that someone with a positive test will actually have the disease, and more likely that the positive test result is a false positive. The relationship between the sensitivity and specificity of the test and the prevalence (pretest probability) can be expressed through the use of Bayes' theorem (see Appendix 2) (11, 14) and the likelihood ratio. The positive likelihood ratio (PLR) estimates the likelihood that a positive test

Table 1.4. Imaging effectiveness hierarchy

Technical efficacy: production of an image or information
Measures: signal-to-noise ratio, resolution, absence of artifacts
Accuracy efficacy: ability of test to differentiate between disease and nondisease
Measures: sensitivity, specificity, receiver operator characteristic curves
Diagnostic-thinking efficacy: impact of test on likelihood of diagnosis in a patient
Measures: pre- and posttest probability, diagnostic certainty
Treatment efficacy: potential of test to change therapy for a patient
Measures: treatment plan, operative or medical treatment frequency
Outcome efficacy: effect of use of test on patient health
Measures: mortality, quality-adjusted life years, health status
Societal efficacy: appropriateness of test from perspective of society
Measures: cost-effectiveness analysis, cost-utility analysis

Adapted with permission from Fryback and Thornbury (36).

result will raise or lower the pretest probability, resulting in estimation of the posttest probability [where PLR = sensitivity/(1–specificity)]. The negative likelihood ratio (NLR) estimates the likelihood that a negative test result will raise or lower the pretest probability, resulting in estimation of the posttest probability [where NLR = (1–sensitivity)/specificity] (38). The likelihood ratio (LR) is not a probability but a ratio of probabilities and as such is not intuitively interpretable. The positive predictive value (PPV) refers to the probability that a person with a positive test result actually has the disease. The negative predictive value (NPV) is the probability that a person with a negative test result does not have the disease. Since the predictive value is determined once the test results are known (i.e., sensitivity and specificity), it actually represents a posttest probability; hence, the posttest probability is determined by both the prevalence (pretest probability) and the test information (i.e., sensitivity and specificity). Thus, the predictive values are affected by the prevalence of disease in the study population.

A practical understanding of this concept is shown in Examples 1 and 2 in Appendix 2. The example shows an increase in the PPV from 0.67 to 0.98 when the prevalence of carotid artery disease is increased from 0.16 to 0.82. Note that the sensitivity and specificity of 0.83 and 0.92, respectively, remain unchanged. If the test information is kept constant (same sensitivity and specificity), the pretest probability (prevalence) affects the posttest probability (predictive value) results.

The concept of diagnostic performance discussed above can be summarized by incorporating the data from Appendix 2 into a nomogram for interpreting diagnostic test results (Fig. 1.3). For example, two patients present to the emergency department complaining of left-sided weakness. The treating physician wants to determine if they have a stroke from carotid artery disease. The first patient is an 8-year-old boy complaining of chronic left-sided weakness. Because of the patient's young age and chronic history, he was determined clinically to be in a low-risk category for carotid artery disease-induced stroke and hence with a low pretest probability of 0.05 (5%). Conversely, the second patient is 65 years old and is complaining of acute onset of severe left-sided weakness. Because of the patient's older age and acute history, he was determined clinically to be in a high-risk category for carotid artery disease-induced stroke and hence with a high pretest probability of 0.70 (70%). The available diagnostic imaging test was unenhanced

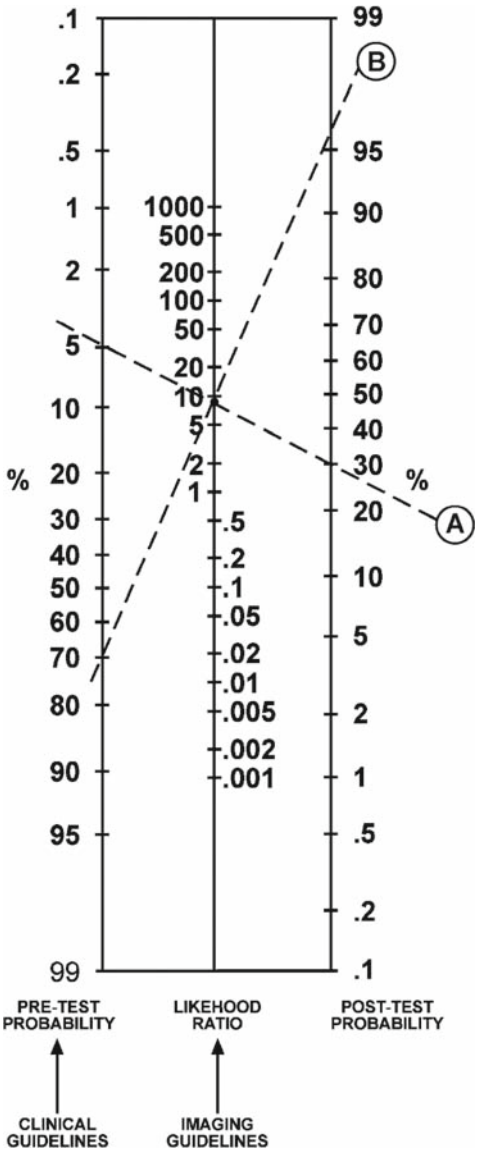

Figure 1.3. Bayes' theorem nomogram for determining posttest probability of disease using the pretest probability of disease and the likelihood ratio from the imaging test. Clinical and imaging guidelines are aimed at increasing the pretest probability and likelihood ratio, respectively. Worked example is explained in the text. (Reprinted with permission from Medina et al. (10).)

head and neck CT followed by CT angiography. According to the radiologist's available literature, the sensitivity and specificity of these tests for carotid artery disease and stroke were each 0.90. The positive likelihood ratio (sensitivity/1–specificity) calculation derived by the radiologist was 0.90/(1–0.90)=9. The posttest probability for the 8-year-old patient is therefore 30% based on a pretest probability of 0.05 and a likelihood ratio of 9 (Fig. 1.3, dashed line A). Conversely, the posttest probability for the 65-year-old patient is greater than 0.95 based on a pretest probability of 0.70 and a positive likelihood ratio of 9 (Fig. 1.3, dashed line B). Clinicians and radiologists can use this scale to understand the probability of disease in different risk groups and for imaging studies with different diagnostic performance. This example also highlights one of the difficulties in extrapolating adult data to the care of children as the results of a diagnostic test may have very different meaning in terms of posttest probability of disease in lower prevalence of many conditions in children.

Jaeschke et al. (38) have proposed a rule of thumb regarding the interpretation of the LR. For PLR, tests with values greater than 10 have a large difference between pretest and posttest probability with conclusive diagnostic impact; values of 5–10 have a moderate difference in test probabilities and moderate diagnostic impact; values of 2–5 have a small difference in test probabilities and sometimes an important diagnostic impact; and values less than 2 have a small difference in test probabilities and seldom have important diagnostic impact. For NLR, tests with values less than 0.1 have a large difference between pretest and posttest probability with conclusive diagnostic impact; values of 0.1 and less than 0.2 have a moderate difference in test probabilities and moderate diagnostic impact; values of 0.2 and less than 0.5 have a small difference in test probabilities and sometimes an important diagnostic impact; and values of 0.5–1 have small difference in test probabilities and seldom have important diagnostic impact.

The role of the clinical guidelines is to increase the pretest probability by adequately distinguishing low-risk from high-risk groups. The role of imaging guidelines is to increase the likelihood ratio by recommending the diagnostic test with the highest sensitivity and specificity. Comprehensive use of clinical and imaging guidelines will improve the posttest probability, hence increasing the diagnostic outcome (10).

III. How to Use This Book

As these examples illustrate, the EBI process can be lengthy (39). The literature is overwhelming in scope and somewhat frustrating in methodologic quality. The process of summarizing data can be challenging to the clinician not skilled in meta-analysis. The time demands on busy practitioners can limit their appropriate use of the EBI approach. This book can obviate these challenges in the use of EBI and make the EBI accessible to all imagers and users of medical imaging.

This book is organized by major diseases and injuries. In the table of contents within each chapter, you will find a series of EBI issues provided as clinically relevant questions. Readers can quickly find the relevant clinical question and receive guidance as to the appropriate recommendation based on the literature. Where appropriate, these questions are further broken down by age, gender, or other clinically important circumstances. Following the chapter's table of contents is a summary of the key points determined from the critical literature review that forms the basis of EBI. Sections on pathophysiology, epidemiology, and cost are next, followed by the goals of imaging and the search methodology. The chapter is then broken down into the clinical issues. Discussion of each issue begins with a brief summary of the literature, including a quantification of the strength of the evidence, and then continues with detailed examination of the supporting evidence. At the end of the chapter, the reader will find the take-home tables and imaging case studies, which highlight key imaging recommendations and their supporting evidence. Finally, questions are included where further research is necessary to understand the role of imaging for each of the topics discussed.

Acknowledgment: We appreciate the contribution of Ruth Carlos, MD, MS, to the discussion of likelihood ratios in this chapter.

IV. Take-Home Appendix 1: Equations

Test result	Present	Outcome	Absent
Positive	a (TP)		b (FP)
Negative	c (FN)		d (TN)
a. Sensitivity		a/(a + c)	
b. Specificity		d/(b + d)	
c. Prevalence		(a + c)/(a + b + c + d)	
d. Accuracy		(a + d)/(a + b + c + d)	
e. Positive predictive value[a]		a/(a + b)	
f. Negative predictive value[a]		d/(c + d)	
g. 95% confidence interval (CI)		$p \pm 1.96\sqrt{\frac{p(1-n)}{n}}$ p = proportion n = number of subjects	
h. Likelihood ratio		$\frac{\text{Sensitivity}}{1-\text{Specificity}} = \frac{a(b+d)}{b(a+c)}$	

[a]Only correct if the prevalence of the outcome is estimated from a random sample or based on an a priori estimate of prevalence in the general population; otherwise, use of Bayes' theorem must be used to calculate PPV and NPV. TP, true positive; FP, false positive; FN, false negative; TN, true negative.

V. Take-Home Appendix 2: Summary of Bayes' Theorem

A. Information before Test × Information from Test = Information after Test
B. Pretest Probability (Prevalence) Sensitivity/1–Specificity = Posttest Probability (Predictive Value)
C. Information from the test also known as the likelihood ratio, described by the Equation: Sensitivity/1–Specificity
D. Examples 1 and 2 predictive values: The predictive values (posttest probability) change according to the differences in prevalence (pretest probability), although the diagnostic performance of the test (i.e., sensitivity and specificity) is unchanged. The following examples illustrate how the prevalence (pretest probability) can affect the predictive values (posttest probability) having the same information in two different study groups.

Equations for calculating the results in the previous examples are listed in Appendix 1. As the prevalence of carotid artery disease

Example 1: Low prevalence of carotid artery disease.

	Disease (carotid artery disease)	No disease (no carotid artery disease)	Total
Test positive (positive CTA)	20	10	30
Test negative (negative CTA)	4	120	124
Total	24	130	154

Example 2: High prevalence of carotid artery disease.

	Disease (carotid artery disease)	No disease(no carotid artery disease)	Total
Test positive (positive CTA)	500	10	510
Test negative (negative CTA)	100	120	220
Total	600	130	730

Results: sensitivity = 500/600 = 0.83; specificity = 120/130 = 0.92; prevalence = 600/730 = 0.82; positive predictive value = 0.98; negative predictive value = 0.55.

increases from 0.16 (low) to 0.82 (high), the positive predictive value (PPV) of a positive contrast-enhanced CT increases from 0.67 to 0.98, respectively. The sensitivity and specificity remain unchanged at 0.83 and 0.92, respectively. These examples also illustrate that the diagnostic performance of the test (i.e., sensitivity and specificity) does not depend on the prevalence (pretest probability) of the disease. CTA, CT angiogram.

References

1. Levin A. Ann Intern Med 1998;128:334–336.
2. Evidence-Based Medicine Working Group. JAMA 1992;268:2420–2425.
3. The Evidence-Based Radiology Working Group. Radiology 2001;220:566–575.
4. Wood BP. Radiology 1999;213:635–637.
5. Poisal JA et al. Health Affairs 2007 (Feb 21): W242–253.
6. Davis K. NEJM 2008;359(Oct 17):1751–1755.
7. Hulley SB, Cummings SR. Designing Clinical Research. Baltimore: Williams and Wilkins, 1998.
8. Kelsey J, Whittemore A, Evans A, Thompson W. Methods in Observational Epidemiology. New York: Oxford University Press, 1996.
9. Blackmore C, Cummings P. AJR 2004;183(5): 1203–1208.
10. Medina L, Aguirre E, Zurakowski D. Neuroimag Clin North Am 2003;13: 157–165.
11. Medina L. AJNR 1999;20:1584–1596.
12. Sunshine JH, McNeil BJ. Radiology 1997; 205:549–557.
13. Black WC. AJR 1990;154:17–22.
14. Sox HC, Blatt MA, Higgins MC, Marton KI. Medical Decision Making. Boston: Butterworth, 1988.
15. Metz CE. Semin Nucl Med 1978;8:283–298.
16. Singer M, Applegate K. Radiology 2001;219: 611–620.
17. Weinstein MC, Fineberg HV. Clinical Decision Analysis. Philadelphia: WB Saunders, 1980.
18. Carlos R. Acad Radiol 2004;11:141–148.
19. Detsky AS, Naglie IG. Ann Intern Med 1990;113:147–154.
20. Doubilet P, Weinstein MC, McNeil BJ. N Engl J Med 1986;314:253–256.
21. Gold MR, Siegel JE, Russell LB, Weinstein MC. Cost-Effectiveness in Health and Medicine. New York: Oxford University Press, 1996.
22. Hillemann D, Lucas B, Mohiuddin S, Holmberg M. Ann Pharmacother 1997;974–979.
23. Medina L, Aguirre E, Bernal B, Altman N. Radiology 2004;230:49–54.
24. Appel LJ, Steinberg EP, Powe NR, Anderson GF, Dwyer SA, Faden RR. Med Care 1990;28:324–337.
25. Evens RG. Cancer 1991;67:1245–1252.
26. Yin D, Forman HP, Langlotz CP. AJR 1995; 165:1323–1328.
27. Medina L, Crone K, Kuntz K. Pediatrics 2001; 108:E101.
28. Ware JE, Sherbourne CD. Medical Care 1992;30:473–483.
29. Jarvik J, Hollingworth W, Martin B, et al. JAMA 2003;2810–2818.
30. Blackmore CC, Magid DJ. Radiology 1997; 203:87–91.
31. Medina L, Aguirre E, Altman N. Acad Radiol 2003;10:139–144.
32. Zou K, Fielding J, Ondategui-Parra S. Acad Radiol 2004;11:127–133.
33. Langlotz C, Sonnad S. Acad Radiol 1998;5(suppl 2):S269–S273.
34. Littenberg B, Moses LE. Med Decis Making 1993;13:313–321.
35. Terasawa T, Blackmore C, Bent S, Kohlwes R. Ann Intern Med 2004;141(7):37–546.
36. Fryback DG, Thornbury JR. Med Decis Making 1991;11:88–94.
37. Blackmore C. Radiology 2005;235(2):371–374.
38. Jaeschke R, Guyatt GH, Sackett DL. JAMA 1994;271:703–707.
39. Malone D. Radiology 2007 242(1);Jan:12–14.
40. Medina LS, Blackmore DD. Evidence-Based Imaging: Optimizing Imaging in Patient. New York: Springer Science+Business Media, 2006.

2

Critically Assessing the Literature: Understanding Error and Bias

C. Craig Blackmore, L. Santiago Medina, James G. Ravenel, Gerard A. Silvestri, and Kimberly E. Applegate

Issues

The keystone of the evidence-based imaging (EBI) approach is to critically assess the research data that are provided and to determine if the information is appropriate for use in answering the EBI question. Unfortunately, the published studies are often limited by bias, small sample size, and methodological inadequacy. Further, the information provided in published reports may be insufficient to allow estimation of the quality of the research. Two recent initiatives, the CONSORT (1) and the STARD (2), aim to improve the reporting of clinical trials and studies of diagnostic accuracy, respectively. However, these guidelines are only now being implemented.

This chapter summarizes the common sources of error and bias in the imaging literature. Using the EBI approach requires an understanding of these issues.

I. What Are Error and Bias?

Errors in the medical literature can be divided into two main types. *Random error* occurs due to chance variation, causing a sample to be different from the underlying population. Random error is more likely to be problematic when the sample size is small. *Systematic error*, or *bias*, is an incorrect study result due to nonrandom

C.C. Blackmore (✉)
Center for Health Care Solutions, Department of Radiology, Virginia Mason Medical Center, Seattle, WA 98111 USA

Reprinted with kind permission of Springer Science+Business Media from Blackmore CC, Medina LS, Ravenel JG, Silvestri GA. Critically Assessing the Literature: Understanding Error and Bias. Medina LS, Blackmore DD (eds): *Evidence-Based Imaging: Optimizing Imaging in Patient Care.* New York: Springer Science+Business Media, 2006.

L.S. Medina et al. (eds.), *Evidence-Based Imaging in Pediatrics*,
DOI 10.1007/978-1-4419-0922-0_2,

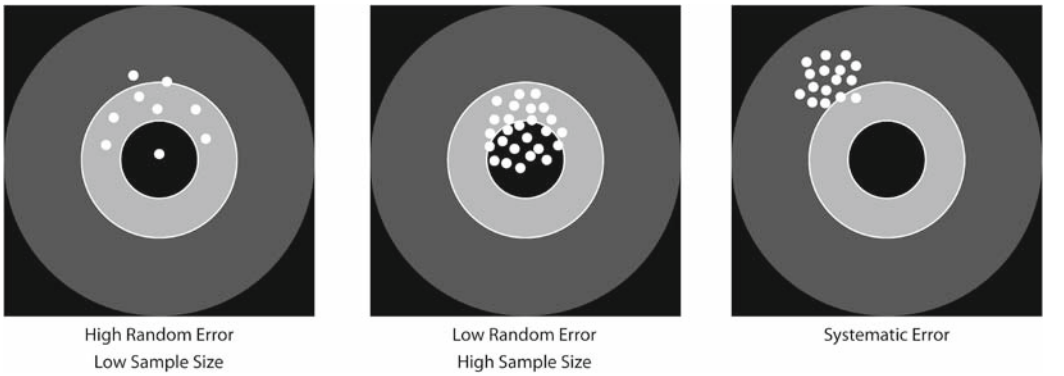

Figure 2.1. Random and systematic errors. Using the bull's-eye analogy, the larger the sample size, the less the random error and the larger the chance of hitting the center of the target. In systematic error, regardless of the sample size, the bias would not allow the researcher to hit the center of the target. (Reprinted with kind permission of Springer Science+Business Media from Blackmore CC, Medina LS, Ravenel JG, Silvestri GA. Critically Assessing the Literature: Understanding Error and Bias. Medina LS, Blackmore DD (eds): *Evidence-Based Imaging: Optimizing Imaging in Patient.* New York: Springer Science+Business Media, 2006.).

distortion of the data. Systematic error is not affected by sample size but is rather a function of flaws in the study design, data collection, and analysis. A second way to think about random and systematic error is in terms of precision and accuracy (3). Random error affects the precision of a result (Fig. 2.1). The larger the sample size, the more precision in the results and the more likely that two samples from truly different populations will be differentiated from each other. Using the bull's-eye analogy, the larger the sample size, the less the random error and the larger the chance of hitting the center of the target (Fig. 2.1). Systematic error, on the other hand, is a distortion in the accuracy of an estimate. Regardless of precision, the underlying estimate is flawed by some aspect of the research procedure. Using the bull's-eye analogy, in systematic error, regardless of the sample size, the bias would not allow the researcher to hit the center of the target (Fig. 2.1).

II. What Is Random Error?

Random error is divided into two main types: Type I, or alpha error, occurs when an investigator concludes that an effect or a difference is present when in fact there is no true difference. Type II, or beta error, occurs when an investigator concludes that there is no effect or no difference when in fact a true difference exists in the underlying population (3).

A. Type I Error

Quantification of the likelihood of alpha error is provided by the familiar p value. A p value less than 0.05 indicates that there is a less than 5% chance that the observed difference in a sample would be seen if there was in fact no true difference in the population. In effect, the difference observed in a sample is due to chance variation rather than a true underlying difference in the population.

There are limitations to the ubiquitous p values seen in imaging research reports (4). The p values are a function of both sample size and magnitude of effect. In other words, there could be a very large difference between two groups under study, but the p value might not be significant if the sample sizes are small. Conversely, there could be a very small, clinically unimportant difference between two groups of subjects or between two imaging tests, but with a large enough sample size, even this clinically unimportant result would be statistically significant. Because of these limitations, many journals are underemphasizing the use of p values and encouraging research results to be reported by way of confidence intervals.

B. Confidence Intervals

Confidence intervals are preferred because they provide much more information than p values. Confidence intervals provide information

about the precision of an estimate (how wide are the confidence intervals), the size of an estimate (magnitude of the confidence intervals), and the statistical significance of an estimate (whether the intervals include the null) (5).

If you assume that your sample was randomly selected from some population (that follows a normal distribution), you can be 95% certain that the confidence interval (CI) includes the population mean. More precisely, if you generate many 95% CIs from many data sets, you can expect that the CI will include the true population mean in 95% of the cases and not include the true mean value in the other 5% (4). Therefore, the 95% CI is related to statistical significance at the $p = 0.05$ level, which means that the interval itself can be used to determine if an estimated change is statistically significant at the 0.05 level (6). Whereas the p value is often interpreted as being either statistically significant or not, the CI, by providing a range of values, allows the reader to interpret the implications of the results at either end (6, 7). In addition, while p values have no units, CIs are presented in the units of the variable of interest, which helps readers to interpret the results. The CIs shift the interpretation from a qualitative judgment about the role of chance to a quantitative estimation of the biologic measure of effect (4, 6, 7).

Confidence intervals can be constructed for any desired level of confidence. There is nothing magical about the 95% that is traditionally used. If greater confidence is needed, then the intervals have to be wider. Consequently, 99% CIs are wider than 95%, and 90% CIs are narrower than 95%. Wider CIs are associated with greater confidence but less precision. This is the trade-off (4).

As an example, two hypothetical transcranial circle of Willis vascular ultrasound studies in patients with sickle cell disease describe mean peak systolic velocities of 200 cm/s associated with 70% of vascular diameter stenosis and higher risk of stroke. Both articles reported the same standard deviation (SD) of 50 cm/s. However, one study had 50 subjects, while the other one had 500 subjects. At first glance, both studies appear to provide similar information. However, the narrower confidence intervals for the larger study reflect greater precision and indicate the value of the larger sample size. For a smaller sample

$$95\%\ \text{CI} = 200 \pm 1.96\left(\frac{50}{\sqrt{50}}\right)$$
$$95\%\ \text{CI} = 200 \pm 14 = 186 - 214$$

For a larger sample

$$95\%\ \text{CI} = 200 \pm 1.96\left(\frac{50}{\sqrt{500}}\right)$$
$$95\%\ \text{CI} = 200 \pm 4 = 196 - 204$$

In the smaller series, the 95% CI was 186–214 cm/s, while in the larger series, the 95% CI was 196–204 cm/s. Therefore, the larger series has a narrower 95% CI (4).

C. Type II Error

The familiar p value alone does not provide information as to the probability of a type II or beta error. A p value greater than 0.05 does not necessarily mean that there is no difference in the underlying population. The size of the sample studied may be too small to detect an important difference even if such a difference does exist. The ability of a study to detect an important difference, if that difference does in fact exist in the underlying population, is called the power of a study. Power analysis can be performed in advance of a research investigation to avoid type II error. To conclude that no difference exists, the study must be powered sufficiently to detect a clinically important difference and have p value or confidence interval indicating no significant effect.

D. Power Analysis

Power analysis plays an important role in determining what an adequate sample size is so that meaningful results can be obtained (8). Power analysis is the probability of observing an effect in a sample of patients if the specified effect size, or greater, is found in the population (3). Mathematically, power is defined as 1 minus beta

(1–β), where β is the probability of having a type II error. Type II errors are commonly referred to as false negatives in a study population. Type I errors, in contrast, are analogous false positives in a study population (7). For example, if β is set at 0.10, then the researchers acknowledge that they are willing to accept a 10% chance of missing a correlation between abnormal computed tomography (CT) angiographic findings in the diagnosis of carotid artery disease. This represents a power of 1 minus 0.10, or 0.90, which represents a 90% probability of finding a correlation of this magnitude.

Ideally, the power should be 100% by setting β at 0. In addition, ideally α should also be 0. By accomplishing this, false-negative and false-positive results are eliminated, respectively. In practice, however, powers near 100% is rarely achievable, so, at best, a study should reduce the false negatives (β) and false positives (α) to a minimum (3, 9). Achieving an acceptable reduction of false negatives and false positives requires a large subject sample size. Optimal power, α and β, settings are based on a balance between scientific rigorousness and the issues of feasibility and cost. For example, assuming an α error of 0.10, your sample size increases from 96 to 118 subjects per study arm (carotid and noncarotid artery disease arms) if you change your desired power from 85 to 90% (10). Studies with more complete reporting and better study design will often report the power of the study, for example, by stating that the study has 90% power to detect a difference in sensitivity of 10% between CT angiography and Doppler ultrasound in carotid artery disease.

III. What Is Bias?

The risk of an error from bias decreases as the rigorousness of the study design and analysis increases. Randomized controlled trials are considered the best design for minimizing the risk of bias because patients are randomly allocated. This random allocation allows for unbiased distribution of both known and unknown confounding variables between the study groups. In nonrandomized studies, appropriate study design and statistical analysis can control only for known or measurable bias.

Detection of and correction for bias, or systematic error, in research is a vexing challenge for both researchers and users of the medical literature alike. Maclure and Schneeweiss (11) have identified 10 different levels at which biases can distort the relationship between published study results and truth. Unfortunately, bias is common in published reports (12), and reports with identifiable biases often overestimate the accuracy of diagnostic tests (13). Careful surveillance for each of these individual bias phenomena is critical, but may be a challenge. Different study designs are also susceptible to different types of bias, as will be discussed in this section as well. Well-reported studies often include a section on limitations of the work, spelling out the potential sources of bias that the investigator acknowledges from a study as well as the likely direction of the bias and steps that may have been taken to overcome it. However, the final determination of whether a research study is sufficiently distorted by bias to be unusable is left to the discretion of the user of the imaging literature. The imaging practitioner must determine if results of a particular study are true, are relevant to a given clinical question, and are sufficient as a basis to change practice.

A common bias encountered in imaging research is that of *selection bias* (14). Because a research study cannot include all individuals in the world who have a particular clinical situation, research is conducted on samples. Selection bias can arise if the sample is not a true representation of the relevant underlying clinical population (Fig. 2.2). Numerous subtypes of selection bias have been identified, and it is a challenge to the researcher to avoid all of these biases when performing a study. One particularly severe form of selection bias occurs if the diagnostic test is applied to subjects with a spectrum of disease that differs from the clinically relevant group. The extreme form of this spectrum bias occurs when the diagnostic test is evaluated on subjects with severe disease and on normal controls. In an evaluation of the effect of bias on study results, Lijmer et al. (13) found the greatest overestimation of test accuracy with this type of spectrum bias.

A second frequently encountered bias in imaging literature is that of *observer bias* (15, 16), also called test-review bias and diagnostic-review bias (17). Imaging tests are largely

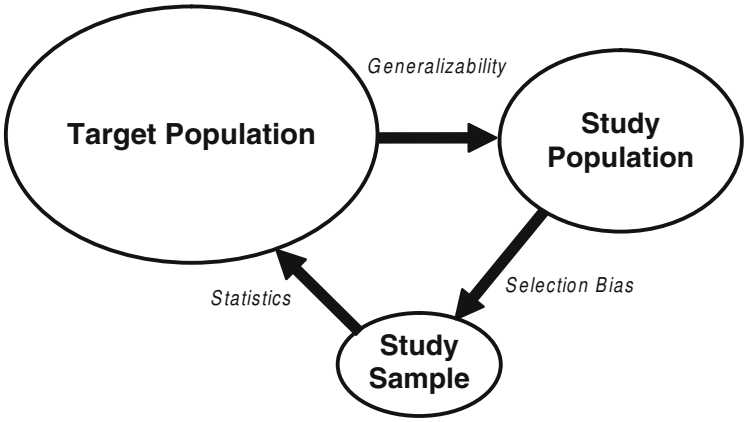

Figure 2.2. Population and sample. The target population represents the universe of subjects who are at risk for a particular disease or condition. In this example, all subjects with abdominal pain are at risk for appendicitis. The sample population is the group of eligible subjects available to the investigators. These may be at a single center or group of centers. The sample is the group of subjects who are actually studied. Selection bias occurs when the sample is not truly representative of the study population. How closely the study population reflects the target population determines the generalizability of the research. Finally, statistics are used to determine what inference about the target population can be drawn from the sample data. (Reprinted with kind permission of Springer Science+Business Media from Blackmore CC, Medina LS, Ravenel JG, Silvestri GA. Critically Assessing the Literature: Understanding Error and Bias. Medina LS, Blackmore DD (eds): *Evidence-Based Imaging: Optimizing Imaging in Patient*. New York: Springer Science+Business Media, 2006.).

subjective. The radiologist interpreting an imaging study forms an impression based on the appearance of the image, not based on an objective number or measurement. This subjective impression can be biased by numerous factors including the radiologist's experience; the context of the interpretation (clinical vs. research setting); the information about the patient's history that is known by the radiologist; incentives that the radiologist may have, both monetary and otherwise, to produce a particular report; and the memory of a recent experience. But because of all these factors, it is critical that the interpreting physician be blinded to the outcome or gold standard when a diagnostic test or an intervention is being assessed. Important distortions in research results have been found when observers are not blinded vs. blinded. For example, Schulz et al. (18) showed a 17% greater outcome improvement in studies with unblinded assessment of outcomes versus those with blinded assessment. To obtain objective scientific assessment of an imaging test, all readers should be blinded to other diagnostic tests and final diagnosis, and all patient-identifying marks on the test should be masked.

Bias can also be introduced by the *reference standard* used to confirm the final diagnosis. First, the interpretation of the reference standard must be made without knowledge of the test results. Reference standards, like the diagnostic tests themselves, may have a subjective component and therefore may be affected by knowledge of the results of the diagnostic test. In addition, it is critical that all subjects undergo the same reference standard. The use of different reference standards (called differential reference standard bias) for subjects with different diagnostic test results may falsely elevate both sensitivity and specificity (13, 16). Of course, sometimes it is not possible or ethical to perform the same reference standard procedure on all subjects. For example, in a recent meta-analysis of imaging for appendicitis, Terasawa et al. (19) found that all of the identified studies used a different reference standard for subjects with positive imaging (appendectomy and pathologic evaluation) than for those with negative imaging (clinical follow-up). It simply would not be ethical to perform appendectomy on all subjects. Likely the sensitivity and specificity of imaging for appendicitis was overestimated as a result.

IV. What Are the Inherent Biases in Screening?

Investigations of screening tests are susceptible to an additional set of biases. Screening case–control trials are vulnerable to *screening selection bias.* For example, lung cancer case–control studies have been performed in Japan, where long-running tuberculosis control programs have been in place. This allowed for the analysis of those who were screened to be matched with a database of matched unscreened controls to arrive at a relative risk of dying from lung cancer in screened and unscreened populations. Because screening is a choice in these studies, selection bias plays a prominent role. That is, people who present for elective screening tend to have better health habits (20). In assessing the exposure history of cases, the inclusion of the test on which the diagnosis is made, regardless of whether it is truly screen or symptom detected, can lead to an odds ratio greater than 1 even in the absence of benefit (21). Similarly, excluding the test on which the diagnosis is made may underestimate screening effectiveness. The magnitude of bias is further reflected in the disease preclinical phase; the longer the preclinical phase, the greater the magnitude of the bias.

Prospective nonrandomized screening trials perform an intervention on subjects, such as screening for lung cancer, and follow them for many years. These studies can give information on the stage distribution and survival of a screened population; however, these measures do not allow an accurate comparison to an unscreened group due to lead time, length time, and overdiagnosis bias (22) (Fig. 2.3). *Lead-time bias* results from the earlier detection of the disease, which leads to longer time from diagnosis and an apparent survival advantage but does not truly impact the date of death. *Length-time bias* relates to the virulence of tumors. More indolent tumors are more likely to be detected by screening, whereas aggressive tumors are more likely to be detected by symptoms. This disproportionally assigns more indolent disease to the intervention group and results in the appearance of a benefit. *Overdiagnosis* is the most extreme form of length-time bias in which a disease is detected and "cured," but it is so indolent that it would have never caused symptoms during life. Thus, survival alone is not an appropriate measure of the effectiveness of screening (23).

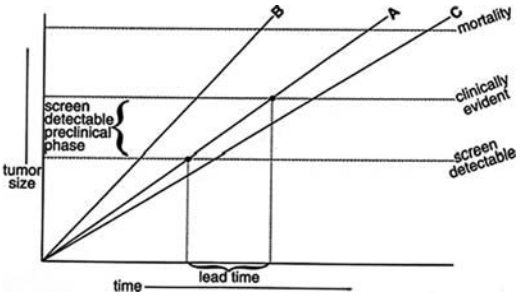

Figure 2.3. Screening biases. For this figure, cancers are assumed to grow at a continuous rate until they reach a size at which death of the subject occurs. At a small size, the cancers may be evident on screening, but not yet evident clinically. This is the preclinical screen-detectable phase. Screening is potentially helpful if it detects cancer in this phase. After further growth, the cancer will be clinically evident. Even if the growth and outcome of the cancer is unaffected by screening, merely detecting the cancer earlier will increase apparent survival. This is the screening lead time. In addition, slower growing cancers (such as **C**) will exist in the preclinical screen-detectable phase for longer than do faster growing cancers (such as **B**). Therefore, screening is more likely to detect more indolent cancers, a phenomenon known as length bias. (Reprinted with kind permission of Springer Science+Business Media from Blackmore CC, Medina LS, Ravenel JG, Silvestri GA. Critically Assessing the Literature: Understanding Error and Bias. Medina LS, Blackmore DD (eds): *Evidence-Based Imaging: Optimizing Imaging in Patient.* New York: Springer Science+Business Media, 2006.).

For this reason, a randomized controlled trial (RCT) with disease-specific mortality as an end point is the preferred methodology. Randomization should even out the selection process in both arms, eliminating the bias of case–control studies and allowing direct comparison of groups that underwent the intervention and those that did not, to see if the intervention lowers deaths due to the target disease. The disadvantage of the RCT is that it takes many years and is expensive to perform. There are two biases that can occur in RCTs and are important to understand: *sticky diagnosis* and *slippery linkage* (24). Because the target disease is more likely to be detected in a screened population, it is more likely to be listed as a cause of death, even if not the true cause. As such, the diagnosis "sticks" and tends to underestimate the true value of the test. On the other hand, screening may set into motion a

series of events in order to diagnose and treat the illness. If these procedures remotely lead to mortality, such as a myocardial infarction during surgery with death several months later, the linkage of the cause of death to the screening may no longer be obvious (slippery linkage). Because the death is not appropriately assigned to the target disease, the value of screening may be overestimated. For this reason, in addition to disease-specific mortality, all-cause mortality should also be evaluated in the context of screening trials (24). Ultimately, to show the effectiveness of screening, not only more early-stage cancers need to be found in the screened group, but also there must be fewer late-stage cancers (stage shift) (22).

V. Qualitative Literature Summary

The potential for error and bias makes the process of critically assessing a journal article complex and challenging, and no investigation is perfect. Producing an overall summation of the quality of a research report is difficult. However, there are grading schemes that provide a useful estimation of the value of a research report for guiding clinical practice. The method used in this book is derived from that of Kent et al. (25) and is shown in Table2.1. Use of such a grading scheme is by nature an oversimplification. However, such simple guidelines can provide a useful quick overview of the quality of a research report.

Table 2.1. Evidence classification for evaluation of a study

Level I: Strong evidence **Studies with broad generalizability to most patients suspected of having the disease of concern: a prospective, blinded comparison of a diagnostic test result with a well-defined final diagnosis in an unbiased sample when assessing diagnostic accuracy or blinded randomized control trials or when assessing therapeutic impact or patient outcomes. Well-designed meta-analysis based on level I or II studies**
Level II: Moderate evidence **Prospective or retrospective studies with narrower spectrum of generalizability, with only a few flaws that are well described so that their impact can be assessed, but still requiring a blinded study of diagnostic accuracy on an unbiased sample. This includes well-designed cohort or case–control studies and randomized trials for therapeutic effects or patient outcomes**
Level III: Limited evidence **Diagnostic accuracy studies with several flaws in research methods, small sample sizes, or incomplete reporting, or nonrandomized comparisons for therapeutic impact or patient outcomes**
Level IV: Insufficient evidence **Studies with multiple flaws in research methods, case series, descriptive studies, or expert opinions without substantiating data**

Reprinted with kind permission of Springer Science+Business Media from Blackmore CC, Medina LS, Ravenel JG, Silvestri GA. Critically Assessing the Literature: Understanding Error and Bias. Medina LS, Blackmore DD (eds): *Evidence-Based Imaging: Optimizing Imaging in Patient*. New York: Springer Science+Business Media, 2006.

Conclusion

Critical analysis of a research publication can be a challenging task. The reader must consider the potential for type I and type II random errors, as well as systematic error introduced by biases including selection bias, observer bias, and reference standard bias. Screening includes an additional set of challenges related to lead time, length bias, and overdiagnosis.

References

1. Moher D, Schulz K, Altman D. JAMA 2001;285:1987–1991.
2. Bossuyt PM, Reitsma J, Bruns D, et al. Acad Radiol 2003;10:664–669.
3. Hulley SB, Cummings SR. Designing Clinical Research. Baltimore: Williams and Wilkins, 1998.
4. Medina L, Zurakowski D. Radiology 2003;226:297–301.
5. Gallagher E. Acad Emerg Med 1999;6:1084–1087.
6. Lang T, Secic M. How to Report Statistics in Medicine. Philadelphia: American College of Physicians, 1997.
7. Gardener M, Altman D. Br Med J 1986:746–750.
8. Medina L, Aguirre E, Zurakowski D. Neuroimag Clin North Am 2003;13:157–165.
9. Medina L. AJNR 1999;20:1584–1596.
10. Donner A. Stat Med 1984;3:199–214.
11. Maclure M, Schneeweiss S. Epidemiology 2001;12:114–122.
12. Reid MC, Lachs MS, Feinstein AR. JAMA 1995;274:645–651.
13. Lijmer JG, Mol BW, Heisterkamp S, et al. JAMA 1999;282:1061–1066.
14. Blackmore C. Acad Radiol 2004;11:134–140.
15. Ransohoff DF, Feinstein AR. N Engl J Med 1978;299:926–930.
16. Black WC. AJR 1990;154:17–22.
17. Begg CB, McNeil BJ. Radiology 1988;167: 565–569.
18. Schulz K, Chalmers I, Hayes R, Altman D. JAMA 1995;273:408–412.
19. Terasawa T, Blackmore C, Bent S, Kohlwes R. Ann Intern Med 2004;141:537–546.
20. Marcus P. Lung Cancer 2003;41:37–39.
21. Hosek R, Flanders W, Sasco A. Am J Epidemiol 1996;143:193–201.
22. Patz E, Goodman P, Bepler G. N Engl J Med 2000;343:1627–1633.
23. Black WC, Welch HG. AJR 1997;168:3–11.
24. Black W, Haggstrom D, Welch H. J Natl Cancer Inst 2002;94.
25. Kent DL, Haynor DR, Longstreth WT Jr, Larson EB. Ann Intern Med 1994;120: 856–871.

3

Radiation Risk from Medical Imaging in Children

Donald P. Frush and Kimberly E. Applegate

Issues

I. Is there a cancer risk from low-level radiation used in medical imaging? What are the uncertainties in the data?
II. What is the estimated risk from a single chest X-ray in a child?
III. What is the estimated risk from a single abdominal CT scan in a child?
IV. Understanding benefit versus risk of imaging tests in well-indicated studies versus those that have very low probability of disease
V. How should I communicate radiation risk from imaging to parents and patients?
VI. Special situation: Increased cancer risk following therapeutic medical radiation

Key Points

- Medical radiation currently accounts for an increasing percentage (approximately 50%) of the total radiation exposure for the US population (previously about 15%) (moderate evidence).
- Children are 2–5 (some cite up to 10) times more sensitive to radiation than adults (moderate evidence).
- There are no data that prove a direct link between low-level radiation from diagnostic imaging and cancer. The best data regarding long-term effects of low-level radiation (100–150 mSv) exposure come from the longitudinal survivor study (LSS) of atomic bomb survivors (moderate evidence).
- Most major medical and scientific organizations accept the linear, no-threshold model as the preferred model for low-level radiation and cancer risk estimation.
- The lifetime risk of fatal cancer from a single (relatively high dose) CT in a child has been estimated to be 1:1000 (limited to moderate evidence).

D.P. Frush (✉)
Professor of Radiology and Pediatrics, Division of Pediatric Radiology, Department of Radiology, Duke Medical Center, Durham, NC 27710, USA

L.S. Medina et al. (eds.), *Evidence-Based Imaging in Pediatrics*,
DOI 10.1007/978-1-4419-0922-0_3,

Definition and Pathophysiology

Medical radiation is used for both diagnostic and therapeutic purposes. The X-ray is an invisible beam of ionizing radiation that passes through the body and is altered by different tissues to create images. Imaging tests that use ionizing radiation include the plain X-ray (or radiograph), fluoroscopy, and the CT scan. Diagnostic imaging uses low-level radiation that is defined, for the purposes of radiation risk, as <100–150 mSv.

Radiation Terminology

Measurements are presented in standard international units (SI=*Systeme Internationale*) (1) (Table 3.1). Incident X-ray radiation *intensity* can be characterized by exposure in coulombs/kg (ionizations in coulombs per mass) or the preferred air kerma in Gray (Gy) (kinetic energy transferred per unit mass). The *absorption* of this radiation intensity is then, simply, the *absorbed dose,* also measured in Gy (the energy transfer will depend on factors including physical properties of the material as well as depth in the body), including skin and other organ doses. The biological *impact* to tissue is represented by *equivalent dose* in Sieverts (Sv), the product of the absorbed dose and a weighting factor (value depends on the type of radiation that causes ionization in tissue with the factor being 1.0 for medical imaging). Finally, the *effective dose equivalent* (alternatively, effective dose) in Sv is the sum of products of dose equivalents multiplied by weighting factors depending on the radiosensitivity of organs exposed. Effective doses represent a whole body equivalent (as if the whole body were exposed) for exposures that may be regional. Because absorbed dose and effective dose represent energy deposition and ionization in tissues, these terms are typically used in discussions of radiation risk in humans.

Radiation Mechanisms of Effect

Ionizing radiation particles include X-rays (photons). These high-energy photons interact with tissue depositing energy at the nuclear level causing ionizations. Ionizations then damage DNA either directly or secondarily through generation of free radicals, especially hydroxyl free radicals. Single-stranded DNA damage is usually repaired but double-stranded damage is more difficult to repair completely. Biological effects may be immediate causing *cell death* (such as radiation necrosis), which may lead to organism death, or consist of *cell damage* leading to other effects such as birth defects or cancer. Cell damage could be due to direct DNA damage but may also be due to other effects such as genomic instability (with additional DNA aberrations in cell progeny) and regulatory mechanisms. For diagnostic imaging levels of radiation dose, the most pertinent bioeffect is carcinogenesis. In short, the development of radiation-induced cancer is a multistep process. In addition to these generalized mechanisms of radiation bioeffects, there are other factors determining susceptibility; for example, there is a genetic basis of cancer in up to 10–15% of childhood cancer (Table 3.2) (2).

Types of Biological Effects

There are two types of biological effects: stochastic and deterministic. Deterministic effects have a threshold below which the effect is not seen (Table 3.3). These effects include cataracts, skin burns, and epilation (hair loss). These types of effects are almost all seen in imaging when interventional procedures are being performed with doses well above the low-level radiation seen in diagnostic imaging. Recently, however, epilation was noted with a diagnostic perfusion and CTA examination (3). Stochastic effects do not have a threshold. The risk of a particular effect increases with increasing radiation dose; however the severity of the effect is independent of dose. Radiation carcinogenesis and radiation-induced genetic damage are stochastic phenomena. For the purposes of this chapter, the stochastic effect of carcinogenesis will be discussed as most literature and attention has been focused on this effect. While other biological effects of low-level radiation have been assessed (4, 5), the overwhelming majority on investigation with low-level radiation deals with cancer risk.

Radiation Doses in Medical Imaging

Radiation doses for the imaging modalities of radiography, fluoroscopy/angiography, and computed tomography vary depending on the type of dose measurement, age of the patient, examination, and techniques used. A detailed discussion of dose ranges for these various modalities is beyond the intent of this chapter; however readers are referred to the UNSCEAR report (6) for a comprehensive review of dose ranges for many of these modalities.

Fluoroscopy and angiography procedures are better described in terms of dose rates, since the dose from these procedures will depend on imaging time, as well as the number of radiographs (CR, DR, or conventional screen film) (7). For the purposes of clinical practice, it can be helpful to describe these common fluoroscopic (and other diagnostic imaging) procedures in terms of dose equivalents compared with chest radiography (Table 3.4). Recently, Thierry-Chef et al. (8) estimated that lifetime risk for developing brain cancer following a variety of neurointerventional procedures in children ranged from 2 to 80% (relative risk of 1.02–1.8).

It is worth mentioning, since CT is a relatively large component of total medical dose, that there are methods for estimating patient dose based on the CT dose index (CTDI) in mGy and the dose length product (DLP) in mGy.cm (the product of CTDI and the length of the scan). It is important to realize that this dose represents only the determination from a phantom and has nothing to do with the individual patient on the scanner. However, conversion factors to change the dose length product into an effective dose estimate are available and have been recently well reviewed by Thomas and Wang (9). In addition, Huda et al. have described a method for converting pediatric CT examination parameters into effective dose estimates for a variety of pediatric CT examinations (10).

Epidemiology and Medical Utilization of Ionizing Radiation

We all are exposed to small amounts of radiation from soil, rocks, building materials, air, water, and cosmic radiation. This naturally occurring background radiation dose is about 3.0 mSv annually. When medical radiation is added to this background, the average dose for the US population is about 6.0 mSv (11). The largest contributors to medical radiation dose are CT scanning (up to one-half of medical exposure) followed by nuclear medicine (about one-quarter of medical exposure). Medical imaging is predominantly used in developed rather than developing nations.

Medical imaging is an extremely important diagnostic tool; in a recent survey, leaders in internal medicine ranked CT and MR imaging as the most important medical innovations in the twentieth century (12). With increased technologic advances and potential applications, the benefits to the patients and society will continue to become more diverse and increase. However, there are inherent risks in those modalities which depend on ionizing radiation for imaging formation, consisting primarily of radiography, fluoroscopy/angiography, and computed tomography in the pediatric population. One of these risks is the potential for cancer development. While there are clearly established relationships between cancer development and radiation from studies of Hiroshima atomic bomb survivors at medium- and high-level exposures (>100–150 mSv), the risks in the lower range are debated. In general, assignment of this risk follows a linear, no-threshold model. This model is accepted by most major medical imaging organizations. There are no data from medical exposures in this range of low-level exposure that directly link diagnostic imaging with cancer development; our understanding of this potential link comes from atomic bomb data, with some additional contribution from epidemiologic studies from higher dose of radiation used for both diagnostic and therapeutic purposes. With these data, there is growing evidence supporting the association with lower level radiation and a significant increased risk of cancer development as predicted by the linear, no-threshold model. This adds support for subscribing to the ALARA principle. This principle of As Low As Reasonably Achievable means that we should use as low a radiation dose as possible to answer the clinical question asked.

Increased Dose from Medical Imaging

While increased use is part of the reason for increasing radiation exposure to the population, technologic advances have also resulted in some of this increase in radiation exposure. Digital technology is now nearly standard for all diagnostic imaging modalities that use ionizing radiation including radiography, fluoroscopy/angiography, and computed tomography. When properly performed, digital technology for radiography should provide for lower (or similar) radiation exposures as the traditional film-based systems. This is not always the case. Often, dose information from computed radiography (CR), digital radiography (DR), and computed tomography images is not displayed nor apparent and monitoring dose based on annotation on the image is difficult. In addition, with film, an overexposure resulted in a dark image serving as a quality control. This does not happen with digital technology; there is no visual manifestation, no "penalty" for overexposures. Collimation can reduce the field of view for the final image and the exposure outside of this field is no longer accounted for as with traditional film-based technology. Similarly, since there is no "film repository" for poor-quality studies, a digital radiograph which is unacceptable may essentially vanish into an unmonitored, electronic wastebasket despite the fact that the patient did receive the dose.

Increased Use of CT Scans

CT scans contribute the highest dose from medical radiation in developed nations. Worldwide, there are an estimated 260,000,000 CT studies annually. The United States accounts for an estimated 25% of all CT exams worldwide, representing 65,000,000 CT examinations each year (6, 13). If we apply a recent estimate that 11% of CT examinations being performed are in children, then the number of annual pediatric CT examinations could be as high as 7.1 million in the United States (14).

Assessing Risk Versus Benefit when Using Medical Imaging in Children

Medical imaging is often now first line in diagnosis of injury and illness in children as well as adults. More simply stated, information obtained from imaging alone can be lifesaving. However, the decision to obtain imaging examinations needs to balance this potential benefit with both established and potential risks. Risks for several of these imaging modalities include bioeffects due to exposure to ionizing radiation. The bulk of pediatric diagnostic imaging that exposes children to ionizing radiation consists of radiography, fluoroscopy/angiography, and computed tomography; radionuclide scintigraphy contributes relatively little to medical dose in children since examinations are relatively infrequent and lower dose compared with adults (i.e., cardiac imaging). As will be discussed later, the radiation dose from imaging can vary and may be relatively high. This is particularly important since imaging use has grown. For example, medical imaging especially computed tomography currently accounts for up to or more than 50% of all of the radiation exposure to the US population (11). This increased use has not gone without continued scrutiny. Brenner and Hall outlined the growing use of CT with respect to potential cancer development late in 2007 (13).

While the topic of medical imaging, radiation exposure, and potential risk is important at all ages, this is especially topical for children. Children are more sensitive to radiation than adults. Accordingly, imaging applications and techniques may need to differ from those in adults to minimize the radiation exposure, in keeping with the ALARA (as low as reasonably achievable) principle (15). However, adult techniques, for example in CT (16), have traditionally been the default. A lack of understanding of radiation risks in children coupled with a neglect of the unique considerations in applications and techniques may shift the balance away from patient benefit.

Therefore, this chapter will discuss radiation risks with medical imaging in children. This material will primarily address what is known about low-level radiation—100–150 mSv (17)—resulting from diagnostic imaging rather than oncologic radiation treatment where radiation bioeffects are clearly present and risks more definitively established due to doses which may be orders of magnitude greater. Some data on radiation therapy for non-oncologic conditions in children will be presented as these doses are

lower and approach low-level radiation. While cumulative doses from diagnostic imaging may exceed the low-level threshold, most material will focus on low-level doses.

The topic of radiation and biological impact is extensive and discussion will be focused on diagnostic imaging in the pediatric population, and will not address fetal exposures. Information will be provided from a perspective of radiology rather than radiation biology, health or radiation physics, or epidemiology. More extensive information on radiation and the potential effects can be found in other comprehensive sources (18). Finally, discussion will not include strategies for dose management, including radioprotectants (19).

Overall Cost to Society

The American health care system costs more than $2.3 trillion annually, more per capita than any other developed nation. The cost of medical imaging is estimated at $100 billion per year and is the fastest growing segment of the health care system, growing at approximately 10–15% annually.

CT and medical imaging use is primarily in the United States and developed nations. Compared to the United States, other developed nations have much lower use and spending on health care in general and imaging in particular, yet have similar life expectancy. The main issue is the number of either unindicated or borderline indicated studies in the United States for ionizing (CT, radiography, fluoroscopy) and non-ionizing (MRI, sonography) imaging studies. Furthermore, there is under-recognition of the harm from false-positive imaging tests.

Goals

The goal of imaging is to diagnose or exclude medical conditions that concern the patient, family, or clinician. Imaging, like any test, should ideally improve patient health outcomes and reduce the intensity and use of resources, especially cost, of care. Diagnostic imaging guides clinicians in management of patients. Imaging tests have both risks and benefits that must be weighed for each patient.

Methodology

Information for this chapter was obtained primarily through a MEDLINE search using PubMed (National Library of Medicine, Bethesda, Maryland, http://www.ncbi.nlm.nih.gov/sites/entrez) from 1968 to January 2008. Keywords are *ALARA (As Low As Reasonably Achievable)*, *pediatric*, *radiation*, *radiation risk*, *CT*, *diagnostic imaging*, and the resultant related fields from this original database.

Discussion of Issues

I. Is There a Cancer Risk from Low-Level Radiation Used in Medical Imaging? What Are the Uncertainties in the Data?

Summary of Evidence: There is strong research evidence for cellular and organism damage from high levels of ionizing radiation (strong evidence). At lower levels of radiation (<100–150 mSv), the linear, no-threshold model suggests increased cancer risk. Although most major medical and scientific organizations accept the linear, no-threshold model as the preferred model for low-level radiation and cancer risk estimation, direct evidence linking medical use of low-level radiation is lacking (insufficient evidence).

In analyzing potential radiation biological effects, there are other considerations in addition to the modeling discussed above, including type of radiation, site (e.g., organ or organ system) specific risks, regional versus whole body exposure, acute versus protracted exposure, and gender and age sensitivity.

Supporting Evidence: Dose from CT represents the largest contribution from medical radiation to developed nation populations. The risk of radiation-induced cancer from CT should be put into context against the statistical risk of developing cancer in the entire population. The average risk of fatal cancer developing over a person's lifetime is approximately 18–22%. So, for every 1,000 children, 180–220 will develop fatal cancer in their lifetime regardless of exposure to medical radiation. The estimated

increased risk of cancer over a person's lifetime from a single CT scan is controversial but has been estimated to be a fraction of this risk (0.03–0.05%); this estimate is based on the model showing that 1 in 1,000 children who undergo abdominal CT may have later fatal cancer induction. It is important to remember that these estimates are population-based rather than for the individual child.

A. Cancer Risk and Radiation Following Diagnostic Medical Imaging

Gonzulea and Darby estimated cancer risk from diagnostic imaging and concluded that the attributable risk in developed countries varied from 0.6, to as high as 3.2% (20), similar to projections reported by Brenner and Hall (11). These projections come under the same scrutiny as with any that base conclusions on longitudinal survivor study (LSS) Hiroshima data and may not reflect contemporary imaging techniques, particularly in children. In addition, there is no provision for the benefit achieved by diagnostic imaging. Ron et al. discuss development of leukemia, thyroid, and breast cancer from diagnostic X-rays (21). For example, one investigation by Doody et al. reported on the association of breast cancer and scoliosis follow-up in childhood, concluding that with a mean dose of 110 mGy, mean exposure age 10.6 years, that there were 70 observed breast cancers versus nearly 36 expected (22). These data are in agreement with those of atomic bomb survivors.

For fluoroscopic and angiographic evaluations, increases in breast cancer in girls undergoing fluoroscopic evaluation for TB have been summarized (14). However, three investigations of cardiac catheterizations in children have not shown an increased risk of cancer (23–25). Doses up to 500 mGy showed no effect (26).

Finally, diagnostic imaging exposes the medical community to radiation dose. Bearrington et al. reported cancer and other causes of mortality for British radiologists from 1897 to 1997 and found no significant increase in morality from all causes reviewed except for cancer in those radiologists in early years (5).

B. CT Scan and Risk

CT examinations, as noted above, provide a relatively high dose per examination compared with other forms of ionizing radiation used in diagnostic medical imaging. The potential risks of cancer development have been outlined by Brenner, Hall, and colleagues (13, 17, 27). In summary, depending on the age of exposure, as well as the technique used, Brenner reports a risk of fatal cancer in up to 1 in 500 children from a single CT examination. Of note, the techniques assumed for this analysis were well beyond those currently advocated as standard (28, 29). Using lower dose (1.0 mSv) biennial screening CT predictions from 2 years of age until death in the cystic fibrosis population, de Jong et al. concluded that while the risk of cancer was small, projected excess relative risk could be 13% at 65 years of age. Again, assumptions are based on LSS data and they point out that there is no assumption of benefit from screening CT (30). Chodick et al. also estimated an excess risk of 0.29% in a population under 18 years of age in Israel (31). Although a large population (in the millions) would likely be needed to assess low-level radiation risk in children, there are an estimated 7,000,000 CT examinations performed in children per year in the United States (32). While these large numbers provide an opportunity for study of low-level doses from diagnostic imaging, the cost of this type of investigation would be prohibitively high given the decades of follow-up required. Alternatively, a retrospective evaluation of those children who have had multiple examinations could be culled for those that have total estimated effective doses at more than 100–150 mSv to see if this subgroup has demonstrated the same risk for cancer that has been shown in the atomic bomb population.

C. Assumptions in Estimating Radiation Risks

In general, medium- and high-level radiation dose effects are linear although recent reports suggest that there may be some nonlinearity at higher effects (33). The issue with radiation from diagnostic imaging is that these doses are low level, and because of potentially small

effects, the data have been less conclusive. There are several possible extrapolation models for cancer risk with low-level radiation. The linear, no-threshold model is in general the most accepted model, being supported by scientific committees, major imaging organizations, and other scientific bodies including the Committee on the Health Risks from Exposure to Low Levels of Ionizing Radiation, Biological Effects of Ionizing Radiation of the National Academy of Sciences (BEIR VII), National Council on Radiation Protection and Measurement (NCRP), International Commission on Radiological Protection (ICRP), American Academy of Pediatrics (AAP), Radiological Society of North America (RSNA), and the Society for Pediatric Radiology (SPR).

D. Increased Radiosensitivity in Children

Children are more radiosensitive than adults. The range quoted is 2–10 times. Preston et al. notes that children are 2–5 times more sensitive (33, 34), and Hall (35) indicates children are up to 10 times more sensitive. Infants are more sensitive than older children and girls are more radiosensitive than boys. Preston et al. (33) notes that the most recent LSS data indicate that the female to male ratio is 1.4 (90% confidence interval 1.1; 1.8) but also points out that this difference disappears when non-gender-specific cancers were analyzed.

E. Nonfatal Cancers

In addition, it should be understood that nonfatal cancer incidence is higher than cancer resulting in fatality. This frequency is about 2 times (21). Part of this is due to the fact that some cancers, such as breast and thyroid, have relatively successful treatment regimes with improved survival.

F. Additional Confounders in Risk Estimation

Finally, these estimations represent an imperfect science due to other confounding variables. Prasad argues that health risks of doses <100 mGy (absorbed dose) in "…humans may not be accurately estimated by any current mathematical model because of numerous inherit environmental, dietary and biological variables that cannot be accounted for in epidemiologic studies. In addition, the expression of radiation-induced damage depends not only on dose, dose rate, LET, fractionation, and protraction but also on repair mechanisms, bystander effects, an exposure to chemical and biological mutagens, carcinogens, tumor promoters, and other toxins as well as radioprotective substances, such as antioxidants" (36).

G. Radiation Doses from Medical Imaging and Uncertainty in Cancer Risks

There is still debate as to whether the linear, no-threshold model is an acceptable model for low-level radiation (recall that this is generally the accepted model) and, what, if any, potential risks exist for the levels of radiation seen with diagnostic imaging. Currently, *there are no data from diagnostic medical imaging modalities that prove the connection between low-level radiation doses and risk of cancer development*. What is discussed, then, are data from other sources, predominantly the atomic bomb LLS, for cancer risk in this low-level range. Brenner et al. goes on to summarize that "the epidemiologic study with the highest statistical power for evaluating low dose risk is the LSS cohort atomic bombs survivors" (17). As discussed previously, the exposure to this population has potential variations from medical imaging exposure in that the atomic bomb radiation consisted of other than just gamma (X-ray equivalent) radiation, acute versus protracted (such as with multiple CT examinations) exposures, and whole body versus regional exposures. That said, the following supports a significant risk of cancer development at low-level exposure.

"For x- or gamma-rays, good evidence of an increase and risk for cancer is shown at acute doses > 50 mSv, and reasonable evidence for an increase and some cancer risks at doses above [approximately] 5 mSv. As expected from basic radiobiology… the doses above which statistically significant risks are seen are somewhat higher for protracted exposures than for acute exposures; specifically, good evidence of an increase in some cancer risks is shown for protracted doses >100 mSv,

and reasonable evidence for an increase in cancer risks at acute doses above [approximately] 50 mSv" (17) (Table 3.5). From Preston et al. (33) ". . .furthermore, there is statistically significant dose response when analyses were limited to cohort members with doses of 0.15 Gy (150 mGy) or less."

One of the difficulties in determining if there is a significant risk of cancer development or mortality from low-level exposures is that this would take a very large population study over a long period of time. For example, solid tumors may take more than three decades to develop. To find an effect may take a long-term study of an exposed population of several million individuals for doses near the 10 mSv range (17). According to Kleinerman (26), "Large population size is usually required to evaluate the risk of cancer, because cancer is a rare outcome, especially in children. In addition, the lower the radiation dose, the large the population size required to detect a radiation effect" (Tables 3.6 and 3.7).

II. What Is the Estimated Risk From a Single Chest X-Ray in a Child?

Summary of Evidence: The dose to a child from a single plain radiograph is very low. Unless these low-dose exams are repeatedly performed in young children, the risk is considered negligable. There is little concern to terminally ill children or to older adults whose life expectancy is less than the latency time to develop cancer from the radiation exposure (several years for leukemia and several decades for solid cancers).

Supporting Evidence: The effective radiation dose from a single chest X-ray in a child is approximately 0.02 mSv (Table 3.4), a very small dose. It is the equivalent of 1 day of natural background radiation and less than the dose from a cross-country flight. Table 3.8 provides a comparison of radiation dose from a single chest radiograph to air travel across the United States.

III. What Is the Estimated Risk from a Single Abdominal CT Scan in a Child?

Summary of Evidence: The dose to a child from a single abdominal CT is approximately 100 times higher than a plain X-ray but still low. When these CT exams are repeatedly performed in children, the risk may be significant. There is little concern in terminally ill children or to older adults whose life expectancy is less than the latency time to develop cancer from the radiation exposure (several years for leukemia and several decades for solid cancers).

Supporting Evidence: As noted above, Table 3.8 shows the dose from a single abdominal CT as compared to natural background, a chest radiograph, and a cross-country flight. When the CT parameters are adjusted for children, the dose is approximately 5 mSv. This represents up to 20 months of natural background dose. Another way of assessing the relative risk of having a CT scan is to compare the theoretical risk of one abdominal CT scan to other risks. The estimated risk of one abdominal CT has been compared to driving a car 7,500 miles (accident risk) or even less distance on a motorcycle. This information shows that the risk of developing cancer related to a single CT scan is very small and helps to put risk in the context of everyday life experiences.

A. The Changing Landscaping of Radiation Dose for Medical Imaging

The use of medical imaging is increasing in developed nations. This does depend somewhat on the modality as radiography and fluoroscopy rates have remained relatively stable. However, there has been a substantial increase in the use of CT in both children and adults. For example, Broder et al. looked at CT use in the emergency department and found that, in children, the use of chest CT increased more than 435% during a 6-year period (2000–2006) while the frequency of emergency room visits increased by only 2% during the same period (Fig. 3.1) (37).

B. Lowering CT Dose in Children

There are a few simple strategies that can lower the radiation exposure to children undergoing CT. These concepts include the following: use pediatric protocols—adjusting the kVp and mA settings based on the child's weight; perform a single scan rather than multiple passes through the child's body—this is usually adequate to answer the clinical question, and scan only the indicated area of the child's body.

IV. Understanding Benefit Versus Risk of Imaging Tests in Well-Indicated Studies Versus Those That Have Very Low Probability of Disease

Summary of Evidence: It is critical to weigh both the benefits and the risks when using any test, including medical imaging with ionizing radiation. The benefit to a patient should outweigh risks. Risk from an imaging test must include the potential for false-positive (and false-negative) results that lead to unnecessary intervention and anxiety, as well as lifetime cancer risk. Because children are more radiosensitive than adults and have longer expected life spans, these considerations may alter the diagnostic work-up and management plan for children undergoing imaging.

What is the benefit–risk of CT in high versus very low risk groups? High-risk children for disease, such as acute trauma, have relatively low risk from CT or its radiation compared to its potential benefit. In low-risk groups for a disease such as low-impact trauma, there is little benefit in using CT and the risk of short-term-increased false-positive results plus long-term radiation risk outweigh any benefit.

Supporting Evidence: Health benefit or lifesaving use of CT has been shown in certain populations that include acute motor vehicle trauma, non-accidental trauma, acute infection, and acute abdominal pain. The appropriate use of imaging has not been well researched or well funded by research agencies.

A. The Example of CT in Children with Headache

Medina and colleagues investigated the clinical role and cost of head CT and MR in children with headache (38). They compared three diagnostic strategies: (a) magnetic resonance imaging (MRI), (b) computed tomography followed by MRI for positive results (CT-MRI), and (c) no neuroimaging with close clinical follow-up in the evaluation of children suspected of having a brain tumor.

They also grouped the children's risk into low, medium, and high for brain tumor prior to imaging. With a high pre-test probability of brain tumor (4% risk), MR imaging of the head was the recommended and cost-effective imaging strategy. When there was an intermediate pre-test probability of brain tumor (0.4%), imaging was very expensive (CT then MR if CT was positive).

When children had chronic headache, the pre-test probability of tumor was low (0.01%), and neither CT nor MR was recommended. Even with high sensitivity and specificity of CT (95%, 95%), the posttest probability of tumor was only 16%. In the short term, this means children are being submitted to a false-positive rate (low positive predictive value). MR imaging would have the same results but avoid ionizing radiation exposure to the child. On the other hand, there is a small risk from sedation or anesthesia in young children undergoing MR that would not be needed with CT. If, however, the study is well indicated, CT has more benefit than risk in the high-risk group of children with headache. CT would reduce short-term morbidity and mortality.

So we emphasize the importance of weighing benefit versus risk. For many other diseases in children, there are low-risk subgroups that get studies ordered that expose them to both high false-positive rates and radiation.

V. How Should I Communicate Radiation Risk from Imaging to Parents and Patients?

Summary of Evidence: There are growing numbers of web sites and published literature that provide both appropriate language and data to

discuss the benefits and risk of medical imaging to consumers. There are survey data that suggest that parents and families both want to know and can understand these issues (39).

Supporting Evidence: The Internet has revolutionized access to scientific and medical information for consumers. There are growing numbers of both scientific and medical web sites that target consumers and include the Image Gently Campaign (www.imagegently.org) for children, the National Cancer Institute (www.cancer.gov/cancertopics/causes/radiation-risks-pediatric-CT), the Health Physics Society (http://hps.org), the American Academy of Pediatrics (www.aap.org), and the American College of Radiology (www.acr.org).

The "Image Gently Campaign" is an educational and awareness campaign created by the Alliance for Radiation Safety in Pediatric Imaging that was formed in July 2007. It is a coalition of health care organizations dedicated to providing safe, high-quality pediatric imaging nationwide. There are four founding members—Society for Pediatric Radiology, American Association of Physicists in Medicine, American College of Radiology, and the American Society of Radiologic Technologists—as well 44 national and international societies in this coalition representing over 500,000 health care professionals in radiology, pediatrics, medical physics, and radiation safety. The site provides information for all stakeholders in medicine. As an example, Table 3.8 shows the relative radiation doses to children for common imaging exams compared to background and airline flight.

Information about radiation and the role of all stakeholders to improve radiation safety in medicine is summarized in a Blue Ribbon Panel article (15). ACR guidelines now include dose estimates for imaging tests and reference levels for acceptable doses in all appropriateness criteria.

Larson and colleagues surveyed parents about their understanding of the benefits and risks from CT for their children. They found that two of three parents knew that CT used ionizing radiation. After they were given an informational brochure 99% reported understanding that CT used ionizing radiation. After reading the brochure, 86% of parents reported that there was a risk of cancer induction from CT yet they remained willing to have their child undergo CT when appropriate (39). They concluded that "A brief informational handout can improve parental understanding of the potential increased risk of cancer related to pediatric CT without causing parents to refuse studies recommended by the referring physician." Families and patients should be encouraged to ask questions about the risks and benefits of CT scans and other imaging tests (40).

The risk of radiation-induced cancer from CT should be put into context against the statistical risk of developing cancer in the entire population. The average risk of fatal cancer developing over a person's lifetime is approximately 18–22%. So, for every 1,000 children, 180–220 will develop cancer in their lifetime regardless of exposure to medical radiation. The estimated increased risk of cancer over a person's lifetime from a single CT scan is controversial but has been estimated to be a fraction of this risk (0.03–0.05%) or 1 in 1,000 children who undergo CT. It is important to remember that these estimates are population based rather than for the individual child.

VI. Special Situation: Increased Cancer Risk Following Therapeutic Medical Radiation

Summary of Evidence: There are known risks of secondary cancer development after medical radiation treatment for both neoplastic and non-neoplastic conditions in children (41) (strong evidence).

Supporting Evidence: There are a number of studies showing increased risk of cancers after radiotherapy that include leukemia, lymphoma, and solid cancers (42). The risk is variable and is related to the primary cancer treatment and other factors. The Children's Oncology Cancer group provides medical recommendations for lifelong follow-up in these children (43).

According to Kleinerman (26) "many of the classic epidemiologic studies of cancer following medical radiation exposure are distinguished by a cohort design, large population size, long-term follow-up of the cohort,

well-characterized dose estimates for individuals, and a wide range of doses in order to estimate a dose-response relationship; studies based on a cohort design are generally less likely to be biased than case control studies that depend on the retrospective collection of data." Ron and colleagues also discuss the advantages and disadvantages of assessing cancer risks in those patients who have relatively high doses for medical therapy of both neoplastic and non-neoplastic conditions (Table 3.9) (44). The advantages of these types of data include that the records are relatively accurate, with data on other potentially confounding medical problems. Radiation is generally always an X-ray (gamma ray) exposure and the region radiated is known. However, disadvantages include confounding factors of underlying diseases. Long-term effects from radiation therapy for cancer in children have recently been reviewed (42).

There are illustrative reports for cancer risk from non-oncologic treatment that are worth reviewing. For example, in a review of six investigations dealing with thyroid cancer, all cohort studies, the author concludes "these studies demonstrate that the thyroid gland is very sensitive to the carcinogenic effects of radiation, characterized by a strong linear dose response." In three of these investigations, the risk was seen with doses as low as 100 mGy. In an additional investigation, a thyroid dose of 90 mGy was associated with a 400% increase in malignant tumors and a 200% increase in those tumors that were benign. A linear dose response was demonstrated in children exposed under the age of 5 years and were significantly more likely to develop tumors than older children (44). Brenner et al. discussed data from pooled studies, including Ron et al. (44) and noted that the thyroid cancer risk was significant at glandular doses as low as 50 mSv (17). Kleinerman also summarizes data demonstrating increased risk of breast cancer seen with therapeutic doses as low as 300 mGy (26).

Take-Home Tables and Figures

Tables 3.1–3.9 and Fig. 3.1 serve to highlight key recommendations and supporting evidence.

Table 3.1. Radiation dose units

Absorbed dose—Gray (Gy)—rad (rad) is prior unit
1 Gy = 100 rad
1 cGy = 1 rad
1 mGy= 100 mrad
Equivalent dose—Sievert (Sv)—rem (rem) is prior unit
Sv = Gy × quality factor (=1)
1 Sv = 100 rem
10 mSv = 1 rem
1 mSv = 100 mrem

Reprinted with permission of Elsevier from Frush DP, Slovis TL. Biological effects of diagnostic radiation on children. In Slovis TL (ed.): Caffey's Pediatric Diagnostic Imaging. Philadelphia: Elsevier, 2007, 29–41.

Table 3.2. Inherited human syndromes associated with sensitivity to X-rays

Ataxia–telangiectasia
Basal cell nevoid syndrome
Cockayne's syndrome
Down syndrome
Fanconi's anemia
Gardner's syndrome
Nijmegan breakage syndrome
Usher's syndrome

Reprinted and adapted with permission of Elsevier from Frush DP, Slovis TL. Biological effects of diagnostic radiation on children. In Slovis TL (ed.): Caffey's Pediatric Diagnostic Imaging. Philadelphia: Elsevier, 2007, 29–41, and from Hall (45).

Table 3.3. Deterministic effects: relatively high-radiation doses needed compared to what is used in diagnostic imaging

Injury	Approximate	Threshold
Skin		
Transient erythema	**2 Gy**	**(200 rad)**
Eyes		
Cataracts (acute)	**>2.0 Gy**	**(>200 rad)**

Reprinted and adapted with permission of Elsevier from Frush DP, Slovis TL. Biological effects of diagnostic radiation on children. In Slovis TL (ed.): Caffey's Pediatric Diagnostic Imaging. Philadelphia: Elsevier, 2007, 29–41, and from Hall (45).

Table 3.4. Estimated medical radiation doses for a 5-year-old child

Imaging area	Effective dose, mSv	Equivalent number of CXRs
Three-view ankle	0.0015	1/14th
Two-view chest	0.02	1
Anteroposterior and lateral abdomen	0.05	2–1/2
Tc-99m radionuclide cystogram	0.18	9
Tc-99m radionuclide bone scan	6.2	310
FDG PET scan	15.3	765
Fluoroscopic cystogram	0.33	16
Head CT	4	200
Chest CT	3	150
Abdomen CT	5	250

CXR indicates chest radiograph; Tc-99m, technetium 99m; FDG PET, fluorodeoxyglucose positron emission tomography. Data were provided by R. Reiman, MD (Duke Office of Radiation Safety [www.safety.duke.edu/RadSafety], written communication, 2006).
Reproduced with permission of the AAP from et al. (40).

Table 3.5. Atomic bomb (longitudinal survivor study) data showing excess solid cancers linked to radiation exposure doses. These data combine children and adults. Atomic bomb (longitudinal survivor study) data 1950–1997

		1950–1997			1991–1997		
Dose (Sv)	People	Deaths	Expected background	Fitted excess	Deaths	Expected background	Fitted excess
<0.005	37,458	3,833	3,844	0	742	718	0
0.005–0.1	31,650	3,277	3,221	44	581	596	12
0.1–0.2	5,732	668	622	39	137	109	10
0.2–0.5	6,332	763	678	97	133	118	24
0.5–1	3,299	438	335	109	75	62	28
1–2	1,613	274	157	103	68	31	27
2+	488	82	38	48	20	8	13
Total	86,572	9,335	8,895	440	1,756	1,642	114

Reprinted with permission from Preston et al. (34).

Table 3.6. Hematopoietic cancer risks and adult diagnostic X-rays

Kaiser-Permanente, Oregon and California, 1956–1982
565 leukemias (358 non-CLL)
318 non-Hodgen's
208 multiple myeloma
Various diagnostic procedures
Exposure data from medical records
RR[a]: Non-CLL=1.4 (0.9–2.2)
NHL=0.99 (0.6—1.6)
MM =1.3 (0.6–3.0); *P*-trend 0.03

[a]2-year lag.
Reprinted with the kind permission of Springer Science+Business Media from Ron (21).
CLL: chronic lymphatic leukemia; NHL: non-Hodgkin's lymphoma; MM: multiple myeloma; RR: relative risk.

Table 3.7. Childhood Cancer risks and diagnostic X-ray exams

Population-based study: Shanghai 1981–1991 642 cancer cases (<15 years); 642 controls Postnatal diagnostic X-ray exposure risks:		
Cancer	**OR**	**95% CI**
Total cancer	1.3	1.0–1.7
Acute leukemia	1.6	1.0–2.6
Brain cancer	1.5	0.8–3.0
Lymphoma	1.3	0.6–22

Cases included prenatal and postnatal diagnostic radiation exposure in children. The odds ratios for total cancer and acute leukemia are significant. Given large confidence intervals for brain cancer and lymphoma, these are not significant.
Reprinted with the kind permission of Springer Science+Business Media from Ron (21).
OR: odds ratio; CI: confidence interval.

Table 3.8. Relative radiation doses for children

Source	Estimated effective dose (mSv)
Natural background radiation	3 mSv per year
Airline passenger (cross-country)	0.04 mSv
Chest X-ray (single view)	0.01 mSv
Head CT	Up to 2 mSv
Chest CT	Up to 3 mSv
Abdominal CT	Up to 5 mSv

Based on US data and adapted from www.imagegently.org.

Table 3.9. Cancer risks following childhood therapeutic irradiation for benign diseases

Cancer site	Benign condition, cohort	No. of irradiated subjects	Mean age (years)	Mean dose (Gy)	ERR/Gy (95% CI)
Thyroid	Tinea capitis, Israel	10,834	7.1	0.1	32 (14–57)
	Tinea capitis, New York	2,224	7.8	0.1	7.7 (<0–60)
	Hemangioma,[a] Gotenburg	11,914	<1.5	0.1	7.5 (0.4–18)
	Hemangioma,[a] Stockholm	14,435	<1.5	0.3	4.9 (1.3–10)
	Enlarged tonsils, Chicago	2,634	4	0.6	2.5 (0.6–26)
	Thymus, Rochester, NY	2,650	<1	1.4	9.1 (3.6–29)
Breast	Hemangioma (pooled)[a]	17,202	0.5	0.3	0.4 (0.2–0.6)
	Thymus, Rochester, NY	1,201	<1	0.7	2.5 (1.1–5.2)
Leukemia	Tinea capitis, Israel	10,834	7.1	0.3	Not available
	Hemangioma (pooled)[a]	28,008	0.5	0.1	1.6 (–0.6 to 5.5)
Brain	Tinea capitis, Israel	10,834	7.1	1.5	4.6 (2.4–9.1)[b]
				1.5	2.0 (0.7–4.7)[c]
	Hemangioma (pooled)[a]	28,008	0.5	0.1	2.7 (1.0–5.6)[d]
Skin	Tinea capitis, Israel	10,834	7.1	6.1	0.7 (0.3–1.4)
	Tinea capitis, New York	2,224	7.8	4.3	1.6 (1.3–2.1)

[a] Radium-226 treatment.
[b] Benign tumor only.
[c] Malignant tumor only.
[d] Benign and malignant tumors combined.
Reprinted with the kind permission of Springer Science+Business Media from Kleinerman (26).
Note that ERR is the excess relative risk (where relative risk=excess relative risk + 1).

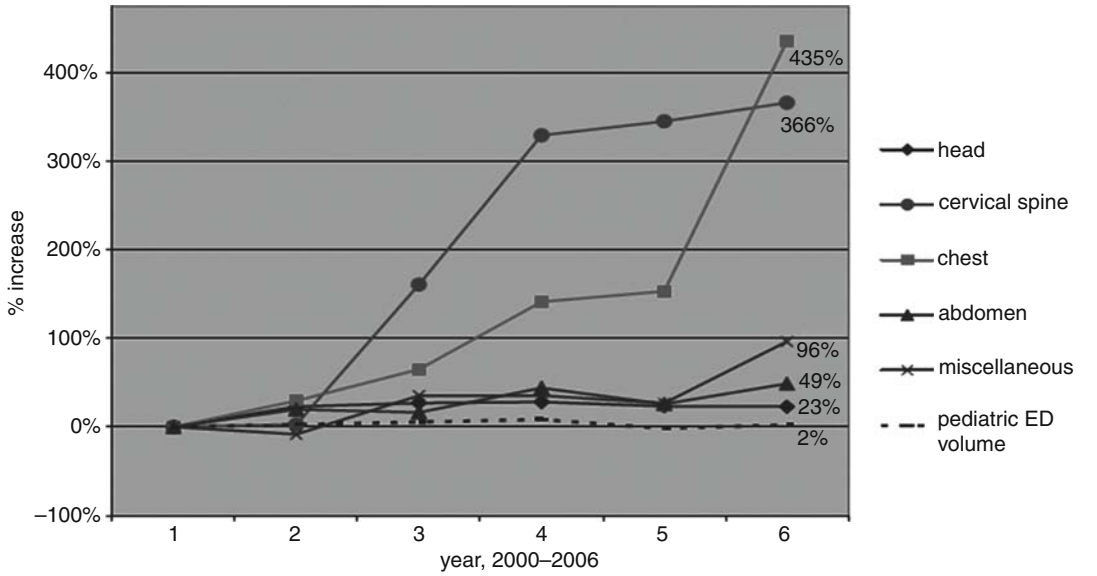

Figure 3.1. Percent increase in various pediatric CT examinations over a 6-year period compared to a 2% increase in visits over the same time period (years 2000–2006). (Reprinted with kind permission of Springer Science+Business Media from Broder and Fordham (37)).

Future Research

- Increase multi-center outcomes research on the health benefits/risks of imaging in children for common conditions (trauma, abdominal pain, infection, and cancer).
- Increase understanding of the trend in utilization of imaging, in particular those with relatively high ionizing radiation doses (e.g., CT, PET) and potential non-ionizing radiation alternative imaging (e.g., sonography, MRI).

References

1. Huda W. Medical Radiation Dosimetry. Categorical Course in Physics: Radiation Dose and Image Quality. Chicago, IL: Radiological Society of North America, 2006; 167–182.
2. Frush DP, Slovis TL. In Slovis TL (eds.). Caffey's Pediatric Diagnostic Imaging. Philadelphia: Elsevier, 2007, 29–41.
3. Imanishi Y et al. Eur Radiol 2005; 15:41–46.
4. Hall HA et al. BMJ 2004; 328:1–5.
5. Berrington A et al. Br J Radiol 2001; 74:507–519.
6. UNSCEAR 2000 Medical radiation exposures, annex D. United Nations Scientific Committee on the Effects of Atomic Radiation Report to the General Assembly; New York.
7. Gaca AM. Pediatr Radiol 2008; 38:285–291.
8. Thierry-Chef I, Simon SL, Miller DL. Pediatr Radiol 2006; 36(14):159–162.
9. Thomas KE, Wang BB. Age-specific effective doses for Pediatric MSCT examinations at a large children's hospital using DLP conversion coefficients; a simple estimation method. Pediatr Radiol. In press.
10. Huda W, Vance A. Am J Roentgenol 2007; 188:540–546.
11. Mettler FA, Thomadsen BR, Bhargavan M et al. Med Phys 2008; n95:502–712.
12. Fuchs VR, Sox HC. Health Affairs 2001; 20: 30–42.
13. Brenner DJ, Hall EJ. NEJM 2007; 357:2277–2284.
14. Mettler FA, Wiest PW, Locken JA et al. J Radiol Prot 2000; 20:353–359.
15. Amis ES Jr. et al. J Am Coll Radiol 2007; 4: 272–284.
16. Paterson A, Frush DP, Donnelly LF. AJR 2001;176(2):297–301.
17. Brenner DJ et al. Proc Natl Acad Sci USA 2003; 25: 100(24):13761–13766.
18. BEIR VII. Health risks from exposure to low levels of ionizing radiation 2006. http://www.nap.edu/openbook.php?isbn=030909156X. Last accessed 1-1-08.
19. Prasad KN, Cole WC, Hasse GM. Exp Biol Med 2004; 229:378–382.
20. Gonzalea AB, Darby S. Lancet 2004; 363:345–351.
21. Ron E. Pediatr Radiol 2002; 32:232–237.

22. Doody MM et al. Spine 2000; 25:2052–2063.
23. Modan B et al. Int J Epidemiol 2000; 29:424–428.
24. Spengler RF et al. Pediatrics 1983; 71:235–239.
25. McLaughlin JR et al. Int J Epidemiol 1993; 22:584–591.
26. Kleinerman RA. Pediatr Radiol 2006; 36(2): 121–125.
27. Brenner DJ et al. AJR 2001; 176:289–296.
28. Donnelly LF et al. Am J Roentgenol 2001; 176:303–306.
29. Frush DP. In Kalra M, Saini S, Rubin G (eds.). MDCT: Form Protocols to Practice. New York: Springer, 2008; 333–354.
30. De Jong PA et al. Am J Respir Crit Care Med 2006; 173:199–203.
31. Chodick G et al. Isr Med Assoc J 2007;9(8): 584–587.
32. Frush DP, Applegate K. J Am Coll Radiol 2004; 1:113–119.
33. Preston DL et al. Radiat Res 2007; 168:1–64.
34. Preston DL et al. Radiat Res 2003; 160:381–407.
35. Hall EJ. Pediatr Radiol 2002; 32:700–706.
36. Prasad KN, Cole WC, Haase GM. Br J Radiol 2004; 77:97–99.
37. Broder J, Fordham L, Warshaver D. Emerg Radiol 2007; 14:227–232.
38. Medina LS, Kuntz KM, Pomperoy S. Pediatrics 2001; 108:255–263.
39. Larson DB, Rader SB, Forman HP, Fenton LZ. Am J Roentgenol 2007 Aug;189(2):271–275.
40. Brody AS, Frush DP, Huda W, Brent RL. Pediatrics 2007 Sep;120(3):677–682.
41. http://www.ncrponline.org/.
42. Larrier N, Lawrence T, Halperin EC. In Slovis T (ed.). Caffey's Pediatric Diagnostic Imaging. Philadelphia: Elsevier, 2007; 13–25.
43. http://www.childrensoncologygroup.org/
44. Ron E et al. Radiat Res 1989; 120:516–531.
45. Hall EJ. Radiobiology for the Radiologist, 5th ed. Philadelphia: Lippincott Williams & Wilkins, 2000.

Part II

Neuroimaging

4

Imaging in the Evaluation of Children with Suspected Craniosynostosis

Daniel N. Vinocur and L. Santiago Medina

Issues

I. What is the role of imaging in the diagnosis of craniosynostosis?
II. What is the cost and cost-effectiveness of imaging in children with suspected craniosynostosis?
III. Is imaging required when the clinical diagnosis has clearly been made?
IV. How often and what intracranial abnormalities are seen in craniosynostosis?
V. What is the role of imaging in the prenatal diagnosis of craniosynostosis?

Key Points

- Plain skull radiography demonstrates moderate to high sensitivity and specificity in craniosynostosis.
- Numerous publications support 3D-CT as the imaging modality with the best diagnostic performance, with reported sensitivities of 96–100%. CT also detects associated intracranial pathology.
- Higher diagnostic performance is obtained with plain films and CT if the studies are of good quality and interpreted by an experienced reviewer.
- Cranial sonography shows preliminary promise as a diagnostic test for craniosynostosis. The evidence is based on small cohorts; hence, larger series are needed before it is routinely used.
- Imaging strategies for children with suspected craniosynostosis should be based on their risk group. In healthy children with head deformity including posterior plagiocephaly, skull radiography is recommended. Syndromes such as Apert, Crouzon, and Pfeiffer nearly always have associated craniosynostosis and hence require 3D imaging for surgical planning.

D.N. Vinocur (✉)
Department of Radiology, Children's Hospital Boston. Harvard Medical School. Boston, Massachusetts
e-mail: daniel.vinocur@childrens.harvard.edu

L.S. Medina et al. (eds.), *Evidence-Based Imaging in Pediatrics*,
DOI 10.1007/978-1-4419-0922-0_4,

- Imaging is not necessary for diagnosis or preoperative planning in isolated craniosynostosis with unequivocal clinical findings. However, in countries with high medicolegal issues, imaging may still be required.
- Intracranial anomalies can be seen in some patients with craniosynostosis but the exact incidence is not well known.
- Small retrospective US and MRI studies demonstrate the feasibility of prenatal diagnosis of craniosynostosis. However, large prospective studies are still required to understand the prenatal role of imaging in craniosynostosis and their effect on postnatal outcome.

Definition and Pathophysiology

Craniosynostosis is the premature fusion of the skull sutures. The resulting asymmetric calvarial growth causes characteristic cranial deformities. The clinical outcome varies between minor cosmetic deformity to severe head growth restriction with mental retardation and cranial palsies (1). Craniosynostosis cases can be classified as non-syndromic (isolated) and syndromic. The exact etiology of this disorder is unknown; however, in several syndromic cases, genetic disorders have been documented (2–4).

Epidemiology

The overall prevalence of craniosynostosis in the general population ranges from 34 to 48 per 100,000 live births (5, 6). Higher incidence has been reported in the state of Colorado, USA (7), but the reason for this difference is unclear. In the general population, syndromic cases of synostosis are less common than non-syndromic cases (8–11). Sagittal followed by coronal synostosis are the most frequent type, accounting for 56 and 22% of the cases, respectively (6). In children with syndromic craniosynostotic disorders, such as Crouzon, Apert, and Pfeiffer syndromes, synostosis is almost universally present (8–11)

Deformational plagiocephaly is defined as the asymmetric flattening of the head due to repeated pressure. Since 1992, there has been an exponential increase in the number of infants seen with deformational posterior plagiocephaly (positional molding) (12, 13). The most likely explanations are the 1992 American Academy of Pediatrics recommendation that infants sleep in the supine position to decrease the risk of sudden infant death syndrome (SIDS) and the increased awareness among pediatricians and other primary care providers of plagiocephaly (14–18). This specific entity usually presents some time after birth, progresses until 6 months of age, and remains stable thereafter (13). The skull deformity is generally considered to be only of cosmetic significance, and in the vast majority of cases it will respond to conservative measures such as changing sleep position or corrective helmets (3, 14).

Overall Cost to Society

We are not aware of studies documenting national costs of diagnosis or treatment of craniosynostosis or deformational plagiocephaly before or after the 1992 recommendations from the American Academy of Pediatrics. The cost of imaging studies and cost-effectiveness analysis are discussed in detail below.

Goals

The overall goal of neuroimaging for infants with suspected craniosynostosis is the early detection and characterization of this entity to enable appropriate treatment. Delayed diagnosis and treatment may lead to (1) cosmetic calvarial deformity which may be difficult to correct or may require more extensive cranioplasty and (2) potentially irreversible neurological impairment (18). Specific imaging goals include detailed characterization of the number of sutures, extent of suture involvement, and complexity of 3D calvarial deformity. Secondary goals include uncovering underlying brain anomalies associated with syndromic

synostotic disorders. More recently, there has been growing interest in the prenatal diagnosis of this disorder.

Methodology

Scientific article search was performed using the Medline/PubMed electronic database (National Library of Medicine, Bethesda, MD) and Ovid (Wolters Klumer, New York, New York) for original research publications discussing the diagnostic performance and effectiveness of imaging strategies in craniosynostosis. The search for neuroimaging-related publications covered the period 1980–November 2007. The search strategy employed different combinations of the following terms: (1) *Craniosynostosis*, (2) *Sensitivity*, (3) *Specificity*, and (4) *Diagnosis*. This review was limited to human studies and the English language literature. The authors performed an initial review of the titles and abstracts of the identified articles followed by full text detailed review of relevant articles.

Discussion of Issues

I. What Is the Role of Imaging in the Diagnosis of Craniosynostosis?

Summary of Evidence: Plain skull radiography demonstrates moderate to high sensitivity and specificity in craniosynostosis (limited to moderate evidence). Numerous publications show 3D-CT as the test with the best diagnostic performance, with reported sensitivities of 96–100% (limited to moderate evidence). Additionally CT allows the detection of associated intracranial pathology. Higher diagnostic performance is obtained when radiographs and CT are of good quality and interpreted by experienced reviewers (limited to moderate evidence). An imaging diagnostic algorithm is summarized in Fig. 4.1. The diagnostic algorithm is based on the clinical differentiation between syndromic and isolated craniosynostosis. In isolated (non-syndromic) cases, we advocate starting with plain radiographs. If the radiographs are negative, clinical follow-up would be indicated. In equivocal cases, or when the radiographs are positive, further characterization with 3D-CT is recommended. Syndromic cases are best evaluated directly with 3D-CT, with surgical consultation indicated in positive cases.

Head sonography shows preliminary promise as a diagnostic test for craniosynostosis. The evidence is based on small cohorts; hence, larger series are needed before routine use in medical practice (limited evidence). Bone scintigraphy has fallen out of use, mainly due to its low accuracy, estimated at 66%. In addition, interpretation of images is complex and requires great expertise (limited evidence).

Supporting Evidence

Skull Radiographs

Plain radiographs are classically considered the first-line imaging modality in craniosynostosis (19, 20). The standard series includes an anteroposterior view, Towne projection, and both lateral views. The low cost per study, low radiation, and universal availability have made it an attractive diagnostic choice (21). However, large prospective studies addressing the diagnostic accuracy of plain radiographs for the detection of craniosynostosis are lacking. In a retrospective study by Cerovac and colleagues, the overall diagnostic accuracy of plain radiography was estimated to be 91% (20) (limited evidence). Vannier and colleagues (22) reported wide ranges of diagnostic accuracies depending on the suture evaluated, ranging from 56% for the metopic suture to 88% for the sagittal suture. Overall sensitivity and specificity were reported between 57 and 80% and 54 and 100%, respectively (limited to moderate evidence). Pilgram et al. showed poor quality radiographic studies had significant decrease in sensitivity and specificity estimated at 60 and 78%, respectively (23) (Table 4.1) (limited to moderate evidence). In an older study from 1985 with 36 patients (18), plain radiography was reported to have an accuracy rate of 89% when compared to surgical inspection and pathologic examination (limited evidence).

Computed Tomography (CT)

The introduction of computed tomography revolutionized the imaging of craniosynostosis. This modality not only depicts the

osseous pathology exquisitely but also allows for the detection of associated intracranial abnormalities, including hydrocephalus and brain developmental anomalies, such as agenesis of the corpus callosum (24). In addition, CT can identify alternative causes for asymmetric cranial morphology, such as brain hemiatrophy and chronic subdural collections (19).

Numerous studies have been published in the literature demonstrating the high diagnostic performance of CT (Table 4.1). Agrawal et al. (25) reported an overall sensitivity of 100% for CT diagnosis of synostosis in 12 infants (limited evidence). A blinded study performed on a relatively small cohort (25 infants) reported that the sensitivity of CT with 3D surface-rendered reconstructions to be in the range of 96–100% (limited evidence) (26). An older study from 1985 using thicker axial slices and no 3D reconstructions (18) reported an overall accuracy for CT diagnosis of 94%. CT reviewer experience and image quality play an important role in the achieved diagnostic performance. Vannier et al. demonstrated sensitivity and specificity of 96.4 and 100%, respectively, for experienced CT reviewers (limited to moderate evidence) (27). They also revealed that less experienced CT reviewers had a significant drop in specificity of the test to 83% (limited to moderate evidence) (Table 4.1) (27). Pilgram et al. demonstrated that poor quality CT studies had a significant decrease in sensitivity and specificity estimated at 73 and 78%, respectively (limited to moderate evidence) (23).

The use and risks of sedation or general anesthesia to perform CT examinations in children have been considered by several authors (20, 21). The overall risk of death from sedation is very low and has been estimated at 1 in one million (28–30). Furthermore, with the advent of spiral and multidetector CT, imaging time has been reduced drastically; hence, most children no longer need sedation for routine head CT.

Imaging post-processing also has an impact on the diagnostic performance of CT. Vannier et al. (22) compared and concluded that 3D shaded rendering of the skull was superior to the combined information from 2D-CT and plain radiography (limited to moderate evidence). In a technical note, Medina (31) reported from a small group of 10 patients the advantages of 3D maximum intensity projections (MIP) in the comprehensive assessment of craniosynostosis (limited evidence).

Ultrasound (US)

Lately growing interest has been placed on ultrasonographic examination for craniosynostosis given its lack of ionizing radiation and need for sedation. However, sonography is operator dependent, requires special technologist training, and is not feasible in infants older than 13 months (32). Technically the examination consists in scanning the sutures with high-frequency transducers (typically 7.5 MHz), utilizing gel as contact medium.

In 2006, Jan Regelsberger and colleagues from Hamburg, Germany, published a small series of 26 patients in which the diagnosis of craniosynostosis was established by ultrasound and confirmed later with CT. The study reported US sensitivity of 100% relative to CT (limited evidence) (32).

Plagiocephaly is a common problem with an estimated prevalence of 20% at 8 months of age (33). There was a sharp increase in posterior plagiocephaly over the last 25 years (13), after the widespread adoption of the AAP infant positioning recommendations to decrease the incidence of SIDS (34). A few articles addressed the use of ultrasound for this specific clinical concern (i.e., unilateral occipital craniosynostosis versus deformational molding) (32, 35). Sze and colleagues (35) published a prospective study of 41 subjects (including controls) to understand the role of US in characterizing posterior plagiocephaly (limited to moderate evidence). Their study correlated ultrasonographic findings with CT results. The overall sensitivity for US diagnosis was 100% and the specificity was 89% (limited to moderate evidence).

Bone Scintigraphy

Older literature emphasized the role of Tc99m-based bone scintigraphy for the diagnosis of craniosynostosis. The literature estimates the overall accuracy of scintigraphy to be approximately 66% (18), which renders it essentially valueless for current practice use. In addition, interpretation of this modality requires expert knowledge regarding the different normal phases of activity along calvarial bone maturation (36).

II. What Is the Cost and Cost-Effectiveness of Imaging in Children with Suspected Craniosynostosis?

Summary of Evidence: Selection of children with suspected craniosynostosis based on their risk group and use of the most appropriate evaluation strategy could maximize clinical and economic outcomes for these patients. A comprehensive cost-effectiveness analysis comparing different imaging strategies in the diagnosis of craniosynostosis was performed by Medina et al. (21) (moderate to strong evidence). In healthy children with head deformity, including posterior plagiocephaly, the skull radiographic strategy had the most reasonable cost per quality-adjusted life year (QALY) gained. Three-dimensional CT was more effective but had a high cost per QALY gained. In children with syndromic craniofacial disorders (high risk), 3D-CT was the most effective strategy and had a reasonable cost per QALY gained. Figure 4.1 summarizes the best imaging approach in suspected craniosynostosis.

Supporting Evidence: Medina et al. (21) performed formal cost-effectiveness analysis (CEA) on diagnostic strategies in children with suspected craniosynostosis (moderate to strong evidence). Three risk groups were analyzed on the basis of the prevalence (pretest probability) of disease: low (completely healthy children; prevalence, 34/100,000), intermediate (healthy children with head deformity; prevalence, 1/115), and high risk (children with syndromic craniofacial disorders (i.e., Crouzon's syndrome or Apert's syndrome); prevalence, 9–10/10). The analysis was based on cost (not charge) expressed in 1999 U.S. dollars. Cost data for the study are shown in Table 4.2.

In the low-risk group, the radiographic plus 3D-CT strategies resulted in a cost per quality-adjusted life year (QALY) gained of more than $560,000. In the intermediate risk group, the radiographic strategy resulted in a cost per QALY gained of $54,600. Three-dimensional CT was more effective than the two other strategies but at a higher cost, with a cost per QALY gained of $374,200. In the high-risk group, 3D-CT (without initial radiographs) was the most effective strategy with a cost per QALY gained of $33,800. Less experienced radiologists and poor-quality studies increased the evaluation cost per QALY gained for all of the risk groups because of decreased effectiveness.

The authors concluded that radiologic screening of completely healthy children (low risk for synostosis) is not warranted because of the high cost per QALY gained for any imaging. In healthy children with head deformity (intermediate risk), the initial workup with radiographs is the most cost-effective choice. Three-dimensional CT is more effective but more expensive. In children with syndromic craniofacial disorders (high risk), 3D-CT was the most cost-effective imaging approach.

III. Is Imaging Required When the Clinical Diagnosis Has Clearly Been Made?

Summary of Evidence: Isolated craniosynostosis with unequivocal clinical findings probably does not warrant preoperative imaging for diagnostic correlation and preoperative planning (moderate evidence), though imaging may be important for medicolegal considerations.

Supporting Evidence: In the setting of growing concern regarding radiation exposure (37), Agrawal et al. (25) studied the usefulness of preoperative imaging of clinically diagnosed isolated sagittal craniosynostosis. In their retrospective study of 114 cases, they correlated clinical diagnosis and pre-surgical imaging (plain radiography and CT) with surgical and pathologic findings and found a correlation of 100% for clinical diagnosis (moderate evidence). Both imaging studies also had a 100% correlation with surgical pathology results. In this preliminary work, they concluded that clinically typical isolated sagittal craniosynostosis does not warrant imaging.

Similarly, Cerovac and colleagues from the Great Ormond Street Hospital for Children in UK (20) published a retrospective series of 109 clinically diagnosed cases of isolated craniosynostosis (non-syndromic) and correlated them with pre-surgical imaging (CT and radiography) and surgical findings. They also demonstrated 100% confirmation of clinical and CT diagnosis (moderate evidence). Furthermore,

they reported no additional treatment benefit from CT in screening for intracranial abnormalities or change in surgical planning.

IV. How Often and What Intracranial Abnormalities Are Seen in Craniosynostosis?

Summary of Evidence: There are few studies addressing this question and those published have been small and without well-defined cohorts. Therefore, intracranial anomalies can be seen in some patients with craniosynostosis but the exact incidence is not well known.

Supporting Evidence: The exact incidence of associated intracranial anomalies in craniosynostosis is not well known. In a study from 1982, Goldstein and Kidd (38) reported on a heterogeneous group of patients with a variety of syndromic and isolated craniosynostosis (limited evidence). In this group, 5 out of 13 patients (38%) demonstrated an associated intracranial abnormality, most commonly hydrocephalus. However, only 1 of the 5 patients with an intracranial abnormality led to change in therapy (insertion of a shunt for hydrocephalus).

On the other hand, Hayward et al. (39) published a selective study of 30 patients with severe craniosynostosis and complex clinical syndromes who had MR imaging. The authors found more associated pathologies with the following prevalence: hindbrain herniation 19/30; syringomyelia 1/30; hydrocephalus 12/30; and non-specified anomalies of cerebral white matter 4/30.

The association of intracranial anomalies with syndromic craniosynostosis has been well established. Crouzon syndrome is associated with chronic tonsillar herniation (Chiari I malformation) in approximately 70% of cases and syringomyelia in 20% of cases. Other associations include hydrocephalus and absent corpus callosum (40).

Apert syndrome has been associated with megalencephaly and stable ventriculomegaly. Interestingly, progressive hydrocephalus appears to be relatively uncommon (20%) (41). Additional associations include agenesis of the corpus callosum/septum pellucidum, encephalocele (42), limbic and gyral malformations, and heterotopic gray matter among others (24, 41).

Finally, Pfeiffer syndrome demonstrates considerable heterogeneity, with subgroups of patients with mild phenotypes without mental retardation (43) to more severe phenotypes associated with mental retardation, hydrocephalus, and Arnold Chiari II malformation (40).

V. What Is the Role of Imaging in the Prenatal Diagnosis of Craniosynostosis?

Summary of Evidence: Small retrospective US and MRI studies in the prenatal diagnosis of craniosynostosis have been published (limited evidence). However, large prospective studies are still required to understand the prenatal role of imaging in craniosynostosis and their effect on parental counseling, surgical planning, and postnatal outcome of these fetuses.

Supporting Evidence: Recently, there has been increasing interest in the antenatal diagnosis of craniosynostosis. Early detection could potentially allow for different interventions, including elective termination of pregnancy in severe syndromic synostosis, elective cesarean section, early postnatal surgery, and perhaps fetal surgery (44).

Ultrasound (US)

In the largest series found in the literature, Delahaye and colleagues (4) performed a retrospective study in 40 fetuses with high risk of craniosynostosis. The inclusion criteria included (1) patients with positive family history of craniosynostosis and (2) those with an abnormal screening obstetrical ultrasound. Abnormal screening ultrasounds were based on altered head measurements and indices. Reported sensitivity and specificity was 100 and 97%, respectively, for this retrospective study (4) (limited evidence).

Miller and colleagues used screening ultrasound (non-targeted) in the second and third trimesters to compile a heterogeneous retrospective cohort of 21 fetuses with craniosynostosis. In this study, the authors correlated postnatal diagnosis with indirect signs of craniosynostosis on screening ultrasound

examinations (cranial geometry and indices). Their study demonstrated poor correlation between routine parameters of a non-dedicated prenatal ultrasound in the proper identification of synostosis (limited evidence). Using cranial geometry and indices, only 15 of the 26 (estimated sensitivity 58%) cases were diagnostic of postnatally documented craniosynostosis (limited evidence) (44).

MRI

Fjortoft and colleagues reviewed the imaging in a small group of 15 fetuses that demonstrated abnormal screening US during the second and third trimesters and were subsequently referred to fetal MRI imaging with the specific suspicion of craniosynostosis. In this cohort, MRI demonstrated 100% sensitivity and specificity when correlated to follow-up postnatal medical records (limited evidence) (45). No prospective MR imaging studies were found.

Take Home Figures and Tables

Figure 4.1 is an algorithm with a suggested diagnostic approach for suspected craniosynostosis.

Tables 4.1 and 4.2 discuss the performance of imaging tests for suspected craniosynostosis and the costs of imaging tests, respectively.

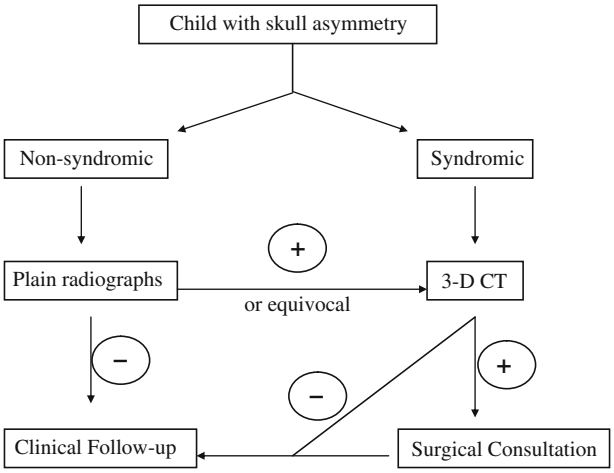

Figure 4.1. Suggested diagnostic approach algorithm. Summary of the best imaging approach according to suspected syndromic versus non-syndromic skull deformity.

Table 4.1. Diagnostic performance of imaging tests

Diagnostic test	Sensitivity (%)	Range	References
Radiographs (good quality)			
Sensitivity (%)	**80**	**57–80**	**(22)**
Specificity (%)	**95**	**54–100**	**(22)**
Radiographs (poor quality)			
Sensitivity (%)	**60**	**40–80**	**(23)**
Specificity (%)	**78**	**56–100**	**(23)**
CT[a,b] (experienced reviewer)			
Sensitivity (%)	**96**	**93–96**	**(26)**
Specificity (%)	**100**	**95–100**	**(26)**
CT[a,b] (less experienced reviewers)			
Sensitivity (%)	**96**	**89–100**	**(26)**
Specificity (%)	**83**	**43–100**	**(26)**
CT (poor quality)			
Sensitivity (%)	**73**	**52–83**	**(23)**
Specificity (%)	**78**	**30–81**	**(23)**

[a]CT with 3D reconstructions.
[b]Good quality.
Modified with permission of the ARRS from Medina et al. (21)

Table 4.2. Cost of imaging tests

Variable	Direct cost ($)	Total cost[a] ($)	Medicaid[b] ($)
Skull radiography	44	76	38
3D-CT	80	191	261
Sedation	70	121	0[c]
CT plus sedation	150	312	261

[a]Medical center cost estimates include direct (fixed and variable) and indirect (overhead) costs.
[b]Medicaid reimbursement (Ohio). This cost was used for the case-based study.
[c]Sedation by nonanesthesiologist is not reimbursed by Medicaid.
Modified with permission of the ARRS from Medina et al. (21)

Imaging Case Studies

Figures 4.2, 4.3, and 4.4 illustrate representative cases of non-syndromic and syndromic craniosynostosis. In addition, a case of the commonly seen non-synostotic plagiocephaly is presented.

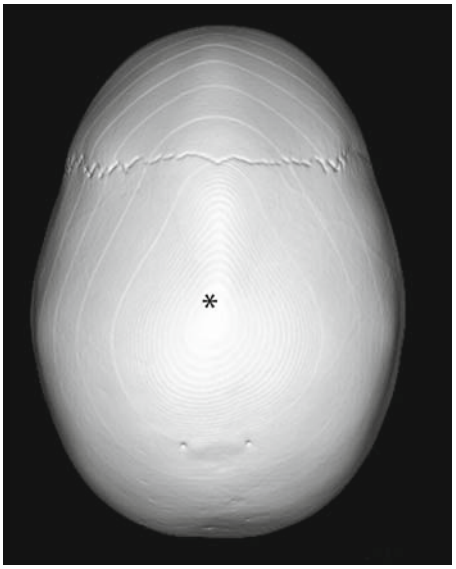

Figure 4.2. Case 1. Another case of isolated sagittal craniosynostosis. Superior view from a 3D-CT reconstruction demonstrating fusion of the sagittal suture (*star*) with associated dolichocephaly.

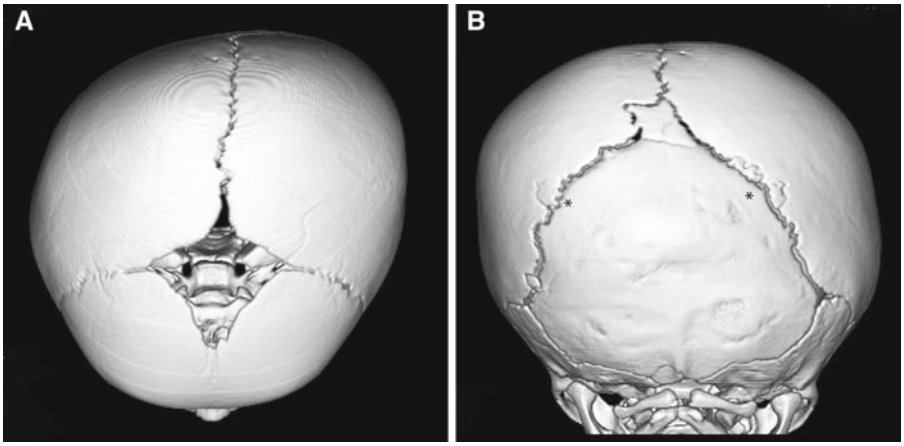

Figure 4.3. Case 2. Non-synostotic occipital plagiocephaly (positional molding or deformational plagiocephaly). A: Superior projection from a 3D-CT reconstruction demonstrating the skull deformity. B: Posterior projection from a 3D-CT reconstruction demonstrating patent lamboid sutures (*stars*).

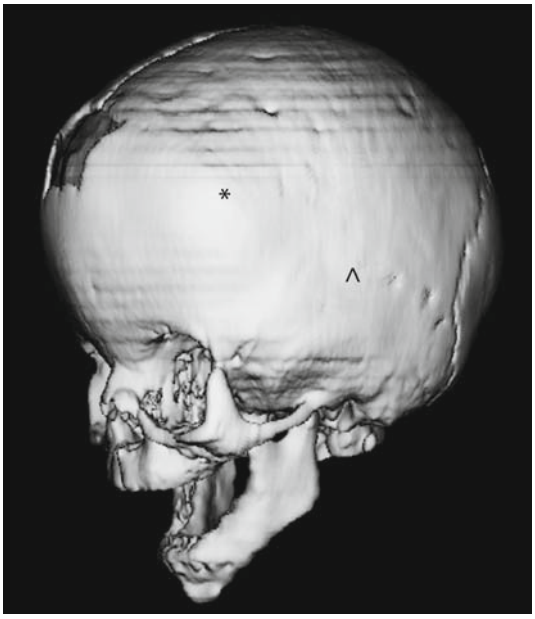

Figure 4.4. Case 3. Apert syndrome. Anterior oblique projection from a 3D-CT reconstruction demonstrating coronal (*star*) and squamosal (^) sutures synostosis. Also note the facial hypoplasia.

Suggested Imaging Protocol for Craniosynostosis

Plain Radiographs

Excellent quality plain films including anteroposterior, Towne, and both lateral radiographs.

CT

Spiral or MDCT with surface rendering and maximum intensity projections.

Axial acquisition with the following suggested parameters.

- 120 kVp
- 200 mA
- Thickness 2.5 mm
- Parenchymal reconstruction: 5 mm with soft tissue algorithm

3D Images: 0.625 mm high-resolution bone reconstruction using 3D volume rendering and high-definition maximum intensity projection.

Future Research

- Large studies are needed to evaluate the role of ultrasound in the diagnosis of craniosynostosis, particularly in the differentiation between this entity and deformational plagiocephaly.
- Further research is required to establish the role of MRI and US in the antenatal diagnosis of craniosynostosis.
- Better-defined cohorts should be studied to determine the incidence of intracranial abnormalities based on the type of synostotic disorder.

References

1. Fernbach SK. Pediatr Radiol 1998 Sep; 28(9):722–728.
2. Blaumeiser B, Loquet P, Wuyts W, Nothen MM. Prenat Diagn 2004 Aug; 24(8):644–646.
3. Van Vlimmeren LA, Helders PJ, van Adrichem LN, Engelbert RH. Euro J Pediatr 2004 Apr; 163(4–5):185–191.
4. Delahaye S, Bernard JP, Renier D, Ville Y. Ultrasound Obstet Gynecol 2003 Apr; 21(4): 347–353.
5. Lajeunie E, Le Merrer M, Bonaïti-Pellie C, Marchac D, Renier D. Am J Med Genet. 1995 Feb 13; 55(4):500–504.
6. Cohen MM Jr. In Cohen MM Jr (ed.): Craniosynostosis: Diagnosis, Evaluation and Management, 2nd ed. New York: Oxford University Press, 2000;112–118.
7. Alderman BW, Fernbach SK, Greene C, Mangione EJ, Ferguson SW. Arch Pediatr Adolesc Med 1997 Feb; 151(2):159–164.
8. Cohen MM Jr. In Cohen MM Jr (ed.): Craniosynostosis: Diagnosis, Evaluation, and Management, 2nd ed. New York: Oxford University Press, 2000;3–50.
9. Cohen MM Jr. In: Cohen MM Jr (ed.): Craniosynostosis: Diagnosis Evaluation, and Management, 2nd ed. New York: Oxford University Press, 2000;51–68.
10. Cohen MM Jr, MacLean RE In Cohen MM Jr (ed.): Craniosynostosis: Diagnosis, Evaluation, and Management, 2nd ed. New York: Oxford University Press, 2000;119–146.
11. Blank CE. Ann Hum Genet 1960;24:151–163.
12. Mulliken JB, Vander Woude DL, Hansen M, LaBrie RA, Scott RM. Plast Reconstr Surg 1999;103:371–380.
13. Jones BM, Hayward R, Evans R, Britto J. BMJ 1997 Sep 20; 315(7110):693–694.
14. Argenta LC, David LR, Wilson JA, Bell WO. J Craniofac Surg 1996;7:5–11.
15. Kane AA, Mitchell LE, Craven KP, Marsh JF. Pediatrics 1996;89:877–885.
16. Turk AE, McCarthy JG, Thorn CHM, Wissoff JH. J Craniofac Surg 1996;7:12–18.
17. Willinger M, Hoffman JH, Hartford RB. Pediatrics 1994;93:814–819.
18. Gellad FE, Haney PJ, Sun JC, Robinson WL, Rao KC et al. Pediatr Radiol 1985; 15(5):285–290.
19. Abrahams JJ, Eklund JA. Clin Plast Surg 1995 Jul; 22(3):373–405.
20. Cerovac S, Neil-Dwyer JG, Rich P, Jones BM, Hayward RD. Br J Neurosurg 2002 Aug; 16(4):348–354.
21. Medina LS, Richardson RR, Crone K. Am J Roentgenol 2002 Jul; 179(1):215–221.
22. Vannier MW, Hildebolt CF, Marsh JL, Pilgram TK, McAlister WH, Shackelford GD et al. Radiology 1989 Dec; 173(3):669–673.
23. Pilgram TK, Vannier MW, Hildebolt CF et al. Radiology 1989;173:675–679.
24. de León GA, de León G, Grover WD, Zaeri N, Alburger PD. Ach Neurol 1987; 44(9):979–982.
25. Agrawal D, Steinbok P, Cochrane DD. Child's Nerv Syst 2006 Apr; 22(4):375–378.
26. Vannier MW, Pilgram TK, Marsh JL, Kraemer BB, Rayne SC, Gado MH et al. Am J Neuroradiol 1994 Nov; 15(10):1861–1869.
27. Vannier MW, Pilgram TK, Marsh JL et al. AJNR 1994;15:1861–1869.
28. Cote CJ. Pediatr Clin North Am 1994;41:31–58.
29. Holzman RS. Pediatr Clin North Am 1994;41:239–256.
30. deDombal F. J R Coll Physicians Lond 1975;9:211–218.
31. Medina LS. Am J Neuroradiol 2000 Nov–Dec; 21(10):1951–1954.
32. Regelsberger J, Delling G, Helmke K, Tsokos M, Kammler G, Kranzlein H et al. J Craniofac Surg 2006 Jul; 17(4):623–625; discussion 626–628.
33. Hutchison BL, Hutchison LA, Thompson JM, Mitchell EA. Pediatrics 2004 Oct;114(4): 970–980.
34. AAP Task Force on Infant Positioning and SIDS Positioning and SIDS Pediatrics. Pediatrics 1992 Jun; 89: 1120–1126.
35. Sze RW, Parisi MT, Sidhu M, Paladin AM, Ngo AV, Seidel KD et al. Pediatr Radiol 2003 Sep; 33(9):630–636.
36. Fernbach SK, Feinstein KA. Neurosurg Clin N Am 1991 Jul; 2(3):569–585.
37. Slovis TL. Pediatrics 2003; 112:971–972.
38. Goldstein SJ, Kidd RC. Comput Radiol 1982 Nov–Dec; 6(6):331–336.
39. Hayward R, Harkness W, Kendall B, Jones B. Scand J Plast Reconstr Surg Hand Surg 1992; 26(3):293–299.
40. Lachman R. Taybi and Lachman's Radiology of Syndromes, Metabolic Disorders, and Skeletal Dysplasias, 5th ed. St. Louis: Mosby, 2006.
41. Cohen MM Jr, Kreiborg S. Am J Med Genet 1990; 35:36–45.
42. Gershoni-Baruch R, Nachlieli T, Guilburd JN. Child's Nerv Syst 1991; 7:231–232.
43. Teebi AS, Kennedy S, Chun K, Ray PN. Am J Med Genet 2002; 107:43–47.
44. Miller C, Losken HW, Towbin R, Bowen A, Mooney MP, Towbin A et al. Cleft Palate-Craniofac J 2002; Jan 39(1):73–80.
45. Fjortoft MI, Sevely A, Boetto S, Kessler S, Sarramon MF et al. Neuroradiology 2007 Jun; 49(6):515–521.

5

Sickle Cell Disease and Stroke

Jaroslaw Krejza, Maciej Swiat, Maciej Tomaszewski, and Elias R. Melhem

Issues

I. What is the role of neuroimaging in acute stroke in children with sickle cell disease (SCD)?
II. What is the role of neuroimaging in children with SCD at risk for their first stroke?
III. What is the role of neuroimaging in prevention of recurrent ischemic stroke in children with SCD?
IV. Are there neuroimaging criteria that indicate that blood transfusions can be safely halted?
V. What is the role of neuroimaging in hemorrhagic stroke in children with SCD?

Key Points

- Implementation of the Stroke Prevention Trial in Sickle Cell Anemia (STOP) primary prevention strategy that uses transcranial Doppler screening resulted in lower rates in stroke admissions in California (limited evidence).
- Presence of silent infarcts on MR scans in asymptomatic children with SCD is associated with higher risk for future stroke (limited evidence).
- The risk of first stroke can be substantially reduced by chronic transfusions in asymptomatic children with SCD and hemoglobin (Hb) SS, in whom intracranial arterial mean velocities are over 200 cm/s on transcranial Doppler examination (strong evidence).
- Management of children with SCD and acute stroke requires immediate non-contrast CT to exclude intracranial hemorrhage (moderate–strong evidence).
- Children with symptoms of stroke and negative CT for hemorrhage require urgent MRI/DWI/MRA to assess the degree and extent of

J. Krejza (✉)
Department of Radiology, Division of Neuroradiology, University of Pennsylvania Philadelphia, PA 19104, USA, and Department of Nuclear Medicine, Medical University of Gdansk, Polond
e-mail: jaroslaw.krejza@uphs.upenn.edu

L.S. Medina et al. (eds.), *Evidence-Based Imaging in Pediatrics*,
DOI 10.1007/978-1-4419-0922-0_5, © Springer Science+Business Media, LLC 2010

brain structural abnormalities and PET/SPECT or MRS to determine the degree of ischemia (moderate evidence).
- Presence of intracranial arterial stenosis and new lesions on MR imaging in patients with stroke history is associated with high risk for recurrent stroke (limited evidence).
- There are no specific neuroimaging findings which can suggest that blood transfusions be safely halted in children with SCD (strong evidence).
- No data were found that evaluate the cost-effectiveness of the different neuroimaging modalities in the evaluation of symptomatic and asymptomatic patients with SCD and suspected stroke (limited evidence).

Definition, Pathophysiology, and Clinical Presentation

Sickle cell disease (SCD) is a family of recessively inherited disorders of hemoglobin (Hb). People who inherit only one sickle gene (HbS) are sickle cell carriers. Sickle cell anemia (SCA) is the most severe form of SCD developing when two sickle genes are inherited (homozygotic HbSS). Clinically significant SCD also arises when people inherit the sickle gene from one parent and another variant Hb gene from the second parent such as HbC (SC) or beta thalassemia gene (Sβ+ or $S\beta^0$). Sickle Hb (HbS), particularly when not carrying oxygen, polymerizes to gel-like consistency, the red blood cell (RBC) becomes more rigid and deformed to less pliable sickle shape (1, 2). The ability of RBC to adopt a new shape becomes the only important factor determining their transit through microcirculation as the viscosity of blood is abnormally increased primarily due to a loss of normal RBCs' deformability (3, 4). Sickle RBCs are much more vulnerable to mechanical stress during passage through the vasculature, resulting in hemolytic anemia. There is also accumulating evidence that activated white blood cells change their rheological properties contributing to SCD pathophysiology (5, 6). Chronically elevated levels of biologic mediators and acute reactants and ongoing activation of the coagulation system associated with persistence of inflammation in sickle subjects, even when they are in "steady state," further increase plasma viscosity and RBC aggregation (4, 7, 8). The viscosity of the oxygenated sickle blood is about 1.5-fold that of normal at equal shear rates but is increased to 10-fold that of normal blood in the deoxygenated state (9).

There is a wide range of values for all RBC indices in chronic SCA (10). The reduction in volume of RBC restricts the oxygen-carrying capacity of Hb, leading to chronic hemoglobin desaturation (11). Children with HbSS are more vulnerable to frequent episodes of pain, chest crisis, stroke (12–15), and delayed growth (16) than those with HbSC or $HbS\beta^0$ thalassemia, who usually have less-severe neurological complications in later life. There is ongoing controversy as to whether stroke is more common in those with sickle cell trait (HbAS) than in the general population.

Stroke is a major cause of morbidity in SCD typically defined as a cerebral vascular accident (CVA) of sudden onset with focal neurological deficit persisting over 24 h, developed either spontaneously or in the context of an acute illness such as infection (17). There is a high risk of CVA recurrence—particularly for patients presenting spontaneously—that is reduced but not eliminated by regular blood transfusion (17, 18).

Both ischemic and hemorrhagic strokes may be encountered as well as common subclinical strokes called "silent infarcts." The typical areas of infarction are the frontal and parietal lobes, particularly in boundary zones of territories supplied by the internal carotid (ICA) and middle (MCA) and anterior (ACA) cerebral arteries whereas the posterior circulation is affected much less frequently. Large-vessel vasculopathy and vaso-occlusion at the microvascular level, which enhances rheological insult, appear to be the dominant mechanisms of stroke in SCD. Not all patients who die after developing

neurological symptoms have large-vessel disease, however. In addition to the typical small necrotic lesions in the border between the cortex and the subcortical white matter, acute demyelination and venous sinus thrombosis have also been documented on MRI (19, 20).

There is a broad spectrum of acute presentation with CVA and other neurological complications in patients with SCD (21–23). Besides clinical stroke, patients with SCD also can have transient ischemic attacks (TIAs) with symptoms and signs resolving within 24 h (21–23), although many of these individuals are found to have had recent cerebral infarction or atrophy on imaging (12). The insidious onset of "soft neurological signs," such as difficulty in tapping quickly, is usually associated with cerebral infarction (24, 25). In addition, seizures (26), coma (27) and headache (28) are common presentations of stroke and CVA in children with SCD. Altered mental status—with or without reduced level of consciousness, headache, seizures, visual loss, or focal signs—can occur in numerous contexts, including infection, shunted hydrocephalus (29), acute chest syndrome (ACS) (30, 31), aplastic anemia secondary to parvovirus (32), after surgery (28, 33), transfusion (34), immunosuppression (35, 36), and apparently spontaneously (37). In one large series of 538 patients with ACS, 3% of children had neurological symptoms at presentation, and such symptoms developed in a further 7–10% in association with ACS (30). These patients are classified clinically as having had a CVA (12), although there is a wide differential of focal and generalized vascular and nonvascular pathologies—often distinguished using acute magnetic resonance techniques (37)—with important management implications (26, 29, 34, 38–41). Sixty-seven percent of those who have had an initial stroke and are not transfused will develop another, most likely within 36 months (42). With each episode, the child is usually left with more residual neurological deficit including some degree of mental retardation.

Epidemiology

SCD is one of the most prevalent genetic disorders and primarily affects people originating from sub-Saharan Africa, the Middle East, the Mediterranean, the Indian subcontinent, the Caribbean and South America, and their descendants in other parts of the world and immigrants from the above countries (43–50). The incidence of SCA in the African American population is 0.2–0.3%; that of SS trait is 9–11% and that of SC disease is 3% (48, 51–54). The sickle gene is present in about 20% of the indigenous black population in Africa (50, 55, 56). Approximately 80,000 African Americans in the USA have SCD. About 1 in 12 African Americans and 1 in 100 Hispanic Americans are carriers of the disease (57). This prevalence has remained constant primarily because the trait provides partial protection against malarial infection from *Plasmodium falciparum* (50, 58, 59). When RBCs containing HbS are deoxygenated, malarial parasites within these cells are destroyed. The parasites by themselves lower the pH causing the cells to sickle faster. Such protection has become irrelevant in the USA where malaria is no longer endemic.

Epidemiology of Stroke

Overall prevalence of stroke in all forms of SCD is 4%, and in those with SCA is 5%. First stroke occurs in all age groups, except for children under 1 year of age. The annual incidence of first stroke is approximately 0.6 per 100 patient-years or 600/100,000/year in SCA children. However, the highest incidence occurs in the first decade of life with rates of 1.02 per 100 patient-years in SCA patients 2–5 years of age and 0.8 in those 6–9 years of age (12). The cumulative risk of first stroke in SCA patients is 11% by the age of 20 years, 15% by age 30, and 24% by age 45 (12). The combined incidence of hemorrhagic and ischemic strokes in a general sample of American children 14 years of age was reported as 3.3 per 100,000 yearly or 0.0033 per 100 patient-years (60). The types of stroke differ between adults and children with SCD. Infarctive strokes are relatively more common in children than in adults while the reverse is true for hemorrhagic stroke. In the Cooperative Study of Sickle Cell Disease (CSSCD) report 9.6% of first strokes in SCD patients under age 20 were hemorrhagic, while 52% of all strokes in those over 20 years were hemorrhagic (12). When compared with their peers, children with

SCD have a 220-fold increase in stroke risk and a 410-fold increase in cerebral infarction.

In the CSSCD, stroke occurred less frequently in the other common genotypes of SCD. Age-adjusted prevalence rates of stroke at study entry were 2.43% for SB0 thalassemia (SCD-Sβ^0), 1.29% for SCD-Sβ^+, and 0.84% for SCD-SC. About 21% of SCD-SC patients who had a stroke were less than 10 years old compared to those with SCD-SS (31% under age 10).

Risk of Stroke

Clinically apparent stroke represents the most significant and recurrent threat to the SCD patient population. When compared with their peers, children with SCD have a 220-fold increase in stroke risk and a 410-fold increase in cerebral infarction; 11% of patients will have a clinically apparent stroke by age 20 years and 24% by age 45 years (12). The risk of first symptomatic stroke is highest during the first decade of life, with an incidence of 1.02% per year between the ages of 2 and 5 years. Moreover, 17–35% of SCD children without a compatible history of a cerebrovascular event have "silent" infarctions detectable with MRI (41, 61, 62). Children with silent infarcts are at higher risk for further ischemia than are SCD children with a normal MRI (41, 61, 62). The Cooperative Study of Sickle Cell Disease (CSSCD) amassed clinical data from October 1978 through September 1988 on a cohort of 4,082 patients with SCD from 23 clinical centers across the USA (12). Subjects were followed for an average duration of 5.2 $\pm$ 2.0 years. The overall incidence of first stroke was 0.46 per 100 patient-years, the age-adjusted incidence of first CVA was 0.61% per 100 patient-years. The incidence and prevalence of CVA is given in Table 5.1.

Epidemiology of Recurrent Stroke

Stroke in SCD has a high tendency to recur. In untransfused patients there is a 67% recurrence rate with 70% of the recurrent strokes occurring within the first 3 years following the initial stroke (42). The high risk of CVA recurrence can be reduced but not eliminated by chronic blood transfusion (18, 63). Estimated risk of stroke of children with SCD receiving blood transfusion therapy for at least 5 years after initial stroke is 2.2 per 100 patient-years (63). There is no sufficient evidence to state that hydroxyurea therapy reduces the risk of stroke (64, 65); however, data from nonrandomized clinical series suggest that hydroxyurea might be an alternative to transfusion for primary stroke prevention (insufficient evidence) (66). Chance of stroke recurrence in SCD patients is given in Table 5.2.

Epidemiology of Silent Infarcts Diagnosed by MRI

Children with silent infarcts are at higher risk for further ischemia than are SCD children with a normal MRI (41, 59, 60). About 17–35% of SCD children without a compatible history of a CVA have "silent" infarctions (41, 63, 67), and up to 25% have silent infarction by adolescence, typically between the ACA and MCA or between MCA and Posterior Cerebral Artery (PCA) territories (41, 68, 69). There is evidence of white matter damage in these border zones, even in those having normal T_2-weighted MRI (70) and no neurological symptoms (24, 25). These patients, however, might have had subtle transient ischemic attacks, headaches, or seizures (69). Cognitive difficulties (71, 72), which commonly affect attention (71) and executive function (73), are common in SCD, sometimes from infancy (73); they can be progressive (74) and are associated with brain abnormalities on MRI (70, 71, 74, 75).

Overall Cost to Society

SCD affects about 72,000 African Americans (54). Nationally, total health-care costs for SCD exceeded $0.9 billion in 1995 (data provided by NHBLI). This estimated cost does not include direct and indirect non-health-related costs, patient's and family member's time lost from school, lost workdays and reduced productivity of the patient, lost earnings of unpaid caregivers, transportation expenses, and income lost from premature death. Moreover, pain, disruption of family life, and stress on the patient and family are not included in the estimate. In 2007 dollars, the total cost may exceed $1.5 billion, which makes SCD one of the most costly genetic disorders in the USA. During the years 1989–1993, there were on average 75,000

hospitalizations per year of patients with SCD for a total direct cost of $475 million per year (in 1996 dollars) (76). Government paid 66% of the cost of hospitalizations. Thus, research into interventions that prevent complications or result in better outpatient management of patients with SCD is important and has great potential for cost savings.

Cost of Screening

STOP research findings and NHBLI recommendations pose challenges to the health-care system. The time on transfusions necessary to decrease the stroke risk for patients with SCD remains unclear. As recommended by NHBLI, every child between the ages of 2 and 16 (approximately half of 72,000 people with SCD) should undergo two transcranial Doppler (TCD) studies a year. Estimated TCD exams cost $21.6 million ($300/TCD) a year, while estimated recommended transfusions cost about $154 million (77, 78).

Cost-Effectiveness Analysis

No data exist concerning cost-effectiveness of assessing the risk of first stroke, of neuroimaging in acute stroke, or of predicting stroke outcome in children with SCD.

Goals

The goal of neuroimaging such as computed tomography (CT), magnetic resonance (MR), positron emission tomography (PET), single photon emission CT (SPECT), and TCD in acute stroke is to document whether the stroke is ischemic or hemorrhagic, to assess the extent of parenchymal abnormalities, and to determine the presence of cerebrovascular changes. However, initiation of neuroprotective therapy, including exchange transfusion therapy to minimize secondary brain damage and neutralize "ischemic cascade," should not be delayed by arrangement for imaging studies. CT without contrast is the primary imaging modality for the assessment of acute stroke because of its 24/7 availability, ease of accessibility, and ability to exclude hemorrhagic causes. MRI and MR engiography (MRA) are recommended for better assessment of extent of infarction and demonstration of cerebrovascular abnormalities. In the case of hemorrhagic stroke, the goal is to identify with conventional angiography an arteriovenous malformation or aneurysm(s) amenable to surgery or catheter intervention. Exchange transfusion prior to invasive angiography is recommended.

The ultimate goal is to preserve brain function in children with SCD. A secondary goal is to prevent the progression of preclinical ischemia to permanent neuronal loss with disability. The first step is to identify young children at high risk of stroke before development of focal neurological deficits. The preferred imaging is dependent upon the neuroradiologist and the institution but typically is large-vessel velocity measurements with transcranial Doppler ultrasound confirmed by conventional MRI or quantitative MRI and MRA (Fig. 5.1). This should be followed by preventive therapy in those with evidence of parenchymal and/or cerebrovascular changes. In patients with neurological symptoms and negative MRI/MRA findings PET or SPECT is recommended.

Methodology

We conducted a systematic review of the literature using a database search of MEDLINE (PubMed, National Library of Medicine, Bethesda, MD) and of Web of Science® (Institute of Scientific Information, Philadelphia, PA) to identify studies dealing with sickle cell disease and stroke and relevant to neuroimaging. The search covered years 1990–2007, using the following key terms: (*1) sickle cell disease* and *(2) stroke*, and one of the following: *exp cerebral ischemia, cerebral infarction, cerebrovascular disorders or cerebrovascular accidents, epidemiology, cost, ultrasound, TCD* or *transcranial Doppler sonography, TCCS* or *transcranial color-coded sonography, TCCD* or *transcranial color-coded duplex sonography, MRI* or *magnetic resonance imaging, MRA* or *magnetic resonance angiography, angiography, DSA*, or *digital contrast angiography, CT* or *computed tomography, PET* or *positron emission tomography, SPECT* or *single photon emission computerized tomography.* There was one randomized controlled trial, no meta-analyses, and no cost analysis of neuroimaging diagnostic

options. We expanded our retrieval to include also clinical trials, cohort studies, multicenter studies, comparative studies, case–control studies, and case reports having more than five subjects for the key question of the age-specific natural history of ischemic stroke. Reviews, letters, hospital bulletins, and single case reports were excluded.

Discussion of Issues

I. What Is the Role of Neuroimaging in Acute Stroke in Children with Sickle Cell Disease?

Summary of Evidence: CT without contrast is the best tool to exclude hemorrhagic stroke in children as well as adults. There is need for a research study, however, to determine whether anatomical MR can replace CT (79, 80). Patients without hemorrhagic stroke should then undergo MRI with DWI and MRA to detect an infarct(s), determine location and extent of ischemic lesions, and presence of large-vessel occlusion/narrowing as soon as possible, the best on emergency basis. Vascular imaging of the neck vasculature with CT or MR angiography to exclude arterial dissection (81) and venous thrombosis should be undertaken within 48 h of presentation with arterial ischemic stroke. MRI and MR angiography become preferable due to noninvasive nature, and no requirement to administer iodinated IV contrast. MR venogram must be specially requested if cerebral venous thrombosis is suspected (82). Imaging from the aortic arch to the intracranial vasculature should be performed in all children with arterial ischemic stroke. Transcranial Doppler (TCD) is not useful in acute stroke (limited evidence) (83–85).

Symptomatic children with negative CT and MR studies should be followed subacutely by PET or SPECT to identify loss of cerebral neuronal metabolic function.

Supporting Evidence

CT

Non-contrast CT provides sufficient information to make decisions about emergency management in hyperacute stroke, i.e., <6 h after onset of symptoms (moderate evidence) (86–89). Unenhanced CT has 57% sensitivity and 100% specificity for acute stroke detection (90). The sensitivity can be improved up to 80% by use of variable window width and center level settings or 10-point topographic scoring system (91). The utility of CTA in acute adult stroke relies on demonstrating occlusion or significant arterial narrowings within intracranial vessels and on evaluating the carotid and vertebral arteries in the neck. The sensitivity of CTA was determined to be 88.5–98% in these aspects (92, 93). The utility of CTA in SCD children with stroke has not been determined.

MRI

MRI with diffusion-weighted imaging (DWI) provides additional useful information on presence of ischemic stroke (moderate evidence) and visualization of silent cerebral infarcts (moderate evidence) (94–96). DWI determine ischemic regions that later progresse to infarction and the volume of acute infarct correlates well with clinical outcome. Based on adults data DWI was reported to have had high sensitivity and specificity of 88–100% and 86–100%, respectively (97–99). DWI is superior to conventional MRI imaging and CT in demonstrating ischemic stroke during the first 24 h after presentation (moderate evidence) (80, 100–102). The pattern of ischemic changes in the brain can be indicative but not specific for a particular stroke etiology (insufficient evidence) (103, 104).

MRA

Like CT angiography, MR angiography (MRA) is useful for detecting intravascular occlusion due to a thrombus and for evaluating the carotid bifurcation in patients with acute stroke. Kandeel and colleagues reported that MRA is 85% accurate when compared to DSA (104). In a study of 22 SCD patients, MRA abnormality in a long segment (6 mm) with reduced distal flow correlated with subclinical infarction, while short focal areas of abnormal MRA most commonly in branching regions showed no associated MRI infarction (105).

More recent data from adults showed that MRA has 70–86% sensitivity for detection of intracranial stenosis compared to DSA, while sensitivity of CTA is higher up 98% (92, 93, 106). Although CTA has better sensitivity than MRA, the advantage of MRA in SCD is that, unlike CTA, it does not require contrast agent, which can be toxic and can exacerbate symptoms in

acute stroke (107). MR spectroscopy allows distinguishing an ischemic lesion from other non-ischemic changes but utility of MRS in hyperacute stroke is limited in children with SCD.

Angiography

Digital subtraction angiography (DSA) is not included in standard acute stroke imaging protocol in children with SCD (108). DSA is accurate in detecting intracranial vascular abnormalities (AVM, aneurysm, dissection, occlusion) and quantifying arterial narrowing (moderate evidence) but is invasive and carries a risk of stroke (109–111). MR and CT angiography are not as accurate as DSA in evaluating vasculature (limited evidence) (112–116), but DSA is performed when endovascular therapy is anticipated.

Nuclear Medicine (PET, SPECT)

PET and SPECT are indicated if CT and MR are negative in patients with clinical stroke to detect the functional activity of the cerebral tissues by using radioactive tracers to indicate glucose metabolism of 2-deoxy-2-[^{18}F]fluoro-D-glucose (FDG) and evaluate microvascular perfusion ([^{15}O]H_2O) (limited evidence) (117, 118). PET studies (117, 119, 120) that have been done in patients with SCD have shown a variety of abnormalities including hypometabolism in frontal areas of the brain and areas of low perfusion that appear normal on MRI. The study of Powars et al. (120) suggested that few patients with SCD have normal PET studies, and areas of hypometabolism in brain regions with normal MR appearance are not uncommon (not sufficient evidence). The authors suggest that PET could be used to select patients for treatment as four patients showed improvement in metabolism and perfusion with transfusion treatment. The most powerful predictor of ischemia in other applications of PET is an increased oxygen extraction fraction, but this application and metabolism measurements remain to be established in children with SCD.

II. What Is the Role of Neuroimaging in Children with Sickle Cell Disease at Risk of Their First Stroke?

Summary of Evidence: Transcranial Doppler sonography (TCD) is currently the most commonly used screening method to identify children with SCD who are at high risk for first stroke. In the Stroke Prevention Trial in Sickle Cell Anemia (STOP) (121) — a multicenter, randomized trial of standard care versus transfusion therapy to prevent first stroke in 130 children with SCD—the transcranial Doppler ultrasonography was employed to identify patients with high risk at stroke based on mean flow velocity measurements in terminal segment of ICA and MCA. Patients with velocities over 200 cm/s, consistent with cerebral arterial narrowing and at high risk of first-time stroke, were enrolled. Those treated with chronic blood transfusions (to keep the hemoglobin above 30%) had 92% lower stroke rate. Based on this trial and its follow-up study (122), the NHLBI recommends TCD screening in children starting at 2 years of age and continue annually if TCD is normal and every 4 months if TCD shows velocity over 170 cm/s but less than 200 cm/s. Asymptomatic children with abnormal TCD results should be retested within 2–4 weeks to confirm abnormality, while transfusion is recommended in symptomatic children and abnormal velocities, as patients with TIA whose symptoms are recognized and reported and with confirmed abnormality on neuroimaging are treated as having had a stroke.

There have been no randomized trials testing preventive treatment after the first stroke. However, a number of case series and a more recent review have reported that the risk of reduction appears to be substantial, reducing at least the recurrence in the first few years from over 50 to around 10% (123–125) (limited evidence).

The stroke risk may vary substantially among children with SCD who have abnormal TCD results, because high velocity can be consistent with arterial narrowing as well as hyperemic high blood flow (126). Although there are no data to stratify the risk of stroke based on presence of narrowing or hyperemia, in both situations higher risk of stroke seems to correlate with increased TCD velocities. The risk of ischemic stroke is also higher in children with silent infarctions on MRI and cerebrovascular disease on MRA.

Supporting Evidence: The use of TCD is currently the most commonly used screening method to identify children at high risk of both first and recurrent stroke (strong evidence) (121, 122, 127). TCD is a safe, noninvasive,

well-tolerated, relatively low-cost procedure in which the velocity of blood flow can be measured in intracranial arteries using an ultrasound probe placed over the temporal bone (128, 129). In comparison with conventional angiography, TCD flow velocity measurements showed a sensitivity of 90% and specificity of 100% for the diagnosis of arterial narrowing greater than or equal to 50% lumen diameter reduction (moderate evidence) (109, 114). The STOP trial showed associations between stroke risk and TCD mean velocities in the MCA or terminal ICA (Table 5.3).

The NHLBI issued a clinical alert recommending TCD screening for cerebrovascular disease every 6 months on all children with SCD between the ages of 2 and 16 and consideration of chronic transfusions in those with two abnormal TCD test results (130). The timing of repeated TCDs is not clearly defined. If TCD is normal annual testing is proposed while every 4 months if TCD is marginal. Children with abnormal TCD results should be retested within 2–4 weeks (limited evidence) (78, 122, 131, 132).

Fullerton et al. (133) evaluated administrative data in California comparing the rates of hospital admissions for the first stroke in children with SCD between the early 1990s (before STOP) and from 1998 to 2000 (after STOP) and found sharp reduction in first stroke admissions (limited evidence). Further reports from STOP I and II trials (131) and two ongoing clinical trials in children with SCD — one testing other approaches to screening, silent infarct documented by MRI (SILENT Cerebral Infarct Multi-Center Clinical Trial) (134), and the other testing hydroxyurea compared with transfusion for secondary stroke prevention (Stroke With Transfusions Changing to Hydroxyurea Trial) (135) — may show improved outcomes in the future.

Imaging TCD has become a widely employed in practice because it allows accurate identification of intracranial arteries in color and placement of a sample volume in a site of arterial segment, where the velocity is the highest. Also imaging TCD allows determination of the angle of insonation and correction of velocity measurements for the error related to more than zero angles. However, there are no data to support that angle-corrected flow velocity measurements are better than uncorrected ones in risk assessment in children with SCD. There are several articles suggesting that imaging TCD flow velocity measurements obtained without correction for the angle of insonation can be used to identify children at high risk for stroke instead of conventional TCD (limited to moderate evidence) (85, 127, 136–140).

Elevation of cerebral blood flow velocities on TCD may precede abnormal findings in MRA (141, 142). MRA is more costly and children under 3 years may require general anesthesia; however, MRA can confirm the presence and extent of cerebrovascular disease in those with elevated TCD velocities (limited evidence) (104, 143, 144).

Risk of Symptomatic Stroke in Children with Silent Infarct on MRI

Data from the CSSCD showed that silent infarction seen on MRI was associated with an increased risk of symptomatic stroke (1.03 per 100 patient-years) and progression of silent infarction (7.06 per 100 patient-years) (moderate evidence) (41, 62, 69). The Silent Cerebral Infarct Multi-Center Clinical Trial, in which estimated number of 204 children with silent infarction seen on MRI will be randomized to chronic blood transfusions or observation, is currently enrolling patients and will report after 2012 (145).

III. What Is the Role of Neuroimaging in Prevention of Recurrent Ischemic Stroke in Children with Sickle Cell Disease?

Summary of Evidence: Recurrent stroke is observed in children with SCD despite proper regimen of transfusion therapy. Arterial stenosis is the main risk factor for recurrent stroke. Elevated cerebral artery mean velocities (>200 cm/s) on TCD and new lesions on MRI or MRA indicate higher risk of recurrent stroke. SCD children should be monitored after first stroke episode with TCD and MRI/MRA although no randomized or controlled data are available to optimize frequency of follow-up.

Supporting Evidence: Two studies found a high risk of stroke recurrence in children who had arterial abnormalities on conventional

angiography (limited evidence) (123, 125). Moyamoya syndrome is characterized by chronic progressive narrowing of proximal segments of intracranial arteries with the characteristic distal collateral network on angiography.

It is a risk factor for stroke recurrence even in those children undergoing regular transfusion (limited evidence) (146, 147). Serial MRI scans in these individuals with pre-existing cerebral damage might show new lesions as well as extension of existing abnormality (148). Some studies show this risk to be reduced after extracranial–intracranial bypass or indirect revascularization (149, 150) (limited evidence). Further studies of these procedures are needed as some researchers have not found progression (151), and the cerebrovascular disease can stabilize as demonstrated on both MRA (152) and TCD (limited evidence) (78).

IV. Are There Neuroimaging Criteria That Indicate That Blood Transfusions Can Be Safely Halted?

Summary of Evidence: Limited data on discontinuation of blood transfusion suggest that halting transfusions increases the risk of stroke. A decision analytic model suggests follow-up of SCD children during transfusion therapy with annual TCD until age 10 years. The model also suggests transfusions until 18 years in children with high risk of stroke. The main risk of prolonged blood transfusions is iron overload which can result in organ failure and death.

Supporting Evidence: The STOP II trial followed the children in STOP I and showed that discontinuation of transfusions led to recurrence of TCD abnormalities and development of new stroke events (moderate evidence) (145, 153). However, only the baseline TCD results were used to determine stroke risk against follow-up observations. Transfusion therapy converts approximately 60% of patients to normal TCD results (153, 154) (moderate evidence). Similar findings were observed on MRA examinations (78) (limited evidence). The STOP II trial concluded that transfusions should not be stopped once TCD results were normal (moderate evidence) (153).

However, 20% of children who discontinued transfusion therapy did not develop abnormal TCD or stroke. Mazumdar et al. performed a decision analysis model to compare various stroke prevention strategies for a hypothetical cohort of 2-year-old children (155), such as (1) annual transcranial Doppler ultrasonography screening until age 16 years with children at high risk for stroke receiving monthly transfusion for life; (2) annual transcranial Doppler ultrasonography until age 16 years with transfusions until age 18 years; (3) biannual transcranial Doppler ultrasonography until age 16 years with transfusions until age 18 years; (4) annual transcranial Doppler ultrasonography until age 10 years with transfusion until age 18 years; (5) one-time screening at age 2 years with transfusion until age 18 years; and (6) no intervention.

The optimal stroke prevention strategy was projected to be annual transcranial Doppler ultrasonography screening until age 10 years with transfusion for children at high risk until age 18 years. Better adherence to chelation therapy would improve life expectancy in all intervention strategies with fewer deaths from iron overload in comparison to other more intensive strategies (155) (limited evidence).

V. What Is the Role of Neuroimaging in Hemorrhagic Stroke in Children with SCD?

Summary of Evidence: Infarctive strokes are relatively more common in children than in adults with SCD while reverse is true for hemorrhagic stroke (12). Primary hemorrhagic stroke is much more devastating and in majority of patients is fatal (12). High leukocyte count and low steady-state Hb concentration were identified to be the main risk factors of hemorrhagic stroke in SCD patients (12). Other potential risk factors are hypertension, treatment with corticoids, previous ischemic stroke, or hypertransfusion (36). CT without contrast is still the first line examination in diagnosing hemorrhagic stroke. In acute intraparenchymal hemorrhage (ICH) the accuracy of MRI examination seems to be similar to accuracy of CT, especially when gradient echo sequences are used (79, 80); however, in patients with subarachnoid hemorrhage (SAH) CT is superior (156). TCD seems to be

ineffective in predicting hemorrhagic stroke (122). The role of TCD in pediatric SAH is unclear though in adults it is used to detect and monitor vasospasm. In cases with ICH DSA is advisable to rule out lesions that should be treated with surgery. In cases with SAH DSA is used to detect ruptured cerebral aneurysms. Hydration and reduction of HbS to less than 30% prior to DSA is the usual method of preparation, and there have been few reports of stroke complications since this practice was initiated.

It is not known if transfusion prevents recurrent hemorrhage. Patients with any form of intracranial bleeding, excepting subdural from trauma, need evaluation for a surgically correctable aneurysm even if the bleeding appears to be primarily intracerebral. If there is no aneurysm then transfusion for at least a year is often recommended, but it is not clear if this helps. Recurrent hemorrhage is less common than recurrent ischemic stroke, partly because more of the first events are fatal.

Supporting Evidence: The Cooperative Study of Sickle Cell Disease (CSSCD) showed about 9.6% of first strokes in SCD-SS patients less than 20 years old were hemorrhagic, compared to 52% of first strokes in those over 20 years old (12). There is nearly a 250-fold increase in the risk of hemorrhagic stroke compared with children under age 20 years (23). In CSSCD study almost all fatal cases (24%) were due to hemorrhagic stroke. However, in the first published series the mortality rate associated with hemorrhagic stroke was over 50% (157), similar to the rate (40%) reported by Strouse et al. (34). Typical clinical presentation of hemorrhagic stroke in SCD includes focal neurological deficits, severe headache, nuchal rigidity, and coma.

The CSSCD study showed that risk of hemorrhagic stroke increases along with decreasing steady-state Hb concentration (RR 1.61 per 1 g/dL decrease) and increasing steady leukocyte count (1.94 per 5×10^9/L increase) (limited evidence) (12). Associations with hypertension, recent blood transfusions, treatment with corticosteroids, previous ischemic stroke, moyamoya, cerebral aneurysms, or acute chest syndrome (ACS) were also reported (insufficient evidence) (34, 39, 146, 158–161).

CT is being used as an initial imaging study. In emergency setting non-contrast CT is adequate and the most cost-effective strategy in diagnosing acute hemorrhagic stroke (moderate evidence) (162). In acute ICH the accuracy of MRI is similar to accuracy of CT, especially with the use of gradient echo sequences (79, 80) (strong evidence). MRI is better than CT in evaluations of chronic hemorrhage (79, 80) (strong evidence). MRI, however, is not feasible in up to 20% acute stroke patients due to contraindications to MRI, impaired consciousness, hemodynamic compromise, vomiting, or agitation, and lack of cooperation (163). To obtain successful MRI results patients often need general anesthesia.

CT should be used if subarachnoid hemorrhage is suspected (156) (insufficient evidence). DSA is used to identify the source of bleeding (164, 165) (limited evidence), but most children require general anesthesia. DSA is invasive, however, and carries risk of stroke (166, 167). CTA and MRA are less accurate then DSA in depicting intracranial vascular anatomy, especially in visualization of tertiary branches and small cerebral arteries (164). The additional advantage of DSA is the potential to initiate therapy such as endovascular coiling of aneurysms and embolization of AVMs. TCD is not effective in predicting hemorrhagic stroke (122); however, TCD can be used to detect and monitor intracranial vasospasm in patients with SAH (168) (limited evidence).

Take Home Figures and Tables

Figure 5.1 shows a decision tree about the role of neuroimaging in the primary prevention against stroke and management of children with sickle cell disease (SCD) with neurological symptoms.

Table 5.1 shows incidence of first stroke and prevalence of CVA in the population of children with sickle cell disease. Table 5.2 shows risk of recurrent stroke in SCD patients. Table 5.3 shows risk for stroke in SCD patients in accordance with initial TCD velocities.

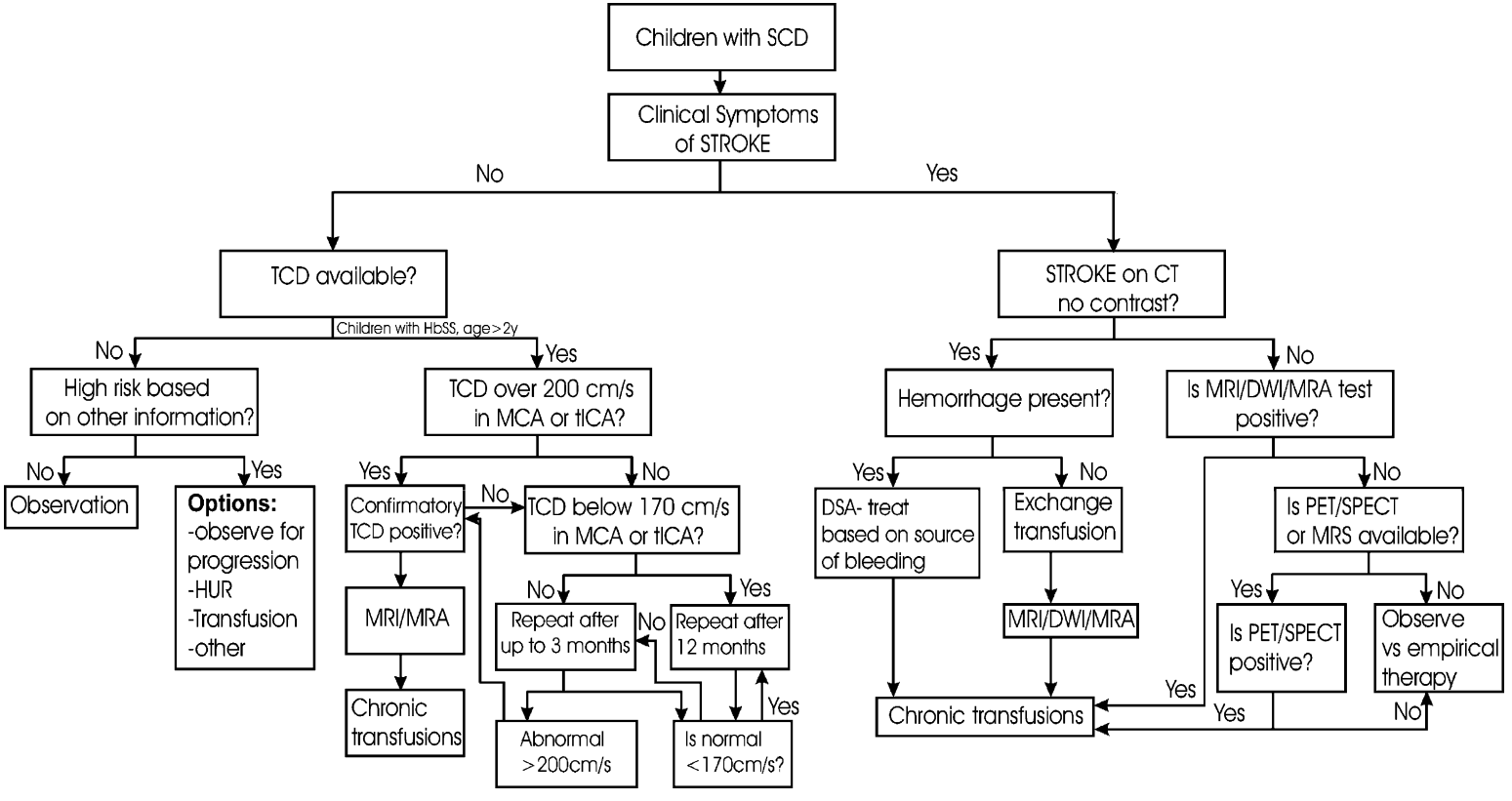

Figure 5.1. Decision tree shows the role of neuroimaging in primary prevention against stroke and management of children with sickle cell disease (SCD) with neurological symptoms. TCD—transcranial Doppler sonography, MRI—magnetic resonance imaging, MRA—MR angiography, DWI—diffusion weighted imaging, PET—positron emission tomography, SPECT—single photon emission computed tomography, DSA—digital subtraction angiography, HUR—hydroxyurea, MCA—middle cerebral artery, ICA—internal carotid artery. Note: optimal frequency of rescreening with TCD is not established; younger children with velocity closer to 200 cm/s should be rescreened more frequently.

Table 5.1. Incidence (in %) of first stroke and prevalence of CVA in the population of children with sickle cell disease

	Hb SS	Hb SC	Hb S-β^+	Hb S-β^0	Total
Overall incidence	0.61	0.17	0.11	0.10	0.46
Age-adjusted incidence	0.61	0.15	0.09	0.08	
Overall prevalence	4.07	0.80	1.48	1.56	3.75
Age-adjusted prevalence	4.01	0.84	1.29	2.43	

Data from Ohene-Frempong et al. (12).

Table 5.2. Risk of recurrent stroke in SCD patients in accordance with initial event

Initial event	Events per 100 patient-years
Symptomatic stroke	
– Before age 20	6.4
– After age 20	1.6
Silent infarct	0.54

Data from Ohene-Frempong et al. (12) and from Balkaran et al. (40).

Table 5.3. Risk of stroke in SCD patients in accordance with initial TCD mean velocities

TCD velocity (cm/s)	Stroke risk (%)
≥200	40
>170	7
<170	2

Data from STOP trial results from Adams et al. (122).

Imaging Case Studies

Case 1

Figure 5.2 presents brain images of an 11-year-old girl with sickle cell disease without neurological deficits.

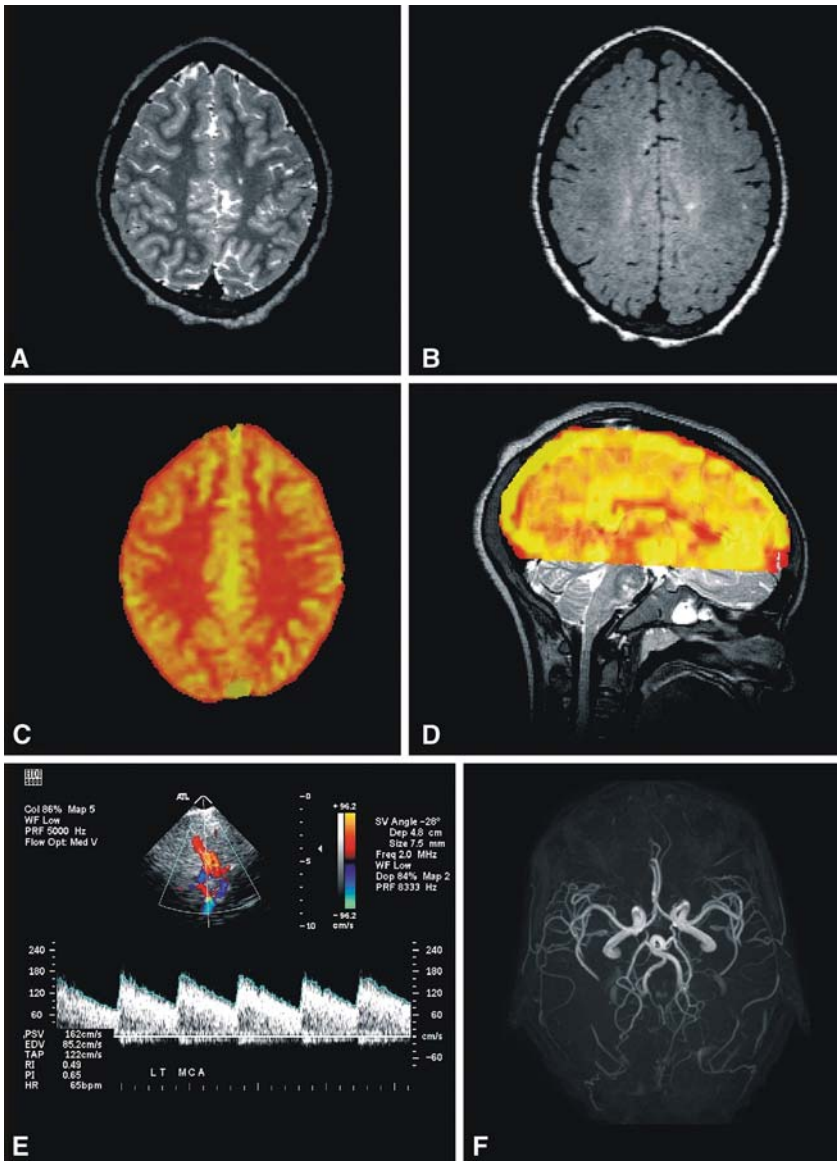

Figure 5.2. Brain images of an 11-year-old female with sickle cell disease (genotype HbSS) without neurological deficits. A: Axial T2-weighted image with small silent lesion located in left parietal region. B: Axial flair image showing the same lesion in left parietal lesion. C: Axial slice of CBF map obtained using arterial spin labeling perfusion MRI coregistered to T1-weighted image. D: Sagittal projection of the CBF map registered to T2-weighted volumetric image; note the high CBF signal in sagittal sinus. E: Image from transcranial color-coded Doppler study of the middle cerebral artery with velocity measurements and angle correction. F: Axial projection of the 3D reconstruction of time-of-flight MRA.

Suggested Imaging Protocol for Sickle Cell Disease and Stroke

Shown in Fig. 5.1.

Future Research

- Is TCD useful to assess the risk of stroke among children with hemoglobin SC and β-thalassemia?
- Is advanced MR imaging helpful to better select SCD patients for chronic transfusions?
- Is advanced MR imaging useful in secondary stroke prediction?
- Is neuroimaging useful to identify children in whom chronic transfusions can be safely stopped?
- Is there a role for PET-CT for better identification of ischemia in children with SCD?

References

1. Pavlakis SG, Kingsley PB, Bialer MG. J Child Neurol 2000;15:308–315.
2. Prohovnik I, Pavlakis SG, Piomelli S, Bello J, Mohr JP, Hilal S et al. Neurology 1989;39: 344–348.
3. Lipowsky H, Cram L, Justice W, Eppihimer M. Microvasc Res 1993;46:43–64.
4. Lipowsky H. Microcirculation 2005;12:5–15.
5. Zhao Y, Chien S, Skalak R, Lipowsky H. Ann Biomed Eng 2001;29:360–372.
6. Dong C, Cao J, Struble E, Lipowsky H. Ann Biomed Eng 1999;27:298–312.
7. Mulivor A, Lipowsky H. Am J Physiol Heart Circ Physiol 2004;286:H1672–H1680.
8. Hebbel RP, Osarogiagbon R, Kaul D. Microcirculation 2004;11:129–151.
9. Kaul DK, Fabry ME, Nagel RL. Blood Rev 1996;10:29–44.
10. Serjeant GR. Br J Haematol 2001;112:3–18.
11. Stuart MJ, Setty BNY. Pediatr Pathol Mol Med 2001;20:27–46.
12. Ohene-Frempong K, Weiner SJ, Sleeper LA, Miller ST, Embury S, Moohr JW et al. Cooperative study sickle cell D. Blood 1998;91:288–294.
13. Embury SH. Microcirculation 2004;11:101–113.
14. Miller ST, Sleeper LA, Pegelow CH, Enos LE, Wang WC, Weiner SJ et al. New Engl J Med 2000;342:83–89.
15. Wethers DL. Am Family Physician 2000;62:1309–1314.
16. Stevens M, Maude G, Beckford M, Grandison Y, Mason K, Taylor B et al. Blood 1986;67:411–414.
17. Scothorn DJ, Price C, Schwartz D, Terrill C, Buchanan GR, Shurney W et al. J Pediatr 2002;140:348–354.
18. Hulbert ML, Scothorn DJ, Panepinto JA, Scott JP, Buchanan GR, Sarnaik S et al. J Pediatr 2006;149:710–712.
19. Garcia J, Anderson M. Crit Rev Neurobiol 1989;4:303–324.
20. Di Roio C, Jourdan C, Terrier A, Artru F. Ann Fr Anesth Reanim 1997;16:967–969.
21. Ganesan V, Prengler M, McShane M, Wade A, Kirkham F. Ann Neurol 2003;53:167–173.
22. Kirkham FJ, Prengler M, Hewes DKM, Ganesan V. J Child Neurol 2000;15:299–307.
23. Earley CJ, Kittner SJ, Feeser BR, Gardner J, Epstein A, Wozniak MA et al. Neurology 1998;51:169–176.
24. Melek I, Akgul F, Duman T, Yalcin F, Gali E. Tohoku J Exp Med 2006;209:135–140.
25. Mercuri E, Faundez J, Roberts I, Flora S, Bouza H, Cowan F et al. Eur J Pediatr 1995;154:150–156.
26. Prengler M, Pavlakis SG, Boyd S, Connelly A, Calamante F, Chong WK et al. Ann Neurol 2005;58:290–302.
27. Huttenlocher P, Moohr J, Johns L, Brown F. Pediatrics 1984;73:615–621.
28. Kirkham FJ, Calamante F, Bynevelt M, Gadian DG, Evans JPM, Cox TC et al. Ann Neurol 2001;49:477–485.
29. Kirkham FJ, Hewes DKM, Prengler M, Wade A, Lane R et al. Lancet 2001;357:1656–1659.
30. Vichinsky E, Neumayr L, Earles A, Williams R, Lennette E, Dean D et al. N Engl J Med 2000;342:1855–1865.
31. Lee KH, McKie VC, Sekul EA, Adams RJ, Nichols FT. J Pediatr Hematol Oncol 2002;24:585–588.
32. Wierenga KJJ, Serjeant BE, Serjeant GR. J Pediatr 2001;139:438–442.
33. Makani J, Meda E, Rwezaula S, Mwamtemi K, Thein SL, Williams T et al. Blood 2006;108:26B.
34. Strouse JJ, Hulbert ML, DeBaun MR, Jordan LC, Casella JF. Pediatrics 2006;118:1916–1924.
35. Coley S, Porter D, Calamante F, Chong W, Connelly A. Am J Neuroradiol 1999;20: 1507–1510.
36. Horton D, Ferriero D, Mentzer W. Pediatr Neurol 1995;12:77–80.
37. Gadian D, Calamante F, Kirkham F, Bynevelt M, Johnson C, Porter D et al. J Child Neurol 2000;15:279–283.
38. Sébire G, Tabarki B, Saunders D, Leroy I, Liesner R, Saint-Martin C et al. Brain 2005;128:477–489.

39. Powars D, Adams R, Nichols F, Milner P, Charache S, Sarnaik S. J Assoc Acad Minor Phys 1990;1:79–82.
40. Balkaran B, Char G, Morris J, Thomas P, Serjeant B, Serjeant G. J Pediatr 1992;120: 360–366.
41. Pegelow C, Macklin E, Moser F, Wang W, Bello J, Miller S et al. Blood 2002;99:3014–3018.
42. Jeffries BF, Lipper MH, Kishore PR. Surg Neurol 1980;14:291–295.
43. Aluoch J, Jacobs P. S Afr Med J 1996;86:982–983.
44. Al-Riyami A, Ebrahim G. J Trop Pediatr 2003;49(Suppl 1):i1–i20.
45. De D. Br J Nurs 2005;14:447–450.
46. Balgir R. J Assoc Physicians India 1996;44: 25–28.
47. Fattoum S. Tunis Med 2006;84:687–696.
48. Hamdallah M, Bhatia A. Lancet 1995;346: 707–708.
49. Kamble M, Chatruvedi P. Indian Pediatr 2000;37:391–396.
50. Williams T, Mwangi T, Wambua S, Alexander N, Kortok M, Snow R et al. J Infect Dis 2005;192:178–186.
51. Petrakis N, Wiesenfeld S, Sams B, Collen M, Cutler J, Siegelaub A. N Engl J Med 1970;282:767–770.
52. Scott R. N Engl J Med 1970;282:164–165.
53. Boyle EJ, Thompson C, Tyroler H. Arch Environ Health 1968;17:891–898.
54. Nietert P, Silverstein M, Abboud M. Pharmacoeconomics 2002;20:357–366.
55. Hicks E, Miller G, Horton R. Am J Public Health 1978;68:1135–1137.
56. Ashley-Koch A, Yang Q, Olney R. Am J Epidemiol 2000;151:839–845.
57. National Human Genome Research Institute. Learning about SCD. Available at: www.genome.gov/10001219.Accessed July 30, 2008.
58. Das L. Indian J Malariol 2000;37:34–38.
59. Rodríguez-Ojea Menéndez A, García de la Osa M. Rev Cubana Med Trop 1992;44:62–65.
60. deVeber G, Roach ES, Riela AR, Wiznitzer M. Semin Pediatr Neurol 2000;7:309–317.
61. Steen R, Emudianughe T, Hankins G, Wynn L, Wang W, Xiong X et al. Radiology 2003;228: 216–225.
62. Miller S, Macklin E, Pegelow C, Kinney T, Sleeper L, Bello J et al. J Pediatr 2001;139: 385–390.
63. Scothorn D, Price C, Schwartz D, Terrill C, Buchanan G, Shurney W et al. J Pediatr 2002;140:348–354.
64. Charache S, Terrin ML, Moore RD, Dover GJ, Barton FB, Eckert SV et al. N Engl J Med 1995;332:1317–1322.
65. Hankins JS, Ware RE, Rogers ZR, Wynn LW, Lane PA, Scott JP et al. Blood 2005;106: 2269–2275.
66. Gulbis B, Haberman D, Dufour D, Christophe C, Vermylen C, Kagambega F et al. Blood 2005;105:2685–2690.
67. Moser F, Miller S, Bello J, Pegelow C, Zimmerman R, Wang W et al. Am J Neuroradiol 1996;17:965–972.
68. Bernaudin F, Verlhac S, Fréard F, Roudot-Thoraval F, Benkerrou M, Thuret I et al. J Child Neurol 2000;15:333–343.
69. Kinney T, Sleeper L, Wang W, Zimmerman R, Pegelow C, Ohene-Frempong K et al. Pediatrics 1999;103:640–645.
70. Baldeweg T, Hogan A, Saunders D, Telfer P, Gadian D, Vargha-Khadem F et al. Ann Neurol 2006;59:662–672.
71. DeBaun M, Schatz J, Siegel M, Koby M, Craft S, Resar L et al. Neurology 1998;50:1678–1682.
72. Watkins K, Hewes D, Connelly A, Kendall B, Kingsley D, Evans J et al. Dev Med Child Neurol 1998;40:536–543.
73. Hogan A, Kirkham F, Prengler M, Telfer P, Lane R, Vargha-Khadem F et al. Br J Haematol 2006;132:99–107.
74. Wang W, Enos L, Gallagher D, Thompson R, Guarini L, Vichinsky E et al. J Pediatr 2001;139:391–397.
75. Schatz J, Buzan R. J Int Neuropsychol Soc 2006;12:24–33.
76. Davis H, Moore RJ, Gergen P. Public Health Rep 1997;112:40–43.
77. Wayne A, Schoenike S, Pegelow C. Blood 2000;96:2369–2372.
78. Bernaudin F, Verlhac S, Coïc L, Lesprit E, Brugières P et al. Pediatr Radiol 2005;35: 242–248.
79. Kidwell C, Chalela J, Saver J, Starkman S, Hill M, Demchuk A et al. JAMA 2004;292: 1823–1830.
80. Fiebach J, Schellinger P, Gass A, Kucinski T, Siebler M, Villringer A et al. Stroke 2004;35: 502–506.
81. Mokri B, Sundt TM Jr, Houser OW, Piepgras DG. Ann Neurol 1986;19:126–138.
82. de Bruijn SF, Stam J. Stroke 1999;30:481–483.
83. Adams R, Nichols F, McKie V, McKie K, Milner P et al. Neurology 1988;38:1012–1017.
84. Brambilla D, Miller S, Adams R. Pediatr Blood Cancer 2007;49:318–322.
85. Seibert J, Miller S, Kirby R, Becton D, James C, Glasier C et al. Radiology 1993;189: 457–466.
86. Switzer J, Hess D, Nichols F, Adams R. Lancet Neurol 2006;5(6):501–512.

87. Kirkham F. Nat Clin Pract Neurol 2007;3: 264–278.
88. Unit CEE. Stroke in Childhood: Clinical Guidelines for Diagnosis, Management and Rehabilitation. http://www.rcplondon.ac.uk/pubs/books/childstroke/childstroke_guidelines.pdf. London: Royal College of Physicians; online November 2004.
89. Winrow N, Melhem E. Neuroimaging Clin N Am 2003;13:185–196.
90. Lev MH, Farkas J, Gemmete JJ et al. Radiology 1999;213:150–155.
91. Lin K, Rapalino O, Law M, Babb JS, Siller KA, Pramanik BK. Am J Neuroradiol 2008;29: 931–936.
92. Katz DA, Marks MP, Napel SA, Bracci PM, Roberts SL. Radiology 1995;195:445–449.
93. Bash S, Villablanca JP, Jahan R, Duckwiler G, Tillis M, Kidwell C et al. Am J Neuroradiol 2005;26:1012–1021.
94. Beyer J, Platt A, Kinney T, Treadwell M. J Soc Pediatr Nurs 1999;4(2):61–73.
95. Pavlakis S, Bello J, Prohovnik I, Sutton M, Ince C, Mohr J et al. Ann Neurol 1988;23:125–130.
96. DeBaun M, Glauser T, Siegel M, Borders J, Lee B. J Pediatr Hematol Oncol 1995;17:29–33.
97. Marks MP, de Crespigny A, Lentz D, Enzmann DR, Albers GW et al. Radiology 1996;199: 403–408.
98. González RG, Schaefer PW, Buonanno FS, Schwamm LH, Budzik RF, Rordorf G et al. Radiology 1999;210:155–162.
99. Lövblad KO, Laubach HJ, Baird AE, Curtin F, Schlaug G, Edelman RR et al. Am J Neuroradiol 1998;19:1061–1066.
100. Mullins M, Schaefer P, Sorensen A, Halpern E, Ay H, He J et al. Radiology. 2002;224:353–360.
101. Lansberg M, Albers G, Beaulieu C, Marks M. Neurology 2000;54(8):1557–1561.
102. Lansberg M, Norbash A, Marks M, Tong D, Moseley M, Albers G. Arch Neurol 2000;57:1311–1316.
103. Rovira A, Grivé E, Alvarez-Sabin J. Eur Radiol 2005;15:416–426.
104. Kandeel AY, Zimmerman RA, Ohene-Frempong K. Neuroradiology 1996;38:409–416.
105. Gillams AR, McMahon L, Weinberg G, Carter AP. Pediatr Radiol 1998;28:283–287.
106. Korogi Y, Takahashi M, Nakagawa T et al. Am J Neuroradiol 1997;18:135–143.
107. Kielpinska K, Walecki J, Giedrojc J, Turowska A, Kordecki K. Acad Radiol 2002;9:283–289.
108. Srinivasan A, Goyal M, Al Azri F, Lum Ch. RadioGraphics 2006;26:S75–S95.
109. Adams R, Nichols F, Figueroa R, McKie V, Lott T. Stroke 1992;23:1073–1077.
110. Dawkins A, Evans A, Wattam J, Romanowski C, Connolly D et al. Neuroradiology 2007;49: 753–759.
111. Rao K, Lee M. Radiology 1983;147:600–601.
112. Coley S, Wild J, Wilkinson I, Griffiths P. Neuroradiology 2003;45:843–850.
113. Qureshi N, Lubin B, Walters M. Expert Opin Biol Ther 2006;6:1087–1098.
114. Verlhac S, Bernaudin F, Tortrat D, Brugieres P, Mage K, Gaston A. Pediatr Radiol 1995;25(Suppl 1):S14–S19.
115. Chooi W, Woodhouse N, Coley S, Griffiths P. Am J Neuroradiol 2004;25:1251–1255.
116. Kandeel A, Zimmerman R, Ohene-Frempong K. Neuroradiology 1996;38:409–416.
117. Reed W, Jagust W, Al-Mateen M, Vichinsky E. Am J Hematol 1999;60:268–272.
118. Powars D, Conti P, Wong W, Groncy P, Hyman C, Smith E et al. Blood 1999;93:71–79.
119. Rodgers GP, Clark CM, Larson SM, Rapoport SI, Nienhuis AW et al. Arch Neurol 1988;45: 78–82.
120. Herold S, Brozovic M, Gibbs J, Lammertsma AA, Leenders KL, Carr D et al. Stroke 1986;17:692–698.
121. Adams R, McKie V, Hsu L, Files B, Vichinsky E, Pegelow C et al. N Engl J Med 1998;339:5–11.
122. Adams R, Brambilla D, Granger S, Gallagher D, Vichinsky E, Abboud M et al. Blood 2004;103:3689–3694.
123. Russell M, Goldberg H, Hodson A, Kim H, Halus J, Reivich M et al. Blood 1984;63:162–169.
124. Pegelow CH, Adams RJ, McKie V, Abboud M, Berman B, Miller ST et al. J Pediatr 1995;126:896–899.
125. Wilimas J, Goff J, Anderson HJ, Langston J, Thompson E. J Pediatr 1980;96:205–208.
126. Ausavarungnirun P, Sabio H, Kim J, Tegeler CH. J Neuroimaging 2006;16:311–317.
127. Adams R, Pavlakis S, Roach E. Ann Neurol 2003;54:559–563.
128. Krejza J, Rudzinski W, Pawlak M, Tomaszewski M, Ichord R, Kwiatkowski J et al. Am J Neuroradiol 2007;28:1613–1618.
129. Adams R. J Pediatr Hematol Oncol 1996;18: 331–334.
130. National Heart L, and Blood Insititute. Clinical alert: periodic transfusions lower stroke risk in children with sickle cell anemia. http://www.nim.nih.gov/databases/alerts/sickle97.html.
131. Lee M, Piomelli S, Granger S, Miller S, Harkness S, Brambilla D et al. Blood 2006;108: 847–852.
132. Bulas D. Pediatr Radiol 2005;35:235–241.
133. Fullerton H, Adams R, Zhao S, Johnston S. Blood 2004;104:336–339.

134. Trial. http://www.clinicaltrials.gov/ct/show/NCT00072761 . CgWsSCIM-CC.
135. http://www.clinicaltrials.gov/ct/show/NCT00122980. CgWsSwTCtHS.
136. Jones A, Seibert J, Nichols F, Kinder D, Cox K, Luden J et al. Pediatr Radiol 2001;31:461–469.
137. Malouf AJ, Hamrick-Turner J, Doherty M, Dhillon G, Iyer R, Smith M. Radiology 2001;219:359–365.
138. McCarville M, Li C, Xiong X, Wang W. Am J Roentgenol 2004;183:1117–1122.
139. Riebel T, Kebelmann-Betzing C, Götze R, Overberg U. Eur Radiol 2003;13:563–570.
140. Lowe L, Bulas D. Pediatr Radiol 2005;35:54–65.
141. Abboud M, Cure J, Granger S, Gallagher D, Hsu L, Wang W et al. Blood 2004;103:2822–2826.
142. Wang W, Gallagher D, Pegelow C, Wright E, Vichinsky E, Abboud M et al. J Pediatr Hematol Oncol 2000;22:335–339.
143. Wiznitzer M, Ruggieri P, Masaryk T, Ross J, Modic M, Berman B. J Pediatr 1990;117:551–555.
144. Gillams A, McMahon L, Weinberg G, Carter A. Pediatr Radiol 1998;28:283–287.
145. Kirkham F, Lerner N, Noetzel M, DeBaun M, Datta A, Rees D et al. Pediatr Neurol 2006;34:450–458.
146. Dobson S, Holden K, Nietert P, Cure J, Laver J, Disco D et al. Blood 2002;99:3144–3150.
147. Ganesan V, Prengler M, Wade A, Kirkham F. Circulation 2006;114:2170–2177.
148. Woodard P, Helton K, Khan R, Hale G, Phipps S, Wang W et al. Br J Haematol 2005;129:550–552.
149. Kirkham F, DeBaun M. Curr Treat Options Neurol 2004;6:357–375.
150. Fryer R, Anderson R, Chiriboga C, Feldstein N. Pediatr Neurol 2003;29:124–130.
151. Walters M, Storb R, Patience M, Leisenring W, Taylor T, Sanders J et al. Blood 2000;95:1918–1924.
152. Steen R, Helton K, Horwitz E, Benaim E, Thompson S, Bowman L et al. Ann Neurol 2001;49:222–229.
153. Adams R, Brambilla D. N Engl J Med 2005;353:2769–2778.
154. Minniti C, Gidvani V, Bulas D, Brown W, Vezina G, Driscoll M. J Pediatr Hematol Oncol 2004;26:626–630.
155. Mazumdar M, Heeney M, Sox C, Lieu T. Pediatrics 2007;120:e1107–e1116.
156. Adams HP Jr, del Zoppo G, Alberts MJ, Bhatt DL, Brass L, Furlan A et al.; American Heart Association; American Stroke Association Stroke Council; Clinical Cardiology Council; Cardiovascular Radiology and Intervention Council; Atherosclerotic Peripheral Vascular Disease and Quality of Care Outcomes in Research Interdisciplinary Working Groups. Stroke 2007;38:1655–1711.
157. Powars D, Wilson B, Imbus C, Pegelow C, Allen J. Am J Med 1978;65:461–471.
158. Diggs LW, Brookoff D. South Med J 1993;86:377–379.
159. Royal JE, Seeler RA. Lancet 1978;2(8101):1207.
160. Stockman JA, Nigro MA, Mishkin MM, Oski FA. N Engl J Med 1972;287:846–849.
161. Henderson JN, Noetzel MJ, McKinstry RC, White DA, Armstrong M et al. Blood 2003;101:415–419.
162. Wardlaw JM, Keir SL, Seymour J, Lewis S, Sandercock PA, Dennis MS et al. Health Technol Assess 2004;8(iii, ix–x):1–180.
163. Singer OC, Sitzer M, du Mesnil de Rochemont R, Neumann-Haefelin T. Neurology 2004;62:1848–1849.
164. Wardlaw JM, White PM. Brain 2000;123:205–221.
165. Chappell ET, Moure FC, Good MC. Neurosurgery 2003;52:624–631.
166. Willinsky RA, Taylor SM, TerBrugge K et al. Radiology 2003;227:522–528.
167. Burger IM et al. Stroke 2006;37;2535–2539.
168. Lysakowski C, Walder B, Costanza MC, Tramèr MR. Stroke 2001;32:2292–2298.

6

Imaging of Hypoxic-Ischemic Encephalopathy in the Full-Term Neonate

Amit M. Mathur and Robert C. McKinstry

Issues

I. What are the clinical features of neonatal hypoxic ischemic encephalopathy (HIE)?
II. What is the optimal time and what are the ideal MRI sequences to image neonatal HIE?
III. Why should infants with neonatal encephalopathy be imaged?
IV. Does the pattern of brain injury on MR help predict outcomes in neonatal HIE?
V. Does cooling alter the pattern of brain injury?

Key Points

- Clinical neurological evaluation of the neonate with depression and/or encephalopathy is nonspecific. The neonatal course may suggest hypoxic-ischemic insult but the clinical examination cannot fully evaluate the extent or severity of the brain injury (moderate evidence).
- The role of ultrasound (US) and computed tomography (CT) in the evaluation of hypoxic-ischemic brain injury at term is limited. Ultrasound could be used to evaluate neonates in the neonatal ICU if the patient is too sick to travel to the MR scanner. CT can be used to assess for traumatic brain injury if there is a history of complicated delivery. CT also plays a role in the acute management of suspected acute intracranial hemorrhage. However, CT and US fall short of MR imaging in the evaluation of the parenchymal changes of hypoxic-ischemic injury (moderate evidence).
- Conventional MR imaging with T1-weighted, T2-weighted and T2*-weighted imaging is more sensitive than US and at least as sensitive as CT for HIE (moderate evidence).

A.M. Mathur (✉)
Department of Pediatrics/Newborn Medicine, Washington University School of Medicine, St. Louis Children's Hospital, St. Louis, MO 63110, USA
e-mail: mathur_a@kids.wustl.edu

L.S. Medina et al. (eds.), *Evidence-Based Imaging in Pediatrics*,
DOI 10.1007/978-1-4419-0922-0_6,

- Diffusion-weighted imaging (DWI) is complementary to conventional MR imaging, improving sensitivity to ischemic injuries during the first week after the ischemic insult (moderate to strong evidence).
- MR spectroscopy (MRS) may detect injuries in the first week after the insult that are otherwise occult. Elevated lactate and decreased NAA predict a poor clinical outcome (moderate to strong evidence).
- FLAIR and contrast-enhanced imaging sequences do not improve sensitivity of the MR exam beyond the other conventional sequences, DWI and MRS (moderate evidence).
- MR imaging holds promise for evaluating prognosis, triaging patients for neuroprotective therapies, and serving as early predication of therapeutic efficacy (limited to moderate evidence).

Definition and Pathophysiology

Hypoxic-ischemic brain injury in term neonates is often preceded by a significant obstetric history (uterine rupture, abruption, cord prolapse, etc.), evidence of impaired placental gas exchange (metabolic acidosis on the cord gas), poor adaptation at birth needing resuscitation (low Apgar scores), presence or development of encephalopathy, and evidence of other end organ injury (e.g., liver or kidney) (1).

Standard of care for this condition has been restricted to maintaining the respiratory/metabolic milieu, keeping the infant normothermic, and treating seizures when they arise. A review of recent multicenter trials has shown improved survival in moderate and severe encephalopathy with both head cooling and body cooling (2).

Recent evidence from clinical and experimental models has demonstrated a biphasic pattern of injury following reversal of the hypoxic-ischemia process (3–5). It has been recognized that the physiologic consequences of hypoxic-ischemia evolve over hours to days. The hypoxic-ischemic cascade results in two phases of energy failure that culminate in brain injury. The "primary" energy failure occurs at the time of the hypoxic-ischemic insult itself, resulting in depletion of high-energy metabolites (ATP and phosphocreatine), progressive depolarization of cells, severe cytotoxic edema, tissue acidosis, and extracellular accumulation of excitatory amino acids due to a failure of reuptake by astroglial cells and also excessive release due to depolarization (6). Loss of ionic homeostasis results in an influx of calcium into cells, triggering a number of destructive pathways by activating lipases, proteases, and endonucleases (7). Once the cerebral blood flow and oxygenation are re-established, the initial metabolic impairments resolve over 30–60 min. This is followed by a latent phase after which there may be complete recovery or development of a secondary phase. Whether injury reversal occurs depends on several factors including the severity of the primary injury, body temperature, substrate availability, preconditioning, and simultaneous disease processes (1). The "secondary" phase of energy failure starts about 6–15 h later and extends over several hours to days. This phase is clinically associated with seizures and a worsening neurological examination. There is secondary cytotoxic edema, excitotoxic amino acid accumulation, mitochondrial failure, altered growth factors and protein synthesis, and apoptotic cell death (8–10).

In term infants with moderate to severe encephalopathy, MR spectroscopy results are consistent with this model of biphasic injury. MR spectroscopy demonstrates normal oxidative metabolism shortly after birth followed by a secondary phase of energy failure. The severity of this secondary phase correlates with neurodevelopmental outcome in these infants (2).

Epidemiology

Neonatal encephalopathy secondary to hypoxic-ischemic injury (HIE) affects 1.6 per 1,000 live term-born infants (American College of Obstetricians and Gynecologists

2003) (11). Perinatal HIE is but one subset of neonatal encephalopathy; other subsets include those resulting from prenatal stroke, infection, cerebral malformation, genetic disorders, and many other conditions. Although there are longitudinal studies that have shown a decrease in the incidence of perinatal HIE in the past few decades, this has not been consistent across different countries. In the United States, the incidence of perinatal HIE in the state of California declined from 14.8 per 1,000 live births in 1991 to 1.3 per 1,000 live births in 2,000 (12). A similar decline was seen in a British hospital from 7.7 per 1,000 live births in the 1970s to 1.9 per 1,000 in the mid-1990s (13, 14). However, a Swedish report showed a slight increase in the incidence of birth asphyxia and neonatal encephalopathy between 1985 and 1991 (15). This difference could reflect a trend in moving away from using the diagnosis of "birth asphyxia" to currently used terminology of "perinatal hypoxic-ischemic encephalopathy" or "neonatal encephalopathy." Perinatal HIE carries an appreciable burden of illness and has a mortality of 15–20% in the newborn period. In addition, 25% of survivors have permanent neurological deficits such as cerebral palsy or mental retardation (16).

Overall Cost to Society

The long-term consequence of neonatal HIE is most commonly cerebral palsy, a nonprogressive disorder of the developing brain principally affecting the motor system. Cerebral palsy affects 2–3 per 1,000 newborns, with a conservative estimate of its impact on society being about $5 billion per year (17). Cerebral palsy can be associated with epilepsy and abnormalities of speech, vision, and intellect. The impact of diseases affecting the newborn is much greater than diseases that affect the elderly because of the burden of disease when one considers mortality, years of life lost, and years of productive life lost. Lifetime costs for all patients with cerebral palsy are estimated to total $11.5 billion (17).

Goals

When a neonate is encephalopathic and hypoxic-ischemic injury is suspected, the goals of the MR imaging study are the following:

- Establish whether the brain development has progressed normally for gestational age. Malformations of cortical development or other significant congenital brain malformations could present with a similar clinical picture.
- Establish timing of injury to assess whether there is evidence for in utero brain injury that preceded events during labor and delivery. Subacute and/or chronic brain injury detected on conventional MR imaging in the first few days of life is likely the result of an unfavorable maternal–fetal milieu rather than HIE related to events during the birthing process.
- Differentiate between the various patterns of HIE in the newborn, and establish the extent and severity of the brain injury. With this information, the NICU team can begin to analyze the potential etiologies (e.g., hypercoaguable state associated with sinus venous thrombosis) and take appropriate measures to minimize further injury.
- Help to establish prognosis for the family and caregivers. Armed with the prognostic information, an appropriate care plan can be developed and early intervention can be initiated to maximize the child's neurological and cognitive potential.

Methodology

The authors queried the MEDLINE database using PubMed (National Library of Medicine, Bethesda, MD) through a combination of the web-based interface (http://www.ncbi.nlm.nih.gov/sites/entrez) and searches performed using Endnote (Thomson Reuters, New York). Initial imaging queries were generated using terms including *magnetic resonance imaging* and *MRI,* limiting the searches with *English, Human,* and *Newborn: birth–1 month*. Terms *hypoxia, ischemia, hypoxic-ischemic, hypoxia-ischemia, HIE,* and *encephalopathy* were added to evaluate the role of MR imaging in the evaluation of the encephalopathic neonate. Specific modifiers included *outcome, prediction,* and *hypothermia*. The role of individual MR sequences was evaluated with the terms *diffusion, perfusion, spectroscopy, FLAIR, T2*, susceptibility, hemorrhage, functional MRI,* and *fMRI.* To expand the

search, each query generated by the PubMed web interface was expanded by following links to related articles, which were then examined for relevance. No limits were placed on the date range of the PubMed search. Therefore, the queries spanned dates from 1950 to June 2008.

Discussion of Issues

I. What Are the Clinical Features of Neonatal HIE?

Summary of Evidence: Clinical neurological evaluation of the neonate with depression and/or encephalopathy is nonspecific. The neonatal course may suggest a hypoxic-ischemic insult, but the clinical examination may not fully reveal the extent or severity of the brain injury (moderate evidence).

Supporting Evidence: The neurological syndrome that accompanies significant neonatal HIE is essential to the diagnosis. The three cardinal features that point to the perinatal origin of HIE include evidence of fetal distress (abnormal fetal heart rate tracing, meconium-stained amniotic fluid), depression at birth, and an overt neonatal neurological syndrome in the first several hours to days of life. The severity of neonatal encephalopathy is assessed using criteria described by Sarnat and Sarnat and modified by Finer (16) (Table 6.1).

The diagnosis of neonatal HIE is based on a detailed history of pregnancy, labor, and resuscitation including fetal acid–base status, neurological examination, metabolic parameters such as hypoglycemia, hyponatremia, hypocalcemia, hypoxemia, lactate level, and acidosis. Non-HIE causes of neonatal encephalopathy such as meningitis or metabolic disorders should be considered (1).

In addition to the history and physical examination, supplementary evaluations including electroencephalography (EEG) and neuroimaging are very important (19).

MR imaging is the most accurate imaging modality in the evaluation of neonatal encephalopathy to assess the timing, extent, and severity of injury (19, 20, 21). Although the advantage with MRI of superlative anatomical detail is tempered by the need to study the infant within a magnet, away from the neonatal intensive care unit (NICU) the information obtained on MRI is superior to other neuroimaging modalities (19).

II. What Is the Optimal Time and What Are the Ideal MRI Sequences to Image Neonatal HIE?

Summary of Evidence: Diffusion-weighted imaging (DWI) is complementary to conventional MR imaging, improving sensitivity to ischemic injuries during the first week after the ischemic insult (moderate to strong evidence).

MR spectroscopy (MRS) may detect injuries in the first week after the insult that are otherwise occult. Elevated lactate and decreased NAA predict a poor clinical outcome (moderate to strong evidence).

FLAIR and contrast-enhanced imaging sequences do not improve sensitivity of the MR exam beyond the other conventional sequences, DWI and MRS (moderate evidence).

See Table 6.2 for a summary of MR imaging evaluation of evolving hypoxic-ischemic injury.

Supporting Evidence: Ideally, neonates with perinatal HIE should have two MR scans. The first scan is optimally performed within 24–48 h of life. Proton spectroscopy is the most sensitive MR technique at this time to identify brain injury, showing elevation of lactate and, in severe cases, a reduction in *n*-acetyl aspartate (NAA) in the cerebral cortex more so than the deep nuclear gray matter (22, 23). MRS detected abnormalities in the deep nuclear gray matter in all six patients on whom it was performed versus conventional T1 and T2 images, which only showed mild edema in 3/7 patients [24]. Diffusion-weighted imaging (DWI) can give false-negative results in up to 30% of infants if performed in the first few hours of delivery (25) and will underestimate the extent of injury if performed in the first 24 h of life. Sensitivity is increased by analyzing apparent diffusion coefficient (ADC) values (26), which can be abnormal even when

DWI does not show abnormalities. An early scan may help guide clinicians in deciding the timing, severity, and extent of injury. Early changes on conventional T1 and T2 images with negative diffusion are likely to indicate an onset of injury remote from birth. This information, along with data from electroencephalographic studies and the clinical course of the infant, is vital for both parents of these infants and neonatologists in deciding the plan of care.

The second scan should be undertaken at 7–10 days of life. At this time, diffusion imaging, T2-weighted spin echo images with long repetition times, and inversion recovery/spoiled gradient echo T1-weighted sequences are preferred for detecting brain injury (27). Affected cortex appears hyperintense on T2-weighted images. T1-weighted images show areas of low signal intensity in the involved cortex. The most obvious finding is the loss of gray–white matter distinction. Injury over the high convexities of the cortex is best visualized in coronal and sagittal planes. An exception is in perirolandic injury where T1-weighted images may show hyperintense signal in the cortex (Fig. 6.1 panel c). The pattern of diffusion abnormalities changes over time. Initial diffusion abnormalities in the deep nuclear gray matter may pseudonormalize by the end of the first week, and new diffusion restriction may become apparent in the corpus callosum (Fig. 6.1) or the posterior limb of the internal capsule (PLIC). This may represent Wallerian degeneration or injury in the "secondary phase" of the cascade of brain injury (28, 29, 30, 31). Some studies have shown that even though ADC values in affected areas may pseudonormalize by the end of the first week (25, 32), FA values remain abnormal (33).

If only one MR scan can be obtained, a scan at 3–4 days of life can help establish timing, extent, and severity of the injury. Specifically, the DWI and ADC will show the maximum deflection from normal neonatal values, the lactate peak of the MR spectrum will remain elevated, and the conventional MR sequences will be abnormal. A single scan at the end of the first week will delineate the injury but will make timing difficult or impossible.

T1- and T2-weighted imaging is a standard part of every MR protocol as they are designed to image the intrinsic relaxation properties of brain water. MR imaging is recommended, when evaluated against cranial sonography and computed tomography, for detection of brain injury in the term newborn (34).

T2*-weighted images are designed to detect small fluctuations in the local magnetic field due to susceptibility effects associated with hemorrhage and/or calcification. Presently, three T2*-weighted options are available: gradient echo (GRE) imaging, echo planar imaging (EPI), and susceptibility-weighted imaging (SWI). EPI has the benefit of extremely fast scan times, followed by GRE and SWI. In terms of sensitivity to small amounts of cerebral hemorrhage, there is a moderate evidence (Level 2) study that SWI is the superior technique (35, 36). However, SWI is time consuming and may not be suitable for evaluation of an unsedated newborn. A moderate evidence (Level 2) study has shown that GRE is more sensitive in the posterior fossa, while both GRE and EPI performed well for detection of supratentorial hemorrhage (37).

The value of FLAIR T2-weighted and contrast-enhanced sequences in the newborn period is a matter of some debate in the literature. There is no strong evidence (level 1) that directly addresses the value of FLAIR. Recent evidence from moderate evidence (Level 2) study directly addressed the relative value of T1, T2, FLAIR, DWI, and contrast-enhanced images in the evaluation of HIE (38). These investigators found that adding FLAIR and contrast-enhanced images to T1, T2, and DWI did not improve detection of HIE. An earlier limited evidence (Level 3) study concluded similarly that FLAIR did not improve detection of HIE, largely due to hypomyelination of the newborn brain (39).

Diffusion MR imaging has received the most attention for the detection HIE in the term neonate (22, 25, 26, 40–52) because of its established utility in adult stroke. Diffusion imaging complements T1-weighted and T2-weighted imaging for detection of the acute injury (Fig. 6.2), the timing of the insult (25, 48), and the associated secondary injury pattern (29–31). Some studies have shown that DWI and ADC during the first week of life are less sensitive than conventional imaging (42, 47), with reported sensitivity as low as 47%.

Others report high sensitivity (100%) with low specificity (20%) (41). However, ADC changes dramatically over the first 2 weeks following an injury (25, 32, 46, 53), with maximum restriction occurring at day 3–4 of life (25) and pseudonormalization of the ADC at the end of the first week (25, 33). Therefore, sensitivity and specificity will be highly dependent on the timing of the exam relative to the injury. At this point, the imaging "gold standard" for HIE remains the conventional MR sequences obtained at 7–10 days of life.

III. Why Should Infants with Neonatal Encephalopathy Be Imaged?

Summary of Evidence: The clinical neurological examination in term neonates with HIE can be subjective and non-specific. Early diagnosis of brain injury is important for both neuroprotective interventions and prognosis. Neuroimaging plays an essential role in the assessment of brain injury in these patients by helping establish the timing and likely cause of injury and the expected neurological outcome (strong evidence).

While sonography (US), computerized tomography (CT), and magnetic resonance imaging (MRI) have all been used in imaging infants with HIE, MRI has emerged as the imaging modality of choice because of lack of ionizing radiation exposure, high inter-observer reliability, and high predictive value of neurodevelopmental outcome (moderate to limited evidence).

Unsedated MRI examination is possible in neonates. In addition to conventional T1- and T2-weighted MR images, MR spectroscopy and diffusion-weighted imaging (with apparent diffusion coefficient maps for quantitative analysis) are needed to establish timing and extent of brain injury (strong evidence).

Supporting Evidence: The central nervous system (CNS) of the neonate may be injured by a number of different mechanisms including hemorrhage, hypoxic-ischemia, hypoglycemia, inborn errors of metabolism, hyperbilirubinemia, and neonatal infections. Neurological assessment of the affected neonate includes assessment for encephalopathy, cranial nerve function, motor function (tone, posture, movement, power, and reflexes), primitive reflexes, and sensory examination. However, because of the immaturity of the CNS in the neonate, this clinical assessment is imprecise. Although it may alert the examiner to the presence or absence of injury, the precise cause of injury and the severity, extent, and location of injury are difficult to establish on clinical grounds alone. Neuroimaging plays a critical role in the assessment of brain injury in these patients (20, 21).

The role of ultrasound (US) and computed tomography in the evaluation of hypoxic-ischemic brain injury at term is limited. Although sonography was shown to be useful in evaluating neonatal HIE with good accuracy (91%) and sensitivity (100%) and but poor specificity (33%) when compared prospectively to MRI in a single series (54), its use has not been routinely recommended in evaluation of neonatal HIE because it is operator dependent and has poor inter-observer reliability (34, 55) (moderate evidence).

CT can be used to assess for traumatic brain injury (fracture or hemorrhage) if there is a history of complicated delivery. However, in a head to head study (56), MRI had better inter-observer agreement and demonstrated findings of HIE as well as CT. Further, MRI eliminates the use of ionizing radiation, a putative cause of malignancy (moderate evidence).

MRI examination is considered an established tool in the evaluation of term neonates with encephalopathy (57). It is the most sensitive and specific technique for examining infants with HIE (58) and is a good predictor of neurodevelopmental outcome (34, 59).

Recent advances in MR imaging of neonates have included the availability of MR-compatible incubator and ventilator systems that can provide a stable environment for the often critically ill and unstable neonate (60). Neonates can be safely and successfully imaged without sedation using standard monitoring with a MR compatible pulse-oximeter and a cardio-respiratory monitor (61). In addition, custom-built coils have dramatically improved signal-to-noise ratios (SNR). MR diffusion imaging including diffusion tensor imaging (DTI), diffusion-weighted imaging (DWI), and fractional anisotropy (FA) provide valuable insights about timing of injury (62, 63, 64),

while MR spectroscopy (MRS) helps evaluate the metabolic state in the injured brain (65, 66, 67) (34). Emerging MR techniques include neonatal perfusion imaging, which non-invasively measures cerebral blood flow, and functional MR imaging, which evaluates brain function and connectivity.

Diffusion-weighted imaging (DWI) is complementary to conventional MR imaging, improving sensitivity to ischemic injuries during the first week after the ischemic insult (62–64).

IV. Does the Pattern of Brain Injury on MR Help Predict Outcome in Neonatal HIE?

Summary of Evidence: While it is accepted that the risk of an abnormal neurodevelopmental outcome increases with the severity of the injury, the pattern of injury on MRI also conveys important prognostic information. In particular, the basal ganglia–thalamus and watershed patterns of injury are associated with impairments in different developmental domains. The basal ganglia–thalamus predominant pattern or abnormal signal intensity in the posterior limb of the internal capsule on MRI is associated with severely impaired motor and cognitive outcomes. Given the frequent occurrence of cerebral watershed injury with the basal ganglia–thalamus predominant pattern, cognitive deficits may result from damage to areas outside the deep gray nuclei themselves. By contrast, newborns with the watershed pattern have predominantly cognitive impairments that often occur without functional motor deficits (moderate evidence).

Supporting Evidence: Selective neuronal necrosis is the most common form of injury following perinatal HIE and is prevalent in almost all cases (16). The distribution of the lesion depends on the severity and duration of the hypoxia-ischemia.

In *severe and prolonged insults*, *diffuse neuronal injury* is seen in the cerebral cortex, hippocampus, deep nuclear gray matter, brainstem, cerebellum, and spinal cord (16, 68). This lesion carries a high mortality (35%) (68), and survivors (65%) are likely to have quadriparesis, severe seizure disorder (10–30%) (19), choreoathetosis, microcephaly, and mental retardation (68).

There is often abnormal signal intensity and restricted diffusion in the posterior limb of the internal capsule (PLIC). Abnormalities in the PLIC are excellent predictors of abnormal outcome in term infants with HIE (59, 69). The internal capsule is an area of great importance in the evaluation of the brain of the newborn infant. It myelinates around term age and is therefore a marker of maturation that is readily identifiable on MRI scans. Absent or abnormal myelination within the posterior portion of the internal capsule is found in many metabolic disorders; it is also a strong predictor of normal and abnormal motor outcome in HIE (28). The absence of normal signal in the PLIC was shown to predict an abnormal outcome with a sensitivity of 0.90, a specificity of 1.0, a positive predictive value of 1.0, and a negative predictive value of 0.87. The test correctly predicted motor outcome in 93% of infants with moderate HIE (59) in more detail correlation of these predictors with outcome.

Prolonged partial insults cause a cerebral cortical-deep nuclear neuronal injury. The affected area includes the parasagittal and periRolandic cortex, hippocampus, basal ganglia, and thalamus. Brainstem involvement may also occur. This pattern is seen in 35–65% of cases of HIE (70). These lesions are associated with predominantly motor deficits with tone and posture abnormalities. Choreoathetoid movements may become apparent between 1 and 4 years of life in these infants (19). Intellectual function is relatively preserved in infants with later onset disease (71). Infants with involvement of the thalamus have associated cognitive delay (72).

Severe and abrupt insults such as those following placental abruption, cord prolapse, or uterine rupture result in a pattern of injury that involves predominantly *deep nuclear gray matter and brainstem.* All surviving infants are likely to develop motor disability in the form of cerebral palsy. Cognitive impairment depends on associated cortical injury that may overlap in 50% of these cases (68, 73). Twenty to thirty percent of infants in this group may require gastrostomy feeding tubes (74).

Parasagittal cerebral injury is another pattern that is predominantly an ischemic lesion in

term infants. The lesions are usually bilateral and involve the cerebral cortex and subcortical white matter in the "watershed areas" between major cerebral arteries (16). This lesion is seen in the setting of *acute hypotension* and is seen in about 45% of surviving infants with HIE (75). It results in spastic quadriparesis along with specific cognitive deficits such as disproportionate disturbance in the development of language or of visual–spatial abilities or both (76).

V. Does Cooling Alter the Pattern of Brain Injury?

Summary of Evidence: Therapeutic hypothermia (whole body or head) is an accepted treatment modality in infants with HIE. It is unclear as to what impact hypothermia has on MR images in these infants (limited evidence).

Supporting Evidence: Two studies have looked at MR changes in infants who underwent therapeutic hypothermia for perinatal HIE. Rutherford et al. looked at MR imaging in 14 infants with HIE who underwent head cooling, 20 infants with body cooling, and 52 noncooled infants with similar severity of HIE (77). They found that both modes of hypothermia were associated with a decrease in basal ganglia and thalamic lesions, which are predictive of abnormal outcome.

Inder et al. analyzed a group of 26 infants with HIE. Infants were randomized to either body cooling or normothermia (78). The hypothermia group had less cortical gray matter signal abnormality on MR imaging. They postulated that there might be differing regional benefits from systemic cooling. Although the studies are difficult to interpret because the initial distribution of injury is not known, there does appear to be a decrease in the amount of injury.

Take Home Tables

Table 6.1 presents grading of neonatal encephalopathy. Table 6.2 discusses MR imaging of evolving hypoxic-ischemic injury.

Table 6.1. Grading of neonatal encephalopathy

Encephalopathy grade	Clinical features
Mild or Stage 1	• Hyperalertness, decreased sleep • Uninhibited reflexes, excessive reaction to stimuli, weak suck but normal tone • Sympathetic overactivity—eyes wide open, decreased blinking, mydriasis • Duration less than 24 h
Moderate or Stage 2	• Lethargy or obtundation (i.e., delayed and incomplete response sensory stimuli), mild hypotonia • Cortical thumbs, suppressed primitive reflexes • Seizures, hypotonia, lethargy • Parasympathetic activation with miosis (even on dim light), heart rate less than 120 beats per minute, increased peristalsis, and copious secretions
Severe or Stage 3	• Stupor response only to strong stimuli with withdrawal or decerebrate posturing only • Rarely coma, severe hypotonia (i.e., flaccidity) • Suppression of deep tendon and primitive (i.e., Moro, tonic neck, oculocephalic, suck) reflexes • Suppression of brainstem reflexes (corneal or gag) • Clinical seizures less frequent than Stage 2

Modified with permission from Sarnat and Sarnat (18).

Table 6.2. MR imaging evaluation of evolving hypoxic-ischemic injury

MR sequence	Day 1	Days 3–4	Day 7	Year 2
T1	–	+	+	±
T2	–	–	+	+
FLAIR	–	–	–	+
DWI/ADC	±	+	–	–
MRS	+	+	±	–

Plus signs indicate that the test is a specific indicator at the time point. Minus signs indicate that the test is insensitive at the specified time point. If inconsistent results have been reported the plus/minus designation is shown.

Imaging Case Studies

Case 1

Figure 6.1 presents images of a neonate with encephalopathy and seizures.

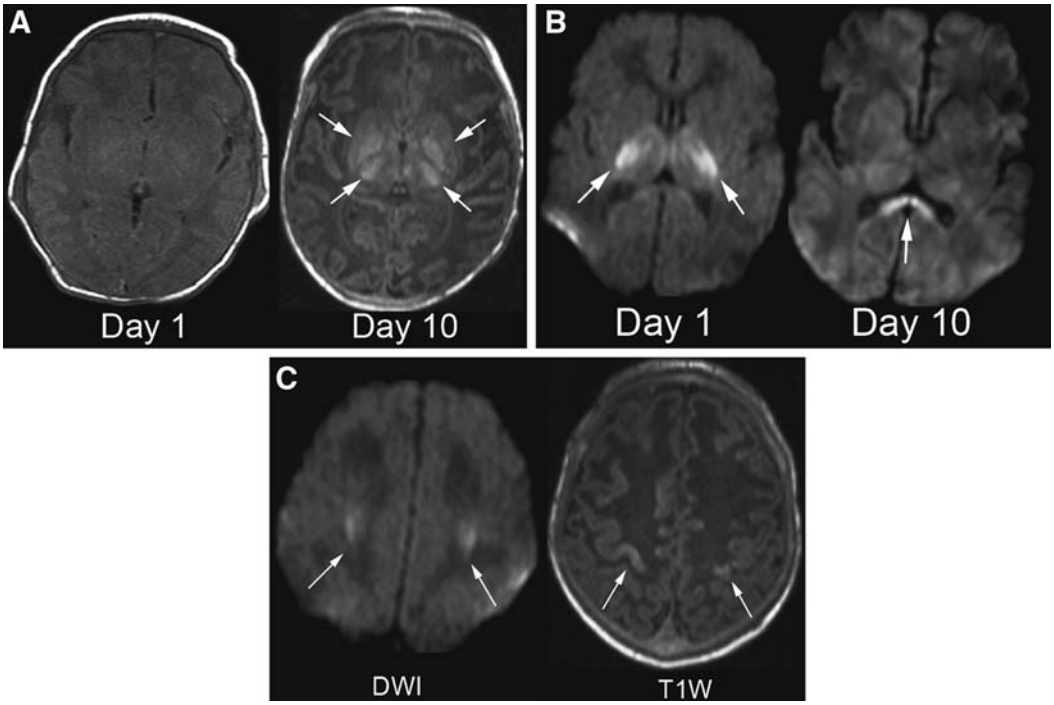

Figure 6.1. A: Neonate with encephalopathy and seizures. T1-weighted images on day 1 of life (*left*) are unremarkable. By day 10, the T1-weighted images demonstrate the classic pattern of deep nuclear gray matter injury (*arrows*). This illustrates that T1-weighted and T2-weighted (not shown) imaging alone are not sensitive to the earliest changes of HIE. B: DWI on day 1 (*left*) shows reduced diffusion in the posterior limb of the internal capsule bilaterally and the adjacent ventrolateral thalami. By day 10 (*right*), those regions have pseudonormalized on DWI and there is early Wallerian degeneration of the splenium of the corpus callosum (*arrow*). C: DWI (*left*) on DOL 1 shows reduced diffusion in the distribution of the corticospinal tracts bilaterally (*arrows*). The T1-weighted images on day 10 show hyperintensity of the cortex bordering the central sulcus. At 1 month, the child was doing well with no further seizures or obvious deficits, which reinforce that MR imaging must be correlated with long-term outcome to assess its true utility. This case illustrates the variable sensitivity of MR by pulse sequence and time after the injury. In addition, the Wallerian degeneration of the splenium of the corpus callosum without overt parieto-occipital injury suggests that not all of the primary injury is evident.

Case 2

Figure 6.2 presents images of a neonate with encephalopathy on DOL 2.

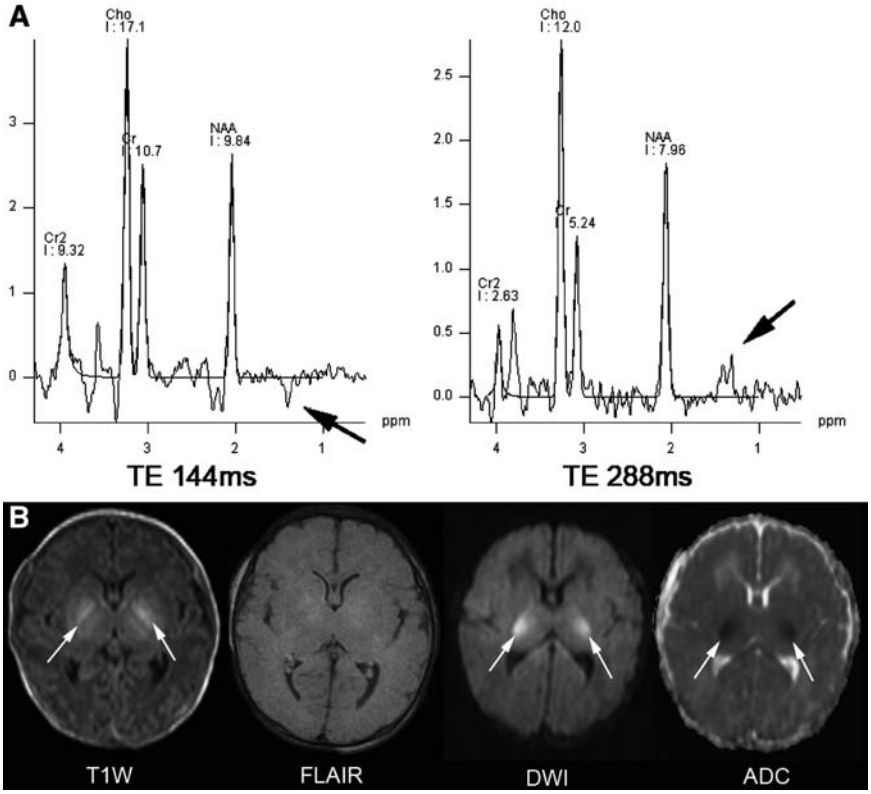

Figure 6.2. **A**: Neonate with encephalopathy on day of life 2. Single voxel PRESS proton MR spectroscopy from the left deep nuclear gray matter region with TE 144 ms (*left*) and TE 288 ms (*right*) shows the characteristic inversion of the lactate doublet at 1.33 ppm. The degree of elevation of the lactate peak is inversely correlated with clinical outcome. **B**: T1-weighted images (*far left*) show subtle abnormality in the deep nuclear gray matter region (*arrows*). FLAIR fails to show the abnormality. DWI and ADC show restricted diffusion in the thalami bilaterally. Despite a neonatal ICU course marked by seizures and abnormal MR imaging and spectroscopy, the neurodevelopment outcome (Bayley Scales of Infant Development) assessed at 1 year of age is within normal limits. Again, the neonatal imaging predicts a poor outcome, yet the clinical assessment is normal 1 year later. If MR is to serve as a predictor of outcome, long-term clinical follow-up studies will be needed to establish the positive and negative predictive values of MR imaging in the newborn period.

Suggested Imaging Protocols for HIE in the Full-Term Neonate

A comprehensive evaluation of neonatal encephalopathy must address the issues discussed above. Has the brain developed normally? Are there signs of subacute/chronic injury? Are there signs of recent brain injury? If brain injury is present, what are the extent and severity of the injury? Are there signs of complication such as hemorrhage or hydrocephalus? Based on the literature cited herein, the suggested MR protocol for evaluation of the term neonate with suspected HIE is

1. T1-weighted images;
2. T2-weighted images;
3. T2*-weighted images;
4. diffusion-weighted images with computation of the apparent diffusion coefficient (ADC); and
5. proton MR spectroscopy.

Future Research

The gaps in our current knowledge point to future research opportunities for MR imaging in neonatal HIE. One shortcoming is that MR imaging on the first day of life does not consistently characterize the severity and extent of HIE that eventually manifests on follow-up MR imaging (25). Advanced MR spectroscopy methods (79) hold promise for predicting severity on the first day of life, but routine MRI and MRS currently underestimate the injury. If MR imaging is to serve as an objective measure for triage of encephalopathic neonates with suspected HIE for novel interventions, then more work needs to be focused on improving sensitivity on day 1 of life. Potential avenues for research include arterial spin label (ASL) perfusion (80) and functional connectivity MRI (81), which have not yet been reported in the evaluation of HIE.

While structural MR imaging with diffusion and MR spectroscopy on days 3–4 of life have shown prognostic value, it remains unproven that early detection of severity and extent of HIE improves patient outcomes. Clinicians and families may initiate rehabilitation programs with the intent of maximizing the child's neurodevelopmental potential. However, the MRI adds cost to the initial evaluation of the neonate, with the presumption that the overall cost to society will be reduced if early intervention yields better outcomes. This still needs to be proven.

Another open question is whether MRI can serve as a surrogate for clinical outcomes in trials of novel therapeutic intervention. MRI could afford significant cost savings in prospective therapeutic trials if interim analyses and short-term outcomes could be based on objective imaging endpoints rather than on neurodevelopmental assessments that may take months or years to reach significance. MR imaging is commonly used to assess endpoints in adult multiple sclerosis trials, and MRI endpoints are central to the design of an ongoing pediatric therapeutic trial (82). An open question remains whether cooling alters the time course of diffusion restriction in HIE. If so, what is the optimal timing of the MR scan if one wants to detect HIE changes in the brain of a neonate who is being cooled?

To date, most studies of HIE attempt to correlate clinical outcome with severity of the injury pattern on MRI. However, there are examples of rule breakers that come through our clinical practice on a regular basis. Why do neonates with a deep nuclear gray matter injury or periventricular white matter injury have seizures? Presumably, the MRI is not detecting the full spectrum of brain injury in this population. How do we avoid the problem of satisfaction of search? What strategies should we pursue to detect brain injury that does not fit one of the classic imaging patterns? Many questions remain unanswered at this point.

References

1. Shankaran S, Laptook AR. Clin Obstet Gynecol Sep 2007;50(3):624–635.
2. Jacobs S, Hunt R, Tarnow-Mordi W, Inder T, Davis P. Cochrane Database Syst Rev 2007(4):CD003311.
3. Lorek A, Takei Y, Cady EB et al. Pediatr Res Dec 1994;36(6):699–706.
4. Penrice J, Cady EB, Lorek A et al. Pediatr Res Jul 1996;40(1):6–14.
5. Gluckman PD, Williams CE. Dev Med Child Neurol Nov 1992;34(11):1010–1014.
6. Gunn AJ, Thoresen M. NeuroRx Apr 2006;3(2):154–169.
7. Siesjo BK. Magnesium 1989;8(5–6):223–237.
8. Fellman V, Raivio KO. Pediatr Res May 1997;41(5):599–606.
9. Liu XH, Kwon D, Schielke GP, Yang GY, Silverstein FS et al. J Cereb Blood Flow Metab Oct 1999;19(10):1099–1108.
10. Tan WK, Williams CE, During MJ et al. Pediatr Res May 1996;39(5):791–797.
11. Gynecologists ACoOa. Neonatal Encephalopathy and Cerebral Palsy: Defining the Pathogenesis and Pathophysiology 2003.
12. Wu YW, Backstrand KH, Zhao S, Fullerton HJ, Johnston SC. Pediatrics Dec 2004;114(6): 1584–1590.
13. Hull J, Dodd KL. Br J Obstet Gynaecol May 1992;99(5):386–391.
14. Smith J, Wells L, Dodd K. Bjog Apr 2000;107(4):461–466.
15. Thornberg E, Thiringer K, Odeback A, Milsom I. Acta Paediatr Aug 1995;84(8):927–932.
16. Volpe JJ. Ment Retard Dev Disabil Res Rev 2001;7(1):56–64.
17. Derrick M, Drobyshevsky A, Ji X, Tan S. Stroke Feb 2007;38(2 Suppl):731–735.

18. Sarnat HB, Sarnat MS. Arch Neurol Oct 1976;33(10):696–705.
19. Volpe JJ. Neurology of the Newborn, 5th ed. Philadelphia: Saunders, 2008,414–427.
20. Barkovich AJ, Hajnal BL, Vigneron D et al. Am J Neuroradiol Jan 1998;19(1):143–149.
21. Kaufman SA, Miller SP, Ferriero DM, Glidden DH, Barkovich AJ et al. Pediatr Neurol May 2003;28(5):342–346.
22. Barkovich AJ, Westmark KD, Bedi HS, Partridge JC, Ferriero DM et al. Am J Neuroradiol Oct 2001;22(9):1786–1794.
23. Hanrahan JD, Cox IJ, Azzopardi D et al. Dev Med Child Neurol Feb 1999;41(2): 76–82.
24. Coskun A, Lequin M, Segal M, Vigneron DB, Ferriero DM et al. Am J Neuroradiol Feb 2001;22(2):400–405.
25. McKinstry RC, Miller JH, Snyder AZ et al. Neurology Sep 24 2002;59(6):824–833.
26. Jissendi Tchofo P, Christophe C, David P, Metens T, Soto Ares G et al. J Neuroradiol Jan 2005;32(1):10–19.
27. Barkovich AJ. Pediatric Neuroimaging, 4th ed. Philadelphia: Lippincott Williams & Wilkins, 2005, 226.
28. Cowan FM, de Vries LS. Semin Fetal Neonatal Med Oct 2005;10(5):461–474.
29. Groenendaal F, Benders MJ, de Vries LS. Semin Perinatol Jun 2006;30(3):146–150.
30. Mazumdar A, Mukherjee P, Miller JH, Malde H, McKinstry RC. Am J Neuroradiol Jun–Jul 2003;24(6):1057–1066.
31. Neil JJ, Inder TE. J Child Neurol Feb 2006;21(2):115–118.
32. Winter JD, Lee DS, Hung RM et al. Pediatr Neurol Oct 2007;37(4):255–262.
33. Ward P, Counsell S, Allsop J et al. Pediatrics Apr 2006;117(4):e619–e630.
34. Ment LR, Bada HS, Barnes P et al. Neurology Jun 25 2002;58(12):1726–1738.
35. Akter M, Hirai T, Hiai Y et al. Acad Radiol Sep 2007;14(9):1011–1019.
36. de Souza JM, Domingues RC, Cruz LC, Jr., Domingues FS, Iasbeck T et al. Am J Neuroradiol Jan 2008;29(1):154–158.
37. Liang L, Korogi Y, Sugahara T et al. Am J Neuroradiol Sep 1999;20(8):1527–1534.
38. Liauw L, van der Grond J, van den Berg-Huysmans AA, Palm-Meinders IH, van Buchem MA et al. Radiology Apr 2008;247(1): 204–212.
39. Sie LT, Barkhof F, Lafeber HN, Valk J, van der Knaap MS. VEur Radiol 2000;10(10):1594–1601.
40. Cowan FM, Pennock JM, Hanrahan JD, Manji KP, Edwards AD. Neuropediatrics Aug 1994;25(4):172–175.
41. Dag Y, Firat AK, Karakas HM, Alkan A, Yakinci C et al. Diagn Interv Radiol Sep 2006;12(3):109–114.
42. Forbes KP, Pipe JG, Bird R. Am J Neuroradiol Sep 2000;21(8):1490–1496.
43. Johnson AJ, Lee BC, Lin W. Am J Roentgenol Jan 1999;172(1):219–226.
44. Khong PL, Tse C, Wong IY et al. J Child Neurol Nov 2004;19(11):872–881.
45. Krishnamoorthy KS, Soman TB, Takeoka M, Schaefer PW. J Child Neurol Sep 2000;15(9): 592–602.
46. Malik GK, Trivedi R, Gupta RK et al. Neuropediatrics Dec 2006;37(6):337–343.
47. Rutherford M, Counsell S, Allsop J et al. Pediatrics Oct 2004;114(4):1004–1014.
48. Soul JS, Robertson RL, Tzika AA, du Plessis AJ, Volpe JJ. Pediatrics Nov 2001;108(5):1211–1214.
49. Takeoka M, Soman TB, Yoshii A et al. Pediatr Neurol Apr 2002;26(4):274–281.
50. Thornton JS, Ordidge RJ, Penrice J et al. Magn Reson Med Jun 1998;39(6):920–927.
51. Wolf RL, Zimmerman RA, Clancy R, Haselgrove JH. Radiology Mar 2001;218(3):825–833.
52. Zarifi MK, Astrakas LG, Poussaint TY, Plessis Ad A, Zurakowski D et al. Radiology Dec 2002;225(3):859–870.
53. van Pul C, Buijs J, Janssen MJ, Roos GF, Vlaardingerbroek MT et al. Am J Neuroradiol Mar 2005;26(3):469–481.
54. Daneman A, Epelman M, Blaser S, Jarrin JR. Pediatr Radiol Jul 2006;36(7):636–646.
55. Blankenberg FG, Loh NN, Bracci P et al. Am J Neuroradiol Jan 2000;21(1):213–218.
56. Robertson RL, Robson CD, Zurakowski D, Antiles S, Strauss K et al. Pediatr Radiol Jul 2003;33(7):442–449.
57. Jyoti R, O'Neil R, Hurrion E. Pediatr Radiol Jan 2006;36(1):38–42.
58. Barkovich AJ. Am J Neuroradiol 1997 Nov–Dec; 18(10):1816–1820.
59. Rutherford MA, Pennock JM, Counsell SJ et al. Pediatrics Aug 1998;102(2 Pt 1):323–328.
60. Bluml S, Friedlich P, Erberich S, Wood JC, Seri I et al. Radiology May 2004;231(2):594–601.
61. Mathur AM, Neil JJ, McKinstry RC, Inder TE. Pediatr Radiol Mar 2008;38(3):260–264.
62. Conturo TE, McKinstry RC, Akbudak E, Robinson BH. Magn Reson Med Mar 1996;35(3):399–412.
63. Le Bihan D, Mangin JF, Poupon C et al. J Magn Reson Imaging Apr 2001;13(4):534–546.
64. Neil JJ, Shiran SI, McKinstry RC et al. Radiology Oct 1998;209(1):57–66.
65. Cappellini M, Rapisardi G, Cioni ML, Fonda C. Radiol Med (Torino) Oct 2002;104(4): 332–340.

66. da Silva LF, Hoefel Filho JR, Anes M, Nunes ML. Pediatr Neurol May 2006;34(5):360–366.
67. Kadri M, Shu S, Holshouser B et al. J Perinatol Apr–May 2003;23(3):181–185.
68. Roland EH, Poskitt K, Rodriguez E, Lupton BA, Hill A. Ann Neurol Aug 1998;44(2): 161–166.
69. Hunt RW, Neil JJ, Coleman LT, Kean MJ, Inder TE. Pediatrics Oct 2004;114(4):999–1003.
70. Kuenzle C, Baenziger O, Martin E et al. Neuropediatrics Aug 1994;25(4):191–200.
71. Saint Hilaire MH, Burke RE, Bressman SB, Brin MF, Fahn S. Neurology Feb 1991;41(2 (Pt 1)): 216–222.
72. Barnett A, Mercuri E, Rutherford M et al. Neuropediatrics Oct 2002;33(5):242–248.
73. Rutherford MA, Ward P, Malamatentiou C. Semin Fetal Neonatal Med Oct 2005;10(5): 445–460.
74. Pasternak JF, Gorey MT. Pediatr Neurol May 1998;18(5):391–398.
75. Miller SP, Ramaswamy V, Michelson D et al. J Pediatr Apr 2005;146(4):453–460.
76. Gonzalez FF, Miller SP. Arch Dis Child Fetal Neonatal Ed Nov 2006;91(6):F454–F459.
77. Rutherford MA, Azzopardi D, Whitelaw A et al. Pediatrics Oct 2005;116(4):1001–1006.
78. Inder TE, Hunt RW, Morley CJ et al. J Pediatr Dec 2004;145(6):835–837.
79. Wang ZJ, Vigneron DB, Miller SP et al. Am J Neuroradiol Apr 2008;29(4):798–801.
80. Wang J, Licht DJ. Neuroimaging Clin N Am Feb 2006;16(1):149–167, ix.
81. Fair DA, Cohen AL, Dosenbach NU et al. Proc Natl Acad Sci U S A Mar 11 2008;105(10): 4028–4032.
82. Vendt BA, McKinstry RC, Ball WS et al. J Digit Imaging Apr 9 2009;22(3):326–343.

7

Evidence-Based Neuroimaging for Traumatic Brain Injury in Children

Karen A. Tong, Udochukwu E. Oyoyo, Barbara A. Holshouser, Stephen Ashwal, and L. Santiago Medina

Issues

I. Which pediatric patients with head injury should undergo imaging in the acute setting?
II. What is the diagnostic performance (sensitivity and specificity) of imaging for injury requiring immediate treatment/surgery?
III. What is the role of imaging in the diagnosis and outcome of children with head trauma?
IV. What is the role of advanced imaging (functional MR, MR spectroscopy, diffusion imaging, SPECT, and PET) in children with traumatic brain injury (TBI)?

Key Points

- Head injury is not a homogeneous phenomenon and has a complex clinical course. There are different mechanisms, varying severity, diversity of injuries, secondary injuries, and effects of age or underlying disease. A highly sensitive clinical decision rule in more than 20,000 children has been derived for the identification of children who should undergo CT imaging after head trauma (moderate evidence).
- The important CHALICE (Children's Head injury Algorithm for the prediction of Important Clinical Events) prediction rule (Fig. 7.1) has the potential to improve and standardize the care of pediatric patients with head injuries (strong evidence).
- Calvarial plain radiographs have a poor sensitivity for identifying pediatric patients with intracranial pathology (moderate to strong evidence) and hence are not recommended unless for highly selected patients with suspected non-accidental trauma. (See Chapters 12 and 13 on non-accidental head injury and non-CNS non-accidental injury, respectively.)
- CT is the mainstay of imaging in the acute period. The majority of evidence relates to the use of CT for detecting injuries that may require

K.A. Tong (✉)
Department of Radiology, Loma Linda University, Loma Linda, CA 92354, USA
e-mail: ktong@llu.edu

L.S. Medina et al. (eds.), *Evidence-Based Imaging in Pediatrics*,
DOI 10.1007/978-1-4419-0922-0_7, © Springer Science+Business Media, LLC 2010

immediate treatment or surgery. Speed, availability, ease of exam, and lesser expense of CT studies remain important factors for using this modality in the acute setting (Table 7.1). Sensitivity of detection also increases with repeat scans in the acute period (strong evidence).

- It is safe to discharge children with TBI home after a negative CT study (moderate to strong evidence).
- The sensitivity and specificity of MRI for brain injury is generally superior to CT, although most studies have been retrospective and few direct comparisons have been performed in the recent decade. CT is clearly superior to MRI for the detection of fractures. MRI outperforms CT in detection of most other lesions (limited to moderate evidence), particularly diffuse axonal injury (DAI). MRI allows more detailed analysis of injuries, including metabolic and physiologic measures, but further evidence-based research is needed. There are few pediatric studies regarding the use of imaging and outcome predictions.
- Accurate prognostic information is important for determining management, but there are different needs for different populations. In severe TBI, information is important for acute patient management, long-term rehabilitation, and family counseling. In mild or moderate TBI, patients with subtle impairments may benefit from counseling and education.

Definition and Pathophysiology

Head trauma is difficult to study because it is a heterogeneous entity that encompasses many different types of injuries that may occur together (Table 7.2). Definitions of age groups, injuries, and outcomes are also variable. Classification of injury severity is usually defined by the Glasgow Coma Scale (GCS) score, a scale ranging from 3 to 15, which is often grouped into mild, moderate, or severe categories. There is inconsistency in timing of measurement, with some investigators using "initial or field GCS" while others use "post-resuscitation GCS." Grouping of GCS scores also vary. There is no universal definition of mild or minor head injury (1) as some use GCS scores of 13–15 (2, 3), while others use 14–15 (1) and still others use only 15. Variable definitions result in inconsistencies in imaging recommendations. Moderate TBI is generally defined by GCS of 9–12. Severe TBI is defined by GCS of 3–8.

Classification and measures of outcome are even more variable. The most commonly used outcome measure is the Glasgow Outcome Scale (GOS) (4). It is an overall measure based on degree of independence and ability to participate in normal activities with the following five categories: (1) death, (2) vegetative state (VS), (3) severe disability, (4) moderate disability, and (5) good recovery. The GOS is often dichotomized although grouping is variable. Recently modified, the extended GOS (5) has eight categories that also account for ability to work. In children, outcomes have been varibly measured using the GOS or other scales such as the Pediatric Cerebral Performence Category Scale (PCPCS) (12). Less common adult outcome scales include the Differential Outcome Scale (DOS) (6), the Rappaport Disability Rating Scale (DRS) (7), the Disability Score (DS) (8), the FIM (Functional Independence Measure) instrument (9), the Supervision Rating Scale (SRS) (10), and the Functional Status Examination (FSE) (11, 12).

Timing of outcome measurement also varies. Some investigators measure outcomes at discharge, 3, 6, or 12 months (or more) after injury. This may be problematic because outcomes often improve with time. However, there is moderate to strong evidence that 6 months is an appropriate time point to measure outcomes for clinical trials (13). Neuropsychological assessment is the most sensitive measure of outcome, although this is difficult to

perform in severely injured patients, resulting in selection bias. There is a wide variety of psychometric scales for various components of cognitive function such as intellect, orientation, attention, language, speech, information processing, motor reaction time, memory, learning, visuoconstructive ability, verbal fluency, mental flexibility, executive control, and personality. Currently, there have been a few studies in children showing relationships between neuroimaging in the acute period and long-term neuropsychological impairment (limited evidence) (14, 15).

Epidemiology

The prevalence of TBI is difficult to determine, because many less severely injured patients are not hospitalized and cases with multiple injuries may not be included. Estimates are often based on existing disabilities. Approximately 1.74 million individuals per year suffer mild TBI that results in a physician visit or temporary disability of at least 1 day (16) and more than 1 million visits per year to emergency departments are for TBI-related injuries in the United States (17). As many as 50% are pediatric patients (18–20). There are more than 230,000 TBI-related hospitalizations/year (17), perhaps up to 500,000/year (21). TBI is responsible for nearly 40% of all deaths from acute injuries (16). There are approximately 50,000 TBI-related deaths/year, in the United States (22). Other studies have demonstrated lower mortality rates (23). The major causes of TBI are falls (28%), motor vehicle accidents (MVA) (20%), struck by vehicles or objects (19%), and assaults (11%). Among children 0 to 14 years, TBI results in an annual estimated 2,685 deaths; 37,000 hospitalizations, and 435,000 emergency department visits (22). Head injuries in child abuse will be discussed in a separate chapter.

Overall Cost to Society

There has been an overall decline in TBI-related deaths, probably from multiple factors including improvements in medical care, use of evidence-based guidelines, and injury prevention efforts (17). An estimated 5.3 million U.S. residents live with permanent TBI-related disabilities (17). Direct costs are estimated at $4 billion/year (16). In 2000, total direct and indirect costs of TBI were estimated at $60 billion/year (22). In the United States, where there are 95,000 hospital admissions from pediatric head injuries, the yearly cost has been estimated at greater than $1 billion (24–26). There are little data on costs of TBI related solely to imaging. There has been one small study (limited evidence) that determined that 60% of patients were found to have additional lesions on MRI, but because none of these additional findings changed management, MRI resulted in a nonvalue-added incremental increase of $1,891 per patient and a $3,152 incremental increase in charges to detect each patient with a lesion not identified on CT (27).

Goals

To detect the presence of injuries that may require immediate surgical or procedural intervention.

To detect the presence of injuries that may benefit from early medical therapy.

To determine the prognosis of patients to tailor rehabilitative therapy or aid family counseling.

Methodology

A search of the Medline/PubMed electronic database (National Library of Medicine, Bethesda, MD) and Ovid (Wolters Klumer, New York, New York) was performed using keywords including (1) head injury, head trauma, brain injury, brain trauma, traumatic brain injury or TBI; and (2) CT, computed tomography, computerized tomography, MR, magnetic resonance, spectroscopy, diffusion, diffusion tensor, functional magnetic, functional MR*, T2*, FLAIR, GRE, gradient echo. A systematic literature review was performed through January 2008. Limits included English language, abstracts, and human subjects. A search of the National Guideline Clearinghouse at www.guideline.gov was also performed

using keywords including (1) head injury, head trauma, brain injury; and (2) parameter, guideline.

Discussion of Issues

I. Which Pediatric Patients with Head Injury Should Undergo Imaging in the Acute Setting?

Summary of Evidence: A highly sensitive clinical decision rule in more than 20,000 children has been derived for the identification of children who should undergo CT imaging after head trauma (moderate evidence). The important CHALICE prediction rule (Table 7.3) has the potential to improve and standardize the care of pediatric patients with head injuries (strong evidence). Calvarial plain radiographs have a poor sensitivity for identifying pediatric patients with intracranial pathology (moderate to strong evidence) and are not recommended unless for patients with suspected non-accidental trauma (28). A recommended decision tree for children with acute head injury is shown in Fig. 7.1.

Supporting Evidence: Multiple studies have now been conducted to determine clinical prediction rules for the identification of which pediatric victims with minor head trauma require imaging. These studies show great promise, but to date, validation has not been completed. The largest study is the recent CHALICE (Children's Head injury Algorithm for the prediction of Important Clinical Events) study conducted by Dunning and colleagues. The CHALICE was a large prospective multicenter diagnostic cohort study in the UK (28) (strong evidence). All children who had a clinically significant head injury (death, need for neurosurgical intervention or abnormality on a CT study) were identified. Abnormalities on CT included intracranial hematomas of any size, cerebral contusion, diffuse cerebral edema, and depressed skull fractures. Simple or non-depressed skull fractures alone were not considered to be significant predictors of intracranial injury (28). Multivariate recursive partitioning on 40 clinical variables was performed. About 22,772 children were recruited over 2.5 years; 56% were under 5 years of age and 65% were male children; 281 children showed an abnormality on CT, 137 had a neurosurgical intervention, and 15 died. The CHALICE (Children's Head injury Algorithm for the prediction of Important Clinical Events) rule was derived (Table 7.3) with a sensitivity of 98% (95% confidence interval (CI) 96–100%) and a specificity of 87% (95% CI 86–87%) for the prediction of clinically significant head injury and requires a CT imaging rate of 14%. Prospective validation of this rule with new cohorts is still pending.

Palchak and colleagues derived a rule based on the evaluation of 2,043 pediatric patients under 18 years who had head trauma and positive findings on history or clinical examination such as loss of consciousness, memory loss, headache, or emesis (29). Of the nine predictive variables studied, abnormal mental status, clinical findings of calvarial fracture, history of emesis, scalp hematoma in children 2 years of age or less, and cephalagia were identified in 96 of 98 patients with a positive intracranial lesion on CT (98% sensitivity, 95% CI 93–100%) (moderate evidence). Greenes and Shutzman (30) performed a prospective study on 608 patients under 2 years of age in a single hospital setting (moderate evidence). Their study demonstrated that pediatric patients with suspected non-accidental trauma, lethargy, or a major scalp hematoma had an increased risk of significant intracranial injury. This study found that loss of consciousness, seizures, or emesis alone were not an adequate predictor of intracranial injury, and furthermore, the absence of clinical symptoms or signs did not fully exclude the possibility of having positive intracranial pathology (30). They allocated patients into four risk groups, with CT imaging recommended in the highest risk group of children who vomited more than three times or had loss of consciousness, lethargy, a high-risk mechanism, or considerable bruising (30). This study and the CHALICE study revealed that it was safe to discharge children with a negative CT study (28, 30).

Haydel and Shembekar (31) in 2003 evaluated the adult New Orleans criteria (32) in children under age 5 years. They studied 175 children with Glasgow Coma Scale of 15 at a single institution. They concluded that the 14 positive CT scans could be identified with this adult

predictive rule (31). The Canadian CT rule for children was proposed by the UK National Institute of Clinical Excellence before the CHALICE study was published (28). The CHALICE group assessed the diagnostic performance of this rule in children (33) to detect intracranial injury and found a sensitivity of 94% (95% CI 91–97%), specificity of 89% (95% CI 89–90%), and a CT ordering rate of 12% (28).

Boran and colleagues (34) studied 421 children with GCS of 15 and without any focal neurological deficit (moderate evidence). Intracranial lesions were noted in 37 cases (8.8%). The clinical parameters associated with an increased incidence of intracranial pathology were posttraumatic seizures and loss of consciousness. However, when patients with these predictive parameters were subtracted, intracranial lesions were still identified in 4.1% of the cases and 1.8% required neurosurgical operation (34). Boran and colleagues (34) also found a low sensitivity of plain radiographs of 43.2% and specificity of 93%. The CHALICE study (28) as well as other studies (35) support the recommendation of not performing skull radiographs except for patients who may have had a non-accidental injury. Calvarial plain radiographs have a poor sensitivity for identifying pediatric patients with intracranial pathology (moderate to strong evidence) (28).

II. What Is the Sensitivity and Specificity of Imaging for Injury Requiring Immediate Treatment/Surgery?

Summary of Evidence: CT is the mainstay of imaging in the acute period. The majority of evidence relates to the use of CT for detecting injuries that may require immediate treatment or surgery. Speed, 24/7 availability, ease of acquisition, and lesser expense of CT studies remain important factors for using this modality in the acute setting. Sensitivity of detection also increases with repeat scans in the acute period (strong evidence).

Supporting Evidence: The incidence of injury-related abnormalities on CT is related to the severity of injury. The incidence of CT abnormalities in moderate head injury (with GCS of 9–13) has been reported to be 61% (36). The sensitivity of CT for detecting abnormalities after severe TBI (GCS below 9) varies from 68 to 94%, while normal scans range from approximately 7 to 12% (37). Several studies have shown that timing of CT studies also affects the sensitivity. Oertel and colleagues (strong evidence) prospectively studied 142 patients with moderate or severe injury, who had undergone more than one CT scan within the first 24 h, and found that the initial CT scan did not detect the full extent of hemorrhagic injuries in almost 50% of patients, particularly if scanned within the first 2 h (38). The likelihood of progressive hemorrhagic injury, potentially requiring surgical intervention, was greatest for parenchymal hemorrhagic contusions (51%), followed by epidural hematoma (EDH) (22%), subarachnoid hemorrhage (SAH) (17%), and subdural hemorrhage (SDH) (11%). Servedei and colleagues (strong evidence) prospectively studied 897 patients with more than one CT scan and found that 16% of patients with diffuse brain injury demonstrated significant evolution of injury. This was more frequent in those patients with midline shift, often evolving to mass lesions (39). Similar results have been seen in retrospective studies (40). Therefore, it is useful to perform repeat CT scans in the acute period, particularly after moderate and severe injury, although the timing has not been clearly determined.

III. What Is the Overall Sensitivity and Specificity of Imaging in the Diagnosis and Prognosis of Children with Head Trauma?

Summary of Evidence: The overall sensitivity and specificity of MRI for brain injury is generally superior to CT, although most studies have been retrospective and very few head-to-head comparisons have been performed. CT is clearly superior to MRI for the detection of fractures. MRI outperforms CT in detection of most other lesions (limited to moderate evidence), particularly diffuse axonal injury (DAI). Because different sequences vary in ability to detect certain lesions, it is often difficult to compare results. MRI allows more detailed analysis of injuries,

including metabolic and physiologic measures, but further evidence-based research is needed.

There are few pediatric studies regarding the use of imaging and outcome prediction. Pediatric TBI patients are known to have different biophysical features, risks, mechanisms, and outcomes after injury. There are also differences between infants and older children, although this remains controversial. Categorization of pediatric age groups is variable and measures of injury or outcomes are inconsistent. The GCS and GOS have been used for pediatric studies, sometimes with modifications (41–43) or with variable dichotomization (41, 44). For infants and toddlers, some investigators have used a Children's Coma Scale (CCS) (45). There are several pediatric adaptations of the GOS, such as the King's Outcome Scale for Childhood Head Injury (KOSCHI) (46), the Pediatric Cerebral Performance Category Scale (PCPCS), or the Pediatric Overall Performance Category Scale (POPCS) (47). Management guidelines are controversial.

Supporting Evidence: MRI has higher sensitivity than CT for intracranial injury, although most comparison studies were performed in the late 1980s and early 1990s (with older generation or lower field scanners). Orrison and colleagues (moderate evidence) retrospectively studied 107 patients with MRI and CT within 48 h and showed that MRI had an overall sensitivity of 97% compared to 63% for CT even when a low-field MRI scanner was used, with better sensitivity for contusion, shearing injury, subdural and epidural hematoma (48). Ogawa and colleagues (moderate evidence) detected more lesions with conventional MRI than CT with the exception of subdural and subarachnoid hemorrhages, in a prospective study of 155 patients, although they were studied at variable time points (49). Other studies (moderate evidence) showed better detection of nonhemorrhagic contusions and shearing injuries (50) and of brainstem lesions (51).

The literature on imaging and prediction of outcome from head injury is limited in pediatric subjects. Importantly, within the pediatric population, age may be a confounding variable or effect modifier for outcomes. Levin and colleagues (moderate evidence) studied 103 children at one of the original four centers participating in the Trauma Coma Databank (TCDB) and found heterogeneity in 6-month outcomes based on age. Worst outcomes were found in the 0–4-year-old patients and best outcomes were found in the 5–10-year-old patients, while adolescents had intermediate outcomes. They suggested that studies involving severe TBI in children should analyze age-defined subgroups rather than pooling a wide range of pediatric ages (52).

There is less literature regarding the utility of imaging in predicting outcome in pediatric TBI compared to adults. Many studies have consisted of relatively small sample sizes and used varying outcome, possibly accounting for conflicting reports regarding outcomes related to TBI in children. There have been several studies evaluating CT in predicting outcome in children with variable results. Suresh and colleagues (moderate evidence) studied 340 children and compared CT findings to discharge GOS outcomes. Progressively worse outcomes were found with fractures, epidural hematoma (EDH), contusion, diffuse head injury, and acute SDH (44). Death occured in 16% of their patients. Hirsch and colleagues (moderate evidence) studied 248 children after severe TBI and compared initial CT findings to the level of consciousness (measured by a modified GCS score) at 1 year after injury. They found that children with normal CT or isolated SDH or EDH were least impaired, while children with diffuse edema had the most impairment. Those with parenchymal hemorrhage, ventricular hemorrhage, or focal edema had intermediate outcomes (53). A study of 82 children (moderate evidence) found that unfavorable prognosis (using a 3-category Lidcombe impairment scale) was more likely to occur after shearing injury or intracerebral/subdural hematomas, whereas a better outcome was more likely in patients with epidural hematoma (54). Another study of 74 children (moderate evidence) found that the presence of traumatic subarachnoid hemorrhage on CT was an independent predictor of poorer discharge outcome ($P< 0.001$) but did not find that DAI or diffuse swelling was associated with outcome. After stepwise logistic regression analysis, CT findings did not have prognostic significance compared to other variables such as GCS and the oculocephalic reflex (42). Another study (moderate evidence)

compared 59 children and 59 adults and found that a CT finding of absent ventricles/cisterns was associated with a slightly lower frequency of poor outcome (6-month GOS) in children, suggesting that diffuse swelling may be more benign in children than adults unless there was a severe primary injury or a secondary hypotensive insult (55).

Bonnier and colleagues studied 50 children with severe TBI before 4 years of age (moderate evidence) (56). TBI severity (initial GCS score or coma duration) was significantly associated with subcortical lesions. A greater deterioration in intellectual quotient over time was noted in patients with subcortical lesions. Sigmund and colleagues studied 40 children with TBI using CT and MRI (moderate evidence) (57). T2-weighted, FLAIR, and susceptibility-weighted MRI findings showed no significant difference in lesion volume between normal and mild outcome groups, but did indicate significant differences between normal and poor and between mild and poor outcome groups. CT revealed no significant differences in lesion volume between any groups. The findings suggest that these MRI findings provide a more accurate assessment of injury severity and detection of outcome-influencing lesions than does CT in pediatric DAI patients (moderate evidence).

Wilde and colleagues studied morphometrics (morphological measurements) using MRI in 16 children with DAI and 16 individually matched uninjured children (limited evidence) (58). Analysis demonstrated significant volume loss in the hippocampus, amygdala, and globus pallidus in the TBI group. Spanos and colleagues studied 16 children 9–16 years of age and 16 demographically matched typically developing children (59). A significant group difference was found in cerebellar white matter volume with children in the TBI group (limited evidence) (59).

Some lesions, such as DAI, are clearly better detected with MRI and have been reported in up to 30% of patients with mild head injury with normal CT (60) (limited evidence). However, sensitivity depends on the sequence, field strength and type of lesion. Gradient echo (GRE) type sequences are best for detecting hemorrhagic DAI, although the proportion of hemorrhagic versus non-hemorrhagic DAI is not truly known. An early report (limited evidence) suggested that less than 20% of DAI lesions were visibly hemorrhagic (61), but this is likely to be erroneously low, due to poor sensitivity of the imaging methods available at that time. Tong and colleagues compared a new susceptibility-weighted imaging (SWI) sequence (at 1.5 T), a modified GRE sequence, and showed significantly better detection of small hemorrhagic shearing lesions compared to conventional GRE (62) (limited evidence). They studied 40 children with TBI using SWI to detect hemorrhage (moderate evidence). Children with lower GCS scores ($\leq$8, n=30) or prolonged coma (>4 days, n=20) had a greater average number (P=0.0007) and volume (P=0.008) of hemorrhagic lesions (63). Scheid and colleagues (moderate evidence) prospectively studied 66 patients using high-field (3.0 T) MRI and found that T2$*$-weighted GRE sequences detected significantly more lesions than conventional T1- or T2-weighted sequences (64). Babikian and colleagues studied 18 children and adolescents 1–4 years after injury using susceptibility weighted imaging (limited evidence). Negative correlations between lesion number and volume with neuropsychologic functioning were shown (14).

The fluid-attenuated inversion recovery (FLAIR) sequence is useful for detecting SAH, SDH, contusions, non-hemorrhagic DAI, and perisulcal lesions, but there are few studies comparing the sensitivity of FLAIR to other sequences. One study (limited to moderate evidence) found that FLAIR sequences were significantly more sensitive than spin echo (SE) sequences (P<0.01) in detection of all lesions studied within 1–36 days (0.5 T), particularly in those who had DAI-type lesions (65).

There have been some studies evaluating MRI for outcome prediction in children with TBI. Prasad and colleagues (moderate evidence) prospectively studied 60 children with acute CT and MRI. Hierarchical multiple regression indicated that the number of lesions, as well as certain clinical variables such as GCS (modified for children) and duration of coma, were predictive of outcomes up to 1 year (modified GOS) (41). Several investigators have studied the correlation between depth of lesion and outcomes, with varying results. Levin and colleagues (moderate evidence) studied 169 children prospectively as well as 82 patients

retrospectively with MRI at variable time points, and showed a correlation between depth of brain lesions and functional outcome (66). Grados and colleagues (moderate evidence) studied 106 children with a SPGR (T1-weighted) MRI sequence obtained 3 months after TBI, and classified lesions into a depth-of-lesion model. They found that depth and number of lesions predicted outcome, although correlation was better with discharge outcomes than 1 year outcomes (67). Blackman and colleagues (moderate evidence) studied 92 children in the rehabilitation setting (using variable imaging modalities) and used a depth-of-lesion classification (based on the Grados model) to study neuropsychological outcomes. They found that this classification had limited usefulness. Although patients with deeper lesions tended to have longer stays in rehabilitation, they were able to "catch up" after sufficient time had elapsed (68). In a recent study of hemorrhagic DAI lesions (moderate evidence), Tong and colleagues found that the degree and location of hemorrhagic lesions correlated with GCS, duration of coma and outcomes at 6–12 months after injury (63). Levin and colleagues (moderate evidence) showed that in children, as in adults, corpus callosum area (measured on subacute MR) correlated with functional outcome. They also found that the size of the corpus callosum decreased after severe TBI in contrast to mild/moderately injured children who showed growth of the corpus callosum on follow-up studies (69).

IV. What Is the Role of Advanced Imaging (Functional MRI, MR Spectroscopy, Diffusion Imaging, SPECT, and PET) in Children with TBI?

Summary of Evidence: There is moderate evidence that MR spectroscopic changes can help predict outcome in children with TBI. SPECT hypoperfusion abnormalities may be an indicator of a worse outcome in children (moderate evidence). Brain PET metabolic abnormalities may predict outcome in children (limited to moderate evidence). Data about functional MRI and diffusion tensor imaging are limited. Large studies are required with these advanced imaging modalities to determine the role and outcome prognosis in children with TBI.

Supporting Evidence: Table 7.1 describes briefly the current imaging methods of TBI including their principle, advantages/limitations, and use. Diffusion-weighted imaging (DWI) has also recently been shown to improve the detection of non-hemorrhagic shearing lesions, although there are only a few small studies describing sensitivity. Hou and colleagues studied 37 adults with TBI and showed that higher apparent diffusion coefficient (ADC) values in normal appearing brain correlated with unfavorable outcomes ($P<0.05$) (moderate evidence) (70). Galloway and colleagues studied 37 children with TBI and showed that the average total brain ADC could correctly predict outcome in 84% of cases (moderate evidence) (71). Schaefer and colleagues studied 26 patients (age range 4–72 years) with closed head injury (limited evidence) (72) and showed a correlation between volume of abnormal signal intensity on DWI and modified Rankin score ($r=0.772$, $P<0.001$) (72). A small study (insufficient evidence) of patients scanned within 48 h found that DWI identified an additional 16% of shearing lesions that were not seen on conventional MRI. The majority of DWI-positive lesions (65%) had decreased diffusion (73). Another descriptive study (limited evidence) characterized several different types and patterns of DWI lesions, although there was no comparison with other MRI sequences or analysis of diffusion changes over time (74). A recent study (limited evidence) found a strong correlation between apparent diffusion coefficient (ADC) histograms and GCS score (75). Few studies have studied the role of diffusion tensor imaging (DTI). Wozniak and colleagues studied 14 children with TBI and 14 controls aged 10–18 years who had DTI studies and neurocognitive evaluations at 6–12 months (76). The TBI group had lower fractional anisotropy (FA) in three white matter regions: inferior frontal, superior frontal, and supracallosal (limited evidence). Supracallosal FA correlated with motor speed and behavior ratings. Parent-reported executive deficits were inversely correlated with FA. A few small studies (insufficient or limited evidence) have shown decreased anisotropy in brain parenchyma of TBI patients (77–79).

Although CT and MR imaging are often limited to observing structural abnormalities associated with TBI, magnetic resonance spectroscopy (MRS) can detect subtle cellular abnormalities that may more accurately estimate the extent of brain injury, particularly DAI. Makaroff and colleagues studied 11 children with TBI (limited evidence) (80). Four children demonstrated elevated lactate and diminished NAA in several regions, indicating global ischemic injury. All four children had seizures, abnormal neurological examination, and required admission to the PICU. In four other children, lactate was detected in least one region, indicating a focal ischemic injury. Two children had seizures and two had abnormal neurological examination. The remaining three children had no evidence of elevated lactate. Clinically no seizures were demonstrated and no PICU admission was required. Holshouser and colleagues performed MRS in 40 children with TBI 1–16 days after injury (moderate evidence) (81). Neurologic outcome was evaluated at 6–12 months after TBI. A logistic regression model demonstrated a significant decrease in the NAA/creatine and increase in the choline/creatine ratios in normal-appearing ($P<0.05$) and visibly injured brain ($P<0.001$). In normal-appearing brain NAA/creatine decreased more in patients with poor outcomes (1.32 $\pm$0.54) than in those with good outcomes (1.61 $\pm$0.50). Babikian and colleagues studied 20 children and adolescents and demonstrated a moderate to strong correlation of decreased NAA and worse cognitive scores (limited evidence) (15). Ashwal and colleagues in 38 children with TBI demonstrated that the occipital glutamate/glutamine in the short echo MRS was significantly increased in TBI when compared with controls (limited evidence) (82). No difference was seen in this ratio between children with good and poor outcome. Ashwal and colleagues studied 38 children and demonstrated that occipital gray matter myoinositol in children was increased with TBI (4.30 ± 0.73) compared with controls (3.53 ± 0.48; $P=0.003$). In addition, patients with poor outcomes 6–12 months after injury had higher myoinositol levels (4.78 ± 0.68) than patients with good outcomes (4.15 ± 0.69; $P=0.05$) (moderate evidence) (83), indicating that myoinositol elevation after pediatric TBI is associated with a poor neurologic outcome. The reasons for the increased myoinositol may be due to astrogliosis or a disturbance in osmotic function. Ashwal and colleagues (moderate evidence) also demonstrated significant decreases in NAA-derived ratios and elevation of Cho/Cre measured in occipital GM within 13 days of neurological insult. These metabolite changes correlated with poor neurological outcome at 6–12 months after injury ($n=52$) (84). In a subgroup of these patients ($n=24$) neuropsychological evaluations were performed at 3–5 years after neurological insult. It was found that these metabolite changes strongly correlated with below average functioning in multiple areas including full scale IQ, memory, sensorimotor, and attention/executive functioning (85).

Single photon emission computed tomography (SPECT) can measure regional cerebral blood flow (CBF) and assess localized perfusion deficits that may correlate with cognitive deficits even in the absence of structural abnormalities. However, SPECT has low spatial and temporal resolution, does not permit imaging of transient cognitive events, and interpretation is often highly subjective. It also uses low ionizing radiation and requires patient cooperation. SPECT studies generally show patchy perfusion deficits, often in areas with no visible injury on CT. One of the largest studies, although retrospective, was performed by Abdel-Dayem and colleagues (moderate evidence) who reviewed SPECT findings in 228 subjects with mild or moderate TBI. They found focal areas of hypoperfusion in 77% of patients. However, there was no comparison to CT or MRI (86). Stamatakis and colleagues (moderate evidence) studied 61 patients with SPECT and MRI, within 2–18 days after injury, and found that SPECT detected more extensive abnormality than MRI in acute and follow-up studies (87). A small study (limited evidence) of patients with persistent post-concussion syndrome after mild TBI found that SPECT showed abnormalities in 53% of patients whereas MRI and CT only showed abnormalities in 9 and 5% respectively (88). A more recent study by Gowda and colleagues (89) studied 28 children and 64 adults with SPECT using technetium Tc99m ethyl cysteinate dimer within 72 h of the traumatic brain injury. The most common abnormality was hypoperfusion of the temporal lobe in children and

the frontal lobe in adults (moderate evidence). A significantly higher number of a perfusion abnormalities were seen in patients with post-traumatic amnesia (P=0.03), loss of consciousness (P=0.02), and post-concussion syndrome (P=0.01) than in patients without these symptoms. CT findings were abnormal in 31 (34%) versus SPECT in 58 (63%). Difference between the SPECT and CT detection rate was statistically significant (P<0.05).

Positron emission tomography (PET) can measure regional glucose and oxygen utilization, CBF at rest, and CBF changes related to performances of different tasks. Spatial and temporal resolution is also limited, although better than SPECT. However, PET is not widely available, uses low ionizing radiation, and requires patient cooperation. A few PET studies have reported various areas of decreased glucose utilization, even without visible injury. Bergsneider and colleagues (limited to moderate evidence) prospectively studied 56 patients with mild to severe TBI, evaluated with 18F fluorodeoxyglucose (FDG)-PET within 2–39 days of injury, 14 of which had subsequent follow-up studies. They describe in this and previous reports that TBI patients demonstrate a triphasic pattern of glucose metabolism changes that consist of early hyperglycolysis, followed by metabolic depression, and subsequent metabolic recovery (after several weeks) (90). Wu and colleagues (91) performed a study evaluating the gray matter and white matter with PET. Fourteen TBI patients and 19 normal volunteers were studied with a quantitative FDG-PET, a quantitative H_2 ^{15}O-PET, and MRI acutely following TBI. The gray to white matter ratios for both FDG uptake rate and changes of glucose metabolic rate were significantly decreased in TBI patients (P<0.001). The changes of glucose metabolic rate decreased significantly in gray matter (P<0.001) but not in white matter (P>0.1). The glucose to white matter ratios of changes in glucose metabolic rate correlated with the initial GCS of TBI patients with r=0.64. The patients with higher changes of glucose metabolic rate (>1.54) showed good recovery a year after TBI. A more recent study by Lupi and colleagues examining PET in 58 consecutive patients, (age range 14–69 years), with 44 having TBI demonstrated a relative hypermetabolic cerebellar vermis as a common finding in the injured brain regardless of the nature of the trauma (92).

There are a few small studies evaluating sensitivity of Xenon CT and even fewer describing the sensitivity of functional MRI (fMRI) or MR perfusion. Newsome and colleagues studied eight children with moderate to severe TBI and eight matched, uninjured control children with fMRI using an N-back task to test effects of TBI on working memory performance and brain activation (limited evidence) (93). Two patterns in TBI patients were seen. Patients whose criterion performance was reached at lower memory loads than control children demonstrated less extensive frontal and extrafrontal brain activation than controls. Patients who performed the same, highest (3-back) memory load as controls demonstrated more frontal and extrafrontal activation than controls. This is a small series and further longitudinal studies are needed.

Take Home Figures and Tables

Figure 7.1 is an algorithm for diagnosing acute head injury in children.

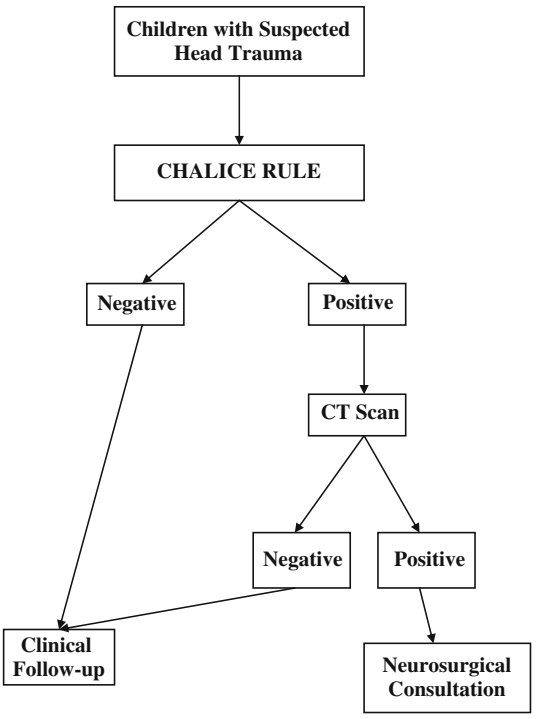

Figure 7.1. Recommended decision tree for children with acute head injury.

Table 7.1 reviews current imaging methods for TBI. Table 7.2 lists types of head injuries. Table 7.3 is a children's head injury algorithm for the prediction of important clinical events (CHALICE) rule.

Table 7.1. Current imaging methods of traumatic brain injury (TBI)

Modality	Principle and advantages/limitations	Use in TBI
CT	Based on X-rays, measures tissue density; rapid, inexpensive, widely available 24/7, ionizing radiation	Detects hemorrhage and "surgical lesions"
Xenon CT perfusion	Inhalation of stable xenon gas which acts as a freely diffusible tracer; requires additional equipment and software that is available only in a few centers	Detects disturbances in CBF due to injury, edema, or infarction
MRI	Uses RF pulses in magnetic field to distinguish tissues, employs many different techniques; currently has highest spatial resolution; complex and expensive	Detection of various injuries, subtle injuries, sensitivity varies with different techniques
MRI—FLAIR	Suppresses CSF signal	Detection of edematous lesions, particularly near ventricles and cortex; as well as extra-axial blood
MRI—T2[a] GRE	Accentuates blooming effect,[a] such as blood products	Detection of small parenchymal hemorrhages
MRI—DWI	Distinguishes water mobility in tissue	Detection of recent tissue infarction or traumatic cell death
MRI—DTI	Based on DWI, maps degree and direction of water diffusion along major fiber bundles; requires special software	Detects impaired connectivity of white matter tracts, even in normal-appearing tissue
MRI—MT	Suppression of "background" brain tissue containing protein-bound H_2O, enhances contrast between water and lipid-containing tissue	May detect microscopic neuronal dysfunction, even in normal-appearing tissue
MRI—MRS	Analyzes chemical composition of brain tissue; requires special software	Metabolite patterns indicate neuronal dysfunction or axonal injury, even in normal-appearing tissue
MR volumetry	Measures volumes of various brain structures or regions; time consuming, requires special software	Detects atrophy of injured tissue, can quantitate progression over time
fMRI	Measures small changes in blood flow related to brain activation; requires cooperative patients	Detects impairment or redistribution of areas of brain activation
MR perfusion (global, non-fMRI)	Measures tissue perfusion using contrast or non-contrast methods; better temporal resolution than PET, SPECT; not as well studied	Detects disturbances in CBF due to injury, edema, or infarction
SPECT	Photon-emitting radioisotopes used to measure CBF. Low ionizing radiation	Detects disturbances in CBF due to injury, edema, or infarction
PET	Positron emitting radioisotopes act as freely diffusible tracers, used to measure CBF, metabolic rate (glucose metabolism or oxygen consumption) or response to cognitive tasks; available only in a few centers. Low ionizing radiation	Detects disturbances in CBF due to injury, edema, or infarction

[a]Blooming effect is usually caused by hemosiderin from a prior hemorrhagic lesion.

Abbreviations: CT, computed tomography; MRI, magnetic resonance imaging; FLAIR, fluid-attenuated inversion recovery; GRE, gradient recalled echo; DWI, diffusion-weighted imaging; DTI, diffusion tensor imaging; MT, magnetization transfer; MRS, magnetic resonance spectroscopy; fMRI, functional magnetic resonance imaging; SPECT, single photon emission computed tomography; PET, positron emission tomography; CBF, cerebral blood flow.

Modified with the kind permission of Springer Science+Business Media from Tong KA, Oyoyo U, Holshouser BA, Ashwal S. Neuroimaging for Traumatic Brain Injury. In Medina LA, Blackmore CC (eds): Evidence-Based Imaging: Optimizing Imaging in Patient Care. New York: Springer Science+Business Media, 2006.

Table 7.2. Types of head injury (excluding penetrating/missile injuries and non-accidental trauma)

Primary injuries

1. **Peripheral, non-intracranial**
   - **Scalp or soft tissue injury**
   - **Facial or calvarial fractures**

2. **Extra-axial**
   - **Extradural or epidural hemorrhage**
   - **Subdural hemorrhage**
   - **Traumatic subdural effusion or "hygroma"**
   - **Subarachnoid hemorrhage**
   - **Intraventricular hemorrhage**

3. **Parenchymal**
   - **Contusion**
     - ☐ **Hemorrhagic**
     - ☐ **Non-hemorrhagic**
     - ☐ **Both**
   - **Shearing injury or "diffuse axonal injury"**
     - ☐ **Hemorrhagic**
     - ☐ **Non-hemorrhagic**
     - ☐ **Both**

4. **Vascular**
   - **Arterial dissection/laceration/occlusion**
   - **Dural venous sinus laceration/occlusion**
   - **Carotid-cavernous fistula**

Secondary injuries

5. **Cerebral edema**
6. **Focal infarction**
7. **Diffuse hypoxic-ischemic injury**
8. **Hydrocephalus**
9. **Infection**

Reprinted with the kind permission of Springer Science+Business Media from Tong KA, Oyoyo U, Holshouser BA, Ashwal S. Neuroimaging for Traumatic Brain Injury. In Medina LA, Blackmore CC (eds): Evidence-Based Imaging: Optimizing Imaging in Patient Care. New York: Springer Science+Business Media, 2006.

Table 7.3. The children's head injury algorithm for the prediction of important clinical events (CHALICE) rule

A computed tomography scan is required if *any* of the following criteria are present:

1. *History*
- **Witnessed loss of consciousness of >5 min duration**
- **History of amnesia (either antegrade or retrograde) of >5 min duration**
- **Abnormal drowsiness (defined as drowsiness in excess of that expected by the examining doctor)**
- **≥3 vomits after head injury (a vomit is defined as a single discrete episode of vomiting)**
- **Suspicion of non-accidental injury (NAI, defined as any suspicion of NAI by the examining doctor)**
- **Seizure after head injury in a patient who has no history of epilepsy**

2. *Examination*
- **Glasgow Coma Score (GCS) <14, or GCS <15 if <1 year old**
- **Suspicion of penetrating or depressed skull injury or tense fontanelle**
- **Signs of a basal skull fracture (defined as evidence of blood or cerebrospinal fluid from ear or nose, "panda eyes", "battle's sign", hemotympanum, facial crepitus, or serious facial injury)**
- **Positive focal neurology (defined as focal neurological abnormality, including motor, sensory, coordination, or reflex abnormality)**
- **Presence of bruise, swelling or laceration >5 cm if <1 year old**

3. *Mechanism*
- **High-speed road traffic accident either as pedestrian, cyclist, or occupant (defined as accident with speed >40 m/h)**
- **Fall of >3 m in height**
- **High-speed injury from a projectile or an object**

If none of the above variables are present, the patient is at low risk of intracranial pathology

Reprinted with permission by BMJ Publishing Group Ltd from Dunning et al. (28).

Imaging Case Studies

Case 1: Example of MR Imaging for Traumatic Brain Injury (TBI)

This case study (Fig. 7.2) illustrates imaging findings of diffuse axonal injury (DAI) in a 10-year-old male struck by a car.

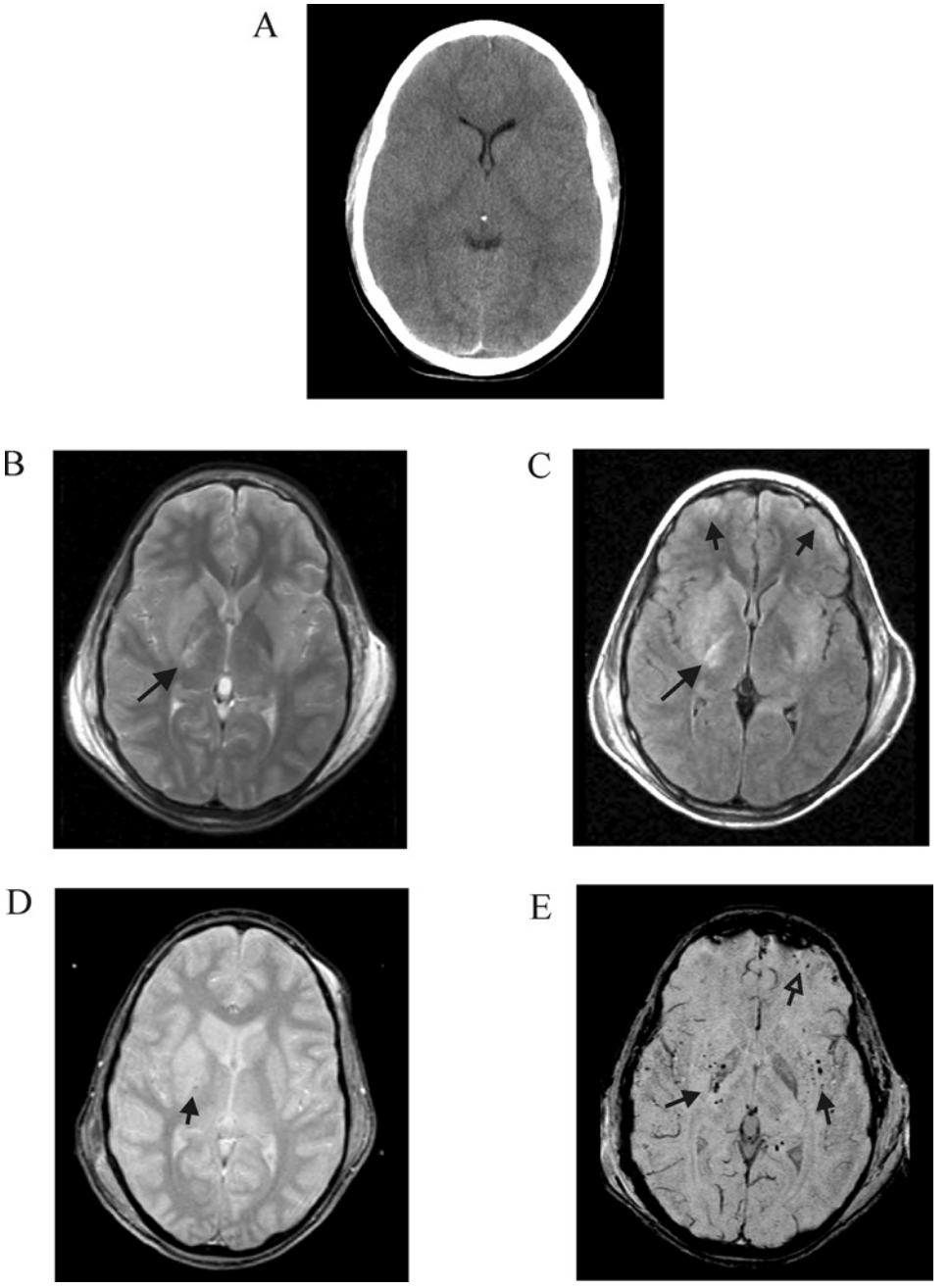

Figure 7.2. Magnetic resonance imaging findings of diffuse axonal injury (DAI) in a 10-year-old boy who was struck by a car. He had an initial GCS score of 3, was in a coma for 11 days, and had elevated ICP. His admission CT scan was normal (**A**). MRI was obtained 2 days after injury. Subtle hyperintense signal is seen in the right basal ganglia and posterior limb of the internal capsule (*arrow*), on the T2-weighted images (**B**). The FLAIR sequence (**C**) accentuates the edema in those areas (*long arrow*), as well as along the periphery of the frontal lobes (*short arrows*). The standard T2*-GRE sequence (D) shows a subtle punctuate hypointense focus in the right internal capsule (*arrow*). The SWI technique (a modified T2*-GRE sequence) shows multiple tiny hemorrhagic foci within the bilateral basal ganglia and capsular white matter (*closed arrows*) as well as within the left frontal contusion (*open arrow*) (E). (Reprinted with the kind permission of Springer Science+Business Media from Tong KA, Oyoyo U, Holshouser BA, Ashwal S. Neuroimaging for Traumatic Brain Injury. In Medina LA, Blackmore CC (eds): Evidence-Based Imaging: Optimizing Imaging in Patient Care. New York: Springer Science+Business Media, 2006.).

Case 2: Example of MR Spectroscopy

This case study (Fig. 7.3) illustrates metabolite changes in single voxel short echo time proton spectra (TE = 20 ms) from a young adult male patient admitted to hospital with severe TBI (GCS of 4) following a motor vehicle accident, compared to a normal age-matched control subject.

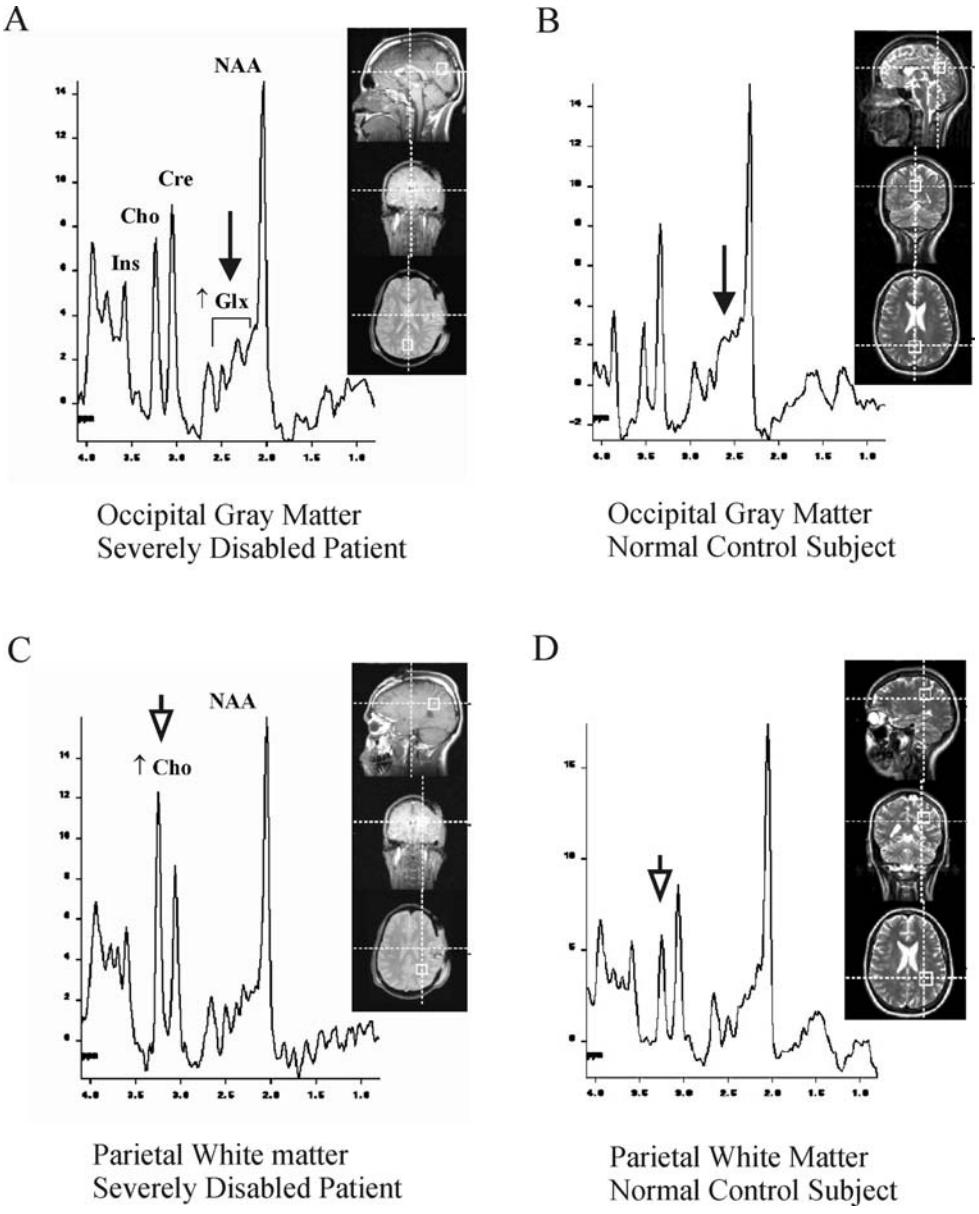

Figure 7.3. Metabolite changes in single voxel short echo time proton spectra (TE = 20 ms) from a young adult male patient hospitalized with severe TBI (GCS of 4) following a motor vehicle accident compared to a normal 27-year-old control subject. (**A**) is taken from occipital gray matter shows increased glutamate/glutamine (Glx) compared to the control spectrum (**B**) (*arrows*). (**C**) is taken from parieto-occipital white matter shows increased choline (Cho) compared to the control spectrum (**D**) (*arrowheads*). Evaluation at 6 months after the injury revealed severe disabilities (GOS of 3) in this patient. (Reprinted with the kind permission of Springer Science+Business Media from Tong KA, Oyoyo U, Holshouser BA, Ashwal S. Neuroimaging for Traumatic Brain Injury. In Medina LA, Blackmore CC (eds): Evidence-Based Imaging: Optimizing Imaging in Patient Care. New York: Springer Science+Business Media, 2006.).

Suggested Protocols for Acute TBI Imaging

CT

Standard and bone algorithms; viewed with brain, intermediate, and bone windows. Axial 5 mm images.

MR

T1-weighted, T2-weighted, FLAIR, T2*-weighted GRE, DWI.

Future Research

- Promising CHALICE pediatric head trauma prediction rule needs to be validated in actual practice.
- Clinical trials have been disappointing in TBI research, perhaps due to different mechanisms of injury included in trials; but also probably due to nonuniformity in classification of injuries and outcomes. There is a need for a consistent, widely accepted classification of information to facilitate comparisons of different groups of patients and institutions. The vast amount of clinical and imaging data may yield elaborate approaches; however, this must be balanced with clinical practicality. The practice guideline should be simple, relevant, reliable, and acceptable to clinicians in routine practice (94).
- More research is needed to develop a multimodal prognostic index for a wide range of disabilities.
- Larger, prospective studies are needed to evaluate the sensitivity, specificity, predictive accuracy, and cost-effectiveness of various neuroimaging methods in TBI.

References

1. Servadei F, Teasdale G, Merry G [on behalf of the Neurotraumatology Committee of the World Federation of Neurosurgical Societies]. J Neurotrauma 2001;18; 657–664.
2. Cushman JG, Agarwal N, Fabian TC, Garcia V, Nagy KK, Pasquale MD et al.; EAST Practice Management Guidelines Work Group. J Trauma 2001;51:1016–1026.
3. Iverson GL, Lovell MR, Smith S, Franzen MD. Brain Inj 2000;14:1057–1061.
4. Jennett B, Bond M. Lancet 1975;1:480–484.
5. Jennett B, Snoek J, Bond MR, Brooks N. J Neurol Neurosurg Psychiatr 1981;44:285–293.
6. van der Naalt J, van Zomeren AH, Sluiter WJ, Minderhoud JM. J Neurol Neurosurg Psychiatr 1999;66:207–213.
7. Rappaport M, Hall KM, Hopkins K, Belleza BS, Cope DN. Arch Phys Med Rehabil 1982;63: 118–123.
8. Schwab K, Grafman J, Salazar AM, Kraft J. Neurology 1993;43:95–103.
9. Guide for the Uniform Data Set for Medical Rehabilitation (including the FIM^{TM} instrument), version 5.1. Buffalo (NY): State Univ New York, 1997.
10. Boake C. Arch Phys Med Rehabil 1996;77: 765–772.
11. Dikmen S, Machamer J, Miller B, Doctor J, Temkin N. J Neurotrauma 2001;18:127–140.
12. Fiser DH. Assessing the outcome of pediatric intensive care. J Pediatr 1992;121:68–74.
13. Choi SC, Barnes TY, Bullock R, Germanson TA, Marmarou A et al. J Neurosurg 1994;81: 169–173.
14. Babikian T, Freier MC, Tong KA, Nickerson JP et al. Peds Neurol 2005;33:184–194.
15. Babikian T, Freier MC, Ashwal S, Riggs ML et al. J MRI 2006;24:801–811.
16. Torner JC, Choi S, Barnes TY. In Marion D (ed): Traumatic Brain Injury. New York: Thieme, 1998; 9–25.
17. Adekoya N, Thurman DJ, White DD, Webb KW. MMWR Surveill Summ 2002;1–14.
18. Teasdale GM. Head injury. J Neurol Neurosurg Psychiatr 1995; 58:526–539.
19. MacMillan R, Jennett B. BMJ 1981; 282: 101–107.
20. Brookes M, MacMillan R, Cully S et al. J Epidemiol Community Health 1990; 44:147–151.
21. Meythaler JM, Peduzzi JD, Eleftheriou E, Novack TA. Arch Phys Med Rehabil 2001;82:1461–1471.
22. www.cdc.gov/ncipc/tbi/TBI.htm2009
23. Swann IJ, Teasdale GM. Trauma 1999;12: 274–278.
24. Kraus JF, Fife D, Cox P et al. Am J Dis Child 1986; 140:687–693.
25. Kraus JF, Rock A, Hemyari P. Am J Dis Child 1990; 144:684–691.
26. Division of Injury Control CfDC. Am J Dis Child 1990; 144:627–646.
27. Fiser SM, Johnson SB, Fortune JB. Am Surg 1998;64:1088–1093.
28. Dunning J, Daly JP, Lomas JP et al. Arch Dis Child 2006; 91:885–891.

29. Palchak M, Holmes J, Vance C et al. Ann Emerg Med 42(4):492–506.
30. Greenes DS, Schutzman SA. Pediatrics 1999; 104:861–867.
31. Haydel MJ, Shembekar AD. Ann Emerg Med 2003; 42:507–514.
32. Haydel MJ, Preston CA, Mills TJ et al. N Engl J Med 2000; 343:100–105.
33. Dunning J, Daly JP, Malhotra R et al. Arch Dis Child 2004; 89:763–767.
34. Boran B, Boran P, Barut N. Pediatr Neurosurg 2006; 42:203–207.
35. Lloyd DA, Carty H, Patterson M et al. Lancet 1997; 349:821–824.
36. Fearnside M, McDougall P. Aust N Z J Surg 1998;68:58–64.
37. The Brain Trauma Foundation. The American Association of Neurological Surgeons. The Joint Section on Neurotrauma and Critical Care. J Neurotrauma 2000;17:597–627.
38. Oertel M, Kelly DF, McArthur D, Boscardin WJ, Glenn TC, Lee JH et al. J Neurosurg 2002;96: 109–116.
39. Servadei F, Murray GD, Penny K, Teasdale GM, Dearden M, Iannotti F et al. Neurosurgery 2000;46:70–75.
40. Stein SC, Spettell C, Young G, Ross SE. Neurosurgery 1993;32:25–30.
41. Prasad MR, Ewing-Cobbs L, Swank PR, Kramer L. Pediatr Neurosurg 2002;36:64–74.
42. Pillai S, Praharaj SS, Mohanty A, Sastry Kolluri VR. Pediatr Neurosurg 2001;34: 98–103.
43. Sganzerla EP, Tomei G, Guerra P, Tiberio F, Rampini PM, Gaini SM et al. Child's Nerv Syst 1989;5:168–171.
44. Suresh HS, Praharaj SS, Indira Devi B, Shukla D, Sastry Kolluri VR. Neurol India 2003;51: 16–18.
45. Raimondi AJ, Hirschauer J. Childs Brain 1984;11:12–35.
46. Crouchman M, Rossiter L, Colaco T, Forsyth R. Arch Dis Child 2001;84:120–124.
47. Fiser DH. J Pediatr 1992;121:69–74.
48. Orrison WW, Gentry LR, Stimac GK, Tarrell RM, Espinosa MC et al. Am J Neuroradiol 1994;15:351–356.
49. Ogawa T, Sekino H, Uzura M et al. Acta Neurochir 1992;55(Suppl.):8–10.
50. Hadley DM, Teasdale GM, Jenkins A, Condon B, Macpherson P, Patterson J et al. Clin Radiol 1988;39:131–139.
51. Gentry LR, Godersky JC, Thompson B, Dunn VD. AJR 1988;150:673–682.
52. Levin HS, Aldrich EF, Saydjari C, Eisenberg HM, Foulkes MA, Bellefleur M et al. Neurosurgery 1992;31:435–443.
53. Hirsch W, Schobess A, Eichler G, Zumkeller W, Teichler H et al. Paediatr Anaesth 2002;12: 337–344.
54. Tomberg T, Rink U, Pikkoja E, Tikk A. Acta Neurochir 1996;138:543–548.
55. Lang DA, Teasdale GM, Macpherson P, Lawrence A. J Neurosurgery 1994;80: 675–680.
56. Bonnier C, Marique P, Van Hout A et al. J Child Neurol 2007;22: 519–529.
57. Sigmund GA, Tong KA, Nickerson JP et al. Pediatr Neurol 2007; 36:217–226.
58. Wilde EA, Bigler ED, Haider JM et al. J Child Neurol 2006; 21:769–776.
59. Spanos GK, Wilde EA, Bigler ED et al. Am J Neuroradiol 2007; 28:537–542.
60. Mittl RL Jr, Grossman RI, Hiehle JF et al. Am J Neuroradiol 1994;15:1583–1589.
61. Gentry LR, Godersky JC, Thompson B. AJR 1988;150: 663–672.
62. Tong K, Ashwal S, Holshouser B, Shutter L, Herigault G, Haacke EM et al. Radiology 2003;227:332–339.
63. Tong K, Ashwal S, Holshouser BA. Ann Neurol 2004; 56:36–50.
64. Scheid R, Preul C, Gruber O, Wiggins C, von Cramon DY. Am J Neuroradiol 2003;24:1049–1056.
65. Ashikaga R, Araki Y, Ishida O. Neuroradiology 1997;39:239–242.
66. Levin HS, Mendelsohn D, Lilly MA, Yeakley J, Song J, Scheibel RS et al. Neurosurgery 1997;40:432–440.
67. Grados MA, Slomine BS, Gerring JP, Vasa R, Bryan N et al. J Neurol Neurosurg Psychiatr 2001;70:350–358.
68. Blackman JA, Rice SA, Matsumoto JA, Conaway MR, Elgin KM, Patrick PD et al. J Head Trauma Rehabil 2003;18:493–503.
69. Levin HS, Benavidez DA, Verger-Maestre K, Perachio N, Song J, Mendelsohn DB et al. Neurology 2000;54: 647–653.
70. Hou DJ, Tong KA, Ashwal S, Oyoyo U, et al. J Neurotrauma 2007;24:1558–1569.
71. Galloway NR, Tong KA, Ashwal S, Oyoyo U, Obenaus A. J Neurotrauma 2008;25: 1153–1162.
72. Schaefer P, Huisman T, Thierry AGM et al. Radiology 2004; 233:58–66.
73. Huisman TAGM, Sorensen AG, Hergan K, Gonzalez RG, Schaefer PW. J Comput Assist Tomogr 2003;27:5–11.
74. Hergan K, Schaefer PW, Sorensen AG, Gonzalez RG, Huisman TAGM. Eur Radiol 2002;12: 2536–2541.
75. Shanmuganathan K, Gullapalli RP, Mirvis SE, Roys S, Murthy P. Am J Neuroradiol 2004;25: 539–544.

76 Wozniak JR, Krach L, Ward E. Arch Clin Neuropsyhcol 2007;22(5):555–568.
77. Ptak T, Sheridan RL, Rhea JT, Gervasini AA, Yun JH et al. AJR 2003;181:1401–1407.
78. Arfenakis K, Haughton VM, Carew JD et al. AJNR 2002;23:794–802.
79. Jones DK, Dardis R, Ervine M, Horsfield MA, Jeffree M et al. Neurosurgery 2000;47:306–314.
80. Makaroff KL, Cecil KM. Care M et al. Pedicatr Radiol 2005; 35:668–676.
81. Holshouser BA, Tong K, Ashwal S et al. 2005; 26:1276–1285.
82. Ashwal S, Holshouser B, Tong K et al. J Neurotrauma 2004; 21:1539–1552.
83. Ashwal S, Holshouser BA, Tong K et al. Pediatr Res 2004;56:630–638.
84. Ashwal S, Holshouser BA, Shu SK, Simmons PL, Perkin RM, Tomasi LG et al. Pediatr Neurol 2000; 23:114–125.
85. Brenner T, Freier MC, Holshouser BA, Burley T, Ashwal S. Pediatr Neurol 2003;28:104–114.
86. Abdel-Dayem HM, Abu-Judeh H, Kumar M, Atay S, Naddaf S, El-Zeftawy H et al. Clin Nucl Med 1998;23:309–317.
87. Stamatakis EA, Wilson JT, Hadley DM, Wyper DJ. J Nucl Med 2002;43:476–483.
88. Kant R, Smith-Seemiller L, Isaac G, Duffy J. Brain Inj 1997;11:115–124.
89. Gowda NK, Agrawal D, Bal C et al. Am J Neuroradiol 2006; 27:447–451.
90. Bergsneider M, Hovda DA, McArthur DL, Etchepare M, Huang SC, Sehati N et al. J Head Trauma Rehabil 2001;16:135–148.
91. Wu HM, Huang SC, Hattori N. J Neurotrauma 2004; 21:149–161.
92. Lupi A, Bertagnoni G, Salgarello M. Clin Nucl Med 2007; 32:445–451.
93. Newsome MR, Scheibal RS, Hunter J et al. Neurocase 2007; 13:16–24.
94. Teasdale G, Teasdale E, Hadley D. J Neurotrauma 1992;9(suppl 1): 249–257.

8

Imaging of Brain Neoplasm

Soonmee Cha

Issues

I. Who should undergo imaging to exclude pediatric brain cancer?
II. What is the appropriate imaging in subjects at risk for pediatric brain cancer?
Special case: How can a tumor be differentiated from a tumor-mimicking lesion?
III. What is the role of proton magnetic resonance spectroscopy (MRS) in the diagnosis and follow-up of brain neoplasms?
IV. Can imaging be used to differentiate post-treatment necrosis from residual tumor?
V. What is the added value of functional MRI (fMRI) in the surgical planning of patients with suspected brain neoplasm or focal brain lesions?

Key Points

- Brain imaging is necessary for optimal localization, characterization, and management of pediatric brain cancer prior to surgery in patients with suspected or confirmed brain tumors (strong evidence).
- Due to its superior soft tissue contrast, multi-planar capability, and bio-safety, magnetic resonance imaging without and with gadolinium-based intravenous contrast material is the preferred method for pediatric brain cancer imaging when compared to computed tomography (moderate evidence).
- The role of proton MR spectroscopy in the diagnosis and follow-up of pediatric brain cancer remains uncertain (insufficient evidence).
- No adequate data exist on the role of imaging in monitoring pediatric brain cancer response to therapy and differentiating between tumor recurrence and therapy-related changes (insufficent evidence).

S. Cha (✉)
Department of Radiology and Biomedical Imaging, University of California San Francisco, San Francisco, CA 94143, USA
e-mail: soonmee.cha@radiology.ucsf.edu

L.S. Medina et al. (eds.), *Evidence-Based Imaging in Pediatrics*,
DOI 10.1007/978-1-4419-0922-0_8,

- There is added value of functional MRI in the surgical planning of patients with suspected brain cancer or focal brain lesion (moderate evidence).

Definition and Pathophysiology

Definition of Brain Cancer

The term brain cancer, or more commonly referred to as malignant brain tumor, is used here to represent all primary and secondary neoplasms of the brain and its covering, including the leptomeninges, dura, skull, and scalp. Pediatric brain cancer is comprised of a variety of central nervous system tumors with a wide range of histopathology, molecular/genetic profile, clinical spectrum, treatment possibilities, and patient prognosis. The pathophysiology of pediatric brain cancer is complex and dependent on various factors, such as histology, molecular and chromosomal aberration, tumor-related protein expression, primary versus secondary origin, and host factors (1–4).

Unique Challenges of Brain Cancer

When compared to systemic cancers (e.g., lung, breast, prostate, colon), brain cancer is unique in several different ways. First, the brain is covered by a tough, fibrous tissue dura matter and a bony skull that protects the inner contents. This rigid covering allows very little, if any, increase in volume of the inner content and, therefore, brain tumor cells adapt to grow in a more infiltrative rather than expansive pattern. This growth pattern limits the disruption to the underlying cytoarchitecture. Second, the brain capillaries have a unique barrier known as the blood–brain barrier (BBB), which limits the entrance of systemic circulation into the central nervous system. Cancer cells can hide behind the protective barrier of BBB, migrate with minimal disruption to the structural and physiologic milieu of the brain, and escape imaging detection since intravenous contrast agent becomes visible when there is BBB disruption, allowing the agent to leak into the interstitial space (5–9).

Epidemiology

The epidemiologic studies of brain cancer suggest that the incidence of pediatric brain cancer is rising but the actual details remain unclear. There are two fundamental problems that might explain the difficulty in elucidating epidemiological changes in pediatric brain cancer. First, the definition and histopathological criteria for each type of primary pediatric brain cancer remain inconsistent and variable. Second, there is a lack of true brain cancer registry that is critical for monitoring incidence and epidemiology. Rather, data from nine registries have been compiled since 1973 by the National Cancer Institute as the Surveillance, Epidemiology, and End Results (SEER) program and extrapolated to represent national data. These data demonstrate an overall incidence of pediatric central nervous system cancer to be 3.5 per 100,000 children less than 15 years of age. Pediatric central nervous system cancers account for about 15–20% of all childhood cancers, and the peak age is 5–8 years old. There is no definitive evidence to suggest any gender or race predilection for pediatric brain tumors. An additional source of epidemiologic information is a report from the Central Brain Tumor Registry of the United States (CBTRUS), a nonprofit agency organized for the purpose of collecting and publishing epidemiologic data for brain tumors (CBTRUS 2002). Syndromes associated with central nervous system tumors are neurofibromatosis type 1 and 2, tuberous sclerosis type 1 and 2, von Hippel–Lindau syndrome, Li–Fraumeni syndrome, nevoid basal cell carcinoma, Turcot's syndrome, Gorlin syndrome, Ataxia-telangiectasia syndrome, Gardner's syndrome, and Down syndrome (10). The molecular genetics of pediatric brain tumors may provide valuable insights into the etiology and biology of these tumors, but the specific genetic alterations for tumor development in a majority of patients remain elusive.

The most common primary pediatric brain cancers are astrocytomas, which account for approximately 50% of all pediatric CNS tumors (11). Pediatric astrocytomas can arise within the optic pathway (15–25%), cerebral hemisphere (12%), spine (10–12%), and brain stem (12%)

(12). Contrary to adult primary brain cancer, which is more common in supratentorial brain, more than half of all pediatric brain cancers occur in infratentorial brain. The most common infratentorial pediatric brain cancer is medulloblastoma/primary neuroectodermal tumor (PNET) (30–35%), closely followed by pilocytic astrocytoma (20–35%), brain stem gliomas (25%), ependymoma (10%), and other miscellaneous types (5%) (12). The long-term survival rates for the two most common types of pediatric brain cancers, namely pilocytic astrocytoma and medulloblastoma, differ substantially in that medulloblastoma tends to have poorer survival especially when it occurs in children younger than 3 years of age or those with metastatic disease at the time of initial diagnosis (12).

Overall Cost to Society

Brain cancer is a rare neoplasm but affects people of all ages (13). It is more common in the pediatric population and tends to cause high morbidity and mortality (12). The overall cost to society in dollar amount is difficult to estimate. There are very few articles in the medical literature that address the cost-effectiveness or overall cost to society in relation to imaging of brain cancer. Kovanlikaya et al. (14) studied the role and cost-effectiveness of surveillance imaging in the management of pediatric patients with brain tumor and found that surveillance imaging is an effective follow-up tool in detecting symptomatic recurrence. One of the few articles that discusses the actual monetary cost to society is a 1998 article by Latif et al. (15) from Great Britain. The team measured the mean costs of medical care for 157 patients with brain cancer in British Pounds. Based on this study, the average cost of imaging was less than 3% of the total, whereas radiotherapy was responsible for greater than 50% of the total cost. The relative contribution of imaging in this study appears unrealistically low, however, and what is not known from this report is what kind and how often imaging was done in these patients with brain cancer during their hospital stay and as out-patients. In addition, the vastly different health care reimbursement structure in Britain and the United States makes interpretation difficult.

Goals

The goals of imaging in pediatric patients with suspected brain cancer depend on when and why the imaging is being conducted; hence, it is critical to determine the main objectives prior to imaging (16). In general there are three goals for imaging in pediatric patients with suspected brain cancer: (1) diagnosis, (2) therapy planning, and (3) post-therapy disease monitoring. First, the initial imaging goal is for diagnosis. Because of its wider availability and quick imaging time, CT is often used for acute presentation, especially in the emergency room setting. Second, the goal of imaging once an abnormality is detected is for treatment planning. For this purpose, MRI with contrast is the test of choice since it has superior soft tissue resolution, multi-planar capability, and lack of ionizing radiation. In addition, if the nature of the brain lesion is still in question after the initial imaging, further imaging with MRI may be necessary to differentiate brain cancer from tumor-mimicking lesions such as infarcts, abscesses, or demyelinating lesions (17–19). Once a preliminary diagnosis of brain cancer is made and other possibilities have been excluded, the next imaging performed is for surgical planning to assist neurosurgeons. In the immediate postoperative period, the two most important imaging objectives are to determine the amount of residual tumor and to assess postoperative complications such as hemorrhage, contusion, or other brain injury. Imaging during or after therapy (radiation therapy and chemotherapy) depends on whether the purpose is for a routine follow-up or for a specific reason, such as clinical deterioration, or change in therapy. In either situation, imaging without and with intravenous contrast agent is standard, but if there is a specific question, such as cancer progression versus therapy-related changes, physiology-based imaging methods such as positron emission tomography (PET), single photon emission computed tomography (SPECT), diffusion and perfusion MR imaging, and/or proton MR spectroscopic imaging are often added to complement anatomic imaging.

Methodology

A MEDLINE search (from 1966 to 2007) was performed using PubMed (National Library of Medicine, Bethesda, Maryland) for original research publications discussing the diagnostic performance and effectiveness of imaging strategies in brain cancer. Keywords included are (1) brain tumor, (2) brain cancer, (3) pediatric, (4) CNS neoplasm, (5) diagnostic imaging, and (6) clinical evaluation. In addition, the following three cancer databases were reviewed:

1. The Surveillance, Epidemiology, and End Results (SEER) program maintained by the National Cancer Institute (www.seer.cancer.gov) for incidence, survival, and mortality rates, classified by tumor histology, brain topography, age, race, and gender. SEER is population-based reference standard for cancer data and collects incidence and follow-up data on malignant brain cancer only.
2. The Central Brain Tumor Registry of the United States (CBTRUS) (www.cbtrus.org) collects incidence data on all primary brain tumors from 11 collaborating state registries; however, follow-up data are not available.
3. The National Cancer DataBase (NCDB) (www.facs.org/cancer/ncdb) serves as a comprehensive clinical surveillance resource for cancer care in the United States. While not population based, the NCDB identifies newly diagnosed cases and conducts follow-up on all primary brain tumors from hospitals accredited by the American College of Surgeons. The NCDB is the largest of the three databases and also contains more complete information regarding treatment of tumors than either the SEER or CBTRUS databases.

Discussion of Issues

I. Who Should Undergo Imaging to Exclude Pediatric Brain Cancer?

Summary of Evidence: Determinationof which children with clinical suspicion of brain cancer should undergo imaging is a complex issue for a number of reasons. First, the three most common clinical symptoms of brain cancer are headache, seizure, and focal weakness—all of which are neither unique nor specific for the presence of brain cancer. Hence, it is difficult to perform a prospective study based on these clinical symptoms to determine whether or not imaging is indicated. Second, the clinical manifestation of brain cancer is heavily dependent on the topography of the lesion. For example, lesions in the motor cortex may have more acute presentation, whereas more insidious onset of cognitive or personality changes are commonly associated with prefrontal cortex tumors. Third, neurocognitive dysfunction may not necessarily be due to a mass lesion within the brain but can also be the secondary effects of systemic disease, chemical or hormonal imbalance, toxic exposure, drug or radiation therapy, or nonorganic neurodegenerative disorder (20, 21).

Despite the aforementioned nonspecific clinical presentation of subjects with brain cancer, there are guidelines one can use to determine who should undergo imaging (Table 8.1). A relatively acute onset of any one of these symptoms that progresses over time should strongly warrant brain imaging, preferably with MRI (strong evidence).

Supporting Evidence: It remains difficult, however, to narrow down the criteria for the "suspected" clinical symptomatology of brain cancer. In a retrospective study of 653 patients with supratentorial brain cancer, Salcman (22) found that the three most common clinical features of brain cancer were headache (70%), seizure (54%), and cognitive or personality change (52%). Similarly, Snyder et al. (23) studied 101 patients who were admitted through an emergency room and discharged with a diagnosis of brain cancer. They found that the three most frequent clinical features were headache (55%), cognitive or personality changes (50%), and ataxia (40%). Headache is by far the most common clinical presentation of brain cancer (24). Unfortunately, however, there are numerous other serious, as well as self-limiting, diseases where headache is the most prevalent presenting symptom. Table 8.1 lists various clinical symptoms that are associated with pediatric brain cancer.

Available evidence suggests that MR imaging is the imaging modality of choice in high-

risk patients with suspected brain cancer (25). Once the subject is identified as high risk for suspected brain cancer, an MRI without and with gadolinium-based contrast agent is the recommended imaging test of choice (strong evidence).

Since CT scanners are more widely available and easily performed than MR scanners, especially in an emergency department setting, it is commonly performed, even though CT is inferior to MR in lesion detection and characterization. There is no evidence to support the combination of CT and MRI improves the outcome nor cost-effective for patients with brain cancer. Table 8.2 lists advantages and limitations of CT and MRI in the evaluation of children with suspected brain cancer.

It should be noted that there is marked difference between adult and pediatric subjects with suspected brain cancer in terms of epidemiology, clinical presentation, tomography of the lesion, histologic tissue type, metastatic potential, and prognosis (26). Headache, posterior fossa symptoms such as nausea and vomiting, ataxia, and cranial nerve symptoms predominate in children due to the fact that the overwhelming majority of pediatric brain cancers occur infratentorially (12).

The two most common types of pediatric brain cancer are medulloblastoma and juvenile pilocytic astrocytoma (JPA), both of which commonly occur in the posterior fossa. Medulloblastomas and other small round blue cell tumors (pineoblastoma, primitive neuroectodermal tumor) have high propensity to spread along the leptomeningeal route within the central nervous system (10). JPAs are also commonly seen in supratentorial brain, especially near the hypothalamic region (26, 27). Prognosis differs vastly depending on the tissue histology and metastatic potential, since medulloblastoma and other small cell tumors tend to have aggressive biology and poor outcome whereas JPAs tend to have more favorable long-term prognosis (1, 12, 13).

Non-migraine, non-chronic headache in a child should raise a high suspicion for an intracranial mass lesion, especially if there are any additional posterior fossa or visual symptoms, and imaging should be conducted without delay. (See Chapter 9 on headache.)

II. What Is the Appropriate Imaging in Subjects at Risk for Pediatric Brain Cancer?

Summary of Evidence: In the high-risk children suspected of having brain cancer, MRI without and with gadolinium-based contrast agent is the imaging modality of choice (Table 8.3). There is no evidence to suggest that the addition of other diagnostic tests, such as CT, catheter angiography, or PET scan, improves either the cost-effectiveness or the outcome in the high-risk group at initial presentation (Table 8.3).

Supporting Evidence: High-risk subjects with pediatric brain cancer are defined as those children with abnormality on initial CT in conjunction with specific symptoms and signs as listed in section "Definition and Pathophysiology." There is strong evidence to suggest that MRI is the diagnostic imaging test of choice in high-risk subjects suspected of having brain cancer (16, 24, 28) (Table 8.3). For example, superiority of MRI over CT in detection of brain cancer has been supported by an animal study done by Whelan et al. (29). As aforementioned, it is not uncommon for a child with suspected brain cancer to undergo unenhanced CT examination as the first imaging, often in an emergency department setting. Unenhanced CT is good for assessing acute intracranial hemorrhage, midline shift/mass effect, or hydrocephalus. CT, however, is not ideal for detecting subtle parenchymal abnormality (16). As seen in Fig. 8.1, in comparing an unenhanced CT and an enhanced MRI, a rather large abnormality can be quite subtle to detect on the CT study due to its inferior soft tissue contrast, whereas the lesion is clearly visible in the MRI. However, CT does have advantage in depicting calcium much better than MRI as can be seen in Fig. 8.1A. Contrast-enhanced CT offers improved sensitivity but the addition of iodinated contrast agent is not without risk of anaphylactic reaction (truly the risk is very low for non-ionic low osmolar contrast in children—moderate to severe reactions are less than 1:10,000). As shown in Fig. 8.2, MRI is superior to CT in its ability to depict brain cancer in multiple planes with greater soft tissue resolution and

without the use ionizing radiation. It is important to note that the addition of MRI contrast agent, gadolinium, is necessary to fully characterize the extent of disease, especially to assess leptomeningeal spread of disease (Fig. 8.2D–F) (Table 8.3). Table 8.4 lists suggested MR imaging protocols for a pediatric subject suspected of having brain cancer. Imaging strategy in pediatric brain cancer subjects should be tailored to the need of clinical management and treatment decisions.

Nuclear Medicine Imaging Tests

There has been tremendous progress in research involving various brain radiotracers, which provide the valuable functional and metabolic pathophysiology of brain cancer. Yet, the question remains as to how best to incorporate radiotracer imaging methods into diagnosis and management of patients with brain cancer. The most widely used radiotracer imaging method in brain cancer imaging is ^{201}Thalium single photon emission computed tomography (SPECT) (Table 8.3). Although very useful, it has a limited role in initial diagnosis or predicting the degree of brain cancer malignancy. Positron emission tomography using ^{18}F-2-fluoro-2-deoxy-D-glucose (FDG) radiotracer can be useful in differentiating recurrent brain cancer from radiation necrosis but, similar to SPECT, its ability as an independent diagnostic and prognostic value above that of MR imaging and histology remains debated (30) (Table 8.3).

In pediatric patients with brain cancer, it is important to assess whether imaging of the entire craniospinal axis is warranted to detect any drop metastases and staging (Table 8.3). This is especially true for children with aggressive neoplasm with high propensity for tumor spread along the cerebrospinal fluid route such as medulloblastoma/PNET and ependymoma.

In pediatric patients with suspected brain metastatic disease, MRI is the imaging test of choice, especially when leptomeningeal spread of disease is considered. CT is indicated when there is suspected calvarial metastasis. Surveillance imaging with MRI is a cost-effective way of monitoring disease stability or symptomatic progression in pediatric patients with brain cancer (14).

Special Case: How Can a Tumor Be Differentiated from a Tumor-Mimicking Lesion?

There are several intracranial disease processes—such as infarcts, radiation necrosis, demyelinating plaques, abscesses, hematomas, and encephalitis—that can mimic brain cancer and pose a diagnostic dilemma on both clinical presentation and conventional magnetic resonance (MR) imaging (18, 31–35). On imaging, any one of these lesions and brain cancer can both demonstrate contrast enhancement, peri-lesional edema, varying degrees of mass effect, and central necrosis.

There are numerous reports in the literature of misdiagnosis and mismanagement of individuals who were erroneously thought to have brain cancer and, in some cases, went on to surgical resection for histopathologic confirmation (36–38). Surgery is clearly contraindicated in these patients and can lead to unnecessary increase in morbidity and mortality. A large acute demyelinating plaque, in particular, is notorious for mimicking an aggressive brain cancer (17, 39). Due to the presence of mitotic figures and atypical astrocytes, this uncertainty occurs not only on clinical presentation and imaging but also on histopathological examination (34). The consequence of unnecessary surgery in subjects with tumor-mimicking lesions can be quite grave, and hence every effort should be made to differentiate them from brain cancer.

Anatomic imaging of the brain suffers from nonspecificity and its inability to differentiate tumor from tumor-mimicking lesions (17). Recent developments in non-anatomic, physiology-based MRI methods, such as diffusion/perfusion MRI and proton spectroscopic imaging, promise to provide information not readily available from structural MRI and improve diagnostic accuracy. However, review of current literature suggests that none of these physiology-based MRI methods have shown sufficient specificity in pediatric brain cancer imaging to alter treatment decision (e.g., avoid tissue diagnosis) or differentiate tumor and tumor-mimicking lesion.

Table 8.5 lists neurological diseases that can mimic brain cancer both on clinical grounds and

on imaging. By using diffusion-weighted imaging, acute infarct and abscess could readily be distinguished from brain cancer since reduced diffusion is seen with the first two entities. Highly cellular brain cancer can have reduced diffusion (40) but may not have the same degree of reduced diffusion as acute infarct or abscess (41–44).

III. What Is the Role of Proton Magnetic Resonance Spectroscopy (MRS) in the Diagnosis and Follow-Up of Brain Neoplasms?

Summary of Evidence: The Blue Cross Blue Shield Association (BCBSA) Medical Advisory Panel concluded that the MRS in the evaluation of suspected brain cancer did not meet the Technology Evaluation Center (TEC) criteria as a diagnostic test, hence further studies in a prospectively defined population are needed. A similar conclusion was obtained by the systematic literature review done by Hollingworth et al. (45). However, the study highlighted two important findings in the literature (1): one large study demonstrating a statistically significant increase in diagnostic accuracy for indeterminate brain lesions from 55%, based on MR imaging, to 71% after analysis of ^{1}H-MR spectroscopy (45) and (2) several studies have found that ^{1}H-MR spectroscopy is highly accurate for distinguishing high- and low-grade gliomas, though the incremental benefit of ^{1}H-MR spectroscopy in this setting is less clear (45).

Supporting Evidence: No systematic review of MRS has been done only for pediatric patients with brain neoplasms. The systematic reviews available include adult and pediatric patients. The Blue Cross and Blue Shield Association (BCBSA) Medical Advisory Panel made the following judgments about whether ^{1}H-MRS for evaluation of suspected brain tumors meets the BCBSA Technology Evaluation Center (TEC) criteria based on the available evidence (46). The Advisory Panel reviewed seven published studies that included a total of up to 271 subjects (47–53). These seven studies were selected for inclusion in the review of evidence because (1) the sample size was at least 10; (2) criteria for a positive test were specified; (3) there was a method to confirm ^{1}H-MRS diagnosis; and (4) the report provided sufficient data to calculate diagnostic test performance (sensitivity and specificity). The reviewers specifically addressed whether ^{1}H-MRS for evaluation of suspected brain tumors meets the following five TEC criteria:

1. The technology must have approval from the appropriate governmental regulatory bodies.
2. The scientific evidence must permit conclusions concerning the effect of the technology on health outcomes.
3. The technology must improve the net health outcomes.
4. The technology must be as beneficial as any established alternatives.
5. The improvement must be attainable outside the investigational settings.

With the exception of the first criterion, the reviewers concluded that the available evidence on ^{1}H-MRS in the evaluation of brain neoplasm was insufficient. The TEC also concluded that the overall body of evidence does not provide strong and consistent evidence regarding the diagnostic test characteristics of MRS in determining the presence or absence of brain neoplasm, both for differentiation of recurrent/residual tumor versus delayed radiation necrosis (53) and for diagnosis of brain tumor versus other non-tumor diagnosis (47, 48, 50–52). Assessment of the health benefit of MRS in avoiding brain biopsy was evaluated in two studies (47, 52), but the results were limited by study limitations. Therefore, human studies conducted on the use of MRS for brain tumors demonstrate that this non-invasive method is technically feasible and suggest potential benefits for some of the proposed indications. However, there is a paucity of high quality direct evidence demonstrating the impact on diagnostic thinking and therapeutic decision making.

The systematic review by Hollingworth et al. showed no articles evaluated patient health or cost-effectiveness (45). Methodologic quality was mixed; most used histopathology as the reference standard but did not specify blinded interpretation of histopathology (45). One large study demonstrated a statistically significant increase in diagnostic accuracy for indeterminate brain lesions from 55%, based on MR imaging, to 71% after analysis of ^{1}H-

MR spectroscopy (45). Several studies have found that ^{1}H-MR spectroscopy is highly accurate for distinguishing high- and low-grade gliomas, though the incremental benefit of ^{1}H-MR spectroscopy in this setting is less clear. Interpretation for the other clinical subgroups is limited by the small number of studies (45).

IV. Can Imaging Be Used to Differentiate Post-treatment Necrosis from Residual/Recurrent Tumor?

Summary of Evidence: No adequate data exist on the role of imaging in monitoring pediatric brain cancer response to therapy and differentiating between tumor recurrence and therapy-related changes (insufficient evidence).

Supporting Evidence: Imaging differentiation of post-treatment necrosis and residual/recurrent tumor is challenging because they can appear similar and can coexist in a single given lesion. Hence, the traditional anatomy-based imaging methods have a limited role in the accurate differentiation of the two entities. Nuclear medicine imaging techniques such as single photon emission computed tomography (SPECT) and ^{18}F-fluorodeoxyglucose (FDG) positron emission tomography (PET) have been proposed as a diagnostic alternative, particularly when co-registered with MRI to provide functional information on tissue metabolism and oxygen consumption, and thus offer a theoretical advantage over anatomic imaging in differentiating tissue necrosis and active tumor. Chao et al. (54) studied 47 patients with brain tumors treated with stereotactic radiosurgery and followed with FDG PET. For all tumor types, the sensitivity of FDG PET for diagnosing tumor was 75% and the specificity was 81%. For brain metastasis without MRI co-registration, FDG PET had a sensitivity of 65% and a specificity of 80%. For brain metastasis with MRI co-registration, FDG PET had a sensitivity of 86% and specificity of 80%. MRI co-registration appears to improve the sensitivity of FDG PET, making it a useful modality to distinguish between radiation necrosis and recurrent brain metastasis (54). Khan et al. (55) studied the value of SPECT versus PET in 19 patients with evidence of tumor recurrence in CT or MR images using both 201TI SPECT and FDG PET imaging and were unable to detect a statistically significant difference in sensitivity or specificity between the two scans. They found both techniques to be sensitive for tumor recurrence for lesions 1.6 cm or larger and concluded that SPECT, given its greater availability, simplicity, ease of interpretation, and lower cost, is a better method of choice (55). However, there is insufficient data to determine whether SPECT, PET, or any other imaging modality can confidently discriminate tumor recurrence from treatment effect.

V. What Is the Added Value of Functional MRI (fMRI) in the Surgical Planning of Patients with Suspected Brain Neoplasm or Focal Brain Lesions?

Summary of Evidence: The addition of fMRI in the surgical planning of patients with suspected brain neoplasm or focal brain lesions can influence diagnostic and therapeutic decision making (moderate evidence).

Supporting Evidence: Functional MRI is a non-invasive tool to assess brain function and has been around since the early 1990s, largely as a research tool with limited clinical availability and application. Over the past several years, however, fMRI has crossed over to the clinical realm and has gained more acceptance as a useful clinical tool. The growing use of fMRI in clinical areas include mapping of critical or eloquent areas such as the motor cortex in patients undergoing brain surgery, early identification of psychiatric disorder, and measurement of the effect of therapies on neurodegenerative and neurodevelopmental disorders. Medina et al. (56) evaluated the effect of adding fMRI on diagnostic work-up and treatment planning in 53 patients with seizure disorders who are candidates for surgical treatment. They found that fMRI results influenced diagnostic and therapeutic decision making. Specifically, the fMRI results indicated language dominance changed, confidence level in identification of critical brain function areas increased, patient and family counseling were altered, and intraoperative mapping and surgical approach were altered (56).

Take Home Tables

Tables 8.1 and 8.2 show clinical symptoms of brain cancer and a comparison of MR/CT, respectively. Table 8.3 shows the sensitivity and specificity of brain tumor imaging. Table 8.4 shows a protocol of MR imaging of suspected brain cancer. Table 8.5 lists lesions mimicking brain cancer.

Table 8.1. Clinical symptoms suggestive of a brain cancer

- **Non-migraine, non-chronic headache of moderate to severe degree (see Chapter 9 on headache)**
- **Partial complex seizure**
- **Focal neurological deficit**
- **Speech disturbance**
- **Cognitive or personality change**
- **Visual disturbance**
- **Altered consciousness**
- **Sensory abnormalities**
- **Gait problem or ataxia**
- **Nausea and vomiting without other gastrointestinal illness**
- **Papilledema**
- **Cranial nerve palsy**

Reprinted with the kind permission of Springer Science+Business Media from Cha S. Imaging of Brain Cancer. In Medina LS, Blackmore CC (eds.): Evidence-Based Imaging: Optimizing Imaging in Patient Care. New York: Springer Science+Business Media, 2006.

Table 8.2. Comparison of CT and MRI

	Advantages	Limitations
Computed tomography (CT)	• Widely available • Short imaging time • Lower cost • Excellent for detection of acute hemorrhage, calcification?, or bony abnormality	• Inferior soft tissue resolution • Prone to artifact in posterior fossa • Ionizing radiation • Risk of allergy to iodinated contrast agent
Magnetic resonance imaging (MRI)	• Multi-planar capability • Superior soft tissue resolution • No ionizing radiation • Safer contrast agent (gadolinium-based) profile	• Higher cost • Not as widely available • Suboptimal for detection of acute hemorrhage or bony/calcific abnormality

Reprinted with the kind permission Springer Science+Business Media from Cha S. Imaging of Brain Cancer. In Medina LS, Blackmore CC (eds.): Evidence-Based Imaging: Optimizing Imaging in Patient Care. New York: Springer Science+Business Media, 2006.

Table 8.3. Diagnostic performance (sensitivity and specificity) of brain tumor imaging

Type of brain cancer	Imaging modality	Sensitivity (%)	Specificity (%)
Primary brain cancer	MRI with contrast	Gold standard	–
	CT with contrast	87	79
Primary brain cancer in children (Medina et al.)	MRI	92	99
	CT	81	92
Brain metastasis	MRI with single dose contrast	93–100	–
	MRI without contrast	36	–
	^{201}Tl SPECT	70	–
	^{18}FDG PET	82	38
Recurrent tumor versus treatment-related necrosis	^{201}Tl SPECT	92	88
	^{18}FDG PET		
	MRI with co-registration	86	80
	MRI without co-registration	65	80

Adapted with permission of Elsevier from Hutter A, Schweyte KE, Bierhals AJ, McKinstry RC. Brain neoplasms: epidemiology, diagnosis, and prospects for cost-effective imaging. Neuroimag Clin N Am 2003;13:237–250.

Table 8.4. MR imaging protocol for a subject with suspected brain cancer

- **3D Localizer**
- **Axial and sagittal pre-contrast T1-weighted imaging**
- **Diffusion-weighted imaging**
- **Axial fluid-attenuated inversion recovery**
- **Axial T2-weighted imaging**
- **Axial, coronal, and sagittal post-contrast T1-weighted imaging**
- **Optional: dynamic contrast-enhanced perfusion MR imaging**
- **Proton MR spectroscopic imaging**

Reprinted with the kind permission of Springer Science+Business Media from Cha S. Imaging of Brain Cancer. In Medina LS, Blackmore CC (eds.): Evidence-Based Imaging: Optimizing Imaging in Patient Care. New York: Springer Science+Business Media, 2006.

Table 8.5. Brain cancer-mimicking lesions

- **Infarct**
- **Radiation necrosis**
- **Abscess**
- **Demyelinating plaque**
- **Subacute hematoma**
- **Encephalitis**

Reprinted with the kind permission of Springer Science+Business Media from Cha S. Imaging of Brain Cancer. In Medina LS, Blackmore CC (eds.): Evidence-Based Imaging: Optimizing Imaging in Patient Care. New York: Springer Science+Business Media, 2006.

Imaging Case Studies

Case 1

Figure 8.1 presents image of an 8-year-old girl with headache and seizure and a pathologic diagnosis of ependymoma.

Figure 8.1. An 8-year-old girl with headache and seizure and a pathologic diagnosis of ependymoma. **A**: Unenhanced CT image through the level of frontal lobe demonstrates a subtle mass lesion in the right frontal lobe associated with scattered areas of calcification (*small black arrows*). **B**: Fluid-attenuated inversion recovery (FLAIR) MR image better demonstrates the large frontal lobe mass (*white arrow*) compressing the adjacent ventricle. **C**: Contrast-enhanced T1-weighted MR image shows heterogeneous enhancement of the mass more intensely involving the lateral portion (*large black arrow*).

Case 2

Figure 8.2 presents images of a 7-year-old girl with nausea and vomiting and a pathologic diagnosis of medulloblastoma.

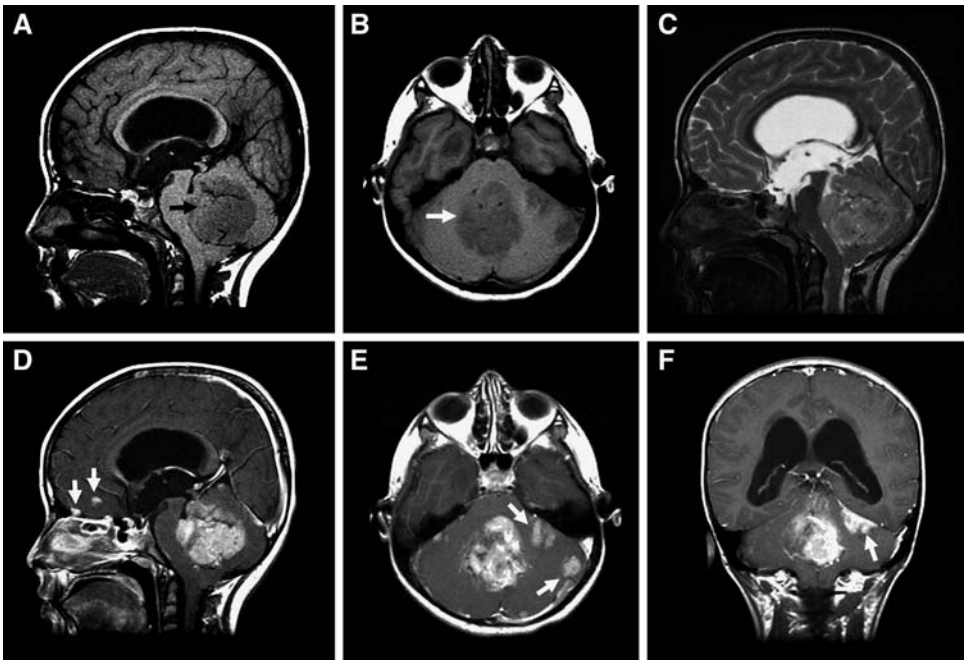

Figure 8.2. A 7-year-old girl with nausea and vomiting and a pathologic diagnosis of medulloblastoma. Sagittal (**A**) and axial (**B**) unenhanced T1-weighted and sagittal T2-weighted (**C**) images of the brain shows a large midline mass (*arrows*) within the posterior fossa near the fourth ventricle. Sagittal (**D**), axial (**E**), and coronal enhanced T1-weighted (**F**) images demonstrate widespread leptomeningeal spread of tumor (*white arrows*) both within supra- and infratentorial brain characteristic of medulloblastoma.

Suggested Imaging Protocols for Brain Neoplasms

Shown in Table 8.4.

Future Research

- Identification and validation of noninvasive imaging biomarkers of tumor activity during and after therapy.
- Development and clinical validation of physiologic MR imaging to assess biologic and molecular features of pediatric brain cancer.
- National database dedicated to epidemiology of pediatric brain cancer.

References

1. Burger PC, Vogel FS. In Burger PC, Vogel FS (eds.). Surgical Pathology of the Central Nervous System and Its Coverings. New York: Wiley, 1982;223–266.
2. Burger PC, Vogel FS, Green SB, Strike TA. Cancer 1985; 56:1106–1111.
3. Kleihues P, Sobin LH. World Health Organization classification of tumors. Cancer 2000; 88:2887.
4. Kleihues P, Ohgaki H. Toxicol Pathol 2000; 28:164–170.
5. Go KG. Adv Tech Stand Neurosurg 1997; 23: 47–142.
6. Sato S, Suga S, Yunoki K, Mihara B. Acta Neurochir Suppl 1994; 60:116–118.

7. Stewart PA, Hayakawa K, Farrell CL, Del Maestro RF. J Neurosurg 1987; 67:697–705.
8. Stewart PA, Magliocco M, Hayakawa K et al. Microvasc Res 1987; 33:270–282.
9. Abbott NJ, Chugani DC, Zaharchuk G, Rosen BR, Lo EH. Adv Drug Deliv Rev 1999; 37: 253–277.
10. Becker LE. Neuroimaging Clin N Am 1999; 9:671–690.
11. Rickert CH, Probst-Cousin S, Gullotta F. Childs Nerv Syst 1997; 13:507–513.
12. Pollack IF. Semin Surg Oncol 1999; 16:73–90.
13. DeAngelis LM. N Engl J Med 2001; 344:114–123.
14. Kovanlikaya A, Karabay N, Cakmakci H, Uysal K, Olgun N et al. Eur J Radiol 2003; 47:188–192.
15. Latif AZ, Signorini D, Gregor A, Whittle IR. Br J Neurosurg 1998; 12:118–122.
16. Ricci PE. Neuroimaging Clin N Am 1999; 9: 651–669.
17. Cha S, Pierce S, Knopp EA et al. Am J Neuroradiol 2001; 22:1109–1116.
18. Kepes JJ. Ann Neurol 1993; 33:18–27.
19. De Stefano N, Caramanos Z, Preul MC, Francis G, Antel JP et al. Ann Neurol 1998; 44: 273–278.
20. Porter RJ, Gallagher P, Thompson JM, Young AH. Br J Psychiatry 2003; 182:214–220.
21. Meyers CA. Oncology (Huntingt) 2000; 14:75–79; discussion 79, 81–72, 85.
22. Salcman M. In Wilkins R, Rengachary S (eds.). Neurosurgery. New York: McGraw-Hill, 1985;579–590.
23. Snyder H, Robinson K, Shah D, Brennan R, Handrigan M. J Emerg Med 1993; 11:253–258.
24. Medina LS, Kuntz KM, Pomeroy S. Pediatrics 2001; 108:255–263.
25. Claussen C, Laniado M, Kazner E, Schorner W, Felix R. Neuroradiology 1985; 27:164–171.
26. Miltenburg D, Louw DF, Sutherland GR. Can J Neurol Sci 1996; 23:118–122.
27. Davis FG, McCarthy BJ. Curr Opin Neurol 2000; 13:635–640.
28. Medina LS, Pinter JD, Zurakowski D, Davis RG, Kuban K et al. Radiology 1997; 202: 819–824.
29. Whelan HT, Clanton JA, Wilson RE, Tulipan NB. Pediatr Neurol 1988; 4:279–283.
30. Benard F, Romsa J, Hustinx R. Semin Nucl Med 2003; 33:148–162.
31. Morgenstern LB, Frankowski RF. J Neurooncol 1999; 44:47–52.
32. Barcikowska M, Chodakowska M, Klimowicz I, Liberski PP. Folia Neuropathol 1995; 33:55–57.
33. Kim YJ, Chang KH, Song IC et al. Am J Roentgenol 1998; 171:1487–1490.
34. Zagzag D, Miller DC, Kleinman GM, Abati A, Donnenfeld H et al. Am J Surg Pathol 1993; 17:537–545.
35. Itto H, Yamano K, Mizukoshi H, Yamamoto S. No To Shinkei 1972; 24:455–458.
36. Babu R, Huang PP, Epstein F, Budzilovich GN. J Neurooncol 1993; 17:37–42.
37. Kurihara N, Takahashi S, Furuta A et al. Clin Imaging 1996; 20:171–177.
38. Nesbit GM, Forbes GS, Scheithauer BW, Okazaki H, Rodriguez M. Radiology 1991; 180: 467–474.
39. Giang DW, Poduri KR, Eskin TA et al. Neuroradiology 1992; 34:150–154.
40. Gauvain KM, McKinstry RC, Mukherjee P et al. Am J Roentgenol 2001; 177:449–454.
41. Chang SC, Lai PH, Chen WL et al. Clin Imaging 2002; 26:227–236.
42. Chan JH, Tsui EY, Chau LF et al. Comput Med Imaging Graph 2002; 26:19–23.
43. Guzman R, Barth A, Lovblad KO et al. J Neurosurg 2002; 97:1101–1107.
44. Schaefer PW. Top Magn Reson Imaging 2000; 11:300–309.
45. Hollingworth W, Medina LS, Lenkinski RE et al. Am J Neuroradiol 2006; 27:1404–1411.
46. Center TE. TEC Bull (Online) 2003;20:23–26.
47. Adamson AJ, Rand SD, Prost RW, Kim TA, Schultz C et al. Radiology 1998; 209:73–78.
48. Rand SD, Prost R, Haughton V et al. Am J Neuroradiol 1997; 18:1695–1704.
49. Shukla-Dave A, Gupta RK, Roy R et al. Magn Reson Imaging 2001; 19:103–110.
50. Kimura T, Sako K, Gotoh T, Tanaka K, Tanaka T. NMR Biomed 2001; 14:339–349.
51. Wilken B, Dechent P, Herms J et al. Pediatr Neurol 2000; 23:22–31.
52. Lin A, Bluml S, Mamelak AN. J Neurooncol 1999; 45:69–81.
53. Taylor JS, Langston JW, Reddick WE et al. Int J Radiat Oncol Biol Phys 1996; 36:1251–1261.
54. Chao ST, SUh JH, Raja S, Lee S, Barnett G. Int J Cancer 2001; 96:191–197.
55. Khan D, Follett KA, Bushnell DL et al. Am J Roentgenol 1994; 163:1459–1465.
56. Medina LS, Bernal B, Dunoyer C et al. Radiology 2005; 236:247–253.

9

Children with Headache: Evidence-Based Role of Neuroimaging

L. Santiago Medina, Michelle Perez, and Elza Vasconcellos

Issues

I. When is neuroimaging appropriate in children with headache?
II. What is the sensitivity and specificity of CT and MR imaging for space-occupying lesions?
III. What is the sensitivity and specificity of imaging in patients with headache and subarachnoid hemorrhage suspected of having an intracranial aneurysm?
IV. What is the role of advance imaging techniques in primary headache disorders?
V. What is the cost-effectiveness of neuroimaging in patients with headache?

Key Points

- Although most headaches in children are benign in nature, a small percentage is caused by serious diseases such as brain neoplasm.
- Neuroimaging is recommended in children with headache and an abnormal neurologic examination or seizures (moderate evidence).
- Sensitivity and specificity of MR imaging are greater than CT for intracranial lesions. For intracranial surgical space-occupying lesions, however, there is no difference in diagnostic performance between MR imaging and CT (limited evidence).
- Conventional CT angiography (CTA) and MR angiography have sensitivities greater than 85% for aneurysms greater than 5 mm. Multidetector CT (MDCT) sensitivity and specificity are greater than 90% for aneurysms greater than 4 mm (moderate evidence).
- MDCTA and digital subtraction angiography (DSA) have similar sensitivities and specificities for aneurysms >4 mm (moderate evidence).

L.S. Medina (✉)
Co-Director Division of Neuroradiology and Brain Imaging, Director of the Health Outcomes, Policy, and Economics (HOPE) Center, Department of Radiology, Miami Children's Hospital, Miami, FL 33155, USA
e-mail: santiago.medina@mch.com

L.S. Medina et al. (eds.), *Evidence-Based Imaging in Pediatrics*,
DOI 10.1007/978-1-4419-0922-0_9, © Springer Science+Business Media, LLC 2010

- Advance brain imaging may help differentiate the different types of primary headache disorders. Preliminary MRI studies in patients with migraine have demonstrated increased iron levels and increased fMRI activation in the midbrain. PET has demonstrated increased uptake in the hypothalamus and phosphorus MRS has revealed mitochondrial dysfunction in those with cluster headaches (limited evidence).

Definition and Pathophysiology

Headaches can be divided into primary and secondary (Table 9.1). Primary causes include migraine, cluster, and tension-type headaches while secondary etiologies include neoplasms, arteriovenous malformations, aneurysm, infection, trauma, and hydrocephalus. Diagnosis of primary headache disorders is based on clinical criteria as set forth by the International Headache Society (1). A detailed history and physical examination help distinguish between primary and secondary headaches. Neuroimaging should aid in the diagnosis of secondary headache disorders. Secondary headaches in children are more likely to present as acute headache, sudden onset in an otherwise healthy child, or as a chronic progressive headache, with gradual increase in frequency and severity. Acute recurrent headaches in an otherwise healthy child most often represent migraine or episodic tension-type headaches (47). Sinus disease is a common cause of acute headache. (See Chapter 11 on acute and chronic sinusitis in children.)

Epidemiology

Pediatric headache is a common health problem in children, with a significant headache reported in more than 75% by the age of 15 years (48). In approximately 50% of patients with migraines, the headache disorder starts before the age of 20 years (2). In the USA, adolescent boys and girls have a headache prevalence of 56 and 74% and a migraine prevalence of 3.8 and 6.6%, respectively (3). A small percentage of headaches in children are secondary in nature.

A primary concern in children with headache is the possibility of a brain tumor (4, 5). Although brain tumors constitute the largest group of solid neoplasms in children and are second only to leukemia in overall frequency of childhood cancers, the annual incidence is low at 3 in 100,000 (5). Primary brain neoplasms are far more prevalent in children than they are in adults (6). They account for almost 20% of all cancers in children but only 1% of cancers in adults (2). Central nervous system (CNS) tumors are the second cause of cancer-related deaths in patients younger than 15 years (7).

Overall Cost to Society

Headache is the most common and one of the most disabling type of chronic pain among children and adolescents (49, 50). The incidence of migraine peaks in adolescence, but the prevalence of migraine continues to increase and is highest in the most productive years of life between the ages of 25 and 55 years (8, 9). The direct and indirect annual cost of migraine in the USA has been estimated at more than $5.6 billion (10). A recent US study showed that migraine families incur far higher direct and indirect healthcare costs (70% higher than non-migraine families) with most of the difference concentrated in outpatient costs (51). Of interest, in families that the sole migraineur was a child versus a parent the total healthcare costs per family were about $600 higher and almost $2,500 higher when both a parent and child were affected (51). Work absence days, short-term disability, and workman's compensation days all were higher among migraine families than among families without a migraineur (51).

Goals

- To diagnose the secondary causes of headache (Table 9.1) so that appropriate treatment can be instituted.
- Exclude secondary etiologies of headache in patients with atypical primary headache disorders.

- Decrease the risk of brain herniation prior to lumbar puncture by excluding intracranial space-occupying lesions.
- Study the role of advance brain imaging in the differentiation of the types of primary headache disorders.

Methodology

MEDLINE search using Ovid (Wolters Klumer US Corporation, New York, NY) and PubMed (National Library of Medicine, Bethesda MD) was used. Systematic literature review was performed from 1966 to January 2008. Keywords included (1) headache, (2) cephalgia, (3) diagnostic imaging, (4) clinical examination, (5) practice guidelines, and (6) surgery. The Cochrane Collaboration had no reviews of imaging for headache.

Discussion of Issues

I. When Is Neuroimaging Appropriate in Children with Headache?

Summary of Evidence: Determination of the appropriateness of imaging is made based on the frequency, pattern, family history, and associated seizure or neurological findings (Table 9.2) (moderate evidence). These guidelines reinforce the primary importance of careful acquisition of the medical history and performance of a thorough examination, including a detailed neurologic examination (11). Among children at risk for brain lesions based on these signs and symptoms, neuroimaging with either MR imaging or CT is valuable in combination with close clinical follow-up (Table 9.2).

Supporting Evidence: In 2002, the American Academy of Neurology and Child Neurology Society published evidence-based neuroimaging recommendations for children (12). Six studies (one prospective and five retrospective) met inclusion criteria (moderate evidence). Data on 605 of 1275 children with recurrent headache who underwent neuroimaging found only 14 (2.3%) with nervous system lesions that required surgical treatment. All 14 children had definite abnormalities on neurologic examination. The recommendations from this study were as follows: (1) neuroimaging should be considered in children with an abnormal neurologic examination or other physical findings that suggest CNS disease. Variables that predicted the presence of a space-occupying lesion included (a) headache of less than 1-month duration, (b) absence of family history of migraine, (c) gait abnormalities, and (e) occurrence of seizures; (2) neuroimaging is not indicated in children with recurrent headaches and a normal neurologic examination; (3) neuroimaging should be considered in children with recent onset of severe headache, change in the type of headache, or if there are associated features suggestive of neurologic dysfunction.

Medina and colleagues (11) performed a 4-year retrospective study of 315 children with no known underlying CNS disease who underwent brain imaging for a chief complaint of headache (moderate evidence). All patients underwent brain MR imaging. Sixty-nine patients also underwent brain CT. Clinical data were correlated with findings from MR imaging and CT and the final diagnosis using logistic regression. Thirteen (4%) patients had surgical space-occupying lesions, including nine malignant neoplasms, three hemorrhagic vascular malformations, and one arachnoid cyst.

In this study, they identified seven independent multivariate predictors of a surgical lesion, the strongest of which were sleep-related headache (odds ratio 5.4, 95% CI: 1.7–17.5) and no family history of migraine (odds ratio 15.4, 95% CI: 5.8–41.0). Other predictors included vomiting, absence of visual symptoms, headache of less than 6 months' duration, confusion, and abnormal neurologic examination findings. The risk of surgical lesion increased with the increased number of these seven factors ($P<0.0001$). No difference between MR imaging and CT was noted in detection of surgical space-occupying lesions, and there were no false-positive or false-negative surgical lesions detected with either modality on clinical follow-up.

In a study by Schwedt and colleagues of 241 pediatric patients with headache who had MRI or CT, 23 patients (9.5%) had findings requiring a change in management (13) (limited to moderate evidence). These included five

sinus disease, four tumors, four old infarcts, three Chiari I, two moyamoya, one intracranial vascular stenosis, one internal jugular vein occlusion, one arteriovenous malformation, one demyelinating disease, and one intracerebral hemorrhage. When sinus disease was excluded, three patients (1.2%) had normal neurologic symptoms and signs and imaging findings that resulted in a change in management (limited to moderate evidence).

II. What Is the Sensitivity and Specificity of CT and MR Imaging for Space-Occupying Lesions?

Summary of Evidence: Sensitivity and specificity of MR imaging is greater than CT for intracranial lesions. For surgical intracranial space-occupying lesions, however, there is no difference between MR imaging and CT in diagnostic performance (moderate evidence). The use of intravenous contrast material after unenhanced CT of the brain in children did not change the diagnosis frequently (moderate evidence).

Supporting Evidence: Sensitivity and specificity of CT and MR imaging for intracranial lesions is shown in Table 9.3. Medina and colleagues (moderate evidence) (11) showed that the overall sensitivity and specificity with MR imaging (92 and 99%, respectively) were higher than with CT (81 and 92%, respectively). Comparison of patients who underwent both MR imaging and CT revealed no significant disagreement between the tests for surgical space-occupying lesions (McNemar test, $P = 0.75$). The US Headache Consortium evidence-based guidelines from systematic review of the literature similarly concluded that MR imaging may be more sensitive than CT in identifying clinically insignificant abnormalities, but MRI imaging may be no more sensitive than CT in identifying clinically significant pathology (14).

A recent study by Branson et al. in 353 children with unenhanced and enhanced CT demonstrated that unenhanced CT of developing brains has high sensitivity and specificity in the diagnosis of pathologic findings (15). Sensitivity, specificity, positive predictive value, and negative predictive value for unenhanced scans were 97, 89, 87, and 97%, respectively (15). The use of contrast material led to a change in the original normal or equivocal diagnosis to an abnormal diagnosis for only 5 (2.7%) of the 183 normal unenhanced scans. Therefore, the use of intravenous contrast material after unenhanced CT of the brain in children did not change the diagnosis frequently (15).

III. What Is the Sensitivity and Specificity of CT and MRI Imaging of Patients with Headache and Subarachnoid Hemorrhage Suspected of Having an Intracranial Aneurysm?

Summary of Evidence: In North America, 80–90% of nontraumatic SAH in older children and adults is caused by the rupture of nontraumatic cerebral aneurysms (16). CT angiography and MR angiography have sensitivities greater than 85% for aneurysms greater than 5 mm. Most recent studies with newer generations of multidetector CT report sensitivity and specificity greater than 90% for aneurysms greater than 4 mm (moderate evidence). Studies that have compared sensitivity and specificity of CTA and digital subtraction angiography (DSA) report similar sensitivities and specificities (moderate evidence). The sensitivity of CTA and MRA examinations drops significantly for aneurysms less than 5 mm.

Supporting Evidence: White et al. (17) searched the literature from 1988 to 1998 to find studies with 10 or more subjects in which the conventional angiography results were compared with noninvasive imaging. They included 38 studies, which scored more than 50% on evaluation criteria by using intrinsically weighted standardized assessment to determine suitability for inclusion (moderate evidence).

The rates of aneurysm accuracy for CT angiography and MR angiography were 89 and 90%, respectively. The study showed greater sensitivity for aneurysms larger than 3 mm than for aneurysms of 3 mm or smaller for CT angiography (96 verses 61%) and for MR angiography (94 versus 38%).

White et al. (18) also performed a prospective blinded study in 142 patients who underwent intra-arterial digital subtraction angiography to detect aneurysms (moderate evidence). Results

were compared with CT angiography and MR angiography. The accuracy rates per patient for the best observer were 87 and 85% for CT angiography and MR angiography, respectively. The accuracy rates for brain aneurysm for the best observer were 73 and 67% for CT angiography and MR angiography, respectively. The sensitivity for the detection of aneurysms 5 mm or larger was 94% for CT angiography and 86% for MR angiography. For aneurysms smaller than 5 mm, sensitivities for CT angiography and MR angiography were 57 and 35%, respectively.

More recent studies using CTA have shown even higher sensitivity and specificity, which may reflect technological improvements. Uysal and colleagues using spiral CT in 32 cases with aneurysm size from 3 to 13 mm (19) reported sensitivity of 97% and specificity of 100% (limited evidence). Teksam and colleagues studied 100 consecutive patients with 113 aneurysms with MDCT (20) and reported sensitivity for detecting aneurysms of less than 4 mm, 4–10 mm, and greater than 10 mm on a per aneurysm basis of 84, 97, and 100%, respectively (moderate evidence). Overall specificity was 88%. Karamessini and colleagues using CTA with 3D techniques in 82 consecutive patients (21) demonstrated sensitivity of 89% and specificity of 100% for CTA and sensitivity of 88% and specificity of 98% for DSA when compared with the reference standard of surgical findings (moderate evidence). Therefore, CTA was equivalent to DSA. Tipper and colleagues with 16-row MDCT in 57 patients with 53 aneurysms (22) reported sensitivity and specificity of 96.2 and 100% for both CTA and DSA, respectively (moderate evidence). In this study, mean diameter of the aneurysm was 6.3 mm with a range of 1.9–28.1 mm (22). Study published by Taschner and colleagues (23) in 2007 in 27 consecutive patients with 24 aneurysms using a 16-row multisection CT angiography (CTA) reported an overall sensitivity and specificity of 100 and 83%, respectively (limited evidence). Study by Papke and colleagues comparing digital subtraction angiography (DSA) with 16-row CTA in 87 patients (24) reported sensitivity and specificity of 98 and 100% for DSA and CTA, respectively (moderate evidence). Yoon and colleagues using 16-row multidetector CTA in 85 patients (25) had overall sensitivity and specificity of 92.5 and 93.3%, respectively (moderate evidence). For aneurysms less than 3 mm, however, sensitivity decreased for reader 1 and reader 2 to 74.1 and 77.8%, respectively (25). More recent study done by Lubicz and colleagues (26) in 54 consecutive patients with 67 aneurysms using a 64-row multisection CT angiography reported an overall sensitivity and specificity of 94 and 90.2%, respectively (moderate evidence). For aneurysms less than 3 mm, CTA had a mean sensitivity of 70.4% (26). Intertechnique and interobserver agreements were good for aneurysm detection with a mean Kappa of 0.673 (26). Agid and colleagues (27) in 73 patients with 47 aneurysms using a 64-row multisection CT angiography reported an overall sensitivity and specificity of 98 and 98%, respectively (moderate evidence).

IV. What Is the Role of Advance Imaging Techniques in Primary Headache Disorders?

Summary of Evidence: High-resolution MR technique using transverse relaxation rates have demonstrated increased tissue iron levels in the brain stem (periaqueductal gray, red nuclei, and substantia nigra in patients with headache disorders (limited evidence). Functional MR has demonstrated activation of the red nuclei and substantia nigra in patients during spontaneous migraine episodes (28, 29) (limited evidence).

In cluster headache disorders, MR phosphorus spectroscopy (^{31}P-MRS) has demonstrated brain mitochondrial dysfunction (30, 31) (limited evidence). PET has demonstrated strong activation in the hypothalamic gray matter in acute cluster headache attacks (32) (limited evidence). In contrast to migraine disorders, there is no brain stem activation during acute cluster headache episodes compared with the resting state (33). These initial studies suggest that although primary headaches such as migraine and cluster headache may share a common pain pathway—the trigeminovascular innervation—their underlying pathogenesis differs significantly (30).

Supporting Evidence: The underlying pathophysiology of migraine disorders is not well

understood (34). Conventional CT and MRI studies are usually normal with no evidence of a structural lesion. Studies have shown involvement of the nociceptive pathways in chronic daily headache and migraine (34). Study by Raskin and colleagues (35) revealed migraine-like headache in patients with electrodes implanted in the periaqueductal gray (PAG) matter. The ventral brain stem has also been identified to be involved in migraine disorders (35). There are also reports of multiple sclerosis plaque (36) and cavernous malformation (37) involving the PAG and causing migraine-like disorders. Imaging studies have been performed to study the iron homeostasis in the midbrain. High-resolution MR techniques have been used to map the transverse relaxation rates R2 (1/T2), R2∗ (1/T2∗), and R2′ (R2∗–R2) in the PAG, red nuclei (RN), and substantia nigra (SN) (38). A positive correlation (r=0.80; P<0.006) was identified between the duration of illness and the increase in R2′ (increased tissue iron levels) for patients with episodic migraine disorders and chronic daily headaches (38, 39) (limited evidence). Another study by Kruit and colleagues (40) in patients studied in a 1.5 T MR scanner revealed higher iron concentrations in the RN and putamen in patients with migraines (limited to moderate evidence); functional MR has demonstrated activation of the RN and SN in patients during spontaneous migraine episodes (28, 29) (limited evidence).

In cluster headache, in vivo MR phosphorus spectroscopy (^{31}P-MRS) has demonstrated brain mitochondrial dysfunction characterized by reduced phosphocreatine levels, an increased ADP concentration, and a reduced phosphorylation potential (30, 31) (limited evidence). In a study of nine patients, PET demonstrated strong activation in the hypothalamic gray matter in acute cluster headache attacks (32) (limited evidence). In contrast to migraine disorders, there is no brain stem activation during acute cluster headache episodes compared with the resting state (33). These initial studies suggest that, although primary headaches such as migraine and cluster headache may share a common pain pathway—the trigeminovascular innervation—their underlying pathogenesis differs significantly (30).

V. What Is the Cost-Effectiveness of Neuroimaging in Patients with Headache?

Summary of Evidence: A CEA study (41) assessed the clinical and economic consequences of three diagnostic strategies in the evaluation of children with headache suspected of having a brain tumor: MR imaging, CT followed by MR imaging for positive results (CT-MR imaging), and no neuroimaging with close clinical follow-up (41). This model suggests that MR imaging maximizes quality-adjusted life years (QALY) gained at a reasonable cost-effectiveness ratio in patients at high risk of having a brain tumor. Conversely, the strategy of no imaging with close clinical follow-up is cost saving in low-risk children. Although the CT-MR imaging strategy maximizes QALY gained in the intermediate-risk patients, its additional cost per QALY gained is high. In children with headache, appropriate selection of patients and diagnostic imaging strategies may maximize quality-adjusted life expectancy and decrease costs of medical workup.

Supporting Evidence: A CEA in children with headaches has been published in Pediatrics (41). A decision-analytic Markov model and CEA were performed incorporating the risk group pretest probability, MR imaging and CT sensitivity and specificity, tumor survival, progression rates, and cost per strategy. Outcomes were based on QALY gained and incremental cost per QALY gained.

The results were as follows: for low-risk children with chronic non-migraine headaches of more than 6 months' duration as the sole symptom (pretest probability of brain tumor, 0.01% [1 in 10,000]), close clinical observation without neuroimaging was less costly and more effective than the two neuroimaging strategies. For the intermediate-risk children, with migraine headache and normal neurologic examination (pretest probability of brain tumor, 0.4% [4 in 1,000]), CT-MR imaging was the most effective strategy but costs more than $1 million per QALY gained compared with no neuroimaging. This cost is not typically justified by health policy makers. For high-risk children with headache of less than 6 months' duration

and other clinical predictors of a brain tumor, such as an abnormal neurologic examination (pretest probability of brain tumor, 4% [4 in 100]), the most effective strategy was MR imaging, with a cost-effectiveness ratio of $113,800 per QALY gained compared with no imaging.

The cost-effectiveness ratio in the high-risk children with headache is in the comparable range of annual mammography for women aged 55–64 years at $110,000 per life-year saved (42), colonoscopy for colorectal cancer screening for persons older than 40 years at $90,000 per life-year saved (42, 43), and annual cervical cancer screening for women beginning at age 20 years at $220,000 per life-year saved (42, 44). Therefore, this CEA model supports the use of MR imaging in high-risk children.

Table 9.1. Common causes of primary and secondary headache

Primary headaches
- **Migraine**
- **Cluster**
- **Tension type**

Secondary headaches
- **Intracranial space-occupying lesions**
  - **Neoplasm**
  - **Arteriovenous malformation**
  - **Abscess**
  - **Hematoma**
- **Cerebrovascular disease**
  - **Intracranial aneurysms**
  - **Occlusive vascular disease**
- **Infection**
  - **Acute Sinusitis**
  - **Meningitis**
  - **Encephalitis**
- **Inflammation**
  - **Vasculitis**
  - **Acute disseminated encephalomyelitis**
- **Increased intracranial pressure**
  - **Hydrocephalus**
  - **Idiopathic Intracranial Hypertension (Pseudotumor cerebri)**

Reprinted with the kind permission of Springer Science+Business Media from Medina LS, Shah A, Vasconcellos E. Adults and Children with Headache: Evidence-Based Role of Neuroimaging. In Medina LA, Blackmore CC (eds): Evidence-Based Imaging: Optimizing Imaging in Patient Care. New York: Springer Science+Business, 2006.

Take Home Tables and Figures

Table 9.1 shows common causes of primary and secondary headaches. Table 9.2 summarizes clinical guidelines in children with headache. Table 9.3 shows the sensitivity and specificity of CT and MRI imaging. Figure 9.1 provides the decision trees for diagnostic workup of children with headache.

Table 9.2. Suggested guidelines for neuroimaging in pediatric patients with headache

- **Persistent headaches of less than 6 months duration**
- **Headache associated with abnormal neurologic examination**
- **Headache associated with seizures**
- **Recent onset of severe headache or change in the type of headache**
- **Persistent headache without family history of migraine**
- **Headaches that persistently awaken a child from sleep or occurs immediately upon awakening.**
- **Family or medical history of disorders that may predispose one to CNS lesions, and clinical or laboratory findings that suggest CNS involvement**

Reprinted with permission of the RSNA from Medina et al. (11).

Table 9.3. Diagnostic performance of imaging

Variable	Baseline (%)	Range (%)	References
Diagnostic tests			
MR imaging	**92**	**82–100**	**(11, 45, 46)**
Sensitivity	**99**	**81–100**	**(11, 46)**
Specificity			
CT			
Sensitivity	**81**	**65–100**	**(11, 45, 46)**
Specificity	**92**	**72–100**	**(11, 45, 46)**

Modified with the kind permission of Springer Science+Business Media from Medina LS, Shah A, Vasconcellos E. Adults and Children with Headache: Evidence-Based Role of Neuroimaging. In Medina LA, Blackmore CC (eds): Evidence-Based Imaging: Optimizing Imaging in Patient Care. New York: Springer Science+Business, 2006.

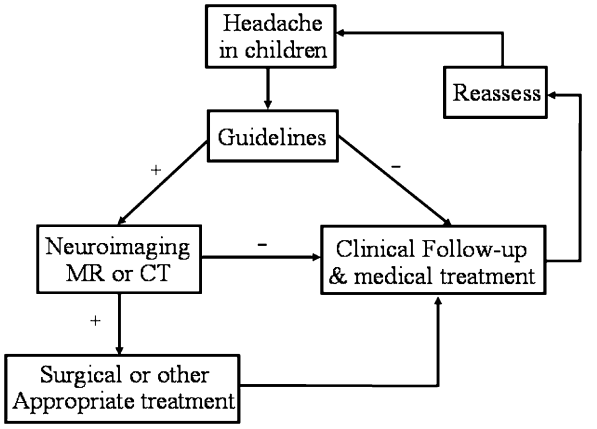

Figure 9.1. Decision tree for use in children with headache. Neuroimaging is suggested for patients who meet any of the signs or symptoms in the guidelines (Table 9.2). For patients who do not meet these criteria or those with negative findings from imaging studies, clinical observation with periodic reassessment is recommended. (Reprinted with permission of the RSNA from Medina et al. (11).).

Imaging Case Studies

Case 1: Colloid Cyst

Patient presented with headache and vomiting (Fig. 9.2).

Case 2: Chiari I

Patient presented with persistent headaches triggered by cough or exertion (valsalva maneuver) (Fig. 9.3).

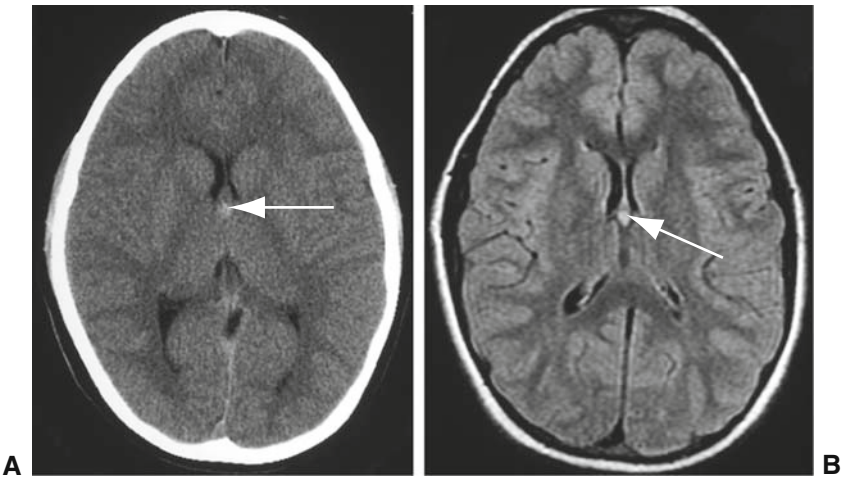

Figure 9.2. **A**: Unenhanced CT shows a small focal lesion with increased density at the level of the foramen of Monro. **B**: Axial flair sequence reveals increased T2-weighted signal in the lesion. No hydrocephalus noted. Neuroimaging findings consistent with colloid cyst. (Reprinted with permission from Medina LS, Shah A, Vasconcellos E. Adults and Children with Headache: Evidence-Based Role of Neuroimaging. In Medina LA, Blackmore CC (eds): Evidence-Based Imaging: Optimizing Imaging in Patient Care. New York: Springer Science+Business, 2006.).

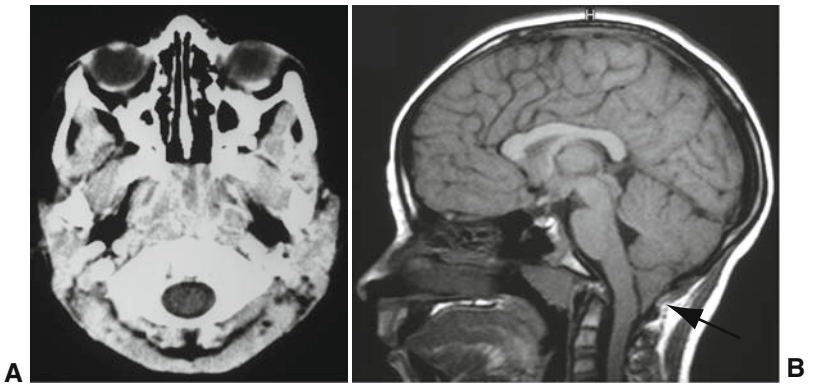

Figure 9.3. **A**: Unenhanced CT at craniocervical junction was interpreted as unremarkable. **B**: Sagittal MRI T1-weighted image reveals pointed cerebellar tonsils extending more than 5 mm below the foramen magnum consistent with Chiari I. No cervical cord hydrosyrinx noted. (Reprinted with the kind permission of Springer Science+Business Media from Medina LS, Shah A, Vasconcellos E. Adults and Children with Headache: Evidence-Based Role of Neuroimaging. In Medina LA, Blackmore CC (eds): Evidence-Based Imaging: Optimizing Imaging in Patient Care. New York: Springer Science+Business, 2006.).

Case 3: Brain Stem Infiltrative Glial Neoplasm

Patient presented with ataxia andheadaches (Fig. 9.4).

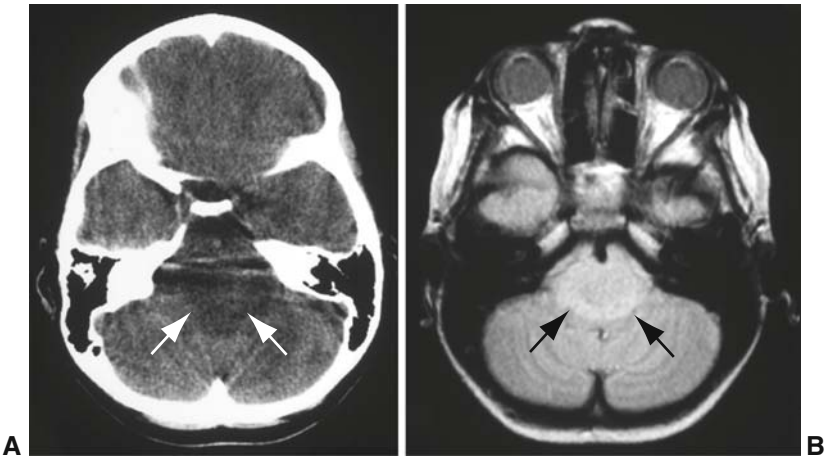

Figure 9.4. **A**: Unenhanced CT through posterior fossa is limited by beam-hardening artifact. A hypo-dense lesion is seen in the pons. **B**: Axial proton density MR image better depicts the anatomy and extent of the lesion without artifact. (Reprinted with the kind permission of Springer Science+Business Media from Medina LS, Shah A, Vasconcellos E. Adults and Children with Headache: Evidence-Based Role of Neuroimaging. In Medina LA, Blackmore CC (eds): Evidence-Based Imaging: Optimizing Imaging in Patient Care. New York: Springer Science+Business, 2006.).

Suggested Imaging Protocols for Headaches

CT Imaging

- CT without contrast. Axial 5–10 mm non-spiral images should be used to assess for subarachnoid hemorrhage, tumor hemorrhage, or calcifications.
- CT with contrast. Axial 5–10 mm non-spiral enhanced images should be used in patients with suspected neoplasm. Infection or other focal intracranial lesion. If indicated, CT angiography can be performed as part of the enhanced CT.

MR Imaging

Basic brain MR protocol sequences include sagittal T1-weighted conventional spin-echo (repetition time, 600 ms; echo time, 11 ms [600/11]), axial proton density-weighted conventional or fast spin-echo (2,000/15), axial T2-weighted conventional or fast spin-echo (3,200/85), axial FLAIR (fluid attenuation inversion recovery) spin-echo (8,800/152, inversion time [TI], 2,200 ms), and coronal T2-weighted fast spin-echo (3,200/85) images. In patients with suspected neoplasm, infection, or focal intracranial lesions gadolinium enhanced T1-weighted conventional spin-echo (600/11) images should be acquired in at least two planes.

Future Research

- Large-scale prospective studies to validate risk factors and prediction rules of significant intracranial lesions in children with headache.
- Large diagnostic performance studies comparing the sensitivity, specificity, and ROC curves of neuroimaging in children with headache.
- Larger studies evaluating the role of advance brain imaging in primary headache disorders such as migraine and cluster headaches.

References

1. Headache Classification Subcommittee of the International Headache Society. Cephalalgia 2004;24(Suppl 1):1–160.
2. Field AG, Wang E. Emerg Clin North Am 1999;17:127–152.
3. Linet MS, Stewart WF, Celentano DD et al. JAMA 1989;261:2211–2216.
4. Honig PJ, Charney EB. Am J Dis Child 1982;136:121–124.
5. The Childhood Brain Tumor Consortium. J Neurooncol 1991;10, 31–46.
6. Rorke L, Schut L. In McLaurin RL (ed.): Pediatric Neurosurgery, 2nd ed. Philadelphia: WB Saunders, 1989; 335–337.
7. Silverberg E, Lubera J. Cancer 1986;36:9–23.
8. Pryse-Phillips W, Findlay H, Tugwell P et al. Can J Neurol Sci 1992;19:333–339.
9. Lipton RB, Stewart WF. Neurology 1993;43: S6–S10
10. de Lissovoy G, Lazarus SS. Neurology 1994;44(Suppl):S56–S62.
11. Medina LS, Pinter JD, Zurakowski D et al. Radiology 1997;202:819–824.
12. Lewis D, Ashwal S, Dahl G et al. Neurology 2002;51:490–498.
13. Schwedt TJ, Guo Y, Rothner AD. Headache 2006; 46(3):387–398.
14. Scott Morey S. Am Family Physician 2000;62:1699–1701.
15. Branson HM, Doria AS, Moineddin R, Shroff M. Radiology 2007;244:838–844.
16. Gentry LR, Gordersky JC, Thopson BH. Radiology 1989; 171:177–187.
17. White PM, Wardlaw JM, Easton V. Radiology 2000;217:361–370.
18. White PM, Teasdale EM, Wardlaw JM et al. Radiology 2001;219 :739–749.
19. Uysal E, Yanbuloglu B, Erturk M, Kilinc BM, Basak M. Diagn Interv Radiol 2005 Jun; 11(2): 77–82.
20. Teksam M, McKinney A, Asis M et al. Am J Neuroradiol 2004 Oct; 25(9):1485–1492.
21. Karamessini MT, Kagadis GC, Petsas T et al. Euro J Radiol 2004 Mar; 49(3):212–223.
22. Tipper G, U-King-Im JM, Price SJ, Trivedi RA et al. Clin Radiol 2005 May; 60(5):565–572.
23. Taschner CA, Thines L, Lernout M et al. J Neuroradiol 2007 Oct; 34(4):243–249.
24. Papke K, Kuhl CK, Fruth M et al. Radiology 2007 Aug; 244(2):532–540.
25. Yoon DY, Lim KJ, Choi CS, Cho BM, Oh SM et al. Am J Neuroradiol 2007 Jan; 28(1):60–67.
26. Lubicz B, Levivier M, Francois O et al. Am J Neuroradiol 2007 Nov–Dec; 28(10):1949–1955.

27. Agid R, Lee SK, Willinsky RA, Farb RI, terBrugge KG. Neuroradiology 2006 Nov; 48(11):787–794.
28. Welch KMA, Cao Y, Aurora SK et al. Neurology 1998, 51:1465–1469.
29. Cao Y, Aurora SK, Vikingstad EM et al. Neurology 2002, 59:72–78.
30. May A, Goadsby PJ. Curr Opin Neurol 1998; 11(3):199–203.
31. Montagna P, Lodi R, Cortelli P. Neurology 1997; 48:113–118.
32. May A, Bahra A, Buchel C, Frackowiak RSJ, Goadsby PJ. Lancet 1998; 351:275–278.
33. Weiller C, May A, Limmroth V, Juptner M, Kaube H et al. Net Med 1995; 1:658–660.
34. Aurora SK. Curr Pain Headache Rep 2003, 7: 209–211.
35. Raskin NH, Hosobuchi Y, Lamb S. Headache 1987, 27:416–420.
36. Haas DC, Kent PF, Friedman DI. Headache 1993, 33:452–455.
37. Goadsby PJ. Cephalgia 2002, 22:107–111.
38. Gelman N, Gorell JM, Barker PB et al. Radiology 1999, 210:759–767.
39. Welch KMA, Nagesh V, Aurora SK, Gelman N. Headache 2001, 41:629–637.
40. Kruit MC, van Buchem MA, Overbosch J et al. Cephalgia 2002, 22:571.
41. Medina LS, Kuntz KM, Pomeroy SL. Pediatrics 2001;108:255–263.
42. Tengs T, Adams M, Pliskin J et al. Risk Anal 1995;15:369–390.
43. England W, Halls J, Hunt V. Med Decis Making 1989;9:3–13.
44. Eddy DM. Gynecol Oncol 1981;12(2 Part 2): S168–S187.
45. Haughton VM, Rimm AA, Sobocinski KA, et al. Radiology 1986; 160:751–755.
46. Orrison WJ, Stimac GK, Stevens EA, et al. Radiology 1991; 181:121–127.
47. Rothner AS. Semin Pediatr Neurol 1995; 2: 109–118.
48. Bille BS. Acta Pediatr 1962; 51(Suppl 136):1–151.
49. Roth-Isigkeit A, Thyen U, Stöven H, Schwarzenberger J, Schmucker P. Pediatrics 2005; 115: e152–162.
50. Peterson CC, Palermo DM. J Pediatr Psychol 2004; 29:331–341.
51. Stang PE, Crown WH, Bizier R, Chatterton ML, White R. Am J Manag Care 2004; 10:313–20.

10

Pediatric Neuroimaging of Seizures

Byron Bernal and Nolan Altman

Issues

I. What is the likelihood of having an abnormal structural finding in neuroimaging in newly diagnosed epilepsy in infancy and childhood?
II. Can neuroimaging predict future seizures or seizure outcome?
III. Is neuroimaging justified in patients with first febrile seizures?
IV. What is the probability to find structural abnormalities in neuroimaging performed in children with temporal lobe epilepsy?
V. What is the role of functional MRI in patients who are candidates for epilepsy surgery?
VI. What is the role of nuclear medicine in children with temporal lobe epilepsy?

Key Points

- Neuroimaging (MRI/CT) in children with seizures rules out life-threatening brain lesions requiring immediate medical or surgical treatment (moderate evidence).
- Magnetic resonance imaging is the neuroimaging study of choice in the workup of first unprovoked seizure (moderate evidence).
- Emergency imaging with CT or MR should be performed in cases of long-lasting post-ictal confusion or focal deficit, in first unprovoked seizure (limited to moderate evidence).
- Magnetic resonance is indicated in children with motor or developmental delays or under 1 year of age with symptomatic seizures (moderate evidence).
- Neuroimaging is not recommended for a simple febrile seizure (limited evidence).
- MRI is more sensitive than CT in detecting temporal lobe pathology (limited evidence).

B. Bernal (✉)
Department of Radiology, Miami Children's Hospital, Miami, FL 33155, USA
e-mail: byron.bernal@mch.com

L.S. Medina et al. (eds.), *Evidence-Based Imaging in Pediatrics*,
DOI 10.1007/978-1-4419-0922-0_10, © Springer Science+Business Media, LLC 2010

- The presence of a focal lesion on MRI is a strong predictor of intractable seizures in children with new onset of temporal lobe epilepsy (TLE) (moderate evidence).
- Abnormal MRI may be found in more than 35% of patients with TLE (moderate evidence).
- Generalized abnormalities in neuroimaging are correlated with higher risk of status epilepticus (moderate evidence).
- Use of fMR increases importantly the post-test probabilities of hemispheric language dominance in patients with epilepsy (Bayesian analysis).

Definition and Pathophysiology

Seizures should be differentiated from epilepsy. A seizure is just a symptom; epilepsy is a disease characterized by recurrent seizures. Children suffering from epilepsy will have by definition "seizures," but not all children with seizures have epilepsy. Seizures may be partial or generalized. In *partial seizures*, a focal origin is suggested by clinical semiology and demonstrated by electroencephalography (EEG). Sometimes the epileptic seizure is not convulsive. Focal non-convulsive seizures consist of sensory phenomena (visual, auditory, olfactory, or body perception) with preserved awareness of the episode. *Complex partial seizures* are seizures without convulsions characterized by lack of awareness of the patient. In contrast to partial seizures, *generalized seizures* are due to generalized discharges of the brain. They produce global motor convulsions and complete lack of awareness of the episode. Grand mal and petit mal absences are typical generalized seizures.

As any other symptom, seizures may have different etiologies, can be accompanied by other symptoms, and recede once the cause is removed. A *symptomatic seizure* is a convulsion that occurs due to a specific etiology such as hypoglycemia or brain tumor. Symptomatic seizures are divided into acute symptomatic and remote symptomatic. *Acute symptomatic* seizures are due to proximate precipitant (drug intoxication, alcohol withdrawal, or viral encephalitis), whereas *remote symptomatic* seizures are caused by pre-existing long-lasting lesions (e.g., cortical dysplasia, ganglioglioma, and hippocampal sclerosis).

In many cases, seizures appear without an evident cause. They are called *non-symptomatic* seizures and could be categorized as cryptogenetic or idiopathic seizures. In cryptogenic seizures, no cause is found after appropriate workup, even though the clinical findings suggest a structural lesion, such as focal clinical signs with EEG correlation. Idiopathic seizures are generalized seizures with no focal electrical or clinical signs. In these cases, a genetic factor is presumed.

The term *unprovoked seizures* is used when the seizures appear without a clinical history, indicating an etiology (acute or remote) in a child with normal neurological examination. The term is used as a temporary diagnosis while the workup is underway, and the seizure can be classified properly.

Two types of seizures are of particular importance in the pediatric population. Children between 6 months and 5 years of age may have seizures with fever not related to meningitis or other infections of the central nervous system (CNS). These seizures are termed *febrile seizures*. Febrile seizures are further divided into simple febrile seizures and complex febrile seizures. Complex febrile seizures are characterized by focal onset, lasting more than 15 min, or occur in multiple episodes (1).

Epidemiology

There is a relative paucity of epidemiologic studies on seizures in the pediatric population. Some of the few studies done have conflicting results due to lack of agreement in the definition of the seizure disorders and diagnostic

workup. For example, incidence and prevalence of seizures vary among studies depending on whether cases with febrile seizures or symptomatic seizures are included or not (2), and also with respect to the country where the study takes place.

Prevalence and Incidence

The prevalence of epilepsy in American children and adolescents is 4.71 per 1,000 inhabitants, according to a study conducted by Cowan et al. (3), based on 1,159 cases recruited in central Oklahoma. In an extensive review of the world literature on the epidemiology of epilepsy in the pediatric population, Levinton and Cowan (4) found the prevalence of epilepsy to be between 4 and 5 per 1,000, despite the variation in sampling methods and case definitions.

The effect of socioeconomic factors and country development on the prevalence or incidence of epilepsy is not clear. There are some reports of high prevalence rates in developing countries (5, 6). A recent report shows prevalence up to 18.4 per 1,000 in a population of 1,742 children between 0 and 19 years of age in a rural area of Honduras (7). In contrast, a study performed in Estonia showed a prevalence rate of 3.6 per 1,000 inhabitants (8), even lower than that found in other developed countries.

Incidence of epilepsy in children ranges among countries, from 52.6 to 151.5 per 100,000 inhabitants (4). Variations may be explained by true ethnic differences but are most likely because of differences in case recruitment and definition.

The incidence of seizures is age dependent, peaking at extremes of life. In neonates and infants, it ranges between 100 and 140 cases per 100,000 (9). The proportions of the different types of epilepsies have been ascertained in some cohort studies. In a 20-year cohort study, done in Tel-Aviv (Israel), of 440 pediatric patients with seizures (from which neonatal seizures were excluded), Kramer and colleagues (10) found the following distribution of seizure types: partial seizures secondarily generalized (20.6%), complex partial seizures (12.5%), simple partial seizures (8.6%), benign rolandic epilepsy (8%); absence seizures 7%; and generalized tonic–clonic seizures (66.6%). The remaining were classified as several different types of idiopathic generalized epilepsy. Another large cohort study in children with epilepsy (309 children) has been conducted in Hong Kong by Kwong and coworkers (11). Forty-two percent of the epilepsy was idiopathic, 16.8% cryptogenetic, and 40.8% remote symptomatic. Seizures were partial in 48.5% of children and generalized in 46.9%. The cumulative incidence of febrile seizures is 2% (12) with a recurrence between 12 and 100%, depending on the number of risk factors involved (13, 14).

Acute non-febrile symptomatic seizures (unprovoked seizures) affect 1 out of 1,000 neonates. The presence of neurodevelopmental abnormalities increases the probability of future unprovoked seizures (15). Complex partial seizures, also known as psychomotor or temporal lobe seizures, are of the utmost importance because they may be suitable for surgical treatment. However, there are no epidemiologic studies of temporal lobe epilepsy in children.

Overall Cost to Society

No data were found in the medical literature on the cost to society in regard to the neuroimaging assessment of seizures in the pediatric population. The best work on the general cost of childhood epilepsy is of Argumosa and Herranz (16). In a critical review, these authors review the costs of epilepsy in the pediatric population. The direct costs per patient per year vary from 869 euros for children with controlled seizures to 11,980 euros for those with refractory epilepsy requiring surgery. The annual cost per child for diagnostic investigation ranges from 86 to 266 euros. These tests include plasma levels of antiepileptic drugs, EEGs, and neuroimaging. The impact of the cost of workup in the United States, which includes neuroimaging, can be inferred from the study of Begley et al. performed in two different regions of North America. Although the study is not focused on the pediatric population, the costs of laboratory and neuroimaging are at least the same as that for adults. The mean annual cost per patient

decreased from $3,157 for the first year to $702 for the second. The costs continue diminishing to $411 in the fourth year (17).

Goals

The main goal of neuroimaging in pediatric seizures is to rule out focal lesions that could threaten the patient's life. Secondary goals of neuroimaging in seizures are the identification of focal brain lesions related to the epileptogenic focus and the rejection or confirmation of a clinical diagnosis.

Methodology

For each of the procedures, i.e., MRI and CT, a systematic review of the literature was performed utilizing PubMed (National Library of Medicine, Bethesda, MD). All searches were limited for publications in the last 20 years (up to December 31, 2007), abstracts available in English, and within the age range of 0–18 years. The following criteria were utilized:

1. ((EBM[Title] OR Evidence[Title]) AND (("seizures"[MeSH Terms] OR seizures[Text Word]) OR ("epilepsy"[MeSH Terms] OR epilepsy[Text Word])))
2. ((Epilepsy[Title] OR seizure[Title]) AND (neuroimaging[Title] OR neuroimage [Title]))
3. ((Epilepsy[Title] OR Seizure [Title]) AND ((MRI [Title]) OR (CT [Title])))
4. Searches 1, 2, and 3 with same key words replacing [Title] by [Text Word]

Titles and abstracts were reviewed to determine appropriateness of content. Articles with less than 30 patients, no standard of reference, or no significant influence on clinical decision making were excluded. Likelihood ratios, probability, sensitivity, specificity, predictors, and techniques were sought and summarized for each procedure.

Of a total of 169 abstracts, 48 abstracts met criteria for full-text reviewing. References of these articles were also utilized if relevant to the search.

Discussion of Issues

I. What Is the Likelihood of having an Abnormal Structural Finding in Neuroimaging in First Unprovoked Seizure or Newly Diagnosed Epilepsy in Infancy and Childhood?

Summary of Evidence: The likelihood of finding a structural abnormality in neuroimaging in first unprovoked seizure ranges between 10 and 34% (moderate evidence). The clinically significant yield is between 3 and 8% (moderate evidence). In first unprovoked temporal lobe epilepsy (TLE), the yield increases to 38–50% (limited to moderate evidence).

The sensitivity to detect structural lesions in TLE is 31% for CT and 64% for MRI (moderate evidence). Emergency imaging with CT or MR should be performed in cases of long-lasting post-ictal confusion or focal deficit. See Table 10.1 for neuroimaging yield in children with first unprovoked seizure.

Supporting Evidence: In a prospective study, Shinnar et al. (18) describe the results of 159 CTs and 59 MRIs performed on 411 children with an apparent first unprovoked seizure (moderate evidence). Forty-five children (21%) had abnormal neuroimaging findings, with similar yields found between generalized and partial seizures. MRI was abnormal in 34% and CT in 22%. In 8 of 27 patients who had both MRI and CT, MRI showed a different or new lesion not seen on the CT. However, only four children were found to have lesions requiring intervention. From these results the authors conclude that in spite of this fact that "the yield in finding acute lesions is low,. . .there is. . ..substantial yield of imaging abnormalities in children with a first unprovoked seizure that may influence prognosis and decision of whether to treat or not." Sharma et al. (19) found in a well-described retrospective study (moderate evidence) clinically significant abnormal neuroimaging in 8% of 475 children with "new-onset afebrile seizures" (95% CI: 6.4–11.8). Two risk factors were associated with a high probability of significant abnormal neuroimaging: the presence of a predisposing condition (such as concurrent mental retardation, lateralized neurological signs, and systemic illness) and focal seizures in

children younger than 33 months of age. One hundred and twenty-one children who conformed to the high-risk group yielded abnormal neuroimaging in 26%. Berg et al. (20) conducted a consortium study in Connecticut (moderate evidence). In this study, 488 of 613 children with newly diagnosed epilepsy were imaged with MRI (388, 63.3%), CT (197, 32.1%), or both (97, 15.8%). Abnormal findings were found in 62 (12.7%); this increased to 15.4% if only partial seizures were computed (20). Similar results were described by Khodapanahandeh and Hadizadeh in a retrospective study of 125 children (limited evidence), where neuroimaging (CT or MRI) found abnormalities in 12 of 119 (10%) children (21).

In a more recent article, Byars et al. (22) explored the yield of MRI in 249 children after the first seizure. Thirty-four children (13.7%) had structural brain abnormalities that possibly were related to their seizures (23). As expected, the authors also found that children who had structural abnormalities had lower cognitive function scores, including IQ, language, and executive functions. Unfortunately, the authors did not differentiate between provoked and unprovoked seizures, so this result should be considered as a global yield of MRI in all cases of first seizure.

If the first seizure is of temporal lobe type (for example, complex partial seizure), the yield of MRI ranges between 38 and 50%. Initially, Harvey et al. (24) (moderate evidence) found structural abnormalities in 24 of 63 (38%) children with new onset of TLE, of whom 8 (13%) showed findings requiring medical intervention. In 2002, Sztriha and coworkers (25), in a prospective cohort study, described a group of 30 children with first-time seizures of temporal origin (moderate evidence). Forty-three percent of the MRI performed showed structural abnormalities. More recently, Spooner et al. (26) described a cohort study of 77 children (moderate evidence) with new-onset epilepsy, of which 64 had the diagnosis of temporal lobe epilepsy (TLE) with more than 7 years of follow-up. Temporal lesions were found in 28 subjects (44% of all cases) including hippocampal sclerosis in 10, tumor in 8, and cortical dysplasia in 7 patients. The yield increased to 48% if only the MRI cases (59) were taken into account. All children with lesions on MRI were not seizure free.

The sensitivity of MRI and CT in detecting structural lesions in pediatric temporal lobe epilepsy (new-onset and chronic TLE) has been assessed by Sinclair et al. (27). In their retrospective study of 42 children (limited evidence) who had MRI (42) and CT (39) exams, neuroimaging was compared with pathology. They found that MRI was abnormal in 27 of 42 children (64%), while CT was abnormal in 12 of 39 (31%) children.

The role of CT in the evaluation of children with new-onset seizures (including febrile seizures) has been studied by Garvey et al. (23) in a retrospective analysis of 99 neurologically normal children (limited evidence) presenting with seizures to the emergency room. Fifty were unprovoked seizures. A total of 19 children had brain abnormalities (19%), 7 of whom required further investigation or intervention. Two risk factors were identified: first unprovoked seizure ($p<0.01$) and focal seizures or focal post-ictal clinical abnormality ($p<0.04$). Similar results have been reported by Maytal et al. (28) in a 1-year retrospective study of 66 patients (limited evidence). Fourteen cases (21%) had abnormal CT results. Two of them prompted immediate therapeutic intervention, as they were children of child abuse with subdural hematomas that were drained.

In 2000, the Quality Standards Subcommittee of the American Academy of Neurology, the Child Neurology Society, and the American Epilepsy Society published practice guidelines in the evaluation of first non-febrile seizures in children (unprovoked seizure) based on EBM (29). Analysis of their results found that a range of 0–7% of children had lesions on CT which changed patient management (i.e., tumors, hydrocephalus, arachnoid or porencephalic cysts, and cysticercosis). The practice guidelines conclude that MRI yields more lesions than does CT but it does not always change medical management. Only a few cases with temporal sclerosis or cortical dysplasia were candidates for epilepsy surgery. The guidelines also conclude that there is insufficient evidence to support the recommendation for routine neuroimaging after the first unprovoked seizure. However, neuroimaging may be indicated in cases of focal seizures associated with clinical neurological findings. If a neuroimaging study is required, MR is the

preferred modality. Emergency imaging with CT or MR should be performed in cases of long-lasting post-ictal focal deficit or in those patients who remain confused several hours after the seizure. MRI should be considered in children less than 1 year of age with significant and unexplained cognitive or motor impairment, partial seizures, or EEG with focal abnormality.

II. Can Neuroimaging Predict Future Seizures or Patient Outcomes?

Summary of Evidence: Focal lesions found by MRI are predictors of intractable seizures in children with new-onset TLE (moderate evidence). Outcome is poor (lack of seizure control) in 50% of patients with diffuse lesions in neuroimaging (limited evidence). Generalized abnormalities in neuroimaging correlate with higher risk of suffering status epilepticus (moderate evidence). Type of cortical dysplasia does not correlate with drug refractoriness or severity of cognitive impairment (insufficient evidence). There are conflicting studies of neuroimaging as a predictor of poor drug treatment response or surgical outcome. See Table 10.2 for neuroimaging as a predictor of seizure outcome.

Supporting Evidence: Seizure outcome and neuroimaging may be correlated in three different ways. First, can the neuroimaging findings predict the probability of treatment success? Second, can neuroimaging results predict cognitive developmental delays or abnormalities? Third, can neuroimaging predict the outcome of neurosurgery in intractable epilepsy?

Neuroimaging as a Predictor of Treatment Outcome

In a prospective study by Spooner et al. (26) (moderate evidence) of 77 patients, it was found that lesions such as hippocampal sclerosis, tumor, and cortical dysplasia found by MRI were predictors of intractable seizures in children with new-onset TLE. One hundred percent of children with lesions on MRI remained with seizures during a follow-up period greater than 10 years. Unfortunately, this observation has not been replicated. The contribution of neuroimaging to detect risk factors to predict if a child will suffer a status epilepticus event (SE) was assessed by Novak et al. (30) (limited evidence). Forty-four patients with symptomatic epilepsy (with demonstrated brain lesions) and one or more status epilepticus events were studied retrospectively and compared to 88 children with the same condition but without SE. Univariate analysis revealed that generalized abnormalities in neuroimaging correlated with higher risk of suffering of an SE (odds ratio = 2.9, $p = 0.03$). The same conclusion was reached by Karasallho et al. (31) in a retrospective study of 83 pediatric patients (limited evidence). The histopathologic outcome effect has also been investigated, although in a very limited manner. In 2006, Mazurkiewicz et al. (32) reported a retrospective study of 46 pediatric subjects (limited evidence) with cortical dysplasia. The authors sought to correlate the type of cortical dysplasia with the clinical outcome. The group consisted of 31 patients with focal cortical dysplasia, 6 with schizencephaly, 4 with heterotopia, 3 with lissencephaly, and 2 with band heterotopia. The authors did not find correlations between the type of cortical dysplasia and the presence of drug-resistant epilepsy or severity of the cognitive impairment.

Neuroimaging as a Predictor of Developmental Outcome

Tekgul et al. (33) studied MRI predictors of neurodevelopmental outcome in a retrospective study of 89 term infants with neonatal seizures (limited evidence). Cerebral dysplasia and global hypoxia–ischemia were associated with poor developmental outcome, especially those who have multifocal or diffuse cortical or subcortical gray matter lesions. Thirty-six infants (40%) had severe cognitive impairment, and 31% had persistence of seizures after intensive care unit discharge. Overall outcome was judged *poor* for 50% of the subjects with diffuse lesions. In contrast, only 1/18 (6%) in the group with normal MRI was graded as having a poor outcome.

Neuroimaging as a Predictor of Epilepsy Surgery Outcome

Seizure outcome of intractable epilepsy was studied in children in a retrospective study of 50 subjects with at least 2 consecutive years of follow-up (34). The study was limited to non-tumor-related partial epilepsy cases (limited

evidence). However, the author found that the only risk factor of poor drug treatment outcome was the presence of focal lesions on neuroimaging (MRI/CT). The opposite was found in surgical cases. Of the 20 patients that underwent epilepsy surgery, 60% had excellent outcome despite them representing 90% of the cases with focal neuroimaging abnormalities. Similar findings have been reported by two small-sample, retrospective studies (35, 36) (limited evidence). These findings, however, conflict with those reported by Hennessy et al. (37). They demonstrated, in a retrospective study of 80 lesions in 234 consecutive temporal resections (limited evidence), that a lesion found on a preoperative CT (followed by "complete histological resection") was not able to predict outcome. Likewise, Goldstein et al. described in a retrospective study of 33 children (limited evidence) that MRI lesions do not predict seizure outcome after temporal lobectomy in childhood (38).

III. Is Neuroimaging Justified in Patients with First Febrile Seizures?

Summary of Evidence: Neuroimaging is not recommended for a simple febrile seizure (limited evidence). There are not enough data to recommend or not recommend neuroimaging in complex febrile seizures. See Table 10.3 for neuroimaging yield in first febrile seizure.

Supporting Evidence: No articles with strong or moderate evidence were found. The role of neuroimaging in febrile seizures and its value to rule out meningitis are summarized by Offringa and Moyer (39) in an evidence-based medicine study (limited evidence). Combining the yield of CT and MRI scans, only 1.2% of 2,100 cases of seizures associated with fever had significant findings (e.g., tumor, malformations, and atrophy). The conclusions of this group are similar to the American Academy of Pediatrics (40) (limited evidence), which suggests that CT or MRI is not recommended for a simple febrile seizure.

Complex febrile seizures may have prognostic implications. Notwithstanding, only one study which met selection criteria was found. Teng and coworkers (41) reported the findings in a retrospective study of 71 children (limited evidence) seen in the ER because of a first complex febrile seizure (as diagnosed and classified by two epileptologists). All subjects had neuroimaging. Fifty-one children (72%) had only one of three features that characterize a complex febrile seizure. Twenty children (28%) had multiple complex features (long duration, involvement of only one side of the body, and long post-ictal state). However, none of the 71 patients had intracranial pathologic conditions on neuroimaging that required emergency intervention.

IV. What Is the Probability of Finding Structural Abnormalities in Neuroimaging Performed in Children with Temporal Lobe Epilepsy (TLE)?

Summary of Evidence: Abnormal MRI may be found in more than 36% of patients with TLE (moderate evidence). MRI is twice as sensitive as CT in detecting temporal lobe pathology (limited evidence) (Fig. 10.2). MRI findings can classify TLE into three categories: developmental lesions, hippocampal sclerosis, and cryptogenic. Therefore, MRI is recommended in the evaluation of TLE. See Table 10.4 for neuroimaging abnormalities in children with temporal lobe epilepsy.

Supporting Evidence: Sixty-three children with new-onset temporal lobe epilepsy were studied by Harvey et al. (moderate evidence) (42). Imaging was performed in 58 (92%) by MRI and 48 (76%) by CT. MRI was abnormal in 23 children (37%). Unilateral hippocampal sclerosis (HS) was seen in 12 (19% of all patients with TLE), bilateral HS in 1, temporal lobe tumor in 8, arachnoid cyst in 1, and cortical dysplasia in 1. CT was abnormal in 23% of cases, including all tumors, but failed to detect all cases of HS. CT demonstrated calcifications of a small hamartoma in the posterior area of the hippocampus in one case that was not detected on MR. Based on neuroimaging findings, the authors proposed to divide partial seizures into three groups: Group I: developmental temporal

lobe epilepsy. This epilepsy is associated with tumors and long-standing, non-progressive cortical lesions such as gangliogliomas, dysembryoplastic neuroepithelial tumors, and pilocytic xanthoastrocytomas. Seizures begin in mid to late childhood (mean age 8.2 years in 10 subjects) and neurobehavioral problems are infrequent. Group II: temporal lobe epilepsy with hippocampal sclerosis (Fig. 10.3). Prior clinical history of neurologically significant insult, such as complicated febrile seizures, hypoxic–ischemic encephalopathy, or meningitis, is usually present. Group III: cryptogenic temporal lobe epilepsy, in whom no etiology could be determined.

This classification was utilized by Sztriha et al. (25) in a cohort study of 30 children (limited evidence). Patients had TLE with onset before age 14. Eight children (28%) had developmental temporal lobe epilepsy, 7 (23%) had hippocampal sclerosis, and 15 (50%) had cryptogenic TLE.

The sensitivity of CT and MRI to detect temporal lobe pathology in TLE was assessed by Sinclair et al. (27) (limited evidence). Forty-two pediatric patients were studied. All patients underwent temporal lobectomy for intractable epilepsy, with histopathology results as the reference standard. MRI was clearly more sensitive than CT. MRI correctly identified the pathology in 27 of the 42 cases (64%), while CT scan did in 12 of 39 cases (31%). However, of 15 cases where the MRIs were reported normal, 10 showed abnormal pathology results, including mesial temporal sclerosis (MTS), porencephaly, and 1 case of ganglioglioma (10 false-negative results). Of seven cases found without pathology, two MRIs were reported abnormal (two false-positive results). CT produced 21 false-negative and 0 false-positive results. Therefore, the sensitivity and specificity of MRI and CT was 71.5%/71.4% and 38.2%/100%, respectively. The authors did not utilize FLAIR sequences and only part of the sample group was scanned utilizing inversion recovery techniques that have increased the yield of MTS and other cortical lesions related with intractable epilepsy in recent years. No studies reporting sensitivity/specificity of FLAIR or high-resolution T2 signal in MRI sequences were found in the pediatric population.

V. What Is the Role of Functional MRI in Patients Who Are Candidates for Epilepsy Surgery?

Summary of Evidence: fMRI influences diagnostic and therapeutic decision making (moderate evidence). fMRI increases importantly the post-test probability of language lateralization. The cost of the non-invasive fMRI study is significantly less than that of the invasive WADA test.

Supporting Evidence: fMRI is a non-invasive MR technique that detects minute signal enhancement produced by blood oxygen level changes associated with brain cortical activity. These signal changes are also known as the BOLD (blood oxygen level-dependent) effect. fMRI only recently has a separate billing code for clinical use after undergoing stringent evaluation as a diagnostic study by the US government. fMRI may replace the intracarotid amobarbital exam (the Wada arteriography test) in the lateralization and location of language in children who are candidates for epilepsy surgery. The vast majority of fMRI papers are based on small samples of adults or a mixture of children and adults. One article that fulfilled our inclusion criteria was the prospective study (moderate evidence) by Medina et al. (43), which assessed the role of fMRI in 60 pediatric candidates for epilepsy surgery. fMRI results altered patient and family counseling in 35 (58%); avoided further studies (including Wada test) in 38 (63%); altered intraoperative mapping plans in 31 (52%); and changed surgical approach plans in 25 (42%) of cases. In five (8%) patients, fMRI averted two-stage surgery. In four (7%) patients, the extent of surgical resection was altered because eloquent language areas were identified close to the seizure focus. The authors concluded that fMRI influences diagnostic and therapeutic decision making.

A Bayesian analysis study has been performed to assess the role of fMRI in determining how this test modifies pretest to post-test probabilities of language dominance in the epilepsy population (44). The study pooled data from studies published between 1995 and 2002 having language fMRI compared with Wada tests

or electrocortical stimulation as the standard of reference. Two hundred and forty cases having both exams were pooled. From the literature review and utilizing the Wada test as the reference study, the authors found that the sensitivity (and specificity) of fMRI in language lateralization was 92.5% (95% CI: 89.1%, 95.9%), and the likelihood ratio was 12.3 [(sensitivity)/(1 – specificity); 95% CI: 8.2, 23.4)]. When the reference standard was the electrocortical stimulation, sensitivity (and specificity) was 90.3% (95% CI: 80–100%), and the likelihood ratio was 9.3 (95% CI: 4, ∞). From the Bayesian analysis, the authors conclude that, in epilepsy patients with right-hand dominance or ambidexterity, the post-test probability (of truly language lateralization in the left hemisphere) is greater than 95%. In the left-handed epilepsy patients, there was high post-test probability (80–97%) of a correlation between functional MR hemisphere activation and definite left-handed language dominance (44).

A cost study of functional MRI and the Wada test has been published (45). The total direct costs of the Wada test ($1,130.01 ± $138.40) and of functional MR imaging ($301.82 ± $10.65) were significantly different (p <0.001) (44). The cost of the more invasive Wada test was 3.7 times higher than that of functional MR imaging (45).

VI. What Is the Role of Nuclear Medicine in Children with TLE Seizures?

Summary of Evidence: PET and ictal SPECT can localize epileptogenic zones in children with TLE (limited evidence).

Supporting Evidence: No large prospective studies have been done addressing the role of nuclear medicine in children with seizure disorders. There is however a retrospective article by Lee et al. (46) describing 21 pediatric patients who had TLE and evaluated with ictal SPECT and interictal PET (limited evidence). PET correctly localized the epileptogenic zone in 20 of 21 patients (95%) and SPECT in 12 of 15 patients (80%).

Take Home Figures

Table 10.1 presents neuroimaging yield in children with first unprovoked seizure. Table 10.2 shows neuroimaging as a predictor of seizure outcome. Table 10.3 shows neuroimaging yield in first febrile seizure. Table 10.4 shows neuroimaging abnormalities in children with temporal lobe epilepsy.

Figure 10.1 represents an algorithm for decision making in children with first febrile seizures.

Table 10.1. Neuroimaging yield in children with first unprovoked seizure

Author	Patients[a]	CT/MRI	Yield (%)	Comments
Shinnar et al. (18)	218	159/59	22/34	Only four children (1.8%) with significant findings
Sharma et al. (19)	475	454/21	8[b]	Predictors of abnormal neuroimaging: predisposing condition and focal seizure in younger than 33 months
Berg et al. (20)	488	294/485	12.7[b]	Three cases had normal CT and abnormal MRI
Khodapanahandeh and Hadizadeh (21)	119	108/11	10[b]	Significant relationship found between partial seizure and abnormal neuroimaging
Byars et al. (22)	249	0/249	14	Structural brain abnormalities correlated with overall low cognitive functioning
TLE				
Sztriha et al. (25)	30	0/30	43.3	Only in first seizure of temporal origin
Spooner et al. (26)	61	3/58	43.8[b]	Yield corrected: 47.5 (see text)
Harvey et al. (24)	63	48/58	38.1[b]	One normal MRI case had CT calcifications in the posterior hippocampus
CT in new-onset seizures including febrile seizures				
Garvey et al. (23)	50	50	19.2	Two predictors of positive yielding: unprovoked seizure, focal seizure
Maytal et al. (28)	66	66	21.2	Two cases required immediate therapeutic intervention

[a]Patients with neuroimaging.
[b]Combined yield.

Table 10.2. Neuroimaging as a predictor of seizure outcome

Author	Cases	Predictor	Outcome	Sensitivity (as reported)	Comments
Spooner et al. (26)	77	Structural lesion on MRI	Poor seizure control	100%	Patient with lesions remained with seizures
Novak et al. (30)	44	Generalized abnormalities on MRI	Status epilepticus (SE)	OR = 2.85, $p = 0.034$	Control group: seizure patients without SE
Mazurkiewicz et al. (32)	46	Cortical dysgenesis	Seizure control	NA	No correlation found
Tekgul et al. (33)	89	Diffuse cerebral dysgenesis	Abnormal development	50%	Poor cognitive outcome
Chen et al. (34).	49	Focal lesions on MRI	Poor seizure control	57[a]	Non-tumor partial epilepsies
Duchowny et al. (35)	31	Focal lesions on MRI	Success of epilepsy surgery	?	Outcome judged in an average of 4.6 years
Hennessy et al. (37)	234	Focal lesion on CT	Success of epilepsy surgery	?	Statistics based on 80 lesions. Not able to predict
Goldstein et al. (38)	33	MRI lesions	Success of epilepsy surgery	?	Not able to predict outcome

[a]Percentage of patients in Class IV outcome with focal neuroimaging abnormality. Class IV defined as at least one seizure per week.
?, not reported.

Table 10.3. Neuroimaging yield in first febrile seizure

Author	Patients	CT/MRI	Yield	Comments
Offringa et al. (30)	2100 (EBM—review)	2100 (combined)	1.2	"Yield" refers only to findings of meningitis
Teng et al. (41)	71	71 (combined)	0	"Yield" refers only to significant findings. All cases were complex partial seizures

Table 10.4. Neuroimaging abnormalities in children with temporal lobe epilepsy

Author	Patients	CT/MRI	Yield	Comments
Harvey et al. (42)	63	48/58	23/36.5	CT failed to detect HS but demonstrated calcifications missed in one case by MRI
Sinclair et al. (27)	42	39/42	31/64	MRI yielded two false positives. Cases controlled with histopathology

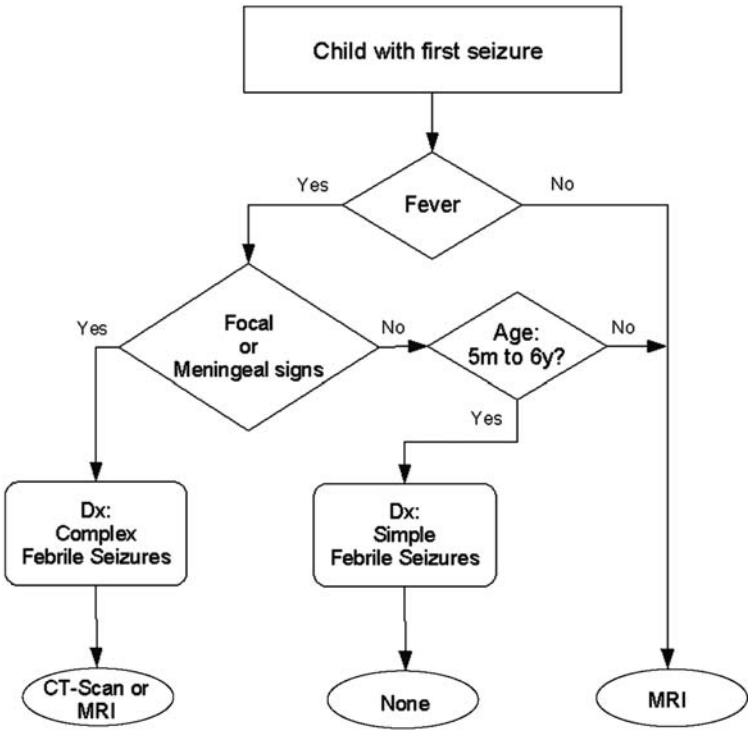

Figure 10.1. Algorithm for decision making in children with first febrile seizure.

Imaging Case Studies

Case 1

Figure 10.2 presents CT and MRI images of a child with epilepsy and postural plagiocephaly.

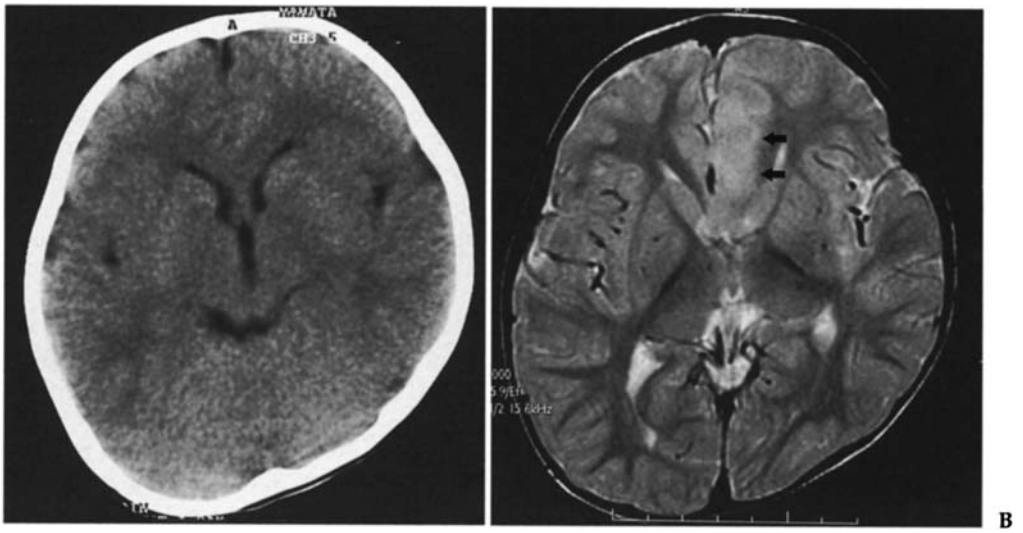

Figure 10.2. Distinct yield between CT and MRI in a case with partial seizures. The axial CT (**A**) is compared to the MR (**B**) in a child with epilepsy and postural plagiocephaly. The CT fails to show the cortical abnormality demonstrated by the T2-weighted MRI sequence. The left parasagittal frontal region corresponds most likely to an area of focal cortical dysplasia characterized by the loss of gray–white matter interface and the increased T2-weighted signal intensity (*arrows*). This focal lesion is associated with a poor outcome with pharmacotherapy and may have a better prognosis with surgery. (Reprinted with kind permission of Springer Science+Business Media from Bernal B, Altman N. Neuroimaging of Seizures. In Medina LA, Blackmore CC (eds.): Evidence-Based Imaging: Optimizing Imaging in Patient Care. New York: Springer Science + Business Media, 2006.).

Case 2

Figure 10.3 presents MRI of a patient with complex partial seizures and left temporal EEG abnormalities.

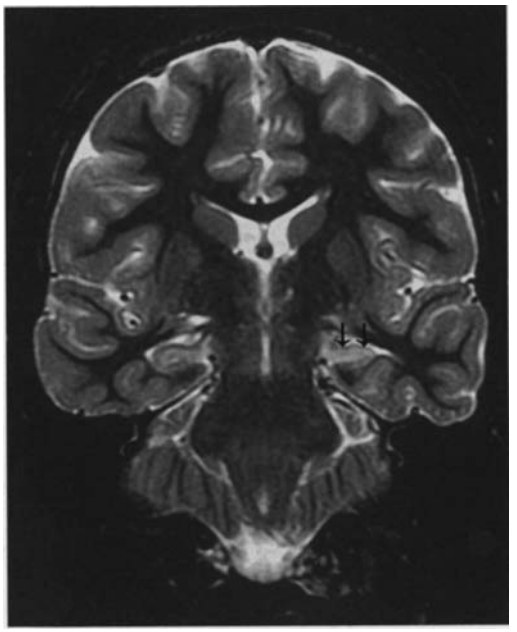

Figure 10.3. Role of MRI in patients with temporal lobe epilepsy (TLE). MRI is positive in 37% of children with TLE. Of this group, more than 50% may have hippocampal sclerosis. The image corresponds to a patient with complex partial seizures and left temporal EEG abnormalities. Coronal image at the level of the temporal lobes demonstrates left hippocampal sclerosis characterized by reduction in size and increased signal intensity (arrows), compared to the normal right hippocampus. (Reprinted with kind permission of Springer Science+Business Media from Bernal B, Altman N. Neuroimaging of Seizures. In Medina LA, Blackmore CC (eds.): Evidence-Based Imaging: Optimizing Imaging in Patient Care. New York: Springer Science + Business Media, 2006.).

Suggested Imaging Protocols for Seizures

CT Scan Brain Protocol for the Study of First Seizure

In the acute or emergent setting, we recommend non-enhanced axial contiguous 5 mm-slice sequence of the entire brain. Radiation doses should follow the ALARA recommendation.

MRI of the Brain for the Workup of Epilepsy and Non-febrile Seizures

The suggested MRI protocol consists of the following sequences:

T1-weighted, sagittal 3D volume 1-mm ST no gap, axial fluid-attenuated inversion recovery, axial dual echo (gradient and spin echo), diffusion-weighted axial, T2-weighted coronal fast spin echo, T2 coronal, oblique, high resolution through the temporal lobe plus contrast T1-weighted axial and coronal sequences.

Future Research

- More studies to understand pediatric seizure disorders other than febrile seizures and temporal lobe epilepsy.
- Studies to determine the sensitivity and specificity of neuroimaging in detecting and categorizing brain lesions are needed.
- More studies on the added value of fMRI are needed in the pediatric population.
- More research is needed in evaluating the role of neuroimaging in first febrile seizures.
- Evaluation of 3T MR in pediatric epilepsy.

References

1. Karande S. Indian J Med Sci 2007;61:161–172.
2. Cowan LD, Leviton A, Bodensteiner JB, Doherty L. Paediatr Perinat Epidemiol 1989;3:386–401.
3. Cowan LD, Bodensteiner JB, Leviton A, Doherty L. Epilepsia 1989;30:94–106.
4. Leviton A. Cowan LD. Neuroepidemiology 1982;1:40–83.
5. Chiofalo N, Kirschbaum A, Fuentes A, Cordero ML, Madsen J. Epilepsia 1979;20:261–266.
6. Gomez JG, Arciniegas E, Torres J. Neurology 1978;28:90–94.
7. Medina MT, Durón RM, Martínez L, Osorio JR, Estrada AL, Zúniga C et al. Epilepsia 2005;46:124–131.
8. Beilmann A, Napa A, Sööt A, Talvik I, Talvik T. Epilepsia 1999;40:1011–1019.
9. Bell GS, Sander JW. Seizure 2001;10:306–314
10. Kramer U, Nevo Y, Neufeld MY, Fatal A, Leitner Y et al. Pediatr Neurol 1998;18:46–50.
11. Kwong KL, Chak WK, Wong SN, So KT. Pediatr Neurol 2001;24:276–282.
12. Hauser WA, Annegers JF, Rocca WA. Mayo Clin Proc 1996;71:576–586.

13. Knudsen FU. Arch Dis Child 1985;60:1045–1049.
14. Offringa M, Bossuyt PM, Lubsen J, Ellenberg JH, Nelson KB, Knudsen FU et al. J Pediatr 1994;124:574–584.
15. Berg AT, Shinnar S. Neurology 1996;47:562–568.
16. Argumosa A, Herranz JL. Epileptic Disord 2004;6:31–40.
17. Begley CE, Lairson DR, Reynolds TF, Coan S. Epilepsy Res 2001;47:205–215.
18. Shinnar S, O'Dell C, Mitnick R, Berg AT, Moshe SL. Epilepsy Res 2001;43:261–269.
19. Sharma S, Riviello JJ, Harper MB, Baskin MN. Pediatrics 2003;111:1–5.
20. Berg AT, Testa FM, Levy SR, Shinnar S. Pediatrics 2000;106:527–532.
21. Khodapanahandeh F, Hadizadeh H. Arch Iran Med 2006;9:156–158.
22. Byars AW, deGrauw TJ, Johnson CS, Fastenau PS, Perkins SM, Egelhoff JC et al. Epilepsia 2007;48:1067–1074.
23. Garvey MA, Gaillard WD, Rusin JA, Ochsenschlager D, Weinstein S, Conry JA et al. J Pediatr 1998;133:664–669.
24. Harvey AS, Berkovic SF, Wrennall JA, Hopkins IJ. Neurology 1997;49:960–968.
25. Sztriha L, Gururaj AK, Bener A, Nork M. Epilepsia 2002;43:75–80.
26. Spooner CG, Berkovic SF, Mitchell LA, Wrennall JA, Harvey AS. Neurology 2006;67:2147–2153.
27. Sinclair DB, Wheatley M, Aronyk K, Hao C, Snyder T, Colmers W et al. Pediatr Neurosurg 2001;35:239–246.
28. Maytal J, Krauss JM, Novak G, Nagelberg J, Patel M. Epilepsia 2000;41:950–954.
29. Hirtz D, Ashwal S, Berg A, Bettis D, Camfield C, Camfield P et al. Neurology 2000;55:616–623.
30. Novak G, Maytal J, Alshansky A, Ascher C. Neurology 1997;49:533–537.
31. KarasalIho Glu S, Oner N, Celtik C, Celik Y, Biner B et al. Pediatr Int 2003;45:429–434.
32. Mazurkiewicz-Bełdzińska M, Szmuda M, Matheisel A. Folia Neuropathol 2006;44: 314–318.
33. Tekgul H, Gauvreau K, Soul J, Murphy L, Robertson R, Stewart J et al. Pediatrics 2006;117: 1270–1280.
34. Chen LS, Wang N, Lin MI. Pediatr Neurol 2002;26:282–287.
35. Duchowny M, Jayakar P, Resnick T, Harvey AS, Alvarez L, Dean P et al. Epilepsia 1998;39: 737–743.
36. Ferrier CH, Engelsman J, Alarcón G, Binnie CD, Polkey CE. J Neurol Neurosurg Psychiatr 1999;66:350–356.
37. Hennessy MJ, Elwes RD, Honavar M, Rabe-Hesketh S, Binnie CD et al. J Neurol Neurosurg Psychiatr 2001;70:450–458.
38. Goldstein R, Harvey AS, Duchowny M, Jayakar P, Altman N, Resnick T et al. J Child Neurol 1996;11:445–450.
39. Offringa M, Moyer VA. West J. Medicine 2001;175:254–259.
40. American Academy of Pediatrics. Provisional Committee on Quality Improvement, Subcommittee on Febrile Seizures. Pediatrics 1996;97:769–772
41. Teng D, Dayan P, Tyler S, Hauser WA, Chan S, Leary L et al. Pediatrics 2006;117: 304–308.
42. Harvey AS, Berkovic SF, Wrennall JA, Hopkins IJ. Neurology 1997;49:960–968.
43. Medina LS, Bernal B, Dunoyer C, Cervantes L, Rodriguez M, Pacheco E et al. Radiology 2005;236:247–253.
44. Medina LS, Bernal B, Ruiz J. Radiology 2007; 242:94–100.
45. Medina LS, Aguirre E, Bernal B, Nolan A. Radiology 2004; 230:49–54.
46. Lee JJ, Kang WJ, Lee DS, Lee JS, Hwang H, Kim KJ et al. Seizure 2005; 14: 213–220.

11

Diagnosis and Management of Acute and Chronic Sinusitis in Children

Yoshimi Anzai and Angelisa Paladin

Issues

I. Is there a role for imaging in the initial diagnosis of uncomplicated acute bacterial sinusitis in children?
II. What is the diagnostic performance of sinus radiography and sinus CT in acute bacterial sinusitis? What diagnostic criteria should we use for acute sinusitis?
III. When are imaging studies indicated for the diagnosis and the management of children with sinusitis?
IV. What is the most cost-effective strategy for the diagnosis and the management of patients with acute sinusitis?
V. What is the role of imaging in children with chronic sinusitis?
VI. Special situation: what is the role of imaging in immunocompromised children?

Key Points

- The clinical signs and symptoms of acute bacterial sinusitis overlap with that of non-specific upper respiratory tract viral infection (strong evidence).
- Children under the age of 6 years should not undergo sinus radiographs due to their limited sinus development (moderate evidence).
- Sinus radiographs are moderately sensitive to diagnose acute bacterial sinusitis compared with sinus puncture and culture (moderate evidence).
- Sinus CT is highly sensitive to diagnose acute bacterial sinusitis but specificity is low in part due to vaguely defined diagnostic criteria in the literature (limited evidence).

Y. Anzai (✉)
Department of Radiology, University of Washington Medical Center, Seattle, WA 98195, USA
e-mail: anzai@u.washington.edu

L.S. Medina et al. (eds.), *Evidence-Based Imaging in Pediatrics*,
DOI 10.1007/978-1-4419-0922-0_11, © Springer Science+Business Media, LLC 2010

- Definitive imaging criteria are the presence of frothy air–fluid levels or complete sinus opacification but do not include mucosal thickening (limited evidence).
- Despite relatively high sensitivity and specificity, imaging is not indicated in the initial diagnostic workup for acute uncomplicated sinusitis, due to cost and radiation dose (strong evidence).
- CT scan is indicated for patients that fail to respond to medical management or with severe symptoms suspicious for complications related to acute sinusitis (moderate evidence).
- In chronic sinusitis, computed tomography is a modality of choice as it provides anatomical roadmaps much better than plain radiography or ultrasound (limited to moderate evidence). Although rare, for children suspected of serious complications, such as intracranial or orbital abscess, MR with contrast is recommended to assist surgical treatment planning.

Definition and Pathophysiology

Acute sinusitis is a bacterial infection of the paranasal sinuses lasting less than 4 weeks. Under normal circumstances, the paranasal sinuses are assumed to be sterile. However, the paranasal sinuses are continuous to nasal mucosa or nasopharynx that is heavily colonized with bacteria. These bacteria are present in low density and removed by the normal mucociliary function of the paranasal sinuses. Normal mucous secretions contain antibodies and, together with mucociliary clearance, work to clear bacteria from the paranasal sinuses. Thus, maintaining the mucociliary flow and an intact local mucosal surface are key host defenses against infection (1).

The common predisposing events that set the stage for acute bacterial sinusitis are an acute viral upper respiratory infection that results in a viral rhinosinusitis (predisposes to approximately 80% of bacterial sinus infections) and an allergic inflammation (predisposes to 20% of bacterial infection). Once the mucosa of the paranasal sinuses swells due to either viral infection or allergy, it causes sinus ostia obstruction, thus interfering with normal mucociliary clearance. This leads to low pressure within the paranasal sinuses, thus further exaggerating mucosal thickening and poor sinus clearance, resulting in acute bacterial sinus infection. *Streptococcus pneumoniae* and *Haemophilus influenza* are two common organisms for acute bacterial sinusitis. Since the widespread use of the heptavalent pneumococcal conjugate vaccine (PCV7) in 2004, pneumococcal strains have declined; thus, *H. influenza* has become a more prevalent organism (2, 3). Other organisms include *Moraxella catarrhalis*, other *Streptococcus* and *Staphylococcus* species.

Epidemiology

Acute sinusitis is one of the most common diagnoses in primary care setting in the United States, affecting 31 million individuals diagnosed each year (4). Fourteen percent of Americans claim to have had a previous diagnosis of sinusitis (5). The prevalence of sinusitis has increased in the last decade due to increased air pollution and resistance to antibiotics. There is no gender difference in sinusitis prevalence. Sinusitis is more common in the Midwest and southern part of the country compared to the coasts.

Acute sinusitis more often affects patients with a history of allergy or asthma. Other patients with high risk of developing acute sinusitis include individuals with defects in immunity (HIV, agammaglobulinemia), delayed or absent mucociliary activity (Karagener's, cystic fibrosis), structural defects (cleft palate), and white blood cell functional abnormalities (chronic granulomatous disease, Wegener's granulomatosis) (6). Dental infections may cause 5–10% of all cases of maxillary sinusitis; the roots of the upper back teeth

(second bicuspid, first and second molars) abut the floor of the maxillary sinus.

Sinusitis affects all age groups. The prevalence of sinusitis among children is even higher than adults and may be as high as 32% in young children (7–9). The average child has between 6 and 8 "cold" episodes annually, and it is estimated that 5–10% of all upper respiratory infections are complicated by sinusitis. Children under the age of 6 years are the most likely to have acute bacterial sinusitis (10).

Acute maxillary sinusitis in adults is characterized by purulent nasal discharge, facial tenderness, headache or toothache, and fever. Children, however, may have less specific symptoms, such as a prolonged daytime cough lasting more than 10 days. The development of paranasal sinuses in children also contributes to diagnostic challenges. The maxillary and the ethmoid sinuses are present at birth. The sphenoid sinuses generally start to pneumatize by the age of 5 years; the frontal sinuses start to develop around the age of 7–8 years (10). Both frontal and sphenoid sinuses continue to develop until late adolescence. Sinus tenderness is not a typical sign observed in pediatric patients with acute sinusitis.

Overall Cost to Society

Sinusitis has a significant economic impact on health-care organizations. In 1992, Americans spent $200 million on prescription medications and more than $2 billion for over-the-counter medications to treat sinusitis (11). There were 11 million doctor visits and 1.3 million outpatient visits due to sinusitis in 1999 (12). Approximately 500,000 sinus surgeries are performed each year. The study using data from AHCPR's 1987 National Medical Expenditure Survey (inflated to 1996 dollars) estimated that overall health-care expenditures attributable to sinusitis were $5.8 billion, mainly from ambulatory and emergency department services and 500,00 surgical procedures performed on paranasal sinuses (13). Approximately 31% ($1.8 billion) of the cost was attributed to treatment expenditures for children 12 years or younger (14). They concluded that sinusitis needed to be recognized as a serious, debilitating, costly disease that warrants precise diagnosis and effective specific therapy (15). This estimate of direct costs does not include indirect costs, such as expense of care of sick children, transportation costs, the value of work time lost, baby-sitting costs, ancillary medication costs, and expenditures for treatment of adverse effects. Clearly, sinusitis imposes a considerable economic burden for the patients and the family. Therefore, improved diagnosis and the use of the most effective agents with the highest tolerability profile will improve outcomes and lower the overall cost of therapy.

It is important to keep in mind that the majority of "sinusitis" is caused by viral upper respiratory tract infection. The symptoms of acute viral sinusitis and allergic rhinitis overlap with that of acute bacterial sinusitis, leading to misdiagnosis. Consequently, acute bacterial sinusitis is overdiagnosed (in as many as 50–60% of cases), and therefore antibiotics are overprescribed in the primary care setting. Clinical studies showed that as many as 60% of patients with cold are prescribed antibiotics (16). The overprescription of antibiotics leads to a widespread antibiotic-resistant infection. Antibiotic-resistant infections are an increasing problem in hospitals in terms of the number of resistant organisms and their prevalence. Consequently, the costs of these infections are also increasing. Antibiotic resistance increases the costs of care in hospitals in various ways including increased length of stay, more admissions to intensive care unit, and more intensive resource use.

Goals

In patients presenting with acute sinusitis symptoms, the goal is to differentiate those with acute bacterial sinusitis who benefit from antibiotics from those with non-specific viral infection. Imaging is not indicated for the initial diagnostic workup for acute sinusitis, due to increasing cost and radiation for pediatric patients. Diagnosis and treatment decision, particularly prescribing antibiotics or not, is often made based on clinical examination for uncomplicated sinusitis.

Imaging is, however, indicated for patients who failed to respond to initial medical management. The goal of imaging at this setting is

to exclude (or include) diagnosis of acute bacterial sinusitis and to assess potential causes of poor mechanical drainage of the paranasal sinuses and complications such as orbital cellulitis or abscess formation (i.e., orbital subperiosteal abscess and anterior cranial fossa abscess).

Methodology: Medline and PubMed

The authors performed a MEDLINE search using PubMed (National Library of Medicine, Bethesda, MD) for data relevant to the diagnostic performance and accuracy of both clinical and radiographic examinations of patients with acute sinusitis. The diagnostic performance of clinical examination (history and physical exam) and clinical outcome was based on a systematic literature review performed in MEDLINE from January 1966 to October 2008. The clinical examination search strategy used the following statements: (1) acute rhinosinusitis, (2) acute bacterial sinusitis, (3) pediatric, (4) children, (5) clinical examination, and (6) outcomes. The review of the current diagnostic imaging literature was done with MEDLINE covering from January 1966 to October 2008 with the following key statements and words: (1) acute bacterial sinusitis, (2) radiograph, (3) CT, and (4) ultrasound, as well as combinations of these search strings. We excluded animal studies and non-English articles.

Discussion of Issues

I. Is There a Role for Imaging in the Initial Diagnosis of Uncomplicated Acute Bacterial Sinusitis in Children?

Summary of Evidence: Diagnosis of acute sinusitis should be made on clinical criteria in children. Radiographic imaging study should not be obtained to diagnose acute sinusitis or to confirm clinical diagnosis of acute sinusitis, particularly in children under the age of 6 years (17). Imaging as an initial diagnostic workup not only substantially increases the cost but also is potentially harmful due to radiation exposure.

It is, however, controversial if sinus radiography is needed as a confirmatory test of acute sinusitis in children older than 6 years with persistent and severe symptoms. Some practitioners may elect to perform sinus radiographs with the expectation that the study may be normal. Normal radiographs are powerful evidence that bacterial sinusitis is not the cause of a child's symptoms. Though solid evidence is lacking, guidelines from the ACR (American College of Radiology) and others state that the diagnosis of uncomplicated acute sinusitis should be made on clinical grounds alone and reserve the use of imaging for situations of medically refractory cases or worsening during the course of antibiotics treatment (18) (http://acsearch.acr.org/) (moderate evidence).

Supporting Evidence: Diagnosis of acute sinusitis should be made on clinical criteria in children who present with upper respiratory symptoms that are either persistent or severe. Clinicians should distinguish acute bacterial sinusitis (ABS) from acute viral rhinosinusitis using clinical diagnostic guidelines (strong evidence).

The clinical diagnostic guidelines for ABS in children are (a) persistent symptoms including nasal or postnasal discharge (of any quality) and daytime cough (which may be worse in night) and (b) symptoms lasting more than 10–14 days but less than 30 days (10). Severe symptoms include a temperature of at least 102°F and purulent nasal discharge present concurrently for at least 3–4 consecutive days in a child who seems ill or toxic (10). Respiratory symptoms related to acute viral sinusitis may not have completely resolved by the 10th day but almost always have peaked in severity and begun to improve. Therefore, persistence of respiratory symptoms without any signs of improvement suggests the presence of bacterial infection. Facial pain is rare and unreliable for children. Periorbital swelling may indicate ethmoid sinusitis. If fever is present in uncomplicated viral infection, it is usually at earlier phase of illness and accompanied by other constitutional symptoms such as headache. Purulent nasal discharge does not appear for several days in uncomplicated viral infection. The concurrent presentation of fever and purulent nasal discharge for at least 3–4 consecutive days helps diagnose acute bacterial sinusitis (17).

Physical examination does not contribute to the diagnosis of acute bacterial sinusitis. Transillumination has little value, and its clinical use is controversial. Sinus aspiration is the gold standard for the diagnosis of acute bacterial sinusitis; but it is an invasive, time-consuming, and potentially painful procedure that should be performed only by a specialist (otolaryngologist) (19).

Radiographic imaging should not be obtained for patients who meet diagnostic criteria for ABS. Imaging studies are not necessary to confirm a diagnosis of clinical acute bacterial sinusitis in children younger than 6 years of age (strong recommendation). In children younger than 6 years of age, clinical history correlates with sinus radiography in 88% of time (20); therefore radiography can be safely omitted for children under age 6 (strong consensus based on limited evidence). The paranasal sinuses are still under development in younger children. Therefore, lack of aeration of the sinuses may be physiological rather than infectious, limiting the accuracy of radiography (21).

For children over 6 years of age with persistent symptoms, the need for radiograph as a confirmatory test of acute sinusitis remains controversial. When an alternative diagnosis is considered, imaging might be useful. Normal radiographs or CT is a powerful evidence that bacterial sinusitis is not the cause of the symptoms (22) (limited evidence).

A practical guideline by AHRQ indicates that imaging study is not warranted when the likelihood of acute sinusitis is either high or low, but imaging is useful when a diagnosis is in doubt (limited evidence).

Sinus CT is indicated for children with acute sinusitis symptoms in the following three conditions: (1) when complications related to sinusitis are suspected, (2) when symptoms persist without response to medical management, and (3) when surgery is considered (strong recommendation based on moderate evidence). Complicated sinusitis is suspected when patients present with ptosis, cranial nerve palsies, and facial and orbital swelling. Contrast-enhanced CT of the sinuses and orbit is recommended when orbital cellulites or periosteal abscess as a complication of sinusitis is suspected (18, 23, 24). Contrast-enhanced MRI is occasionally recommended when intracranial extension, such as epidural empyema or brain abscess, is suspected (21, 25–28) (limited evidence).

II. What Is the Diagnostic Performance of Sinus Radiography and Sinus CT in Acute Bacterial Sinusitis? What Diagnostic Criteria Should We Use for Acute Sinusitis?

Summary of Evidence: Although the diagnosis of acute sinusitis should be made on clinical grounds, the accuracy of such clinical diagnosis is not well documented compared with the gold standard of direct sinus puncture. Compared with sinus radiography as the gold standard, clinical diagnosis has moderate accuracy (moderate evidence) (13). Summary receiver operating characteristics (SROC) is used to represent the accuracy of a diagnostic test, where one is perfect accuracy and 0.5 is no better than the flip of a coin. The area under the curve (AUC) of clinical diagnosis compared with sinus radiograph is 0.74 (29). Compared with sinus puncture as the gold standard, sinus radiography offers moderate ability to diagnose acute sinusitis (SROC area 0.83) (moderate evidence) (30–34). No single study comparing CT or MR with sinus puncture to evaluate the accuracy of CT or MR for acute sinusitis was found. Given CT and MRI's superior spatial and soft tissue resolution to radiography, both are likely more sensitive for detection of acute sinusitis, but specificity is questionable. Lack of definitive diagnostic criteria for sinus disease makes it difficult to interpret studies investigating specificity of sinus CT or MRI.

Sinus puncture performed by an otolaryngologist is the gold standard; however, it is rarely performed due to its invasiveness and cost. An inexpensive, simple, and accurate diagnostic test is needed to better differentiate patients who need antibiotics from those with nonspecific viral illness. Good, high-quality evidence for acute uncomplicated sinusitis in children is limited. Diagnostic modalities show poor concordance. More evidence is needed for defining the optimal treatment and diagnostic methods for this common condition (35) (insufficient evidence).

Supporting Evidence: The most accurate and cost-effective way to diagnose acute sinusitis remains uncertain. The diagnosis of acute sinusitis is often made based on clinical grounds, but the accuracy of such clinical diagnosis is not well documented. Engels et al. performed a meta-analysis of diagnostic tests for acute sinusitis that showed clinical history and physical examination had moderate ability to identify patients with positive radiography (SROC area 0.74) (33).

Using sinus opacity or the presence of an air–fluid level as the criterion for sinusitis, sinus radiography had sensitivity of 0.73 and specificity of 0.80. Compared with sinus puncture and aspiration as the gold standard, sinus radiography offers moderate ability to diagnose acute sinusitis (SROC area 0.83). Another systematic review performed by Varonen et al. published concurrently with Engels et al. study focused on adult patients suspected of acute maxillary sinusitis. They compared sinus radiography, ultrasound, and clinical examination with sinus puncture as the gold standard and concluded that sinus radiography was a more accurate method for diagnosing acute sinusitis (SROC area of 0.82) than clinical examination. Clinical examination even by experienced physicians was less reliable (area under SROC is 0.75) (34). Using sinus puncture as the gold standard, Berg and Carenfelt reported that clinical examination had a sensitivity of 66% and specificity of 79% in the setting of emergency clinic (36). Sinus radiograph is accurate than clinical examination for diagnosis of acute bacterial sinusitis. However, clinical application for sinus radiograph as an initial workup is not justified due to its costs and radiation exposure.

In Europe, A-mode ultrasound is used to diagnose acute maxillary sinusitis in primary care setting with moderately strong accuracy (SROC area of 0.80) (30, 34, 37). Savolainen et al. reported among 234 patients suspected of maxillary sinusitis that ultrasound had a sensitivity of 81% and specificity of 72%, as compared with sinus puncture (38). Ultrasound waves are transmitted to the sinus, then reflected back from the interface of two different media. A sinus cavity filled with secretions results in an echo in the display screen. It is insensitive to mucosal thickening of the sinus (39).

Computed tomography (CT) provides superior assessment of all paranasal sinuses compared with sinus radiograph (40). However, CT has not been directly compared with sinus puncture for assessment of diagnostic accuracy (33, 34). Given the invasiveness of sinus puncture and the need for otolaryngology referral (additional cost), sinus CT can be used as a proxy of sinus puncture. Sinus CT is considered more sensitive than sinus radiograph for diagnosis of acute sinusitis. A study comparing sinus plain radiograph and CT in 47 consecutive patients showed that sinus radiograph had a high specificity but markedly low sensitivity for disease in the ethmoid, frontal, and sphenoid sinuses (41). The sensitivity of sinus radiograph for maxillary sinus was 80% in this study. Another study enrolled 134 patients with suspected sinusitis who underwent a single Waters view of sinus, and CT revealed that plain film has markedly low sensitivity for a disease outside of maxillary sinus. The sensitivity and specificity of Waters view compared with CT for maxillary sinus disease was 67.7% and 87.6%, respectively (42). They recommended the use of a low-dose, high-resolution CT scan of the paranasal sinuses (moderate evidence). The problem is its lack of specificity data of sinus CT, compared with sinus puncture. A question is if CT scan overdiagnoses sinusitis.

Another reason that accuracy of sinus CT remains uncertain and controversial is lack of definitive diagnostic criteria. Diagnostic criteria of sinus radiography for acute sinusitis are complete opacification and sinus air–fluid level. Diagnostic criteria considered positive for acute sinusitis on sinus CT are not well defined but usually include mucosal thickening greater than 4 mm, any degree of sinus opacification, and any type of fluid level. Mild mucoperiosteal thickening can be found on head CT in patients without any sinusitis-related symptoms in up to 40% of individuals (43). Gwaltney et al. reported on CT scan of 31 patients with self-diagnosed common cold. They found that 87% of 31 patients had occlusion (or mucosal thickening) of ethmoid infundibulum, and 65% of patients had mucosal abnormality in maxillary sinuses (44). It is of paramount importance to define what CT findings constitute acute bacterial sinusitis. The only specific CT finding to indicate acute sinusitis is a frothy, bubbly

air–fluid level, which indicates purulent secretion within the sinuses (21). Waterish smooth air–fluid level may be nasal secretion without bacterial infection or clear secretion related to allergic rhinitis (45). Complete opacification of a sinus with bone thickening may indicate chronically obstructed sinus rather than acute sinusitis (46).

For children under 6 years whose paranasal sinuses are still under development, mucosal thickening or fluid level may be physiological, rather than acute sinusitis. This is another reason that imaging test should be reserved for when complicated sinusitis is suspected or alternative diagnosis is suggested in cases of poor response to medical therapy (10).

III. When Are Imaging Studies Indicated for the Diagnosis and the Management of Children with Sinusitis?

Summary of Evidence: Imaging studies, sinus radiography, and CT or MR are normally not indicated as the initial diagnostic workup for uncomplicated acute sinusitis. Imaging studies are indicated when patients do not respond to medical management, when diagnosis is in doubt, or when complications related to sinusitis are suspected.

Sinus CT should be performed in children who present with complications of acute bacterial sinusitis or who have very persistent or recurrent disease not responding to medical management. When patients do not respond to medical management, the patients may have mechanical obstruction that prevents restoration of mucociliary clearance, such as a polyp or structural anomalies of the nasal cavity and sinuses.

Sinusitis is a self-limiting disease with complete cure in most cases. However, serious complications still do occur in a small percentage (3.7–11%) of these patients with acute sinusitis (47). When patients with sinusitis symptoms present with orbital swelling, ptosis, visual changes, cranial nerve palsies, and mental status changes, contrast-enhanced CT and/or MR is recommended to diagnose orbital cellulitis/abscess, epidural or subdural empyema, cavernous sinus thrombosis, and intracranial extension of infection (28).

When surgery is considered for patients with recurrent or medically refractory disease, detailed sinus CT is indicated to define the bony anatomy, including the osteomeatal complex, and correlated with patients' clinical symptoms (48, 49) (limited evidence).

Supporting Evidence: Sinusitis is a common condition among pediatric patients and in most cases is a self-limited disease. Most cases of sinusitis resolve completely with appropriate antibiotic therapy. Children with complicated acute sinusitis have severe symptoms, including high fever, intense headache that is above or behind the eye, periorbital swelling, or pressure over the face. Complicated acute sinusitis results from a delay in initiating treatment, antibiotic-resistant infection, and incomplete treatment. Immunocompromised patients, such as those with cystic fibrosis, often present with extensive sinus infection. The incidence of sinusitis-related complications remains indeterminate as many literatures reporting sinusitis-related complications were case series or case reports. A retrospective review from a single institution revealed that 5.3% of ENT emergencies were sinusitis complications. Among them, orbital complications were the most common (62%), followed by acute subdural empyema (23%) and meningitis (15%) (50). Among the transplant patients, patients with graft versus host disease (GVHD) were 4.3 times more likely than patients without GVHD to develop sinusitis post-transplant (51).

These include intraorbital complications, such as orbital cellulitis and subperiosteal abscess, cavernous sinus thrombosis, epidural empyema, meningitis, cerebritis, and brain abscess. Therefore, contrast-enhanced CT or MR is indicated when patients with sinusitis symptoms present with orbital swelling, proptosis, visual changes, and cranial nerve palsies (27, 52, 53). Clary et al. investigated the accuracy of sinus CT for orbital abscess as compared with surgical exploration in 19 patients and reported that CT had a sensitivity of 93% and specificity of 67% (54).

With the advent of antibiotics, the incidence of orbital cellulitis is low. Approximately 3% of sinusitis progresses to orbital cellulitis (40). This

can be divided into preseptal and postseptal cellulitis. The septum is defined as the medial orbital periosteal reflection attaching to the medial eyelid at the tarsal plate. The majority of orbital cellulitis is either due to direct spread from ethmoid sinusitis through porous lamina papyracea or through the valveless anterior and posterior ethmoid veins (40). The periosteum of the medial orbital wall is loosely attached to the lamina papyracea; as such, it often forms subperiosteal abscess or phlegmon. Clinically, these patients may present with deviation of the globe or proptosis. Cavernous sinus thrombosis results from infection of the midface, orbit, and sinonasal cavity. This may lead to cranial nerve palsies and blindness. In the setting of orbital cellulitis, the presence of cranial nerve palsies involving cranial nerve III, IV, V, and/or VI raises the suspicion of cavernous sinus thrombosis. Contrast-enhanced CT or MR shows an engorged superior ophthalmic vein. Enhancing cavernous carotid artery may stand out from the surrounding thrombosed cavernous sinus (55–58).

Intracranial spread of sinus infection most commonly originates from frontal or sphenoid sinusitis (59, 52). Intracranial extension of infection is facilitated by the abundant valveless emissary venous plexus of the posterior frontal sinus, known as Behcet's plexus. Infection spreads through the sinus to dura, meninges, and parenchyma, resulting in epidural or subdural empyema, meningitis, cerebritis, and brain abscess (55). Contrast-enhanced brain MR is recommended when intracranial spread of sinusitis is suspected (52, 55). One study comparing diagnostic accuracy of CT, MR, and clinical diagnosis for sinusitis-related complications revealed that the diagnostic accuracy was 82% for clinical assessment compared with 91% for CT for orbital complications. For patients with intracranial complications, meningitis was the most common diagnosis, and MRI was more accurate (97%) in determining the diagnosis than CT (87%) or clinical findings (82%). Both CT and MR have improved the management and outcomes of patients who have sinusitis with complications (60).

Surgery of the sinuses or nasal passage may be considered for patients who do not respond to medical management for sinusitis. Sinus CT is the primary imaging test and provides detailed images of sinus anatomy in multiple planes. Attention should be paid to the status of the osteomeatal complex, particularly the curvature and the superior extension of the uncinate process. Sinus CT often reveals various anatomical variations, such as nasal septum deviation or concha bullosa. A study evaluating anatomical variations of sinuses on CT revealed that 64.9% of 202 patients had anatomical variations. The significance of such anatomical variant remains uncertain, as these anatomical variations are often seen in patients without any sinusitis symptoms (61).

IV. What Is the Most Cost-Effective Strategy for the Diagnosis and the Management of Patients with Acute Sinusitis?

Summary of Evidence: The most cost-effective method to manage patients presented with mild to moderate symptoms of acute sinusitis is to use clinical guidelines and treat with first-line antibiotic therapy (59). For patients with severe symptoms or high disease prevalence population, empirical antibiotic treatment is cost effective. This leads to many unnecessary antibiotic prescriptions that lead to antibiotic-resistant infection.

Cost-effectiveness analysis (CEA) comparing four different management strategies (empirical antibiotics, no antibiotics, clinical diagnosis, or sinus CT-based treatment) of adult acute sinusitis revealed that empirical antibiotic therapy is most cost effective from the societal perspective, as patients return to normal life more quickly, offsetting the upfront cost of antibiotics (62, 63). From the payer's perspective, clinical diagnosis-based treatment was the most cost-effective strategy (62). The effectiveness of antibiotic therapy in children remains controversial. The study results depend highly on the inclusion criteria of the study population. Antibiotic therapy was effective for patients with radiographically confirmed pediatric acute sinusitis, but little or no effect is seen when patients were selected based on clinical diagnosis (9) (moderate evidence). This is likely due to the fact that some of these patients had viral infection, therefore potentially diluting the effectiveness of antibiotic therapy (64).

A full sinus CT instead of screening or limited sinus CT is recommended for patients with

chronic sinusitis who undergo sinus surgery. The screening sinus CT for preoperative assessment was thought to be inadequate for operative planning (65).

Supporting Evidence: A diagnostic workup strategy for any disease should be directly connected to its management of the disease. Although sinusitis is a self-limiting disease in most cases, undertreating acute sinusitis may lead to rare but serious complications. Children remain sick longer, thus requiring additional cost for childcare, time away from work for parents, loss of productivity of parents, transportation, and over-the-counter medications (63). Overtreating sinusitis may result in unnecessary costs and adverse effects from antibiotic therapy, such as allergic reaction or gastrointestinal disturbance, as well as future development of antibiotic-resistant infection. Treating viral illness with antibiotic should not change the natural history of sinusitis, other than reduced quality of life from adverse drug effects. Accurate diagnosis by CT scan improves effectiveness of antibiotic therapy, by selecting patients who benefit from antibiotics. However, such additional benefit is too small to justify the additional cost of CT scan and the additional risks from radiation exposure in children.

The effectiveness of antibiotic therapy in children remains controversial. The results depend highly on the study inclusion criteria. Antibiotic therapy was found effective for patients with radiographically confirmed acute sinusitis (moderate evidence). Patients treated with antibiotics recovered more quickly than those under placebo (20). On the third day of treatment, 83% of children receiving antibiotics were cured or improved compared with 51% of the children in the placebo group. However, little or no effect is seen in antibiotic treatment when patients were selected based on clinical diagnosis alone. A study by Garbutt (9) challenged the notion that children having acute sinusitis based on clinical ground will benefit from antibiotic therapy. Since "sinusitis patients" defined by clinical diagnosis include children with viral infection, the effectiveness of antibiotics is diluted.

The American Academy of Pediatrics clinical practice guidelines for the management of sinusitis show that children with mild and moderate symptoms who do not attend day care should receive the usual dose of amoxicillin (17). Those patients who (a) do not improve while receiving the usual dose of amoxicillin, or (b) have recently been treated with antibiotics, or (c) have illness that is moderate to severe, or (d) attend day care should receive high dose of amoxicillin with clavulanate. Higher doses of amoxicillin are effective for *S. pneumoniae* species that are intermediate in resistance to penicillin, and potassium clavulanate is effective against β-lactamase-producing *H. influenza* and *M. catarrhalis*. Children with penicillin allergy should receive cefuroxime, cefpodoxime, cefdinir, azithromycin, or clarithromycin.

The AAP guidelines make no recommendations about the use of antihistamines, decongestants, and intranasal steroids based on limited or controversial data (10).

V. What Is the Role of Imaging in Children with Chronic Sinusitis?

Summary of Evidence: Clinical diagnosis of chronic sinusitis is even more difficult than that of acute sinusitis. Children with chronic sinusitis have relatively vague symptoms that overlap with viral upper respiratory infection, allergy, and migraine. Imaging plays an important role in excluding diagnosis or identifying anatomical causes leading to sinusitis. Computed tomography is a modality of choice as it provides anatomical road maps much better than plain radiography or ultrasound (limited to moderate evidence). Although rare, for children suspected of serious complications such as intracranial or orbital abscess, MR with contrast is recommended to assist surgical treatment planning.

Supporting Evidence: Chronic sinusitis is defined as sinusitis symptoms lasting more than 12 weeks. The diagnosis of chronic sinusitis is difficult because of relatively non-specific signs and symptoms that overlap with viral upper respiratory infection and allergy. Children or adolescents with chronic headache are often misdiagnosed as sinus headache and receive sinus medication (66). Imaging plays a major role in making or excluding diagnosis or assessing the anatomy of sinuses leading to recurrent or chronic infection (67).

In terms of the choice of imaging for children with chronic sinusitis, sinus radiography was reported to overestimate abnormalities. In a study which performed sinus radiography and CT in 34 children with chronic sinusitis, sinus radiography (Waters and occipitomental views) overestimated ethmoid sinus disease in 24% and maxillary sinus disease in 56% (68) (limited evidence). Sinus CT provides details on anatomy as well as the extent of disease better than sinus radiography and remains the imaging study of choice for patients with chronic sinusitis. CT scan is often performed in children who remain symptomatic following multiple courses of antibiotics in order to diagnose or rule out the presence of obstructive lesion interfering mucociliary clearance.

If sinus CT is completely normal in children who are suspected of having chronic sinusitis, diagnosis can be excluded. When sinus CT shows a focal intranasal mass with unilateral sinus opacification, this may lead to evaluation by endoscopy for possible surgical resection. The problem lies, however, when sinus CT shows mild, non-specific, diffuse mucosal thickening without correlation with clinical symptoms; in terms of facial pain, or tenderness, it is difficult to determine if sinusitis contributes to patients' clinical symptoms.

A study comparing CT scan findings of 60 children aged 2–12 with chronic sinusitis with 50 control subjects who underwent CT scan for indications other than sinusitis found that mucoperiosteal thickening is a highly prevalent finding seen in 60% of patients and 46% of control groups (limited to moderate evidence). Early-stage (mild) mucoperiosteal thickening was present in the majority of children who had sinus CT (98% of control and 85% of children with chronic sinusitis) (69). Certain anatomical variations are thought to contribute causality of chronic sinusitis as these variations may interfere with sinus drainage pathways. These include, but are not limited to, nasal septum deviation, concha bullosa, and Haller cells. Significance of anatomic variations in children is still controversial as these findings can be seen in asymptomatic subjects (70).

Medical management remains the cornerstone for children with chronic sinusitis. Indication for sinus surgery is controversial. No prospective randomized trial comparing medical management with surgery has been reported. The decision regarding the need for sinus surgery should not be solely based on imaging abnormalities. A study investigating the impact of sinus CT on therapeutic decision making by otolaryngologists showed that the concordance between CT abnormalities and patient's symptoms and the obstruction of osteomeatal complex are the main predictors of favorable surgical treatment (71). Sinus surgery may be performed in children with nasal obstruction from polyposis or refractory sinusitis aggravating asthma (72). Outcome assessment for 308 children with chronic sinusitis after sinus surgery revealed that endoscopic sinus surgery improved outcomes in 2-year follow-up in the intermediate stages of chronic sinusitis (stages II and III out of stages I–IV) (73). Some study suggested the use of IV antibiotics for children who have failed to respond to traditional oral antibiotic therapy (74).

VI. Special Situation: What Is the Role of Imaging in Immunocompromised Children?

Summary of Evidence: Invasive fungal sinusitis (IFS) has been increasingly seen in immunocompromised children. The incidence has increased in accordance with increased use of antibiotics, steroids, chemotherapy, and radiation treatment. IFS is a difficult disease to treat. CT findings that are characteristic of IFS include mucoperiosteal thickening associated with bone erosion or extrasinus soft tissue invasion to orbit or retroantral fat pad. CT is helpful for planning of surgical debridement. However, diagnosis of IFS should not be solely based on CT, as CT findings suggestive of IFS, bone erosion, or extrasinus invasion are often absent in an earlier course of disease (75). With a high clinical suspicion, rigid nasal endoscopy with biopsy is recommended for early diagnosis (75). Complete surgical resection and reversal of neutropenia are critical elements for improved outcomes.

Supporting Evidence: Invasive fungal sinusitis (IFS) is a rare but life-threatening disease in children with underlying immunocompromised disease. Incidence has been increasing in accordance with expansion of transplant medicine and progress in antineoplastic

medication for hematological malignancies. Common fungal organisms seen in immunocompromised children include aspergillosis, mucormycosis, and zygomycosis. IFS often spreads directly to the brain via vascular channels or is blood borne from pulmonary infection. Abscess formation along blood vessels often causes thrombosis of vessels, leading to neurological deficit (76). Therefore, when immunocompromised patients present with stroke type of symptoms, intracranial involvement of IFS is highly suspected. IFS in immunocompromised children has a high mortality rate and requires early diagnosis and treatment.

Imaging study such as sinus CT plays an important role in demonstrating the extent of disease, the degree of bone destruction, the orbital invasion, the extrasinus soft tissue invasion, and the vascular encasement. When intracranial involvement is suspected, such as epidural abscess/phlegmon, cerebritis, or septic emboli, brain MR with and without contrast is essential to make a diagnosis and plan appropriate surgical management. MR allows differentiation of direct cerebral invasion from multiple brain abscess or septic emboli. Venous sinus thrombosis is also another serious complication that can be diagnosed with MR and MR venogram.

However, classic CT findings of IFS are often absent in earlier course of disease. Retrospective review of CT findings in 23 immunocompromised patients (limited evidence) with confirmed IFS showed that many patients had mucoperiosteal thickening of sinuses (21/23), but bone erosion (8/23) or orbital invasion (6/23) was seen only in more advanced IFS. They found that disease was frequently unilateral (21/23). Thus, clinician should not rely solely on imaging to make a diagnosis of IFS. With a high index of suspicion, early nasal endoscopy and biopsy and initiation of antifungal therapy are critical to improve prognosis.

Treatment for IFS includes surgical debridement, followed by high-dose antifungal treatment, and attempts to correct underlying immunocompromised state are essential for improved survival.

Take Home Figures and Tables

Figure 11.1 demonstrates an algorithm for the management of a child with acute sinusitis.

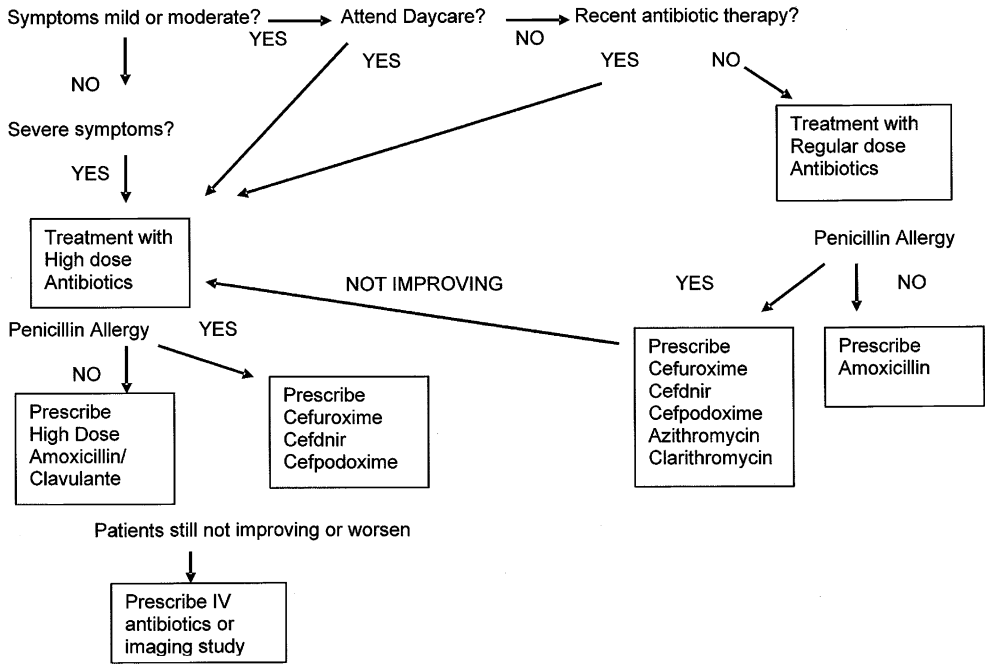

Figure 11.1. Management of acute sinusitis in children.

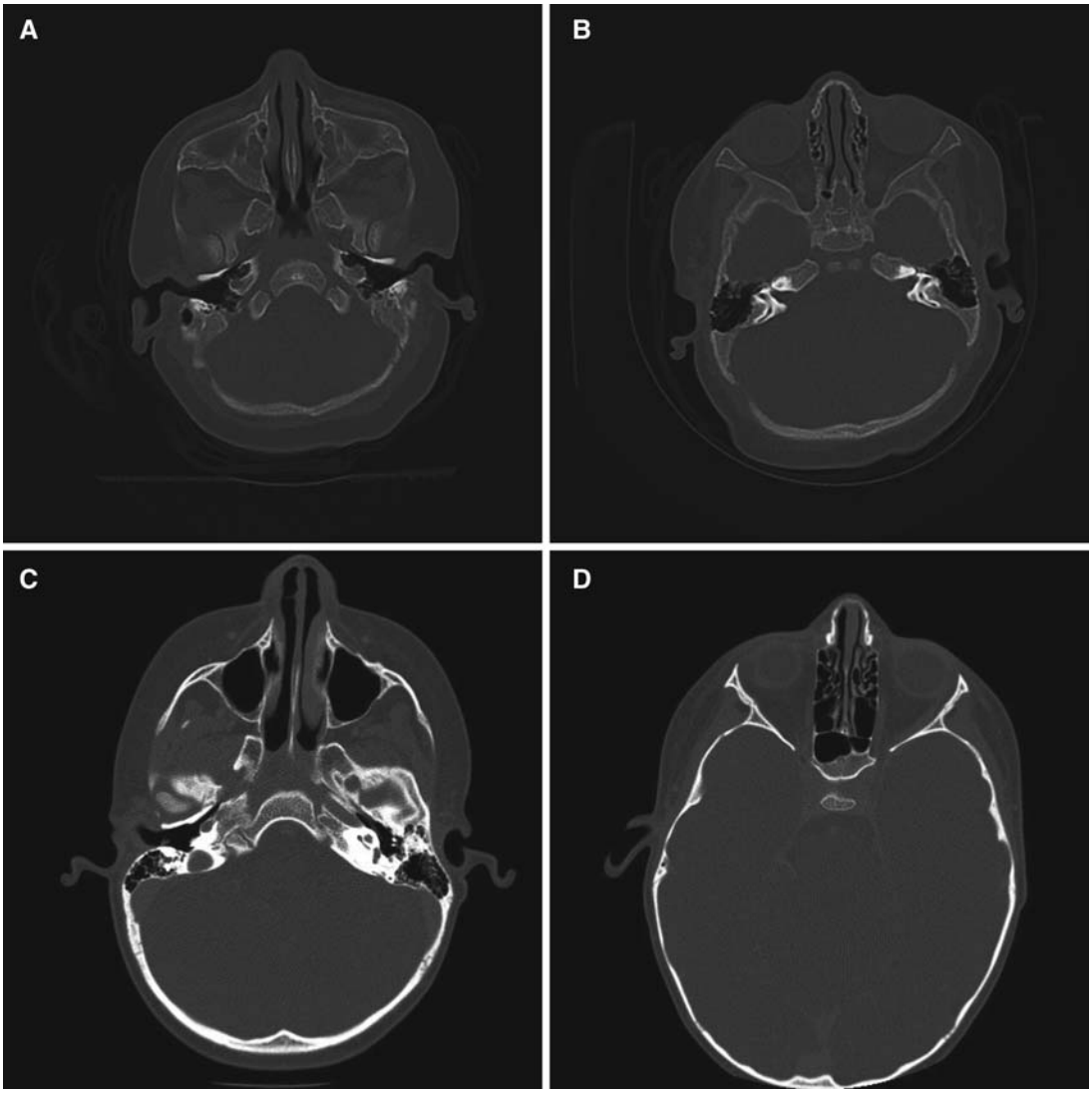

Figure 11.2 Normal development of paranasal sinuses. **A**: 0–1-year maxillary sinus. **B**: 0–1-year ethmoid sinuses. **C**: 3–4-year maxillary sinus. **D**: 3–4-year ethmoid and sphenoid sinuses. **E**: 6–8-year maxillary and ethmoid sinuses. F: 6–8-year sphenoid sinuses. **G**: 14–18-year maxillary and ethmoid sinuses. **H**: 14–18-year sphenoid sinuses.

Figure 11.2 demonstrates the normal development of paranasal sinuses. Table 11.1 gives the definition of acute sinusitis. Table 11.2 presents the clinical signs/symptoms of acute bacterial sinusitis vs. viral upper respiratory infection. Table 11.3 is a summary table of diagnostic performance of imaging and clinical examinations for diagnosing acute sinusitis in children.

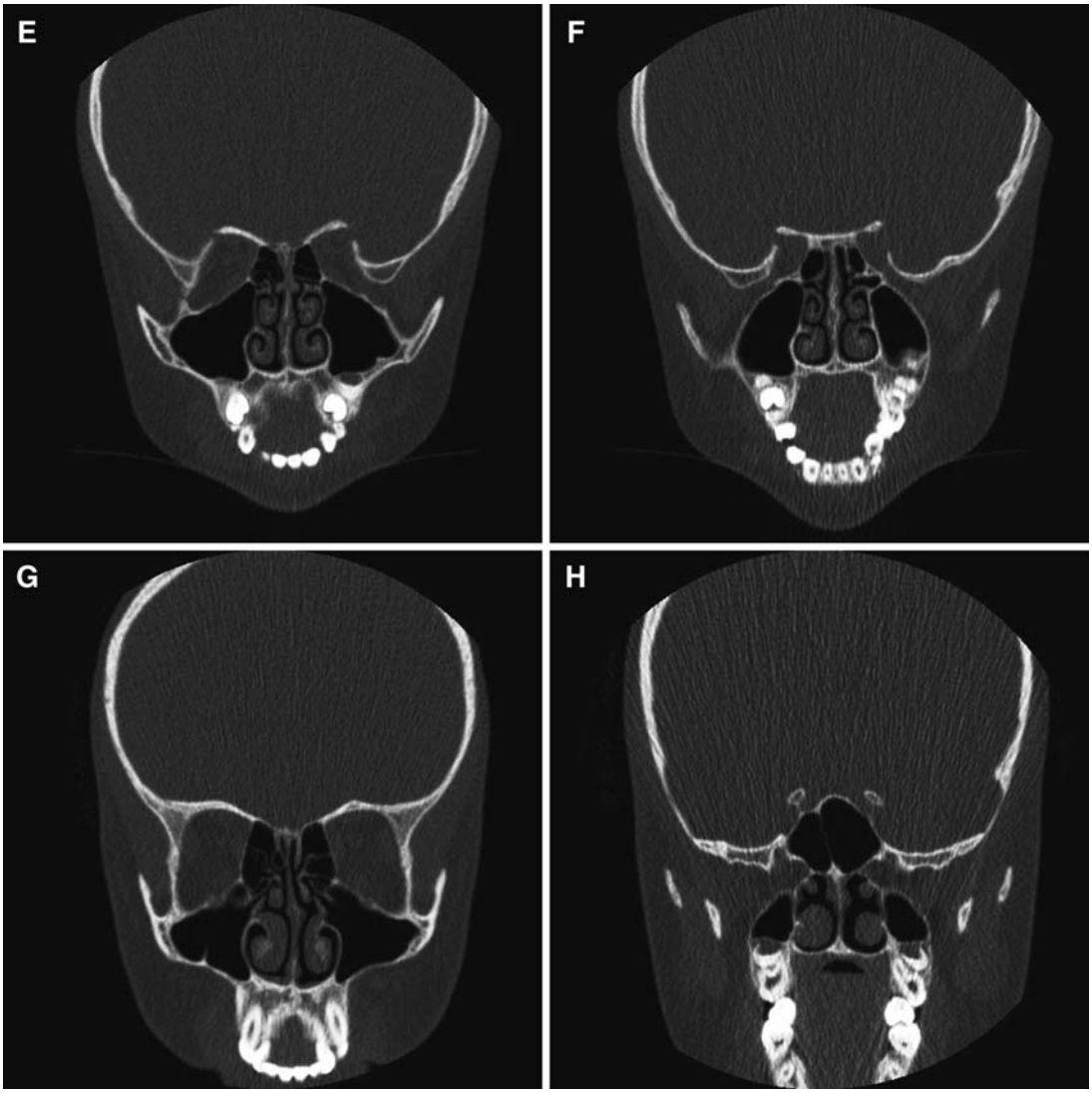

Figure 11.2. *Continued*

Table 11.1. Definition of acute bacterial sinusitis (acute sinusitis) in children

Acute sinusitis **Infection of the paranasal sinuses lasting less than 30 days that presents with either *persistent or severe symptoms*** ***Persistent symptoms* are those that last longer than 10–14 days. Such symptoms include nasal or postnasal discharge, daytime cough (which may be worse at night), or both** ***Severe symptoms* include a temperature of at least 102°F and purulent nasal discharge present concurrently for at least 3–4 consecutive days in a child who seems ill**

Table 11.2. Acute bacterial sinusitis vs. viral upper respiratory infection. Clinical signs and symptoms

	Acute bacterial sinusitis	Viral URI
Duration of illness	Longer than 10–14 days	Usually less than 5–7 days
Symptoms	Persistent or worsening after mild resolution (double sickening)	Improved or resolved by 10 days
Fever	Concurrent presentation of high fever and nasal discharge	Earlier in illness and later nasal discharge
Headache	Severe headache behind eyes	Mild headache
Facial pain	Unilateral pain But not reliable for small children	Mild or absent

Table 11.3. Summary table of diagnostic performance of imaging and clinical examinations for diagnosing acute sinusitis in children (only those using sinus puncture as gold standard)

	Sensitivity (95% CI)	Specificity (95% CI)	References
Physical exam only	0.66 (0.58–0.73)	0.79 (0.73–0.87)	(15, 33, 34, 34, 36)
Radiographs	0.87 (0.85–0.88)	0.89 (0.85–0.91)	(31–34)
Ultrasound	0.85 (0.84–0.87)	0.82 (0.80–0.83)	(30, 32, 35, 37, 38)
CT: No study assessing accuracy of CT using sinus puncture as the gold standard			
CT (orbital abscess)	0.93	0.67	(5)

Imaging Case Studies

Figures 11.3 and 11.4 show images of various sinus findings and diagnoses and complications of acute sinusitis, respectively.

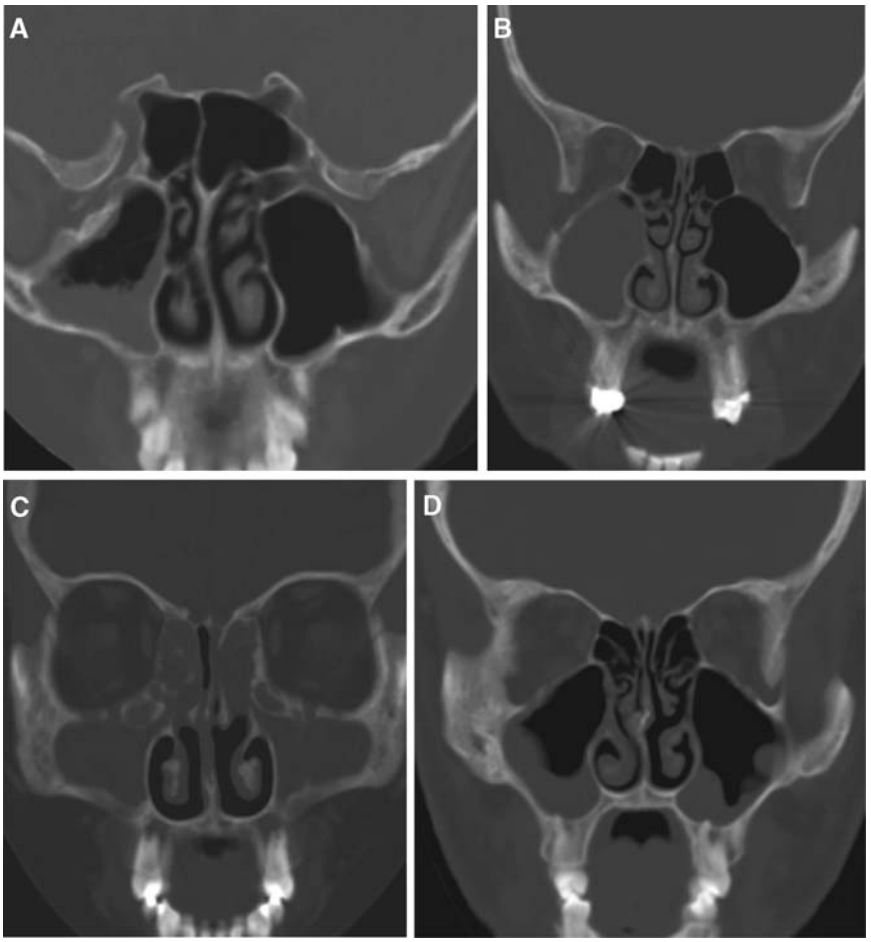

Figure 11.3. Various imaging findings and suggested diagnosis. **A**: Air–fluid level in the right maxillary sinus: findings highly suspicious of acute bacterial sinusitis. **B**: Near-complete opacification of right maxillary sinus in a patient suspected of acute sinusitis. **C**, **D**: Diffuse mucosal swelling and opacification of maxillary and ethmoid sinuses with thickening of bone walls in a patient with sinonasal polyposis.

Figure 11.4. Imaging of sinusitis complications. **A**: A patient with fungal infection involving ethmoid sinuses complicated with left cavernous sinus thrombosis. **B**: Coronal image shows extension of infection to the medial left orbit associated with focal bone erosion. **C**: A young patient presented with headache and mental status change. Non-contrast head CT shows focal air near the fluid collection in the base of the left frontal lobe. **D**: Sagittal reformatted image shows an expansive sphenoid sinus with adjacent pneumocephalus. **E**: Contrast-enhanced, fat-suppressed coronal image shows a focal epidural abscess adjacent to the left sphenoid sinus, underneath the air pocket. This patient was thought to have left sphenoid mucocele with intracranial ruptured, resulting in epidural abscess.

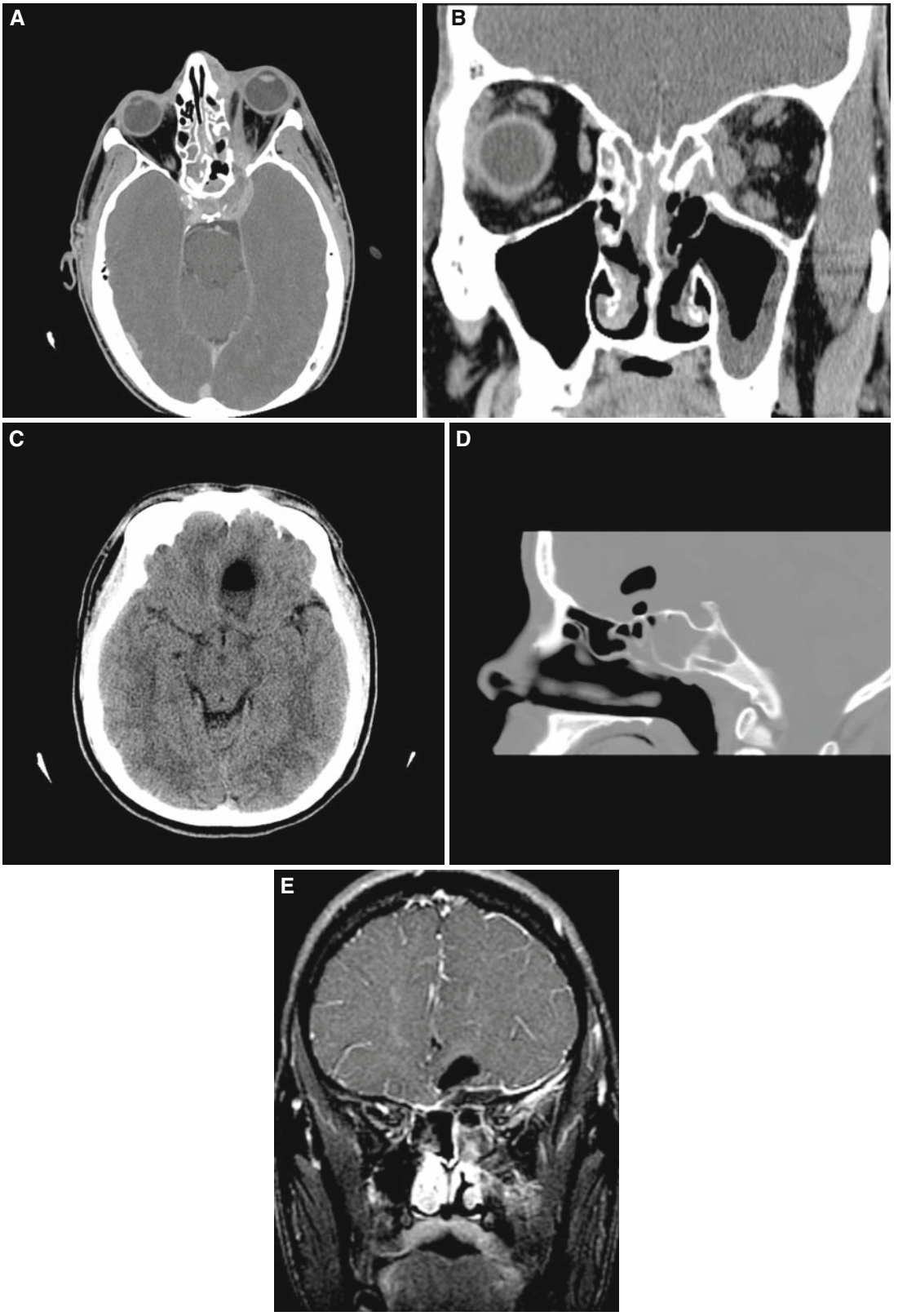

Figure 11.4. *Continued*

Suggested Imaging Protocols for Children Clinically Suspected of Acute Sinusitis

Sinus Radiographs

Sinus radiographic series has been rapidly replaced by the limited sinus CT for evaluation of sinusitis. However, some pediatricians still order sinus radiograph, likely due to either lower costs or easier access to radiographs than CT. In order to visualize and assess all paranasal sinuses, at least three views of sinus are required. These include Waters view, Caldwell view, and lateral view. In children under the age of 6 years, the ACR (appropriateness criteria) states that radiographs of the paranasal sinuses are both not indicated and technically difficult to perform. For recurrent infection, some clinicians order a single Waters view to evaluate the maxillary sinuses.

Low-Dose Screening Sinus CT

Low mA and low kVp are most widely used for the assessment of sinus infection in our institution, when available, reducing radiation dose compared with the standard CT (77). Screening sinus CT demonstrates air–fluid level or sinus opacification, as well as adjacent soft tissue abnormalities and mastoid and middle ear fluid collection.

MDCT allows rapid acquisition of axial images through paranasal sinuses with thin collimation ($\leq$5 mm), in supine position using 100 mAs and 120 kVp. Reconstruction of these images in the coronal plane is routinely performed. No intravenous contrast is necessary unless there is a suspected complication such as orbital abscess or epidural empyema. No sedation is needed for these rapidly acquired CTs.

MRI

When MR is needed to assess intracranial complications, the following sequences should be included: Axial FLAIR, Axial Diffusion, Axial T2 FSE, pre- and postcontrast T1 multiplanar images. Fat suppression should be used for the assessment of postcontrast images in order to better visualize cavernous sinuses, orbital apex, skull base, as well as epidural and subdural spaces.

Future Research

- Large clinical study correlating imaging and clinical findings with sinus aspiration and treatment outcomes.
- Develop non-invasive strategies to accurately diagnose acute sinusitis in children, particularly imaging that differentiates bacterial infection from viral infection or allergic inflammation.
- Determine optimal duration of antibiotic therapy for children with acute bacterial sinusitis.

References

1. Kennedy DW. Otolaryngol Head Neck Surg 1990;103:884–886.
2. Fletcher MA, Fritzell B. Vaccine 2007;25:2507–2512.
3. Brook I. Int J Pediatr Otorhinolaryngol 2007;71:1653–1661.
4. Lethbridge-Cejku M, Schiller JS, Bernadel L. Vital Health Stat 2004;10:1–151.
5. Willett LR, Carson JL, Williams JW, Jr. J Gen Intern Med 1994;9:38–45.
6. Senior BA, Kennedy DW, Tanabodee J, Kroger H, Hassab M, Lanza D. Laryngoscope 1998;108: 151–157.
7. Ioannidis JP, Lau J. Pediatrics 2001;108:E57, 51–58.
8. Clement PA, Bluestone CD, Gordts F, Lusk RP, Otten FW, Goossens H et al. Int J Pediatr Otorhinolaryngol 1999;49:S95–S100.
9. Garbutt JM, Goldstein M, Gellman E, Shannon W, Littenberg B. Pediatrics 2001;107:619–625.
10. American Academy of Pediatrics. Clinical practice guideline: management of sinusitis. Pediatrics 2001;108:798–808.
11. Collins JG. Vital Health Stat 10 1997:1–89.
12. NCHS. National Center for Health Statistics: Sinusitis. 2002.
13. Rosenfeld RM, Andes D, Bhattacharyya N, Cheung D, Eisenberg S, Ganiats TG et al. Otolaryngol Head Neck Surg 2007;137:S1–S31
14. Ray NF, Baraniuk JN, Thamer M, Rinehart CS, Gergen PJ, Kaliner M et al. J Allergy Clin Immunol 1999;103:408–414
15. Lau J, Zucker D, Engles EA, Balk E, Barza M, Terrin N et al. Diagnosis and Treatment of Acute Bacterial Rhinosinusitis, Rockville, MD: Agency for Health Care Policy and Research, 1999:1–38.
16. Brooks I, Gooch WM, 3rd, Jenkins SG, Pichichero ME, Reiner SA, Sher L et al. Ann Otol Rhinol Laryngol Suppl 2000;182:2–20.

17. Nash D, Wald E. Pediatr Rev 2001;22: 111–117.
18. McAlister WH, Parker BR, Kushner DC, Babcock DS, Cohen HL, Gelfand MJ et al. Radiology 2000;215(Suppl):811–818.
19. Wald ER. Am J Med Sci 1998;316:13–20.
20. Wald ER, Chiponis D, Ledesma-Medina J. Pediatrics 1986;77:795–800.
21. Diament MJ. J Allergy Clin Immunol 1992;90:442–444.
22. Reider JM, Nashelsky J. J Fam Pract 2003;52:565–567; discussion 567.
23. Kronemer KA, McAlister WH. Pediatr Radiol 1997;27:837–846.
24. Howe L, Jones NS. Clin Otolaryngol Allied Sci 2004;29:725–728.
25. Dessi P, Champsaur P, Paris J, Moulin G. Rev Laryngol Otol Rhinol (Bord) 1999;120: 173–176.
26. Eufinger H, Machtens E. J Craniomaxillofac Surg 2001;29:111–117.
27. Eustis HS, Mafee MF, Walton C, Mondonca J. Radiol Clin North Am 1998;36:1165–1183, xi.
28. Mafee MF, Tran BH, Chapa AR. Clin Rev Allergy Immunol 2006;30:165–186.
29. Williams JW, Jr., Simel DL, Roberts L, Samsa GP. Ann Intern Med 1992;117:705–710.
30. Revonta M, Blokmanis A. Sinusitis. Can Fam Physician 1994;40:1969–1972, 1975–1976.
31. van Buchem FL, Knottnerus JA, Schrijnemaekers VJ, Peeters MF. Lancet 1997;349:683–687.
32. Laine K, Maatta T, Varonen H, Makela M. Rhinology 1998;36:2–6.
33. Engels EA, Terrin N, Barza M, Lau J. J Clin Epidemiol 2000;53:852–862.
34. Varonen H, Makela M, Savolainen S, Laara E, Hilden J. J Clin Epidemiol 2000;53:940–948.
35. Ioannidis JP, Lau J. TPediatrics 2001;108:E57.
36. Berg O, Carenfelt C. Acta Otolaryngol 1988;105:343–349.
37. Berg O, Carenfelt C. Laryngoscope 1985;95: 851–853.
38. Savolainen S, Pietola M, Kiukaanniemi H, Lappalainen E, Salminen M et al. Acta Otolaryngol Suppl 1997;529:148–152.
39. Varonen H, Savolainen S, Kunnamo I, Heikkinen R, Revonta M. Rhinology 2003;41:37–43.
40. Som PM. Neuroradiology 1985;27:189–201.
41. Aalokken TM, Hagtvedt T, Dalen I, Kolbenstvedt A. Dentomaxillofac Radiol 2003;32: 60–62.
42. Konen E, Faibel M, Kleinbaum Y, Wolf M, Lusky A, Hoffman C et al. TClin Radiol 2000;55: 856–860.
43. Glasier CM, Ascher DP, Williams KD. Am J Neuroradiol 1986;7:861–864.
44. Gwaltney JM, Jr., Phillips CD, Miller RD, Riker DK. C N Engl J Med 1994;330:25–30.
45. Berg O, Bergstedt H, Carenfelt C, Lind MG, Perols O. Ann Otol Rhinol Laryngol 1981;90:272–275.
46. April MM, Zinreich SJ, Baroody FM, Naclerio RM. Laryngoscope 1993;103:985–990.
47. Vazquez E, Creixell S, Carreno JC, Castellote A, Figueras C, Pumarola F et al. Curr Probl Diagn Radiol 2004;33:127–145.
48. Kennedy DW, Senior BA. Otolaryngol Clin North Am 1997;30:313–330.
49. Jiannetto DF, Pratt MF. Laryngoscope 1995;105:924–927.
50. Ali A, Kurien M, Mathews SS, Mathew J. Singapore Med J 2005;46:540–544.
51. Thompson AM, Couch M, Zahurak ML, Johnson C, Vogelsang GB. Bone Marrow Transplant 2002;29:257–261.
52. Grundmann T, Weerda H. Laryngorhinootologie 1997;76:534–539.
53. Larson TL. Semin Ultrasound CT MR 1999;20:379–390.
54. Clary RA, Cunningham MJ, Eavey RD. Ann Otol Rhinol Laryngol 1992;101:598–600.
55. Reid JR. Pediatr Radiol 2004;34:933–942.
56. Unlu HH, Aslan A, Goktan C, Egrilmez M. Auris Nasus Larynx 2002;29:69–71.
57. Nawashiro H, Shimizu A, Shima K, Chigasaki H, Kaji T, Doumoto E et al. Neurol Med Chir (Tokyo) 1996;36:808–811.
58. Rochat P, von Buchwald C, Wagner A. Rhinology 2001;39:173–175.
59. Fountas KN, Duwayri Y, Kapsalaki E, Dimopoulos VG, Johnston KW, Peppard SB et al. South Med J 2004;97:279–282; quiz 283.
60. Younis RT, Anand VK, Davidson B. Laryngoscope 2002;112:224–229.
61. Bolger WE, Butzin CA, Parsons DS. Laryngoscope 1991;101:56–64.
62. Anzai Y, Jarvik JG, Sullivan SD, Hollingworth W. Am J Rhinol 2007;21:444–451.
63. Balk EM, Zucker DR, Engels EA, Wong JB, Williams JW, Jr., Lau J. J Gen Intern Med 2001;16:701–711.
64. Combs JT. Pediatrics 2001;108:1387–1388.
65. Franzese CB, Stringer SP. Am J Rhinol 2004;18:329–334.
66. Senbil N, Gurer YK, Uner C, Barut Y. J Headache Pain 2008;9:33–36.
67. Triulzi F, Zirpoli S. Pediatr Allergy Immunol 2007;18(Suppl 18):46–49.
68. Lee HS, Majima Y, Sakakura Y, Inagaki M, Sugiyama Y et al. Nippon Jibiinkoka Gakkai Kaiho 1991;94:1250–1256.
69. Cotter CS, Stringer S, Rust KR, Mancuso A. Int J Pediatr Otorhinolaryngol 1999;50:63–68.

70. Al-Qudah M. Int J Pediatr Otorhinolaryngol 2008;72:817–821.
71. Anzai Y, Weymuller EA, Jr., Yueh B, Maronian N, Jarvik JG. Arch Otolaryngol Head Neck Surg 2004;130:423–428.
72. Daele JJ. Acta Otorhinolaryngol Belg 1997;51:285–304.
73. Lieu JE, Piccirillo JF, Lusk RP. Otolaryngol Head Neck Surg 2003;129:222–232.
74. Adappa ND, Coticchia JM. Am J Otolaryngol 2006;27:384–389.
75. DelGaudio JM, Swain RE, Jr., Kingdom TT, Muller S, Hudgins PA. Arch Otolaryngol Head Neck Surg 2003;129:236–240.
76. Nadkarni T, Goel A. J Postgrad Med 2005;51(Suppl 1):S37–S41.
77. Hagtvedt T, Aalokken TM, Notthellen J, Kolbenstvedt A. Eur Radiol 2003;13:976–980.

12

Imaging of Nonaccidental Head Injury

Yutaka Sato and Toshio Moritani

Issues

I. What are the clinical findings that raise suspicion of nonaccidental head injury (NAHI) to direct further imaging?
II. Can imaging help to predict nonaccidental head injury?
III. Can CT and MR imaging help to determine the timing of injury?
IV. What is the sensitivity and specificity of CT and MRI?
V. How should the newer MR imaging techniques be used?

Key Points

- Head injury is the most common cause of death from nonaccidental trauma, and the majority of NAHI occurs in infants under age 1 year; its clinical presentation is nonspecific (moderate evidence).
- NAHI is suspected when the magnitude of the injury demonstrated clinically or on neuroimaging is discrepant with the history provided (moderate evidence).
- Subdural hematoma is the most commonly associated pathology with NAHI (moderate evidence).
- None of the intracranial pathology is specific or pathognomonic for NAHI.
- Temporal evolution of subdural hematoma associated with NAHI is dynamic and complex. For the best estimation of injury timing, comparison of CT and MRI and correlation with follow-up studies are often needed.
- CT is the standard of care for the initial evaluation of NAHI. CT readily demonstrates intracranial pathology requiring immediate treatment (moderate evidence).
- MRI should be performed once the patient is stabilized. Overall, MRI is more sensitive than CT for diagnosis, documentation, characterization, and prognostication of intracranial pathology associated with NAHI (limited evidence).

Y. Sato (✉)
Department of Radiology, University of Iowa, Iowa City, IA 52242, USA
e-mail: yutaka-sato@uiowa.edu

L.S. Medina et al. (eds.), *Evidence-Based Imaging in Pediatrics*,
DOI 10.1007/978-1-4419-0922-0_12, © Springer Science+Business Media, LLC 2010

Definition and Pathophysiology

Nonaccidental head injury (NAHI), the shaking impact syndrome, is most commonly seen among children under 3 years of age, with the majority occurring during the first year (1, 2). Because of anatomic and developmental differences in the brain and skull of young children, the mechanisms and types of brain injury are distinctly different from that seen in older children and adults (3–5).

Rotational acceleration is considered as the primary mechanism of diffuse, severe, and often life-threatening brain injury, including diffuse axonal injury (DAI) with disruption of axons and tearing of bridging veins, which causes subdural hematoma (SDH) and/or subarachnoid hemorrhage (SAH) and is often associated with retinal hemorrhage.

Impact loading causes focal strains at the site of impact, deforming the skull and generating the pressure waves in the brain. At the site of impact, scalp hematoma, skull fracture, focal SDH/SAH, and cortical contusion may occur. Impact injuries, except epidural hematoma, are usually not life threatening.

The term "shaken-baby" syndrome was coined by Caffey to explain a constellation of clinical findings of severe NAHI of infants with retinal hemorrhage, SDH/SAH, and little or no external cranial trauma (6, 7). Repetitive, "pure" rotational acceleration of the head on the weak infant's neck was considered as a mechanism of injury. There has been controversy over whether "shaking" alone can cause fatal brain injury; some consider that violent shaking alone causes serious or fatal injuries, but many instances of "shaken-baby" syndrome demonstrate clinical, radiological, and/or autopsy evidence of blunt impact to the cranium (8, 9). Thus, the term "shaken-impact" syndrome may more accurately reflect the mechanisms of injury observed (2).

The infant skull is easily deformable because it consists of thin calvarial bones separated by soft membranous sutures and fontanelles. Also, the partially myelinated infant's brain is more deformable. Recent investigation based on biomechanical analysis emphasizes the more significant role of deformation-mediated impact response rather than impact-induced rotational acceleration force as the critical injurious mechanism for an infant brain (3).

The focal injury to the craniovertebral junction has recently been proposed as the mechanism of traumatic brain injury unique to young infants. Significant deformation and shearing of the cervicomedullary junction and surrounding soft tissue occur during violent shaking (10, 11). Geddes et al. suggested that violent shaking without impact may cause focal axonal injury of the brainstem and upper cervical cord and/or epidural hematoma in the craniovertebral junction, resulting in traumatic apnea. This, in turn, causes secondary global hypoxic brain injury and generalized brain edema (12–14).

Geddes et al. further proposed that SDH can be caused by a combination of severe brain hypoxia, brain swelling, and raised central pressure; however, this hypothesis is not fully accepted (15–17).

Epidemiology

Seven to 19% of physically abused victims suffer from CNS injury in the United States, and approximately 1,500 will die and 18,000 will be left with serious disability every year (18–20). Most NAHIs occur in infants and toddlers. Nine to 14% of child head injuries are caused by inflicted trauma, and boys are more commonly affected than girls (21, 22). The incidence of serious or fatal NAHI in children less than 1 year of age is approximately 1 in 3,300 (21); since many cases of NAHI are mild or moderate in severity, the incidence is probably significantly higher. Head injury is the leading cause of child abuse fatality and accounts for up to 80% of fatal child abuse injuries at the youngest ages (23). Accidental HI is uncommon in infancy. Ninety-five percent of serious CNS injuries in infants less than 1 year of age are attributable to abuse (24). Approximately 80% of deaths caused by traumatic head injury in infants and children younger than 2 years were the result of NAHI (25). Among the victims of severe NAHI, evidence of prior child abuse is common (26).

Mortality rate of severe NAHI is approximately 60%, and morbidity includes mental retardation, cortical blindness, spasticity, seizures, and microcephalus (16, 22).

Overall Cost to Society

The cost of child abuse to society is considerable. According to the report released by *Prevent Child Abuse America* (27) in 2008, the United States spent $103.8 billion annually in response to child abuse, of which $33.1 billion is for the direct (immediate intervention) and $70.7 billion is for the indirect (long-term) costs (see Chapter 13 on non-CNS child abuse).

There are no data available on the social cost of imaging for NAHI.

Goals

The goals of imaging are as follows:

- diagnose conditions requiring immediate treatment and intervention;
- fully document the nature and extent of NAHI;
- assist in the determination of timing of NAHI;
- diagnose clinically unsuspected NAHI among victims with extensive evidence of extracranial abuse.

Methodology

A medical search was performed using PubMed (National Library of Medicine, Bethesda, Maryland) for original research publications discussing the clinical diagnosis, imaging, and effectiveness of imaging strategies in NAHI. The search covered the period from 1966 to December 2007. The search strategy employed different combinations of the following terms: (1) child abuse, (2) head injury, (3) brain injury, (4) head trauma, (5) inflicted injury, (6) diagnosis, and (7) therapy or surgery or etiology. Additional articles were identified by reviewing the reference list of relevant publications, identifying appropriate authors, and using the citation indices for MeSH terms. This review was limited to human studies and English-language literature. The authors performed a critical review of the title and abstracts of the identified articles followed by a review of the full text in articles that were relevant.

Discussion of Issues

I. What Are the Clinical Findings that Raise Suspicion of NAHI to Direct Further Imaging?

Summary of Evidence: The clinical presentation of NAHI is nonspecific (moderate evidence). NAHI is suspected when the magnitude of the injuries demonstrated clinically or on neuroimaging is discrepant with the history provided (Moderate Evidence). Also, NAHI should be suspected when retinal hemorrhage is present (moderate evidence). Low threshold for neuroimaging is recommended when physical abuse is suspected in a young child less than 1 year of age (limited evidence).

Supporting Evidence: The clinical presentation of NAHI is nonspecific and misleading. An accurate history is rarely provided, and the story may change with time (moderate evidence) (28, 29). An alleged injury mechanism in the history is often incompatible with the nature and magnitude of injury demonstrated by imaging and inconsistent with the developmental physical ability of the victim. The majority of victims are less than 3 years of age (1, 2). However, rare incidents of "shaken-baby" syndrome have been reported in older children. Salehi-Had et al. reported four fatal cases of older children of age 2.5–7 years who had acute SDH and RH without evidence of impact trauma (30). Approximately 30–70% of NAHIs demonstrate simultaneous fractures (19), and 40% of fatal NAHIs have a previous history or imaging/autopsy evidence of previous head trauma (26, 31).

A victim with a milder case of NAHI may have a history of poor feeding, vomiting, lethargy, and/or irritability of days' or weeks' duration. In a retrospective review of 173 children less than 3 years of age with NAHI, Jenny et al. found that 31% of victims had been misdiagnosed during previous visit(s) as gastroenteritis, influenza, possible sepsis, and otitis media (moderate evidence) (28).

In more severe cases, a victim becomes immediately symptomatic and clearly identifiable as head trauma with lethargy, seizures, and coma without lucid interval. Respiratory difficulty often progresses to apnea or bradycardia

requiring cardiopulmonary resuscitation (moderate evidence). In a retrospective cohort study by Willman et al. (32) of 95 children with fatal accidental HI, all but one of the children had an immediate decreased level of consciousness. One exceptional case with an enlarging epidural hematoma had a "lucid interval." There is no evidence of a prolonged "lucid interval" in children with SDH and brain edema.

Retinal hemorrhage is one of the cardinal features of NAHI (moderate evidence). In 75–90% of NAHI cases, unilateral or bilateral retinal hemorrhages are present (33). Numerous preretinal, intraretinal, and subretinal hemorrhages extending out to the edges of the retina and/or the splitting of the retina (retinoschisis) are particularly indicative of shaken-baby syndrome (34). Retinal hemorrhage is not pathognomonic for NAHI and occasionally is seen in association with other causes including accidental trauma, cardiopulmonary resuscitation, and paroxysmal coughing episode (35). Johnson et al. (36) reported only 2 cases of RH among 215 children with severe accidental HI. Schloff et al. reported 2 cases of RH among 57 children with intracranial hemorrhage from nonabuse causes (37). Sezen (38) reported 14% occurrence of less severe form of RH in normal newborns, which regress to normal rapidly in 4–6 weeks.

Adoption of a lower clinical threshold for performing neuroimaging was recommended when physical abuse is suspected or when "high-risk" criteria including rib fractures or multiple fractures are present in a young child, particularly when they are less than 1 year of age (39, 40) (limited evidence).

II. Can Imaging Help to Predict NAHI?

Summary of Evidence: SDH is the most commonly associated pathology with NAHI (moderate evidence). Other pathologic and imaging findings frequently associated with NAHI include complex skull fractures, diffuse and multifocal SDH, interhemispheric SDH, SDH with mixed density, traumatic diffuse axonal injury, and severe brain swelling. Evidence of previous injuries, such as atrophy and ventricular enlargement, is often seen in addition to the acute findings associated with NAHI described above (moderate evidence). None of the individual pathologic findings are unique or pathognomonic for NAHI, and image findings should be closely correlated with history, clinical findings, physical ability of the victim, and social background.

Supporting Evidence: Many comprehensive neuroradiologic reviews are available and should be used as references (41–46).

Child abuse causes approximately 10% of skull fractures in the pediatric population in general and 30% in children less than 2 years of age (47, 48). Minor domestic accidents rarely cause skull fractures (moderate evidence) (49, 50). Warrington et al. analyzed 11,466 questionnaires regarding domestic accidents occurring in the first 6 months of life and found the rate of concussion or fracture to be less than 1%. Falls from bed and seats did not result in skull fractures (51). Complex skull fractures, such as fractures crossing suture, diastatic fractures, depressed fractures, and comminuted fractures in premobile infants without history of violent trauma, should raise suspicion of NAHI (limited evidence) (24, 48, 52). Such fractures, however, have been observed in infants with impact to the vertex, impact against more than one surface, fall or drop down stairs, and an adult or older child falling onto an infant.

NAHI is the predominant cause of SDH in infancy (53), and SDH is the most common associated intracranial pathology in NAHI (moderate evidence). In a retrospective chart review of 173 children less than 3 years of age diagnosed with NAHI, Jenny et al. found the following injuries: SDH (87%), diffuse parenchymal brain injury (45%), localized brain contusion (37%), skull fracture (32%), and epidural hematoma (2%) (28).

Reece and Sege (54) in 287 children's head injury series (age 1 week–6.5 years) reported the prevalence of SDH in 46% of abused children compared with 10% of accidental injury. Hobbs et al. reported that 57% of SDHs seen among infants of age 0–2 years are caused by NAHI, as opposed to 4% by accident (53). Also, in a prospective, longitudinal analysis of CT/MRI findings of inflicted (n=31) and noninflicted (n=29) childhood traumatic head injury, Ewing-Cobbs et al. found statistically significant higher frequency of SDH and evidence

of previous injuries among the inflicted injury group (55). The incidence of isolated SDH/SAH as the only gross finding in fatal AHI is less than 2%, while it is 90–98% in NAHI (23). Other causes of SDH are listed in Table 12.1 and should be excluded with a combination of clinical history and relevant laboratory investigation. SDH may result from birth (moderate evidence). Looney et al. (56) reported that 26% of 76 asymptomatic term infants (65 vaginally delivered and 23 with cesarean delivery) who underwent MRI had focal SDH near the tentorium and parafalcine location. None, however, had interhemispheric SDH.

Diffuse subdural hematoma (SDH) involving bilateral convexity, interhemispheric fissure, and posterior fossa is a sign of violent trauma-producing impulsive loading to the bridging veins by rotational acceleration. The volume of noncontact SDH, which is relatively small ranging from 2 to 15 ml, does not, in and of itself, manifest symptoms and almost never causes death by its mass effect (limited evidence) (23). Contact SDH on the contrary tends to be focal and monocentric and seen under the site of impact.

Presence of SDHs of different ages suggests trauma of a repetitive nature and heightens the possibility of NAHI (limited evidence) (57).

Interhemispheric SDH was considered as highly specific for abusive injury (limited evidence). Zimmerman et al. reported a 69% prevalence of parietooccipital interhemispheric SDH in a retrospective CT review of 26 abused children and suggested as a sign of NAHI (58). However, accidental injury with significant rotational acceleration in the sagittal plane, such as a violent fall or a motor vehicle accident, also causes interhemispheric SDH (59).

Mixed-density SDH is more frequently seen among NAHI, while homogenous hyperdense SDH is more frequent in AHI (limited evidence) (57, 59).

Epidural hematoma is not a specific indicator of NAHI (limited evidence) (1, 19, 60).

Cortical contusions often seen in older children with violent accidental HI are less frequently seen in infants with NAHI. When present, they are seen in the cortex underneath the impact site. Likely sites for cortical contusions caused by the differential displacement of the brain and the skull (gliding contusions) include the temporal tips and frontal bases adjacent to the skull base and parasagittal cerebral cortex along the cerebral falx.

Traumatic diffuse axonal injuries are commonly seen in the corpus callosum, especially in the splenium, the gray–white junction especially of the superior frontal gyri, the periventricular areas, and the dorsolateral quadrants of the rostral brainstem. Occasionally, gross parenchymal tear is seen at the gray–white junction (61). This injury is unique to infants with blunt head trauma and most commonly seen in the frontal and anterior parietal lobes. This lesion can be overlooked both by CT and at autopsy, but is reliably demonstrated by sonography (62).

Severe swelling of the brain suggests a poor prognosis (limited evidence). Among profoundly traumatized infants, Cohen reported an unusual pattern of brain edema on CT that involves the cerebral cortex and the subcortical white matter in diffuse and symmetric fashion with relative density preservation of the deep white matter, basal ganglia, thalami, brainstem, and cerebellum and applied the term "reversal sign" (63).

Another unique CT pattern to predict poor outcome is "tin ear" syndrome described by Hanigan et al., who reported three fatal cases of NAHI, age ranging from 24 to 36 months, in which unilateral diffuse cerebral edema is associated with ipsilateral SDH and bruises and lacerations about the ear, resulting from a severe blow (64).

Even though traumatic axonal injury to the cervicomedullary junction and injury to the craniocervical osseoligamentous structure are postulated as a unique cause of the brain pathology of NAHI (10–14), there are only anecdotal reports of such injury demonstrated on neuroimaging and there is not enough evidence to support systematic spine imaging to investigate such injury without additional suggestive clinical or radiological evidence.

NAHI carries a significantly worse clinical outcome than does accidental HI. Early clinical and neuroimaging findings in NAHI are of prognostic value for neurodevelopmental outcome (limited evidence). In a retrospective medical chart review of 23 NAHI cases, Bonnier et al. reported that the presence of intraparenchymal lesions demonstrated on CT

and/or MRI in the first 3 months was significantly associated with neurodevelopmental impairment (65).

III. Can CT and MR Imaging Help to Determine Timing of Injury?

Summary of Evidence: The evolution of SDHs associated with NAHI is dynamic and complex. For the best estimation of injury timing, comparison of CT and MRI and correlation with follow-up studies are often needed.

Supporting Evidence: Scalp edema/hematoma becomes evident several hours to 24 h after the impact injury. Nonvisualization of scalp edema on a single neuroimaging on arrival should not be taken as absence of impact injury.

Skull fracture is a poor index of timing of injury because of the lack of periosteal reaction during healing.

On CT examination, the classical description of temporal evolution of SDH can be simplified as summarized in Table 12.2. The time course of the evolution may vary considerably from patient to patient and from location of SDH in the same patient, however (66–68). Subdural collection with septation, mixed density, and layering suggests rehemorrhage.

MRI evolution of hemoglobin products in the SDH roughly follows that of parenchymal hematoma (limited evidence) (69, 70). The evolution of intraparenchymal hematoma on MRI is summarized in Table 12.3. The signal pattern of evolving SDH generally follows the one of intraparenchymal hematomas in the acute and subacute stage with slower rate because of higher oxygen tension of the subdural space. The chronic SDH is isointense to slightly hypointense relative to gray matter on T1-weighted images and hyperintense on T2-weighted images. Hemosiderin is rarely seen in chronic SDH.

Gradient-refocused echo sequence is the most sensitive to detect the presence of hemoglobin product with prominent hypointensity, but signal characteristics do not change significantly according to the age of hematoma and thus cannot be used for timing of injury.

The temporal evolution of SDH should be reevaluated applying the newer anatomic and physiologic knowledge of the dural membrane (57, 71, 72). SDH is most often located in the inner layer of the dura matter (dural border cell layer) adjacent to the arachnoid membrane. Histologically, there is no actual or potential subdural "space" in humans. In the border cell layer, the bridging veins are less protected against the shearing force. Furthermore, there appears to be continuous and/or progressive bleeding or effusion upon resolving acute SDH in this "intradural" space after the initial trauma, which is further facilitated by intracranial hypotension caused by ongoing brain atrophy and treatment to decrease intracranial pressure (71, 72). So the evolution of the SDH is dictated not only by the degradation of hemoglobin products of the initial hematoma but also by the dynamic physiologic phenomena taking place in the space, including clot matrix formation, changes in red blood cell concentration due to packing, changes in RBC hydration, retraction of clots, effusion of serous fluid through traumatized dura, escaped CSF into the subdural space through the torn arachnoid membrane, and rebleeding (limited evidence) (57).

Occasionally, a subdural collection is hypodense, similar to CSF density in acute injury (limited evidence) (57, 59, 73, 74). Acute subdural hygroma is considered as the result of exudate collection in the dural membrane. SDH in anemic patients also may show low attenuation.

Mixed-density SDH is more commonly seen in SDH in NAHI and is traditionally considered "acute hemorrhage in the chronic hematoma," i.e., evidence of repeated injury, i.e., NAHI. However, the following possibilities should also be entertained: (1) acute SDH mixed with CSF leaked through arachnoid tear, (2) a mixture of subdural hygroma and hematoma, (3) low-density SDH with thrombosed cortical veins, and (4) sedimentation in the SDH (limited evidence) (57, 59).

Because of the complexity involving the timing determination, comparison between CT and MRI and follow-up studies, either CT or MR, are often necessary for accurate estimation of injury timing.

In addition to the acute findings associated with NAHI discussed above, attention should also be paid to more subtle evidence of previous brain injury. Ewing-Cobbs et al.

performed a prospective longitudinal study of 20 NAHI and 20 accidental H1 victims of less than 6 years of age and reported the statistically significant higher prevalence of brain injury (up to 45%)—namely the presence of brain atrophy, ventriculomegaly, and subdural hygroma among the NAHI group (55).

IV. What Is the Sensitivity and Specificity of CT and MRI?

Summary of Evidence: CT is a sensitive imaging test for SDH and skull fracture. CT is the preferred imaging modality for the evaluation of acute NAHI, adequately demonstrating injuries that need urgent intervention. Serial CT during the acute phase improves detection of intracranial hemorrhage (moderate evidence). MRI should be performed within a few days if the clinical symptoms are disproportionate to CT findings. MRI without gadolinium is more sensitive and specific than CT in the screening of subacute or chronic head injury and should be the primary imaging modality used (moderate evidence). MRI is superior to CT in determining prognosis (limited evidence).

Supporting Evidence: The imaging tool that should be used initially in the cases of suspected acute child abuse is CT (65, 75). CT is relatively sensitive and specific for detecting the presence of intracranial hemorrhage, including parenchymal contusional hemorrhage, subdural and epidural hematoma, and subarachnoid hemorrhage. The sensitivity of CT for detecting abnormalities after severe traumatic brain injury in adult patients varies from 68 to 94%, while normal scans range from 7 to 12% (76). CT is adequate for demonstrating lesions that require surgery (77) (moderate evidence); however, CT often fails to reveal nonhemorrhagic parenchymal injuries and brain edema. Serial CT scans are useful to detect progressive intracranial hemorrhage after head injury. Oertel et al. studied 142 adult patients with moderate or severe head injury who had undergone more than one CT scan and found that the initial CT did not detect the full extent of hemorrhage in 50% of patients (78) (moderate evidence).

MRI generally has a higher sensitivity and specificity for detecting brain parenchymal injury (79, 80) (moderate evidence). In a retrospective study of 107 adult patients with acute traumatic brain injury, MRI performed within 48 h of injury had an overall sensitivity of 97% compared to 63% for CT, with better sensitivity for hemorrhagic and nonhemorrhagic contusions, shearing injuries, and subdural and epidural hematomas (79). MRI is more sensitive to detect hypoxic–ischemic injury, shearing injuries, lesions caused by direct impact, compression, and penetration injuries in NAHI (77, 81–86) (moderate evidence). In a study involving 19 cases of child abuse, subdural hematomas, cortical contusions, and shearing injuries were demonstrated with particular advantage with MRI (77).

T2*-weighted images using gradient echo (GRE) sequences are more sensitive in detecting blood products than is conventional MRI (87). FLAIR (fluid-attenuated inversion recovery) sequences consist of an inversion recovery pulse to null the signal from CSF and a long echo time to produce heavily T2-weighted images. FLAIR is as sensitive as, or more sensitive than, CT in the evaluation of acute subarachnoid hemorrhage (88). MRI with its multiplanar capability is more sensitive than CT in detecting small SDH or subarachnoid bleeds. Diffusion-weighted imaging (DWI) is sensitive in detecting acute and subacute parenchymal injuries including hypoxic–ischemic injury and nonhemorrhagic DAI (85, 89–92).

MRI yields more information than CT in demonstrating the distribution and mechanisms of injury in NAHI and provides better prognostication when performed between 0.5 and 3 months after injury (65) (limited evidence). Usefulness of serial MR imaging in young patients with head trauma has not been established. Single photon emission computed tomography (SPECT) and positron emission tomography (PET) permit in vivo assessment of regional blood flow and metabolism. However, the spatial and temporal resolution is limited and not widely available.

V. How Should the Newer MR Imaging Techniques Be Used?

Summary of Evidence: Use of newer MR imaging techniques including DWI, susceptibility-weighted imaging, and MR spectroscopy may

improve the clinical care and management of children with traumatic brain injury (limited evidence). These techniques better characterize the nature, mechanism, and evolution of injuries that lead to progressive neurodegeneration, recovery, or subsequent plasticity. DWI is especially useful in the early detection of acute and subacute brain parenchymal injury (moderate evidence).

Supporting Evidence

Diffusion-Weighted Imaging

DWI is sensitive to alteration in diffusion of water molecules and can discriminate vasogenic and cytotoxic brain edema. There are more free interstitial water molecules in vasogenic edema (increased ADC), while there are restricted water molecules in the cellular edema (decreased ADC). DWI is more sensitive than conventional MRI in detecting early changes of NAHI and more extensive involvement of acute or subacute brain parenchymal injury (85, 89–93) (moderate evidence). Suh et al. retrospectively evaluated 18 children within 5 days of presentation, and 89% showed abnormalities on DWI. In 81% of positive cases, DWI revealed more extensive brain injury than did conventional MRI (90). DWI characteristics of the normal brain in young infants differ significantly from those in adults (94). ADC values in both gray and white matter of young infants are considerably higher than in adults, reflecting the high water content of the pediatric brain (95). Abnormalities of the pediatric brain become apparent on DWI (hyperintensity on DWI is associated with decreased ADC) within a few hours after injury before they appear on T2-weighted images. In adults, abnormalities become apparent on T2-weighted images within 24 h. In the undermyelinated infant brain with increased water content, however, "DWI-positive and T2-negative" duration of parenchymal injury may last up to 48–72 h, even up to 1 week in some cases. The parenchymal abnormalities displayed on DWI can be far more extensive than are detected on other sequences. The parenchymal hyperintensity on DWI with a decreased ADC value mainly represents cytotoxic brain edema in acute and subacute ischemia, which is usually irreversible, and results in necrosis or neuronal apoptotic cell death. An optimal window level setting is essential for accurate diagnosis. Quantifying the ADC value is useful to detect extensive parenchymal abnormalities (Fig. 12.1). The severity of abnormality on DWI correlates with the patient's outcome (90) (limited evidence).

Diffusion Tensor Imaging

Diffusion tensor imaging (DTI) allows evaluation of the white matter tract by demonstrating the intrinsic directionality of water diffusion in the white matter (anisotropy). DTI demonstrates normal myelination earlier than does conventional MR imaging (96, 97). The anisotropic pattern is nonspecific and varies depending on the extent of edema, gliosis, myelination, and the irregularity of axonal orientation. DTI may contribute to the early evaluation of NAHI (limited evidence). Most DTI studies in TBI have been performed on adult patients. In a study of 20 adults within 7 days of trauma, reduction of fractional anisotropy (FA) values in the internal capsules and corpus callosum correlated better with the Glasgow Coma Scale and the Rankin Scale scores than with the ADC values of DWI (98). In a study of five adults within 24 h of trauma, FA revealed regions of reduced anisotropy, while other MRI sequences were normal (99).

DTI potentially increases early detection of parenchymal injury in NAHI, but not enough bodies of evidences exists in the literature.

Susceptibility-Weighted Imaging

Susceptibility-weighted imaging (SWI) is a newer gradient echo sequence that is more sensitive than T2*-weighted gradient echo sequence in detecting susceptibility-related effects of blood products, especially hemorrhagic diffuse axonal injury (100, 101). SWI may contribute to the evaluation of hemorrhagic parenchymal lesions in NAHI (limited evidence). In 40 children and adolescents with mild to severe TBI and DAI, the number and the volume of hemorrhagic lesions demonstrated on SWI were significantly correlated with the patient's outcome (87).

MR Spectroscopy

MR spectroscopy (MRS) allows noninvasive in vivo analysis of neurochemicals and metabolites and has shown potential for providing prognostic information in pediatric patients with head injury (102–104) (limited evidence). In a study of 54 pediatric patients with NAHI, MRS showed decreased *N*-acetyl aspartate (NAA) (decreased neuronal activity), increased choline (breakdown product of myelin and cell membranes), and increased lactate (metabolic acidosis) (103). The degree of these changes seems to be related to the severity of brain damage and prognosis (102, 103, 105–109) (limited evidence). In 38 children with TBI, significantly increased myoinositol (product reflecting glial cell proliferation) and glutamate/glutamine (Gx) were observed when compared to controls (105). In experimental studies of acute subdural hematomas in the infant rat, the glutamate concentration in the extracellular fluid of the cortex was increased more than seven times over the base level (110). Gx levels peak early after injury and then fall rapidly (111, 112). This grading may become important in the future since the neuroprotective effects of several kinds of selective glutamate receptor antagonists have been reported in animal studies (113–115).

Take Home Tables

Table 12.1 shows the differential diagnoses for SDH. Table 12.2 shows the evolution of subdural hematoma on CT. Table 12.3 shows evolution of intraparenchymal hematoma on MR primary.

Table 12.1. Differential diagnosis of SDH

- **NAHI**
- **Accidental HI**
- **Perinatal**
  Fetal
  Traumatic delivery
  "Normal" vaginal delivery (56)
- **Aneurysms, arteriovenous malformations**
- **Arachnoid cyst**
- **Meningitis**
- **Coagulopathies: vitamin K deficiency (116)**
- **Metabolic disorders**
  Glutaric aciduria type I (117, 118)
  Galactosemia
  Pyruvate carboxylase deficiency
  Menkes disease (119)
- **Hypernatremia**
- **Paroxysmal cough with increased intrathoracic pressure (120)**

Table 12.2. Evolution of subdural hematoma on CT

~3 h	**Iso- to hypodense to brain**
~7 days	**Hyperdense**
~1 month	**Isodense**
1 month	**Hypodense**

Table 12.3. Evolution of intraparenchymal hematoma on MR primary

	T1-weighted	T2-weighted	Hb products
~12 h	**Iso- to hypointense**	**Hyper-**	**Oxy-Hb**
~3 days	**Hypo-**	**Hypo-**	**Doxy-Hb**
~7 days	**Hyper-**	**Hypo-**	**Met Hb (intracellular)**
~1 month	**Hyper-**	**Hyper-**	**Met HB (extracellular)**
~1 month	**Hypo-**	**Hypo-**	**Hemosiderin, ferritin**

Imaging Case Studies

Case 1

Figure 12.1 shows the advantage of DWI in demonstrating parenchymal injury in NAHI.

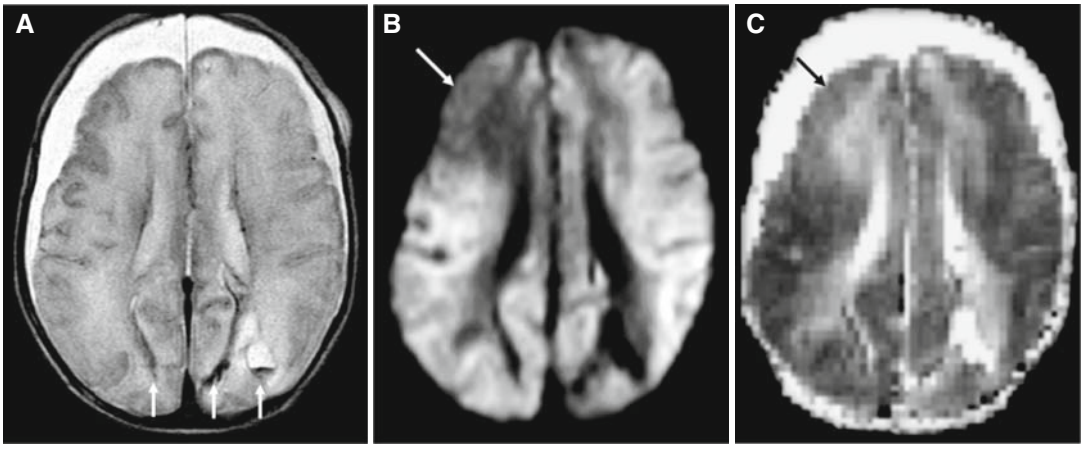

Figure 12.1. MRI of a 2-month-old boy with NAHI. **A**: T2-weighted image shows intraparenchymal hemorrhages (*arrows*) and bilateral frontal chronic subdural hematomas. **B**: DWI shows extensive parenchymal abnormalities. There is diffuse increased signal in both hemispheres with relative sparing of the right frontal area (*arrow*) and deep white matter adjacent to the ventricle. **C**: Calculated ADC values are decreased (0.26–0.45 $\times$ 10^{-3}/mm^2 per s) in the abnormal parenchyma.

Case 2

Figure 12.2 represents imaging of SDHs of different ages.

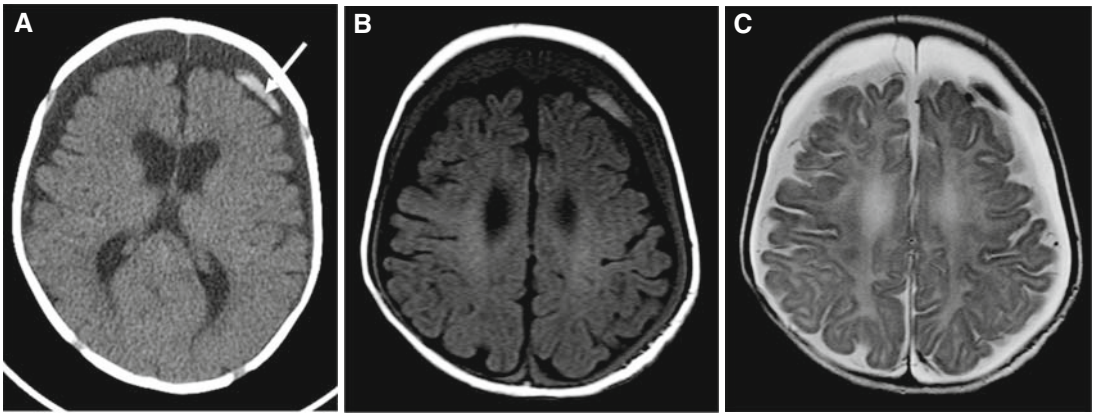

Figure 12.2. A 4-month-old infant with NAHI. CT (**A**), axial T1- (**B**) and axial T2-weighted image (**C**) show bilateral chronic SDH and subacute SDH in the left convexity (*arrow*).

Suggested Imaging Protocols for Nonaccidental Head Injury

Neuroimaging in the setting of suspected abuse depends on the child's age, signs, and symptoms. Consensus opinion by experts formulated the ACR Appropriateness Criteria® (121) and provided a guideline:

(1) Children 2 years of age or younger with suspicion of abuse without focal signs and symptoms: skeletal survey including AP and lateral radiographs of skull.
(2) Children 2 years of age or younger with histories of head trauma without neurologic deficits: brain CT or MRI for documentation of abuse.
(3) Children up to 5 years of age with neurologic signs and symptoms:
(a) unstable patients: noncontrast CT to detect lesions requiring urgent intervention, followed by MRI once stabilized;
(b) stable patients: MRI.
(4) Suggested MRI sequences include sagittal T1, axial T1, FLAIR, T2, T2*-GRE, DW1/ADC, and contrast-enhanced T1 in axial and coronal planes.

In addition, neuroimaging, either CT or MRI, is recommended among the young infants less than 1 year of age when they are found to have multiple fractures or rib fractures.

Future Research

- To better define the temporal evolution of SDH on newer MRI protocols and CT equipment for better dating.
- To better understand the unique biomechanics of the traumatic brain injury of infants correlating biomechanical, anatomical, pathological, and imaging data.
- To determine the advantages, limitations, and pitfalls of newer imaging techniques including DWI, DTI, SWI, and MR spectroscopy.
- Assessment of the effects of imaging on the patient's prognosis, outcome, and costs of diagnosis and management.
- To define newer imaging guidelines for NAHI incorporating recent neuroscientific and neuroimaging advancement including serum- and CSF biochemical markers (122).
- To understand the cost-effectiveness of screening head CT in asymptomatic infants with physical abuse.

References

1. Duhaime AC, Alario AJ, Lewander WJ et al. Pediatrics 1992;90(2 Pt 1):179–185.
2. American Academy of Pediatrics: Committee on Child Abuse and Neglect. Pediatrics 2001;108(1):206–210.
3. Goldsmith W, Plunkett J. Am J Forensic Med Pathol 2004;25(2):89–100.
4. Hymel KP, Bandak FA, Partington MD, Winston KR. Child Maltreat 1998;3(2):116–128.
5. Pierce MC, Bertocci GE, Berger R, Vogeley E. Neurosurg Clin N Am 2002;13(2):155–168.
6. Caffey J. Am J Dis Child 1972;124(2):161–169.
7. Caffey J. Pediatrics 1974;54(4):396–403.
8. Duhaime AC, Gennarelli TA, Thibault LE, Bruce DA, Margulies SS et al. J Neurosurg 1987;66(3):409–415.
9. Cory CZ, Jones BM. Med Sci Law 2003;43(4):317–333.
10. Morison CN, Minns RA. In Minns RA, Brown JK (eds.): Shaking and Other Non-Accidental Head Injuries in Children. London: Mac Keith, 2005,109–146.
11. Hadley MN, Sonntag VK, Rekate HL, Murphy A. Neurosurgery 1989;24(4):536–540.
12. Geddes JF, Hackshaw AK, Vowles GH, Nickols CD, Whitwell HL. Brain 2001;124(Pt 7): 1290–1298.
13. Geddes JF, Vowles GH, Hackshaw AK, Nickols CD, Scott IS et al. Brain 2001;124(Pt 7): 1299–1306.
14. Shannon P, Smith CR, Deck J, Ang LC, Ho M et al. Acta Neuropathol 1998;95(6):625–631.
15. Geddes JF, Tasker RC, Hackshaw AK et al. Neuropathol Appl Neurobiol 2003;29(1):14–22.
16. Punt J, Bonshek RE, Jaspan T, McConachie NS, Punt N et al. Pediatr Rehabil 2004;7(3):173–184.
17. Geddes JF, Tasker RC, Adams GG, Whitwell HL. Pediatr Rehabil 2004;7(4):261–265.
18. U.S. Department of Health and Human Services, Administration on Children, Youth and Families (ed.). Child Maltreatment 2003. Washington, DC: U.S. Government Printing Office; 2005.
19. Merten DF, Osborne DR, Radkowski MA, Leonidas JC. Pediatr Radiol 1984;14(5):272–277.
20. Tsai FY, Zee CS, Apthorp JS, Dixon GHJ. Comput Tomogr 1980;4(4):277–286.

21. Keenan HT, Runyan DK, Marshall SW et al. JAMA 2003;290(5):621–626.
22. Dashti SR. Pediatr Neurosurg 1999;31(6): 302–306.
23. Case ME, Graham MA, Handy TC, Jentzen JM, Monteleone JA, National Association of Medical Examiners Ad Hoc Committee on shaken baby syndrome. Am J Forensic Med Pathol 2001;22(2):112–122.
24. Billmire ME, Myers PA. Pediatrics 1985;75(2):340–342.
25. Bruce DA, Zimmerman RA. Pediatr Ann 1989;18(8):482–484, 486–489, 492–494.
26. Alexander R, Crabbe L, Sato Y, Smith W, Bennett T. Am J Dis Child 1990;144(1):58–60.
27. Wang CT, Holton J. Total estimated cost of child abuse and neglect in the United States. Prevent Child Abuse America Web site. Updated September 2007. Accessed August 15, 2008.
28. Jenny C, Hymel KP, Ritzen A, Reinert SE, Hay TC. AMA 1999;281(7):621–626.
29. Duhaime AC, Partington MD. Neurosurg Clin N Am 2002;13(2):149–154, v.
30. Salehi-Had H, Brandt JD, Rosas AJ, Rogers KK. Pediatrics 2006;117(5):e1039–e1044.
31. Kleinman PK, Marks SC Jr, Richmond JM, Blackbourne BD. Am J Roentgenol 1995;165(3):647–650.
32. Willman KY, Bank DE, Senac M, Chadwick DL. Child Abuse Negl 1997;21(10):929–940.
33. Morad Y, Kim YM, Armstrong DC, Huyer D, Mian M et al. Am J Ophthalmol 2002;134(3):354–359.
34. Levin AV. Neurosurg Clin N Am 2002;13(2):201–211, vi.
35. Aryan HE, Ghosheh FR, Levy ML. J Clin Neurosci 2005;12(6):624–631.
36. Johnson DL, Braun D, Friendly D. Neurosurgery 1993;33(2):231–234; discussion 234–235.
37. Schloff S, Mullaney PB, Armstrong DC et al. Ophthalmology 2002;109(8):1472–1476.
38. Sezen F. Br J Ophthalmol 1971;55(4):248–253.
39. Laskey AL, Holsti M, Runyan DK, Socolar RR. J Pediatr 2004;144(6):719–722.
40. Rubin DM, Christian CW, Bilaniuk LT, Zazyczny KA, Durbin DR. Pediatrics 2003;111(6 Pt 1):1382–1386.
41. Kleinman PK, Barnes PD. In Kleinman PK (ed.): Diagnostic Imaging of Child Abuse, 2nd ed. St. Louis: Mosby, Inc., 1998;285–342.
42. Barnes PD, Krasnokutsky M. Top Magn Reson Imaging 2007;18(1):53–74.
43. Barnes PD. Top Magn Reson Imaging 2002;13(2):85–93.
44. Lonergan GJ, Baker AM, Morey MK, Boos SC. Radiographics 2003;23(4):811–845.
45. David TJ. Pediatr Radiol 2008;38(Suppl 3): S370–S377.
46. Jaspan T. Pediatr Radiol 2008;38(Suppl 3): S378–S387.
47. Johnstone AJ, Zuberi SH, Scobie WG. J Accid Emerg Med 1996;13(6):386–389.
48. Hobbs CJ. Arch Dis Child 1984;59(3):246–252.
49. Helfer RE, Slovis TL, Black M. Pediatrics 1977;60(4):533–535.
50. Nimityongskul P, Anderson LD. J Pediatr Orthop 1987;7(2):184–186.
51. Warrington SA, Wright CM, ALSPAC Study Team. Arch Dis Child 2001;85(2):104–107.
52. Meservy CJ, Towbin R, McLaurin RL, Myers PA, Ball W. Am J Roentgenol 1987;149(1): 173–175.
53. Hobbs C, Childs AM, Wynne J, Livingston J, Seal A. Arch Dis Child 2005;90(9):952–955.
54. Reece RM, Sege R. Arch Pediatr Adolesc Med 2000;154(1):11–15.
55. Ewing-Cobbs L, Kramer L, Prasad M et al. Pediatrics 1998;102(2 Pt 1):300–307.
56. Looney CB, Smith JK, Merck LH et al. Radiology 2007;242(2):535–541.
57. Hymel KP, Jenny C, Block RW. Child Maltreat 2002;7(4):329–348.
58. Zimmerman RA, Bilaniuk LT, Bruce D, Schut L, Uzzell B et al. Radiology 1979;130(3): 687–690.
59. Tung GA, Kumar M, Richardson RC, Jenny C, Brown WD. Pediatrics 2006;118(2):626–633.
60. Shugerman RP, Paez A, Grossman DC, Feldman KW, Grady MS. Pediatrics 1996;97(5):664–668.
61. Lindenberg R, Freytag E. Arch Pathol 1969; 87(3):298–305.
62. Jaspan T, Narborough G, Punt JA, Lowe J. Pediatr Radiol 1992;22(4):237–245.
63. Cohen RA. Am J Roentgenol 1986;146(1): 97–102.
64. Hanigan WC, Peterson RA, Njus G. Pediatrics 1987;80(5):618–622.
65. Bonnier C, Nassogne MC, Saint-Martin C, Mesples B, Kadhim H et al. Pediatrics 2003;112(4):808814.
66. Bergström M, Ericson K, Levander B, Svendsen P. J Comput Assist Tomogr 1977;1(4):449–455.
67. Lee KS, Bae WK, Bae HG, Doh JW, Yun IG. J Korean Med Sci 1997;12(4):353–359.
68. Dias MS, Backstrom J, Falk M, Li V. Pediatr Neurosurg 1998;29(2):77–85.
69. Bradley WG. Radiology 1993;189(1):15–26.
70. Fobben ES, Grossman RI, Atlas SW et al. Am J Roentgenol 1989;153(3):589–595.
71. Haines DE. Anat Rec 1991;230(1):3–21.
72. Haines DE, Harkey HL, al-Mefty O. Neurosurgery 1993;32(1):111–120.

73. Joy HM, Anscombe AM, Gawne-Cain ML. Clin Radiol 2007;62(7):703–706.
74. Wells RG, Sty JR. Arch Pediatr Adolesc Med 2003;157(10):1005–1010.
75. Duhaime AC, Christian CW, Rorke LB, Zimmerman RA. N Engl J Med 1998;338(25): 1822–1829.
76. The Brain Trauma Foundation. The American Association of Neurological Surgeons. The Joint Section on Neurotrauma and Critical Care. J Neurotrauma 2000;17(6–7):597–627.
77. Sato Y, Yuh WT, Smith WL, Alexander RC, Kao SC et al. Radiology 1989;173(3):653–657.
78. Oertel M, Kelly DF, McArthur D et al. J Neurosurg 2002;96(1):109–116.
79. Orrison WW, Gentry LR, Stimac GK, Tarrel RM, Espinosa MC et al. Am J Neuroradiol 1994;15(2):351–356.
80. Ogawa T, Sekino H, Uzura M et al. Acta Neurochir Suppl (Wien) 1992;55:8–10.
81. Ball WS Jr. Radiology 1989;173(3):609–610.
82. Dias MS, Backstrom J, Falk M, Li V. Pediatr Neurosurg 1998;29(2):77–85.
83. Chabrol B, Decarie JC, Fortin G. Child Abuse Negl 1999;23(3):217–228.
84. Blumenthal I. Postgrad Med J 2002;78(926): 732–735.
85. Poussaint TY, Moeller KK. Neuroimaging Clin N Am 2002;12(2):271–294, ix.
86. Gerber P, Coffman K. Childs Nerv Syst 2007;23(5):499–507.
87. Tong KA, Ashwal S, Holshouser BA et al. Ann Neurol 2004;56(1):36–50.
88. Stuckey SL, Goh TD, Heffernan T, Rowan D. Am J Roentgenol 2007;189(4):913–921.
89. Parizel PM, Ceulemans B, Laridon A, Ozsarlak O, Van Goethem JW et al. Pediatr Radiol 2003;33(12):868–871.
90. Suh DY, Davis PC, Hopkins KL, Fajman NN, Mapstone TB. Neurosurgery 2001;49(2):309–318; discussion 318–320.
91. Biousse V, Suh DY, Newman NJ, Davis PC, Mapstone T et al. Am J Ophthalmol 2002;133(2):249–255.
92. Chan YL, Chu WC, Wong GW, Yeung DK. Pediatr Radiol 2003;33(8):574–577.
93. Field AS, Hasan K, Jellison BJ, Arfanakis K, Alexander AL. Am J Neuroradiol 2003;24(7):1461–1464.
94. Tanner SF, Ramenghi LA, Ridgway JP et al. Am J Roentgenol 2000;174(6):1643–1649.
95. Morriss MC, Zimmerman RA, Bilaniuk LT, Hunter JV, Haselgrove JC. Neuroradiology 1999;41(12):929–934.
96. Neil JJ, Shiran SI, McKinstry RC et al. Radiology 1998;209(1):57–66.
97. Wimberger DM, Roberts TP, Barkovich AJ, Prayer LM, Moseley ME et al. J Comput Assist Tomogr 1995;19(1):28–33.
98. Huisman TA, Schwamm LH, Schaefer PW et al. Am J Neuroradiol 2004;25(3):370–376.
99. Arfanakis K, Haughton VM, Carew JD, Rogers BP, Dempsey RJ et al. Am J Neuroradiol 2002;23(5):794–802.
100. Haacke EM, Cheng NY, House MJ et al. Magn Reson Imaging 2005;23(1):1–25.
101. Grados MA, Slomine BS, Gerring JP, Vasa R, Bryan N et al. J Neurol Neurosurg Psychiatr 2001;70(3):350–358.
102. Holshouser BA, Ashwal S, Luh GY et al. Radiology 1997;202(2):487–496.
103. Ashwal S, Holshouser BA, Shu SK et al. Pediatr Neurol 2000;23(2):114–125.
104. Brenner T, Freier MC, Holshouser BA, Burley T, Ashwal S. Pediatr Neurol 2003;28(2): 104–114.
105. Ashwal S, Holshouser B, Tong K et al. J Neurotrauma 2004;21(11):1539–1552.
106. Ashwal S, Babikian T, Gardner-Nichols J, Freier MC, Tong KA et al. Arch Phys Med Rehabil 2006;87(12 Suppl 2):S50–S58.
107. Yeo RA, Phillips JP, Jung RE, Brown AJ, Campbell RC et al. J Neurotrauma 2006;23(10):1427–1435.
108. Babikian T, Freier MC, Ashwal S, Riggs ML, Burley T et al. Magn Reson Imaging 2006;24(4):801–811.
109. Hunter JV, Thornton RJ, Wang ZJ et al. Am J Neuroradiol 2005;26(3):482–488.
110. Bullock R, Butcher SP, Chen MH, Kendall L, McCulloch J. J Neurosurg 1991;74(5): 794–802.
111. Schuhmann MU, Stiller D, Thomas S, Brinker T, Samii M. Acta Neurochir Suppl 2000; 76:3–7.
112. Zhang H, Zhang X, Zhang T, Chen L. Clin Chem 2001;47(8):1458–1462.
113. Duhaime AC, Gennarelli LM, Boardman C. J Neurotrauma 1996;13(2):79–84.
114. Ikonomidou C, Qin Y, Labruyere J, Kirby C, Olney JW. Pediatr Res 1996;39(6): 1020–1027.
115. Smith SL, Hall ED. J Neurotrauma 1998; 15(9):707–719.
116. Brousseau TJ, Kissoon N, McIntosh B. J Emerg Med 2005;29(3):283–288.
117. Bishop FS, Liu JK, McCall TD, Brockmeyer DL. J Neurosurg 2007;106(3 Suppl):222–226.
118. Gago LC, Wegner RK, Capone A Jr, Williams GA. Retina 2003;23(5):724–726.
119. Nassogne MC, Sharrard M, Hertz-Pannier L et al. Childs Nerv Syst 2002;18(12):729–731.

120. Geddes JF, Talbert DG. Neuropathol Appl Neurobiol 2006; 32, 625–634.
121. Slovis TL, Smith WL, Strain JD et al. Suspected physical abuse—child. ACR Appropriateness Criteria®. American College of Radiology Web Site. http://www.acr.org. Updated 2005. Accessed April 30, 2008.
122. Berger RP, Kochanek PM, Pierce MC. Child Abuse Negl 2004;28(7):739–754.

Part III

Musculoskeletal Imaging

13

Evidence-Based Imaging in Non-CNS Nonaccidental Injury

Rick R. van Rijn, Huub G.T. Nijs, Kimberly E. Applegate, and Rob A.C. Bilo

Issues

I. What are the radiological findings in skeletal nonaccidental injury?
II. What is the preferred imaging modality for the diagnosis of nonaccidental skeletal injury?
III. What is the role of repeat surveys in skeletal nonaccidental injury?
IV. What is the role of sibling screening with skeletal survey?
V. What is the role of postmortem imaging?
VI. How well can we date fractures?
VII. What is the role of imaging in abdominal trauma in NAI?

Key Points

- Child abuse is a serious health problem with severe long-term consequences and high societal costs (strong evidence).
- Child abuse is both underdetected and underreported, and the role of imaging is a critical part of the investigation of abuse (moderate evidence).
- Radiographic skeletal survey is the main diagnostic tool in the diagnosis of skeletal injuries in both living and dead children (moderate evidence).
- Repeat skeletal surveys can clarify and substantiate initially equivocal findings (moderate evidence).
- Skeletal scintigraphy can be used as an adjunct to the skeletal survey (moderate evidence).
- Infant deaths are most likely due to head trauma, whereas toddlers are more likely to die from blunt abdominal trauma (strong evidence).

R.R. van Rijn (✉)
Department of Radiology, Emma Children's Hospital/Academic Medical Centre Amsterdam, Meibergdreef 9, Amsterdam 1105 AZ, The Netherlands
e-mail: r.r.vanrijn@amc.uva.nl

L.S. Medina et al. (eds.), *Evidence-Based Imaging in Pediatrics*,
DOI 10.1007/978-1-4419-0922-0_13, © Springer Science+Business Media, LLC 2010

Definition and Pathophysiology

According to the World Health Organization (WHO), child maltreatment is defined as "Child maltreatment, sometimes referred to as child abuse and neglect, includes all forms of physical and emotional ill-treatment, sexual abuse, neglect, and exploitation that results in actual or potential harm to the child's health, development or dignity. Within this broad definition, five subtypes can be distinguished—physical abuse; sexual abuse; neglect and negligent treatment; emotional abuse; and exploitation" (1).

Risk factors for child abuse can be broadly divided into three categories: social/environmental, parent or caregiver related, and child related (2). Of the social factors, poverty is the most important risk factor, although it is unclear whether the stress related to poverty is a true risk factor or whether the heightened attention from, e.g., social services leads to overreporting. Important caregiver-related factors include substance abuse, emotional immaturity, mental health problems, stress, poverty, and a parental history of child abuse (3, 4). In a population of 194 children (median age 6 months), Starling et al. evaluated the relation between perpetrators and their victims. In 153 (79%) cases, it was possible to identify the perpetrator, and in 68%, the perpetrators were male; 45% were the biological fathers. The median age of the children abused by males (5 months) was significantly younger compared to the median age of those abused by females (10 months) (p=0.003) (5).

Although the child can be seen only as a victim, there are certain child-related factors that increase the risk of child abuse and that relate to more intensive care needs due to chronic health issues such as prematurity, congenital disorders, and cerebral palsy (6).

Epidemiology

The scope of this problem was addressed in 2003 by Lord Laming in his report on the death of Victoria Climbie (a case that had much media attention in the United Kingdom), in which he stated "I have no difficulty in accepting the proposition that this problem (deliberate harm to children) is greater than that of what are generally recognized as common health problems in children, such as diabetes or asthma" (7). Child abuse is both underdetected and underreported.

Another difficulty in assessing the incidence of child abuse is the well-recognized problem of underreporting, due to physician barriers and limited knowledge of signs and symptoms of child abuse (8, 9). This implies that there is only limited evidence for the true incidence of child abuse. The World Health Organization (WHO) has estimated, through the use of limited country-level data, that worldwide in 2002, almost 53,000 children died as a result of homicide (insufficient evidence) (10). The WHO further estimates that 40 million children are abused worldwide each year (11). In the United States in 2005, there were 3,600,000 reports of abuse, of which 17% were due to physical abuse and approximately 1,500 deaths attributed to child abuse (moderate–strong evidence) (12). There is no difference in abuse incidence by gender of the child. It is of importance to note that the majority of abused children (75%) have no history of prior abuse (13).

In a retrospective chart review of 6,186 trauma patients younger than 18 years, over an 8-year period, 7% (n = 453) of the patients were admitted for nonaccidental trauma (NAT) in Denver, Colorado (14). Children admitted for NAT were significantly younger, 12 vs. 76 months ($p < 0.05$), and more severely injured, with average injury severity score 18 vs. 9 ($p<0.05$). There was an increased mortality rate for NAT of 9.7% compared to 2.2% for AT ($p< 0.05$) (moderate evidence). In a population-based, case–control study, Schnitzer and Ewigman analyzed the Missouri Child Fatality Review Program data of all children <5 years of age who died in Missouri between January 1, 1992 and December 31, 1999 (15). From this population, a subset of 901 children who died as a result of an injury or undetermined cause were selected. In this subset, 149 deaths caused by inflicted injuries were identified. At the time of death, the majority of the children were below the age of 1 year (58%), 75% less than 2 years old, and 90% were less than 3 years old (moderate evidence). Infant deaths are most likely due to head trauma, whereas toddlers are more likely to die from blunt abdominal trauma (strong evidence) (16).

Although child abuse is a clinical diagnosis, imaging plays an important role in the diagnosis of physical child abuse. Approximately 94% of all skeletal fractures from abuse occur in children under the age of 3 years (17). Up to 80% of all rib fractures are occult findings; hence, radiological studies can also shed light on the incidence of child abuse (18). Loder and colleagues reviewed the causes of femoral fractures in a large retrospective cohort and showed that out of 1,076 femoral fractures in children younger than 2 years of age, 15% were due to child abuse (limited evidence) (19).

Overall Cost to Society

In child abuse detection, investigation, prosecution, protection, and long-term care, there are two main components attributing to the cost to society: direct costs related to treatment and investigations, and long-term indirect costs. Total direct and indirect costs to American society for child abuse is estimated at $258 million per day or $92 billion annually (20).

Direct Costs

A 2001 Prevent Child Abuse America report estimates that these costs are $24 billion annually (20). An analysis of the database of the United States 1999 Nationwide Inpatient Sample of the Healthcare Costs and Utilization Project showed that, on average, those children coded with abuse or neglect spent twice the number of days in hospital (8.2 vs. 4.0), had twice the number of diagnoses (6.3 vs. 2.8), had more procedures (1.3 vs. 0.8), and had double the total charges ($19,266 vs. $9,513) compared to those children not coded with abuse or neglect (Strong Evidence) (21). The authors reported that the total hospitalization costs related to child abuse or neglect for 1999 amounted to $92 million. These data do not include the pre- and posthospitalization healthcare costs for abused children.

Indirect Costs

Indirect costs include juvenile and adult criminal activity, mental illness, substance abuse, domestic violence, loss of productivity due to unemployment and underemployment, special education services, and increased use of the health-care system. Prevent Child Abuse America estimated that these costs are more than $69 billion per year (2001).

Walker et al. studied a group of women within one health maintenance organization (HMO) containing 163,844 women and found that a history of childhood abuse was significantly correlated with increased adult healthcare costs. They estimated that the total annual costs of childhood abuse in adult health care amounted to 8.2 million Canadian dollars (22). Tang and colleagues assessed the influence of child abuse on the pattern of adult health-care use in Ontario, Canada (23). They found that women with a history of abuse report double the mean annual health-care costs, i.e., 775 Canadian dollars (95% CI 504–1,045 Canadian dollars) compared to a mean cost of 400 Canadian dollars in women with no history of abuse (95% CI 357–443 Canadian dollars).

Although not directly intended to assess the cost of health care, one of the most important studies on the long-term effects of child abuse is the adverse childhood event (ACE) study by Felitti et al. (moderate evidence) (24). This influential study showed a strong relationship between the number of ACE and the number of health risk factors for leading causes of death in adults.

Goals

Imaging is used for both the social and legal investigation of these children and their environment and for medical treatment. The role of the radiologist and imaging in children with clinically suspected abuse is to

- detect findings which are suggestive of child abuse in suspected and unsuspected cases;
- distinguish findings indicative of child abuse from other pathologies (differential diagnosis) and normal variants in cases of suspected child abuse;
- determine if a fracture or an injury is consistent with the clinical information presented by the caretakers;
- date fractures as far as reasonably can be expected.

One might also argue that, in conjunction with the primary clinician and health-care team caring for the abused child, the radiologist should work with investigative agencies to provide appropriate imaging information and recommendations in suspected child abuse.

Methodology

The authors performed a Medline search on PubMed (National Library of Medicine, Bethesda, MD), date ranging from 1950 to 2005–2008. The search was restricted to human studies and the languages were restricted to English, German, French, and Dutch. Additionally, the TRIP (http://www.tripdatabase.com/) database was used.

The search strategy used the following key statements: *Medical Subject Heading Terms [Mesh], Diagnostic Imaging, Ultrasonography, Tomography, X-Ray Computed, Magnetic Resonance Imaging, Radionuclide Imaging, Cost–Benefit Analysis, Musculoskeletal System, Growth Plate, Bone Fractures, Wounds and Injuries, Rib Fractures, Abdomen, Intestines, Siblings,* and *Child Abuse.* Separate search terms were *skeletal survey* and *blunt abdominal trauma*, as well as combinations of these search strings. Related articles on PubMed were also screened for relevance.

Discussion of Issues

I. What Are the Radiological Findings in Skeletal Nonaccidental Injury?

Summary of Evidence: Fractures are the second most common findings in child abuse after dermatologic findings such as bruises, contusions, and burns (25). Nevertheless, radiological findings are rarely the absolute proof of child abuse, if evaluated without their context. Children with fractures resulting from NAI are significantly younger than children with accidental trauma. In a retrospective analysis by Roaten et al., NAI victims had a mean age of 12 months compared to 76 months in accidental trauma (14).

Differentiating between abusive fractures and nonabusive fractures is in most cases possible only by examining in great detail the clinical scenario regarding whether it is plausible for the specific child to have the specific fracture in the specific circumstances. Physical abuse as a cause of injuries is typically a conclusion after excluding alternatives, based on medical, social, and sometimes criminal investigations, unless the abuse has been observed by an independent eyewitness.

It is mandatory that the radiologist evaluates the characteristics of the fracture, with knowledge of the clinical history in cooperation with other specialists such as pediatricians and, if available, forensic pediatricians (Table 13.1). In determining whether a child's fracture is the result of abuse, one needs to understand or hypothesize the injury mechanism if no history of the injury is forthcoming from the caretaker (26). The reporting radiologist should be aware of the differential diagnosis of imaging findings in cases of suspected NAI (Table 13.2).

Supporting Evidence: Fractures resulting from physical abuse can be found throughout the whole skeleton; they are likely to be multiple and can show diverse stages of healing (strong evidence) (26–29). In the majority of cases, no external physical findings, e.g., bruises, are present (moderate evidence) (30, 31).

The most common fractures in child abuse are long bone fractures, where the femur and humerus are most commonly involved (20% of abused children with fractures) (32). In most diaphyseal fractures, there is an oblique or a spiral component, in which only a segment of the fracture will be seen tangentially on the radiograph. The underlying mechanism for spiral fractures is a torsion force.

Some fractures, like classical metaphyseal lesions (CMLs), and locations, like posterior rib fractures, are more suspicious than others, compared to clavicular fractures or a toddler's fracture in an ambulatory child.

Synonyms for CML include the corner or the bucket handle fracture. CMLs are regarded as highly predictive of intentional injury because of the known fracture biomechanics (shearing force, perpendicular to the bone across the metaphysis), their almost exclusive presence in children under the age of 2 years, and the limited differential diagnosis. CMLs are seen in 39–50% of children under the age of 18 months who have a skeletal survey because of child abuse (strong evidence) (33–35).

Rib fractures are considered highly predictive of child abuse in the absence of accidental trauma or certain skeletal diseases (e.g., osteogenesis imperfecta). Williams and Connolly formulated the following clinical conclusions regarding rib fractures, based on an analysis of reliable medical literature (36):

- In children with rib fractures, the likelihood of nonaccidental injury decreases with increasing age.
- Rib fractures in children less than 3 years of age are highly predictive of nonaccidental injury.

In a retrospective analysis, Barsness et al. assessed the positive predictive value (PPV) of rib fractures for child abuse in young children (<3 years) (37). In their study, the positive predictive value (PPV) of a rib fracture as an indicator of nonaccidental trauma was 95%. The positive predictive value increased to 100% once historical and clinical circumstances excluded all other causes of rib fractures (moderate evidence).

Their study also showed the following:

- Multiple rib fractures are more likely to be seen in child abuse compared to single fractures.
- Child abuse was more likely in the presence of posterior rib fractures (43% of NAI cases compared to 6% of accidental trauma cases).
- Rib fractures were the only skeletal finding in 29% of all NAI children.

Based on extensive experience that has been helpful in the investigation of fractures (limited evidence), Kleinman has published an overview of the specificity of fractures in children related to child abuse (Table 13.3) (32).

In neonates, one should consider the possibility of birth-related trauma, and there have been rare reports of single posterior rib fractures in neonates (in nearly all cases, these were large babies with a difficult delivery) (38–43). The rarity of birth-related rib fractures is shown in five studies on birth trauma, totaling 115,756 live births, which reported no cases of rib fractures (44–48).

II. What Is the Preferred Imaging Modality for the Diagnosis of Nonaccidental Skeletal Injury?

Summary of Evidence: See Table 13.4 for a summary of evidence on the diagnostic performance of imaging for suspected skeletal and abdominal injuries in NAI.

Conventional radiography, consisting of the skeletal survey, has historically been and continues to be the mainstay for imaging of suspected child abuse. The American College of Radiography (ACR) has defined the skeletal survey as "A skeletal survey is a systematically performed series of radiographic images that encompasses the entire skeleton or those anatomic regions appropriate for the clinical indications" (49). These surveys should include both the axial and the appendicular skeleton, depicting each anatomic region on separate radiographs, and guidelines have been established by the ACR (Table 13.5) as well as by the British Society of Paediatric Radiology (Table 13.6) (50, 51). Additional radiographic views are indicated in case of equivocal lesions.

Bone scintigraphy is used as a complementary test for the detection of occult fractures, especially in Australasia and North America but less so in Western Europe, (moderate evidence) (49, 52, 53). Like the skeletal survey, bone scintigraphy requires meticulous technique to achieve optimal sensitivity and specificity. Bone scintigraphy has higher sensitivity for fractures of the ribs particularly posterior ones but lower sensitivity for skull and metaphyseal corner fractures (52, 53).

While ultrasonography (54–56) and magnetic resonance imaging (57, 58) avoid ionizing radiation in the detection of occult fractures, these examinations can be time consuming and costly and reported studies have small sample sizes (insufficient evidence). Postmortem whole-body MRI may play a complementary role with autopsy. The role of CT in the diagnosis of skeletal occult fractures in child abuse has not been reported. However, CT may play a role in severe trauma, dating rib fractures, or postmortem evaluation (limited evidence) (59–61).

Supporting Evidence

Conventional Radiology

In 2006, Kemp et al. published a critical appraisal of all literatures pertaining to radiological investigations in NAI (52). Of 427 articles reviewed by members of the Welsh child protection systematic review group, 34 were included in the final analysis. The collected data were not sufficiently homogenous to enable meta-analysis (limited evidence). Five studies found that bone scintigraphy had the highest sensitivity (see section on bone scintigraphy). Two studies stated that the skeletal survey alone had the highest sensitivity (53, 62). Kemp et al. concluded that neither study alone detected all the fractures. Mandelstam et al. showed that the skeletal survey compared to bone scintigraphy was superior in detecting metaphyseal fractures (p=0.007) and skull fractures (p=0.02) (53). In the ACR appropriateness criteria, the skeletal survey was ranked most appropriate by the expert panel (limited evidence) (63).

With respect to the inclusion of oblique radiographs of the ribs (this is one of the major differences between the ACR and the BSPR guidelines), Ingram et al. performed an RCT and found that the addition of oblique views of the chest increased the sensitivity for the detection of rib fractures by 17% (95% CI 2–36%) and the specificity by 7% (95% CI 2–13%) (64).

With the introduction of Picture Archiving and Communication Systems, concern was raised about the use of digital images in the diagnosis of child abuse. Kleinman et al. demonstrated that in a laboratory setting, digital radiology performed comparably to high-detail film-screen imaging (65). Offiah et al. reported on the effect of varying degrees of edge enhancement and method of digital image display on fracture detection in suspected NAI (66). They could not find a significant difference between the different imaging methods and concluded that diagnostic accuracy depended mostly on observer-related factors. This is supported by the retrospective analysis by Carty and Pierce in which 51/435 (11.7%) cases were initially missed on the skeletal survey (67).

Bone Scintigraphy

Bone scintigraphy should not be performed within the first 48 h after injury due to known risk of false negatives. Kemp et al. found five publications stating that overall bone scintigraphy was more sensitive than the skeletal survey; one of these studies excluded skull fractures (a well-known pitfall for bone scintigraphy) (35, 68–71). Bone scintigraphy had a higher diagnostic yield in more anatomical complex locations such as the pelvis and the feet. In addition, bone scintigraphy is also better than skeletal survey in the detection of soft tissue trauma (limited evidence) (72). In the study by Mandelstam et al., only 7/20 (35%) classic metaphyseal lesions showed increased uptake on the bone scintigraphy (mild evidence) (53). In this study, 70% of all fractures were detected on both bone scintigraphy and skeletal survey, 20% only on bone scintigraphy, and 10% only on the skeletal survey.

Bone scintigraphy may be used to augment the number of fractures identified, which has been shown to influence the rate of criminal convictions of the abuser (71). Sty and Starshak used meticulous bone scintigraphy technique to document more fractures than a limited skeletal survey (11 radiographs) in a comparative study of 261 children. Bone scintigraphy had a sensitivity of 84% as compared to the skeletal survey sensitivity of 73%.

In the ACR appropriateness criteria, no consensus on the use of bone scintigraphy was reached by the expert panel, that it is "Indicated when a clinical suspicion of abuse remains high and documentation is still necessary" (63).

Ultrasonography

There have been limited case reports on the use of ultrasonography in the detection of single occult fractures but none that survey the entire skeletal system (54–56, 73). There is insufficient evidence to use ultrasonography for screening for occult fractures.

Computed Tomography

No references to the use of CT in the detection of non-CNS fractures in suspected cases of child abuse were found. As a rough rule, CT doses are approximately 100 times higher than those for plain radiographs, raising concern about later cancer induction. Accordingly,

CT for this diagnosis is unlikely to become routine. However, CT may be of use in special situations such as severe trauma or postmortem evaluation. In a study of 45 pediatric trauma patients, Renton et al. compared CT with chest radiographs; 18/45 (40%) cases had findings only at CT, including 2 patients with rib fractures (limited evidence) (61). Traub et al. retrospectively analyzed a cohort of 141 trauma patients, mean age 47 years (range 17–89 years) with major blunt trauma (59). Chest radiography showed 47 (33%) rib fractures, 5 (4%) scapula fractures, and 0 (0%) sternum fractures compared to chest CT which showed 68 (48%, $p<0.001$), 12 (9%, $p=0.016$), and 10 (7%, $p<0.001$), respectively (limited evidence).

Magnetic Resonance Imaging

MRI may be used to clarify inconclusive clinical or radiographic findings; for example, negative radiographs of the elbow or the shoulder in the immature skeleton may not show cartilaginous injuries or nondisplaced fractures (74). With the advent of whole-body Short Tau Inverse Recovery (STIR) MRI and its relatively short scan times, whole-body imaging in children has become possible. Several authors have suggested its use in the diagnosis of occult fractures (75, 76). Two case reports have been published regarding the use of whole-body STIR (WB-STIR) in the detection of musculoskeletal lesions in child abuse (insufficient evidence) (57, 58). A study comparing WB-STIR to the skeletal survey in 16 children (mean age 9 months; range 1.5–37) with suspected inflicted injury was presented (77). Mean interval between skeletal survey and WB-STIR was 2 days (range 0–13). The sensitivity of WB-STIR for fractures of the rib was 75% (33/44); metaphyseal corner 67% (2/3); metaphysis 100% (1/1), diaphysis 100% (6/6); and parietal skull 100% (1/1). Eleven rib fractures were missed, however, all in patients with multiple rib fractures and at least one other rib fracture was detected on WB-STIR in each case. In three different patients, WB-STIR detected fractures that were not identified on initial skeletal survey.

Cost and Cost-Effectiveness Analysis Studies

No robust large formal cost-effectiveness analysis has been performed. Only one study could be found which reported, be it only marginally, on the cost of diagnostic imaging in suspected child abuse. Ellerstein and Norris published a retrospective analysis of 331 skeletal surveys, in which 38 cases (12%) showed signs of child abuse (limited evidence) (78). In 30 cases, this was already known or suspected, in 8 cases the survey provided new information. Based on their finding, they calculated that it cost US$ 33,000 to identify these 8 cases. Given the long-term costs of child abuse, the skeletal survey may be a cost wise examination (limited evidence) (22–24).

III. What Is the Role of Repeat Surveys in Skeletal Nonaccidental Injury?

Summary of Evidence: A skeletal survey for child abuse may be negative or inconclusive, even if performed adequately, especially when acute fractures are present (50, 79). Therefore, the use of follow-up radiological investigation has been advocated (mild–moderate evidence), in which case the entire skeletal survey with the exception of radiographs of the skull is repeated after approximately 14 days.

Supporting Evidence: Zimmerman et al. report on 48 children who were enrolled in a prospective study (80). Additional information regarding skeletal trauma was obtained in 22 of 48 patients (46%). Twenty-seven previously undetected fractures were seen in 11 patients (18 rib, 4 scapular, 2 metaphyseal, 1 clavicular, 1 fibular, and 1 ulnar fractures). In two cases, the follow-up exam influenced the diagnosis; in both cases a definite diagnosis of child abuse could be made (moderate evidence).

Kleinman et al. report on a retrospective study in 23 children (81). In 61% of the follow-up exams, additional information was provided, either on the number or on the dating of fractures. Out of 19 additional fractures found on follow-up exam, 13 were initially not noted on skeletal survey. The remaining six fractures were initially considered equivocal (limited evidence). The authors concluded that follow-up skeletal survey is warranted to "provide a thorough and accurate assessment of osseous injuries" in children with suspected abuse (81).

Cost and Cost-effectiveness Analysis Studies

Reported cost-effectiveness analysis studies on the use of repeat skeletal surveys are not available. It can be assumed that in cases in which repeat surveys are advised by the radiologist (e.g., after negative or equivocal findings with a suspected history in children below the age of 2 years), a higher number of true positives regarding child abuse may be found (50). This may result in substantially lower future societal costs, by far higher than the cost of repeat skeletal surveys.

IV. What Is the Role of Sibling Screening with Skeletal Survey?

Summary of Evidence: A recent survey showed that physicians involved in child abuse perceive that findings of abuse in index children are sufficient to warrant medical examination of most contact children (in the same household) (82). In a retrospective study by Hamilton-Giachritsis and Browne in 795 siblings from a cohort of 400 "index" children, in 37% of cases, maltreatment was not limited to the index case but to all siblings and in 20%, maltreatment was specifically directed at some but not all siblings (83). Given these data, siblings, under the age of 2 years, of index children should undergo a skeletal survey (moderate evidence). The British Society of Paediatric Radiology state in their guidelines that in cases of proven NAI in the index child, siblings under the age of 3 years should undergo a skeletal survey (51).

Supporting Evidence: Only one study could be found in which siblings underwent a skeletal survey. Day et al. evaluated 70 index cases and 6 siblings (insufficient evidence) (84). The siblings' ages ranged from 1 to 36 months, although three (50%) were under 12 months of age. One (17%) of the siblings' surveys (a twin) was positive. In their systematic review, Kemp et al. could find no evidence for the use of the skeletal survey in siblings (moderate evidence) (52).

V. What Is the Role of Postmortem Imaging?

Summary of Evidence: In cases of sudden infant death syndrome (infants aged 1 month–1 year) or otherwise unexplained death of a young child, a thorough clinical workup is mandatory (85). In this workup, skeletal survey has a definite role as metaphyseal corner fractures and posterior rib fractures may be missed on autopsy (86). The skeletal survey in deceased children should be of the same high quality as in living children and should be performed according to the ACR or BSPR guidelines. When this occurs, the pathologist can focus on areas of concern and plan the extent of the bone and soft tissue preparation based on the skeletal survey.

Supporting Evidence: Arnestad et al. retrospectively reviewed 309 cases of sudden unexpected death in infancy and early childhood (0–3 years) (87, 88). In 73 cases, an explainable cause of death was found. Of these, 7 (10%) were due to neglect or abuse and 10 (14%) were due to homicide. In their study, radiology showed signs of child abuse in three (4%) children (limited evidence). In a retrospective study by McGraw et al., 106 consecutive postmortem radiography studies were reviewed (89). In 14 cases, the diagnosis was of NAI; in seven children, radiography showed a total of 26 fractures; 24 (92%) were metaphyseal corner fractures (MCFs). The authors did not specify the number of MCF detected at autopsy (Limited Evidence). Klotzbach et al. compared postmortem radiography to autopsy and found a total of 44 osseous lesions; 27 fractures were diagnosed by postmortem skeletal survey, and 5 recent rib fractures were suspected (90). Radiology mainly failed to show acute, lateral, and anterior rib fractures (limited evidence).

Whole-body MRI as a complementary tool to the autopsy is being investigated in both adults and children (91, 92).

VI. How Well Can We Date Fractures?

Summary of Evidence: Radiologic dating of fractures in the context of child protection, whether in a medical or in a forensic setting, is possible to a certain extent but is not an exact enterprise. Evidence shows considerable overlap in radiologic features appearing over time following fracture occurrence. A time frame of weeks rather than days should be used and explained as such to investigating agencies. Recent fractures can be differentiated from subacute and

old fractures, which may be useful for assessing the consistency of the history offered. The key findings (moderate evidence) most consistently agreed upon are the following (32, 93–95):

1. Appearance of periosteal reaction indicates early healing (minimum 1 week in newborn, 14 days in older children).
2. Presence of hard callus indicates subacute healing phase (minimum 2–3 weeks, peak 3–6 weeks, with a long time distribution tail afterward).
3. Signs of remodeling indicate late healing phase (minimum 8 weeks).
4. Exceptions for dating fractures on the basis of callus formation are fractures of the skull and classical metaphyseal lesions.

Supporting Evidence: Fracture dating was addressed in a systematic review by Prosser et al. (moderate evidence) (96). An extensive search in literature resulted in 1,556 titles that were reviewed systematically by a large (and varying) group of specialists. Only three studies could be included, reflecting data on 189 children (only 56 children were younger than 5 years; the age group most vulnerable for abuse), with variable age ranges and a variable number of radiographs per child. All three studies were categorized as "longitudinal." However, in the study of Cumming (93), the mean number of radiographs per child was one, which seems contradictory. The key findings are quite similar to the often-quoted table by Kleinman et al., which was based on extensive personal experience (insufficient evidence) (32). In this publication, formation of soft callus and hard callus was noted between 10 and 21 days and 14 and 92 days, respectively, after the incident.

More research is needed to assess the possible role of factors influencing the appearance and/or the disappearance of reported radiologic features such as type of bone involved, age below 5 years (and in subcategories, i.e., 0.6, 2, 5 years), prior nutrition state, repeated abuse, refracturing, underlying bone disease, and casting vs. delay in immobilization of fractures.

VII. What Is the Role of Imaging in Abdominal Trauma in NAI?

Summary of Evidence: Historically, the focus of radiological imaging in relation to NAI has been on intracranial and skeletal injuries. Abdominal trauma is a relatively infrequent finding in children with reported rates from 1.7 to 7.2% in all trauma patients (97). However, the severity of these injuries is reflected in the high mortality rate, which has been reported to range from 10 to 50% (moderate evidence) (98–100). Blunt abdominal trauma represents the most common cause of death from abuse in toddlers (ages 1–3 years) (32).

The clinical presentation of blunt abdominal trauma (BAT) overlaps common benign conditions, such as vomiting from gastroesophageal reflux or viral gastroenteritis, making diagnosis difficult, especially in younger (nonverbal) children. In contrast to accidental trauma, splenic injury is less common than liver injury (101, 102). GI tract injury most commonly occurs in the duodenum (with or without associated pancreatic injury), followed in decreasing order by jejunum (usually proximal), ileum, colon, and stomach.

Supporting Evidence: The main evidence is found in the pediatric trauma literature, although there have been studies focused solely on abdominal injury in NAI. Overall, the most common and most sensitive imaging test for the detection of abdominal trauma in the United States is MDCT (moderate evidence). Most evidence is presented in publications addressing specific injuries in separate organs, as summarized in the following paragraphs.

Bowel and Mesenteric Injury

Bowel injury and especially duodenal injury have been linked to NAI by several authors (98, 103–106). Upper GI series has poor sensitivity (54%) but excellent specificity (98%) and should not be used to rule out duodenal perforation (limited evidence) (107). The role of sonography in the diagnosis of intestinal injury is limited, with only a few case reports (insufficient evidence) (108–110).

With respect to imaging of bowel injury, CT is the most widely applied technique (105, 108,

111–117). Three studies presented data enabling the construction of 2×2 tables of a total of 1,694 trauma patients (adults as well as children) (112–114). The CT findings of mesenteric focal fluid, bowel wall thickening, and increasing free fluid suggest bowel injury. Free intraperitoneal air is a specific but uncommon finding. With respect to bowel and mesenteric injury, MDCT yields a combined sensitivity of 74%, specificity of 99%, positive predictive value of 87%, and a negative predictive value of 99% (112–114). CT is the exam with the highest diagnostic performance to identify bowel and mesenteric injury (moderate evidence).

Hepatic, Splenic, and Renal Injury

Abdominal MDCT is a well-accepted technique to grade hepatic, splenic, and renal injuries that provides risk data for further bleeding and avoids unnecessary surgical exploration (113, 114, 116, 118–120). Most solid organ injuries are managed nonoperatively. With the increasing use of transcatheter arterial embolization techniques, CT also plays an important role in guiding the interventional radiologist (limited evidence) (121–126).

Pancreatic Injury

Pancreatic injuries are challenging to detect as the classic triad of fever, leukocytosis, and elevation of serum lipase levels is rarely identified in children. The use of CT in the initial stage has been debated, and a delayed study to diagnose and manage the complications of pseudocyst or abscess is indicated (limited evidence) (127, 128). MRI has been advocated to depict the biliary tree and pancreatic duct, mainly in order to guide endoscopic retrograde pancreatography (limited evidence) (129).

Take Home Tables

Table 13.1 presents evaluation of fractions in young children. Table 13.2 presents differential diagnosis of NAI. Table 13.3 presents radiologic findings highly predictive of child abuse. Table 13.4 discusses the diagnostic performance of imaging for suspected skeletal and abdominal injuries in NAI.

Table 13.1. Evaluation of fractures in young children

Fracture	Type Location Number Date (known and unknown recent and old fractures) Other injuries
Child	Age and developmental stage Underlying pathology
History	Plausibility of the history: • Age and developmental stage • Accidental vs. nonaccidental fractures • Disease-related fractures vs. nonaccidental fractures • Fracture biomechanics

Table 13.2. Differential diagnosis of NAI

Collagen synthesis disorders	Osteogenesis imperfecta Copper deficiency Menkes syndrome
Bone mineralization disorders	Rickets X-linked hypophosphatasia Prematurity Malabsorption disorders Neuromuscular disorders
Radiological findings without fractures	Physiological subperiosteal new bone formation Congenital syphilis Osteomyelitis Bone tumors Leukemia Caffey's disease (infantile cortical hyperostosis) Vitamin C deficiency (scurvy) Methotrexate or prostaglandin E treatment

Table 13.3. Radiologic findings highly predictive of child abuse

	Type and location of fracture
Highly predictive	Classic metaphyseal lesions Rib fractures, especially posterior Scapular fractures Spinous process fractures Sternal fractures
Moderately predictive	Multiple fractures, especially bilateral Fractures of different ages Epiphyseal separations Vertebral body fractures and subluxations Digital fractures Complex skull fractures
Common but low predictive value	Subperiosteal new bone formation Clavicular fractures Long bone shaft fractures Linear skull fractures

Reprinted with permission of the author and Elsevier from Kleinman (32).

Table 13.4. Summary of evidence: diagnostic performance of imaging for suspected skeletal and abdominal injuries in NAI

	Sensitivity (%)	Specificity (%)	References
All fractures			
Skeletal survey (11 views)	73		(71)
Repeat skeletal survey	46–61[a]		(80, 81)
Bone scan	84		(71)
Rib fractures			
Oblique views[b]	17	7	(64)
Classic metaphyseal lesion			
Bone scan[c]	35		(53)
Mesenteric/bowel injuries			
CT	74	99	(112–114)

[a]Percentage of additional findings at repeat survey at 2 weeks.
[b]Percentage increase above routine frontal and lateral chest radiographs.
[c]Bone scan detected only 35% of those found at skeletal survey.

Imaging Case Studies

Case 1

Figure 13.1 demonstrates a case of a 24-day-old boy admitted to the hospital with a fracture of the left humerus.

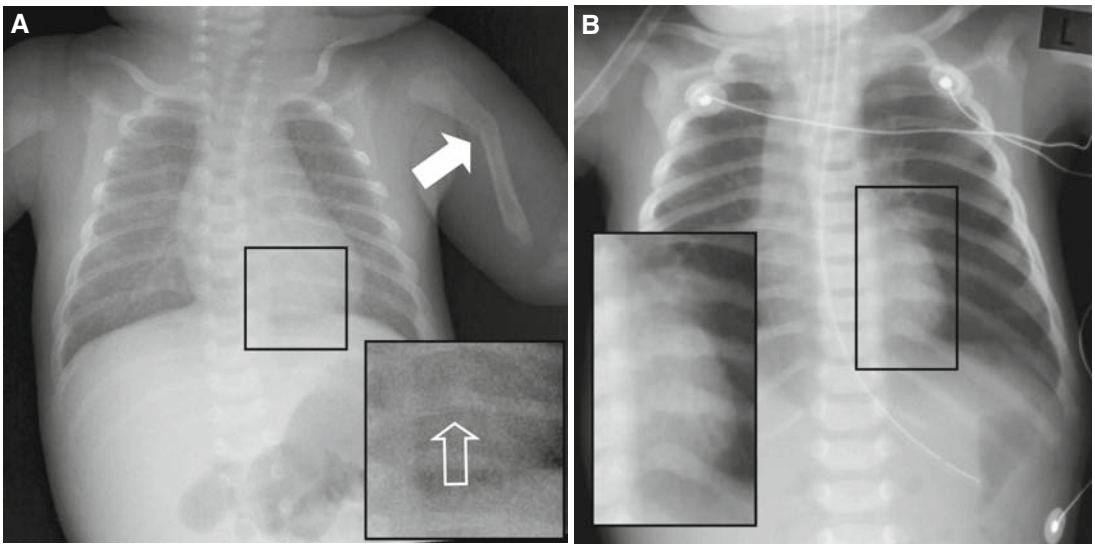

Figure 13.1. A 24-day-old boy admitted to the hospital with a fracture of the left humerus (*solid arrow*) (**A**). Note the acute rib fracture (see inset—*open arrow*), which was initially missed. A radiograph of the chest obtained 67 days after the initial chest radiograph showed numerous healing rib fractures (**B**).

Case 2

Figure 13.2 demonstrates a case of a 2-year-old boy who presented at the emergency department after a witnessed fall from a counter.

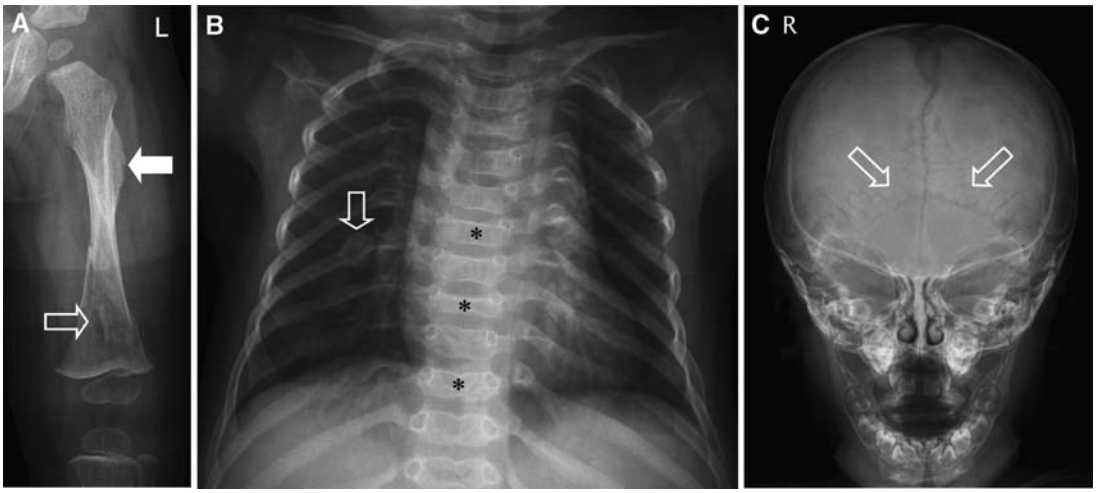

Figure 13.2. A 2-year-old boy presented at the emergency department after a witnessed fall from a counter. A radiograph of the left femur (**A**) shows an acute oblique fracture of the distal femur (*open arrow*) but also callus formation proximal to the fracture (*solid arrow*). A skeletal survey was performed which shows rib fractures (**B**, *open arrow*) and vertebral fractures (*asterisk*). The radiograph of the skull shows Wormian bones (**C**, *open arrows*). Based on imaging features and genetic analysis, a diagnosis of osteogenesis imperfecta was established. NAI was ruled out.

Suggested Imaging Protocols for Non-CNS Nonaccidental Injury

Tables 13.5 and 13.6 present the complete skeletal survey according to the ACR and the BSPR.

Table 13.5. Complete skeletal survey according to the American College of Radiology

Axial skeleton	Appendicular skeleton[a]
Thorax (AP and lateral), to include ribs, thoracic, and upper lumbar spine	Humeri (AP)
Pelvis (AP), to include the mid lumbar spine	Forearms (AP)
Lumbosacral spine (lateral)	Hands (PA)
Cervical spine (AP and lateral)	Femora (AP)
Skull (frontal and lateral), additional views if needed—oblique or Towne view	Lower legs (AP) Feet (PA) or (AP)

[a] Additional views if needed: views centered on joints or lateral views.

Reprinted with permission of the American College of Radiology (ACR) from ACR practice guideline for skeletal surveys in children on www.acr.org . No other representation of this guideline is authorized without express written permission from the American College of Radiology.

Table 13.6. Complete skeletal survey according to the British Society of Paediatric Radiology

Axial skeleton	Appendicular skeleton[a]
AP thorax, right and left oblique views of the ribs	Humeri (AP)
Pelvis (AP)	Forearms (AP)
Lumbosacral spine (lateral)	Hands (PA)
Cervical spine (lateral)	Femora (AP)
Skull (frontal and lateral), Towne view if occipital injury suspected	Lower legs (AP) Feet (AP)

[a]Lateral coned views of the elbows, wrists, knees, and ankles may demonstrate metaphyseal injuries in greater detail. The consultant radiologist should decide this at the time of checking the films with radiographers.
Reprinted with permission of the British Society of Paediatric Radiologists from NAI standard for skeletal surveys on www.bspr.org.uk/nai.htm.

Future Research

The critical gaps in the evidence include the following:

- The sensitivity and specificity of whole-body MRI and CT in nonaccidental injury should be evaluated in controlled trials/verified cases.
- Radiological dating of fractures
  - Role of CT in dating fractures
- Standardization in terminology of the radiological findings and in methodology of imaging techniques.
- Role of postprocessing and computer-aided diagnostic (CAD) techniques in increasing early detection and interpretation of fractures (applies for both conventional radiography and CT).
- Role of skeletal surveys in siblings of index children.

References

1. WHO. Child maltreatment. http://www.who.int/topics/child_abuse/en/.
2. Bethea L. Am Fam Physician 1999; 59:1577–1585.
3. Cappelleri JC, Eckenrode J, Powers JL. Am J Public Health 1993; 83:1622–1624.
4. Desai S, Arias I, Thompson MP, Basile KC. Violence Vict 2002; 17:639–653.
5. Starling SP, Sirotnak AP, Heisler KW, Barnes-Eley ML. Child Abuse Negl 2007; 31:993–999.
6. Sidebotham P, Heron J. Child Abuse Negl 2006; 30:497–522.
7. Laming, H. The Victoria Climbié inquiry. http://www.victoria-climbie-inquiry.org.uk/; Date accessed: 10-1-2007.
8. Flaherty EG, Sege R. Pediatr Ann 2005; 34:349–356.
9. Slovis TL. Acad Radiol 1995; 2:728–729.
10. WHO. The United Nations Secretary General's Study on Violence Against Children. A/61/299 ed, 2007.
11. World Health Organization [WHO] Department of Injuries and Violence Prevention. Prevention of child abuse and neglect: making the links between human rights and public health. Geneva, 2001.
12. Centres for Disease Control and Prevention. Child maltreatment. 2008.
13. Children's Bureau Administration on Children Youth and Families. Child maltreatment 2006, 2008.
14. Roaten JB, Partrick DA, Nydam TL et al. J Ped Surg 2006; 41:2013–2015.
15. Schnitzer PG, Ewigman BG. Pediatrics 2005; 116:687–693
16. Bruce DA, Zimmerman RA. Pediatr Ann 1989; 18:482–494.
17. Herndon WA. J Pediatr Orthop 1983; 3:73–76.
18. Chapman S. J R Soc Med 1990; 83:67–71.
19. Loder RT, O'Donnell PW, Feinberg JR. J Pediatr Orthop 2006; 26:561–566.
20. Prevent Child Abuse America. Total estimated cost of child abuse and neglect in the United States: statistical evidence. http://member.preventchildabuse.org/site/DocServer/cost_analysis.pdf?docID=144&JServSessionIdr007=esnmlgova3.app2b; Date accessed: 24-4-2008.
21. Rovi S, Chen PH, Johnson MS. Am J Public Health 2004; 94:586–590.
22. Walker EA, Unutzer J, Rutter C et al. Arch Gen Psychiatr 1999; 56:609–613.
23. Tang B, Jamieson E, Boyle M, Libby A, Gafni A et al. Soc Sci Med 2006; 63:1711–1719.
24. Felitti VJ, Anda RF, Nordenberg D et al. Am J Prev Med 1998; 14:245–258.
25. McMahon P, Grossman W, Gaffney M, Stanitski C. J Bone Joint Surg Am 1995; 77:1179–1183.
26. Pierce MC, Bertocci GE. Clin Ped Emerg Med 2006; 7:143–148.
27. Hobbs CJ, Hanks HGI, Wynne JM. Child Abuse and Neglect – A Clinician's Handbook, New York: Churchill Livingstone, 1993.

28. Leventhal JM, Thomas SA, Rosenfield NS, Markowitz RI. Am J Dis Child 1993; 147: 87–92.
29. Worlock P, Stower M, Barbor P. BMJ 1986; 293:100–102.
30. Mathew MO, Ramamohan N, Benet GC. BMJ 1998; 317:1117–1118.
31. Valvano T, Binns H, Flaherty E, Leonhardt D. The reliability of bruising in predicting which fractures are caused by child abuse 3140. 5 ed, 2006.
32. Kleinman PK. Diagnostic Imaging of Child Abuse, 2nd edn. St. Louis: Mosby, 1998.
33. Kleinman PK, Marks SC, Blackbourne B. Am J Roentgenol 1986; 146:895–905.
34. Lonergan GJ, Baker AM, Morey MK, Boos SC. Radiographics 2003; 23:811–845.
35. Merten DF, Radlowski MA, Leonidas JC. Radiology 1983; 146:377–381.
36. Williams RL, Connolly PT. Arch Dis Child 2004; 89:490–492.
37. Barsness KA, Cha ES, Bensard DD et al. J Trauma 2003; 54:1107–1110.
38. Barry PW, Hocking MD. Arch Dis Child 1993; 68:250.
39. Bulloch B, Schubert CJ, Brophy PD, Johnson N, Reed MH et al. Pediatrics 2000; 105:E48.
40. Durani Y, DePiero AD. Ann Emerg Med 2006; 47:210–215.
41. Hartmann RW, Jr. Arch Pediatr Adolesc Med 1997; 151:947–948.
42. Rizzolo PJ, Coleman PR. J Fam Pract 1989; 29:561–563.
43. Thomas PS. Ann Radiol (Paris) 1977; 20: 115–122.
44. Alexander JM, Leveno KJ, Hauth J et al. Obstet Gynecol 2006; 108:885–890.
45. Bhat BV, Kumar A, Oumachigui A. Indian J Pediatr 1994; 61:401–405.
46. Gudmundsson S, Henningsson AC, Lindqvist P. BJOG 2005; 112:764–767.
47. Levine MG, Holroyde J, Woods JR, Jr., Siddiqi TA, Scott M, Miodovnik M. Obstet Gynecol 1984; 63:792–795.
48. Rubin A. Obstet Gynecol 1964; 23: 218–221.
49. American College of Radiology (ACR). ACR practice guideline for skeletal surveys in children. www.acr.org ; Date accessed: 17-6-0008.
50. American College of Radiology (ACR). Standards for skeletal surveys in children. Research 1997:51–54.
51. British Society of Paediatric Radiologists. NAI standard for skeletal surveys. www.bspr.org.uk/nai.htm; Date accessed: 1-9-2007.
52. Kemp AM, Butler A, Morris S et al. Clin Radiol 2006; 61:723–736.
53. Mandelstam SA, Cook D, Fitzgerald M, Ditchfield MR. Arch Dis Child 2003; 88:387–390.
54. Smeets AJ, Robben SG, Meradji M. Pediatr Radiol 1990; 20:566–567.
55. Nimkin K, Kleinman PK, Teeger S, Spevak MR. Pediatr Radiol 1995; 25:562–565.
56. Markowitz RI, Hubbard AM, Harty MP, Bellah RD, Kessler A, Meyer JS. Pediatr Radiol 1993; 23:264–267.
57. Elterman T, Beer M, Girschick HJ. J Child Neurol 2007; 22:170–175.
58. Stranzinger E, Kellenberger CJ, Braunschweig S, Hopper R, Huisman TAGM. Eur J Radiol Extra 2007; 63:43–47.
59. Traub M, Stevenson M, McEvoy S et al. Injury 2007; 38:43–47.
60. Alkadhi H, Wildermuth S, Marincek B, Boehm T. J Comput Assist Tomogr 2004; 28: 378–385.
61. Renton J, Kincaid S, Ehrlich PF. J Pediatr Surg 2003; 38:793–797.
62. Pickett WJ, Faleski EJ, Chacko A, Jarrett RV. South Med J 1983; 76:207–212.
63. Slovis TL, Smith W, Kushner DC et al. Radiology 2000; 215(Suppl.):805–809.
64. Ingram JD, Connell J, Hay TC., Strain JD, Mackenzie T. (2000). Oblique radiographs of the chest in nonaccidental trauma Emerg Radiol 2007; 7:42–46.
65. Kleinman PK, O'Connor B, Nimkin K et al. Pediatr Radiol 2002; 32:896–901.
66. Offiah AC, Moon L, Hall CM, Todd-Pokropek A. Clin Radiol 2006; 61:163–173.
67. Carty H, Pierce A. Eur Radiol 2002; 12: 2919–2925.
68. Conway JJ, Collins M, Tanz RR. Semin Nucl Med 1993; 23:321–333.
69. Haase GM, Ortiz VN, Sfanakis GN. J Trauma 1980; 20:873–875.
70. Jaudes PK. Pediatrics 1984; 73:166–168.
71. Sty JR, Starshak RJ. Radiology 1983; 146: 369–375.
72. Howard JL, Barron BJ, Smith GG. Radiographics 1990; 10:67–81.
73. Lewis D, Logan P. J Clin Ultrasound 2006; 34:190–194.
74. Major NM, Crawford ST. AJR Am J Roentgenol 2002; 178:413–418.
75. Hargaden G, O'Connell M, Kavanagh E, Powell T, Ward R, Eustace S. Am J Roentgenol 2003; 180:247–252.
76. Kellenberger CJ, Epelman M, Miller SF, Babyn PS. Radiographics 2004; 24:1317–1330.
77. Evangelista P, Barron C, Goldberg A, Jenny C, Tung G. MRI STIR for the Evaluation of Nonaccidental Trauma in Children. 2912.433 ed, 2006.
78. Ellerstein NS, Norris KJ. Pediatrics 1984; 74:1075–1078.

79. Kleinman PK, Marks SC, Jr., Nimkin K, Rayder SM, Kessler SC. Radiology 1996; 200: 807–810.
80. Zimmerman S, Makoroff K, Care M, Thomas A, Shapiro R. Child Abuse Negl 2005; 29: 1075–1083.
81. Kleinman PK, Nimkin K, Spevak MR et al. Am J Roentgenol 1996; 167:893–896.
82. Campbell KA, Bogen DL, Berger RP. Arch Pediatr Adolesc Med 2006; 160:1241–1246.
83. Hamilton-Giachritsis CE, Browne KD. J Fam Psychol 2005; 19:619–624.
84. Day F, Clegg S, McPhillips M, Mok J. J Clin Forensic Med 2006; 13:55–59.
85. Hymel KP. Committee on child abuse and neglect NAoME. Pediatrics 2006; 118: 421–427.
86. Norman MG, Smialek JE, Newman DE, Horembala EJ. Perspect Pediatr Pathol 1984; 8:313–343.
87. Arnestad M, Vege A, Rognum TO. Forensic Sci Int 2002; 125:262–268.
88. Kleinman PK, Blackbourne BD, Marks SC, Karellas A, Belanger PL. N Engl J Med 1989; 320:507–511.
89. McGraw EP, Pless JE, Pennington DJ, White SJ. Am J Roentgenol 2002; 178:1517–1521.
90. Klotzbach H, Delling G, Richter E, Sperhake JP, Puschel K. Int J Legal Med 2003; 117:82–89.
91. Griffiths PD, Paley MN, Whitby EH. Lancet 2005; 365:1271–1273.
92. Roberts IS, Benbow EW, Bisset R et al. Histopathology 2003; 42:424–430.
93. Cumming W. J Can Assoc Radiol 1979; 30:33.
94. Islam O, Soboleski D, Symons S, Davidson LK, Ashworth MA, Babyn P. Am J Roentgenol 2000; 175:75–78.
95. Yeo LI, Reed MH. Can Assoc Radiol J 1994; 45:16–19.
96. Prosser I, Maguire S, Harrison SK, Mann M, Sibert JR et al. Am J Roentgenol 2005; 184: 1282–1286.
97. Trokel M, Discala C, Terrin NC, Sege RD. Child Maltreat 2004; 9:111–117.
98. Trokel M, Discala C, Terrin NC, Sege RD. Pediatr Emerg Care 2006; 22:700–704.
99. Cooper A, Floyd T, Barlow B et al. J Trauma 1988; 28:1483–1487.
100. Sivit CJ, Taylor GA, Eichelberger MR. Radiology 1989; 173:659–661.
101. Gornall P, Ahmed S, Jolleys A, Cohen SJ. Arch Dis Child 1972; 47:211–214.
102. Ledbetter DJ, Hatch EI, Jr., Feldman KW, Fligner CL, Tapper D. Arch Surg 1988; 123:1101–1105.
103. Champion MP, Richards CA, Boddy SA, Ward HC. Arch Dis Child 2002; 87:432–433.
104. Gaines BA, Shultz BS, Morrison K, Ford HR. J Pediatr Surg 2004; 39:600–602.
105. Peters E, LoSasso B, Foley J, Rodarte A, Duthie S, Senac MO, Jr. Pediatr Crit Care Med 2006; 7:551–556.
106. Wood J, Rubin DM, Nance ML, Christian CW. J Trauma 2005; 59:1203–1208.
107. Timaran CH, Daley BJ, Enderson BL. J Trauma 2001; 51:648–651.
108. Chao HC, Kong MS. J Clin Ultrasound 1999; 27:284–286.
109. Lorente-Ramos RM, Santiago-Hernando A, Del Valle-Sanz Y, Rjonilla-Lopez A. J Clin Ultrasound 1999; 27:213–216.
110. Grassi R, Pinto A, Rossi G, Rotondo A. Acta Radiol 1998; 39:52–56.
111. Albanese CT, Meza MP, Gardner MJ, Smith SD, Rowe MI et al. J Trauma 1996; 40: 417–421.
112. Butela ST, Federle MP, Chang PJ et al. Am J Roentgenol 2001; 176:129–135.
113. Stuhlfaut JW, Soto JA, Lucey BC et al. Radiology 2004; 233:689–694.
114. Allen TL, Mueller MT, Bonk RT, Harker CP, Duffy OH et al. J Trauma 2004; 56:314–322.
115. Desai KM, Dorward IG, Minkes RK, Dillon PA. J Trauma 2003; 54:640–645.
116. Brody JM, Leighton DB, Murphy BL et al. Radiographics 2000; 20:1525–1536.
117. Strouse PJ, Close BJ, Marshall KW, Cywes R. Radiographics 1999; 19:1237–1250.
118. Rathaus V, Pomeranz A, Shapiro-Feinberg M, Zissin R. Emerg Radiol 2004; 10:190–192.
119. Ruess L, Sivit CJ, Eichelberger MR, Taylor GA, Bond SJ. Pediatr Radiol 1995; 25:321–325.
120. Marco GG, Diego S, Giulio A, Luca S. Eur J Radiol 2005; 56:97–101.
121. Hagiwara A, Yukioka T, Ohta S, Nitatori T, Matsuda H et al. Am J Roentgenol 1996; 167: 159–166.
122. Hagiwara A, Yukioka T, Ohta S et al. Am J Roentgenol 1997; 169:1151–1156.
123. Hagiwara A, Sakaki S, Goto H et al. J Trauma 2001; 51:526–531.
124. Yao DC, Jeffrey RB, Jr., Mirvis S et al. Am J Roentgenol 2002; 178:17–20.
125. Willmann JK, Roos JE, Platz A et al. Am J Roentgenol 2002; 179:437–444.
126. Kitase M, Mizutani M, Tomita H, Kono T, Sugie C et al. Vasa 2007; 36:108–113.
127. Bosboom D, Braam AW, Blickman JG, Wijnen RM. Eur J Radiol 2006; 59:3–7.
128. Gupta A, Stuhlfaut JW, Fleming KW, Lucey BC, Soto JA. Radiographics 2004; 24:1381–1395.
129. Mattix KD, Tataria M, Holmes J et al. J Pediatr Surg 2007; 42:340–344.

14

Imaging of Spine Disorders in Children: Dysraphism and Scoliosis

L. Santiago Medina, Diego Jaramillo, Esperanza Pacheco-Jacome, Martha C. Ballesteros, Tina Young Poussaint, and Brian E. Grottkau

Issues

Spinal Dysraphism

I. How accurate is imaging in occult spinal dysraphism (OSD)?
II. What are the clinical predictors of OSD?
III. What are the natural history and role of surgical intervention in OSD?
IV. What is the cost-effectiveness of imaging in children with OSD?

Scoliosis

I. How should the radiographic evaluation of scoliosis be performed?
II. What radiation-induced complications result from radiographic monitoring of scoliosis?
III. What is the role of magnetic resonance imaging in idiopathic scoliosis?

Key Points

Spinal Dysraphism

- The prevalence of occult spinal dysraphism (OSD) ranges from as low as 0.34% in children with intergluteal dimples to as high as 46% in newborns with cloacal malformation (moderate evidence).
- *Radiographs are relatively insensitive and nonspecific for this diagnosis.* MRI and ultrasound have high overall diagnostic performances (i.e., sensitivity and specificity) in children with suspected OSD (moderate evidence).
- Early detection and prompt neurosurgical correction of OSD may prevent upper urinary tract deterioration, infection of dorsal dermal sinuses, or permanent neurologic damage (moderate and limited evidence).

L.S. Medina (✉)
Co-Director, Division of Neuroradiology and Brain Imaging, Director of the Health Outcomes, Policy, and Economics (HOPE) Center, Department of Radiology, Miami Children's Hospital Miami, FL 33155, USA
e-mail: santiago.medina@mch.com

L.S. Medina et al. (eds.), *Evidence-Based Imaging in Pediatrics*,
DOI 10.1007/978-1-4419-0922-0_14, © Springer Science+Business Media, LLC 2010

• Cost-effectiveness analysis suggests that, in newborns with suspected OSD, appropriate selection of patients and diagnostic strategy may increase quality-adjusted life expectancy and decrease cost of medical workup (moderate evidence).

Scoliosis

- Radiographic measurements of scoliosis are reproducible, particularly when the levels of the end plates measured are kept constant (moderate evidence). Unexpected findings on radiographs are unusual (limited evidence).
- Radiographic monitoring of scoliosis results in a clear increase in the radiation-induced cancer risk, particularly to the female breast (moderate evidence). It also results in a high dose of radiation to the ovaries and worsens reproductive outcome in females (moderate evidence). Therefore, it is very important to reduce the radiation exposure. Posteroanterior projection greatly reduces exposure. Some digital systems also decrease radiation.
- Significant controversy exists on the use of MRI in "idiopathic" scoliosis. MRI is recommended for children at higher risk of CNS lesions: (1) patients with idiopathic scoliosis and an abnormal neurological exam; (2) children under the age of 11 years; and (3) patients with levoconvex or atypical curves (limited to moderate evidence). However, exceptions to these rules have been reported in the literature (limited to moderate evidence). Therefore, patients with scoliosis considered for surgical intervention should have preoperative MRI to avoid the potential irreversible neurological complications that could occur if any underlying CNS lesion was undetected or misdiagnosed.

Definition and Pathophysiology

Spinal Dysraphism

Spinal dysraphism is a wide spectrum of congenital anomalies that results from abnormal development of one or more of the midline mesenchymal, bony and neural elements of the spine (1). This entity can be divided into open and closed spina bifida. Open spina bifida is characterized by a dorsal herniation of all or part of the spinal content without full skin coverage. Open spina bifida entities include meningocele and myelomeningocele. Closed or occult spinal dysraphism (OSD) is characterized by a spinal anomaly covered with skin and hence with no exposed neural tissue (2, 3). OSD spectrum includes dorsal dermal sinus, thickened filum terminale, diastematomyelia, caudal regression syndrome, intradural lipoma, lipomyelocele, lipomyelomeningocele, anterior spinal meningocele, and other forms of myelodysplasia (Figs. 14.3 and 14.4).

Scoliosis

Scoliosis is defined as an abnormal spinal curvature most apparent in the coronal plane (4). Scoliosis can be classified as idiopathic, congenital, neuromuscular, or degenerative. Most pediatric cases are idiopathic in nature. Idiopathic scoliosis is further subdivided according to the age at which the disease presents: infantile (birth to 3 years), juvenile (4–9 years), and most commonly adolescent (10 years and beyond) (5). Congenital scoliosis is caused by vertebral anomalies of embryologic etiology (e.g., hemivertebra, butterfly, or block vertebra) (6). Neuromuscular scoliosis is typically seen in cerebral palsy and muscular dystrophy.

Scoliosis can also be seen in disorders such as neurofibromatosis (Figs. 14.5 and 14.6) and Marfan syndrome (4). Degenerative scoliosis is primarily a disease of adults.

Conus Medullaris Position

Controversy has existed about the normal position of the conus medullaris. The normal level of the conus medullaris was thought to vary with the age of the child (7–9). Cross-sectional imaging studies, however, indicate that the normal conus medullaris position can vary from the middle of T11 to the bottom of L2 by the age of 2 months (7, 9) and probably at birth (7, 10). More recent study by Soleiman and colleagues (11) studied 635 adult patients with no spinal deformity and demonstrated the mean position of the tip of the conus medullaris at the level of the middle third of L1. The range extended from the lower third of T11 to the upper third of L3 (11). Although a spinal cord terminating at these normal levels can be tethered (8), the conus that terminates caudal to the L2–L3 disc space is at much higher risk of being tethered (7, 9, 12). Neuroimaging can define the anatomical location of the conus medullaris but the concept and word of "tethered" is a neurophysiological concept which requires clinical input (13). Small fibrolipomas in the filum terminale may be seen in untethered as well as tethered cords. Five to six percent of normal individuals can have variable amounts of fat in the filum terminale (14, 15).

Epidemiology

Spinal Dysraphism

Three percent of neonates have major central nervous system or systemic malformations (16). Furthermore, 5–15% of pediatric neurology hospital admissions are related to cerebrospinal anomalies (17). The incidence of neural tube defects in the United States is 1.2–1.7 per 1,000 births (18, 19). Almost half of neural tube defects are caused by anencephaly (0.6–0.8 per 1,000 births), and the majority of the remaining are caused by spinal dysraphism (0.5–0.8 per 1,000 births) (18, 19). Occult spinal dysraphism is the most prevalent spinal axis malformation (20) and the most common indication for spinal imaging in children (21). Occult spinal dysraphic lesions are commonly associated with urinary tract anomalies (22). One well-recognized risk factor for this disorder is folate deficiency in the mother.

The clinical spectrum of occult dysraphism is broad, ranging from skin stigmata such as a dimple, sinus tract, hairy patch, or hemangioma to motor, bladder, or bowel dysfunction (23–25). About 50–80% of occult spinal dysraphic cases exhibit a dermal lesion (15–28). However, 3–5% of all normal children have skin dimples (29, 30).

Scoliosis

Adolescent idiopathic scoliosis, by far the most common form, has a prevalence between 0.5 (31) and 3% (31, 32) and occurs more often in females. In a UK study of 15,799 children and young adolescents, Stirling and colleagues (31) found that the prevalence ratio of girls to boys was 5.2 [95% confidence interval (CI), 2.9–9.5]. In a study of 26,947 students, Rogala et al. (33) found that for curves ranging from 6 to 10°, the girl-to-boy ratio was 1:1, whereas the ratio was 5.4:1 for curves greater than 20°. The more severe the curve, the greater the predominance of girls over boys. Infantile scoliosis constitutes approximately 8% of idiopathic scoliosis, whereas juvenile scoliosis represents 18% (34). Male predominance is seen in infantile scoliosis. Congenital scoliosis is caused by failure of segmentation and normal formation of spinal elements (4). In a series of 60 cases of congenital scoliosis, Shahcheraghi and Hobbi (6) found that the most common type of anomaly was a hemivertebra (failure of formation), and that the most severe deformity was associated with a unilateral unsegmented bar (failure of segmentation) with a contralateral hemivertebra.

The etiology of adolescent scoliosis remains a mystery; however, some principles are generally agreed upon (34):

1. The progression of scoliosis is related to severity and skeletal maturity. The younger the onset and the greater the severity of the curve, the faster the progression. Although previously it was believed that scoliosis remained stable after skeletal maturity was attained, Weinstein and Ponseti (35) demonstrated that 68% of curves worsened after bone maturity.

2. The typical scoliosis curve is not associated with pain or neurologic signs and symptoms. Painful curves, especially if rapidly progressive or if associated with an atypical curve pattern, are frequently caused by underlying diseases (36).
3. Less than 10% of the curves require treatment (37).

Goals

Spinal Dysraphism

In patients with spinal dysraphism, the goal of imaging is to detect early neurosurgical correctable occult dysraphic lesions in order to prevent neurologic damage, upper urinary tract deterioration, and potential infection of the dorsal dermal sinuses.

Scoliosis

In patients with scoliosis, the goal of imaging is to detect and characterize the type of curve and its severity, to track disease progression and monitor changes related to treatment, and to identify those cases in which occult etiologies exist (4).

Methodology

The authors performed a MEDLINE search using Ovid (Wolters Kluwer U.S. Corporation, NY City) and PubMed (National Library of Medicine, Bethesda, MD) for data relevant to the diagnostic performance and accuracy of both clinical and radiographic examination of patients with occult spinal dysraphism or scoliosis during the years 1966–January 2008. Animal studies and non-English articles were excluded. The titles, abstracts, and full text of the relevant articles were reviewed at each step.

Discussion of Issues in Spinal Dysraphism

I. How Accurate Is Imaging in Occult Spinal Dysraphism?

Summary of Evidence: Several studies have shown that MRI and ultrasound have better overall diagnostic performances (i.e., sensitivity and specificity) than do plain radiographs (moderate evidence) for detection of occult spinal dysraphism (21, 26, 38, 39). The sensitivity of spinal MRI and ultrasound has been estimated at 95.6 and 86.5%, respectively (31, 39). The specificity of spinal MRI and ultrasound has been estimated at 90.9 and 92.9%, respectively (21, 39). Conversely, the sensitivity and the specificity of plain radiographs have been estimated at 80 and 18%, respectively (26, 38).

Supporting Evidence: The diagnostic performance of the imaging tests available is shown in detail in Table 14.1.

II. What Are the Clinical Predictors of Occult Spinal Dysraphism (OSD)?

Summary of Evidence: The prevalence of OSD ranges from as low as 0.34% in children with intergluteal dimples to as high as 46% in newborns with cloacal malformation (moderate evidence). Table 14.2 summarizes the spectrum of occult spinal dysraphism into low-, intermediate-, and high-risk groups.

Supporting Evidence: Children in the low-risk group included those with simple skin dimples as the sole manifestation or newborns of diabetic mothers. Intergluteal dimples over the sacrococcygeal area rarely extend into the spinal canal (40–42). Caudal regression syndrome occurs at higher rates in children born to diabetic mothers (43). The prevalence (pretest probability) of a dysraphic lesion among low-risk patients has been estimated at 0.3–3.8% (Table 14.2). In the low range (0.3%) are children with low intergluteal dimples, while in the upper range (3.8%) are children with higher lumbosacral dimples (19, 26, 31) (moderate and limited evidence).

Children in the intermediate-risk group included those with complex skin stigmata (hairy patch, hemangiomas, lipomas, and well-defined dorsal dermal sinus tracks) or low and intermediate anorectal malformations. The prevalence (pre-test probability) of a dysraphic lesion among intermediate-risk patients has been estimated at 27–36% (Table 14.2)

(moderate evidence). Children in the high-risk group included those with high anorectal malformations, cloacal malformation, and cloacal exstrophy. The prevalence (pre-test probability) of a dysraphic lesion among high-risk patients has been estimated at 44–100% (Table 14.2) (moderate evidence).

III. What Are the Natural History and Role of Surgical Intervention in Occult Spinal Dysraphism?

Summary of Evidence: Early detection and prompt neurosurgical correction of occult spinal dysraphism may prevent upper urinary tract deterioration, infection of dorsal dermal sinuses, or permanent neurologic damage (44–48) (moderate and limited evidence). Several studies have demonstrated that motor function, urologic symptoms, and urodynamic patterns may be improved, stabilized, or prevented by early surgical intervention in patients with occult spinal dysraphism (49, 50) (moderate and limited evidence). The surgical outcome may be better if intervention occurs before the age of 3 years (49–51) (moderate and limited evidence). Spinal neuroimaging, therefore, has the important role of determining the presence or the absence of an occult spinal dysraphic lesion so that appropriate surgical treatment can be instituted in a timely manner.

At our institution, occult dysraphic lesions diagnosed in the newborn period are usually operated at the age of 2–3 months. Therefore, if ultrasound is indicated, it is performed in the early newborn and infancy period to avoid a limited sonographic window from posterior element mineralization (52, 53). If MRI is required, it is usually performed a few days before surgery.

Supporting Evidence: In the newborn period, most children with OSD are neurologically asymptomatic (29). Symptoms from occult spinal dysraphism are often not apparent until the child becomes older and is ambulating (29) (moderate evidence). The most common clinical presentations for occult dysraphic patients later in life include delay in walking, delay in the development of sphincter control, asymmetry of the legs or abnormalities of the feet (i.e., pes cavus and pes equinovarus), and pain in the lower extremities or back (44, 45, 49, 54–57).

Several studies have demonstrated improvement of the multiple symptoms associated with occult dysraphism if surgical intervention is performed (49–51) (moderate and limited evidence). However, there are differences in outcome depending on the timing of surgery (51). Using surgical outcome data from the study by Satar and colleagues (51), in the children diagnosed and surgically treated before the age of 3 years, 60% became asymptomatic, 30% were unchanged, and 10% worsened. Conversely, the same study data for the children diagnosed and surgically treated after the age of 3 years demonstrated that 27% became asymptomatic, 27% improved, 27% were unchanged, and 19% worsened (51).

Dysraphic patients with a central nervous system communicating dorsal dermal sinus (i.e., 10% of all dysraphic patients) are at risk for infection (26). The most dreaded infection is meningitis. Meningitis in the patient with a communicating dorsal dermal sinus may be caused by gram-negative or anaerobic bacteria (58, 59). The meningitis mortality rate in patients with communicating dorsal dermal sinus ranges between 1 and 12% (57–61) (limited evidence).

Severely symptomatic patients with dysraphism are at high risk of upper urinary tract deterioration (30, 62). In this population, up to 15% may have upper urinary tract deterioration (30, 62) and of those with progressive renal damage, 7.5% may develop end-stage renal disease over a 10-year period if undiagnosed (30, 62) (limited evidence).

IV. What Is the Cost-Effectiveness of Imaging in Children with Occult Spinal Dysraphism?

Summary of Evidence: Cost-effectiveness analysis suggests that, in newborns with suspected OSD, appropriate selection of patients and diagnostic strategy may increase quality-adjusted life expectancy and decrease cost of medical workup (30).

Supporting Evidence: A cost-effectiveness analysis (CEA) in children with occult spinal

dysraphism has been published in *Pediatrics* (30). This study assessed the clinical and economic consequences of four diagnostic strategies, MRI, ultrasound, plain radiographs, and no imaging with close clinical follow-up, in the evaluation of newborns with suspected occult spinal dysraphism (30).

A decision-analytic Markov model and cost-effectiveness analysis was performed incorporating (1) pre-test or prior probability of disease in three different risk groups, (2) sensitivity and specificity of diagnostic tests, and (3) morbidity and mortality rates of early versus late diagnosis and treatment of dysraphism. Outcomes were based on quality-adjusted life year (QALY) gained and incremental cost per QALY gained.

Medina and colleagues (30) found that in low-risk children with intergluteal dimple or newborns of diabetic mothers (pre-test probability=0.3–0.34%), ultrasound was the most effective strategy with an incremental cost-effectiveness ratio of $55,100 per quality-adjusted life year (QALY) gained. The cost for QALY is less than $100,000 and hence considered a reasonable cost-effective strategy. For children with lumbosacral dimples who have a higher pre-test probability of 3.8%, ultrasound was less costly and more effective than MRI, plain radiographs, or no imaging with close clinical follow-up.

In intermediate-risk newborns with low anorectal malformation (pre-test probability 27%), ultrasound was more effective and less costly than radiographs and no imaging. However, MRI was more effective than ultrasound at an incremental cost-effectiveness ratio of $1,000 per QALY gained. Therefore, this diagnostic strategy has a very low cost per QALY gained. In the high-risk group that included high anorectal malformation, cloacal malformation, and exstrophy (pre-test probability 44–46%), MRI was actually cost saving when compared with the other diagnostic strategies.

For the intermediate-risk group, the CEA was sensitive to the costs and diagnostic performances (sensitivity and specificity) of MRI and ultrasound. Lower MRI cost or greater MRI diagnostic performance improved the cost-effectiveness of the MRI strategy, while lower ultrasound cost or greater ultrasound diagnostic performance worsened the cost-effectiveness of the MRI strategy. Therefore, individual or institutional expertise with a specific diagnostic modality (MRI versus ultrasound) may influence the optimal diagnostic strategy.

Discussion of Issues in Scoliosis

I. How Should the Radiographic Evaluation of Scoliosis Be Performed?

Summary of Evidence: Radiographic measurements of scoliosis are reproducible, particularly when the levels of the vertebral body end plates measured are kept constant at each radiographic study over time (moderate evidence). Unexpected findings on radiographs are unusual (limited evidence) (4).

Supporting Evidence: Many articles have addressed the variability in measurement of the Cobb angle in adolescent idiopathic scoliosis. In a 1990 study by Morrisy and colleagues (67), four orthopedic surgeons performed six measurements on 50 frontal radiographs. The 95% CIs were 4.9°, and the variation was greatest when the end-plate vertebrae were not preselected (moderate evidence). Similar variability was noted in the sagittal and coronal planes. Carman and colleagues (68) had five observers perform two measurements on 28 radiographs showing kyphosis or scoliosis and found 95% CIs of 8° for scoliosis and 7° for kyphosis (Moderate Evidence). A more recent study (69) comparing manual versus computer-assisted radiographic measurements (24 radiographs, six observers) found a statistically significant difference between the 95% CIs of manual measurements (3.3°) and computer-generated measurements (2.6°).

Variability is greater for congenital scoliosis versus idiopathic scoliosis. Using six observers and 54 radiographs, Loder and colleagues (70) found 95% CIs of 11.8° (moderate evidence).

The contribution of radiologists' reports of scoliosis radiographs to clinical management was studied by Crockett and colleagues (71). These investigators retrospectively reviewed 161 charts and analyzed them for the presence or the absence of information about certain key parameters. There was no mention of how the review was done or whether there was any

attempt to correct for bias. Radiologists added information in 1.9% of the cases that, although not specified, was not deemed clinically significant (limited evidence) (71).

II. What Radiation-Induced Complications Result from Radiographic Monitoring of Scoliosis?

Summary of Evidence: Patients with severe scoliosis are monitored with the use of serial radiographs that expose the body to radiation. Radiographic monitoring of scoliosis results in a clear increase in the radiation-induced cancer risk, particularly to the breast (4) (moderate evidence). It also results in a high dose of radiation to the ovaries and worsens reproductive outcome in females (4) (moderate evidence). Therefore, it is very important to reduce the radiation exposure. Posteroanterior projection greatly reduces exposure, and some digital systems also decrease radiation (72).

Supporting Evidence: In 2000, Morin Doody and colleagues (73) published a retrospective cohort study of 5,573 female patients with scoliosis diagnosed before the age of 20 years. The average length of follow-up was 40.1 years, with complete follow-up in 89%. The average number of radiographs per patient was 24.7 (range, 0–618), and the mean estimated cumulative radiation dose to the breast was 10.8 cGy (range, 0–170). This dose is equivalent to 54 two-view mammograms (average breast dose of 2 mGy) (0.2 cGy). Seventy-seven breast cancer deaths were observed compared with 45.6 expected deaths on the basis of US mortality rates. Women with scoliosis had a 1.7-fold risk of dying of breast cancer (95% CI, 1.3–2.1) when compared with the general population. The data suggested that radiation was the causative factor, with risk increasing significantly with the number of radiographic exposures and the cumulative radiation dose (moderate evidence). Potential confounding was noted because the severity of disease was related to radiation exposure and reproductive history; patients with more severe disease were less likely to become pregnant and had a greater risk of breast cancer.

In a large retrospective cohort study of 2,039 patients, Levy and colleagues (74) found an excess lifetime cancer risk of 1–2% (12–25 cases per 1,000 population) among women (moderate evidence). The same group suggested that supplanting the anteroposterior (AP) view with the posteroanterior (PA) view would result in a three- to sevenfold reduction in cumulative doses to the thyroid gland and the female breast, three- to fourfold reductions in the lifetime risk of breast cancer, and a halving of the lifetime risk of thyroid cancer (75). The same cohort of women was evaluated for adverse reproductive outcomes (76). Of the initial group of 1,793 young women evaluated for scoliosis between 1960 and 1979, 1,292 women returned questionnaires in 1990. This cohort was compared with a reference group of 1,134 women selected randomly from the general population. The adolescent idiopathic scoliosis cohort had a higher risk of spontaneous abortions [odds ratio (OR), 1.35; 95% CI, 1.06–1.73] (moderate evidence). The odds of unsuccessful attempts at pregnancy (OR, 1.33; 95% CI, 0.84–2.13) and of congenital malformations in their offspring (OR, 1.2; 95% CI, 0.78–1.84) were also higher but not statistically significant (moderate evidence).

Digital radiography seems to reduce radiation exposure. The results are varied (77–79), and the technology is evolving (limited evidence). Recent studies report an 18-fold reduction with some systems (72) versus an almost twofold increase with others (80).

III. What Is the Role of Magnetic Resonance Imaging in Idiopathic Scoliosis?

Summary of Evidence: Significant controversy exists on the use of MR in idiopathic scoliosis. (1) Patients with idiopathic scoliosis and an abnormal neurological exam; (2) children under the age of 11 years; and (3) patients with levoconvex or atypical curves are at higher risk of CNS lesions and hence MRI is recommended (limited to moderate evidence). However, significant exceptions to these rules have been reported in the literature (limited to moderate evidence). Therefore, patients with scoliosis considered for surgical intervention should have preoperative MRI to avoid the potential

irreversible neurological complications that could occur if any underlying CNS lesion was undetected or misdiagnosed.

Supporting Evidence: Cheng and colleagues (81) studied 36 healthy control subjects, 135 patients with moderately severe adolescent idiopathic scoliosis (Cobb angle less than 45°), and 29 similar patients with Cobb angles greater than 45°. All of the patients were evaluated prospectively with MR imaging looking specifically for tonsillar ectopia and with somatosensory-evoked potentials. Tonsillar herniation was found in none of the controls versus 4 of 135 (3%) and 8 of 29 (27.6%) of the two scoliotic groups ($P<0.001$) (moderate evidence). Similarly, the percentages of patients with abnormal somatosensory-evoked potentials were 0, 11.9, and 27.6%, respectively. There was a significant association between tonsillar ectopia and abnormal somatosensory function ($P<0.0011$; correlation coefficient, 0.672) (moderate evidence). Tonsillar ectopia was defined as any inferior displacement of the tonsils, and none of the patients had a displacement greater than 5 mm, which is considered the usual threshold for the diagnosis (82–84).

Several studies have addressed the prevalence of MR abnormalities in patients with severe idiopathic scoliosis who are otherwise asymptomatic. Do and colleagues (85) studied a consecutive series of 327 patients with idiopathic scoliosis requiring surgical intervention (average preoperative curve of 57°) but without neurologic findings. The patients, aged 10–19 years, were evaluated from the base of the skull to the sacrum. Seven patients had abnormal MR images, including two with syrinx, four with Chiari malformation type I, and one with a fatty vertebral body. None of them required specific treatment for these findings (moderate evidence). In four other cases, equivocal MR findings necessitated additional workup. In a similar prospective double-blinded study of 140 patients evaluated preoperatively, Winter et al. (86) found four patients with abnormalities, three with Chiari I malformations, and one with a small syrinx, none of whom required treatment. In another study of MR examinations performed preoperatively, Maiocco et al. (87) found 2 of 45 patients with syrinx, one requiring decompression (moderate evidence).

To study whether the severity of the curve increased the risk of associated abnormalities, O'Brien et al. (88) performed MR evaluation on 33 consecutive patients with adolescent idiopathic scoliosis and Cobb angles greater than 70°. No neural axis abnormalities were found (limited evidence).

In a recent prospective study by Maenza (89) of 56 patients with juvenile and adolescent scoliosis, 11 patients (19.6%) had spinal axis lesions (Chiari I, $n=5$; Chiari I and syringomyelia, $n=4$; diastematomyelia and tethered cord, $n=1$; and tethered cord, $n=1$) (moderate evidence). In this group, the right and left thoracic curve patterns were seen in the same number of patients (4 of 11 each) (89) (moderate evidence). Thirty-six percent of the patients in this group were under the age of 11 years. Four patients (7.1%) had intracranial lesions (Dandy Walker syndrome, $n=1$; hydrocephalus, $n=2$; and cerebellar angioma, $n=1$). Four of the 15 patients (26.7%) with CNS abnormalities (spinal axis or intracranial lesions) had a normal neurological exam. Aria and colleagues found in 1,059 patients with scoliosis screened with MRI a total of 43 patients with syringomyelia and 38 of them associated with a Chiari I (90) (moderate evidence). Charry and colleagues found in 25 patients with scoliosis and syringomyelia, 10 patients with a levothoracic and 9 patients with a dextrothoracic curve pattern (limited evidence) (91).

Several studies have shown that, with scoliosis types that are different from the typical adolescent idiopathic form, there is a high prevalence of neural abnormalities (4). Of 30 consecutive children with congenital scoliosis studied by Prahinski and colleagues (92), nine had syringomyelia. Of these children, one required release of the tethered cord and one correction of a diastematomyelia (limited evidence). Two studies of prepubertal children suggest a high incidence of neural abnormalities in juvenile and infantile scoliosis. In a study of 26 consecutive children aged less than 11 years, Lewonowski and colleagues (93) found 5 (19.2%) with abnormalities of the cord. Three required surgical intervention, two with hydromyelia, and one with a mass (93) (limited evidence). Gupta and colleagues (94) found that 6 of 34 patients under 10 years of age studied prospectively had neural axis abnormalities, including two patients with

syrinx requiring syringopleural shunting (one with a Chiari I malformation). Other abnormalities included dural ectasia, tethered cord, and a brainstem astrocytoma (limited evidence).

In a retrospective review of 95 patients with idiopathic scoliosis who had been studied for various indications, Schwend and colleagues (95) found that 12 had a syrinx, 1 a cord astrocytoma, and 1 dural ectasia (limited evidence). Left thoracic scoliosis was the most important predictor of abnormality (10 abnormalities in 43 patients). Mejia and colleagues (96) then performed a prospective study (level 2) of 29 consecutive patients with idiopathic left thoracic scoliosis, finding only two with syrinx and no other abnormalities (limited evidence). Barnes and colleagues (36) retrospectively analyzed 30 patients with atypical idiopathic scoliosis and found 17 abnormalities in 11 patients, including seven cases of syringohydromyelia and five Chiari I malformations (Limited Evidence).

Take Home Figures and Tables

How Should Physicians Evaluate Newborns with Suspected Occult Spinal Dysraphism?

The decision tree in Fig. 14.1 reinforces the primary importance of a careful acquisition of a medical history and performance of a thorough examination in newborns with suspected spinal dysraphism (30). For those patients in the high-risk group, imaging of the spine with MRI is recommended. For those patients in the intermediate-risk group, imaging of the spine with MRI or ultrasound is suggested, while in the low-risk group, the strategies of ultrasound or no imaging may be indicated. Selection between these two strategies per risk group may be based on individual and institutional diagnostic performance and cost per test. In newborns with suspected occult dysraphism, appropriate selection of patients for imaging based on these risk groups may maximize health outcomes for patients and improve health-care resource allocation.

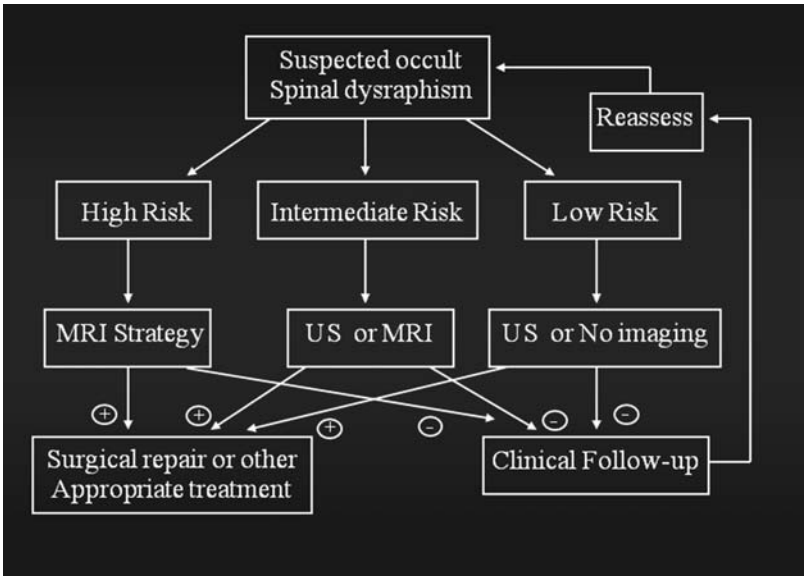

Figure 14.1. Suggested decision tree for use in newborns with suspected occult spinal dysraphism. For those patients in the high-risk group, MRI is recommended. For patients in the intermediate-risk group, ultrasound (US) or MRI is the strategy of choice, while for the low-risk group, ultrasound or no imaging is recommended. For patients with negative imaging studies, close clinical follow-up with periodic reassessment is recommended. (Reproduced with permission from Medina LS, Crone K, Kuntz KM. Newborns with suspected occult spinal dysraphism: a cost-effectiveness analysis of diagnostic strategies. Pediatrics. 2001;108:E101. Copyright © 2001 by the AAP.).

Tables 14.1 and 14.2 discuss the diagnostic performance of imaging tests in children with occult spinal dysraphism and the risk groups for occult spinal dysraphism, respectively.

Table 14.1. Diagnostic performance of imaging tests in children with occult spinal dysraphism

Variable	Baseline value (%)	95% Confidence interval[a] (%)	References
Ultrasound			
Sensitivity	86.5	75–98	(30, 39)
Specificity	92.0	84–100	(30, 39)
MRI			
Sensitivity	95.6	89.8–99.7	(20, 30)
Specificity	90.9	75.7–98.1	(20, 30)
Plain radiographs			
Sensitivity	80	80–100	(26, 30, 38)
Specificity	18	11–25	(30, 38)

[a]95% confidence intervals were estimated from the available literature.

Modified with kind permission of Springer Science+Business Media from Medina LS, Jaramillo D, Pacheco-Jacome E, Ballesteros MC, Grottkau BE. Imaging of Spine Disorders in Children: Dysraphism and Scoliosis. In Medina LS, Blackmore CC (eds.): Evidence-Based Imaging: Optimizing Imaging in Patient Care. New York: Springer Science+Business Media, 2006.

Table 14.2. Risk groups for occult spinal dysraphism

Variable	Baseline risk (%)	References
Low-risk group		
Offsprings of diabetic mothers	0.3	(30, 63–65)
Intergluteal dimples	0.34	(15, 30)
Lumbosacral dimple	3.8	(29)
Intermediate-risk groups		
Low anorectal malformation	27	(66)
Intermediate anorectal malformation	33	(66)
Complex skin stigmata[a]	36	(29)
High-risk group		
High anorectal malformation	44	(66)
Cloacal malformation	46	(22)
Cloacal exstrophy	100	(22)

[a]Hemangiomas, hairy patches, and subcutaneous masses.

Modified with kind permission of Springer Science+Business Media from Medina LS, Jaramillo D, Pacheco-Jacome E, Ballesteros MC, Grottkau BE. Imaging of Spine Disorders in Children: Dysraphism and Scoliosis. In Medina LS, Blackmore CC (eds.): Evidence-Based Imaging: Optimizing Imaging in Patient Care. New York: Springer Science+Business Media, 2006.

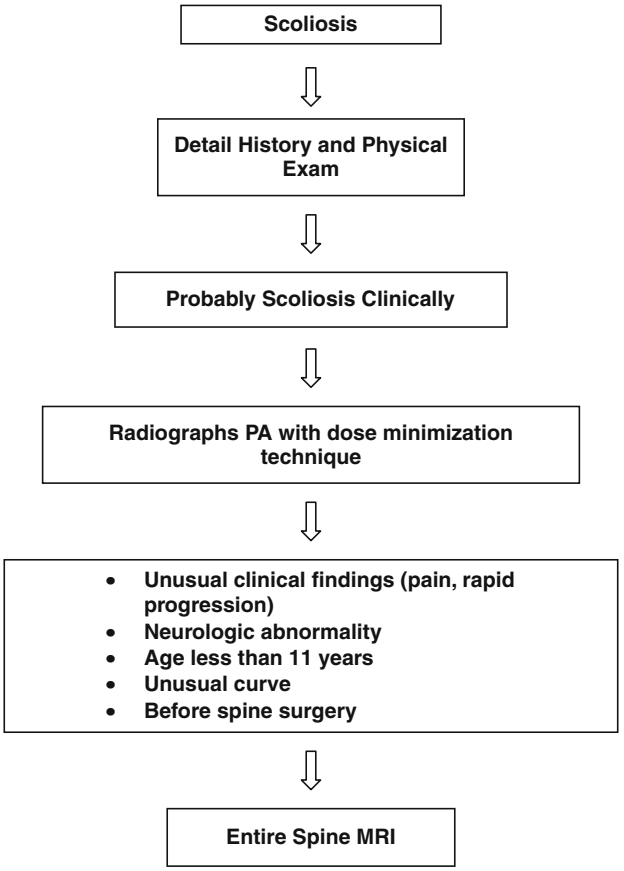

Figure 14.2. Suggested decision tree for use in patients with suspected scoliosis. Decision tree emphasizes the importance of clinical history, physical exam, and radiographs in determining the need for MRI. (Modified with kind permission of Springer Science+Business Media from Medina LS, Jaramillo D, Pacheco-Jacome E, Ballesteros MC, Grottkau BE. Imaging of Spine Disorders in Children: Dysraphism and Scoliosis. In Medina LS, Blackmore CC (eds.): Evidence-Based Imaging: Optimizing Imaging in Patient Care. New York: Springer Science+Business Media, 2006.).

How Should Scoliosis Be Evaluated?

Figure 14.2 summarizes the decision tree for patients with suspected scoliosis.

Imaging Case Studies

Case 1: Spinal Dysraphism

Imaging case study illustrates a child with skin stigmata (Fig. 14.3) who has an occult dysraphic lesion of the intradural lipoma type (Fig. 14.4).

Figure 14.3. Photograph of the lower back reveals skin discoloration, hairy patch, and dorsal lipoma. (Reprinted with kind permission of Springer Science+Business Media from Medina LS, Jaramillo D, Pacheco-Jacome E, Ballesteros MC, Grottkau BE. Imaging of Spine Disorders in Children: Dysraphism and Scoliosis. In Medina LS, Blackmore CC (eds.): Evidence-Based Imaging: Optimizing Imaging in Patient Care. New York: Springer Science+Business Media, 2006.).

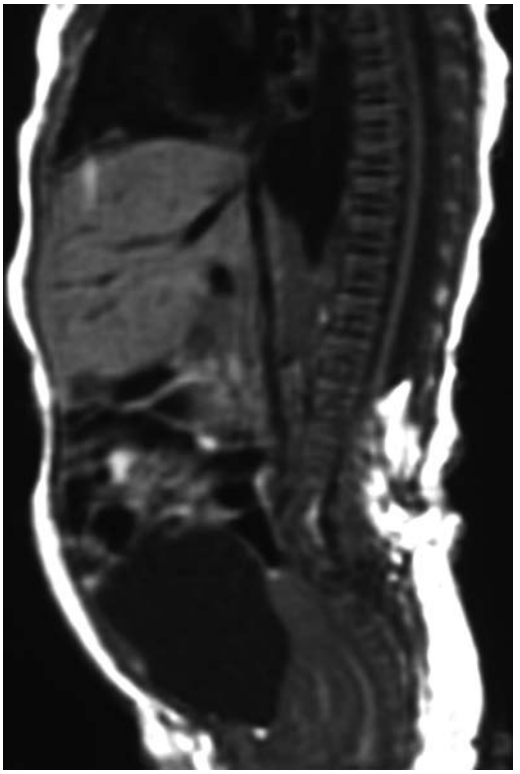

Figure 14.4. Sagittal T1-weighted imaging shows a dorsal lipoma extending into the spinal canal with an associate low-lying conus medullaris. (Reprinted with kind permission of Springer Science+Business Media from Medina LS, Jaramillo D, Pacheco-Jacome E, Ballesteros MC, Grottkau BE. Imaging of Spine Disorders in Children: Dysraphism and Scoliosis. In Medina LS, Blackmore CC (eds.): Evidence-Based Imaging: Optimizing Imaging in Patient Care. New York: Springer Science+Business Media, 2006.).

Case 2: Scoliosis

Imaging case study illustrates a child with atypical levoconvex thoracic scoliosis (Fig. 14.5) who has neurofibromatosis type 1 with underlying plexiform neurofibromas(Fig. 14.6).

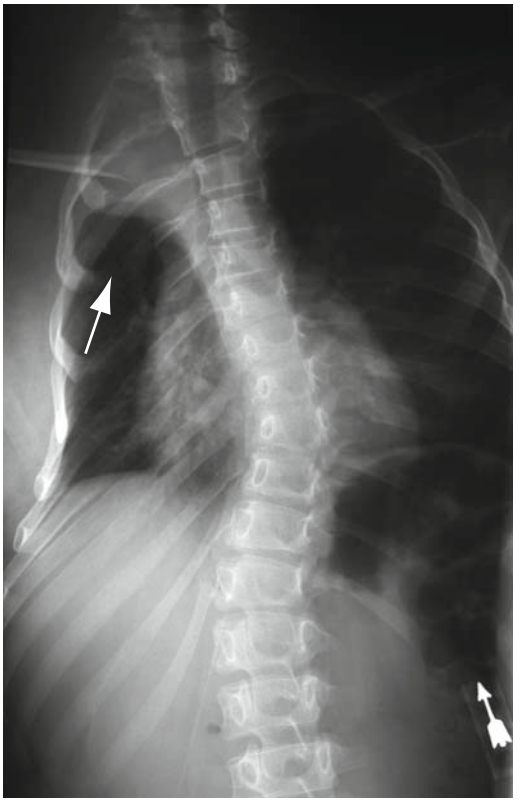

Figure 14.5. Frontal radiograph of the spine reveals atypical levoconvex thoracic scoliosis and right thoracic apical mass. (Reprinted with kind permission of Springer Science+Business Media from Medina LS, Jaramillo D, Pacheco-Jacome E, Ballesteros MC, Grottkau BE. Imaging of Spine Disorders in Children: Dysraphism and Scoliosis. In Medina LS, Blackmore CC (eds.): Evidence-Based Imaging: Optimizing Imaging in Patient Care. New York: Springer Science+Business Media, 2006.).

Figure 14.6. Coronal T2-weighted image shows a large right neck and chest plexiform neurofibroma. (Reprinted with kind permission of Springer Science+Business Media from Medina LS, Jaramillo D, Pacheco-Jacome E, Ballesteros MC, Grottkau BE. Imaging of Spine Disorders in Children: Dysraphism and Scoliosis. In Medina LS, Blackmore CC (eds.): Evidence-Based Imaging: Optimizing Imaging in Patient Care. New York: Springer Science+Business Media, 2006.).

Suggested Imaging protocols for Spinal Dysraphism and Scoliosis

Spinal Dysraphism

Spinal Ultrasound

Should be performed before the age of 3 months to avoid limited acoustic window from mineralization of posterior elements. An experienced operator should perform the study using a high-frequency 5–15 MHz linear array transducer (52).

Entire Spine MRI

A retrospective case–control study including 101 patients (moderate evidence) suspected of having occult lumbosacral dysraphism demonstrated that conventional three-plane, T1-weighted lumbosacral MR imaging in children and young adults provided better diagnostic information than did a fast-screening, two-plane, T1-weighted MRI because of its higher specificity and interobserver agreement (21). T2-weighted images in the axial and sagittal plane are often added to the protocol to assess intrinsic cord abnormalities. Intravenous paramagnetic contrast is not routinely used unless the patient has a communicating dorsal dermal sinus tract or clinical concerns of underlying infection.

Scoliosis

Scoliosis Radiographs

Should be performed only when clinically indicated. Using the posteroanterior projection greatly reduces exposure, and some digital systems also decrease radiation (4, 72). Use of gonads and breast lead shields further decreases the radiation exposure.

Entire Spine MRI

Patients with scoliosis may represent an imaging challenge. In patients with scoliosis being evaluated with MRI, the entire spine should be covered. Three-plane, T1- and T2-weighted images should be obtained with different obliquities to optimize imaging information. Another approach is to obtain three-dimensional FSE volumetric imaging. Weinberger and colleagues (97) recommend using a TR of 500 ms, TE_{eff} of 21 ms, echo train length (ETL) of 8, 20–38 cm field of view, 256 $\times$ 256 in-plane matrix, 1 mm sagittal partition thickness, one excitation, and 16 kHz of receive bandwidth. Intravenous paramagnetic contrast is important in the evaluation of intramedullary and extramedullary neoplasm.

Future Research

- Formal cost-effectiveness analysis of imaging in children with scoliosis.
- Further development of low- or no-radiation imaging techniques for patients with scoliosis.

- Large series studying the role of MRI in scoliosis.

References

1. Pacheco-Jacome E, Ballesteros MC, Jayakar P, Morrison G, Ragheb J et al. Neuroimag Clin N Am 2003;13:327–334.
2. Soonawala N, Overweg-Plandsoen WCG, Brouwer OF. Clin Neurol Neurosurg 1999;101:11–14.
3. Tortori-Donati P, Cama A, Rosa ML, Andreussi L, Taccone A. Neuroradiology 1990;31: 512–522.
4. Jaramillo D, Poussaint TY, Grottkau BE. Neuroimag Clin N Am 13 2003; 335–341.
5. Oestreich AE, Young LW, Young Poussaint T. Skeletal Radiol 1998;27(11):591–605.
6. Shahcheraghi GH, Hobbi MH. J Pediatr Orthop 1999;19(6):766–775.
7. DiPietro MA. Radiology 1993;188:149–153.
8. Rowland Hill CA, Gibson PJ. Am J Neuroradiol 1995;16:469–472.
9. Wilson DA, Prince JR. Am J Neuroradiol 1989;10:259–262.
10. Beek FJ, de Vries LS, Gerards LJ, Mali WP. Neuroradiology 1996;38(Suppl):S174–S177.
11. Soleiman J, Demaerel P, Rocher S et al. Spine 30(16): 1875–1880.
12. Barson AJ. J Ana 1970;106:489–497.
13. Warder DE, Oakes WJ. Neurosurgery 1993;33:374–378.
14. Haworth JC, Zachary RB. Lancet 1955;2:10–14.
15. Milhorat TH, Miller JI. In Avery GB, Fletcher MA, Mhairi GM (eds.): Neonatology, 4th edn. Philadelphia: J.B. Lippincott, 1994;1155–1163.
16. Kalter H, Warkany J. N Engl J Med 1983;308: 424–431.
17. Bird TD, Hall JG. Neurology 1977;27:1057–1060.
18. Vintzileos AM, Ananth CV, Fisher AJ, Smulian JC, Day-Salvatore D, Beazoglou T et al. Am J Obstet Gynecol 1999; 180(5):1110–1114.
19. Knight GJ, Palomaki GF. In Elias S, Simpson JL (eds.): Maternal Serum Screening for Fetal Genetic Disorders, New York: Churchill Livingstone, 1992;41–58.
20. Egelhoff JC, Prenger EC, Coley BD. In Ball W Jr. (ed.): Pediatric Neuroradiology, Philadelphia: Lippincott-Raven Publishers, 1997;717–778.
21. Medina LS, Al-Orfali M, Zurakowski D, Poussaint TY, DiCanzio J et al. Radiology 1999;211:767–771.
22. Appignani BA, Jaramillo D, Barnes PD, Poussaint TY. Am J Roentgenol 1994;163: 1199–1203.
23. Raghavan N, Barkovich AJ, Edwards M, Norman D. Am J Roentgenol 1989;152:843–852.
24. Brophy JD, Sutton LN, Zimmerman RA, Bury E, Schut L. Neurosurgery 1989;25:336–340.
25. Moufarrij NE, Palmer JM, Hahn JF, Weinstein MA. Neurosurgery 1989;25:341–346.
26. Volpe JJ. Neurology of the Newborn, 4th edn. Philadelphia: W.B. Saunders, 2001.
27. Hoffman HJ, Hendrick EB, Humphreys RP. Childs Brain 1976;2:145–155.
28. Hoffman HJ, Taecholarn C, Hendrick EB, Humphreys RP. J Neurosurg 1985;62:1–8.
29. Kriss VM, Desai NS. Am J Roentgenol 1998;171:1687–1692.
30. Medina LS, Crone K, Kuntz KM. Pediatrics 2001;108:E101.
31. Stirling AJ, Howel D, Millner PA, Sadiq S, Sharples D et al. J Bone Joint Surg Am 1996;78(9):1330–1336.
32. Newton PO, Wenger DR. In Morrissy RT, Weinstein SL (eds.): Lovell & Winter's Pediatric Orthopaedics, 5th edn. Philadelphia: Lippincott Williams & Wilkins, 2000;677–740.
33. Rogala EJ, Drummond DS, Gurr J. J Bone Joint Surg Am 1978;60(2):173–176.
34. Al-Arjani AM, Al-Sebai MW, Al-Khawashki HM, Saadeddin MF. Saudi Med J 2000;21(6):554–557.
35. Weinstein SL, Ponseti IV. J Bone Joint Surg Am 1983;65(4):447–455.
36. Barnes PD, Brody JD, Jaramillo D, Akbar JU, Emans JB. Radiology 1993;186(1):247–253.
37. Weinstein SL. Spine 1999;24(24):2592–2600.
38. Horton D, Barnes P, Pendleton BD, Polly M. J Okla State Med Assoc 1989;82:15–19.
39. Rohrschneider WK, Forsting M, Darge K, Tröger J. Radiology 1996;200:383–388.
40. Powell KR, Cherry JD, Hougen TJB, Blinderman EE, Dunn MC. J Pediatr 1975;87:744–750.
41. Byrd SE, Darling CF, McLone DG. Radiol Clin North Am 1991;29:711–752.
42. Herman TE, Oser RF, Shackelford GD. The role of neonatal spinal sonography. Clinical Pediatrics 1993;32:627–628.
43. Estin MD, Cohen AR. Neurosurg Clin N Am 1995;6:377–391.
44. Kaplan JO, Quencer RM. Radiology 1980;137:387–391.
45. McLone DG, Naidich TP. In McLaurin RL, Schut L Venes JL, Epstein F (eds.) Surgery of the Developing Nervous System, Philadelphia: W.B. Saunders Co, 1989,71–96.
46. Yamada S, Iacono RP, Andrade T, Mandybur G, Yamada BS. Neurosurg Clin N Am 1995;6: 311–323.
47. Davis PC, Hoffman JC, Ball TI, Wyly JB, Braun IF, Fry SM et al. Radiology 1988;166:679–685.

48. Scatliff JH, Kendall BE, Kingsley DPE, Britton J, Grant DN et al. Am J Neuroradiol 1989;10: 269–277.
49. Pang D, Wilberger JE. J Neurosurg 1982;57:32–47.
50. Fone PD, Vapnek JM, Litwiller SE, Couillard DR, McDonald CM, Boggan JE et al. J Urol 1997;157.
51. Satar N, Bauer SB, Shefner J, Kelly MD, Darbey MM. J Urol 1995;154:754–758.
52. Coley BD, Siegel MJ. In Siegel MJ (ed.): Pediatric Sonography, Philadelphia: Lippincott Williams & Wilkins, 2002; 671–698.
53. Rubin JM, Di Pietro MA, Chandler WF et al. Radiol Clin North Am 1988;26:1–27.
54. Page LK. In Wilkins RH, Rengachary SS (eds.): Neurosurgery, New York: McGraw Hill, 1992;2053–2058.
55. Westcott MA, Dynes MC, Remer EM, Donaldson JS, Dias LS. Radiographics 1992;12:1155–1173.
56. Atala A, Bauer SB, Dyro FM et al. J Urol 1992;148:592–594.
57. Reigel DH, Tchernoukha, K., Bazmi B, Kortyna R, Rotenstein D. Pediatr Neurosurg 1994;20:30–42.
58. Law DA, Aronoff SC. Pediatr Infect Dis J 1992; 11:968–971.
59. Rogg JM, Benzil DL, Haas RL, Knuckey NW. Am J Neuroradiol 1993;14:1393–1395.
60. DiTullio MVJr. . Surg Neurol 1977;7:351–354.
61. Feigen RD, Cherry JD. Textbook of Pediatric Infectious Diseases, 2nd edn. Philadelphia: W.B. Saunders Co, 1987.
62. Capitanucci ML, Iacobelli BD, Silveri M, Mosiello G, De Gennaro M. Eur J Pediatr Surg 1996;6(Suppl 1):25–26.
63. Mills JL. Teratology 1982;25:385–394.
64. Rusnak SL, Discoll SG. Pediatrics 1965;35: 989–995.
65. Becerra JE, Khoury MJ, Cordero JF, Ericson JD. Pediatrics 1990;85:1–9.
66. Long FR, Hunter JV, Mahboubi S, Kalmus A, Templeton JM. Radiology 1996;200:377–382.
67. Morrissy RT, Goldsmith GS, Hall EC, Kehl D, Cowie GH. J Bone Joint Surg Am 1990;72(3): 320–327
68. Carman DL, Browne RH, Birch JG. J Bone Joint Surg Am 1990;72(3):328–333.
69. Shea KG, Stevens PM, Nelson M, Smith JT, Masters KS et al. Spine 1998;23(5):551–555.
70. Loder RT, Urquhart A, Steen H, Graziano G, Hensinger RN, Schlesinger A et al. J Bone Joint Surg Br 1995;77(5):768–770.
71. Crockett HC, Wright JM, Burke S, Boachie-Adjei O. Idiopathic scoliosis. Spine 1999;24(19):2007–2009; discussion 2010.
72. Kalifa G, Charpak Y, Maccia C, Fery-Lemonnier E, Bloch J, Boussard JM et al. Pediatr Radiol 1998;28(7):557–561.
73. Morin Doody M, Lonstein JE, Stovall M, Hacker DG, Luckyanov N et al. Spine 2000;25(16): 2052–2063.
74. Levy AR, Goldberg MS, Hanley JA, Mayo NE, Poitras B. Health Phys 1994;66(6): 621–633.
75. Levy AR, Goldberg MS, Mayo NE, Hanley JA, Poitras B. Spine 1996;21(13):1540–1547; discussion 1548.
76. Goldberg MS, Mayo NE, Levy AR, Scott SC, Poitras B. Epidemiology 1998;9(3):271–278.
77. Kalmar JA, Jones JP, Merritt CR. Spine 1994;19(7):818–823.
78. Kling TF, Jr., Cohen MJ, Lindseth RE, De Rosa GP. Spine 1990;15(9):880–885.
79. Stringer DA, Cairns RA, Poskitt KJ, Bray H, Milner R et al. Pediatr Radiol 1994;24(1):1–5.
80. Geijer H, Beckman K, Jonsson B, Andersson T, Persliden J. Radiology 2001;218(2): 402–410.
81. Cheng JC, Guo X, Sher AH, Chan YL, Metreweli C. Spine 1999;24(16):1679–1684.
82. Barkovich AJ, Wippold FJ, Sherman JL, Citrin CM. Am J Neuroradiol 1986;7(5):795–799.
83. Elster AD, Chen MY. Radiology 1992;183(2): 347–353.
84. Mikulis DJ, Diaz O, Egglin TK, Sanchez R. Radiology 1992;183(3):725–728.
85. Do T, Fras C, Burke S, Widmann RF, Rawlins B et al. J Bone Joint Surg Am 2001;83–A(4):577–579.
86. Winter RB, Lonstein JE, Heithoff KB, Kirkham JA. Spine 1997;22(8):855–858.
87. Maiocco B, Deeney VF, Coulon R, Parks PF, Jr. Spine 1997;22(21):2537–2541.
88. Brien MF, Lenke LG, Bridwell KH, Blanke K, Baldus C. Spine 1994;19(14):1606–1610.
89. Maenza RA. J Pediatr Orthop Sept 2003; 12(5):295–302.
90. Arai S, Ohtsuka Y, Moriya H, Kitahara H, Minami S. Scoliosis associated with syringomyelia. Spine 1993; 18:1591–1592.
91. Charry O, Koop S, Winter RB, Lonstein J, Denis F et al. J Pediatr Orthop 1994; 14:309–317.
92. Prahinski JR, Polly DW, Jr., McHale KA, Ellenbogen RG. J Pediatr Orthop 2000;20(1):59–63.
93. Lewonowski K, King JD, Nelson MD. Spine 1992;17(6 Suppl):S109–S116.
94. Gupta P, Lenke LG, Bridwell KH. Spine 1998;23(2):206–210.
95. Schwend RM, Hennrikus W, Hall JE, Emans JB. J Bone Joint Surg Am 1995;77(1):46–53.
96. Mejia EA, Hennrikus WL, Schwend RM, Emans JB. J Pediatr Orthop 1996;16(3):354–358.
97. Weinberger E. Murakami J, Shaw D, White K, Radvilas M et al. J Comput Assist Tomogr 1995;19:721–725.

15

Imaging of the Spine for Traumatic and Nontraumatic Etiologies

C. Craig Blackmore

Issues

I. Who should undergo imaging of the cervical spine following trauma?
II. Who should undergo imaging of the thoracic and lumbar spine following trauma?
III. Who should undergo imaging for nontraumatic back pain?
IV. Special case: spondylolysis

Key Points

- Imaging in older children and adolescent victims of trauma should be limited to those who have any of the following criteria: (1) altered neurologic function, (2) intoxication, (3) midline posterior bony cervical spine tenderness, and (4) other painful distracting injury (moderate evidence).
- In contrast to adults, children with back pain should undergo evaluation to understand the cause of back pain. Imaging is clearly indicated in children and adolescents when infection, tumor, or scoliosis is suspected. Imaging is probably not indicated in subjects with symptoms of relatively short duration and intensity and in whom the physical examination is benign (insufficient evidence).
- Spondylolysis should be suspected in adolescent athletes with exercise-induced low back pain. Because spondylolysis may not be apparent on radiography, SPECT or CT is indicated if clinical suspicion is high (limited evidence).

C.C. Blackmore (✉)
Department of Radiology, Virginia Mason Medical Center, Seattle, WA, USA
e-mail: craig.blackmore@vmmc.org

L.S. Medina et al. (eds.), *Evidence-Based Imaging in Pediatrics*,
DOI 10.1007/978-1-4419-0922-0_15, © Springer Science+Business Media, LLC 2010

Definition and Pathophysiology

Cervical spine injury patterns in children are profoundly affected by the anatomy, biomechanics, and mechanisms of injury, all of which change as the child matures. Further, injuries in this age group are most common in the upper cervical spine (1–3) and may be dislocations and purely ligamentous disruptions. From the National Pediatric Trauma Registry, 84% of injured subjects 8 years of age and younger had upper cervical spine injuries (C1–C4) (1). In the NEXUS study, all four cervical spine injuries in young children were at the C2 level or higher (2).

The cervical spine achieves adult size by age 10, though complete fusion of the vertebral bodies does not occur until the mid-teenage years. In older children and adolescents, the patterns and mechanisms of injury parallel those of young adults, with increasing proportion of lower cervical spine injuries resulting from motor vehicle crashes (2, 4).

Data on thoracic and lumbar spine fractures in children are even more limited. Lower spine fractures occur generally as a consequence of high-energy trauma, with Chance or flexion distraction-type injuries at the thoracolumbar junction being relatively more common (5, 6).

Nontraumatic low back pain is a relatively common condition in both children and adults. Though extensively studied in the adult population, relatively less is known about the prevalence, etiology, and significance of back pain in the pediatric age group.

The etiology of nontraumatic low back pain in children and adolescents is not well understood. Etiological studies have grouped the factors associated with pediatric back pain into four broad categories: anthropometry, lifestyle factors, mechanical, and psycho social/behavioral fractures. All of these factors are somewhat controversial (7). Among the anthropometry factors that have been implicated are height, rate of growth, and spinal mobility, though the evidence supporting all of these factors is somewhat in conflict. The primary lifestyle factors that have been implicated include participation in sports, specifically weight lifting, skiing, and gymnastics (8–11), though, conversely, sedentary activity has also been implicated (12). The main mechanical fracture that has attracted much attention is the use of heavy school backpacks. Currently, the American Academy of Pediatrics recommends that backpacks not exceed 10–20% of the child's body weight, though this recommendation is based on limited evidence (13, 14). Finally, as in adults, psychosocial factors appeared to have a role (7).

Pediatric back pain can be grouped into broad categories. In addition to trauma, spondylolysis and spondylolisthesis are important causes of pediatric back pain, particularly in athletes (10, 11). Scoliosis and spinal dysraphism may also contribute to back pain. (See Chapter 14 on scoliosis and spine dysraphism.) In addition, benign and malignant bone tumors and infections can be the etiology of both chronic and acute symptomatology. (See Chapter 17 on osteomyelitis.) Finally, degenerative conditions, though less frequently seen than in adults, can also occur in the pediatric age group, including disk herniations and disk and endplate degeneration.

Epidemiology

In children under the age of 8, cervical spine injuries are uncommon (15–17). The National Emergency X-Radiography Utilization Study (NEXUS) included 818 individuals with cervical spine fracture. However, only four of these were 8 years of age or younger (2). There are no reliable data on the prevalence of thoracic or lumbar spine fractures in children.

The prevalence of low back pain in pediatric patients is not clearly established. A prospective study in Belgium of children 9–12 years of age demonstrated that 18% who had not reported back pain at baseline had at least one episode over the 2-year study (14). However, a meta-analysis of published lifetime prevalence studies performed by Jeffries et al. (18) found a range of 5–74% (18, 19).

Overall Cost to Society

Data on the cost of pediatric back pain are not available. There are estimates that back pain in the United States in adults costs more than $90 billion per year, though the relevance of this figure to the pediatric group is unclear (20).

Goals

The primary role of imaging in trauma is to exclude an unstable spinal injury. The primary role of imaging in nontraumatic back pain is to exclude a serious underlying pathological condition as an explanation for the child's pain.

Scoliosis and painful congenital deformities will be considered in a separate chapter. Additionally, infection including diskitis and vertebral osteomyelitis will be covered in this textbook in the appropriate chapter on bone infections. This chapter will focus on traumatic causes of back pain as well as on spondylolysis and spondylolisthesis.

Methodology

The author performed a MEDLINE search using PubMed (National Library of Medicine, Bethesda, MD) to identify publications reporting data on indications for imaging and imaging diagnostic performance for subjects at risk for traumatic spine injury and for those reporting nontraumatic back pain. The search time frame was January 1, 1980 to December 31, 2008. The study was limited to human, pediatric subjects, and English language publications. Additional references were searched from the identified papers.

Discussion of Issues

I. Who Should Undergo Imaging of the Cervical Spine Following Trauma?

Summary of Evidence: The NEXUS clinical prediction rule is a reasonable method of identifying which older children and adolescents should undergo cervical spine imaging after trauma. Imaging should be performed in subjects with (1) altered neurologic function, (2) intoxication, (3) midline posterior bony cervical spine tenderness, and (4) distracting injury (moderate evidence). There are no reliable data on when imaging is indicated in younger children (insufficient evidence). Radiography can appropriately be used to exclude cervical spine fracture in children, though cervical spine CT may be useful in high-risk subjects. In younger children, CT should be limited to the upper cervical spine (limited evidence).

Supporting Evidence: Evidence for who should undergo imaging is less complete in children than in adults. Determination of clinical predictors of injury in pediatric subjects is complicated by the decreased incidence of injury in children, requiring larger sample size for adequate study (4, 21). In addition, children may sustain serious cervical cord injuries that are not radiographically apparent (4, 21). Among adult clinical prediction rules, the Canadian Clinical Prediction Rule development study excluded children (22). The NEXUS trial included children, but there were only 30 injuries in subjects under age 18 and only 4 in subjects under age 9 (2, 23). Although no pediatric injuries were missed in the NEXUS study, the sample size was too small to adequately assess the sensitivity of the prediction rule in this group. Further validation of a pediatric version of the NEXUS was performed at a single academic pediatric trauma center in the United States. In 647 trauma victims age 3 or older, injuries were found in approximately 2%, of whom four required operative fixation. No missed injuries were reported (24).

A pediatric adaptation of the NEXUS is thus a reasonable approach, suggesting that imaging is indicated only when subjects have any of the following: (1) altered neurologic function, (2) intoxication, (3) midline posterior bony cervical spine tenderness, and (4) distracting injury (moderate evidence) (24). In addition, imaging is warranted in subjects under age 3 who are at risk for cervical spine injury, as the NEXUS cannot be reliably applied in these subjects (limited evidence).

Comparison of CT versus radiography has not been well explored in children. Radiography has accuracy for cervical spine fracture of approximately 94% (25), similar to adults (26). The odontoid view and flexion extension radiographs contribute little in young children (27–29). CT is likely more accurate than radiography but does encompass higher radiation doses and higher costs (30). The cost-effectiveness analysis of Blackmore and colleagues excluded children (26, 31, 32), as did the studies of the Harborview high-risk cervi-

cal spine criteria (31, 32). Further, the lower frequency of injury in children (2, 4) and the increased radiosensitivity of pediatric subjects (33) suggest that cost-effectiveness results from adults may not be relevant.

A reasonable approach to pediatric cervical spine imaging is the Harborview protocol (Fig. 15.1). Overall, radiography is adequate to exclude cervical spine fracture in most younger children (30, 34) (limited evidence). However, the use of upper cervical CT in high-risk younger children (35) who are getting head CT is probably reasonable, as the time and the cost are minimal, and the thyroid can be spared the CT radiation dose if imaging is limited to the upper cervical spine (insufficient evidence). In addition, upper cervical spine injuries are more common than lower cervical injuries in younger children (Fig. 15.2) (1–3).

II. Who Should Undergo Imaging of the Thoracic and Lumbar Spine Following Trauma?

Summary of Evidence: There are no clinical prediction rules validated in children for the determination of when imaging is indicated. However, a reasonable approach is to image when any of the following are present: (1) complaints of thoracolumbar spine pain, (2) thoracolumbar spine pain on midline palpation, (3) decreased level of consciousness, (4) abnormal peripheral nerve examination, (5) distracting injury, and (6) intoxication (moderate evidence). No reliable data exist on when to image in younger children (insufficient evidence). Compared to adults, younger children are less likely to localize pain and may have pain referred to the spine from intra-abdominal causes, particularly renal (infection and obstruction).

Supporting Evidence: Data on appropriate indications for thoracolumbar spine imaging in children are limited. The adult clinical prediction rule from Holmes and colleagues did enroll children. However, the actual number of children in the study is not reported (36). The youngest patient enrolled in the small clinical prediction rule validation trial by Hsu et al. was 14 years of age (37).

Given the 100% sensitivity in adults, it is reasonable to employ the Holmes clinical prediction rule in older children and perform imaging when any of the following clinical predictors are met: (1) complaints of thoracolumbar spine pain, (2) thoracolumbar spine pain on midline palpation, (3) decreased level of consciousness, (4) abnormal peripheral nerve examination, (5) distracting injury, and (6) intoxication (moderate evidence). In younger children, the criteria would have to be modified ad hoc to meet the clinical perception of the child's ability to provide reasonable responses and the clinical picture (insufficient evidence). The specificity of the Holmes prediction rule in adults was low (3.9%), so it is not expected that the use of this prediction rule would decrease unnecessary imaging (36).

III. Who Should Undergo Imaging for Nontraumatic Back Pain?

Summary of Evidence: There are no validated clinical prediction rules for determining which subjects with nontraumatic low back pain should undergo imaging. However, imaging is clearly indicated if there is clinical concern for infection, tumor, or scoliosis. Imaging is probably not indicated in subjects without concern for one of the preceding entities, in whom the pain has been of relatively short duration and intensity and in whom the physical examination is benign (insufficient evidence).

Spondylolysis is relatively common in adolescent athletes and should be suspected when pain develops in such subjects. Because spondylolysis may not be apparent on radiography, SPECT or CT may be warranted (limited evidence).

Supporting Evidence: There are no quality clinical trials on the value of imaging in children and adolescents with nontraumatic back pain. In addition, there are no validated clinical prediction rules for determining which children and adolescents should undergo imaging. Evidence supporting the use of imaging is mainly epidemiological, based on the relatively high yield for imaging in selected groups. Several studies from the 1980s reported that diagnosable pathology could be found in 52–84% of

children with back pain (19, 38, 39). However, a more recent paper by Bhatia et al. revealed pathology in only 22% (40). The reason for this difference is not clear, but it may be that there is increasing reporting of uncomplicated mechanical back pain in children, leading to more frequent imaging of children with no vertebral pathology.

Imaging is indicated in patients who may be at risk for vertebral osteomyelitis or diskitis (see Chapter 17) and in those with scoliosis (see Chapter 14). Risk factors for these conditions include fever, malaise, weight loss, neurological deficit, focal deformity, and pain at night (13, 41, 42). In addition, imaging is indicated when a significant scoliosis is present (see Chapter 14).

Among children and adolescents who have a short duration of pain and no antecedent history of significant trauma, and without physical findings on examination that put the child into a high-risk category for one of the diagnoses above, imaging can be withheld. Though substantiating evidence is lacking, a reasonable list of risk factors that might promote imaging includes point tenderness over the bony elements, particularly the pars interarticularis, radicular pain, abnormal neurologic examination, and pain with spinal flexion and extension (13) (insufficient evidence).

In a small prospective study of 87 patients seen by a single pediatric orthopedic surgeon by Felman et al., the predictors of constant pain, night pain, radicular pain, and abnormal neurologic examination could be combined into a clinical prediction rule to define subjects at high risk for underlying pathologic diagnosis (spondylolisthesis, scoliosis, tumor, disc degeneration, dysraphism). Patients with none of these predictors had only a 19% probability of underlying pathology, while patients of all four predictors had a probability of 100% for an underlying specific diagnosis. These results have not been validated, but the results may be useful in identifying subjects in whom additional imaging is indicated, after negative radiography (43) (limited evidence).

When imaging is indicated, radiography will almost always be the initial imaging modality of choice. The accuracy of radiography is not established. However, a recent protective study by Bhatia et al. determined that among 13 patients in this series, 10 had definitive diagnosis by radiography, with the remainder requiring CT, bone scan, or MRI (40). Similarly, in the Feldman et al. study, of 31 subjects with specific pathological diagnoses, 21 were diagnosed by initial radiography, with an additional 10 being diagnosed by MRI performed for high clinical suspicion. Thus in this small study, radiography has a sensitivity of 68% (21 of 31) for clinically important conditions (43). The specificity of radiography has not been documented. Despite the relatively modest accuracy of radiography, however, the relatively low radiation, low cost, and availability make this the initial imaging modality of choice. CT is the preferred imaging modality when spondylolysis is suspected. Bone scan is useful when symptoms are difficult to localize or if the acuteness of findings on other imaging evaluation is in question. MRI is the imaging modality of choice for infection, tumor, or neural element pathology (limited evidence).

IV. Special Case: Spondylolysis

Spondylolysis is the leading cause of low back pain in adolescents after exclusion of patients in whom no specific diagnosis can be made. In the Bhatia et al. study, spondylolysis accounted for 11% of patients presenting with low back pain (40). The overall prevalence of spondylolysis may be as high as 4.4% in small children and 6% in adults (44). It is particularly prevalent in athletes, specifically gymnasts, weight lifters, skiers, runners, and swimmers (8–12), and is the cause of back pain in an estimated 50% of cases (45, 46). Spondylolysis may be acute or chronic. Acute spondylolysis may be precipitated by exercise and may be amenable to conservative therapy (11). The prognosis and treatment in chronic spondylolysis or in spondylolisthesis is less clear.

There is no consensus on the appropriate imaging evaluation of spondylolysis, and multiple modalities may be required in some individuals (45, 47–49). Unfortunately, however, reliable data on the sensitivity and specificity of any imaging modality in this clinical setting are lacking. Though often the initial imaging, radiography is considered relatively insensitive for spondylolysis (50). CT scanning has

been promoted as an effective method for determining the acuteness of spondylolysis and for determining the potential for bony healing and the extent to which healing has occurred (11, 50, 51). The accuracy of CT for staging and following spondylolysis may be increased by performing thin-section scanning in the plane of the pars articularis with angled reformations (Fig. 15.3). However, reliable data on CT accuracy do not exist (48, 50) (insufficient evidence).

SPECT scan may be more sensitive for the diagnosis of spondylolysis (52), but it is less specific and provides less detailed anatomic information (53). Scintigraphy may also help differentiate painful acute spondylolysis from chronic spondylolysis that is not a cause of pain (54, 55). MRI (56–59) and PET-CT (60) show promise but have not been well evaluated in this population (insufficient evidence).

A reasonable imaging approach for suspected spondylolysis is initial imaging with radiography, followed by SPECT if no other cause of pain is identified and the subject is at high risk. If SPECT is negative, then no further imaging is indicated. However, if SPECT is positive, thin-section CT can be performed to define and stage the lesion (limited evidence).

Take Home Figures and Tables

Figure 15.1 demonstrates imaging protocol for pediatric blunt trauma. Table 15.1 discusses the pediatric modification of the NEXUS cervical spine imaging clinical prediction rule, and Table 15.2 discusses thoracolumbar spine imaging criteria.

Table 15.1. Pediatric modification of the NEXUS cervical spine imaging clinical prediction rule

Imaging of the cervical spine is not necessary if all of the following are met (in children aged 3 years and older):
1. Absence of midline cervical tenderness
2. Normal level of alertness
3. Absence of painful, distracting injury
4. No evidence of intoxication
5. Normal neurologic exam

Data from Hoffman et al. (23).
Adapted with permission from Anderson et al. (24).

Table 15.2. Thoracolumbar spine imaging criteria

Thoracolumbar spine imaging is not indicated in communicative children if all of the following are absent:
1. Thoracolumbar spine pain
2. Thoracolumbar spine tenderness on midline palpation
3. Decreased level of consciousness
4. Abnormal peripheral nerve examination
5. Distracting injury
6. Intoxication

Adapted with permission of Wiley-Blackwell from Holmes et al. (5). Reprinted with the kind permission of Springer Science+Business Media from Blackmore CC, Avey GD. Imaging of the Spine in Victims of Trauma. In Medina LS, Blackmore CC (eds): Evidence-Based Imaging. New York: Springer Science+Business Media, 2006.

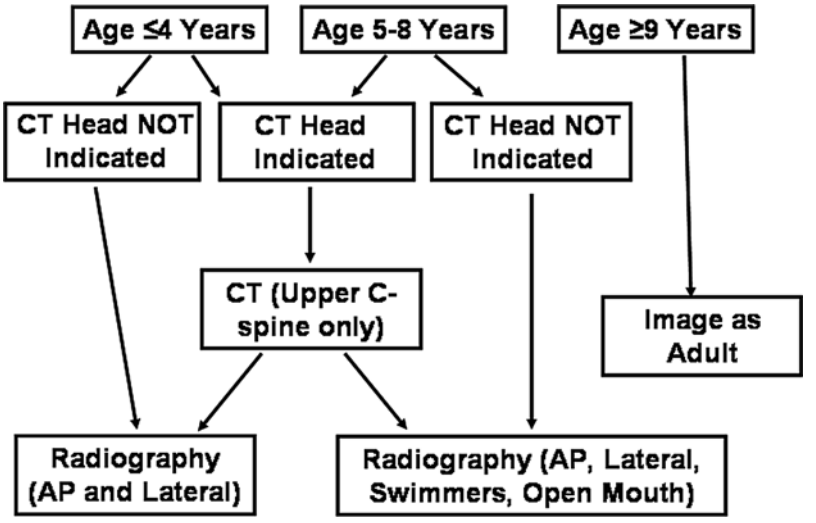

Figure 15.1. Pediatric imaging protocol for blunt trauma from Harborview Medical Center.

Imaging Case Studies

Case 1

Figure 15.2 represents a case of atlantooccipital subluxation with occipital condyle fracture in a 9-year-old boy.

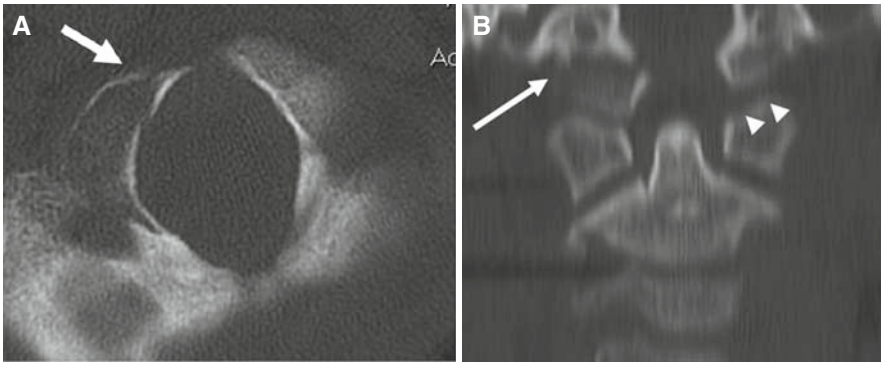

Figure 15.2. Atlantooccipital subluxation with occipital condyle fracture in a 9-year-old boy. **A:** Axial CT demonstrates right occipital condyle fracture (*arrow*). **B:** Coronal reformation demonstrates the right occipital condyle fracture (*arrow*) as well as widening at the left atlantooccipital joint (*arrowheads*).

Case 2

Figure 15.3 represents a case of spondylolysis in a 15-year-old female.

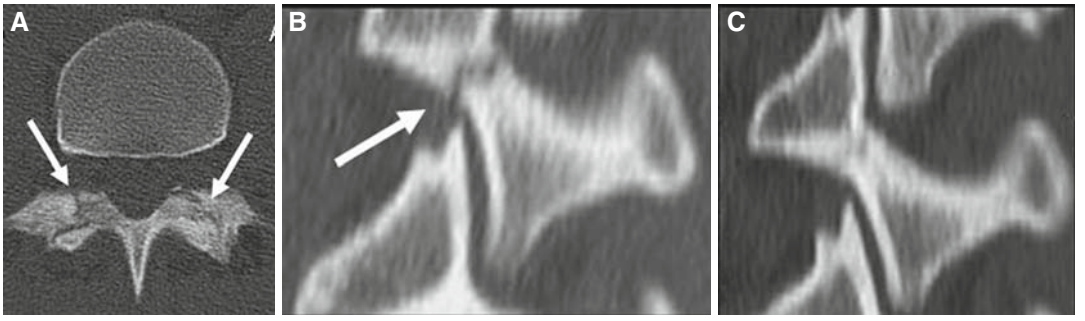

Figure 15.3. Spondylolysis in a 15-year-old female. Initial axial CT (**A**) shows irregular linear lucencies through the bilateral pars interarticularis (*arrows*). Angled thin-section oblique reformation (**B**) demonstrates smooth margins indicating an acute injury (*arrow*). Follow-up CT 4 months later reveals near-complete healing (**C**) on angled thin-section oblique reformation.

Future Research

- Development and validation of clinical prediction rules for the determination of which pediatric victims of acute trauma should undergo imaging of the cervical, thoracic, and lumbar spine.
- Development and validation of clinical prediction rules for determining who should be imaged in nontraumatic pediatric low back pain.
- Determination of the accuracy of various imaging modalities for the diagnosis, staging, and prognosis of spondylolysis.
- Development of fast MRI protocols for the evaluation and staging of spondylolysis in adolescent athletes to avoid radiation from repeated CT scanning.

References

1. Patel JC et al. J Pediatr Surg 2001; 36(2): 373–376.
2. Viccellio P et al. Pediatrics 2001; 108:E20.
3. Cirak B et al. J Pediatr Surg 2004; 39(4):607–612.
4. Kokoska E et al. J Pediatric Sur 2001; 36:100–105.
5. Holmes JF et al. Acad Emerg Med 2001; 8: 866–872.
6. Samuels LE, Kerstein MD. J Trauma 1993; 34(1): 85–89.
7. Jones GT, Macfarlane GT. Arch Dis Child 2005; 90: 312–316.
8. Rossi F, Dragoni S. Radiographics 2001; 66: 699–707.
9. Soler T, Calderon C. Am J Sports Med 2000;28: 57–62.
10. Micheli LJ, Wood R. Arch Pediatr Adolesc Med 1995; 149:15–18.
11. Standaert CJ, Herring SA. Arch Phys Med Rehabil 2007;88:537–540.
12. Ogon M.et al. Clin Orthop Related Res 2001; 390:151–162.
13. Bernstein RM,Cozen H. Am Fam Physician 2007;76: 1669–1676.
14. Szpalski M. et al. Eur Spine J 2002; 11:459–464.
15. Anderson JM, Schutt AH. Mayo Clin Proc 1980; 55(8):499–504.
16. Apple JS et al. Pediatr Radiol 1987; 17(1): 45–49.
17. Hamilton MG, Myles ST. J Neurosurg 1992; 77(5): 700–704.
18. Jeffries LJ, Milanese SF, Grimmer-Somers KA. Spine 2007; 32: 2630–2637.
19. Sjolie AN. Spine 2004;21: 2452–2457.
20. Sammer M, and Jarvik JG. Imaging of adults with low back pain in the primary care setting, in Medina LS, and Blackmore CC (eds). Evidence Based Imaging: Optimizing Imaging for Patient Care, Springer, New York, 2006.
21. Finch G, Barnes M. J Pediatric Orthop 1998; 18:811–814.
22. Stiell I et al. JAMA 2001; 286:1841–1848.
23. Hoffman J. et al. N Eng J Med 2000; 343(2): 94–99.
24. Anderson RA. et al. J Neurosurg 2006; 105: 361–364.
25. Baker C, Kadish H, Schunk JE. Am J Emerg Med 1999; 17(3):230–234.
26. Blackmore CC et al. Radiology 1999; 212(1): 117–125.
27. Buhs C et al. J Pediatr Surg 2000; 35(6):994–997.
28. Dwek JR, Chung CB. Am J Roentgenol 2000; 174(6):1617–1619.
29. Ralston ME. et al. Acad Emerg Med 2001; 8(3): 237–245.
30. Adelgais KM. et al. Acad Emerg Med 2004; 11: 228–236.
31. Blackmore CC et al. Radiology 1999; 11: 759–765.
32. Hanson JA.et al. AJR 2000; 174: 713–718.
33. National Health effects of exposure to low levels of ionizing radiation: BEIR V. 1990, Washington, DC: National Academy Press.
34. Hernandez JA, Chupik C, Swischuk LE. Emerg Radiol 2004;10(4): 176–178.
35. Keenan HT et al. Am J Roentgenol 2001; 177(6):1405–1409.
36. Holmes JF et al. J Emerg Med 2003; 24(1): 1–7.
37. Hsu JM, Joseph T, Ellis AM. Injury 2003; 34(6):426–433.
38. Turner PG, Hancock PG, Green JH. Spine 1989; 14: 812–814.
39. King HA, Tufel D. Orthop Trans 1986; 10(9–10).
40. Bhatia NN et al. J Pediatr Orthop 2008; 28: 230–233.
41. Wilne S et al. Lancet Oncol 2007; 8: 685–695.
42. Garg S, Dormans JP. J Am Acad Orthop Surg 2005; 13(6):372–381.
43. Feldman DS et al. J Pediatr Orthop 2006; 26:353–357
44. Frederickson BE et al. J Bone Joint Surg Am 1984; 66: 699–707.
45. Sassmannshausen G, Smith BG. Clin Sports Med 2002; 21(1):121–132.
46. DePalma MJ, Bhargava A. Curr Sports Med Rep 2006; 5(1):44–49.
47. Standaert CJ, Herring SA. Br J Sports Med 2000;34(6): 415–422.
48. McCleary MD, Congeni JA. Curr Sports Med Rep 2007; 6(1):62–66.
49. Waicus KM, Smith BW. Curr Sports Med Rep 2002; 1(1):52–58.
50. Congeni J, McCulloch J, Swanson K. Am J Sports Med 1997; 25(2):248–253.

51. Fujii K et al. J Bone Joint Surg Br 2004; 86: 225–231.
52. Sanpera, I. and J.L. Beguiristain-Gurpide, J Pediatr Orthop, 2006; 26:221–225.
53. Garces GL et al. Int Orthop 1999;23(4):213–215.
54. Elliott S, Hutson MA, Wastie ML. Clin Radiol 1988; 39(3): 269–272.
55. Lowe J et al. Spine 1984; 9(6):653–655.
56. Bennett DL, Nassar L, DeLano MC. Skeletal Radiol 2006; 35(7): 503–509.
57. Masci L et al. Br J Sports Med 2006;40(11): 940–946; discussion 946.
58. Udeshi UL, Reeves D. Clin Radiol 1999; 54(9): 615–619.
59. Campbell RS, Grainger AJ. Clin Radiol 1999; 54(1): 63–68.
60. Ovadia D et al. J Pediatr Orthop 2007; 27(1): 90–93.

16

Imaging for Early Assessment of Peripheral Joints in Juvenile Idiopathic Arthritis

Elka Miller and Andrea Doria

Issues

I. What is the diagnostic performance of radiography in juvenile idiopathic arthritis (JIA)?
II. What is the diagnostic performance of MRI and ultrasound (US) in JIA?
III. Can MRI and/or US (diagnostic tests) accurately detect synovial hypertrophy in JIA children?
IV. Can cross-sectional imaging modalities (MRI and/or US) accurately demonstrate evidence of cartilage degeneration?
V. Is there an association between imaging (US or/and MRI) evidence of cartilage degeneration and clinical response to treatment?
VI. What is the diagnostic accuracy of peripheral quantitative ultrasound (QUS) and peripheral computed tomography (pQCT) to detect bone changes in children with JIA?

Key Points

- Plain radiographs are the standard imaging tools for the diagnosis of JIA; however, they show low sensitivity (50%) and moderate specificity (85%) for detection of cartilage destruction (strong evidence).
- Both MRI and ultrasound (US) can detect synovial hypertrophy, cartilage erosions, and joint effusion in peripheral joints of children with JIA. Ultrasound is less sensitive than MRI for assessment of both soft tissue findings (sensitivity 62%) and superficial cartilage loss (sensitivity 60%) (moderate evidence).
- Both MRI and ultrasound can demonstrate clinically meaningful response to treatment (moderate evidence).
- Although dual-energy X-ray absorptiometry (DEXA) is the most commonly used quantitative imaging method for assessing bone mass, no standardized pediatric normative DEXA database is currently

E. Miller (✉)
Department of Radiology, The Hospital for Sick Children, Toronto, ON M5G 1X8, Canada
e-mail: elkaavimiller@gmail.com

L.S. Medina et al. (eds.), *Evidence-Based Imaging in Pediatrics*,
DOI 10.1007/978-1-4419-0922-0_16, © Springer Science+Business Media, LLC 2010

available for children under the age of 5 years and for hips and wrists of older children. Therefore, other imaging techniques such as peripheral quantitative ultrasound (QUS) and computed tomography (pQCT) have been investigated as alternative techniques to DEXA for evaluation of osteopenic changes in pediatric arthropathies. pQCT is more sensitive than QUS for evaluation of bone density changes (insufficient evidence) but has the disadvantage of using ionizing radiation.
- Overall, MRI is the imaging modality of choice for evaluation of joints in children with JIA. However, US can be an excellent initial imaging tool for evaluation of young children who otherwise would require sedation for MR imaging (moderate evidence).

Definition and Pathophysiology

Juvenile idiopathic arthritis (JIA) is a nonmigratory chronic monoarticular or polyarticular arthropathy of childhood. The diagnostic criteria for JIA include disease onset prior to the age of 16 years, presence of arthritis in one or more joints for at least 6 weeks, onset type defined by the type of disease in the first 6 months of diagnosis (Table 16.1), and exclusion of other forms of juvenile arthritis (1). It may be associated with systemic manifestations that include fever, erythematous rashes, nodules, leukocytosis and, less commonly, iridocyclitis, pleuritis, pericarditis, anemia, fatigue, and growth failure (2). At the time of presentation, other causes of inflammation should be excluded. JIA differs from the adult type of rheumatoid arthritis (RA) because of the age of presentation, its preference for large joints, tendency for generating joint contractures and muscle wasting, and its association with extra-articular manifestations (3).

Although the etiology of JIA is unknown, some believe that it is multifactorial, given the heterogeneity of presentations and course of the disease. Juvenile idiopathic arthritis is characterized by an acute synovitis that leads to synovial proliferation and formation of a highly cellular pannus (4). The pannus erodes the adjacent articular cartilage and subchondral bone, leading to centripetal articular destruction, i.e., the articular damage starts at the periphery of the joint and progresses toward its center. Despite the fact that JIA is usually transient and self-limited, without active synovitis in adulthood, up to 10% of children become severely disabled in adulthood. The disease process leads to joint instability, subluxation, and ankylosis (5–7). Disturbance of the overall joint growth can be consequent to the disease itself and/or to the treatment (8).

The classification and the terminology of JIA have been issues for disagreement in the scientific community. In the past, two major sets of criteria for diagnosis and classification of JIA were used. In North America, the American College of Rheumatology (ACR) classified the subtypes of JRA into oligoarticular (pauciarticular), polyarticular, and systemic. In Europe, the European League Against Rheumatism (EULAR) classified all childhood arthritis into pauciarticular, polyarticular or systemic, juvenile rheumatoid arthritis (positive rheumatoid factor), juvenile ankylosing spondylitis, and juvenile psoriatic arthritis. The need for a universally accepted system of classification of childhood arthritis led to the development of the International League of Associations of Rheumatologists Taskforce. A new internationally accepted classification system was established in 1997 (Table 16.1) (1, 9) and the previously used terms juvenile chronic arthritis and juvenile rheumatoid arthritis were incorporated under the term juvenile idiopathic arthritis (JIA).

Epidemiology

Juvenile idiopathic arthritis is the most common chronic musculoskeletal disease of childhood, occurring worldwide. The incidence and the prevalence of JIA range, respectively, between 5–18 and 30–150 per 100,000 children under the age of 16 in Europe and North America

(10). Twice as many girls as boys have JIA (11). Although few data are available on geographic or racial groups of JIA patients, Hanson et al. (12) studies suggest that in the United States there are proportionately fewer African-American than Caucasian children with JIA. Onset of JIA before 6 months of age is distinctly unusual; nevertheless, the age at onset is often quite young, with the highest frequency occurring between 1 and 3 years of age (13).

Radiographic changes are seen most frequently in patients with JIA who have a polyarticular course (14, 15). The presence of polyarthritis is an essential requirement for patient inclusion in controlled trials of second-line or biologic agents (16, 17).

Large joints are most commonly affected in this disease. The knee is the most frequently affected joint followed by the ankle. Occasionally children may develop changes in the cervical spine or temporomandibular joint (8). It has been suggested that patients with JIA with polyarthritis and wrist disease are at high risk of experiencing radiographic progression (18). The wrist is the most vulnerable site for early radiographic changes in patients with JIA (15, 19).

Overall Cost to Society

Limited data are currently available in the medical literature on the overall cost to the society of clinical follow-up of JIA patients with MRI. A recent systematic review on the economic burden of rheumatoid arthritis in adults (20) showed that the economic impact of this disease is substantial as determined by all 14 studies reviewed. Average annual medical costs were reported to range from US $5,720 to US $5,822. Medication constituted between 8% and 24% of total medical costs, physician visits between 8 and 21%, and in-patient stays between 17 and 88%. No information about costs related to imaging for diagnosis or follow-up of rheumatoid arthritis was however available in this review. Bernatsky et al. (21) reported that the total difference in annualized average direct medical costs for children with JIA vs controls (asthmatic children) was CND $1,686 (95% confidence interval, $875, $2,500). JIA subjects had substantially higher costs compared to controls concerning medication use, visits to specialists and allied health-care professionals, and diagnostic tests. With specific regard to diagnostic tests (including imaging, laboratory, and pulmonary function testing), the total difference in annualized average costs was CND $170 (95% confidence interval, $97, $244), approximately 10% of the total direct medical costs. In spite of the relatively small percentage of costs for diagnostic tests in comparison to the total costs in the management of JIA as noted in a single study (21) (insufficient evidence), repeated imaging has the potential to have an economic impact on the follow-up of JIA patients.

Clinical and Laboratory Predictors

The clinical and laboratory tests that are currently available for assessment of JIA are poor for characterization of early inflammatory, hypoxic, and vascular changes, which are the primary physiologic events involved in the disease.

Radiography is the traditional standard for assessment of established joint damage including soft tissue changes, bone erosions, joint space narrowing, joint subluxation, misalignment, or ankylosis. However, so far no single laboratory or imaging marker has adequately reflected the spectrum of events involved in the process of inflammatory arthritis.

Goals

The goals of imaging in children with suspected or confirmed JIA are to (a) exclude alternative diagnoses although this may be challenging, given the poor specificity of findings (Table 16.2); (b) document initial and progressive disease in the joints; (c) determine treatment effects by showing relative changes in joint appearance over time; and (d) detect potential complications of the disease or the therapy (22).

Conventional radiography remains the standard practice imaging modality for evaluation of disease progression in JIA (22). However, only indirect signs of synovial inflammation and cartilage degeneration can be identified with this imaging modality and are detected only in late stages of the disease (23).

In this chapter we will focus on the role of conventional ultrasound (US) and MRI but will

also comment on the potential role of quantitative ultrasound (QUS) and peripheral quantitative computed tomography (pQCT) for evaluation of bony density changes in osteoporotic patients.

Methodology[1]

An electronic search of the literature was performed by the authors who identified studies relevant to the diagnostic accuracy of cross-sectional imaging (US, CT, and MRI) for assessment of JIA. The MEDLINE (January 1966 to April 2007), the EMBASE (January 1980 to April 2007), the DARE database of the National Health Service Center for Reviews and Dissemination (1st quarter 2007), and the Cochrane Library databases (1st quarter 2007) were searched through OVID by using a validated search strategy.

The following articles were excluded: (I) imaging considered as the reference standard measure for assessment of the diagnostic accuracy of radiographic or clinical findings; (II) case reports and case series, surveys, pictorial essay, comments, cost evaluations, decision analysis models and review papers; (III) studies that reported axial joint disease (sacroiliac joint or temporomandibular joint); (IV) papers written in languages other than English, French, German, Italian, Spanish, and Portuguese.

We applied the QUADAS (*quality assessment of studies of diagnostic accuracy included in systematic reviews*) guidelines for assessment of the selected articles in diagnostic accuracy (24).

Discussion of Issues

I. What Is the Diagnostic Performance of Radiography in JIA?

Summary of Evidence: The diagnosis of JIA is clinically based. Radiographs are used for baseline and follow-up assessment of the joint involvement and its progression. It allows exclusion of other disorders such as fractures, tumors, and congenital disorders that can produce symptoms similar to JIA at presentation. However, plain radiographs are usually insensitive to the early changes of the disease.

Supporting Evidence: Radiography has advantages over MRI, which include its low cost, widespread availability, helpfulness in differential diagnosis, reasonable reproducibility, and validated assessment methods. Nevertheless, radiography is not sensitive (sensitivity 50%; strong evidence, Table 16.3 in detecting early cartilage deterioration) as compared with MRI (reference standard measure). It is fairly specific (specificity, 85%; strong evidence, Table 16.3) for diagnosis of osteochondral abnormalities (Table 16.3), provides projectional superimposition, and uses ionizing radiation (25).

II. What Is the Diagnostic Performance of US and MRI in JIA?

Summary of Evidence: The use of cross-sectional imaging such as US and unenhanced MRI in the initial diagnostic evaluation of JIA holds the potential for improved diagnostic accuracy. US and unenhanced MRI are fairly sensitive in assessing the morphologic status of soft tissues, cartilage, and subchondral bone compared to the gold standard for imaging, contrast-enhanced MRI (moderate evidence) (Tables 16.4 and 16.5).

US has the potential for more accurate assessment of synovial thickness changes over time in JIA knees as compared with clinical follow-up (moderate evidence) (Tables 16.6 and 16.7).

Supporting Evidence

Ultrasound

Ultrasound is safe, relatively inexpensive, noninvasive, dynamic, and does not use ionizing radiation. It also has the benefit of not requiring sedation in children. However, US has reduced reliability compared to MRI because it can visualize only the peripheral cartilage and it is operator dependent with regard to the imaging acquisition and interpretation (26).

[1] This section is adapted with permission from Miller E, Roposch A, Uleryk E, Doria AS. Juvenile idiopathic arthritis of peripheral joints: Quality of reporting of diagnostic accuracy of conventional MRI. Acad Radiol 2009;16 (6):739–757.

This fact is particularly important for less common applications of US such as musculoskeletal evaluations. In addition, there is lack of standardization of ultrasound techniques for assessment of growing joints in the literature and this imaging technique is unable to visualize the central aspect of the joint if high-resolution transducers are employed.

Data on the diagnostic accuracy of US in children with JIA are limited. Assessment of joint effusion, synovial hypertrophy, and cartilage erosions by ultrasound can provide information about the severity of the disease. Ultrasound can differentiate between joint effusion and synovial hypertrophy (22), the latter appearing as a hypoechoic irregular thickening of the synovial membrane. Erosions and focal or diffuse thinning of the articular cartilage can also be detected, however only peripherally in the joint. Color Doppler ultrasound enables the detection of perisynovial hyperemia. Studies in children (27, 28) have demonstrated the ability of color and power Doppler sonography, with or without intravenous injection of contrast agents, to estimate synovial activity in JIA. Resistive indices and fraction of color pixels may be used as quantitative measurements of the blood flow (29). Specifically, contrast-enhanced sonography holds potential for detection of active synovial inflammatory disease in subclinical JIA patients guiding early treatment (27).

The number of studies on diagnostic accuracy of US for assessment of JIA available in the literature is limited (n=8 in this systematic review). There is very limited information in our review (a single study, small sample size) about the diagnostic performance of US as compared with MRI (sensitivity for joint effusion 62% and for superficial cartilage destruction 60%) (moderate evidence) (Table 16.4). Most studies that used US for assessment of JIA in the literature were limited to the evaluation of the knee and hip joints (27, 28, 30–34) (moderate evidence); however, US can also be used for assessment of smaller joints such as hands (35). Note is made that previous studies (36) demonstrated the value of evaluating wrists and hands in JIA children since loss of flexion of the wrists and radial deviation in the metacarpophalangeal joints are more frequent in children than in adults with rheumatoid arthritis.

MRI

MRI plays an important role in assessing the presence or the absence of synovitis, in establishing the extent of the disease in a given joint, and in assessing outcomes either at a given timepoint or repeatedly over time. Contrast-enhanced MRI is a sensitive imaging tool for evaluation of JIA (expert opinion), demonstrating synovial hypertrophy and cartilage degeneration which can only be indirectly evaluated by plain radiography (37). In this review, only two papers (38, 39) compared MRI with a reference standard measure (arthroscopy) for assessment of the diagnostic performance of MRI in JIA (criterion validity). In one paper (38), the authors mentioned a single true-positive case (1 out of 30 patients [3%]) in which arthroscopy confirmed femoral and tibial cartilage thinning. In the other papers (39), the authors reported 1 out of 21 cases (5%) that represented a true-negative result upon comparison with arthroscopy, another single case (5%) that represented a false-positive result (the partial anterior cruciate ligament tear depicted on MRI was not seen at arthroscopy), and a third single case (5%) that represented a false-negative result (the lateral meniscus tear seen at arthroscopy was not depicted by MRI). In these two studies, the limited sample size in which the diagnostic performance of MRI could be assessed precludes a formal calculation of diagnostic performance indices. Gylys-Morin et al.'s study (38), however, demonstrated a suboptimal ability of MRI to discriminate between patients with JIA and control subjects as the area under the curve of receiver operating characteristic curves representing the accuracy of MRI as a discriminative index was 0.60 (95% CI: 0.47–0.73, p=0.07).

Unenhanced MRI, however, holds suboptimal to borderline sensitivity (73% joint effusion; 50–80% deep cartilage involvement) for diagnosis of peripheral JIA joints (moderate evidence, poor sample size) (Table 16.5).

MRI has two main limitations: the long time for imaging acquisition, requiring sedation in young children, and the restricted coverage of the body if dedicated extremity coils are used, which can be a limiting factor when there is clinical involvement of more than one joint.

III. Can US and/or MRI (Diagnostic Tests) Accurately Detect Synovial Hypertrophy in JIA Children?

Summary of Evidence: Both diagnostic tests are accurate imaging tools for detection of synovial hypertrophy in the peripheral large (knees, ankles, elbows, and hips) and small (hands/wrists and feet) joints of children with JIA (moderate evidence for US and MRI) (Tables 16.8 and 16.9).

Supporting Evidence

Ultrasound

Most of the information on the accuracy of US for assessment of synovial hypertrophy in JIA was obtained from studies in knees. Ultrasound can be applied as an objective method for detection of synovial thickness, being able to demonstrate either regular or irregular thickening of the synovial membrane (Table 16.6). Thickness of the synovial membrane of knees > 5 mm on US is suggestive of active disease (27, 30–32) (moderate evidence). Ultrasound can also be used to evaluate the disease course during therapy. Sureda et al. (30) reported synovial hypertrophy during follow-up in 17 of 48 joints (35%) of JIA patients in clinical remission (mean synovial thickness, 4.5 ± 1.6; range, 1.8–8.3 mm). In this study (30), no significant differences in synovial thickness were noted between patients with clinically active disease and those in clinical remission, but there were statistically significant differences ($p<0.001$) in the thickness of the synovial membrane of control subjects and of patients of two JIA groups (active and inactive disease). Gray-scale results of Doria et al. (27) corroborated Sureda et al. (30) results with regard to maximum synovial thickness of knees when symptomatic and asymptomatic subgroups of JIA patients were compared. Furthermore, Doria et al. (27) showed that the maximum synovial membrane thickness of patients with asymptomatic joints but with laboratory evidence of active disease was significantly greater than the maximum synovial membrane thickness of control subjects ($p=0.002$) (moderate evidence).

Color and power Doppler ultrasound can help in the evaluation of the vascularity of the synovial/perisynovial tissues. This topic was explored by three studies that used unenhanced sonography (28, 34, 35) and by one contrast-enhanced sonography study (27) that demonstrated increased number of synovial vessels representing increased pannus vascularity in active JIA patients (moderate evidence). The possibility of using microbubble-based contrast-enhanced color Doppler ultrasound for evaluation of synovial changes in JIA was previously investigated (27). The authors of this study reported significant differences in peak contrast enhancement [(mean pixel intensity values at maximum contrast enhancement–unenhanced mean pixel values)/unenhanced mean pixel values] in children with active ($p=0.004$) and subclinical ($p=0.0001$) JIA, but not in asymptomatic JIA patients ($p=0.06$) and control subjects ($p=0.25$). Patients with clinically asymptomatic disease but with serum chemistry levels of active disease can benefit from identification of subclinical disease with contrast-enhanced sonography (limited evidence). Currently, microbubble agents are used in the clinical setting mainly for cardiac imaging diagnosis and they are not approved for other uses in the United States. According to a recent FDA report (40), the diagnostic information that can be provided by using Definity (Perflutren Lipid Microsphere) or Optison (Perflutren Protein-Type A Microspheres for Injection) may, in certain situations, justify the risk for serious cardiopulmonary reactions, even in those patients at high risk for these reactions and in some patients for whom the use of these products was contraindicated. Nevertheless, patients with pulmonary hypertension or unstable cardiopulmonary conditions must be closely monitored during and for at least 30 min postadministration of these microbubble contrast agents.

Few studies in the literature have correlated changes in synovial thickness of JIA patients over time with their corresponding clinical outcome (28, 30, 33) (Table 16.7). The results of these studies demonstrated that upon clinical improvement over time, the synovial thickness measurements tended to reduce in the interim (moderate evidence).

MRI

MRI is an excellent tool for detection of synovial hypertrophy (pannus) and joint

effusions (moderate evidence). In unenhanced MR imaging, fast spin-echo (FSE) with heavily T2-weighted sequences allow excellent contrast between the hyperintense joint effusions and the hypointense pannus (22, 41). Fat-suppressed, T1-weighted sequences provide good discrimination between pannus and joint effusion (42, 43).

Use of Intravenous Contrast Material

Pannus can enhance after intravenous contrast administration depending on the inflammatory status of the joint. The use of intravenous contrast material helps to differentiate between fluid and synovial thickening since pannus exhibits rapid contrast enhancement (44–50) (moderate evidence). At this point, however, there is insufficient evidence to support the assumption that quantitative enhancement of synovium in patients with known JIA can grade the level of disease activity, suggest the JIA subtype, or predict synovial changes over time after treatment (47, 51, 52) (insufficient evidence).

With regard to challenges of the clinical use of gadolinium, we should note that only joints that are imaged immediately or soon after the injection will benefit from the qualitative assessment that results from the use of contrast. Previous studies have recommended that imaging acquisition should occur within 5 min after contrast material administration to capture peak synovial enhancement and prevent volume overestimation due to contrast material diffusion into the joint space. Delays in imaging compromise the differentiation of synovium from joint fluid (38, 53, 54). If multiple joints are being imaged at a given time in polyarticular JIA patients, the assessment of contrast-enhanced soft tissues in secondary joints (evaluated after scanning the primary joint) may not be an accurate measure of their inflammatory status.

Radiologists should also be aware of potential gadolinium–DTPA-related reactions in patients with impaired renal function such us the development of nephrogenic systemic fibrosis (55).

Synovial Thickness and Volume Measures

Synovial thickness $\geq$3 mm is a sensitive and specific MRI criterion for active synovitis in knees of JIA patients (38). Changes in synovial thickness over time on MRI correlate with clinical progression or improvement of inflammation in the joint (51, 56) (moderate evidence). Gardner-Medwin et al. (57) evaluated MRI examinations of clinically unaffected joints in 10 children with oligoarthritis within 4 months of presentation. Four of these children (40%) developed arthritis in other joints over a median of 4 (range 3–6) months after the MRI scan. Three out of these four children (75%) developed clinical features in the previously normal knee 4–11 months after MRI. Four other children had a persistent monoarthropathy. All four had normal MRI. Two children had reactive arthritis. The authors concluded that MRI can distinguish between patients with persistent monoarthritis and those who developed further clinical arthritis up to 1 year later.

Previous studies in JIA showed that measures of synovial volume obtained after the administration of gadolinium correlate well with synovial thickness measurements and with the degree of clinical swelling of the joints (38, 46, 47) (moderate evidence). These results are supported by the results of studies in adult RA, in which MRI-determined synovial membrane volumes were shown to be closely related to the rate of progressive joint destruction and to be valuable as markers of joint disease activity and predictors of progressive joint destruction (58). Although this information is not available in JIA, studies in adult RA demonstrated that MRI-determined synovial volumes correlated moderately (Spearman's sigma, 0.55, $p<0.001$) with the overall histologic assessment of synovial inflammation (59). The main limitations of synovial volumetric measurements are the long postprocessing time required for data analysis and the potential inter- and intraobserver variability that may be present in manual analyses. Computerized measurement of magnetic resonance imaging joint volumes in adult RA, however, demonstrates excellent intraobserver reliability and interoccasion reliability (60).

IV. Can Cross-Sectional Imaging Modalities (US and/or MRI) Accurately Demonstrate Evidence of Cartilage Degeneration?

Summary of Evidence: Both MRI and US are able to demonstrate cartilage abnormalities (moderate evidence) (Tables 16.8 and 16.9). US can

detect thinning or blurring of the margins of the articular cartilage (moderate evidence). The use of ultrasound to assess smaller joints such as wrist, hands, and feet, which are initially affected in JIA, should be further investigated.

Although previous studies have used contrast-enhanced MRI as the reference standard measure for detection of cartilage abnormalities with unenhanced MRI (38, 44, 56, 61), to our knowledge, no previous studies have evaluated the range of normal thickness of the articular cartilage in joints of children of different age groups. This lack of information in the literature limits the specificity of diffuse thinning of cartilage in joints of JIA children of different ages.

Supporting Evidence: There are differences in the cartilage of children and adults. In adults, the cartilage of the articular surface is avascular, protecting the underlying bone from inflammation. This anatomic characteristic results in the development of the typical marginal erosions of RA. In children, the ossification of the skeleton is closely related to the vascularity of the epiphyseal and physeal cartilage. The unossified epiphysis and the very immature physis are supplied by nonanastomotic vessels that run within canals (62). As a result, when an inflammatory process involves immature joints, increased vascularity takes place in the epiphyseal cartilage (22, 35, 38) (moderate evidence).

Detection of cartilage changes with MRI tends to be more reliable in older children than in younger children (63) because of the presence of immature growth cartilage in joints of younger children (64), which makes the distinction between cartilage abnormalities and normal growth changes problematic in some cases. No previous studies have evaluated the range of normal thickness of the articular cartilage in joints of children of different age groups either with MRI or US. This lack of information in the literature makes difficult the assessment of diffuse thinning of cartilage in joints of JIA children of different ages.

Barnewolt et al. (62) evaluated gadolinium-enhanced MR images of 80 normal epiphyses in 48 neonates, infants, and children and reported that gadolinium enhancement allowed differentiation between physeal and epiphyseal cartilage and revealed epiphyseal vascular canals. Enhancement proved to be greater in the physeal than in the epiphyseal cartilage ($p< 0.001$). In the unossified epiphysis, the vascular canals were mainly parallel. After the development of the secondary ossification center, these canals tended to present with a radial pattern ($p<0.0001$). Also, physeal enhancement decreased with physeal closure. This study also confirms the normal tendency for thinning of the articular cartilage with maturity.

Ultrasound

The appearance of the normal articular cartilage on US is of a hypoechoic band that presents with sharp margins. The involvement of the articular cartilage by JIA can be appreciated by thinning or blurring of the joint margins, depending on the stage of the disease. Limitations on the use of US for evaluation of the cartilage include the impossibility for assessing the entire joint (peripheral and central aspects) with high-resolution transducers and the difficulty in obtaining reproducible measurements of cartilage thickness, given differences in measurements according to the degree of obliquity of the joints during imaging acquisition.

Abnormalities of cartilage were reported in several studies on JIA. Sureda et al. (30) reported blurring of the margins in 36 of the 56 (64%) cases of clinically active knee involvement and in 15 of 48 (31%) cases of remission. Cellerini et al. (33) reported abnormalities of the articular cartilage such as irregular and blurred edges in 5 of 49 (10%) knee joints. Shahim et al. (28) reported a significant negative correlation (r=–0.45, $p<0.05$) between cartilage thickness in knee joints and disease duration. In the study by Barbuti et al. (32), the articular cartilage outline appeared blurred in 36% of patients with active knee disease. Finally, Karmazyn et al. (35) reported signs of articular destruction (bone erosions or cartilage thinning) in 25 of 200 (13%) metacarpophalangeal joints of JIA patients (moderate evidence). In none of three studies was a significant difference in the thickness of the knee cartilage noted between JIA patients and controls (30, 32, 33) (moderate evidence). Nevertheless, differences in the sharpness of the cartilage were noted between JIA joints in remission and controls (30, 33).

Further investigation is required to determine the normal thickness of the cartilage in healthy

children of different ages using a standardized ultrasound protocol for acquisition of measurements (65) at given degrees of flexion of the joints. Without this information, it will be challenging to evaluate the presence of diffuse thinning of the articular cartilage in JIA joints in future clinical trials.

MRI

In comparison with US, MRI has the advantage of providing higher contrast resolution for visualization of the cartilage, with the ability of demonstrating the entire extension of the articular cartilage in different planes and of differentiating epiphyseal, physeal, and articular cartilage in young children (62). Superficial or deep, peripheral or central cartilaginous lesions are well visualized with MRI (38, 44, 50, 51, 56, 61, 66, 67) (moderate evidence).

The administration of intravenous MR contrast material may enable the identification of striated or linear enhancement of the cartilage. This characteristic enhancement can either represent a normal pattern of vessels or relate reactive hyperemia to the adjacent soft tissue inflammation (62). Recognizing normal patterns of cartilage on contrast-enhanced MRI may avoid false-positive interpretations of MRI examinations. Previous studies (44, 56, 66) showed that the use of gadolinium facilitates the evaluation of cartilage thickness and erosion in acute and subacute JIA, but it is unlikely to add any information to the unenhanced status of the cartilage in chronic or advance disease (61) (moderate evidence).

Morphologic evidence of cartilage destruction is best investigated with intermediate-weighted, fast spin-echo and 3D gradient-echo (MPGR), fat-saturated sequences (moderate evidence) (38, 47, 51, 57). Recent studies support the hypothesis that regional variation in cartilage water concentration and collagen orientation generates differences in mobility of water in the cartilage, which can be measured with T2 relaxation time maps (functional MRI). Kight et al. (67) compared T2 map values of the distal femoral weight-bearing cartilage between 18 girls with JIA and controls and reported that the average of T2 relaxation times was significantly higher in girls with JIA, which may reflect cartilage microstructure differences that occur in JIA.

Two articles (44, 56) reported an association between severity of clinical pain in the joint and degree of cartilage destruction on MRI [$p<0.05$ (37)] (moderate evidence) (Table 16.9).

V. Is There an Association Between Imaging (US or/and MRI) Evidence of Cartilage Degeneration and Clinical Response to Treatment?

Summary of Evidence: Although imaging can be used to monitor the anatomic status of cartilage during and after treatment, there is insufficient evidence that MRI and/or US can predict the future status of the cartilage after the use of therapeutic agents (insufficient evidence) (Tables 16.8 and 16.9).

Supporting Evidence

Ultrasound

Imaging is able to evaluate the response to treatment by measuring synovial thickness (hypertrophy) and to determine the optimal location and route for topical steroid injection. However, few articles have evaluated the effect of treatment on the cartilage from the imaging perspective. Sureda et al. (30) reported that 2 out of 16 (12.5%) patients had marked clinical improvement with corresponding decrease in cartilage thickness (insufficient evidence).

MRI

Three out of 18 (17%) studies that used MRI for assessment of JIA in our review evaluated the effect of treatment. Of them, two out of three (67%) studies used intraarticular steroid injection and one (33%) used conservative medical treatment. In one study (45), the joints of 21 consecutive JIA patients who did not respond to nonsteroidal anti-inflammatory treatment underwent intraarticular corticosteroid injection in the knee, ankle, and elbow joints. In 12 out of 21 (57%) patients who had a follow-up MRI performed 13 months after treatment, no new anatomic abnormalities since the pretreatment MRI were found at the follow-up MRI and the cartilage integrity appeared well preserved. Another study (66) that used intraarticular steroids to treat JIA knees and hips in 10 patients (15 joints) with JIA reported that 1 out of 10 (10%) patients had replacement

of the articular cartilage by enhancing pannus with almost complete resolution of cartilage changes posttreatment. The authors of this study assumed that the cartilage changes represented infiltration rather than cartilage destruction. Cakmakci et al. (51) assessed the cartilage status of joints in 21 JIA patients after medical treatment and reported that 2 out of 18 (11%) knees showed a decrease in the number of cartilage lesions on the 3–6-month follow-up MRI (Table 16.9) (insufficient evidence). In this study, MRI scores devised by the authors showed progression in eight knees, while clinical assessment demonstrated equivalence in seven knees and progression in one knee of corresponding patients. Although an MRI scoring system has been developed and validated for assessment of rheumatoid arthritis in adults, no such scoring system has been validated for use in children. There was moderate to strong correlation between clinical and MRI scores according to progression, with improvement and equivalent findings of 0.5 and 0.7 in 1–3 months and 3–6 months, respectively. In the group of patients whose MRI examinations demonstrated interval progression between 0 and 3 months, increased synovial hypertrophy (n=1 knee), synovial effusion (n=5), cartilage lesions (n=3), and epiphyseal lesions (n=2) were identified. Further MRI research using the adult RA cartilage scoring system in JIA children may help to define the role of MRI.

VI. What Is the Diagnostic Accuracy of Peripheral Quantitative Ultrasound (QUS) and Peripheral Computed Tomography (pQCT) to Detect Bone Changes in Children with JIA?

Summary of Evidence: Reduced bone mineral density (BMD), changes in bone geometry, and decrease in muscular bulk are well-recognized findings in children and adolescents with JIA, and occur either as a result of the disease itself or in response to prolonged systemic corticosteroid therapy (disease treatment). Although dual-energy X-ray absorptiometry (DEXA) remains the most commonly used imaging technique for assessing bone mass in children, no standardized pediatric normative DEXA database is currently available for children under the age of 5 years and for hips and wrists of older children. Therefore, other imaging techniques have been investigated as alternative methods *to detect bone changes in children with JIA.* Peripheral quantitative computed tomography (pQCT) seems to be accurate for discrimination between cortical and trabecular bone (insufficient evidence). Further studies are required to improve our understanding of the value of quantitative ultrasound (QUS) in the assessment of JIA joints (insufficient evidence) (Table 16.10).

Supporting Evidence: Bony alterations in joints of children with JIA involve both juxtaarticular and generalized osteopenia. Juxtaarticular osteopenia usually occurs in the early stages of JIA and is secondary to the local inflammatory hyperemia with direct effect on the subchondral bone. Diffuse osteopenia reflects chronicity and it is typically associated with the reduced volume of the surrounding soft tissues and muscles (68).

Dual-Energy X-ray Absorptiometry (DEXA)

In contrast to available information in adults, no generally accepted definitions for osteoporosis and osteopenia are currently available for children, and a *Z* score (obtained with comparison to age- and sex-matched controls) is used. Several imaging methods are currently available for diagnosis of osteoporosis in children and adolescents (69).

Dual-energy X-ray absorptiometry (DEXA), peripheral quantitative computed tomography (pQCT), and bone ultrasound are imaging techniques used to evaluate the bone mineral content. The goal of these modalities is to measure the bone mineral content (BMC) in children in order to quantify the deficits in bone mineral associated with the various disorders that cause osteopenia in children.

Currently, the most commonly used quantitative radiologic method for assessing bone mass is DEXA. DEXA has several advantages, such as fast scanning, low cost, low radiation dose, and applicability to clinically relevant sites of osteoporotic fracture. However, DEXA provides two-dimensional imaging of 3D objects, does not distinguish between trabecular and cortical bone (70), and is size dependent (a potential

problem in growing children). A further drawback is that in vivo bone strength is related to bone quality as well as to bone density (71–73). Finally, no standardized pediatric normative DEXA database is currently available for children under the age of 5 years and for hips and wrists of older children. For older children, the control standard measures used for comparison of measurements of the bone mineral density of the spine vary according to standards predefined by different DEXA units' manufacturers. Also, there are insufficient supportive data on correlations between this technique and clinical outcome of different pathological process (69, 74–76), most likely due to the heterogeneity of pathologic processes in which osteopenia can be present in pediatric musculoskeletal disorders.

Quantitative Ultrasound (QUS)

Quantitative ultrasound is a radiation-free imaging technique that measures the transmission of US waves through bone and has been proposed for assessment of bone density (77, 78). Only three clinical trials using this technique in JIA were found in the literature (Table 16.10) (insufficient evidence). Two studies (66.7%) (69, 70) reported promising results. One of them (79) compared the broadband US attenuation (BUA) by bone in the left calcaneus in 67 children with chronic rheumatic diseases, 46 of them with JIA. At baseline, mean BUA values and *Z* scores were significantly lower in the patient group than in controls: 41.84 ± 21.64 vs 61.69 ± 17.42 dB/MHz ($p<0.001$); *Z* score -0.91 ± 1.07 vs 0.09 ± 0.62 in controls ($p<0.001$). At 1-year follow-up, BUA values in the patient group were significantly increased compared to baseline values (BUA 46.43 ± 21.51 dB/MHz; $p=0.002$). No significant differences were found in *Z* scores. The authors concluded that US bone analysis at the calcaneus is a useful tool in the assessment and monitoring of bone status in children with chronic rheumatic diseases.

The second study (80) compared QUS at midtibia to DEXA in assessing generalized osteoporosis in 22 patients with JIA. Spine and total body BMD measured by DEXA correlated significantly with the tibia speed of sound (SOS) (spine: $r = 0.57$, $p<0.007$; total body: $r = 0.68$, $p<0.001$). The mean spine BMD was lower in JIA patients compared to normal ranges (mean *Z* score of –1.19). BMD *Z* scores were negatively associated with disease duration. Patients receiving systemic steroids were associated with lower *Z* scores.

In the study with negative results (81), the authors measured phalangeal bone US in 49 children with JIA (oligoarticular, polyarticular, and systemic). No significant deficits were noted in the amplitude-dependent speed of an ultrasound signal (Ad-SOS) of JIA patients compared to the SOS of the reference population. The finger width was reduced only in patients with polyarticular JIA. There was significant correlation between the Ad-SOS and the finger width ($r=0.233$, $p=0.012$), but no significant correlation between the standard deviation score of the Ad-SOS and the standard deviation score of the finger width ($r=-0.060$, $p=0.084$). The authors concluded that phalangeal US was strongly dependent on bone size (insufficient evidence).

Peripheral Quantitative Computed Tomography (pQCT)

Peripheral quantitative computed tomography (pQCT) is another technique for assessment of bone, which allows for three-dimensional measurements of appendicular bones such as tibia and radius. This technique uses a low-energy (38 keV) X-ray tube and the effective radiation dose is approximately 0.2 μSv from a radiation source of 45 kV at 150 μA (82, 83). pQCT measures volumetric BMD and is not influenced by bone size. It allows separate analysis of cortical and trabecular bone and determination of bone's geometric parameters such as cortical area and thickness, as well as muscle cross-sectional area (84).

Roth et al. (82) evaluated the musculoskeletal system in 57 children with JIA and reported that children in all subgroups of JIA presented with significantly reduced muscle cross-sectional area, which was strongly correlated with muscle force and abnormalities in geometric parameters of bone, including a significant reduction in cortical thickness. Trabecular density was affected only in the polyarticular JIA group, and cortical density was normal in all subgroups. The thinned bony cortices might predispose to fractures even though cortical bone density itself is normal.

Bechtold et al. (85) used pQCT to evaluate the forearm bone mass, density, and geometry

as well as the forearm muscle in 17 patients with JIA receiving treatment with growth hormone (GH) for 3.8 ± 1.1 years compared with an untreated age- and sex-matched control group ($n = 17$). Compared with untreated JIA patients, GH-treated JIA patients had significant higher bone mineral content as well as total cross-sectional area (CSA), cortical CSA, and muscle CSA. A significant difference between groups for height-corrected cortical and muscle areas was seen only in male patients. Cortical CSA relative to muscle CSA was not different between groups. These findings were compatible with an anabolic effect of GH on muscle and bone development (insufficient evidence).

Take Home Figures and Tables

Figure 16.1 is an algorithm for investigation of monoarticular juvenile idiopathic arthritis joints

Tables 16.1 to 16.10 discuss classification system of juvenile idiopathic arthritis, imaging mimics of JRA, performance of conventional radiographs, performance of ultrasound, performance of unenhanced MRI, ultrasound measurements of synovial thickness at the level of the suprapatellar bursa, correlation of clinical and sonographic outcomes, levels of evidence of diagnostic accuracy for ultrasound, MRI, QUS, and evidence-based strength of recommendations, respectively.

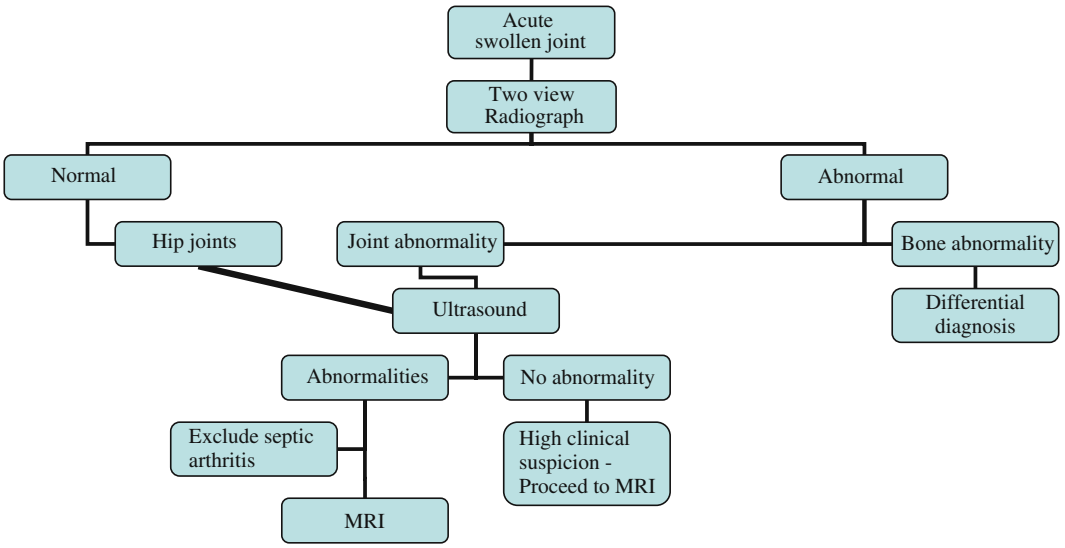

Figure 16.1. Algorithm for investigation of monoarticular juvenile idiopathic arthritis joints. Because small hip joint effusions are easily missed on radiography, ultrasound is indicated in case of clinical suspicion of arthritis. Indications for ultrasound evaluation in other joints (hands/wrists, knees, ankles, elbows) include assessment of effusion in large joints and synovitis in small joints. Because the value of ultrasound to assess articular cartilage in JIA has not been fully assessed, in case of clinical suspicion of cartilage damage, an MRI is recommended. Once the diagnostic performance of both ultrasound and contrast-enhanced MRI are further investigated, one will be able to decide which imaging modality is more accurate for diagnosis of synovial and osteochondral abnormalities in JIA patients who do not respond well to therapy. Currently, centers with expertise in both ultrasound and MRI tend to use MRI for assessment of large and small joints in JIA patients who are unlikely to need sedation and ultrasound for younger patients. Once ultrasound acquisition protocols and scales for assessment of joints are validated for use in children, and the value of this imaging modality for evaluation of cartilage is objectively determined, ultrasound may become part of the routine follow-up of unresponsive JIA patients. (Adapted with permission of Elsevier from Cohen PA, Job-Deslandre CH, Lalande G, Adamsbaum C. Overview of the radiology of juvenile idiopathic arthritis (JIA). Eur J Radiol 2000; 33: 94–101.).

Table 16.1. International league against rheumatism (ILAR) classification system of juvenile idiopathic arthritis

Classification of juvenile idiopathic arthritis (Durban, 1997)
Onset <16 years Duration: 6 weeks Subtypes: 1. Systemic arthritis 2. Oligoarthritis Persistent Extended 3. Polyarthritis (rheumatoid factor negative) 4. Polyarthritis (rheumatoid factor positive) 5. Psoriatic arthritis 6. Enthesitis-related arthritis 7. Other a. Does not meet criteria for any of categories 1–6 b. Meets criteria for more than one of categories 1–6

Table 16.2. Imaging mimics of JRA

Imaging finding	Differential diagnosis	
Joint effusion	Traumatic synovitis; infectious/septic arthritis; hemophilic arthropathy; acute transient synovitis	Acute rheumatic fever; intraarticular osteoid osteoma; connective tissue disorders
Soft tissue swelling	Infectious/septic arthritis; hemophilic arthropathy; diabetic cheiroarthropathy; NOMID; sarcoid	Synovial hemangioma; PVNS; CAP syndrome; spondyloarthropathies
Osteoporosis	Juvenile osteoporosis; multifocal osteolysis; leukemia; collagen vascular disease	Hemophilic arthropathy; infectious arthritis
Joint space loss	Traumatic joint dislocation; septic arthritis; hemophilic arthropathy; avascular necrosis; Kniest dysplasia; idiopathic chondrolysis	Progressive pseudorheumatoid chondrodysplasia; slipped femoral capital epiphyses; osteoid osteoma
Ankylosis	Spondyloarthropathies; traumatic arthritis; infectious arthritis	Iatrogenic
Bony erosions	Hemophilic arthropathy; septic arthritis; spondyloarthropathies; synovial osteochondromatosis	Carpal osteolysis; CAP syndrome; PVNS
Periostitis	Trauma including abuse; osteomyelitis; spondyloarthropathies; osteoid osteoma	Goldbloom's syndrome; hypertrophic osteoarthropathy; leukemia; sickle-cell dactylitis
Growth disturbances; epiphyseal overgrowth	Hemophilic arthropathy; trauma; tuberculous/fungal arthropathy; spondyloarthropathies	NOMID; Legg–Perthes disease; skeletal dysplasias; Turner syndrome
Growth arrest	Turner syndrome; frostbite damage	
Dysplastic changes	CAP syndrome; mucopolysaccharidosis; mucolipidosis	Kniest dysplasia

PVNS = pigmented villonodular synovitis, CAP = camptodactyly–arthropathy–pericarditis syndrome, NOMID = neonatal-onset multisystem inflammatory disease.

Reprinted with the kind permission of Springer Science+Business Media from Wihlborg C, Babyn P, Ranson M, Laxer R. Radiologic mimics of juvenile rheumatoid arthritis. Pediatr Radiol 2001; 31:315–326.

Table 16.3. Diagnostic performance of conventional radiography (reference standard measure: MRI)

Article	Level of evidence	Sensitivity	Specificity	PPV	NPV
Herve-Somma et al. (44)	Moderate				
Superficial cartilage destruction (n=17)		0.29			
Deep subchondral involvement (n=4)		1.0 (n <10)			
El-Miedany et al. (56)	Moderate				
Superficial cartilage destruction (n=5)		0.40 (n<10)			
Deep subchondral involvement (n=17)		0.18			
Murray et al. (61)	Moderate				
Superficial cartilage destruction (n=5)		1.0 (n <10)	0.50 (n<10)	0.83 (n <10)	1.0 (n <10)
Deep subchondral involvement (n=10)		0.90 (n<10)	1.0 (n <10)	1.0 (n <10)	0.50 (n <10)
Gylys-Morin et al. (38)	Strong				
Superficial cartilage destruction (bone erosions) (Ref. standard: contrast-enhanced MRI) (n=23)		0.50	0.85	0.2	0.96

Table 16.4. Diagnostic performance of ultrasound (reference standard measure: MRI)

Article	Level of evidence	Sensitivity
El-Miedany et al. (56)	Moderate	
Joint effusion (n=38)		0.62
Superficial cartilage destruction (n=5)		0.60
Deep subchondral involvement (n=17)		0.24

Abbreviation: n=number of cases.

Table 16.5. Diagnostic performance of unenhanced MRI (reference standard measure: contrast-enhanced MRI)

Articles	Level of evidence	Sensitivity	Specificity	PPV	NPV
Herve-Somma et al. (44)	Moderate				
Joint effusion (mild)		0.73			
Joint effusion (large)				0.77	
Superficial cartilage destruction		0.24			
Deep subchondral involvement		0.50 (n<10)			
Murray et al. (61)	Moderate				
Superficial cartilage destruction		1.0 (n <10)	0.33 (n <10)	0.71 (n <10)	1.0 (n <10)
Deep subchondral involvement		0.8 (n=10)	1.0 (n =10)	1.0 (n =10)	0.33 (n =10)
El-Miedany et al. (56)	Moderate				
Superficial cartilage destruction		1.0 (n <10)		0.5 (n <10)	
Deep subchondral involvement		0.71		1.0	

Abbreviation: n=number of cases.

Table 16.6. Ultrasound measurements of synovial thickness at the level of the suprapatellar bursa (knee joint) in juvenile idiopathic arthritis patients and asymptomatic controls

Articles	Synovial thickness (mm) (US)	Synovial thickness (mm) (US)	Synovial thickness (mm) (US)	Synovial thickness (mm) (US)	P value
	Active disease—JIA	Inactive disease—JIA	Asymptomatic joints/laboratory evidence of active disease—JIA	Control subjects	
Sureda et al. (30)	5.2 ± 2.5	4.5 ± 1.6	–	Not visualized	<0.001 between control and two groups
Barbuti et al. (32)	6	–	–	2.7	–
Doria et al. (27)	5.6 ± 2.6 p=0.001	1.7 ± 0.6 p=0.13	2.8 ± 1.2 p=0.002	1.4 ± 0.3	
Frosch et al. (31)	5.8 ± 1.9	5.2± 2.6	–	–	Not significant

Abbreviations: JIA=juvenile idiopathic arthritis, US=ultrasound.

Table 16.7. Correlation of clinical and sonographic (synovial thickness) outcomes over time

Articles	Total *n* of JIA patients	No. of patients with follow-up US	Joint	Timepoint of follow-up (months)	Interval clinical change	Interval US change (synovial thickness)
Sureda et al. (30)	36	16/18 (44% in relation to total number of patients)	Knee	12	Improved (*n*=10)	No change (*n*=10) and decrease (*n*=6)
		6/18 (17% in relation to total number of patients)			Worsening (*n*=6)	Increase (*n*=6)
Cellerini et al. (33)	49	10	Knee	1–15	Improved (*n*=9)	Decrease (*n*=8)
					Worsening (*n*=1)	Increase (*n*=1)
Shahin et al. (28)	30	14	Knee	–	Improved (*n*=13)	Decrease (*n*=13)

Abbreviations: JIA=juvenile idiopathic arthritis, US=ultrasound, *n*=number.

Table 16.8. Levels of evidence on diagnostic accuracy of ultrasound for assessment of juvenile idiopathic arthritis as per Canadian Task Force (Appendix) and evidence-based strength of recommendations. Quality assessment of articles was based on the quality assessment of studies of diagnostic accuracy (QUADAS) tool

Maneuver	Diagnostic accuracy	Quality of articles/levels of evidence[a]	Recommendations
1. Diagnostic accuracy of US to detect synovial hypertrophy in JIA children (27–35)	Eight articles assessed construct validity of US for evaluation of synovium. Six articles assessed synovial thickness (five moderate and one substantial quality). Two articles (one moderate and one substantial quality) evaluated the use of color and power Doppler. The use of IV contrast was effective for measuring mean color pixel intensity in active and quiescent disease (one article—moderate quality). Six articles correlated the degree of disease activity with the US findings (Five moderate and one substantial quality)	One substantial, seven moderate quality studies Seven case–control/cross-sectional studies and one cross-sectional study. Two studies assessed responsiveness of the ultrasound technique to therapy Overall rating: Level II-2	Moderate evidence
2. Diagnostic accuracy of US to detect cartilage degeneration in JIA (28, 30, 32, 33, 35)	Five articles assessed cartilage with US (one substantial, four moderate quality)	One substantial, four moderate quality studies Four case–control studies and one cross-sectional study (only cases) Overall rating: Level II-2	Moderate evidence
3. Association between US evidence of cartilage degeneration and clinical response to treatment (30)	Only one article of moderate quality reported two cases with clinical improvement and corresponding decrease in cartilage thickness	One moderate quality article Case–control study Overall rating: Level II-2	Insufficient evidence (in quantity) (association between US evidence of cartilage degeneration and clinical response to treatment and prediction role of US on future status of the cartilage after treatment)

[a]Level of evidence defined in Appendix.

Abbreviations: JIA=juvenile idiopathic arthritis, US=ultrasound, IV=intravenous.

Data from Harris RP et al. (86) and Whiting et al. (24).

Table 16.9. Levels of evidence on diagnostic accuracy of MRI for assessment of juvenile idiopathic arthritis as per Canadian Task Force (Appendix) and evidence-based strength of recommendations. Quality assessment of articles was based on the quality assessment of studies of diagnostic accuracy (QUADAS) tool

Maneuver	Diagnostic accuracy	Quality of articles/levels of evidence[a]	Recommendations
1. Diagnostic accuracy of MRI to detect synovial hypertrophy in JIA children (38, 44–52, 56, 57)	Twelve articles assessed the construct validity of MRI for evaluation of synovium. The use of IV contrast was effective for qualitative assessment as mentioned in seven articles (four moderate, two poor, and one substantial quality). Five articles assessed synovial thickness (three moderate, one poor, and one substantial quality). Three articles calculated synovial volume (two moderate and one substantial quality)	Two substantial, seven moderate, three poor quality articles Eight prospective cohort studies and four case–control studies Overall rating: Level II-2: $n=12$	Grade B—Moderate evidence (assessment of synovium using *qualitative* MRI) Grade I—Insufficient evidence (in quantity and quality) (assessment of synovium using *quantitative* MRI)
2. Diagnostic accuracy of MRI to detect cartilage degeneration in JIA (38, 44, 50, 51, 56, 61, 67)	Eight articles assessed the detection of cartilaginous lesions with MRI (one substantial, five moderate, two poor quality articles). Two moderate quality and one poor quality article reported the effectiveness of IV contrast. Recent articles added the use of MPGR (one substantial and one moderate article) or fat suppression sequences (one substantial and two moderate quality article) to the ongoing protocol	One substantial, five moderate, and two poor quality studies Four prospective cohorts and four case–control studies Overall rating: Level II-2: $n=8$	Grade B—Moderate evidence
3. Association between MRI evidence of cartilage degeneration and clinical response to treatment (45, 51, 66)	Three articles of moderate quality assessed cartilage response to treatment. One article mentioned improvement of MRI findings in all 21 children treated with IAS. Another article using medical treatment reported MR improvement of cartilage lesion in 2/18 knees	Three moderate quality studies Two cohort studies and one case–control study Overall rating: Level II-2: $n=3$	Grade I—Insufficient evidence (in quantity) (association between US evidence of cartilage degeneration and clinical response to treatment and prediction role of MRI on future status of the cartilage after treatment)

[a]Level of evidence defined in Appendix.

Abbreviations: JIA=juvenile idiopathic arthritis, US=ultrasound, MRI=magnetic resonance imaging, IV=intravenous, IAS=intraarticular steroids.

Data from Harris et al. (86) and Whiting et al. (24).

Adapted with permission from Miller E, Uleryk E, Doria AS. Evidence-based outcomes of studies addressing diagnostic accuracy of MRI of juvenile idiopathic arthritis. AJR 2009; 192:1209–1218.

Table 16.10. Levels of evidence on diagnostic accuracy of quantitative ultrasound (QUS) and peripheral quantitative computed tomography (pQCT) for assessment of juvenile idiopathic arthritis as per Canadian Task Force (Appendix) and evidence-based strength of recommendations. Quality assessment of articles was based on the quality assessment of studies of diagnostic accuracy (QUADAS) tool

Maneuver	Diagnostic accuracy	Quality of articles/levels of evidence	Recommendations
1. Diagnostic accuracy of quantitative ultrasound to detect bone alteration in JIA children (79–81)	Three articles assessed construct validity. Two articles (one moderate and one poor quality study) showed either good correlation between total body BMD and SOS QUS measurements or decreased BUA in JIA joints. One article (moderate quality) failed to demonstrate differences between the SOS in fingers of patients with JIA and control subjects	Two moderate and one poor quality studies Case–control/cross-sectional studies Overall rating: Level II-2	Grade I—Insufficient evidence (in quantity and quality)
2. Diagnostic accuracy of peripheral quantitative CT to detect bone alterations in JIA children (82, 83, 85, 87)	Four articles assessed construct validity. Three articles of substantial quality reported that patients with JIA had decreased bone density compared to controls. One article (moderate quality) reported improved bone parameters in JIA patients receiving growth hormone	Three substantial and one moderate quality studies Cross-sectional studies Overall rating: Level II-2	Grade I—Insufficient evidence (in quantity)

Abbreviations: JIA=juvenile idiopathic arthritis, BMD=bone mineral density, BUA=broadband ultrasound attenuation, QUS=quantitative ultrasound, SOS=seed of sound; CT=computed tomography.
Data from Harris et al. (86) and Whiting et al. (24).

Imaging Case Studies

Case 1

Figure 16.2 shows a case of a 7 year-old girl with new onset of significant left thenar atrophy, swelling around the wrist, and limited motion.

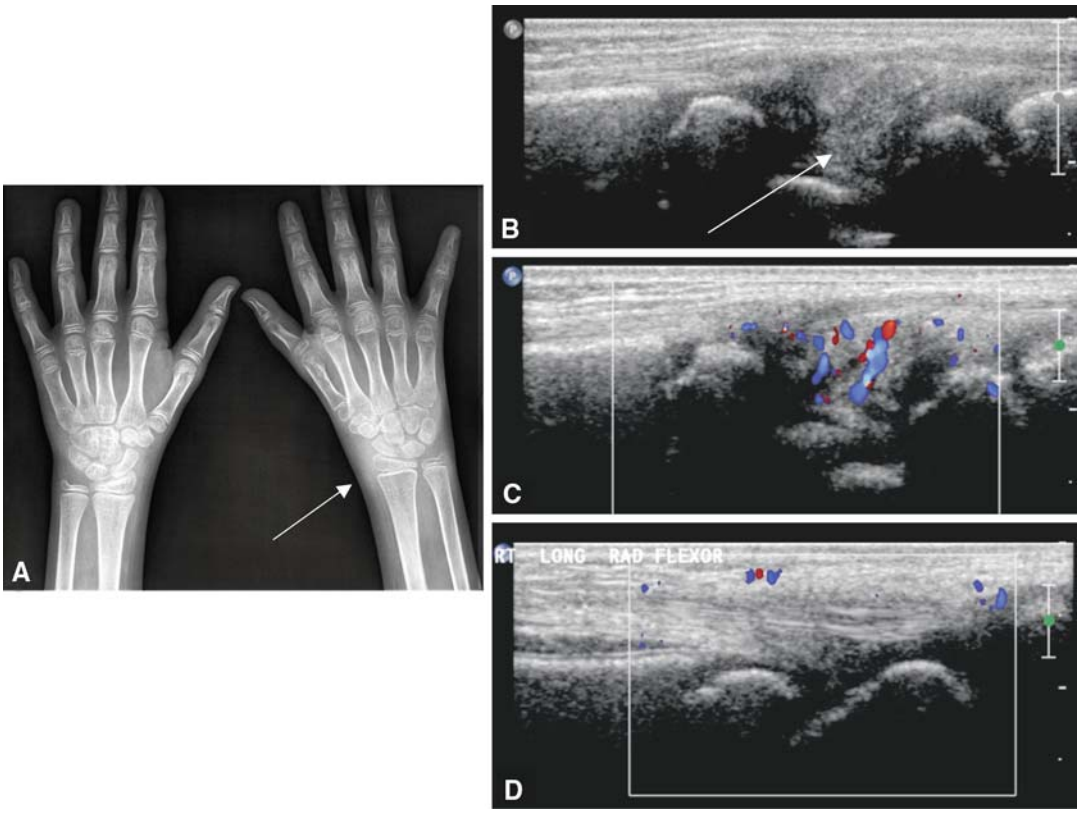

Figure 16.2. A 7-year-old girl with new onset of significant left thenar atrophy, swelling around the wrist, and limited motion. She received a subsequent diagnosis of ANA-negative and RF-negative juvenile idiopathic arthritis. Plain film of hands (**A**) demonstrates minimal lateral soft tissue swelling around the left wrist (*arrow*). Longitudinal ultrasound images of the radial aspect of her left wrist demonstrated increase echoes within the synovium tissue (*arrow*) (**B**) and increased flow on color Doppler ultrasound (**C**). **D** represents the unaffected contralateral side.

Case 2

Figure 16.3 is the case of a 14-year-old boy with polyarticular juvenile idiopathic arthritis presenting with an acutely swollen right elbow.

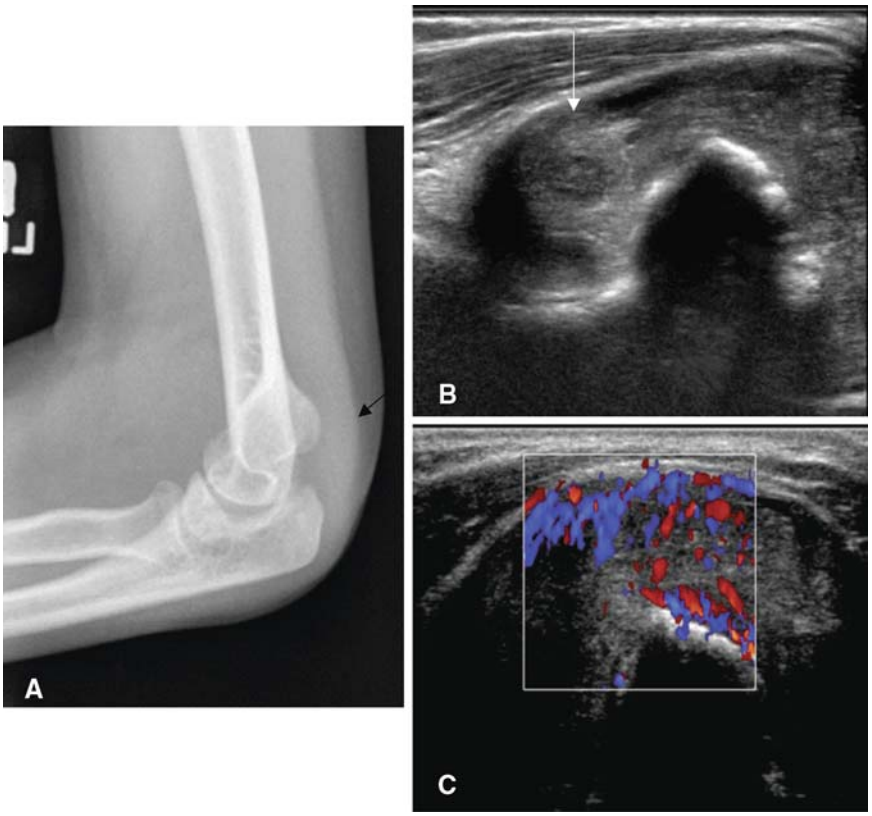

Figure 16.3. A 14-year-old boy with polyarticular juvenile idiopathic arthritis presenting with an acutely swollen right elbow. A lateral plain radiograph shows mild right posterior soft tissue swelling (*arrow*) (**A**). Transverse ultrasound images of the posterior right elbow demonstrate synovial thickening on gray-scale imaging (*arrow*) (**B**) with increased flow on color Doppler scans (**C**).

Case 3

Figure 16.4 is the case of a 12-year-old girl with active juvenile idiopathic arthritis presenting with persistent pain and reduced range of motion of the left wrist.

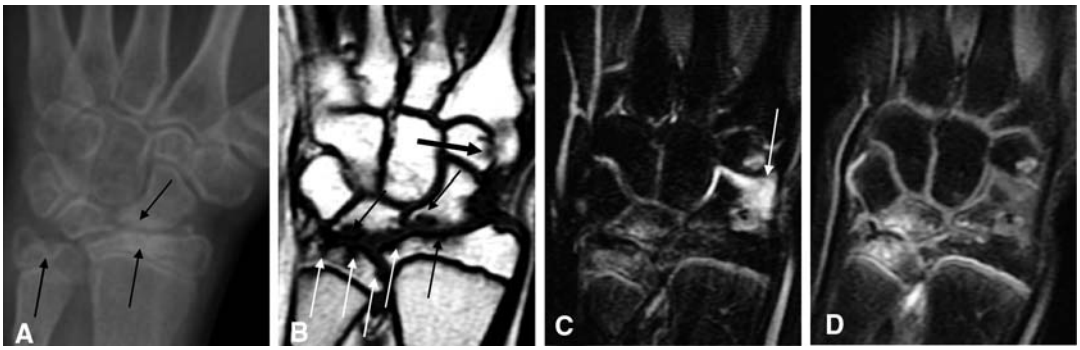

Figure 16.4. A 12-year-old girl with active juvenile idiopathic arthritis presenting with persistent pain and reduced range of motion of the left wrist. The frontal radiograph (**A**) and the MRI examination (**B**–**D**) were acquired 6 months apart. Unenhanced coronal T1-weighted (**B**), inversion recovery (**C**) images and contrast-enhanced T1-weighted images of the left wrist obtained with fat saturation (**D**) show the presence of multiple cortical erosions (*arrows*) in the scaphoid bone, lunate, trapezoid, and epiphysis of the distal radius and ulna. Joint effusion (*arrow*) is noted in the radioulnar joint and surrounding the scaphoid (**C**). There is high signal in the bone marrow on inversion recovery images in keeping with bone marrow edema involving the epiphysis of the ulna, the lunate, and the proximal scaphoid (**C**). Enhancement postinjection of gadolinium is noted in the scaphoid, the lunate, and the epiphysis of the distal ulna and at a lesser extent, the epiphysis of the distal radius (**D**). (Reprinted with kind permission from Springer Science+Business Media from Doria AS, Babyn PS, Feldman B. A critical appraisal of radiographic scoring systems for assessment of juvenile idiopathic arthritis. Pediatr Radiol 2006; 36:759–772.).

Suggested Imaging Protocols for Juvenile Idiopathic Arthritis

Ultrasound

Longitudinal and transverse scans of affected joints should be performed in comparison to the contralateral joint or to similar joints in case of hands and feet. High-resolution linear transducers (10–15 MHz) are suggested. For gray-scale US assessment, the image depth should be adjusted to the size of the joint. The operator should document synovium of bursae, fluid, adjacent soft tissues, and cartilage. The maximum synovial membrane thickness should be obtained by applying firm compression of the transducer on the region of interest of the joint. Color Doppler parameters may include low filter, pulse repetition frequency of 700 Hz, and color gain settings of 60% (27). Power Doppler instead of color Doppler should be considered if low probability of motion artifacts during the scanning. Comparison of the synovial vascularity with the contralateral side is helpful in monoarthritis. When evaluating the knee joints, the child can lie in supine position with the knee in 30° flexion. The position of the transducer in sagittal and axial planes of US acquisition of knees and ankles was described elsewhere (65). For scanning of hands, the patient is examined in upright position with the hand of interest placed on a cushion, relaxed, and pronated. The region of interest of the wrist/hand is scanned in the longitudinal and transverse planes. Metacarpo/metatarsophalangeal joints are typically assessed in the regions that are accessible from the dorsal side.

MRI

Large Joints (Knees, Ankles, Elbows, Shoulders)
A suggested protocol includes unenhanced sagittal spin-echo (SE) T1-weighted (TR 418 ms, TE 12 ms, slice thickness 3 mm, FOV 100 mm, matrix 184 × 256, 2 acquisitions), sagittal turbo SE T2-weighted (TR 4,200 ms, TE 96 ms, echo train 7, slice thickness 3 mm, FOV 100 mm, matrix 154 × 256, 2 acquisitions), sagittal fat-suppressed 3D gradient echo (TR 50 ms, TE 11 ms, flip angle 40°, slice thickness 1.5 mm, FOV 100 mm, matrix 228 × 256, 1 acquisition), and coronal short tau inversion recovery (STIR) (TI 150 ms, TR 4,500 ms, TE 60 ms, slice thickness 4 mm, FOV 113 mm, matrix 198 × 256, 3 acquisitions) images. Immediately after the intravenous administration of gadolinium–DTPA (0.1 mmol/kg), axial or sagittal T1-weighted, fat-saturated images should be obtained. The images should be acquired using an extremity coil.

For hips, the suggested planes are axial and coronal.

Small Joints (Wrists, Hands, Feet)
This protocol includes unenhanced imaging of the patient's symptomatic wrist, hand, or foot (91): unenhanced axial T1-weighted SE (TR 420 ms, TE 13 ms, slice thickness 3 mm, gap 0 mm, 2 acquisitions), axial T2-weighted FSE fat-saturated (TR 3,760 ms, TE 12 ms, TI 150 ms, slice thickness 3, gap 0 mm, 2 acquisitions), coronal T1-weighted SE (TR 680 ms, TE 14 ms, slice thickness 3 mm, gap 0 mm, 1 acquisition), coronal T2-weighted fat-saturated or short tau inversion recovery (STIR) (TR 3,760 ms, TE 12 ms, TI 150 ms, slice thickness 3 mm, gap 0 mm, 2 acquisitions), axial and coronal 3D spoiled gradient-recalled (SPGR) fat-saturated images (TR 23 ms, TE 6 ms, slice thickness 1.5 mm). After intravenous administration of gadolinium–DTPA (0.1 mmol/kg), axial T1-weighted fat-saturated images should be obtained. We recommend the use of field of view (FOV) of 10 cm or smaller, whenever possible, and matrix of at least 256 × 192. The following areas should be included in the FOV: distal radioulnar, radiocarpal, and intercarpal joints, metacarpal bases for wrist scanning, and dedicated regions of interest for hands and feet.

Future Research

The following topics require further investigation:

- Assessment of early joint damage in small joints (hands and feet) with US and/or MRI.
- MRI and/or US evaluation of the long-term effect of therapy on early diagnosed JIA.
- Comparison of MRI and/or US findings and clinical findings in JIA patients and controls using a standardized MR and US protocol for acquisition of images.
- Validation of MRI and US scoring systems for interpretation of findings in JIA.
- Assessment of the predictive value of MRI and/or US findings in prospective clinical trials of early JIA using specific treatment algorithms.
- Evaluation of temporal progression of asymptomatic joints in children affected with JIA.
- Use of functional MR imaging for improved characterization of the cartilage morphology, structure, and function in children with JIA.
- Larger studies on pQCT and QUS with adequate sample size.
- Determination of the normal thickness of the articular cartilage according to age in healthy children using a standardized protocol for acquisition of measurements on US and MRI.

Appendix

Grading of levels of evidence as per Canadian Task Force (86).

I. Evidence obtained from at least one properly randomized controlled trial.

II-1. Evidence obtained from well-designed controlled trials without randomization.

II-2. Evidence obtained from well-designed cohort or case–control analytic studies, preferably from more than one center or research group.

II-3. Evidence obtained from multiple time series with or without the intervention; dramatic results in uncontrolled experiments could be regarded as this type of evidence.

III. Opinions of respected authorities, based on clinical experience; descriptive studies and case reports or reports of expert committees.

References

1. Petty RE. Rev Rhum Engl Ed 1997; 64:161S–162S.
2. Hollister J. In Hay WW, Levin MJ, Sondheimer JM, Deterding RR (eds.): Current Diagnosis & Treatment in Pediatrics, 18th edn. New York: Lange Medical Books/McGraw – Hill Medical Publishing Division, 2007.
3. Wright D. In Morrissy R, Weinstein S (eds.): Lovell & Winter's Pediatric Orthopedics, 6th edn. Philadelphia: Lippincott Williams & Wilkins, 2006; 406–410.
4. Yulish BS, Lieberman JM, Newman AJ, Bryan PJ, Mulopulos GP et al. Radiology 1987; 165: 149–152.
5. Minden K, Niewerth M, Listing J et al. Arthritis Rheum 2002; 46:2392–2401.
6. Zak M, Pedersen FK. Rheumatology (Oxford) 2000; 39:198–204.
7. Packham JC, Hall MA. Rheumatology (Oxford) 2002; 41:1440–1443.
8. Davidson J. Eur J Radiol 2000; 33:128–134.
9. Fink CW. J Rheumatol 1995; 22:1566–1569.
10. Gare BA. Baillieres Clin Rheumatol 1998; 12: 191–208.
11. Aaron S, Fraser PA, Jackson JM et al. Arthritis Rheum 1985; 28: 753–758.
12. Hanson V, Kornreich HK, Bernstein B et al. Arthritis Rheum 1977; 20(Suppl):184.
13. Cassidy JT, Petty RE. In Cassidy JT, Petty RE (eds): Textbook of Pediatric Rheumatology, 3rd edn. Philadelphia: W.B. Saunders Company, 1995: 133–223.
14. Ravelli A. Clin Exp Rheumatol 2004; 22:271–275.
15. Oen K. Best Pract Res Clin Rheumatol 2002; 16:347–360.
16. Lovell DJ, Giannini EH, Reiff A et al. Pediatric Rheumatology Collaborative Study Group. N Engl J Med 2000; 342:763–769.
17. Ruperto N, Murray KJ, Gerloni V et al. Arthritis Rheum 2004; 50:2191–2201.
18. Cassone R, Falcone A, Rossi F et al. Clin Exp Rheumatol 2004; 22:637–642.
19. Lang BA, Schneider R, Reilly BJ, Silverman ED, Laxer RM. J Rheumatol 1995; 22:168–173.
20. Cooper NJ. Rheumatology (Oxford) 2000; 39: 28–33.
21. Bernatsky S, Duffy C, Malleson P, Feldman DE, St Pierre Y, Clarke AE. Arthritis Rheum 2007; 57:44–48.
22. Lamer S, Sebag GH. Eur J Radiol 2000; 33:85–93.
23. Kaye JJ. Radiology 1990; 177:601–608.
24. Whiting P, Rutjes AW, Reitsma JB, Bossuyt PM, Kleijnen J. BMC Med Res Methodol 2003; 3:25.
25. Babyn P, Doria AS. Rheum Dis Clin North Am 2007;33:403–440.
26. Joshua F, Lassere M, Bruyn GA et al. J Rheumatol 2007; 34:839–847.
27. Doria AS, Kiss MH, Lotito AP et al. Pediatr Radiol 2001;31:524–531.
28. Shahin AA, el Mofty SA, el Sheikh EA et al. Z Rheumatol 2001;60:148–155.
29. Klauser A, Frauscher F, Schirmer M et al. Arthritis Rheum 2002;46:647–653.
30. Sureda D, Quiroga S, Arnal C, Boronat M, Andreu J et al. Radiology 1994; 190:403–406.
31. Frosch M, Foell D, Ganser G, Roth J. Ann Rheum Dis 2003; 62:242–244.
32. Barbuti D, Bergami G, Vecchioli Scaldazza A. Radiol Med (Torino) 1997; 93:27–32.
33. Cellerini M, Salti S, Trapani S, D'Elia G, Falcini F et al. Pediatr Radiol 1999; 29:117–123.
34. Shahin AA, Shaker OG, Kamal N, Hafez HA, Gaber W et al. Rheumatol Int 2002; 22:84–88.
35. Karmazyn B, Bowyer SL, Schmidt KM et al. Pediatr Radiol 2007; 37:475–482.
36. Granberry WM, Mangum GL. J Hand Surg [Am] 1980; 5:105–113.
37. Graham TB. Curr Opin Rheumatol 2005; 17: 574–578.
38. Gylys-Morin VM, Graham TB, Blebea JS et al. Radiology 2001; 220:696–706.
39. Ramsey SE, Cairns RA, Cabral DA et al. J Rheumatol 1999; 26:2238–2243.
40. Website: http://www.fda.gov/CDER/drug/InfoSheets/HCP/microbubbleHCP.htm; September 3, 2008.
41. Winalski CS, Palmer WE, Rosenthal DI, Weissman BN. Radiol Clin North Am 1996; 34:243–258.
42. Peterfy CG, Majumdar S, Lang P, van Dijke CF, Sack K et al. Radiology 1994; 191:413–419.
43. Peterfy CG. Curr Opin Rheumatol 2003; 15: 288–295.
44. Herve-Somma CM, Sebag GH, Prieur AM, Bonnerot V, Lallemand DP. Radiology 1992; 182: 93–98.
45. Huppertz HI, Tschammler A, Horwitz AE, Schwab KO. J Pediatr 1995; 127:317–321.
46. Graham TB, Laor T, Dardzinski BJ. J Rheumatol 2005; 32:1811–1820.
47. Workie DW, Graham TB, Laor T et al. Pediatr Radiol 2007; 37:535–543.
48. Nistala K, Babar J, Johnson K et al. Rheumatology (Oxford) 2007; 46:699–702.
49. Remedios D, Martin K, Kaplan G, Mitchell R, Woo P et al. Br J Rheumatol 1997; 36:1214–1217.
50. Uhl M, Krauss M, Kern S et al. Acta Radiologica 2001; 42:6–9.
51. Cakmakci H, Kovanlikaya A, Unsal E. Pediatric Radiol 2001; 31:189–195.
52. Workie DW, Dardzinski BJ, Graham TB, Laor T, Bommer WA, O'Brien KJ. Magn Reson Imaging 2004; 22:1201–1210.

53. Yamato M, Tamai K, Yamaguchi T, Ohno W. J Comput Assist Tomogr 1993; 17:781–785.
54. Ostergaard M, Klarlund M. Ann Rheum Dis 2001; 60:1050–1054.
55. Swaminathan S. N Engl J Med 2007; 357: 720–722.
56. El-Miedany YM, Housny IH, Mansour HM, Mourad HG, Mehanna AM et al. Joint, Bone, Spine: Revue du Rhumatisme 2001; 68: 222–230.
57. Gardner-Medwin JM, Killeen OG, Ryder CAJ, Bradshaw K, Johnson K. J Rheumatol 2006; 33:2337–2343.
58. Ostergaard M, Hansen M, Stoltenberg M et al. Arthritis Rheum 1999; 42:918–929.
59. Ostergaard M, Stoltenberg M, Lovgreen-Nielsen P, Volck B, Jensen CH et al. Arthritis Rheum 1997; 40:1856–1867.
60. Bird P, Lassere M, Shnier R, Edmonds J. Arthritis Rheum 2003; 48:614–624.
61. Murray JG, Ridley NTF, Mitchell N, Rooney M. Clin Radiol 1996; 51:99–102.
62. Barnewolt CE, Shapiro F, Jaramillo D. Am J Roentgenol 1997; 169:183–189.
63. Doria AS, Babyn PS, Lundin B et al. Haemophilia 2006; 12:503–513.
64. Kilcoyne RF, Nuss R. Haemophilia 2003; 9 (Suppl 1):57–63; discussion 63–54.
65. Zukotynski K, Jarrin J, Babyn PS et al. Haemophilia 2007; 13:293–304.
66. Eich GF, Halle F, Hodler J, Seger R, Willi UV. Pediatr Radiol 1994; 24:558–563.
67. Kight AC, Dardzinski BJ, Laor T, Graham TB. Arthritis Rheum 2004; 50:901–905.
68. Johnson K. Pediatr Radiol 2006; 36:743–758.
69. Gilsanz V. Eur J Radiol 1998; 26:177–182.
70. Gomberg BR, Saha PK, Song HK et al. IEEE Trans Med Imaging 2000; 19:166–174.
71. Cody DD, Goldstein SA, Flynn MJ et al. Spine 1991; 16:146–154.
72. Lang SM, Moyle DD, Berg EW et al. J Bone Joint Surg [Am] 1988; 70:1531–1538.
73. Mosekilde L, Bentzen SM, Ortoft G, et al. Bone 1989; 10:465–470.
74. Gilsanz V, Wren T. Pediatrics 2007; 119 (Suppl 2):S145–S149.
75. Henderson CJ, Specker BL, Sierra RI, Campaigne BN, Lovell DJ. Arthritis Rheum 2000; 43:531–540.
76. Wren TA, Liu X, Pitukcheewanont P, Gilsanz V. J Pediatr 2005; 146:776–779.
77. Njeh CF, Boivin CM, Langton CM. Osteoporos Int 1997; 7:7–22.
78. Prins SH, Jorgensen HL, Jorgensen LV, Hassager C. Clin Physiol 1998; 18:3–17.
79. Falcini F, Bindi G, Simonini G et al. J Rheumatol 2003; 30:179–184.
80. Njeh CF, Shaw N, Gardner-Medwin JM, Boivin CM, Southwood TR. J Clin Densitom 2000; 3: 251–260.
81. Scheunemann I, Dannecker GE, Roth J. Rheumatology (Oxford) 2006; 45:1125–1128.
82. Roth J, Palm C, Scheunemann I, Ranke MB, Schweizer R et al. Arthritis Rheum 2004; 50: 1277–1285.
83. Bechtold S, Ripperger P, Dalla Pozza R, Schmidt H, Hafner R et al. Osteoporos Int 2005; 16: 757–763.
84. Njeh CF, Genant HK. Arthritis Res 2000; 2: 446–450.
85. Bechtold S, Ripperger P, Bonfig W, Pozza RD, Haefner R et al. J Clin Endocrinol Metab 2005; 90:3168–3173.
86. Harris RP, Helfand M, Woolf SH et al. Am J Prev Med 2001; 20:21–35.
87. Felin EM, Prahalad S, Askew EW, Moyer-Mileur LJ. Arthritis Rheum 2007; 56:984–994.

17

Imaging of Hematogenous Osteomyelitis and Septic Arthritis in Children

Boaz Karmazyn, John Y. Kim, and Diego Jaramillo

Issues

I. What is the diagnostic performance of the different imaging studies in acute hematogenous osteomyelitis (AHOM)?
II. What is the diagnostic performance of the different imaging studies in the evaluation of subperiosteal and soft tissue abscesses associated with AHOM?
III. What is the diagnostic performance of the different imaging studies in chronic osteomyelitis?
IV. What is the diagnostic performance of the different imaging studies in septic hip arthritis?

Key Points

- When signs and symptoms of osteomyelitis cannot be localized, bone scintigraphy is the preferred imaging (limited evidence).
- MRI is the imaging modality of choice for evaluation of AHOM when symptoms are localized (limited evidence).
- PET FDG/CT is the imaging modality of choice for evaluation of chronic osteomyelitis (limited evidence, based on studies on adult population).
- Ultrasound is the imaging modality of choice for evaluation of hip joint effusion in septic hip (limited–moderate evidence).
- No data were found in the medical literature on the cost-effectiveness of the different imaging modalities in the evaluation of hematogenous osteomyelitis and septic joint.

B. Karmazyn (✉)
Department of Pediatric Radiology, Assistant Professor of Radiology, 702 Barnhill Drive, Room 1053, Indiana University School of Medicine, Riley Hospital for Children, 702 Barnhill Drive, Room 1053, Indianapolis, IN 46202, USA
e-mail: bkarmazy@iupui.edu

L.S. Medina et al. (eds.), *Evidence-Based Imaging in Pediatrics*,
DOI 10.1007/978-1-4419-0922-0_17, © Springer Science+Business Media, LLC 2010

Definition and Pathophysiology

Osteomyelitis is an infection of the bone. The root word *osteon* (bone) and *myelo* (marrow) are combined with *itis* (inflammation) to define the clinical state of bone infected with microorganisms (1). Clinical presentation depends on many variables including age, pathogen, anatomical site of infection, and presence or absence of any underlying disorder or situation (1–6). Acute osteomyelitis is characterized by the relatively abrupt onset of clinical symptoms and signs. Acute hematogenous osteomyelitis (AHOM) is an infection of the bone that is rapid in onset after blood-borne pyogenic organisms settle in the metaphysis. It most commonly affects children. Chronic osteomyelitis (COM) is a persistent bone infection of the low-grade type (4). It is more common in adults secondary to trauma or surgery. A sequestrum represents a segment of necrotic bone that is separated from the living bone by granulation tissue (1). An involucrum is a layer of living bone that has formed around dead bone. Cloaca is an opening on the involucrum (1). Brodie abscess is a sharply delineated focus of infection. It is lined by granulation tissue and frequently surrounded by eburnated bone (1).

Routes of infection include hematogenous spread, spread by contiguity, and direct infection by a penetrating wound (1–6). Hematogenous spread is the most common route in children, usually seeding the metaphyses of long bones due to sluggish blood flow patterns in this region (1–6). In children less than 18 months of age, transphyseal vessels allow metaphyseal infections to cross the physis and infect the epiphyses and joints. The most common bones affected by AHOM are the tibia and the femur (6). The most common organism is *Staphylococcus aureus* (*S. aureus*), followed by *β -hemolytic streptococcus, Streptococcus pneumoniae, Escherichia coli,* and *Pseudomonas aeruginosa* (1–3). In recent years, methicillin-resistant *S. aureus* (MRSA) became a common pathogen in community-acquired osteomyelitis in children. The MRSA AHOM is more commonly associated with lung infection and deep venous thrombosis (7–11). Tuberculous osteomyelitis remains a major cause of skeletal infection in less developed countries (12).

The clinical presentation of osteomyelitis in the neonate differs from that seen in older children (13, 14). Because of immaturation of the immune response, inflammatory response is not well localized. Signs and symptoms are initially nonspecific or may be related to sepsis (13). Toddlers can present with limping, pseudoparalysis, or pain on passive movement (1–6). Standard laboratory tests, such as sedimentation rate and CRP, are usually elevated (1–6, 15, 16). Serial blood cultures are reported to be positive in 32%–60% of cases (1–6, 15, 16). Occasionally, direct aspiration of bone material may be needed for diagnosis. These aspirations can yield positive cultures in 87% of cases (17).

Acute septic arthritis is a bacterial infection of a joint. Most cases arise from hematogenous spread or contiguous spread from adjacent osteomyelitis in the metaphysis (18–23). The most common organism is *S. aureus* (18–23). The prognosis worsens with delayed treatment due to destruction of the physis and articular cartilage secondary to lytic enzymes (22) and osteonecrosis (21, 22). This can lead to growth arrest, limb deformity, permanent joint malalignment, and early degenerative joint disease (21, 22).

Septic arthritis is a medical emergency. The hip joint is most commonly involved. A combination of clinical findings and laboratory tests including leukocytosis, fever, inability to bear weight, elevated erythrocyte sedimentation rate (ESD), and C-reactive protein can differentiate between septic hip arthritis and nonbacterial arthritis in 80%–90% of the cases (24, 25). In undetermined cases, ultrasound can be used to detect hip joint effusion and guide joint aspiration to differentiate between septic hip and transient synovitis (26–30). Septic hip is unlikely in the absence of hip effusion (26–29).

Epidemiology

The annual incidence of osteomyelitis in more developed countries is around 1/5,000 (3). Approximately 50% of cases occur in children younger than 5 years of age, and, of these, 25% are under 1 year of age (1–3). AHOM is more common in boys than girls, by a ratio of 2:1 (1–3). Although a single bone is usually affected, polyostotic involvement has been

reported in up to 6.8% of cases in infants and in 22% of neonates (13, 14, 31).

Half of the cases of septic arthritis occur in children less than 3 years of age (31). Children with septic arthritis have concomitant osteomyelitis in 42%–48% of the cases (32, 33). There is no significant difference in the incidence between boys and girls (32).

Overall Cost to Society

No data were found in the medical literature on the overall cost to society from the diagnosis, treatment, and complications of acute hematogenous osteomyelitis or septic arthritis. Although there are several cost-effective analyses evaluating the type, extent, and route of antibiotic administration in the treatment of osteomyelitis and septic arthritis, no cost-effectiveness data were found in the literature, specifically incorporating imaging strategies in the management of acute hematogenous osteomyelitis or septic arthritis.

Goals

In acute hematogenous osteomyelitis and septic arthritis, the goal is early diagnosis and treatment to prevent the long-term sequelae of these diseases, which include growth arrest, limb deformity, joint instability, joint destruction, ankylosis, and early degenerative joint disease. The standard treatment of osteomyelitis includes intravenous antibiotics followed by oral antibiotics. Surgical debridement may be necessary for osteomyelitis if frank pus can be aspirated from the bone, if there is necrotic bone present, or if there is failure to respond to antibiotic therapy (1–6). Septic arthritis usually requires surgical therapy in order to decompress the intraarticular pressure (32–34). Response to treatment is monitored clinically and with erythrocyte sedimentation rate and C-reactive protein. Imaging may be needed to evaluate for complications.

Methodology

The authors searched MEDLINE (January 1966 to June 2008), EMBASE (January 1980 to June 2008), and the Cochrane Library databases using OVID for data relevant to the diagnostic performance and accuracy of imaging evaluation of pediatric patients with hematogenous osteomyelitis and septic arthritis. The search strategy used medical subject headings: (1) osteomyelitis; (2) arthritis, infectious; (3) child (0–18 years); (4) ultrasonography; (5) radionuclide imaging; (6) radiography; (7) tomography, X-ray computed; and (8) magnetic resonance imaging. We excluded animal studies and non-English articles. If insufficient literature was found on pediatric population, a search was performed on adult population (Table 17.1).

Discussion of Issues

I. What Is the Diagnostic Performance of the Different Imaging Studies in Acute Hematogenous Osteomyelitis (AHOM)?

Summary of Evidence: The diagnostic performance of the various imaging for AHOM is summarized in Table 17.2. Plain radiographs are neither sensitive nor specific in the diagnosis of early AHOM (1–3). However, their low cost, ready availability, and ability to exclude other diseases (e.g., fractures, tumors) that can produce similar symptoms argue for their continued use as the initial evaluation (limited evidence) (35–38). In addition, in the appropriate clinical circumstance when plain radiographs demonstrate metaphyseal lytic lesion, no other imaging workup is necessary (limited evidence) (1–6, 37).

Several studies have shown that MRI and radionuclide bone scintigraphy have high sensitivity for detection of osteomyelitis (limited evidence) (39–45). Their relative merits have not been established. Bone scintigraphy has the advantage of whole-body imaging when symptoms cannot be localized, but has decreased specificity (limited evidence) (46–52). White blood cells (WBC) labeled with 111-In and ^{99m}Tc-HMPAO are more specific than bone scan for diagnosis of osteomyelitis (limited evidence) (1–6). Their main value is in the evaluation of osteomyelitis in the presence of prosthesis or after surgery when artifacts and postoperative changes make cross-sectional studies less valuable (1–6). In recent studies, 18F-FDG PET was reported (53, 54) to have

higher sensitivity for acute osteomyelitis as compared to bone scan, but at higher cost (insufficient evidence) (54). MRI is the preferred imaging method for the evaluation of AHOM when symptoms are localized (limited evidence) (55–61). Whole-body MRI is an emerging alternative to bone scintigraphy. It has mainly been used for the evaluation of bone metastasis, but there is not yet enough experience with the use of whole-body MRI for the evaluation of multifocal osteomyelitis (62–64) (insufficient evidence).

Supporting Evidence

Plain Radiographs

Initial radiographs can detect deep soft tissue swelling and loss of soft tissue planes as early as 48 hours after the onset of symptoms, but bone destruction is usually not detectable until 7–21 days after the onset of symptoms (1–6, 34–36, 65). 30%–50% of bone destruction is required before a lytic lesion is apparent (1–6). Radiographic evidence for osteomyelitis includes bone destruction and periostitis. Bone destruction may appear as an area of permeative destruction and lucency that may be associated with surrounding bone sclerosis (1–6).

The most important differential diagnosis is malignancy. Lytic bone lesion with laminated periosteal reaction was described in leukemia, Ewing's sarcoma, langerhans cell histiocytosis, and chronic recurrent multifocal osteomyelitis (66).

The sensitivity and the specificity of plain radiographs are 43%–75% and 75%–83%, respectively (limited evidence) (1–6, 36–38, 67). In the appropriate clinical settings, if bone destruction is detected, no further imaging may be necessary (limited evidence) (37).

Nuclear Medicine Imaging

Bone Scintigraphy

Technetium-99 M-labeled phosphates or phosphonates such as methylene diphosphonate (^{99m}Tc-MDP) are most commonly used for the diagnosis of AHOM (1–6, 42–52). These compounds bind to hydroxyapatite crystal. Uptake is increased with increased blood flow and increased osteoblastic activity. The increased uptake in the early (perfusion), intermediate (blood pool), and late (bone uptake) phases is typical for osteomyelitis (46–52).

The overall sensitivity and specificity of radionuclide bone scanning are 73%–100% and 73%–79% (limited evidence) (39–43, 46, 51). In the neonate, however, the sensitivity of radionuclide bone scanning is decreased, ranging from 32% to 87% (68, 69). More than 90% of the positive bone scans are "hot," with increasing uptake of ^{99m}Tc-MDP. Less commonly, decreased uptake ("cold" foci) is detected in AHOM (47, 50).

Advantages of bone scintigraphy include the ability to detect AHOM early (generally within 48 hours of onset of symptoms), high sensitivity, no requirement for sedation, imaging of the entire body, and relatively low cost. The ability to image the entire skeleton is ideal if symptoms cannot be localized or if there is polyostotic disease (limited evidence) (36, 40, 41, 69–71).

Gallium

Galium-67 binds to plasma proteins such as transferrin and lactoferrin. It is therefore deposited in areas of inflammation because of leaky capillaries and uptake by white blood cells and bacteria. Scan imaging is performed 48 hours after injection, but occasionally can be performed at 24 hours. The reported sensitivity of gallium scan has ranged from 25% to 80%, with a specificity of 67% (insufficient evidence) (72).

Leukocyte Scintigraphy

White blood cell scan can be done with 111-indium-labeled white blood cells or 99m Tc-hexamethylpropyleneamine oxime-labeled white cells. There is a need to take 20–40 ml of blood from the patient for WBC scan, and this is one of the reasons it is uncommonly used in pediatrics. Compared to bone scan, there is improved specificity (80%–90%). WBC scan is useful in patients who have prostheses when artifact can interfere with cross-sectional studies, and bone scan is not specific due to the expected increased uptake (limited evidence) (1–6).

FDG-PET

The 18F-FDG positron emission tomography (PET) is a relatively novel imaging technique for the evaluation of osteomyelitis. In acute and

subacute osteomyelitis and soft tissue infection, sensitivities of 98% and specificities in the range of 75%–99% have been reported (insufficient evidence) (54, 73).

MR Imaging

The ability of MRI to demonstrate AHOM with high sensitivity and specificity as well as joint effusion and fluid collections made MRI the best test for AHOM when symptoms are localized. The sensitivity and the specificity of MRI are 82%–100% and 75%–96% (limited evidence) (37, 58–65). MRI has the advantage of both high sensitivity and specificity. It can also display high-resolution images and evaluate for complications such as abscesses, joint effusions, and soft tissue extension that would require surgical intervention (64, 65). The disadvantages include higher cost relative to bone scintigraphy and prolonged imaging time which may require sedation. Whole-body MRI is a new application, used particularly in the evaluation of metastases. However, it can be performed to evaluate multifocal sites of infection (insufficient evidence) (62–64).

II. What Is the Diagnostic Performance of the Different Imaging Studies in the Evaluation of Subperiosteal and Soft Tissue Abscesses Associated with Acute Hematogenous Osteomyelitis?

Summary of Evidence: Most patients respond clinically to systemic antibiotics within 48 hours. If there is no clinical response to therapy, repeat imaging should be considered to exclude complications that would require surgical intervention such as abscess collections or necrotic tissue (limited evidence) (1–6).

Cross-sectional studies (CT scan, MRI, and ultrasound) may be necessary for the evaluation of soft tissue extension and complications. MR has the highest sensitivity for early detection of osteomyelitis and better delineates soft tissue spread of infection and abscess formation (limited evidence) (1–6, 74).

Ultrasound has high sensitivity for detection of subperiosteal abscess (limited evidence) (75–78). This could be particularly useful in the evaluation of AHOM in premature infants who are too fragile and unstable to withstand other cross-sectional studies.

Supporting Evidence: The use of ultrasound in osteomyelitis has been reported in few small series (75–78). In these series, ultrasound had high sensitivity for detection of subperiosteal and soft tissue fluid collections and can guide their aspirations (limited evidence) (75–78). However, ultrasound cannot evaluate the bone marrow and, therefore, may miss the diagnosis of osteomyelitis. The sensitivity to osteomyelitis was reported in a range of 46%–74% with a specificity range of 63%–100% (76, 78).

CT scan could be used for the evaluation of complications of osteomyelitis if the MRI study is not available or contraindicated (1–6, 74, 79, 80). It can demonstrate soft tissue and subperiosteal abscesses (insufficient evidence) (1–6, 74, 79, 80).

MRI is more sensitive than CT scan for the evaluation of soft tissue complications (insufficient evidence) (1–6, 74). MRI is especially valuable in imaging osteomyelitis of the pelvis as it is often associated with soft tissue abscesses (limited evidence) (81–83).

III. What Is the Diagnostic Performance of the Different Imaging Studies in Chronic Osteomyelitis?

Summary of Evidence: The diagnostic performance of the various imaging for chronic osteomyelitis is summarized in Table 17.3. A small percentage of children with osteomyelitis remain refractory to therapy, leading to chronic osteomyelitis (COM) (1–6). COM is seen more commonly in adults with osteomyelitis secondary to trauma or surgery. The evidence for the use of imaging in the evaluation of COM derives mainly from the adult population. The clinical diagnosis in these patients could be difficult as symptoms are typically indolent (4). Imaging findings that may indicate COM include Brodie abscess, cloaca, and sequestrum (1–6). These can be detected by plain radiographs; however, CT is more sensitive in the detection of these complications (limited evidence) (1–3, 84–86).

In COM that complicates trauma or surgery, the imaging diagnosis is challenging. MRI is

very sensitive for the detection of the bone marrow changes in COM. However, in the setting of post-trauma or post-surgery COM, the specificity is limited as MRI cannot differentiate between fibrovascular scarring and active osteomyelitis (limited evidence) (87–89).

Several nuclear medicine studies have been used for the detection of COM. These include bone scintigraphy, gallium-67, indium-11 or Tc-99m, and labeled leukocytes (87, 88). In the evaluation of the axial skeleton COM, WBC scan is limited as it may produce areas of "cold" foci that are difficult to detect and are nonspecific (insufficient evidence) (88).

In the evaluation of COM, 18F-FDG PET has the highest sensitivity and specificity and, therefore, is considered the study of choice for the diagnosis of COM (limited evidence) (87–92).

Supporting Evidence: Radiographs may demonstrate findings suggestive of COM such as Brodie abscess and sclerosis. These findings are nonspecific (84). The sensitivity for the detection of sequestrum is low compared to CT scan (insufficient evidence) (85). CT, although sensitive for the detection of sequestrum, cannot differentiate well between active infected COM and changes related to bone remodeling (86).

The diagnosis of COM could be difficult especially if superimposed on changes due to trauma or surgery (87, 88). Meta-analysis study comparing MRI, radionuclide imaging, and 18F-FDG PET for the diagnosis of COM demonstrated the following sensitivity and specificity: ^{99m}Tc-MDP 61% and 25%, WBC scintigraphy 78% and 77%, MRI 84% and 60%, and 18F-FDG PET 96% and 91%, respectively (87). Meta-analysis comparing MRI, 18F-FDG PET, and radionuclide imaging of COM resulted in the following sensitivity and specificity for peripheral open fractures and prosthetic joint infection: gallium-67 70% and 82%, ^{99m}Tc-MDP 89% and 89%, 111-In WBC 83% and 84%, MRI 88% and 85%, and 18F-FDG PET 94% and 87%, respectively (88).

In a prospective study of 30 patients, COM was proven in 11/36 regions of suspected skeletal infection and subsequently excluded in 25/36 regions (92). 111-In WBC scintigraphy was positive in only 2 of the 11 regions with COM. Seven of the false-negative results were in the axial skeleton. 18F-FDG PET detected all regions (11/11) with COM. 18F-FDG PET and 111-In WBC were each false positive in two cases (92).

These studies, therefore, suggest that 18F-FDG PET is the imaging study of choice for the diagnosis of COM (low evidence) (87–92) (Table 17.3).

IV. What Is the Diagnostic Performance of the Different Imaging Studies in Septic Hip Arthritis?

Summary of Evidence: The sensitivity of plain radiographs for hip joint effusion is low (limited evidence) (28).

Ultrasound is highly sensitive for the evaluation of hip effusion (limited evidence) (27–30). However, it cannot distinguish between infectious (septic arthritis) and other noninfectious causes of joint effusions (27–30). The absence of hip effusion by ultrasound is reliable for exclusion of septic hip (limited to moderate evidence) (27–30). Rare exceptions have been reported if symptoms were less than 24 hours (29).

MRI is highly sensitive for joint effusion. Several studies suggest that MRI can differentiate between septic hip arthritis and transient synovitis, based on the presence of bore marrow edema or decreased perfusion of the femoral lead (insufficient evidence) (93, 94).

Supporting Evidence

Radiography

Pelvic radiography is usually the first imaging performed for evaluating a child with suspected septic hip joint. The "joint space" seen on plain radiograph in the immature bone represents the nonossified femoral head, the articular cartilage, and the true joint space. Indirect signs for joint effusion include lateral displacement of the femoral head (distance of the ossified femoral head from the pelvis teardrop) and displacement of the fat pads. The sensitivity of plain radiograph for joint effusion is low (limited evidence) (28).

Ultrasonography

Ultrasound is highly sensitive for the evaluation of joint effusion (27–30). No ultrasound characteristics, including complexity of the fluid, quantity of fluid, and adjacent hyperemia on color Doppler imaging, have shown to be

definitive in distinguishing septic arthritis versus other noninfectious causes of joint effusions (27–30). The absence of hip effusion by ultrasound is reliable for exclusion of septic hip (limited to moderate evidence) (27–30).

MR Imaging

MRI is highly sensitive for hip joint effusion. Several studies demonstrated that bone marrow edema in the femur is associated with septic hip (93). Another finding that correlated with septic hip is decreased femoral hip enhancement (94). Those findings are based on small series of patients. The evidence is, therefore, insufficient. In addition, the use of MRI may not be practical due to costs and availability in an urgent situation.

Take Home Figure

What Are the Roles of the Imaging Modalities in the Evaluation of Acute Osteomyelitis and Septic Arthritis?

The decision tree in Fig. 17.1 outlines the role of each imaging modality in the evaluation of suspected osteomyelitis. The plain radiograph is the initial imaging evaluation due to its relative low cost, rapid acquisition, and ready availability. If there is frank evidence for osteomyelitis on the radiograph, immediate antibiotic therapy can be instituted and further imaging may not be necessary, as up to 80% of patients are successfully treated with antibiotics alone.

If the radiograph is negative for osteomyelitis and there are no localizing symptoms clinically, radionuclide bone scintigraphy is the next imaging modality, based on its ability to provide whole-body imaging.

If there are localized symptoms, MRI would be a better choice due to higher resolution, more specificity, and ability to immediately evaluate for complications.

In chronic osteomyelitis, especially in the axial skeleton, 18F-FDG PET is the preferred imaging modality.

If acute symptoms are referable to the hip, an ultrasound can be performed to rapidly evaluate for the presence of an effusion and also to provide image-guided joint aspiration. See the decision tree in Fig. 17.2.

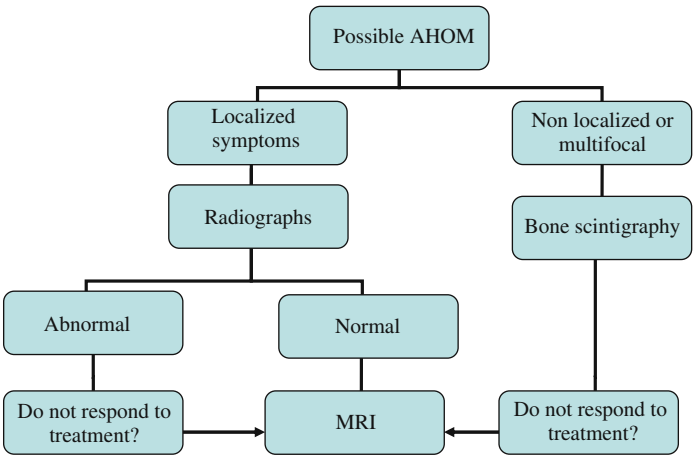

Figure 17.1. Algorithm for imaging suspected osteomyelitis in the pediatric population.

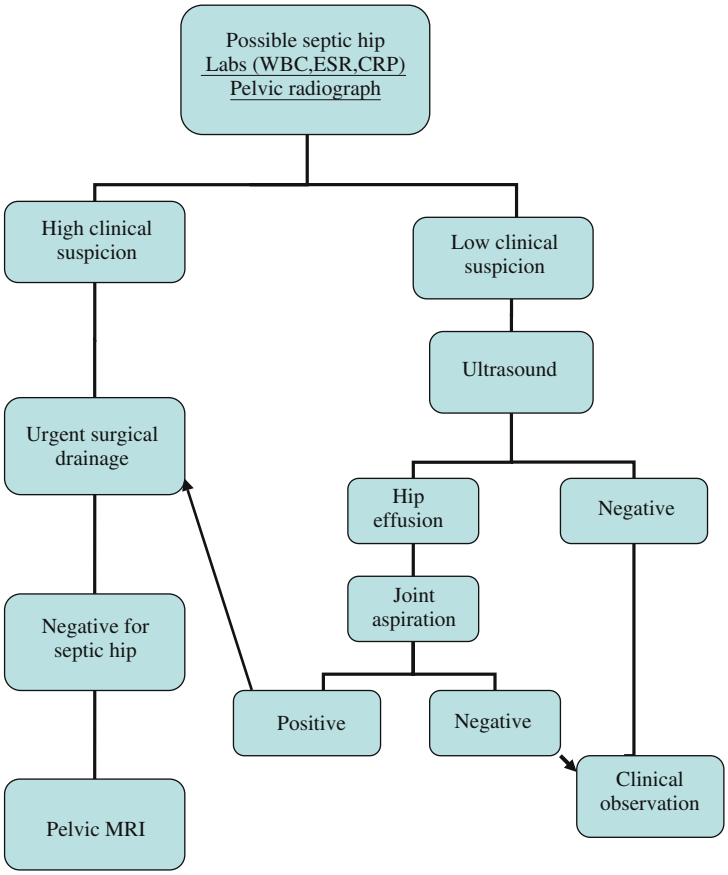

Figure 17.2. Algorithm for imaging suspected septic hip arthritis in the pediatric population (WBC, white blood cell; ESR, erythrocyte sedimentation rate; CRP, C-reactive protein).

Table 17.1 summarizes the literature search on osteomyelitis and septic arthritis. Table 17.2 discusses the diagnostic performance characteristics of imaging studies for acute hematogenous osteomyelitis. Table 17.3 discusses the diagnostic performance characteristics of imaging studies for chronic osteomyelitis.

Table 17.1. Summary of the literature search on osteomyelitis and septic arthritis (January 1966–October 2008)

Type of study	Number of manuscripts
Meta-analysis	2
Case series	99
Case reports	189
Reviews	29

Table 17.2. Diagnostic performance characteristics of imaging studies for acute hematogenous osteomyelitis based on studies in children and adults

	Sensitivity (%)	Specificity (%)
Plain radiograph (36–38, 67)	43–75	75–83
Ultrasound (75–78)	46–74	74–100
^{99m}TC bone scintigraphy (39–43, 46, 51, 68, 69)	73–100 (32–87% in infants)	73–79
MRI (37, 58–65)	82–100	75–96
18F-FDG PET (54, 73)	98	75–79

Table 17.3. Diagnostic performance characteristics of imaging studies for chronic osteomyelitis based on meta-analysis of 23 studies mainly in the adult population

	Sensitivity (%)	Specificity (%)
WBC scintigraphy	78	71
^{99m}TC bone scintigraphy	61	25
MRI	84	60
18F-FDG PET	96	91

Data from Termaat et al. (87).

Imaging Case Studies

Case 1

Figure 17.3 is a case of a 2-month-old male with distal right femoral osteomyelitis who presented with flexion at the right hip and knee.

Figure 17.3. A 2-month-old male with distal right femoral osteomyelitis presented with flexion at the right hip and knee. He did not move his right hip for 8 days. Plain radiograph of the right femur demonstrates distal metaphyseal lucency (*arrow*).

Case 2

Figure 17.4 is a case of a 4-year-old female with right septic hip who presented to the emergency room with fever and decreased weight bearing on the right leg.

Figure 17.4. A 4-year-old female with right septic hip who presented to the emergency room with fever and decreased weight bearing on the right leg. Hip ultrasound demonstrates a large hip effusion. Pus was drained from the joint.

Case 3

Figure 17.5 presents the case of a 3-year-old male with CA-MRSA sepsis, osteomyelitis of the right parietal bone, epidural abscess, septic pulmonary embolism, pyomyositis, and multifocal osteomyelitis.

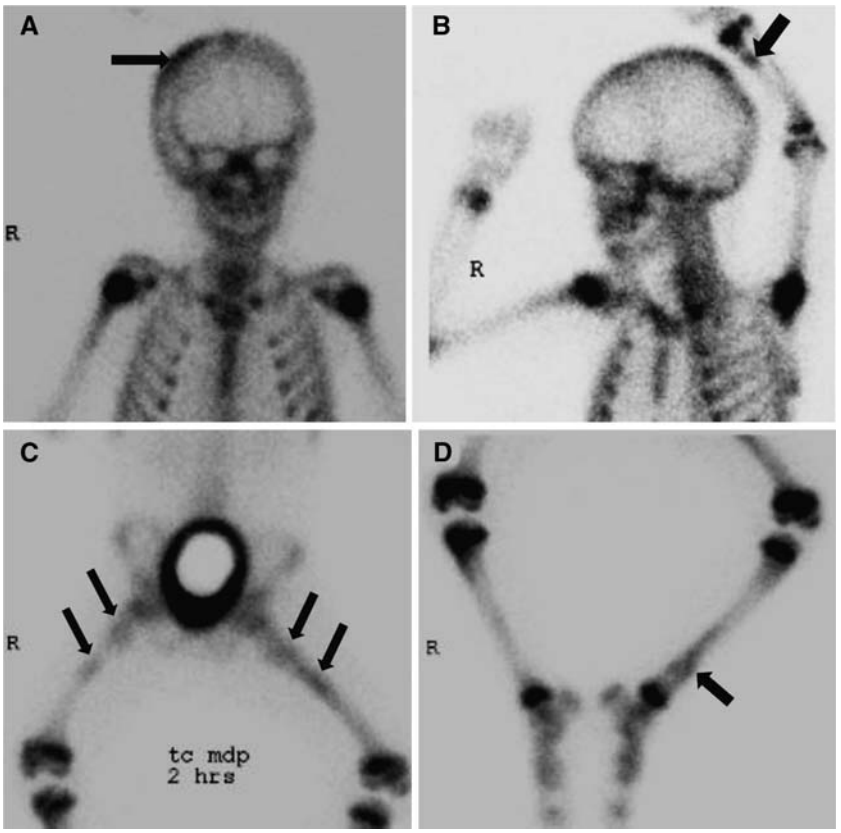

Figure 17.5. A 3-year-old male with CA-MRSA sepsis, osteomyelitis of the right parietal bone, epidural abscess, septic pulmonary embolism, pyomyositis, and multifocal osteomyelitis. He had a close hair cut at home and presented a few days later with swelling of the head and neck and refused to ambulate. ^{99m}Tc-MDP bone scan demonstrates increased uptake in the right parietal bone (**A**, *arrow*), the distal left radius (**B**, *arrow*), both femurs (**C**, *arrows*) and distal left tibia (**D**, *arrow*), compatible with multifocal osteomyelitis.

Case 4

Figure 17.6 shows the case of an 8-year-old female with left femur osteomyelitis and large subperiosteal abscess who presented with a 5-day history of fever and left leg pain that became increasingly worse.

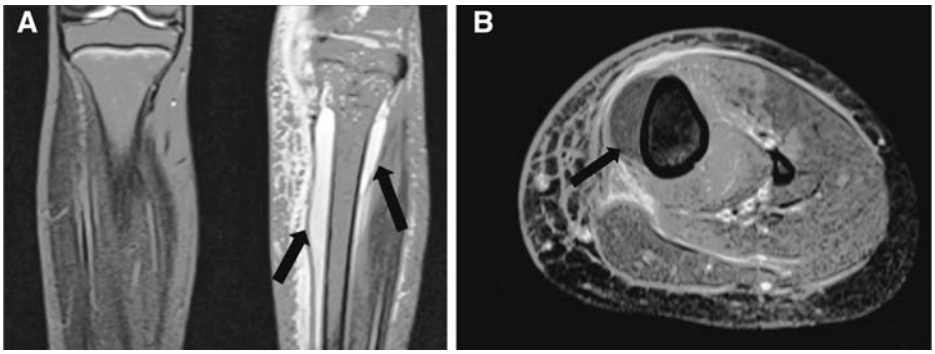

Figure 17.6. An 8-year-old female with left femur osteomyelitis and large subperiosteal abscess who presented with a 5-day history of fever and left leg pain that became increasingly worse. **A**: Coronal MRI STIR shows extensive high heterogenous bone marrow signal involving the proximal left tibial metadiaphysis and epiphysis, muscle and subcutaneous edema. A large subperiosteal abscess is demonstrated on both the coronal STIR (A, *black arrows*) and the axial T1 SE, fat suppression postcontrast (**B**, *arrow*). Incision and drainage were performed for both the tibial osteomyelitis and the subperiosteal abscess.

Suggested Imaging Protocols for Hematogenous Osteomyelitis and Septic Arthritis in Children

Radiography

At least two orthogonal views of the body part of interest. Views of the opposite limb may be useful for comparison to detect subtle changes.

Should be performed on all patients with suspected osteomyelitis or septic arthritis to evaluate for destruction, as well as exclude other pathologies such as tumors or fractures.

Radionuclide Bone Scintigraphy

Three-phase radionuclide bone scintigraphy with Tc-99m-labeled MDP. Planar images during blood flow and soft tissue phases. Planar images of extremities and SPECT images of the axial skeleton during bone phase. Should be used if symptoms are nonlocalizing or if there is suspicion for polyostotic disease.

MRI

Axial T1 SE and T2 FSE with fat saturation, coronal STIR and T1 SE, and axial and coronal T1 SE with fat saturation after intravenous gadolinium. Sagittal images are optional and dependent on location of bone and soft tissueabnormalities.

Should be performed if there are localizing symptoms.

Ultrasound

Linear transducer high-frequency probe (7–17 MHz). Compare with opposite joint for symmetry. Ultrasound should be performed to evaluate for joint effusion and joint aspiration. Most commonly used for the hip joint.

Future Research

- Can the use of whole-body MR imaging technique obviate the need for radionuclide scintigraphy in the evaluation of multifocal osteomyelitis?
- Can MR with gadolinium provide more information than ultrasound in the evaluation of septic arthritis?
- Can findings on imaging (plain film, MR, ultrasound) predict the likelihood of success

of medical therapy alone or provide early triage to surgical therapy?
- Does PET-CT have a role in the evaluation of acute osteomyelitis?

References

1. Pineda C, Vargas A, Rodríguez AV. Infect Dis Clin North Am 2006;4: 789–825.
2. Blickman JG, van Die CE, de Rooy JW. Eur Radiol 2004;14(Suppl 4): L55–L64.
3. Steer AC, Carapetis JR. Paediatr Drugs 2004; 6(6):333–346.
4. Oudjhane K, Azouz EM. Radiol Clin North Am 2001; 39(2): 251–266.
5. Faden H, Grossi M. Am J Dis Child 1991; 145(1): 65–69.
6. Kao HC, Huang YC, Chiu CH, Chang LY, Lee ZL, Chung PW et al. J Microbiol Immunol Infect 2003; 36(4):260–265.
7. Arnold SR, Elias D, Buckingham SC, Thomas ED, Novais E, Arkader A et al. J Pediatr Orthop 2006; 26(6):703–708.
8. Browne LP, Mason EO, Kaplan SL, Cassady CI, Krishnamurthy R et al. Pediatr Radiol 2008;38(8):841–847.
9. Dohin B, Gillet Y, Kohler R, Lina G, Vandenesch F, Vanhems P et al. Pediatr Infect Dis J 2007; 26(11):1042–1098.
10. Gillet Y, Vanhems P, Lina G, Bes M, Vandenesch F, Floret D et al. Clin Infect Dis 2007;1;45(3):315–321.
11. Martínez-Aguilar G, Avalos-Mishaan A, Hulten K, Hammerman W, Mason EO Jr et al. Pediatr Infect Dis J 2004; 23(8):701–706.
12. Teo HE, Peh WC. Pediatr Radiol 2004; 34(11): 853–860.
13. McPherson DM. Neonatal Netw 2002; 21(1):9–22
14. Offiah AC. Euro J Radiol 2006; 60(2): 221–232.
15. Dormans JP, Drummond DS. J Am Acad Orthop Surg 1994; 2(6):333–341.
16. Nixon GW. Am J Roentgenol 1978; 130(1): 123–129.
17. Howard CB, Einhorn M, Dagan R, Yagupski P, Porat S. J Bone Joint Surg Br 1994; 76(2): 311–314.
18. Barton LL, Dunkle LM, Habib FH. Am J Dis Child 1987; 141(8): 898–900.
19. Azou EM, Greenspan A, Marton D. Skeletal Radiol 1993; 22(1): 17–23.
20. Welkon CJ, Long SS, Fisher MC, Alburger PD. Pediatr Infect Dis 1986; 5(6): 669–676.
21. Choi IH, Shin YW, Chung CY, Cho TJ, Yoo WJ et al. J Bone Joint Surg Am 1990 72(8): 1150–1165.
22. Betz RR, Cooperman DR, Wopperer JM, Sutherland RD, White JJ Jr, Schaaf HW et al. J Pediatr Orthop 1990;10(3): 365–372.
23. Alderson M et al. J Bone Joint Surg Br 1986; 68(2): 268–274.
24. Kocher MS, Mandiga R, Zurakowski D, Barnewolt C, Kasser JR. J Bone Joint Surg Am 2004;86(8):1629–1635.
25. Caird MS, Flynn JM, Leung YL, Millman JE, D'Italia JG et al. J Bone Joint Surg Am 2006;88(6):1251–1257.
26. Zurakowski D, Kasser JR. J Bone Joint Surg Am 1999: 81(12): 1662–1670.
27. Zawin JK, Hoffer FA, Rand FF, Teele RL. Radiology 1993;187(2):459–463.
28. Zamzam MM. J Pediatr Orthop B 2006; 15(6):418–422.
29. Miralles M, Gonzalez G, Pulpeiro JR, Millán JM, Gordillo I, Serrano C et al. Am J Roentgenol 1989; 152(3):579–582.
30. Gordon JE, Huang M, Dobbs M, Luhmann SJ, Szymanski DA et al. J Pediatr Orthop 2002; 22(3):312–316.
31. Asmar BI. Infect Dis Clin North Am 1992; 6(1): 117–132.
32. Caksen H, Oztürk MK, Uzüm K, Yüksel S, Ustünbaş HB et al. Pediatr Int 2000; 42(5): 534–540.
33. Perlman MH, Patzakis MJ, Kumar PJ, Holtom P. J Pediatr Orthop 2000; 20(1): 40–43.
34. Wang CL, Wang SM, Yang YJ, Tsai CH, Liu CC. J Microbiol Immunol Infect 2003; 36(1): 41–46.
35. Zucker MI, Yao L. West J Med 1992; 156(3): 297–298.
36. Bonakdar-pour A, Gaines VD. Orthop Clin North Am 1983; 14(1): 21–37.
37. Jaramillo D, Treves ST, Kasser JR, Harper M, Sundel R et al. Am J Roentgenol 1995; 165(2): 399–403.
38. Gold R. Pediatr Infect Dis J 1995; 14(6): 555.
39. Duszynski DO, Kuhn JP, Afshani E, Riddlesberger MM Jr. Radiology 1975; 117(2): 337–340.
40. Gelfand MJ, Silberstein EB. JAMA 1977;237(3): 245–257.
41. Hankins JH, Flowers WM, Jr. J Miss State Med Assoc 1978; 19(1):10–12.
42. Nelson HT, Taylor A. Eur J Nucl Med 1980; 5(3):267–269.
43. Erasmie U, Hirsch G. Z Kinderchir 1981; 32(4): 360–366.
44. McAndrew PT, Clark C. BMJ 1998; 316(7125): 147.
45. Middleton MS. Am J Roentgenol 1988; 151(3): 612–613.
46. Sullivan DC, Rosenfield NS, Ogden J, Gottschalk A. Radiology 1980; 135(3): 731–736.

47. Wald ER, Mirro R, Gartner JC. Clin Pediatr (Phila) 1980; 19(9): 597–601.
48. Jones DC, Cady RB. J Bone Joint Surg Br 1981; 63-B(3): 376–378.
49. Berkowitz ID, Wenzel W. Am J Dis Child 1980; 134(9): 828–830.
50. Handmaker H. Radiology 1980;135(3): 787–789.
51. Barron BJ, Dhekne RD. Clin Nucl Med 1984; 9(7): 392–393.
52. Park HM, Rothschild PA, Kernek CB. Am J Roentgenol 1985; 145(5): 1079–1084.
53. Kälicke T, Schmitz A, Risse JH, Arens S, Keller E, Hansis M et al. Eur J Nucl Med 2000; 27(5):524–528.
54. Stumpe KD, Dazzi H, Schaffner A, von Schulthess GK. Eur J Nucl Med 2000;27(7): 822–832.
55. Modic MT, Pflanze W, Feiglin DH, Belhobek G. Radiol Clin North Am 1986; 24(2): 247–258.
56. Unger E, Moldofsky P, Gatenby R, Hartz W, Broder G. Am J Roentgenol 1988; 150(3): 605–610.
57. Morrison WB, Schweitzer ME, Bock GW, Mitchell DG, Hume EL, Pathria MN et al. Radiology 1993; 189(1): 251–257.
58. Fletcher BD, Scoles PV, Nelson AD. Radiology 1984; 150(1): 57–60.
59. Berquist TH, Brown ML, Fitzgerald RH Jr, May GR. Magn Reson Imaging 1985; 3(3): 219–230.
60. Dangman BC, Hoffer FA, Rand FF, O'Rourke EJ. Radiology 1992; 182(3): 743–747.
61. Mazur JM, Ross G, Cummings J, Hahn GA Jr, McCluskey WP. J Pediatr Orthop 1995; 15(2): 144–147.
62. Mentzel HJ, Kentouche K, Sauner D, Fleischmann C, Vogt S, Gottschild D et al. Eur Radiol 2004; 14(12): 2297–2302.
63. Laffan EE, O'Connor R, Ryan SP, Donoghue VB. Pediatr Radiol 2004 Jun;34(6):472–480.
64. Darge K, Jaramillo D, Siegel MJ. Whole-body MRI in children: Current status and future applications. Eur J Radiol 2008; 68(2): 289–298.
65. Capitanio MA, Kirkpatrick JA. Am J Roentgenol Radium Ther Nucl Med 1970; 108(3): 488–496.
66. Wenaden AE, Szyszko TA, Saifuddin A. Clin Radiol 2005;60(4):439–456.
67. Kaye JJ. Pediatr Ann 1976; 5(1): 11–31.
68. Ash JM, Gilday DL. J Nucl Med 1980; 21(5): 417–420.
69. Bressler EL, Conway JJ, Weiss SC. Radiology 1984; 152(3): 685–688.
70. Handmaker H, Leonards R. Semin Nucl Med 1976; 6(1): 95–105.
71. Connolly LP, Connolly SA, Drubach LA, Jaramillo D, Treves ST. J Acute Nucl Med 2002; 43(10): 1310–1316.
72. Deysine M Robinson R Rafkin H Teicher I Silver L et al. Ann Surg 1974; 180(6): 897–901.
73. Stumpe KD, Strobel K. Q J Nucl Med Mol Imaging 2006;50(2):31–42.
74. Kaiser S, Jorulf H, Hirsch G. Acta Radiol 1998 Sep;39(5):523–531.
75. Abiri MM, Kirpekar M, Ablow RC. Radiology 1989; 172(2):509–511.
76. Azam Q, Ahmad I, Abbas M, Syed A, Haque F. Acta Orthop Belg 2005; 71(5): 590–596.
77. Riebel TW, Nasir R, Nazarenko O. Radiology; 1996; 26(4):291–297.
78. Nath AK, Sethu AU. Br J Radiol 1992; 65(776):649–652.
79. Kuhn JP, Berger PE. Radiology 1979;130(2): 503–506.
80. Gold RH Hawkins RA Katz RD. Am J Roentgenol 1991;157(2):365–370.
81. Pretorius ES, Fishman EK. Radiol Clin North Am 1999; 37(5):953–974.
82. Karmazyn B, Loder RT, Kleiman MB, Buckwalter KA, Siddiqui A, Ying J et al. J Pediatr Orthop 2007;27(2): 158–164.
83. Connolly SA, Connolly LP, Drubach LA, Zurakowski D, Jaramillo D. Am J Roentgenol 2007 Oct;189(4):867–872.
84. Lopes TD, Reinus WR, Wilson AJ. Invest Radiol 1997; 32(1):51–58.
85. Wing VW, Jeffrey RB Jr, Federle MP, Helms CA, Trafton P. Radiology 1985; 154(1) :171–174.
86. Tumeh SS, Aliabadi P, Seltzer SE, Weissman BN, McNeil BJ. Clin Nucl Med 1988; 13(10): 710–715.
87. Termaat MF, Raijmakers PG, Scholten HJ, Bakker FC, Patka P et al. J Bone Joint Surg Am 2005; 87(11):2464–2471
88. Prandini N, Lazzeri E, Rossi B, Erba P, Parisella MG et al. Nucl Med Commun 2006; 27(8): 633–644.
89. Guhlmann A, Brecht-Krauss D, Suger G, Glatting G, Kotzerke J, Kinzl L et al. Radiology 1998; 206(3):749–754.
90. Zhuang H, Duarte PS, Pourdehand M, Shnier D, Alavi A. Clin Nucl Med 2000; 25(4):281–284.
91. Kälicke T, Schmitz A, Risse JH, Arens S, Keller E, Hansis M et al. Eur J Nucl Med 2000; 27(5): 524–528.
92. Meller J, Köster G, Liersch T, Siefker U, Lehmann K, Meyer I et al. Eur J Nucl Med Mol Imaging 2002; 29(1):53–56.
93. Lee SK, Suh KJ, Kim YW, Ryeom HK, Kim YS, Lee JM et al. Radiology 1999;211(2):459–465.
94. Kwack KS, Cho JH, Lee JH, Cho JH, Oh KK et al. Am J Roentgenol 2007; Aug;189(2): 437–445.

18

Imaging of Pediatric Bone Tumors: Osteosarcoma and Ewing Sarcoma

Geetika Khanna

Issues

I. What is the recommended imaging approach for evaluation of suspected bone tumors?
II. What is the best imaging modality for local staging of pediatric bone sarcomas?
III. Do imaging findings of the primary tumor have prognostic significance?
IV. What is the frequency of skip bone metastases and what is the best imaging modality to detect them?
V. What imaging studies should be performed for staging of pediatric bone sarcomas?
VI. What is the best imaging method to assess response to chemotherapy?
VII. What is the appropriate imaging protocol for posttreatment surveillance of these malignancies?

Key Points

- The initial imaging test for suspected bone tumors is radiography. Some lesions can be definitely determined to be benign (nonaggressive) based on radiography alone, but in other cases, surgical excision or biopsy will be necessary for diagnosis (limited evidence).
- Local staging of bone sarcomas is best performed with contrast-enhanced MRI. Precontrast T1-weighted images best depict intraosseous extent, while postcontrast images evaluate soft tissue component and joint invasion (moderate to limited evidence).
- *Prognosis*: Large tumor size is a poor prognostic factor for both OS and ES and correlates with the presence of distant metastases (moderate evidence). Intensity of uptake on PET may correlate with prognosis/survival (limited evidence).

G. Khanna (✉)
Washington University School of Medicine, 510 S. Kings highway, Campus Box 8131-MIR, St Louis, MO 63110
e-mail: geetika.khanna@iuowa.edu

L.S. Medina et al. (eds.), *Evidence-Based Imaging in Pediatrics*,
DOI 10.1007/978-1-4419-0922-0_18,

- Skip metastases in the bone are best detected on T1-weighted MR images (moderate evidence).
- *Staging*: Chest CT is essential to detect lung metastases. Detection of bone metastases is best performed with scintigraphy for OS and with FDG-PET for ES (moderate to limited evidence).
- While reduction of tumor size correlates with response in Ewing's sarcoma, this is not true for OS. The role of imaging in assessing response to chemotherapy remains limited (moderate evidence).
- Optimal posttreatment imaging surveillance protocols are not well defined. The recommendations from the children's oncology group have been summarized.

Definition and Pathophysiology

Osteosarcoma and Ewing's sarcoma account for approximately 90% of pediatric malignant bone tumors (1, 2). OS is an osteoid-producing tumor that most commonly occurs in the metaphysis (90%), though it can occur in the diaphysis (9%) or epiphysis (1%) of bone as well (3). ES is a small, round, blue cell tumor that can arise in the bone or soft tissues. Osseous ES has been classically described as occurring in the diaphysis (33%), though the metadiaphyseal location is actually more common (44%) (4).

Conventional OS is a high-grade, intramedullary tumor that comprises 75% of OSs (3). These tumors are typically large (>6 cm) with osteoid matrix production giving a fluffy density, aggressive periosteal reaction, Codman's triangle, and a soft tissue mass. Less common are the parosteal (3% of cases), periosteal (1%), and telangiectatic (10%) variants of OS. Telangiectatic OS is characterized by multiple, aneurysmally dilated, blood-filled cavities with high-grade, sarcomatous cells in the periphery. It has been shown to have similar prognosis as high-grade conventional OS (5). Parosteal OS is the most common surface OS that classically arises from the posterior aspect of the distal femur (6). It is a low-grade tumor with an excellent prognosis (7). Its typical radiographic appearance is that of a dense mineralized lobulated mass attached to the outer cortex by a broad-based stalk. Periosteal OS, the next most common surface OS, tends to involve the diaphysis of long bones (8). Although it is associated with a better prognosis than conventional or high-grade surface OS, periosteal OS is a malignant tumor that tends to recur and metastasize.

Ewing's sarcoma can have a mixed lytic–sclerotic pattern (75%) or a purely lytic appearance (25%) (9). Plain films and CT can show a spiculated periosteal reaction (50%) or a Codman's triangle (27%). Cortical permeation and destruction is seen in 31 and 42%, respectively, whereas cortical thickening is seen in 20%. The most characteristic finding on MRI is the presence of a large soft tissue mass.

Patients with bone malignancies may present with pain, functional impairment, or soft tissue mass (1). In addition, children with ES can have systemic symptoms, such as fever, anemia, weight loss, and elevated erythrocyte sedimentation rate, which can mimic osteomyelitis.

The pathogenesis of these tumors remains unclear. Identified risk factors for OS are exposure to ionizing radiation and genetic conditions like familial retinoblastoma and Li-Fraumeni syndrome. The increased risk of OS among patients with hereditary retinoblastoma and those with Li-Fraumeni syndrome points to pathogenetic roles of p53 and RB tumor suppressor genes (1). About 95% of patients with ES have a t(11;22) or t(21;22) translocation (10).

Epidemiology

Malignant bone tumors are rare worldwide, with approximately 650–700 cases diagnosed each year in the United States in children 0–19 years of age (11, 12). They account for 3–5% of cancers diagnosed in children under 15 years of age and 7–8% of those in adolescents

15–19 years of age (13). The incidence rates of OS and ES have not changed significantly between 1987 and 2001 in the United States (12). The two most common types of malignant bone tumors in children are OS and ES, accounting for 51 and 41% of all pediatric bone malignancies, respectively. The overall rates for OS and ES are 4.6 and 3.0 cases per million children of 0–19 years of age in the United States, respectively (12). All types of bone tumors are very rare before the age of 4 years with a peak incidence at the age of 13 years in girls and 15 years in boys. The incidence in young adults (20–24 years of age) is substantially lower than that at the peak in adolescence (14). The rate of bone sarcomas is somewhat higher in males than in females (ratio 1.2:1) (11).

OS and ES have striking contrasts in their incidence patterns, particularly with respect to race and location. While OS occurs at roughly the same rate among blacks and whites, ES is 11 times more common in white children as compared to blacks (15). With regard to location, while 80% of OS cases occur around the knee, 45% of ES occur in the central skeleton and 30% in the lower limbs (11). These facts have given significant insight into the etiologic investigations of these malignancies. It appears that bone growth and development play an important role in the occurrence of OS (16). The racial disparity in the occurrence of ES and its relatively uniform distribution in the body suggest a genetic predisposition.

Though the survival rate of bone sarcomas has improved significantly over the last two decades, it remains lower than that for childhood cancers overall. The 5-year survival rate for bone cancers in children is 65% compared to 76% for all pediatric malignancies (12). Survival is only slightly higher for OS than for ES, with respective 5-year survival rates of 64.3 and 61.5%.

Overall Cost to Society

There are very limited data in the literature regarding the cost of imaging pediatric bone sarcomas. The costs would include imaging for detection of a suspected malignant bone tumor, initial staging, assessing response to therapy prior to surgery, and the cost of surveillance imaging. We were able to find one study from Stockholm evaluating the cost of surveillance MRI performed over the period 1997–2001 (17). However, this study comprised primarily an adult population and included both low-grade and high-grade musculoskeletal sarcomas. Surveillance MRI was performed 6 months, 1 year, and then annually after surgery for 5 years. The authors concluded that surveillance MRI was cost-effective with a cost just under £6,000 per recurrence detected.

Goals

The ultimate goal of imaging is to decrease the morbidity and mortality of children from malignant bone tumors. This would be achieved by timely detection of tumors, accurate local staging to allow limb-sparing surgery, and detection of metastases to provide appropriate therapy. An imaging method that would allow early and accurate differentiation between good responders and nonresponders would help tailor chemotherapy to individual patients. Finally, surveillance imaging would be effective only if it helps improve survival in a cost-effective fashion.

Methodology

The author searched the literature for both primary literature (scientific articles) and secondary literature (evidence-based reviews) on this topic. The National Library of Medicine (NLM) database, MEDLINE, was searched using the PubMed search engine for primary evidence over the period 1966–2008. Articles were retrieved using the following medical subject heading (MeSH) terms that applied to the clinical question: (1) OS; (2) Ewing's sarcoma; (3) imaging; (4) MRI or magnetic resonance imaging; (5) CT or computed tomography; (6) scintigraphy; and (7) PET or positron emission tomography. The following limits were applied to restrict the focus of our search: humans, English language, and all children. The title and abstracts of the retrieved papers were reviewed to find relevant literature. The bibliographies of these articles were also reviewed to identify any other relevant papers.

Discussion of Issues

I. What Is the Recommended Imaging Approach for Evaluation of Suspected Bone Tumors?

Summary of Evidence: The initial evaluation of an osseous lesion should start with plain radiographs. In most cases the diagnosis can be established on plain radiographs, and advanced imaging is performed for staging/preoperative planning (limited evidence).

Supporting Evidence: The initial evaluation of a suspected bone lesion should include two orthogonal plain radiographs of the entire lesion. Plain radiography is the most important imaging tool in determining the biologic activity and very often histology of bone lesions. Imaging features to consider in the interpretation of radiographs include pattern of bone destruction, margin of lesion, presence and nature of matrix, cortical erosion, presence and type of periosteal reaction, and presence of associated soft tissue mass. Lodwick et al. have shown that radiographs can be used to estimate rate of growth of focal bone lesions (18). They showed that a permeative or moth-eaten appearance can be seen in 88% of OS and 83% ES cases secondary to their aggressive nature. Most OSs have a radiographic appearance that poses little diagnostic dilemma, while ES can mimic osteomyelitis both radiographically and clinically. In a series of 50 OS patients, 35 had a mixed lytic–blastic appearance, 8 were lytic, and 7 were purely lytic (19). OS tends to violate the cortex resulting in aggressive periosteal reaction. Various terms have been used to describe this aggressive pattern of periosteal reaction, including Codman triangle, laminated, hair-on-end, or sunburst pattern. Aggressive periosteal reaction can be seen in 80–90% of osteosarcoma cases (3). Laminated periosteal reaction has been described in 57% of ES patients (20). Approximately 96% of ESs are poorly marginated on radiographs and 76% have a permeative component (20). In a review of 64 patients (mean age 17.9 years) with ES, 75% of cases were shown to have a mixed sclerotic–lytic appearance, with an aggressive spicular periosteal reaction present in 50% of cases and a laminated periosteal reaction seen in 14% of cases (9). However, we were unable to find any data on the accuracy or predictive value of these imaging characteristics in differentiating malignant from benign bone lesions.

II. What Is the Best Imaging Modality for Local Staging of Pediatric Bone Sarcomas?

Summary of Evidence: In patients diagnosed with OS or ES, MRI is the imaging modality of choice for local staging. Precontrast T1-weighted images are best suited to evaluate for the extent of marrow replacement and transphyseal extension. Evaluation of intraarticular extension, muscular compartment involvement, and neurovascular encasement is best performed with postcontrast MR imaging (limited to moderate evidence).

Supporting Evidence: Accurate delineation of local tumor extent is essential in planning limb-sparing surgery for children with bone sarcoma. Local staging involves determination of the extent of intraosseous disease, evaluating for extension across physis and into the joint space, muscular compartment involvement by the soft tissue mass, and encasement of the neurovascular bundle. For soft tissue sarcomas, the anatomic site determines the extent of surgical resection and the need for additional therapies.

There is moderate evidence to suggest that MR has higher accuracy than CT and bone scintigraphy to determine the intraosseous extent of tumor (21). T1-weighted MR images have been shown to have the highest accuracy in determining the intraosseous extent of marrow replacement (22, 23). In a prospective study of 56 patients, Bloem et al. reported MR to have an accuracy of 98% in the detection of neurovascular bundle involvement by tumor, as compared to 82% for CT and 74% for angiography. However, the difference was not statistically significant (21). In the same study, MR was reported to have a sensitivity of 96% (95% CI: 91–99%) and a specificity of 99% (95% CI: 97–100%), as compared to a sensitivity of 71% (95% CI: 63–79%) and a specificity of 93% (95% CI 89–95) for CT in the detection of muscular involvement.

MRI has been shown to depict transphyseal extension with high sensitivity but low specificity (23) (24) (25) (limited evidence). Hoffer et al. found T1-weighted images to have a specificity of 60% in evaluating for transphyseal extension of tumor, as compared to 40% for STIR (short tau inversion recovery) images (24). Both sequences however had 100% sensitivity in detecting transphyseal extension in their study of 40 children with OS. In another study of 20 children with newly diagnosed OS, MRI using T1-weighted and STIR images was shown to have 100% sensitivity and 50% specificity in detecting epiphyseal involvement by tumor (23). The accuracy of MRI in determining transphyseal extension can be affected by peritumoral edema. While tumor is dark on T1-weighted images and causes architectural distortion, peritumoral edema has intermediate signal on T1-weighted images and does not distort normal bone architecture. Both are, however, bright on T2-weighted images and both can show enhancement (24) (limited evidence).

There is limited evidence for the role of MRI in evaluating intraarticular extension. Schima et al. evaluated the efficacy of preoperative MR in detecting joint involvement in 46 OS patients (mean age 20.5 years) (26). They found postcontrast T1-weighted images to be most useful with a reported sensitivity of 100% and specificity of 69%. Extraosseous tumor growth causing displacement of the joint capsule may result in a false-positive diagnosis of joint invasion. Postcontrast T1-weighted images have been shown to be most useful in evaluating intraarticular extension, while T2-weighted images are limited as peritumoral edema can have similar signal characteristics as the tumor itself. In detecting tumor involvement of the joint, the presence of a joint effusion had a positive predictive value of 27% and a negative predictive value of 92% (26) (limited evidence).

III. Do Imaging Findings of the Primary Tumor Have Prognostic Significance?

Summary of Evidence: Tumor size, as estimated on radiographs or advanced imaging, has been shown to be a significant prognostic factor in OS and ES patients (moderate evidence).

Supporting Evidence

Anatomic Imaging

There is moderate evidence that absolute tumor volume estimated on plain radiographs is an important risk factor and can be used to stratify OS patients for risk-adapted therapy (27, 28). In a study of 128 OS patients (children and adults), Bieling et al. showed that none of 19 patients with an absolute tumor volume 70 cc and only 4 of 53 with an absolute tumor volume 150 cc relapsed, while in patients with an absolute tumor volume more than 150 cc, the relapse rate was 40–60% (27). These initial studies were based on measurements obtained on plain films. In a more recent study of 42 patients, Kaste et al. showed that tumor volume and anteroposterior tumor depth as measured on MRI were statistically significant predictors of overall survival and event-free survival in children with nonmetastatic OS (29). They showed that patients with tumor volumes >150 cc were 3.6 times more likely to die compared to patients with smaller tumor volumes (95% CI: 0.9–13.9). The estimated 5-year overall survival for patients with tumor volume 150 cc was 87.5 $\pm$6.9% compared to 61.1 $\pm$ 12.1% for those with tumor volume >150 cc (limited evidence). However, Lee et al. found that tumor size adjusted for body surface area was a better prognostic factor than absolute tumor size as measured on MRI (30) (limited evidence).

Studies performed on ES patients have also shown a negative correlation between tumor volume at presentation and patient outcome (31, 32) (limited to moderate evidence). Reports from the European Intergroup Cooperative Ewing's sarcoma study group have shown that tumor volumes >100 ml have a statistically significant association with the presence of metastatic disease at presentation ($p < 0.0001$) (31). The outcome of patients with tumor volume under 200 ml has been shown to be a prognostic factor in determining disease-free survival and progression-free survival (32).

Functional Imaging

The role of *dynamic MRI* in determining tumor behavior is still under investigation. Preliminary studies suggested that tumor

vascularity estimated by dynamic vector magnitude on dynamic-enhanced MRI may correlate with response to therapy; however, these results were not confirmed in subsequent studies from the same group (33, 34) (limited to insufficient evidence).

Other imaging modalities that have been used to evaluate tumor behavior at diagnosis include *thallium 201 scintigraphy* and *FDG-PET*. Studies have suggested that presence of a central donut of photopenia on Tl-201 scintigraphy correlates with aggressive tumor behavior and negatively impacts survival (35, 36) (limited to insufficient evidence). In a study of 40 children with OS, Kaste et al. showed that 3-year estimates of event-free survival were 63.3 ± 11.6% for patients whose tumors exhibited a donut shape, compared to 94.4 ± 5.9% for patients without the donut shape. Several studies have shown a correlation between tumor aggressiveness and histologic grading with 18-FDG uptake on PET (37–39) (moderate evidence). A retrospective study of FDG-PET in 209 adults with sarcomas showed a statistically significant difference in disease-free survival between patients with tumors whose baseline SUVmax was more than 6 and those with tumors whose SUVmax was less than 6 (40). In a study including 52 patients with osteogenic sarcoma, an association between standardized uptake value (SUV) and overall survival has also been shown (40).

In summary, at this time, there is limited evidence suggesting that intensity of uptake on FDG-PET may have a prognostic value.

IV. What Is the Frequency of Skip Bone Metastases and What Is the Best Imaging Modality to Detect Them?

Summary of Evidence: T1-weighted MRI has been shown to be the most accurate for detection of skip metastases (moderate evidence).

Supporting Evidence: Skip metastases are defined as synchronous smaller foci of tumor occurring in the same bone anatomically separate from the primary lesion or as synchronous smaller foci of tumor on the opposing side of the joint (41, 42). The reported incidence of skip metastases in children with OS ranges from 1.8 to 25% (41–45). Skip metastases have been reported to be less common in children with Ewing's sarcoma (46). The outlook for patients with OS who present with skip metastasis is poor with a 5-year survival probability of 50% (43). MRI has been reported to be the most sensitive imaging technique for detection of skip metastases (43) (moderate evidence). The sensitivity of MRI for detection of skip lesions has been reported to be 83%, followed by 46% for (technetium 99 m) bone scans. The limited spatial resolution of bone scintigraphy may account for its lower accuracy in differentiating the primary tumor mass from skip metastases. The same study reported the sensitivity of radiography and CT in the detection of skip metastases at 36 and 50%, respectively (43). There is limited information on the role of PET in the detection of skip lesions at this time.

V. What Imaging Studies Should Be Performed for Staging of Pediatric Bone Sarcomas?

Summary of Evidence: The most common sites of metastatic disease from pediatric sarcomas are lungs, bone marrow, and bone. Chest CT is the imaging modality of choice for detection of lung metastases (moderate evidence). Recent data suggest that FDG-PET should replace bone scintigraphy for detection of bone marrow/bone disease in patients with ES (limited evidence). However, bone scintigraphy remains more sensitive than PET in the detection of distant disease in OS (moderate evidence).

Supporting Evidence: In a study of 215 patients with OS, the prevalence of metastatic disease at diagnosis has been reported to be 15%. The most common sites of metastases are the lungs and bone. The prevalence of metastatic disease in ES is higher and virtually all patients with ES are believed to have micrometastases at presentation. Up to 30% of ES patients have visible metastases at the time of initial presentation (47). The common sites of detectable metastases in ES are lungs, followed by bone and bone marrow (4). The presence of metastatic disease is a significant predictor of survival (28, 48). The 5-year survival rate is less than 40% for ES patients with lung metastases and less than 20%

for patients with bone marrow infiltration (49). Hence, detection of metastases and exact staging are essential for the best possible treatment and outcome.

Lung Metastases

For detection of lung metastases, the accuracy of chest CT remains the highest (50). Radiography has been shown to have a sensitivity of 32% in the detection of all pulmonary metastases as compared to chest CT (51). In a study of 71 patients with OS and ES, Franzius et al. found PET to have a sensitivity of 0.50 and a specificity of 0.98, while CT had a sensitivity of 1 and a specificity of 0.76 (52).The sensitivity of FDG-PET is particularly low in the detection of lesions smaller than 7 mm in size (52, 53) (moderate to limited evidence). This is likely due to the long acquisition time of PET, resulting in blurring due to breathing motion and due to partial volume effects.

Bone Metastases

Detection of bone metastases in ES and OS has predominantly been performed with Tc-99m-methylene diphosphonate (MDP) bone scintigraphy. However, recently FDG-PET has been shown to be superior to bone scintigraphy for the detection of bone metastases from Ewing's sarcoma (54). In a study of 49 ES with osseous metastases, the sensitivity, specificity, and accuracy of FDG-PET and bone scan were 1.00, 0.96, and 0.97 and 0.68, 0.87, and 0.82, respectively (55). The same study had five cases of OS with metastatic disease, none of which were detected by FDG-PET. So, the authors concluded that bone scintigraphy is more sensitive in the detection of osseous metastases from OS (55). Another prospective multicenter study compared the accuracy of PET and conventional imaging (including CT, MRI, and bone scintigraphy) for staging of pediatric sarcomas (53). This study found FDG-PET and conventional imaging to be equally sensitive (90%) for detection of metastatic disease in OS patients, while PET performed significantly better in the evaluation of ES (sensitivity 88% compared to 37% for conventional imaging including scintigraphy, $p<0.01$) (moderate evidence). A possible explanation for the high scintigraphic detection rate of skeletal OS metastases is the production of osteoid and osteoblastic activity. ES, however, tends to infiltrate the bone marrow and has predominantly osteolytic activity.

Whole-body MRI has also been used to stage pediatric sarcomas. The limited evidence that is available at this time suggests that though whole-body MRI maybe more sensitive than scintigraphy in the detection of marrow metastases, it is less sensitive than PET (56). The American College of Radiology Imaging Network has conducted a prospective study to compare the diagnostic performance of whole-body fast MRI with that of conventional imaging [the combination of chest CT, scintigraphy (bone or MIBG), and abdominal/pelvic CT/MRI as indicated] for detecting distant metastases in staging non-CNS small cell solid tumors in the pediatric population. The study has completed accrual and the results of this multicenter study are pending (http://www.acrin.org).

VI. What Is the Best Imaging Method to Assess Response to Chemotherapy?

Summary of Evidence: There is moderate evidence that conventional MRI has limited role in assessing response in OS. Tumor volume assessment on conventional MRI correlates with response in ES patients (moderate evidence). The role of molecular imaging techniques such as dynamic MRI, diffusion-weighted MRI, thallium scintigraphy, and PET is still under investigation. Both DEMRI and PET show promise in improved assessment of tumor response to treatment.

Supporting Evidence: The treatment of pediatric bone sarcomas is based on neoadjuvant chemotherapy designed to treat micrometastatic disease and reduce primary tumor volume to facilitate surgical resection. The degree of necrosis following induction chemotherapy is a major prognostic factor in predicting event-free survival (57–60). OS patients with histological evidence of less than 10% viable tumor postchemotherapy are classified as good responders. As histological evaluation is feasible only after surgery, there is a strong need for an imaging method to

noninvasively quantify tumor necrosis during chemotherapy.

Plain Radiographs

The role of radiography in evaluating response to treatment remains limited (moderate evidence). While some authors have reported that increasing soft tissue mass size and increased bone destruction are indicative of poor response (28), these findings have not been unanimously confirmed (61). Holscher et al. evaluated the role of radiography in assessing response to therapy in 22 patients with OS (61). The radiologic parameters studied included change in tumor diameter, definition of intraosseous and extraosseous margins, presence of pseudocapsule, development of ossification/calcification, periosteal reaction, cortical involvement, and development of fracture. They did not find a statistically significant association between any of the above parameters and histologic response to therapy. In another study of 47 pediatric patients with OS, Lawrence et al. found statistically significant association between poor histological response and an increase or no change in size of the soft tissue mass ($p<0.01$) and an increase in bone destruction ($p<0.02$) as evaluated on radiography (28). The above two radiographic features in combination had a sensitivity of 80% and a specificity of 66% in predicting poor response to chemotherapy.

MR Imaging

Magnetic resonance imaging is routinely used for initial and posttherapy evaluation of sarcomas. While an increase in tumor volume has been shown to correlate with poor histological response in OS (PPV 85–92%), decreased or unchanged tumor volume are unreliable predictors of good response (PPV 56–62%) (62, 63). This may be because tumor shrinkage for OS requires active resorption of the osteoid matrix by osteoclasts. There is moderate evidence that the change in tumor volume, as estimated on MRI, in ES patients correlates with chemotherapy-induced tumor necrosis (64, 65). In a study of 50 ES patients, the median reduction in tumor volume was 64% in cases with no viable tumor seen postchemotherapy excision, as compared to 11% reduction in tumor volume in excised tumors that showed no necrosis after therapy (64).

No significant correlation has been found between change in volume response and patient survival in pediatric sarcomas (28, 33, 64). Also, the length of intramedullary signal abnormalities does not vary in response to chemotherapy (23). Hence, tumor measurements performed during chemotherapy have a limited prognostic significance. Several studies have shown no correlation between T1, T2, or postcontrast signal intensity and tumor response to therapy (65, 66) (moderate evidence).

There is insufficient evidence at this time regarding the role of diffusion-weighted imaging in differentiating necrotic from viable tumor (67, 68). In viable tumor cells, the cell membranes are intact restricting molecular diffusion. In contrast, breakdown of cell membranes in necrotic tumor cells allows free diffusion and an increase in the mean free path length of the diffusion molecules. In a study of 18 sarcoma patients (16 OS, 2 ES), the change in the apparent diffusion coefficient (ADC) value postchemotherapy has been shown to be statistically greater in the group that manifested tumor necrosis greater than 90%, as compared to those with less tumor necrosis ($p=0.003$) (67). However, this needs to be confirmed in larger studies.

Dynamic MRI

There are several studies evaluating the role of dynamic contrast-enhanced MRI (DEMRI) in evaluating response of sarcoma patients to therapy (66). Viable tumor tends to show early enhancement within 10–20 s of injection or within 6 s of contrast reaching a neighboring vessel. Lack of enhancement or late enhancement favors necrotic tumor or therapy-related changes (69). The slope of the signal intensity vs. time curve on DEMRI has been shown to correlate with the degree of necrosis during and after chemotherapy (70, 71). In a study of 20 sarcoma patients, Fletcher et al. showed that all histologically responsive tumors had slopes of 40% per minute or less after completion of chemotherapy (70). Two-compartmental pharmacokinetic models that can take into account contrast uptake and washout have been tested to evaluate tumor response to therapy. The initial results are promising for evaluation of pediatric sarcomas (71). The routine use of these techniques is currently limited due to lack

of standardization and sophistication of post-processing mathematical models (insufficient evidence).

Thallium Scintigraphy

There is limited evidence favoring the use of thallium-201 scintigraphy for evaluation of OS response to chemotherapy (72, 73). Tl-201 is a potassium analog that enters tumor cells via the adenosine triphosphatase system. The avidity of OS for Tl-201 reflects the cellular activity and to a lesser extent the tumor perfusion. Investigators from Memorial Sloan-Kettering Cancer Center evaluated the change in pre- and post-therapy tumor to background uptake ratio in 24 OS patients. They found a statistically significant correlation between the change in Tl-201 uptake intensity and the histologically determined grade of necrosis (72).

FDG-PET

FDG-PET has been used to evaluate the response of bone sarcomas to therapy (74). Most of these are single-center studies with small sample sizes (limited evidence). In their studies on pediatric bone sarcomas, Hawkins et al. have shown that the posttherapy standardized uptake value (SUV) and the ratio of the posttherapy SUV to pretherapy SUV correlate with histological assessment of response to chemotherapy (75). In another study of 36 ES patients, they showed that a postchemotherapy SUV of <2.5 was predictive of progression-free survival independent of initial disease stage (76).They found the positive predictive value of posttherapy SUV of <2.5 for a favorable histological response to be 79%, while the negative predictive value for an unfavorable response was 40% (moderate to limited evidence).

VII. What Is the Appropriate Imaging Protocol for Posttreatment Surveillance of These Malignancies?

Summary of Evidence: There are insufficient data regarding the most cost-effective protocol for surveillance imaging. The recommendations of the children's oncology group for surveillance of OS and ES are summarized (77) (insufficient evidence).

Supporting Evidence: The aim of posttreatment surveillance imaging is to detect tumor recurrence/relapse prior to the patient becoming symptomatic. It is the current approach that asymptomatic detection will aid detection of a small tumor burden at an early enough stage that remission of relapsed tumor can still be achieved. However, the benefits of early detection are unproven and need to be balanced with the costs of multiple investigations and the risks of radiation exposure and sedation/anesthesia required for imaging in children. Ultimately, the imaging protocol can be considered effective only if it improves survival of children with malignancies.

MRI is being routinely used for local recurrence and several studies have shown its role in the detection of local recurrence (78–80). However, the sensitivity and specificity of MRI for differentiating posttherapy changes from residual/recurrent tumor remains low (81). In a study of 24 pediatric patients with soft tissue sarcoma, Kaste et al. reported the sensitivity of magnetic resonance imaging for detecting residual tumor at 78%, specificity at 86%, with a positive predictive value of 0.78, and a negative predictive value of 0.86 (81). Also, whether detection of asymptomatic recurrence by MRI improves survival still needs to be investigated (82). Comparison of chest X-rays and CT scans has shown that the latter can detect lung metastasis at an earlier stage (51, 83). However, these studies did not analyze if the use of CT improves the chance for a successful relapse compared with a follow-up program using chest X-rays alone. CT carries a higher radiation and economic burden compared to chest X-rays. There is need for a prospective study to answer this question. FDG-PET has been shown to aid the diagnosis of local recurrence in small case series (84, 85). Its molecular imaging capabilities can be especially useful when anatomical imaging is limited by therapy-related structural changes or hardware-producing artifact (Fig. 18.2). There is insufficient evidence supporting the role of FDG-PET in the surveillance of pediatric sarcomas at this time.

Take Home Tables

Tables 18.1, 18.2, 18.3, and 18.4 cover the diagnostic performance of imaging tests in the

evaluation of OS and ES, each focusing on one of the following, respectively: MRI/CT in local staging of primary bone sarcoma, sensitivity for detection of skip bony metastases, sensitivity for detection of lung metastases with 95% CI, and sensitivity for detection of osseous metastases.

Table 18.1. Diagnostic performance of imaging tests in the evaluation of OS and ES: imaging performance of MRI and CT in local staging of primary bone sarcoma

		Sensitivity (95% CI)	Specificity
Extension into muscle	MR	96% (91–99%)	99% (97–100%)
	CT	71% (63–79%)	93% (89–95%)
Neurovascular bundle involvement	MR	100% (69–100%)	98% (88–100%)
	CT	33% (8–70%)	93% (81–98%)
Intraarticular extension	MR	94% (71–100%)	97% (86–100%)
	CT	93% (68–100%)	94% (82–99%)

Data from Bloem et al. (21).

Table 18.2. Diagnostic performance of imaging tests in the evaluation of OS and ES: sensitivity for detection of skip bony metastases

Plain radiographs	CT	Bone scan	MRI
36% (8/22)	50% (5/10)	46% (11/24)	83 (15/18)

Data from Kager et al. (43).

Table 18.3. Diagnostic performance of imaging tests in the evaluation of OS and ES: sensitivity for detection of lung metastases with 95% CI

	Plain radiographs	CT[a]	PET
Sensitivity	32% (N/A)	100% (82–100%)	50% (27–73%)
Specificity	(N/A)	76% (63–87%)	98% (90–100%)

[a]Conventional imaging was defined as CT, MRI, bone scintigraphy, and ultrasound in this reference.
Any lesion ≥5 mm or more than one lesion <5 mm classified as positive.
Data from Vanel et al. (51) and Franzius et al. (52).

Table 18.4. Diagnostic performance of imaging tests in the evaluation of OS and ES: sensitivity for detection of osseous metastases

	Conventional imaging[a] (%)	PET (%)
OS	90	90
ES	37	88 (p<0.01)

[a]Conventional imaging was defined as CT, MRI, bone scintigraphy, and ultrasound in this reference.
Data from Volker et al. (53).

Imaging Case Studies

Case 1

Figure 18.1 presents the case of a 5-year-old boy with 6 days of leg pain.

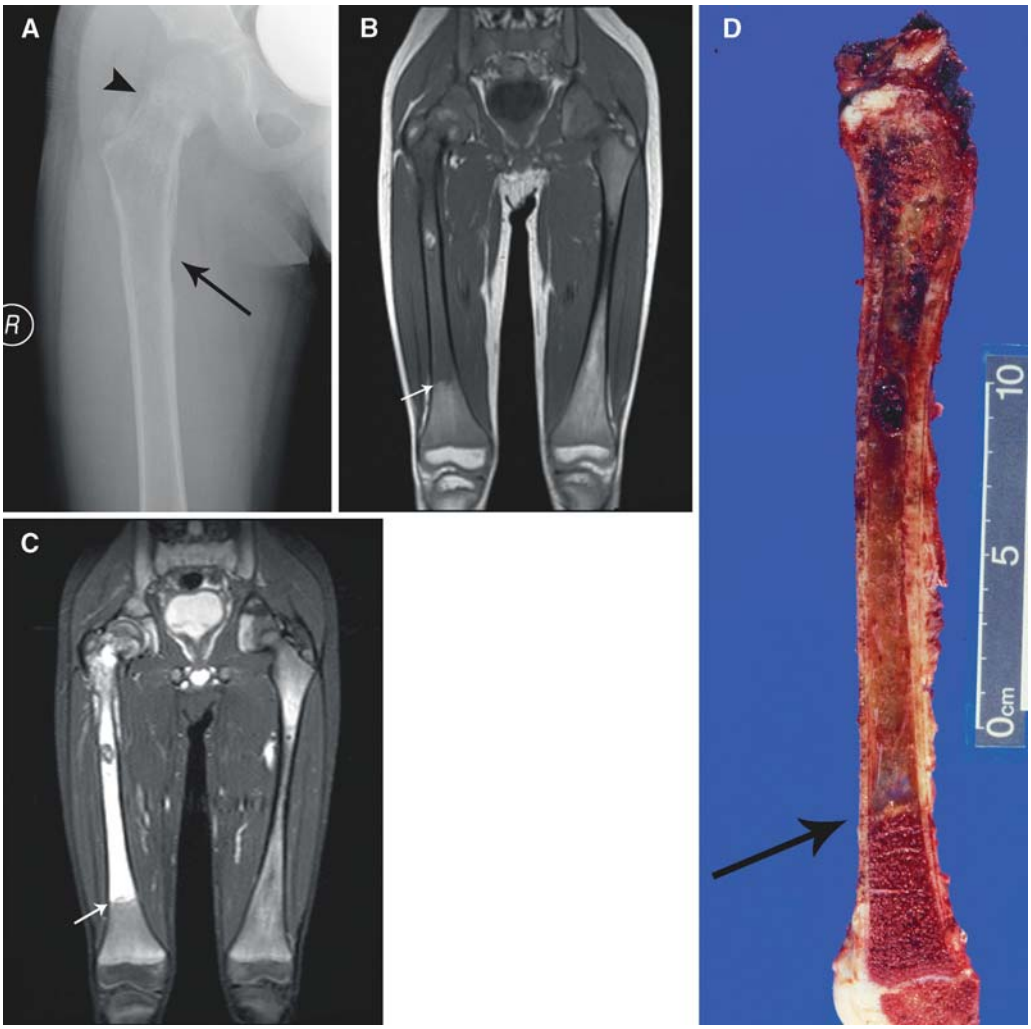

Figure 18.1. A 5-year-old boy with 6 days of leg pain. Radiograph shows interrupted periosteal reaction (**A**, *arrow*) concerning aggressive lesion with a pathologic neck fracture (**A**, *arrow head*). Coronal T1 (**B**) and fat-saturated T2 (**B**) weighted images show marrow replacement extending to the distal shaft. Amputation specimen (**D**) confirms tumor extension into the distal shaft. (Pathology: Ewing's sarcoma.).

Case 2

Figure 18.2 presents the case of a 15-year-old girl with knee prosthesis, postchemotherapy, and surgery for osteosarcoma.

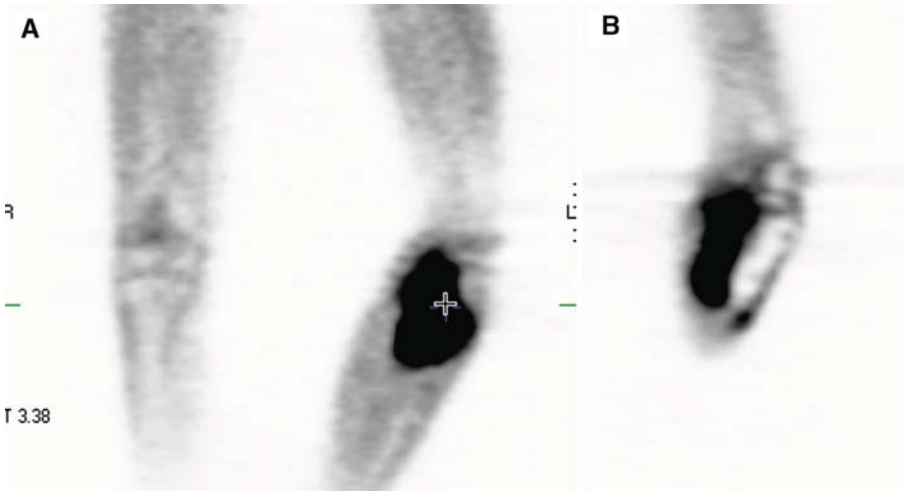

Figure 18.2. A 15-year-old girl with knee prosthesis, postchemotherapy, and surgery for osteosarcoma. FDG-PET (**A**) AP view of both knees and (**B**) lateral view of the left knee show a hypermetabolic focus posterior to the tibia highly concerning recurrence. Ultrasound-guided biopsy confirmed recurrent osteosarcoma.

Suggested Imaging Protocols for Osteosarcoma and Ewing's Sarcoma

Imaging guidelines were formulated by the Children's Oncology Group (77).

Osteosarcoma Imaging Evaluation at Baseline

Anatomic Imaging

1. AP and lateral view of the involved bone.
2. MRI with contrast to determine the extent of disease.
   a. Small field of view images for local extent.
   b. Large field of view images to include whole bone to evaluate for skip lesions.
3. Chest CT for lung metastasis.

Functional Imaging

1. Bone scintigraphy for staging.
2. FDG-PET is recommended but not required.

OS Baseline After Surgery

1. AP and lateral radiographs within 2 weeks of surgery.
2. MRI with contrast 3–4 months after local control.

OS Surveillance During Chemotherapy

1. AP and lateral radiographs of the tumor site (approximately halfway through chemotherapy).
2. Chest CT (approximately halfway through chemotherapy).
3. MRI with contrast at the end of chemotherapy (earlier if symptoms or abnormal imaging, or any intervention planned).
4. Scintigraphy at the end of chemotherapy (earlier if symptoms or abnormal imaging, or any intervention planned).
5. FDG-PET at the end of chemotherapy recommended (earlier if symptoms or abnormal imaging, or any intervention planned).

OS Surveillance After Chemotherapy

1. Radiographs of local site q 3 months for 2 years, q 6 months × 6, then q 12 months × 5.

2. Chest CT q 3 months for 2 years, q 6 months × 6, then q 12 months × 2.
3. Chest 2 views q 12 months × 5 (starting after last chest CT).
4. MRI with contrast of primary site (recommended if symptoms or abnormal imaging).
5. Whole-body imaging with bone scan and/or FDG-PET (recommended if symptoms or abnormal imaging).

ES Imaging Evaluation at Baseline

Anatomic Imaging

1. AP and lateral radiographs of the involved bone.
2. MRI with contrast to determine extent of disease.
a. Small field of view images for local extent.
b. Large field of view images to include whole bone to evaluate for skip lesions.
3. Chest CT for lung metastasis.

Functional Imaging

1. Bone scintigraphy for staging.
2. FDG-PET for staging of Ewing's sarcoma (especially if bone scan negative).

ES Baseline After Surgery

1. AP and lateral radiographs within 2 weeks of surgery.
2. MRI with contrast 3–4 months after local control.

ES Surveillance During Chemotherapy

1. AP and lateral view of the tumor site (approximately 50% through chemotherapy).
2. Chest CT (approximately 50% through chemotherapy).
3. MRI with contrast at the end of chemotherapy (earlier if symptoms or abnormal imaging, or any intervention planned).
4. Scintigraphy at the end of chemotherapy (earlier if symptoms or abnormal imaging, or any intervention planned).
5. FDG-PET at the end of chemotherapyrequired if baseline bone scan is negative in ES (earlier if symptoms or abnormal imaging, or any intervention planned).

ES Surveillance After Chemotherapy

1. Radiographs of local site q 3 months for 2 years, q 6 months × 6, then q 12 months × 5.
2. Chest 2 views q 3 months for 2 years, q 6 months × 6, then q 12 months × 5.
3. Chest CT recommended if radiographs abnormal.
4. MRI with contrast of primary site (recommended if symptoms or abnormal imaging).
5. Whole-body imaging with bone scan and/or FDG-PET (recommended if symptoms or abnormal imaging).

Future Research

- Can the use of PET/CT replace the need for a multimodality surveillance protocol?
- Does posttreatment imaging surveillance improve survival in children with OS and ES?
- What is the most cost-effective imaging protocol for surveillance of these malignancies?
- Is there a difference in outcome for lung metastasis detected on chest CT vs. chest X-ray?
- Understanding the role of molecular imaging techniques to assess tumor aggressiveness and response to therapy.

References

1. Arndt CA, Crist WM. N Engl J Med 1999; 341:342–352.
2. Meyer JS, Mackenzie W. Pediatr Radiol 2004; 34:606–613.
3. Murphey MD, Robbin MR, McRae GA, Flemming DJ, Temple HT, Kransdorf MJ. Radiographics 1997; 17:1205–1231.
4. Grier HE. Pediatr Clin North Am 1997; 44: 991–1004.
5. Weiss A, Khoury JD, Hoffer FA et al. Cancer 2007; 109:1627–1637.
6. Okada K, Frassica FJ, Sim FH, Beabout JW, Bond JR, Unni KK. J Bone Joint Surg Am 1994; 76: 366–378.
7. Kaste SC, Fuller CE, Saharia A, Neel MD, Rao BN, Daw NC. Pediatr Blood Cancer 2006; 47: 152–162.
8. Murphey MD, Jelinek JS, Temple HT, Flemming DJ, Gannon FH. Radiology 2004; 233:129–138.

9. Peersman B, Vanhoenacker FM, Heyman S et al. Jbr-Btr 2007; 90:368–376.
10. Denny CT. Cancer Invest 1996; 14:83–88.
11. Ries LA. Cancer Incidence and survival among children and adolescents: United States SEER Program 1975–1995. Bethesda, MD: National Cancer Institute, 1999.
12. Ries LA. SEER Cancer Statistics Review 1975–2001. Bethesda, MD: National Cancer Institute, 2004.
13. Stiller CA, Bielack SS, Jundt G, Steliarova-Foucher E. Eur J Cancer 2006; 42:2124–2135.
14. Wu XC, Chen VW, Steele B et al. J Adolesc Health 2003; 32:405–415.
15. Gurney JG, Severson RK, Davis S, Robison LL. Cancer 1995; 75:2186–2195.
16. Price CH. J Bone Joint Surg Br 1958; 40-B: 574–593.
17. Watts AC, Teoh K, Evans T, Beggs I, Robb J, Porter D. J Bone Joint Surg Br 2008; 90: 484–487.
18. Lodwick GS, Wilson AJ, Farrell C, Virtama P, Dittrich F. Radiology 1980; 134:577–583.
19. Hudson TM, Schiebler M, Springfield DS, Hawkins IF, Jr., Enneking WF, Spanier SS. Skeletal Radiol 1983; 10:137–146.
20. Reinus WR, Gilula LA, Committee I. RadioGraphics 1984; 4:929–944.
21. Bloem JL, Taminiau AH, Eulderink F, Hermans J, Pauwels EK. Radiology 1988; 169:805–810.
22. Gillespy T, 3rd, Manfrini M, Ruggieri P, Spanier SS, Pettersson H, Springfield DS. Radiology 1988; 167:765–767.
23. Onikul E, Fletcher BD, Parham DM, Chen G. Am J Roentgenol 1996; 167:1211–1215.
24. Hoffer FA, Nikanorov AY, Reddick WE et al. Pediatr Radiol 2000; 30:289–298.
25. Norton KI, Hermann G, Abdelwahab IF, Klein MJ, Granowetter LF, Rabinowitz JG. Radiology 1991; 180:813–816.
26. Schima W, Amann G, Stiglbauer R et al. Am J Roentgenol 1994; 163:1171–1175.
27. Bieling P, Rehan N, Winkler P et al. J Clin Oncol 1996; 14:848–858.
28. Lawrence JA, Babyn PS, Chan HS, Thorner PS, Pron GE, Krajbich IJ. Radiology 1993; 189:43–47.
29. Kaste SC, Liu T, Billups CA, Daw NC, Pratt CB, Meyer WH. Pediatr Blood Cancer 2004; 43: 723–728.
30. Lee JA, Kim MS, Kim DH et al. Pediatr Blood Cancer 2008; 50:195–200.
31. Hense HW, Ahrens S, Paulussen M, Lehnert M, Jurgens H. Ann Oncol 1999; 10:1073–1077.
32. Miller ME, Emerson L, Clayton F et al. J Clin Oncol 2007; 25:4845–4848.
33. Miller SL, Hoffer FA, Reddick WE et al. Pediatr Radiol 2001; 31:518–523.
34. Reddick WE, Bhargava R, Taylor JS, Meyer WH, Fletcher BD. J Magn Reson Imaging 1995; 5: 689–694.
35. Kaste SC, Billips C, Tan M et al. Pediatr Radiol 2001; 31:251–256.
36. McCarville MB, Barton EH, Cameron JR et al. Am J Roentgenol 2007; 188:572–578.
37. Kern KA, Brunetti A, Norton JA et al. J Nucl Med 1988; 29:181–186.
38. Adler LP, Blair HF, Makley JT et al. J Nucl Med 1991; 32:1508–1512.
39. Folpe AL, Lyles RH, Sprouse JT, Conrad EU, 3rd, Eary JF. Clin Cancer Res 2000; 6:1279–1287.
40. Eary JF, O'Sullivan F, Powitan Y et al. Eur J Nucl Med Mol Imaging 2002; 29:1149–1154.
41. Enneking WF, Kagan A. Cancer 1975; 36: 2192–2205.
42. Enneking WF, Kagan A. Clin Orthop Relat Res 1975:33–41.
43. Kager L, Zoubek A, Kastner U et al. J Clin Oncol 2006; 24:1535–1541.
44. Sajadi KR, Heck RK, Neel MD et al. Clin Orthop Relat Res 2004:92–96.
45. Wuisman P, Enneking WF. J Bone Joint Surg Am 1990; 72:60–68.
46. Jiya TU, Wuisman PI. Acta Orthop 2005; 76: 899–903.
47. Marec-Berard P, Philip T. Pediatr Blood Cancer 2004; 42:477–480.
48. Kaste SC, Pratt CB, Cain AM, Jones-Wallace DJ, Rao BN. Cancer 1999; 86:1602–1608.
49. Gerth HU, Juergens KU, Dirksen U, Gerss J, Schober O, Franzius C. J Nucl Med 2007; 48:1932–1939.
50. Cohen M, Grosfeld J, Baehner R, Weetman R. Am J Roentgenol 1982; 139:895–898.
51. Vanel D, Henry-Amar M, Lumbroso J et al. Am J Roentgenol 1984; 143:519–523.
52. Franzius C, Daldrup-Link HE, Sciuk J et al. Ann Oncol 2001; 12:479–486.
53. Volker T, Denecke T, Steffen I et al. J Clin Oncol 2007; 25:5435–5441.
54. Gyorke T, Zajic T, Lange A et al. Nucl Med Commun 2006; 27:17–24.
55. Franzius C, Sciuk J, Daldrup-Link HE, Jurgens H, Schober O. Eur J Nucl Med 2000; 27: 1305–1311.
56. Daldrup-Link HE, Franzius C, Link TM et al. Am J Roentgenol 2001; 177:229–236.
57. Hudson M, Jaffe MR, Jaffe N et al. J Clin Oncol 1990; 8:1988–1997.
58. Huvos AG, Rosen G, Marcove RC. Arch Pathol Lab Med 1977; 101:14–18.
59. Picci P, Bohling T, Bacci G et al. J Clin Oncol 1997; 15:1553–1559.
60. Rosen G, Caparros B, Huvos AG et al. Cancer 1982; 49:1221–1230.

61. Holscher HC, Hermans J, Nooy MA, Taminiau AH, Hogendoorn PC, Bloem JL. Skeletal Radiol 1996; 25:19–24.
62. Holscher HC, Bloem JL, Nooy MA, Taminiau AH, Eulderink F, Hermans J. Am J Roentgenol 1990; 154:763–769.
63. Holscher HC, Bloem JL, Vanel D et al. Radiology 1992; 182:839–844.
64. Abudu A, Davies AM, Pynsent PB et al. J Bone Joint Surg Br 1999; 81:317–322.
65. van der Woude HJ, Bloem JL, Holscher HC et al. Skeletal Radiol 1994; 23:493–500.
66. Erlemann R, Sciuk J, Bosse A et al. Radiology 1990; 175:791–796.
67. Hayashida Y, Yakushiji T, Awai K et al. Eur Radiol 2006; 16:2637–2643.
68. Uhl M, Saueressig U, Koehler G et al. Pediatr Radiol 2006; 36:1306–1311.
69. van der Woude HJ, Bloem JL, Verstraete KL, Taminiau AH, Nooy MA, Hogendoorn PC. Am J Roentgenol 1995; 165:593–598.
70. Fletcher BD, Hanna SL, Fairclough DL, Gronemeyer SA. Radiology 1992; 184: 243–248.
71. Dyke JP, Panicek DM, Healey JH et al. Radiology 2003; 228:271–278.
72. Imbriaco M, Yeh SD, Yeung H et al. Cancer 1997; 80:1507–1512.
73. Ohtomo K, Terui S, Yokoyama R et al. J Nucl Med 1996; 37:1444–1448.
74. Franzius C, Sciuk J, Brinkschmidt C, Jurgens H, Schober O. Clin Nucl Med 2000; 25:874–881.
75. Hawkins DS, Rajendran JG, Conrad EU, 3rd, Bruckner JD, Eary JF. Cancer 2002; 94:3277–3284.
76. Hawkins DS, Schuetze SM, Butrynski JE et al. J Clin Oncol 2005; 23:8828–8834.
77. Meyer JS, Nadel HR, Marina N et al. Pediatr Blood Cancer 2008; 51:163–170.
78. Vanel D, Lacombe MJ, Couanet D, Kalifa C, Spielmann M, Genin J. Radiology 1987; 164:243–245.
79. Vanel D, Shapeero LG, De Baere T et al. Radiology 1994; 190:263–268.
80. Kauffman WM, Fletcher BD, Hanna SL, Meyer WH. Magn Reson Imaging 1994; 12: 1147–1153.
81. Kaste SC, Hill A, Conley L, Shidler TJ, Rao BN, Neel MM. Clin Orthop Relat Res 2002:204–211.
82. Korholz D, Verheyen J, Kemperdick HF, Gobel U. Med Pediatr Oncol 1998; 30:52–58.
83. Pass HI, Dwyer A, Makuch R, Roth JA. J Clin Oncol 1985; 3:1261–1265.
84. Arush MW, Israel O, Postovsky S et al. Pediatr Blood Cancer 2007; 49:901–905.
85. Franzius C, Daldrup-Link HE, Wagner-Bohn A et al. Ann Oncol 2002; 13:157–160.

19

Imaging for Knee and Shoulder Injuries

Ricardo Restrepo and Christopher Schettino

Issues

Issues in Imaging the Pediatric Knee

I. What is the role of radiographs in children with an acute knee injury and possible fracture?
II. When should MRI be used in children with suspected meniscal, ligamentous, or articular cartilage injuries?
III. What is the role of imaging in the evaluation of osteochondritis dissecans?
IV. What is the role of imaging in the evaluation of discoid lateral meniscus (DLM)?

Issues in Imaging Children with Acute Shoulder Injury

I. When is radiography indicated for children with acute shoulder injury?
II. What is the role of MRI in shoulder dislocation?

Key Points

Knee

- Knee radiographs of the acutely injured knee in the emergency department are rarely useful for determining therapy, except in patients with any of the following conditions: isolated tenderness of the patella, tenderness at the head of fibula, inability to flex 90°, inability to bear weight both immediately and in the emergency department for a total of four steps, or if the patient is an adult aged 55 or older (strong evidence).
- Physical examination by an experienced pediatric physician is as accurate as an MRI to diagnose articular cartilage injury, discoid lateral meniscus, anterior cruciate ligament tears, and medial meniscal tear (limited evidence). An MRI is likely more accurate for lateral meniscal tears. However, if the MRI study is interpreted by a physician

R. Restrepo (✉)
Pediatric Radiologist, Fellowship Director, Department of Radiology, Miami Children's Hospital, Miami, FL 33155, USA
e-mail: ricres1@aol.com

L.S. Medina et al. (eds.), *Evidence-Based Imaging in Pediatrics*,
DOI 10.1007/978-1-4419-0922-0_19,

experienced with the skeletally immature patient, the accuracy could be superior, and additional associated pathology can be identified (limited evidence).
- An MRI in the setting of osteochondritis dissecans plays an important role in a specific subgroup of patients where it is imperative to assess the integrity of the overlying cartilage (limited evidence).
- An MRI in the setting of discoid lateral meniscus plays a role in identifying the state of the meniscus in order to assess surgical reparability and also to identify superimposed pathology, such as articular cartilage damage (limited evidence).

Shoulder

- The use of radiography to evaluate children with first-time acute shoulder trauma is to confirm a fracture or a dislocation and to evaluate the alignment and possible extension into the physeal plate (limited evidence).
- The use of radiography to evaluate patients with suspected recurrent atraumatic shoulder dislocation is unnecessary in most cases (limited evidence). Furthermore, selective imaging strategies may be able to reduce the number of pre-reduction and/or post-reduction radiographs required in suspected first-time or traumatic shoulder dislocations (limited evidence).
- Identification of labral and glenohumeral ligament tears is important especially in patients with a history of shoulder dislocations, as they have a high recurrence rate. No dedicated MRI or Magnetic Resonance Arthrogram (MRA) studies have been done in children. However, studies in adults show that MR arthrogram has a high sensitivity and specificity to identify and classify these lesions (limited to moderate evidence). This information is useful to the orthopedic surgeon in preoperative planning of joint stabilization procedures.

Definition and Pathophysiology

The Knee

Osteochondritis Dissecans

Osteochondritis dissecans (OCD) is a localized injury or condition affecting an articular surface that involves separation of a segment of cartilage and subchondral bone (1). OCD most commonly affects the weight-bearing surface of the femoral condyles, with 85% occurring in the lateral aspect of the medial femoral condyle close to the intercondylar groove. Thirteen percent occur in the inferocentral aspect of the lateral femoral condyle and 2% in the anterior aspect of the lateral femoral condyle. OCD rarely occurs in the femoral sulcus/femoral trochlea, accounting for 2% as well (2). There is an association between OCD of the lateral femoral condyle and OCD of the discoid meniscus (3–6). The etiology of OCD is controversial, and many hypotheses have been formulated, including trauma, ischemia, defects of ossification, and genetic causes. It probably results from a combination of factors (1, 4).

There are two subgroups of OCD according to the fusion state of the physeal plate: juvenile (JOCD) with open physeal plates and adult type (AOCD) with closed plates. The average age for OCD of the knee at the time of diagnosis is between 11 and 14 years for the juvenile type. The age of presentation for the adult form ranges between 17 and 36 years; however, it may occur at an earlier stage if the physeal plate is closed (4). Because of a tendency to heal, the juvenile type has a better prognosis and is usually treated conservatively (1, 7). On the other hand, when conservative management fails, a more aggressive operative treatment is advocated. The goal of operative treatment is to stimulate healing once an unstable lesion is identified (1, 4, 7–9).

Discoid Lateral Meniscus

The normal lateral meniscus has much more variability in size, thickness, shape, and mobility than the normal medial meniscus. The lateral meniscus is generally more circular than the medial meniscus and covers a larger portion of the articular surface. It averages approximately 12 mm in width and 4–5 mm in height; if it is thicker and wider, a Discoid Lateral Meniscus (DLM) is present (10). The classification and types of DLM are of utmost importance. DLM can be stable or unstable. The stable ones have normal posterior attachments and are subdivided into complete and incomplete type by the amount of tibial plateau coverage, which is larger with the complete type. The presence of a discoid meniscus is suggested on an MRI when three or more 5-mm-thick consecutive sagittal sections demonstrate continuity of the meniscus between the anterior and the posterior horn. The unstable or Wrisberg type may have a discoid or a normal shape but lacks its posterior attachments.

The clinical presentation varies according to the type. Many stable lateral meniscal variants are asymptomatic and are found incidentally. These usually become symptomatic due to a tear, and the presentation is similar to any other lateral meniscal tear (pain, swelling, and mechanical symptoms like giving way and locking).

The snapping knee syndrome is likely related to an unstable meniscal variant. It is usually found in a child under 10 years of age with intermittent popping and snapping within the knee, producing an audible clunk (11–13). The treatment of a DLM depends also on its type and whether it is associated with a tear. If a DLM is discovered with no tear, it must be considered a normal variant and should be left intact. If a tear is associated with a complete or an incomplete type, partial meniscectomy is advocated. The traditional treatment for the Wrisberg type has been total meniscectomy, but recently arthroscopic attachment has been performed (11, 14).

The Shoulder

The most obvious difference between the pediatric and the adult skeleton is the presence of growth plates. The growth and the change that occur at the growth plate facilitate remodeling of fractures and contribute to rapid healing; however, damage to the physis itself can lead to deformity secondary to asymmetrical growth. Pediatric bone is highly cellular and porous, and it contains a large amount of collagen and cartilage compared to adult bone. The larger amount of collagen leads to a reduction in tensile strength and prevents the propagation of fractures. The tensile strength of pediatric bone is less than that of the ligaments, so children are more likely to have bone fractures that would cause only ligamentous injuries in adults (15). Fractures around the shoulder in children are rarely operative. However, it is important for the practicing orthopedic surgeon to differentiate nonoperative from urgent, potentially operative injuries. Missing such an injury in the pediatric population could be potentially life threatening or could lead to long-term disability (16).

The rotator cuff in juveniles is more elastic and lacks the degenerative changes typically seen in the older population. In adolescents most rotator cuff tears involve overhead throwing sports, as they are part of overuse syndromes (17–19). In adults, the most common cause of rotator cuff tears is primary impingement by the acromioclavicular joint, which is extremely uncommon in pediatric patients (20).

Epidemiology

Acute Knee Trauma

Approximately 0.3% of the US population seeks medical care for an acute knee injury each year. These injuries are most frequently seen in adolescents and young males and are usually precipitated by sports (36%), twisting, bending, or stepping motions (27%) or falls (21%) (21). Half of all children aged 5–18 years in the United States are thought to participate in organized sports programs. This means that an estimated 30 million school-age children are involved in sports, a substantial increase over the past two decades. A study by Burt et al. estimated an average of 2.6 million emergency room visits for sports-related injuries per year for individuals aged 5–24 years. Across all ages, the peak incidence of emergency room visits for sports-related injuries occurs at ages 5–14 years and decreases gradually with age. It is estimated that 38% of high school children and 34% of middle school children will sustain a physical

activity-related injury that will be treated by a doctor or a nurse (22, 23).

Osteochondritis Dissecans

Osteochondritis dissecans of the knee has an incidence estimated at between 0.02 and 1.2% and typically manifests between 10 and 15 years of age. The incidence of OCD has increased with the introduction of organized sports at younger and younger ages. Like virtually all traumatic injuries, OCD is twice as common in males as in females, which is related to the predominance of males in organized competitive sports. Bilateral presentation occurs in between 15 and 30% of the cases (24).

Discoid Lateral Meniscus

The reported prevalence of DLM varies depending on the method of investigation, selection criteria, and patient population. The prevalence in two studies of symptomatic patients who underwent open meniscectomy ranged from 2 to 5%. Arthroscopic studies have recorded prevalence varying from 0.4 to 16.6% (12). Arthroscopic studies may be more accurate in estimating the true prevalence as asymptomatic DLMs are included. Cadaveric studies suggest a prevalence ranging from 0 to 7% (11). The reported prevalence of discoid lateral meniscus ranges from 1.5 to 4.6% of symptomatic knees (25). Bilateral discoid menisci have been reported between 5 and 20% (11, 25).

Acute Shoulder Trauma

Less than 2% of all traumatic glenohumeral shoulder dislocations occur in patients younger than 10 years of age, and about 20% occur in patients between the ages of 10 and 20 years. Adolescents with shoulder instability have a much higher recurrence rate of dislocation than do adults, with rates ranging from 70 to 100%. Chronic instability and recurrent dislocation cause articular damage, leading to glenohumeral arthropathy in the long term; and in the short term, they produce persistent symptoms that interfere with daily activities (10, 26).

Musculoskeletal injuries of the shoulder in competitive adolescents are common and include acute traumatic injuries such as clavicular and proximal humeral fractures and, in older adolescents, acromioclavicular joint separation. Rotator cuff injuries are far less common in children than in adults. Less than 1% of rotator cuff tears occur in patients under the age of 20 years (16, 20, 27).

Overall Cost to Society

No data were found on the overall cost to society considering only pediatric patients and using the diagnosis of acute knee or shoulder injury, shoulder dislocation, osteochondritis dissecans, or discoid lateral meniscus. However, some data regarding the overall cost to society for shoulder and knee injuries in adult and pediatric patients state that the direct cost of health care for musculoskeletal problems is about 1% of the gross national product in several industrialized countries (28), although we found no convincing estimates of the total societal costs for knee and shoulder problems.

The Knee

In the year 2001, knee symptoms and injuries were the primary reason for 1.5 million (1.4%) of all emergency room visits in the United States (29). Furthermore, knee symptoms and injuries led to an estimated 861,000 (1.0%) hospital outpatient department visits and 13.8 million (1.6%) office visits to physicians (29). Knee problems are, therefore, in the top 15 most frequent reasons for consulting a physician, second only to back pain among musculoskeletal problems.

The Shoulder

Medical care visits for shoulder problems are less frequent. In total, shoulder symptoms and injury lead to 1.2 million (1.1%) emergency room visits, 425,000 (0.5%) outpatient visits, and 8.9 million (1.0%) office visits (29).

Goals

The decision to use the less expensive diagnostic tests should be based on whether the physician thinks using the test will do any of the following:

1. Confirm or expand the present diagnosis.

2. Change the diagnosis in such a way that the proposed treatment plan is altered.
3. Be used to formulate a therapeutic decision.

The Knee

The goal of knee radiographs in children with acute injury is to identify fractures and effusions and exclude uncommon causes of pain.

The goal of imaging children with osteochondritis dissecans is to confirm the diagnosis and to serve as a baseline for monitoring response to treatment.

The goal of an MRI is to evaluate cartilaginous structures of the knee, such as meniscus and articular surface cartilage not seen on conventional radiographs.

The Shoulder

The goals of imaging in children with acute shoulder trauma are to confirm the presence of a fracture or a dislocation and to evaluate the alignment of the fracture and physeal plate involvement, as well as to confirm a dislocation in questionable cases.

Methodology

Our initial search strategy identified systematic literature reviews of knee and shoulder imaging studies. We initially searched the Medline database using the PubMed interface for abstracts published between January 1966 and October 2008 with the text word *knee* or *shoulder* and the PubMed designation of a systematic review [systematic (s)b]. From this group, we selected several key articles reviewing the role of imaging. An additional search tailored to children was made using the words *knee* or *shoulder* and *children* or *pediatric patient*. We found only three key, exclusively "pediatric" articles reviewing the role of imaging the knee (30–32). Our search strategy used the following key words: *acute knee and shoulder trauma*, *osteochondritis dissecans*, *discoid lateral meniscus*, *shoulder dislocation*, *imaging*, *MRI* or *Magnetic Resonance Imaging*, as well as combinations of these words. When possible, we obtained and reviewed the full text of all relevant English language articles identified. We then searched the articles cited by these systematic reviews to identify the relevant primary studies.

Discussion of Issues: Knee

I. What Is the Role of Radiographs in Children with an Acute Knee Injury and Possible Fracture?

Summary of Evidence: The role of radiographs is to diagnose fractures and knee effusions that are associated with internal knee derangements (ligament, meniscal, or cartilaginous injuries). Acute knee trauma provides a common diagnostic quandary in emergency departments. Fractures are present in 4–12% of adults and 4–5% of children presenting with knee injuries (33–36), and yet radiography may be requested in excess of 70% of cases (37). In many cases, plain radiography is all that is required to allow the clinician to proceed with conservative therapy if negative.

Several guidelines are available to help clinicians target imaging at high-risk patients. The Ottawa Knee Rules (OKRs) are a clinical prediction guideline for when to perform radiographs, and they have been adapted for use in children over the age of 5 years. The OKRs were highly sensitive and specific for the need for knee radiographs to diagnose fractures (strong evidence).

Supporting Evidence: Frontal and bent knee lateral routine views are performed for knee trauma to exclude fracture and to detect a knee effusion suggesting internal derangement.

There are five clinical decision rules to guide clinicians on when to order knee radiography following trauma in order to save costs and avoid unnecessary radiation; these are called the Ottawa Knee Rules (Table 19.1) (38–41). These decision rules focus variously on patient age (adults), injury mechanism, inability to ambulate, and other clinical signs, such as fibular head tenderness. The optimal threshold for radiography requests will depend on the trade-off between the clinical and possible legal consequences of a missed fracture compared to the time, cost, and radiation exposure from radiographs. Appropriately, these decision rules place great emphasis on sensitivity at the expense of specificity.

To date, the OKR (40, 42) has undergone the most extensive validation. Other decision rules may have greater specificity, but they have not yet been validated by independent investigators. The OKR suggests that radiography should be performed on the acutely injured knee when the patient has one or more of the following criteria: (1) is of age 55 or older; (2) isolated tenderness of the patella (no other knee bone tenderness); (3) tenderness of the head of the fibula; (4) inability to flex the knee to 90°; and (5) inability to bear weight both immediately and in the emergency department for four steps.

A recent systematic review by Hollingworth et al. (43) found 11 studies evaluating the diagnostic accuracy of the OKR (44). Six of these studies were suitable for inclusion of a meta-analysis, and four were considered to be of high quality. The mean sensitivity of the OKR in these studies was 98.5% and the specificity was 48.6% (44). While this provides strong evidence (Level 1) that the OKR is sensitive at predicting fracture, it does not prove that it is a cost-effective method of organizing care. On the other hand, if it is indeed as sensitive as reported, it significantly reduces cost.

The applicability of the OKR has been studied as well. The diagnostic performance of the OKR may be altered in the skeletally immature knee due to open growth plates and secondary ossification centers, resulting in different injury patterns (45). The ability to bear weight was originally considered not as valid in children due to lack of patient cooperation. Two case series have studied the applicability of the OKR to children (35, 46). In the largest study involving 750 children aged 2–16, Bulloch et al. found that the OKR was 100% sensitive (95% CI, 94.9–100%) in predicting the 70 fractures observed and 43% specific (95% CI, 39.1–46.5%). Due to the small numbers of children in the youngest age category, these authors endorsed the OKR in children 5 years of age or more. In a smaller study conducted by Khine et al., the OKR correctly predicted 12 of 13 fractures observed in 234 children aged 2–18 years. The one missed injury was a nondisplaced fracture of the proximal tibia in an 8 year old. Overall, the similarity between these two studies and evaluations conducted in adults provide reassurance that the OKR is valid in children (Level 2—moderate evidence). More recently, in a prospective multicenter cohort study by Moore et al. that included 146 patients between 3 and 18 years of age, it was found that the ability to bear weight would have decreased the use of radiography by 53% without missing any fractures. No additional value to the rule was found by adding assessment of the ability to flex the knee or bony tenderness. No reference to cost was made on this study. With this refinement, the sensitivity of the OKR was 1.0 and the specificity 0.59. However, there is not yet sufficient evidence to demonstrate the cost effectiveness of applying the OKR to children (limited evidence) (36).

Based on these multicenter trials in children, several authors have speculated that adherence to the OKR would reduce the use of knee radiography in the emergency room by 31–53%. Patients who are not imaged spend less time in the emergency department and have lower follow-up cost than their counterparts who were referred for radiography. However, these estimates rely on the assumption that clinicians would rigidly follow the OKR and would not be swayed by fears of missed diagnoses or patient expectations of radiographs (35, 36, 46).

II. When Should MRI Be Used in Children with Suspected Meniscal, Ligamentous, or Articular Cartilage Injuries?

Summary of Evidence: The accuracy of MRI in the diagnosis of internal knee derangements is well established in adults but is less well characterized in children and adolescents. When interpreting knee MRI in children, one must be aware of the transient morphological changes that occur during growth that can alter the appearance of intra-articular structures on MRI. This in part may account for the low accuracy of the formal interpretation of the MRI scans by the radiologist. Pediatric radiologists are more familiar with the appearance of the pediatric knee, and their expertise helps decrease the number of inaccurate reports.

Intra-articular lesions are being seen with increased frequency in the pediatric age group (30), in part because of more aggressive and single sport activities from an early age. There

is evidence (moderate strength evidence) that a clinical exam is more sensitive and specific than an MRI in the diagnosis of most knee problems in children, including medial collateral ligament tears, discoid lateral meniscus, ACL tear, and articular cartilage injury, when performed by a skilled practitioner, such as a pediatric orthopedic surgeon (moderate evidence). A more recent study has shown that additional important information can be obtained from an MRI when results are reviewed by a physician who also has access to the physical exam findings and is familiar with the morphology of the immature knee (31).

Supporting Evidence

Clinical Exam

The accuracy of clinical joint line tenderness in adolescents for the diagnosis of meniscal tears was evaluated in a study by Eren where 104 male patients between 18 and 20 years of age (mean age 19.2 years) with suspected meniscal tear underwent arthroscopy. The authors concluded that joint line tenderness as a test study for lateral meniscal tear is accurate (96%), sensitive (89%), and specific (97%), but for medial meniscal tear, the rates were lower with 62, 56, and 68%, respectively (moderate evidence) (47). This is in accordance with the findings made by Kocher et al. discussed in the next section (30).

MR Imaging

When interpreting knee MRIs in children, one must be aware of the transient morphological changes that occur during growth, which can alter the appearance of intra-articular structures on an MRI. Postnatally, the meniscus undergoes gradual change, specifically decreasing vascularity and progressive adaptation of the collagen-fiber arrangement to biomechanical stress. The radiologist should be familiar with these normal pediatric changes to avoid false-positive interpretations (31).

Stanitski studied 28 children (aged 8–17 years) to correlate clinical, MRI, and arthroscopic findings (moderate evidence). In this small, retrospective, unblinded study, the authors considered arthroscopy as the reference standard. In this study, a highly positive correlation (79%) was found between clinical and arthroscopic findings of ACL tear, meniscal tear, and articular cartilage tear. A highly negative correlation was found between arthroscopic and magnetic resonance imaging findings, as 20 of the 28 patients (71%) had either false-positive (+) or false-negative (–) results. These authors found that very experienced clinicians (knee surgeons) provided greater sensitivity and specificity for injuries to the ACL, menisci, and articular cartilage than did an MRI. In this particular setting, an MRI added little to the treatment and outcome in their patient group. This author believes that MRIs are overused and are not cost effective when compared to a skilled examiner (limited evidence). The sensitivity and specificity estimates from this review are in Tables 19.2 and 19.3 (32).

In the study by Kocher et al., the diagnostic performance of clinical examination and selective MRI in the evaluation of intra-articular knee disorders in children and adolescents was tested (Level 1). He included 118 knees in 113 patients from 3.1 to 16 years of age. The diagnoses included in the study were ACL tear, medial and lateral meniscal tears, osteochondritis dissecans, and lateral discoid meniscus. The study found no significant difference ($p < 0.05$) between a clinical examination and an MRI with arthroscopic findings for overall sensitivity (clinical 71.2%; MRI 72%) and overall specificity (clinical 91.5%; MRI 93.5%). Stratified analysis of sensitivity and specificity for the five major diagnoses revealed significant differences between a clinical examination and an MRI only for lateral discoid meniscus sensitivity (clinical 88.9%; MRI 38.9%; $p = 0.002$) and medial meniscal tear specificity (clinical 80.7%; MRI 92%; $p = 0.0280$). In this series it was concluded that clinical examination and selective MRI had similar overall diagnostic performance. Clinical examination was more sensitive for lateral discoid meniscus, while selective MRI was more specific for medial meniscal tear (moderate evidence), as depicted in Table 19.4.

The diagnostic performance of both clinical examination and MRI was age related in this study, with diminished accuracy in the pediatric age group compared to the adolescent age group, as shown in Table 19.5. Potential explanations hypothesized included difficulty in obtaining an accurate history, difficulty in localizing the symptoms, lack of patient cooperation and relaxation during examination,

lack of recognition of significant injuries, and the more varied differential diagnoses associated with these age groups (30).

As a result of the questioned utility of MRIs in the diagnosis of pediatric knee disorders, in part attributed to the morphologic changes during growth and the low accuracy of the formal interpretation of the MRI by radiologists, a study by Luchmann et al. challenged these assertions. They found that integration of patient information/clinical data with an orthopedic surgeon's review of the actual MR images in children and adolescent patients improves the identification of pathological disorders, including ACL tear, lateral meniscal tear, osteochondritis dissecans, and discoid lateral meniscus, giving a value to knee MRIs. On the other hand, this study questioned the necessity for and the appropriateness of a routine interpretation of an MRI of the knee in children and adolescents by a radiologist (strong evidence) (31).

III. What Is the Role of Imaging in the Evaluation of Osteochondritis Dissecans?

Summary of Evidence: As in most disease processes, the key factor for symptom resolution and minimal sequelae is early diagnosis and early intervention, whether medical or surgical. The distinguishing factor in the treatment of OCD is the physeal plate, as the adult type has a significantly worse prognosis and rarely heals without operative intervention. Most children with OCD and open physis can be successfully managed nonoperatively. The juvenile type that does not heal with conservative treatment or the adult type should be treated surgically (1, 24).

The clinical Wilson sign has a very poor sensitivity for diagnosing OCD. It may be used to monitor and follow patients that had a positive sign at presentation, as the disappearance correlates well with healing. AP, lateral, and tunnel-view radiographs should always be used as the first imaging modality to evaluate OCD. MRI is the only noninvasive diagnostic tool that can reveal the state of the overlying cartilage as well as evidence of fragment loosening and detachment in patients with OCD (limited evidence). MRI should be reserved for patients with open physis and mechanical symptoms, persistent pain after nonoperative management, and/or equivocal symptoms, such as locking or giving way (48–50). The literature agrees on two factors that have an important impact on the prognosis as it pertains to the development of secondary osteoarthritis: the age of the patient, i.e., whether the epiphyseal plate is closed, and the state of the cartilage, i.e., whether the overlying cartilage is intact (51, 52). An MRI is particularly useful to evaluate the stability of the lesion, the presence of cartilaginous loose bodies, and the size of the articular cartilage defects if chondrocyte transplantation is a therapeutic option (8, 51, 52). An MRI may also identify additional superimposed intra-articular pathology including early degenerative changes that can be a source of clinical confusion.

Supporting Evidence

Clinical Signs

The clinical Wilson sign to diagnose OCD is elicited by flexing the knee to 90°, internally rotating the tibia, and then slowly extending the knee. A positive Wilson sign causes pain at approximately 30° of flexion that is relieved by external rotation of the tibia (1, 53). In a study by Conrad and Stanitski, 32 patients were evaluated and divided in juvenile and adolescent groups. Of the juvenile group, only 23.5 and 26.7% of the adolescent group had a positive initial sign. On the other hand, patients with an initially positive sign during the pretreatment period have a negative sign after healing, making it helpful in clinical monitoring during treatment (conservative or surgical) and for lesion resolution. This was not applicable to lesions located in the lateral femoral condyle (53). Aichroth reported extremely poor sensitivity of the Wilson test, with only 7 of 100 patients with OCD yielding a positive test result (5). There are no studies correlating the Wilson sign with MRI findings in patients with OCD.

The Role of Radiographs

There is agreement that when OCD is suspected, a radiograph of the knee should be obtained to confirm the diagnosis and determine the location of the lesion and the state of the physeal plate (1, 54–56). The routine protocol should include three views: AP, lateral, and tunnel view. This latter view is more

accurate to depict lesions in the most common location that can be missed on the other two views (8, 57, 58). The question to answer is not what modality is used to diagnose OCD (plain radiograph vs. MRI), but what the role of each one is. The major drawbacks of plain radiographs are its inability to visualize the articular cartilage (hence not providing any information of the state of the overlying cartilage) and the inability to assess the stability of a lesion (52, 59). It is certain that most patients with the juvenile type of OCD tend to heal with conservative management and no sequelae (Figure 19.1). Conservative treatment includes restriction of sports activity and limited weight bearing for 6–8 weeks. It is in this group of patients that initial plain radiograph to confirm the diagnosis and MRI to evaluate the integrity of the cartilage may suffice (48, 49, 52). If there is clinical progression of the symptoms or a persistent positive Wilson sign, as well as a chondral defect on the MRI, arthroscopy with cartilage drilling and/or lesion fixation are recommended (48, 52, 60). In an evaluation of 76 knees, Linden reported no significant complications in patients with a history of juvenile-type OCD who had been treated before skeletal maturity (61).

The Role of MRI

The MRI staging of OCD is important to identify stable or unstable lesions. This factor is important to decide which patients will undergo arthroscopy and surgery. Several classifications have been developed using radiographs, MRI, and arthroscopy. Please refer to Table 19.6 for the original MRI classification by Di Paola et al. (62) and a more recent classification which compiles several versions published in a pediatric radiology journal (49) (Table 19.7).

In a study by O'Connor et al. (59) in which 33 knees of 31 patients were analyzed, the MRI accuracy to stage a lesion as unstable was 85% when compared with the arthroscopic findings. The authors considered a high T2 signal line (Figure 19.2) as a predictor of instability in the presence of a cartilage breach on the T1 sequence. These authors in their conclusion recommended the use of an MR classification system that correlates with the arthroscopic finding. The MR classification used was the one described by Di Paola et al. (62). They were able to improve the accuracy of MRI for staging the OCD lesion from 45 to 85% by interpreting the high T2 signal line as a predictor of instability only when accompanied by a breach in the articular cartilage on the T1WI (59).

IV. What Is the Role of Imaging in the Evaluation of Discoid Lateral Meniscus?

Summary of Evidence: The diagnosis is made mainly on the clinical grounds, even though in younger patients the physical exam is more difficult and less reliable. There is no pediatric study stating the exact sensitivity or specificity of a physical exam in younger children. Plain radiographs play no role in the evaluation of DLM in children (63, 64). When interpreting MRI of the knees in children, special attention must be paid to discoid lateral meniscus to avoid missing this diagnosis (Figure 19.3). Even though there are no exclusive pediatric studies evaluating the tear pattern of discoid lateral meniscus, MRI may still play a role in providing information about the type of discoid meniscus and the state of that meniscus, which would help for surgical planning (limited evidence). A detailed description of the tear is imperative as surgical planning is based on the meniscal tear pattern and degeneration.

Supporting Evidence: Despite the fact that physical examination in young children is more difficult, the sensitivity for diagnosing DLM has been reported as 90% with a specificity of 98% (8, 30). There are no exclusive pediatric studies evaluating the incidence of a tear in symptomatic patients with DLM. MRI plays a role in identifying both DLM and the presence and type of meniscal tear for surgical planning (64). The shape of the meniscus in DLM makes it more prone to tear/degeneration even in the absence of trauma, and it may tear at a younger age. In a study by Rohren et al. that included knee MRI examinations of 1,250 patients, both children and adults, 49 were found to have DLM. The frequency of isolated tears in DLM was twice that of the comparison group (20.45% vs. 9.9%), a statistically significant difference ($p = 0.02$) (64). In a study

by Kim of 771 patients that included discoid lateral menisci and normal-shaped menisci, 2.3% of patients younger than 10 years and 21.8% of the teens with DLM had a tear. There were no tears in patients younger than 10 years for normal-shaped menisci and fewer in the knees of teens. Tears without a history of trauma occurred in 9.5% of normal-shaped lateral meniscus and 53% of DLM, indicating vulnerability of DLM to tear without injury. In normal-shaped menisci, longitudinal tears within the substance were the most common, accounting for 36.4%, whereas peripheral tears were the most common in DLM, accounting for 43.2% (65).

An MRI may help in the planning of a surgical approach by identifying which patients will respond favorably to partial meniscectomy based on the state of the meniscus; this is given by the tear pattern and associated degeneration. MRI is useful in identifying and characterizing intrasubstance tears and degeneration in symptomatic stable DLM (11, 66–69). In a retrospective study by Hamada et al. that included 18 menisci, it was shown that intrameniscal regions of high signal intensity and flattening of the shape on MR images corresponded to an intrasubstance tear or degeneration of the lateral discoid meniscus not detectable by arthroscopy. The detection of these findings is very important as it can affect the surgical plan and support the preoperative role of MRI in the evaluation of DLM (66).

In a retrospective study by Bin et al. of 108 cases of patients with discoid meniscus between 6 and 71 years of age, the tear pattern was evaluated and further characterized according to the type of discoid meniscus, showing a significant difference (p <0.001). These findings help in deciding and planning (subtotal or total meniscectomy vs. partial meniscectomy). The treatment of the different tears found in DLM should be individualized, and factors such as location of the tear, clinical presentation, extent of the tear, and associated intra-articular findings should affect the choice of treatment (68).

In a prospective study by Ryu et al. of 77 patients that included children and adults of ages ranging from 10 to 67 years, knees were studied for the diagnosis of DLM and tear patterns. MRIs showed a PPV of 92% for DLM and a PPV of 57% for discoid meniscal tears. Peripheral tears alone and peripheral tears with horizontal tears were the most common types of tears (28%). Multiple tears were common (48%), and displacement of the torn segment was present in 78% of the cases. This supported a poor correlation (57%) between the prospective MRI diagnosis of discoid meniscal tears and arthroscopic findings. Sensitivity and specificity, parameters that are independent of the prevalence and that can thus be extrapolated to the general population, could not be calculated from the information provided in this article. Possible explanations for the poor performance of the prospective MRI interpretation include the high incidence of multiple tears (48%) in the DLM and the fact that DLMs are prone to degeneration because of their abnormal structure (70).

The very rare Wrisberg variant of DLM is more difficult to diagnose on arthroscopy. A preoperative suggestion of this diagnosis may alert the surgeon who confirms it at arthroscopy, demonstrating the hypermobility (10). The decision to operate, the surgical approach, and the technique all may be altered by a preoperative diagnosis of a Wrisberg DLM (10, 11, 13, 14, 71).

Cost-Effectiveness Analysis

No studies analyzing the impact of knee MRIs on cost and patient quality of life exclusively in pediatric patients were found for osteochondritis dissecans or for discoid lateral meniscus.

Discussion of Issues: Shoulder

I. When Is Radiography Indicated for Children with Acute Shoulder Trauma?

Summary of Evidence: Due to the presence of growth plates and the decreased tensile strength of bone in children, which make them more prone to fractures, the main purpose of plain radiographs in acute traumatic injury to the shoulder is to confirm the presence of a fracture and to evaluate the alignment and involvement of the physeal plate to avoid long-term disability. Most of the fractures are diagnosed readily using conventional radiographs (limited evidence). There is also limited

evidence regarding the sensitivity and specificity of a physical exam to diagnose a fracture and/or a dislocation around the shoulder in children. Radiography should be targeted to those patients with obvious shoulder deformity and point tenderness (limited evidence). However, more research is needed to validate these guidelines and to provide direct comparisons of selective imaging strategies to demonstrate the cost-effectiveness (72).

Conventional teaching advocates both pre- and post-reduction radiographs for patients with clinically suspected shoulder dislocation, and survey data confirm that many hospitals follow this recommendation (73). However, more recent limited research in adults suggests that radiographs are not necessary in most patients with recurrent atraumatic dislocation. Furthermore, the pre-reduction radiograph may be omitted in traumatic joint dislocations, provided that the clinician is confident of the diagnosis (limited evidence). There is a high recurrence rate in children after the first episode of dislocation (moderate evidence). Chronic instability and recurrent dislocation cause articular damage, leading to glenohumeral arthropathy in the long term and producing symptoms that interfere with routine daily life activities in the short term.

Supporting Evidence

Acute Trauma

In a retrospective study by Rivara et al., 189 children (209 extremities) between 1 and 15 years of age with acute trauma to the upper and lower extremities were evaluated. Among the several clinical criteria used, the authors found that there were definite physical signs in children closely correlating with finding a fracture on an extremity radiograph obtained for trauma. The two best discriminators for upper extremity fracture in this study were gross deformity and point tenderness. From the values provided on that study, no sensitivity or specificity could be generated (72). Many other studies that include adults evaluate the role of radiographs in the setting of shoulder pain, including acute trauma. For example, a retrospective study conducted in a North American Medical Center found that radiographs were performed in 59% of emergency department patients with shoulder pain (74). Twenty percent of these radiographs provided therapeutically important information (defined as glenohumeral dislocation, fracture, severe acromioclavicular joint separation, infection, or malignancy).

In the adolescent, the clinician may be more worried about possible dislocation, especially in those with recurrent episodes where the chance of recurrent dislocation is high.

Dislocation and Recurrence

In a retrospective cohort study by Dietch et al. (26) that included 32 patients between 11 and 18 years of age, the recurrence rate of shoulder dislocation and instability was 75%. In a retrospective study by Marans et al. that included 21 patients with open physes, 100% had one or more episodes of recurrent dislocation (75). In a third study of 33 patients between 12 and 17 years of age by Postacchini et al., recurrent dislocation occurred in 86% of the cases (76).

We did not find studies for only pediatric patients that evaluated the usefulness of radiographs in children with suspected shoulder dislocation or after dislocation reduction.

Hendey has demonstrated that, for adult patients with suspected recurrent relatively atraumatic dislocation, physicians were certain of the dislocation in more than 90% of cases (77). In every case this preimaging confidence was justified by radiographic evidence of dislocation without fracture. After reduction of these atraumatic dislocations, physicians were also confident that relocation had been achieved in more than 90% of patients; again this was subsequently radiographically confirmed in all cases. Although this work requires validation, it does provide limited evidence (Level 3) that radiographs are not routinely indicated in recurrent dislocation.

Opinions differ for suspected traumatic or first-time dislocations. Some have suggested that many post-reduction radiographs are not diagnostically or therapeutically useful when the pre-reduction radiograph demonstrates dislocation without fracture (77–79). In 53 patients with simple dislocation and clinically successful relocation, Hendey reported that all post-reduction radiographs confirmed the reduction and found no unsuspected fractures. Others have argued that it is more practical to eliminate the pre-reduction radiograph when the

physician is certain of the clinical diagnosis of dislocation (80). Omitting the pre-reduction radiograph enables prompt joint relocation, which would, in any case, be the preferred management even if Hill-Sachs lesions, Bankart lesions, or greater tuberosity fractures are later demonstrated on the post-reduction radiograph. Shuster et al. estimated that eliminating the pre-reduction radiograph would remove approximately 30 min from the delay between presentation and reduction (80).

Either of the strategies described above will significantly reduce radiograph utilization at centers which routinely image pre- and post-reduction. There is currently insufficient evidence (Level 4) to choose definitively between these selective imaging strategies; both have potential drawbacks. In high-energy injury mechanisms, omitting the pre-reduction radiograph risks an iatrogenic displacement of an unrecognized fracture of the humeral neck during the attempted reduction (81). Conversely, some physicians are reluctant to eliminate the post-reduction radiograph for fear of missing a fracture not evident on initial imaging or of overlooking a failed reduction (80).

II. What Is the Role of MRI in Shoulder Dislocation?

Summary of Evidence: Identification of labral and glenohumeral ligament tears is important, especially in patients with a history of shoulder dislocations, as they have a high recurrence rate. No dedicated MRI or MRA studies have been done in children. However, studies in adults show that MR arthrogram has a high sensitivity and specificity to identify and classify these lesions (moderate evidence). This information is useful to the orthopedic surgeon in preoperative planning of joint stabilization procedures.

Supporting Evidence: Given the high rate of recurrence after dislocation due to shoulder instability, MR arthrogram (MRA) may play an important role in evaluating the shoulder before surgery. It has been proven in cadaveric studies that the inferior glenohumeral ligament functions as the major stabilizing restrain and that the glenoid labrum is primarily important as the site of ligamentous attachment. There are no studies evaluating the use of shoulder MRI or MR arthrogram to evaluate the labrum or glenohumeral ligaments in pediatric patients with instability.

Even though rotator cuff pathology is not common in children and adolescents, the glenoid labrum and glenohumeral ligaments are commonly affected after a dislocation, leading to joint instability. Anteroinferior shoulder dislocation is the most common cause of shoulder instability. The glenohumeral ligaments, particularly the inferior glenohumeral ligament, are currently believed to be the major passive stabilizing structures of the shoulder. The glenoid labrum functions more as a site of ligamentous attachment. The labrum tears as it is avulsed by the glenohumeral ligaments at the time of injury.

Since different types of anterior labroligamentous lesions require different surgical procedures, preoperative discrimination of these lesions is very important. Furthermore, results of several investigations on arthroscopic procedures showed that a strong anterior band of the inferior glenohumeral ligament and an arthroscopically good delineation of the anterior labrum and associated glenohumeral ligament complex were predictors of a favorable postoperative outcome (82). The goal of performing arthroscopic and open stabilization of anterior glenohumeral instability is to re-establish the continuity of the inferior glenohumeral ligament complex to the glenoid. Thus, several authors have suggested the use of proper selection criteria to obtain optimal results after arthroscopic stabilization (82).

The role of unenhanced MRI in the detection of anterior labral injuries has mixed results with wide differences in accuracy and sensitivity ranging from 69 to 100% (82). MRA has the capability to identify labral tears that could predispose to future dislocations and articular cartilage damage. However, MR arthrogram with the injection of intra-articular gadolinium has shown superior results as joint distension helps significantly in evaluating the complex shoulder anatomy. In two consecutive prospective studies, Palmer et al. found a high sensitivity and specificity of MR arthrogram for the diagnosis of labral and glenohumeral ligament tears in adult patients with anterior instability when compared with operative reports (83, 84). In the

first study of 48 patients, they found 91% sensitivity and 93% specificity in the diagnosis of labral tears when compared with arthroscopy or open surgery (83). In the second study of 121 patients, they found 92% sensitivity and specificity for labral tears. In the same study, inferior labroligamentous lesions enabled prediction of anterior instability with a 76% sensitivity and 98% specificity (84).

Chandnani et al. in a retrospective study evaluated 46 adult patients with shoulder instability, impingement, and pain of unknown cause. They found that in the detection of tears of the superior, middle, and inferior glenohumeral ligament, MR arthrogram had a sensitivity of 100, 89, and 88%, respectively. The specificity of this technique in the identification of a normal superior, middle, and inferior glenohumeral ligament was 94, 88 and 100%, respectively. Tears of the superior, anterior, inferior, and posterior portions of the labrum were identified with a sensitivity of 89, 97, 92, and 100%, respectively. Conversely, the normal superior, anterior, inferior, and posterior portions of the labrum were identified with a specificity of 88, 86, 100, and 100%, respectively. In this study, arthroscopic findings were considered the standard of reference (85).

In a more recent study by Waldt et al. of 104 adult patients using arthroscopy as the reference standard, labroligamentous lesions were detected and correctly classified at MR arthrography with sensitivities of 88 and 77%, specificities of 91 and 91%, and accuracies of 89 and 84%, respectively (82). These data are summarized in Tables 19.8, 19.9, and 19.10.

Take Home Tables

Tables 19.1–19.10 discuss clinical prediction rules for radiography of acute knee injury, clinical exam correlation with arthroscopy, MRI interpretation with arthroscopy, diagnostic performance of clinical examination and MRI by injury, diagnostic performance of clinical examination and MRI by age group, arthroscopic and MRI classification of OCD, MRI classification of OCD, diagnostic performance of MR arthrography for detection of glenohumeral ligament tears and labral tears, and the accuracy of MR arthrography in the depiction of anteroinferior labroligamentous injuries.

Table 19.1. Clinical prediction rules for radiography of acute knee injury

Clinical prediction rule	Criteria for radiography	Sensitivity (%)	Specificity (%)	References
Ottawa knee rule (42)	• Isolated tenderness of patella (no other bone tenderness) or • Tenderness at the head of fibula or • Inability to flex 90° or • Inability to bear weight both immediately and in the emergency department for four steps	99 (44)	49 (44)	(33–35, 37, 40, 46, 86–91)
Pittsburgh rule (39)	• Fall or blunt trauma and age <12 (or >50) or • Fall or blunt trauma and inability to walk four weight-bearing steps in emergency department	99 (34)	60 (34)	(34, 39, 41)
Fagan and Davies (38)	Two or more of the following: • Effusion • Hemarthrosis • Not able to bear weight in the department (includes touch weight bearing as nonweight bearing) • History of direct trauma to the knee • Point bony tenderness at the patella, tibial plateau, femoral condyles, or the head of fibula • Age over 55 years	95 (22)	62 (22)	23 (22)
Weber et al. (41)	Patient does not need radiograph if • Able to walk without limping • Twist injury without effusion	100 (41)	34 (41)	(41)

Modified with kind permission of Springer Science+Business Media from Hollingworth W, Dixon AK, Jenner JR. Imaging for Knee and Shoulder Problems. In Medina LS, Blackmore CC (eds.): Evidence-Based Imaging: Optimizing Imaging in Patient Care. New York: Springer Science + Business Media, 2006.

Table 19.2. Clinical exam correlation (percent) with arthroscopy findings by type of injury ($N = 28$)

Test	ACL	Meniscus	Articular	Overall
Sensitivity	91	93	50	84
Specificity	100	92	100	98
Positive predictive value	100	93	100	96
Negative predictive value	94	92	88	90
Accuracy	96	92	89	

Adapted with permission of SAGE Publications from Stanitski (32).

Table 19.3. MRI interpretation (percent correlation) with arthroscopic findings (note that there was no evaluation of PCL injuries)

Test	ACL	Meniscus	Articular	Overall
Findings by type of injury				
Sensitivity	75	50	0	50
Specificity	100	45	100	87
Positive predictive value	100	50	45	70
Negative predictive value	84	50	78	75
Accuracy	89	37	78	

Adapted with permission of SAGE Publications from Stanitski (32).

Table 19.4. Diagnostic performance of clinical examination and MRI by injury

	Sensitivity (%)		Specificity (%)	
Diagnosis	Clinical	MRI	Clinical	MRI
ACL tear	81	75	90	94
Medial meniscal tear	62	79	80	92
Lateral meniscal tear	50	67	89	82
Osteochondritis dissecans	77	91	98	97
Lateral discoid meniscus[a]	89	39	98	100
Overall	71	72	92	94

[a]Statistically significant.
Adapted with permission of SAGE publications from Kocher et al. (30).

Table 19.5. Diagnostic performance of clinical examination and MRI by age group

	Sensitivity		Specificity	
Diagnostic method	<12 years	>12 years	<12 years	>12 years
Clinical examination #	77	68	93	91
MRI[a]	62	78	90	96

[a]Statistically significant.
Adapted with permission of SAGE publications from Kocher et al. (30).

Table 19.6. Arthroscopic and MRI classification of OCD

Grade	MRI
I	No break in articular cartilage; thickening of articular cartilage
II	Articular cartilage breached, low signal rim behind fragment indicating fibrous attachment
III	Articular cartilage breached with high T2 signal changes behind fragment, suggesting fluid behind the lesion
IV	Loose body with defect of articular surface

Reprinted with permission of Elsevier from Di Paola et al. (62).

Table 19.7. MRI classification of OCD (Hughes)

Stage	Description
I	Localized subchondral bone marrow edema with no changes in the overlying cartilage
II	In situ fragmentation of the subchondral bone with still intact overlying cartilage. A linear high T2 signal outlines the defect
III	Same as III, but there is edema and thinning of the overlying cartilage
IVa	Same as III, but the linear high T2 signal extends through the cartilage
IVb	Osteochondral fragment is displaced from subchondral parent bone, forming a loose body

Stages I to III are considered stable with no articular cartilage defect.
Adapted with kind permission of Springer Science+Business Media from Hughes et al. (49).

Table 19.8. Diagnostic performance of MR arthrography for detection of glenohumeral ligament tears

	Superior gleno-humeral ligament tear (%)	Middle gleno-humeral ligament tear (%)	Inferior gleno-humeral ligament tear (%)
Sensitivity	100	89	88
Specificity	94	88	100
Accuracy	94	91	97

Data from Chandnani et al. (85).

Table 19.9. Diagnostic performance of MR arthrography for detection of labral tears

	Superior labrum (%)	Anterior labrum (%)	Inferior labrum (%)	Posterior labrum (%)
Sensitivity	89	97	92	100
Specificity	88	86	100	100
Accuracy	89	95	96	100

Data from Chandnani et al. (85).

Table 19.10. Accuracy of MR arthrography in the depiction of anteroinferior labroligamentous injuries

Parameter	Value (%)
Sensitivity	88
Specificity	91
Negative predictive value	88
Positive predictive value	91
Accuracy	89

Adapted with permission of the Radiological Society of North America from Waldt et al. (82).

Imaging Case Studies

Case 1

Figure 19.1 shows MRI of osteochondritis dissecans: Sagittal PD image of the medial knee in a child with pain.

Figure 19.1. Osteochondritis dissecans on MRI. Sagittal PD image of the medial knee in a child with pain. There is a subchondral area of abnormal signal intensity. The overlying cartilage is preserved, indicating a stable lesion. Grade I by Di Paola Classification.

Case 2

Figure 19.2 shows MRI of osteochondritis dissecans: Sagittal PD image through the medial femoral condyle.

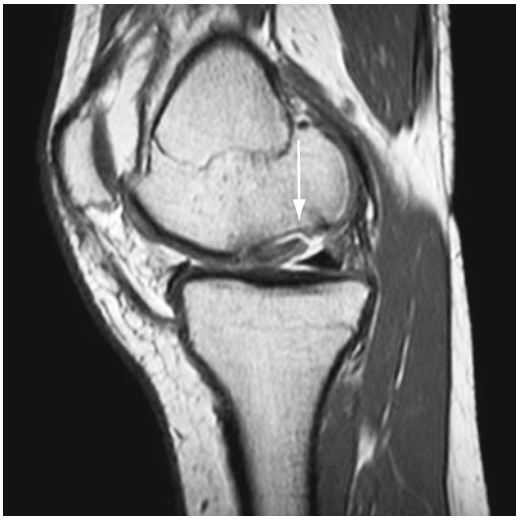

Figure 19.2. Osteochondritis dissecans on MRI. Sagittal PD image through the medial femoral condyle shows an elliptically shaped, osteochondral defect with disruption of the overlying articular cartilage (*arrow*). The bright synovial fluid outlining the defect makes this lesion unstable (Di Paola Grade III) and unlikely to heal with conservative therapy.

Case 3

Figure 19.3 shows discoid lateral meniscus on MRI.

Figure 19.3. Discoid lateral meniscus on MRI. Coronal PD image with fat saturation of the left knee shows a markedly thickened lateral meniscus extending medially close to the intercondylar notch consistent with a lateral discoid meniscus without a tear.

Suggested Imaging Protocol for the Knee and the Shoulder

The Knee

Figure 19.4 shows a diagnostic algorithm for imaging of the knee.

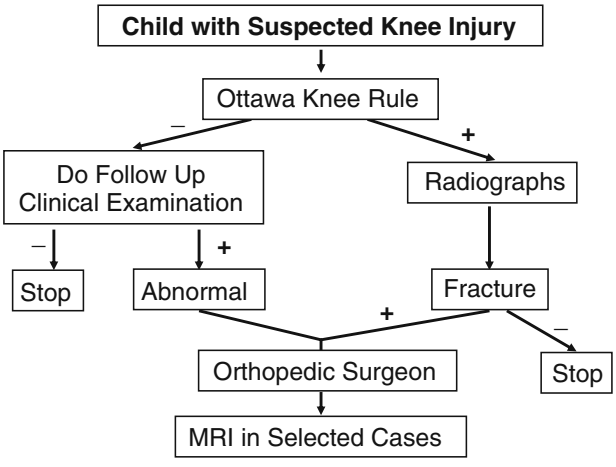

Figure 19.4. Algorithm for imaging of child with suspected knee injury.

Radiography
AP and lateral views usually suffice. The lateral view is with bent knee if possible and is obtained as a "shoot through" to see an effusion or a fluid/fluid level. Tunnel view is not recommended in children unless to evaluate osteochondritis dissecans; sunrise view is recommended for suspected lateral patellar dislocation.

MRI
MRI with the knee coil in the three orthogonal planes is desirable. Typical protocol includes sagittal, fat-suppressed, T2-weighted, and proton density sequences to evaluate the menisci and articular cartilage; coronal T1 and fat-suppressed PD sequences; fat-suppressed, PD-weighted axial series. Intra-articular gadolinium is used only when suspected unstable osteochondritis dissecans is not clearly seen on the routine protocol.

The Shoulder

Radiography
AP view of the glenohumeral joint, which includes the acromioclavicular joint and either a Y or an oblique view. The axial view is ideal to exclude dislocation, but it may be difficult if the patient cannot fully abduct the arm.

Future Research

We believe that future research should focus on the following:

The Knee

- Providing appropriate training for clinicians to implement the Ottawa Knee Rule in children while monitoring patient outcomes and cost-effectiveness.
- Defining diagnostic thresholds for the cost-effective use of MRI for internal knee derangement (meniscal, ligamentous, and cartilaginous injuries) in primary vs. specialist care settings in the pediatric population.

The Shoulder

- Validate the sensitivity, specificity, and therapeutic impact of clinical prediction rules for radiographic evaluation of children with acute shoulder pain in the emergency department.

References

1. Schenck RC Jr., Goodnight JM. J Bone Joint Surg (Am) 1996;78-A(3):439–456.
2. Obedian RS, Grelsamer RP. Clin Sports Med 1997;16:157–174.
3. Mitsuoka T, Shino K, Hamada M, Horibe S. Arthoscopy 1999;15(1):20–26.
4. Hefti F, Beguiristain J, Krauspe R et al. J Pediatr Orthop Part B 1999;8:231–245.
5. Aichroth PJ. Bone Joint Surg (Br) 1971;53(3): 440–447.
6. Deie M, Ochi M et al. J Pediatr Orthop 2006;26(1):79–82.
7. Cahill BR. J Am Acad Orthop Surg 1995;3: 237–247.
8. Cain EL, Clancy WG. Clin Sports Med 2001;20(2):321–342.
9. Robertson W, Kelly BT, Green DW. Cur Opin Pediatr 2003;15:38–44.
10. Kelly BT, Green D. Cur Opin Pediatr 2002;14: 54–61.
11. Jordan MR. J Am Acad Orthop Surg 1996;4:191–200.
12. Woods GW, Whelan JM. Clin Sports Med 1990;9(3):695–706.
13. Andrish JT. J Am Acad Orthop Surg 1996;4: 231–237.
14. Singh K, Helms CA, Jacobs MT, Higgins LD. AJR 2006;187:384–387.
15. Carson S, Woolridge D et al. Pediatr Clin N A 2006;53:41–67.
16. Bishop J, Flatow E. Clin Orthop Relat Res 2005; 432:41–48.
17. Tarkin IS, Morganti CM, et al. Am J Sports Med 2005;33:596–601.
18. Wolff AB, Sethi P et al. J Am Acad Orthop Surg 2006;14(13):715–725.
19. Morag Y, Jacobson JA et al. Radiographics 2006;26:1045–1065.
20. Emery K. Clin Sports Med 2006;25:543–568.
21. Yawn BP, Amadio P, Harmsen WS, Hill J, Ilstrup D et al. J Trauma 2000;48(4):716–723.
22. Adirim TA, Cheng TL. Sports Med 2003;33(1): 75–81.
23. Burt CW, Overpeck MD. Ann Emerg Med 2001;37(3):301–306.
24. Gomol, A. Orthopedics 2007;30:487.
25. Connolly B, Babyn PS. Can Assoc Rad J 1996;47(5):347–354.
26. Dietch J et al. Am J Sports Med 2003;31(5): 758–763.

27. Tuite M. Magn Reson Imaging Clin N Am 2003; 11(3):207–219.
28. Woolf AD, Pfleger B. Bull World Health Organ 2003;81(9):646–656.
29. National Center for Health Statistics (US). National hospital ambulatory medical care survey: 2001. Hyattsville, MD: National Center for Health Statistics (US), 2003.
30. Kocher MS, Dicanzio J, Zurakowski D, Micheli LJ. Am J Sports Med 2001;29(3):292–296.
31. Luhmann S, Schootman M, Gordon JE, Wright RW. J Bone Joint Surg 2005;87-A(3):497–502.
32. Stanitski CL. Am J Sports Med 1998;26(1):2–6.
33. Matteucci MJ, Roos JA. J Emerg Med 2003;24(2):147–150.
34. Seaberg DC, Yealy DM, Lukens T, Auble T, Mathias S. Ann Emerg Med 1998;32(1):8–13.
35. Khine H, Dorfman DH, Avner JR. Ped Emerg Care 2001;17(6):401–404.
36. Moore B. J Emerg Med 2005;28(3): 257–261.
37. Stiell IG, Wells GA, Hoag RH, Sivilotti ML, Cacciotti TF, Verbeek PR et al. JAMA 1997;278(23):2075–2079.
38. Fagan DJ, Davies S. Injury 2000;31(9):723–727.
39. Seaberg DC, Jackson R. Am J Emerg Med 1994;12(5):541–543.
40. Stiell IG, Greenberg GH, Wells GA, McKnight RD, Cwinn AA, Cacciotti T et al. Ann Emerg Med 1995;26(4):405–413.
41. Weber JE, Jackson RE, Peacock WF, Swor RA, Carley R et al. Ann Emerg Med 1995;26(4): 429–433.
42. Stiell IG, Greenberg GH, Wells GA, McDowell I, Cwinn AA, Smith NA et al. JAMA 1996;275(8):611–615.
43. Hollingworth W. In Medina LS, Blackmore CC (eds): Evidence Based Imaging, New York: Springer, 2006;273–293.
44. Bachmann LM, Haberzeth S, Steurer J, ter Riet G. Ann Intern Med 2004;140(2):121–124.
45. Tepper KB, Ireland ML. Instr Course Lect 2003;52:667–676.
46. Bulloch B, Neto G, Plint A, Lim R, Lidman P, Reed M et al. Ann Emerg Med 2003;42(1):48–55.
47. Eren OT. Arthroscopy 2003;19(8):850–854.
48. De Smet A, Ilahi OA, Graf BK. Skeletal Radiol 1997;26:463–467.
49. Hughes JA, Cook JA, Churchill MA, Warren ME. Pediatr Radiol 2003;33:410–417.
50. Pill SG, Ganley TJ et al. J Pediatr Orthop 2003;23:102–108.
51. Bohndorf K. Eur Radiol 1998;8:103–112.
52. Yoshida S, Ikata T, Takai H et al. Clin Orthop Rel Res 1998; 46: 162–170.
53. Conrad JM, Stanitski CL. Am J Sports Med 2003;31(5):777–778.
54. Cepero S, Ullot R, Sastre S. J Pediatr Orthop Part B 2005;14:24–29.
55. Williams JS, Bush-Joseph CH, Bach BR. Am J Knee Surg 1998;11(4): 221–232.
56. Milgram JW. Radiology 1978;126:305–311.
57. Jerosch J, Hoffstetter L, Reer R. Acta Orthop Belg 1996;62(2):83–89.
58. Wall E, Von Stein D. Orthop Clin N Am 2003;34:341–353.
59. O'Connor MA, Palaniappan M, Khan N, Bruce CE. J Bone Joint Surg (Br) 2002;84-B:258–262.
60. Kocher MS, Micheli Lj, Yaniv M et al. Am J Sports Med 2001; 29(5): 562–566.
61. Linden B. J Bone Joint Surg (Am) 1977;59: 769–776.
62. Di Paola J, Nelson DW, Colvine MR. Arthoscopy 1991;7:101–104.
63. Kim S-J, Moon S-H et al. Arthroscopy 2000;16(5): 511–516.
64. Rohren EM, Kosarek FJ, Helms CA. Skeletal Radiol 2001;30:316–320.
65. Kim JM. J Korean Orthop Assoc 1997;32(3): 658–661.
66. Hamada M, Shino K, Kawano K, Araki Y, Matsui Y et al. Arthroscopy 1994;10(6):645–653.
67. Araki Y, Ashikaga R, Fujii K, Ishida O, Hamada M, Ueda J et al. Eur J Rad 1998; 27:153–160.
68. Bin SI, Kin JC, Kim JM, Park SS, Han YK. Knee Surg Sports Traumatol Arthros 2002; 10: 218–222.
69. Raber DA, Friederich NF, Hefti F. J Bone Joint Surg (Am) 1998;80-A(11):1579–1586.
70. Ryu KN, Kim AS, Ahn JW et al. AJR 1998;171:963–967.
71. Aichroth PM, Patel DV. J Bone Joint Surg (Br) 1991;73-B:932–936.
72. Rivara F, Parish RA et al. Pediatrics 1986;78(5):803–807.
73. te Slaa RL, Wijffels MP, Marti RK. Eur J Emerg Med 2003;10(1):58–61.
74. Fraenkel L, Lavalley M, Felson D. Am J Emerg Med 1998;16(6):560–563.
75. Marans HJ, Angel KR et al. J Bone Joint Surg 1992;74A:1242–1244.
76. Postacchini F, Gumina S et al. J Shoulder Elbow Surg 2000;9(6):470–474.
77. Hendey GW. Ann Emerg Med 2000;36(2): 108–113.
78. Harvey RA, Trabulsy ME, Roe L. Am J Emerg Med 1992;10(2):149–151.
79. Hendey GW, Kinlaw K. Ann Emerg Med 1996;28(4):399–402.
80. Shuster M, Abu-Laban RB, Boyd J. Am J Emerg Med 1999;17(7):653–658.
81. Demirhan M, Akpinar S, Atalar AC, Akman S, Akalin Y. Injury 1998;29(7):525–528.

82. Waldt S, Burkart A, Imhoff AB, Bruegel M et al. Radiology 2005; 237:578–583.
83. Palmer WE, Brown JH, Rosenthal Di. Radiology 1994 190: 645–651.
84. Palmer WE, Carlowitz PL. Radiology 1995, 197:819–825.
85. Chandnani VP, Gagliardi A, Murnane TG et al. Radiology 1995: 196:27–32.
86. Szucs PA, Richman PB, Mandell M. Acad Emerg Med 2001;8(2):112–116.
87. Kec RM, Richman PB, Szucs PA, Mandell M, Eskin B. Acad Emerg Med 2003;10(2):146–150.
88. Ketelslegers E, Collard X, Vande Berg B, Danse E, El-Gariani A, Poilvache P et al. Eur Radiol 2002;12(5): 1218–1220.
89. Emparanza JI, Aginaga JR. Ann Emerg Med 2001;38(4):364–368.
90. Tigges S, Pitts S, Mukundan S, Jr., Morrison D, Olson M, Shahriara A. AJR Am J Roentgenol 1999;172(4):1069–1071.
91. Richman PB, McCuskey CF, Nashed A, Fuchs S, Petrik R, Imperato M et al. J Emerg Med 1997;15(4):459–463.

20

Developmental Dysplasia of the Hip

Marc S. Keller, Els L.F. Nijs, and Kimberly E. Applegate

Issues

I. What are the clinical findings of developmental dysplasia of the hip (DDH) and how effective are clinicians at detecting them?
II. What is the natural history in undetected DDH?
III. How accurate is US imaging in depicting hip anatomy and DDH?
IV. How effective is imaging in the diagnosis and treatment of DDH?
V. Is there a case for US screening of all newborns to detect DDH?

Key Points

- Skilled clinical examiners are capable of detecting the vast majority of developmental dysplasia of the hip (DDH) in neonates, and this remains the primary screening method in the United States. Ultrasound (US) is no better than these examiners but may improve DDH diagnosis or exclusion for less-experienced clinical examiners (strong evidence).
- The great majority of hips with neonatal laxity will spontaneously become normal (strong evidence). Of the newborns labeled as DDH by either clinical or US screening, about 90% will spontaneously become normal without treatment (strong evidence). When there is a displaced femoral head and acetabular dysplasia found from late-appearing DDH in a toddler or a preschooler, this usually will lead to an unfavorable long-term result and the need for corrective orthopedic procedures (strong evidence).
- The main aim of health care in DDH is to detect and treat DDH early and in doing so avoid multiple corrective procedures and prevent lifelong hip disease with significant costs (strong evidence).
- US hip imaging in neonates and infants, whether the static or the dynamic method, is highly sensitive to DDH when done by experienced operators but is not specific (false positives). The low

M.S. Keller (✉)
Department of Radiology, Children's Hospital of Philadelphia, Philadelphia, PA 19104, USA
e-mail: kellerm@email.chop.edu

L.S. Medina et al. (eds.), *Evidence-Based Imaging in Pediatrics*,
DOI 10.1007/978-1-4419-0922-0_20, © Springer Science+Business Media, LLC 2010

specificity leads to overtreatment, excessive imaging, and higher costs. Like the clinical exam, the use of hip US may not prevent late DDH (moderate evidence).
- Hip US for DDH evaluation should not be performed prior to age 3 weeks due to normal neonatal hip laxity that produces high false-positive rates (moderate evidence).
- Conflicting data remain concerning the role of general neonatal or infant population US hip screening with regard to late emergence of DDH and its cost-effectiveness (moderate evidence).

Definition and Pathophysiology

Developmental dysplasia of the hip (DDH) is a term that includes a variety of conditions in the developing fetal, neonatal, and infant hip. The inciting pathology is agreed to be abnormal laxity of the hip joint leading to subsequent displacement of the femoral head. The sustained subluxation or dislocation of the femoral head over time does not permit normal development of the acetabulum and results in a predictable pattern of acetabular growth disturbance that is termed hip dysplasia (strong evidence). In the current era, with clinical newborn screening nearly universal, the incidence of neonatal hip instability is in the range of about 1–2%. Nearly all of neonatal laxity can be shown to be transient hip joint instability with spontaneous stabilization within the first few weeks of life due to maternal hormones and not true DDH, which has an incidence closer to 0.1–0.2% (1–5) (strong evidence). Hip joints that show more displacement for more time tend to exhibit more dysplasia.

Epidemiology

Studies have shown DDH six times more often in girls than boys and occurring 60% in the left hip, 20% in the right hip, and 20% bilaterally (6). Some parts of the world have higher incidences of DDH than others, and there appear to be both genetic and environmental effects (strong evidence). According to the Centers for Disease Control (CDC), the Caucasian rate is 1.7/1,000 live births and for blacks, it is significantly lower at 0.54/1,000 live births.

Some countries or regions have higher incidences of DDH identified. In other parts of the world where infants are carried with their hips in abduction from early in life, lower rates of DDH may be noted. It seems that cultural infant hip abduction may modify the natural history of early instability and clinically noted dysplasia (moderate evidence). On balance, the reported incidence of abnormal neonatal clinical examinations indicative of neonatal laxity ranges from 1 to 2%, of which perhaps only one-tenth are true cases of DDH, creating a DDH incidence of 0.1–0.2% (2, 3, 7–9) (strong evidence).

In all areas of the world, a breech position found just before birth is a risk factor for DDH with an odds ratio of 5.5 (10) (strong evidence).

Family history of DDH and the presence of neonatal clubfoot or torticollis are each thought to increase the risk for DDH (1, 11–14) (moderate evidence).

A number of childhood conditions have DDH as a comorbidity, although not presenting in the typical neonatal and infant manner as noted above. For example, 35% of children with cerebral palsy will develop DDH (15). Other notable conditions with development of hip dysplasia would include myelodysplasia, arthrogryposis, caudal regression syndrome, Larsen syndrome, Stickler syndrome, multiple epiphyseal dysplasia, Trevor disease, spondyloepiphyseal dysplasias, metatropic dysplasia, and some of the mucopolysaccharidoses, particularly Morquio disease (16).

Overall Cost to Society

Concerning the primary clinical problem of DDH, promptly detecting and treating young infants leads to excellent outcomes (strong evidence). Early treatment is nonoperative as well as lower in cost. Organized programs that have used US screening of large populations consistently seem to overdiagnose DDH based upon either immature acetabular morphology or detection of laxity, leading to overtreatment, repeated imaging, and higher costs in a group that would not have emerged clinically and would not have needed this care (17) (moderate evidence). Furthermore, in most studies, early US general population screening has not eradicated the appearance of late DDH cases (4, 5, 18–25) (strong evidence).

Using a brief, well-established, and accurate clinical examination to screen neonates would seem intuitively most cost-effective without the added costs of routine imaging, unless the costs of screening are less than the costs of treating cases of late appearance of DDH, some of which will require multiple surgeries, hospitalizations, and even some hip replacements as adults (26–40). At least two studies show that the use of US hip screening in the general population helped to efficiently diagnose and to care for children with DDH and was not associated with higher health-care costs (26, 41) (moderate evidence).

Goals

The main aim of imaging is to detect and treat DDH early and in doing so avoid multiple corrective procedures and prevent lifelong hip disease with significant costs (strong evidence). The aims of imaging in evaluating DDH are several. Initial imaging must be able to depict the important anatomy along with morphologic and dynamic alterations. Care in early US examinations must be taken to learn and to appreciate variations in immature morphology and normal ranges of laxity in order to avoid overtreatment. The confirmation of hip reductions in treatment devices is an important and useful function of US imaging (6, 27–37). In children who have had surgery and spica cast applications, brief, tailored, low-dose CT examinations or MRI studies are key in confirming successful reductions prior to patient discharge. Lastly, use of radiographic and cross-sectional images is all needed in the accurate preoperative assessments of children with late detection of DDH and subsequent corrective operations as well as in the evaluation and care of postoperative complications (38–40, 42).

Methodology

The authors performed a MEDLINE search using PubMed (National Library of Medicine, Bethesda, MD) to retrieve information concerning clinical and imaging diagnosis and treatment of children with developmental dysplasia of the hip (DDH). The systematic literature review performed in MEDLINE looked at the 10-year period from 1998 to 2008. The search strategy used the following terms: (1) developmental dysplasia of the hip; (2) humans; (3) clinical trial; (4) meta-analysis; (5) randomized controlled trial; (6) review; (7) English language; (8) all infants: birth–23 months; (9) all children: 0–18 years.

Discussion of Issues

I. What Are the Clinical Findings of DDH and How Effective Are Clinicians at Detecting Them?

Summary of Evidence: The clinical examination techniques of neonatal and infant hip examination are well described and have been used for over 40 years (43, 44). The group of clinically described findings includes limited range of motion, abnormal skin creases, unequal limb lengths, palpable grinding, and the Barlow and Ortolani signs. The Barlow sign is appreciated during neonatal hip flexion and adduction when posterior stress along the axis of the femur produces palpable posterior displacement of the femoral head from the acetabulum. Ortolani's sign is a low-pitched palpable thud or clunk appreciated during hip abduction, indicating the reduction of the posteriorly

dislocated femoral head back into the acetabulum. Examination early in life is key, for the Barlow and Ortolani signs are useful only during the first months.

While examiners with experience produce excellent results (5) (strong evidence), clinical observation study of less-experienced personnel performing neonatal hip examinations finds their assessments to be considerably less reliable (45) (limited evidence). The specificity of a normal examination approaches 100% (1). However, review of reported prevalence of neonatal clinical hip instability has yielded a range of 1.6–28.5/1,000 (4). The skill of experienced examiners is believed to improve sensitivity (1). In addition, examination by knowledgeable examiners has been shown to yield very low late appearance of DDH incidences ranging from 0.01 to 0.2% (1–5) (strong evidence).

A small number of babies with normal initial clinical examinations will later develop DDH; therefore, repeat clinical examinations are recommended.

Supporting Evidence: While all of the clinical hip findings above are listed in the performance of the neonatal and infant hip evaluations, the detection of them has not been shown to be synonymous with the actual diagnosis of DDH. Clinical screening for DDH is performed in the first 1–2 days after birth and serially at follow-up well-baby checks. About 1–2% of the neonates will be shown to have only neonatal laxity which will spontaneously correct over the course of several weeks and without treatment. Such self-limited hip instability is a common finding in newborns (46). A variety of publications with follow-ups ranging from 2 weeks to 6 months have found that 80–97% of milder neonatal abnormal hip findings normalize without treatment (2). Some of the large clinical studies have designed the use of selective US hip imaging in the assessment of babies with a family history of DDH, breech presentation at birth, foot deformity, and the detection of neonatal laxity (5). In these instances, selective US imaging of the hips is utilized as an extension of the historical and clinical assessment and not as a screening examination. In one randomized controlled study of 15,529 infants seen by experienced clinical examiners, the specificity of a normal clinical examination was high, with only 0.65/1,000 late appearance of DDH (5).

The experience of the clinical examiner is not a trivial issue. Studies show that experienced confident neonatal and infant hip examiners have excellent clinical results and need to refer very few babies to imaging as noted above. Less-skilled personnel have more questions, less confidence, and a more liberal use of imaging to provide a second opinion behind their assessments. Prevalence of DDH in some clinical series has been reported as high as 168–200/1,000 infants, while most series suggest ranges of 0.1–7/1,000 (2). As will be discussed below, imaging tends to result in higher treatment rates of infant hips and is shown by most studies to increase health-care expense from overtreatment (47, 48).

II. What Is the Natural History of Undetected DDH?

Summary of Evidence: Of the newborns labeled as DDH by either clinical or US screening, about 90% will spontaneously become normal without treatment (2, 3) (strong evidence). When there is a displaced femoral head and acetabular dysplasia found from late-appearing DDH in a toddler or a preschooler, this usually will lead to an unfavorable long-term result and the need for corrective orthopedic procedures (1–5, 49) (strong evidence). Currently unknown is how untreated hips with a mild degree of dysplasia will fare in the long run as practitioners seem unwilling to test this. A key uncertainty created by US imaging is the significance of milder abnormalities such as neonatal laxity, immature acetabula, and milder dysplasia without instability, which has led to a tendency of clinicians to treat and follow up on all of these infants. The value, if any, of this early detection remains unknown (30, 35, 47) (moderate evidence).

Supporting Evidence: The pathophysiology of DDH can be viewed as a combination of mobility and morphology. Excessive mobility is described as laxity, subluxation, or dislocation. Displaced femoral heads may be reducible or irreducible. Acetabula can be normal,

immature, or have varying degrees of severity of dysplasia. The greater the degree of abnormal femoral head mobility and the longer the time period of hip instability, the more dysplastic the acetabulum is likely to be.

Better than 96% of infant hips that are treated early in life, within 6–8 weeks from birth, by observation or by using dynamic or fixed abduction splints, tend to become readily stabilized and regress their dysplastic changes in short order (5). The small remainder goes on to need additional procedures such as adductor tenotomies or open reductions and placement in hip spicas. Most rarely, infants detected early with DDH may come to innominate osteotomy for realignment of an abnormal acetabulum to allow for better femoral head coverage and hip stability (50–56). The most common complication from treatment is avascular necrosis of the femoral head. It occurs in approximately 0.25% if treatment begins before the age of 6 months and 10.9% if treatment begins after 6 months (10).

Conversely, children in whom the diagnosis of DDH is delayed beyond 3–6 months have a much poorer prognosis. Review of several studies of older toddlers with delayed DDH diagnoses finds only 28% with good outcomes (moderate evidence). When followed to young or middle adulthood over 30–40 years, 41–43% have degenerative hip disease, 60% have disturbed proximal femoral growth, and 11–14% have total hip replacement or hip arthrodesis (2, 3) (moderate evidence). The case for the importance of diagnosing DDH as early as possible is clear.

III. How Accurate Is US Imaging in Depicting Hip Anatomy and DDH?

Summary of Evidence: In neonates and infants, no significant controversy remains that hip sonography is an excellent and accurate method to image the normal hip and the anatomy of DDH. All initial skepticism of the 1980s has vanished concerning this point. Of the two methods used, the static and the dynamic, both appear to work well. Better evidence (strong evidence) exists to support the static method owing to the preponderance of European studies (4, 5, 20, 21, 23, 25, 26, 35, 49), but no sizeable randomized controlled trials in North America have been performed. No study has been performed to pit the static method vs the dynamic method, but investigators do not seem inclined to pursue this as an important question.

Sonographic exams depend on the experience of the operator. One large study in the Netherlands of hip US in 7,236 infants reported a sensitivity of 88.5%, a specificity of 96.7%, a positive predictive value of 61.6%, and a negative predictive value of 99.4% (57).

Supporting Evidence: The initial studies regarding hip sonography as reported by Graf and colleagues in Austria emphasized extremely detailed classification of sonographic hip anatomy in normal, immature, and dysplastic hips with accompanying alpha and beta angles describing quantitative measures of acetabular bony angle and position of the lateral acetabular labrum in a static hip via a standardized coronal view with the baby in a lateral decubitus position. The method has been validated repeatedly in large studies (1–5) (strong evidence), but clinical use has tended to deemphasize the need for the original painstakingly detailed classifications and subclassifications. Success in clinical use has reduced the categories in many studies to normal, immature, mild dysplasia, and more severe dysplasia with femoral head displacement while tending not to quantitate the alpha and beta angles, which have been shown to be difficult to reproduce among examiners (5, 49) (moderate evidence).

The dynamic method described in the United States with Harcke as its most experienced proponent acknowledges all of the morphologic acetabular changes described by Graf but creates images both in the coronal and transverse planes and, in addition, parallels the clinical orthopedic examination by imaging during relaxed hip flexion, with neutral hip position, and during stress using a Barlow maneuver (hip flexion, hip adduction, and posteriorly directed mild stress). In the dynamic method, the degree of hip stability or instability is reported in the different positions and is combined with a qualitative description of acetabular morphology (29, 30) (moderate evidence).

Morin et al. added a quantitative descriptor of bony acetabular coverage over the femoral head in the coronal plane that is used by some practitioners and investigators. Normal coverage is lowest (45–50%) in the newborn and normally increases with time (58) (limited evidence).

In 1993, a meeting was held with both Graf and Harcke present and with each acknowledging the validity of both methods. Agreement allowed the creation of recommendations combining the strengths of each into a standardized US hip examination and largely ending the controversy about two methods that both seemed to work. The aftermath of this summit focused subsequent investigation on studying DDH and not the competition between two examination methods.

Interestingly, this combined assessment, which indeed appears to be accurate and valid in practice, has been adopted as a performance standard of the American College of Radiology and the American Institute of Ultrasound in Medicine largely based on expert recommendations (59) (limited evidence).

IV. How Effective Is Imaging in the Diagnosis and Treatment of DDH?

Summary of Evidence: In neonates and young infants with cartilage dominating the femoral head and acetabular structures, US hip imaging is the most accurate noninvasive method to portray hip anatomy and dynamics and to detect DDH. In older infants and toddlers with femoral ossification centers and more acetabular bone that limits the use of US, radiographs become the imaging method for detection and treatment follow-up.

Contrast arthrography remains a very accurate examination but one that is not in general diagnostic use except to assess for intraoperative reductions and before applying spica casts. Limited postreduction low-exposure CT studies or limited rapid MRI scans are effectively used after intraoperative hip reductions and spica applications to ensure satisfactory reductions prior to patient discharge. In older children and adolescents with either delayed DDH diagnosis or with long-term complications requiring additional surgery for hip coverage or stabilization, volumetric CT examinations with 3D and MIP reformatted images are very useful for preoperative planning (6, 27–30, 38–40, 42).

Supporting Evidence

Sonography

The problem of late emergence of DDH was the impetus to develop US hip imaging. Clinical hip screening detected the great majority of cases; nevertheless, late appearance of hip dislocations with dysplasia continued. Despite educational programs designed to teach this new method, late appearances of hip dysplasia did not decrease. Similar findings appeared in a number of studies; in fact, this unexpected result led to a change in both thinking and terminology about the condition, formerly called congenital dysplasia of the hip (CDH) which was changed to developmental dysplasia of the hip (DDH) to reflect that not all of these cases were congenital and diagnosable at the time of birth (1) (strong evidence).

While learning that US hip screening did not readily eradicate late appearance of DDH was a disappointment, the question remained about what was the role of hip sonography which had eventually become accepted as accurate imaging within its first 10–15 years of use. The preponderance of current evidence shows that not only hip sonography is anatomically and dynamically accurate, but the sensitive portrayal of findings tends to lead to overtreatment and higher health-care costs. One study evaluating the diagnostic accuracy of hip US found in 7,236 Netherlands infants a sensitivity of 88.5%, a specificity of 96.7%, a positive predictive value of 61.6%, and a negative predictive value of 99.4% (57). Armed with US images showing degrees of hip laxity, subluxation, and mild dysplasia, physicians tend to conservatively follow-up on these infants in whom natural history shows will spontaneously revert to normal almost always. However, the emotion revolving around possible missed cases of DDH creates an environment of caution, with clinical and imaging follow-up. In this regard, US has less than ideal sensitivity for a screening test (48). Some studies however have shown that the use of hip sonography can reduce the rate of

infant hip splinting without adverse effects (47, 49) (moderate evidence).

Plain Radiographs

By 4–6 months of age, radiography becomes the primary imaging modality, for the nucleus of the femoral head ossifies at approximately 4 months (50th percentile) with a normal range of 2–8 months (60). The ossific nucleus is visible on sonography several weeks before its radiographic appearance, and as the center develops and enlarges, the ossific femoral head nucleus obscures medial acetabular sonographic landmarks.

An anteroposterior view of the hips in neutral position is routinely used in the evaluation of DDH. One main goal of radiography is evaluating the relationship of the femoral head and metaphysis to the acetabulum. The lines of Hilgenreiner, Perkins, and Shenton serve as visual guides to recognize an abnormal relationship, particularly when the femoral head is still unossified. The acetabular angle is an often used objective measurement in the diagnosis and follow-up of DDH. Normally, it is less than 30° in newborns and then decreases with age. The reported 95% tolerance interval for intraobserver variability, however, is 8.35° with interobserver variability exceeding this number, which casts doubt on the reliability of this angle measurement based on a single reading (61, 62). In a small series of seven children (14 nonoperated hips with DDH) with a mean age of 7.3 years (range 3.3–10.5 years), the acetabular index was measured on radiography and compared with MRI with a significant correlation with a Spearman correlation coefficient of 0.88 (95% confidence interval, 0.61–0.96; $p<0.001$) and a mean difference between the two measures of $0.36 \pm 6.5°$ (limited evidence). In addition, the osseous and cartilaginous acetabular indexes as measured by MRI had a significant correlation with a Spearman correlation coefficient of 0.88 (95% confidence interval, 0.80–0.98; $p<0.001$). Based on these results the authors suggest that plain radiography is still an appropriate tool for follow-up of the nonoperated hip with DDH and may be a good indicator of hip cartilaginous development (63). In the older child, two other measurements can be assessed: the coverage of the ossified femoral head by the bony acetabular roof can be quantified and the center–edge angle (C–E angle) can be measured.

Computed Tomography (CT)

Starting in the early 1980s, CT has been used to evaluate the postreduction femoral head position in spica casts, instead of plain radiography. CT has a twofold advantage over plain radiography. The hip after reduction can be evaluated directly in the axial and coronal planes, and CT images are not significantly degraded by the overlying spica cast. A digital scout view is first obtained to plan a limited series of narrow collimation images at very low dose through the hips. In the normally positioned hip, the quality of reduction is assessed by the CT equivalent of Shenton's line. There should be a smooth arc formed by the anterior aspect of the femoral neck and the anterior aspect of the pubic bone. Also, the center of the concentrically reduced femoral head lies directly lateral to the anterior ischial junction with the triradiate cartilage (64). In addition the degree of dysplasia can be evaluated. While the normal hip will have a smooth, round-shaped acetabulum with a well-defined posterior lip, the dysplastic hip lacks this round shape and the posterior acetabulum will often be straightened without a well-defined border. Dysplastic acetabula will usually show the low attenuation of the fibrofatty pulvinar tissue medially.

A more complete pelvic CT may be used to plan pelvic osteotomy. The protocol used for this type of CT is different in that the axial images will be obtained with 2.5–3 mm collimation or less and more anatomic coverage is needed to reconstruct in 2D and 3D. Measurements of the acetabular roof, cartilage thickness, acetabular rotation, and acetabular version can all be assessed for surgical planning.

MR Imaging (MRI)

MRI is not frequently used for evaluation of DDH. For example, the postreduction hip in spica cast MR imaging requires longer scanning time in comparison to CT and the potential need for sedation or anesthesia. A brief scan protocol has been described by Laor et al. in a small number of patients (65) in which her team did not use sedation or anesthesia. The main

advantage of MRI is better cartilage anatomical detail.

Femoroacetabular impingement and labral tears are increasingly recognized as a cause of hip pain or disability in adolescents and young adults, and they are fairly common in late DDH. The preferred imaging modality is MR arthrography, which is performed by injecting dilute gadolinium solution in the hip joint followed by MRI. MRI findings of impingement include edema and cyst formation in the acetabular rim and cartilage or labral degeneration or tear. In DDH the labrum is typically hypertrophic and may have associated tears or paralabral cysts.

AVN of the femoral head, the most common complication of treatment, is well evaluated by MRI (66).

V. Is There a Case for US Screening in Newborns to Detect DDH?

Summary of Evidence: Universal screening of newborns with ultrasound is performed in some European countries. In most of the larger studies, the use of general screening has tended to reduce but has not eradicated the rare but persistent late emergence of DDH in older infants and toddlers (moderate evidence). Some of the smaller studies, however, claim to use US screening and follow-up efficiently and cost-effectively to detect early DDH and prevent the appearance of late cases. In North America, neither the United States nor the Canadian government believes that current evidence supports universal US hip screening for DDH (48).

Supporting Evidence: Rosendahl et al. found in a study of nearly 12,000 Norwegian infants that late DDH appeared in 0.3/1,000 in an US screened group vs 1.3/1,000 in a clinically screened cohort (57). This result was not statistically significant but a trend suggesting a four-fold reduction in late DDH from US screening. In a study of 15,529 babies, Holen et al. found late DDH in 0.13/1,000 infants with universal US screening vs 0.65/1,000 in a clinically examined group with selective US use, again showing a trend but not reaching statistical significance (5). One of the very interesting and important points that emerge from studying this question is that skill of the clinical and US examiners is exceedingly important. Observational study of clinical examinations hints that the degree of skill and sophistication of neonatal hip examiners is quite variable and that novices, not surprisingly, do not examine as well as more experienced practitioners (18, 19, 65). The results of having less-experienced personnel do these examinations can lead either to a higher rate of missed DDH or to a more liberal use of imaging as a check upon weak clinical skills in order not to miss the diagnosis or to reassure the presence of normal. In a study focusing on routine newborn clinical examination quality in England, the quality of hip examination performed by midwives and senior house officers was sometimes rated poor by the attending physicians. However, the midwives performed better than did the senior house officers. A κ value of 0.42 showed only moderate agreement between the opinion of attending physicians and midwives (45).

With sonography, skill and experience also play an important role, for again, a less-experienced imager is more likely to miss some findings or be tentative with declaring physiologic neonatal hip laxity or acetabular immaturity as normal and instead recommending another interval US hip imaging. This tendency toward being conservative has been shown to lead to hip splinting of infants who in all likelihood would have spontaneously stabilized without treatment or additional imaging (2, 3). Unnecessary splinting is not innocuous, since 1–4% of treated infants may develop avascular necrosis of the femoral head as a result of flexion and abduction positioning (48).

In some of the larger studies described above, experienced clinical hip examiners had excellent results in evaluating thousands of babies with only 0.65/1,000 late detection of DDH (diagnosis made after 1 month of age) and were helped by the US screening only in a limited number of cases with additional risk factors such as neonatal laxity, breech presentation, foot deformity, and family history of hip disease (5).

In routine practice, clinical and US imaging examiners have a range of skill levels so that the results achieved in a specialized center

running a focused infant hip study may not be readily duplicated in all communities. In most of the world, clinical screening of neonates and infants is still likely to dominate DDH detection with US imaging used to evaluate those with abnormal examinations, those with questionably abnormal results, those with risk factors, and in follow-up examinations of hip reduction devices in children under treatment.

Take Home Figures and Tables

Figure 20.1 presents an algorithm for imaging protocol in DDH. Figure 20.2 shows different categories of DDH. Figure 20.3 shows normal hip sonogram vs posterolateral displacement of the femoral head. Table 20.1 presents a summary of diagnostic performance in infants with DDH.

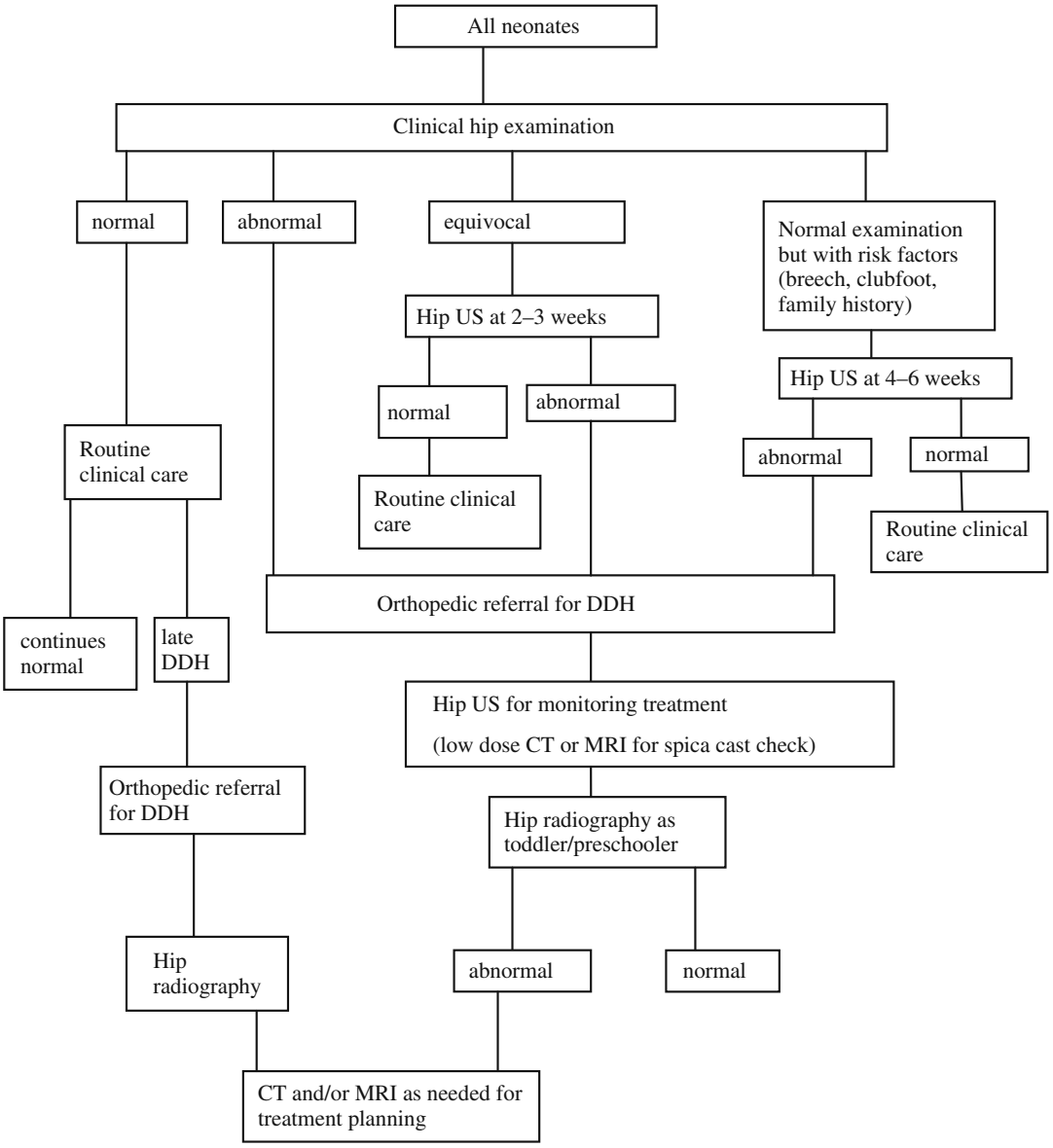

Figure 20.1. Algorithm for imaging in DDH.

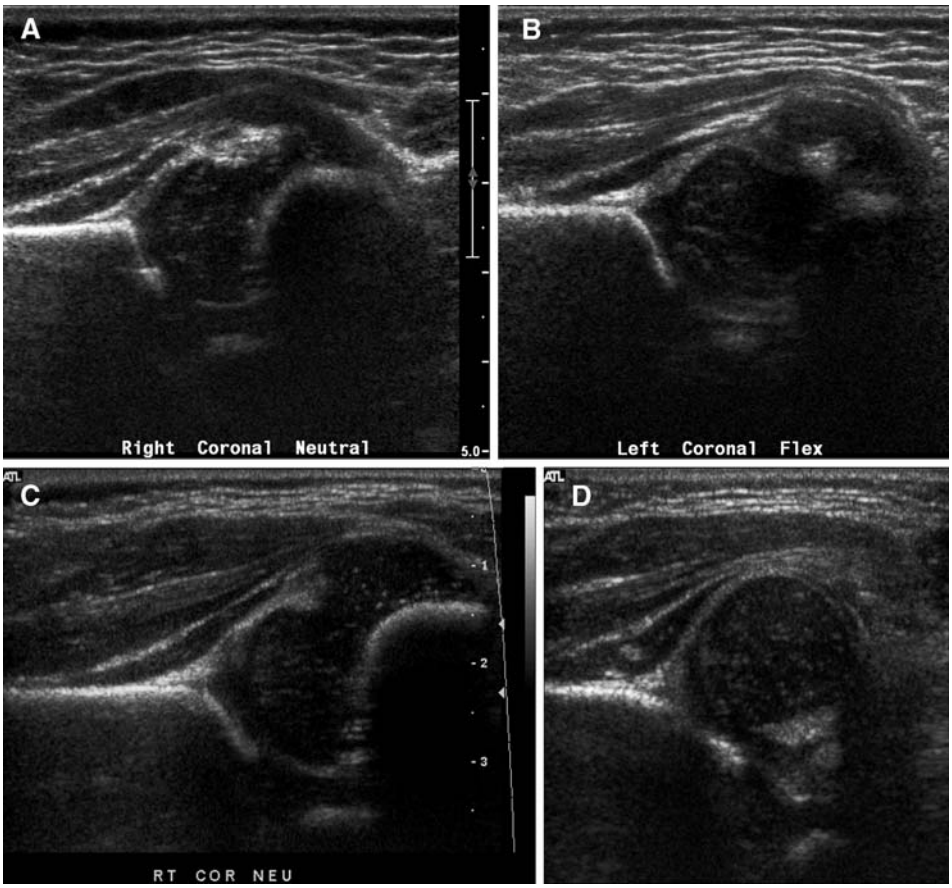

Figure 20.2. Coronal hip sonograms depicting basic categories. **A**: Normal. **B**: Immature, with minimally diminished superolateral rim ossification. **C**: Mild dysplasia without femoral head displacement. **D**: Dysplasia with femoral head displacement, deficient acetabular rim ossification, thickened labrum and pulvinar.

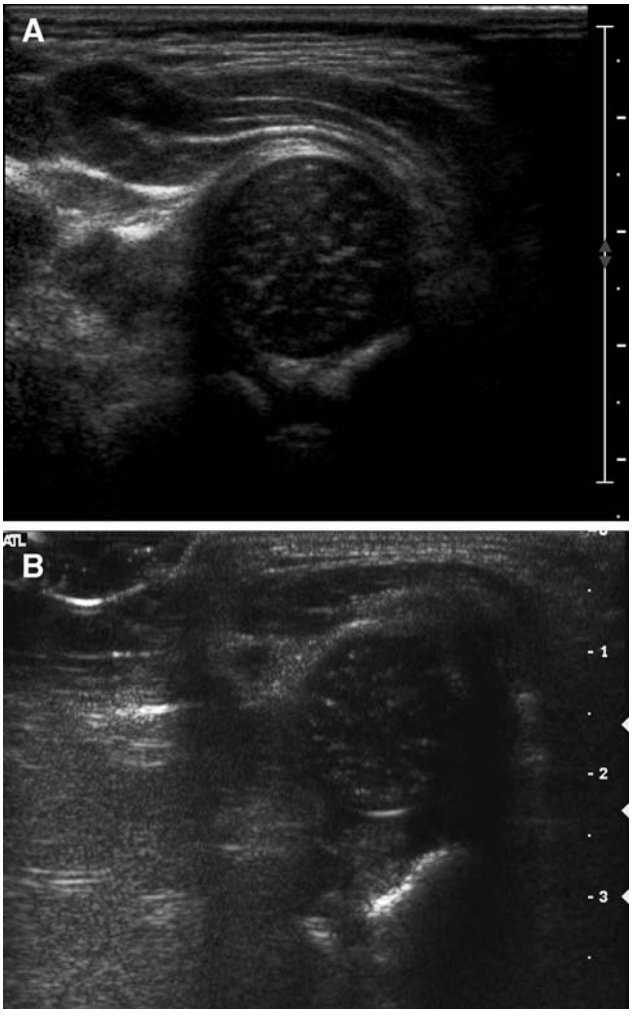

Figure 20.3. **A**: Normal transverse neutral hip sonogram. **B**: Posterolateral displacement of femoral head in transverse neutral view.

Table 20.1. Summary of diagnostic performance in infants with DDH

Screening test	Sensitivity (%)	Specificity (%)	
Clinical exam (reference standard was sonography for all references)			
Limited abduction	70	90	(67)
Limited abduction[a]	69	54	(24)
Orthopedic specialist	97	14	(68)
Sonography	89 (22, 67)	97 (57)	PPV 62%, NPV 99% (57)

[a]Age >3 months.

PPV=positive predictive value; NPV=negative predictive value.

Imaging Case Studies

Case 1

Figure 20.4 presents a case depicting hip laxity without dysplasia

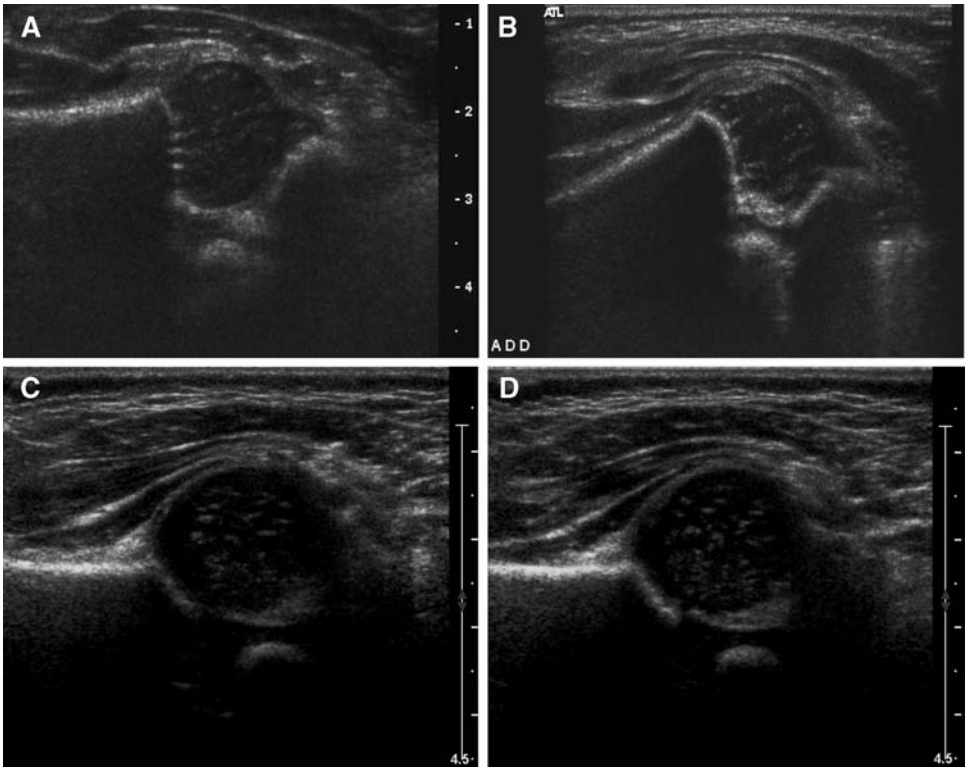

Figure 20.4. Transverse (**A**) flexion–abduction and (**B**) flexion–adduction views along with coronal (**C**) flexion–abduction and (**D**) flexion–adduction views depicting hip laxity without dysplasia. Evidence shows that follow-up imaging is unnecessary.

Case 2

Figure 20.5 presents a limited axial CT study according to the principles of www.imagegently.org.

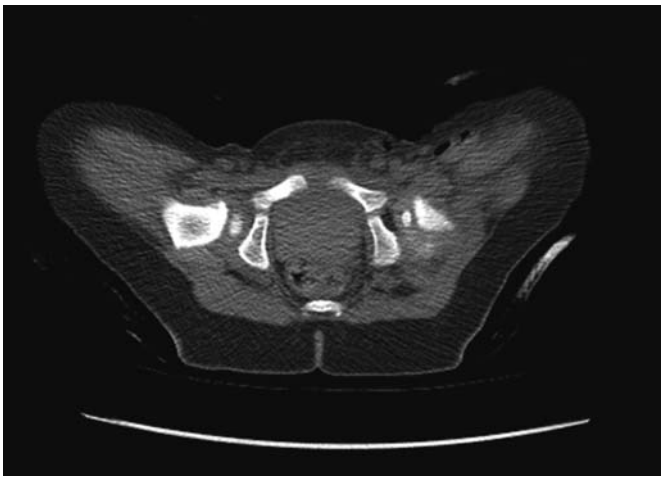

Figure 20.5. Low mAs limited axial CT study to confirm reduction in spica in line with principles of www.imagegently.org. Despite image noise, note sufficient detail at 10 mAs to identify postoperative air from adductor tenotomy and fatty pulvinar at the base of dysplastic left acetabulum.

Suggested Imaging Protocols for Developmental Dysplasia of the Hip

Screening for DDH

- Birth–6 months: hip sonography (coronal view—neutral and stress, transverse view—flexion and stress)
- 6 months and older: hip radiography (AP radiograph of the pelvis and hips)
- Assessing reduction in Pavlik harness: hip sonography (coronal and transverse views—"as is" and within safe zone adduction restriction of harness)
- Assessing reduction in spica cast: low-dose CT (digital radiograph scout view and limited axial imaging through hips) or tailored MRI
- Routine preschooler assessment after treatment: hip radiography
- Surgical planning to address DDH in older child: hip radiography; low-dose MDCT with 3D, and MPR (multiplanar reconstructions) or MRI (arthrography optional)

Future Research

- Can the rare late case of DDH be prevented?
- Cost-effectiveness analysis on the role of screening hip US in high-risk newborns.
- Cost-effectiveness analysis of universal screening hip US.
- Is nontreatment of the sonographic finding of mild acetabular dysplasia with a stable hip a safe practice or will it lead to late case emergence of DDH?
- What is the best way to improve both clinical and sonographic DDH examination skills?

References

1. Eastwood D M. Lancet 2003;361(9357): 595–597.
2. Kocher MS. Am J Orthop 2000;29(12): 929–933.
3. Kocher MS. Am J Orthop 2001; 30(1): 19–24
4. Dezateux C, Rosendahl K. Lancet 2007;369(9572): 1541–1552.
5. Holen K, Tegnander A et al. J Bone Joint Surg Br 2002;84-B(6): 886–890.

6. Hennrikus WL. Pediatr Ann 1999;28(12): 740–746.
7. Patel H, Care CPFOPH. CMAJ 2001;164(12): 1669–1677.
8. Storer SK, Skaggs DL. Am Fam Physician 2006;74(8): 1310–1316.
9. Witt C. Adv Neonatal Care 2003; 3(2): 65–75.
10. Lehmann HP, Hinton R, Morello P et al. Pediatrics 2003;105 (4): e57.
11. Guille JT, Pizzutillo PD et al. J Am Acad Orthop Surg 2000;8(4): 232–242.
12. Hobbs DL, Mickelsen W et al. Radiol Technol 2007;78(5): 423–428.
13. Lee MC, Eberson CP. Orthop Clin N Am 2006;37(2): 119–132.
14. Scherl SA. Pediatrics in Review 2004;25(2): 52–62.
15. Soo B, Howard J, Boyd RN et al. J Bone Joint Surg Am 2006; 88(1): 121–129
16. Taybi H, Lachman RS. Radiology of Syndromes, Metabolic Disorders, and Skeletal Dysplasias, 4th edn. St. Louis: Mosby-Year Book, 1996.
17. Woolacott, NF, Puhan MA et al. BMJ 2005;330(7505): 1413–1418.
18. French L, Dietz F. Am Fam Physician 1999;60(1): 177–184.
19. Goldberg MJ. Pediatrics in Review 2002;22(4): 131–134.
20. Kohler G, Hell A. Swiss Med Wkly 2003;133(35–36): 484–487.
21. Puhan MA, Woolacott N et al. Ultraschall Med (Stuttgart, Germany: 1980) 2003;24(6): 377–382.
22. Roovers EA.M, Boere-Boonekamp M et al. Arch Dis Child Fetal Neonatal Ed 2005;90(1): F25–F30.
23. Rosendahl K, Toma P. Euro Radiol 2007;17(8): 1960–1967.
24. Shipman SA, Helfand M et al. Pediatrics 2006;117(3): e557–e576.
25. Toma P, Valle M et al. Euro J Ultrasound 2001;14(1): 45–55.
26. Gray A, Elbourne D et al. J Bone Joint Surg Am 2005;87(11): 2472–2479.
27. Bellah R. Radiol Clin N Am 2001;39(4): 597–618.
28. Grissom LE, Harcke HT. Curr Opin Pediatr 1999;11(1): 66–69.
29. Harcke H. Clin Orthop Relat Res 2005;434: 71–77.
30. Harcke HT, Grissom LE. Radiol Clin N Am 1999;37(4): 787–796.
31. Hosny G, Koizumi W et al. J Pediatr Orthop B 2002;11(3): 204–211.
32. Hubbard AM. Radiol Clin N Am 2001;39(4): 721–732.
33. Portinaro N, Pelillo F et al. J Pediatr Orthop 2007;27(2): 247–250.
34. Smergel E, Losik SB et al. Ultrasound Q 2004;20(4): 201–216.
35. Synder M, Harcke HT et al. Orthop Clin N Am 2006;37(2): 141–147.
36. Wedge JH. J Bone Joint Surg 2003; American Volume 85-A(8): 1623–1623.
37. Wientroub S, Grill F. J Bone Joint Surg Am 2000;82(7): 1004.
38. Abril J, Berjano P et al. J Pediatr Orthop B 1999;8(4): 264–267.
39. Aoki K, Mitani S et al. J Orthop Sci 1999;4(4): 255–263.
40. Dillon JE, Connolly SA et al. Magn Reson Imaging Clin N Am 2005;13(4): 783–797.
41. Clegg J, Bache CE et al. J Bone Joint Surg Br 1999;81-B(5):852–857.
42. Murray KA, Crim JR. Semin Ultrasound CT MR 2001;22(4): 306–340.
43. Ortolani M. La Pediatr 1937;45;129–131.
44. Barlow TG. J Bone Joint Surg Br 1962;44; 292–294.
45. Bloomfield L, Rogers C et al. J Med Screen 2003;10: 4.
46. Gardiner HM, Clarke NM, Dunn PM. J Pediatr Orthop 1990; 10(5):633–637.
47. Wood M, ConboyV et al. J Pediatr Orthop 2000;20(3): 302–305.
48. Force, USPST. Am Fam Physician 2003;73(11): 1992–1996.
49. Elbourne D, Dezateux C et al. Lancet 2002;360(9350): 2009–2017.
50. Forlin E, Munhoz da Cunha LA et al. Orthop Clin N Am 2006;37(2): 149–160.
51. Ganger R, Radler C et al. J Pediatr Orthop B 2005;14(3): 139–150.
52. Gillett CA. AORN J 2002;75(4): 737.
53. Gillingham BL, Sanchez AA et al. J Am Acad Orthop Surg 1999;7(5): 325–337.
54. Kim S, Frick S et al. J Pediatr Orthop 1999;19(4): 438–442.
55. Macnicol M, Bertol P. J Pediatr Orthop B 2005;14(6): 415–421.
56. Trousdale R. Clin Orthop Relat Res 2004; 429: 182–187.
57. Rosendahl K, Markestad T, Lie RT. Pediatrics 1994; 94: 47–52.
58. Morin C, Harcke HT, MacEwen GD. Radiology 1985; 157: 673–677.
59. American College of Radiology Appropriateness Criteria. Developmental Dysplasia of the Hip- Child. http://www.acr.org/SecondaryMainMenuCategories/quality_safety/app_criteria/pdf/ExpertPanelonPediatricImaging/DevelopmentalDysplasiaoftheHipChildDoc1.aspx

60. Garn SM, Rohmann CG, Silverman FN. Med Radiogr Photogr 1967; 43(2):45–66.
61. Kay RM, Watts HG, Dorey FJ. J Pediatr Orthop 1997;17(2):170–173.
62. Spatz DK, Reiger M, Klaumann M et al. J Pediatr Orthop 1997;17(2):174–175.
63. Pirpiris M, Payman KR, Otsuka NY. J Pediatr Orthop 2006; 26(3):310–315.
64. Hernandez RJ. Radiology 1984;150: 266–268.
65. Laor T, Roy DR, Mehlman CT. J Pediatr Orthop 2000;20:572–574.
66. Grissom L, Harcke HT, Thacker M. Clin Orthop Relat Res 2008;466:791–801.
67. Jari S, Paton RW, Srinivasan MS. JBJS 2002; 84-B: 104–107.
68. Dogruel H, Atalar H, Yavuz O, Sayli U. Int Orthop 2008;32(3);415–419.

21

Slipped Capital Femoral Epiphysis

Martin H. Reed and G. Brian Black

Issues

I. What is the diagnostic performance of radiographs in the initial diagnosis of slipped capital femoral epiphysis (SCFE)?
II. What is the diagnostic performance of magnetic resonance imaging in the initial diagnosis of SCFE?
III. What is the diagnostic performance of ultrasound imaging in the initial diagnosis of SCFE?
IV. What is the role of CT in preoperative planning?
V. What is the imaging method of choice in suspected avascular necrosis associated with the treatment of slipped capital femoral epiphysis?

Key Points

- If there is clinical suspicion of slipped capital femoral epiphysis (SCFE), pelvic radiographs of both hips in neutral and lateral views should be obtained (limited evidence).
- CT may be of value for preoperative planning if there is severe SCFE (limited evidence).
- If there is clinical concern about avascular necrosis of the femoral head in the postoperative period, MRI can be used to confirm the diagnosis (limited evidence).

Definition and Pathophysiology

Slipped capital femoral epiphysis is a disorder of the proximal femur which occurs in adolescence in which the proximal femoral metaphysis is displaced superiorly and anteriorly through the physis on the proximal femoral epiphysis (1). The etiology of the condition is not known, but endocrine changes which occur during adolescence probably play a role in this

M.H. Reed (✉)
Department of Diagnostic Imaging University of Manitoba Health Sciences Centre/Children's Hospital, Winnipeg MB R3A 1S1 Canada
e-mail: mreed@hsc.mb.ca

L.S. Medina et al. (eds.), *Evidence-Based Imaging in Pediatrics*,
DOI 10.1007/978-1-4419-0922-0_21,

condition (1). Obesity is a significant risk factor for SCFE. At least 50% of children with SCFE are above the 95th percentile for weight (1). A recent Scottish study correlated an increasing incidence of SCFE with increasing obesity in the same age group (2). Obesity also increases the risk of bilateral disease (1), and it is related to an earlier age of onset (1, 2). Varus position and retroversion of the proximal femur are also predisposing factors (1, 3, 4). A variety of endocrine disorders predispose to this condition, particularly hypothyroidism and growth hormone deficiency (1, 5). An association with Down Syndrome has also been suggested (6). SCFE may be bilateral although the frequency of this occurring is uncertain, ranging from 18 to 63% in different studies (1).

Two types of SCFE are recognized. An acute SCFE is one that occurs in a patient with symptoms for less than 3 weeks, although there may be up to 3 months history of mild prodromal symptoms. Radiographically, these patients usually have a joint effusion and no evidence of metaphyseal remodeling. Patients with chronic SCFE, which comprise approximately 85% of cases, usually have symptoms of more than 3 weeks of increasing pain or pain extending down the thigh, sometimes to the knee. The primary complaint may be of knee pain. These patients often limp. These symptoms may vary in severity over time. Metaphyseal remodeling and severity of the slip are generally increased with longer symptoms (1).

SCFE can also be classified as stable or unstable. A stable SCFE is one in which a child is able to walk with or without crutches, and radiologically these patients have signs of metaphyseal remodeling and usually no evidence of an effusion. In a case of unstable SCFE, the child is unable to walk even with the aid of crutches. On imaging, there will usually be a joint effusion and no evidence of metaphyseal remodeling. Patients with an unstable SCFE have a much higher risk of avascular necrosis (AVN) of the femoral head, a complication of this condition (1). Another rare but recognized complication of SCFE is chondrolysis, which is usually related to penetration of the fixating pin or screw through the articular cortex to involve the articular cartilage (1). There is also some evidence that the more severe forms of SCFE predispose to degenerative arthritis (1).

The prognosis for a patient with SCFE depends on the severity of the slip prior to treatment and the type of treatment. The outcome is good in mild cases treated with a single screw, but severe preoperative deformity, AVN, and chondrolysis all predispose to early degenerative arthritis and eventual need for total hip replacement (1).

Epidemiology

Slipped capital femoral epiphysis occurs most commonly in the early adolescent period. In one recent study, the average age of onset for males was 12.7 years and for females 11.1 years (7). It is more common in males than females, with an incidence of 13.25 per 100,000 for boys and 8.07 per 100,000 for girls in the same study (7). The average age of onset is similar for all races, but there are significant variations in incidences between races. The condition is most common in blacks with an incidence of almost four times that in whites. It is also at least twice as common in Hispanics as Whites and slightly more common in Asian children or Pacific Islanders. It is less common in Native Americans than in Whites (7). In the United States, there is a geographic variation, with higher incidence rates in the Northeast and West compared to the Midwest and South (7). Interestingly, there is also a seasonal variation, with the incidence being slightly higher in the summer north of 40° latitude and slightly higher in the winter south of 40° latitude (7).

Overall Cost to Society

There is no information in the literature on the cost to society of slipped capital femoral epiphysis or the imaging for slipped capital femoral epiphysis. Much of the costs of SCFE occur in adulthood when functional limitations and hip replacement occur. However, one study showed significant lower cost of care for children with SCFE when they were treated at a children's hospital as compared to a community hospital (8).

Goals

The goals of imaging are to diagnose SCFE and to help determine the stability of the SCFE if it

is present. Imaging is also used to follow these patients after surgery in order to help assess for any complications including avascular necrosis.

Methodology

A PubMed search was undertaken using the terms *slipped capital femoral epiphysis and epidemiology, cost and cost-effectiveness, radiography, magnetic resonance imaging, computed tomography, nuclear medicine,* and *ultrasound*. A search for slipped capital femoral epiphysis with the limitation of review articles was also undertaken. All searches had the limits of English language and human placed on them. There were no date limits to any of the searches. The searches were completed in November 2008.

Discussion of Issues

I. What Is the Diagnostic Performance of Radiographs in the Initial Diagnosis of Slipped Capital Femoral Epiphysis?

Summary of Evidence: Currently, the standard diagnostic imaging modality for SCFE is pelvic radiography. Two views of both hips are necessary, one with the hips in a neutral position and one with both hips in a lateral position (the frog-leg view) (limited evidence).

Supporting Evidence: There is no information in the literature on the accuracy of radiography for the diagnosis of slipped capital femoral epiphysis. However, radiography has been in use clinically for this indication for decades, so accuracy is presumed to be reasonable. There is also little evidence in the literature on when imaging is indicated in children with hip pain. There are currently no validated or well-developed clinical prediction rules for the use of imaging in pediatric hip pain (insufficient evidence).

The standard radiograph series for SCFE consists of an AP radiograph of the entire pelvis as well as a lateral view of the hips (the "frog-leg" view) (Fig. 21.1). There is some information supporting the importance of the lateral view of the hip for the diagnosis of this disorder. In Cowell's series, in 14% of 55 patients, the diagnosis could be made only on the lateral view (9). Loder undertook a study with a femur model and showed that the lateral view, including the commonly used frog-leg lateral projection, is accurate in showing slipped capital femoral epiphysis (limited evidence) (10). Billing et al. described and carefully defined a reproducible lateral view of the proximal femur. He studied 95 normal children and 100 children with SCFE, and showed that the measurements obtained with the lateral view were highly reproducible and diagnostically superior to a conventional frog-leg lateral view ($p < 0.05$) (limited evidence) (11).

On radiographs, in patients with SCFE, the proximal femoral growth plate appears widened and poorly defined. A line drawn along the lateral margin of the femoral neck with the hips in the neutral position should intersect the lateral margin of the proximal femoral epiphysis. In patients with SCFE, this line will pass lateral to the epiphysis (12) (insufficient evidence) (Fig. 21.1C). On the neutral view of the femur, there may be a crescentic region of increased density seen below the proximal femoral physis. As a result of the anterior slip of the proximal femoral metaphysis, the epiphysis is superimposed on the metaphysis and creates this "blanch sign" (13) (insufficient evidence).

The angle between the line drawn perpendicularly through the center of the epiphysis and another line drawn through the center of the femoral neck, the epiphyseal–shaft angle, on the lateral view of the proximal femur can be used to classify the severity of SCFE into mild, less than 30°; moderate, 30°–50°; and severe, greater than 50° (Fig. 21.1D) (1). Carney and Liljenquist assessed the reliability of this measurement in 108 hips and showed that intraobserver variability was ±5.9° (14) (moderate evidence).

II. What Is the Diagnostic Performance of Magnetic Resonance Imaging in the Initial Diagnosis of Slipped Capital Femoral Epiphysis?

Summary of Evidence: MRI accurately diagnoses slipped capital femoral epiphysis, and it may be more accurate in both assessing the severity of SCFE and showing abnormalities predictive of SCFE ("pre-slip"), prior to the slip

actually occurring (insufficient to limited evidence).

Supporting Evidence: Umans et al. studied 13 patients with 15 symptomatic hips using radiography, MRI, and CT. Apart from physeal widening, MRI also showed synovitis and marrow edema. Physeal widening was also seen on one patient with normal radiographs who was presumed to have a "pre-slip" (limited evidence) (15). In a retrospective study, Tins et al. reviewed the radiographs and preoperative MRI examinations of 14 patients with 15 cases of SCFE. MRI did not demonstrate any more cases of SCFE than radiography (16). Lalaji et al. reported two patients who had distortion of the physis and bone marrow edema demonstrated on the MRI and who subsequently went on to develop SCFE. They suggest that this is evidence that MRI can demonstrate abnormalities predictive of impending SCFE, "pre-slip" (insufficient evidence) (17).

III. What Is the Diagnostic Performance of Ultrasound Imaging in the Diagnosis of Slipped Capital Femoral Epiphysis?

Summary of Evidence: In experienced hands, ultrasound may be used to diagnose slipped capital femoral epiphysis (insufficient evidence). The presence of hip effusion on ultrasound imaging may predict an unstable hip (insufficient evidence).

Supportive Evidence: Magnano et al. in a prospective study of 21 symptomatic patients, all of whom had radiographs and 19 who had ultrasound examinations, suggested that ultrasound might be more accurate, because they had three false-negative radiographic examinations and one false-negative ultrasound examination (insufficient evidence) (18). Castriota-Scanderbeg and Orsi studied three patients sonographically who had acute SCFE and showed an anterior displacement of the metaphysis on the epiphysis in each case (insufficient evidence) (19). Kallio and colleagues have published three papers on the value of ultrasound in the assessment of SCFE (20–22). In the largest series of 55 hips in 45 patients, ultrasound showed anterior displacement of the metaphysis on the epiphysis in 50 hips, ranging from mild to severe. Five other patients had "advanced remodeling" of the metaphysis so that the degree of metaphyseal displacement could not be assessed accurately (limited evidence) (22). Ultrasound also demonstrates the presence of joint effusions in patients with unstable SCFE (19, 22), but its accuracy in the depiction of joint effusions has not been determined (insufficient evidence).

IV. What Is the Role of CT in Preoperative Planning?

Summary of Evidence: Computerized tomography (CT) may allow more accurate assessment of the severity of the SCFE if a corrective osteotomy of the femoral neck is being considered (limited evidence).

Supporting Evidence: Some authors recommend a corrective femoral neck osteotomy for the treatment of severely displaced SCFE (1). Richolt et al. suggested that CT with 3D reconstruction is a more accurate method of measuring the degree of angulation and displacement, which will determine if an osteotomy is needed. They studied prospectively 23 patients with 31 SCFEs using both X-ray and CT and showed that the shaft–physis angles were overestimated an average of 10.1° on X-rays (limited evidence) (23). Cohen et al. in a similar study of 19 hips with SCFE also concluded that CT was more accurate than X-rays for measurement (limited evidence) (24). In an earlier study of 20 hips with chronic SCFE, Guzzanti and Falciglia concluded that if the hip was carefully positioned for the lateral view, measurements on X-ray could be as accurate as on CT (limited evidence) (25), but Richolt suggested that it was difficult to place patients with severe SCFE in the position described by Guzzanti and Falciglia (23).

V. What Is the Imaging Method of Choice in Suspected Avascular Necrosis Associated with the Treatment of Slipped Capital Femoral Epiphysis?

Summary of Evidence: MRI has become the imaging test of choice to diagnose AVN

earlier than does plain radiography in postoperative patients with SCFE. Bone scintigraphy is an accurate method that is used less today due to the ease and availability of MR without the need for contrast and ionizing radiation (insufficient to limited evidence).

Supporting Evidence: MRI has become the imaging test of choice for the *early* diagnosis of avascular necrosis (AVN) of the femoral head. (For more complete discussion, please see Chapter 22.) Scintigraphy can be used early in the diagnosis when plain films are normal, although MRI has become the modality of choice in this situation.

There is very little literature on the imaging of AVN in patients with SCFE. Strange-Vognsen et al. performed preoperative bone scans on 26 patients with 31 involved hips. In 18 of the hips with SCFE, there was increased activity on the bone scan and in 13 there was normal uptake. The preoperative scan did not correlate with postoperative development of AVN in any patient, and the authors did not recommend preoperative bone scans (limited evidence) (26). Fragniere et al. prospectively studied 61 patients with SCFE who had Tc-99m bone scans carried out early in the postoperative period (average 9 days, range 3–28 days). Three of these patients developed AVN, confirmed by follow-up X-rays. In one of these, abnormalities were evident radiographically at the time of the bone scan and in another the radiograph was normal, although the bone scan showed evidence of AVN. No details were given about the third patient (insufficient evidence) (27).

Staatz et al. used contrast-enhanced MRI to evaluate the vascularization of the femoral head in 11 consecutive children with SCFE. One child had an avascular zone in the epiphysis preoperatively, but this was completely vascularized after surgery. One other patient developed AVN postoperatively, which was demonstrated by MRI (insufficient evidence) (28).

Take Home Tables

Table 21.1 details the imaging approach for children with suspected SCFE.

Table 21.1. Imaging approach in children with suspected SCFE

Clinical situation	Recommended imaging	Strength of evidence
Diagnosis of SCFE	Two-view X-rays of both hips	Insufficient evidence
Preoperative planning	Low-dose MDCT with 3D reformat	Limited evidence
Diagnosis of AVN	MRI or nuclear medicine	Insufficient evidence

Case Imaging Studies

Case 1

Figure 21.1 presents the case of a 10-year-old girl with SCFE on the right.

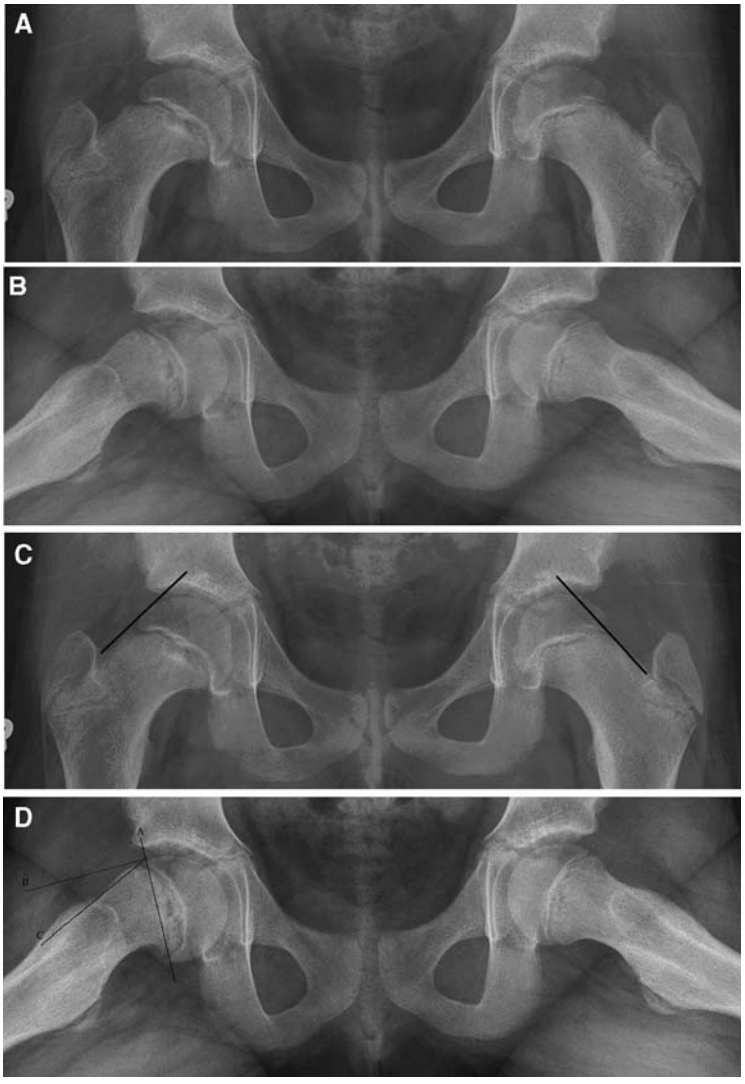

Figure 21.1. A 10-year-old girl with SCFE on the right, neutral (**A**) and frog-leg lateral (**B**) views. Note that the slip is better seen on the lateral view (**B**). A line drawn along the lateral aspect of the femoral neck passes through the margin of the epiphysis on the normal side but not on the side of the SCFE (**C**). D. The epiphyseal–shaft angle. A line is drawn across the physis (a). A second line (b) is drawn perpendicular to (a), and a third line is drawn parallel to the femoral shaft (c) to intersect (b). The angle between (b) and (c) is the epiphyseal–shaft angle.

Suggested Imaging Protocols for Slipped Capital Femoral Epiphysis

Radiographs

Radiographs of the pelvis (including both hips), both neutral and lateral views, should be obtained in all patients that have signs or symptoms suggestive of SCFE.

CT

CT may be of help in preoperative planning for patients with severe SCFE. For surgical planning, 2D axial, coronal, and sagittal images and 3D reformats are used. A low-radiation dose technique should be used.

MRI and Nuclear Medicine

In the postoperative period if there is concern about AVN, MRI or nuclear medicine could be used to confirm the diagnosis. MR imaging using a T1-weighted sequence may be adequate, and gadolinium contrast is not required but may improve early detection of AVN.

Future Research

Should MRI be used as the initial diagnostic imaging modality for SCFE to avoid radiation?

- Is ultrasound accurate enough to be used to exclude the diagnosis of SCFE?
- When is imaging necessary to exclude SCFE in children with hip pain?

References

1. Loder RT, Aronsson DD, Weinstein SL, Breur GJ et al. Instr Course Lect 2008; 57:473–498.
2. Murray AW, Wilson NIL. J Bone Joint Surg 2008; 90:92–94.
3. Fishkin Z, Armstrong DG, Shah H, Patra A, Mihalko WM. J Pediatr Orthop 2006; 26:291–294.
4. Gomez-Benito MJ, Moreo P, Perez MA, Paseta O et al. J Biomech 2007; 40:3305–3313.
5. Loder RT, Wittenberg B, DeSilva G. J Pediatr Orthop 1995; 15:349–356.
6. Dietz FR, Albanese SA, Katz DA, Dobbs MB et al. J Pediatr Orthop 2004; 5:508–513.
7. Lehmann CL, Arons RR, Loder RT, Vitale MG. J Pediatr Orthop 2006;26:286–290.
8. Smith JT, Price C, Stevens PM, Masters KS et al. J Pediatr Orthop 1999; 19:553–555.
9. Cowell HR. Clin Orthop Rel Res 1966; 48:89–94.
10. Loder RT. J Pediatr Orthop 2001; 21:488–494.
11. Billing L, Bogren HG, Wallin J. Pediatr Radiol 2002; 32:423–430.
12. Klein A, Joplin RJ, Reidy JA, Hanelin J. J Bone Joint Surg Am 1952; 34:233–239.
13. Steel HH. J Bone Joint Surg Am 1986; 68:920–922.
14. Carney BT, Liljenquist J. J Surg Orthop Adv 2005; 14:165–167.
15. Umans H, Liebling MS, Moy L, Haramati N et al. Skeletal Radiol 1998; 27:139–144.
16. Tins B, Cassar-Pullicino V, McCall I. Eur J Radiol 2008;doi:10.1016.
17. Lalaji A, Umans H, Schneider R, Mintz D et al. Skeletal Radiol 2002; 31:362–365.
18. Magnano GM, Lucigrai G, De Filippi C, Castriota Scanderberg A. et al. Radiol Med 1998; 95: 16–20.
19. Castriota-Scanderbeg A, Orsi E. Skeletal Radiol 1993; 22:191–193.
20. Kallio P, Lequesne GW, Paterson DC, Foster BK et al. J Bone Joint Surg (Br) 1991; 73: 884– 889.
21. Kallio PE, Paterson DC, Foster BK, Lequesne GW. Clin Orthop Rel Res 1993; 294:196–203
22. Kallio PE, Mah ET, Foster BK, Paterson DC et al. J Bone Joint Surg (Br)1995; 77:752–755.
23. Richolt JA, Hata N, Kikinis R, Scale D et al. J Pediatr Orthop 2008; 28:291–296.
24. Cohen MS, Gelberman RH, Griffin PP, Kasser JR et al. J Pediatr Orthop 1986; 6:259–264.
25. Guzzanti V, Falciglia F. J Pediatr Orthop 1991; 11:6–12.
26. Strange-Vognsen H, Wagner A, Dirksen K, Rabol A et al. Acta Orthop Belgica 1999; 65:33–38.
27. Fragniere B, Chotel F, Vargas Barreto B, Berard J. J Pediatr Orthop Part B 2001; 10:51–55.
28. Staatz G, Honnef D, Kochs A, Hohl C et al. Eur Radiol 2007; 17:163–168.

22

Imaging of Legg–Calvé–Perthes Disease in Children

Neil Vachhani, Andres H. Peña, and Diego Jaramillo

Issues

I. What is the role of imaging in the diagnosis of Legg–Calvé–Perthes (LCP) disease?
II. Can plain radiographs establish the prognosis of the disease?
III. Is MRI the best imaging modality to determine the extent of disease and establish important predictors in Legg–Calvé–Perthes disease?
IV. Can patterns of healing and reperfusion assessed by scintigraphy, US, or MRI predict the ultimate outcome of the disease?

Key Points

- Two-view pelvic radiographs remain the primary diagnostic tool when there is clinical suspicion for Legg–Calvé–Perthes (LCP) (limited evidence).
- The radiographic evaluation of LCP is based at presentation on the presence or the absence of the lateral pillar (the degree of preservation of the height of the lateral third of the femoral head) and after healing on the degree of deformity of the femoral head (moderate evidence).
- The pattern of reperfusion as determined by scintigraphy and MRI is an important determinant of the prognosis (moderate evidence).
- MRI has proven more useful than other modalities to detect the extent of marrow involvement, the damage to the physis and metaphysis, and the femoroacetabular relationships (limited to moderate evidence).
- CT and US do not have a primary role in diagnosing LCP (moderate evidence).

N. Vachhani (✉)
Department of Radiology, Children's Hospital of Philadelphia, Philadelphia, PA 19104, USA
e-mail: vachhanin@email.chop.edu

L.S. Medina et al. (eds.), *Evidence-Based Imaging in Pediatrics*,
DOI 10.1007/978-1-4419-0922-0_22, © Springer Science+Business Media, LLC 2010

Definition and Pathophysiology

Legg–Calvé–Perthes (LCP) disease is idiopathic necrosis of the immature proximal femur in children. Synonyms for Legg–Calvé–Perthes disease include juvenile osteochondritis, coxa plana, and LCP. It is generally acknowledged that an interruption of the blood supply to the femoral head is the cause of the necrosis although the etiology of the avascularity is unclear (1). The lack of vascularization of the proximal femur causes deformity of the cartilaginous femoral epiphysis and decreased containment of the femoral head within the acetabulum, leading to early and severe osteoarthritis. The goal of treatment is to prevent deformity with adequate containment of the femoral head by the acetabulum.

Multiple factors have been associated with LCP, including delayed skeletal maturity, abnormal growth, short stature, low birth weight, social and economic deprivation, trauma, congenital anomalies, and possible genetic etiologies (2–6).

The wide variety of etiologic factors that have been suggested speak for our current ignorance about the cause of the disease. Many believe that etiologic factors operate either prenatally such as maternal smoking (7) or during the first few years of life, possibly in relation to a hypercoagulable state (8) or a history of toxic synovitis (9).

Poor prognostic predictors include increased age of onset, female gender, and bilaterality. Children that present before 6 years of age generally have a benign course, whereas those presenting after 8 years of age fare less well (10–13). These findings were recently confirmed in a nationwide study performed by Wiig et al. in Norway, which showed age at the time of diagnosis to be the second strongest predictor of outcome, with those presenting before 6 years of age having a better outcome regardless of operative or nonoperative treatment (3).

Epidemiology

The incidence of LCP varies within different regions and population groups from 0.2 to 29.4 per 100,000 per year (14). It is four times more common in boys. The disease is generally detected between 5 and 10 years of age, although girls usually present at a slightly earlier age. It is more common in children of Caucasian origin (5) and uncommon in Asian countries (14). Bilateral disease occurs in approximately 10–15% of patients, with each hip being affected at different times (asynchronous disease).

LCP has an insidious onset, often with a variable clinical presentation. The disease can present initially as hip or knee pain, or sometimes as a painless limp or stiffness and decreased range of motion of hip joint. The differential diagnosis is vast and can include transient hip synovitis, Meyer's dysplasia, multiple epiphyseal dysplasia, hypothyroidism, sickle cell disease, Gaucher's disease, etc. Unlike sickle cell disease and Gaucher's disease, the marrow in LCP is otherwise normal. Unlike multiple epiphyseal dysplasia and hypothyroidism, only the affected femoral epiphysis is abnormal.

At the time of diagnosis, approximately 90% of patients have pain or discomfort with a mean duration of symptoms being 4 months (3). This suggests that the detection of asymptomatic disease is less important because unsuspected LCP presents only sporadically. LCP is a major cause of degenerative disease of the hip in adult males, with radiographic signs of osteoarthritis developing by the third and fourth decades and degenerative disease usually by age 70.

Overall Cost to Society

No exact figures are known as to the overall cost to society from LCP. Although a cost exists from the significant disability related to joint pain, decreased movement, and decreased participation in athletic activities associated with LCP both during the course of the disease and into adulthood, a more significant cost is related to the residual deformity of the hip as a sequela of LCP as it can lead to a debilitating osteoarthritis that presents earlier in life. It has been shown that osteonecrosis in general is the cause of 5–12% of total hip arthroplasties (15).

From a treatment standpoint, it has been shown that for those patients diagnosed with LCP before the age of 6, the prognosis does not change regardless of treatment modality,

suggesting that more conservative measures may be employed (13).

Goals

The goals of imaging in patients with suspected Legg–Calvé–Perthes disease are (1) to accurately diagnose the disease, (2) to evaluate the extent of epiphyseal involvement, and (3) to assess the residual deformity. LCP is a self-limiting disease, and the goal of therapy is to minimize deformity. This is attained by maximizing containment of the femoral head during healing and preserving the congruity of the joint surfaces while the disease is ongoing.

Methodology

The authors performed a MEDLINE search using the electronic database PubMed (National Library of Medicine, Bethesda, MD) for original research publications discussing the diagnostic performance and effectiveness of imaging relevant to Legg–Calvé–Perthes disease. The search covered the period 1966 to October 2008. The search strategy involved combinations of the following terms: (1) Legg–Calve–Perthes; (2) diagnosis; (3) etiology; (4) treatment *or* surgery. No time limits were applied for the searches. Non-English articles were excluded.

Discussion of Issues

I. What Is the Role of Imaging in the Diagnosis of Legg–Calvé–Perthes Disease?

Summary of Evidence: Although plain radiographs remain the primary imaging tool in the diagnosis of LCP, the literature is based on those patients that have been diagnosed with the disease based predominately on radiographic criteria, which can lag behind the initial insult or patient symptoms. The percentage of patients presenting with LCP without radiographic findings is unknown (limited evidence).

Supporting Evidence

Plain Radiographs

Conventional radiographs still remain the primary diagnostic tool in the diagnosis of patients with a clinical suspicion for LCP. Although specific for advanced disease, radiographs exhibit a low sensitivity in the detection of early disease (15).

LCP progresses through multiple pathologic stages before healing that can be visualized radiographically as described by Waldenstrom. Stage 1 is the necrotic phase in which the affected femoral head shows increased density and may appear slightly smaller than the contralateral side. A subchondral fracture may also be present. Stage 2 is the fragmentation phase with fragmentation and collapse of the femoral epiphysis. Stage 3 is the reossification phase in which the affected femoral head begins to reossify. Stage 4 is the remodeling phase which describes the final shape of the femoral head and neck.

Although these stages can be visualized radiographically, these findings can lag behind the initial vascular insult by as much as 14 months (16), and the percentage of patients presenting with a normal radiograph and findings of LCP by scintigraphic or MRI findings is unknown.

Pain in the groin or thigh and limping are the most common early symptoms (16). According to Lamer et al., 3 of 23 children with hip pain and limping had MR abnormalities and no radiographic evidence of LCP, but findings consistent with the disease (17) (limited evidence). Most studies, however, include only patients who have been diagnosed with LCP because of abnormal radiographs, including the 95 hips evaluated scintigraphically by Van Campenhout et al. (18). The corollary is that since there is no agreed upon imaging reference standard for the diagnosis of the disease, it is impossible to determine what is the prevalence of radiographically negative LCP.

Scintigraphy

Bone scintigraphy has been shown to have a sensitivity of 98% and a specificity of 95% in the diagnosis of Legg–Calvé–Perthes disease (19). Scintigraphic imaging plays a role in the diagnosis of LCP based on the premise that radioactivity indicates the presence of perfusion

and metabolism within the bone that is studied (20). Although an extremely sensitive technique, newer modalities such as MRI have been shown to be just as sensitive while providing better detection of the extent of femoral head involvement without the use of ionizing radiation (21).

Ultrasound

Ultrasound may be used initially to exclude other potential etiologies such as synovitis or a hip effusion. Although it has been shown that ultrasound can be as sensitive as MRI in determining the degree of subluxation of the femoral head using criteria such as the cartilaginous acetabular head index (limited evidence), the prognosis of these findings is still unclear (22, 23). Additionally, MRI has proven to be more sensitive in evaluating reperfusion of the femoral head.

CT Scan

The role of computed tomography in the diagnosis of LCP relies on the better visualization of osseous structures than plain radiographs. It has been shown that the staging of LCP on the basis of plain radiographs is upgraded in 30% of patients (24). With MRI and bone scintigraphy having proven to be more sensitive modalities as well as the increased ionizing radiation, only a limited role exists for the use of CT scanning in the diagnosis of LCP.

Arthrography

Arthrography is a means to evaluate the contours of the joint capsule that allows evaluation of the acetabular and femoral epiphyseal cartilage. It has been well documented, first by arthrography and subsequently with MRI, that there is increased hypertrophy of the acetabular and femoral epiphyseal cartilage when compared to the nonaffected side. In addition, there is increased accuracy in evaluating containment of the femoral head compared to plain radiographs (limited evidence) (25, 26).

Providing maximum containment of the femoral head to heal within the acetabulum provides the basis of treatment in Legg–Calvé–Perthes disease. Arthrography has been predominately used to evaluate the femoroacetabular relationship to determine the best positioning to provide maximum containment of the femoral head. Studies performed by Jaramillo et al. and subsequently by Weishaupt et al. using MRI in different stages of abduction, adduction, and flexion showed MRI to be comparable to arthrography in evaluating the femoroacetabular relationship (limited evidence) (27, 28).

Although comparable to MRI in multiple facets, arthrography is invasive by nature and has been used predominately as an intraoperative planning tool.

II. Can Plain Radiographs Establish the Prognosis of the Disease?

Summary of Evidence: The most important factors in Legg–Calvé–Perthes disease in establishing prognosis are the age at presentation and the extent of disease, which have been classified extensively using plain radiographs. The two classifications that have shown to be the most predictive of overall outcome as well as have shown good inter- and intraobserver reliability are the lateral pillar classification and the Stulberg classification (moderate evidence).

Supporting Evidence: Many classification systems have been developed using radiographic criteria to categorize and predict the outcome of Legg–Calvé–Perthes disease. Of these, a few classifications have become prevalent on the basis of an ability to accurately predict outcome and good interobserver reliability.

In 1971, Catterall proposed a classification system based on the involvement of the femoral epiphysis. Catterall group I had involvement only of the anterior epiphysis (seen best on the frog-leg lateral radiograph); Catterall group II showed central segment fragmentation and collapse; Catterall group III showed involvement of the lateral portion of the femoral epiphysis; and Catterall group IV had involvement of the entire femoral head. The Catterall classification had fallen out of favor due to poor interobserver reliability, especially if diagnosed too early in the disease process (10). A modification of this classification, developed first by Salter and Thomson and then recently by Wiig et al., divides patients into two groups,

with group 1 representing <50% necrosis of the femoral head and group 2 representing >50% necrosis of the femoral head. Wiig et al. has reported that this classification was the strongest radiographic predictor of long-term prognosis (12).

The lateral pillar classification is based on the degree of preservation of the height of the lateral third of the femoral head, also called the "lateral pillar." The integrity of the lateral pillar is crucial to weight bearing; this is also the zone where revascularization begins. Most authorities believe that collapse of the lateral pillar is the most important predictor of a poor outcome. Type A hips show preservation of the full height of the lateral pillar; Type B hips demonstrate some lucency of the lateral femoral head with preservation of a height between 50 and 100% of the original height of the lateral pillar; and Type C hips demonstrate loss of more than 50% of the lateral pillar. The lateral pillar classification was recently modified by Herring et al., creating a new category termed the Type B/C border group which falls between these two groups, showing either a very narrow lateral pillar that is greater than 50% of the original height or a lateral pillar with very little ossification but with at least 50% of the original height (10).

The Stulberg classification is useful to grade the outcome of the disease based on sphericity of the femoral head and femoroacetabular congruency. Class I is characterized by a femoral head of normal appearance; class II shows a slightly deformed femoral head with less than 2 mm deviation from a circular shape; class III shows an ovoid femoral head, coxa magna, shortened femoral neck, or an abnormally steep acetabulum; class IV is characterized by a flattened femoral head and acetabulum, with abnormalities of the neck; and class V shows a flattened femoral head, usually with central collapse, with normal neck and acetabulum. Classes I and II generally are not prone to arthritis, classes III and IV have aspherical congruency and are prone to moderate arthritis in late adulthood, and class V (with aspherical incongruency) usually develops severe arthritis before the age of 50 (13).

Herring et al. (10) and subsequently Rosenfield et al. (29) reviewed a large population of children with LCP. In the children presenting before the age of 6, 80% had a good result (29). Only children with a B/C or C lateral pillar involvement had a less favorable prognosis (moderate evidence).

In a large prospective multicenter study of the effect of treatment on outcome in which 451 hips were evaluated, Herring et al. showed no difference between treated and untreated groups in patients under 8 years of age. Only lateral pillar B and B/C groups over age 8 had significantly better results with surgery (moderate evidence) (1).

A recent prospective multicenter study in Norway by Wiig et al. showed similar results with patients presenting before age 6 having a markedly better outcome, with no significant difference in outcome regardless of treatment in those with more than 50% of femoral head necrosis. Significant associations were also identified between the lateral pillar classification and the Stulberg outcome, with 70% of hip classified as A under the lateral pillar classification having spherical heads at 5-year follow-up. Additionally, there was a significant association between the Stulberg outcome and the level of activity, with a strong association between Stulberg class IV and V and more limited walking and reduced sporting ability (moderate evidence) (12).

In evaluating long-term outcome, a study by Shah et al. showed that the Stulberg grade assigned to a patient did not change between healing and skeletal maturity in 88% of patients. In those that did change, it either improved or deteriorated by one grade, with all but one changing between grade I and grade II, neither of which is prone to arthritis (limited evidence) (30).

III. Is MRI the Best Imaging Modality to Determine the Extent of Disease and Establish Important Predictors in Legg–Calvé–Perthes?

Summary of Evidence: MRI has shown to be an excellent imaging modality in the diagnosis and staging of Legg–Calvé–Perthes disease. MRI is able to determine the extent and prognosis of LCP earlier than plain radiographs. Dynamic contrast-enhanced imaging and imaging in

multiple positions allow a less invasive, nonionizing method in evaluating LCP, although it is an expensive imaging modality and may require sedation in younger children (limited evidence).

Supporting Evidence: Although outcome is predicted by plain radiographic classification (Catterall, lateral pillar, or Stulberg classifications), these classifications are based on the radiographic appearance during the later (fragmentation and beyond) stages of the disease. Abnormalities on MRI may precede radiographic abnormalities by several months, but usually radiographs are abnormal at the time of presentation. It is possible that earlier detection and therapy will improve containment and long-term prognosis (12).

De Sanctis et al. established four prognostic indicators on MRI and correlated them with outcome based on the Stulberg classification. MRI abnormalities included the extent of osteonecrosis, lateral extrusion, physeal involvement, and metaphyseal abnormalities. Physeal abnormality was the strongest correlated parameter with outcome based on a Spearman coefficient ($S = 0.84$ for Stulberg class; $S = 0.91$ for total score) (limited evidence) (31, 32).

Metaphyseal cysts may be strictly confined to the metaphysis or extend into the physis and metaphysis (33). Cysts, seen in slightly less than half of the patients, are more frequent with advanced disease. Both metaphyseal abnormalities and physeal interruption on MRI were associated with subsequent growth disturbance. A retrospective study involving 23 patients showed by multivariate analysis that the probability of subsequent growth arrest was 100% when both epiphyseal and metaphyseal abnormalities were present, 75% when only physeal interruption was present, and 50% when only metaphyseal cystic changes were detected (34) (limited evidence).

MRI has proven to be extremely sensitive in the evaluation of bone marrow. The lipid within the normal bone marrow shows characteristic high T1 signal intensity and intermediate T2 signal intensity on MRI. The marrow signal changes in MRI more clearly determine the extent and location of necrosis than do findings identified radiographically (limited to moderate) (35–37).

A prospective study performed by Uno et al. involving 40 patients comparing MRI and scintigraphy demonstrated that MRI showed the extent of the involved femoral epiphysis more clearly than did scintigraphy (limited evidence) (38). An additional prospective study performed by Kaniklides et al. involving 22 patients comparing plain radiographs, MRI, scintigraphy, and arthrography demonstrated MRI to be superior to plain radiographs and scintigraphy in defining the extent of involvement of the femoral head (limited evidence) (21).

IV. Can Patterns of Healing and Reperfusion Assessed by Scintigraphy, US, or MRI Predict the Ultimate Outcome of the Disease?

Summary of Evidence: Patterns of healing and reperfusion in Legg–Calvé–Perthes disease are based on either the recanalization of existing vessels which are seen along the lateral column of the femoral epiphysis or the neovascularization of the epiphyseal vessels which arise at the base of the epiphysis. These findings were initially described scintigraphically, which demonstrated excellent positive predictive value in determining outcome. More recent studies have shown a better depiction of these findings using dynamic contrast-enhanced subtraction MRI (moderate to limited evidence). Due to this as well as its lack of ionizing radiation and its wide availability, MRI has essentially replaced scintigraphy for the diagnosis of LCP.

SupportingEvidence

Scintigraphy

Conway proposed that the pattern of reperfusion determines the prognosis in LCP. If the reperfusion occurs peripherally along the lateral column, the head reforms normally and without growth arrest. However, if the reperfusion occurs across the physis, scintigraphic activity is seen at the base of the epiphysis, and there is a poorer prognosis. Comte et al. performed a prospective scintigraphic study involving 58 patients evaluated by the Conway

classification (A = appearance of lateral column formation, B = appearance of activity from the base of epiphysis) (19, 20, 39). The absence of lateral column activity (B pathway) equated with a 97% probability of poor outcome, while preservation of lateral column activity (A pathway) indicated only a 15% probability of poor outcome (moderate evidence). Hyperactivity of the metaphyseal growth plates indicated a probability of poor outcome of 92%, though with low sensitivity. Additional evidence by Van Campenhout et al. showed a statistically significant correlation between the A pathway and a good prognosis using the lateral pillar radiographic classification, although further studies showed only moderate intraobserver (k= 0.573) and interobserver (k= 0.525) agreement, less than that seen with the lateral pillar classification (limited to moderate evidence) (18, 40).

Ultrasonography

The use of color and power Doppler techniques with ultrasound has been useful in depicting tissue vascularity. US contrast agents, although not currently approved in the United States, have improved the ability of detecting vascularity in low flow states (41).

Doria et al. studied revascularization comparing contrast-enhanced power Doppler sonography with scintigraphy. The results demonstrated that the effect of scintigraphic stages on the overall proximal femoral vascularity visualized on power Doppler US does not seem to be relevant. Contrast-enhanced power Doppler US imaging improves visualization of epiphyseal flow from revascularization but cannot differentiate recanalized (type A) from neovascularized (type B) vessels as is possible with scintigraphy (41, 42). Ultrasound thus plays a limited role in determining the extent as well as establishing prognosis in LCP.

MRI

Dynamic gadolinium-enhanced subtraction MRI has shown similar patterns of enhancement as those described in the Conway classification (43). Lamer et al. compared MRI and scintigraphy in the evaluation of reperfusion. They found that both techniques agreed in depicting epiphyseal necrosis and metaphyseal abnormality; however, revascularization in the lateral and medial column and transphyseal reperfusion were better depicted with MRI (limited evidence) (17). In this study, scintigraphic reperfusion preceded the loss of containment of the femoral head by an average of 3 months.

In conclusion, MRI can help diagnose confusing cases of LCP early, assess the severity of epiphyseal and physeal involvement, and define the extent of residual epiphyseal and acetabular deformity later in the disease.

Take Home Figures and Tables

Table 22.1 details predictors of LCP and Fig. 22.1 presents an algorithm for imaging protocol for LCP.

Table 22.1. Predictors of Legg–Calvé–Perthes disease

Imaging modality	Finding	Outcome	References
Radiographic	Presence of lateral pillar of femoral head	Improved	(10)
Radiographic	Stulberg classification	Improved with greater femoral head sphericity and femoral–acetabular congruency	(13)
Scintigraphy	Absence of lateral column activity	Poorer	(18, 40)
MRI	Abnormal perfusion pattern	May precede radiographic outcome findings by months	(12)
MRI and scintigraphy	Epiphyseal necrosis and metaphyseal abnormality	Poorer	(17)

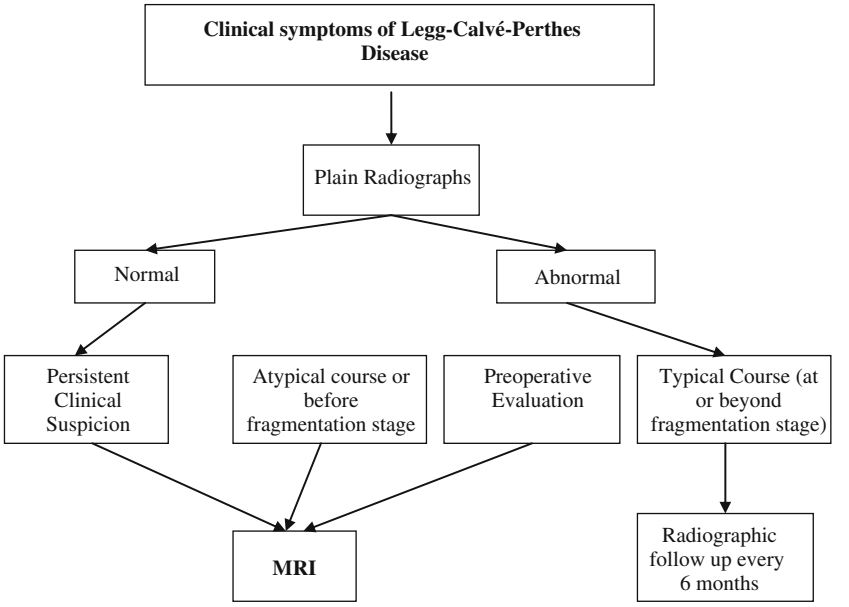

Figure 22.1. Algorithm for imaging in cases of suspected Legg–Calvé–Perthes disease.

Imaging Case Studies

Case 1

Figure 22.2 presents a case of a 9-year-old boy with known LCP.

Figure 22.2. Frontal radiograph of the pelvis shows marked osteonecrosis of the right hip with almost complete absence of the femoral ossification center, collapse of the lateral pillar, sclerosis and irregularity of the physis, and lateral uncovering of the femoral neck.

Case 2

Figures 22.3 and 22.4 present the case of a 6-year-old boy with right hip and leg pain.

Suggested Imaging Protocol for Legg–Calvé–Perthes Disease in Children

See Fig. 22.1.

Future Research

- Define the predictive value of abnormal perfusion and diffusion MR imaging on epiphyseal outcome.
- Develop automated 3D imaging techniques to evaluate deformity.
- Evaluate the role of various techniques to evaluate cartilage integrity (T2 shading or dGEMRIC) in predicting subsequent osteoarthritis.

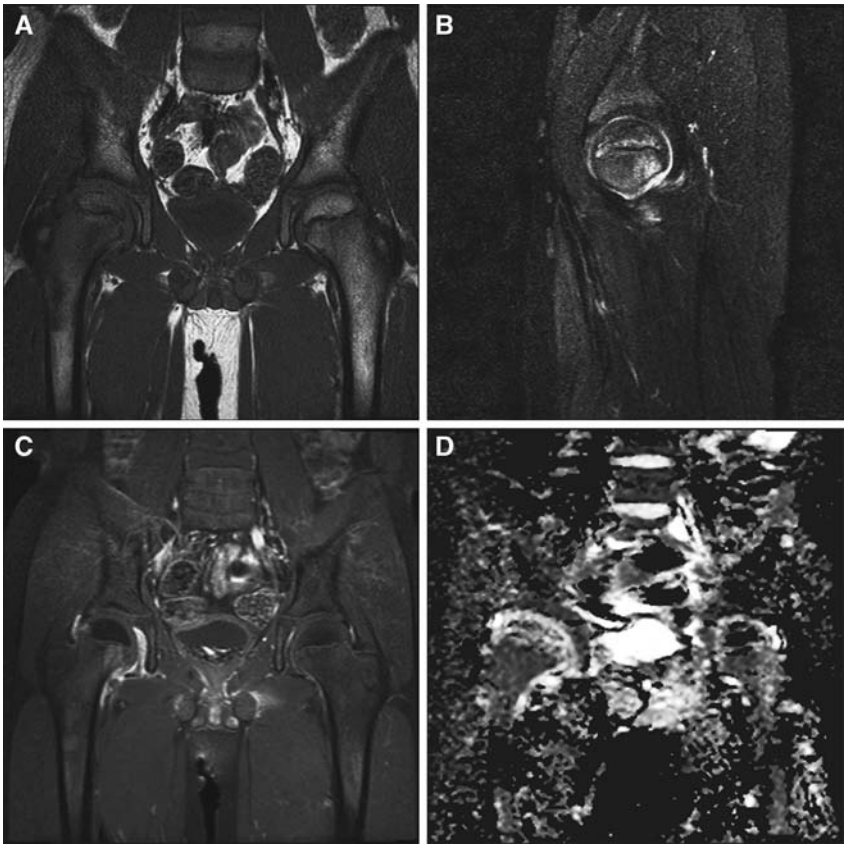

Figure 22.3. Initial MRI evaluation. **A**: Coronal T1-weighted image shows decreased signal intensity of the epiphyseal fatty marrow. **B**: Sagittal STIR image shows diffuse involvement of the femoral head. **C**: Contrast-enhanced T1-weighted image shows global decrease in perfusion of the right hip. **D**: ADC map image shows diffusely increased diffusion throughout the femoral head.

Figure 22.4. AP radiograph taken 3 months later showing collapse and sclerosis of the right femoral epiphysis and a metaphyseal cyst.

References

1. Herring JA, Kim HT, Browne R. J Bone Joint Surg Am 2004; 86-A(10): 2121–2134.
2. Kealey WD et al. J Bone Joint Surg Br 2000; 82(2): 167–171.
3. Wiig O et al. J Bone Joint Surg Br 2006; 88(9): 1217–1223.
4. Epidemiology of Perthe's disease. Arch Dis Child 2000; 82(5): 385.
5. Sharma S, Sibinski M, Sherlock DA. J Bone Joint Surg Br 2005; 87(11): 1536–1540.
6. Su P et al. Arthritis Rheum 2008; 58(6): 1701–1706.
7. Bahmanyar S et al. Pediatrics 2008; 122(2): e459–e464.
8. Balasa VV et al. J Bone Joint Surg Am 2004; 86-A(12): 2642–2647.

9. Hochbergs P et al. Acta Radiol 1998; 39(5): 532–537.
10. Herring JA, Kim HT, Browne R. J Bone Joint Surg Am 2004; 86-A(10): 2103–2120.
11. Van den Bogaert G et al. J Pediatr Orthop B 1999; 8(3): 165–168.
12. Wiig O, Terjesen T, Svenningsen S. J Bone Joint Surg Br 2008; 90(10):1364–1371.
13. Stulberg SD, Cooperman DR, Wallensten R. J Bone Joint Surg Am 1981; 63(7): 1095–1108.
14. Rowe SM et al. J Bone Joint Surg Br 2005; 87(12): 1666–1668.
15. Malizos KN et al. Eur J Radiol 2007; 63(1): 16–28.
16. Gross GW, Articolo GA, Bowen JR. Semin Musculoskelet Radiol 1999; 3(4): 379–391.
17. Lamer S et al. Pediatr Radiol 2002; 32(8): 580–585.
18. Van Campenhout, Moens AP, Fabry G. J Pediatr Orthop B 2006; 15(1):6–10.
19. Tsao AK et al. J Pediatr Orthop 1997; 17(2): 230–239.
20. Conway JJ. Nucl Med 1993;23(4): 274–295.
21. Kaniklides C et al. Acta Radiol 1995; 36(4): 434–439.
22. Stucker MH, Buthmann J, Meiss AL. Ultraschall Med 2005; 26(5):406–410.
23. Stuecker MH, Meiss AL. Ortop Traumatol Rehabil 2004; 6(5): 582–588.
24. Khan AN et al. Legg–Calvé–Perthes Disease. Emedicine 2008, cited May 28, 2008.
25. Sales de Gauzy J et al. J Pediatr Orthop B 1997; 6(4): 235–238.
26. Rush BH., Bramson RT, Ogden JA. Radiology 1988; 167(2): 473–476.
27. Jaramillo D et al. Radiology 1999; 212(2): 519–525.
28. Weishaupt D et al. Am J Roentgenol 2000; 174(6): 1635–1637.
29. Rosenfeld SB, Herring JA, Chao JC. J Bone Joint Surg Am 2007; 89(12): 2712–2722.
30. Shah H, Siddesh ND, Joseph B. J Pediatr Orthop 2008; 28(7): 711–716.
31. de Sanctis N, Rega AN, Rondinella F. J Pediatr Orthop 2000; 20(4): 455–462.
32. de Sanctis N, Rondinella F. J Pediatr Orthop 2000; 20(4): 463–470.
33. Song HR et al. J Pediatr Orthop 2000; 20(5): 557–561.
34. Jaramillo D et al. Radiology 1995; 197(3): 767–773.
35. Bos CF, Bloem JL, Bloem RM. J Bone Joint Surg Br 1991; 73(2):219–224.
36. Henderson RC et al. J Pediatr Orthop 1990; 10(3): 289–297.
37. Lahdes-Vasama T et al. Pediatr Radiol 1997; 27(6): 517–522.
38. Uno A et al. J Pediatr Orthop 1995; 15(3): 362–367.
39. Comte F et al. J Nucl Med 2003; 44(11): 1761–1766.
40. Van Campenhout A, Moens P, Fabry G. Acta Orthop Belg 2007; 73(2): 196–199.
41. Doria AS et al. J Pediatr Orthop 2002; 22(4): 471–478.
42. Doria AS et al. Pediatr Radiol 2000; 30(12): 871–874.
43. Sebag G et al. Pediatr Radiol 1997; 27(3): 216–220.

23

Fractures of the Ankle

Martin H. Reed and G. Brian Black

Issues

I. What are the clinical indications for obtaining the X-ray ankle series following trauma in a child?
II. What is the diagnostic performance of computed tomography in the investigation of ankle fractures in children?
III. What is the diagnostic performance of MRI in the investigation of ankle injuries in children?
IV. What is the diagnostic performance of ultrasound in the investigation of ankle injuries in children?

Key Points

- Most ankle injuries in children do not require imaging (strong evidence).
- A three-view radiographic series of the ankle is indicated only in children who (a) have pain near the malleoli and (b) have an inability to bear weight immediately after the injury and in the Emergency Department or (c) have bone tenderness at the posterior edge or the tip of either malleolus (strong evidence). There is insufficient evidence to guide use of evidence in children too young to provide reliable history and physical exam.
- CT is useful for surgical planning in children with complex ankle fractures; MRI may also be used but may be less available and may require sedation.
- MRI is the imaging modality of choice for evaluation of (a) ligamentous injuries, (b) occult injuries, such as talar dome fracture, and (c) possible premature physeal closure (limited evidence).
- Ultrasound has no proven role in the imaging of acute ankle trauma in children (insufficient evidence).

M.H. Reed (✉)
Department of Diagnostic Imaging University of Manitoba Health Sciences Centre/Children's Hospital, Winnipeg, MB R3A 1S1, Canada
e-mail: mreed@hsc.mb.ca

L.S. Medina et al. (eds.), *Evidence-Based Imaging in Pediatrics*,
DOI 10.1007/978-1-4419-0922-0_23, © Springer Science+Business Media, LLC 2010

Definition and Pathophysiology

For the purposes of this chapter, fractures of the ankle will be defined as fractures involving the metaphysis, the growth plate, or the epiphysis of the distal tibia and fibula. Prior to growth plate closure, Salter–Harris Types I–IV fractures of the distal tibia occur. The higher the SH number, the higher the risk of premature closure of the growth plate.

Type II fractures are most common (Fig. 23.1) (Table 23.1) (1). A characteristic fracture pattern, which is seen in adolescents, is the juvenile Tillaux fracture, a Salter–Harris Type III fracture of the lateral aspect of the distal tibia (2). An unusual growth plate injury that occurs in the distal tibia is the triplane fracture (3). This injury is characterized by a fracture line through the metaphysis in the coronal plane, which is visible on the lateral view, an extension of the fracture through the growth plate in the axial plane, and a further extension through the epiphysis in the sagittal plane best seen on the frontal view (Fig. 23.2). This fracture can be thought of as a combination of a Salter–Harris Type II and a Salter–Harris Type III fracture. Characteristically, this fracture occurs in adolescence also.

A Pilon fracture is an intra-articular fracture of the distal tibia with an associated articular disruption and usually other injuries. These fractures are rare in the pediatric age group, although they occasionally occur in adolescents. The prognosis in this age group may be better than in adults (insufficient evidence) (4).

Salter–Harris Type I fractures are thought to be the most common fractures involving the distal fibula, but these are difficult to diagnose radiologically because they are characteristically nondisplaced. Other growth plate injuries of the distal fibula are quite uncommon. Avulsion fractures of the tip of the lateral malleolus can occur (5).

Epidemiology

Ankle fractures are common in both children and adults. The incidence of ankle fractures in children in Britain ranges from 4.2 per 10,000 person-years (6) to 10.3 per 10,000 person-years (7). The incidence of ankle fractures in children increases year by year throughout childhood (6, 7). The incidence is higher in boys than girls, particularly in older children (6, 7). Ankle fractures comprise between 3 and 5% of all pediatric fractures and 15% of physeal injuries (6, 7).

Overall Cost to Society

There is no information about the overall societal cost of ankle fractures in children. There is also no information on the cost-effectiveness of the use of the Ottawa Ankle Rule in children, but Anis et al. estimated that the implementation of the Ottawa Ankle Rule for the radiography of ankles following trauma in adults would result in savings of between US $600,000 and US $3,000,000 per 100,000 patients in the United States and of CAN $700,000 per 100,000 patients in Canada (8).

Goals

The goals of imaging are to detect or exclude fractures accurately, to help to determine appropriate treatment, and to aid in surgical planning when necessary. In addition, imaging is essential for follow-up if there is clinical concern that premature physeal closure is occurring.

Methodology

A PubMed search was undertaken using the following terms: *ankle, tibia, fibula, epidemiology, cost, radiography, computed tomography, magnetic resonance imaging,* and *ultrasound.* Limits placed on all searches included the following: English language only, humans only, and all children (0–18 years). There was no date limit on the search. The searches were all completed in October 2008.

Discussion of Issues

I. What Are the Clinical Indications for Obtaining the Ankle X-ray Series Following Trauma in a Child?

Summary of Evidence: A well-validated clinical prediction rule provides guidance for which children should undergo ankle radiography in the setting of acute trauma. Imaging is indicated only in children who meet the criteria of the pediatric modification of the Ottawa Ankle Rule (strong evidence). The criteria are the following:
Following an injury, radiography of the ankle is indicated only in children who have pain near the malleoli and at least one of the following:

(a) inability to bear weight immediately after the injury and in the Emergency Department for four steps;
(b) bone tenderness at the posterior edge or the tip of either malleolus.

Supporting Evidence: Ian Stiell and his group carried out a multicenter, prospective study using a multivariate analysis technique to establish the Ottawa Ankle Rule in adults. This rule identifies the symptoms and signs most likely to predict the presence of a fracture. Without these signs, a fracture is very unlikely (sensitivity 100%, specificity 40.1%) (9). Stiell and associates validated this rule with a prospective multicenter study involving 12,777 adults 18 years of age and older (10), and it has been independently validated by several other studies as well (11, 12).

The rule has also been validated with minor modifications for use in children: in the United States, in one study of 71 patients (sensitivity 100%, specificity 32%) (13) and in another study of 195 patients by Clark and Tanner (sensitivity 83%, specificity 50%) (14), in one Canadian study of 671 patients (sensitivity 100%, specificity 24%) (15), and in one English study of 432 patients (sensitivity 98.3%, specificity 46.9%) (16) (Table 23.2). The sensitivity of the rule was not quite as good in the series by Clark and Tanner (14) as it was in the other three studies. Five of 30 (17%) fractures would have been missed in that study using the Ottawa Ankle Rule, but the authors did not state why they were missed or what type of fractures were missed (14).

Boutis et al. proposed and assessed a more detailed decision rule, classifying the findings on physical examination into low and high risk. A low-risk clinical examination comprised isolated pain or tenderness with or without edema or ecchymosis in the region of the distal fibula below the level of the joint line and in the regions of the adjacent ligaments (17). Fractures in this region are always stable and are treated on the basis of clinical findings rather than radiologic findings. Therefore, patients with low-risk findings may not need to be radiographed. Of the 381 children in the low-risk category in this two-center study, none had a high-risk fracture requiring surgery, whereas 54 of the 226 children in the high-risk category had fractures, 45 of which were high risk potentially requiring surgery (17). Using the rule that children with a low-risk examination do not need to be radiographed would have reduced the number of radiographs obtained by 62.8% compared to a reduction of only 12% using the Ottawa Ankle Rule (17). This guideline has not been validated by an independent prospective study (limited evidence).

II. What Is the Diagnostic Performance of Computed Tomography in the Investigation of Ankle Fractures in Children?

Summary of Evidence: Computed tomography is of value in the preoperative assessment of complex distal tibial epiphyseal fractures because it shows more accurately the degree of comminution and the severity of displacement than do ordinary X-rays (Fig. 23.2) (insufficient evidence). This examination would normally be ordered by an orthopedic surgeon.

Supporting Evidence: Brown et al. retrospectively studied 51 patients who had had CT scans to evaluate triplane fractures. This type of imaging showed the detailed anatomy of the fractures and the precise degree of displacement of the fragments (3). Cutler et al., in a study of 62 patients with distal tibial physeal fractures, showed that CT scans helped in more accurately positioning screws used for internal fixation (18).

Benefits of using CT for treatment planning include improved anatomic detail, especially of the articular surfaces, and improved visualization of bones that often are not well seen by radiography if there is overlying cast/splint material. Relative to radiography, CT has both higher cost and radiation exposure. The role of CT in other specific fracture types has not been adequately explored, although it may be useful in Pilon fracture treatment planning.

III. What Is the Diagnostic Performance of Magnetic Resonance Imaging in the Investigation of Ankle Injuries in Children?

Summary of Evidence: MRI detects more injuries, including injuries of the bone marrow, stress injuries, and ligamentous injuries, than do radiographs. However, there is no evidence that its routine use affects the acute management of ankle fractures in children (limited evidence). Like CT, it may be of value in providing more detailed assessment of the anatomy of complex fractures preoperatively (limited evidence). It is the imaging modality of choice for the assessment of premature physeal (growth plate) closure (limited evidence).

Supporting Evidence: Lohman et al. (19), in a prospective study of 60 children 7 years of age and older with ankle injuries who were all examined with X-rays and MRIs, found one false-negative and one false-positive fracture of the tibia on X-ray and 11 false-positive and 4 false-positive fractures of the fibula on radiographs. Twenty-two of the patients had bone bruises, mostly associated with ligamentous injuries, none of which was seen on radiographs. However, they concluded that routine MRI examination of children with mild ankle injuries was not indicated, although MRI was useful for showing the anatomy of complex fractures in detail (limited evidence). Seifert et al. (20) prospectively studied 22 patients, 10–16 years of age, with distal tibial fractures using X-ray and MRI. Ten of these cases were thought to require internal fixation based on the X-rays and 15 based on the MRIs because X-ray underestimated the degree of displacement of the fragments in five patients. They therefore recommended MRI in all Salter type III and IV fractures and all triplane fractures of the distal tibia (limited evidence). They comment that CT can also be used, but they prefer MRI because it avoids radiation. Bone bruises or ligamentous damage were also shown in eight patients only by MRI, but these findings did not affect management of the patients.

MRI can also be used to evaluate premature closure of the distal tibial epiphysis following an acute ankle injury by accurately demonstrating the site and degree of the fusion. Ecklund and Jaramillo (21) studied 43 children with post-traumatic physeal bars of the distal tibia and Sailhan et al. (22) studied 14 patients, both in larger series of premature physeal fusion at a variety of sites. MRI visualized the sites and sizes of the physeal bridges well, and in Sailhan's series, the MRI findings correlated well with the surgical findings in eight patients (22) (limited evidence).

IV. What Is the Diagnostic Performance of Ultrasound in the Investigation of Ankle Injuries in Children?

Summary of Evidence: Ultrasound may be of value in detecting fractures not visible on X-rays in children following trauma (insufficient evidence). Sonography is also able to detect ankle joint effusions and in experienced hands, it can detect ligamentous or tendon injuries (insufficient evidence).

Supporting Evidence: Simanovsky et al. (23) prospectively studied 20 children aged 5–13 years who had no fractures seen on radiographs following ankle trauma. They found seven minor fractures in these patients with ultrasound, all of which were confirmed by follow-up radiographs (insufficient evidence). Two other studies assessed the accuracy of ultrasound in the diagnosis of fractures around the ankle, both including adults as well as children. Singh et al. studied 114 patients aged 10–80 years, 27 of whom had fractures detected by ultrasound. Twenty-three of these were

visible on the initial X-rays and four were confirmed on follow-up X-rays (limited evidence) (24). In a study by Wang et al. of 268 patients (aged 8–63 years), 24 fractures were identified sonographically that had not been seen on the initial X-rays, although they were visible in retrospect (insufficient evidence) (25).

Take Home Tables

Table 23.1 presents the Salter–Harris classification of physeal fractures of the distal tibia. Tables 23.2 and 23.3 discuss the Ottawa Ankle Rule for children and its diagnostic performance.

Table 23.1. Physeal fractures of the distal tibia (Salter–Harris classification)

Type	Percentage (%)
Type I	6
Type II	46
Type III	25
Type IV	10
Miscellaneous	12

Reprinted with permission from MacNealy et al. (1).

Table 23.2. Diagnostic performance of the Ottawa Ankle Rule in children

Author	Patients (*N*)	Sensitivity (%)	Specificity (%)	Strength of evidence
Chande (13)	71	100	32	Moderate
Plint et al. (15)	670	100	24	Strong
Libetta et al. (16)	761	98.3	46.9	Strong
Clark et al. (14)	195	83	50	Moderate

Table 23.3. The Ottawa Ankle Rule for children[a]

Following trauma, a child should receive ankle radiographs if
There is pain around the malleoli and either
a. Inability to bear weight for four steps both immediately following the trauma and at the time of examination
b. Bone tenderness at the posterior edge or the tip of the lateral or medial malleolus

[a]For children aged 2–16 who can verbalize pain.
Data from Chande (13), Clark and Tanner (14), Plint et al. (15), and Libetta et al. (16).

Imaging Case Studies

Case 1

Figure 23.1 presents a case of a Salter Type II fracture in a 12-year-old boy.

Figure 23.1. Salter Type II fracture in a 12-year-old boy. There is a fracture of the metaphysic of the distal tibia.

Case 2

Figure 23.2 presents a case of a triplane fracture in a 14-year-old boy.

Figure 23.2. Triplane fracture in a 14-year-old boy. A, B: Frontal and lateral X-rays. The metaphyseal component of the fracture in the coronal plane (C) is more clearly seen on the CT scan as is the epiphyseal component in the sagittal plane (D) as well as the degree of separation of the fragments. The extension through the growth plate in the axial plane is best seen on the sagittal (E) and coronal (F) reconstructions. These also show that a triplane fracture can be thought of as a combination of a Salter Type II fracture (E) and a Salter Type III fracture (F).

Suggested Imaging Protocol for Fractures of the Ankle

Radiographs

A three-view series of radiographs of the ankle (AP view, internal oblique or Mortise view, and lateral view) is the initial imaging study of choice following trauma in children. It is indicated only if the child presents with pain around the malleoli and if either of the following two signs is present:

a. inability to bear weight for four steps both immediately following the trauma and at the time of examination;
b. bone tenderness at the posterior edge or the tip of the lateral or medial malleolus (Table 23.3).

CT and MRI

In cases of complex fractures of the distal tibia, CT or MRI may provide better details of the anatomy prior to surgery; MRI is useful for the assessment of premature physeal closure. The MDCT can be performed with low-dose technique to minimize radiation exposure.

Future Research

- To understand the barriers to implementation of the Ottawa Ankle Rule in the clinical setting (both Emergency Department and outpatient).
- To prospectively validate the decision rule developed by Boutis et al. (17).
- To determine the role of MRI in the management of acute ankle injuries in children.
- To assess the potential role of ultrasound in the diagnosis of ankle injuries in children.

References

1. MacNealy GA, Rogers LF, Hernandez R, Poznanski AK. AJR 1982; 138:683–689.
2. Horn BD, Crisci K, Krug M, Pizatillo PD et al. J Pediatr Orthop 2001;21:162–164.
3. Brown SD, Kasser JR, Zurakowski D, Jaramillo D. AJR 2004; 183:1489–1495.
4. Letts M, Davidson D, McCaffrey M. J Pediatr Orthop 2001;21:20–26.
5. Ogden JA, Lee J. J Pediatr Orthop 1990; 10: 306–316.
6. Lyons RA, Delahunty AM, Kraus D, Heaven M et al. Inj Prev 1999; 5:129–132.
7. Cooper C, Dennison EM, Leufkens HG, Bishop N et al. J Bone Miner Res 2004; 19: 1976–1981.
8. Anis AH, Stiell IG, Stewart DG, Laupacis A. Ann Emerg Med 1995; 26:422–428.
9. Stiell IG, Greenberg GH, McKnight RD et al. Ann Emerg Med 1992; 4:384–390.
10. Stiell I, Wells G, Laupacis A, Brison R et al. Multicentre Ankle Rule Study Group. BMJ 1995; 311:594–597.
11. Auleley GR, Kerboull L, Durieux P, Cosquer M et al. Ann Emerg Med 1998; 32:14–18.
12. Auleley GR, Ravaud P, Giraudeau B, Kerboull L et al. JAMA 1997; 25:1935–1939.
13. Chande VT. Arch Pediatr Adolesc Med 1995; 149:255–258.
14. Clark KD, Tanner S. Ped Emerg Care 2003; 19: 73–78.
15. Plint AC, Bulloch B, Osmond MH, Stiell I et al. Acad Emerg Med 1999; 6:1005–1009.
16. Libetta C, Burke D, Brennan P, Yassa J. J Accid Emerg Med 1999; 16:342–344.
17. Boutis K, Komar L, Jaramillo D, Babyn P et al. Lancet 2001; 358:2118–2121.
18. Cutler L, Molloy A, Dhukuram V, Bass A. J Bone Joint Surg Br 2004; 86:239–243.
19. Lohman M, Kivisaari A, Kallio P, Puntila J et al. Skeletal Radiol 2001; 30:504–511.
20. Seifert J, Matthes G, Hinz P, Paris S et al. J Pediatr Orthop 2003; 23: 727–732.
21. Ecklund K, Jaramillo D. Am J Roentgenol 2002; 178:967–972.
22. Sailhan F, Chotel F, Guibal AL, Gollogly S et al. Eur Radiol 2004; 14:1600–1608.
23. Simanovsky N, Hiller N, Leibner E, Simanovsky N. Pediatr Radiol 2005; 35: 1062–1065.
24. Singh AK, Malpass S, Walker G. Arch Emerg Med 1990; 7:90–94.
25. Wang CL, Shieh JY, Wang TG, Hsieh FJ. J Clin Ultrasound 1999; 27:421–425.

Part IV

Chest Imaging

24

Evidence-Based Approach to Imaging of Congenital Heart Disease

Rajesh Krishnamurthy and Pranav Chitkara

Issues

I. What is the role of conventional chest radiography in initial diagnosis of congenital heart disease (CHD)?
II. What is the role of routine daily chest radiography in the pediatric intensive care unit and in the immediate post-operative period for CHD?
III. How does MRI compare with echocardiography (echo) in evaluating right ventricular (RV) size and function in CHD?
IV. Can MRI determine clinical outcome and timing of pulmonary valve replacement in repaired Tetralogy of Fallot (TOF)?
V. Can MRI replace routine cardiac catheterization in the evaluation of patients undergoing single-ventricle repair?
VI. What is the role of CT in CHD?

Key Points

- Chest radiographs do not function as a screening test for suspected CHD in neonates. If CHD cannot be excluded by clinical examination, echo is the preferred modality (moderate evidence).
- In patients with CHD, chest radiography has low accuracy for diagnosis of specific cardiac lesions (moderate evidence) but provides ancillary information regarding pulmonary vascularity which is helpful in initial management.
- Routine daily chest radiographs are useful in the setting of pediatric and neonatal intensive care units and in the immediate post-operative period after repair of CHD (moderate evidence).
- MRI should be considered the gold standard for evaluation of RV size and function in the setting of CHD (strong evidence). Two-dimensional echo measurements of RV size and mass correlate poorly with MRI parameters (moderate evidence). Three- and four-dimensional echo

R. Krishnamurthy (✉)
EB Singleton Department of Diagnostic Imaging, Texas Children's Hospital, Baylor College of Medicine, Houston, TX 77030, USA
e-mail: rxkrishn@texaschildrens.org

L.S. Medina et al. (eds.), *Evidence-Based Imaging in Pediatrics*,
DOI 10.1007/978-1-4419-0922-0_24, © Springer Science+Business Media, LLC 2010

hold promise for measurement of RV volume and mass in the setting of CHD, but further study is required (limited evidence).
- MRI parameters (RV end-diastolic volume, RV end-systolic volume, and biventricular ejection fraction) and EKG parameters (QRS duration on the resting EKG of >180 msec) are the best predictors of adverse clinical outcome in patients with treated tetralogy of Fallot (moderate evidence). The optimal timing of pulmonary valve replacement for patients with corrected TOF is undetermined but is influenced by MRI parameters of RV size and function (indexed RV volume and RV ejection fraction).
- MRI can replace cardiac catheterization for routine evaluation of cardiovascular morphology and function prior to superior cavopulmonary connection in the majority of patients undergoing single-ventricle repair (moderate evidence).
- The role of multidetector CT is mainly as a problem-solving tool when MRI is contraindicated, limited, or not available (limited evidence). MDCT is accurate for diagnosing coronary artery anomalies, coarctation, and post-operative complications, but concerns regarding high radiation exposure has limited its use.

Introduction, Pathophysiology, and Definitions

Historically, conventional radiography played an important role in infants with CHD. The status of pulmonary vascularity on radiography along with clinical status determined the nature of palliative therapy at birth. Final palliation was based on the morphologic and physiologic diagnoses determined during initial palliative surgery, as well as the clinical status of the patient, and frequently involved invasive monitoring and cardiac catheterization. The advent of echo in the 1970s led to a revolution in the noninvasive diagnosis of heart disease and coincided with the introduction of several new surgical techniques that not only prolonged survival in complex CHD but also led to adoption of these techniques by centers around the world. Echo became the mainstay of diagnosis and follow-up for CHD, with cardiac catheterization being used as a trouble-shooting modality and to determine chamber pressures, oxygen saturation, and pulmonary vascular resistance prior to surgery. CT and MRI were late entrants to the field in the 1980s and have made rapid strides since then, being driven by technological breakthroughs that resulted in successful cardiac and respiratory motion correction and dramatic improvements in spatial and temporal resolution. MRI has rapidly established itself as a complementary modality to echo in a wide variety of clinical scenarios where echo is either hindered by lack of acoustic windows or is unable to provide all the necessary information for therapeutic decision-making. It has also decreased the need for routine diagnostic cardiac catheterization prior to surgery. The use of CT in children has been restricted due to the increased susceptibility of children to radiation, but has carved a niche for itself in situations where MRI is contraindicated (pacemakers) or inadequate (vascular coils, coronary stenosis). In this chapter, we will explore some questions relevant to radiologists and cardiologists who are involved in imaging of CHD. The most common clinical scenarios incorporating the use of conventional radiography, MRI, and CT are considered. Due to the large scope of the chapter, discussions of epidemiology and cost are generalized to the entire field of CHD rather than to specific issues like TOF or single-ventricle repair. Brief discussions of pathophysiology and goals of treatment are provided in the section on each clinical issue where applicable.

Epidemiology

Estimates of prevalence (1) of congenital heart disease range from 4 to 8 per 1,000 live-born

infants. In adults (defined as >18 years), the prevalence of CHD ranges from 2 to 4 per 1,000. The prevalence of severe CHD (which includes TOF, truncus arteriosus, transposition complexes, and single ventricle) is approximately 1.45 per 1,000 children and 0.38 per 1,000 adults, accounting for 12 and 9% of all CHD lesions in children and adults, respectively. ASD, VSD, and PDA are the most prevalent lesions. In the year 2000, 49% of those alive with severe CHD were adults.

Overall Cost to Society

Since low mortality and good long-term outcome are commonplace for most CHD, hospital-based mortality is not a sensitive parameter to judge outcome. Almost every CHD has low-risk and high-risk groups, which determine duration of hospitalization and cost of treatment (2). For instance, patients undergoing VSD repair who were younger than 6 months of age at the time of the repair, who required preoperative hospital stays of longer than 7 days before surgical repair, or who had Down's syndrome had a less favorable cost picture than patients who were older than 2 years, who had short (less than 4 days) preoperative hospitalization, or who did not have Down's syndrome. There are limited population-based data on the cost of congenital heart disease to society. One population-based study (3) of 10,569 patients with CHD in 27 states calculated median total hospital charges of $53,828 per patient. They identified a small subset of high resource users that accounted for 40% of all charges, with risk factors including greater disease complexity, younger age at surgery, prematurity, the presence of other anomalies, and admission during the weekend. Actual cost measures related to diagnostic evaluation are difficult to separate from total hospital costs and are subject to significant geographic variation (3).

Goals

The goals of imaging in the setting of congenital heart disease (CHD) are to identify subjects with CHD, establish the need for treatment and the optimal mode of treatment, define anatomy and hemodynamics for treatment planning, monitor for complications after treatment, and determine the optimal timing of repeat intervention. The role of MRI is to supplement the diagnostic information on echo and replace catheterization where possible. Echo is quite successful at delineating intracardiac anatomy and function in the preoperative period. But, there are numerous examples in the neonatal period and early childhood where the lack of optimal acoustic windows results in inadequate characterization of the extracardiac vasculature by echo. Hence, the vast majority of indications for MRI in the preoperative situation deal with the extracardiac vasculature. Examples include aortic coarctation, anomalous pulmonary veins, scimitar syndrome, systemic venous anomalies, branch pulmonary artery stenosis, aortopulmonary collaterals, anomalous coronary arteries, etc. Following permanent palliation of CHD, the goals of imaging change considerably. Information regarding cardiac function and flow becomes more important than information regarding morphology. The goals of post-operative imaging include serial assessment of ventricular and valvular functions; surveillance of grafts, conduits, and baffles; early detection of complications; and determining timing of surgical intervention. The failure rate with echo increases in the post-operative setting when acoustic windows diminish. MRI provides several advantages over echo in assessment of cardiovascular function and flow in this subgroup, including large field of view 3-D morphologic imaging with high spatial resolution, serial accurate and reproducible measurements of ventricular function with no geometric assumptions, and accurate flow velocity/volume quantification, including Qp/Qs, stroke volumes, and regurgitant fractions.

Methodology

The authors performed a MEDLINE search using PubMed (National Library of Medicine, Bethesda, MD) for data regarding the use of diagnostic modalities and therapeutic decision-making in the setting of common clinical

scenarios in CHD. A systematic literature review was performed from January 1966 to August 2008. The clinical scenarios are listed in the issues section. For each clinical scenario, the search strategy used the following key statements and words: (1) *Clinical scenario* (for example, TOF), (2) *Terms related to the clinical scenario* (for example, RV size, RV function, pulmonary regurgitation), (3) *Diagnosis*, (4) *MRI* or *Magnetic Resonance Imaging*, (5) *Echocardiography*, (6) *Catheterization* or *intervention*, (7) *Treatment*, (8) *Decision-making*, as well as combinations of these search strings.

Discussion of Issues

I. What Is the Role of Conventional Chest Radiography in Initial Diagnosis of CHD?

Summary of Evidence: Chest radiographs do not function as a screening test for suspected CHD in neonates. Conventional radiographs are not helpful in the workup of an asymptomatic patient with a cardiac murmur. If CHD cannot be excluded by clinical examination, echo is the preferred diagnostic modality (moderate evidence).

In neonates with CHD, chest radiography has low accuracy for diagnosis of specific cardiac lesions (moderate evidence) but provides ancillary information regarding pulmonary vascularity which is helpful in initial management.

Supporting Evidence: During radiologic assessment of chest radiographs in 98 children with an asymptomatic heart murmur, a low reproducibility and accuracy were found with respect to the presence or absence of heart disease (4). The mean inter- and intra-observer kappa values were less than 0.6, mean sensitivity was 0.3, mean predictive value of a positive test was 0.4, and mean predictive value of a negative test was 0.8. The consequence is a false-positive radiologic assessment in 60% of the patients causing unnecessary anxiety and further examinations. Similarly, a false-negative assessment occurred in 20%, resulting in omission of relevant investigations and timely identification of the heart defect. Because of this low accuracy, the authors concluded that the use of chest radiographs in the initial evaluation of the asymptomatic child with a heart murmur cannot be recommended. If a heart defect cannot be excluded by clinical examination, echo should be performed (4).

Another retrospective study (5) found that a screening chest film for CHD in 128 consecutive neonates with suspected heart disease had a low sensitivity for structural heart disease (26–59%), a low negative predictive value (46–52%), and worse sensitivity among low birth weight and preterm infants. Chest films do not function as a screening test for neonates with suspected heart disease and echo should be considered.

The overall measure of accuracy in distinguishing specific congenital cardiac lesions among 13 patient categories representing different congenital heart diseases was 71%. At such low accuracy, chest films alone are not diagnostic of specific cardiac lesions (6). The chest radiographs have also been shown not to influence clinical management in 68 asymptomatic neonates with a cardiac murmur (7).

Traditional teaching holds that specific types of CHD can be diagnosed on the chest radiograph through pattern recognition. A number of characteristic patterns have been described like "egg on a string" appearance in transposition of great arteries (Fig. 24.1A), a "boot-shaped" heart in tetralogy of Fallot, and a "snowman" appearance in supra-cardiac total anomalous pulmonary venous connection among others. This morphologic approach is not useful clinically because specific types of CHD rarely occur in isolation, and a number of factors modify the manifestations of a particular CHD on a neonatal chest radiograph, including severity of the lesion, associated conditions, status of the ductus, shape of the thymus, and morphology of the lungs and chest wall.

However, in patients with documented CHD, the status of the pulmonary vascularity is an important clue to physiology and helps to determine the type of initial palliation. For example, in the example in Fig. 24.1B, the patient has a combination of diagnoses on echocardiography

that could potentially result in congestive failure (mitral atresia), increased vascularity (double outlet right ventricle), or reduced vascularity (pulmonary stenosis). The chest radiograph shows decreased pulmonary vascularity, which enabled the choice of pulmonary blood flow augmentation with a modified Blalock–Taussig shunt as the appropriate initial palliative procedure. Although chest radiography is commonly used in the neonatal period to determine the choice of initial palliation, this aspect has not been studied in rigorous fashion.

II. What Is the Role of Routine Daily Chest Radiography in the Pediatric Cardiac Intensive Care Unit and in the Immediate Post-operative Period for CHD?

Summary of Evidence: Routine daily chest radiographs are useful in the setting of pediatric intensive care units and in the immediate post-operative period after repair of CHD (moderate evidence).

Supporting Evidence: It is important to limit the dosage of radiation neonates receive by performing only necessary and beneficial radiologic imaging (8). There are two approaches to the use of chest radiography in the pediatric intensive care unit (9):

1. Performing routine daily chest radiographs in all patients who have cardiopulmonary issues or are mechanically ventilated *in addition to* on-demand radiographs based on clinical status.
2. Obtaining chest radiographs only following a change in clinical status.

A large number of adult critical care physicians may doubt the value of daily routine chest radiography but still practice that strategy (10). Studies involving *adult* patients in the ICU appear to be conflicting but overall tend to favor non-utilization of daily routine chest radiography (Table 24.1) (11–15). The limited studies involving *pediatric* ICU patients seem to indicate that daily chest radiography has significant clinical value. However, this area needs more research.

Pediatric Studies

In a prospective study in a pediatric ICU (16) in which 353 routine chest radiographs in 101 patients were examined, 23% of chest radiographs resulted in significant alterations in management, 43% had unpredicted pulmonary findings, and 46% showed unpredicted appliance malpositions. Therefore, it was concluded that routine daily and post-appliance placement chest radiographs have significant clinical value in the pediatric ICU.

Two prospective studies (17, 18) in pediatric intensive care units evaluating the diagnostic value of routine chest radiographs also revealed a high frequency of malpositioned medical devices and changes in radiologic cardiopulmonary status. In a study analyzing 174 CXRs in 74 patients (18), 16% of endotracheal tubes, 23% of central venous lines, and 15% of nasogastric tubes were malpositioned. Changes in cardiopulmonary status, after the initial film, were noted in 63%. More children showed worsening of the radiologic cardiopulmonary status rather than an improvement. Therefore, the study also supported the importance of routine CXRs in critically ill pediatric patients (moderate evidence).

III. How Does MRI Compare with Echocardiography in Evaluating RV Size and Function in CHD?

Summary of Evidence:

1. MRI should be considered the gold standard for assessment of right ventricular (RV) size and function in the setting of CHD (strong evidence).
2. Two-dimensional (2-D) echocardiographic measurements of RV size and mass correlate poorly with MRI parameters (moderate evidence).
3. Three- and four-dimensional echocardiographies hold promise for measurement of RV volume and mass, but further study is required (limited evidence).

Supporting Evidence: The right ventricle (RV) is the most important determinant of outcome in many congenital heart diseases before and after surgical correction. Adults with repaired tetralogy of Fallot and significant chronic pulmonary

regurgitation are at risk for progressive right ventricular dilatation and dysfunction. Other groups that need assessment of RV size and function include left-to-right shunts, conditions involving a systemic RV like l-transposition of great arteries, and following intra-atrial repair of d-transposition of great arteries (Fig. 24.2), Ebstein's disease, and cardiomyopathy. RV size and function can be monitored over time with excellent precision and accuracy using MRI (Table 24.2). Cardiac MRI has shown good inter-study reproducibility in large study groups, not only for assessment of left ventricular parameters but also for the more complex-shaped right ventricle (19–22). MRI shows good inter-study reproducibility for RV functional parameters in healthy subjects, patients with heart failure, and patients with hypertrophy, which suggests that MRI is reliable for serial RV assessment (19). Another recent study examined the reproducibility of MR-derived RV measurements in patients with congenital heart disease and dilated right ventricles and demonstrated high reproducibility in patients with both normal and abnormal volume loads (20). Such high intra- and inter-observer reproducibilities further establish the utility of MRI in diagnosis and longitudinal follow-up of heart disease affecting the right ventricle.

Although MRI is considered the gold standard, it is still expensive, has limited availability, and requires significant expertise to acquire and interpret the images. The use of 2-D, 3-D, and 4-D echocardiographies has been tested as an alternative to MRI in a number of studies.

Current 2-D echocardiographic assessment of RV function is at best an estimate. There is a lack of an adequate geometric model to quantify RV function by 2-D echocardiography (23). The irregular crescentic shape of the RV does not allow the use of geometric assumptions that are used for the left ventricle. The most recent study on this topic (24) evaluated three groups of patients: a normal RV group (group 1), a repaired tetralogy of Fallot group (group 2), and an unrepaired atrial septal defect and/or partially anomalous pulmonary venous connection group (group 3). It evaluated the accuracy of the American Society of Echocardiography guidelines for 2-D quantitative assessment of right ventricular size and function against MRI-derived RV volumes in patients with congenital heart disease. There was weak correlation between 2-D RV measurements by echocardiography and MRI-derived RV volumes (group 1: $r = 0.15–0.54$, group 2: $r=0.33–0.61$, group 3:$r=0.32–0.85$). Most 2-D RV parameters were smaller by echocardiography vs. MRI. The difference between 2-D RV measurements by echocardiography and MRI-derived RV volumes was more pronounced in the RV volume overload groups.

The introduction of volume-rendered 3-D reconstruction of echocardiography images provides a tool for the direct measurement of cardiac chambers, not based on geometric assumptions (25, 26). Real-time 3-D imaging is referred to as 4-D imaging.

A recent study (27) aimed to determine the accuracy of 3-D echocardiography to measure RV volumes in pediatric patients with secundum atrial septal defects compared with direct volume measurements performed during intervention. It was determined that 3-D echo provides an accurate measurement of RV volume in pediatric patients with RV volume overload (correlation of 0.93 and 0.91 for end-systolic and end-diastolic volumes, respectively).

Three-dimensional echocardiography (3-D echo) by freehand scanning provides highly accurate measurements of left ventricular mass and volume using the piecewise smooth subdivision surface reconstruction method. The complexity of right ventricular (RV) geometry presents a challenge in accurate 3-D assessments of its physical parameters. The mean difference between 3-D and true mass was 3.4 g, or 5.4% of the mean true mass. It was concluded that RV mass and volume can be measured accurately from 3-D echocardiograms acquired using freehand scanning and reconstruction by the piecewise smooth subdivision method (28).

A newly developed 4-D right ventricular analysis method (29) for computing RV volumes for both 3-D ultrasound and magnetic resonance images was tested. New software aided delineation of the RV free wall, tricuspid valve, RV outflow tract, and apex on 3-D echo volumes. Although there was a slightly higher variability measuring right ventricular ejection fraction (RVEF) and volumes obtained

by US compared with MRI, both imaging methods showed closely correlated results (correlation of 0.98 and 0.99 for end-systolic and end-diastolic volumes, respectively). The new RV analysis software validated the accuracy of 4-D echo RV volume data compared with MRI.

The main limitation with 3-D echocardiography is the lack of optimal acoustic windows in older patients and in the post-operative setting, and future research should focus on this patient population.

IV. Can MRI Determine Clinical Outcome and Timing of Pulmonary Valve Replacement in Repaired Tetralogy of Fallot?

Summary of Evidence: MRI parameters (RV end-diastolic volume and biventricular ejection fraction) and length of the QRS duration on EKG are the best predictors of adverse clinical outcome in the late post-operative period after repair of tetralogy of Fallot (moderate evidence). The optimal timing of pulmonary valve replacement for patients with corrected TOF is undetermined but is influenced by MRI parameters of RV size and function (indexed RV volume and RV ejection fraction).

Supporting Evidence: Repair of TOF often results in chronic pulmonary regurgitation (PR) and RV dilation, which have been linked to late morbidity and mortality related to prolongation of the QRS duration with increased risk of malignant ventricular arrhythmias, atrial arrhythmias, heart failure, and sudden death (30). Although right ventricular volume load due to severe pulmonary regurgitation can be tolerated for years, the compensatory mechanisms of the right ventricular myocardium ultimately fail. RV dysfunction may become irreversible if the volume load is not eliminated or reduced. Many centers now recommend early pulmonary valve replacement before symptoms of heart failure develop (31, 32). Restoration of pulmonary valve competence results in improvement of right ventricular function, incidence of arrhythmias, and exercise capacity. Apart from surgical replacement of the pulmonary valve, a percutaneous option for pulmonary valve replacement has been recently introduced and promises to have a major impact on treatment strategy of TOF (33). Current clinical guidelines for valve replacement include the onset of symptoms, progressive RV dilation, progressive tricuspid valve regurgitation, or diminishing exercise capacity.

MRI Predictors of Adverse Clinical Outcome in Repaired Tetralogy of Fallot

MRI (Fig. 24.3) is considered the gold standard for anatomical and functional evaluation of corrected tetralogy of Fallot (34). Phase-contrast MRI can reliably grade pulmonary regurgitation and can detect restrictive RV physiology (35). MRI accurately evaluates the morphology of the RV outflow tract and branch pulmonary arteries (36).

One study (37) aimed to determine independent predictors of major adverse clinical outcomes late after TOF repair during follow-up evaluated by MRI. Twenty-two major adverse outcomes occurred in 18 patients—with death in 4, sustained ventricular tachycardia in 8, and increase in NYHA class in 10. Multivariate analysis identified RV end-diastolic volume and LV ejection fraction as independent predictors of outcome. LV ejection fraction could be replaced by RV ejection fraction <45%. QRS duration greater than 180 msec also predicted major adverse events and correlated with RV size. It was concluded that severe RV dilatation and either LV or RV dysfunction assessed by MRI predicted major adverse clinical events.

In another study (38), the clinical, laboratory, and MRI data of 100 consecutive patients with repaired TOF (median 21 years after repair) were analyzed. Moderate or severe LV or RV systolic dysfunction, but not PR fraction or RV diastolic dimensions, was independently associated with impaired clinical status in long-term survivors of TOF repair.

One study (39) examined the relationship among biventricular hemodynamics, pulmonary regurgitant fraction (PRF), right

ventricular outflow tract (RVOT) aneurysm or akinesia, and baseline and surgical characteristics in 85 adults with repaired TOF using MRI vs. 26 matched healthy controls. Patients with repaired TOF had higher right ventricular end-diastolic volume index, right ventricular end-systolic volume index, right ventricular mass index, and lower RV ejection fraction and LV ejection fraction compared to controls. Pulmonary regurgitation and RVOT aneurysm/akinesia were independently associated with RV dilation. Left ventricular systolic dysfunction correlated with RV dysfunction, suggesting an unfavorable ventricular–ventricular interaction. They concluded that measures to maintain or restore pulmonary valve function and avoid RVOT aneurysm/akinesia are mandatory for preserving biventricular function late after repair of TOF.

Timing of Pulmonary Valve Replacement

The timing of pulmonary valve replacement (PVR) in adult patients with repaired tetralogy of Fallot remains controversial. Since MRI is currently the best means of serial monitoring and predicting adverse clinical outcome in patients with treated TOF, it will become an important means of selecting candidates suitable for surgical vs. transcatheter pulmonary valve replacement (33) and to follow them after treatment. An MRI study (40) in 17 adult patients with repaired tetralogy of Fallot revealed a statistically significant decrease in right ventricular (RV) volume at a mean follow-up of 21 months after pulmonary valve replacement and RV systolic function remained unchanged. In no patients with an RV end-diastolic volume >170 ml/m^2 or an RV end-systolic volume >85 ml/m^2 before pulmonary valve replacement were RV volumes "normalized" after surgery.

A recent study (41) analyzed the influence of pulmonary regurgitation severity and RV size and function before PVR on the outcome of RV size and function after PVR. Pulmonary regurgitation was not related to RV dimensions and function before PVR. Moreover, severity of pulmonary regurgitation did not influence changes in RV dimensions after PVR. The indexed RV end-systolic volume before PVR best predicted the indexed RV end-systolic and end-diastolic volumes after PVR. Timing of PVR should be based on indexed RV end-systolic volume and corrected RV ejection fraction rather than on severity of pulmonary regurgitation.

Another recent study (42) sought to investigate the optimal timing of pulmonary valve replacement by analyzing preoperative thresholds of right ventricular volumes above which no decrease or normalization of RV size takes place after surgery. After surgery, RV volumes decreased with a mean of 28%; however, RV ejection fraction did not change significantly. In addition, it appeared that higher preoperative RV volumes were independently associated with a larger decrease in RV volumes. Receiver-operating characteristic analysis revealed a cut-off value of 160 mL/m^2 for normalization of RV end-diastolic volume or 82 mL/m^2 for RV end-systolic volume. Overall, a threshold above which RV volumes did not decrease after surgery was not found. However, normalization could be achieved when preoperative RV end-diastolic volume was <160 mL/m^2 or RV end-systolic volume was <82 mL/m^2.

V. Can MRI Replace Routine Cardiac Catheterization in the Evaluation of Patients Undergoing Single-Ventricle Repair?

Summary of Evidence: MRI may replace cardiac catheterization for routine evaluation of cardiovascular morphology and function prior to superior cavopulmonary connection in the majority of patients undergoing single-ventricle repair (moderate evidence).

Supporting Evidence: Almost 10% of congenital heart defects belong to the family of functionally univentricular hearts. Most cases are fatal if surgical intervention does not occur. Typically palliation is done by a series of operations that result in passive systemic venous return to the pulmonary circulation and a

functional single ventricle supporting the systemic circulation. The bidirectional Glenn procedure or the superior cavopulmonary anastomosis involves anastomosis of the SVC to the pulmonary artery and is usually performed in infancy as a staged procedure before the Fontan procedure. It provides a controlled source of pulmonary blood flow while volume unloading the systemic ventricle. Routine cardiac catheterization before bidirectional Glenn operation is considered the standard of care in these patients (43). The main goals of the procedure include assessment of anatomic and hemodynamic suitability for surgery. However, cardiac catheterization is associated with morbidity and exposure to ionizing radiation. Moreover, retrospective studies have demonstrated that patients are rarely excluded from bidirectional Glenn operation on the basis of findings at cardiac catheterization (44, 45). Hence, MRI (Fig. 24.4) has been proposed as an alternative to cardiac catheterization for routine evaluation of cardiovascular morphology and function prior to the bidirectional Glenn procedure (44).

A randomized clinical trial of 82 patients comparing MRI and cardiac catheterization in this patient population (46) showed that in selected patients with single-ventricle physiology considered for a bidirectional Glenn operation, there is no detectable differences in immediate and short-term post-operative outcomes between the MRI and catheterization groups. The study also found that routine cardiac catheterization is associated with higher rates of minor adverse events (78 vs. 5%; $p<0.001$), longer hospital stay (median 2 days vs. 1 day; $p<0.001$), and higher hospital charges ($34,477 vs. $14,921; $p<0.001$) than MRI. The authors also implied that routine measurement of pulmonary vascular resistance is not necessary before bidirectional Glenn operation. Furthermore, this imaging strategy was applicable for the majority of patients presenting for Glenn operation; only 10% of eligible patients were excluded based on the following criteria: pulmonary vein stenosis, pulmonary hypertension, severe ventricular dysfunction, severe atrioventricular valve regurgitation, known large aortopulmonary or venous collateral vessels, or coarctation of the aorta. These conditions are generally considered to warrant catheterization for hemodynamic assessment or transcatheter intervention. The authors state that the findings of this study follow a trend in which routine preoperative catheterization has been supplanted by noninvasive strategies for a variety of congenital heart lesions (47–52).

VI. What Is the Role of CT in CHD?

Summary of Evidence: Multidetector CT (MDCT) has been used to diagnose coronary artery anomalies, coarctation, and other diseases of the extracardiac vasculature. Apart from its use in the setting of coronary artery anomalies, there are limited data on its diagnostic efficacy in congenital heart disease (limited evidence).

Concerns regarding radiation exposure have limited the use of MDCT as a primary diagnostic modality for CHD. CT has been used mainly as a problem-solving tool in the setting of contraindications, limitations, or non-availability of MRI.

Supporting Evidence: Although echocardiography is the initial diagnostic modality for patients with suspected congenital heart disease, in some patients this modality can be limited in its ability to define the coronary arteries and the extracardiac vasculature. MRI imaging boasts excellent anatomic and functional assessment capabilities, but has limited availability, requires sedation, is time consuming, and contraindicated or inadequate in patients with pacemakers and vascular coils. MRI enjoys a clear superiority over CT for evaluation of intracardiac anatomy, flow, and function. However, in situations where the clinical question is restricted to the morphology of the extracardiac vasculature, including the coronaries, pulmonary arteries, aorta, pulmonary or systemic veins, CT is comparable to MRI. The strengths of MDCT complement the weaknesses of MRI. CT is rapid, with a reduced need for sedation; is efficacious in the setting of metallic hardware, pacemakers, and coils; is widely available and provides better definition of small vessels and higher order branches (Fig. 24.5). CT has the potential to assess patency of stents or metallic prostheses

placed across pulmonary arteries, baffles, coronary arteries, and aortic branches. One important advantage of CT angiography, when compared to contrast angiography or even MR angiography, is the ability to visualize the vessel wall. CT also provides better delineation of the airway, mediastinal abnormalities, and the pulmonary parenchyma. CT has proven to be clinically useful as an adjunct to echocardiography or magnetic resonance imaging (53, 54). Examples of indications appropriate for CT include, but are not limited to, evaluation of total or partial anomalous pulmonary venous return, pulmonary vein stenosis, systemic and pulmonary venous anatomy in heterotaxy, branch pulmonary artery stenosis, confluence and size of branch pulmonary arteries, and the presence of systemic–pulmonary arterial collaterals in pulmonary atresia, vascular rings, anomalous coronaries, and the presence and severity of coarctation (55).

One study (56) compared cardiac CT and transthoracic echocardiography (TTE) in CHD to determine their advantages and limitations. Electron beam CT (EBCT) and TTE findings were found to be concordant in patients below 1 year of age. EBCT was not accurate for detecting anomalies of cardiac chambers (sensitivity of 0.68 and specificity 0.58) but was useful for evaluation of the great arteries (sensitivity of 0.91 and specificity of 0.85). It was concluded that EBCT delineates findings related to systemic venous return and coronary vessels. However, TTE was found to be more suitable for intracardiac anatomy, including the cardiac valves and septal defects.

A recent study (57) of 16 patients assessed the reliability of MDCT angiography and 3-D reconstruction in patients with coarctation of the aorta. The sensitivity of MDCT diagnosis for coarctation of the aorta was 100%, which was higher than that of echocardiography (87.5%). It was concluded that CTA with 3-D reconstruction represents a reliable noninvasive technique for the assessment of coarctation and may serve as a noninvasive diagnostic tool before intervention or surgical treatment.

Congenital anomalous coronary arteries, although rare, are a well-recognized cause of myocardial ischemia and sudden death in children and young adults, with an increased prevalence in patients with congenital heart disease, especially TOF, TGA, and congenitally corrected TGA. Defining the presence and the exact proximal course of the coronary arteries with respect to the aorta and pulmonary artery is essential because this is the most important indicator of risk of ischemia and determines treatment. The spatial resolution of CT is superior to MRI, with the ability to reconstruct up to 0.4 mm in the *z*-axis. Studies have shown that CT is superior to MRI for evaluation of coronary artery stenosis. Coronary CTA using MDCT is an established means of detecting anomalous origin of the coronary arteries (58–64). MDCT is particularly advantageous in patients presenting with acute symptoms including palpitations, dizziness, atypical or typical exertional chest pain, and dyspnea on exertion, especially in young athletes (59). Some authors advocate that CT should be used as a first-line modality for coronary artery anomalies (61).

In situations where there is a need for serial evaluation, as in monitoring of aortic root dilatation in TOF or after a Ross procedure, size of coronary aneurysms in Kawasaki's disease, or aortic wall thickness in familial hypercholesterolemia, MRI may be a better choice than CT because of the risk of cumulative radiation dose associated with CT (55).

But, there are limited quantitative data on the diagnostic accuracy of CT in CHD. A number of questions regarding the clinical utility of CT and MRI in congenital heart disease remain unanswered. Multi-institutional clinical trials are required to clarify the role of CT.

Take Home Tables

Table 24.1 discusses adult studies of routine chest radiography in the intensive care setting. Table 24.2 discusses accuracy and reproducibility of MRI for evaluation of RV functional parameters.

Table 24.1. Adult studies of routine chest radiography in the intensive care setting

Study	Material	Results	Comment
Hornick et al. (11)	Routine post-operative chest radiograph after cardiac bypass surgery in 100 adult patients	Non-indicated CXR demonstrated a significant finding in only 1/89 cases. Post-op CXR was of value only to clarify or confirm clinical findings or to check the position of an intra-aortic balloon catheter	Routine immediate post-op CXR, in the absence of a clinical indication, has little clinical yield
Mets et al. (12)	Prospective comparative study between routine and on-demand radiography in 338 adult cardiac surgery patients in the ICU and post-ICU setting	Elimination of daily routine CXR led to decrease in total number of CXR obtained per patient per day in the ICU and did not change the utilization of on-demand CXR based on clinical need	Routine radiography in adult ICU and post-ICU setting not indicated
Krivopal et al. (13)	Prospective randomized study of routine vs. indicated chest radiography in 94 adult patients receiving mechanical ventilation > 48 hours	Significant cost savings and decreased radiation exposure among those undergoing CXR only when clinically indicated	Routine radiography not associated with reduced ICU or hospital length of stay or with reduced mortality
Hall et al. (14)	Prospective study comparing new findings on 538 routine CXR vs. clinical examination in 74 mechanically ventilated patients	65.8% of radiographs did not disclose any new findings. However, in 17.6%, new major findings were discovered only by chest radiography	Findings supported use of routine daily chest radiography in mechanically ventilated patients
Marik et al. (15)	Prospective study of 471 routine CXR in 200 consecutive patients in a medical ICU	37% of radiographs resulted in change in therapy. Intubated patients more likely to benefit from routine CXR	Routine daily CXR justified in critically ill patients

Table 24.2. Accuracy and reproducibility of MRI for evaluation of RV functional parameters

Study	Material	Results	Comment
Grothues et al. (19)	60 subjects (47 male; 20 healthy volunteers, 20 with heart failure, 20 with ventricular hypertrophy) underwent two CMR studies for assessment of RV functional parameters	Interstudy reproducibility for all groups 6.2% for RV end-diastolic volume, 14.1% for RV end-systolic volume, 8.3% for RV EF, and 8.7% for RV mass. LV reproducibility better than RV for all measures but statistically significant only for EF ($p<0.01$)	MR is reliable for serial RV assessment
Mooij et al. (20)	Inter- and intra-observer reproducibility of biventricular mass, volume, ejection fraction (EF), and stroke volume (SV) measurements in 60 patients with normal RV volumes (20) and dilated RV due to ASD (20) and repaired tetralogy of Fallot (20)	High inter-observer (0.94–0.99) and intra-observer (0.96–0.99) intra-class correlation coefficients for RV and LV mass, volume, and stroke volume measurements. RV and LV EF less reproducible (0.79–0.87). Higher variability for RV mass relative to LV	MR measurements of RV size and function highly reproducible in patients with both normal and abnormal volume load
Helbing et al. (21)	Comparison between RV and LV stroke volumes, and between RV and LV stroke volumes, and AV valve inflow and great artery stroke volumes in 20 patients with CHD affecting RV, and 22 normal controls aged 5–16 years	Close correlation between RV vs. LV stroke volumes ($r = 0.96$) and RV stroke volume vs. great artery ($r = 0.97$) or tricuspid flow ($r = 0.97$) was observed with small inter-observer and intra-observer variability	MR imaging provides accurate noninvasive measurements of RV function in healthy children and patients with (operated) CHD
Beygui et al. (22)	Assess accuracy and reproducibility of MRI-derived RV mass, volume, and function. In vivo study with postmortem correlation in nine pigs. In vivo study in 15 volunteers and 25 patients with coronary artery disease	High correlation between MRI-derived RV mass and RV weight ($r = 0.98$, bias = 2.5 g), intra- and inter-observer measurements of RV mass, EDV, ESV, and EF, inter-study measurements of RV functional parameters, and MRI-derived right and left ventricular stroke volumes	Assessment of the RV mass, volume, and function by routine breath-hold gradient echo MRI is accurate and highly reproducible

Imaging Case Studies

Case 1

Figure 24.1 presents the utility of chest radiograph in a case of a neonate with d-transposition of the great arteries and in a neonate with complex cyanotic congenital heart disease, including mitral atresia, total anomalous pulmonary venous connection to the coronary sinus, double outlet right ventricle, and pulmonary stenosis.

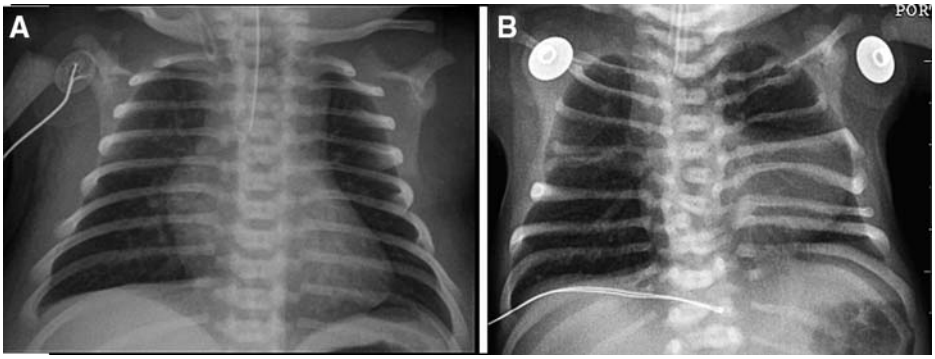

Figure 24.1. Utility of chest radiography in CHD. **A**: Chest radiograph of a neonate with d-transposition of the great arteries, appearing as an "egg on a string" appearance of the heart and mediastinum. This pattern-based approach to cardiac morphology is inaccurate and is rarely helpful for clinical management. Cardiac morphology is determined by echocardiography in the neonatal period while the chest radiograph sheds light on physiology. **B**: Neonate with complex cyanotic congenital heart disease, including mitral atresia, total anomalous pulmonary venous connection to the coronary sinus, double outlet right ventricle, and pulmonary stenosis. The chest radiograph demonstrated decreased pulmonary vascularity, which enabled decision-making regarding initial palliative treatment. The pulmonary blood flow was augmented using a modified Blalock–Taussig shunt.

Case 2

Figure 24.2 shows MRI for evaluation of the systemic right ventricle after intra-atrial repair of d-transposition of the great arteries.

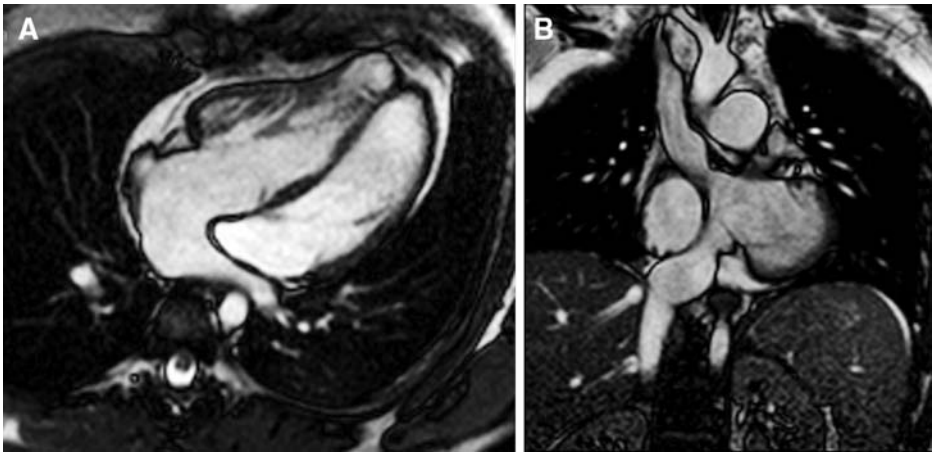

Figure 24.2. MRI for evaluation of the systemic right ventricle after intra-atrial repair of d-transposition of the great arteries. **A**: Four-chamber view of the heart showing hypertrophy of the systemic RV as well as patency of the pulmonary venous baffle coursing toward the right side of the heart. **B**: "Trouser"-like appearance of the superior and inferior limbs of the systemic venous baffle after a Senning procedure.

Case 3

Figure 24.3 shows MRI for evaluation of repaired tetralogy of Fallot.

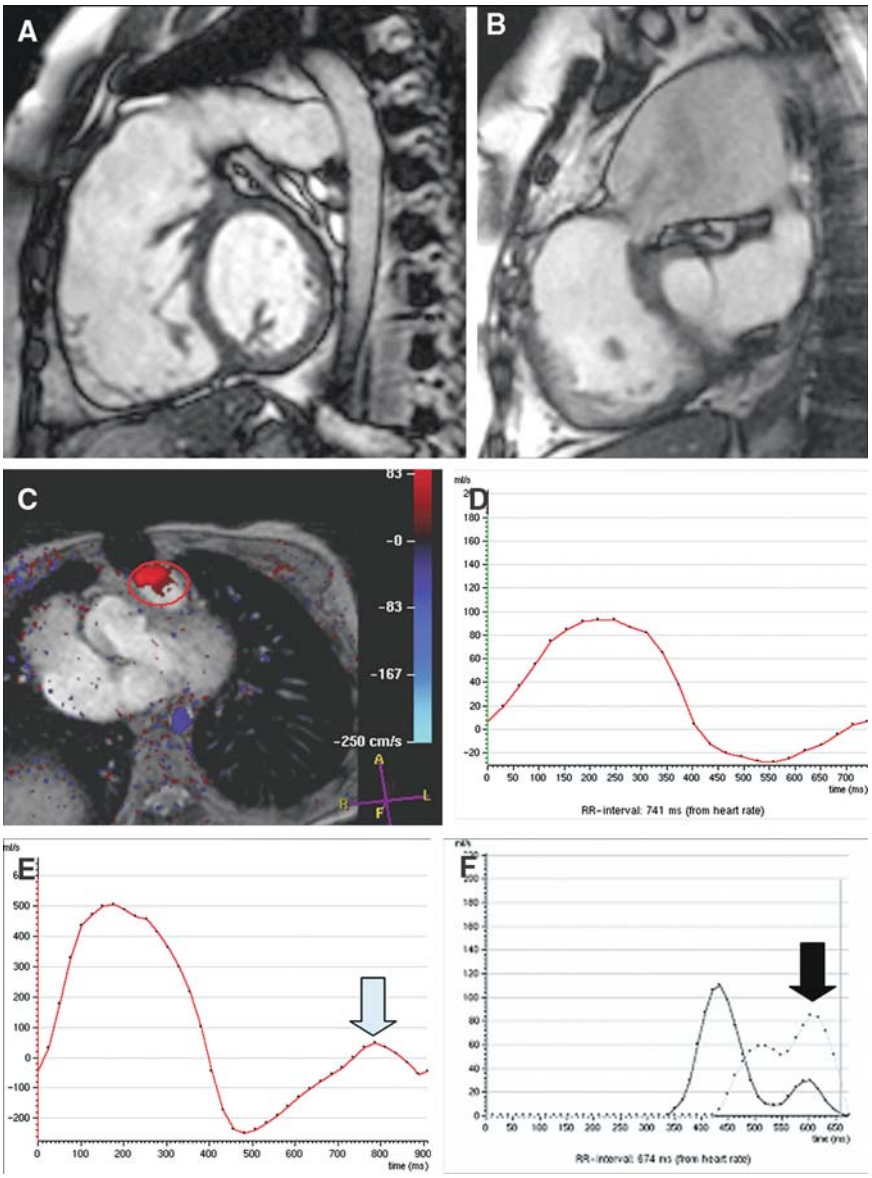

Figure 24.3. MRI for evaluation of repaired tetralogy of Fallot. **A**: Short axis view of the heart showing severe RV dilatation with mild flattening of the interventricular septum. Systolic function of the RV was diminished, with an ejection fraction of 42%. **B**: Recurrent right ventricular outflow tract obstruction in a patient with treated TOF, showing a dephasing jet arising at the obstruction, with aneurysmal dilatation of the RVOT. **C, D**: Phase-contrast imaging of the pulmonary artery demonstrating severe pulmonary regurgitation. **E, F**: Diminished diastolic function of the RV in a patient with treated TOF. E demonstrates end-diastolic forward flow within the main pulmonary artery (*white arrow*), while 3f demonstrates reversal of the E:A ratio of the tricuspid valve. This is due to increasing RV stiffness, causing diminished early diastolic filling (E), and predominant RV filling (*black arrow*) occurring during atrial systole (A).

Case 4

Figure 24.4 presents an MRI evaluation prior to superior cavopulmonary anastomosis in a patient with hypoplastic left heart syndrome.

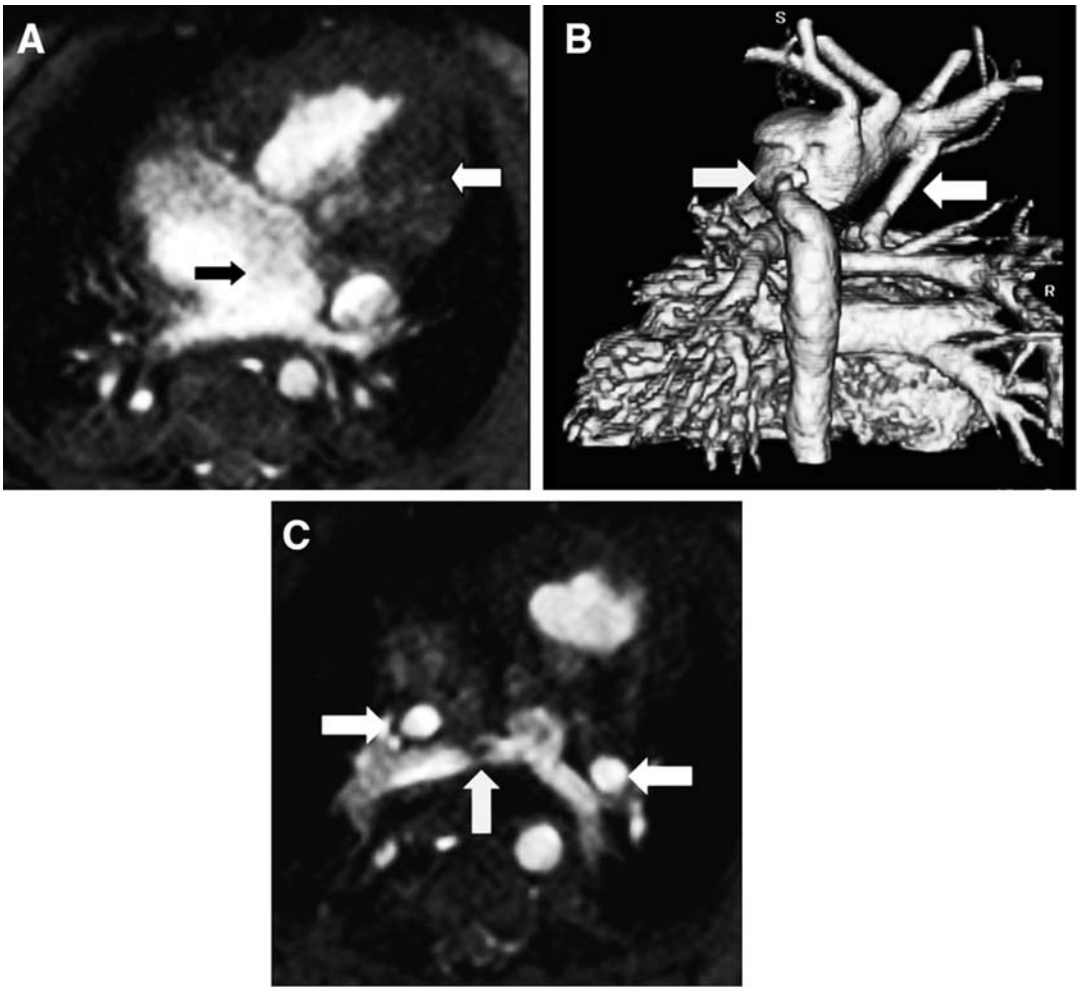

Figure 24.4. MRI evaluation prior to superior cavopulmonary anastomosis in a patient with hypoplastic left heart syndrome. **A**: Four-chamber view of the heart showing a functional single RV and severe hypoplasia of the LV (*white arrow*). Following an atrial septectomy (*small black arrow*) the pulmonary venous return is diverted to the RV, which functions as the systemic ventricle following a Norwood 1 procedure. **B**: Posterior view of a volume-rendered 3-D MRA showing severe recurrent coarctation (*left arrow*) after a Norwood 1 procedure. A modified Blalock–Taussig shunt (*right arrow*) is also noted supplying the pulmonary arteries. **C**: Unobstructed branch pulmonary arteries. *Central arrow* points to the dephasing jet within the right pulmonary artery at the insertion of the modified BT shunt. The *left* and *right arrows* point to bilateral SVCs in this patient, which would require performance of a bilateral bidirectional Glenn shunt.

Case 5

Figure 24.5 presents utility of CT angiography in congenital heart disease.

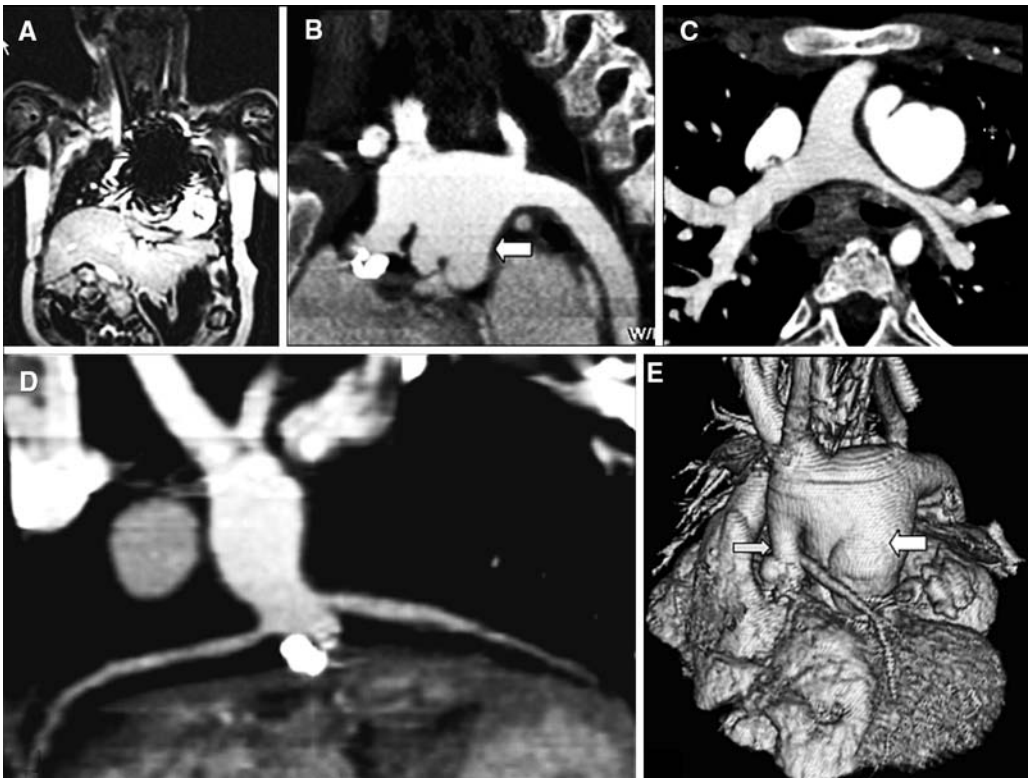

Figure 24.5. Utility of CT angiography in congenital heart disease. Four-month-old male after a Norwood 1 procedure for hypoplastic left heart syndrome. A metallic endovascular coil was placed in the region of the native aortic valve due to the presence of persistent aortic regurgitation after surgery. This resulted in a large artifact on an attempted screening MRI prior to a Norwood 2 procedure (**A**). An EKG-gated CT angiogram was performed instead, which demonstrated an unobstructed neo-aorta (*arrow*), and aortic arch (**B**), unobstructed branch pulmonary arteries (**C**), and a normal appearance of the coronary arteries (**D**). A 3-D volume-rendered image (**E**) provides an overview of the morphology, including the hypoplastic native aorta (*left arrow*), neo-aorta (*right arrow*), and the left coronary artery.

Suggested Protocols for Imaging of Congenital Heart Disease

MRI Protocol for Repaired Tetralogy of Fallot

- Axial black blood imaging for overview of chest anatomy.
- Axial thin-slice (3–4 mm) cine segmented k-space gradient echo or cine SSFP for evaluation of branch pulmonary arteries.
- Cine SSFP in vertical long axis, four chamber, RVOT, and short-axis planes for functional evaluation.
- Phase-contrast imaging of the ascending aorta, RVOT for PR fraction, branch pulmonary arteries for differential pulmonary flow, AV valves for regurgitant fraction, and diastolic function assessment.
- Three-dimensional gadolinium-enhanced MR angiogram for the extracardiac vasculature.

MRI Protocol for Patients Undergoing Single-Ventricle Repair Prior to Superior and Total Cavopulmonary Connection

- Axial and/or coronal thin-slice (2–3 mm) black blood imaging for overview of chest anatomy.
- Axial thin-slice (3–4 mm with overlap) cine segmented k-space gradient echo or cine SSFP for evaluation of branch pulmonary arteries, systemic veins, and pulmonary veins.
- Cine SSFP in vertical long axis, four-chamber, and short axis planes for intracardiac morphology and function.
- Phase-contrast imaging for Qp:Qs, differential pulmonary blood flow, AV valve regurgitant fraction, and diastolic function assessment.
- Three-dimensional gadolinium-enhanced MR angiogram for the extracardiac vasculature.

Future Research

- The role of chest radiography in determining the need for palliation and the nature of initial palliation in patients with functional single ventricle and left-to-right shunts.
- Prospective randomized study of routine radiography compared with on-demand radiography in specific pediatric cardiac conditions in the ICU setting with outcome measures.
- Validity of newer MRI techniques for ventricular volumetry and functional evaluation, including real-time, free-breathing, and single breath-hold cine 3-D sequences.
- Normal MRI age-, sex-, and race-based nomograms for biventricular volumetry, mass, and function.
- Use of automated software algorithms for RV functional processing.
- Optimal interval between MRI studies for serial follow-up of patients with repaired TOF.
- MRI evaluation of diastolic function in TOF and in conditions with a systemic RV as a means of predicting adverse clinical outcome.
- Optimal timing and patient selection for surgical vs. percutaneous pulmonary valve replacement using MRI parameters.
- Use of MRI for decision making regarding single vs. biventricular repair or transplantation in patients with borderline ventricular size and myocardial dysfunction.
- MRI vs. routine catheterization prior to total cavopulmonary connection (Fontan procedure) for assessment of anatomic and hemodynamic suitability for surgery.
- Serial neurologic and cardiac MR imaging of patients undergoing single-ventricle repair for predicting long-term outcome.

References

1. Marelli AJ, Mackie AS, Ionescu-Ittu R, Rahme E, Pilote L. Circulation 2007;115(2): 163–172.
2. Ungerleider RM, Bengur AR, Kessenich AL, Liekweg RJ, Hart EM et al. Ann Thorac Surg 1997; 64(1):44–48; discussion 49.
3. Connor JA, Gauvreau K, Jenkins KJ. Pediatrics 2005; 116(3):689–695.
4. Birkebaek NH, Hansen LK, Elle B, Andersen PE, Friis M et al. Pediatrics 1999; 103(2):E15.
5. Fonseca B, Chang RK, Senac M, Knight G, Sklansky MS. Pediatr Cardiol 2005; 26: 367–372, .
6. Laya BF, Goske MJ, Morrison S, Reid JR, Swischuk L et al. Pediatr Radiol 2006; 36: 677–681.
7. Oeppen RS, Fairhurst JJ, Argent JD. Clinical Radiol 2002; 57:736–740.
8. Pedrosa de Azevedo AC, Osibote AO, Bastos Boechat MC. Appl Radiat Isot 2006; 64(12): 1637.
9. Graat ME, Stoker J, Vroom MB, Schultz MJ. J Intensive Care Med 2005; 20(4):238–246.
10. Graat ME, Hendrikse KA, Spronk PE, Korevaar JC, Stoker J et al. BMC Med Imaging 2006; 18: Hornick PI, Harris P, Cousins C, Taylor KM, Keogh BE. 6–8.
11. Hornick PI, Harris P, Cousins C, Taylor KM, Keogh BE. Ann Thorac Surg 1995; 59:1150–1154.
12. Mets O, Spronk PE, Binnekade J, Stoker J, de Mol BA et al. J Thorac Cardiovasc Surg 2007; 134(1):139–144.
13. Krivopal M, Shlobin OA, Schwartzstein RM. Chest 2003; 123(5):1607–1614.
14. Hall JB, White SR, Karrison T. Crit Care Med 1991; 19(5):689–693.
15. Marik PE, Janower ML. Am J Crit Care 1997; 6(2):95–98.

16. Hauser GJ, Pollack MM, Sivit CJ, Taylor GA, Bulas DI et al. Pediatrics 1989 Apr; 83(4):465–470. Erratum in: Pediatrics 1989; 84(1):17.
17. Plötz FB, Valk JW. Pediatrics 2002; 110(2 Pt 1):421; author reply 421.
18. Valk JW, Plötz FB, Schuerman FA, van Vught H, Kramer PP et al. Pediatr Radiol 2001; 31(5): 343–347.
19. Grothues F, Moon JC, Bellenger NG, Smith GS, Klein HU et al. Am Heart J 2004; 147: 218–223.
20. Mooij CF, de Wit CJ, Graham DA, Powell AJ, Geva T. J Magn Reson Imaging 2008; 28(1): 67–73.
21. Helbing WA, Rebergen SA, Maliepaard C et al. Am Heart J 1995; 130:828–837.
22. Beygui F, Furber A, Delépine S, Helft G, Metzger JP et al. Int J Cardiovasc Imaging 2004; 20(6): 509–516.
23. Schwerzmann M, Samman AM, Salehian O, Holm J, Provost Y et al. Am J Cardiol 2007; 99(11):1593–1597.
24. Lai WW, Gauvreau K, Rivera ES, Saleeb S, Powell AJ et al. Int J Cardiovasc Imaging 2008; 24(7): 691–698.
25. Grison A, Maschietto N, Reffo E, Stellin G, Padalino M et al. J Am Soc Echocardiogr 2007; 20(8):921–929.
26. Sheehan FH, Bolson EL. Catheter Cardiovasc Interv 2004; 62(1):46–51.
27. Heusch A, Lawrenz W, Olivier M, Schmidt KG. Cardiol Young 2006; 16(2):135–140.
28. Hubka M, Mantei K, Bolson E, Coady K, Sheehan F. Comput Cardiol 2000; 27:703–706.
29. Niemann PS, Pinho L, Balbach T, Galuschky C, Blankenhagen M et al. J Am Coll Cardiol 2007; 50(17):1668–1676.
30. Gatzoulis MA, Balaji S, Webber SA, Siu SC, Poile C et al. Lancet 2000; 356:975–981.
31. Geva T. Semin Thorac Cardiovasc Surg Pediatr Card Surg Ann 2006:9; 11–22.
32. Therrien J, Webb GD, Siu S. J Am Coll Cardiol 2000; 36:1670–1675.
33. Mulder BJM, de Winter RJ, Wilde AAM. Neth Heart J 2007; 15(1):3–4.
34. Samyn MM, Powell AJ, Garg R, Sena L, Geva T. J Magn Reson Imaging 2007; 26(4): 934–940.
35. van den Berg J, Wielopolski PA, Meijboom FJ, Witsenburg M, Bogers AJ et al. Radiology 2007; 243(1):212–219.
36. Ghez O, Tsang VT, Frigiola A, Coats L, Taylor A et al. Eur J Cardiothorac Surg 2007; 31(4): 654–658.
37. Knauth AL, Gauvreau K, Powell AJ, Landzberg MJ, Walsh EP et al. Heart 2008; 94:211–216.
38. Geva T, Sandweiss BM, Gauvreau K, Lock JE, Powell AJ. J Am Coll Cardiol 2004; 43: 1068–1074.
39. Davlouros PA, Kilner PJ, Hornung TS, Li W, Francis JM et al. J Am Coll Cardiol 2002; 40: 2044–2052.
40. Therrien J, Provost Y, Merchant N, Williams W, Colman J et al. Am J Cardiol 2005; 95(6): 779–782.
41. Henkens IR, van Straten A, Schalij MJ. Ann Thorac Surg 2007; 83:907–911.
42. Oosterhof T, van Straten A, Vliegen HW, Meijboom FJ, van Dijk AP et al. Circulation 2007; 116:545–551.
43. Nakanishi T. Pediatr Cardiol 2005; 26(2):159–161.
44. Fogel MA. Pediatr Cardiol 2005; 26(2): 154–158.
45. Ro PS, Rychik J, Cohen MS, Mahle WT, Rome JJ. J Am Coll Cardiol 2004; 44(1):184–187.
46. Brown DW, Gauvreau K, Powell AJ, Lang P, Colan SD et al. Circulation 2007; 116(23): 2718–2725.
47. Muthurangu V, Taylor AM, Hegde SR, Johnson R, Tulloh R et al. Circulation 2005; 112: 3256–3263.
48. Festa P, Ait Ali L, Bernabei M, De Marchi D. Cardiol Young 2005; 15(Suppl 3):51–56.
49. Freed MD, Nadas AS, Norwood WI, Castaneda AR. J Am Coll Cardiol 1984; 4:333–336.
50. Lipshultz SE, Sanders SP, Mayer JE, Colan SD, Lock JE. J Am Coll Cardiol 1988; 11: 373–378.
51. Pfammatter JP, Berdat PA, Carrel TP, Stocker FP. Ann Thorac Surg 1999; 68:532–536.
52. Prakash A, Powell AJ, Krishnamurthy R, Geva T. Am J Cardiol 2004; 93:657–661.
53. Achenbach S, Daniel WG. Herz 2007 Mar; 32(2):97–107.
54. Gilkeson RC, Ciancibello L, Zahka K. AJR2003; 180(4):973–980.
55. Sena L, Krishnamurthy R, Chung T. In Lucaya J, Strife JL (eds.). Pediatric Chest Imaging, 2nd ed. Berlin: Springer Publishers, 2007.
56. Beier UH, Jelnin V, Jain S, Ruiz CE. Catheter Cardiovasc Interv 2006; 68(3):441–449.
57. Hu XH, Huang GY, Pa M, Li X, Wu L et al. Pediatr Cardiol 2008; 29(4):726–731.
58. Ropers D, Moshage W, Daniel WG, Jessl J, Gottwik M et al. Am J Cardiol 2001; 87: 193–197.
59. Deibler AR, Kuzo RS, Vohringer M, Page EE, Safford RE et al. Mayo Clin Proc 2004; 79(8): 1017–1023.
60. Kacmaz F, Ozbulbul NI, Alyan O, Maden O, Demir AD et al. Coron Artery Dis 2008; 19(3):203–209.

61. Srinivasan KG, Gaikwad A, Kannan BR, Ritesh K, Ushanandini KP. J Med Imaging Radiat Oncol 2008; 52(2):148–154.
62. Dogan OF, Karcaaltincaba M, Yorgancioglu C, Demircin M, Dogan R et al. Heart Surg Forum 2007; 10(1):E90–E94.
63. Waite S, Ng T, Afari A, Gohari A, Lowery R. J Thorac Imaging 2008; 23(2): 145–147.
64. Saremi F, Channual S, Abolhoda A, Gurudevan SV, Narula J et al. Am J Roentgenol 2008; 190(6):1569–1575.

25

Congenital Disease of the Aortic Arch: Coarctation and Arch Anomalies

Jeffrey C. Hellinger, Luisa F. Cervantes, and L. Santiago Medina

Issues

I. Which clinical symptoms and signs may suggest the presence of coarctation or an aortic arch anomaly?
II. What is the natural history of thoracic aorta coarctation and aortic arch anomalies?
III. What are the diagnostic performances of imaging modalities used to evaluate suspected coarctation and aortic arch anomalies?

Key Points

Coarctation

- Evaluation of upper versus lower extremity blood pressure is an important diagnostic tool in the evaluation of coarctation. Systolic blood pressure of upper extremities greater than that of lower extremities merits further diagnostic workup (limited to moderate evidence).
- Associated cardiovascular anomalies are common in patients with coarctation and impact the presenting clinical symptoms, the age of clinical presentation, and the clinical outcome (moderate evidence).
- In newborns and infants with appropriate acoustic window, echocardiogram is the study of choice with sensitivity >90% (limited to moderate evidence).
- In older children, contrast-enhanced MR angiography (MRA) is superior to transthoracic echocardiography and other MR imaging techniques for the diagnosis of congenital coarctation and obstructive aortic arch anomalies (moderate to strong evidence).
- CT angiography (CTA) offers comparative performance to MRA and can be used for the diagnosis and surgical planning when MRA is not available or is contraindicated (limited evidence).

J. C. Hellinger (✉)
Department of Radiology, Children's Hospital of Philadelphia, University of Pennsylvania School of Medicine, Philadelphia, PA 19104, USA
e-mail: jchellinger@yahoo.com

L.S. Medina et al. (eds.), *Evidence-Based Imaging in Pediatrics*,
DOI 10.1007/978-1-4419-0922-0_25, © Springer Science+Business Media, LLC 2010

- Conventional angiography is no longer routinely used for diagnosing coarctation but is reserved for endovascular treatment with balloon angioplasty or stent placement (limited evidence).

Aortic Arch Anomalies: Vascular rings and Pulmonary Slings

- The clinical presentation of a symptomatic vascular ring or a pulmonary sling may result from tracheal compression, esophageal compression, or both. Symptoms and signs are typically respiratory in infants and children, whereas they are esophageal in adults (limited to moderate evidence).
- Associated cardiac abnormalities occur in up to one-third of patients with aortic arch anomalies (moderate evidence).
- Preoperative evaluation of aortic arch anomalies should also address the presence of tracheomalacia. Unrecognized tracheomalacia can lead to negative surgical outcome and persistent symptoms.
- MRI–MRA and CTA have the highest diagnostic performance (sensitivity and specificity) followed closely by the esophagram in evaluating aortic arch vascular rings (limited to moderate evidence).
- Esophagram can readily detect vascular ring but has lower sensitivity for pulmonary sling (limited evidence).
- Conventional angiography is no longer routinely used for the diagnosis of vascular rings (limited evidence).

Definition

Congenital disease of the aortic arch includes coarctation and aortic arch anomalies. Tubular hypoplasia and interrupted aortic arch are additional obstructive lesions which often occur with coarctation and should be considered in a clinical differential diagnosis. Suspected aortic arch anomalies warrant investigations to exclude a vascular ring or a pulmonary sling. Fundamental understanding and prompt diagnosis for both coarctation and aortic arch anomalies are important as they can lead to increased patient morbidity and mortality and decreased patient longevity.

Thoracic Aorta Coarctation

Coarctation of the aortic arch is focal, eccentric obstructive narrowing involving the isthmus. The narrowing may be located at (juxtaductal), just above (preductal), or just below (postductal) the site of insertion of the ductus arteriosus (1). In children less than 1 year of age, the preductal type predominates, while in those children greater than 1 year of age, the postductal type predominates (2). The narrowing results from an abnormal sling of fibromuscular ductal tissue which extends from the dorsal, superior–posterior margin of the isthmus, opposite the ductal ostium, and encircles the medial and lateral walls of the aorta back toward the ostium (3). In addition to tubular hypoplasia of the aortic arch and an interrupted aortic arch, other associated cardiovascular abnormalities include bicuspid aortic valve, left to right shunts (i.e., ventricular septal defects), and left-sided obstructive cardiac lesions (i.e., congenital mitral atresia, hypoplastic left ventricle, subaortic stenosis, and aortic atresia). Depending on the level and degree of the aortic obstruction, the patency of the ductus arteriosus, and the age of the patient, collateral arterial pathways develop to direct flow below the obstruction. Key pathways include the subclavian, internal mammary, thoracodorsal, and intercostal arteries.

It is hypothesized that as the left subclavian artery migrates cephalad through differential growth of the dorsal aorta, the ductal ostium from the sixth arch is pulled into the aorta, forming the circumferential sling. Obstruction occurs when there is postnatal constriction of the ductus arteriosus (4, 5). While this may be an isolated occurrence, it is theorized that

when there is decreased antegrade flow in the ascending aorta and the proximal aortic arch, there is reversal in flow from the ductus arteriosus across the isthmus to the aortic arch and supra-aortic arteries, resulting in an alteration of the "branch point" angulation and accentuation of the cephalad migration (4–6). The left to right shunts and left-sided obstructive cardiac lesions lead to decreased ascending aortic flow, accounting for their high association with tubular hypoplasia, interrupted aortic arch, and coarctation. Right-sided obstructive cardiac lesions, such as right ventricular outflow tract obstruction, pulmonary stenosis, and pulmonary atresia, protect against developing coarctation, as there is dominant antegrade isthmus flow with diminished pulmonary to aortic flow across the ductus arteriosus (7, 8).

Vascular Ring

A vascular ring is a developmental aortic arch anomaly in which the trachea and the esophagus are surrounded and either compressed or effaced by vessels, ligaments, or both. The ring may be complete or incomplete. The surrounding structures include the aortic arch or arches, aortic arch branch arteries, pulmonary branch arteries, ductus arteriosus, and ligamentum arteriosum. The vascular rings may occur with a normal left-sided arch, a double aortic arch, a right-sided aortic arch, or a cervical aortic arch, depending on the number and side of the aortic arch(es), the course and side of the descending aorta, and the origin and course of the aortic arch branch arteries, the pulmonary branch arteries, and the ductus or the ligament arteriosum.

Vascular rings result from abnormal persistence and involution of primitive brachial arch segments. Among the six arch segments, it is most commonly due to abnormalities involving the third, fourth, and sixth arches. Classification is based on Edwards' hypothetical embryologic double aortic arch model (9).

The normal left-sided aortic arch with a left descending aorta and the left-sided ligament arteriosum are formed by regression of the right and persistence of the left fourth arches, eighth dorsal aorta segments, and sixth dorsal arches, respectively. Left aortic arch (LAA) anomalies include an aberrant right subclavian artery (ARSCA) and a circumflex descending aorta. In both instances, the anomalous arterial structures have a retroesophageal course. The ring is formed when the ligamentum arteriosum is right sided. With an LAA–ARSCA, the right ligament is indicated by the presence of a Diverticulum of Kommerell.

A double aortic arch (DAA) is a complete vascular ring. It results from the persistence of both the right and the left fourth arches and the dorsal aortae. The right arch is often dominant in size and located higher than the left arch. Symmetrical arches can occur and less commonly, the left arch may be atretic with a fibrous segment distal to the takeoff of one or both of the left arch branch arteries. Rarely, the right arch may be atretic. The right arch typically supplies the right common carotid and brachiocephalic arteries and the left supplies the left common carotid and brachiocephalic arteries. The descending aorta is often on the left but the proximal descending aorta can occur on the right or course midline. The ligament is usually left sided. Less commonly, it can be right sided or bilateral. Pulmonary arteries are normal.

A right aortic arch (RAA) occurs from persistence of the right and regression of the left fourth arches and eighth dorsal aorta segments, respectively. Four variations may arise: aberrant left subclavian artery (ALSCA), aberrant left brachiocephalic artery (ALBCA), mirror-image branching, and a circumflex left descending aorta. In each instance, a vascular ring occurs when the ligamentum arteriosum is left sided. With a retroesophageal ALSCA or ALBCA, a diverticulum of Kommerell signifies the contralateral ligament. With mirror-image branching, a ring forms when a left ligament courses retroesophageal. While the ligament may not be visualized, morphologically, a small leftward-facing dimple at the proximal descending aorta indicates the takeoff of the ligament (10).

A cervical arch occurs when the aortic arch is positioned above the thoracic inlet. It is thought to result when the third arch forms the basis for aortic arch development, rather than the fourth. This may occur with both right and left third arches, leading to the potential formation of left-sided, right-sided, and double aortic arch anomalies and vascular rings. Most commonly,

however, it occurs with a persistent right third aortic arch and a right dorsal aorta (11).

Pulmonary Sling

A pulmonary sling is a specific type of vascular ring in which the left pulmonary artery arises from the right pulmonary artery, crosses back to the left chest between the trachea and the esophagus, and produces symptoms from tracheal compression. It occurs as a result of left sixth ventral arch involution. The left pulmonary artery develops directly from the right pulmonary artery. While right and left ligaments are possible, only a left ligament will lead to a complete vascular ring. In this instance, the ligament passes between the main or right pulmonary artery and the left descending aorta.

Epidemiology

The incidence of congenial heart disease ranges between 2.2 and 8.8 per 1,000 live births (12–16). Depending on the study population and inclusion of minor lesions, the incidence of congenital heart disease may reach 12–75 per 1,000 live births (15, 17). Both coarctation and aortic arch anomalies account for low percentages of these congenital lesions.

Coarctation

Coarctation occurs in 1.8–9.8% of reported congenital heart disease, with most studies showing an incidence of 5–6% (12–17). About 6.3–7.5% of critically ill infants presenting with congenital heart disease may have coarctation (18, 19). Males predominate with a male-to-female ratio of 1.2–2.3:1 (12, 20–27). About 14–23% of patients present at less than 1 year of age (23, 26–29), while 21–38% may present during childhood (ages 1–10) (23, 27–29), 19–20% during adolescence (ages 11–18) (23, 27), and 17–21% during young adulthood (ages 19–29) (23, 27). About 10–16% present during the fourth decade of life (ages 30–40), while 9–10% are diagnosed beyond age 40 (23, 27). Among infants with newly diagnosed coarctation, 15% will present within the first 48 hours of life, while nearly 60% will warrant diagnostic evaluation within the first two weeks of life (12).

Among pediatric patients with coarctation, associated cardiovascular anomalies may occur in 44–84% (20, 22, 30). The majority of anomalies occur in infants and young children less than 2 years of age. About 67% of lesions will occur in patients less than 1 year of age (20), while up to 68–71% will occur by 2 years of age (20, 22). This results in 67–89% of infants less than 1 year of age (20, 23) and up to 78–87% (20, 22) of patients less than 2 years of age having an associated congenital lesion. This is in comparison to 21–54% of patients greater than 2 years of age having associated congenital heart disease (20, 22).

Prevalent lesions include patent ductus arteriosus (58–80%) (12, 20, 31, 32), aortic tubular hypoplasia (33–49%) (31, 32), bicuspid aortic valve (27–63%) (28, 30–33), ventricular septal defects (16–53%) (12, 20, 30–32), atrial septal defects (6–27%) (20, 30–32), aortic valvular disease (7–37%) (12, 20, 30–32), mitral valvular disease (3–26%) (12, 20, 30–32), and transposition of the great arteries (1–8%) (20, 30–32).

Most cases of coarctation occur sporadically, but both environmental factors and genetic causes are postulated. Supporting the former, bimodal seasonal peak incidence is reported to occur between September and November and January and March (21). For the latter, concordance in monozygotic twins, autosomal dominant transmission, and high first-degree relative transmission have been described (34–36). The relationship between coarctation and left ventricular outflow tract obstructive lesions is postulated to occur through a single gene mutation (37). Common associated chromosomal syndromes include trisomy 13, trisomy 18, and 45 XO karyotype (1).

Aortic Arch Anomaly

Aortic arch anomalies occur in 0.5–1.6% (13, 18) of congenital heart disease presentations. Review of surgical case series over the past 20 years found that males have a slightly greater prevalence than females (1.2:1) (38–46). Depending on the severity of vascular compression and the presence of cardiovascular and noncardiovascular comorbid congenital disease, presentation may occur during the neonatal period, infancy, childhood, or young adulthood. However, review of surgical case

series found that most patients first exhibit respiratory symptoms by 1 year of age (range 4.5–20 months, average 12 months) (39–41, 43, 44, 46, 47). In a retrospective review of 35 symptomatic pediatric patients (2 weeks to 17.5 years), McLaughlin et al. reported that diagnosis was made by 6 months of age in 34% and by 12 months of age in 63%. About 37% of patients were diagnosed with an aortic arch anomaly after 1 year of age (47).

The most common symptomatic anomalies are a double aortic arch (49%, range 36–72%) and a right aortic arch with a left ligamentum/ductus arteriosum (28%, range 8–49%). Less frequent symptomatic anomalies include innominate artery compression (10%, range up to 3.3–27%), left aortic arch with an aberrant right subclavian artery (8%, range up to 1.7–20%), and pulmonary sling (5%, range up to 1.8–12.5%) (38–44, 46–48). With a double aortic arch, right dominance occurs in 66% (range 37–81%), left dominance in 16% (range 10–20%), and codominance in 17% (range 3–53%) (38, 43–45, 47). With a right aortic arch–left ligamentum, a diverticulum of Kommerell occurs in 15–21% (43, 45).

In reported case series, associated congenital heart abnormalities were found to occur in 12–32% (average 18%) of patients with aortic arch anomalies (38, 40, 42–45, 48, 49). Common abnormalities include ventricular septal defects (37%, range 18–71%), patent ductus arteriosus (21%, range 0–57%), right-sided obstructive lesions (including Tetralogy of Fallot; 18%, range 0–23%), coarctation (9%; range 0–40%), and atrial septal defects (3%, range 0–14%) (38, 40, 42–45, 49). Analysis showed that 50% (range 0–70%) of these lesions occurred with a right aortic arch–left ligament, 33% (range 10–50%) with a double aortic arch, 9.7% (range 0–70%) with an aberrant right subclavian artery, 3.6% (range 0–10.5%) with a pulmonary sling, and 3.6% (range 0–20%) with innominate artery compression. Among patients with a right aortic arch–left ligament and a double aortic arch, authors reported a prevalence of 23% (range 19–42%) and 12% (range 3–43%), respectively, for associated congenital heart lesions (38, 42–45, 48).

Tracheomalacia may occur in up to 53% of patients with symptomatic aortic arch anomalies (50). Defining tracheomalacia as a tracheal cross-sectional area reduction by greater than 50% in expiration as compared to inspiration, Lee et al. found in a two-reader analysis of 15 patients with aortic arch anomalies undergoing 16- or 64-channel dynamic inspiratory–expiratory multidetector-row CT that 8 patients with tracheomalacia had an average reduction of 87% (range 60–100%). The seven patients without tracheomalacia had an average reduction of 8.2% (range 0.2–27%). Tracheomalacia occurred in 100% of patients with innominate artery compression, 33% of patients with a double aortic arch, and 20% of patients with a right aortic arch and an aberrant left subclavian artery. Nine of the study patients underwent bronchoscopy, confirming the presence of tracheomalacia in seven patients and excluding tracheomalacia in the other two patients (50). In a retrospective surgical review of 29 patients undergoing double aortic arch repair, Shanmugam et al. achieved similar results. Thirty-one percent of their study patients had tracheomalacia (49) (limited to moderate evidence).

Pulmonary slings are associated with tracheal abnormalities including tracheal rings, tracheomalacia, and right upper lobe bronchus. In a retrospective review of 12 patients who underwent surgical repair for pulmonary sling, Backer et al. reported 42% to have tracheal rings (51). Horvath et al. found 40% of pulmonary sling patients to have severe tracheomalacia (52). In a study by Chen et al., all patients with a left pulmonary artery sling presented with tracheal stenosis (100%), and there was a high incidence of right tracheal bronchus (22%), right lung hypoplasia (22%), persistent left superior vena cava (22%), and left patent ductus arteriosus (39%) (53). In a more recent retrospective review of surgical experience for pulmonary sling (31 patients), Oshima et al. found 100% of the patients to have short- (29%) and long (81%)-segment tracheal stenosis from tracheal rings, while 19% had a right tracheal bronchus (54).

There is no reported seasonal variance for the birth prevalence of aortic arch anomalies. Turner et al. reported 4% of patients with arch anomalies to have 22q11 deletion (46). This compares to 35% of patients with chromosome 22q11 deletion potentially having an aortic arch anomaly (55).

Overall Cost to Society

Limited information was found in the medical literature regarding cost-effective diagnostic algorithms for coarctation. In a retrospective review comparing MRI and echocardiography obtained in young children prior to balloon angioplasty for coarctation, Mendelsohn et al. found no significant difference between either modality to provide quantitative analysis for required treatment planning. However, MRI defined collateral flow with greater accuracy while echocardiography was superior for intracardiac anatomy. An "echo-first" protocol followed by MRI for nondiagnostic echocardiograms would incur higher cost than if the workup proceeded directly to MRI for cases when it was felt echocardiography would be limited or nondiagnostic (56). Therrien et al. evaluated cost-effective sensitivities of clinical office visits, chest radiography, echocardiography, exercise stress testing, and MRI to detect recoarctation or aneurysms in a cohort of patients who previously underwent surgical repair. The authors concluded that clinical visit with MRI was the most cost-effective strategy. Clinical evaluation with screening echocardiography and an MRI for positive echocardiograms cost only slightly more; however, 3% of recoarctation or aneurysms may have been missed on screening echocardiography (57).

No data were found in the medical literature regarding overall cost to society for diagnosis, treatment, and sequelae of aortic arch anomalies. Both diagnostic and treatment algorithms are discussed in the literature, but no cost-effectiveness data were found specifically incorporating imaging strategies in the diagnosis and management of symptomatic patients with suspected vascular ring, pulmonary sling, or other aortic arch anomalies.

Goals

For both coarctation and aortic arch anomalies, early diagnosis and intervention are paramount to minimizing morbidity and mortality. Initial diagnosis and treatment planning should be made with high accuracy and confidence, utilizing a minimum number of modalities. Investigations should limit redundant data accumulation and minimize the use of invasive modalities and radiation. When radiation modalities are employed, dose reduction strategies should always be employed.

Imaging evaluation of the congenital aortic arch lesions focuses on structural morphology and flow analysis. Primary interpretation addresses the caliber of the ascending aorta; the location, number, sidedness, and caliber of the arch(es); the number, course, and caliber of the aortic arch branches; the patency and caliber of the isthmus; the course and patency of the descending aorta; and the course and caliber of pulmonary branch arteries. The ductus is classified as patent or closed. If coarctation is identified, the narrowing is classified in relation to the ductus and collateral flow is assessed. If an aortic arch anomaly is detected and the duct is closed, ligament sidedness is determined by recognition of a diverticulum of Kommerell or a ductal nimple. For both coarctation and aortic arch anomalies, search is made for associated cardiovascular and noncardiovascular abnormalities. For vascular rings and pulmonary slings, the compressed tracheal and esophageal segments are characterized by location, length, and degree (qualitative and quantitative). Consideration is given to the assessment of tracheobronchial structural properties and airway dynamics and exclusion of tracheobronchomalacia and complete cartilaginous tracheal rings. Central airways and the esophagus should be assessed for fluid and debris. Consideration may also be given to assessment of aspiration, airway disease, and pneumonia. Alternative causes of tracheoesophageal narrowing, including cardiac chamber, pulmonary arteries, aortic arch, and innominate artery, extrinsic compression, should be excluded. Postoperative and postendovascular evaluation should assess patency of the aorta and branch arteries and exclude aneurysms, pseudoaneurysms, and iatrogenic aortic injury. In addition, for those patients who have undergone stent placement, stent migration and fatigue should be excluded.

Methodology

For data regarding the diagnostic performance of clinical and radiographic examinations of

patients with suspected coarctation and aortic arch anomalies, a MEDLINE search was performed using PubMed (National Library of Medicine, Bethesda, MD). Imaging and treatment outcome literature review was based upon searches up to January 2009. Search methodology used the following statements: (1) coarctation, (2) vascular ring, (3) pulmonary sling, (4) hypertension, (5) congestive heart failure, (6) respiratory distress, (7) recurrent infection, (8) dysphasia, (9) surgical repair, (10) balloon angioplasty, (11) endovascular stents, (12) ultrasound, (13) echocardiogram, (14) esophagram, (15) MRI and MR angiography, and (16) CT angiography.

Discussion of Issues

I. Which Clinical Symptoms and Signs May Suggest the Presence of Coarctation or an Aortic Arch Anomaly?

Coarctation

Summary of Evidence: Coarctation results in aortic flow obstruction and increased left ventricular afterload. The alterations in systemic perfusion, along with activation of sympathetic and renin–angiotensin systems, in turn lead to increased blood pressure. Most clinical signs and symptoms are a direct manifestation of this process. Two other sources for presentation are valvular disease (aortic and mitral) and infectious endocarditis. Clinical presentation during the neonatal period, infancy, childhood, adolescence, or adulthood depends on the location of the coarctation, the rate of ductal closure, the severity of the coarctation, the presence of collateral arteries, and the presence and type of cardiac lesion. Neonates and young infants may present with lethargy, poor feeding tolerance, failure to thrive, congestive heart failure, renal insufficiency, and circulatory collapse (shock), while pediatric patients beyond the neonatal period in addition to lethargy, poor feeding tolerance, and failure to thrive, more commonly present with fatigue, exertional dyspnea, claudication, chest pain, headaches, dizziness, epistaxis, fevers, and/or asymptomatic hypertension (limited to moderate evidence). Detection of a systolic murmur, diminished femoral pulses, and elevated upper relative to lower extremity blood pressure are important clinical findings in the evaluation of coarctation (limited to moderate evidence). Upper extremity systolic blood pressure greater than the lower extremity systolic blood pressure merits further diagnostic workup (limited to moderate evidence).

Supporting Evidence: In a review of 80 patients (2 weeks to 49 years old) who underwent surgical repair for coarctation, Kish et al. found that 100% of patients less than 3 months of age presented with congestive heart failure; only 9% of those greater than 3 months had cardiac dysfunction (25).

A study by Cheatham et al. reported that in patients less than 2 years of age (78% having congenital heart anomalies), 75% presented with heart failure, while 3% had fatigue and 9% failure to thrive as the main presenting symptom. In Cheatham's cohort of pediatric patients greater than 2 years of age (21% having congenital heart anomalies), 8% presented with heart failure, while 15% had fatigue, 10% claudication, and 10% failure to thrive (22). In a clinicopathologic study of 84 patients beyond 1 year of age (range 1–49 years old, mean 17 years old), including 48 with isolated coarctation and 36 with associated cardiac lesions, Glancy et al. reported that the most common presenting symptoms included dyspnea (44%), claudication (39%), fatigue (27%), epistaxis (19%), chest pain (18%), and headaches (18%). Only 18% presented with heart failure—all of whom had an associated cardiac lesion (58).

Regarding physical exam findings, 74–95% of patients are reported to have elevated blood pressure above that of age-matched populations, while 88–100% have a systolic murmur and 85–96% have decreased femoral pulses (22, 23, 25, 58) (limited to moderate evidence). Liberthson found that 72% of pediatric patients <1 year of age and 83% of patients between 1 and 18 years of age have blood pressure exceeding the 90th percentile (23) (limited to moderate evidence). In a retrospective review of 108 infants surgically treated for coarctation over 12 years, Glass et al. reported 84% of clinical diagnoses could be made by palpating femoral arteries (i.e., diminished pulses) and obtaining blood pressure readings in the upper and

lower extremities (2) (limited to moderate evidence). In a study of 40 children (mean age 11 years) including 20 healthy controls, Rahaila et al. demonstrated that the value to warrant further diagnostic imaging evaluation was a blood pressure 5–10 mmHg higher in the arm than in the leg (59) (limited to moderate evidence). Park et al. compared blood pressure gradients and pulsed Doppler recordings in 74 healthy children and 21 children with preoperative or postoperative aortic coarctation. The authors concluded that (1) if the systolic pressure in the calf or the thigh was lower than that in the arm, the presence of aortic coarctation was suspicious and (2) if the arm systolic pressure minus calf systolic pressure and/or arm systolic pressure minus thigh systolic pressure is greater than the mean plus two standard deviation for normal children, the diagnosis of aortic coarctation is likely (60) (limited to moderate evidence).

Aortic Arch Anomaly

Summary of Evidence: The clinical presentation of a vascular ring or a pulmonary sling reflects the severity of compression on the trachea, esophagus, or both. The age of presentation correlates indirectly with the degree of narrowing. Respiratory symptoms are more prevalent among infants and young children, while esophageal symptoms are more common among older children, adolescents, and adults. As there are no direct vascular signs or symptoms, a high index of suspicion is necessary to reach a correct working differential diagnosis (limited to moderate evidence).

Supporting Evidence: Review of surgical experience over the past 40 years finds that most patients present with respiratory symptoms (91%, range 80–100%), including stridor (53%, range 42–100%), recurrent infections (32%, range 21–47%), respiratory distress (26%, range 0–78%), wheezing (21%, range 0–86%), and cough (13%, range 0–24%) (limited to moderate evidence). Gastrointestinal complaints are less frequent occurring in 36% of patients (range 15–60%), mostly adults. Dysphagia (54%, range 0–100%), feeding difficulties (28%, 0–100%), and failure to thrive (8%, range 6–46%) are most common (38, 40–46, 61, 62). Multiple authors have shown that more severe constrictions (as with a double aortic arch) manifest in younger patients with stridor, respiratory distress, and feeding difficulties, while less severe lesions, as found in older patients, result in recurrent infections and dysphagia (38, 42, 46). When there are associated cardiac defects, cardiac symptoms will also be present. Kocis et al. reported murmurs (10%), congestive heart failure (8%), cyanosis (3%), cor pulmonale (2%), and chest pain (2%) to be most common among the cohort of 19% presenting with cardiac symptoms (43).

II. What Is the Natural History of Thoracic Aorta Coarctation and Aortic Arch Anomalies?

Coarctation

Summary of Evidence: In the neonatal period, the inability to develop collateral flow as the aorta constricts leads to left heart dysfunction and potentially pulmonary hypertension and right heart dysfunction with enlarged cardiac chambers. This is exacerbated by comorbid congenital heart lesions (limited to moderate evidence). Diminished cardiac output can lead to fatigue during feedings, renal insufficiency, and systemic shock. The feeding intolerance can result in failure to thrive. For those with sufficient compensatory collateral flow that delays presentation until later in life, secondary cardiovascular complications will develop as a result of the systemic hypertension, potential valvular disease, and potential bacterial endocarditis (moderate evidence). For all patients, unrepaired coarctation increases patient morbidity and mortality, reducing expected life expectancy as compared to the general population (moderate evidence). Medical management is first initiated to maintain ductal arteriosum patency, to control hypertension, and/or to control cardiac function. Definitive patient management requires surgical repair. In select patients, endovascular therapy is an option with balloon angioplasty, stent placement, or both. While surgery improves patient survival, patients may have residual hypertension placing them at risk for subsequent cardiovascular disorders, including coronary artery disease, ischemic heart disease, congestive heart failure, aortic valvular disease, aortic root dilatation, aortic aneurysms, aortic rupture, aortic dissection, cerebrovascular ischemia,

cerebral hemorrhage, and bacterial endocarditis. Age at the time of coarctation repair is a determining factor for operative mortality, recoarctation, and residual hypertension. To optimize surgical outcome and minimize potential future cardiovascular risk, elective coarctation repair is recommended in early childhood and should not be delayed past 10 years of age (limited to moderate evidence).

Supporting Evidence: In an autopsy review of 304 patients who did not undergo surgical repair, Campbell found that nearly 90% of patients died prior to 50 years of life. Causes of death included congestive heart failure, aortic rupture, intracranial hemorrhage, and bacterial endocarditis. The mean age of death was calculated to be 34, as compared to 71 for the control population (63). In a study reviewing a 12-year surgical experience for coarctation in infants less than 1 year of age, Glass et al. reported a 50% mortality rate if coarctation was not repaired and appropriate medical management initiated. Fifty-three percent of the deaths occurred in neonates less than 4 weeks of age (2). Following surgical repair for coarctation, Bobby et al. showed that surgical repair increased life expectancy but did not achieve that of the expected general population. In comparison to Campbell et al., 70% of patients reached the sixth decade of life and 50% were alive at 70 years of age. Survival data from two studies examining patients following surgery reveal 79% to be alive at 40 years (28) and 74% at 44 years (64), with a mean age of death of 34 and 37 years, respectively.

Pediatric surgical repair for coarctation most commonly consists of resection with direct end-to-end anatomists (70–97%) or extended end-to-side anastomosis (30%). Other options include interposition graft (1–3%), patch aortoplasty (3–5%), and left subclavian flap transposition (5%) (22, 65, 66). Depending on the age in which repair is undertaken and the surgical technique, operative mortality over the past 40 years for pediatric patients has been reported to range between 2 and 41% (2, 20, 22, 30, 65–68). Various groups have shown mortality to be highest in infants less than 1 year (19–45%) (2, 30, 66). In a review of 333 operative pediatric cases, Tawes et al. reported that mortality reached 45% in patients less than 1 year and was significantly lower in infants older than 1 (2.6%). Preductal coarctation, multiple congenital heart lesions, and congestive heart failure were prevalent in the cohort of demised infants (20, 33). In more recent surgical experience, Williams et al. reported mortality rates of 25% for infants less than 1 year with complex congenital heart disease and only 4% for those with isolated coarctation (66).

Recoarctation has been reported to occur in 4–26% of pediatric patients (20, 22, 30, 65, 67, 69). Several studies have shown recoarctation to have a higher rate in infants less than 1 year. Among 248 patients who survived operative repair, Tawes et al. reported that 21 patients (8%) developed recoarctation over 2 months to 16 years. Ninety-five percent were less than 1 year, yielding a recoarctation rate among surviving infants of 20% as compared to 0.6% rate for those older than 1 year (20). Sorland et al. found a recoarctation rate of 57% among infants less than 1 year as compared to 17% for those operated after 1 year (65). Similarly, Rostad et al. reported a rate of 52% for infants and 14% for those older than 1 year (67). Applying actuarial analysis for infants who underwent coarctation repair, Williams et al. found that recoarctation occurred in 54% within 7 years (66).

Examining outcome data from pediatric surgical review series found that isolated late hypertension occurs in 12.5–21% (22, 23, 65, 69). Multiple authors have reported that the prevalence of late hypertension increases with the age at the initial operation and that a greater degree of blood pressure normalization is achieved when repair occurs in early childhood. Liberthson et al. found a prevalence of 6% when operated at 1–5 years of age, 27% at 6–10 years of age, 33% during adolescence, 51% during young adulthood, and 44% after 30 years of age (23). Cohen et al. reported that the lowest prevalence was achieved when the coarctation repair occurred under 9 years of age (70). Toro-Salazar et al. found similar results. However, in addition to an age of less than 9 years, these authors reported that the presence of hypertension at the first postoperative clinic visit and the development of postoperative paradoxical hypertension were independent risk factors. Long-term survival was highest when surgery occurred between 1 and 5 years of age (28).

Aortic Arch Anomaly

Summary of Evidence: Chronic tracheoesophageal compression from an unrepaired vascular ring or a pulmonary sling may result in persistent respiratory and gastrointestinal dysfunction. Secondary upper airway abnormalities and intrathoracic airway obstruction may lead to exercise intolerance, apnea, cyanosis, and recurrent upper and lower respiratory infections, while continuous esophageal compression may result in feeding intolerance, failure to thrive, and aspiration. Surgical repair is definitive management to relieve symptoms. This consists of dividing the vascular ring and in the case of a pulmonary sling, reimplanting the left pulmonary artery. In the majority of cases, the surgical approach is a left thoracotomy. Residual tracheal narrowing may occur from intrinsic pathology and/or extrinsic compression. Postoperatively, pulmonary function testing (PFT) can be applied to initially screen for central airway (tracheal) obstruction (intrinsic or extrinsic). Intrinsic tracheomalacia and tracheal rings may cause persistent narrowing and symptoms, leading to postoperative morbidity and mortality. Additional surgical procedures such as aortopexy, tracheal segmental resection, and tracheoplasty may be required at the time of anomaly repair to treat both tracheomalacia and tracheal rings (limited to moderate evidence).

Supporting Evidence: In a retrospective review of 69 patients who underwent surgical repair for tracheobronchial compression, Horvath et al. reported high preoperative morbidity related to late diagnosis. One hundred percent had recurrent respiratory infections treated with antibiotics. In 35%, preoperative management required endotracheal ventilation with 12.5% of these patients necessitating tracheostomy (52).

Repair of a vascular ring or a pulmonary sling is approached from a left thoracotomy in 87% of patients (range 57–93%), a right thoracotomy in 7% (range 1–41%), and a median sternotomy in 6% (range 2–9%) (38, 40–42, 44, 49). Operative mortality ranges between 3 and 7% (40–42, 44, 46, 49, 52). Rivilla et al., Horvath et al., Shanmugam et al., and Turner et al. each individually reported that tracheomalacia was a significant contributing factor in all cases of patient demise in their respective surgical experiences (40, 46, 49, 52). Mclaughlin et al. reported that 50% of patients requiring postoperative tracheostomy had significant tracheomalacia (47), while Turner et al. reported that 100% of patients requiring a tracheostomy had tracheomalacia (46).

Regarding long-term clinical surveillance and outcome, surgical repair achieves symptomatic relief in 80% (range 70–95%) of patients. Among the 20% (range 5–30%) of patients with residual symptoms, 36% (range 17–100%) may have tracheomalacia (38, 42, 44, 47, 49). Horvath et al. applied PFTs in 15% of surviving patients to screen for central airway obstruction. Thirty percent of these patients were found to have decreased peak expiratory flow rates, warranting advanced imaging to assess for residual narrowing (52).

III. What Are the Diagnostic Performances of Imaging Modalities Used to Evaluate Suspected Coarctation and Aortic Arch Anomalies?

Coarctation

Summary of Evidence: Chest radiography has a low to moderate sensitivity, depending of the age of the patient, the degree of coarctation, and the presence of associated cardiac anomalies. It is useful to assess the heart size, screen for congestive heart failure, and exclude other potential etiologies. In isolated coarctation, key diagnostic findings include aortic rib notching and a "figure of 3" contour (limited evidence). In neonates and infants with optimal acoustic window, echocardiography has a high sensitivity of >90% for coarctation (moderate evidence). In older children, contrast-enhanced MR angiography is superior to transthoracic echocardiography and other MR imaging techniques for the diagnosis of congenital coarctation and obstructive aortic arch anomalies (moderate to strong evidence). CT angiography is a useful and sensitive alternative modality to MRA when MRI may be contraindicated (i.e., aortic stent) or not available (limited to moderate evidence).

Supporting Evidence: Glancy et al. reported 51% of chest radiographs to have rib notching. Seventy-two percent were in patients with isolated coarctation. Rib notching correlated inversely with the aortic lumen and directly with the patient's age (58). Similarly, Kish et al.

found that in patients greater than 3 months of age with coarctation, 59% had rib notching. The "figure of 3" aortic contour has sensitivity as low as 4% on routine chest radiography (25), increasing to 64% if oral contrast is given (58). In isolated coarctation, the heart size is most often normal (63%) or mildly enlarged (35%). In distinction, in 94% of patients with associated cardiac lesions, the heart is enlarged (58). Kish et al. in a retrospective review of 80 patients (2 weeks to 49 years) found that 92% of neonates presenting at less than 3 months of age had cardiomegaly as compared to 44% of patients greater than 3 months of age (25).

The largest series found comparing multiple imaging modalities is from Ming et al. (moderate to strong evidence). Contrast-enhanced MR angiography, ECG-gated T1-weighted spin-echo imaging, and gradient-echo cine imaging were performed for the diagnosis of congenital obstructive aortic arch anomalies in 416 patients (age range 3 days to 12 years, mean age 2.4 years). Transthoracic echocardiography was performed in all patients prior to the 1.5 T MR examination. Standard of reference was based on final diagnosis at surgery and/or conventional catheterization angiography. Congenital obstructive aortic arch anomalies were diagnosed in 213 patients and ruled out in 203 patients. Among the 213 patients with anomalies, coarctation of the aorta was diagnosed in 174, interruption of aortic arch in 35, and persistent fifth aortic arch with fourth aortic arch interruption in 4 patients. Diagnostic sensitivity, specificity, and accuracy of contrast-enhanced MR angiography were 98% (208/213), 99% (201/203), and 98% (409/416), respectively. Diagnostic sensitivity, specificity, and accuracy of transthoracic echocardiography were 88% (187/213), 92% (186/203), and 90% (373/416), respectively. The same diagnostic parameters for ECG-gated T1-weighted imaging and gradient-echo cine imaging were 89% (189/213), 84% (170/203), and 86% (359/416), respectively (71).

In an echocardiogram study by Smallhorn et al., echocardiography correctly predicted the presence of coarctation in 45 of 48 neonates and infants (sensitivity 93.75%) (72). Huhta et al. studied 261 consecutive infants and children with congenital heart disease (age 1 day to 20 years, mean 3.3 years) (moderate evidence). In 255 patients (98%), complete visualization of the ascending and descending aorta was possible by two-dimensional transthoracic echocardiographic examination. One or more significant aortic arch anomalies were present on angiograms in 116 of 255 patients (46%) and were detected by two-dimensional echocardiography in 110 (sensitivity 95%, specificity 99%). Of those with coarctation, 27 out of 29 cases were diagnosed correctly (93.1%) (73).

Nihoyannopoulos et al. studied 540 consecutive patients prospectively aged 2 days to 15 years with a mean of 2 months (moderate evidence). Standard of reference was subsequent cardiac catheterization and angiography. At angiography, 51 patients had aortic arch obstruction; of these, 35 had juxtaductal coarctation, 15 isthmic hypoplasia, and 1 a type B interrupted aortic arch. The presence of arch obstruction was correctly diagnosed with two-dimensional echocardiography in 45 of 51 patients for an overall sensitivity of 88%. Echocardiography defined a juxtaductal coarctation in 33 of 35 patients and isthmic hypoplasia in 13 of 15 patients (sensitivity 94 and 73%, respectively). Among the 489 patients without aortic arch obstruction, echocardiography incorrectly diagnosed the presence of such obstruction in 9 patients (overall specificity 98%) (74).

A more recent echocardiography study from 2005 using the carotid–subclavian artery index has been reported (limited evidence). Sixty-three patients (47 neonates and 16 infants) and 23 controls were evaluated. The ratio of the aortic arch diameter to the left subclavian artery (carotid–subclavian artery index) was significantly smaller in patients with coarctation. A cutoff point at 1.5 showed a sensitivity of 97.7 and 94.7%, and a specificity of 92.3 and 100% for neonates and young infants, respectively. The positive predictive value for coarctation was 97.7 and 100% for neonates and infants, respectively (75).

It is important to determine pressure gradient at the level of the coarctation (76). Catheter angiography continues to be the standard reference to quantify pressure gradients. However, phase contrast MRI provides reliable noninvasive data for determining pressure gradients at the coarctation site. Nielsen et al. retrospectively reviewed 31 patients referred for assessment of native or recurrent coarctation.

By logistic regression analysis, the following variables predicted a hemodynamically significant coarctation gradient (>20 mm Hg): (a) smallest aortic cross-sectional area from gadolinium-enhanced 3D MR angiography and (b) heart rate-corrected mean flow deceleration in the descending aorta measured by phase-velocity cine. The combination of these variables had a sensitivity of 95%, specificity of 82%, and an area under the receiver–operator characteristic curve of 0.938. In a subsequent validation study, the prediction model correctly classified 9 of 10 patients, with no false negatives (76).

A retrospective review of 16 pediatric patients (15 days to 2 years) by Hu et al. compared 16-channel multidetector-row CT angiography to color Doppler echocardiography using operative findings as the reference standard. CTA achieved an overall sensitivity of 100 with an 87.5% sensitivity for axial interpretation and 100% sensitivity using multiplanar and three-dimensional (3D) reconstructions. Color Doppler echocardiography had a sensitivity of 87.5% (limited to moderate evidence) (77).

Aortic Arch Anomaly

Summary of Evidence: Diagnostic algorithms are designed to first investigate the pulmonary system and upper gastrointestinal tract with a secondary aim of excluding a vascular ring or a sling. Algorithms utilize chest radiographs, barium esophagrams, echocardiography, angiography, and bronchoscopy. MRI–MRA and CTA have the highest diagnostic performance (sensitivity and specificity) followed closely by the esophagram in evaluating aortic arch vascular rings (limited to moderate evidence). However, the esophagram may not detect pulmonary slings, for which cross-sectional vascular imaging is required (limited evidence). Chest radiography is most helpful to establish arch sidedness and exclude parenchymal abnormalities. Invasive bronchoscopy is reserved for direct assessment of the airway and exclusion of tracheomalacia.

Supporting Evidence: Chest radiography is performed as part of the initial evaluation. It is readily accessible and exposes patients to minimal radiation. While it is a rapid means to determine arch sidedness, detect airway narrowing, and assess for atelectasis, pneumonia, bronchial wall thickening, and air trapping, it has a low sensitivity for detection of a symptomatic vascular ring or a pulmonary sling. Recognition of a right aortic arch or an eccentric (unilateral or bilateral) tracheal narrowing should raise suspicion for a ring (47). In a retrospective review of 24 patients (mean age 4.5 months, range birth to 8.7 years) presenting with symptomatic vascular rings, Turner et al. reported a sensitivity of only 4% (46) (limited evidence).

The esophagram is essential for evaluating the upper gastrointestinal tract in patients who have feeding difficulties and dysphasia. Search is made for a retro- or anteroesophageal concave impression. The retroesophageal impression may reflect a double aortic arch, an aberrant subclavian artery, an aberrant brachiocephalic artery, or a circumflex aorta. The anteroesophageal impression would suggest a pulmonary sling. Rivilla et al. found that the esophagram could diagnose esophageal compression in 90% of cases, depicting the impression on the esophagus and its relationship to the trachea (40, 47). Both Chun et al. (41) and Turner et al. (46) found esophagrams to have a sensitivity of 95% in diagnosing aortic arch anomalies (limited evidence). In a retrospective clinical review of 82 patients with aortic arch anomalies, Woods et al. reported that most diagnoses could be made by the esophagram in conjunction with echocardiography. The esophagram was limited in detecting a pulmonary sling as well as innominate artery compression (44).

Echocardiography may be used as a screening modality or as an adjunct means to confirm the diagnosis following a positive esophagram. However, echocardiography may not always depict intrathoracic vascular and nonvascular structures in their entirety, as needed for surgical planning. Echocardiography is dependent on the operator and an appropriate acoustic window to display the aortic arch, isthmus, and branch vessels (78). An adequate acoustic window is more often obtained in newborns and young infants than in older children and adults. Echocardiography is most useful for diagnosing associated congenital heart disease. Among 15 of 24 pediatric patients with a known vascular ring, Turner et al. found echocardiography to have a sensitivity of only 47% (46) (limited evidence).

Until recently, catheter angiography has been considered the standard means to angiographically evaluate aortic arch anomalies. While catheter angiography provides a direct vascular display of the thoracic aorta, arch anatomy, and branch arteries to facilitate diagnosis and treatment planning, it is an invasive study that requires sedation or anesthesia, is dependent on iodinated contrast, and generates potentially moderate to high radiation exposure. Turner et al. found catheter angiography to have a sensitivity of 100% (46) (limited evidence).

MRI–MRA and CTA have replaced conventional angiography in most algorithms requiring angiography. The diagnostic capability of MRA and CTA is equivalent to the diagnostic capability of catheter angiography and both are noninvasive. In addition, both can evaluate associated congenital heart lesions, can generate three-dimensional angiographic displays, and can depict the aortopulmonary–tracheoesophageal topographic relationship for diagnosis and treatment planning. MRI–MRA and CTA directly evaluate the aortic arch anomaly and the etiology and degree of central tracheoesophageal compression (79) (limited evidence).

MRI is advantageous over CTA in that aortic arch and aberrant artery flow dynamics can be quantified and the exam is performed without radiation or iodinated contrast medium. MRI, however, is not always readily accessible for timely diagnostic evaluations and is not applicable to all patients, as select implantable devices preclude its use and ferromagnetic susceptibility artifact can render portions of or the entire exam nondiagnostic. MRI has limited spatial resolution, particularly for evaluating peripheral airways and lung parenchyma. Complete exams with functional and hemodynamic sequences may take up to 45–60 minutes, often necessitating sedation for pediatric cases. In a study consisting of 18 subjects with congenital aortic arch anomalies, Kersting-Sommerhoff et al. showed that MRI can provide sufficient anatomic information for the effective, noninvasive evaluation of patients with congenital aortic arch anomalies (limited evidence) (80). In a recent study of 11 infants and children, Greil et al. established that noninvasive 3D MRI using 3D double-slab FISP MR angiography is effective in diagnosing vascular rings and slings in free-breathing infants and children without intravenous contrast agent or associated radiation exposure (limited evidence) (81). In a retrospective review of 22 patients, Eichorn et al. found MRA to have sensitivities and specificities of 100% for diagnosing an aortic arch anomaly (79). Turner et al (46), and Shanmugam et al. (49) achieved accuracies of 100% in the cohort of patients who underwent MRI (limited evidence). MRI is recommended for pulmonary sling evaluation (44, 82).

CT angiography is advantageous for its high spatial resolution and rapid acquisition time. For most pediatric patients with a suspected aortic arch anomaly, it obviates the need for sedation and anesthesia. CTA is most advantageous for simultaneous evaluation of central and peripheral airways and the lung parenchyma. Tracheobronchomalacia, tracheal rings, atelectasis, pneumonia, and air trapping can all be assessed. Although CTA is dependent on radiation and iodinated contrast medium, low radiation dose and low contrast medium protocols can and should be employed for safe practice. Eichorn et al. found CTA to have sensitivities and specificities of 100% for diagnosing an aortic arch anomaly (79). Turner et al. achieved an accuracy of 100% in the select patients who had a CTA (40). Shanmugam et al. (49) utilized CT angiography to evaluate 11 out of 29 patients with a double aortic arch, reporting 100% accuracy (limited evidence). CT is also recommended as an option to evaluate for a pulmonary sling (44). With regard to diagnosing tracheomalacia with CT, Lee et al. reported 100% sensitivity with dynamic inspiratory–expiratory, low-dose acquisitions (50) (limited evidence).

Although invasive, bronchoscopy offers the direct means to diagnose and evaluate tracheal narrowing and tracheomalacia. With this method, arch anomalies are diagnosed indirectly by recognizing the location of narrowing and determining that it is from extrinsic compression. While bronchoscopy may demonstrate a pulsating mass at the level of extrinsic compression, it cannot define the entire anatomical morphology of the arch anomaly. Supporting its application for evaluating tracheomalacia in this patient population, Shanmugam et al. reported that 14 out of 29 patients with a double aortic arch underwent preoperative bronchoscopy. 64% of these patients had tracheomalacia (49). Iatrogenic bronchial

wall edema during bronchoscopy may exacerbate tracheal narrowing and symptoms (limited evidence).

Take Home Figures

What Is the Diagnostic Imaging Workflow for Suspected Thoracic Aorta Coarctation?

The diagnostic algorithm for suspected coarctation is shown in Fig. 25.1. Chest radiography is recommended as the first imaging modality. For an infant, a single frontal anterior–posterior projection is obtained. For all other patients, frontal and lateral views are recommended. If the patient is an infant or a young child, or if the chest exam reveals cardiomegaly, congestive heart failure, or both, echocardiography should be performed. For all other patients or if echocardiography has a suboptimal acoustic window, MRI with MRA is the study of choice. CT angiography should be obtained if there are contraindications to MRI, MRI is not

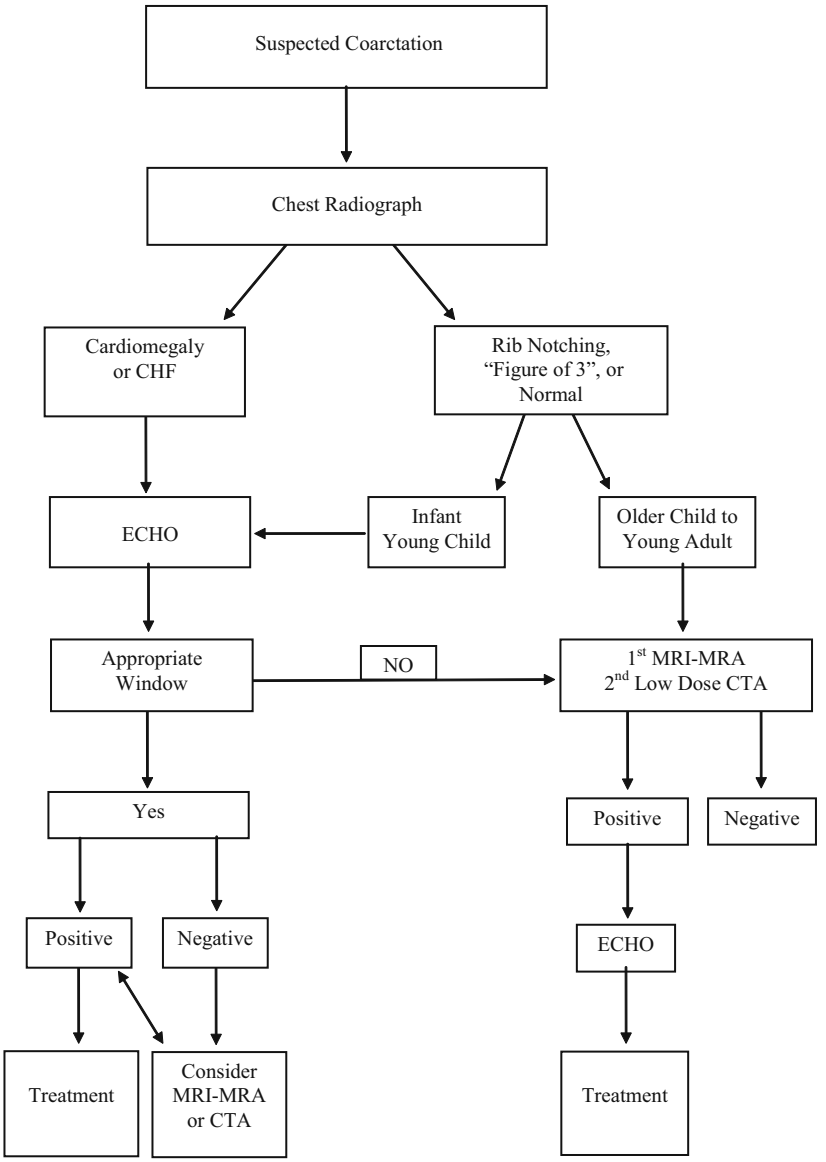

Figure 25.1. Diagnostic algorithm for suspected coarctation.

available, or if the patient is at a high sedation risk. Following a positive MRI–MRA or CTA, prior to surgical or endovascular repair, echocardiography is recommended as a second screening modality to assess cardiac morphology and function and exclude congenital heart defects. If diagnosis is first made by echocardiography, MRI–MRA or CTA may be considered prior to intervention.

What Is the Diagnostic Imaging Workflow for a Suspected Aortic Arch Anomaly?

As shown in Fig. 25.2, modality consideration reflects the dominating clinical symptoms. If respiratory symptoms predominate, noninvasive advanced angiography is recommended. As no radiation is utilized, MRI with MRA is the

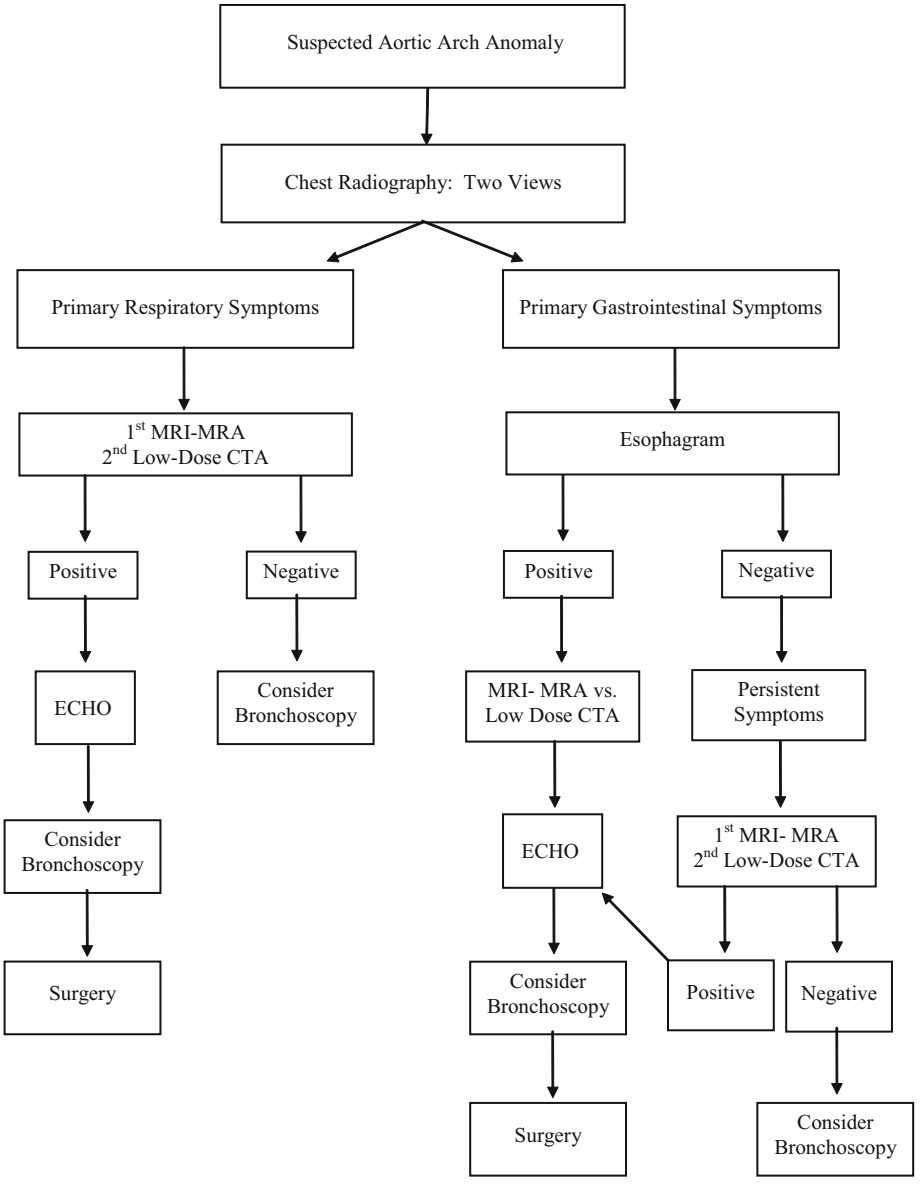

Figure 25.2. Diagnostic algorithm for suspected aortic arch anomaly.

study of choice. However, if there is a high suspicion for tracheomalacia, there are suspected lung parenchymal abnormalities, or the patient is at a high sedation risk, CT angiography is the study of choice. In addition, if MRI is contraindicated or MRI is not available, CT angiography is recommended. When gastrointestinal symptoms predominate, an esophagram is recommended as the first imaging modality. A positive esophagram should be followed by an MRI–MRA or a CTA based upon the criteria described above. Echocardiography is warranted after a positive MRI–MRA or CTA to assess cardiac morphology and function and exclude congenital heart lesions. If symptoms persist following a negative esophagram, consideration should be given to either MRI-MRA or CTA. If the airway has not been adequately characterized and tracheomalacia, tracheal rings or both have not been excluded, either prior to surgical repair or following a negative MRI-MRA or CTA, invasive bronchoscopy should be considered.

Take Home Tables

Tables 25.1 and 25.2 discuss the imaging performances for coarctation and arch anomalies, respectively.

Table 25.1. Diagnostic imaging performance for coarctation

Imaging modality	Sensitivity (%)	Specificity (%)	Accuracy (%)	References
3D MRA	98	99	98	(71)
MRI – ECG gated T1-weighted and gradient-echo CINE	89	84	86	(71)
CTA	100	100	100	(77)
Transthoracic ECHO	94	98	98	(74)
neonate to early adolescence	88	92	90	(73)
neonate to late adolescence	93	100	98	(73)

Table 25.2. Diagnostic imaging performance for aortic arch anomalies

Imaging modality	Sensitivity (%)	Specificity (%)	Accuracy (%)	References
3D MRA	100	100	100	(79)
CTA	100	100	100	(46)
	100	100	100	(49)*
Esophagram	95	NA	NA	(41)
	95	NA	NA	(46)
Transthoracic ECHO	47	NA	NA	(46)

*Patients limited to those with a double aortic arch.

Imaging Case Studies

Case 1

Figure 25.3 presents a case of a 17-year-old male who presented with asymptomatic hypertension and elevated upper extremity systolic blood pressure relative to the lower extremity.

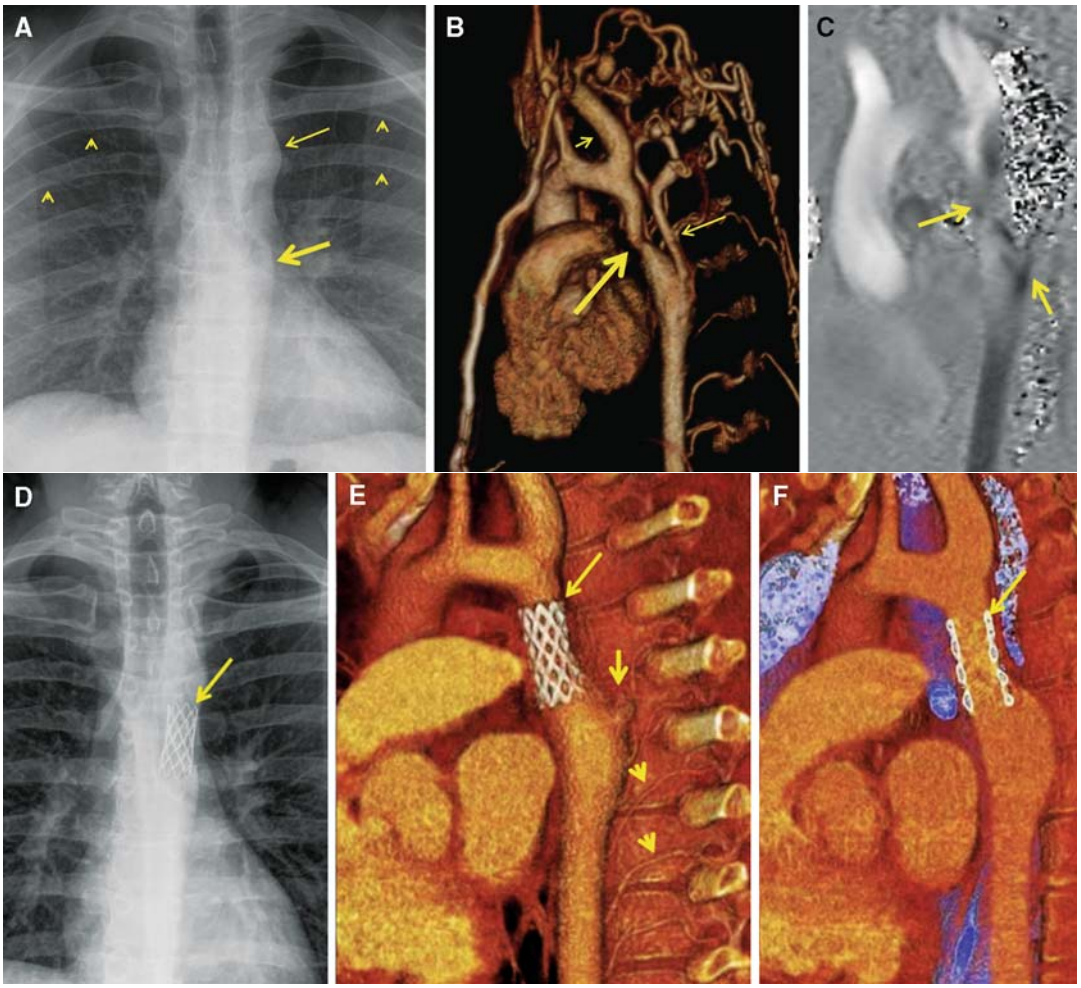

Figure 25.3. **A–F** are selected images from a 17-year-old male who presented with asymptomatic hypertension and elevated upper extremity systolic blood pressure relative to the lower extremity. A frontal chest (**A**) radiograph demonstrates bilobed convex prominence of the proximal descending aortic shadow (*arrows*) with multiple ribs showing sclerosis and notching (*arrowheads*). High-resolution 3D MRA (**B**) confirms high-grade juxtaductal coarctation (*thick arrow*) and dilation of the subclavian artery (*short arrow*) and aorta proximal to the narrowing as well as poststenotic dilatation of the descending aorta immediately distal to the narrowing. The dilated segments conform to the bilobed "figure of 3" radiographic appearance of the aortic shadow with proximal (*thin arrow*) and distal (*thick arrow*) aortic enlargement relative to the coarctation. In B, note the robust collateral network consisting of aortic arch branch arteries, intercostal arteries, and a dominant post-coarctation collateral artery (*thin arrow*). Phase contrast MRI (**C**) was applied to quantify collateral flow. Note the turbulent flow (signal) across the coarctation and the retrograde flow through the post-coarctation-dominant collateral branch artery into the descending aorta. The patient was managed with endovascular bare stent placement (**D–F**, *thin arrows*). A surveillance non-ECG-gated chest CT angiogram shows appropriate positioning (**E, F** volume-rendered images) and wide patency (**F**) of the stent. Note the decompression of the dominant post-coarctation collateral artery (*short arrow*). Mid and distal descending aorta intercostal arteries remain patent (*arrowheads*).

Case 2

Figure 25.4 shows images from a 19-month-old male who presented with feeding intolerance and gastroesophageal reflux.

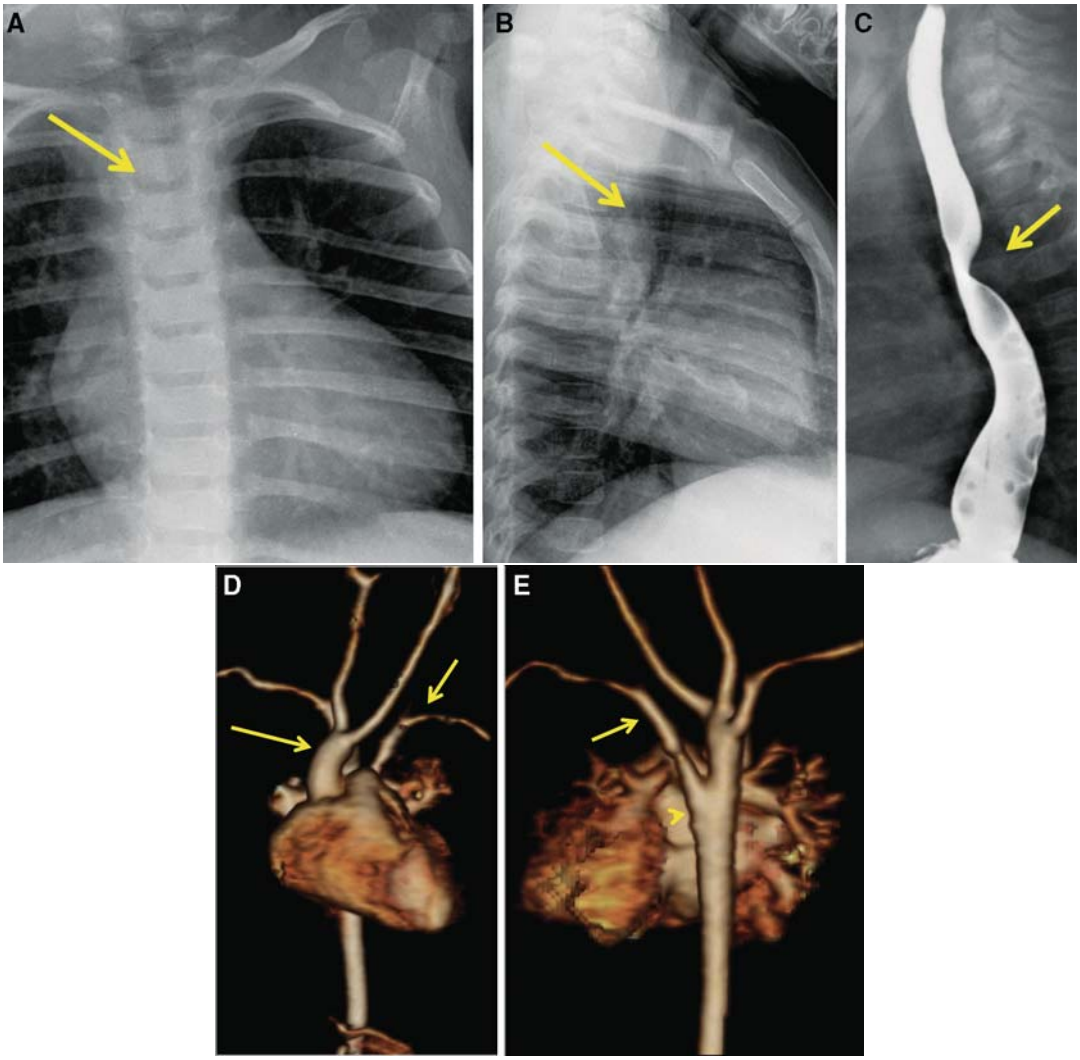

Figure 25.4. **A–E** are selected images from a 19-month-old male who presented with feeding intolerance and gastroesophageal reflux. Chest radiography demonstrates a right aortic arch (**A**, *arrow*; RAA) with anterior displacement of the mid to distal trachea (**BC**, *arrow*), indicating a retroesophageal versus retrotracheal artery. Volume-rendered images from a high-resolution 3D MRA (**DE**) confirm the RAA (**D**, *long arrow*) with an aberrant left subclavian artery (**DE**, *short arrow*). A posterior projection demonstrates a small diverticulum of Kommerell, indicating a complete ring formed by a left-sided ligamentum arteriosus (**E**, *arrowhead*).

Suggested Imaging Protocols for Coarctation and Arch Anomalies

Plain Radiograph

Frontal anterior–posterior projections are obtained for infants. For other pediatric patients, frontal and lateral views are recommended. Exam should be performed in inspiration. If air trapping is suspected, bilateral decubitus views can be obtained.

Esophagram

Multiprojectional real-time barium swallow is performed with dose reduction strategies. Search is made for posterior or anterior indentation of the esophagus to determine the presence of a ring or a sling, respectively.

MRI

Bright and dark blood MRI sequences are obtained followed by CINE short- and long-axis imaging through the heart, pulmonary arteries, and thoracic aorta. For an aortic arch anomaly, focused dark blood imaging is recommended through the trachea to evaluate for narrowing. For coarctation, phase contrast imaging is performed to assess the hemodynamics of the coarctation and collateral flow. Aortic valve short-axis CINE and phase contrast imaging should be performed to assess the number of leaflets and exclude stenosis, insufficiency, or both. Gadolinium is administered and a 3D MRA is acquired in the coronal or the sagittal plane. Images are transferred to a workstation for interpretation using advanced imaging techniques, including multiplanar reformations (MPR), curved planar reformations (CPR), volume rendering (VR), and maximum intensity projections (MIP).

CTA

High-resolution axial images are acquired using low-dose techniques. Acquisition is timed such that pulmonary arteries, thoracic aorta, and aortic branch arteries are opacified. Images are transferred to a workstation for interpretation using advanced 3D visualization techniques.

Echocardiogram

For an appropriate acoustic window, two-dimensional gray scale and color Doppler CINE imaging is performed through the heart, thoracic aorta, aortic branch arteries, and pulmonary arteries. In select cases, if there is available technology, 3D imaging can be considered to assist in depicting complex anatomy.

Future Research

- Evaluate advanced MR and CT angiography protocols using the latest generation of MR and CT scanners and workstation technology to determine diagnostic performance.
- Multimodality cost-effective analysis for evaluation of suspected coarctation and aortic arch anomalies.

References

1. Rosenberg HS. Pediatr Pathol 1990; 10(1–2): 103–115.
2. Glass IH, Mustard WT et al. Pediatrics 1960; 26:109–121.
3. Ho SY, Anderson RH. Br Heart J 1979; 41(3): 268–274.
4. Krediet P. Acta Morphol Neerl Scand 1965; 6:207–212.
5. Momma K, Takao A et al. Jpn Circ J 1982; 46(2):174–183.
6. Hutchins GM. Am J Pathol 1971; 63(2): 203–214.
7. Rudolph AM, Heymann MA et al. Am J Cardiol 1972; 30(5): 514–525.
8. Shinebourne EA, Elseed AM. Br Heart J 1974; 36(5): 492–498.
9. Edwards J. Med Clin North Am 1948; 32: 925–949.
10. Weinberg PM. J Cardiovasc Magn Reson 2006; 8(4):633–643.
11. Davies M, Guest PJ. Br J Radiol 2003; 76(907):491–502.
12. Large group/organigation report (1980). Report of the new England Regional Infant Cardiac Program. *Pediatrics* 1980; 65(2 Pt 2):375–461.
13. Samanek M, Slavik Z et al. Pediatr Cardiol 1989; 10(4):205–211.
14. Samanek M, Voriskova M. Pediatr Cardiol 1999; 20(6):411–417.
15. Hoffman JI, Kaplan S. J Am Coll Cardiol 2002; 39(12):1890–1900.

16. Goetzova J, Benesova D. Cor Vasa 1981; 23(1): 8–13.
17. Bolisetty S, Daftary A et al. Med J Aust 2004; 180(12):614–617.
18. Dorfman AT, Marino BS et al. Pediatr Crit Care Med 2008; 9(2):193–202.
19. Rothman A. Curr Probl Pediatr 1998; 28(2):33–60.
20. Tawes RL Jr, Aberdeen E et al. Circulation 1969; 39(5 Suppl 1):I173–I184.
21. Miettinen OS, Reiner ML et al. Br Heart J 1970; 32(1):103–107.
22. Cheatham JE Jr, Williams GR et al. Am J Surg 1979; 138(6):889–893.
23. Liberthson RR, Pennington DG et al. Am J Cardiol 1979; 43(4):835–840.
24. Ou P, Celermajer DS et al. J Am Coll Cardiol 2007; 49(8):883–890.
25. Kish GF, Tenekjian VK et al. Am Surg 1981; 47(1):26–30.
26. Bobby JJ, Emami JM et al. Br Heart J 1991; 65(5):271–276.
27. Koller M, Rothlin M et al. Eur Heart J 1987; 8(7):670–679.
28. Toro-Salazar OH, Steinberger J et al. Am J Cardiol 2002; 89(5):541–547.
29. Stewart AB, Ahmed R et al. Br Heart J 1993; 69(1):65–70.
30. Kappetein AP, Zwinderman AH et al. J Thorac Cardiovasc Surg 1994; 107(1):87–95.
31. Demircin M, Arsan S et al. J Cardiovasc Surg (Torino) 1995; 36(5):459–464.
32. Becker AE, Becker MJ et al. Circulation 1970; 41(6):1067–1075.
33. Tawes RL Jr, Berry CL et al. Br Heart J 1969; 31(1):127–128.
34. Sehested J. Br Heart J 1982; 47(6):619–620.
35. Beekman RH, Robinow M. Am J Cardiol 1985; 56(12):818–819.
36. Loffredo CA, Chokkalingam A et al. Am J Med Genet A 2004; 124A(3):225–230.
37. Wessels MW, Berger RM et al. Am J Med Genet A 2005; 134A(2):171–179.
38. Bertolini A, Pelizza A et al. J Cardiovasc Surg (Torino) 1987; 28(3):301–312.
39. Hartyanszky IL, Lozsadi K et al. Eur J Cardiothorac Surg 1989; 3(3):250–254.
40. Rivilla F, Utrilla JG et al. Z Kinderchir 1989; 44(4):199–202.
41. Chun K, Colombani PM et al. Ann Thorac Surg 1992; 53(4):597–602; discussion 602–603.
42. van Son JA, Julsrud PR et al. Mayo Clin Proc 1993; 68(11):1056–1063.
43. Kocis KC, Midgley FM et al. Pediatr Cardiol 1997; 18(2):127–132.
44. Woods RK, Sharp RJ et al. Ann Thorac Surg 2001; 72(2):434–438; discussion 438–439.
45. Backer CL, Mavroudis C et al. J Thorac Cardiovasc Surg 2005; 129(6):1339–1347.
46. Turner A, Gavel G et al. Eur J Pediatr 2005; 164(5):266–270.
47. McLaughlin RB Jr, Wetmore RF et al. Laryngoscope 1999; 109(2 Pt 1):312–319.
48. Anand R, Dooley KJ et al. Pediatr Cardiol 1994; 15(2):58–61.
49. Shanmugam G, Macarthur K et al. Asian Cardiovasc Thorac Ann 2005; 13(1):4–10.
50. Lee EY, Zurakowski D et al. J Thorac Imaging 2008; 23(4):258–265.
51. Backer CL, Idriss FS et al. J Thorac Cardiovasc Surg 1992; 103(4):683–691.
52. Horvath P, Hucin B et al. Eur J Cardiothorac Surg 1992; 6(7):366–371; discussion 371.
53. Chen SJ, Lee WJ et al. Ann Thorac Surg 2007; 84(5): 1645–1650.
54. Oshima Y, Yamaguchi M et al. Ann Thorac Surg 2008; 86(4):1334–1338.
55. McElhinney DB, McDonald-McGinn D et al. Pediatrics 2001; 108(6):E104.
56. Mendelsohn AM, Banerjee A et al. Cathet Cardiovasc Diagn 1997; 42(1):26–30.
57. Therrien J, Thorne SA et al. J Am Coll Cardiol 2000; 35(4):997–1002.
58. Glancy DL, Morrow AG et al. Am J Cardiol 1983; 51(3):537–551.
59. Rahaila E et al. Clinical Physiol 2001; 21(1): 100–104.
60. Park MK et al. Pediatrics 1993; 91: 761–765.
61. Sebening C, Jakob H et al. Thorac Cardiovasc Surg 2000; 48(3):164–174.
62. Shah RK, Mora BN et al. Int J Pediatr Otorhinolaryngol 2007; 71(1):57–62.
63. Campbell M. Br Heart J 1970; 32(5): 633–640.
64. Brouwer RM, Erasmus ME et al. J Thorac Cardiovasc Surg 1994; 108(3):525–531.
65. Sorland SJ, Rostad H et al. Acta Paediatr Scand 1980; 69(1):113–118.
66. Williams WG, Shindo G et al. J Thorac Cardiovasc Surg 1980; 79(4):603–608.
67. Rostad H, Abdelnoor M et al. J Cardiovasc Surg (Torino) 1989; 30(6):885–890.
68. Van Son JA, Falk V et al. J Card Surg 1997; 12(3):139–146.
69. Nanton MA, Olley PM. Am J Cardiol 1976; 37(5):769–772.
70. Cohen M, Fuster V et al. Circulation 1989; 80(4):840–845.
71. Ming Z, Yumin Z et al. J Cardiovasc Magn Reson 2006; 8(5):747–753.
72. Smallhorn JF, Huhta JC et al. Br Heart J 1983; 50(4):349–361.

73. Huhta JC, Gutgesell HP et al. Circulation 1984; 70(3):417–424.
74. Nihoyannopoulos P, Karas S et al. J Am Coll Cardiol 1987; 10(5):1072–1077.
75. Dodge-Khatami A, Ott S et al. Ann Thorac Surg 2005; 80(5):1652–1657.
76. Nielsen JC, Powell AJ et al. Circulation 2005; 111(5):622–628.
77. Hu XH, Huang JY et al. Pediatr Cardiol 2008; 29(4):726–731.
78. Lillehei CW, Colan S. J Pediatr Surg 1992; 27(8):1118–1120; discussion 1120–1121.
79. Eichhorn J, Fink C et al. Z Kardiol 2004; 93(3):201–208.
80. Kersting-Sommerhoff BA, Sechtem UP et al. Am J Roentgenol 1987; 149(1):9–13.
81. Greil GF, Kramer U et al. Pediatr Radiol 2005; 35(4):396–401.
82. Newman B, Meza MP et al. Pediatr Radiol 1996; 26(9):661–668.

26

Imaging Evaluation of Mediastinal Masses in Infants and Children

Edward Y. Lee

Issues

I. What are the clinical findings that raise suspicion for possible mediastinal masses in infants and children?
II. What is the diagnostic performance of the major methods to image infants and children with mediastinal masses?
III. Which imaging approach is most appropriate in differentiating normal thymus from abnormal anterior mediastinal masses in infants?
IV. Which imaging modality is best equipped to evaluate anterior mediastinal masses in infants and children?
V. Which imaging modality is most appropriate for evaluating middle mediastinal masses in infants and children?
VI. What is the recommended imaging approach for evaluating neurogenic tumors in the posterior mediastinum in infants and children?
VII. What is the role of PET in the management of childhood lymphomas?

Key Points

- The most common chest masses are located within the mediastinum in infants and children. Approximately 80% of mediastinal masses consist of malignant lymphoma, benign thymic enlargement, teratomas, foregut cysts, and neurogenic tumors in the pediatric population (moderate evidence).
- Mediastinal masses in the pediatric population are often asymptomatic. However, infants and children may also present with clinical symptoms characteristic of a particular type of mediastinal mass (limited to moderate evidence).

E.Y. Lee (✉)
Department of Radiology, Children's Hospital Boston, Harvard Medical School, Boston, MA 02115, USA
e-mail: edward.lee@childrens.harvard.edu

L.S. Medina et al. (eds.), *Evidence-Based Imaging in Pediatrics*,
DOI 10.1007/978-1-4419-0922-0_26,

- Mediastinal masses are typically detected and localized on frontal and lateral chest radiographs, the initial imaging modality of choice. Further evaluation can be performed with ultrasound, CT, or MRI depending on a combination of clinical presentation, age of patient, and location of the mass (i.e., anterior, middle, or posterior mediastinum) (moderate evidence).
- In infants, prominent but normal thymus can be differentiated from neoplasm or other masses by ultrasound after initial evaluation with chest radiographs (limited evidence).
- CT and MRI have similar sensitivity for further evaluation of a mediastinal mass. While CT is preferable to MRI for evaluating lung masses and calcification in a mass, MRI is preferable to CT for evaluating chest wall involvement (limited to moderate evidence).
- In evaluating mediastinal vascular anomalies presenting as middle mediastinal masses in pediatric population, both CT angiography (CTA) and MR angiography (MRA) are excellent diagnostic imaging tests (moderate evidence).
- Magnetic resonance imaging (MRI) is the preferred test in evaluating posterior mediastinal masses since most are neurogenic and have possible intraspinal extension (limited evidence).
- PET is useful in the initial staging, monitoring interim treatment response, and reassessment after completed treatment in pediatric patients with lymphoma (moderate evidence).

Definition and Pathophysiology

The mediastinum is defined anatomically as the portion of the body within the thorax located between the pleural spaces (1–10). It is bordered by the thoracic inlet superiorly, the diaphragm inferiorly, the sternum anteriorly, and the vertebral column posteriorly. With the exception of the lungs, the mediastinum contains all of the organs and tissues within the chest including the thymus gland, the chest portion of the trachea and esophagus, the great vessels, the heart, lymph nodes, fat, and nerves (1–10). Within each of these organs and structures, mediastinal masses in infants and children can arise from a wide variety of conditions including congenital anomalies, benign and malignant neoplasms, infection, which often present complex diagnostic and therapeutic dilemmas (6, 11–24). In both infants and children, mediastinal masses are associated with variable signs and symptoms depending on the underlying primary pathologic condition and functional compromise of both structures within the mediastinum and the lung (5, 11, 14, 22, 25).

In order to narrow the differential diagnosis, the precise location of a suspected mediastinal mass must be identified. The mediastinum is traditionally divided into three compartments on the lateral chest radiograph: anterior, middle, and posterior (Fig. 26.1) (1, 2, 4, 7, 8, 10). The *anterior mediastinal compartment* is the space bordered anteriorly by the sternum and posteriorly by the pericardium. The predominant anatomic structures and tissues located within the anterior mediastinum are the thymus gland, anterior (prevascular) lymph nodes, and fat. Although experts differ over the exact boundaries between the middle and posterior mediastinal compartments, it is generally agreed that the *middle mediastinal compartment* is the space between the anterior border of the pericardium and an imaginary line drawn 1 cm posteriorly to the anterior border of the vertebral bodies (2). The middle mediastinal compartment contains the heart, great vessels, tracheobronchial tree and esophagus (both are of embryonic foregut origin), lymph nodes, fat, and nerves. The *posterior mediastinal compartment* is the space bordered anteriorly by an imaginary line drawn

1 cm posterior to the anterior border of the vertebral bodies and posteriorly by the posterior paravertebral gutters. The posterior mediastinal compartment contains the paravertebral autonomic (sympathetic and parasympathetic) nerve chain and intercostal nerves, fat, lymph nodes, as well as the thoracic vertebral column.

Epidemiology

The mediastinum is the most common location of chest masses in infants and children (4). In infants (0–2 years), mediastinal masses are located within the anterior mediastinum in 24%, middle mediastinum in 12%, and posterior mediastinum in 49% as presented in Table 26.1 (26). While thymic hyperplasia (18%) is the most common anterior mediastinal mass, neuroblastoma (39%) is the most common posterior mediastinal mass in infants (26). Middle mediastinal masses are predominantly due to duplication cysts (such as bronchogenic or esophageal duplication cyst).

In contrast, mediastinal masses are found most frequently within the anterior mediastinum in children aged 2–18 years accounting for 46% of 508 children with mediastinal masses as presented in (Table 26.2) (4, 25, 27). Of the anterior mediastinal masses, malignant lymphomas, teratomas, and benign thymic enlargement accounted for the majority (85%). Of the 508 pediatric mediastinal masses, approximately 20% were located within the middle mediastinum (Table 26.2). Developmental malformations of the embryonic foregut (such as bronchogenic cyst, esophageal duplication cyst) or lymphadenopathy constituted the majority of middle mediastinal masses (Table 26.2). Approximately 34% of pediatric mediastinal masses were posterior, of which 88% were of neurogenic origin (Table 26.2) (4, 25, 27).

In infants and children, the incidence of different types of mediastinal masses largely depends on the age of the patients. For example, thymic hyperplasia is the most common anterior mediastinal masses (18%) in infants but rarely present in children unless related to prior chemotherapy treatment (i.e., rebound thymic hyperplasia). Lymphoma (with incidence of 1.6 per 100,000 among children living in the United States) is the most common anterior mediastinal mass in older children; however, it rarely occurs in infants or children under 5 years of age (28). Although definite differentiation among the different neurogenic tumor types in infants and children is not possible on the basis of imaging appearance, age of the patient is often the most helpful information. Neuroblastoma is typically seen in infants and younger children (<5 years), ganglioneuroblastoma often occurs in children between 5 and 10 years of age, and ganglioneuroma is typically present in older children and adolescents (29).

Overall Cost to Society

No discussion was found in the medical literature on the overall cost to society from the diagnosis and management of mediastinal masses in infants and children. Although different methods of diagnosing mediastinal masses are evaluated and reviewed (4–10, 13, 23, 30–40), the cost-effectiveness of incorporating imaging strategies in the management of mediastinal masses in infants and children has not been specifically addressed.

Goals

The goals of diagnostic imaging in evaluating mediastinal masses in infants and children include the following:

1) identifying the mass and determining its location within the anterior, middle, or posterior mediastinum;
2) characterizing the mass;
3) delineating its extent and relationship to vascular structures, spinal canal, and chest wall;
4) providing appropriate differential diagnostic considerations and most likely diagnosis; and
5) developing a plan for further patient management.

To accomplish these goals, it is imperative first to understand the various imaging features of mediastinal masses on chest radiographs and second to determine which imaging modality (or modalities) will aid in reaching a definitive diagnosis. This, in turn, will

1) prevent unnecessary additional imaging studies associated with exposure to ionizing radiation (i.e., plain radiographs and CT—a particularly important consideration in imaging a pediatric population);
2) minimize potential side effects from the administration of intravenous contrast material and sedation associated with cross-sectional imaging (CT and MRI); and, most importantly,
3) expedite the delivery of appropriate treatment options that result in improved patient outcomes.

Methodology

The author performed a MEDLINE search using PubMed (National Library of Medicine, Bethesda, MD) for data relevant to the diagnostic performance and accuracy of both clinical and radiographic examinations of infants and children with mediastinal masses. The diagnostic performance of the clinical examination (i.e., history and physical exam) was based on a systematic literature review performed in MEDLINE (National Library of Medicine, Bethesda, MD) during the years from 1966 to June 2008. The clinical examination search strategy used the following key statements and words: *mediastinal mass, symptoms, infants*, and *children* as well as combinations of these search strings. The review of the current diagnostic imaging literature was done with MEDLINE covering the years from 1966 to June 2008. The search strategy used the following key statements and words: *mediastinal mass, infants, children, plain radiographs, ultrasound, CT or computed tomography, MRI or magnetic resonance imaging, PET or positron emission tomography*, and *imaging* as well as combinations of these search strings. Next, mediastinal masses were divided into three main categories: *anterior mediastinum, middle mediastinum*, and *posterior mediastinum*. A further search was performed using each of these three categories or combinations thereof with key statements and words as stated previously. Following a preliminary review of titles and abstracts, the author identified the most relevant publications and reviewed these in full along with additional articles distilled from their respective bibliographies. This chapter was limited to human studies and English language literature.

Discussion of Issues

I. What Are the Clinical Findings that Raise Suspicion for Possible Mediastinal Masses in Infants and Children?

Summary of Evidence: Approximately 50% of pediatric patients with mediastinal masses are asymptomatic (7, 41–43). The clinical presentations of remaining symptomatic pediatric patients with mediastinal masses can be non-specific. However, in some infants and children with mediastinal masses who present with specific symptoms, imaging decisions based on individual clinical presentations may lead to timely, accurate diagnoses and proper patient management (limited to moderate evidence).

Supporting Evidence: In infants and children with mediastinal masses, clinical findings vary widely depending on the specific underlying diagnosis and degree of involvement of adjacent mediastinal structures. Close to half of affected patients ultimately diagnosed with mediastinal masses are clinically asymptomatic, especially posterior ones (7, 41–43). The remaining patients with mediastinal masses usually present with symptoms. Harris et al. reported that pain (53%), dyspnea (17%), malaise or weakness (10%), and chest pressure (3%) are some of the common symptoms in their study consisting of 30 pediatric and adult patients with mediastinal masses (44).

Although the majority of symptoms in children with mediastinal masses are somewhat non-specific, certain symptoms can often suggest specific mediastinal masses in symptomatic pediatric patients (limited to moderate evidence) (7, 41–43). For example, respiratory symptoms such as wheeze, cough, and dyspnea indicate possible airway compromise due to extrinsic compression from an anterior mediastinal mass (e.g., lymphoma); congenital anomalies of the heart or great vessels (e.g., vascular rings and slings) in the middle mediastinum; or developmental malformations involving tracheobronchial tree and esophagus

in the middle mediastinum (e.g., duplication cysts) (limited to moderate evidence) (7, 11, 20–22, 45). Separate chapters (Chapters 24 and 25) will discuss appropriate imaging of congenital heart disease and vascular rings and slings.

Infants and children with neurogenic tumor (virtually all neuroblastoma or ganglioneuroblastoma in the pediatric population) in the posterior mediastinum are often asymptomatic and detected incidentally on chest radiographs or other imaging studies performed for other reasons. However, they can also present with

1) clinical signs of disseminated disease including irritability, weight loss, fever, and/or bone pain;
2) more specific symptoms such as opsoclonus–myoclonus syndrome, which involves ataxia with involuntary muscle and eye movements; or, even less commonly,
3) Horner's syndrome, which is characterized by ptosis, myosis, and anhydrosis secondary to thoracic apical or cervical masses (limited to moderate evidence) (42, 46–50).

In addition, spinal canal invasion by neurogenic tumor in the posterior mediastinum can present with symptoms of cord compression. In a retrospective study consisting of 66 infants and children with neurogenic tumors of the thorax, Ribet and Cardot reported that approximately 12% of thoracic neurogenic tumors in infants and children are associated with cord compression (limited to moderate evidence) (51).

II. What Is the Diagnostic Performance of the Major Methods to Image Infants and Children with Mediastinal Masses?

Summary of Evidence: When evaluating a mediastinal mass, the two-view chest radiographs (posteroanterior and lateral views) are usually the first diagnostic imaging choice due to its widespread availability, relative low cost, and easy acquisition (moderate to strong evidence) (3, 4, 7, 9, 10, 42). Chest radiographs are very sensitive for the detection of mediastinal masses. However, they are rarely specific. To reach a definitive diagnosis, additional imaging (i.e., ultrasound, CT, or MRI) is almost always required (moderate evidence). Ultrasound is generally used to confirm prominent, but normal thymus in infants. Cross-sectional imaging such as CT or MRI can be used to evaluate the remaining mediastinal masses in the pediatric population. CT is often more readily available and rarely requires sedation, particularly with state-of-the-art multi-detector CT (MDCT). Although both CT and MRI are helpful in evaluating mediastinal masses, MRI has advantages over CT in

1) avoidance of ionizing radiation exposure,
2) evaluating posterior mediastinal neurogenic tumor with possible intraspinal extension, and
3) as a problem-solving tool for identifying foregut duplication cysts with high attenuation on non-contrast CT (limited evidence).

CT angiography (CTA) and MR angiography (MRA) have shown utility in evaluating mediastinal masses due to underlying mediastinal vascular anomalies such as vascular rings and slings (moderate evidence). In children with lymphoma, PET is currently used for staging, early response assessment during treatment, and response assessment after completion of therapy. Diagnostic performance of imaging in infants and children with mediastinal masses is presented in Table 26.3.

Supporting Evidence

Chest Radiographs

Mediastinal masses in infants and children are typically first detected on chest radiographs with a relatively high degree of accuracy, depending on the size and location of a given mass. In a retrospective evaluation of 30 pediatric and adult patients with mediastinal masses, Harris et al. showed that chest radiographs (posteroanterior and lateral views) were able to detect mediastinal masses in 29 (97%) of the 30 patients studied (limited evidence) (44). In a larger retrospective study of 105 children and adults, Adegboye et al. reported that all mediastinal masses were initially identified on chest radiographs, supporting the utility of chest radiographs as an initial imaging study choice for evaluating mediastinal masses (limited to moderate evidence) (52). However, in another study of 128 patients aimed at

predicting the pathologic diagnosis of anterior mediastinal masses, Ahn et al. reported only a 36% accuracy in defining the type of mass (limited to moderate evidence) (53). These studies demonstrate that while chest radiographs are useful in detecting mediastinal masses, they are limited in their ability to establish a specific diagnosis; hence, further imaging by ultrasound, CT, or MR is typically needed to further characterize a given mediastinal mass and narrow the differential diagnosis (moderate evidence).

Ultrasound (US)

The utility of ultrasound in diagnosing mediastinal masses may lie somewhere between the established role of chest radiographs and that of cross-sectional imaging studies such as CT and MRI, particularly in infants younger than 12 months. Infants have unossified sternal and costal cartilages, providing acoustic windows large enough to permit evaluation of anterior mediastinal structures and a relatively large thymus (4, 54–57).

Although ultrasound is somewhat operator dependent, it offers several advantages in evaluating anterior mediastinal masses in infants and young children, especially when compared to the more expensive cross-sectional imaging modalities, CT and MRI. Unlike CT and MRI, ultrasound provides *real-time* evaluation and it can be performed portably, *without* sedating the patient, and *without* inserting intravenous angiocatheters for contrast administration. Most importantly, US can be performed *without* the potentially harmful effects of ionizing radiation that is delivered by CT.

In infants initially diagnosed with a widening of the superior mediastinum on chest radiographs, ultrasound may aid in differentiating the normal thymus from a true mediastinal mass, thus obviating the need for further evaluation by CT or MRI, as detailed under Issue III below. However, in evaluating middle and posterior mediastinal compartments, and in evaluating older children (>8 years old) whose acoustic windows are limited, it is generally believed that ultrasound has limited value in assessing these mediastinal masses; hence, cross-sectional imaging by CT or MRI is typically required following initial evaluation on chest radiographs where suspected mediastinal masses have been identified.

Computed Tomography (CT)

CT plays an important role in further characterizing mediastinal masses seen on chest radiographs in infants and children, particularly masses located in the anterior and middle mediastinal compartments. Ginaldi et al. demonstrated that CT provides the most consistently accurate information when they compared CT to chest radiographs in 37 pediatric patients with various chest masses (limited to moderate evidence) (58). In a study of mediastinal abnormalities in 23 pediatric patients, Siegel et al. showed that in 82% of the patients studied, CT provided more diagnostic information than chest radiographs alone (limited to moderate evidence) (30). Specifically, CT was useful in differentiating abnormal masses from benign processes (e.g., normal developmental anomalies) and in demonstrating the full extent of a malignant tumor (30). The additional information generated by CT, in turn, affected the clinical management of 65% of study patients (30). The superior diagnostic utility of CT is also supported by Graeber et al., whose retrospective review of 42 patients with mediastinal masses demonstrated that in 88% of cases, CT accurately predicted the nature, size, location, and involvement of other organs by mediastinal masses (limited to moderate evidence) (59).

With recent advances in computed tomography technology such as multi-detector row CT (MDCT), CT has assumed an expanded role in evaluating mediastinal masses in the pediatric population. Indeed, MDCT can now offer increased temporal and spatial resolution, faster scan times, decreased sedation rate, and sophisticated post-processing techniques including multiplanar reformations and 3D reconstructions (60–62). With respect to mediastinal vascular imaging, the imaging capability of CT angiography (CTA) is presently equivalent or superior to conventional angiography, making rapid and accurate diagnoses of mediastinal vascular anomalies and associated central airway anomalies/abnormalities possible. For example, in a study of 14 children and young adults by Lee et al., CT was shown to have >94% accuracy in evaluating mediastinal aortic

vascular anomalies with multiplanar reformations (i.e., coronal and sagittal reformations) and 3D reconstructions (limited evidence) (63). However, given the potentially harmful effects of ionizing radiation associated with CT, this modality should be used only when necessary in the pediatric population, especially among patients for whom repeated imaging studies may be required (e.g., children with neoplasm).

Magnetic Resonance Imaging (MRI)

Due to its superior ability to characterize soft tissues in exquisite detail, but *without* the effects of ionizing radiation, MRI has become an important diagnostic imaging modality for evaluating mediastinal masses in the pediatric population. The utility of MRI in evaluating mediastinal masses has been well established (31, 64, 65). In a retrospective study consisted of a total 75 pediatric and adult patients with mediastinal masses, von Schulthess et al. demonstrated the utility of MR in evaluating mediastinal masses, particularly with respect to (1) confirming presence, (2) delineating morphology, and (3) depicting encroachment or displacement of adjacent blood vessels or airways within the mediastinum (moderate evidence) (31). In a study of 13 pediatric patients with posterior mediastinal masses, Siegel et al. reported the ability of MRI to accurately evaluate tumors and any associated intraspinal extension—preoperative findings that are essential for successful surgical intervention and patient management (limited evidence) (32).

MR is also useful in confirming the cystic nature of some mediastinal masses, which may appear solid on CT due to their high proteinaceous content (e.g., bronchogenic and esophageal duplication cysts) (limited evidence) (2, 9, 23, 34, 66–68). Lastly, MRI, when combined with magnetic resonance angiography (MRA), is useful in identifying mediastinal vascular anomalies or abnormalities presenting as mediastinal masses (limited to moderate evidence) (69–72). However, MRI, particularly when compared to other cross-sectional imaging modalities such as CT, has several disadvantages including relatively high cost, more image artifacts due to cardiac and respiratory motion, poor spatial resolution, limited ability to demonstrate calcification, and the need for greater sedation in children.

Positron Emission Tomography (PET)

PET is a non-invasive functional imaging modality using the 2-fluoro-2-deoxy-(18 fluorine)-D-glucose (^{18}FDG), which has been shown a great promise in evaluating pediatric patients with lymphoma (73–81). Although other imaging modalities (e.g., chest radiographs, CT, and MRI) are more commonly used for assessing the extent of lymphoma involvement in pediatric patients, they have been limited for the following:

1. detecting tumor involvement in normal-sized lymph nodes;
2. discriminating between fibrous scar and necrotic tissue from active tumor in residual masses after treatment; and
3. evaluating disease involvement in extra-nodal sites (e.g., liver or bone marrow) (73, 81–85).

In the pediatric population with lymphoma (particularly Hodgkin's lymphoma), PET is currently used for staging, early response assessment during treatment, and response assessment after completion of therapy (73–85). Furthermore, PET (with its high sensitivity for detecting the metabolic activity of actively growing cancer cells) and CT (with its ability to visualize detailed anatomic structures) can be "fused" together. This hybrid PET/CT imaging can provide complete information on cancer location and metabolic activity (86, 87).

III. Which Imaging Approach Is Most Appropriate in Differentiating Normal Thymus from Abnormal Anterior Mediastinal Masses in Infants?

Summary of Evidence: In infants, typically younger than 12 months, a normal thymus can vary widely in appearance (i.e., size and symmetry). Thus, it is sometimes confused with a mediastinal mass on chest radiographs. Under these circumstances, ultrasound can be used to identify a normal, albeit large or asymmetric, thymus, thereby obviating the need for further imaging, biopsies, and/or surgery

(limited evidence). However, in cases of ectopic thymic tissue in the neck, a correct diagnosis is usually made by evaluating its connection and similarity to normal thymus with CT or MR in multiple planes. MR is preferable in infants and children due to both the ease of distinguishing the signal characteristics of the thymus and avoidance of ionizing radiation exposure (limited evidence).

Supporting Evidence: In infants, the thymus is quite large in comparison to other structures in the chest. As the child develops, the thymus becomes smaller, reaching its triangular "adult" configuration generally by age 5 (88, 89). As a general rule, the thymus should not be visible on a chest radiograph after age 10 years and on CT after age 40 years. Occasionally, the relatively large thymus or its asymmetric or variable shape in infants is mistaken for a mediastinal mass on chest radiographs. Further complicating the diagnosis, the thymus can also assume an ectopic location due to interrupted migration from the brachial clefts in the neck during thymic embryogenesis. In an autopsy study of 3,236 children, Bale and Sotelo-Avila reported that the incidence of abnormally positioned thymic tissue was 1% (moderate evidence) (90).

In infants and young children with an acoustic window large enough to permit evaluation of the thymus, an ultrasound study can usually establish whether the structure initially identified on chest radiographs is either a normal thymus or a true anterior mediastinal mass. In a prospective evaluation of the thymus in 140 infants and children (newborn to 8 years old), Liang and Huang reported that normal thymus was easily and clearly visualized with ultrasound in the majority (95%) of cases (moderate evidence) (91). Likewise, Adam and Ignotus's prospective ultrasound study of the thymus in healthy children showed visualization of the normal thymus in 47 of 50 (94%) children ranging in age from 2 to 8 years (limited to moderate evidence) (92). Normal thymic features on ultrasound include (1) homogeneous echotexture, (2) mild hypoechogenicity relative to adjacent thyroid gland or liver, (3) smooth and well-marginated border due to a fibrous outer capsule, and (4) a pliable organ that moves with respiration and cardiac pulsation (54, 93).

Although confirmation of normal thymus on ultrasound generally obviates the need for further imaging studies in children, when the normal thymus cannot be clearly visualized on ultrasound, or when an aberrant thymus is suspected, further imaging with CT or MRI may provide a definite diagnosis. The normal thymus is located within the anterior mediastinum; however, it can extend into the suprasternal neck region, as well as into the middle and posterior mediastinum as one contiguous, lobulated, and pliable structure (i.e., an ectopic location) (94–100). Under these circumstances, the thymus can be difficult to evaluate comprehensively on ultrasound. However, cross-sectional imaging such as CT (particularly with the recent introduction of MDCT) or MRI can depict the continuity between ectopically positioned and normally positioned thymic tissues with great certainty (limited evidence) (101–103). Because of its superior soft-tissue characterization and lack of ionizing radiation, MRI is ideally suited for assessing aberrant thymus in infants and children, even though it is more expensive than CT on a *per study* basis, requires sedation in most children under 6 years, and is less available in smaller hospitals and healthcare facilities.

IV. Which Imaging Modality Is Best Equipped to Evaluate Anterior Mediastinal Masses in Infants and Children?

Summary of Evidence: In an effort to make a correct diagnosis of anterior mediastinal masses in a pediatric population, both CT and MRI are used to further characterize a mass (moderate evidence). Although both CT and MRI are equally highly sensitive in evaluating lymphoma and germ cell tumor overall, CT is superior to MRI in assessing lung parenchymal involvement and associated calcification (limited to moderate evidence) (38). MRI, on the other hand, is superior to CT in evaluating chest wall involvement although image

quality is sometimes degraded by the motion and may be a disadvantage of MRI (limited to moderate evidence) (104). The current most common practice is using MDCT for characterizing anterior mediastinal masses in children beyond infancy with CT protocol following the ALARA (as low as reasonably achievable) concept.

Supporting Evidence: Once a mass is localized within the anterior mediastinum on chest radiographs, subsequent imaging is based on several factors including clinical presentation, patient age, and radiographic findings. As mentioned previously in the discussion of Issue III, ultrasound is the ideal modality for distinguishing a normal thymus in infants from a suspected mediastinal mass (54, 91–93). In evaluating germ cell tumor as well as lymphoma, the most common anterior mediastinal malignancy in children, CT is superior to MRI in evaluating lung parenchymal involvement and associated calcification (38). In a study of 45 patients with mediastinal masses, Batra et al. compared CT and MRI and concluded that while CT was superior for displaying calcification within a mass in eight patients and for demonstrating associated lung abnormality in four patients, MRI and CT were equally effective in demonstrating mediastinal lesions (limited to moderate evidence) (38). On the other hand, MRI is more sensitive than CT in assessing chest wall involvement as demonstrated by Bergin et al. in their retrospective study comparing CT and MRI in 28 patients with newly diagnosed or recurrent thoracic lymphoma for chest wall involvement (limited to moderate evidence) (104).

V. Which Imaging Modality Is Most Appropriate for Evaluating Middle Mediastinal Masses in Infants and Children?

Summary of Evidence: Once a suspected mass is localized within the middle mediastinum on chest radiographs, further evaluation with cross-sectional imaging such as CT or MRI is typically required. Although both CT and MRI are useful in evaluating middle mediastinal masses, in circumstances where foregut duplication cysts (which are sometimes solid in appearance on CT due to their high proteinaceous content) must be differentiated from solid mediastinal masses (i.e., primary neoplasms and lymphadenopathy), MRI can be an effective problem-solving imaging tool (limited evidence) (2, 9, 23, 34, 66–68). In cases of mediastinal vascular anomalies, both CT angiography and MR angiography are excellent diagnostic imaging choices (moderate evidence) (63, 105–107).

Supporting Evidence: The middle mediastinum is the least common location of mediastinal masses accounting for approximately 12.1% (in infants) and 20% (in children) of the total including adenopathy (secondary to infection, primary neoplasm [i.e., lymphoma], and metastatic disease) and foregut duplication cysts (i.e., bronchogenic cysts, esophageal duplication cysts, and neurenteric cysts) (4, 25, 27). Once a mass is detected on chest radiographs, either CT or MRI can be used to confirm diagnosis and further characterize the mass. MRI can be used as a problem-solving tool for confirming the cystic nature of mediastinal masses (i.e., foregut duplication cysts). On MRI images, these lesions typically show low to intermediate MR signal intensity on T1-weighted images and markedly increased signal intensity on T2-weighted images with lack of central contrast enhancement—imaging characteristics that are useful in differentiating solid-appearing cysts on CT from solid neoplasms or lymphadenopathy in the middle mediastinum (2, 9, 23, 34, 66–68). Murayama et al. evaluated and characterized the MR signal intensity patterns of 26 cystic mediastinal masses, demonstrating that varying T1-weighted MR signal intensity reflects the composition of the intracystic fluid, which is helpful in confirming and differentiating cystic mediastinal masses (limited evidence) (68).

Vascular structures within the middle mediastinum can also present as middle mediastinal masses. Unlike acquired vascular masses (e.g., aneurysms) in adults, middle mediastinal vascular masses in infants and children are typically congenital anomalies of the great

vessels such as vascular rings and slings (9, 10, 21, 22, 70–72, 108). In evaluating mediastinal vascular anomalies of childhood, cross-sectional imaging by CT or MRI with vascular imaging protocols (i.e., CTA and MRA) and 2D/3D image reconstructions are currently the preferred initial imaging tests. In a study consisting of 18 subjects with congenital aortic arch anomalies, Kersting-Sommerhoff et al. showed that MR can provide sufficient anatomic information for the effective, non-invasive evaluation of patients with congenital aortic arch anomalies (limited evidence) (105). In a recent study of 11 infants and children, Greil et al. established that non-invasive 3D MRI techniques such as 3D double-slab FISP MR angiography are effective (100% accuracy) in diagnosing vascular rings and slings in free-breathing infants and children without intravenous contrast agent or associated radiation exposure (limited evidence) (106). CT angiography protocol combined with 2D and 3D reconstructions has also proven useful in evaluating mediastinal vascular anomalies in infants and children. For example, in a study of 14 children and young adults, Lee et al. demonstrated improved diagnostic accuracy (96%) in evaluating mediastinal aortic vascular anomalies by utilizing 2D and 3D CT reconstructions (compared to axial CT images alone) (limited evidence) (63). Information obtained from CTA and MRA generally obviates the need for further imaging by conventional angiography, which, up until now, has been considered the "gold standard" in evaluating mediastinal vascular anomalies. In a recent study of 22 pediatric patients with mediastinal vascular anomalies (i.e., vascular rings and slings), Eichhorn et al. compared the diagnostic capability of conventional angiography, CTA, and MRA (correlated with intraoperative findings, when available) (107). Their findings suggest that CTA or MRA is equivalent to the diagnostic capability of conventional angiography (limited evidence). In addition, both CTA and MRA are more accurate than conventional angiography in detecting airway- and esophageal compression-associated mediastinal vascular anomalies (limited evidence) (107). They concluded that CTA and MRA are non-invasive, accurate, and robust techniques for preoperative evaluation of mediastinal vascular anomalies (107).

VI. What Is the Recommended Imaging Modality for Evaluating Neurogenic Tumors in the Posterior Mediastinum in Infants and Children?

Summary of Evidence: Once neurogenic tumors in the posterior mediastinum are detected on chest radiographs, both CT and MRI can be used for confirming diagnosis, determining the extent of disease, and assessing changes after treatment (6–10, 24, 31–33, 37, 109). Moreover, because of its superior ability to detect concomitant intraspinal tumor extension, MRI is currently the single best imaging modality for evaluating neurogenic tumors originating in the posterior mediastinum (limited to moderate evidence) (32, 109).

Supporting Evidence: Posterior mediastinal masses account for approximately 34% of all mediastinal masses (4, 25, 27). Among posterior mediastinal masses, most are neurogenic in origin in both infants and children, arising from the nerve ganglion, nerve sheath, or other nervous tissue (4, 25, 27). Among neurogenic lesions, sympathetic chain ganglion cell tumors (i.e., neuroblastoma, ganglioneuroblastoma, and ganglioneuroma) predominate (4, 5, 9, 37, 42). Although differentiating posterior mediastinal sympathetic chain ganglion cell tumors from one another is challenging, age of patient is often helpful. While neuroblastoma and ganglioneuroblastoma occur in the first decade of life, ganglioneuromas are commonly seen in older children and adolescents (29).

Although plain radiographs occasionally show typical imaging characteristics of posterior mediastinal neurogenic tumors (i.e., smooth, well-marginated, and elongated paraspinal soft-tissue masses with speckled internal calcifications growing in a vertical direction [superior-to-inferior] often associated with posterior rib erosions) (9), further cross-sectional imaging by CT or MRI is generally required to confirm diagnosis, determine the extent of disease, and assess changes following treatment.

Until recently, CT has been utilized as the primary diagnostic imaging modality in

assessing patients with posterior mediastinal neurogenic tumors. In current best practice, however, MRI has supplanted CT in evaluating possible intraspinal extension that sometimes occurs when the primary neurogenic tumor spreads through the neural foramina and into the spinal canal. In a study consisting of 240 mediastinal neurogenic tumors, Akwari et al. reported that intraspinal extension can be seen in approximately 8% of patients with posterior mediastinal neurogenic tumors (moderate evidence) (110). Siegel et al. demonstrated that MR may be more helpful than CT in evaluating posterior mediastinal tumors because of the likelihood of intraspinal extension in a study of 18 children with mediastinal masses (limited evidence) (32). In a retrospective, multi-institutional investigation of thoracic neuroblastoma in 26 children, Slovis et al. also suggest that MR imaging is the optimal test for evaluating the extent of thoracic neuroblastoma, particularly for intraspinal extension (achieving 100% sensitivity in detecting intraspinal extension of thoracic neuroblastoma with MRI versus 88% sensitivity with CT) (limited to moderate evidence) (109).

VII. What Is the Role of PET in the Management of Childhood Lymphomas?

Summary of Evidence: PET is a non-invasive diagnostic imaging modality, complementary to conventional cross-sectional imaging (e.g., CT or MRI) in the initial staging of pediatric patients with newly diagnosed lymphoma (moderate evidence). There is moderate evidence that PET is more sensitive than cross-sectional imaging (e.g., CT or MRI) at disease detection (staging) in adults. The role of PET for monitoring treatment response in children with lymphoma is not yet clearly established; however, it will likely have an important role on interim patient management and outcome (limited to moderate evidence). PET is more accurate than other cross-sectional imaging modalities (e.g., CT or MRI) in the reassessment of children after complete treatment for lymphoma (moderate evidence).

Supporting Evidence: PET is a nuclear medicine imaging study, which can detect pairs of gamma rays emitted by a positron-emitting radionuclide (tracer) that is chemically incorporated into a biologically active molecule and then injected into the living subject. Three-dimensional or functional images of tracer concentration within the body can subsequently be produced by computer analysis and image reconstruction algorithm. PET, used as an initial diagnostic imaging modality, changed disease stage in up to 33% pediatric patients with lymphoma (74, 78, 111). Montravers et al. showed that PET in comparison to conventional imaging modalities (consisting of various imaging modalities but at least one CT study of the chest, abdomen, and pelvis) detected more disease sites, resulting in upstaging of disease in 50% of children with Hodgkin's and non-Hodgkin's lymphoma (limited evidence) (74). This finding was supported by another study performed by Hermann et al. who compared whole-body PET with CT in the initial staging of children with Hodgkin's lymphoma (78). They found that PET resulted in a change in disease stage in 28% and treatment modification in 22% (limited evidence) (78). Recently, Miller et al. also confirmed that the use of PET during diagnostic staging results in change in staging in approximately 33% of children with Hodgkin's and non-Hodgkin's lymphoma (limited to moderate evidence) (111). For evaluation of extra-nodal involvement (such as spleen, bone, and bone marrow) in children with lymphoma, PET is superior to conventional cross-sectional imaging modalities (limited to moderate evidence) (74, 78, 80, 112).

Currently, published studies related to the use of PET for evaluation of early treatment response in children with lymphoma are limited. However, there are several studies which showed promising results. Montravers and colleagues showed that residual activity (i.e., incomplete resolution) at previously known disease sites correlated with persistent viable disease in their PET study obtained during treatment of lymphoma in children (limited evidence) (74). This was further supported by Miller and colleagues who demonstrated an excellent prognostic ability of interim PET scan in children with lymphomas (111). In their study, they showed that 95% (19 out of 20

patients) who had a negative PET study during their chemotherapy were found to be disease free for an average period of 14.5 months (limited to moderate evidence) (111). In contrast, further progression of disease was seen in all three patients with interim positive PET study (111).

PET is a functional imaging modality that has a promising ability for tissue characterization (i.e., ability to discriminate between viable residual tumor and necrotic/fibrous scar tissue) in the residual mass at the end of treatment. Montavers et al. demonstrated the usefulness of PET as a reliable imaging modality of choice for assessing the nature of residual mass after treatment of lymphoma by showing 93% negative predictive value (limited evidence) (74). Their finding was subsequently supported by Edeline et al., who demonstrated 100% negative predictive value of PET in their prospective study consisting of 11 children with Hodgkin's lymphoma and negative PET (limited evidence) (113). Most recently, Hernandez-Pampaloni et al. showed similar sensitivity but higher specificity, positive predictive value, and negative predictive value with PET (78, 98, 94, and 90%, respectively) in comparison to CT (79, 88, 90, and 46%, respectively) in their study consisting of 24 children with histologically proven lymphomas (18 Hodgkin's and 6 non-Hodgkin's lymphomas) (limited to moderate evidence) (114).

Take Home Figures

What Are the Various Roles of the Principal Imaging Modalities in Evaluating Mediastinal Masses in Infants and Children?

Figure 26.1 presents the three compartments of mediastinum on the lateral chest radiograph.

The decision tree in Fig. 26.2 outlines the various roles of the four major imaging modalities in evaluating mediastinal masses in infants and children that are either clinically suspected or detected based on chest radiographs. Chest radiographs are the initial imaging modality of choice because of its widespread availability, low cost, and rapid acquisition. The choice of the next imaging modality is typically guided by a combination of clinical presentation, age of the patient, and location of the mass (i.e., anterior, middle, and posterior mediastinum) as viewed on chest radiographs.

For anterior mediastinal masses in infants, ultrasound can aid in confirming the diagnosis of normal thymus. In cases of aberrant thymus that cannot be definitely diagnosed with ultrasound in infants, CT or MRI can be subsequently used for further evaluation. In children, either CT or MRI can be used to evaluate an anterior mediastinal mass.

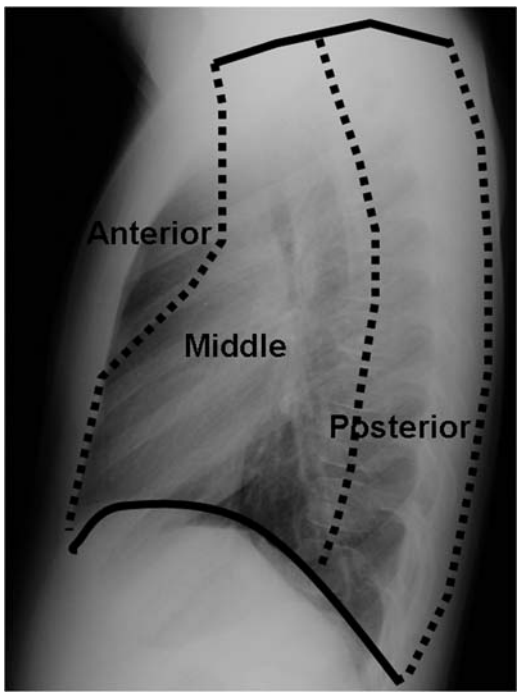

Figure 26.1. Three compartments of mediastinum on the lateral chest radiograph. The mediastinum is traditionally divided into three compartments on the lateral chest radiograph: anterior, middle, and posterior. The anterior mediastinal compartment is the space bordered anteriorly by the sternum and posteriorly by the pericardium. The middle mediastinal compartment is the space between the anterior border of the pericardium and an imaginary line drawn 1 cm posterior to the anterior border of the vertebral bodies. The posterior mediastinal compartment is the space bordered anteriorly by an imaginary line drawn 1 cm posterior to the anterior border of the vertebral bodies and posteriorly by the posterior paravertebral gutters. Anterior = anterior mediastinum. Middle = middle mediastinum. Posterior = posterior mediastinum.

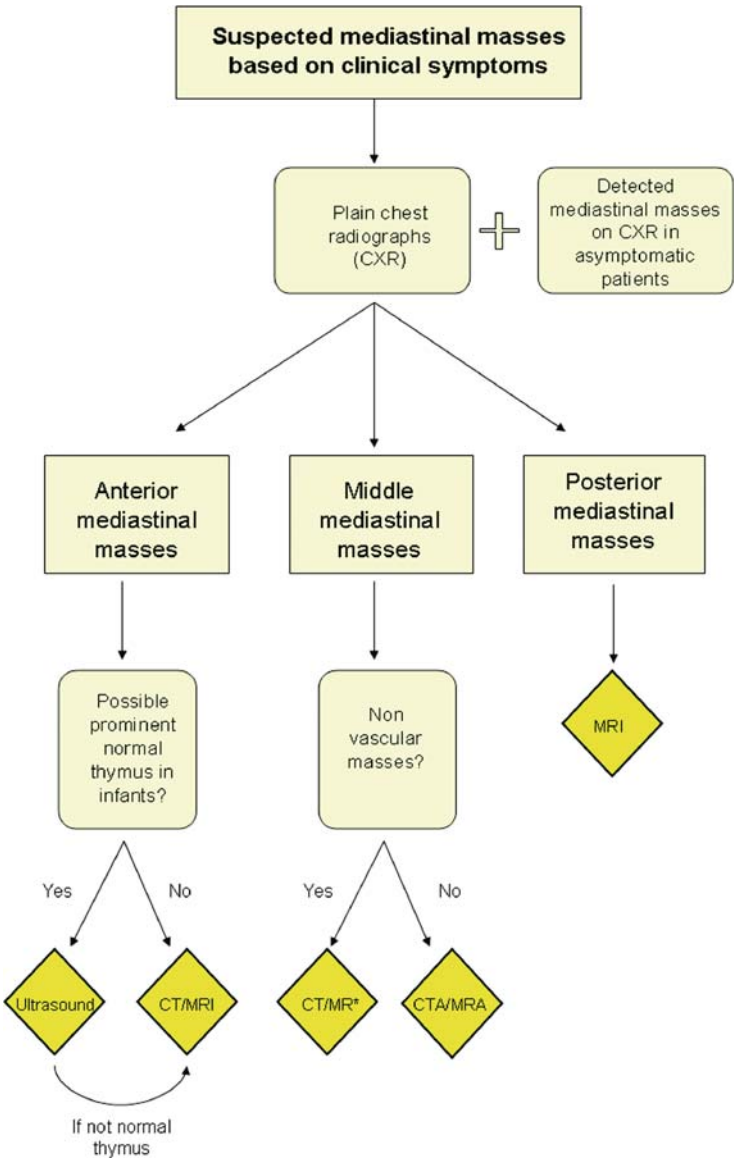

Figure 26.2. Algorithm for imaging mediastinal masses in infants and children. *Preferred as a problem-solving tool for evaluation of solid-appearing foregut duplication cysts on CT.

In infants and children whose middle mediastinal mass is suspected to be non-vascular, CT or MRI can be used for further evaluation. MRI, in addition, can be used as a problem-solving tool for confirming prior CT studies of solid-appearing duplication cysts located within the middle mediastinum. If the middle mediastinal mass is suspected to be vascular in origin, CTA or MRA should be considered.

In infants and children diagnosed with posterior mediastinal masses, particularly those with neurogenic tumors, MRI is the preferred imaging modality.

For evaluation of children with lymphoma, PET can be a useful functional imaging modality for staging, assessment of early treatment response, and assessment after completion of therapy. PET can be used for staging, early response assessment during treatment, and response assessment after completion of therapy in pediatric patients with lymphoma.

Take Home Tables

Tables 26.1 and 26.2 discuss primary mediastinal masses (location and prevalence) in infants (0–2 years) and children (2–18). Table 26.3 discusses the diagnostic performance of infants and children with mediastinal masses.

Table 26.1. Primary mediastinal masses in infants (0–2 years): location and prevalence (prevalence sums to 100% but not all tissue types were stated)

Location/type of mass	Prevalence (%)
Anterior	
Thymic hyperplasia	6
Teratoma	2
Other	16
Total	24
Middle	
Duplication cyst	4
Other	8
Total	12
Posterior	
Neuroblastoma	13
Ganglioneuroblastoma	2
Plexiform neurofibroma	1
Other or mixed neurogenic	33
Total	49
Other	
Angiomatous malformation	4
Undifferentiated sarcoma	1
Other	10
Total	15

Data from Pokorny and Sherman (26).

Table 26.2. Primary mediastinal masses in children (2–18 years): location and prevalence

Location/type of mass	[a]Prevalence (%)
Anterior	
Malignant lymphoma (non-Hodgkin/Hodgkin)	23
Thymus (benign enlargement, ectopy)	6
Teratoma	10
Other (angioma, cardiovascular, thymic cyst, thymoma, substernal thyroid, mesenchymal tumor, histiocytosis X)	–
Total	46
Middle	
Foregut cysts (bronchogenic, enteric)	11
Lymphadenopathy (lymphoma, granulomatous)	–
Other (angioma, cardiovascular, mesenchymal tumor)	–
Total	20
Posterior	
Neurogenic tumor (ganglion cell, nerve cell)	30
Other (angioma, lymphoma, foregut cyst, mesenchymal tumor)	–
Total	34

[a]Prevalences were not available for all types of masses but sum to 100%.

Data from King et al. (25, 27).

Courtesy of David F. Merten, MD; reprinted with the permission of the Am J Roentgenol from Merten (4).

Table 26.3. Diagnostic performance for infants and children with mediastinal masses

Study	Sensitivity	Specificity	References	Evidence
CXR•	97–100%	N/A	(44, 52)	Limited/moderate
US*	94–95%	N/A	(91, 92)	Limited/moderate
CT overall	100%	N/A	(58)	Limited/moderate
CT intraspinal°	88%	N/A	(109)	Limited/moderate
MRI overall	100%	N/A	(31, 32)	Limited/moderate
MRI intraspinal°	100%	N/A	(109)	Limited/moderate

•Patient population consisted of both children and adults.

*Evaluation of thymus in infants and children (newborn to 8 years old).

°Intraspinal extension of posterior mediastinal neurogenic tumors

Note: PET is not included since the primary use of PET in pediatric population is currently limited to the evaluation of mediastinal neoplasm (e.g., lymphoma) instead of evaluating all mediastinal masses.

Imaging Case Studies

Case 1

Figure 26.3 presents a case of a 2-month-old male infant who presented with wheezing and coughing.

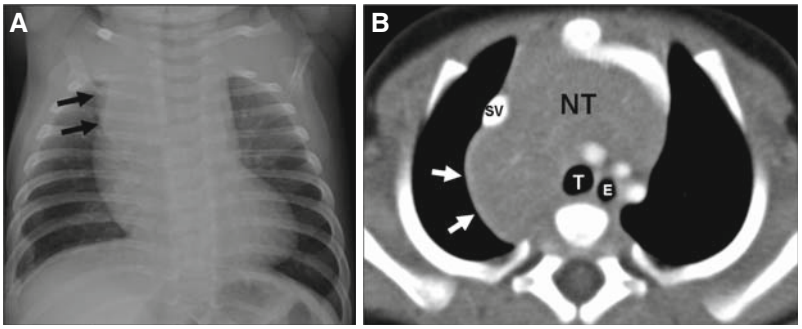

Figure 26.3. **A**: A 2-month-old male infant who presented with wheezing and coughing. Frontal chest radiograph showing soft-tissue density (*arrows*) located in the right superior mediastinum raised the possibility of an anterior mediastinal mass. **B**: Subsequently obtained contrast-enhanced axial MDCT image confirmed the diagnosis of normal thymus (NT) with an extension (*arrows*) into the posterior mediastinum between superior vena cava (SV) and trachea (T). Homogeneous attenuation and contiguity with a normal thymus located within the anterior mediastinum helped to make a correct diagnosis. E = esophagus.

Case 2

Figure 26.4 presents a case of a 10-year-old girl who presented with right-sided chest pain.

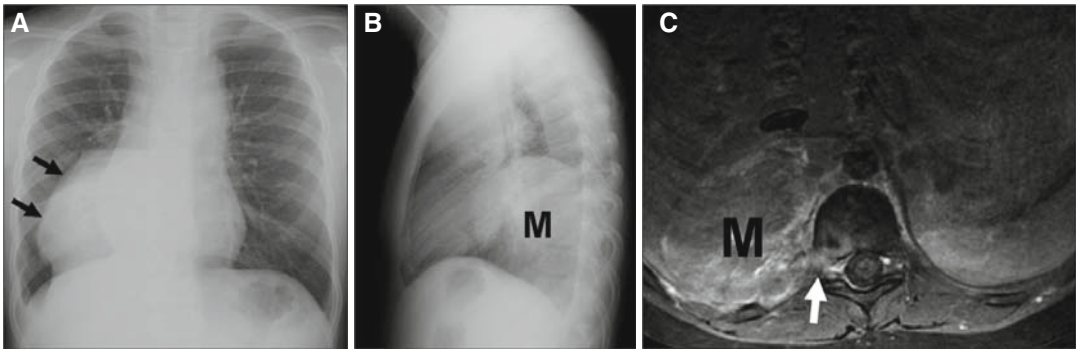

Figure 26.4. **A**: A 10-year-old girl who presented with right-sided chest pain. Frontal chest radiograph shows a large mass in the right hemithorax (*arrows*). **B**: Lateral chest radiograph confirms the location of this mass (M) within the posterior mediastinum. **C**: Axial postcontrast T1-weighted MRI image shows a large heterogeneously enhancing right paraspinal mass (M) with associated intraforaminal extension (*arrow*) at T10–T11 level. Surgical pathology confirmed the diagnosis of neuroblastoma.

Suggested Imaging Protocols

Plain Radiographs

PA and lateral views of the chest are the initial evaluation of mediastinal masses in infants and children. For young infants in whom the lateral chest radiograph cannot be easily obtained, AP view of the chest radiograph may suffice.

Ultrasound

The choice of ultrasound transducer with optimal frequency depends on (1) patient age, (2) mediastinal mass location, and (3) the planned approach. To achieve optimal sonographic imaging evaluation in neonates and infants, a high-resolution 10–15 MHz linear-array transducer in a transsternal, parasternal, or intercostal approach should be used. However, a 2–7 MHz linear-array or sector transducer is typically required for better soft-tissue penetration in children and adolescents. In characterizing the lesion, imaging in at least two planes is recommended and color flow may aid in demonstrating associated internal vascularity or anomalous vessels.

CT

CT should be performed at the lowest possible radiation exposure without affecting diagnostic imaging quality (i.e., weight-based mAs and kVp, thin collimation [<1 mm], and fast table speed [<1 sec]). For non-vascular mediastinal masses in infants and children, imaging is acquired with intravenous contrast and reformatted in 2D (MPR) in both mediastinal and lung window settings. For vascular masses (e.g., vascular rings and slings), the CT angiography protocol is used with 2D (MPR) and 3D reconstructions (for mediastinal vessels and central airways).

MRI

For non-vascular masses, the MRI protocol consists of axial FRFSE T2 fat saturation, axial T1 or DIR, coronal FRFSE T2 fat saturation, coronal 3D MR angiography SPGR (with gadolinium), and axial and coronal T1 fat saturation (after gadolinium) typically using eight channel cardiac coils. With respect to vascular mediastinal lesions, the MRI protocol includes axial, sagittal, and coronal oblique FSEDIR as well as sagittal 3D MRA SPGR (with gadolinium). Ideally, a breath-holding/respiratory trigger should be used for FRFSE sequence. If patients are sedated, a breath-hold sequence may be used without needing cooperation of breath-hold. ECG gating and breath-holding must be used for a DIR sequence.

PET

The patient preparation prior to PET study in pediatric patients with lymphoma includes the following:

1) avoiding any form of caffeine (including soda, tea, chocolate), nicotine, or alcohol (12 hours prior to study);
2) refraining from any strenuous exercise (24 hours before the study);
3) preventing from any solid food or fluid (4 hours prior to the study); and
4) avoiding cold temperatures (12 hours before the study).

In general, younger children (<6 years old) have difficulty staying still for the entire PET study (which typically takes 30–50 minutes) and require sedation to cooperate fully with the test. After arrival at the nuclear medicine department, the patient will remain in a heated room for 30 minutes and the patient's blood sugar level is checked. Then 2-(^{18}F)-fluoro-2-deoxy-D-glucose (^{18}F-FDG) (150 Ci/kg) is administered intravenously. After the injection, the patient waits approximately 1 hour, empties his/her bladder, and lies on the PET scanner table. Trans-axial images are obtained from the base of skull level to the mid thigh level. Once trans-axial image acquisition is completed, trans-axial images are transferred to the image workstation, where they can be reconstructed into multiplanar (i.e., coronal and sagittal reformations) and 3D whole-body MIP (maximum intensity projection) images. Subsequently, fusion software can be used to co-register PET images and CT images to produce a "PET/CT fusion" images.

Future Research

- Large-scale prospective diagnostic performance studies comparing the sensitivities, specificities, and predictive accuracies of

prevailing imaging modalities (e.g., ultrasound, CT, and MRI) aimed at evaluating mediastinal masses in infants and children.
- Cost analysis and outcome assessment of the various types of diagnostic imaging modalities for evaluating mediastinal masses in infants and children.
- Large prospective studies to determine the indications and limitations of new imaging technologies such as PET and hybrid PET/CT for evaluating infants and children with lymphoma.

Acknowledgments: This work was supported in part by a GE-AUR Research Award, a Society of Thoracic Radiology Research Grant, and a Society for Pediatric Radiology Research Grant. The author would like to sincerely thank pediatric pulmonologist Dr. Debra Boyer and pediatric surgeon Dr. Christopher Weldon for their insightful comments and suggestions.

References

1. Heitzman ER. The Mediastinum. Berlin: Springer-Verlag, 1988.
2. McAdams HP, Erasmus JJ, Tarver RD Spritzer CE. In Haaga JR, Lanzieri CF, Gilkeson RC (eds.). CT and MR Imaging of the Whole Body, 4th ed. St. Louis, MO: Mosby Inc., 2003:937–996.
3. Webb WR. In Webb WR, Higgins CB (eds.). Thoracic Imaging, 1st ed. Philadelphia, PA: Lippincott Williams & Wilkins, 2005:175–270.
4. Merten DF. AJR 1992; 158(4):825–832.
5. Meza MP, Benson M, Slovis TL. Radiol Clin North Am 1993; 31(3):583–604.
6. Buckley JA, Vaughn DD, Jabra AA et al. Crit Rev Diagn Imaging 1998; 39(5):365–392.
7. Laurent F, Latrabe V, Lecesne R et al. Eur Radiol 1998; 8(7):1148–1159.
8. Erasmus JJ, McAdams HP, Donnelly LF, Spritzer CE. Magn Reson Imaging Clin North Am 2000; 8(1):59–89.
9. Williams HJ, Alton HM. Paediatr Respir Rev 2003; 4(1):55–66.
10. Whitten CR, Khan S, Munneke GJ, Grubnic S. Radiographics 2007; 27(3):657–671.
11. Simpson I, Campbell PE. Prog Pediatr Surg 1991; 27:92–126.
12. Grosfeld JL, Skinner MA, Rescorla FJ et al. Ann Surg Oncol 1994; 1(2):121–127.
13. Brown LR, Aughenbaugh GL. AJR 1991; 157(6):1171–1180.
14. Jaggers J, Balsara K. Semin Thorac Cardiovasc Surg 2004; 16(3):201–208.
15. Billmire DF. Semin Pediatr Surg 1999; 8(2): 85–91.
16. Billmire DF. Semin Pediatr Surg 2006; 15(1): 30–36.
17. Billmire DF. Surg Clin North Am 2006; 86(2):489–503.
18. Billmire D, Vinocur C, Rescorla F et al. J Pediatr Surg 2001; 36(1):18–24.
19. Dominguez-Malagon H, Perez Montiel D. Semin Diagn Pathol 2005; 22(3):230–240.
20. Kanemitsu Y, Nakayama H, Asamura H et al. Surg Today 1999; 29(11):1201–1205.
21. Berrocal T, Madrid C, Novo S et al. Radiographics 2004; 24(1):e17.
22. McLaughlin RB Jr, Wetmore RF, Tavill MA et al. Laryngoscope 1999; 109(2 pt 1):312–319.
23. Jeung MY, Gasser B, Gangi A et al. Radiographics 2002; 22 Spec No:S79–S93.
24. Lee JY, Lee KS, Han J et al. J Comput Assist Tomogr 1999; 23(3):399–406.
25. King RM, Telander RL, Smithson WA et al. J Pediatr Surg 1982; 17:512–520.
26. Pokorny WJ, Sherman JO. J Thorac Cardiovasc Surg 1974; 68(6):869–875.
27. Ravitch MM. In Welch KJ, Randolph JG, Ravitch MM, O'Neill JA Jr, Rowe MI (eds.). Pediatric Surgery, 4th ed. Chicago: Year Book Medical, 1986; 602–618.
28. Incidence Rates, Lymphoma. Childhood Cancer, Chapter II: Rates and Risk Factors for Specific Childhood Cancers, http://www.state.nj.us/health/cancer/child/chap2d.htm. Published February 1999. Accessed July 10, 2008.
29. Siegel MJ. In Siegel MJ (ed.). Pediatric Body CT. Philadelphia: Lippincott Williams & Wilkins, 2008; 37–39.
30. Siegel MJ, Sagel SS, Reed K. Radiology 1982; 142(1):149–155.
31. von Schulthess GK, McMurdo K, Tsholakoff D et al. Radiology 1986; 158(2):289–296.
32. Siegel MJ, Nadel SN, Glazer HS, Sagel SS. Radiology 1986; 160(1):241–244.
33. Casamassima F, Villari N, Fargnoli R et al. Radiother Oncol 1988; 11(1):21–29.
34. Kornreich L, Horev G, Ziv N, Grunebaum M. Eur J Pediatr 1992; 151(1):38–41.
35. Wernecke K, Potter R, Peters PE, Koch P. AJR 1988; 150(5):1021–1026.
36. Wernecke K, Vassallo P, Potter R, Luckener HG, Peters PE. Radiology 1990; 175:137–143.
37. Kawashima A, Fishman Ek, Kuhlman JE, Nixon MS. Radiographics 1991; 11(6): 1045–1067.

38. Batra P, Brown K, Collins JD et al. J Natl Med Assoc 1991; 83(11):969–974.
39. Stein SM, Cox JL, Hernanz-Schulman M, Kirchner SG, Heller RM. South Med J 1992; 85(7): 735–742.
40. Ikezoe J, Takeuchi N, Johkoh T et al. Radiat Med 1992; 10(5):176–183.
41. Batra P, Brown K, Steckel R. Am J Surg 1988; 156(1):4–10.
42. Duwe BV, Sterman DH, Musani AI. Chest 2005; 128(4):2893–2909.
43. Bower RJ, Kiesewetter WB. Arch Surg 1977; 112(8):1003–1009.
44. Harris GJ, Harman PK, Trinkle JK, Grover FL. Ann Thorac Surg 1987; 44(3):238–241.
45. Ahrens B, Wit J, Schmitt M et al. J Thorac Cardiovasc Surg 2001; 122(5):1021–1023.
46. Grosfeld JL, Baehner RL. World J Surg 1980; 4(1):29–37.
47. Posner JB. J Pediatr Hematol Oncol 2004; 26(9):553–554.
48. Janss A, Sladky J, Chatten J, Johnson J. Med Pediatr Oncol 1996; 26(4):272–279.
49. Mahoney NR, Liu GT, Menacker SJ et al. Am J Ophthalmol 2006; 142(4):651–659.
50. Zafeiriou DI, Economou M, Koliouskas D et al. Eur J Paediatr Neurol 2006; 10(2):90–92.
51. Ribet ME, Cardot GR. Ann Thorac Surg 1994; 58(4):1091–1095.
52. Adegboye VO, Brimmo AI, Adebo OA et al. West Afr J Med 2003; 22(2):156–160.
53. Ahn JM, Lee KS, Goo JM et al. J Thorac Imaging 1996; 11(4):265–271.
54. Kim OH, Kim WS, Kim MJ et al. Radiographics 2000; 20:653–671.
55. Liu P, Daneman A, Stringer DA. Can Assoc Radiol J 1988; 39:198–203.
56. Liang CD, Huang SC. J Formos Med Assoc 1997; 96(9):700–703.
57. Adam EJ, Ignotus PI. AJR 1993; 161(1):153–155.
58. Ginaldi S, Cunningham G, Davis LJ, Singleton EB. J Comput Tomogr 1981; 5(6):511–518.
59. Graeber GM, Shriver CD, Albus RA et al. J Thorac Cardiovasc Surg 1986; 91(5):662–666.
60. Lee EY, Siegel MJ. J Thorac Imaging 2007; 22(3):300–309.
61. Lee EY, Siegel MJ. In Boiselle PM, Lynch DA (eds.). CT of the Airways. Totowa, NJ: Humana, 2008; 351–380.
62. Lee EY, Boiselle PM, Cleveland RH. Radiology 2008; 247:632–648.
63. Lee EY, Siegel MJ, Hildebolt CF et al. AJR 2004; 182(3):777–784.
64. Webb WR, Gamsu G, Stark DD, Moon KL, Moore EH. AJR 1984; 143:723–727.
65. Gamsu G, Stark DD, Webb WR, Moore EH, Sheldon PE. Radiology 1984; 151:709–713.
66. Nakata H, Egashira K, Watanabe H et al. J Comput Assist Tomogr 1993; 17(2):267–270.
67. Gaeta M, Vinci S, Minutoli F et al. Eur Radiol 2002; 12:181–189.
68. Murayama S, Murakami J, Watanabe H et al. J Comput Assist Tomogr 1995; 19(2): 188–191.
69. Neimatallah MA, Ho VB, Dong Q et al. J Magn Reson Imaging 1999; 10(5):758–770.
70. Hernandez RJ. Magn Reson Imaging Clin North Am 2002; 10(2):237–251.
71. Ho VB, Corse WR, Hood MN, Rowedder AM. Semin Ultrasound CT MR 2003; 24(4):192–216.
72. Russo V, Renzulli M, La Palombara C, Fattori R. Eur Radiol 2006; 16:676–684.
73. Shankar A, Fiumara F, Pinkerton R. Eur J Cancer 2008; 44(5):663–673.
74. Montravers F, McNamara D, Landman-Parker J et al. Eur J Nucl Med Mol Imaging 2002; 29(9):1155–1165.
75. Hudson MM, Krasin MJ, Kaste SC. Pediatr Radiol 2004; 34(3):190–198.
76. Wegner EA, Barrington SF, Kingston JE et al. Eur J Nucl Med Mol Imaging 2005; 32(1):23–30.
77. Depas G, De Barsy C, Jerusalem G et al. J Nucl Med Mol Imaging 2005; 32(1):31–38.
78. Hermann S, Warmanns D, Pixberg M et al. Nuklearmedizin 2005; 44(1):1–7.
79. Tatsumi M, Cohade C, Nakamoto Y, Fishman EK, Wahl RL. Radiology 2005; 237(3):1038–1045.
80. Kabickova E, Sumerauer D, Cumlivska E et al. Eur J Nucl Med Mol Imaging 2006; 33(9): 1025–1031.
81. Amthauer H, Furth C, Denecke T et al. Klin Padiatr 2005; 217(6):327–333.
82. Jerusalem G, Beguin Y, Fassotte MF et al. Blood 1999; 94:429–433.
83. Canellos GP. J Clin Oncol 1988; 6:931–933.
84. Gdeedo A, Van Schil P, Corthouts B, Van Mieghem F, Van Meerbeeck J, Van Marck E. Eur Respir J 1997; 10:1547–1551.
85. Cheson BD, Horning SJ, Coiffier B et al. J Clin Oncol 1999; 17:1244–1253 [Erratum in J Clin Oncol. 2000, 18, 2351].
86. Kwee TC, Kwee RM, Nievelstein RA. Blood 2008; 111(2):504–516.
87. Nanni C, Rubello D, Castellucci P et al. Biomed Pharmacother 2006; 60(9):593–606.
88. Francis IR, Glazer GM, Bookstein FL, Gross BH. AJR 1985; 145:249–254.
89. St Amour TE, Siegel MJ, Glazer HS, Nadel SN. J Comput Assist Tomogr 1987; 11(4):645–650.
90. Bale PM, Sotelo-Avila C. Pediatr Pathol 1993; 13(2):181–190.
91. Liang CD, Huang SC. J Formos Med Assoc 1997; 96(9):700–703.
92. Adam EJ, Ignotus PI. AJR 1993; 161(1):153–155.

93. Han BK, Babcock DS, Oestreich AE. Radiology 1989; 170:471–474.
94. Park JJ, Kim JW, Kim JP et al. Auris Nasus Larynx 2006; 33(1):101–105.
95. Spigland N, Bensoussan AL, Blanchard H, Russo P. J Pediatr Surg 1990; 25(11): 1196–1199.
96. Scott KJ, Schroeder AA, Greinwald JH Jr. Arch Otolaryngol Head Neck Surg 2002; 128(6): 714–717.
97. De Foer B, Vercruysse JP, Marien P et al. JBR-BTR 2007; 90(4):281–283.
98. Tovi F, Mares AJ. Am J Surg 1978; 136(5): 631–637.
99. Koumanidou C, Vakaki M, Theophanopoulou M et al. Pediatr Radiol 1998; 28:987–989.
100. Krysta MM, Gorecki WJ, Miezynski WH. J Pediatr Surg 1998; 33(4):632–634.
101. Cohen MD, Weber TR, Sequeira FW, Vane DW, King H. Radiology 1983; 146(3):691–692.
102. Cory DA, Cohen MD, Smith JA. Radiology 1987; 162(2):457–459.
103. Slovis TL, Meza M, Kuhn JP. Pediatr Radiol 1992; 22(7):490–492.
104. Bergin CJ, Healy MV, Zincone GE, Castellino RA. J Comput Assist Tomogr 1990; 14(6): 928–932.
105. Kersting-Sommerhoff BA, Sechtem UP, Fisher MR, Higgins CB. AJR 1987; 149(1):9–13.
106. Greil GF, Kramer U, Dammann F et al. Pediatr Radiol 2005; 35(4):396–401.
107. Eichhorn J, Fink C, Delorme S, Ulmer H. Z Kardiol 2004; 93:201–208.
108. Russo V, Renzulli M, Buttazzi K, Fattori R. Eur Radiol 2006; 16:852–865.
109. Slovis TL, Meza MP, Cushing B et al. Pediatr Radiol 1997; 27(3):273–275.
110. Akwari OE, Payne WS, Onofrio BM, Dines DE, Muhm JR. Mayo Clin Proc 1978; 53:353–358.
111. Miller E, Metser U, Avrahami G, et al. J Comput Assist Tomogr 2006; 30:689–694.
112. Furth C, Denecke T, Steffen I et al. J Pediatr Hematol Oncol 2006; 28:501–512.
113. Edeline V, Bonardel G, Brisse H et al. Leuk Lymphoma 2007; 48:823–826.
114. Hernandez-Pampaloni M, Takalkar A, Yu JQ, Zhuang H, Alavi A. Pediatr Radiol 2006; 36:524–531.

27

Imaging of Chest Infections in Children

Garry Choy, Phoebe H. Yager, Natan Noviski, and Sjirk J. Westra

Issues

I. What are the clinical presentation and predictors of chest infections in children and which findings raise the suspicion for complications?
II. When are chest radiographs useful in children with suspected pneumonia?
III. How does chest radiography compare to cross-sectional imaging in the evaluation of chest infections in children? When is chest CT indicated?
IV. What is the role and diagnostic performance of imaging studies (radiography, ultrasound, CT) for the treatment planning of complicated pneumonia with empyema and pleural effusions?
V. What are the relative roles of imaging studies in medical therapy, minimally invasive intervention such as thoracostomy or thoracentesis, and surgical treatment for pneumonia complicated by pleural involvement?

Key Points

- Imaging studies have limited value in the differentiation between viral and bacterial lower respiratory tract infections (moderate evidence).
- CT provides more information than plain radiographs for complicated pulmonary infections with empyema, pleural effusion, or bronchopleural fistula (moderate evidence).
- In immunocompromised patients, CT has been shown to characterize the type of infection better than plain radiographs (moderate evidence).
- Ultrasound has an advantage over CT in the identification and characterization of complicated effusions (moderate evidence).

S.J. Westre (✉)
Department of Radiology, Massachusetts General Hospital, Boston, MA 02114, USA
e-mail: swestra@partners.org

L.S. Medina et al. (eds.), *Evidence-Based Imaging in Pediatrics*,
DOI 10.1007/978-1-4419-0922-0_27, © Springer Science+Business Media, LLC 2010

- Early detection and therefore intervention for pleural complications of pneumonia are critical and can result in better outcomes (moderate evidence).
- Early surgery (VATS) is more cost-effective than thoracotomy (without or with image guidance) in the treatment of empyemas in children (strong evidence).

Definition and Pathophysiology

Pneumonia is defined as an infection of the lungs. Acute respiratory infections are the most common infection of the human host. The majority of these are of the upper respiratory tract, but infections of the lower respiratory tract are frequent challenges for clinicians caring for children. Most of these illnesses are mild, and patients suffering from them are appropriately cared for in an ambulatory setting, but a small number are ill enough to require hospitalization and some die. Thus, lower respiratory tract infections, particularly pneumonia, constitute a major health problem both in the United States and throughout the world. Bacterial pneumonias make up only a small number of lower respiratory tract infections but have the highest mortality rates. The infectious agents responsible for pneumonia and lower respiratory tract infection can be divided into bacterial, viral, fungal, mycobacterial, and atypical causes. Incidence of specific pathogens differs by age (Table 27.1). The most common pathogens in children are *Streptococcus pneumoniae* and *Haemophilus influenzae*, followed by *Staphylococcus aureus* and *Streptococcus pyogenes* (1–5). In particular, *S. aureus* and gram-negative pathogens can affect newborns and malnourished children (5). Viral illnesses such as respiratory syncytial virus (RSV), influenza, parainfluenza, and adenovirus have been identified in approximately a quarter of children with pneumonia (5). The potential complications of pneumonia include parapneumonic (pleural) effusion, empyema, or abscess. Empyema is treated either medically, surgically, or with placement of drainage tubes. Abscesses and necrotizing pneumonias are usually treated medically, but interventional procedures such as drainage tube placement might sometimes be used.

Pleural Effusion and Empyema

A pleural effusion is broadly defined as an abnormal collection of fluid in the space between the parietal and visceral pleuras and may arise from a variety of processes that alter the normal flow and absorption of pleural fluid. The most common causes of pleural effusions in children are pneumonia (parapneumonic effusion), congenital heart disease, and malignancy. A diagnostic or therapeutic thoracentesis is usually indicated to determine the nature of the effusion as well as to relieve associated dyspnea and respiratory compromise.

An empyema is characterized by the presence of pus, with polymorph nuclear leukocytes and fibrin, in the pleural space. Nearly one-half of all children with pneumonia will develop parapneumonic effusions, but fewer than 5% of these effusions progress to empyema. However, the incidence of empyema complicating community-acquired pneumonia is increasing, which causes significant childhood morbidity (6). Progression of a pleural effusion to empyema is through a three-stage evolution: (1) exudative, (2) fibrinopurulent, and (3) organization. Most commonly pleural effusions do not progress beyond the exudative phase and resolve with antibiotics alone (4, 7). The second stage is heralded by the arrival of bacteria, by pleural invasion from the contiguous pneumonic process. Progression occurs with polymorph accumulation and fibrin deposition; membrane formation occurs and the developing empyema may become compartmentalized or loculated. The chemistry profile of pleural fluid is characterized by a decrease in pH and glucose concentrations and an increase in lactate dehydrogenase concentration (LDH). The most common organisms encountered in pleural fluid in children are *S. aureus, S. pneumoniae, H. influenzae,* and *S. pyogenes* (1–5). If a fibropurulent pleural effusion is not

adequately treated, then the third organizing phase develops. Fibroblasts grow into the exudate from the visceral and parietal pleural surfaces. An inelastic membrane is formed, which and may encase the lung and pleura, with the potential to restrict respiration. The thick exudate may drain spontaneously through the chest wall or into the lungs, causing a bronchopleural fistula. Other infectious complications of empyema include bacteremia and pericarditis by direct extension or bacteremic seeding, and pneumothorax.

Lung Abscess

A lung abscess is an accumulation of inflammatory cells accompanied by tissue destruction or necrosis that produces one or more large cavities in the lung. It is arbitrary to designate larger cavities by the term lung abscesses and smaller, multiple cavities with similar histology by the term necrotizing pneumonia. Necrotizing pneumonia is an acute fulminating infection of the lung parenchyma, characterized by vascular thrombosis and rapid tissue breakdown leading to multiple thin-walled cavities. Pulmonary abscess is a more chronic thick-walled cavity in the lung, usually encountered in patients with chronic debilitating states. Anaerobic bacteria and *S. aureus* are most frequently implicated with the formation of a lung abscess. Complications of lung abscess include rupture into adjacent compartments, which occurs more frequently with *S. aureus.* Localized bronchiectasis may also occur as a complication.

Epidemiology

According to the WHO, there are over 150 million cases of pneumonia annually in the world in children less than 5 years of age (8). In the United States, 20 million hospitalizations in the pediatric population occur, although many are of viral etiology (8). Each year in the developed nations, 5–10% of children under the age of 5 years will develop pneumonia (5). The incidence of pneumonia in children is approximately 34–40 per 1,000 (9). Approximately one-half of children younger than 5 years with community-acquired pneumonia require hospitalization (10). Complicated pneumonia such as necrotizing pneumonia and abscess formation has been noted to increase in incidence over the years between 1990 and 2005 (11, 12). Parapneumonic effusions complicate pneumonia between 36 and 56% of cases with an incidence between 0.4 and 0.6 per 1,000 cases (13). Empyema complicates an estimated 0.6% of all childhood pneumonias, resulting in an incidence of 3.3 per 100,000 children (6). Unlike in the adult population, most pediatric patients recover without mortality whereas in adults, the mortality rate has been reported to be up to 20% (6, 11). There has been an emergence of community-acquired methicillin-resistant *S. aureus* (MRSA) in pediatric pneumonia, originally thought to be mainly hospital acquired (14). An aggressive infection, MRSA pneumonia, has been reported to present with high fever, leukopenia, rapidly progressing respiratory distress, development of multilobar infiltrates with effusions, and empyema (15, 16). Intravenous antibiotics are first-line therapy and surgical treatment may be needed in patients with MRSA pneumonia complicated by empyema (15).

Overall Cost to Society

In the adult population in Europe, the cost to society resulting from uncomplicated pneumonia is estimated at $8 billion, with 1.1 million cases per year (17). Childhood pneumonias are a frequent cause of doctor visits, antibiotics prescriptions, loss of work days of parents, and reduction of quality of life (18). For example, the mean number of work days lost by mothers ranged between 0.2 and 4.2 days (18). No additional specific US pediatric cost data were found in the literature. However, there has been one cost-effectiveness analysis reported, related to pneumonia with pleural involvement, treated by either thoracentesis, chest tube/pleural drain placement, or video-assisted thoracoscopic surgery (VATS) (13).

Length of hospitalization has been compared between different treatment strategies of parapneumonic effusions, or empyema. In a randomized controlled trial, gross total cost of hospitalized patients requiring intervention to treat parapneumonic effusions has been demonstrated to be approximately equal for treatment with VATS versus chest tube placement, resulting in total charges of approximately

$21,947 versus $19,714 on average, respectively. However, hospital length of stay was on average 6 days for patients who underwent VATS and 13 days for patients who underwent chest tube placement (13).

Goals

The main goal in imaging pulmonary infections is early diagnosis. This will aid in early and adequate treatment and may prevent potential complications. When there is pleural effusion, imaging guides appropriate management. The standard treatment of pneumonia and its complications may include all or part of the following: antibiotics, thoracentesis, chest tube placement, fibrinolytic therapy, or surgical debridement of empyema. Severe cases of empyema, for example, often require surgical decortication if there is failure to respond to antibiotic treatment, thoracentesis, or chest tube placement. Appropriate diagnosis and treatment must aim to minimize risk to patients, including that related to ionizing radiation exposure, interventional procedure complications, and surgical complications.

Methodology

The review of the current diagnostic imaging literature was done using PubMed/MEDLINE covering the years January 1980–December 2008. The search strategy used the following key statements and words: *pediatric, children, neonate, neonatal, pneumonia, empyema, pleural effusion, abscess, VATS*. We excluded non-English journal articles, case reports, animal studies, and basic science articles.

Discussion of Issues

I. What Are the Clinical Presentation and Predictors of Chest Infections in Children, and Which Findings Raise the Suspicion for Complications?

Summary of Evidence: Clinical presentation and diagnosis of pneumonia vary with age and pathogen, with tachypnea being the single most predictive sign (moderate evidence).

The clinical exam does not reliably diagnose pneumonia nor distinguish between viral and bacterial pneumonias (moderate evidence).

Supporting Evidence: The goal of clinical evaluation is to confirm the clinical diagnosis and to assess severity of disease (10). The typical presentation is cough and respiratory distress, sometimes with fever and muscle aches. History, physical examination, laboratory testing, and radiographic testing are the primary components of the diagnostic workup. History focuses on assessment of age, presence of fever, chest pain, dyspnea, immunizations, duration of symptoms, exposure to sick contacts, and recent travel. In a study of 110 children with respiratory infections, tachypnea emerged as the best clinical sign for identifying pneumonia, with a sensitivity of 74% and a specificity of 67% (19). Although there may be findings suggestive of either viral or bacterial pneumonia, the clinical exam does not reliably diagnose pneumonia nor distinguish between viral and bacterial pneumonias. Models that have been tested in adult populations based only on clinical information in the absence of imaging do not reliably predict the presence of pneumonia (20).

Laboratory evaluation includes a complete blood count and leukocyte differentiation. In children with severe symptoms or if outbreak is suspected, microbiology of sputum and blood cultures may be useful (21, 22). The diagnosis of pneumonia is often confirmed and defined by the presence of a lung opacity on chest radiography. Accepted indications for a chest radiograph include severe disease, confirmation of non-specific clinical findings, assessment of complications, and exclusion of other thoracic causes of respiratory symptoms (23, 24).

In the neonatal period, pneumonia is virtually always due to bacteria, particularly group B *Streptococcus* as well as *E. coli, H. influenzae*, and –*Listeria monocytogenes* (25). Physical findings and clinical signs of pneumonia are often nonspecific but include fever, temperature instability, difficulty feeding, and restlessness (10). In this population, viral pneumonia is rare due to conferred maternal antibody protection, whereas bacterial pneumonia is most frequently due to pathogens acquired during labor and delivery and is more prevalent in premature babies. In keeping with dropping maternal antibody levels, viral childhood pneumonia occurs

at a peak between 2 months and 2 years of age (7). Presenting signs and symptoms in this age group remain non-specific and include cough, fever, temperature instability, abnormal leukocyte count, findings of sepsis, and respiratory distress (10). In older children from 2 years to 18 years of age, bacterial infections become relatively more common. In addition to previously mentioned symptoms, pleuritic chest pain may occur (7, 10). In a retrospective case series of 79 patients who presented with at least one symptom of fever, cough, sputum production, chest pain, dyspnea, or course crackles, pneumonia was diagnosed using chest radiography as the gold standard in 24 (prevelance: 30%) (26). In this study group, a combination of all four symptoms of fever, cough, sputum, and course crackles yielded a sensitivity and specificity of 91.7 and 92.7% for clinical detection of pneumonia.

Viral Versus Bacterial Pneumonia

If possible, differentiation between bacterial and viral etiologies of pneumonia would be helpful for treatment decisions. As mentioned previously, age is an important criterion. In bacterial infection, pulmonary findings are most commonly limited to one anatomic area on physical examination, and symptoms include fever, moderate-to-severe respiratory distress, and chest pain (27). Primary viral infection is considered more likely if symptoms include wheezing (27). There is a gradual onset of symptoms such as fever, congestion, rhinorrhea, and wheezing (27–29). Children with viral pneumonias also tend not to appear as toxic as those with bacterial pneumonia (28). In addition, viral illnesses may often precede bacterial infection (27).

Lung response to an infective antigen may be more age specific than antigen (i.e., bacteria versus viral) dependent. Virkki et al. performed a study in 254 children admitted with diagnosis of community-acquired pneumonia to evaluate the role of chest radiography, total white blood cell count, serum C-reactive protein, and erythrocyte sedimentation rate (30). They found that 71% of children with lobar opacities demonstrate laboratory evidence of a bacterial infection, but interstitial opacities were seen with approximately equal frequencies in viral and bacterial pneumonias. Of children less than 2 years, 38% had bacterial infections and 60% viral, whereas in older children bacterial pneumonias were more prevalent (49%) than viral (22%), the remainder being of mixed etiology. Likewise, Korppi et al. performed a study of 61 children treated for radiologically and microbiologically confirmed viral or bacterial pneumonia (31). Chest radiographs were independently reviewed by two radiologists, and they found that 74% of the patients with alveolar and 62% with interstitial pneumonias had bacterial infection. An interstitial pattern of pneumonia on chest radiographs is therefore nonspecific: it could be due to viral (26%), bacterial (30%), or mixed (44%) etiologies. Hence, distinguishing between viral and bacterial pneumonias in pediatric patients remains problematic, given the number of clinical and radiographic findings that overlap.

Parapneumonic effusions and empyema in children are complications and follow acute bacterial pneumonias (12, 32). Rare causes of empyema include distant spread from other sources of infection such as osteomyelitis of the ribs, septic emboli, and lung abscesses. Children typically present ill-appearing, febrile, and with unilateral chest signs (12, 32).

II. When Are Chest Radiographs Useful in Children with Suspected Pneumonia?

Summary of Evidence: Chest radiographs may have a role in evaluating for pneumonia in the clinical presentation of fever of unknown origin (limited evidence).

Chest radiographs are sufficiently sensitive and highly specific for the diagnosis of community-acquired pneumonia (moderate evidence).

Imaging studies have limited value in the differentiation between viral and bacterial lower respiratory tract infections (moderate evidence).

Supporting Evidence

Fever of Unknown Origin

There are currently varying data regarding the utility of chest radiographs for fever of unknown origin. Only 0–3% of infants

with fever of unknown origin had a positive chest radiograph demonstrating pneumonia, and therefore chest radiography appears to have limited utility in this age group (33, 34). This contrasts with a prospective study of 278 children aged less than 5 years with fever and leukocytosis, to determine the incidence of radiographic findings of pneumonia, which was found not only in 40% of those with clinical findings suggestive of pneumonia but also in 26% of those without clinical evidence of pneumonia. Accounting for the 53 children in whom no chest radiograph was taken and who were presumed to not have pneumonia, this study estimated the minimum incidence of clinically occult pneumonia in this population as 19% (35).

Neonatal Pneumonia

Chest radiographs are commonly used in the neonatal intensive care unit, but the radiographic findings of neonatal pneumonia substantially overlap with those of other causes of the neonatal respiratory distress syndrome. Although evidence for this practice is lacking, a negative chest radiograph result allows the neonatologists to stop antibiotic treatment at 3 days of age, if other tests are also negative.

Community-Acquired Pneumonia

Chest radiography is the standard first-line imaging tool for the evaluation of suspected pulmonary infections, particularly in suspected community-acquired pneumonias. However, a Cochrane review of a randomized trial of 522 children, aged 2 months to 5 years, performed by Swingler and Zwarenstein failed to demonstrate any evidence that chest radiography improves outcome in ambulatory children with lower respiratory tract infection (36). Up to 10% of pediatric patients with proven pulmonary infection can have a normal chest radiograph (sensitivity 90%) (17). Table 27.2 summarizes the test characteristics of the only three studies in which complete sensitivity and specificity data of chest radiography are available: reported sensitivities range between 71 and 87% and specificities from 90 to 98% (37–39). In a few more limited studies, sensitivity and specificity values were not directly specified, but accuracy was reported to range between 58 and 77% (38–40).

In the evaluation of children with pneumonia, frontal views are most useful when lobar (bacterial) pneumonia is present. When pneumonia has been defined as "a focus of streaky or confluent lung opacity," the sensitivity and specificity of the frontal view alone were 85 and 98%, respectively. For opacities that are confluent and lobar in distribution (not streaky or non-segmental/non-lobar), the sensitivity and specificity increased to 100% (37). However, this study also suggested that non-lobar types of infiltrates will be underdiagnosed in 15% of patients if only the frontal view is used.

Differentiation of Bacterial and Viral Pneumonias

When viral causes of respiratory infection such as bronchiolitis are suspected, chest radiographs may not be needed in uncomplicated cases. In a retrospective study of 298 patients in an urban children's hospital at the University of Colorado by Roback et al., clinicians did not typically obtain chest radiographs in first-time wheezing episodes, whereas there was a higher utilization of radiographs in patients with elevated temperature, absence of family history of asthma, and localized wheezing on physical examination (40). Perlstein et al. developed a publication of a set of evidence-based guidelines, as implemented at the Children's Hospital of Cincinnati, that demonstrated 20% decrease in the number of chest radiographs ordered (40, 41). In another study of 72 adult patients by Graffelman et al. in the primary care setting, limited value was found using chest radiography in predicting the etiology of viral versus bacterial lower respiratory infections. The positive predictive value and the negative predictive value for bacterial infection were 75 and 57%, respectively (42).

III. How Does Chest Radiography Compare to Cross-Sectional Imaging in the Evaluation of Chest Infections in Children? When Is Chest CT Indicated?

Summary of Evidence: Chest CT is not warranted in uncomplicated pneumonia (moderate evidence).

CT provides more information than plain radiographs for complicated pulmonary infections with empyema, pleural effusion, or bronchopleural fistula (moderate evidence).

In immunocompromised patients, CT has been shown to characterize the type of infection better than plain radiographs (moderate evidence).

Supporting Evidence: Given satisfactory performance of chest radiographs in uncomplicated community-acquired pneumonias, CT is not recommended for evaluation of pulmonary infections without empyema, pleural effusion, or bronchopleural fistula.

Pneumonia with Complications (Table 27.3)

Several studies (43–50) have demonstrated that CT can often add information to the diagnosis, particularly in fungal infections and in complicated pneumonia cases. In a case series of 42 immunocompetent children, chest radiography was suboptimal in detecting abscesses, bronchopleural fistulae, fluid loculations, and parenchymal involvement when compared to CT (51). Chest radiograph accuracy rates were reported as follows: fluid loculations (42%), abscess formation (40%), bronchopleural fistulae (33%), and parenchymal involvement (84%). A limitation of this study is the lack of reported sensitivity and specificity values. Donelly and Klosterman performed a study of 56 patients with complicated pneumonia who were not responding to treatment. Chest CT was compared to a chest radiograph performed earlier on the same day. CT scans were evaluated for the presence of cavitary necrosis, abscess, bronchopleural fistula, cavitation, loculated pleural effusions, malpositioned chest tube, pericardial effusion, or bronchial obstruction (50). All 56 CT scans demonstrated at least one of the above findings that were not seen on chest radiographs (50). A total of 110 findings were seen on CT and not on chest radiography, with an average of approximately two findings per CT scan. Parenchymal complications totaled 40 and pleural complications 37. In another retrospective analysis of 17 children who underwent both CT scanning and chest radiography, evidence of cavity necrosis is often seen on CT before or in the absence of findings on chest radiographiy (52).

Immunocompromised Children with Pneumonia

In the high-risk immunocompromised patients, it is absolutely critical to have a high sensitivity, as failure to detect results in failure to treat and subsequent high mortality (45). CT has been shown to have higher accuracy than plain radiography for early detection of pneumonia in immunocompromised and hospitalized patients (45, 48). For example, in a series of 48 patients (median age of 11 years and range of 2–19 years), chest radiographs and CT were rated independently by three experienced radiologists and subsequently correlated with biopsy or bronchoscopic washing results. CT was shown to identify more true-positive cases of bacterial and fungal pneumonias than radiography (91 versus 85%). Unfortunately, no detailed numbers of sensitivity and specificity were cited (45). In 87 adult patients with febrile neutropenia (median age 47, range 18–80 years), CT detected pneumonia 5 days on average earlier than chest radiographs and was more sensitive in the detection of poorly defined opacities, ill-defined nodules, consolidation, ground-glass opacities, pleural effusions, cavitations, and bullae (53). For the evaluation of children who are severely ill or immunocompromised for fungal infections and *Pneumocystis carinii* pneumonia (PCP), CT can add value. Janzen et al., in a retrospective review of 45 children who underwent both CT and chest radiography, found that the first-choice diagnosis was correct in 44% on chest CT and correct in 30% on chest radiography ($p < 0.05$) (49). Equivocal or normal chest radiographs are common, reported up to 39% in patients with PCP infection and up to 10% of patients with known pulmonary disease (17). CT can aid in the detection of fungal infections via identification of nodules, cavitation, ground-glass opacities, and halo effect (45–47). CT can play an important role such as in evaluating pulmonary aspergillosis and candidal pneumonias (45). In another study to evaluate if CT adds information to chest radiography, 33 cases were reviewed retrospectively (54). It was found that in 16 cases CT added no additional useful information, but in 17 cases CT added confidence and changed management (biopsy, changing antibiotics, bronchoscopy).

Nosocomial Infections and MRSA Pneumonia

In the case of nosocomial infections, such as multidrug-resistant infections (MRSA pneumonia), CT offers a rapid and decisive diagnosis (14). For aspiration pneumonias, chest radiographs alone are usually adequate for diagnosis and to ensure resolution. The primary role of imaging has been the detection and monitoring of complications from the pneumonia.

IV. What Is the Role and Diagnostic Performance of Imaging Studies (Radiography, Ultrasound, and CT) for Treatment Planning of Complicated Pneumonia with Empyema and Parapneumonic Effusions?

Summary of Evidence: Chest imaging can be used to distinguish between the exudative and organizing phases of pleural effusion, through demonstration of atypical layering patterns on decubitus radiography, complexity of pleural fluid on ultrasound, and loculations of heterogeneous fluid on CT (moderate evidence).

Ultrasound has an advantage over CT in the identification and characterization of complicated effusions, also being more cost-effective and not employing ionizing radiation (moderate evidence).

Supporting Evidence: The diagnosis of pleural effusion can be readily achieved via radiography, ultrasound, or CT. There are several studies evaluating the prognostic implications of the use of ultrasound versus CT and the implications for treatment decisions. Ultrasound can be helpful in both prognosis and treatment decisions. It is a low-cost test, widely available, portable, does not use ionizing radiation, and rarely requires sedation. This has to be contrasted to CT, which has a relatively high radiation dose, in the order of 100 times that of a chest radiograph. Ultrasound is effective in demonstrating "high-grade" effusions containing septations, fronds, loculations, and debris. US depiction of the thickness and number of these septations predicts the success of chest tube drainage (55). CT assists in providing a global assessment for pre-therapy planning, including the ability to demonstrate size, possible loculations, and the extent of lung involvement, including abscess formation or necrosis (51). Kearney et al. demonstrated in a retrospective review of 50 patients who underwent both US and CT that, although both US and CT have effective roles, neither technique reliably identified the stage of pleural effusions or predicted whether patients would require surgical intervention (56).

Donnelly et al. have shown in a retrospective review of 30 patients who received a chest CT with subsequent pleural fluid analysis that CT characteristics of a parapneumonic effusion do not allow one to predict empyema and distinguish it from a transudative process (57, 58). Experienced radiologist reviewers rated the presence of pleural enhancement (seen in 100% of empyemas and in 89% of transudative effusions), pleural thickening (57 and 56%, respectively), abnormal extrapleural space (66 and 67%, respectively), and extracostal chest wall edema (33 and 56%, respectively) (57).

A retrospective analysis of 46 pediatric patients with empyema by Ramnath et al. found that early sonographic evaluation of parapneumonic effusions led to decreased hospital length of stay for high-grade effusions and effective triage into two groups, operative (20 patients) versus non-operative treatment (26 patients) (55). Operative therapy included video thoracotomy, open decortication, or pleural debridement, and non-operative therapy included antibiotics alone with or without thoracentesis or chest tube placement. When the ultrasound detected high-grade effusions (evidence of organization such as fronds, septations, or loculations), the hospitalization stay was shorter (8.6 days) for patients eventually treated operatively, compared to those who were not (16.4 days). In non-operated patients in whom ultrasound revealed low-grade effusions, there was no significant difference in hospital stay length between patients treated with antibiotics alone and chest tube drainage (55). In another study, ultrasound has also been shown to be quite effective in identifying empyemas (59). In this prospective study of 1640 febrile patients admitted to the ICU, 94 patients underwent 118 ultrasound-guided thoracenteses for pleural effusions, identified by chest radiography and ultrasound. In 11/31 studies where a

complex septated pattern and in all four where a diffusely hyperechoic pattern was reported, empyemas were confirmed with thoracentesis. On the other hand, in none of the remaining 83 studies where an anechoic or complex non-septated/hypoechoic pattern was reported were empyemas diagnosed.

V. What Are the Relative Roles of Imaging in Medical Therapy, Minimally Invasive Intervention such as Thoracotomy or Thoracentesis, and Surgical Treatment for Pneumonia Complicated by Pleural Involvement?

Summary of Evidence: Early detection of complicated pneumonia by imaging and subsequently early intervention result in better patient outcomes (moderate evidence).

Currently, there is no strong evidence to support or not support fibrinolytic therapy for childhood empyema in conjunction with image-guided interventions (insufficient evidence). While it may result in more rapid treatment response, side effects and the pain from this treatment limit its current use.

There is strong evidence in the surgical literature that early surgery (VATS) is more cost-effective than thoracotomy (without or with image guidance) in the treatment of empyemas in children (strong evidence).

Supporting Evidence

Image-Guided Thoracentesis and Chest Tube Placement

As pleural effusions evolve, antibiotic therapy alone may not be sufficient. More aggressive intervention is often required. Beyond antibiotics, minimally invasive therapy with image-guided thoracentesis or chest tube drainage may be necessary. Thoracentesis is a standard procedure for the management of pleural effusions in adults. However, in children, thoracentesis is not easily performed as this procedure requires cooperation and frequently sedation. Patients treated with thoracentesis have been reported to require additional interventions due to recurrence (4, 6, 60). For example, Tu et al. found in 94 ICU patients with a pleural effusion suspected to have empyema that additional interventions were often needed; a total of 118 image-guided thoracentesis procedures were performed in this group (59). A prospective study of 67 patients with empyemas found that single chest tube placement versus repeated thoracentesis had no significant difference in outcome, thereby supporting that in children early thoracotomy tube drainage is preferred to thoracentesis, in order to avoid repeat interventions (61). In this study, the patients were prospectively divided into two treatment arms: chest tube placement (32 patients) and ultrasound-guided thoracentesis (35 patients). As assessed by chest radiography, the amount of fluid drained, the number of days that the patient was febrile, and the duration of antibiotic therapy, no statistical differences were found between both treatment arms.

Thoracentesis or single chest tube placement may not be beneficial in the presence of loculations and adhesions by fibrin. The aim of using fibrinolytic therapy in such cases is to improve drainage of pus by lysis of the fibrinous bands.

Fibrinolysis

A recent meta-analysis has shown that, in adults, intrapleural fibrinolytic therapy confers significant benefit in reducing the requirements for surgical intervention for patients in the early studies included in the review, but not in the more recently published studies (62). Separate subgroup analysis of proven loculated/septated effusions suggests a potential overall treatment benefit with fibrinolytics, but these results should be treated with caution. In children, fibrinolytic therapy has been reported in three studies with about 64 cases (63). There were no in-hospital deaths. The aggregate data revealed a failure rate of 9.3% and a complication rate of 12.5%. One of the studies was a 10-center randomized prospective study of urokinase undertaken by the British Paediatric Respiratory Society Empyema Study Group (64). They reported a slight reduction in length of stay in hospital compared to the saline group (7.4 versus 9.5 days). However, a major surgical concern with this therapy is that patients may be more likely to fail rescue VATS, as it has been suggested that urokinase

causes intrapleural adhesions to become very adhesive (6).

Beyond Image-Guided Thoracentesis or Thoracotomy: Surgery

In cases not amenable to minimally invasive image-guided procedures such as thoracentesis or simple chest tube placement without or with fibrinolysis, surgical interventions including video-assisted thorascopic surgery (VATS) or thoracotomy can be effective options (13, 63). VATS is a relatively safe and effective treatment for complicated pleural effusion and empyema.

Early intervention with VATS can result in better outcomes (13, 65). Luh et al., using VATS, described an 86.3% satisfactory result in 234 patients with complicated pneumonia with effusions or empyema (65). In a prospective randomized trial, Kurt et al. found that early intervention with VATS was superior to conventional thoracotomy drainage (13). These surgical papers may be biased toward operative in favor of image-guided intervention. However, even a meta-analysis, performed to evaluate primary operative versus non-operative therapy in children with empyema, suggested a more favorable response with early surgical intervention (VATS or thoracotomy) (63). In this meta-analysis, primary operative therapy was associated with lower in hospital mortality rate, re-intervention rate, length of stay, time with tube thoracotomy, and time of medical therapy when compared to medical management.

Take Home Tables and Figures

Tables 27.1, 27.2, and 27.3 show data on infectious pneumonia by age, diagnostic performance of clinical exam and chest radiography in detection of pneumonia in non-immunocompromised patients, and a literature review of CT diagnostic performance in all populations of pediatric patients, respectively.

Table 27.1. Infectious pneumonia by age

	0–4 weeks	4–8 weeks	8–12 weeks	12 weeks–4 years	5-Year adolescence
Etiology (in the order of prevalence)	**– Group B *Streptococcus*, – gram-negative enteric bacteria, –*Listeria monocytogenes***	**–*Chlamydia trachomatis*, –Viruses (RSV, parainfluenza) –*Streptococcus pneumoniae*, –*Bordetella pertussis*, –Group B *Streptococcus*, –gram-negative enteric bacteria, –*Listeria monocytogenes***	**–*Chlamydia trachomatis*, –Viruses (RSV, parainfluenza) –*Streptococcus pneumoniae*, –*Bordetella pertussis***	**–Viruses (RSV parainfluenza, Influenza, adenovirus, rhinovirus), –*Streptococcus pneumoniae*, –*Haemophilus influenzae* (non-type B), –*Moraxella catarrhalis*, –group A *Streptococcus*, –*Mycoplasma pneumoniae*, –*Mycobacterium tuberculosis***	**–*Mycoplasma pneumoniae*, –*Chlamydia pneumoniae*, –*Streptococcus pneumoniae*, –Viruses (RSV parainfluenza, Influenza, adenovirus, rhinovirus), –*Mycobacterium tuberculosis***

Modified with permission of Elsevier from Lichenstein R, Suggs AH, Campbell J. Emerg Med Clin North Am 2003; 21: 437–451.

Table 27.2. Diagnostic performance of clinical exam and chest radiography in detection of pneumonia in non-immunocompromised patients

Clinical exam:

Author	Year	Study size	Finding	Sensitivity (%)	Specificity (%)
Palafox et al. (19)	2000	110	Tachypnea	74	67
Okimoto et al. (26)	2006	79	If all of following present: fever, cough, sputum production, dyspnea	91.7	92.7

Chest Radiography

Author	Year	Study size	Sensitivity (%)	Specificity (%)	PPV (%)	NPV (%)
Rigsby et al. (37)	2004	240	85	98	n/a	n/a
Lamme et al. (38)	1986	179	81–87	95–96	n/a	n/a
Patenaude et al. (39)	1995	373	71	90	n/a	n/a
Graffelman et al. (20)	2007	129	n/a	n/a	75	57

Summary: Reported sensitivities range between 71 and 87% and specificities from 90 to 98% (37, 38, 39).

Table 27.3. Review of literature on CT diagnostic performance in all populations of pediatric patients (community-acquired pneumonias, immunocompromised patients): Evidence table

Author	Year	Study size	Objective	Study type	Conclusions
Kuhlman et al. (47)	1987	10	To evaluate whether CT findings impacted clinical decision making	Case series	CT directly affected patient management in 7; CT demonstrated the halo sign in 8/9 patients with early CT scans; fluffy masses, cavitation, or air crescent signs in 5/7 patients with serial CT scans
Mori et al. (46)	1991	55	To compare chest radiography and chest CT in febrile bone marrow transplant patients for evaluation of pulmonary infection	Case series	CT scans demonstrating nodules in febrile BMT patients strongly indicate fungal infection Negative CT studies suggest extrapulmonary infection CT appears to add useful information to radiographic analysis during the assessment of febrile episodes in BMT patients
Barloon et al. (54)	1991	33	To assess if CT added specificity to plain chest radiography	Case series	16 cases, CT added no additional useful information but in 17 cases, CT added confidence and changed management (biopsy, changing antibiotics, bronchoscopy)
Janzen et al. (49)	1993	45	To compare CT and chest radiography in diagnosis of pneumonia in immunocompromised patients (non-AIDS)	Case series	For CT, sensitivity and specificity in detecting pulmonary complications was 100 and 98% For chest radiography, sensitivity and specificity in detecting pulmonary complications was 98 and 93% CT was correct in first-choice diagnosis in 44% and chest radiograph was correct in 30% CT identified the diagnosis within the top three differential considerations in 70% and chest radiography in 53% Chest radiographs and CT scans have comparable sensitivity CT is superior to chest radiography in differential diagnosis
Winer-Muram et al. (45)	1997	48	To determine the diagnostic accuracy of chest radiographs versus chest CT in patients during treatment for hematologic malignancies	Case series	Both chest radiographs and CT have satisfactory accuracies for fungal pneumonia or cryptogenic organizing pneumonia CT identified more true-positive cases than did chest radiographs

Table 27.3. *Continued*

Author	Year	Study size	Objective	Study type	Conclusions
Heussel et al. (53)	1997	87	To assess usefulness of CT in early detection of pneumonia in neutropenic patients with unknown infection or non-specific chest radiographs	Case series	CT detected pneumonia 5 days earlier than chest radiography Probability of pneumonia being detected on chest radiographs during a 7-day follow-up of an abnormal CT was 31%, whereas this probability was only 5% when the initial CT was normal
Donnelly et al. (57)	1997	30	To compare CT findings of parapneumonic effusions treated with thoracentesis, thoracoscopy, or both, to determine whether these CT findings can reliably differentiate empyemas from transudative parapneumonic effusions in children	Case series	None of individual CT findings or a composite score of findings could accurately differentiate empyema from transudative parapneumonic effusions Pleural enhancement was found in 100% of empyema and 89% of transudative effusions Pleural thickening was found in 57% of empyema and 56% in transudative effusions Abnormal extrapleural space was found in 66% of empyema and 67% of transudative effusions Extracostal chest wall edema was found in 33% of empyemas and 56% of transudative effusions
Donnelly et al. (50)	1998	56	To investigate usefulness of CT in evaluating children who do not respond appropriately to treatment for pneumonia when chest radiography is non-contributory	Case series	CT yielded findings related to parenchymal and pleural complications not seen on chest radiography (pericardial effusion, bronchial obstruction, cavitary necrosis, abscess, decreased enhancement, bronchopleural fistula, or cavity) All CT scans showed at least one significant finding (100% yield) not seen on radiography
Donelly et al. (52)	1998	17	To describe sequential clinical and radiographic findings of cavitary necrosis by CT	Case series	CT effective in identifying loss of lung architecture, decreased enhancement, and multiple cavities with thin, non-enhancing walls CT often detects evidence of cavitary necrosis complicating pneumonia before chest radiographs do

Figure 27.1 is a diagnostic and therapeutic imaging workup algorithm for pneumonia with pleural effusion in immunocompetent children. Figures 27.2 and 27.3 show the role of ultrasound and CT in empyema. Figure 27.4 shows how CT can be used to differentiate empyema from lung abscess.

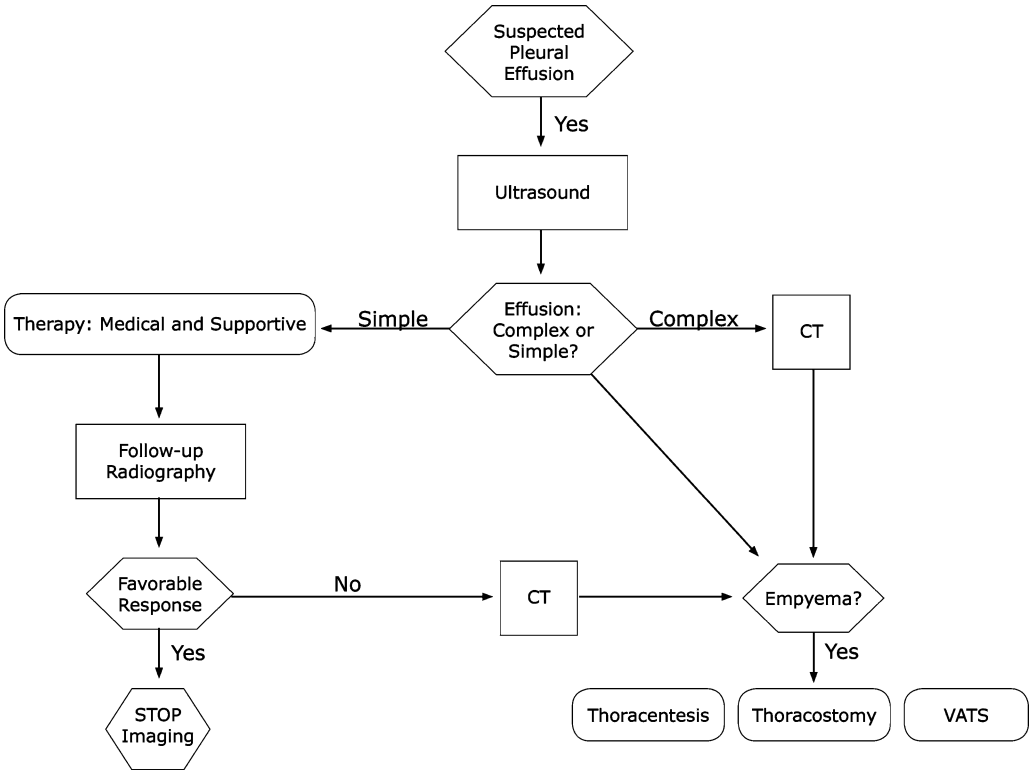

Figure 27.1. Diagnostic and therapeutic imaging workup algorithm for pneumonia with pleural effusion in immunocompetent children.

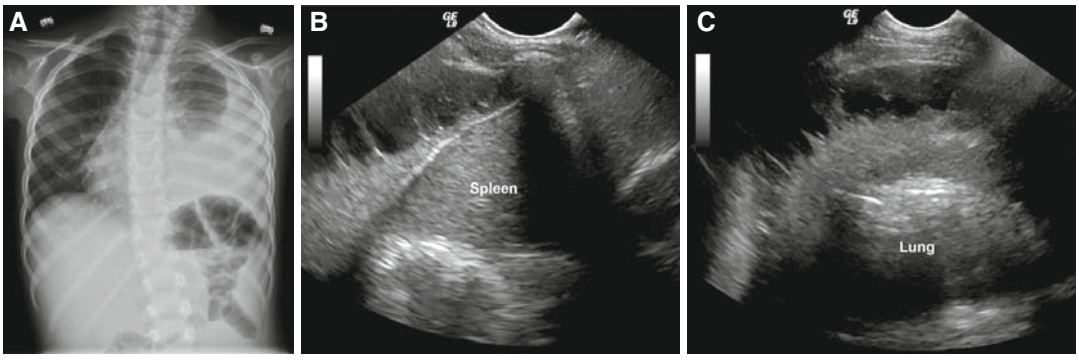

Figure 27.2. Empyema: role of ultrasound. Chest radiograph (**A**) shows left-sided pleural collection. Ultrasound images (**B, C**) demonstrate this collection to be complex (grade 2), with loculations, echogenic fluid, and fibrous adhesions.

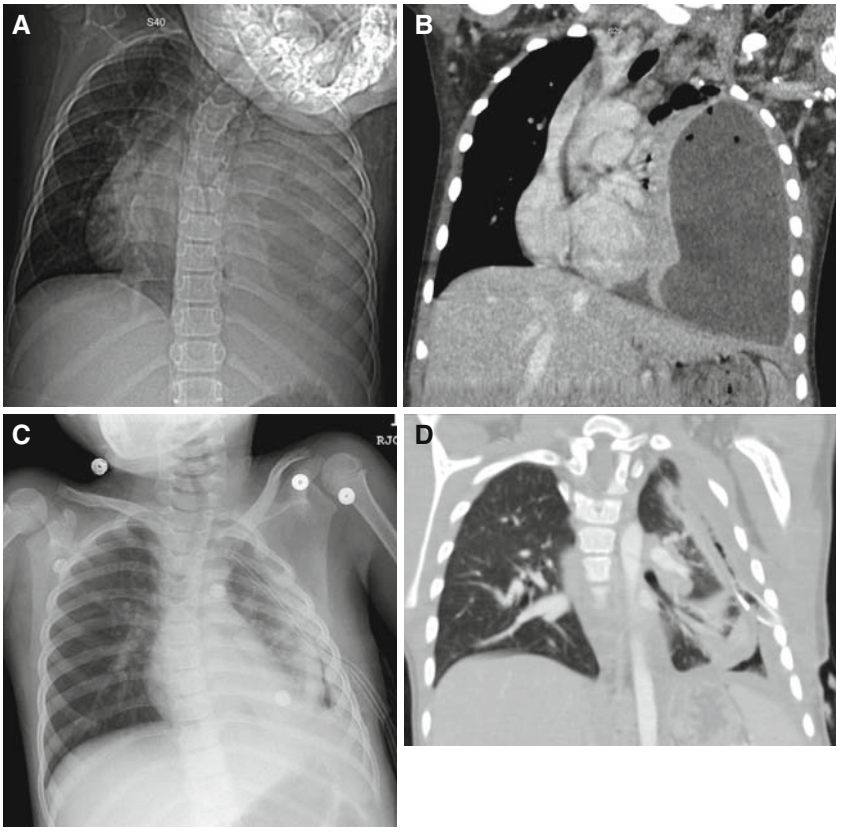

Figure 27.3. Empyema: role of CT. Radiograph (**A**) and CT (**B**) demonstrate left-sided pleural collection with mass effect, consistent with empyema. Radiograph (**C**) and CJ (**D**) following chest tube placement show thickening of the visceral pleura consistent with pleural, fibrosis (organization phase, grade 3), preventing full expansion of the left lung.

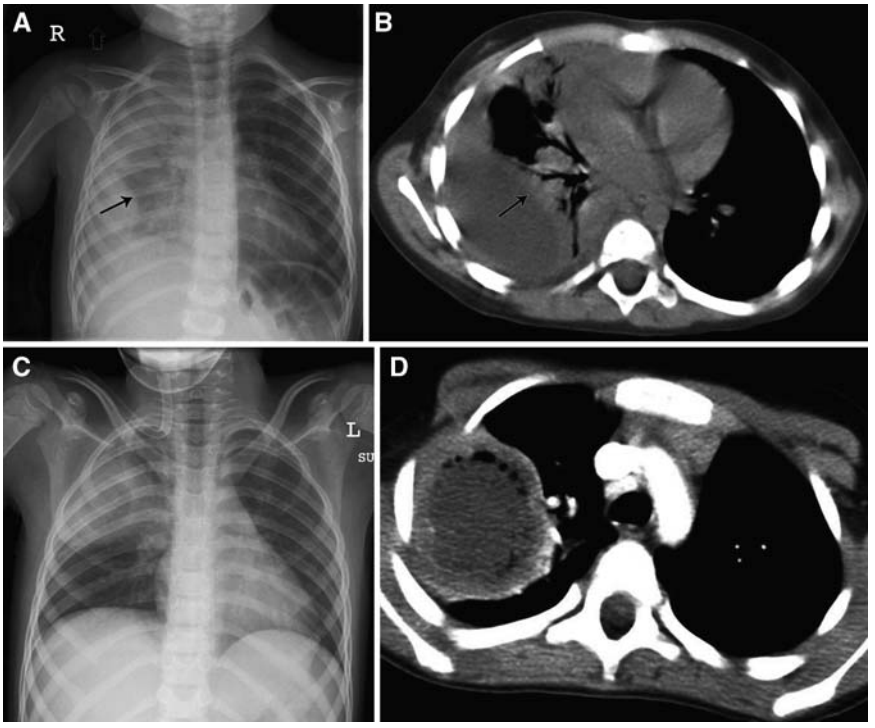

Figure 27.4. Use of CT to differentiate empyema from lung abscess. Radiograph (**A**) and CT (**B**) demonstrate a fluid collection with mass effect on the lung (*arrows*), which forms an obtuse angle with the pleura, consistent with a pleural abscess (empyema). Radiograph (**C**) and CT (**D**) demonstrate a gas- and fluid-containing lung mass, which forms a sharp angle with the pleura, confirming its intraparenchymal location.

Case Imaging Studies

Case 1

Figure 27.5 presents CT in a child with acute lymphatic leukemia with ARDS.

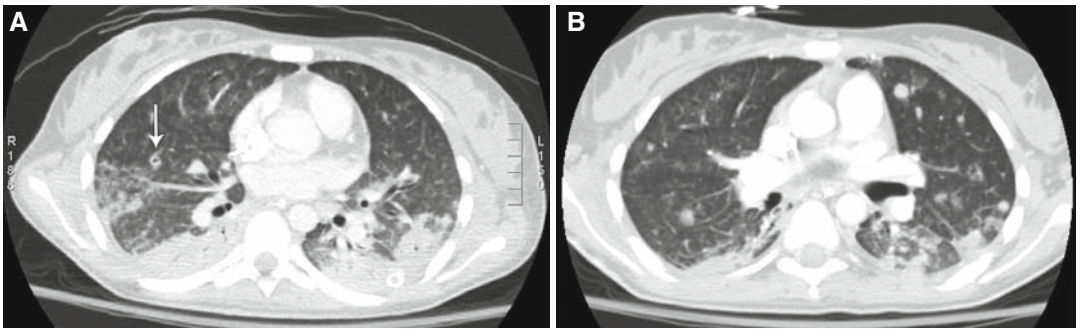

Figure 27.5. CT in a child with acute lymphatic leukemia with ARDS: multiple pulmonary nodules, several of which are cavitating (*arrow*), findings that raise specificity for opportunistic fungal infection.

Suggested Imaging Protocols

Radiography

Posterior–anterior (PA) and lateral views are optimal whenever possible. Anterior–posterior (AP) views are also very useful. In suspected effusions, decubitus views can be useful in distinguishing free-flowing pleural fluid versus loculated fluid collections. However, in the presence of extensive pulmonary parenchymal consolidation, the value of decubitus films to identify loculated versus free pleural fluid is severely limited.

Ultrasound

Technique includes screening of the whole pleural space, not just the lung bases. Lower frequency (3.5–7 MHz) sector transducers are used initially for more overview through inter- and subcostal scanning; higher frequency (10–12.5 MHz) linear transducers are helpful for more detail in the near field, prior to marking for needle placement (66).

Chest CT

In chest infections, use of intravenous contrast is almost always indicated. Lower mA techniques (and kVp reduction in small children) can be used than in the abdomen, due to the high intrinsic contrast of lung parenchyma; further dose reduction is possible with follow-up of large lesions (abscess, empyema pockets) and for checking the position of chest tubes. Coronal reformats and 3D renditions (virtual bronchoscopy) are sometimes helpful tools prior to bronchoscopy or surgery.

Future Research

- What is the cost-effectiveness of CT in management of empyema and parapneumonic effusions?
- Can findings on imaging (plain radiography, ultrasound, CT) predict likelihood of success of various interventions for complications of pneumonia?
- How can ultrasound, a non-irradiating modality, be utilized more in the evaluation of pulmonary infection and its complications?
- What is the role of MR, a more expensive but non-ionizing modality, for evaluation of pulmonary infection complications (67)?
- A prospective clinical trial to compare the benefits (including cost-effectiveness) of optimal image-guided intervention (with fibrinolysis) to early surgery (VATS) for the treatment of empyemas in children.

References

1. Chonmaitree T, Powell KR. Clin Pediatr (Phila) Jun 1983; 22(6):414–419.
2. Freij BJ, Kusmiesz H, Nelson JD, McCracken GH, Jr. Pediatr Infect Dis Nov–Dec 1984; 3(6):578–591.
3. Hardie W, Bokulic R, Garcia VF, Reising SF, Christie CD. Clin Infect Dis Jun 1996; 22(6): 1057–1063.
4. Buckingham SC, King MD, Miller ML. Pediatr Infect Dis J Jun 2003; 22(6):499–504.
5. CDC.gov. Pneumonia among Children in Developing Countries. http://www.cdc.gov/ncidod/DBMD/diseaseinfo/pneumchilddevcount_t.htm
6. Jaffe A, Balfour-Lynn IM. Pediatr Pulmonol Aug 2005; 40(2):148–156.
7. Kuhn J. Caffey's Pediatric Diagnostic Imaging, Vol I, 10 ed. Philadelphia: Mosby, 2004.
8. Rudan I, Boschi-Pinto C, Biloglav Z, Mulholland K, Campbell H. Bull World Health Organ May 2008; 86(5):408–416.
9. Murphy TF, Henderson FW, Clyde WA Jr, Collier AM, Denny FW. Am J Epidemiol Jan 1981; 113(1):12–21.
10. Margolis P, Gadomski A. JAMA Jan 28, 1998; 279(4):308–313.
11. Sawicki GS, Lu FL, Valim C, Cleveland RH, Colin AA. Eur Respir J Jan 23, 2008.
12. Barnes NP, Hull J, Thomson AH. Pediatr Pulmonol Feb 2005; 39(2):127–134.
13. Kurt BA, Winterhalter KM, Connors RH, Betz BW, Winters JW. Pediatrics Sep 2006; 118(3):e547–e553.
14. Vilar J, Domingo ML, Soto C, Cogollos J. Eur J Radiol Aug 2004; 51(2):102–113.
15. Kilbane BJ, Reynolds SL. Pediatr Emerg Care Feb 2008; 24(2):109–114; quiz 115–107.
16. Buescher ES. Curr Opin Pediatr Feb 2005; 17(1):67–70.
17. Franquet T. Eur Respir J Jul 2001; 18(1):196–208.
18. Shoham Y, Dagan R, Givon-Lavi N et al. Pediatrics May 2005; 115(5):1213–1219.
19. Palafox M, Guiscafre H, Reyes H, Munoz O, Martinez H. Arch Dis Child Jan 2000; 82(1):41–45.

20. Graffelman AW, le Cessie S, Knuistingh Neven A, Wilemssen FE, Zonderland HM, van den Broek PJ. J Fam Pract Jun 2007; 56(6):465–470.
21. McCracken GH, Jr. Pediatr Infect Dis J Sep 2000; 19(9):924–928.
22. Ostapchuk M, Roberts DM, Haddy R. Am Fam Physician Sep 1, 2004; 70(5):899–908.
23. Swingler GH, Hussey GD, Zwarenstein M. Lancet Feb 7, 1998; 351(9100):404–408.
24. Alario AJ, McCarthy PL, Markowitz R, Kornguth P, Rosenfield N, Leventhal JM. J Pediatr Aug 1987; 111(2):187–193.
25. Barnett ED Klein JO. Infectious Diseases of the Fetus and Nerborn Infant, 6th ed. Philadelphia: Elsevier Saunders Company, 2006.
26. Okimoto N, Yamato K, Kurihara T et al. Respirology May 2006; 11(3):322–324.
27. McIntosh K. N Engl J Med Feb 7 2002; 346(6):429–437.
28. Turner RB, Lande AE, Chase P, Hilton N, Weinberg D. J Pediatr Aug 1987; 111(2):194–200.
29. McCarthy PL. Curr Opin Pediatr Oct 1996; 8(5):427–429.
30. Virkki R, Juven T, Rikalainen H, Svedstrom E, Mertsola J, et al. Thorax May 2002; 57(5):438–441.
31. Korppi M, Kiekara O, Heiskanen-Kosma T, Soimakallio S. Acta Paediatr Apr 1993; 82(4): 360–363.
32. King S, Thomson A. Br Med Bull 2002; 61: 203–214.
33. Slater M, Krug SE. Emerg Med Clin North Am Feb 1999; 17(1):97–126, viii–ix.
34. Haney PJ, Bohlman M, Sun CC. Am J Roentgenol Jul 1984; 143(1):23–26.
35. Bachur R, Perry H, Harper MB. Ann Emerg Med Feb 1999; 33(2):166–173.
36. Swingler GH, Zwarenstein M. Cochrane Database Syst Rev 2005(3):CD001268.
37. Rigsby CK, Strife JL, Johnson ND, Atherton HD, Pommersheim W, Kotagal UR. Pediatr Radiol May 2004; 34(5):379–383.
38. Lamme T, Nijhout M, Cadman D et al. CMAJ Feb 15, 1986; 134(4):353–356.
39. Patenaude Y, Blais C, Leduc CP. Invest Radiol Jan 1995; 30(1):44–48.
40. Roback MG, Dreitlein DA. Pediatr Emerg Care Jun 1998; 14(3):181–184.
41. Perlstein PH, Kotagal UR, Bolling C et al. Pediatrics Dec 1999; 104(6):1334–1341.
42. Graffelman AW, Willemssen FE, Zonderland HM, Neven AK, Kroes AC, van den Broek PJ. Br J Gen Pract Feb 2008; 58(547):93–97.
43. Winer-Muram HT, Rubin SA, Kauffman WM et al. Clin Radiol Dec 1995; 50(12):842–847.
44. Winer-Muram HT, Rubin SA, Fletcher BD et al. Radiology Oct 1994; 193(1):127–133.
45. Winer-Muram HT, Arheart KL, Jennings SG, Rubin SA, Kauffman WM, Slobod KS. Radiology Sep 1997; 204(3):643–649.
46. Mori M, Galvin JR, Barloon TJ, Gingrich RD, Stanford W. Radiology Mar 1991; 178(3): 721–726.
47. Kuhlman JE, Fishman EK, Burch PA, Karp JE, Zerhouni EA, Siegelman SS. Chest Jul 1987; 92(1):95–99.
48. Katz DS, Leung AN. Clin Chest Med Sep 1999; 20(3):549–562.
49. Janzen DL, Padley SP, Adler BD, Muller NL. Clin Radiol Mar 1993; 47(3):159–165.
50. Donnelly LF, Klosterman LA. Am J Roentgenol Jun 1998; 170(6):1627–1631.
51. Tan Kendrick AP, Ling H, Subramaniam R, Joseph VT. Pediatr Radiol Jan 2002; 32(1):16–21.
52. Donnelly LF, Klosterman LA. Am J Roentgenol Jul 1998; 171(1):253–256.
53. Heussel CP, Kauczor HU, Heussel G, Fischer B, Mildenberger P, et al. Am J Roentgenol Nov 1997; 169(5):1347–1353.
54. Barloon TJ, Galvin JR, Mori M, Stanford W, Gingrich RD. Chest Apr 1991; 99(4):928–933.
55. Ramnath RR, Heller RM, Ben-Ami T et al. Pediatrics Jan 1998; 101(1 Pt 1):68–71.
56. Kearney SE, Davies CW, Davies RJ, Gleeson FV. Clin Radiol Jul 2000; 55(7):542–547.
57. Donnelly LF, Klosterman LA. Am J Roentgenol Jul 1997; 169(1):179–182.
58. Donnelly LF. Radiol Clin North Am Mar 2005; 43(2):253–265.
59. Tu CY, Hsu WH, Hsia TC et al. Chest Oct 2004; 126(4):1274–1280.
60. Mitri RK, Brown SD, Zurakowski D et al. Pediatrics Sep 2002; 110(3):e37.
61. Shoseyov D, Bibi H, Shatzberg G et al. Chest Mar 2002; 121(3):836–840.
62. Cameron R, Davies HR. Cochrane Database Syst Rev 2008(2):CD002312.
63. Avansino JR, Goldman B, Sawin RS, Flum DR. Pediatrics Jun 2005; 115(6):1652–1659.
64. Thomson AH, Hull J, Kumar MR, Wallis C, Balfour Lynn IM. Thorax Apr 2002; 57(4): 343–347.
65. Luh SP, Chou MC, Wang LS, Chen JY, Tsai TP. Chest Apr 2005; 127(4):1427–1432.
66. Coley BD. Radiol Clin North Am Mar 2005; 43(2):405–418.
67. Coskun A, Koc A, Yikilmaz A. Comparison of MRI with short imaging sequences and CXR for evaluation of pneumonia in pediatric patients. Program and abstracts of the Radiological Society of North America 93rd Scientific Assembly and Annual Meeting. Chicago:2007.

28

Imaging of Asthma in Children

D. Gregory Bates

Issues

I. Are chest radiographs indicated in patients with acute asthma?
II. What are the radiographic findings of importance in uncomplicated versus complicated asthma?
III. What is the role of CT in patients with asthma?

Key Points

- Airway inflammation is universal to all asthmatics and the degree of the inflammation corresponds to the severity of disease. Bronchoconstriction plays a limited role in the etiology of asthma (moderate evidence).
- There has been a sharp rise in the prevalence, morbidity, mortality, and economic burden both within the United States and globally over the past 40 years, particularly in children (moderate evidence).
- Despite the considerable knowledge with regard to the pathology of asthma, the costs of asthma represent a large burden to society, both nationally and internationally (moderate evidence).
- The majority of patients presenting with asthma can be diagnosed clinically by medical history and physical examination; the need for chest radiographs in acute asthma is limited to a minority of patients (limited to moderate evidence).
- Pulmonary function testing underestimates the degree of bronchial inflammation and may be insufficient for surveillance criteria (limited evidence).

D.G. Bates (✉)
Department of Radiology, The Ohio State University College of Medicine and Public Health, Nationwide Children's Hospital, Columbus, OH 43205, USA
e-mail: david.bates@nationwidechildrens.org

L.S. Medina et al. (eds.), *Evidence-Based Imaging in Pediatrics*,
DOI 10.1007/978-1-4419-0922-0_28, © Springer Science+Business Media, LLC 2010

- No data were found in the medical literature that evaluate the cost-effectiveness of imaging in asthma (insufficient evidence).
- The value of the chest radiograph should be to diagnose complications, to establish a precipitating cause for an asthmatic attack, and to exclude alternate diagnoses that resemble asthma (moderate evidence).
- High-resolution computed tomography (HRCT) is a non-invasive technique capable of demonstrating and quantifying both the anatomic and physiologic changes in the lungs of asthmatic patients (moderate evidence).

Definition and Pathophysiology

Following the initial description by Sir William Osler (1) in 1892, the definition of asthma has been frequently revised throughout the past century as our understanding of asthma's complex pathophysiology continues to evolve. In infancy, there continues to be limited information about the underlying immunopathology of asthma. Beyond the age of 3 years, the diagnosis of asthma becomes progressively more defined (2). Beyond 6 years, the definition of asthma, defined by the National Heart, Lung, and Blood Institute (NHLBI) in 1997, is accepted as "a chronic inflammatory disorder of the airways in which many cells and cellular elements play a role, in particular, mast cells, eosinophils, T lymphocytes, macrophages, neutrophils, and epithelial cells. In susceptible individuals, this inflammation causes recurrent episodes of wheezing, breathlessness, chest tightness, and coughing, particularly in the night or in the early morning. These episodes are usually associated with widespread but variable airflow obstruction that is often reversible either spontaneously or with treatment. The inflammation also causes an associated increase in the existing bronchial hyperresponsiveness to a variety of stimuli" (3, 4). Any or all of these features may be present in the asthmatic patient, although the absolute minimum criterion for the diagnosis of asthma remains controversial.

Over the last decade, our understanding of the pathophysiology of asthma has progressed rapidly. Once thought to be a primary disorder of smooth muscle, asthma is now recognized primarily as an inflammatory disease in which the airway architecture is modified by cellular inflammation, smooth muscle and myofibroblastic hyperplasia, goblet cell hyperplasia, and reorganization of the extracellular matrix resulting in subepithelial fibrosis. This inflammatory process represents an inappropriate immune response to common allergens in genetically susceptible individuals. The inflammatory response in the asthmatic lung is characterized by infiltration of the bronchial mucosa by mast cells, lymphocytes, and eosinophils. Activation of these cells results in a cascade of inflammatory mediators that individually or in concert induce changes in the airway geometry and produce the symptoms of the disease. This inflammatory response is the primary cause of airway hyperreactivity and variable airway obstruction characteristic of asthma. Airway inflammation is universal to all asthmatics and the degree of the inflammation corresponds to the severity of disease.

T lymphocytes are the primary mediators of the allergic inflammatory response in asthmatics. Following presentation of the antigen to the T cells, a unique set of cytokines is produced, of which the interleukins (IL) play a significant role. These interleukins are responsible for the stimulation of mucosal mastocytosis, eosinophilia, and IgE production. Mast cell degranulation releases vasoactive mediators, chemotactic factors, and cytokines that enhance activation of inflammatory cells, cause microvascular leakage, increase mucous production, and induce bronchoconstriction. Eosinophils induce hyperresponsiveness in the airways by direct cytotoxic injury to epithelial cells, which normally produce enzymes that degrade the neuropeptides responsible for airway tone, as well as epithelial-derived relaxing factor. This antigenic stimulation of cytokines

appears to be genetically controlled and is established during early childhood. Asthma is linked to a region of chromosome 5q, on which the genes for IL-4, IL-5, and IL-13 are localized (5).

Epidemiology

There has been a sharp increase in the prevalence, morbidity, mortality, and economic burden both within the United States and globally over the past 40 years, particularly in children. Currently, approximately 300 million people worldwide have asthma, with the prevalence rate increasing by 50% every decade. In children (defined as ages 0–17 years), prevalence rates of >10% are now seen in developed countries, which increases to >30% in developing regions of the world. In North America, 10% of the population has asthma, approximately 35.5 million individuals (6, 7). In 1997, the National Health Interview Survey (NHIS) redesigned the household survey that served as the primary source of national asthma prevalence estimates. This redesign created a break in the time series and therefore has complicated assessment of recent trends in asthma prevalence. The previous trend of increasing asthma-associated morbidity and mortality that occurred during the period from 1980 to 1995 appears to have plateaued for certain measures (8–10).

The most recent statistics released by the National Center for Health Statistics (NCHS) in 2005 estimate the *current asthma* prevalence at approximately 7.7% of the US population (22.2 million people). Rates are lower in higher age groups: 8.9% of children (6.5 million) had asthma compared to 7.2% of adults (15.7 million). In children, asthma prevalence has increased from 3.6% in 1980. Asthma prevalence for boys (10%) is 30% higher than that for girls (7.8%). The gap between African-Americans and white non-Hispanic children has progressively widened from 15% higher asthma prevalence in 1980–1981, 26% higher in 1995–1996, to 44% higher in 2000. Children aged 0–4 years had the most rapid growth in asthma prevalence during this time period (9, 11).

Asthma Attack Prevalence

Asthma attack prevalence measures the percentage of the populations who had at least one attack over the past 12 months. It is a rough estimate of the percentage of symptomatic persons, at a given point in time, who may have poorly controlled asthma and are therefore at risk of adverse outcomes such as emergency department visits or hospitalization (11). Currently, there are no national measures of asthma incidence or the rate at which people develop asthma over a period of time. The current asthma attack prevalence is estimated at 4.2% of people (12.2 million). Among those with asthma, about 55% had at least one asthma attack in the previous year. Asthma attack prevalence is lower in older age groups: 5.2% of children (3.8 million) compared to 3.9% of adults (8.4 million). Males (5.9%) have an asthma attack rate 30% higher than females (4.5%) (11). In children, the asthma attack prevalence remained stable from 1997 to 2000 (9).

Lifetime Asthma Diagnosis

Lifetime asthma diagnosis (ever been diagnosed as having asthma by a physician) is estimated at 11.2% of people, encompassing 23 million adults and 9 million children. Among all race and ethnicity groups, Puerto Ricans are 95% more likely to have ever been diagnosed with asthma than non-Hispanic Caucasians. Mexicans have the lowest lifetime asthma risk. When considering race only, African-Americans are about 20% more likely to be diagnosed with asthma than Caucasians. In children 0–17 years, males (14.6%) were more likely to have an asthma diagnosis than females (10.6%) (11).

The Center for Disease Control (CDC) report on the asthma morbidity and mortality rates from 1960 to 1995 demonstrated an increasing trend in missed days of school and work, and racial disparities in asthma emergency department visits, hospitalizations, and deaths (12). These statistics have been most recently corroborated by the NCHS, who estimate school days missed due to asthma in children 5–17 years to be 12.8 million days in 2003 (11). In 2004, children had 7.0 million visits to a physician's office or hospital outpatient department (950

visits/10,000 population), and emergency department (ED) visits totaled 754,000 (103 visits/10,000 population). Hospitalizations for childhood asthma totaled 198,000 (27 hospitalizations/10,000 population). The asthma death rate for children had increased 3.4% per year from 1980 to 1998, but recent trends show a decline in asthma deaths to 186 (2.5 deaths/1,000,000 population) in 2004. Risk factors associated with a higher rate of outpatient visits, emergency room visits, and hospitalizations include younger age, female sex, and African-American race. Mortality risks are higher in older children (11–17 years), male sex, and African-American race (11, 13).

Overall Cost to Society

No cost-effectiveness data were found in the medical literature incorporating imaging strategies for the management of asthma. In the United States, the total direct costs (medications, office, and emergency room visits, and hospitalization) and indirect costs (loss of school or work days, lost productivity, restricted activity, and premature retirement) of asthma have increased from approximately 4.5 billion dollars in 1985 to 12.7 billion dollars in 1998. Current estimates show the direct costs accounted for 58% and the indirect costs 42% of the total expenditure (14). Notable changes reflected during this period include a decrease in hospitalization costs (reflecting a decrease in the length of stay and not a decrease in the total number of admissions), and medication costs have replaced hospital costs as the largest component of the direct costs. The average estimate in annual cost per adult with asthma increased 2.9% during this time period, but the cost per child decreased by 15.5%. The reason for this pattern may reflect increasing asthma prevalence in patients with milder disease (15).

Emergency room visits and hospitalizations are major expenditures related to asthma care. The economic burden of asthma disproportionately affects those with the most severe disease (16). In a survey of approximately 35,000 patients, Malone et al. in 1987 found that less than 20% of patients with severe asthma were responsible for greater than 80% of the total direct costs (17). Hospitalizations made up more than 74% of direct expenditures related to asthma care for children 0–4 years of age. Hospitalization expenditures are proportionately the lowest for children 5–17 years of age, but they tend to use more medication and ER services (17).

Although our understanding of the pathophysiology of asthma continues to evolve, the fundamental cause for the disorder and reasons for its increased prevalence remain largely unknown. Allergic sensitization, genetics, and environmental influences all play a role in the development of the disease in susceptible individuals (6, 7). The rising costs of asthma represent a large burden to society, both nationally and internationally. As the direct and indirect costs of asthma continue to rise, the field of health economics has shifted toward how to best utilize available resources and therapeutic strategies to improve care (14). Because only a small proportion of those with asthma are consuming the majority of resources, interventions aimed at these high-cost patients could be an effective strategy in reducing the morbidity and cost of asthma (18). Non-invasive methods that could identify disease and allow introduction of earlier, more effective treatment are needed to curtail the current trends in asthma.

Methodology

A MEDLINE search was performed using Ovid for original research publications discussing the performance and effectiveness of imaging strategies in asthma. The search covered the years 1959 to October 2007. The search strategy employed different combinations of the following terms: (1) *asthma*, (2) *children, age's under 18 years*, (3) *diagnostic imaging*, (4) *economic costs*, and (5) *prevalence*. Additional articles were identified by reviewing the reference lists of relevant papers, identifying appropriate authors, and using citation indices for MeSH terms. This review was limited to human studies and the English language literature. The author performed an initial review of the titles and abstracts of the identified articles followed

by the review of the full text in articles that were deemed relevant.

Discussion of Issues

I. Are Chest Radiographs Indicated in Patients with Acute Asthma?

Summary of Evidence: There is considerable debate in the literature regarding the usefulness of the chest radiograph in the management of the pediatric patient with asthma. The majority of patients presenting with asthma can be diagnosed clinically by medical history and physical examination and tend to respond rapidly to bronchodilator therapy, thus suggesting that chest X-ray is needed in a minority of patients (19) (moderate evidence). The chest radiograph plays a limited role in establishing the diagnosis of asthma, although a variety of manifestations of the disease may be visible on chest radiographs in a significant number of patients. The value of the chest radiograph is in diagnosing complications, establishing a precipitating cause for an attack, and excluding alternate diagnoses that resemble asthma (20).

Supporting Evidence: Prior to the early 1980s, the chest radiograph was considered to play an important role in the evaluation of pediatric asthma (21–30). Recommendations from this cohort of studies were principally derived from hospitalized patients. Abnormal chest radiographs were identified in 43–76% of children hospitalized with asthma (21, 23, 29). When hyperinflation was excluded, radiographic abnormalities were identified in 21–31% of patients, parenchymal consolidation being the most commonly reported complication. Despite the fact that the majority of the radiographs were normal or had no affect on patient management, these early studies concluded that chest radiography made a significant contribution in the evaluation of the hospitalized child with asthma and therefore should be routinely obtained in all patients on admission in order to guide subsequent therapy. These studies provided early, but limited, information on the contribution of chest radiographs in the management of children hospitalized with asthma.

Following the early 1980s, a shift occurred in the recommendation for the chest radiograph as a routine diagnostic procedure in the patient with acute asthma (19, 31–39). These studies evaluated the asthmatic patient and the need for chest radiographs in three major clinical scenarios: the newly diagnosed asthmatic, the emergency room patient, and those requiring hospitalization.

In the outpatient setting, Gershel et al. evaluated the value of the routine chest radiograph in children during acute first attacks of asthma. Radiographs of 5.7% had positive findings other than those seen in uncomplicated asthma. They concluded that for the vast majority of children with a first episode of wheezing, routine chest radiography does not add information that appreciably alters the care of the patient or leads to the diagnosis of unsuspected but clinically important disease in children over 1 year of age (34) (moderate evidence). Hederos et al. studied 60 preschool children (0–6 years old) with newly diagnosed asthma and with relatively greater risk for permanent illness. Seven (11%) of the patients had abnormal X-rays, but none of the findings led to any change in the treatment and all follow-up radiographs were normal (39) (limited evidence).

In the emergency room setting, Rushton compared chest radiographic abnormalities in 391 asthmatic patients treated successfully in the emergency room versus those requiring hospitalization. They found no differences in the radiographic abnormalities between the two groups. The information obtained from the chest X-ray "did not provide sufficient data to alter the acute emergency room management of those asthma patients successfully treated as outpatients or those failing to respond and requiring hospitalization" (32) (moderate evidence). Dalton reviewed the radiographic abnormalities in 135 patients presenting to the emergency room with acute asthma exacerbation. Significantly abnormal radiographs were identified in 15% of children, greater than 50% of these representing pneumonia. They concluded that the need for chest radiography in the management of acute asthma is indicated only after careful clinical evaluation and if there is little or no known improvement after initial treatment (35) (moderate evidence). Tsai et al. conducted a prospective study comparing 445

hypoxemic patients (oxygen saturation <93% on room air) versus non-hypoxemic emergency room patients presenting with an acute asthma exacerbation. While radiographic abnormalities were statistically more common in hypoxemic asthmatics compared to those who were non-hypoxemic, there was no statistical association between any radiographic finding in hypoxemic asthmatics and duration of hypoxemia, hospital length of stay, and admission to the Pediatric Intensive Care Unit (PICU) (38) (moderate evidence).

In the hospital setting, Brooks et al. evaluated 128 asthmatic children hospitalized following failed emergency room treatment. The total incidence of radiographic abnormalities was 64.1%, but only 4.7% were compatible with pneumonia. The chest radiograph was recommended in particularly ill-appearing patients, those failing to respond appropriately to standard emergency room therapy, or if the diagnosis was anything other than uncomplicated asthma (31) (moderate evidence). Dawson and Capaldi evaluated 100 children hospitalized for acute asthma attacks who had a chest X-ray versus 100 children who did not have a chest X-ray. The two groups were matched for age, sex, severity of illness, and in clinical measures of disease. Their findings suggest that the age of the child, time or day of the week at presentation, or severity of the illness did not determine the decision to order a routine X-ray in acute asthma. "The lack of written information about the indication for and the results of the film in the records suggest that the ordering of a chest film is a reflex action, with little thought being given to its value. Ordering of a routine chest X-ray appears to be an ineffective and inefficient use of radiology and an unnecessary expense" (36) (moderate evidence).

Buckmaster and Boon in a retrospective review designed criteria on when *not* to order a chest radiograph in children presenting with acute asthma as opposed to the majority of the literature which typically evaluates the yield of the chest radiograph (how many CXR showed a positive finding). A chest radiograph was considered unnecessary when *all* of the following criteria were met:

1. The child was a known asthmatic.
2. The assessing doctors' diagnosis was asthma.
3. The child was responding to asthma therapy.
4. There was no suspicion of pneumothorax documented by the physician.
5. The child was not admitted to the intensive care unit.

In the 12 months prior to implementation of the guidelines, 466 children were evaluated for acute asthma. Two hundred and sixty patients had a CXR, of which 211 (81.1%) were deemed unnecessary when the criteria were applied. During the 6-month period following the implementation of the program, 197 children presented with acute asthma. Seventy-two had a chest radiograph, of which 56 (78%) were deemed unnecessary. However, the percentage of all children presenting with asthma who had unnecessary chest radiographs fell from 45.3% (211/466) to 28.4% (56/197). If the guidelines had been adhered to completely, the number of patients undergoing chest radiography in the after group would have fallen to 16/197 (8%). Failure to follow guidelines includes uncertainty in diagnosis, fears of litigation, desire to move children through the emergency department, the ready availability of the test, and many others. These authors showed that an unacceptably high rate of unnecessary chest radiographs are ordered in patients presenting to the ED with asthma and that through an educational program a statistical reduction in the rate of ordering radiographs can be achieved (19) (moderate evidence).

II. What Are the Radiographic Findings of Importance in Uncomplicated Versus Complicated Asthma?

Summary of Evidence: A number of radiographic findings have been associated with asthma. The findings can be classified into two main categories as follows: (1) those that are not critical to patient management (*uncomplicated asthma*—hyperinflation, peribronchial thickening, streaky or subsegmental atelectasis, and transient pulmonary hypertension) and (2) those that are critical to patient management (*complicated asthma*—lobar atelectasis, pneumonia, pneumomediastinum, and pneumothorax) (34, 40). A wide variation in the

incidence of abnormal radiographic findings is reported in the literature, depending on both the population studied (hospitalized versus non-hospitalized) and the inclusion or exclusion of non-critical radiographic abnormalities.

Supporting Evidence

Uncomplicated Asthma

Hyperinflation is the most common abnormality and is identified radiographically as hyperexpansion, flattening of the diaphragms, increased retrosternal lucency, anterior bowing of the sternum, and bulging of the intercostal rib spaces (41). The reported incidence in hospitalized patients ranges from 12 to 72% (25, 27–29, 31, 37) and from 5 to 48% (26, 30, 32, 35, 38) in the emergency room. Hyperinflation may fluctuate rapidly as the asthma worsens or is relieved and is occasionally found during symptom-free periods (25). There is poor correlation between the degree of hyperinflation and the severity of the asthma attack (29, 40) or the patient's responsiveness to therapy (32, 40). Simon et al. reported that 95% of the radiographs were normal in patients with intermittent asthma, but only 66% were normal in patients with constant asthma (26) (moderate evidence).

Bronchial wall thickening is usually transient and represents visibility of the walls of secondary bronchi beyond the mediastinum, resulting in parallel line shadows or ring shadows when seen on end. This finding is not specific to asthma and can be identified in infection, bronchiectasis, cystic fibrosis, and pulmonary edema (40). Bronchial wall thickening is more common in asthmatic patients with superimposed acute viral infections and in those with constant asthma (20). Viral infections are in fact the most common cause of acute asthma attacks and hospitalization for asthma in the pediatric age group, and it is likely that the peribronchial thickening and "infiltrates" seen on radiographs are related to the viral infection that precipitated the attack (28, 40). The reported incidence of bronchial wall thickening varies between 11 and 85% (26, 28, 31, 32, 38). Brooks et al. reviewed 128 hospitalized patients and grouped the patients into five categories based on radiographic findings. Peribronchial thickening was equally distributed among all groups, had no effect on patient management, and therefore was not considered a significant radiologic abnormality (31) (moderate evidence).

Prominent perihilar vascular markings are more often seen in pediatric than adult asthmatics (40). The etiology is believed to be transient pulmonary hypertension (40), although no clinical, electrocardiographic, or cardiac catheterization data are available to confirm or exclude this theory (20). Simon et al. reported that 12% of patients with moderate to severe constant asthma had a combination of overinflation and enlarged hilar vessels (26) (moderate evidence).

Atelectasis results from bronchial obstruction, most often as a consequence of mucous plugging. Children have a smaller caliber and reduced elastic recoil of inflamed airways, and reduced number and size of the pores of Kohn and canals of Lambert (40). Both result in an increased likelihood of mucous plugging and more frequent atelectasis, respectively. The spectrum of atelectasis ranges from microscopic to multilobar. Involvement of only part of one or more lobes results in linear or discoid atelectases that resemble viral infection (20). This subsegmental atelectasis is regarded as a noncritical finding, whereas segmental or lobar atelectasis is a critical finding (34). Atelectasis is seen more frequently in younger children (28, 32), with a reported incidence of approximately 3–36% (28, 29, 31–34, 38) (limited to moderate evidence).

Complicated Asthma

The most frequent finding in complicated asthma is pneumonia. Bacterial infection has no statistical association with wheezing, unlike the common association with viral infections, respiratory syncytial virus (RSV) in infants, and parainfluenza, rhinovirus, and mycoplasma in older children. While bacterial colonization occurs in chronic asthmatics, there is no correlation between colonization and acute asthma exacerbation in children or adults (41). The reported radiographic incidence of pneumonia (airspace disease or parenchymal consolidation) in both inpatients and outpatients ranges from 0 to 31% (21–23, 27–35, 37–39) (limited to moderate evidence). Early studies reported the highest incidence of pneumonia (20–31%) in children with asthma requiring

hospitalization (21–23, 28, 29), although these articles poorly differentiated bacterial and viral pneumonias and atelectasis as a cause of consolidation.

The reported incidence of pneumomediastinum varies between 0 and 15% of patients and may be underreported (28). There is a bimodal distribution peaking at ages 4–6 and 13–18 years (40). The extent of the pneumomediastinum correlates with the severity of the attack (40). The postulated mechanism of pneumomediastinum is mucous plugging or infection that causes a check valve obstruction that increases intraalveolar pressure during a deep inspiration, cough or Valsalva maneuver resulting in alveolar rupture. The interstitial air dissects along the perivascular sheaths toward the hilum and ruptures into the mediastinum (40). Eggleston et al. reported that 15% of patients over the age of 10 years developed pneumomediastinum while none were seen less than 2 years of age. They speculated that older patients are able to generate higher intrathoracic pressures, and because their respiratory rates are generally lower than younger patients, these pressures are maintained over longer periods and could be responsible for their susceptibility to mediastinal emphysema (28) (moderate evidence).

Pneumothorax is an uncommon occurrence in asthmatics, with a reported incidence of 0–3% of patients (25, 28, 31, 34, 35, 37, 41, 42). Pneumothorax occurs following rupture of alveoli along the pleural surface permitting escape of air directly into the pleural space. The pleura ruptures at transpulmonary pressures of 200 mm of mercury, a tension not attained by forced expiration even in the most severe paroxysms of coughing. In severe chronic asthma, the pleura becomes thinner and may rupture with sudden increases in transthoracic pressure, such as excessive positive pressure ventilation (43) (limited to moderate evidence). Pneumothorax may occur in association with pneumomediastinum, is more frequent in patients with long-standing disease, is responsible for a significant mortality in intubated asthmatics on positive pressure ventilation, and has a higher recurrence rate in patients with a history of previous pneumothorax. Sudden death may occur secondary to massive lung collapse (40).

III. What Is the Role of CT in Patients with Asthma?

Summary of Evidence: HRCT of the lungs can provide useful information about many diffuse lung diseases and can allow a specific pulmonary diagnosis with a reasonable degree of confidence (44). HRCT manifestations of asthma include bronchial wall thickening, narrowing of the bronchial lumen, regions of decreased attenuation and vascularity on inspiratory scans and air trapping on expiratory scans, bronchiectasis, emphysema, atelectasis, pneumonia, and mucoid impaction (45). Expiratory CT provides complementary information to that of both conventional full-inspiration CT and pulmonary function testing. Expiratory CT scanning is the most sensitive means of detecting subtle air trapping and may aid in directing further diagnostic workup. Combining suspended full-inspiration and end-expiration CT reveals the major physiologic consequences of airway diseases, particularly diseases of smaller airways beyond the segmental branches (46) (moderate evidence).

Supporting Evidence: Chronic inflammation heals through a remodeling process that leads to structural changes of the airways in asthmatic patients. The remodeling process involves thickening of the airway by fibrosis and an increase in smooth muscle and mucous gland mass (45). Airway inflammation is difficult to measure directly in children. Pulmonary function tests are indirect measure of inflammation and are made inaccurate by variable bronchoconstriction over time. Bronchoalveolar lavage with fiberoptic bronchoscopy is problematic in children, and tissue biopsy is rarely performed in clinical practice. There is no well-established method of assessing the activity of inflammation in children's lungs as a means to guide treatment of asthma with anti-inflammatory agents (47). HRCT is capable of demonstrating both the anatomic and physiologic changes in the lungs of asthmatic patients. Thin-section CT is able to resolve anatomic details of the lung on the order of 0.2–0.3 mm, corresponding to bronchial wall thickness of 0.2 mm and a diameter of 2 mm or larger. This represents the proximal seventh to ninth airway generations (48).

Nuhoglu et al. was the first to report the HRCT findings in 16 asthmatic children not responding as expected to inhaled steroids with or without persistent auscultatory findings. Chest radiographs were abnormal in 9 (56%) patients and HRCT was abnormal in 12 (75%) patients. Irreversible findings on HRCT included bronchiectasis, bronchial wall thickening, and fibrotic retractions. They concluded that thoracic HRCT scanning may be a helpful adjunct in the evaluation of a child with asthma and atypical clinical findings (49) (limited evidence).

Ketai et al. evaluated bronchial wall thickening with low-dose HRCT in 18 age-matched control patients and 21 children with moderately severe but stable asthma during periods free from clinical bronchoconstriction in an attempt to define the presence of bronchial wall thickening due to airway remodeling. Bronchoconstriction causes apparent bronchial wall thickening by decreasing the diameter of the bronchus, thereby increasing the wall thickness relative to the bronchial size. Bronchial wall thickness and bronchial wall area were measured and the percentage wall area (bronchial wall area divided by bronchial cross-sectional area) was calculated. Both quantitative measurements and qualitative assessment of HRCT scans demonstrated asthmatic subjects to show a greater wall thickness to outer bronchial diameter and asthmatic airways with an outer diameter of 6–10 mm to have a greater wall thickness than similar-sized airways in healthy subjects. They concluded that moderate to severe stable asymptomatic asthmatics have evidence of bronchial wall thickening, independent of a physiologic bronchodilator response, that is related to airway inflammation or remodeling rather than bronchoconstriction (47) (moderate evidence).

Pifferi et al. in a prospective study evaluated whether 32 asthmatic children with increased residual volume (RV) after 3 months of anti-inflammatory treatment correlated with the detection of low-density areas on HRCT (similar to emphysema) that might indicate bronchiolar remodeling. Functional tests such as RV have been shown to correlate with air trapping measured by quantitative HRCT in adults with asthma. HRCT evaluation in adult studies has shown persistence of low lung density after acute asthmatic attacks and after prolonged treatment with corticosteroids. The HRCT findings resemble emphysema, although the low-attenuation areas were probably not caused by alveolar disruption but by extensive peribronchial fibrosis with cicatricial emphysema and loss of lung recoil. Both the inspiratory and expiratory HRCT were abnormal in 10 (31.2%) children showing persistent low-density areas despite normalization of pulmonary function test (PFT) values and a significant reduction in eosinophilic cationic protein (ECP), an inflammatory marker particularly valuable for monitoring chronic asthma during steroid therapy. This study is the first to identify that there may be structural changes in the lung in chronic pediatric asthma patients not readily detectable by pulmonary function testing (50) (moderate evidence).

Marchac et al. evaluated bronchial wall thickening on HRCT in children with difficult-to-treat asthma and persistent symptoms despite treatment. Children with this condition are likely to have bronchial inflammation and therefore to have a greater risk of remodeling. HRCT findings were compared with clinical status and lung function data. Twenty-seven patients with moderate and severe asthma were compared to 21 age-matched control patients. A bronchial wall thickening score was devised based on the number of visible bronchi at three determined levels on HRCT. Bronchial wall thickening scores were similar in the moderate and severe asthmatic groups but significantly higher than the control group. This persistence of inflammation in patients with difficult-to-treat asthma and persistent symptoms therefore subjects patients to a higher risk of permanent remodeling and sequelae. Like Pifferi et al. (50), they also found no correlation between HRCT scores and respiratory function, including FEV_1 (reflecting proximal bronchial obstruction) and $FEF_{25–75}$ (reflecting obstruction of small airways). Since the fundamental criterion for the non-invasive surveillance and adaptation of asthma treatment is respiratory function, pulmonary function testing may underestimate the degree of bronchial inflammation and thus be insufficient for surveillance. In contrast to adults with severe asthma, no mucoid impaction, emphysema, areas of hyperlucency, bronchiectasis, or sequellar line shadows were

identified. They concluded that HRCT could be used in association with clinical and lung function data to assess the severity in patients with persistent asthma, to identify patients with a higher risk of subsequent airway remodeling, and to assist in decision-making to optimize treatment of inflammation (51) (moderate evidence).

De Blic et al. in a prospective pilot study evaluated 37 children with severe asthma to determine if bronchial wall thickening on HRCT correlates with markers of bronchial inflammation and remodeling. Using the same bronchial wall thickness scoring system as developed by Marchac et al. (51), a significant correlation was identified between bronchial wall thickening and reticular basement membrane (RBM) thickening on endobronchial biopsy and exhaled nitrous oxide production (eNO) by the airway wall as measured by chemiluminescent NO analyzer. Thickening of the lamina reticularis is diagnostic of asthma and appears to reflect thickening of the entire airway wall, including the airway smooth muscle. Increased eNO has both relaxation and antiproliferative effects on airway smooth muscle and may reflect an adaptive response to the airway remodeling. This is the first study to suggest a concordance between radiologic findings and a classic parameter of remodeling (RBM thickness) as well as a relatively new marker (eNO). HRCT scanning is a non-invasive technique that might prove valuable for quantifying airway remodeling in children with severe asthma (52) (moderate evidence).

Take Home Tables

Tables 28.1 and 28.2 discuss indications for chest radiograph and HRCT in asthma, respectively.

Table 28.1. Indications for chest radiograph in asthma

1. Acute onset of wheezing with no prior history of asthma
2. Severe asthma (status asthmaticus) or poor response to treatment
3. Clinical suspicion for complicated asthma
4. Prior to intubation and positive pressure ventilation

Table 28.2. Indications for HRCT in asthma

1. Asthma and atypical clinical manifestations
2. Poor response to bronchodilators or conventional inhaled corticosteroid therapy
3. Patients with high risk for airway remodeling
4. Assessment of bronchial inflammation as a means to optimize treatment and evaluate efficacy of treatment

Imaging Case Studies

Case 1

Figure 28.1 presents a case of a 3-year-old male with asthma with cough, wheezing, and hypoxia.

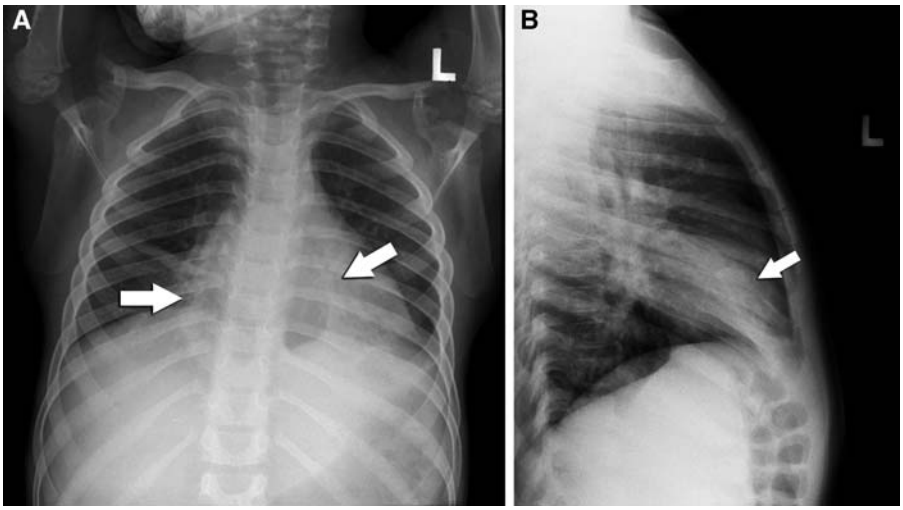

Figure 28.1. A 3-year-old male with asthma presenting with cough, wheeze, and hypoxia. Frontal (**A**) and lateral (**B**) radiographs of the chest demonstrating peribronchial thickening and subsegmental atelectasis (*arrows*) of the right middle lobe and left lower lobe. Radiographs demonstrate findings of uncomplicated asthma.

Case 2

Figure 28.2 presents the case of a 4-year-old female with poorly controlled asthma.

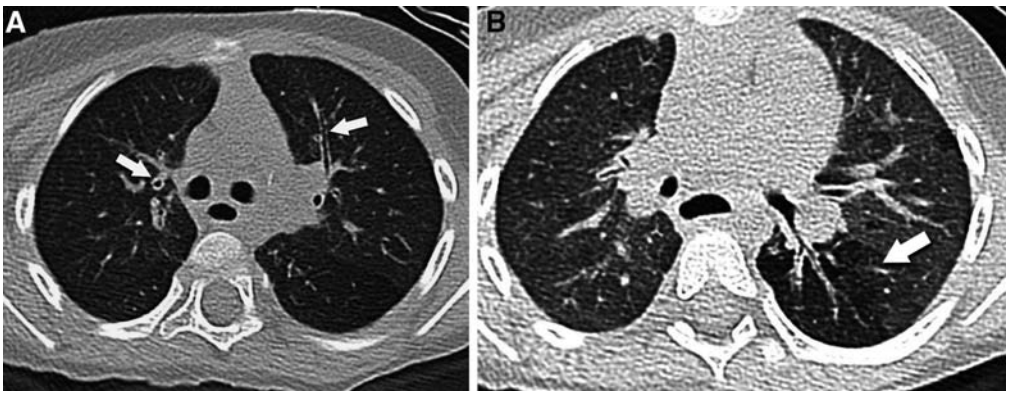

Figure 28.2. A 4-year-old female with poorly controlled asthma. Single-slice HRCT of the chest during inspiration (**A**) demonstrates bilateral, central bronchial wall thickening (*arrows*). Similar HRCT slice obtained in expiration (**B**) demonstrates segmental air trapping in the superior segment of the left lower lobe (*arrow*).

Suggested Protocol for Imaging for Asthma in Children

Chest Radiograph

For children that can stand or sit upright: PA and lateral radiograph. For other children and infants: supine AP and lateral radiograph.

HRCT

HRCT is performed without the need for intravenous contrast and at low radiation dose compared to conventional chest CT. High resolution is simply thinner axial and coronal reconstructions ($\leq$ 2 mm) from a volumetric acquisition of images during full-inspiration breath-hold. Selective 1–2 mm axial slices could then be obtained in full expiration to improve detection of air trapping. Lower kVp and mAs settings can be used and this depends on the size of the child: infants and young children: 90–100 kVp and 20–50 mAs; older children: 110–120 kVp and 50–75 mAs.

Future Research

- Is there a role for MRI of lung function or to assess lung volumes in asthmatics (which avoids ionizing radiation)?
- When is the lateral chest radiograph valuable in children with uncomplicated and complicated asthma?

References

1. Osler W. The Principles and Practice of Medicine. New York: D Appleton and Company, 1892.
2. Warner JO, Naspitz CK. Pediatr Pulmonol 1998 Jan; 25(1):1–17. Review.
3. National Asthma Education and Prevention Program. *Expert Panel Report 2: Guidelines for the Diagnosis and Management of Asthma*. National Institutes of Health Publication No. 97-4051. Bethesda, MD, 1997.
4. National Asthma Education and Prevention Program. *Expert Panel Report: Guidelines for the Diagnosis and Management of Asthma*. National Institutes of Health Publication No. 91-3642. Bethesda, MD, 1991.
5. Willis-Karp M. Annu Rev Immunol 1999; 17:255–281. Review.
6. Bramam SS. Chest 2006 Jul; 130(1 Suppl):4S–12S. Review.
7. Masoli M, Fabian D, Holt S et al. Allergy 2004; 59:469–478.
8. From the Centers of Disease Control and Prevention. MMWR Morb Mortal Wkly Rep 2000; 49(40):908–911.
9. Akinbami LJ, Schoendorf KC, Parker J. Am J Epidemiol 2003; 158(2):99–104.
10. From the Centers for Disease Control and Prevention. JAMA 2000; 284(18):2312–2313.
11. Akinbami L. Adv Data 2006 Dec 12;(381): 1–24.
12. Mannino DM, Homa DM, Pertowski CA et al. MMWR CDC Surveill Summ 1998; 47(1):1–27.
13. Akinbami LJ, Schoendorf KC. Pediatrics 2002 Aug; 110(2 Pt 1):315–322.
14. Weiss KB, Sullivan SD. J Allergy Clin Immunol 2001; 107:3–8.
15. Weiss KB, Sullivan SD. J Allergy Clin Immunol Sept 2000.
16. Stanford R, McLaughlin T, Okamoto LJ. Am J Respir Crit Care Med 1999; 160:211–215.
17. Malone DC, Lawson KA, Smith DH. Pharm Pract Manage Q 2000; 20:12–20.
18. Smith DH, Malone DC, Lawson KA et al. Am J Respir Crit Care Med 1997; 156:787–793.
19. Buckmaster A, Boon R. J Paediatr Child Health 2005 Mar; 41(3):107–111.
20. Alford BA, Armstrong P. Curr Probl Diagn Radiol 1983 May–Jun ; 12(3):1–38.
21. Royle H. Br Med J 1952 Mar 15; 1(4758): 577–580.
22. Richards W, Patrick JR. Am J Dis Child 1965 Jul; 110:4–23.
23. Dworetsky M, Philson AD. J Allergy 1968 Apr; 41(4):181–194.
24. Simon G. In: Principles of Chest X-ray Diagnosis, 3rd ed. London: Butterworths.
25. Rebuck AS. Australas Radiol 1970 Aug; 14(3):264–268.
26. Simon G, Connolly N, Littlejohns DW et al. Thorax 1973 Mar; 28(2):115–123.
27. Hodson ME, Simon G, Batten JC. Thorax 1974 May; 29(3):296–303.
28. Eggleston PA, Ward BH, Pierson WE et al. Pediatrics 1974 Oct; 54(4):442–449.
29. Gillies JD, Reed MH, Simons FE. Can Assoc Radiol 1978 Mar; 29(1):28–33.
30. Gillies JD, Reed MH, Simons FE. J Can Assoc Radiol 1980 Mar; 31(1):45–47.
31. Brooks LJ, Cloutier MM, Afshani E. Chest 1982 Sep; 82(3):315–318.
32. Rushton AR. Clin Pediatr (Phila) 1982 Jun ; 21(6):325–328.
33. Zieverink SE, Harper AP, Holden RW et al. Radiology 1982 Oct; 145(1):27–29.

34. Gershel JC, Goldman HS, Stein RE et al. N Engl J Med 1983 Aug 11; 309(6):336–339.
35. Dalton AM. Arch Emerg Med 1991 Mar; 8(1):36–40.
36. Dawson KP, Capaldi N. Aust Clin Rev 1993; 13(4):153–156.
37. Ismail Y, Loo CS, Zahary MK. Singapore Med J 1994 Apr; 35(2):171–172.
38. Tsai SL, Crain EF, Silver EJ et al. Pediatr Radiol 2002 Jul; 32(7):498–504. Epub 2002 Mar 29.
39. Hederos CA, Janson S, Andersson JS et al. Pediatr Allergy Immunol 2004 Apr; 15(2):163–165.
40. Blair DN, Coppage L, Shaw C. J Thorac Imaging 1986 Mar; 1(2):23–35.
41. Joregensen JR, Falliers CJ, Bukantz SC. Pediatrics 1963 May; 31:824–832.
42. Zulkifli A, Kamal AA. Med J Malaysia 1980 Dec; 35(2):164–165.
43. Bierman CW. Am J Dis Child 1967 Jul; 114(1): 42–50.
44. Jensen SP, Lynch DA, Brown KK et al. Clin Radiol 2002 Dec; 57(12):1078–1085.
45. Silva CI, Colby TV, Muller NL. Am J Roentgenol 2004 Sep; 183(3):817–824.
46. Stern EJ, Frank MS. AJR Am J Roentgenol 1994 Jul; 163(1):37–41.
47. Ketai L, Coutsias C, Williamson S et al. Acad Radiol 2001 Mar; 8(3):257–264.
48. Goldin JG, McNitt-Gray MF, Sorenson SM et al. Radiology 1998 Aug; 208(2):321–329.
49. Nuhoglu Y, Bahceciler N, Yuksel M et al. Ann Allergy Asthma Immunol 1999 Mar; 82(3): 311–314.
50. Pifferi M, Caramella D, Ragazzo V et al. J Pediatr 2002 Jul; 141(1):104–108.
51. Marchac V, Emond S, Mamou-Mani T et al. Am J Roentgenol 2002 Nov; 179(5):1245–1252.
52. de Blic J, Tillie-Leblond I, Emond S et al. J Allergy Clin Immunol 2005 Oct; 116(4): 750–754.

Part V

Abdominal Imaging

29

Imaging of Clinically Suspected Malrotation in Children

Kimberly E. Applegate

Issues

I. What are the clinical predictors of malrotation and volvulus?
II. Who should undergo imaging? What is the diagnostic performance of imaging in the diagnosis or exclusion of malrotation?
III. How should the UGI series be performed? What imaging is appropriate in indeterminate cases?
IV. Special situation: The older child (at low risk?)
V. Special situation: The child with heterotaxy syndrome

Key Points

- Malrotation of the bowel is associated with risk of intestinal volvulus and can be fatal (strong evidence). Volvulus is a surgical emergency that is treated with the Ladd procedure (strong evidence).
- Infants and children diagnosed with symptomatic malrotation (without volvulus) should undergo Ladd procedure to fix the bowel and prevent future volvulus and intestinal obstruction from Ladd's bands (moderate evidence).
- Although consensus is lacking, asymptomatic children beyond infancy should undergo prophylactic Ladd procedure to avoid catastrophic midgut volvulus (limited evidence).
- The imaging test of choice is the upper gastrointestinal (UGI) series to diagnose or exclude malrotation (moderate evidence).
- 15–30% of UGI studies in children are indeterminate for malrotation versus normal variation due to the overlap of normal findings with malrotation, the lack of consensus on UGI positive findings and technique, and the lack of consensus for when surgeons should perform prophylactic Ladd procedure (insufficient evidence).

K.E. Applegate (✉)
Vice Chair of Quality and Safety, Department of Radiology, Emory University School of Medicine, 1364 Clifton Rd NE, Suite D112, Atlanta, GA 30322, USA
e-mail: keapple@emory.edu

L.S. Medina et al. (eds.), *Evidence-Based Imaging in Pediatrics*,
DOI 10.1007/978-1-4419-0922-0_29, © Springer Science+Business Media, LLC 2010

Definition and Pathophysiology

Malrotation is a congenital, abnormal rotation of the bowel, usually both small and large bowels, within the peritoneal cavity. There is accompanying abnormal fixation by mesenteric bands, or there is absence of fixation of portions of the bowel and this leads to an increased risk of acute or chronic volvulus, obstruction, and bowel necrosis. Malrotation has been diagnosed prenatally as well as incidentally at autopsy in the elderly (1, 2). Intestinal malrotation covers the entire range of intestinal anomalies from readily apparent omphalocele in the newborn to asymptomatic "nonrotation" of the large and small bowels in an adult. While the large majority of individuals become clinically symptomatic as infants, an important minority occurs beyond infancy and without the typical clinical presentation of bilious vomiting (3–5).

The greatest concern in the patient with malrotation is volvulus. When there is malrotation, the mesenteric attachment of the midgut (the bowel from the ligament of Treitz to the distal transverse colon) is abnormally short or deficient. The gut can then twist clockwise around the SMA and lead either to intermittent abdominal distention and pain or acute bowel necrosis and perforation if the twist remains fixed (2, 6, 7). Catastrophic volvulus results in ischemia of the entire midgut and if the patient survives, they will need total parenteral nutrition until small bowel transplant.

Epidemiology

While pediatric healthcare workers are universally aware of the devastating potential complications from malrotation, it is not a common condition. The Centers for Disease Control and Prevention (CDC) survey registry of birth defects estimates that the prevalence of malrotation in infants under the age of 1 year is 3.9 per 10,000 live births (8). Pediatric surgeons report that malrotation occurs more frequently, in approximately 1 in 500 live births in the United States, although this rate likely overestimates true incidence due to selection bias (9, 10). There is a slight male predominance in malrotation incidence but no significant difference in incidence in Caucasian versus black infants in the United States.

Malrotation is a diagnosis usually made in the newborn and young infant; 60–75% of cases occur within the newborn period and up to 90% of cases occur within the first year of life (5, 10–13). Malek and Burd used a national inpatient sample and excluded incidental Ladd procedures to estimate the incidence of urgent Ladd procedures in both infants and older children. They reported 5.3 per 1,000,000 or 362 annual cases of urgent Ladd procedures in American children older than 1 year, representing only 10% of all cases (5). Therefore, there are approximately 3620 cases or 53 per 1,000,000 American children who undergo urgent Ladd procedure for malrotation each year.

Malrotation has a variable presentation and appearance, making it more difficult to have consensus on its clinical diagnosis and management (14–17). The classic presentation of malrotation associated with either duodenal obstructive bands or midgut volvulus in the newborn is bilious vomiting (7, 10, 18). Volvulus is more common in infants and associated with a high rate of bowel necrosis and resection—44% and with high mortality—28% (19). When there is midgut volvulus and small bowel necrosis, the baby may have short gut syndrome and dependence on total parenteral nutrition. Mortality in affected newborns was approximately 30% in the 1950s and 1960s (12, 19) but since then has markedly decreased to 3–5% today (19, 20).

The Ladd procedure is the standard surgery to treat malrotation with or without volvulus in infants and children. The surgeon detorses the volvulus (usually in a counterclockwise fashion), cuts the adhesive and, sometimes obstructing peritoneal bands, places the colon in the left abdomen and the small bowel in the right abdomen, and performs an incidental appendectomy. There is a small risk of recurrent volvulus with reports of 5% (21), 3.5% (22), and 1.8% (23).

Associated congenital anomalies are common, reported in up to 62% of cases, and usually involve the gastrointestinal tract (Table 29.1) (9, 13). The most commonly reported anomalies not only involve the duodenum (atresia and web), in 10% of cases, but also include Meckel's diverticulum, other intestinal stenoses or atresias, and Hirschsprung's disease (10, 13, 20).

There are a number of syndromes that have a higher risk of malrotation that include Down's syndrome and the heterotaxy syndrome (Table 29.2). Malrotation is obligate with omphalocele, gastroschisis, and left-sided congenital diaphragmatic hernia.

Overall Cost to Society

The cost of the imaging, evaluation, and care of patients with suspected malrotation in the United States is unknown. Since it is a rare condition with less than 400 urgent Ladd procedures per year, the cost of acute care is likely low. However, long-term costs and impact on quality of life for the minority with short gut syndrome and multivisceral transplants would be significant as well as readmissions both in the short term and in the long term for bowel obstruction caused by mesenteric adhesions (24). Murphy and Sparnon (24) report 26% of patients who underwent Ladd procedure at a tertiary hospital were readmitted within 6 months after Ladd procedure while 13% of patients required multiple readmissions and at least one surgery each to lyse adhesions. Neonates are more likely to develop adhesions compared to older children and adults.

Goals

In acutely symptomatic infants and children, the immediate goal of initial bowel imaging is to detect potentially life-threatening volvulus, enabling urgent surgical intervention and preventing bowel ischemia that may lead to either death or short gut syndrome in those who survive. Imaging to detect those infants and children with malrotation who are at risk of life-threatening volvulus is performed to allow non-urgent surgical treatment with the Ladd procedure. Additional imaging studies, such as repeat UGI series or enema to document the position of the cecum, may be performed to further characterize indeterminate results.

Methodology

A MEDLINE search was performed using PubMed (National Library of Medicine, Bethesda, Maryland) for original research publications discussing the diagnostic performance and effectiveness of imaging strategies in. Clinical predictors of malrotation with volvulus were also included in the literature search. The search covered the years 1966 to June 2008. The search strategy employed different combinations of the following terms: (1) *malrotation*, (2) *volvulus*, (3) *radiography* or *imaging* or *gastrointestinal series*, (4) *sensitivity* and *specificity*, (5) *intestinal obstruction*. Additional articles were identified by citation indices and review of the reference lists of relevant papers. This review was limited to human studies and the English language literature. The author performed an initial review of the titles and abstracts of the identified articles followed by review of the full text in articles that were relevant.

Discussion of Issues

I. What Are the Clinical Predictors of Malrotation and Volvulus?

Summary of Evidence: Neonates will present with vomiting that is either bilious or will progress to bilious in 95% of cases (13, 20, 25). Most neonates have volvulus at surgery (moderate evidence). Most children older than 1 year have abdominal pain as the major presenting symptom. However, the presentation of malrotation in older children is much more varied and non-specific and this leads to long delays in diagnosis (moderate evidence). There are no clinical or imaging predictors for volvulus in patients with malrotation, although some subtypes of malrotation have higher risk of volvulus than others (moderate evidence).

Supporting Evidence: The hallmark of malrotation presenting in the neonate is bilious emesis (20, 25). When malrotation presents with bilious emesis, there is likely volvulus or bowel obstruction from adhesive bands. Bilious emesis suggests obstruction below the insertion of the common bile duct and in the newborn should be attributed to bowel obstruction until proven otherwise. It can be seen in any cause of bowel obstruction from the duodenum to the rectum (e.g., Hirschsprung's disease) as well as ileus (26, 27). However, in two series of neonates with bilious emesis, only 20% (26, 27) and 38%

(27, 28) of them had intestinal obstruction that required surgery.

Approximately 10% of symptomatic malrotation will occur beyond infancy. Catastrophic volvulus of the midgut (with bowel ischemia), while less common than that in infants, occurs in both children and adults (28–32). In children older than 1 year, the clinical presentation is quite variable and leads to long delays in diagnosis—with reports up to 5 years (34–36). Most children older than 1 year have abdominal pain as the major presenting symptom which is non-specific. Abdominal physical exam is unremarkable in 85% of these children at initial presentation (25). The absence of abdominal distension, presence of diarrhea, or a normal abdominal radiograph do not exclude malrotation. The range of reported presentations of malrotation with or without volvulus include chronic intermittent pain, vomiting, failure to thrive, chylous ascites, diarrhea, malabsorption, internal hernia, malnutrition, mesenteric lymphocele, pneumonia, and pneumatosis (11–14, 36–38). Malrotation is also reported incidentally in asymptomatic adults (13, 32, 39).

II. Who Should Undergo Imaging? What Is the Diagnostic Performance of Imaging in the Diagnosis or Exclusion of Malrotation?

Summary of Evidence: All infants and children with clinical suspicion of malrotation should undergo UGI series if they are clinically stable. The upper gastrointestinal (GI) series examination is the gold standard for radiographic diagnosis of malrotation and volvulus and it is often the only imaging test performed (11–13, 20, 40) (moderate evidence). The technique and interpretation must be meticulous to diagnose or exclude malrotation because of the variation of normal that overlaps malrotation. There is a lack of consensus in the radiology community on which images and views are necessary although the American College of Radiology has a pediatric UGI guideline (41). Published case series from single institutions report false-positive rates of approximately 15% and false-negative rates of 3–7% for the diagnosis of malrotation on UGI (10, 15, 42–45) (Table 29.3).

Supportive Evidence: When an infant presents with signs and symptoms that strongly suggest malrotation with volvulus, surgeons will not use imaging and take the infant directly to the operating room. If the clinical presentation is less acute, they may request an abdominal radiograph and UGI series.

Abdominal Radiographs

While commonly performed in infants and children with vomiting, plain radiographs are neither sensitive nor specific for the diagnosis of malrotation with volvulus. Radiographs of patients with malrotation and volvulus range from normal to distal bowel obstruction (11–13, 18, 46). When volvulus or obstruction is present, the most common appearance is of gas in the stomach and a paucity or total lack of other bowel gas.

UGI Series

The UGI series is a fluoroscopic study with barium (or in very ill patients, sometimes iodinated contrast is used) to visualize the anatomy and peristalsis of the stomach and duodenum. It is an inexpensive, easy to perform, and widely available test. The UGI series remains the imaging gold standard for the diagnosis of malrotation with or without volvulus. Yet, when compared to surgical findings, there are known false-positive and false-negative results (Table 29.3). Long et al. reported a 15% false-positive rate in a series of 81 infants and children undergoing a Ladd procedure after UGI study reported malrotation (limited evidence). They also stated that the most common reason for false-positive UGIs was the failure to recognize normal variations that mimic malrotation. These variations include a "wandering" duodenum, a mobile duodenum, and "duodenum inversum" (42, 43). The inferior displacement of the normal duodenal–jejunal junction (DJJ) is often seen in infants and children from dilated adjacent stomach, small and large bowels, the presence of a feeding tube, as well as from enlargement of the spleen or liver (3). Finally, the UGI study has known false-negative results reported 2–7% of the time (Table 29.3). Long notes that in those 2% of the malrotated cases with a normal position of the DJJ, the cecal position was not normal (42, 43).

Contrast Enema

The contrast or barium enema was the primary imaging test to diagnose or exclude malrotation in the mid-twentieth century until research showed the UGI to be more accurate (6, 7, 40, 47). The enema is performed to show the position of the entire colon but in particular to show whether the cecum is normally positioned in the right lower quadrant of the abdomen. Problems with this approach include (a) the presence of a variant of normal, the mobile cecum in 15% of all age groups, (b) the laxity of peritoneal ligaments in infants and young children may allow the cecum to be displaced by dilated bowel, a cause of false positive, and finally, (c) normal cecal position in 13–40% of malrotated patients (Table 29.3). Compare this false-negative rate for the enema of 13–40% to that of the UGI false-negative rate of 2–7%. The false-positive rate of enema (13%) (15) is similar to that for UGI (15%). While the enema is not the preferred imaging test for malrotation, it is useful in uncertain cases at UGI to document cecal position.

Cross-Sectional Imaging (US, CT, and MR)

Diagnostic performance of the relative positions of the SMA and SMV on US (and cross-sectional) imaging is lower than that of the UGI but can reveal malrotation in children with non-specific abdominal symptoms. The SMV is normally located anteriorly and to the patient's right of the SMA. When the SMV is to the left, this relationship is the reverse of normal or if the SMV is directly anterior to the SMA, it raises the possibility of malrotation (48–51). When the SMV is directly anterior to the SMV, Dufour et al. reported that 28% of these cases had malrotation (50). False positives occur and include patients with scoliosis. Further, up to one-third of cases of malrotation have a normal SMA–SMV relationship (50, 51). Finally, the technical feasibility of visualizing the SMA/SMV relationship depends on the ability of the sonographer, the cooperation of the child, and the amount of overlying bowel gas that may obscure it. An US study of over 300 children showed that in 26% it could not depict the SMA/SMV relationship (48). Therefore, ultrasound is inadequate for this diagnosis (limited to moderate evidence).

Similar to US, the SMA/SMV anatomic relationship has been reported in normal and malrotated patients using CT and MR (52–55). In one CT study of 166 patients, 89% of normal patients had a normal SMA/SMV relationship (55).

Volvulus: Diagnostic Performance of UGI, Sonography, and CT

Volvulus can be an intermittent phenomenon and therefore its imaging detection does not always correlate with the surgical findings in several series. The UGI study has a sensitivity of 54% (56) to 79% (57). On UGI, a corkscrew appearance with proximal duodenal obstruction is the typical finding indicating volvulus. The "Z" shape of the duodenum can mimic volvulus but represents malrotation and duodenal obstruction from Ladd's bands (58).

Imaging is specific for the finding of a swirling pattern of small bowel and mesentery around the SMA and has been reported with sonography and CT in addition to UGI. Several reports describe the "whirlpool" sign first on US (59, 60) and then on CT of midgut volvulus confirmed at surgery (61).

III. How Should the UGI Series Be Performed? What Imaging Is Appropriate in Indeterminate Cases?

Summary of Evidence: The UGI series must be performed with careful attention to anatomic detail that includes the patient positioning and the limited use of barium. It is critical to be familiar with the variation of normal and the subtle signs of malrotation (42, 43, 57, 62) (limited evidence).

Supporting Evidence: The critical anatomy that the UGI documents is the position of the duodenal–jejunal junction (DJJ) which is located to the left of the left vertebral body pedicle at the L1 or L2 level and posterior on the lateral view. There is overlap of the UGI appearance of subtle malrotation with that of normal variations and some estimate that 15% (3) to 30% (13) of UGI studies may be indeterminate. Long noted that the most common reason for false-positive UGIs was the failure to recognize normal variations that mimic malrotation. These variations

include a "wandering" duodenum, a mobile duodenum, and "duodenum inversum" (13, 18, 42, 43, 62). One of the most common reasons for false-positive UGI is the inferior displacement of the DJJ (42, 43, 57). The inferior displacement of the normal duodenal–jejunal junction (DJJ) is often seen in infants and children from dilated adjacent stomach, small and large bowels, as well as from enlargement of the spleen or liver. Sizemore also noted that inferior displacement of the DJJ causes false positives but also found that the jejunal position results in both false positives and negatives (57). When the jejunum is located in the right upper abdomen, the radiologist was more likely to report malrotation even if the DJJ is normally positioned. Equally, when the jejunum is located normally in the left upper abdomen, the radiologist was more likely to report a normal UGI study even with abnormal DJJ position.

Katz and colleagues described seven signs of malrotation on UGI series in infants and young children (62). The presence of one of these signs may not be abnormal, but the presence of more than one should raise suspicion of malrotation and perhaps further imaging. One finding of interest was the ability of the radiologist to manually displace the normal DJJ position because of normal laxity of the peritoneal ligaments in children under the age of 4 years. It should not be surprising then that extrinsic "masses" such as gastric distention, small bowel distention, and splenomegaly will displace the normal duodenum and lead to false positives in the unaware (3, 63, 64). Feeding tubes may also displace the normal DJJ (3).

A number of different approaches have been described in the literature to decrease the false-positive and false-negative results on UGI (3, 13, 18). The goal is to document normal mesenteric attachments for the midgut by inferring the position of the ligament of Treitz. No imaging currently shows this ligament and therefore we use the position of the visualized DJJ instead. The second, third, and fourth portions of the duodenum are retroperitoneal and therefore posterior in the abdomen on lateral view. On frontal view, the DJJ is normally located to the left of the left vertebral body pedicle at L1 or L2 level. It is important to document this position on both the frontal and lateral views. On the lateral view, the distal duodenum should remain posterior to the stomach. When the third portion of the duodenum courses anteriorly, it suggests malrotation. Koplewitz and Daneman reported that 70% of proven malrotation cases had this finding (65).

There are a number of reasons that the DJJ may be displaced, particularly inferiorly displaced, on the frontal projection. This displacement is not uncommon in normal infants and young children who have lax peritoneal ligaments that allow mobility of the small bowel. Premature infants are more likely to have a horizontal position of their stomach that orients the duodenal bulb more superiorly than the DJJ. An overdistended stomach from too much barium or air from a crying baby will inferiorly displace the DJJ. Small bowel obstruction, splenomegaly, and scoliosis may displace the DJJ on UGI. Other suggested techniques to optimize the diagnostic performance of the UGI include (a) to document the first pass of barium through the duodenum under fluoroscopic observation, (b) avoid overfilling the stomach with barium, (c) when in doubt, review other imaging studies, (d) perform delayed abdominal radiographs to document the position of the cecum.

What Imaging Is Appropriate in Indeterminate UGI Cases?

Up to 30% of UGI studies may be indeterminate in young infants (3, 13). Either the imaging is not clearly normal or abnormal *or* the clinical presentation does not match the UGI study findings. When uncertainty exists about whether the DJJ position is a normal variant or malrotation, either repeat UGI examination or evaluation of the cecal position may be helpful in indeterminate cases. The simplest solution is to continue the UGI series by following the barium course through the small bowel to document cecal position. In young infants it can be difficult to distinguish small from large bowel so that either an enema (if urgent) or a repeat UGI is recommended. In hospitalized infants, repeat UGI examination (often possible the following day) can be preformed via nasogastric tube which allows control of the amount of barium needed and limits fluoroscopy time. Alternatively, an enema can be performed on the same day to document the cecal position.

The recommended action will depend on the urgency of definitive diagnosis and the degree of clinical suspicion for malrotation. The imaging choice should be performed in conjunction with the referring clinician.

IV. Special Situation: The Older Child (at Low Risk?)

Summary of Evidence: The risk of symptomatic volvulus, either acute or chronic, from malrotation in an older child (beyond infancy) or adult is real but low. Unfortunately, there are no clinical or imaging predictors for volvulus in those patients with malrotation, although some subtypes of malrotation have higher risk of volvulus than others (moderate evidence). Given the reports of catastrophic acute volvulus in older children, and one decision analytic model, prophylactic Ladd procedure is recommended in both symptomatic and asymptomatic children (limited evidence).

Supporting Evidence: Approximately 10% of urgent Ladd procedures in the United States are performed in children beyond infancy and in adults (5). Older children and adults with symptomatic malrotation are a heterogeneous and poorly defined group, with many clinical presentations. Some may present with catastrophic volvulus while others will have years of abdominal complaints. There is no argument that those with acute volvulus undergo Ladd procedure. There is less consensus to perform a Ladd procedure prophylactically in those children (and adults) with less acute or no symptoms.

Small case series of malrotation with acute midgut volvulus are reported in both older children and adults by many surgeons (11, 12, 28–31, 33, 34, 45, 66–68). The clinical manifestations in older patients are often much less straightforward than are those in neonates and encompass a wide variety of signs and symptoms (15, 28–32). This situation has led to controversy and confusion in the literature about whether older children and adults need surgical intervention (18, 45). Most published case series recommend prophylactic Ladd procedure in both symptomatic (11, 12, 28, 33, 66) and incidentally detected malrotation (33, 34, 45, 66–68) in children, but others recommend a watch and wait approach (38).

At present, there is no method for predicting which patients will develop volvulus as a result of malrotation. Given this situation and the often confusing manifestations in older children, it is important that subtle abnormalities in the upper GI series be documented and discussed with the referring clinician and patient. Long average delays of 1.7 years (34), 2.3 years (33), and up to 5 years (35) in the diagnosis of malrotation in symptomatic children after infancy document the challenges of diagnosing the condition in older patients. Symptoms of malrotation in older children and adults range from acute abdominal pain and vomiting to mild intermittent pain and malabsorption (11–13, 17, 32, 63, 69, 70). Other reported manifestations and complications of malrotation include short gut syndrome, feeding difficulties, diarrhea, small bowel obstruction, adhesive bands, internal hernia, malnutrition, failure to thrive, chylous ascites, mesenteric lymphocele, pneumatosis, and pneumonia (11–14, 18, 36, 37). Malrotation also may be an incidental imaging finding, especially in adults (15, 32, 39).

Malek and Burd used Markov decision analysis to understand treatment options for children (beyond infancy) with asymptomatic malrotation. They used a national sample and data on mortality from volvulus and elective surgery to compare quality-adjusted life expectancy for children who undergo Ladd procedure and those who do not. They showed gains in quality-adjusted life expectancy that were the highest if asymptomatic malrotation was treated at the age of 1 year rather than observation. These gains persisted but decreased when the Ladd procedure was performed in older children, up to age 20 years. In adults, the model showed the preferred treatment strategy to be no surgery (4).

V. Special Situation: The Infant or Child with Heterotaxy Syndrome

Summary of Evidence: Infants with heterotaxy syndrome typically have complex congenital heart disease that results in high morbidity and mortality. Most of these infants also have malrotation. Controversy exists on whether

these infants should undergo UGI study and elective Ladd procedure given their higher risk of post-operative complications from their complex heart disease and other medical problems.

Supportive Evidence: Heterotaxy syndrome (also termed asplenia and polysplenia or situs ambiguous) is defined as visceral malposition and dysmorphism that is associated with indeterminate cardiac atrial arrangement. Most infants and children diagnosed with heterotaxy syndrome will have congenital heart disease and many will have severe complex lesions (71, 72). Mortality for the asplenia type of heterotaxy is as high as 80% in the first year of life (71, 72). Therefore, controversy exists regarding the role of UGI series screening and prophylactic Ladd procedure not only in these infants with malrotation but also in those who have complex heart disease and other medical conditions. Small case series show that most (sometimes all) children with heterotaxy will have malrotation and some develop acute midgut volvulus that requires urgent Ladd procedure (73–76).

Small case series show a risk of midgut volvulus in heterotaxy syndrome infants with known malrotation. These authors also conclude that screening UGI studies should be performed in all heterotaxy infants (insufficient evidence) (73–75, 77). The UGI will not only diagnose malrotation but also detect duodenal obstructions from either Ladd's bands or associated duodenal stenoses. Some authors also recommend prophylactic Ladd procedure in a select group of these infants that are stable from the cardiac disease (75, 77). There is insufficient evidence to suggest that all heterotaxy infants should undergo Ladd procedure given the severe congenital heart disease in many that results in either early mortality or high risk of post-operative complications and mortality from this elective procedure.

Take Home Tables

Tables 29.1, 29.2, 29.3, and 29.4 present, respectively, syndromes associated with malrotation, anomalies reported with malrotations, diagnostic performance of imaging for malrotation, and diagnostic performance of imaging for volvulus. Figure 29.1 presents a normal UGI series in an infant.

Table 29.1. Syndromes associated with intestinal malrotation

Apple peel intestinal atresia
Brachmann-de Lange syndrome
Cantrell syndrome
Cat eye syndrome
Chromosomal abnormalities (13, 18, 21, etc.)
Coffin-Siris syndrome
Down's Syndrome
Familial intestinal malrotation
FG syndrome
Heterotaxy syndrome (asplenia, polysplenia)
Marfan syndrome
Meckel syndrome
Mobile cecum syndrome
Prune belly syndrome

Adapted with permission from Taybi H, Lachman R. Radiology of syndromes, metabolic disorders, and skeletal dysplasias, 3rd ed. Chicago, IL: Yearbook Medical Publishers, 1990; 825–826.

Table 29.2. Associated anomalies reported with malrotation

Absence of kidney and ureter
Biliary atresia
Congenital diaphragmatic hernia
Duodenal or small bowel stenosis or atresia
Duodenal web
Gastroschisis
Hirschsprung's disease
Imperforate anus
Intestinal pseudoobstruction
Intussusception
Malabsorption
Meckel's diverticulum
Omphalocele
Pyloric stenosis

Adapted with permission from Jamieson and Stringer (13).

Table 29.3. Diagnostic performance of imaging for malrotation (based on single institution case series with references in parentheses)

Test	Sensitivity (%)	Specificity (%)
UGI series (range)	93–98	85–93
	93 (44, 68)	85 (15)
	95 (10)	85 (42, 43)
	97 (15)	93 (79)
	98 (42, 43)	
	98 (78)	
Barium enema (abnormal cecal position) (range)	60–87	
	87 (57)	87 (15)
	84 (42, 43)	
	80 (56)	
	69 (44)	
	68 (80)	
	60 (68)	
Ultrasound of SMA–SMV relationship (on axial view)	67 (51, 55)	79 (78)
	67 (50)	
	98* (78)	

*Does not include those patients where the SMA/SMV were not visible due to overlying bowel gas.

Table 29.4. Diagnostic performance of imaging for volvulus (reference in parentheses)

	Sensitivity	Specificity
UGI	54% (56)–79% (57)	98% (57)
Whirlpool sign* on US	83% (81)–92% (60)	100% (60)

*Defined as the swirling appearance, usually in a clockwise direction, of the small bowel, mesentery and vessels indicating volvulus.

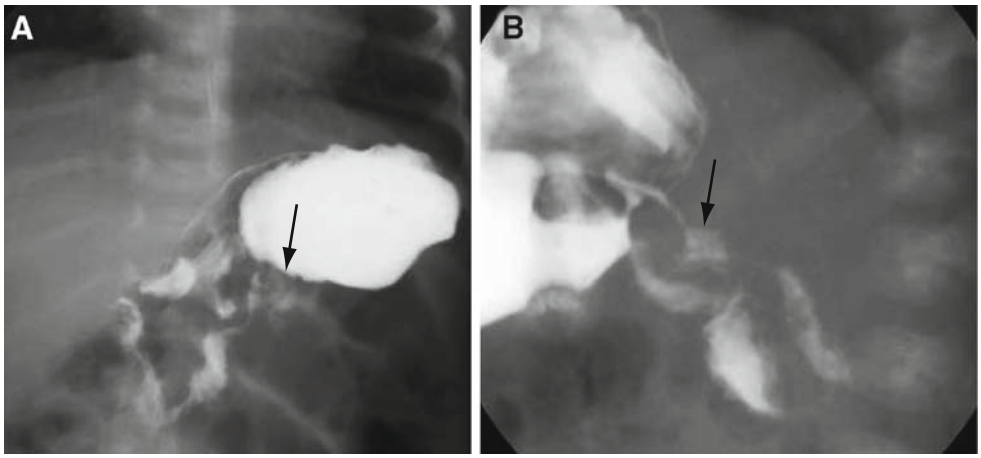

Figure 29.1. Normal UGI series in an infant with the *arrows* showing the position of the normal duodenal–jejunal junction (DJJ) on both antero-posterior (**A**) and lateral views (**B**). The ligament of Treitz position is inferred by the DJJ position. UGI criteria for normal DJJ position are to be located left of the left vertebral body pedicle at the level of the inferior aspect of the duodenal bulb on frontal projection. On the lateral view, the second through fourth portions of the duodenum are retroperitoneal and located posteriorly with the DJJ at the level of the duodenal bulb (reprinted with permission of The Radiological Society of North America from Applegate et al. (3)).

Imaging Case Studies

Cases 1 and 2

Figure 29.2 presents malrotation in two different children: a 3-month-old female with gagging and coughing with feeding; an older child who had bilious vomiting.

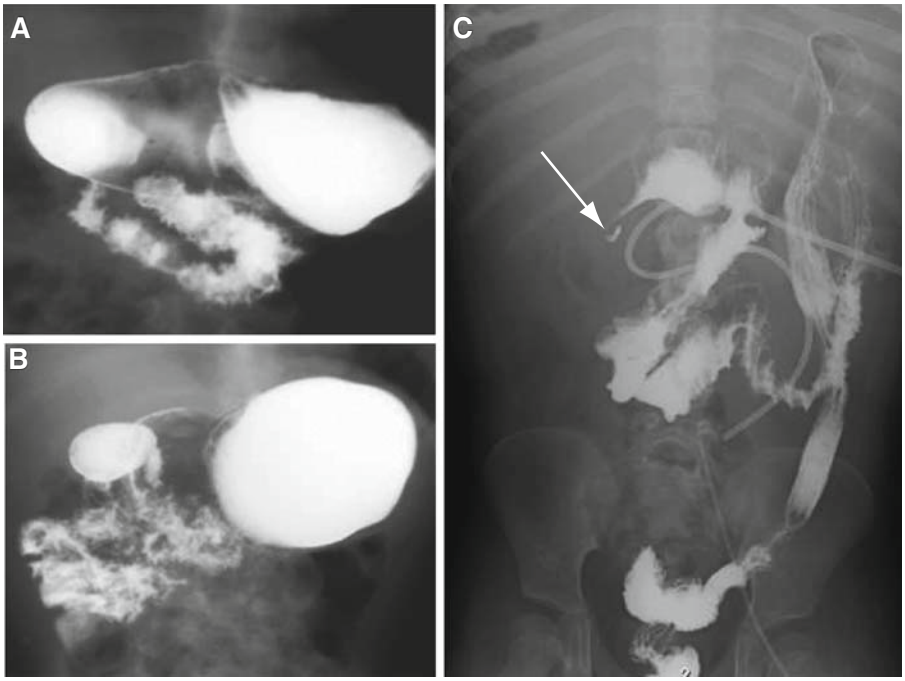

Figure 29.2. Malrotation in two different children. (**A)** and (**B)** are a UGI series of a 3-month-old female with gagging and coughing with feeding. UGI/SBFT demonstrated the DJJ over the left pedicle inferior to the level of the pylorus (**A**). This appearance raised the question of malrotation. Delayed images demonstrated the small bowel to lay in the right abdomen (**B**) and the cecum to lie in the left upper quadrant, confirming the presence of malrotation. At surgery, this infant was malrotated and underwent a Ladd procedure with appendectomy. (**C, D**) An older child who had bilious vomiting underwent a delayed film (**C**) after gastric tube injection that demonstrates the cecum in the epigastric regions and therefore the inferred short small bowel mesentery due to its close proximity to the duodenum (arrow showing barium-filled appendix) (reprinted with permission of The Radiological Society of North America from Applegate et al. (3)).

Suggested Imaging Protocol for Clinically Suspected Malrotation in Children

- UGI series is the preferred single imaging test. Should include true frontal and lateral views to document the position of the entire duodenum and the duodenal–jejunal junction.
- If UGI series is indeterminate, (a) repeat the UGI on a subsequent day or (b) either perform a contrast enema or continue the UGI series with small bowel follow-through to document the position of the cecum.

Future Research

- Consensus on standard technique and explicit criteria for the diagnosis or exclusion of malrotation on UGI series.
- Consensus on explicit criteria for the diagnosis or exclusion of malrotation at laparotomy.
- Decision analysis and consensus on the role of Ladd procedure for (a) children beyond infancy who present with asymptomatic or atypical symptoms for malrotation and (b) infants with heterotaxy syndrome.

References

1. Yoo SJ, Park KW, Cho SY, Sim JS, Hhan KS. Ultrasound Obstet Gynecol 1999 Mar; 13(3):200–203.
2. Dott NM. Br J Surg 1923; 11:251–286.
3. Applegate KE, Anderson JA, Klatte E. RadioGraphics 2006; 26:1485–1500.
4. Malek MM, Burd RS. Am J Surg 2006 Jan; 191(1):45–51.
5. Malek MM, Burd RS. J Pediatr Surg 2005 Jan; 40(1):285–289.
6. Ladd WE. N Engl J Med 1932; 206:277–283.
7. Ladd WE. N Engl J Med 1936; 215:705–708.
8. http://www.cdc.gov/mmwr/PDF/ss/ss4201.pdf
9. Stewart DR, Colodny AL, Daggert WC. Surgery 1976; 79:716–720.
10. Torres AM, Ziegler MM. World J Surg 1993; 17:326–331.
11. Berdon WE. Pediatr Radiol 1995; 25:101–103.
12. Berdon WE, Baker DH, Bull S et al. Radiology 1970; 96:375–383.
13. Jamieson D, Stringer D. In Babyn PS (ed.). Pediatric Gastrointestinal Imaging and Intervention, 2nd ed. Hamilton, ON: Decker, 2000; 311–332.
14. Howell CG, Vozza F, Shaw S et al. J Pediat Surg 1982; 17:469–473.
15. Dilley AV, Pereia J, Shi ECP et al. Pediatr Surg Int 2000; 16:45–49.
16. Janik JS, Ein SH. J Pediatr Surg 1979; 14:670–674.
17. Brandt ML, Pokorny WJ, McGill CW et al. Am J Surg 1985; 150:767–771.
18. Strouse PJ. Pediatr Radiol 2004 Nov; 34(11): 837–851.
19. Rescorla FJ, Shedd FJ, Grosfeld JL et al. Surgery 1990; 108:710–716.
20. Ford EG, Senac MO Jr, Srikanth MS et al. Ann Surg 1992; 215:172–178.
21. Stauffer UG, Herrmann P. J Pediatr Surg 1980 Feb; 15(1):9–12.
22. Feitz R, Vos A. J Pediatr Surg 1997; 32:1322–1324.
23. Nair R, Hadley GP. S Afr J Surg 1996 May; 34(2):73–75.
24. Murphy FL, Sparnon AL. Pediatr Surg Int 2006 Apr; 22(4):326–329.
25. Millar AJ, Rode H, Cywes S. Seimin Pediatr Surg 2003; 12:229–236.
26. Lilien LD, Srinivasan G, Pyati SP, Yeh TF, Pildes RS. Am J Dis Child 1986 Jul; 140(7):662–664.
27. Godbole P, Stringer MD. J Pediatr Surg 2002; 37:909–911.
28. Dietz DW, Walsh RM, Grundfest-Broniatowski S et al. Dis Colon Rectum 2002 45:1381–1386.
29. Fukuya T, Brown BP, Lu CC. Dig Dis 1993; 38:438–444.
30. Rao PL, Katariya RN, Rao PG, Sood S. J Assoc Physicians India 1977; 25:493–497.
31. Yanez R, Spitz L. Arch Dis Child 1986; 61: 682–685.
32. Balthazar EJ. Am J Roentgenol 1976; 126:358–367.
33. Maxon RT, Franklin PA, Wagner CW. Am Surg 1995; 61:135–138.
34. Spigland N, Brandt ML, Yazbeck S. J Pediatr Surg 1990; 25:1139–1142.
35. el-Gohari MA, Cook RC. Z Kinderchir 1984; 39:237–241.
36. West KW, Rescorla FJ, Grosfeld JL et al. J Pediatr Surg 1989; 24:818–822.
37. Zimmerman LM, Laufman H. Ann Surg 1953; 138:82–91.
38. Mehall JR, Chandler JC, Mehall RL et al. J Pediatr Surg 2002; 37:1169–1172.
39. Zissin R, Rathaus V, Oscadchy A et al. Abdom Imaging 1999; 24:550–555.
40. Simpson AJ, Leonidas JC, Krasna IH et al. J Pediatr Surg 1972; 7:243–252.

41. http://www.acr.org/SecondaryMainMenuCategories/quality_safety/guidelines/pediatric/pediatric_contrast_upper_gi.aspx
42. Long FR, Kramer SS, Markowitz RI, Taylor GE. Radiographics 1996; 16:547–556; discussion 556–560.
43. Long FR, Kramer SS, Markowitz RI, Taylor GE, Liacouras CA. Radiology 1996; 198:775–780.
44. Lin JN, Lou CC, Wang KL. J Formos Med Assoc 1995 Apr; 94(4):178–181.
45. Gohl ML, DeMeester TR. Am J Surg 1975; 129:319–323.
46. Kassner EG, Kottmeier PK. Pediatr Radiol 1975; 4:28–30.
47. Steiner GM. Br J Radiol 1978; 51:406–413.
48. Weinberger E, Winters WD, Liddell RM et al. Am J Roentgenol 1992; 159:825–828.
49. Gaines PA, Saunders AJS, Drake D. Clin Radiol 1987; 38:51–53.
50. Dufour D, Delaet MH, Dassonville M et al. Pediatr Radiol 1992; 22:21–23.
51. Zerin JM, DiPietro MA. Radiology 1992; 183:693–694.
52. Chou CK, Mak CW, Hou CC et al. Abdom Imaging 1997; 22:477–482.
53. Nichols DM, Li DK. Am J Roentgenol 1983; 141:707–708.
54. Shatzkes D, Gordon DH, Haller JO et al. J Comput Assist Tomogr 1990; 14:93–95.
55. Zerin JM, DiPietro MA. Radiology 1991; 179: 739–742.
56. Seashore JH, Touloukian RJ. Arch Pediatr Adolesc Med 1994; 148:43–46.
57. Sizemore A, Rabbani KZ, Ladd A, Applegate KE. Pediatr Radiol 2008; 38(5):518–528.
58. Ablow RC, Hoffer FA, Seashore JH et al. Am J Roentgenol 1983; 141:461–464.
59. Pracros JP, Sann L, Genin G, Tran-Minh VA, Morin de Finfe CH et al. Pediatr Radiol 1992; 22:18–20.
60. Shimanuki Y, Aihara T, Takano H, Moritani T, Oguma E et al. Radiology 1996; 199: 261–264.
61. Aidlen J, Anupindi SA, Jaramillo D, Doody DP. Pediatr Radiol 2005 May; 35(5):529–531.
62. Katz ME, Siegel MJ, Shackelford GD et al. Am J Roentgenol 1987; 148:947–951.
63. Taylor GA, Teele RL. Pediatr Radiol 1985; 15: 392–394.
64. Lim-Dunham JE, Ben-Ami T, Yousefzadeh DK. Am J Roentgenol 1999; 173:979–983.
65. Koplewitz BZ, Daneman A. Pediatr Radiol 1999 Feb; 29(2):144–145.
66. Cohen Z, Kleiner O, Finaly R, Mordehai J, Newman N et al. Isr Med Assoc J 2003 Mar; 5(3): 172–174.
67. Powell DM, Othersen B, Smith CD. J Pediatr Surg 1989; 24:777–780.
68. Prasil P, Flageole H, Shaw KS et al. J Pediatr Surg 2000; 35:756–758.
69. Friedland GW, Mason R, Poole GJ. Radiology 1970; 95:363–368.
70. Berardi RS. Surg Gynecol Obstetr 1980; 151: 113–124.
71. Phoon CK, Neill CA. Am J Cardiol 1994; 73: 581–587.
72. Gutgesell HP. In Garson A Jr, Bricker JT, McNamara DG (eds.). The Science and Practice of Pediatric Cardiology. Philadelphia: Lea and Febiger, 1990; 1280–1299.
73. Applegate KE, Goske MJ, Pierce G et al. Radiographics 1999; 19:837–852.
74. Ditchfield MR, Hutson JM. Pediatr Radiol 1998; 28:303–306.
75. Chang J, Brueckner M, Touloukian RJ. J Pediatr Surg 1993 Oct; 28(10):1281–1284; discussion 1285.
76. Lee SE, Kim HY, Jung SE, Lee SC, Park KW et al. J Pediatr Surg 2006 Jul; 41(7):1237–1242.
77. Tashjian DB, Weeks B, Brueckner M, Touloukian RJ. J Pediatr Surg 2007 Mar; 42(3):528–531.
78. Orzech N, Navarro OM, Langer JC. J Pediatr Surg 2006; 41:1005–1009.
79. Beasley SW, De Campo JF. Australas Radiol 1987; 33:376–383.
80. Slovis TL, Klein MD, Watts FB. Surgery 1980; 87:325–330.
81. Pracros JP, Sann L, Genin G, Tran-Minh VA, Morin de Finfe CH et al. Pediatr Radiol 1992; 22:18–20.

30

Imaging of Infantile Hypertrophic Pyloric Stenosis (IHPS)

Marta Hernanz-Schulman, Barry R. Berch, and Wallace W. Neblett III

Issues

I. What are the clinical findings that raise the suspicion for IHPS and direct further investigation?
II. What is the diagnostic performance of the clinical and imaging examinations in IHPS?
III. Is there a role for follow-up imaging in uncertain cases?
IV. What is the natural history of IHPS and patient outcome with medical therapy versus surgical therapy?

Key Points

- In advanced cases, the clinical presentation of IHPS is typical. However, in early cases, the presentation may overlap with other causes of vomiting, particularly gastroesophageal reflux.
- Clinical examination by palpation of the pyloric mass (olive) is specific but less sensitive than imaging depending on the examiner and may be time consuming (moderate evidence).
- US is the preferred diagnostic imaging test in experienced hands (moderate to strong evidence).
- US is highly sensitive and specific to the diagnosis of IHPS, does not require radiation or additional gastric filling, and can be diagnostic within a few minutes. However, it requires operator and diagnostic expertise (moderate evidence).
- If US is negative, UGI series or nuclear medicine to evaluate for reflux may be necessary, depending on clinically assessed need to document presence and degree of reflux.

M. Hernanz-Schulman (✉)
Department of Diagnostic Imaging, Vanderbilt Children's Hospital, Monroe Carell Jr Children's Hospital at Vanderbilt, Nashville, TN 37232, USA
e-mail: marta.schulman@vanderbilt.edu

L.S. Medina et al. (eds.), *Evidence-Based Imaging in Pediatrics*,
DOI 10.1007/978-1-4419-0922-0_30,

- UGI is effective in diagnosis of IHPS but may be time consuming, utilizes radiation which is of particular concern when fluoroscopic time is lengthy, and requires additional filling of the stomach, with the potential for aspiration.

Definition, Clinical Presentation, and Pathophysiology

IHPS is a condition that develops within the 2nd to 12th week of postnatal life, in which there is abnormal thickening of the muscle and mucosa of the antropyloric portion of the stomach, leading to gastric outlet obstruction, protracted "projectile" vomiting, dehydration, electrolyte loss, and eventual emaciation (1, 2). The clinical presentation is dependent on the length of symptoms and initially can be confused with onset or exacerbation of reflux. Vomiting is at first intermittent, but increases to follow all feedings. As the frequency of vomiting increases, there is loss of fluid as well as hydrogen ion and chloride, with hypochloremic alkalosis, paradoxical aciduria as the kidney attempts to conserve sodium at the expense of hydrogen ion, and decreased urine output. The child is voraciously hungry, often gnawing his fists, and as weight loss and starvation supervene, the distended stomach and vigorous peristaltic waves may be visible through the emaciated body habitus.

The pathophysiology of IHPS remains elusive, despite the relatively high prevalence of this condition and the success of modern surgical management. Particular attention has been paid to the hypertrophied muscle, and multiple abnormalities have been identified. When compared to control specimens, the muscular layer has been found to have increased expression of insulin-like growth factor-I messenger RNA, increased platelet-derived, and insulin-like growth factors. Further, it is deficient in interstitial cells of Cajal, in the quantity of nerve terminals and markers for nerve-supporting cells, in peptide-containing fibers, and in messenger RNA production for nitric oxide synthase as well as in nitric oxide synthase activity (3–12). It is therefore hypothesized that, as a consequence of the abnormal innervation of the muscle, there is failure of muscle relaxation, increased synthesis of growth factors, and muscle hyperplasia, hypertrophy, and obstruction.

On the other hand, the hypergastrinemia hypothesis suggests that a genetically influenced congenital increase in parietal cells initiates a cycle of increased acid production, repeated pyloric contraction, and decreased gastric emptying, with histopathologic muscle abnormalities as secondary events. Data supporting these contentions include induction of IHPS in puppies with pentagastrin infusion (13), the development of IHPS after inception of feeding (14), the thickening of the antropyloric mucosa and submucosal edema and cellular infiltrates (1, 2, 15), the development of IHPS with prokinetic agents such as erythromycin (15), and the resolution of the lesion and histopathologic abnormalities after obstruction is surgically relieved (16). However, further research is needed to extricate the etiology and pathophysiology of this intriguing condition from the multiplicity of associated findings and confounding variables.

Epidemiology

Ninety-five percent of cases of IHPS present between the 3rd and 12th week of life, with a peak age at presentation of 4 weeks. The diagnosis is rare earlier than 10 days of life. The epidemiology of IHPS is variable, influenced by genetics and dependent on racial and geographic extraction. The genetic influence is likely to be polygenic, explaining the familial link. No single locus has been found to account for the greater than fivefold increase in incidence among first-degree relatives (17). Male and female children of affected mothers carry a 20 and 7% risk of developing IHPS, respectively, while male and female children

of affected fathers carry a lower respective risk of 5 and 2.5%. Probandwise concordance in monozygotic and dizygotic twins is 0.25–0.44 and 0.05–0.10, respectively (18). The discordance in the incidence of pyloric stenosis among monozygotic twins suggests an environmental factor not yet identified. Among white populations of northern European extraction, the incidence of IHPS is approximately 2–5 per 1,000 live births, with a male:female ratio ranging from 2.5:1 to 5.5:1. This incidence falls by 20–30% among Caucasians in India and among Black (0.7 per 1,000 live births) and Asian populations.

An association has been described between pyloric stenosis and malrotation, esophageal atresia, and obstructive lesions of the urinary tract. Higher birth order, low birth weight, higher maternal age, and maternal educational status have also been described in association with pyloric stenosis (19).

Overall Cost to Society

The costs to society of caring for infants with IHPS vary with the decision tree for diagnosis, with the type of surgery performed, with the skill of the physicians involved, and with the rate of complications. In a retrospective study of 234 patients suspected of IHPS, White and colleagues (20) determined that the mean total charges for their patients with IHPS were $2,454, with a potential savings of $100 per patient in a model in which diagnostic imaging was applied after clinical evaluation by surgery, so long as the surgeon's sensitivity to palpate the olive was at least 38%. This model assumes that no further imaging will be performed if an olive is not palpated by the surgeon. A multi-institutional study by Campbell and colleagues (21) outlined minimum total hospital charges of $1,614 for patients with open pyloromyotomy and $5,075 for patients with laparoscopic pyloromyotomy. However, mean charges were $11,245 for open and $11,307 for laparoscopy surgery, largely secondary to complicating and comorbid events. In a retrospective study of 780 patients in North Carolina, Pranikoff et al. (22) found that mean hospital charges for patients treated for IHPS by general surgeons were $5,121, whereas the charges for those treated by pediatric surgeons were $4,496. This was compounded by the incidence of complications, which were significantly greater in the general surgeon group (2.9 versus 0.5%) and which raised the charges from $4,806 to $6,592. Safford et al. also showed that patients treated both by high-volume surgeons and at high-volume hospitals have improved outcomes at less cost (23).

Cost analyses have been performed that show (a) there is added cost without benefit if imaging is performed after positive palpation of the olive (20); (b) lower costs if patients are treated on a clinical pathway (24); and (c) UGI series as the initial test may be cost-effective when pyloric stenosis prevalence is low (25, 26) (limited evidence). However, to our knowledge, no studies have been published that assess the cost of surgical consult and surgeon's time in palpating the olive, versus performance of an imaging study, such as US, when the condition is initially suspected by the pediatrician or primary care physician or that have assessed the time delay in scheduling an outpatient surgical clinic appointment and its impact on patient care and its cost.

Goals

In patients with IHPS, the goal of imaging is to diagnose the condition as quickly and noninvasively as possible, so that treatment may be begun before electrolyte abnormalities, dehydration, and weight loss supervene.

Methodology

The authors performed a MEDLINE search using PubMed (National Library of Medicine, Bethesda, MD) for data relevant to the diagnostic performance and accuracy of both clinical and radiographic examinations of patients suspected of IHPS, as well as the surgical and medical therapy for this condition. The diagnostic performance of the clinical examination (history and physical exam) and surgical outcome was based on a systematic literature review performed in MEDLINE (National Library of Medicine, Bethesda, MD) during the years 1966–June 2008. The search strategy used

the following statements: (1) *pyloric stenosis*, (2) *US*, (3) *UGI*, (4) *clinical examination*, (5) *surgery*, (6) *laparoscopic surgery*, (7) *medical therapy.*

Discussion of Issues

I. What Are the Clinical Findings that Raise the Suspicion for IHPS and Direct Further Investigation?

Summary of Evidence: The classic presentation of IHPS is that of nonbilious, often projectile vomiting in a young child 3–12 weeks of age. In severe cases, starvation may arise, with indirect hyperbilirubinemia and electrolyte abnormalities including hypochloremia, sodium and potassium imbalances, and alkalosis or acidosis. In emaciated children, the distended peristalsing stomach may be visible in the hypochondrium.

Supporting Evidence: The clinical presentation of IHPS is that of nonbilious vomiting in young infants. This scenario can be confusing, as reflux is common in this age group and is the major diagnostic differential. In patients with IHPS, forceful vomiting sometimes described as "projectile" develops acutely or as an exacerbation of preexistent reflux. The episodes of vomiting are initially intermittent but progress to follow all or nearly all meals, and the infant may develop hematemesis with protracted vomiting, believed to be related to gastritis. Unlike patients with gastroenteritis, patients with IHPS are voraciously hungry. Starvation can exacerbate low glucuronyl transferase activity, and indirect hyperbilirubinemia may be present in 1–2% of patients. Electrolyte abnormalities (hypochloremic alkalosis and sodium and potassium deficits) are more specific findings which can be masked by dehydration. Renal mechanisms supervene to maintain intravascular volume by conservation of sodium at the expense of hydrogen ion, leading to aciduria in the face of systemic alkalosis; sodium may also be conserved at the expense of potassium, exacerbating potassium deficits. Emaciation in these infants is no longer common, but when it occurs, the distended stomach and active peristaltic activity may be visible in the hypochondrium.

In the vomiting infant, measurement of serum electrolyte levels can help differentiate the child with IHPS from the child with vomiting secondary to reflux. However, these findings are seen late in the course of the condition and are correlated with more severe dehydration. In a retrospective study of 65 infants with IHPS (27), investigators found that bicarbonate levels are normal in 29%, moderately elevated in 34%, and markedly elevated in 25%. Patients with elevated bicarbonate levels showed the most severe dehydration, the lowest chloride levels, the highest percentage of low urinary pH, and had the longest duration of symptoms. There was a decrease in bicarbonate levels in 12.3% of patients; these patients had otherwise normal electrolytes, the least dehydration, and the shortest duration of symptoms. The authors postulate that a slight metabolic acidosis from lack of nutrition occurs in IHPS, before the classic overlay of electrolyte disturbances supervenes secondary to gastric losses. In a subsequent study of 216 infants (28), the authors found that the alkalotic and hypochloremic infants had a significantly longer duration of illness, sodium, potassium, and chloride deficits. These sicker patients also had a higher percentage of palpable olives, and overrepresentation of female and black infants, likely because of a lower suspicion of IHPS in these populations.

Therefore, the patient with IHPS will present with new onset or exacerbation of postprandial nonbilious vomiting, with more advanced cases demonstrating dehydration, elevated serum bicarbonate, with chloride, sodium, and potassium deficits, and paradoxical aciduria. The evidence indicates that the typical electrolyte disturbances of IHPS occur later in the evolution of this condition, and that heightened clinical suspicion and further investigation before the full constellation of findings has appeared will aid in reaching the goal of early treatment.

II. What Is the Diagnostic Performance of the Clinical and Imaging Examinations in IHPS?

Summary of Evidence: Clinical examination has moderate sensitivity for pyloric stenosis of 72–74%, although this may be decreasing as reliance upon imaging increases and the

diagnosis is made earlier. The specificity of abdominal palpation is high at 97–99%. Clinical examination is operator dependent, and may be time-consuming, requiring 10–29 minutes of palpation for high diagnostic sensitivity.

Ultrasound has high sensitivity and high specificity, approaching 100% in experienced hands. Ultrasound can be performed rapidly, without patient preparation. However, ultrasound is highly operator dependent.

UGI is considered to have high sensitivity and high specificity, although modern data are lacking. UGI has less operator dependency than ultrasound but does require the use of ionizing radiation, which can be prolonged when there is poor gastric emptying.

In general, physical examination will be the first evaluation for suspected pyloric stenosis. When palpation for the olive is negative, US is the preferred initial imaging test. However, when there is little or no experience with using US for this diagnosis, UGI is the preferred imaging test (moderate evidence).

Supporting Evidence

Clinical Palpation

The clinical examination in IHPS refers to the ability to palpate the pyloric mass or olive. The mainstay imaging examination for IHPS was the UGI or barium meal, standardized in 1932 by Meiweissen and Sloof (29); in 1977, US was first reported in the diagnosis of IHPS (30) and has now become the preferred diagnostic imaging modality for this condition. The sensitivity of each of these examinations varies with the skill of the examiner, particularly for clinical palpation and for US.

Success in palpating the enlarged pylorus is not easy in most circumstances and is possible only if the infant is calm. The use of a pacifier, decompression of the stomach via orogastric tube (which moves the pylorus more anteriorly), or a small feeding (5% dextrose in water) have been described as helpful. The examiner should be willing to commit 10–20 minutes of time in order to successfully palpate the pylorus, and repeat examinations may be required (31). The frequency of diagnosis by successful palpation of the pyloric mass has decreased over the past two decades; this is believed to be due in part to the time commitment needed for successful physical examination, the ease and reliability of the noninvasive US study, and the younger age at diagnosis today, addressed later in this section.

In a prospective investigation of 116 infants with vomiting, the physical examination was successful in 80% of 75 patients with proven IHPS. In this study, the physical examination had a sensitivity of 72%, specificity of 97%, positive predictive value of 98%, and negative predictive value of 61% (32).

In one retrospective study of 212 patients seen between 1974 and 1977 and of 187 patients seen between 1988 and 1991, Macdessi and Oates (33) found that the pyloric mass was successfully palpated by the surgeons in 99% of patients in the earlier group and in 79% of the patients in the second group; however, among the nonsurgeons to whom the patients initially presented, the pyloric mass was palpated in 47% of patients in the earlier group and in 33% of patients in the later group.

In another retrospective study of 234 patients, 150 of whom had pyloric stenosis, the pyloric mass was successfully palpated in 111 patients, with one false-positive examination, for a sensitivity of 74% and a specificity of 99%. However, the sensitivity ranged between 31 and 100% among the five surgeons in the group (20). Some authors suggest sedation in order to increase sensitivity of the manual examination, which increased from 70 to 100% after sedation in a reported series of 10 patients with IHPS (34).

Abdominal Radiographs

Abdominal radiographs, if obtained, typically reveal a distended stomach with scarcity of bowel gas distal to the stomach. However, this is not a sensitive diagnostic test, and findings would need to be confirmed by palpation, US, or UGI. Therefore, if pyloric stenosis is suspected, this examination only adds delay and radiation exposure and is not recommended.

UGI Examination

The UGI examination is performed by introduction of a positive oral contrast agent, typically barium, into the stomach and observation of the abnormal antropyloric channel during passage of the contrast. The fluoroscopic

examination can be lengthy, as diagnosis is dependent on passage of contrast through the abnormal channel, which can be markedly delayed. In addition, it necessitates further distension of the stomach with contrast, or passage of an orogastric tube to decompress the stomach, which allows improved visualization by eliminating dilution of the contrast by the gastric contents.

When performed by an experienced radiologist, the UGI is accurate in the diagnosis and exclusion of IHPS. There are few investigations today that specifically address the sensitivity and specificity of UGI in IHPS. In a study of 46 patients without a palpable olive published in 1967, UGI was diagnostic in 44 (96%) (35). These authors found the double track sign and string sign to be present in more than one-half of the patients, while beak, shoulder, and pyloric tit signs were present in slightly less than half; 7% of the patients had complete obstruction, with no passage of contrast from the stomach 30 minutes after completion of the fluoroscopic examination. There were no false positives in this series; however, without visualization of the muscle layer, overlap of IHPS and pylorospasm can lead to confusion between these two conditions. Continued fluoroscopy until the antropyloric channel opens can lead to protracted length of the examination and increased radiation exposure, even in infants without IHPS. In one patient reported by Hernanz-Schulman et al. (36) who did not have IHPS, findings in the UGI examination were diagnostic of the condition, although the US findings, which were not diagnostic of IHPS, resulted in surgery correctly not being performed. In that study, 45 UGIs were performed following US; the calculated UGI specificity was 98%. When there is little or no experience with the use of US for diagnosing pyloric stenosis, the UGI is the recommended initial imaging test.

Ultrasound Examination

The US examination, similar to abdominal palpation, requires a skilled and experienced examiner. Unlike the clinical examination, US is not time consuming, and diagnosis by an experienced examiner can be made very quickly, even in a hungry, crying infant, and without need to empty the stomach with an orogastric tube. Unlike the UGI examination, US diagnosis is not dependent upon gastric emptying, and both the lumen and the outer muscle are directly visualized. The child does not need to drink and there is no radiation exposure.

Uncertainty in the US diagnosis arises when absolute reliance is placed upon measurements of the antropyloric channel, with changing sensitivity and specificity based on the measurements used and the prevalence of the condition (37). The measurements most often used include muscle thickness, length of the hypertrophied pyloric channel typically termed pyloric length, and pyloric diameter. Analysis of the literature on this subject must be viewed with the understanding that the technique has evolved in unison with the equipment and our ability to visualize increasing details of the antropyloric junction.

The initial and seminal report of US for the diagnosis of IHPS, reported in the *New England Journal of Medicine* in 1977 (30), consisted of five patients examined with a static B-scanner and used the pyloric diameter, which ranged between 1.8 and 2.8 cm, with a mean of 2.3 cm. With the advent of real-time scanners soon thereafter, muscle thickness began to be reported as an important component of this diagnosis.

In a prospective study of 200 infants with vomiting (38) scanned with a mechanical sector transducer operating at 7.5 mHz, Stunden et al. found a mean muscle thickness of 3.4 mm, with a range of 3–5 mm, a mean pyloric length of 22.3 mm with a range of 18–28 mm, and a pyloric diameter of 13.3 mm, with a range of 9–19 mm in positive cases. In their work, these investigators found the pyloric length the most discriminatory criterion, with a cut-off value at 18 mm. They additionally identified the importance of real-time evaluation, the lack of opening of the channel in patients with IHPS, and the variability in size of the normal channel secondary to normal muscular contractions. Using these criteria, these authors were able to discriminate between patients with and without IHPS with 100% success rate, without false-positive or false-negative results. In their patient population, a pyloric mass was palpated in two patients who had normal US examinations and subsequently were proven not to have IHPS.

In a subsequent study including 323 sonographic examinations scanned at 5.0 or 7.5 mHz, Blumhagen and colleagues (39) found an accuracy of 99.4% for US, despite classifying a positive case diagnosed as "suspicious" and a case diagnosed by sonography 4 days later, both scanned at 5.0 mHz, as false negatives. There were no false positives. In 8% of the normal patients, clinical examination had been false positive (specificity 91%). These authors found a mean muscle thickness of 4.8 with a range of 3.5–6.0 mm and a mean pyloric length of 17.8 with a range of 11–25 mm. They found some overlap in the pyloric length and identified muscle thickness as the criterion with the higher discriminatory value.

Graif et al. (40) examined a control group of 22 infants with gastrointestinal symptoms, and 22 patients suspected of IHPS, of whom 17 were shown to have IHPS. These investigators found a mean muscle thickness of 4.5, with a range of 3–6 mm, and pyloric length of 22.1 with a range of 16–26 mm. In the control group, mean muscle thickness was 2.3 with a range of 1.9–3.5 mm, and pyloric length was 12 with a range of 8–16 mm.

In a retrospective study of 145 consecutive infants with vomiting, O'Keefe et al. (41) determined that muscle thickness of 3 mm or greater is diagnostic of IHPS, while muscle thickness was <2 mm in 100% of normal patients and <1.5 mm in 98% of these normals. When appropriate referral for surgical therapy is taken as the endpoint of the examination, the sensitivity and specificity of US was 100 and 99%, respectively.

These results were validated in a study of 152 consecutive patients scanned with linear transducers at 7.5 mHz, with non-palpable olive on initial physical examination. Hernanz-Schulman et al. (36) found that in the 66 patients with IHPS, a muscle thickness of 3 mm or greater was diagnostic of IHPS in their patient population, with no false-positive examinations. In the 77 normal patients, muscle thickness was evaluated only during the time when the antrum was relaxed and measured 1 mm or less in all the patients. There were no false-negative studies. These investigators identified seven patients in whom the muscle thickness ranged between 1.3 and 2.7 mm; these patients were observed and did not develop IHPS; although the muscle thickness in these patients did not reach 3 mm, the canal length overlapped with that of patients with IHPS. These authors also described thickening of the mucosa within the channel lumen, and protrusion into the gastric antrum, termed the antral nipple sign, variability in the thickness of the muscle of the unrelaxed normal antrum, as well as in the muscle thickness and pyloric length in patients with IHPS within the abnormal range.

III. Is There a Role for Follow-Up Imaging in IHPS?

Summary of Evidence: Initially described as congenital hypertrophic pyloric stenosis, IHPS is now known to be a condition that develops after birth. The rate at which pyloric stenosis evolves is not known nor is it known whether pylorospasm is always a self-resolving condition, or whether it is one of the initial steps in the development of pyloric stenosis in some patients. Therefore, in the small minority of patients with equivocal findings, if symptoms do not resolve, a repeat examination is important to assess for the development of IHPS (limited evidence).

Supporting Evidence: In the retrospective evaluation of 145 consecutive patients, O'Keefe et al. (41) found six (4%) patients with equivocal findings and borderline muscle measurements >2 and <3 mm. In two of these patients, IHPS developed, with follow-up examination demonstrating a change in muscle thickness from 2 to 4 mm 2 weeks later. Two patients had pylorospasm that resolved; one patient had milk allergy and one patient had eosinophilic gastroenteritis.

In a prospective Doppler study of vascularity of the pyloric muscle and mucosa, Hernanz-Schulman and colleagues (36) identified one child who was referred at 2 weeks for US evaluation of vomiting secondary to family history and heightened clinical suspicion. The initial examination found a muscle thickness of 2.8 mm with intermittent opening of the canal, which increased to 3.5 mm at 5 weeks of age without canal opening, at which time the diagnosis of IHPS was made and confirmed at surgery. In a manuscript addressing the accuracy of various muscle measurements, O'Keefe and colleagues illustrate the

maturation of pyloric stenosis over a 2-week period, in an infant initially presenting at 5 weeks of age (41).

How long should one wait until a repeat sonogram is requested? The answer is not known; at this time, following the child's clinical status, requesting a follow-up examination is reasonable if initial findings lie in the borderline group as described previously, and the child's symptoms do not resolve, or exacerbate.

IV. What Is the Natural History of IHPS and Patient Outcome with Medical Therapy Versus Surgical Therapy?

Summary of Evidence: Although pyloromyotomy has been widely used and has been successful in the management of IHPS for the past century, experience with nonoperative management has been reported (42). However, the excellent outcomes achieved with the Ramstedt procedure have resulted in little enthusiasm for a nonoperative approach, particularly in North America. This procedure allows rapid return to oral feeding, with average length of stay in North America of less than 2 days.

Several recent publications from Japan have reported resurgent interest in medical therapy for this disorder (43–45). The theory that muscular spasm is a contributing factor to hypertrophy has led to trials of atropine (intravenous and oral) as the primary treatment. However, this approach has not been consistently successful, often requiring subsequent pyloromyotomy, and has the disadvantages of requirement for prolonged hospitalization, necessity of skilled nursing care, and careful follow-up while the patient is receiving this medication. Another approach has been endoscopic or image-guided balloon dilatation; however, these techniques are less reliable and do not convey significant advantage over standard operative surgical treatment but may have a limited application in rare patients in whom surgery may be contraindicated.

Supporting Evidence: In a prospective trial of 34 patients, Yamataka and colleagues (45) treated 14 patients with incremental doses of oral atropine, escalating to intravenous medication as needed, and 20 patients with pyloromyotomy. The stomach was decompressed via NG tube prior to each dose of atropine and trial feedings. Treatment was successful in 20/20 surgical cases and in 12/14 atropine patient cases (85%), with 2 patients requiring subsequent pyloromyotomy. Mean time to full feeds in the surgical group was 2.7 days with a range of 2–3 days and 5.3 days with a range of 1–10 days in the atropine group.

In a prospective trial of 85 patients with IHPS, Kawahara and colleagues (44) treated 52 patients medically with fixed doses of IV atropine, followed by oral atropine, and 33 patients with surgery. Medical therapy was successful in 87% of these, with the remaining needing pyloromyotomy with a mean hospital stay of 15 days and a range of 7–28 days. In the patients successfully treated, atropine was given for a mean of 51 days and a range of 29–137 days. Hospital stay was 13 days with a range of 6–36 days. Complications in this group consisted of urinary tract infection, upper respiratory tract infection, and transient increase in serum aspartate aminotransferase. Among the surgical group, mean hospital stay was 5 days, with a range of 4–29 days. Complications included wound infection in four patients requiring hospitalization in three, mucosal perforation in one patient, and postoperative hemorrhage resulting in hypoxic encephalopathy in one patient with hemophilia.

Balloon dilatation in infants with IHPS has been attempted unsuccessfully in a limited number of patients (46). However, it was reported to be successful in three infants with persistent vomiting after conventional pyloromyotomy (47).

The success of the muscle-splitting surgical correction of IHPS described by Ramstedt in 1912 (48) is unchallenged. However, the surgical approach to the pyloric mass has evolved from an upper midline laparotomy to an incision in the right hypochondrium and circumumbilical incision. In 1991, Alain reported laparoscopic pyloromyotomy in 20 infants, introducing a new approach to the Ramstedt procedure (49). Several retrospective and prospective studies have been performed comparing

complications, postoperative recuperation, length of hospital stay, and expense between these operations. Mucosal perforation, a complication of both procedures, is more problematic with laparoscopy, as it may be unrecognized and require reoperation. On the other hand, wound infection appears to be slightly less with laparoscopy in some series. Although cosmetic results are superior with laparoscopy, the data to date suggest that once the learning curve for the laparoscopic approach is mastered, there is little difference in the overall outcome between these two procedures (21, 50–53).

Take Home Figures and Tables

Figure 30.1 is an algorithm for diagnosis of infants suspected of IHPS. Table 30.1 shows performance of diagnostic imaging in IHPS.

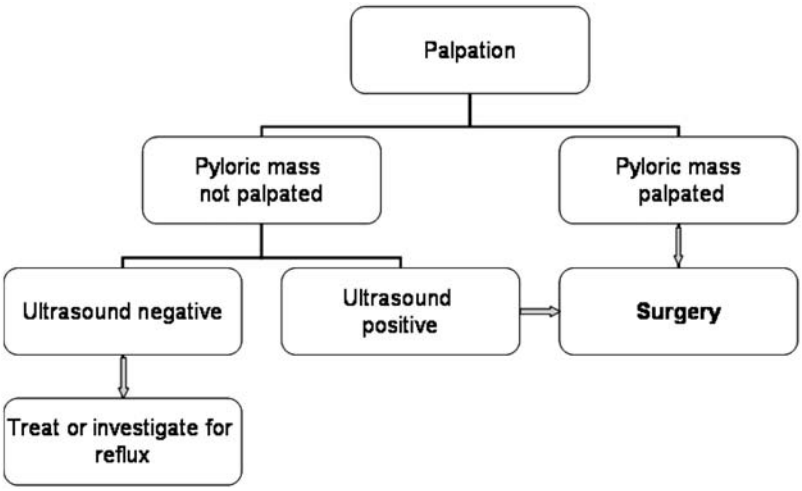

Figure 30.1. General algorithm for diagnosis of infants suspected of IHPS.

Table 30.1. Performance characteristics of diagnostic examinations in IHPS

	Sensitivity (%)	Specificity (%)
Palpation by surgeon*	31–99 (mean 72.5) (20, 32–34, 37, 39)	85–99 (mean 93) (20, 32, 37, 39)
By nonsurgical clinician	26–47 (mean 37) (33, 37)	
Ultrasound (in experienced hands)	97–100 (mean 99) (20, 32, 36, 38–41)	99–100 (mean 99.8) (20, 32, 36, 38–41)
UGI	90–100 (mean 95) (20, 33, 35)	99 (20)

*Reference (37). Assumption that palpation of olive pre-US examination was done by clinicians and post-US examination was done by surgeons, although actual examiner is not specified.
References in parentheses

Imaging Case Studies

Case 1

Figure 30.2 presents a sonogram of an infant with IHPS.

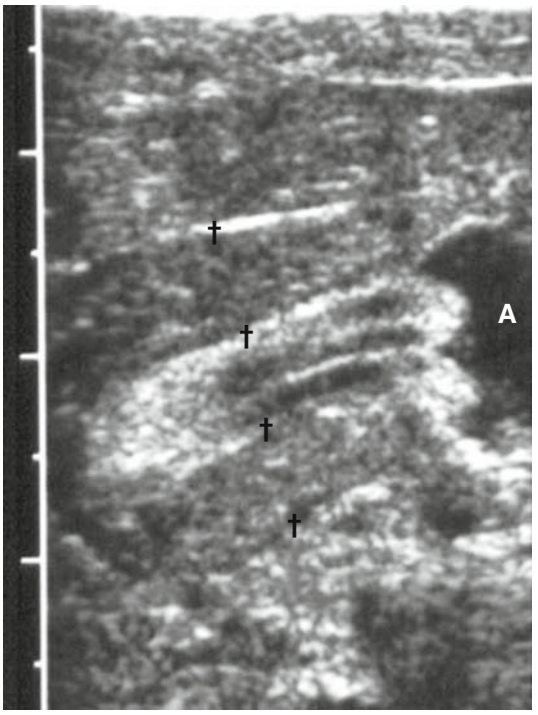

Figure 30.2. US of infant with IHPS. The length of the antropyloric channel with abnormally thickened muscle is 18 mm and the muscle (between cross-hairs) measures 4.5 mm in thickness. The thickened mucosa protrudes into the fluid-filled antrum (A).

Case 2

Figure 30.3 presents a UGI of an infant with IHPS.

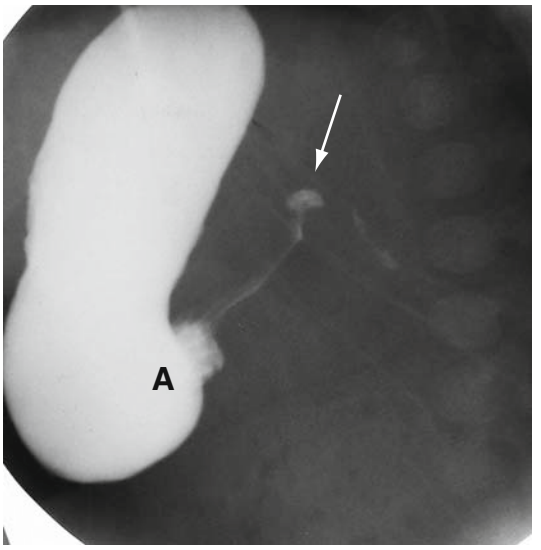

Figure 30.3. UGI of infant with IHPS. The antropyloric portion of the stomach is narrowed by the thickened muscle, and contrast is seen coursing between the interstices of the thickened and compressed mucosa. A = antrum; *arrow* points to the duodenal bulb.

Future Research

- Further research on the etiology of IHPS may prevent the condition or allow more effective and rapid medical management.
- Given the fact that pyloric ultrasound is the current standard of reference, further studies are required to determine learning curve and skills for general radiologists to be proficient with pyloric ultrasound.

References

1. Hernanz-Schulman M et al. J Ultrasound Med 1995; 14(4):283–287.
2. Hernanz-Schulman M et al. Am J Roentgenol 2001; 177(4):843–848.
3. Kobayashi H, O'Briain D, Puri P. J Ped Surg 1994; 29:651–654.
4. Kusafuka T, Puri P. Pediatr Surg Int 1997; 12(8):576–579.

5. Langer JC, Berezin I, Daniel EE. J Pediatr Surg 1995; 30(11):1535–1543.
6. Malmfors G, Sundler F. J Pediatr Surg 1986; 21(4):303–306.
7. Ohshiro K, Puri P. J Pediatr Surg 1998; 33(2): 378–381.
8. Ohshiro K, Puri P. Pediatr Surg Int 1998; 13: 253–255.
9. Okazaki T et al. J Ped Surg 1994; 29:655–658.
10. Vanderwinden J et al. NEJM 1992; 327: 511–515.
11. Vanderwinden JM et al. Gastroenterology 1996; 111(2):279–288.
12. Wattchow D et al. Gastroenterology 1987; 92: 443–448.
13. Dodge JA, Karim AA. Gut 1976; 17(4): 280–284.
14. Rollins MD et al. Arch Dis Child 1989; 64(1): 138–139.
15. Callahan MJ et al. Pediatr Radiol 1999; 29(10):748–751 [MEDLINE record in process].
16. Vanderwinden JM et al. J Pediatr Surg 1996; 31(11):1530–1534.
17. Schechter R, Torfs CP, Bateson TF. Paediatr Perinat Epidemiol 1997; 11(4):407–427.
18. Carter CO. Br Med Bull 1976; 32(1):21–26.
19. Applegate MS, Druschel CM. Arch Pediatr Adolesc Med 1995; 149(10):1123–1129.
20. White MC et al. J Pediatr Surg 1998; 33(6): 913–917.
21. Campbell BT et al. J Pediatr Surg 2007; 42(12):2026–2029.
22. Pranikoff T et al. J Pediatr Surg 2002; 37(3): 352–356.
23. Safford SD et al. J Pediatr Surg 2005; 40(6): 967–972; discussion 972–973.
24. Michalsky MP et al. J Pediatr Surg 2002; 37(7):1072–1075; discussion 1072–1075.
25. Hulka F et al. J Pediatr Surg 1997; 32(11): 1604–1608.
26. Olson AD, Hernandez R, Hirschl RB. J Pediatr Surg 1998; 33(5):676–681.
27. Touloukian RJ, Higgins E. J Pediatr Surg 1983; 18(4):394–397.
28. Breaux CW Jr, Hood JS, Georgeson KE. J Pediatr Surg 1989; 24(12):1250–1252.
29. Meuwissen T, Slooff J. Maandschr.v. kindergeneesk 1933; 2:557–569.
30. Teele RL, Smith EH. N Engl J Med 1977; 296(20):1149–1150.
31. Grosfeld JL, Coran AG, Fonkalsrud EW (eds.). Pediatric Surgery, 6th ed. Philadelphia: Mosby, 2006.
32. Godbole P et al. Arch Dis Child 1996; 75(4): 335–337.
33. Macdessi J, Oates R. BMJ 1993; 306:553–555.
34. Freund H et al. Lancet 1976; 1(7982):473.
35. Shuman FI, Darling DB, Fisher JH. J Pediatr 1967; 71(1):70–74.
36. Hernanz-Schulman M et al. Radiology 1994; 193(3):771–776.
37. Yip WC, Tay JS, Wong HB. J Clin Ultrasound 1985; 13(5):329–332.
38. Stunden RJ, LeQuesne GW,Little KE. Pediatr Radiol 1986; 16(3):200–205.
39. Blumhagen JD et al. Am J Roentgenol 1988; 150(6):1367–1370.
40. Graif M et al. Pediatr Radiol 1984; 14(1):14–17.
41. O'Keeffe FN et al. Radiology 1991; 178(3): 827–830.
42. Hernanz-Schulman M. Radiology 2003; 227(2):319–331.
43. Kawahara H et al. Arch Dis Child 2002; 87(1): 71–74.
44. Kawahara H et al. J Pediatr Surg 2005; 40(12):1848–1851.
45. Yamataka A et al. J Pediatr Surg 2000; 35(2): 338–341; discussion 342.
46. Hayashi AH et al. J Pediatr Surg 1990; 25(11):1119–1121.
47. Khoshoo V et al. J Pediatr Gastroenterol Nutr 1996; 23(4):447–451.
48. Ramstedt C. Med Klin 1912; 8:1702–1705.
49. Alain JL, Grousseau D, Terrier G. Surg Endosc 1991; 5(4):174–175.
50. Fujimoto T et al. J Pediatr Surg 1999; 34(2): 370–372.
51. Hall NJ et al. Ann Surg 2004; 240(5):774–778.
52. Leclair MD et al. J Pediatr Surg 2007; 42(4): 692–698.
53. St Peter SD et al. Ann Surg 2006; 244(3): 363–370.

31

Intussusception in Children: Diagnostic Imaging and Treatment

Kimberly E. Applegate

Issues

I. What are the clinical predictors of intussusception? What are the clinical predictors of reducibility and bowel necrosis? Who should undergo imaging?
II. Which imaging studies should be performed? What is the diagnostic performance of abdominal radiographs and sonograph? What are the pathologic lead points?
III. How should therapeutic enema be performed? Where should patients be treated? What are the complications of enema therapy? What are the surgical management and complications? What is the cost-effectiveness analysis?
IV. What is the appropriate management in recurrent cases?
V. Special case: Intussusception limited to the small bowel
VI. Special case: Intussusception with a known lead point mass

Key Points

- Children with clinically suspected intussusception should undergo enema reduction after surgical consultation. The only absolute contraindications to enema are signs of peritonitis on clinical exam or free air on abdominal radiographs. Air enema has better overall reduction rates than liquid enema, but the outcome depends on the experience of the radiologist (moderate evidence).
- Barium should not be used due to the poorer outcomes compared with iodinated liquid contrast in those children who perforate (moderate evidence).

K.E. Applegate (✉)
Vice Chair of Quality and Safety, Department of Radiology, Emory University School of Medicine,
1364 Clifton Rd NE, Suite D112, Atlanta, GA 30322, USA
e-mail: keapple@emory.edu

L.S. Medina et al. (eds.), *Evidence-Based Imaging in Pediatrics*,
DOI 10.1007/978-1-4419-0922-0_31,

- Ultrasound (US) should be the primary imaging modality in the initial diagnosis of intussusception because it is a non-invasive test with high sensitivity and specificity. US also plays a role in the evaluation of reducibility of intussusception, presence of a lead point mass, potential incomplete reduction after enema, and of intussusception limited to small bowel (limited evidence).
- Abdominal radiographs have poor sensitivity for the detection of intussusception but may serve to screen for other diagnoses in the differential diagnosis, such as constipation, and for free peritoneal air. For evaluating children with a low probability for intussusception, sonography is the preferred screening test (limited evidence).
- The use of delayed repeat enema for the reduction of intussusception shows promise, but there are few data on the appropriate methods or time (limited evidence).
- For recurrence of intussusception, including multiple recurrences, enema is the preferred method for reduction (limited evidence).

Definition and Pathophysiology

Intussusception is an acquired invagination of the bowel into itself, usually involving both small and large bowel, within the peritoneal cavity. The more proximal bowel that herniates into more distal bowel is called the intussusceptum and bowel that contains it is called the intussuscipiens. It is an emergent condition where delay in diagnosis is not uncommon and leads to an increased risk of bowel perforation, obstruction, and necrosis. There may be an accompanying pathologic lead point mass in approximately 5% of children (1). Intestinal intussusception may occur along the entire length of the bowel from the duodenum to prolapse of intussuscepted bowel through the rectum. It can also range from classic clinical presentations to asymptomatic transient intussusception seen increasingly on multichannel CT studies of the abdomen for other indications (2). Most cases are "idiopathic" in that the etiology of the intussusception is due to hypertrophied lymphoid tissue in the terminal ileum which results in ileocolic intussusception. Some reports have suggested a viral etiology, most commonly adenovirus but also enterovirus, echovirus, and human herpes virus 6 (3). The clinical signs and symptoms of intussusception are often non-specific and overlap with those of gastroenteritis, malrotation with volvulus, and, in older children, Henoch–Schonlein Purpura (HSP). The large majority of clinically symptomatic cases occur in the infant and toddler, with a peak age of 5–9 months, although it has been reported on prenatal imaging and may occur in children who present without the typical clinical presentation of vomiting, bloody stools, palpable abdominal mass, and colicky abdominal pain (4). The classic triad of colicky abdominal pain, vomiting, and bloody stools is present in less than 25% of children (5–7).

Epidemiology

Intussusception is the most common cause of small bowel obstruction in children and occurs in at least 56 children per 100,000 per year in the United States (8). It is second only to pyloric stenosis as the most common cause of gastrointestinal tract obstruction in children. It occurs in boys more than girls at a ratio of 3:2. Some papers have reported associations with viruses, particularly adenovirus, although lack of seasonality suggests more than one pathogen (4, 8). Delay in diagnosis and treatment is not uncommon, making enema reduction less successful, bowel resection more likely, and death due to bowel ischemia possible (1, 4, 9, 10). There were 323 intussusception-associated deaths in American infants reported to the Centers for Disease Control (CDC) between 1979 and 1997. In a review of administrative discharge data of intussusception-associated hospitalizations and deaths in the United States,

Parashar and colleagues (8) noted a peak age of 5–7 months, with two-thirds of patients under age 1 year, no consistent seasonality, hospitalization rates of approximately 56 per 100,000 children, and a general trend toward fewer hospitalizations over the past two decades. The mortality rates also decreased over this time period, from 6.4 per 1,000,000 to 2.3 per 1,000,000 live births. They also reported an increased risk of intussusception-related deaths among infants whose mothers were <20 years old, unmarried, nonwhite, and had less than a grade 12 education. The authors concluded that these data suggest reduced access or delay in seeking care contributed to the risk of death. They did not investigate costs or rates of surgical versus enema reductions.

In another paper comparing worldwide data, Meier and colleagues noted that the most important difference between industrialized and developing countries' outcomes was the delay in presentation for treatment and consequent lower rates of enema reduction and higher rates of surgical mortality (18%) from bowel necrosis (10).

Rotavirus Vaccine

Shortly after the first and only rotavirus vaccine was introduced in the United States in 1998 for routine vaccination of infants at ages 2, 4, and 6 months, several reports to the Centers for Disease Control (CDC) suggested an association between the vaccine and intussusception. This was noted particularly within 2 weeks after vaccination with the first dose. The vaccine was removed from the world market in 1999 (11). Although controversial, subsequent investigations have not found a higher rate of intussusception after rotavirus vaccination (12, 13). A new rotavirus vaccine is currently under development (14).

Overall Cost to Society

No data have been identified detailing the total cost to society of intussusception. Three recent surveys have documented practice patterns for the evaluation of intussusception (4, 15, 16). In centers without pediatric radiologists, the enema is the initial and often only imaging test performed for both diagnosis and treatment. In contrast, at the 2004 SPR annual meeting, a survey of pediatric radiologists showed that 57% now use sonography for initial diagnosis prior to enema (15). Overall, the total hospital cost for children with intussusception treated with surgery is approximately four times that of those treated with enema (17–19).

Goals

The goal of initial bowel imaging is early detection of intussusception to enable enema reduction of the intussusception. Additional imaging studies may be performed to further characterize indeterminate results. The ultimate goal that radiologists should strive for is non-operative reduction for all children with idiopathic intussusception (approximately 95% cases), but delay in presentation and diagnosis makes this goal elusive.

Methodology

A MEDLINE search was performed using PubMed (National Library of Medicine, Bethesda, Maryland) for original research publications discussing the diagnostic performance and effectiveness of imaging strategies in intussusception. Clinical predictors of intussusception were also included in the literature search. The search covered the years 1966 to June 2008. The search strategy employed different combinations of the following terms: (1) *intussusception*, (2) *children, ages under 18 years*, (3) *diagnosis*, (4) *therapy* or *surgery* or *etiology.* Additional articles were identified by reviewing the reference lists of relevant papers, identifying appropriate authors, and use of citation indices for MeSH terms. This review was limited to human studies and the English language literature. The author performed an initial review of the titles and abstracts of the identified articles followed by review of the full text in articles that were relevant.

Discussion of Issues

I. What Are the Clinical Predictors of Intussusception? What Are the Clinical Predictors of Reducibility and Bowel Necrosis? Who Should Undergo Imaging?

Summary of Evidence: At this point there are no reliable clinical prediction models that can accurately identify all patients with intussusception (limited evidence). Determination of which children should undergo imaging and which should not undergo imaging has not been studied in formal prospective trials.

Supporting Evidence

What Are the Clinical Predictors of Intussusception?

Ideally, children with intussusception should be diagnosed early to avoid bowel necrosis and surgery. However, one report found that only 50% of children were correctly diagnosed at initial presentation to a healthcare provider (20). The classic triad of colicky abdominal pain (58–100% cases), vomiting (up to 85% cases), and bloody stools is present in less than 25% of children (5, 21). Guaiac positive stool is present in 75% of children with intussusception (7, 22). Vomiting or diarrhea may lead to dehydration, which exaggerates lethargy. The mixture of stool, blood, and blood clots has been described as "current jelly stools" and is suggestive of intussusception.

Kupperman and colleagues published a cross-sectional study that evaluated the clinical factors that might predict intussusception in 115 children (23) (limited evidence). Using multivariate logistic regression and bootstrap sample analysis, they not only found that the presence of highly suggestive abdominal radiographs, rectal bleeding, and male sex were independent predictors of intussusception but also noted that these factors were not specific. Harrington and colleagues investigated the positive and negative clinical predictors of intussusception in a prospective cohort study (5) (moderate evidence). They recorded signs and symptoms in 245 children and correlated them with sonographic and enema findings. Significant positive predictive factors for intussusception were the presence of right upper quadrant mass, gross blood in stool, guaiac positive stool, and the triad of colicky abdominal pain, vomiting, and right upper quadrant mass. They were unable to identify significant negative predictors. Klein and colleagues reviewed clinical history, physical exam, and radiographic findings to develop a prediction model of children with possible intussusception (24) (moderate evidence). Their univariate analysis identified several known factors associated with intussusception, including vomiting, abdominal pain, palpable abdominal mass, guaiac positive stool, and rectal bleeding. However, they concluded that they were "unable to develop a prediction model that would reliably identify all patients with the diagnosis of intussusception. Previously identified predictors of intussusception remain important in increasing suspicion of this important diagnosis. At this point there is no reliable prediction model that can accurately identify all patients with intussusception."

What Are the Clinical Predictors of Reducibility and Bowel Necrosis?

The most important factor that decreases the reduction rate of enema is a longer duration of symptoms. This finding is supported by multiple case series. A significant delay is typically 48 hours, but some reports suggest 24 or 72 hours as either one of several factors or the single factor predicting unsuccessful enema reduction (4, 25). Other factors associated with lower reduction rates include age less than 3 months, dehydration, small bowel obstruction, and intussusception encountered in the rectum (25% reduction rate) (4, 20, 21, 25, 26) (limited evidence).

II. Which Imaging Studies Should Be Performed?

Summary of Evidence: Ultrasound has higher accuracy in the diagnosis of intussusception than plain radiographs. Ultrasound also has higher diagnostic accuracy in identifying pathologic lead points than plain radiographs or enema. The role of ultrasound findings in predicting success of reduction is not well known with available literature. Given current evidence, the diagnostic approach should include

(a) abdominal radiographs if concern for other diagnoses or for perforation; (b) sonography for diagnosis or exclusion of intussusception; (c) if positive, a surgical consult should be obtained prior to the enema reduction attempt; and (d) air enema reduction (or if no experience with the air technique, liquid enema) (moderate evidence).

Supporting Evidence

What Is the Diagnostic Performance of Abdominal Radiographs?

The presence of a curvilinear mass within the course of the colon (the crescent sign), particularly in the transverse colon just beyond the hepatic flexure, is a nearly pathognomonic sign of intussusception. The absence of bowel gas in the ascending colon is one of the most specific sign of intussusception on radiographs (27). However, small bowel gas located in the right abdomen on radiographs may mimic ascending colon or cecal gas. Radiographs have low sensitivity and specificity, even when viewed by experienced pediatric radiologists (27, 28) (limited evidence). Sargent and colleagues (26) reported 45% sensitivity in 60 children when evaluated prospectively by pediatric radiologists, using the enema as the reference standard (Table 31.1). Others report similar poor sensitivity in the detection of intussusception (4). In a survey of the SPR 2004 attendees, Daneman found that 79% obtain radiographs, but this practice may not be under the control of radiologists (15). Only 10% of pediatric radiologists in this survey preferred radiographs for the diagnosis.

What Is the Diagnostic Performance of Sonography?

Intussusception can be reliably diagnosed when a "donut," "target," or "pseudokidney" sign is seen using linear transducer sonography (29–32). The optimal US technique in this population is well described (30–34). There are no known contraindications or complications resulting from US for this purpose. US also plays a role in the evaluation of reducibility of the intussusception, the presence of a pathologic lead point (PLP) mass, intussusception limited to small bowel, to diagnose or exclude residual intussusception after enema, and to identify alternative diagnoses (5, 31, 33, 34) (limited evidence). In a 2004 survey, 57% of North American pediatric radiologists reported the use of sonography to diagnose intussusception as compared to 93% of European pediatric radiologists in a 1999 survey (15, 35).

Sonography screening in children has been suggested to reduce cost, radiation exposure, and both patient and parental anxiety/discomfort with enema (34) (limited evidence). Published series from single institutions suggest high accuracy, approaching 100% in experienced hands, with sensitivity of 98–100% and specificity of 88–100% (5, 31, 36, 37) (limited evidence) (Table 31.1). Eshed and colleagues found similar abilities in sonographic diagnosis of intussusception for staff radiologists as well as senior and junior radiology residents: sensitivity and specificity were 85 and 98% for staff radiologists, 75 and 96% for senior residents, and 83 and 97% for junior residents, respectively (38). Given that the theoretical cost-effectiveness of sonography is dependent on the prevalence of intussusception, optimization of imaging will require stratification of subjects into different levels of probability of intussusception (39). However, data are lacking for such stratification. Henrikson and colleagues noted a trend of decreased prevalence of intussusception (22%) in those children referred for enema and began sonographic screening (limited evidence). In their small series of 38 children, they were able to avoid 19 enemas in those with negative sonography, resulting in savings in both radiation exposure (an average of 8.2 mGy for negative enemas) and hospital charges (34). Future cost-effectiveness modeling research will be needed to define the population that should undergo sonography.

What Are the Sonographic Predictors of Reducibility and Bowel Necrosis?

Del-Pozo and colleagues performed sonography in 145 children with intussusception and found that fluid seen inside the intussusception represented trapped peritoneal fluid and was associated with significantly fewer reductions on enema and with bowel ischemia at surgery (40, 41) (limited evidence).

Some US reports have noted that thicker bowel wall was associated with fewer enema reductions (31, 42), but others did not find

this association (41). Lack of color Doppler signal in the intussuscepted bowel wall suggested bowel ischemia in several small series (43–45). Free intraperitoneal fluid in small or moderate amounts is present in approximately half of children with intussusception and is not a contraindication for enema (32). There are conflicting reports that free peritoneal fluid is associated with fewer reductions (4, 21, 25, 33, 46). Some descriptive studies report that the presence of lymph nodes trapped in the intussusception is associated with fewer reductions (33, 47). For these US findings, due to the conflicting reports and/or small series, the evidence is inconclusive.

What Are the Pathologic Lead Points?

Approximately 5–6% of intussusceptions in children are caused by pathologic lead points (PLP) which are due to either focal masses or diffuse bowel wall abnormality. The most common focal PLPs are (in decreasing order of incidence) Meckel's diverticulum, duplication cyst, polyp, and lymphoma (1, 4, 48) (limited evidence). Diffuse PLPs are most commonly associated with cystic fibrosis or Henoch–Schonlein Purpura. Although the common teaching remains that focal PLPs are more common in older children, this is somewhat misleading. The relative prevalence of PLP with intussusception is higher in children over the age of 3 years, particularly for lymphoma. However, the absolute number of PLP in infants versus older children is approximately equal (1).

The detection of lead points by imaging remains problematic (49), although US is the non-invasive standard of reference. 66% of PLPs may be identified at US (50) and that of 40% of PLPs may be diagnosed on liquid enema (4). Air enema has a lower rate of detection of PLP of 11% (51), so that some researchers suggest that US be used afterward to search for PLP (4) (limited evidence).

III. How Should Therapeutic Enema Be Performed?

Summary of Evidence: The air enema is considered superior at reduction, cleaner (based on appearance of peritoneal cavity at surgery when perforation occurs), safer, and faster, with less radiation when compared to liquid enema (22, 52–56) (moderate evidence). The recurrence rates for air versus liquid enema reductions do not differ (both are approximately 10%). The "rule of threes" used to guide liquid enema technique is supported by limited evidence. Barium is no longer the liquid contrast medium of choice due to the risk of barium peritonitis, infection, and adhesions when perforation occurs during the enema (22, 46, 53, 57). Neither sedation nor medications increase the enema success rate (limited evidence). Direct comparison of reduction with fluoroscopy versus ultrasound has not been studied (insufficient evidence).

Supporting Evidence: There are multiple investigations of success rates for enema reduction, although most are retrospective. Seventy-one published studies of this question were largely Level-3 (limited evidence) investigations consisting of unselected but often consecutive case series. The average reduction rate for these 71 published studies was 74%. In 19 series with at least 150 children each, retrospective analysis demonstrated reduction rates averaging 80%, range 53–96% (25) (Table 31.2). The largest series from China, using air enema in 6,396 children, reported reduction rates of 95% (55) (limited evidence). However, while the air enema may be preferred in experienced hands, the liquid enema is also safe and effective. The air enema technique is well described in the literature (54, 56, 58). Briefly, the enema tip should be placed within the child's rectum and taped in place with abundant tape. The child is placed in a prone position to allow the radiologist or assistant to squeeze the buttocks closed and prevent air from leaking. Air is rapidly insufflated into the colon under fluoroscopic observation. Once the intussusception is encountered, its reduction is followed fluoroscopically until it is completely reduced. Air should flow freely from the cecum into the distal small bowel loops to signify complete reduction. One critical safety issue is to keep air pressure below a maximum limit of 120 mmHg to avoid the risk of perforation (22, 46, 56).

Air Versus Liquid Enema

Two randomized trials comparing outcomes with air versus liquid enema technique exist,

yet their conclusions differ, with one stating there is no difference and the other showing the air enema superior to liquid enema (59, 60) (moderate evidence). In 1999, Hadidi and El Shah reported that air had a higher reduction rate than liquid enema (p=0.01). Children were randomized with less than 48 hours of symptoms to saline reduction under sonographic guidance (n=47), air (n=50), or barium (n=50) under fluoroscopic guidance (59). In 1993, Meyer and colleagues randomized 101 children to air (n=50) or barium (n=51) enema and found success rates of 76% for air and 63% for liquid enema (60). The results were not statistically significant but do support air as being more effective. In addition, the trial used sedation and had lower reduction rates than those not using sedation (25). The authors abandoned the use of sedation after this study. The use of sedation may reduce the intraabdominal pressure children create by the Valsalva maneuver and is reported to improve reducibility at enema (46, 56). More recent reports of air reduction show better results than liquid enema reduction (1). The superior air enema results may be due to the level of experience of those who use air reduction techniques as well as the presence of higher intraluminal pressure for air as compared to standard hydrostatic reduction (61, 62).

In a 1991 survey of American pediatric radiology chairs, Meyer found that only 24% were using air enema but 64% used barium and 12% water-soluble contrast (16) as compared to 35% of international pediatric radiologists who used air enema (63). More recently, in 2004, 65% of American pediatric radiologists reported using air enema, 33% used liquid enema (water-soluble contrast or barium), and 3% used liquid enema with sonographic guidance (15). Some pediatric radiologists will use air for children older than 3 months but for younger infants, especially neonates, they prefer liquid contrast due to the greater differential diagnosis in this group (25).

All children should have surgical consultation prior to enema (a) to assess for peritoneal signs precluding enema, (b) to identify children who cannot be reduced with enema or who are found to have perforation, and (c) for post-reduction management. Prior to enema reduction, dehydration should be treated with intravenous fluid resuscitation. Children with evidence of peritonitis, shock, sepsis, or free air on abdominal radiographs are not candidates for enema. Radiologists should strive for enema reduction rates of 80%, but it will depend on their patient population (moderate evidence). Several reports estimate that the rate of spontaneous reduction based on sonographic and/or enema diagnosis prior to surgery is 10% (1, 21, 42, 51) (limited evidence).

Bratton and colleagues suggest that more experienced radiologists and caregivers at children's hospitals decrease the risk of surgical reduction, length of hospital stay, and cost of care (17) (moderate evidence). Surgical management is performed when the patient is too unstable (shock, dehydration, sepsis) for enema reduction, when the enema is unsuccessful, or when PLP is diagnosed.

The Rule of Threes

A general guideline to the liquid enema technique, often taught to radiology residents, is the "rule of threes": three attempts of 3-minute duration, with the liquid enema bag at 3 feet above the fluoroscopy table. There is little evidence to support this rule, particularly regarding the height of the enema bag (25, 64). Many experienced pediatric radiologists alter this general guide in response to the clinical status of the patient and the movement of the intussusceptum mass achieved with the initial enema (21, 64). For example, if the intussusception is partially reduced to where it most frequently hangs up, at the ileocecal valve, some radiologists will make further or longer attempts and/or raise the enema bag above 3 feet. The exam is tailored to the patient and performed in conjunction with the surgeon involved.

Radiation Dose

The dose deposited will depend on a number of factors, including the type of fluoroscopy equipment, the use of pulsed fluoroscopy, and the fluoroscopy time (1, 46). A 1993 study reported a very low mean effective dose of 0.055 mSv for enema reduction of an intussusception (65). Experienced pediatric radiologists using air enema averaged 95 seconds of fluoroscopy time to reduce an intussusception and

42 seconds to exclude one in a child without intussusception (56). Air enema radiation doses average one-third to one-half less the dose for liquid enema (46).

Alternative Enema Approaches

A number of different approaches have been described to try to improve intussusception reduction on enema that include sedation, anesthesia, use of glucagon, manual palpation, and delayed repeat enema. In the past, sedation and sometimes anesthesia were commonly used to improve reduction rates but case series showed no improvement (16, 66, 67) (limited evidence). In a 1991 survey Meyer found that only 10% of respondents used sedation either always or almost always (16) as compared to 54% of international pediatric radiologists, and those using sedation reported lower reduction rates (59). Therefore, few pediatric radiologists currently use sedation in the United States. Glucagon was shown not to improve enema reduction rates in one study (68) and is no longer used (16). The use of manual palpation has been suggested to improve intussusception reduction at enema but has not been systematically studied (46, 69). One study by Grasso et al. reported a reduction rate of 76% when manual palpation was used, less than the average of 80% in large series (69).

Fluoroscopy Versus Sonography

In the West (i.e., North America, parts of Europe, Australia), fluoroscopy is almost always used during enema reduction. There are other reports, primarily from Asia, on the use of sonography with either water (70–76) or air (77–79) that show reduction rates as high as or higher than those using fluoroscopy. However, the experience level required for these techniques has not been studied nor has the ability of sonography to detect perforations (limited evidence).

Delayed Repeat Enema

In the small percent of children who fail initial enema reduction, delayed repeat enema may avoid the need for surgical reduction. The use of delayed attempts at between 30 minutes and 19 hours after initial attempt has shown promise in increasing the success of enema reductions (80–84) (limited evidence). These four small series showed further reduction rates of 50–82% by waiting at least 30 minutes prior to further attempts at enema reduction. Further research to understand optimal timing and technique for delayed repeat enemas is needed. Daneman and Navarro, with the largest reported experience to date, suggest a delay of 2–4 hours until further research yields more rigorous guidelines (25). The child must remain clinically stable and be appropriately monitored during this time interval. Delayed enema should not be performed if the initial enema does not move the intussusception at all (25, 83).

Where Should Patients Be Treated?

Bratton and colleagues performed a retrospective cohort analysis of all children hospitalized with intussusception in the state of Washington from 1987 through 1996 (17) (moderate evidence). They investigated whether the rate of surgical management for these children varied by hospital pediatric caseload, measured by the annual number of pediatric hospital admissions. By reviewing the discharge data of all 507 children, they found an overall rate of surgical reduction of 53%, with 20% undergoing bowel resection. Rates of surgical reduction varied by pediatric caseload from 36% at hospitals with large pediatric caseloads to nearly double, 64%, at hospitals with low pediatric volumes. Children who underwent surgery versus enema reduction had similar gender and median age characteristics, but those who had bowel resection were more likely to have coexisting conditions. Median cost of hospital care for these children was $5,724 for surgical reduction and $1,184 for enema reduction.

What Are the Complications of Enema Therapy?

The most important potential complication of enema is bowel perforation. Sixty-six published studies of this question were largely Level-3 (limited evidence) investigations consisting of unselected but often consecutive case series. The mean perforation rate was 0.8% (Table 31.2). In 18 case series with at least 150 children each, perforation rates averaged 0.6%, with a range of 0–1.6% (25). There were no statistically

significant differences between air and liquid enema perforation rates (Table 31.3). When these averages were weighted to reflect the sample size of each published study, the perforation rates were even lower, at 0.3% for all 66 studies and 0.2% for the larger studies.

Ultimately, however, the risk of perforation depends on each radiologist's patient population and technique. Though determination of clinical predictors of perforation is complicated by lack of prospective studies, the one acknowledged key factor is symptom length greater than 48 hours. Several reports in both pig models and children suggest that there may be preexisting focal perforation in the necrotic intussuscipiens or, less commonly, the intussusceptum that is rarely radiographically apparent as free air (20, 22, 25, 85–88) (moderate evidence). The most common site is at or just proximal to the intussusception in the transverse colon (88). Perforations with air tend to be smaller than those with liquid enema although the overall perforation rates are similar (22, 86).

In 1989, Campbell surveyed enema techniques and complications of North American pediatric radiologists (89). Respondents' combined experience was 14,000 intussusception enemas. Although they did not report enema reduction rates, the combined perforation rate was 0.39% (55/14,000), with only one death. This study remains the basis for the risk of perforation that is explained to parents for consent prior to enema reduction (one in 250 to one in 300) (limited evidence).

Barium is no longer the liquid contrast medium of choice for reduction of intussusception due to the risk of barium peritonitis, infection, and adhesions when perforation occurs during the enema (22, 46, 53, 57) (moderate evidence). While iodinated contrast is now preferred and is considered a safer agent than barium, one should be aware that it may produce fluid and electrolyte shifts if perforation occurs since contrast is absorbed from the peritoneum.

One complication unique to air enema is the tension pneumoperitoneum. In an early report, two deaths occurred from this complication, leading the proponents of air enema to advise having an 18-gauge needle readily available in the fluoroscopy room for emergent decompression (25, 46, 53). Although theoretically possible, there have been no reports of air embolism.

What Are the Surgical Management and Complications?

Depending on the patient population, approximately 20–40% of children who undergo surgical reduction of their intussusception will require bowel resection (20% reference 17; 30–40% reference 1). If we estimate that 20% of children with intussusception will fail enema reduction and undergo surgical reduction, then only 4–8% of all children will require bowel resection. Ideally, only this population should need surgical intervention.

Short-term complications from laparotomy include infection and bowel perforation. The long-term risk of small bowel obstruction from adhesions is approximately 8% for neonates and 3–5% for those children older than 1 month (90).

Cost-Effectiveness Analysis

There are no known rigorous economic analyses on diagnosis and treatment strategies for intussusception, although one study evaluated the cost savings of more aggressive enema reduction compared to surgical reduction (19). Stein and colleagues analyzed single institution billing records of 703 children with intussusception to compare government DRG reimbursements of hospital care in Australia (limited evidence). In 1993 Australian dollars, the government paid, on average, $727 for enema reduction and $4,514 for surgical reduction in hospital care. With the broader indications for enema and the increased use of air, they noted decreased use of surgical reduction at their institution: in 1983, 65% children underwent surgical reduction decreasing to 25% in 1992 (19). Ironically, the authors noted that hospital profit, however, is greater for surgical reductions.

IV. What Is Appropriate Management in Recurrent Cases?

Summary of Evidence: Intussusception recurrence rates average 10% in large series, with a range of 5.4–15.4% (1, 91), regardless of air versus liquid enema technique (moderate evidence). The recurrence rates are =5% when surgical reduction is performed, presumably

due to the development of adhesions (92). Repeat enema is both safe and effective in recurrent intussusception (1, 46, 92, 93) as long as the child remains clinically stable (limited evidence). There is insufficient evidence to support any particular approach beyond the performance of the enema and referral to a surgeon for shared decision-making with the patient.

Supporting Evidence: Fifty percent of children who develop recurrent intussusception will present within 48 hours, although recurrences have been reported up to 18 months later (53) (limited evidence). No clear risk factors are known for why some children have recurrences although some have focal PLP. In those with PLP, children with diffuse bowel abnormality such as cystic fibrosis, Henoch-Schonlein Purpura, or celiac disease may be treated with enema reduction more aggressively than those with focal PLPs.

The risk of PLP in children with recurrent intussusception is low. In one large series of 763 children, it was 8% (5/69) (53), only slightly higher than the reported 5–6% incidence of PLP at first presentation of intussusception (1) (insufficient evidence). No predictive clinical factors have been identified for PLP in these children with recurrent intussusception. Reduction with air enema was possible in 95% of recurrences in the largest reported experience (1, 53) (limited evidence).

When there is concern for PLP, sonography may play an important role and may detect 60% of PLPs (1, 44, 92) (limited evidence). While US will not detect all PLPs, the risk of missing a PLP without other signs or symptoms to guide management is unlikely (48). Ein reviewed 1,200 intussusception cases covering 40 years' experience at one institution to analyze this risk. When the enema failed to detect lymphoma as a PLP, Ein noted the presence of clinical signs of illness of greater than 1 week, patient age greater than 3 years, weight loss, and palpable mass in all of these children (limited evidence).

In a randomized, double-blind trial comparing 144 children who received intramuscular corticosteroids versus 137 who received placebo before air enema reduction, Lin and colleagues reported significantly fewer intussusception recurrences at 6 months (3) (moderate evidence). In both groups, the initial reduction rate was 85%. There were no recurrences in the children who received dexamethasone, compared to 5% in the placebo group. They hypothesized that steroids decreased the volume of mesenteric adenopathy and lymphoid hyperplasia in the terminal ileum and thus the risk of recurrence. However, further investigation of the risks and benefits of this intervention is needed.

V. Special Case: Intussusception Limited to the Small Bowel

With the increasing use of multi-detector CT scanners, radiologists are reporting more frequent presence of small, asymptomatic small bowel–small bowel intussusception (2, 94) (limited evidence). These intussusceptions are typically transient and, since the children are asymptomatic, they are of no known clinical significance.

There is little evidence in the literature regarding the optimal diagnosis and treatment of symptomatic intussusception limited to the small bowel. Most authors agree, however, that the diagnosis is more difficult both clinically and radiologically (1, 21, 26). Small bowel intussusceptions are unlikely to have associated abdominal mass or rectal bleeding. Treatment is virtually always surgical reduction. Special risk factors for small bowel intussusception include the early post-operative period after either intraperitoneal or retroperitoneal surgery, the presence of long enteric feeding tubes, diffuse PLP (cystic fibrosis or HSP), and small bowel polyps (1, 26, 95) (limited evidence).

VI. Special Case: Intussusception with a Known Lead Point Mass

The optimal imaging approach to children with intussusception and known PLP is unknown. However, Daneman surveyed the SPR members at their 2004 annual meeting and found that 76% of respondents attempt reduction

in these patients (15). Some surgeons may request enema reduction in these children to partially reduce the intussusception and perhaps decrease the laparotomy incision size (82). There is insufficient evidence to support any particular approach beyond referral to a surgeon for shared decision-making with the patient and, if requested, the performance of an enema (25, 59, 93).

Take Home Tables

Table 31.1 summarizes the sensitivity and specificity of diagnostic imaging for intussusception. Table 31.2 summarizes the published intussusception enema reduction rates and perforation rates. Table 31.3 summarizes the comparison of air versus liquid contrast enema reduction and perforation rates.

Table 31.1. Summary of sensitivity and specificity of diagnostic imaging for intussusception

Test	Sensitivity (%)	Specificity (%)
Abdominal radiographs*	45	–
Ultrasound#	98–100	88–100
Enema^	100	100

*Data from references (4) and (27).
#Data from references (5, 31, 36, 37).
^Reference standard for ileocolic intussusception (does not include intussusception limited to small bowel); see reference 25.
(Reprinted with the kind permission of Springer Science+Business Media from Applegate KE. Intussusception in children: Diagnostic imaging and treatment. In Santiago LS, Blackmore CC (eds.) Evidence-Based Imaging: Optimizing Imaging in Patient Care. New York: Springer Science+Business Media, 2006.)

Table 31.2. Summary of published intussusception enema reduction rates and perforation rates. Summary data include a weighted average measure of reduction and perforation rates based on publications with at least 150 pediatric cases. The enema techniques varied and included air versus liquid media, with sonographic or fluoroscopic guidance

	All Studies			Studies with cases>150		
Rates	Number of studies	Mean (SD)	Wt mean (SD)	Number of studies	Mean (SD)	Wt mean (SD)
Reduction (%)	71	74.1 (16.8)	87.3 (12)	19	79.6 (12.5)	89.5 (9.3)
Perforation (%)	66	0.8 (1.4)	0.3 (0.7)	18	0.6 (0.8)	0.2 (0.4)

Wt mean=weighted mean; SD=standard deviation.
Data from Daneman and Navarro (25).
(Reprinted with the kind permission of Springer Science+Business Media from Applegate KE. Intussusception in children: Diagnostic imaging and treatment. In Santiago LS, Blackmore CC (eds.) Evidence-Based Imaging: Optimizing Imaging in Patient Care. New York: Springer Science+Business Media, 2006.)

Table 31.3. Summary comparison of air versus liquid contrast enema reduction and perforation rates. Note that while the liquid contrast media reduction rates are lower, a number of these studies are older than the newer air enema reports. There was no significant difference in perforation rates

		All studies			Studies with cases >150		
		Number of studies	Mean (SD)	Wt mean (SD)	Number of studies	Mean (SD)	Wt mean (SD)
Reduction (%)	Pneumatic	32	82.1 (11.9)	91.4 (5.2)	10	86.4 (6.3)	92.2 (3.3)
	Hydrostatic	39	67.5 (17.6)	69.1 (15.2)	9	72.1 (13.7)	70.0 (14.1)
	p-value		<0.001	<0.0001	0.009	<0.0001	
Perforation (%)	Pneumatic	31	1.0 (1.5)	0.3 (0.6)	11	0.8 (0.9)	0.2 (0.4)
	Hydrostatic	35	0.6 (1.4)	0.4 (1.0)	7	0.3 (0.6)	0.2 (0.4)
	p-value		0.30	0.53	0.28	0.99	

p-values are based on the *t*-test.
Data from Daneman and Navarro (25).
(Reprinted with the kind permission of Springer Science+Business Media from Applegate KE. Intussusception in children: Diagnostic imaging and treatment. In Santiago LS, Blackmore CC (eds.) Evidence-Based Imaging: Optimizing Imaging in Patient Care. New York: Springer Science+Business Media, 2006.)

Imaging Case Study

Case 1

Figures 31.1 and 31.2 present the case of a 9-month-old boy who comes to the emergency department with a 1-day history of irritability, vomiting, and intermittent crying.

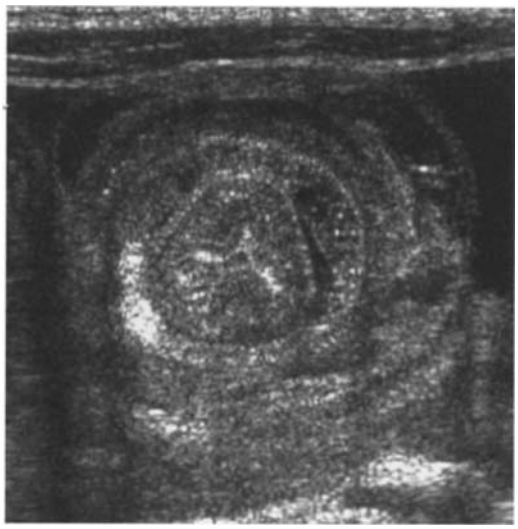

Figure 31.1. Linear sonography of the right mid–lower abdomen demonstrates the target sign of bowel intussusception. There is bowel within bowel and thickened walls of these loops due to edema. No primary lead point (PLP) is identified. (Reprinted with the kind permission of Springer Science+Business Media from Applegate KE. Intussusception in Children: Diagnostic Imaging and Treatment. In Santiago LS, Blackmore CC (eds.) Evidence-Based Imaging: Optimizing Imaging in Patient Care. New York: Springer Science+Business Media, 2006).

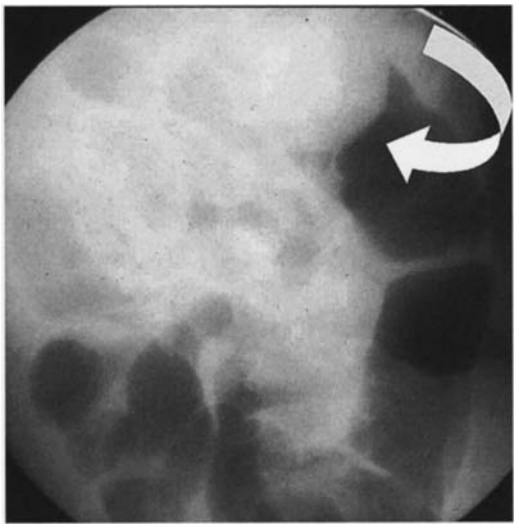

Figure 31.2. The appearance of the intussusception at air enema reduction. The intussusception is encountered at the hepatic flexure, with the baby in a prone position (*arrow*). Air is insufflated into the rectum to push the intussusception retrograde until it is no longer seen on fluoroscopy and there is air in multiple loops of small bowel. (Reprinted with the kind permission of Springer Science+Business Media from Applegate KE. Intussusception in Children: Diagnostic Imaging and Treatment. In Santiago LS, Blackmore CC (eds.) Evidence-Based Imaging: Optimizing Imaging in Patient Care. New York: Springer Science+Business Media, 2006).

Suggested Imaging Protocol for Intussusception in Children

Ultrasound for Clinically Suspected Intussusception

If there is a concern for alternative diagnoses such as constipation, 1–2 view abdominal radiographs (supine or prone and decubitus) (limited evidence). The abdomen is scanned with a 5 mHz or higher linear transducer using the graded compression technique and a bowel or high-contrast application package. All four quadrants of the abdomen must be scanned, typically in transverse planes, beginning with the right upper quadrant, to exclude an intussusception mass.

Air Enema for Reduction

Prior to performing the enema, consult the surgeon (moderate evidence). [If no experience with air or few cases seen per year, then perform liquid enema with water-soluble contrast using the guide of the "rule of threes" described previously.] The enema tip without a balloon should be placed within the child's rectum and taped in place with abundant tape. With the child prone, the radiologist squeezes the buttocks closed to prevent air leak. Air is rapidly insufflated into the colon under fluoroscopic observation until the intussusception is completely reduced, when air flows freely from the cecum into the distal small bowel loops. Air pressure must remain below a maximum limit of 120 mmHg to avoid the risk of perforation. Repeat enema for recurrences, including multiple recurrences (limited evidence).

Future Research Studies

- Investigate the optimal technique and timing of delayed, repeat enema reduction.
- Investigate the role of corticosteroids to decrease the rate of recurrence in a prospective controlled trial.
- Perform cost-effectiveness analyses (CEA) of the role of US for the diagnosis of intussusception. This investigation would include the question: At what disease prevalence or individual case probability is US cost-effective prior to enema?

References

1. Navarro O, Daneman A. Pediatr Radiol 2004; 34:305–312.
2. Strouse PJ, DiPietro MA, Saez F. Pediatr Radiol 2003 May; 33(5):316–320. Epub 2003 Feb 26.
3. Lin SL, Kong MS, Houng DS. Eur J Pediatr 2000 Jul; 159(7):551–552.
4. Daneman A, Navarro O. Pediatr Radiol 2003; 33:79–85.
5. Harrington L, Connolly B, Hu X, Wesson DE, Babyn P et al. J Pediatr 1998 May; 132(5):836–839.
6. Lai AH, Phua KB, Teo EL, Jacobsen AS. Ann Acad Med Singapore 2002 Jan; 31(1):81–85.
7. Losek JD, Fiete RL. Am J Emerg Med 1991 Jan; 9(1):1–3.
8. Parashar UD, Holman RC, Cummings KC, Staggs NW, Curns AT et al. Pediatrics 2000 Dec; 106(6):1413–1421.
9. Berlin L. Am J Roentgenol 1998; 170:1161–1163.

10. Meier DE, Coln CD, Rescorla FJ, OlaOlorun A, Tarpley JL. World J Surg 1996 Oct; 20(8): 1035–1039; discussion 1040.
11. CDC and Prevention. MMWR Morb Mortal Wkly Rep 1999; 48:1007.
12. Chang HG, Smith PF, Ackelsberg J, Morse DL, Glass RI. Pediatrics 2001 Jul; 108(1):54–60.
13. Rennels MB, Parashar UD, Holman RC, Le CT, Chang HG et al. Pediatr Infect Dis J 1998 Oct; 17(10):924–925.
14. Dennehy PH, Bresee JS. Infect Dis Clin North Am 2001 Mar; 15(1):189–207.
15. Daneman A. Personal communication, SPR meeting 2004 unpublished survey.
16. Meyer JS. Pediatr Radiol 1992; 22:323–325.
17. Bratton SL, Haberkern CM, Waldhausen JH, Sawin RS, Allison JW. Pediatrics 2001 Feb; 107(2):299–303.
18. Leonidas JC. Am J Roentgenol 1985 Oct; 145(4):665–669.
19. Stein JE, Beasley SW, Phelan E. Aust N Z J Surg 1997 Jun; 67(6):330–331.
20. Beasley S. Pediatr Radiol 2004; 34:302–304.
21. Littlewood Teele R, Vogel SA. Pediatr Surg Int 1998 Dec; 14(3):158–162. Review.
22. Shiels WE II, Kirks DR, Keller GL, Ryckman FR, Daugherty CC et al. Am J Roentgenol 1993; 160:931–935.
23. Kuppermann N, O'Dea T, Pinckney L, Hoecker C. Arch Pediatr Adolesc Med 2000 Mar; 154(3):250–255.
24. Klein EJ, Kapoor D, Shugerman RP. Clin Pediatr (Phila) 2004 May; 43(4):343–347.
25. Daneman A, Navarro O. Pediatr Radiol 2004; 34:97–108.
26. Sargent MA, Babyn P, Alton DJ. Pediatr Radiol 1994; 24(1):17–20.
27. West KW, Stephens B, Vane DW, Grosfeld JL. Surgery 1987 Oct; 102(4):704–710.
28. Eklof O, Hartelius H. Pediatr Radiol 1980 Jul; 9(4):199–206.
29. Bowerman RA, Silver TM, Jaffe MH. Radiology 1982; 143:527–529.
30. Lee HC, Yeh HJ, Leu YJ. J Pediatr Gastroenterol Nutr 1989 Apr; 8(3):343–347.
31. Pracros JP, Tran-Minh VA, Morin de Finfe CH, Deffrenne-Pracros P, Louis D et al. Ann Radiol (Paris) 1987; 30(7):525–530.
32. Swischuk LE, Hayden CK, Boulden T. Pediatr Radiol 1985; 15:388–391.
33. Del-Pozo G, Albillos JC, Tejedor D, Calero R, Rasero M et al. RadioGraphics 1999; 19:299–319.
34. Henrikson S, Blane CE, Koujok K, Strouse PJ, DiPietro MA et al. Pediatr Radiol 2003; 33: 190–193.
35. Schmit P, Rohrschneider WK, Christmann D. Pediatr Radiol 1999 Oct; 29(10):752–761.
36. Shanbhogue RLK, Hussain SM, Meradji M, Robben SGF, Vernooij JEM et al. J Pediatr Surg 1994; 29:324–328.
37. Verschelden P, Filiatrault D, Garel L, Grignon A, Perreault G et al. Radiology 1992; 184:741–744.
38. Eshed I, Gorenstein A, Serour F, Witzling M. Pediatr Radiol 2004; 34:134–137.
39. Bhisitkul DM, Listernick R, Shkolnik A et al. J Pediatr 1992 Aug; 121(2):182–186.
40. Del-Pozo G, Gonzalez-Spinola J, Gomez-Anson B, Serrano C, Miralles M et al. Radiology 1996; 201:379–383.
41. Britton I, Wilkinson AG. Pediatr Radiol 1999 Sep; 29(9):705–710.
42. Swischuk LE, John SD, Swischuk PN. Radiology 1994; 192:269–271.
43. Lagalla R, Caruso G, Novara V, Derchi LE, Cardinale AE. J Ultrasound Med 1994 Mar; 13(3): 171–174.
44. Lam AH, Firman K. Pediatr Radiol 1992; 22(2):112–114.
45. Lim HK, Bae SH, Lee KH, Seo GS, Yoon GS. Radiology 1994; 191:781–785.
46. Kirks DR. Radiology 1994; 191:622–623.
47. Koumanidou C, Vakaki M, Pitsoulakis G, Kakavakis K, Mirilas P. Am J Roentgenol 2002; 178:445–450.
48. Ein SH. J Pediatr Surg 1976 Apr; 11(2):209–211.
49. Miller SF, Landes AB, Dautenhahn LW et al. Radiology 1995; 197:493–496.
50. Navarro O, Dugougeat F, Kornecki A, Shuckett B, Alton DJ et al. Pediatr Radiol 2000 Sep; 30(9):594–603.
51. Kornecki A, Daneman A, Navarro O, Connolly B, Manson D et al. Pediatr Radiol 2000; 30:58–63.
52. Beasley SW, Glover J. J Pediatr Surg 1992 Apr; 27(4):474–475.
53. Daneman A, Alton DJ, Ein S, Wesson D, Superina R et al. Pediatr Radiol 1995; 25:81–88.
54. Gu L, Alton D, Daneman A, Stringer DA, Liu P et al. Am J Roentgenol 1988; 150: 1345–1348.
55. Guo JZ, Ma XY, Zhou QH. J Pediatr Surg 1986; 21:1201–1203.
56. Shiels WE II, Maves CK, Hedlund GL, Kirks DR. Radiology 1991; 181:169–172.
57. Hernanz-Schulman M, Foster C, Maxa R, Battles G, Dutt P et al. Pediatr Radiol 2000 Jun; 30(6):369–378.
58. Stringer MD, Pablot M, J Brereton. J Surg 1992; 79:867–876.
59. Hadidi AT, El Shal N. J Pediatr Surg 1999; 34: 304–307.
60. Meyer JS, Dangman BS, Buonomo C, Berlin JA. Radiology 1993; 188:507–511.
61. Sargent MA, Wilson BP. Pediatr Radiol 1991; 21(5):346–349.

62. Zambuto D, Bramson RT, Blickman JG. Radiology 1995; 196:55–58.
63. Katz ME, Kolm P. Pediatr Radiol 1992; 22: 318–322.
64. McAlister WH. Radiology 1998 Mar; 206(3): 595–598. Review.
65. Thomas RD, Fairhurst JJ, Roberts PJ. Clin Radiol 1993 Sep; 48(3):189–191.
66. Suzuki M, Hayakawa K, Nishimura K, Koide M, Tateishi S et al. Radiat Med 1999 Mar–Apr; 17(2):121–124.
67. Touloukian RJ, O'Connell JB, Markowitz RI, Rosenfield N, Seashore JH et al. Pediatrics 1987 Mar; 79(3):432–434.
68. Franken EA, Smith WL, Chernish SM, Campbell JB, Fletcher BD et al. Radiology 1983; 146: 687–689.
69. Grasso SN, Katz ME, Presberg HJ. Radiology 1994; 191:777–779.
70. Gonzalez-Spinola J, Del Pozo G, Tejedor D, Blanco A. J Pediatr Surg 1999 Jun; 34(6): 1016–1020.
71. Khong PL, Peh WC, Lam CH, Chan KL, Cheng W et al. Radiographics 2000 Sep–Oct; 20(5):E1.
72. Peh, WCG, Khong PL, Chan KL, Lam C, Cheng W et al. Am J Roentgenol 1996; 167:1237–1241.
73. Riebel TW, Nasir R, Weber K. Radiology 1993; 188:513–516.
74. Rohrschneider WK, Troger J. Pediatr Radiol 1995; 25:530–534.
75. Wang GD, Liu SJ. J Pediatr Surg 1988 Sep; 23(9):814–818.
76. Woo SK, Kim JS, Suh SJ, Paik TW, Choi SO. Radiology 1992; 182:77–80.
77. Gu L, Zhu H, Wang S, Han Y, Wu X et al. Pediatr Radiol 2000 May; 30(5):339–342.
78. Todani T, Sato Y, Watanabe Y, Toki A, Uemura S et al. Z Kinderchir 1990 Aug; 45(4):222–226.
79. Yoon CH, Kim HJ, Goo HW. Radiology 2001; 218:85–88.
80. Connolly B, Alton DJ, Ein SH, Daneman A. Pediatr Radiol 1995; 25:104–107.
81. Gorenstein A, Raucher A, Serour F, Witzling M, Katz R. Radiology 1998; 206:721–724.
82. Navarro OM, Daneman A, Chae A. Am J Roentgenol 2004 May; 182(5):1169–1176.
83. Sandler AD, Ein SH, Connolly B, Daneman A, Filler RM. Pediatr Surg Int 1999; 15(3–4):214–216.
84. Saxton V, Katz M, Phelan E, Beasley SW. J Pediatr Surg 1994 May; 29(5):588–589.
85. Armstrong EA, Dunbar JS, Graviss ER, Martin L, Rosenkrantz J. Radiology 1980; 136:77–81.
86. Blane CE, DiPietro MA, White SJ, Klein ME, Coran AG et al. J Can Assoc Radiologists 1984; 35:113–115.
87. Daneman A, Alton DJ, Lobo E, Gravett J, Kim P et al. Pediatr Radiol 1998 Dec; 28(12):913–919.
88. Mercer S, Carpenter B. Can J Surg 1982; 25: 481–483.
89. Campbell JB. Pediatr Radiol 1989; 19:293–296.
90. Janik JS, Ein SH, Filler RM, Shandling B, Simpson JS et al. J Pediatr Surg 1981; 16:225–229.
91. Champoux AN, Del Beccaro MA, Nazar-Stewart V. Arch Pediatr Adolesc Med 1994; 148: 474–478.
92. Ein SH. J Pediatr Surg 1975; 10:751–755.
93. Katz M, Phelan E, Carlin JB, Beasley SW. Am J Roentgenol 1993 Feb; 160(2):363–366.
94. Cox TD, Winters WD, Weinberger E. Pediatr Radiol 1996; 26:26–32.
95. Hughes UM, Connolly BL, Chait PG, Muraca S. Pediatr Radiol 2000 Sep; 30(9):614–617.

32

Imaging of Appendicitis in Pediatric Patients

Erin A. Cooke and C. Craig Blackmore

Issues

I. What is the accuracy of imaging for diagnosing acute appendicitis in children?
II. In which cases of suspected pediatric appendicitis is imaging indicated?
III. What is the effect of imaging on the rate of negative appendectomy in pediatric patients with suspected appendicitis?
IV. What is the role of imaging in managing pediatric perforated appendicitis?
V. What is the effect of imaging pediatric patients with suspected appendicitis on health-care costs?

Key Points

- In pediatric patients, CT demonstrates superior sensitivity compared to ultrasound in diagnosis of appendicitis, with similar specificities of these modalities (moderate evidence).
- A protocol of initial use of ultrasound followed by CT for negative or equivocal cases may be warranted in order to minimize the risks of ionizing radiation (moderate evidence).
- The presence of an elevated absolute neutrophil count, nausea, or maximal tenderness in the right lower quadrant shows high sensitivity but poor specificity in identifying pediatric patients with appendicitis (moderate evidence). These patients may benefit from imaging.
- There is conflicting evidence regarding the effect of imaging on the rate of negative appendectomy, but the more valid studies suggest that there is a decrease in the rate with use of preoperative imaging (moderate evidence).
- Preliminary data suggest that preoperative imaging may be able to differentiate between cases of perforated and nonperforated appendicitis.

E.A. Cooke (✉)
Department of Radiology, Virginia Mason Medical Center, Seattle, WA 98101, USA
e-mail: radeac@vmmc.org

L.S. Medina et al. (eds.), *Evidence-Based Imaging in Pediatrics*,
DOI 10.1007/978-1-4419-0922-0_32,

Additionally, imaging may lead to a decrease in the perforation rate and may be useful in predicting clinical outcomes in patients who present with perforation (limited evidence).
- The data examining the financial impact of imaging pediatric patients with suspected appendicitis are inconclusive (insufficient evidence).

Definition and Pathophysiology

Appendicitis is defined as inflammation of the vermiform appendix, usually caused by obstruction of the appendiceal lumen (1, 2). Obstruction leads to bacterial overgrowth and an increase in intraluminal pressure, which in turn causes a decrease in mural perfusion. The resulting inflammation and decrease in vascular perfusion can lead to gangrene and perforation. Delayed diagnosis can result in serious complications, including gross perforation, abscess formation, peritonitis, wound infection, sepsis, infertility, adhesions, and bowel obstruction (3, 4).

Epidemiology

Acute appendicitis is the most common reason for abdominal surgery in pediatric patients (3–5) and is diagnosed in 1–8% of children presenting with abdominal pain to the emergency department (2, 4). There are approximately 70,000–90,000 pediatric cases of appendicitis yearly in the United States (1, 6). The estimated incidence ranges from 75 to 233 per 100,000 pediatric patients per year, with males affected more commonly than females at a rate of 1.4 to 1.0 (5). It is more common in 10- to 19-year-old patients although it can present even in children under 1 year old (3, 5). The rate of perforation in pediatric patients ranges from 23 to 73% in various series and is higher in young children (2–4, 7).

Overall Cost to Society

Acute appendicitis is a very common reason for pediatric hospitalization and incurs significant costs in terms of health-care resources. For pediatric patients, appendectomy is the most common surgical procedure performed in the hospital for non-neonatal- or non-pregnancy-related conditions (6). Nationwide, an average of 238 pediatric appendectomies are performed daily (6). Annually, appendicitis accounts for approximately 87,000 pediatric hospital stays in the United States, representing 4.2% of all hospital stays for pediatric illness (6). Appendicitis is the second most common reason for hospitalization for children and adolescents 6–17 years old. The aggregate total charges related to care of pediatric patients with appendicitis nationwide sum to over $800,000,000 annually (6). At an institutional level, a retrospective chart review by Garcia Pena et al. showed that 308 pediatric patients who were observed for possible appendicitis collectively accumulated 487 inpatient observation days, with per-patient cost of $5,831 (8).

Goals

The goals of imaging in suspected acute appendicitis are to determine if the patient has appendicitis, enable earlier diagnosis, and identify complications, such as perforation or abscess, which may change surgical management.

Methodology

A recent meta-analysis on the performance of ultrasonography (US) and computed tomography (CT) for the diagnosis of appendicitis in pediatric populations was performed by Doria et al. (9). In this meta-analysis, a literature search was performed for articles from January 1986 to December 2004 that used US, CT, or both as diagnostic tests for appendicitis in children. The literature search used Medline, Embase, CINAHL, the Cochrane Database of Systematic Reviews, the Cochrane Controlled Trials Register, the American College of Physicians Journal Club database, and manual search for relevant articles. Medical subject headings included *appendicitis*, *appendix*, *sonography*, *ultrasonography, computed tomography*, and *computed*

tomography scan. Both prospective and retrospective studies were included. Clinical variables, technical factors, and test performance were appraised by three readers, and statistical analyses were performed, including pooled point estimates and 95% confidence intervals for the sensitivity and specificity of US or CT for the diagnosis of appendicitis.

To examine the more recent literature as well as studies not included by Doria et al., we performed a literature search of English language articles from 1990 through January 2008 using the Medline database and the MeSH terms *appendicitis and diagnostic imaging and either child, adolescent*, or *child-preschool*. The bibliographies of relevant articles were searched for other potentially relevant articles. Studies were included if they were either prospective or retrospective evaluations of CT or graded compression ultrasound in patients 18 years or younger, with outcomes measured by surgical, pathological, or clinical follow-up.

Discussion of Issues

I. What Is the Accuracy of Imaging for Diagnosing Acute Appendicitis in Children?

Summary of Evidence: CT is more sensitive than ultrasound with similar specificity (moderate evidence) (Table 32.1).

A protocol of US followed by CT in negative or equivocal subjects may achieve similar sensitivity and specificity to CT alone, with less radiation exposure (moderate evidence).

A protocol of US followed by CT if negative may be cost-effective for the evaluation of pediatric patients suspected of having appendicitis (moderate evidence).

There are no reliable data to support the use of abdominal radiographs in the diagnosis of acute appendicitis (insufficient evidence).

Supporting Evidence: Abdominal radiography is generally considered to be both insensitive and nonspecific in the diagnosis of acute appendicitis, although there are limited data to support this (4). Some studies have indicated that abdominal radiographs are either normal or misleading in approximately 77% of children with appendicitis and that they rarely affect management (2). Many of the findings that can be seen with appendicitis, such as localized ileus, bowel obstruction, and a right lower quadrant soft tissue mass, are very nonspecific. The purportedly most specific finding, that of a calcified appendicolith, is seen only in approximately 5–15% of patients with appendicitis versus in less than 1–2% of children without appendicitis (1, 2).

Cross-section imaging, therefore, is the mainstay of image-guided diagnosis. A recent meta-analysis by Doria et al. (9) found 26 prospective and retrospective trials of graded compression US and/or CT in pediatric patients (mean age range of 7–12 years) with suspected acute appendicitis. Studies included results from ultrasound only, CT only, or combined ultrasound and CT in 6,850, 598, and 1,908 patients, respectively. The mean sample prevalence of appendicitis from these trials was 0.31 for both US and CT articles (range 0.15–0.75). The weighted perforation rate in positive appendicitis cases was 26.5%.

This meta-analysis identified eight studies of CT in pediatric patients, which demonstrated a pooled sensitivity of 94% [95% confidence interval (CI), 92–97%], a combined specificity of 95% (95% CI, 94–97%), and a summary diagnostic odds ratio of 239 (95% CI, 118–487). For the extracted data, the positive and negative likelihood ratios were 18.8 and 0.06, respectively (5). When these test specifications were applied to a population with the mean prevalence of appendicitis found in the trials examined by Doria et al. (31%), the positive predictive value was 89% and the negative predictive value was 97%.

There were 23 studies of graded compression ultrasound that met inclusion criteria in the Doria et al. study. With one outlier removed, the pooled sensitivity of ultrasound in pediatric populations was 88% (95% CI, 86–90%), the pooled specificity was 94% (95% CI, 92–95%), and the summary diagnostic odds ratio was 202 (95% CI, 159–258). The positive and negative likelihood ratios were 14.7 and 0.13, respectively (5). The positive predictive value of graded compression ultrasound was 87%, and the negative predictive value was 95% using the mean prevalence of 31% for calculations.

Thus, in patients with suspected acute appendicitis in whom further evaluation with

imaging is desired, the Doria et al. article demonstrated that there is a significant difference in the weighted pooled sensitivities in favor of CT use, with no significant difference in specificity of CT compared to US. However, as the authors noted, pediatric patients in general demonstrate greater sensitivity to ionizing radiation which is produced with CT scanning. This radiation risk of CT use must be weighed against the risk of additional false-negative cases with US.

Several limitations were identified in the examined studies, including potential verification and selection bias, which could result in falsely inflated sensitivity and specificity estimates. The degree of differential verification bias is probably similar between CT and US since patients with negative imaging results were likely to be managed nonoperatively regardless of modality. Additional difficulties in analysis included lack of randomization of patients to imaging groups. Generalizability may also be an issue as CT was more commonly studied in North America whereas ultrasound was more prevalently used in Europe and Asia. In addition, relatively few children under the age of 5 years were included in many of the studies, so that the results may not hold true for infants and preschool-age children.

In review of the literature since the Doria et al. paper, a single prospective trial examining CT in pediatric patients with suspected acute appendicitis was identified (10). This 2005 study of 94 patients of ages 6–17 who were admitted to the hospital for observation for possible appendicitis found that CT with rectal contrast demonstrated a sensitivity of 100%, specificity of 98%, positive predictive value of 90%, and negative predictive value of 100% for those 53 patients in whom the appendix was visualized. The investigators labeled those studies in which the radiologist could not identify the appendix as positive for possible appendicitis. Given the relatively small sample size, these results are consistent with the results of the Doria et al. meta-analysis, although the absence of data on many subjects in whom the appendix was not visualized limits the data.

Ideally, an imaging protocol would combine the sensitivity of CT with the lack of ionizing radiation afforded by US in order to maximize diagnostic accuracy while minimizing patient risk. In our literature search, two prospective studies were identified which examined the combination of graded compression ultrasound as the initial imaging followed by CT study if the appendix was not visualized by ultrasound or if the ultrasound was inconclusive for the diagnosis of appendicitis (11, 12). These trials enrolled a total of 585 patients with a prevalence of appendicitis ranging from 23 to 43% with a pooled prevalence of 39%. The sensitivity varied from 77 to 97% with a pooled sensitivity of 95% (95% CI, 83–100%). The range of specificity was 89–99%, with a pooled result of 93% (95% CI, 97–97%). As expected, these series demonstrated a greater sensitivity and lower specificity when the combined US followed by CT results were considered than when the US data were considered alone. Another randomized trial of 600 patients compared results of CT and ultrasound versus ultrasound alone in a pediatric population (13). This study demonstrated similar results to the two aforementioned series, with the combined CT and ultrasound protocol demonstrating a sensitivity of 99% and specificity of 89% while ultrasound alone showed a sensitivity of 86% and specificity of 95%.

An additional consideration in deciding on the use of US versus CT is patient body habitus. An elevated body mass index (BMI) can limit visualization of the appendix with ultrasound, with nonvisualization of the appendix in 79% of overweight children compared to 33% in normal weight and 25% in underweight children (5). The majority of studies evaluating diagnostic imaging do not report weight or BMI, and thus it is difficult to define a cut-off as to which children of a given weight would benefit more from CT than from US. A retrospective study by Grayson et al. found that increased intraperitoneal fat was correlated with a significantly increased likelihood of visualizing a normal appendix on CT of pediatric patients (14).

A recent formal cost-effectiveness analysis by Wan and colleagues compared a protocol based on US followed by CT if negative to the use of CT and US alone. The Markov decision analytic model indicated that the incremental cost-effectiveness ratio (ICER) of the US followed by CT protocol was below $10,000 in both male and female pediatric patients (15). This falls well below the threshold of societal willingness to

pay $50,000. Thus, the protocol of US followed by CT was found to be a cost-effective imaging strategy (moderate evidence).

II. In Which Cases of Suspected Pediatric Appendicitis Is Imaging Indicated?

Summary of Evidence: A clinical prediction rule that relies on signs and symptoms in conjunction with basic laboratory values may be useful in identifying subjects who do not need imaging (Table 32.2). This prediction rule has been validated at a single institution (moderate evidence).

The high sensitivity (96–98%) of the clinical prediction rule indicates that a negative result effectively excludes appendicitis. The low specificity (32–36%) of the clinical prediction rule indicates that imaging should be performed in patients suspected of having appendicitis as a confirmatory exam prior to treatment.

Supporting Evidence: Clinical exam and serum laboratory testing remain the standard initial method of determining which subjects may have appendicitis. However, given the historical rates of both missed diagnosis and unnecessary laparotomy, a number of investigators have attempted to formalize the clinical exam into a valid scoring tool or decision rule for deciding which subjects are at risk of appendicitis. In 1986, Alvarado introduced a tool termed the MANTRELS criteria for the scoring of appendicitis risk in adults (1). However, diagnostic accuracy in children was only <80%, with significant inter-provider variability in the successful use of these criteria (1). Thus, efforts toward developing a useful pediatric decision rule remain ongoing.

More recent efforts have focused on using clinical and laboratory examination as a triage tool to determine which subjects should undergo imaging. Kharbanda and colleagues developed a clinical decision rule to identify children at low risk for appendicitis so that ideally these patients could avoid imaging (16). They performed a prospective cohort study of 601 pediatric patients with suspected appendicitis presenting to the ED. Pediatric emergency medicine attendings completed standardized data collection forms for each patient prior to imaging, and using these data two clinical decision rules (CDR) were created with logistic regression and recursive partitioning. These decision rules were subsequently validated in a consecutive group of 176 patients (Table 32.2). Developed with logistic regression, the first CDR identified the following clinical factors as helpful in determining pretest probability of appendicitis: nausea (two points), right lower quadrant pain (two points), migration of pain (one point), difficulty walking (one point), rebound tenderness/pain on percussion (two points), and absolute neutrophil count (ANC) $>6.75 \times 10^3/\mu L$ (six points). A score of greater than six points was found to have a sensitivity of 96% and a specificity of 36% in identifying patients with acute appendicitis. The second CDR, developed using recursive partitioning, identified the presence of ANC$>6.75 \times 10^3/\mu L$, nausea, or maximal tenderness in the right lower quadrant to have a sensitivity of 98% and specificity of 32% in identifying patients with appendicitis. It was determined that application of these rules could have allowed for clinical management without need for diagnostic imaging in groups that did not fall into these categories given the low risk of appendicitis, reducing use of CT by 20%. Limitations in this study include the potential for inter-observer variability and lack of validation in other locations.

Garcia Pena et al. also performed recursive partitioning analysis of a retrospective cohort of 958 children with equivocal acute appendicitis, who were risk stratified into three groups based on clinical signs and symptoms and laboratory values (17). Three different management guidelines with subsequent modeling of outcomes were developed. Outcomes included the number of negative appendectomies and missed or delayed diagnoses of appendicitis. The authors showed that management guidelines with more selective use of imaging could reduce the number of imaging exams ordered with minimal increase in the negative appendectomy rate and the number of missed diagnoses of appendicitis. However, these guidelines were not validated, so the effectiveness in clinical practice is uncertain.

Thus, these clinical decision rules show promise, particularly those developed by

Kharbanda et al., given that they have been validated in a pediatric population. However, the reliability and validity in other settings have yet to be demonstrated, an area for future research.

III. What Is the Effect of Imaging on the Rate of Negative Appendectomy in Pediatric Patients with Suspected Appendicitis?

Summary of Evidence: There is conflicting evidence regarding the effect of imaging on the rate of negative appendectomy, but the more valid studies suggest there is a decrease in the rate with use of preoperative imaging, in particular CT (moderate evidence).

Supporting Evidence: While preoperative diagnostic imaging has the potential to increase diagnostic accuracy and reduce the rate of negative appendectomy, there have been conflicting data regarding the effect of imaging on the rate of finding a normal appendix by pathology following appendectomy. Historically, before the advent of routine CT and US use, history and physical exam were the key to the diagnosis of appendicitis and were associated with an approximately 20% negative appendectomy rate (18).

In our literature search evaluating the rates of negative appendectomy following the use of imaging, no prospective studies were identified. Of the retrospective studies, we excluded those with no control group and those with nonconsecutive enrollment. In addition, studies that used a concurrent nonimaged control group were excluded, as nonimaged subjects were likely substantially different clinically from the imaged group, making the comparison of limited value. Thus, as no valid concurrent controlled studies exist, our evaluation was limited to those studies which compared negative appendectomy rates (NAR) before the widespread use of imaging to those after the routine implementation of imaging, as this seemed to be the most valid comparison.

Three studies met these criteria. In the retrospective study by Rao et al., a consecutive group of 129 pediatric patients from 1992 to 1995, before introduction of appendiceal CT, were compared to a group of 59 patients in 1997, after establishment of a standard appendiceal CT protocol (19). All of the patients in both groups underwent appendectomy. The NAR dropped with the advent of appendiceal CT availability, from 10 to 5% in boys and from 18 to 12% in girls. The second study, from Boston Children's Hospital by Garcia Pena et al., compared a retrospective cohort of consecutive patients admitted for suspected appendicitis before the use of a US–CT protocol to a prospective cohort who were evaluated during the time when the US–CT protocol was in use (20). The protocol involved obtaining US on all patients with equivocal appendicitis, followed by CT for equivocal or inconclusive US cases. The NAR dropped from 14.7% in the first group to 4.1% in the second group ($p<0.001$). A third study, also from Children's Hospital Boston, found a decrease in the NAR from 11 to 5.5% ($p=0.03$) with the use of selective CT or US imaging in the context of a clinical practice guideline compared to a control group of patients before the frequent utilization of imaging at their institution (21). However, this study evaluated the entire protocol and not the effects of imaging alone, and thus other factors could have contributed to this result. One potential limitation of these three studies is the possible lack of generalizability as they were performed at urban academic institutions.

Although these three studies all noted a decrease in the NAR with preoperative imaging, data from other studies are not consistent with this. Perhaps the most persuasive is from a retrospective population-based analysis by Flum and colleagues of data from the Washington State hospital discharge database from 1987 to 1998 (22). They found that the population-based incidence of unnecessary nonincidental appendectomy did not change significantly over time for the 85,790 adult and pediatric patients who underwent appendectomy over that 12-year time period, in spite of increasing availability of CT, US, and laparoscopy for presurgical evaluation. Mean patient age was 32.1 years (standard deviation of 18.6 years). A subgroup analysis of children under the age of 5 years showed no significant change in misdiagnosis rates over time as well. Thus, their data did not support their initial supposition

that increased use of imaging would lead to a decrease in the NAR over time. However, it is noted that the investigators were unable to determine the rates of US and CT use with the information available from the database, so the actual patterns of imaging use are uncertain. In addition, the study data are from the time period prior to the use of modern multi-detector CT scanners.

Thus, data on the effect of imaging on negative appendectomy rates are inconsistent at this point. No multi-center or prospective data are available. Also, changes in technology over time may confound results, particularly with regard to CT, which has evolved from single to multi-detector technique with reformations in multiple planes. Though clearly imperfect, the three studies we identified in which nonconcurrent control groups were used are the most valid available reports in terms of study design, and these do indicate a modest decrease in the NAR with imaging. Still, the effect of imaging on the NAR is still somewhat unclear, and a prospective randomized trial has yet to be performed assessing this.

IV. What Is the Role of Imaging in Managing Pediatric Perforated Appendicitis?

Summary of Evidence: Preliminary data suggest that preoperative imaging may be able to differentiate between cases of perforated and nonperforated appendicitis. Additionally, imaging may lead to a decrease in the perforation rate and may be useful in predicting clinical outcomes in patients who present with perforation (limited evidence).

Supporting Evidence: The identification of perforation in patients with appendicitis is an important part of clinical management as this subset has a significantly higher rate of complications, including peritonitis, abscess formation, sepsis, and even death, not to mention increased associated costs of care associated with increased observation time and use of hospital resources. Pediatric patients have a higher incidence of perforated appendicitis than adults, as they tend to pose more of a diagnostic dilemma due to nonspecific signs and symptoms and, in the very young, limited communication skills (9). A wide range of pediatric appendiceal perforation rates have been reported in the literature, from 14 to 88% (1, 7, 8, 13, 23–26). Younger children are significantly more likely to present with perforated appendicitis compared to older children, such that one retrospective review of 769 pediatric patients found a 72% rate of perforation in children under the age of 5 years compared to 22% in those 5 years or older (7). Cases of perforation are also significantly more costly than nonperforated appendicitis cases. One study found an average cost of $16,882 (in 1997 U.S. dollars) per case of perforated appendicitis compared to $5,202 per case of nonperforated appendicitis at their institution (8). Naturally, a purported goal of preoperative imaging is therefore to lead to an earlier diagnosis of appendicitis, thereby allowing for earlier surgical management before perforation is allowed to occur, given that most cases of appendicitis progress to perforation if untreated. Additionally, preoperative imaging could also aid in identifying those patients who already have perforated and thus more accurately direct nonsurgical management if that is deemed most appropriate.

To date there have been limited studies assessing the diagnostic capability of preoperative imaging in determining the presence of perforated appendicitis versus nonperforated appendicitis. In terms of the use of US, a 1992 retrospective review of 71 pediatric appendicitis cases with an incidence of 37% perforation found that the best predictors of perforation were the absence of visualization of the normally echogenic submucosal layer ($p<0.05$) and the presence of a loculated, periappendiceal, or pelvic fluid collection ($p<0.05$) (27). Additionally, a prospective study of 70 pediatric patients with suspected appendicitis who underwent preoperative US found that of those patients with a uniformly hypoechoic appearance of the appendix, 75% had perforation at surgery. As for the utility of CT in this matter, a 2005 retrospective review of 86 consecutive pediatric and adult patients who underwent preoperative CT found that extraluminal air and moderate or severe periappendiceal inflammatory stranding were both statistically significant predictors for perforation and associated with increased length of hospitalization

($p<0.001$) (28). The results of this particular study may not necessarily be applicable to children.

Some authors have postulated that US diagnosis of appendicitis may be more difficult in cases of perforation. For example, a 2001 retrospective review found that of 14 cases in their series with a false-negative US, 9 of these patients turned out to have perforated appendicitis (26). However, the Doria et al. meta-analysis reported that the sensitivity of US for the diagnosis of appendicitis is actually improved in cases of perforated appendicitis compared to nonperforated cases (9). Although these results are in conflict, the statistical strength of the meta-analysis would suggest that this result is more reliable.

Regarding the potential ability of preoperative imaging to affect perforation rates, there have been discrepancies in reported rates of perforation in those patients who undergo preoperative imaging compared to those who do not have preoperative imaging. A 2002 study at Boston Children's Hospital of 854 pediatric patients examined perforation rates before and after the implementation of a preoperative US and CT protocol (in which CT was performed in indeterminate US cases) and reported a statistically significant drop in the perforation rate from 35 to 15.5% following the introduction of the preoperative imaging protocol ($p<0.001$) (20). Similarly, a retrospective review comparing a group of 112 patients who presented with appendicitis before the introduction of routine appendiceal CT use to a group of 55 patients after routine CT use was implemented found a trend toward decrease in the perforation rate after the introduction of preoperative CT from 23 to 15%, although this was not statistically significant (19). In contrast, a 2001 retrospective study of 299 patients and a 2002 retrospective review of 118 patients who underwent appendectomy found no statistically significant difference in perforation rates between those patients who had preoperative imaging and those who did not (18, 25). However, it is possible that there was significant selection bias, with those patients who underwent imaging possibly being more ill or having atypical presentations leading to a delay in diagnosis, which could have substantially affected these results, as could the small sample sizes. Again, in the absence of a randomized clinical trial, the use of the historical control group may be the more accurate method of assessing this issue, suggesting that preoperative imaging may indeed lead to a decrease in the perforation rate.

Imaging may be useful in predicting clinical outcomes in patients who present with perforation. A 2007 retrospective review of 34 pediatric patients with perforated appendicitis treated nonoperatively with IV antibiotics and in some cases with CT-guided percutaneous drainage correlated clinical outcomes with admission CT findings. These investigators found that the presence of fluid collections in three or more sectors (a sector being defined as one of the four abdominal quadrants or the pelvis) correlated significantly with clinical failure of nonoperative management ($p<0.05$), with such collections being present in 50% of patients with failure and in only 10% with a successful recovery (29). As of note, no correlation with outcomes was documented between the presence of an appendicolith, extraluminal air, collection size, or collection complexity and outcome. Of course, this study is limited given the small sample size, nonconsecutive patient selection, selection bias, and non-generalizability, and further investigation in this area is needed.

In summary, there have been no large-scale trials to fully assess the role of imaging in the management of perforated appendicitis, but findings to date hold promise for the future. Multi-center trials are needed to address the existing discrepancies. Additionally, imaging criteria to predict outcomes in patients with perforated appendicitis need to be developed to help direct management in terms of surgical versus nonsurgical management.

V. What Is the Effect of Imaging Pediatric Patients with Suspected Appendicitis on Health-Care Costs?

Summary of Evidence: The data examining the economic impact of imaging pediatric patients with suspected appendicitis suggest that imaging may decrease health-care costs, but the data are not conclusive (limited evidence).

Supporting Evidence: The data examining the cost impact of imaging in pediatric patients with suspected appendicitis are limited. Since patients with equivocal appendicitis have traditionally been admitted for observation, it has been postulated that use of imaging could decrease costs by allowing for more patients to be definitely diagnosed as negative in terms of appendicitis and sent home. However, no formal cost-effectiveness analyses are available.

A prospective cohort study of 94 pediatric patients to be admitted for observation for possible appendicitis found that if all of the patients who had a normal appendix clearly visualized on CT had been discharged to home, the admission rate would have decreased by 41.8% with no missed diagnoses given the high accuracy of CT (10). This could have theoretically resulted in considerable savings, as the mean length of hospital stay was 2.0 days.

In contrast, a retrospective review of 197 consecutive children who underwent appendectomy found no significant improvement in diagnostic accuracy or outcome in imaged compared to nonimaged groups, with a delay in surgical treatment (12.1 hours in imaged group versus 5.4 hours in nonimaged group, $p<0.0001$) and a 26% increase in hospital charges, from $11,791 (imaged) compared to $9360 (nonimaged, $p=0.001$) (30). However, significant selection bias between the nonimaged and the imaged groups is likely, with the nonimaged group representing more typical cases that could be taken directly to the operating room. In addition, this study did not include the potential cost impact from avoiding surgery or observation on subjects without appendicitis who had negative imaging.

A paper by Garcia Pena et al. used a decision analytic model to examine a retrospective consecutive cohort of children admitted to the hospital for observation for suspected appendicitis (8). Three proposed strategies for patient management were evaluated using empirical data from this cohort, which demonstrated sensitivity and specificity of CT for appendicitis of 97 and 97% in imaged patients. All three of the protocols involved getting CT scans of children who, under the practice of the time, would have simply been admitted for observation without CT imaging. Costs for average charges from 1997 were applied to each situation and were calculated using the average hospital charge data. The total cost per patient using the traditional practice strategy was $5,831, compared to $3,813 if CTs were obtained in all patients and those with negative exams sent home. This second strategy would have resulted in the same number of projected missed appendicitis cases and a decrease in the NAR. Two additional strategies involved admitting and getting CTs in all and getting CTs only in patients with elevated WBC count. These strategies resulted in projected costs per patient of $5,277 and $5,140, respectively. It was found that all three proposed CT strategies would have reduced the number of observation days, surgeries, negative laparotomies, and cost per patient compared to traditional practice. The analysis was also repeated for a range of sensitivities from 80 to 100%, with no change in the relative ordering of the strategies. These modeling data have not been validated in actual practice.

Garcia Pena et al. also completed a prospective cohort study of 139 children with equivocal clinical findings of acute appendicitis (31). Subjects were evaluated with US, and those with negative or unequivocal US findings then had CT with rectal contrast. Surgical management plans were recorded before imaging, following US, and following CT, and total hospital direct and indirect costs incurred or saved were determined at each point. The imaging protocol resulted in total cost savings of $565 per patient, in this cohort with a 36% prevalence of appendicitis.

These limited data suggest that there could be cost savings associated with imaging pediatric patients with suspected appendicitis, but the exact effects are unclear, particularly given our present inconclusive knowledge of the effects of imaging on the negative appendectomy rate and clinical decision making.

Take Home Tables

Table 32.1 discusses the sensitivity and specificity of imaging in pediatric patients with suspected acute appendicitis. Table 32.2 discusses

the clinical decision rule for prediction of pediatric patients at elevated risk for acute appendicitis.

Table 32.1. Sensitivity and specificity of imaging in pediatric patients with suspected acute appendicitis

	Sensitivity (%)	Specificity (%)	PPV (%)[4]	NPV (%)[4]
Ultrasound[1]	88	94	87	95
CT[1]	94	95	89	97
Ultrasound followed by CT[2]	95	93	86	98
Clinical data[3]	98	32	39	97

[1] Data from reference (9).
[2] Data derived from references (11–13). If the appendix is not visualized by ultrasound or if the ultrasound is inconclusive for the diagnosis of appendicitis, then CT is obtained.
[3] Calculated using data from reference (17). These results may not be achievable in routine clinical practice as they have only been validated in a single pediatric population.
[4] Calculated using a prevalence of appendicitis of 31%, the mean sample prevalence of appendicitis from the reference (9) meta-analysis as well as the prevalence of appendicitis in the reference (16) validation set.

Table 32.2. Clinical decision rule for prediction of pediatric patients at elevated risk for acute appendicitis

Presence of any of the following three factors has a sensitivity of 98% and specificity of 32% in identifying pediatric patients with appendicitis: **- Absolute neutrophil count (ANC)>6.75 $\times$ $10^3/\mu L$** **- Nausea** **- Maximal tenderness in the right lower quadrant**

Data from Kharbanda et al. (16).

Imaging Case Studies

Case 1

Figure 32.1 presents the case of a 10-year-old girl in the emergency department complaining of less than 24 hours of periumbilical abdominal pain as well as nausea and emesis.

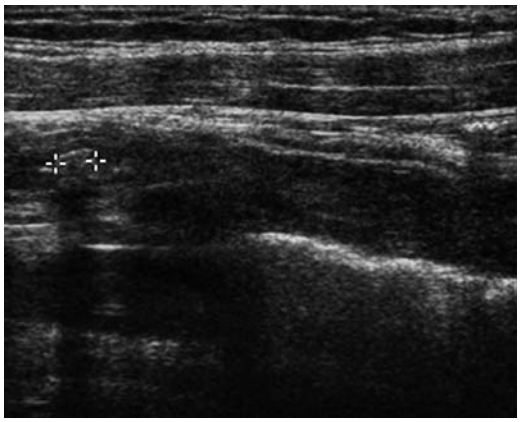

Figure 32.1. A 10-year-old female presented to the emergency department complaining of less than 24 hours of periumbilical abdominal pain as well as nausea and emesis. On physical exam, she was afebrile and demonstrated right lower quadrant tenderness with guarding. Laboratory evaluation revealed an elevated white blood cell count of 16,700 cells/mm^3. This ultrasound was obtained, demonstrating a blind-ending, noncompressible tubular structure in the right lower quadrant compatible with a dilated appendix measuring 13 mm in diameter and containing an echogenic, shadowing fecalith. On appendectomy, gross and histological findings established the presence of a nonperforated but friable, suppurative appendix.

Case 2

Figure 32.2 presents the case of a 17-year-old male in the emergency department complained of abdominal pain, initially periumbilical and subsequently right lower quadrant, and nausea for several hours.

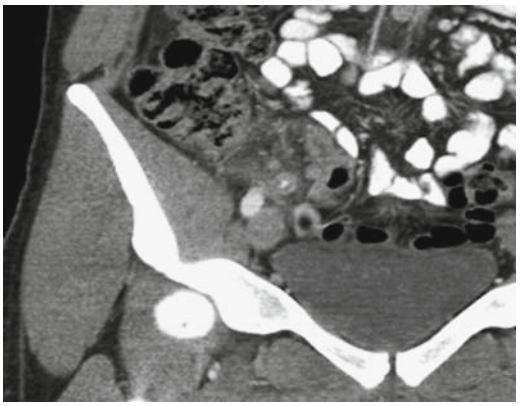

Figure 32.2. A 17-year-old male presenting to the emergency department complained of abdominal pain, initially periumbilical and subsequently right lower quadrant, and nausea for several hours. On physical exam, he was afebrile and demonstrated right lower quadrant tenderness with voluntary guarding. White blood cell count was mildly elevated at 11,200 cells/mm^3. This CT demonstrated a dilated, 12 mm appendix with mild wall thickening and inflammatory changes in the periappendiceal fat. Gross examination of the appendix at appendectomy several hours later revealed a nonperforated, dilated appendix with a fecalith obstructing its tip.

Suggested Imaging Protocols for Suspected Appendicitis

There is no consensus in the literature as to the ideal CT protocol with respect to the use of intravenous contrast, oral contrast, rectal contrast, or non-contrast technique, with varying reports of the efficacy of these protocols (3, 23, 24, 32–36). There is also significant variability in terms of recommendations regarding focused imaging of the appendiceal region versus complete scan of the abdomen and pelvis, with tradeoffs between radiation dose and more complete exam (35, 37). In general, CT protocols are very institutional dependent, and the best technique for a given patient may vary depending on his/her ability to tolerate administration of oral or rectal contrast and if there are any contraindications to intravenous contrast. However, the most commonly used protocol is a complete scan of the abdomen and pelvis with both oral and intravenous contrasts.

Future Research

- Multi-center validation of proposed clinical decision rules aimed at determining when imaging indicated in pediatric patients with suspected appendicitis is still needed.
- The data regarding the effect of imaging on the negative appendectomy rate in pediatric patients are in conflict. Resolution of this question is critical to determining the effect of imaging on patient outcome.
- Additional studies are needed to confirm the role of imaging in managing pediatric patients with perforated appendicitis.
- The ability of imaging to influence medical decision making is not well established.
- Relatively little is known regarding the overall cost and cost-effectiveness of imaging pediatric patients with suspected acute appendicitis.

References

1. Brennan GDG. CJEM 2006; 8:425–432.
2. Rothrock SG, Pagane J. Ann Emer Med 2000; 36:39–51.
3. Sivit CJ, Applegate KE. Semin US, CT, MRI 2003; 24:74–82.
4. Kwok MY, Kim MK, Gorelick MH. Pediatr Emer Care 2004; 20:690–698.
5. Puig S, Staudenherz A, Felder-Puig R, Paya K. Sem Roent 2008; 22–28.
6. Agency for Healthcare Research and Quality (AHRQ). Care of Children and Adolescents in U.S. Hospitals: HCUP Fact Book No. http://www.ahrq.gov/data/hcup/factbk4/factbk4.htm#why.
7. Rodriguez DP, Vargas S, Callahan MJ et al. AJR 2006; 186:1158–1164.
8. Garcia Pena BM, Taylor GA, Lund DP, Mandl KD. Pediatrics 1999; 104:440–446.
9. Doria AS, Moineddin R, Kellenberger C et al. Radiology 2006; 241:83–94.
10. Acosta R, Crain E, Goldman HS. Pediatr Radiol 2005; 35:495–500.

11. Teo EL et al. Singapore Medi J 2000; 41:387–392.
12. Garcia Pena BM, Mandl KD, Kraus SJ et al. JAMA 1999; 282:1041–1046.
13. Kaiser S, Frenckner B, Jorulf HK. Radiology 2002; 223:633–638.
14. Grayson DE, Wettlaufer JR, Dalrymple NC, Keesling CA. AJR 2001; 176:497–500.
15. Wan MJ, Krahn M, Unger WJ et al. Abstract in Press in Radiology. Cost-Effectiveness of Ultrasonography versus Computed Tomography in the Diagnosis of Acute Appendicitis: A Markov Decision Analytic Model, 2008.
16. Kharbanda AB, Taylor GA, Fishman SJ, Bachur RG. Pediatrics 2005; 116:709–716.
17. Garcia Pena BM, Cook EF, Mandl KD. Pediatrics 2004; 113:24–28.
18. Bendeck SE, Nino-Murcia M, Berry GJ, Jeffrey RB. Radiology 2002; 225:131–136.
19. Rao PM, Rhea JT, Rattner DW et al. Ann Surg 1999; 229:344–349.
20. Garcia Pena BM, Taylor GA, Fishman SJ, Mandl KD. Pediatrics 2002; 110:1088–1093.
21. Smink DS, Finkelstein JA, Garcia Pena BM, et al. J Pediatr Surg 2004; 39:458–463.
22. Flum DR, Morris A, Koepsell T, Dellinger EP. JAMA 2001; 286:1748–1753.
23. Hoecker CC, Billman GF. J Emer Med 2005; 28:415–421.
24. Kharbanda AB, Taylor GA, Bachur RG. Radiology 2007; 243:520–526.
25. Applegate KE, Sivit CJ, Salvator AE et al. Radiology 2001; 220:103–107.
26. Ang A, Chong NK, Daneman A. Pediatric Emergency Care 2001; 17:334–340.
27. Quillin SP, Siegel MJ, Coffin CM. AJR 1992; 159:1265–1268.
28. Foley TA, Earnest F, Nathan MA et al. Radiology 2005; 235:89–96.
29. Levin T, Whyte C, Borzykowski R et al. Pediatr Radiol 2007; 37:251–255.
30. York D, Smith A, Phillips JD, von Allmen D. J Pediatr Surg 2005; 40:1908–1911.
31. Garcia Pena BM, Taylor GA, Fishman SJ, Mandl KD. Pediatrics 2000; 106:672–676.
32. Balthazar EJ, Birnbaum BA, Yee J et al. Radiology 1994; 190:31–35.
33. Lowe LH, Penney MW, Stein SM et al. AJR 2001; 176:31–35.
34. Fefferman NR, Bomsztyk E, Yim AM et al. Radiology 2005; 237:641–646.
35. Mullins ME, Kircher MF, Ryan DP, et al. AJR 2001; 176:37–41.
36. Kaiser S, Finnbogason T, Jorulf HK et al. Radiology 2004; 231:427–433.
37. Fefferman NR, Roche KJ, Pinkney LP et al. Radiology 2001; 220:691–695.

33

Imaging of Inflammatory Bowel Disease in Children

Sudha Anupindi, Rama Ayyala, Judith Kelsen, Petar Mamula, and Kimberly E. Applegate

Issues

I. What are the important clinical predictors of IBD?
II. What is the diagnostic performance of current endoscopic techniques in the evaluation of patients with IBD: Lower, upper endoscopies and wireless capsule endoscopy (WCE)?
III. What is the diagnostic performance of current imaging modalities in evaluating IBD of the small bowel (barium small bowel follow–through, CT, MR, US, enteroclysis)?
IV. Complications of IBD (intra-abdominal abscess, intestinal fistulae, strictures and small bowel obstruction, primary sclerosing cholangitis [PSC]): Which imaging should be performed and what is its diagnostic performance?
V. What are the most important imaging features that lead to surgery in a child with Crohn's disease (CD) or ulcerative colitis (UC)?
VI. What are the role and risk of repeat imaging in monitoring IBD status and response to treatment?
VII. Special situation: Which imaging modality provides the best performance for the evaluation of perianal/perirectal disease in Crohn's disease?

Key Points

- Children with clinically suspected IBD should have both upper and lower endoscopies as part of the initial workup (strong evidence). Fluoroscopic small bowel follow-through studies are typically performed as part of the initial diagnosis (limited evidence).
- Wireless capsule endoscopy (WCE) is a safe, moderately sensitive test for the detection of small bowel inflammatory changes and should be utilized in patients without small bowel obstruction and when other diagnostic small bowel exams are negative. However, the specificity

S. Anupindi (✉)
Department of Radiology at the Children's Hospital of Philadelphia, University of Pennsylvania School of Medicine, Philadelphia, PA 19104, USA
e-mail: anupindi@email.chop.edu

L.S. Medina et al. (eds.), *Evidence-Based Imaging in Pediatrics*,
DOI 10.1007/978-1-4419-0922-0_33,

and positive predictive value need to be further established (limited evidence).
- MRI is superior to CT and is the preferred initial diagnostic and follow-up imaging exam of perirectal and perianal disease in Crohn's disease (CD) patients (moderate–strong evidence).
- About 70–80% of CD patients and 30–40% of UC patients will require surgery for disease refractory to medical therapy, or severe disease with complications, or risk of malignancy (UC) (moderate evidence).
- Repeat imaging with SBFT and CT results in significant ionizing radiation exposure and risk of later cancer induction so that alternative imaging methods, MRI and US, should be used (limited evidence).

Definition and Pathophysiology

Inflammatory bowel disease (IBD), comprised of the well-recognized Crohn's disease (CD) and ulcerative colitis (UC), is one of the most serious, chronic gastrointestinal (GI) conditions affecting the growth, social well-being, and education in children worldwide. The pathogenesis is not completely understood; however, the general accepted hypothesis is that IBD occurs as the result of an inappropriate and exaggerated mucosal immune response to common environmental antigens including commensal microflora in a genetically susceptible host. Up to 25% of children with IBD will have a primary degree relative with this diagnosis. Generally both conditions result in suppurative inflammation of the bowel that results in abdominal pain, diarrhea (sometimes bloody), weight loss, and growth disturbance.

UC is a diffuse chronic mucosal inflammation of the mucosa that is limited to the colon and invariably affects the rectum in an uninterrupted fashion, although 5% of UC patients have backwash ileitis. In contrast, CD features segmental transmural inflammation and fibrosis involving the entire GI tract. In 10% of cases a third entity termed "indeterminate colitis" (IC) is used when a firm diagnosis of CD or UC cannot be made. Although the etiology for IBD is not clear, some risk factors include first-degree relatives, smoking, NSAIDs, oral contraceptives. Several infectious agents that have been proposed as causative agents although with great controversy include *Listeria monocytogenes*, *Chlamydia trachomatis*, *Escherichia coli*, Cytomegalovirus, *Saccharomyces cerevisiae*, and *Mycobacterium avium paratuberculosis* (1, 2).

Epidemiology and Diagnosis

In the pediatric population, defined as ages 1–17, the incidence of IBD in North America is approximately 2/100,000 for UC and 4.5/100,000 for CD (1). The U.S. prevalence of CD and UC combined is estimated to be 400 cases per 100,000 persons and these numbers are on the rise (2). Twenty-five percent of all IBD presents in the pediatric age group. The peak age of onset is in the adolescent years, with 4% of pediatric IBD cases occurring before the age of 5 years and 20% before the age of 10 years (3). While IBD incidence is equal in males and females, it occurs more commonly in the developed world and, in urban compared to rural areas, is higher in Caucasians, followed by African Americans and occurs less commonly in Asians and Hispanics.

One million Americans have IBD. There is a higher predisposition of IBD in northern latitudes than southern latitudes. Worldwide the incidence of IBD is increasing. There is minimal emerging data from Asia, Pacific regions, and South America; however, the incidence in these regions is not as great as that in North America or Europe. The current descriptive data are derived from European (Scotland and Sweden) and North American cohorts (4).

No single test can diagnose IBD. Patients presenting with signs and symptoms that suggest IBD, such as bloody or non-bloody diarrhea, or weight loss need to be evaluated with supportive laboratory testing, such as hemoglobin, albumin, inflammatory markers such as erythrocyte sedimentation rate (ESR) and C-reactive protein (CRP), stool cultures, radiographic studies, and endoscopy. Patients

may appear ill on physical exam with some findings including pallor secondary to anemia, and pharyngeal aphthous lesions. The abdominal exam may be normal, non-specific, or have "fullness" in right lower quadrant, indicating inflamed terminal ileum or thickened bowel. On perianal and rectal exam, the frequency of the findings of perianal/perirectal skin tags, fissures, and fistulae is 2–4.5% in newly diagnosed CD patients (1). Upper endoscopy, colonoscopy with biopsies, and radiologic studies are performed for confirmation of diagnosis. The differentiating features at biopsy are listed in Table 33.1.

Overall Cost to Society

A review of the current literature reveals that the overall cost burden of CD to society is quite high and a substantial portion of the direct costs is attributed to hospitalizations. There are several cost-effective analyses evaluating the overall cost to society regarding hospitalization and treatment (i.e., surgery), as well as loss of time from school and work. However, no cost-effectiveness data were found in the literature specifically incorporating imaging strategies in the evaluation and management of IBD. The total economic burden of CD in the United States is estimated to be between $10.9 and $15.5 billion (5). The estimated cost per patient with CD in the United States is close to $18–19,000 annually (5). The severity of the disease is directly proportional to the cost by as much as three- to ninefold, higher in children with severe disease than those with mild disease. Data from 1990 reported a total annual medical cost for patients with UC in the United States as approximately $0.4–0.6 billion (6). In keeping with annual inflation and rising medical costs this estimate is much higher today. Only a single study assessed the economic costs of different diagnostic exams including imaging studies but the focus was primarily on capsule endoscopy (7). Imaging costs are barely mentioned separately in the reviewed citations but it is presumed that it is a significant portion of the costs, as imaging is widely used to help determine medical versus surgical treatment (2, 8, 9) (limited evidence).

Goals

The diagnosis of IBD encompasses use of clinical, tissue diagnosis, and imaging. The goals of imaging in IBD are to primarily determine the extent of small bowel involvement, assess complications, and help determine patients who are candidates for surgery. Using conventional endoscopic techniques (with the exception of emerging capsule endoscopy), the small bowel is difficult to assess and therefore imaging is relied upon. Imaging plays a key role in assessing complications such as abscesses, fistulae, strictures, and obstruction, which would require intervention. Patients with CD who present with acute exacerbations resulting in hospitalizations often require CT and MR imaging to evaluate the current status of disease and possible complications. These imaging techniques are used to help determine who might benefit from surgery.

Methodology

The authors performed a MEDLINE search using PubMed (National Library of Medicine, Bethesda, MD) for data relevant to the diagnostic performance and accuracy of both clinical and imaging examinations of patients with inflammatory bowel disease (IBD). The cost analysis of diagnosis, treatment, and imaging strategies of IBD was searched on MEDLINE (National Library of Medicine, Bethesda, MD) using the following search criteria for the period 1990–2008: (1) *Inflammatory bowel disease*; (2) *diagnosis*; (3) *treatment*; (4) *health economics*; (5) *hospital costs*; (6) *imaging costs.* The diagnostic performance of the clinical examination (history and physical exam) and the surgical outcome were based on a systematic literature review performed in MEDLINE (National Library of Medicine, Bethesda, MD) during the years 1990–2008. The clinical examination search strategy used the following statements: (1) *Inflammatory bowel disease*; (2) *Crohn's disease*; (3) *ulcerative colitis*; (4) *pediatric*; (5) *children*; (6) *epidemiology* or *physical examination* or *endoscopy* or *colonoscopy* or *capsule endoscopy*; (7) *treatment* or *surgery*. The review of the current diagnostic imaging literature was done with MEDLINE covering the years 1990–September 2008. The

search strategy used the following key statements and words: (1) *Inflammatory bowel disease*, (2) *Crohn's disease*, (3) *ulcerative colitis*, (4) *MRI* or *magnetic resonance imaging*, (5) *computed tomography* or *CT*, (5) *ultrasound*, (6) *PET imaging*, (7) *imaging*, as well as combinations of these searches. We excluded animal studies and non-English articles.

Discussion of Issues

I. What Are the Important Clinical Predictors of IBD?

Summary of Evidence: The clinical signs and symptoms of IBD, although variable between UC and CD, most commonly include abdominal pain, diarrhea, weight loss, fever, hematochezia (in UC), and growth failure [10]. These are the most common predictive signs and symptoms occurring in more than 90% of the cases (moderate evidence).

Routine blood and inflammatory markers including, but not limited to, cell blood count (CBC), erythrocyte sedimentation rate (ESR), and C-reactive protein (CRP) are sensitive but not specific for IBD; however, serologic antibody studies such as perinuclear antineutrophil cytoplasm antibodies (pANCA) and anti-*S. cerevisiae* antibodies (ASCA-IgA and IgG) have a high degree of specificity (10, 11).The sensitivity and specificity of ASCA has been estimated as 37 and 97%, respectively, for the diagnosis of CD, whereas for the diagnosis of UC, the sensitivity and specificity of pANCA has been reported as 55 and 89% (10) (moderate evidence). When history, physical, and laboratory studies suggest ongoing symptoms not explained by infection, endoscopy is needed to diagnose (11) (strong evidence).

Supportive Evidence: IBD peak incidence is between 15 and 35 years. A delay in diagnosis is common and can be between 5 months and 2 years. Growth failure in children is identified in 10–40% of patients with IBD at presentation and is more common in CD. Atypical presentations occur in 10–20% of patients. Approximately 4% of IBD patients present with arthritis, usually pauciarticular and involving the large joints. Younger children are more likely to have atypical clinical presentations. In addition, 10% of patients with CD may initially present with perianal abscesses or fistulae or unusual dermatological manifestations such as erythema nodosum or pyoderma gangrenosum (12).

Laboratory Markers

There is also variability in the biological laboratory markers in children with IBD. There is usually an increased concentration of CRP, ESR, fecal calprotectin (FC) and a low albumin, anemia, and neutrophil leukocytosis (13). Certain autoantibodies such as pANCA and ASCA are abnormal in IBD, but the utility of these markers to diagnose IBD is limited by low sensitivity (10). The pANCA is detected in 50–80% of UC patients and 10–40% of CD patients while ASCA is detected in 46–70% of CD patients and only 6–12% of UC patients (11) (moderate evidence). These markers are useful to predict the risk of stricture or perforation and to distinguish Crohn's from UC patients since UC patients more often will have elevated levels of pANCA whereas Crohn's patients are more likely to have ASCA elevated (14). Canani and colleagues showed that if the values of FC, ANCA/pANCA, and bowel US were all negative, the probability of having IBD was 0.69%. If the laboratory exams described above were normal, this was a good negative predictive value for IBD (10, 11, 15, 16) (moderate evidence).

Children Under Age 5 Years

In a large analysis by Heyman et al. IBD specific symptoms were seen in 3% (37/1370 patients) of children less than 1 year of age (17). The serologic markers were poor indicators of disease in younger children than in older children (18). Growth failure, as a presenting symptom, is more common in children with CD than UC or IC (P=0.004). It has been estimated that 5% of fever of unknown origin (FUO) in children is due to IBD (18). Chronic fever is associated with CD but not with UC and vomiting has been associated with CD but not with UC in children less than 5 years old (18) (strong evidence).

II. What Is the Diagnostic Performance of Current Endoscopic Techniques in the Evaluation of Patients with IBD: Lower, Upper Endoscopies and Wireless Capsule Endoscopy (WCE)?

Summary of Evidence: Lower and upper endoscopic techniques are the primary tests used to diagnose or exclude IBD (moderate to strong evidence). Wireless capsule endoscopy (WCE), a newer technique, used to evaluate small bowel disease, has a high diagnostic yield compared to other modalities (limited evidence).

Colonoscopy with ileoscopy, defined as terminal ileum (TI) intubation, should be performed in the initial workup of IBD (strong evidence). This technique is the preferred way to both visualize mucosa and biopsy the colon and TI for diagnosis. Between 60 and 80% of the colonoscopies will have successful ileal intubation in children (19). Colonoscopy assesses disease severity, extent, evidence of disease complications (fistulae, ulceration) and allows surveillance of cancer, more common in UC. CT colonography (CTC) is not used for the evaluation of IBD; it is used to detect polyps (20).

Esophagogastroduodenoscopy (EGD) has an important place in the initial workup of IBD (21). Previously, EGD was not routinely performed unless a patient exhibited symptoms suggesting upper gastrointestinal disease such as dysphagia, nausea, vomiting, or oral aphthous ulcers. It has become widely accepted only within the last decade with increasing recognition that UC, CD, and indeterminate colitis patients have upper GI tract inflammation (21, 22).

Supporting Evidence

Lower Endoscopy

Endoscopic biopsy data show up to 85% of patients with CD have terminal ileal disease. In a minority of adult patients (15–25%), CD is confined to the colon (23).

Ileal intubation (ileoscopy) is a vital part of the colonoscopy as the TI may be the only area of CD in up to 23% of pediatric Crohn's patients (24). Two or three biopsies are taken from each region of the bowel. Biopsy needs to be performed even if the colon and TI macroscopically appear normal. Histologic diagnosis of CD is made when there is segmental involvement characterized by transmural inflammation, congested serosa, aphthous ulcers, granulomas and ulceration leading to nodularity. In distinction, UC does not show granulomas but has continuous bowel changes (Table 33.1) (25).

Colonoscopy with ileoscopy has been shown to be a safe, feasible, and accurate procedure. In a retrospective review of all colonoscopies performed in 164 children referred for suspicion of IBD, the percentage of successful ileoscopies increased from 20% in 1994 to 66% in 2000 (19). The rate of bowel perforation is estimated at 0.2%.

Upper Endoscopy

Overall upper gastrointestinal tract inflammation is most common in the stomach, followed by esophagus and duodenum in children with IBD (22). Both CD and UC may have upper GI tract inflammation.

The incidence of an abnormal upper endoscopy in children with IBD is significant. A retrospective study of 115 patients with IBD (CD and UC) over a 7-year period revealed abnormal upper endoscopic findings in 64% of 82 subjects with CD and in 50% of the 34 subjects with UC. Findings included ulcers (20%), erythema (25%), and erosions (42%) in the esophagus, gastric mucosa, and duodenum. The most common finding, erosions, was more often seen in the stomach (22%) and duodenum (14%) (21). In a control blinded study evaluating endoscopic biopsies in IBD patients, Tobin et al. showed that esophagitis, gastritis, and duodenitis occurred more commonly in CD patients. Esophagitis occurred in 72% of CD, 50% of UC; gastritis in 92% of CD, 69% of UC; and duodenitis in 33% CD, 23% UC patients.

The histologic identification of granulomas is pathopneumonic for CD and can help distinguish it from UC. In a large series of 376 CD patients at a Children's Hospital, granulomas were found on endoscopic biopsies in 48% of all patients, the majority (61%) untreated. De Matos et al. found the presence of granulomas correlated with anti-*S. cerevisiae* antibodies, hypoalbuminemia, perianal disease, and gastritis at presentation ($p = 0.03$, $p = 0.008$, $p = 0.03$, and $p = 0.001$) (24).

As seen in the terminal ileum, microscopic mucosal disease can be present in the absence of symptoms. In a prospective study of 54 children with IBD upper gastrointestinal inflammation was seen in 29/54 (22 CD, 7 UC) (22). However, nine (31%) of these patients were asymptomatic. Thus in all patients strongly suspected to have either CD or UC, EGD in conjunction with lower endoscopy is recommended at initial diagnosis (strong evidence).

Wireless Capsule Endoscopy (WCE)

Summary of Evidence

Wireless capsule endoscopy employs a small, ingestible capsule containing a videochip, transmitter, and battery. The capsule will pass through bowel and appear in the stool within 24–48 hours. An average of 55,000 video images are transmitted to a portable device and downloaded to a computer for interpretation. WCE is used in patients with suspected small bowel pathology (Crohn's, polyps, unexplained hemorrhage) not seen in conventional studies. WCE is a safe and well-tolerated exam in adolescents and adults (26, 27) (limited evidence). In recent studies, WCE was also safe in infants and small children but the 25-mm-sized capsule must be placed in the stomach under endoscopic guidance (26, 28). The biggest risk with capsule endoscopy is capsule impaction above a small bowel stricture. To minimize this risk, small bowel lumen patency is initially evaluated by SBFT, patency capsule, or enterography (CT or MR).

While WCE is equivalent or superior to other modalities in the evaluation of known ileal Crohn's disease, it is expensive and typically reserved for patients with unexplained GI bleeding or a hereditary polyposis syndrome (limited evidence).

Supporting Evidence: WCE has higher sensitivity than conventional small bowel exams (SBFT) or MDCT for the diagnosis of CD of the small bowel and for diagnosis of a cause of bowel hemorrhage when endoscopy is negative. Based on recent adult literature, capsule endoscopy has the highest diagnostic yield for identifying small bowel disease from any cause (including Crohn's) with a sensitivity of 87% versus only 13% for all other imaging modalities (29). The capsule appears to have greater sensitivity in identifying small bowel ulceration or stricture than conventional fluoroscopic barium studies and enteroclysis. In an adult study of 17 patients suspected or known to have non-obstructive CD at the Mayo Clinic in Scottsdale, CD was detected by WCE in (12/17) 71%, by ileoscopy in (11/17) 65%, by CT enterography in (9/11) 53%, and by SBFT in only (4/17) 24% (27). It is advocated that WCE may be helpful in identifying non-obstructive CD when SBFT and ileoscopy are negative or inconclusive (27).

Currently WCE is not routinely used in the identification of CD in children. However, it has a role beyond IBD in diagnosing obscure small bowel lesions accurately in children over the age of 10 years. In a prospective study by Guilhon de Araujo et al., WCE correctly diagnosed or excluded a bleeding source, small-bowel polyps, or Crohn's disease of the small bowel in 29 of 30 children (30).

There are limitations and pitfalls with WCE which can lead to false positives or false negatives. Small children need the capsule placed by endoscopy and extra-intestinal abnormalities cannot be assessed. Limitations include submucosal lesions mimicking normal folds, poor localization of the pathology, capsule retention in patients with asymptomatic strictures, rapid transit resulting in decreased sensitivity, or slow transit which outlasts the capsule battery life (7–8 hours). Also mucosal erosions can be seen in 14% of normal patients and in 28% of NSAID users (31, 32).

III. What Is the Diagnostic Performance of Current Imaging Modalities in Evaluating IBD of the Small Bowel (Small Bowel Follow-Through, CT, MR, US, Enteroclysis)?

Summary of Evidence: There are multidimensional considerations for which imaging test is the best to evaluate a child that include the patient's age and comfort, availability of the exam, radiation dose, and cost. Imaging studies are categorized as follows: conventional includes radiographs, small bowel follow-through (SBFT), multidetector CT (MDCT);

newer imaging comprised of enterography using CT/MR, and enteroclysis CT (CTE), or MR (MRE); and finally ultrasound. Despite the many new imaging tests, SBFT remains the most common initial exam performed (limited evidence).

Children with abdominal pain from IBD or its complications (particularly, abscess or bowel obstruction) may have conventional MDCT performed. However, it does not have a strong role in the diagnosis of IBD as it has a low sensitivity and specificity because of collapsed, underfilled bowel. CT enterography has improved sensitivity and specificity when compared with CT with positive enteral contrast. MR enterography has become increasingly desirable because of the lack of ionizing radiation and its high diagnostic accuracy.

The role of enteroclysis (CT or MRI) is to detect partial small bowel obstruction from either adhesions or stricture. CTE is more sensitive than fluoroscopic enteroclysis (FE) and has largely replaced it where CT is readily available. CT enteroclysis (CTE) should be reserved for complex cases of CD when a partial obstruction (from adhesion or stricture) is highly suspected but other imaging has been negative. MR enteroclysis has been shown to have high diagnostic performance in children but is not widely available and requires experienced personnel, nasal intubation, and sedation making it less practical. Like MRE, US may be used in the first assessment of a child with IBD and in monitoring disease but requires experienced and dedicated personnel.

Supporting Evidence

Abdominal Radiographs

Radiographs are used to evaluate for any patient with acute abdominal pain or in those with known IBD where complications are suspected such as bowel obstruction, free intraperitoneal air, and overall stool burden. Radiographs have no role in diagnosing IBD. The findings of "thumb-printing" (suggesting bowel wall edema or inflammation) and dilated bowel loops are non-specific (33).

Small Bowel Follow-Through (SBFT)

The SBFT exam involves giving the patient oral barium taking immediate and delayed images of the upper gastrointestinal tract and entire small bowel until the contrast reaches the cecum. Relative to ileoscopy, SBFT is not only less sensitive but also inexpensive, widely available, easy to perform, and requires no sedation in diagnosing CD (19, 27) (moderate evidence). The diagnostic capability of SBFT in detecting CD in the small bowel has been conflicting in the literature. In a pediatric study of 84 subjects, the SBFT had a low sensitivity in detecting TI involvement, sensitivity of 45%, specificity of 96% (19). In an adult study by Hara et al. small bowel CD was detected in 4/17 patients (24%) (27). In an older pediatric study (n=46) a sensitivity of 90% and specificity 96% in detection of CD in the small bowel was reported (34). The former two studies appear to reveal more realistic data as poor bowel opacification leads to equivocal exams, and substantial intra- and interobserver variations in interpretation are present (35). In a prospective blinded study of 30 adults with CD the extent of CD and the presence of complications were imaged and compared by both SBFT and MR barium enterography (36). MRI has provided additional information in eight patients. SBFT revealed superficial mucosal lesions seen on MRI, but extra-intestinal pathology, colorectal disease, and potential to distinguish active from chronic disease were far better on MRI (36).

Multidetector CT (MDCT)

MDCT is performed using a low-dose technique with weight-based parameters, after the ingestion of a positive oral contrast agent and administration of IV contrast. CT adds information on extra-intestinal findings of UC and CD; from the earliest publications by Jabra et al. MDCT has had a high sensitivity but low specificity for bowel wall thickness (37, 38). Jabra et al. defined the role of CT as aiding in the management of children with known CD with changing clinical symptoms (limited evidence). CT is the most common examination used for assessing complications of CD such as abscesses, peritonitis, post-operative leaks, and anastomotic issues and has demonstrated a high sensitivity and specificity. These points and the diagnostic performance of CT are discussed in detail under Issue 4, a focus on complications of IBD.

Enterography

Enterography (CT or MR) differs from the conventional CT and MR studies in that a large volume (1,000 ml) of neutral oral contrast agent is given over 1 hour followed by acquisition of a routine intravenously enhanced abdominopelvic CT or MR. The main advantage is that the particular enteric contrast agents used not only result in more bowel distension compared to the conventional enteric agents but also provide low density on CT and low signal on MR imaging of the bowel lumen to allow improved depiction of the bowel wall.

A few CT enterography studies have included a small number of adolescents and the focus of these studies has been to describe data or correlate CT findings with biological markers of inflammation (limited evidence). In one retrospective adult study by Bodily et al. 96 patients underwent CT enterography with enteric water contrast and IV contrast and ileoscopy with or without biopsy. CT results were compared to endoscopic and histological data. CT enterography had a sensitivity of 90% for the detection of CD based on the quantitative mural enhancement which correlated with active CD on endoscopy and biopsy (39). In a large retrospective review of adult CT enterography studies by Paulsen and colleagues (n=700), the sensitivity of CT enterography to detect IBD was >85% when the reference standard was fluoroscopic enteroclysis or SBFT. However, when compared to endoscopy or surgery results, the sensitivity was between 77 and 92% (40).

The data on MR enterography versus the gold standard ileocolonoscopy are promising but limited in children. The key advantage of MRE is its lack of radiation exposure. In a prospective study by Laghi et al. 75 children with IBD underwent ileocolonoscopy and MR enterography with a PEG solution. MRI had a sensitivity of 84% and specificity of 100% in detecting ileitis and differentiating it from other inflammatory conditions (41). Pilleul and colleagues examined 62 patients (median age 14 years) who had suspected or known CD and all underwent MR enterography with an oral preparation of mannitol solution. Imaging was compared to endoscopy and biopsy data. MRI had a sensitivity of 83% and a specificity of 100% in the diagnosis of CD and also identified complications in eight patients (42). There was also a positive correlation between bowel wall thickening and the Pediatric Crohn's Disease Activity Index (PCDAI), ($P = 0.003$). Borthne et al. performed MR in 43 patients suspected of having CD using oral mannitol. MR compared with endoscopy had a sensitivity of 81%, specificity of 100%, and diagnostic accuracy of 90% (43). MR enterography is equally comparable to higher sensitivity compared to CT and US in detection of small bowel CD. Current limitations of MR are the artifacts from respiratory motion and bowel peristalsis and lack of patient cooperation leading to poor bowel distension (limited–moderate evidence).

Enteroclysis (MR or CT)

Enteroclysis is distinct from enterography in that it achieves maximal luminal distention by placement of a duodenal or jejunal tube for high volume, controlled contrast administration. This critical difference improves the detection of partial small bowel obstruction and polyps compared to routine CT or MR and enterography. CT enteroclysis (CTE) combines the advantages of MDCT and enteroclysis. CT enteroclysis has replaced the conventional fluoroscopic technique in many centers and consists of sedation and placement of a feeding tube into the duodenum. A variety of contrast media can be used (water, iodinated contrast, methylcelluose). Once the contrast reaches the cecum the patient is transferred from the fluoroscopic room to CT to undergo a routine abdominopelvic CT (35). CTE is more sensitive and superior to fluoroscopic enteroclysis (FE) and may have a lower radiation dose as reported in an early study by Bender et al. (44, 45). In this adult study CTE was performed to evaluate partial SBO and the sensitivity and specificity for localizing the site of obstruction were 82% and 88%, respectively (45). Brown et al. have recently published data evaluating the safety, feasibility, and outcomes of CTE in 175 children and comparing it with FE. CTE added additional diagnostic information over CT and FE and altered surgical management in 28% of the patients (44). The importance of a normal enteroclysis study in excluding an abnormality is an important clinical consideration. Barloon and colleagues followed 83 adults who had

a normal enteroclysis for 3 years to assess its negative predictive value. Only six were found to have small bowel pathology, meaning that the enteroclysis had a 93% negative predictive value for ruling out any disease (46).

For many children and adults with IBD, repeat imaging is the norm rather than the exception. The main advantage of MR enteroclysis over CTE is the lack of ionizing radiation. The main disadvantage is the motion artifacts, as well as higher cost and possible delay in imaging patients that must be moved from fluoroscopy rooms to the MRI room. A recent evidence-based review of MR enteroclysis shows that this procedure has high diagnostic accuracy in children. Darbari et al. looked at 58 pediatric patients and found a positive predictive value of 96%, negative predictive value of 92%, and overall sensitivity and specificity of 96 and 92%, respectively, for the evaluation of IBD (47). However, MR enteroclysis is not universally available or practical. Currently there are no strong evidence-based studies comparing MR enteroclysis with capsule endoscopy or CT enteroclysis in children (limited evidence).

Ultrasound

Ultrasound (US) of the bowel is performed using a high-frequency transducer with gray scale and color-Doppler compression technique. US oral contrast agents as well as intravenous contrast agents (SICUS) to evaluate the small bowel are not available in the United States but are widely used in Europe. Their use increases the sensitivity and specificity of diagnosing CD over the conventional US techniques (48). Several studies using duplex and color Doppler show improved detection of inflammation of the bowel wall in IBD patients.

Alison and colleagues tabulated the diagnostic effectiveness of US for the few existing studies in children, which have small sample sizes (n=21, n=26). The overall sensitivity of US in detecting bowel IBD is 74–93%, specificity 78–93%; for terminal ileal bowel wall thickening and for stenosis the sensitivity is 85% (48). The variability of these numbers results from both the operator's experience and different cut-off values for abnormal bowel wall thickness.

Absence of bowel wall thickening, particularly when imaging the terminal ileum, has a good negative predictive value for CD. Increased bowel wall thickness in the colon proximal to the rectum and in the terminal ileum has a good positive predictive value for IBD, although it is not specific. In a double-blinded prospective study in 44 children who had endoscopy (n=33) or SBFT (n=25), US of ileal and colonic bowel wall was performed and compared to results of colonoscopy, biopsy, and barium studies (49). US showed significant difference in bowel wall thickness which correlated with active disease on endoscopy. Bowel wall thickness measurements >2.9 mm in the colon or >2.5 mm in the terminal ileum reliably indicated moderate or severe inflammation in children with IBD (49) (limited evidence). In experienced hands, US is an inexpensive imaging tool that avoids ionizing radiation exposure to both diagnose and assess treatment response of the terminal ileum.

IV. Complications of IBD (Intra-abdominal Abscess, Intestinal Fistulae, Strictures and Small Bowel Obstruction, Primary Sclerosing Cholangitis [PSC]): Which Imaging Should Be Performed and What Is Its Diagnostic Performance?

Summary of Evidence: The most common complications of Crohn's disease include abscesses, strictures, fistulae, growth failure, decreased bone mineral density, and delayed puberty. On the other hand, patients with ulcerative colitis are at increased risk for toxic megacolon, peritonitis, and primary sclerosing cholangitis (PSC). Approximately 15–20% of adult patients with ulcerative colitis develop a fulminant colitis and 5% develop toxic megacolon (50). Toxic megacolon, perforation with peritonitis, and mucosal dysplasia are overall rare in children. Because the complications of CD are more frequent than those seen in UC, our discussion will focus primarily on the CD complications with a brief note on the importance of PSC in children.

When imaging complications, CT is preferred in emergent settings specifically for detecting small bowel obstruction, abscesses, peritonitis, post-operative leaks, anastomotic strictures, and perforation (37, 44). To minimize ionizing radiation exposure, US and MRI are

recommended for repeat imaging at follow-up (limited to moderate evidence).

Supporting Evidence

Intra-abdominal Abscess

Intra-abdominal abscesses occur in approximately 10% of children with CD (51). It is rare in children with UC unless it is after colectomy. The most common location of an abscess is the right lower quadrant. However, they can also occur anywhere in the peritoneal cavity, abdominal wall, retroperitoneum, iliopsoas, and subphrenic regions. In nearly 50% of patients, the abscesses occur near an anastomosis following surgical resection. MDCT is the imaging test of choice for the detection of these abscesses unless they are limited to the abdominal wall when US may be sufficient.

Sensitivity and specificity of contrast-enhanced CT in detecting intra-abdominal abscesses in patients with severe CD was 87 and 95%, respectively (52). In experienced hands and using meticulous technique, the sensitivity and specificity of US in detecting abscesses in these same patients was 91 and 85%, respectively (52). CT showed higher specificity and positive predictive value [37]. There are both more false negatives (due to overlying bowel gas) and more false positives (fluid-filled bowel loops) with US and it requires more time and experience than CT.

In a small study, MR enterography had a sensitivity of 100%, in detecting abscesses compared to US (89%) (53). MR enteroclysis, although not performed in children for abscess evaluation, is also sensitive for the detection of abscesses, 100% sensitivity (54) (moderate evidence).

Intestinal Fistulae

The incidence of fistula is also approximately 10% in children, less than that of adults (30%). The gold standard for detection of fistulae is surgery. Using imaging, the gold standard to detect them is CT or MR (limited evidence).

Both CT and MR can detect small bowel fistulae in approximately 70% of patients although reports vary based on experience, technique, and patient populations. The sensitivity of US in the detection of fistulae varies from 31 to 87%. In a prospective study of 213 patients with CD, the US findings of fistulae were compared to surgical data and US showed a sensitivity of 87% and specificity of 90% (55). In patients with internal fistulae, CT showed a sensitivity and specificity of 68 and 91%, respectively, whereas MRI has an overall sensitivity of 87%. MDCT is more accurate for detecting enterovesical and enterocutaneous fistulae and sinus tracts from the bowel to the psoas muscle (50). For fistulae and abscesses extending into the perirectal and perianal regions, MRI is the test of choice with the highest sensitivity and specificity (56, 57) (limited evidence).

Strictures and Small Bowel Obstruction

Development of strictures is a big concern in children, primarily with Crohn's disease. Symptomatic strictures can lead to partial or complete small bowel obstruction and often surgery. In the emergent setting, conventional CT is recommended for assessment of bowel obstruction. In children with subacute or chronic symptoms, CT or MR enteroclysis best detect partial small bowel obstructions. This topic is addressed in more detail in the issue of imaging features leading to surgery (see Issue V).

Primary Sclerosing Cholangitis (PSC)

Any child who presents with PSC should have an evaluation for IBD. PSC is more commonly seen in patients with UC rather than CD. Equally, a child with IBD and elevated liver enzymes may need sonography to evaluate for dilated biliary ducts and if needed MRCP for the diagnosis. PSC is more prevalent in CD than originally thought. According to one adult series the incidence of PSC is 2–7% in UC rather than 0.7–3.4% in CD (58). Approximately 5% of patients with ulcerative colitis are found to have primary sclerosing cholangitis, whereas 75% of patients with primary sclerosing cholangitis are found to have UC. Although these numbers are primarily from data in adults, they are comparable to the limited reports in children. Feldstein and colleagues reported that in 52 children with PSC, 81% had IBD, and in 20% of these children PSC was diagnosed before IBD, thereby setting the impetus for an IBD workup in any child with PSC (58) (moderate evidence). MRCP is the diagnostic study of choice for the evaluation of PSC; when positive, a liver biopsy is not required (limited evidence).

V. What Are the Most Important Imaging Features That Lead to Surgery in a Child with Crohn's Disease and Ulcerative Colitis?

Summary of Evidence: Despite improvements in medical therapies, 70–80% of patients with CD will require an operation, whereas only 30–40% of UC patients will ultimately need surgery (59, 60). The main indications for surgery in a child with CD are (1) small bowel obstruction, SBO (complete or partial) that does not respond to medical therapy; (2) small bowel strictures with associated obstruction; and rarely (3) bowel perforation, appendicitis, or abscess formation (59). When these issues particularly impact the child's growth and development, surgery is warranted. In UC patients, surgery is warranted for the following reasons in the order of most common to least common: (1) disease refractory to medical management, (2) severe disease with complications, (3) risk of malignancy (60). Malignancy requires a colectomy and is a strong concern in adults but rare in children.

Supporting Evidence: The evidence in the pediatric surgical literature determining who needs surgery is limited to a few studies with small sample sizes. The existing large cohort studies evaluate only adults. In a large study by Hurst and colleagues including 513 adult patients, the indications for surgery were the following: failure of medical management in 220, obstruction in 94, intestinal fistula in 68, mass in 56, abscess in 33, peritonitis in 9, and bleeding in 7 (61). Unlike in adults, the impact on a child's growth and development is a vital part of surgical decision making. In one pediatric study, the decision for surgery in up to 50% of the patients was based on the presence of failure of medical therapy with significant growth retardation rather than a mechanical obstruction (62). In a small study of 26 patients, Dokucu et al. described chronic intestinal dysmotility and poor absorption with growth failure as an indication for surgery in 13 children, whereas the remaining 13 had surgery secondary to chronic mechanical intestinal obstruction (63) (limited evidence).

Role of Conventional Barium Fluoroscopy and Multidetector CT

Summary of Evidence: The imaging features of small bowel obstruction include dilated small bowel loops, a decompressed colon, and small bowel air–fluid levels. A symptomatic stricture requires surgery. The presence of a persistently narrowed, smooth walled, and non-thickened segment of bowel with proximal bowel dilatation represents a stricture. The imaging studies most commonly utilized until recently for evaluation of strictures and obstruction have been SBFT and MDCT. MDCT is the imaging test of choice for SBO with high sensitivity for a complete SBO in children but is less likely to detect a partial SBO (Table 33.2) (64) (limited evidence).

Supporting Evidence: Overall conventional fluoroscopic barium imaging is the least accurate in identifying strictures compared with surgical results. Otterson et al. retrospectively reviewed barium studies and surgical records of 118 patients having a total of 230 strictures. The data show that fluoroscopic exams incorrectly estimated the number of small bowel strictures in 43/118 (36%) patients (65). The original work by Jabra et al. has shown that MDCT is both sensitive and specific in diagnosing SBO in children, sensitivity 87%, specificity 86% (66). In this retrospective review MDCT correctly identified the level of obstruction in 12/14 scans, 86% of the cases, and etiology of obstruction in 14/30 scans, 47% of the cases (moderate evidence).

Role of Enteroclysis (CT/MR) and Enterography (CT/MR)

Summary of Evidence: In adults, enteroclysis has been shown to be the most accurate in diagnosing small bowel obstructions in CD (67–69). More recent publications in the pediatric imaging literature report that fluoroscopic enteroclysis (FE) and CT enteroclysis (CTE) are more sensitive and specific in detecting small bowel strictures, partial bowel obstruction, and adhesions compared to conventional SBFT and MDCT, especially in children with IBD (44). MR enteroclysis (MREC) and MR enterography (MRE) have comparable high sensitivity for the

detection of stenoses/strictures (54, 69). In comparison, US has a moderate but lower sensitivity for the detection of ileal stenoses/strictures and post-operative reoccurrences (48). Both accessibility and experience often limit these specialized exams to tertiary care centers.

Supporting Evidence: In adults the sensitivity and specificity of CT enteroclysis (CTE) in accurately diagnosing a small bowel obstruction approaches 100% (Table 33.3) (67, 68). In a recent study by Brown et al. comparing FE and CTE with conventional imaging, FE and CTE added diagnostic information (identification of partial SBO and for CT, extra-intestinal abnormalities) over conventional exams such as SBFT. In particular, CTE definitively identified the etiology of small bowel obstruction, secondary to adhesion, internal hernia, or stricture and changed the surgical management in 28% of patients (44).

MR enteroclysis (MREC) has been shown to be equally sensitive to CTE. Masseli and colleagues found no difference in diagnostic ability of MR enteroclysis and MR enterography to detect stenoses (69). MREC like other enteroclysis procedures requires sedation, nasal–duodenal/jejunal tube placement, and contrast administration. MR enterography is a practical alternative to CT enterography with equal overall sensitivity (limited evidence).

VI. What Are the Role and Risk of Repeat Imaging in Monitoring IBD Response to Treatment?

Summary of Evidence: Imaging is very important for assessing Crohn's disease activity and complications, particularly to investigate the cause of abdominal pain, vomiting, weight loss, or fever; to select or change therapy; and to plan surgery. The imaging modalities most commonly used for follow-up include SBFT and CT because they are non-invasive, widely available, and reproducible. However, in experienced hands, US and MRI have comparable diagnostic accuracy and should be considered to avoid repeated exposure to ionizing radiation. Some children with UC or indeterminant IBD will also need repeat imaging to assess their disease complications but to a lesser frequency than children with CD.

Supporting Evidence: The exact frequency of repeat imaging is not known, but based on current CT literature it is not insignificant. Repeat imaging is primarily performed in children with CD rather than UC and the radiation risk in this population is a big concern. A recent study by Gaca et al. (70) demonstrated that the effective dose (ED) from an abdominopelvic CT was approximately twice that of an average SBFT exam. One important point in this study is that the ED of SBFT studies was calculated based on institutional protocol and equipment, but with varying practices and varying number of images acquired elsewhere, this may potentially lead to ED values larger or equal to that of a CT. In this study of 176 children with CD, 78% of the patients had 0–1 SBFT and 74% patients had over 1.1 CT scans over a follow-up time frame of 3 years and 11 months. Only one patient had an excessive number of SBFT and CTs. The advantages of CT in monitoring these children are clear. CT is a fast, readily available, well-tolerated exam with high sensitivity for evaluation of complications in the emergency setting. Jabra et al. reported that CT should be the first line of imaging in a child with changing clinical symptoms (37). In a separate report of 18 patients with a diagnosis of IBD (including CD, UC, and IC), Jamien and colleagues reported that the sensitivity of MDCT for identifying disease in the small bowel was equal to or greater than that of barium studies (71). When isolated TI or colonic disease is present or if CT has demonstrated an abscess, US with color Doppler can be used to follow these patients (48, 72). In the follow-up evaluation of the extent of bowel involvement or for abscesses and strictures, MRI can be very helpful. A prospective meta-analysis by Horsthuis et al. (73) comparing performance of US, MR, leukocyte-tagged scintigraphy, CT, and PET in the diagnosis of IBD revealed no significant differences in diagnostic accuracy among these techniques [19]. A total of 33 studies out of a search of 1,406 articles, in both the pediatric and adult literature, were evaluated in this meta-analysis and reviewed by two independent reviewers. A minimum of 15 patients were included in the reviewed studies and there were

no age limits on the search. In this study sensitivity for the diagnosis of IBD by each modality per segment of diseased bowel was 73.5% (US), 70.4% (MR), 67.4% (CT), with specificity of 92.7% (US), 94% (MR), 90.2% (CT). CT proved to be significantly less sensitive and specific for intestinal and extra-intestinal pathologies. A limitation of these European studies included in this meta-analysis is that overall CT is much less frequently used in Europe and their experience is superior to North America in US and MRI imaging of bowel. The benefits of CT need to be carefully weighed against the potential long-term risks of radiation dose (74). When possible, based on indication, availability, experience, and cost, an alternative equally diagnostic test, US and MRI, should be obtained in patients requiring repeat imaging (limited–moderate evidence).

VII. Special Situation: Which Imaging Modality Provides the Best Performance for the Evaluation of Perianal/Perirectal Disease in Crohn's Disease?

Summary of Evidence: Pelvic MRI with gadolinium contrast enhancement is the imaging modality of choice for the evaluation of perianal disease, fistula, and adjacent abscesses (limited evidence). It is non-invasive and there is no concern for motion in the pelvis; therefore, high-resolution, high-contrast multiplanar images are feasible without sedation and little patient preparation. Exact differentiation of the sphincter muscles with high-resolution, contrast-enhanced sequences is a requirement for the detection of disorders of the anal canal and the perianal tissues (75). Perianal inflammation occurs overall in about 50% patients with CD. Lifetime risk of a patient with CD to develop a perianal fistula is approximately 20–40% (76) and the rate of recurrence is high. A recurrence rate of up to 48% has been reported in adults with tracts and abscesses inactive and healed after 1 year and up to 60% at 2 years of treatment (77, 78). Although fistulae are less common in children as compared to adults, the lack of ionizing radiation makes MRI ideal, especially when re-imaging children.

Supporting Evidence: A *pelvic* MRI for perianal disease is performed without any endorectal instrumentation or enteric contrast, only intravenous contrast. Perianal inflammation has several manifestations including (1) perirectal wall thickening and inflammation, (2) external cutaneous fistulae and tracts, (3) complex internal fistulae from the bowel to bowel, to bladder, or vagina with frank abscess formation.

Based on the current imaging literature, MR imaging is superior to anal endosonography (EUS/AES), CT, or surgical evaluation in showing disease extent but the optimal approach may be to combine two studies (57, 76). A prospective blinded study in 34 adult patients with CD compared the diagnostic accuracy of EUS, MRI, and rectal exam under anesthesia to identify and classify fistulae (76). The authors reported that the accuracy of identifying a fistula was the greatest, 100%, with any two tests combined rather than one exam alone. MR imaging is also superior to surgical evaluation for predicting clinical outcome (57, 77). In an evidence-based review in adult populations, Sahni et al. described the performance of MRI for the evaluation of perianal disease in CD patients. They concluded that MRI was able to distinguish between simple disease, limited to the perirectal region without fistula, and complex disease, defined as the presence of fistulae and abscesses. MRI overall has a 97% sensitivity and 96% specificity for detection of perianal fistulae (Table 33.4) (57). Essary and colleagues have shown that MRI in children can help differentiate perianal fistulae from other inflammatory conditions such as pilonidal sinus (56) (moderate evidence).

Take Home Tables and Figures

Table 33.1 shows endoscopic, histological, and bio-marker differences between CD and UC. Table 33.2 shows diagnostic performance of imaging in small bowel obstruction (adults). Table 33.3 shows MDCT small bowel obstruction diagnostic accuracy in children. Table 33.4 shows diagnostic performance of MRI for evaluation of perianal disease. Figures 33.1 and 33.2 are algorithms of imaging protocols for CD and US, respectively.

Table 33.1. Endoscopic, histological, and biomarker differences between CD and UC

Modality	CD	UC
Endoscopy and visualization of oral and/or perianal regions	Ulcers (aphthous, linear, or stellate Cobblestoning Skip lesions Strictures Fistula Abnormalities in oral and/or perianal regions Segmental distribution	Ulcers Erythema Loss of vascular pattern Granularity Friability Spontaneous bleeding Pseudopolyps Continuous with variable proximal extension from rectum
Histology	Submucosal (biopsy with sufficient submucosal tissue) or transmural involvement (surgical specimen) Crypt distortion Ulcers, crypt distortion Crypt abscess Granulomas (non-caseating, non-mucin) Focal changes (within biopsy) Patchy distribution (biopsies)	Mucosal involvement Crypt abscess Gobler cell depletion Mucin granulomas (rare) Continuous distribution
Bio-markers		
pANCA detection in IBD	10–40% of CD patients	50–80% of UC patients
ASCA detection in IBD	46–70% of CD patients	6–12% of UC patients

Table 33.2. Diagnostic performance of imaging in small bowel obstruction (adults)

Modality	Sensitivity (%)	Specificity (%)	References
Radiographs (n=78)	46–69	57	(79)
CT abdomen (n=78;55)	57–64	63–79	(79, 80, 81)
High grade	81		(80)
Low grade	48		(80)
CT enteroclysis CTE versus CT (n=15)	100	100	(79)

Table 33.3. MDCT small bowel obstruction diagnostic accuracy in children

Modality	Sensitivity (%)	Specificity (%)	References
MDCT abdomen (n=81)	87	86	(64)

Table 33.4. Diagnostic performance of MRI for evaluation of perianal disease ($N = 34$)

Modality	Sensitivity (%)	Specificity (%)	Positive predictive value (%)	Negative predictive value (%)
MRI	97	96	97	96
AES (anal endosonography)	92	85	89	89
Clinical exam (under anesthesia)	75	64	73	67

Data from Schwartz et al. (76).

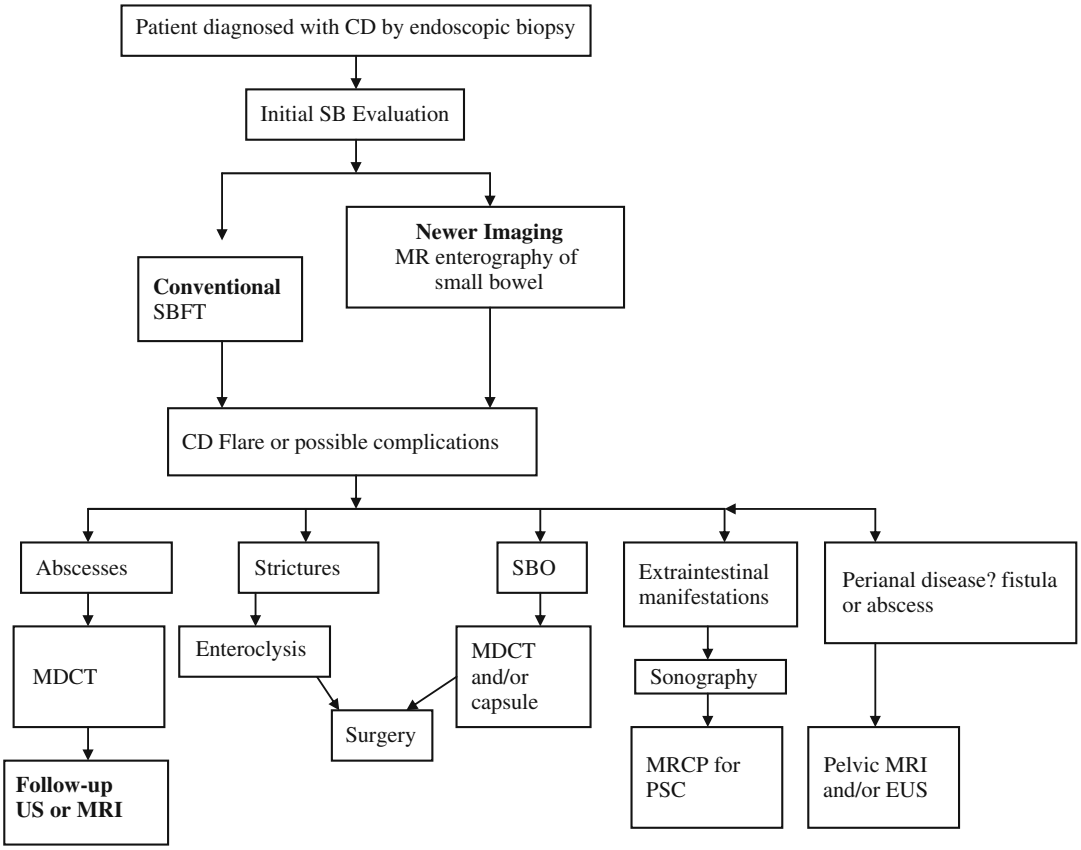

Figure 33.1. Clinical imaging pathways for CD.

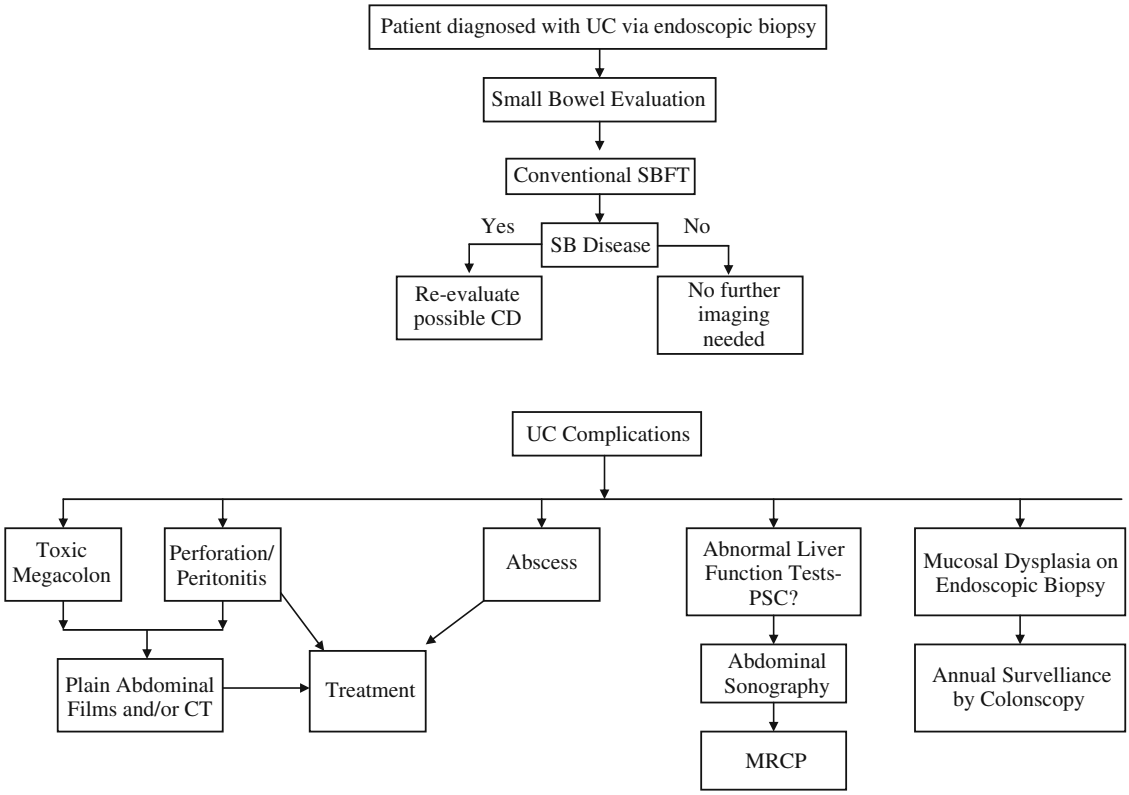

Figure 33.2. Clinical imaging pathways for UC.

Imaging Case Studies

Case 1

Figure 33.3 presents a CT scan of Crohn's disease in a 14-year-old boy complicated by large fistula entering into an even larger abscess in the anterior abdominal wall.

Figure 33.3. CT scan of Crohn's disease in a 14-year-old boy complicated by large fistula entering into an even larger abscess in the anterior abdominal wall. Axial contrast-enhanced CT image of the abdomen demonstrates an enterocutaneous fistula (**F**) arising from an abnormal loop of ileum (**B**) leading to a large abscess (**A**) in the anterior abdominal wall.

Case 2

Figure 33.4 presents CT and MRI of large perianal fistula with abscess in a 10-year-old girl who presented with acute abdominal pain and a new diagnosis of Crohn's disease.

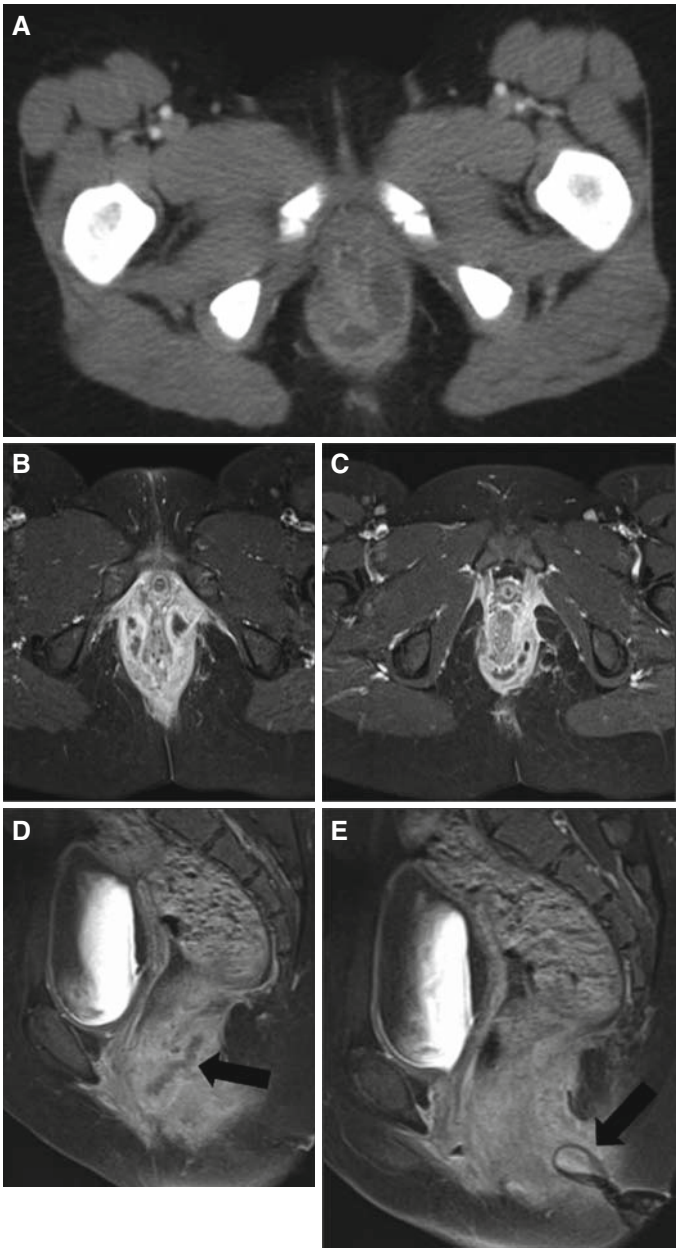

Figure 33.4. MRI of large perianal fistula with abscess in a 10-year-old girl who presented with acute abdominal pain and a new diagnosis of Crohn's disease. **A** is the initial axial MDCT image of the perianal inflammation and small abscesses around her anus. **B** and **C** demonstrate the superior image contrast of the findings on axial MRI with gadolinium and fat saturation technique. There are both exuberant inflammation (enhancement) and small abscesses that nearly circumscribe the anus. **D** demonstrates the perianal abscesses on sagittal view MRI (*black arrow*). **E** shows the superficial position of the drain (*black arrow*) relative to the more deep position of the perianal abscess. She had a large amount of stool in her colon and rectum. She required diverting colostomy to successfully treat her perianal disease.

Case 3

Figure 33.5 presents a case of Crohn's disease in a 12-year-old girl with worsening abdominal pain.

Figure 33.5. Crohn's disease in a 12-year-old girl with worsening abdominal pain. She underwent enteroclysis to evaluate for partial small bowel obstruction. The fluoroscopic enteroclysis image shows that the terminal ileum is strictured (*black arrow*). It produced dilation of the ileum proximal to it and required surgical resection.

Suggested Imaging Protocols for Inflammatory Bowel Disease in Children

Definition of Imaging Techniques

Upper gastrointestinal study with SBFT

UGI/SBFT

A patient is given barium orally and immediate images of the esophagus, stomach, and proximal small bowel are acquired. Then delayed images every 30–45 minutes are obtained of the small bowel until the endpoint when the contrast reaches the cecum. The radiologist will compress the bowel intermittently to evaluate for abnormalities and to assess function of the small bowel loops. The most important anatomy to document on compression spot imaging is the terminal ileum, the most likely area of Crohn's disease.

Enterography (MDCT, MR)

The patient is given oral contrast (20 cc/kg) such as polyethylene glycol, or VoLumen, neutral contrast agents that provide more sustained bowel distention. The patient is given a large volume of contrast to drink over 1 hour. A CT or MRI study is performed after the 1-hour period using a standard institutional CT low-dose protocol with IV contrast.

Enteroclysis (CT, MR)

Three types of enteroclysis exist. All require nasal intubation with sedation for placement of a feeding tube into the duodenum or jejunum for high-volume contrast delivery. Unlike other imaging exams, enteroclysis can achieve the maximum luminal distension of the small bowel. Conventional fluoroscopic enteroclysis (FE) requires contrast administration with a controlled flow rate and careful spot images taken under direct fluoroscopy. MR enteroclysis requires routine MR imaging of the entire abdomen and pelvis in the coronal and axial planes after contrast delivery, whereas CT enteroclysis requires a combination of fluoroscopy and CT. The enteric contrast is instilled under brief fluoroscopic guidance and then the patient undergoes a routine abdominopelvic CT.

Wireless Capsule Endoscopy (WCE)

This procedure is comprised of a 2.5 cm, ingestible capsule containing a videochip, transmitter, and battery. The capsule will pass through the bowel and will evacuate through the stool within 24–48 hours. An average of 55,000 video images are transmitted to a portable device and downloaded to a computer where images are reviewed.

General IBD Algorithm

In a patient suspected to have IBD, the initial workup includes a physical examination, laboratory testing, followed by upper and lower endoscopies for pathological diagnosis and imaging of the small bowel. There is no set rule that endoscopy precedes or follows imaging studies. Endoscopy with biopsy can

determine if the patient has IBD and further classify the patient as CD, UC, or indeterminate. If the endoscopy results are normal, but there is continued concern for IBD, small bowel evaluation should be performed to exclude disease limited to the small bowel, including further laboratory tests or newer techniques such as capsule endoscopy. In some situations imaging of the small bowel by either SBFT or MDCT is performed before endoscopy and may yield information to direct the gastroenterologist especially if the disease process is something other than IBD, i.e., malrotation or malabsorption.

Clinical and Imaging Pathways for CD and UC

See algorithms presented in Figs. 33.1 and 33.2.

Future Research

- Determine the value of both current and as-yet unidentified serologies in the diagnosis and follow-up of IBD.
- Further understanding regarding the role of genetics in IBD.
- Cost-effective analyses on imaging strategies in the evaluation of inflammatory bowel disease activity both at diagnosis and in symptomatic children.
- Large pediatric cohort studies to optimize the techniques of MRI and US to avoid ionizing radiation.
- The role of double-balloon enteroscopy in children with IBD.
- The role of PET and PET–CT in the evaluation of IBD needs to be defined as it can provide both functional and anatomical information.

References

1. Kugathasan S, Judd RH, Hoffmann RG, Heikenen J, Telega G et al. J Pediatr. 2003 Oct; 143(4):525–531.
2. Loftus EV, Jr. Gastroenterology 2004 May; 126(6):1504–1517.
3. Baldassano RN, Piccoli DA. Gastroenterol Clin North Am 1999 Jun; 28(2):445–458.
4. Saeed S, Kugathasan S. In Mamula P, Markowitz JE, Baldassano RN (eds.). Pediatric Inflammatory Bowel Disease. New York, NY: Springer Science and Business Media, 2008; 45–49.
5. Yu AP, Cabanilla LA, Wu EQ, Mulani PM, Chao J. Curr Med Res Opin 2008 Feb; 24(2):319–328.
6. Hay AR, Hay JW. J Clin Gastroenterol 1992 Jun; 14(4):318–327.
7. Goldfarb NI, Pizzi LT, Fuhr JP, Jr., Salvador C, Sikirica V et al. Dis Manag 2004 Winter;7(4): 292–304.
8. Cohen RD, Thomas T. Gastroenterol Clin North Am 2006 Dec; 35(4):867–882.
9. Bassi A, Dodd S, Williamson P, Bodger K. Gut 2004 Oct; 53(10):1471–1478.
10. Hugot JP, Bellaiche M. Pediatr Radiol 2007 Sep 25.
11. Gupta SK, Fitzgerald JF, Croffie JM, Pfefferkorn MD, Molleston JP et al. Inflamm Bowel Dis 2004 May;10(3):240–244.
12. Rabizadeh S, Oliva-Hemker M. In Mamula P, Markowitz JE, Baldassano RN (eds.). Pediatric Inflammatory Bowel Disease. New York, NY: Springer Science and Business Media, 2008; 94–95.
13. Solem CA, Loftus EV, Jr., Tremaine WJ, Harmsen WS, Zinsmeister AR et al. Inflamm Bowel Dis 2005 Aug; 11(8):707–712.
14. Papp M, Norman GL, Altorjay I, Lakatos PL. World J Gastroenterol 2007 Apr 14; 13(14): 2028–2036.
15. Dubinsky MC, Seidman EG. Curr Opin Gastroenterol 2000 Jul; 16(4):337–342.
16. Canani RB, de Horatio LT, Terrin G, Romano MT, Miele E et al. J Pediatr Gastroenterol Nutr 2006 Jan; 42(1):9–15.
17. Heyman MB, Kirschner BS, Gold BD, Ferry G, Baldassano R et al. J Pediatr 2005 Jan; 146(1): 35–40.
18. Mamula P, Telega GW, Markowitz JE, Brown KA, Russo PA et al. Am J Gastroenterol 2002 Aug; 97(8):2005–2010.
19. Batres LA, Maller ES, Ruchelli E, Mahboubi S, Baldassano RN. J Pediatr Gastroenterol Nutr 2002 Sep; 35(3):320–323.
20. Anupindi S, Perumpillichira J, Jaramillo D, Zalis ME, Israel EJ. Pediatr Radiol 2005 May; 35(5):518–524.
21. Abdullah BA, Gupta SK, Croffie JM, Pfefferkorn MD, Molleston JP et al. J Pediatr Gastroenterol Nutr 2002 Nov; 35(5):636–640.
22. Castellaneta SP, Afzal NA, Greenberg M, Deere H, Davies S et al. J Pediatr Gastroenterol Nutr 2004 Sep; 39(3):257–261.
23. Horsthuis K, Bipat S, Bennink RJ, Stoker J. Radiology 2008 Apr; 247(1):64–79.
24. De Matos V, Russo PA, Cohen AB, Mamula P, Baldassano RN et al. J Pediatr Gastroenterol Nutr 2008 Apr; 46(4):392–398.

25. Russo P. In Mamula P, Markowitz JE, Baldassano RN (eds.). Pediatric Inflammatory Bowel Disease. New York, NY: Springer Science and Business Media, 2008; 245–248.
26. de′ Angelis GL, Fornaroli F, de′ Angelis N, Magiteri B, Bizzarri B. Am J Gastroenterol 2007 Aug; 102(8):1749–1757; quiz 8, 58.
27. Hara AK, Leighton JA, Heigh RI, Sharma VK, Silva AC et al. Radiology 2006 Jan; 238(1): 128–134.
28. Arguelles-Arias F, Caunedo A, Romero J, Sanchez A, Rodriguez-Tellez M et al. Endoscopy 2004 Oct; 36(10):869–873.
29. Maglinte DD, Sandrasegaran K, Chiorean M, Dewitt J, McHenry L et al. Am J Roentgenol 2007 Aug; 189(2):306–312.
30. Guilhon de Araujo Sant'Anna AM, Dubois J, Miron MC, Seidman EG. Clin Gastroenterol Hepatol 2005 Mar; 3(3):264–270.
31. Hara AK. Abdom Imaging 2005 Mar–Apr; 30(2):179–183.
32. Maglinte DD. Radiology 2005 Sep; 236(3): 763–767.
33. Taylor GA, Nancarrow PA, Hernanz-Schulman M, Teele RL. Pediatr Radiol 1986; 16(3): 206–209.
34. Lipson A, Bartram CI, Williams CB, Slavin G, Walker-Smith J. Clin Radiol 1990 Jan; 41(1):5–8.
35. Applegate KE, Maglinte DD. Pediatr Radiol 2008 May; 38(Suppl 2):S272–S274.
36. Bernstein CN, Greenberg H, Boult I, Chubey S, Leblanc C et al. Am J Gastroenterol 2005 Nov; 100(11):2493–2502.
37. Jabra AA, Fishman EK, Taylor GA. Radiology 1991 May;179(2):495–498.
38. Jabra AA, Fishman EK, Taylor GA. Am J Roentgenol 1994 Apr; 162(4):975–979.
39. Bodily KD, Fletcher JG, Solem CA, Johnson CD, Fidler JL et al. Radiology 2006 Feb; 238(2): 505–516.
40. Paulsen SR, Huprich JE, Fletcher JG, Booya F, Young BM et al. Radiographics 2006 May–Jun; 26(3):641–657; discussion 57–62.
41. Laghi A, Borrelli O, Paolantonio P, Dito L, Buena de Mesquita M et al. Gut 2003 Mar;52(3): 393–397.
42. Pilleul F, Godefroy C, Yzebe-Beziat D, Dugougeat-Pilleul F, Lachaux A et al. Gastroenterol Clin Biol 2005 Aug–Sep; 29(8–9):803–808.
43. Borthne AS, Abdelnoor M, Rugtveit J, Perminow G, Reiseter T et al. Eur Radiol 2006 Jan; 16(1): 207–214.
44. Brown S, Applegate KE, Sandrasegaran K, Jennings SG, Garrett J et al. Pediatr Radiol 2008 May;38(5):497–510.
45. Bender GN, Timmons JH, Williard WC, Carter J. Invest Radiol 1996 Jan; 31(1):43–49.
46. Barloon TJ, Lu CC, Honda H, Berbaum KS. Abdom Imaging 1994 Mar–Apr; 19(2): 113–115.
47. Darbari A, Sena L, Argani P, Oliva-Hemker JM, Thompson R et al. Inflamm Bowel Dis 2004 Mar; 10(2):67–72.
48. Alison M, Kheniche A, Azoulay R, Roche S, Sebag G et al. Pediatr Radiol 2007 Nov; 37(11):1071–1082.
49. Bremner AR, Griffiths M, Argent JD, Fairhurst JJ, Beattie RM. Pediatr Radiol 2006 Sep; 36(9): 947–953.
50. Carucci LR, Levine MS. Gastroenterol Clin North Am 2002 Mar; 31(1):93–117, ix.
51. The key complications of Crohn's Disease.http://www.ccfa.org. Accessed November 2008.
52. Maconi G, Sampietro GM, Parente F, Pompili G, Russo A et al. Am J Gastroenterol 2003 Jul; 98(7):1545–1555.
53. Potthast S, Rieber A, Von Tirpitz C, Wruk D, Adler G et al. Eur Radiol 2002 Jun; 12(6): 1416–1422.
54. Ryan ER, Heaslip IS. Abdom Imaging 2008 Jan–Feb; 33(1):34–37.
55. Gasche C, Moser G, Turetschek K, Schober E, Moeschl P et al. Gut 1999 Jan; 44(1): 112–117.
56. Essary B, Kim J, Anupindi S, Katz JA, Nimkin K. Pediatr Radiol 2007 Feb; 37(2):201–208.
57. Sahni VA, Ahmad R, Burling D. Abdom Imaging 2008 Jan–Feb; 33(1):26–30.
58. Feldstein AE, Perrault J, El-Youssif M, Lindor KD, Freese DK et al. Hepatology 2003 Jul; 38(1):210–217.
59. Allmen D. In Mamula P, Markowitz JE, Baldassano RN (eds.). Pediatric Inflammatory Bowel Disease. New York, NY: Springer Science and Business Media, 2008;455–465.
60. Mattei P, Rombeau JL. In Mamula P, Markowitz JE, Baldassano RN (eds.). Pediatric Inflammatory Bowel Disease. New York, NY: Springer Science and Business Media, 2008; 469–481.
61. Hurst RD, Molinari M, Chung TP, Rubin M, Michelassi F. Surgery 1997 Oct; 122(4):661–667; discussion 7–8.
62. Patel HI, Leichtner AM, Colodny AH, Shamberger RC. J Pediatr Surg 1997 Jul; 32(7): 1063–1067; discussion 7–8.
63. Dokucu AI, Sarnacki S, Michel JL, Jan D, Goulet O et al. Eur J Pediatr Surg 2002 Jun; 12(3): 180–185.
64. Jabra AA, Fishman EK. Abdom Imaging 1997 Sep–Oct; 22(5):466–470.
65. Otterson MF, Lundeen SJ, Spinelli KS, Sudakoff GS, Telford GL et al. Surgery 2004 Oct; 136(4):854–860.

66. Jabra AA, Eng J, Zaleski CG, Abdenour GE, Jr., Vuong HV et al. Am J Roentgenol 2001 Aug; 177(2):431–436.
67. Maglinte DD, Sandrasegaran K, Lappas JC. Radiol Clin North Am 2007 Mar; 45(2): 289–301.
68. Maglinte DD, Sandrasegaran K, Lappas JC, Chiorean M. Radiology 2007 Dec; 245(3): 661–671.
69. Masselli G, Brizi MG, Menchini L, Minordi L, Vecchioli Scaldazza A. Radiol Med (Torino) 2005 Sep; 110(3):221–233.
70. Gaca AM, Jaffe TA, Delaney S, Yoshizumi T, Toncheva G et al. Pediatr Radiol 2008 Mar; 38(3):285–291. Epub 2008 Jan 5.
71. Jamieson, DH et al. AJR 2003; 180 (5): 1211–1216.
72. Spalinger J, Patriquin H, Miron MC, Marx G, Herzog D et al. Radiology 2000 Dec; 217(3): 787–791.
73. Horsthuis K, Bipat S, Bennink RJ et al. Radiology 2008;247(1):64–79.
74. CT and Radiation Dose. http//www.imagegently.com/CT accessed Sept 2008.
75. Schaefer O, Oeksuez MO, Lohrmann C, Langer M. J Comput Assist Tomogr 2004 Mar–Apr; 28(2):174–179.
76. Schwartz DA, Wiersema MJ, Dudiak KM, Fletcher JG, Clain JE et al. Gastroenterology 2001 Nov; 121(5):1064–1072.
77. Darge K, Anupindi SA, Jaramillo D. Magn Reson Imaging Clin N Am 2008 Aug; 16(3):467–478, vi.
78. Makowiec F, Jehle EC, Starlinger M. Gut 1995 Nov; 37(5):696–701.
79. Maglinte DD, Reyes BL, Harmon BH et al. AJR 1996;167(6):1451–1455.
80. Maglinte DD, Gage SN, Harmon BH. Radiology 1993;188(1):61–64.
81. Walsh SE, Bender GN, Timmons JH. Emerg Radiol 1998; 5:29–37.

34

Pediatric Abdominal Tumors: Neuroblastoma

Marilyn J. Siegel

Issues

I. What are the clinical findings that raise the suspicion for neuroblastoma?
II. What is the diagnostic performance of the different imaging studies in the assessment of the primary tumor mass in patients with neuroblastoma?
III. What are the essential features that need to be assessed by imaging studies in patients with neuroblastoma for surgical planning and staging?
IV. What is the diagnostic performance of the different imaging studies in the detection of regional disease in patients with neuroblastoma?
V. What is the diagnostic performance of the different imaging studies in the detection of distant metastases in patients with neuroblastoma?
VI. Special situations: the child who presents with opsoclonus-myoclonus syndrome or intractable watery diarrhea

Key Points

- The clinical presentation of neuroblastoma can be nonspecific and sometimes confusing (strong evidence).
- The features that need to be evaluated on imaging studies for surgical planning or staging in neuroblastoma are tumor location, regional tumor extent (including vascular encasement, midline extension, regional lymph node involvement), and skeletal or liver metastases (strong evidence).
- Ultrasonography, computed tomography (CT), and magnetic resonance imaging (MRI) have high sensitivity for tumor detection and moderate specificity (strong evidence).

M.J. Siegel (✉)
Mallinckrodt Institute of Radiology, Washington University Medical School, St. Louis, MO 63110, USA
e-mail: siegelm@mir.wustl.edu

L.S. Medina et al. (eds.), *Evidence-Based Imaging in Pediatrics*,
DOI 10.1007/978-1-4419-0922-0_34,

- CT and MRI have moderate sensitivity for detection of regional tumor extent and are superior to sonography for this determination (limited to moderate evidence).
- MRI, bone scintigraphy, metaiodobenzylguanidine (MIBG) scintigraphy and fluoro-2-deoxy-D-glucose positron emission (FDG-PET) imaging have high sensitivity for detecting bone/bone marrow metastases (moderate to strong evidence).
- MRI, MIBG scintigraphy, and FDG-PET imaging have high sensitivity for detecting non-skeletal metastases (moderate to strong evidence).
- No data were found in the medical literature that evaluate the cost-effectiveness of the different imaging modalities in the evaluation of these tumors.

Definition and Pathophysiology

Neuroblastoma is a small, blue, round cell tumor derived from the primordial neural crest cells that give rise to the sympathetic nervous system of childhood (1, 2). The most common sites of origin are the adrenal medulla (35%), extra-adrenal paraspinal ganglia in the abdomen and pelvis (30–35%), and posterior mediastinum (20%) (1, 2). Less common sites are the pelvis (2–3%) and neck (1–5%). In approximately 1% of patients, a primary tumor is not found. Histologically, neuroblastoma consists of neuroblasts, which are small round sympathetic cells that contain dark and indistinct nucleoli. Characteristically, the tumor cell nuclei are arranged in rosettes. An unequivocal diagnosis of neuroblastoma is made from tissue sampling and light microscopy, electron microscopy, or immunohistology *or* by the combination of a bone marrow aspirate or biopsy that shows unequivocal tumor cells *and* increased serum or urinary catecholamines or metabolites. The vast majority of these tumors secrete catecholamines, vanillylmandelic acid (VMA), and homovanillic acid (HVA). There is extensive variability in the clinical behavior of neuroblastoma, ranging from spontaneous regression, differentiation into benign ganglioneuroma, to fatal disease (1, 2). Several histologic, biologic (genetic), and biochemical hallmarks of neuroblastoma have important prognostic features. Histologic features associated with an unfavorable outcome are cellular or stromal immaturity and an elevated mitosis-karyorrhexis index (3). Biologic markers associated with aggressive tumor behavior and a worse outcome are amplification of the N-myc oncogene (4–6), diploid changes (normal or near-normal DNA content) (6, 7), partial deletions of chromosome 1 and 11, and gains of chromosome 17 (8–10). Biochemical markers associated with worse prognosis include elevated serum levels of lactate dehydrogenase, ferritin, and neuron-specific enolase (1, 11, 12). Approximately 50–69% of patients will have metastases at presentation, most commonly to cortical bone, bone marrow, liver, or lymph nodes (1, 2) (strong evidence).

Epidemiology

Neuroblastoma is the most common extracranial solid tumor of childhood, accounting for 8–10% of all childhood cancers (1, 13). The prevalence is about one case per 7,000 live births, and there are approximately 800 new cases of neuroblastoma annually in the United States (1, 13). Neuroblastoma is slightly more common in boys than girls, with a male to female ratio of 1.1:1 (1). The median age at diagnosis is about 19 months. Approximately 40% of patients are infants; 90% are under 5 years of age; and 98% are under 10 years of age (1, 2). The incidence rate of the disease in children under 1 year of age is about 35 per million but declines rapidly with age to about 1 per million between ages 10 and 14. The etiology of neuroblastoma is unknown. In rare cases, neuroblastoma may be familial, exhibiting an autosomal dominant pattern of inheritance, possibly related to an abnormality in the short arm of chromosome 16 (16p12-13) (14,

15). In this subset of patients, the median age of diagnosis is 9 months. Although rare, neuroblastoma may occur in patients with other disorders, including Hirschsprung disease and neurofibromatosis type 1 (NF1). The natural history of neuroblastoma varies most closely with histologic, biologic, and biochemical factors, tumor stage, and patient age. Patients younger than 12 months of age have a better prognosis, even with metastatic disease, than those older than 12 months of age (16, 17). The prognosis for neuroblastoma is based on low-, intermediate-, or high-risk disease (1.2) (strong evidence).

Overall Cost to Society

Although there are several analyses evaluating the cost-effectiveness of chemotherapy in the treatment of neuroblastoma, no cost-effectiveness data were found in the literature specifically incorporating imaging strategies in the management of this tumor.

Goals

In neuroblastoma, the goal of imaging is determination of the site of tumor origin, local disease extent, and distant tumor spread. The current imaging evaluation of patients with neuroblastoma consists of abdominal sonography, chest radiography, computed tomography (CT), and/or magnetic resonance imaging (MRI) for detection and local staging of the primary tumor and bone scintigraphy or metaiodobenzylguanidine scintigraphy (MIBG) for detection of skeletal or marrow metastases. The most common staging system for neuroblastoma is the International Neuroblastoma Staging System (INSS) (Table 34.1) (18, 19). This classification takes into account radiological findings, clinical findings, and bone marrow examination.

Methodology

The author performed a MEDLINE search using PubMed (National Library of Medicine, Bethesda, MD) for data relevant to the diagnostic performance and accuracy of both clinical and imaging examination of patients with neuroblastoma. The diagnostic performance of the clinical and imaging examinations was based on a systematic literature review performed in MEDLINE (National Library of Medicine, Bethesda, MD) during the years 1975–2007. The clinical examination search strategy used the following key words: (1) *neuroblastoma*; (2) *clinical physical examination*; (3) *epidemiology*; (4) *treatment* or *chemotherapy* or *surgery.* The review of the current diagnostic imaging literature was performed using the following words: (1) *neuroblastoma*; (2) *ultrasound*; (3) *computed tomography* or *CT*; (4) *magnetic resonance imaging* or *MRI*; (5) *metaiodobenzylguanidine* or *MIBG scintigraphy*; (6) *indium-111 pentetreotide* or *octreotide* or *somatostatin receptors*; (7) *fluoro-2-deoxy-d-glucose positron emission tomography* or *FDG scanning*, as well as combinations of these search strings. Animal studies and non-English articles were excluded.

Discussion of Issues

I. What Are the Clinical Findings that Raise the Suspicion for Neuroblastoma?

Summary of Evidence: Clinical finding leads of neuroblastoma are generally nonspecific. Patients can be asymptomatic or symptomatic with clinical complaints related to the primary tumor, local or metastatic disease, or a paraneoplastic syndrome. In asymptomatic patients, the tumor can be detected incidentally on antenatal ultrasonography (20–22), post-natal screening of urinary catecholamine metabolites (1, 23–25), physical examination, or imaging studies obtained for other indications (strong evidence).

Supporting Evidence: The most common clinical presentation of abdominal neuroblastoma is an abdominal mass (1, 2). Abdominal distention, anorexia, and vomiting are also frequent features of abdominal involvement. Other complaints include paraplegia and urinary or fecal retention or incontinence from neural

foraminal invasion and nerve compression and hypertension due to catecholamine production or encasement or stretching of the renal artery leading to activation of the renin–angiotensin system. Patients with primary thoracic and cervical neuroblastoma can present with dysphagia, stridor, or Horner syndrome (ipsilateral ptosis, pupillary constriction, and anhydrosis) (26) (strong evidence).

Signs and symptoms related to metastatic disease include proptosis and periorbital ecchymosis; bone pain, limp, or arthritis-type complaints; hepatomegaly; and nontender, bluish subcutaneous nodules (1) (strong evidence). Paraneoplastic syndromes include opsoclonus-myoclonus syndrome and watery diarrhea. Opsoclonus-myoclonus is characterized by jerking movements of the eyes and extremities and ataxia and may represent an immune-mediated antitumor host response, which leads to production of antineural antibodies that cross-react with cerebellar tissue (27–29). It is seen in approximately 2% of patients and is associated with a thoracic primary tumor and a better prognosis. Watery diarrhea results from tumor production of vasointestinal peptides (strong evidence).

Approximately 90% of patients with neuroblastoma have increased serum or urinary levels of catecholamines or their metabolites, particularly vanillylmandelic acid (VMA) and homovanillic acid (HVA).

II. What Is the Diagnostic Performance of the Different Imaging Studies in the Assessment of the Primary Tumor Mass in Patients with Neuroblastoma?

Summary of Evidence: Imaging is performed to confirm the presence of a mass and its site or origin and to identify local and metastatic disease for treatment planning. Ultrasonography, CT, and MRI have equal sensitivity for the detection of the primary abdominal mass in patients with neuroblastoma and its organ of origin (strong evidence).

Supporting Evidence: The sensitivity of ultrasonography, CT, and MRI for detection of the primary mass in patients with neuroblastoma is nearly 100%, which is not surprising given the large mean diameter of the tumor (6–8 cm mean diameter) (30–33) (strong evidence). In a prospective study by Siegel et al. of 129 patients suspected of having neuroblastoma, the sensitivity and specificity of both CT and MRI were 100 and 85%, respectively (33). For detection of very small thoracic or retroperitoneal tumors, CT and MRI have theoretical advantages by comparison with chest radiography and ultrasonography, respectively, because of their superior resolution (insufficient evidence).

III. What Are the Essential Features that Need to Be Assessed by Imaging Studies in Patients with Neuroblastoma for Surgical Planning and Staging?

Summary of Evidence: An understanding of the clinical findings that are important for treatment planning and staging is essential to understand the role of imaging. Key factors in planning surgical resection are tumor location and relationship to major vessels, nerves, and organs. Key factors in the INSS classification for neuroblastoma staging are the regional extent of tumor spread, particularly unilateral or bilateral involvement and nodal involvement, and the presence or absence of distant metastases (18, 19) (strong evidence).

Supporting Evidence: Knowledge of vascular encasement and intraspinal extension are critical factors in planning gross tumor resection. Vascular encasement can be a contraindication to total surgical resection because of the risk of loss of vital structures or significant postoperative morbidity. Surgical complications have been reported in 5–25% of patients with neuroblastoma related to surgical resection of the primary abdominal tumor at diagnosis (34). Commonly encountered complications related to vascular encasement include nephrectomy, operative hemorrhage, and injury to renal or mesenteric vessels. Intraspinal extension of neuroblastoma associated with spinal symptoms requires either urgent treatment

with chemotherapy and steroids or a laminectomy alone or in combination with radiation therapy to reduce cord compression prior to tumor resection of debulking (1, 2) (strong evidence).

Knowledge of the presence of regional and distant disease is pivotal for tumor staging. Locally, the status of regional lymph nodes and midline extension needs to be assessed. Ipsilateral nodes correspond to INSS stage 2 disease. Unilateral tumor with contralateral lymph nodes or midline extension indicates INSS stage 3 disease. Assessment of distant metastases to liver and skeleton is critical because these upgrade the tumor to INSS stage 4 or 4S (18, 19) (strong evidence).

IV. What Is the Diagnostic Performance of the Different Imaging Studies in the Detection of Regional Disease in Patients with Neuroblastoma?

Summary of Evidence: Ultrasonography is sensitive for detecting neuroblastoma, but it cannot reliably identify local extension (30–32) (limited evidence). CT and MRI have moderate sensitivity for assessing local tumor extent (33, 35–37) (limited to moderate evidence).

Supporting Evidence: Ultrasonography has limited value in demonstrating the extent of vessel encasement, involvement of retroperitoneal and retrocrural nodes, and intraspinal tumor extension compared with CT and MRI (2, 32). In one retrospective series of 42 neonates, infants, and children with abdominal masses, including 19 neuroblastomas, by Pfluger et al., MR angiography and color Doppler sonography showed the entire course of unaffected vessels in 88 and 58% of patients, respectively. MRA showed 79% and color Doppler ultrasonography 66% of displaced vessels (32) (limited evidence).

Due to their superior contrast and spatial resolution, CT and MRI have advantages compared with ultrasonography in evaluating the local extent of a primary neuroblastoma (limited to moderate evidence) (33–37). In a prospective multi-institutional study of 45 of 88 patients with proven neuroblastomas who qualified for analysis of extent of local disease, Siegel et al. reported positive predictive values (PPV) (sensitivity) and negative predictive values (NPV) for CT in detection of midline extension of 73 and 83%, respectively. For MRI, corresponding PPV and NPV were 81 and 79%. PPV and NPV for CT in detection of local nodes were 20 and 95%, respectively. For MRI, corresponding PPV and NPV were 19 and 99%, respectively (33) (moderate evidence). The limitation of this study was that it was designed to evaluate distant disease, not local disease, and the prevalence of local disease was relatively low.

MRI appears to be superior to CT for identifying intraspinal extension (35–37). In a small series of four children with neural foraminal invasion, MRI and CT had sensitivities of 100 and 25%, respectively (37) (limited evidence).

V. What Is the Diagnostic Performance of the Different Imaging Studies in the Detection of Distant Metastases in Patients with Neuroblastoma?

Summary of Evidence: About 50–60% of patients with neuroblastoma have distant metastases, most often to cortical bone, bone marrow, liver, and lymph nodes (1, 2, 38). Plain radiographs are not sensitive or specific for detection of skeletal metastases (moderate evidence). Bone scintigraphy is sensitive for detecting skeletal metastases, but it has low specificity and, moreover, it cannot detect nonosseous lesions (moderate evidence). MRI, MIBG scintigraphy, and FDG-PET imaging are superior to conventional radiographic imaging and bone scintigraphy for assessing skeletal and non-skeletal involvement (moderate to strong evidence). CT and MRI are sensitive for detection of liver metastases, but their relative merits have not been established.

Supportive Evidence: CT is generally recognized as a sensitive study for detection of hepatic lesions. However, the sensitivity for detection of neuroblastoma metastases specifically has not been established. The sensitivity of MRI for detecting hepatic involvement is reported to be 100% (35, 39), although these

results are limited by small sample size (limited evidence).

Technetium (Tc)-99m-labeled dimercaptophosphonate (MDP) scintigraphy has been a commonly performed study for detection of skeletal metastases since the 1970s. 99mTc-MDP scans are more sensitive than conventional skeletal radiography for detection of skeletal metastases. The sensitivity of radionuclide imaging is reported to be about 90%, compared with a sensitivity of 35–70% for radiographic skeletal survey (40–42). Primary tumor can also concentrate tracer (90% sensitivity), but this has no clinical significance (40).

MRI can be performed as a dedicated study for evaluation of localized bone pain or as whole-body imaging for detection of distant metastases and stage 4 disease, including skeletal and nonskeletal involvement. The performance characteristics of MRI are good for detecting metastases with sensitivity of approximately 85–100% (33, 43–45) (strong evidence). In a prospective multi-institutional study of 88 children with newly diagnosed neuroblastoma, Siegel et al. reported areas under the ROC curves for MRI, scintigraphy, and CT for diagnosis of bone and bone marrow metastases of 0.86, 0.85, and 0.59, respectively (33) (strong evidence). For diagnosis of all stage 4 disease (skeletal and nonskeletal), the areas under the ROC curves for MRI, CT, and scintigraphy were 0.85, 0.81, and 0.83, respectively (33). The true-positive values (sensitivity) for MRI and CT in the detection of all stage 4 disease were 83 and 43%, respectively, and the true-negative values for MRI and CT were 88 and 97%, respectively. Other studies with smaller sample size have shown similar results. In a study of 36 children with a variety of malignant tumors, including neuroblastoma, by Goo et al. (43), the sensitivity and positive predictive values for skeletal metastasis were 99 and 94%, respectively, for whole-body MRI, 26 and 94%, respectively, for bone scintigraphy, 25 and 100%, respectively, for ^{123}I-MIBG scintigraphy, and 10 and 43%, respectively, for CT (43). Sensitivity for extraskeletal soft tissue metastases was 60% for whole-body MRI. In a prospective study of seven children with small cell tumors, including neuroblastoma, by Mazumdar et al., the sensitivity of MRI for identifying skeletal and soft tissue metastases was 100% (44). In addition, MRI detected more marrow metastases than did scintigraphy (44).

MIBG is an analog of catecholamine precursors that is taken up by catecholamine-producing tumors (46–51). ^{123}I-MIBG is preferable to ^{131}I-MIBG because of lower radiation dose to the patient, better image resolution, and superior sensitivity. ^{123}I-MIBG will localize to sites of neuroblastoma in 90–95% of patients, including the primary tumor and metastases in bone, bone marrow, and lymph nodes (46, 49, 51). Causes of false-negative studies are intense physiologic activity in salivary glands, liver, myocardium, bowel, normal adrenal medulla, and neck muscles causing non-visualization of pathologic lesions (49, 51, 52). False-positive results have been associated with hepatic hemangiomas, focal nodular hyperplasia, and physiologic uptake in normal liver and intestine (49, 51, 52) (limited to moderate evidence). Several studies with small number of patients (n<30) have suggested that MIBG scintigraphy demonstrates more lesions than bone scintigraphy (48, 50) (limited to moderate evidence). The specificity of MIBG for neuroblastoma in the appropriate clinical context is greater than 95% (moderate evidence) (53). In a study of 100 children with suspected neural crest tumors, only 4% (4/100) of non-sympathomedullary tumors showed MIBG uptake, of which only 2% were of non-neural crest origin (53).

^{111}Indium pentetreotide (octreotide), a radiolabeled somatostatin analog, has an affinity for binding to the somatostatin receptors in neuroblastomas (54). Scans are more frequently positive in undifferentiated tumors and in tumors associated with elevated urinary catecholamines. Imaging with ^{111}In-pentetreotide is less sensitive than imaging with MIBG (55–57). The sensitivity of pentetreotide for detection of the primary tumor is approximately 55–70% (55–57) (limited to moderate evidence). In a study of seven patients with neuroblastoma or ganglioneuroblastoma by Shalaby-Rana et al., the overall sensitivity for detection of primary or metastatic disease was 57% (four of seven) for ^{111}In-pentetreotide and 86% (six of seven) for MIBG scintigraphy (56). In another study of 88 children with histologically proven neuroblastoma or ganglioneuroblstoma, ^{111}In-pentetreotide was less sensitive in

detecting tumor tissue that was ^{123}I-MIBG (64 vs. 94%) (57). The relatively poor sensitivity of ^{111}In-pentetreotide and its variable uptake limits its usefulness in the evaluation of patients with neuroblastoma.

Fluoro-2-deoxy-D-glucose positron emission tomography (FDG-PET) reflects the increased glycolytic rate of tumor cells and uptake is proportional to tumor cell burden and tumor cell proliferation (58–60). Based on limited data, FDG-PET imaging appears to be as sensitive as MIBG in detection of the primary tumor and metastases in patients with neuroblastoma (58–60) (limited to moderate evidence). In a series of 17 patients reported by Shulkin et al., 16 of 17 (95%) patients exhibited tumor uptake of FDG (60). In a study of 51 patients with high-risk disease (n-MYC amplified unresectable disease in all age groups or stage 4 disease regardless of biology in patients >18 months old) reported by Kushner et al., PET scan findings correlated well with disease status as determined by standard imaging tests, bone marrow testes, urine VMA and HVA levels, and clinical history (58). In that study, PET was superior to MIBG imaging for identifying small lesions (e.g., foci in ribs or vertebral bodies), matched or surpassed the sensitivity of MIBG scans for detecting extracranial skeletal lesions, and showed more osteomedullary (bone and bone marrow) abnormalities than 99mTc-MDP bone scans. A limitation of PET scanning is the poor visualization of lesions in the cranial vault, because of the normally high physiologic activity in brain. Causes of false-positive scans include physiologic uptake in bowel, thymus, urinary tract, normal adrenal gland, hyperactive bone marrow, and sites of inflammation (58). The role of FDG-PET in staging neuroblastoma is still uncertain, but preliminary data suggest that it is an attractive staging modality in patients with neuroblastoma.

VI. Special Situations: The Child Who Presents with Opsoclonus-Myoclonus Syndrome or Intractable Watery Diarrhea

Summary of Evidence: Several paraneoplastic syndromes have been associated with localized and disseminated neuroblastoma, including opsoclonus-myoclonus syndrome, intractable diarrhea, and flushing associated with hypertension. These findings have been attributed to metabolic and immunological disturbances associated with the tumor.

Supporting Evidence: The opsoclonus-myoclonus syndrome, also referred to as myoclonic encephalopathy of infants, is characterized by acute cerebellar and truncal ataxia and random eye movements (dancing eyes) (61, 62). It occurs in up to 4% of patients with newly diagnosed neuroblastoma. Conversely, up to 50% of children with this syndrome may have neuroblastoma (1). The primary tumor is most commonly found in the posterior mediastinum (50% of cases), but it may be found anywhere along the sympathetic chain. The majority of patients with opsoclonus-myoclonus syndrome have favorable outcomes with respect to their tumor. However, most have long-term neurologic deficits that can progress even after removal of the tumor (61, 62) (moderate to strong evidence).

Intractable watery diarrhea associated with hypokalemia and dehydration is a result of tumor secretion of vasoactive intestinal peptide (VIP). Most patients with tumor-related diarrhea and hypertension have histologically mature tumors (either ganglioneuroma or ganglioneuroblastoma) and favorable outcomes (63, 64). Surgical resection of the tumor leads to resolution of symptoms (moderate to strong evidence).

Take Home Figures and Tables

What Are the Roles of the Imaging Modalities in the Evaluation of Wilms Tumor?

The decision tree in Figure 34.1 outlines the role of each imaging modality in the evaluation of suspected neuroblastoma. Ultrasonography is the initial imaging study to confirm the presence of an abdominal or pelvic mass due to its relative low cost, rapid acquisition, and ready availability (Figure 34.2). Chest radiography is often the initial imaging study for detection of thoracic neuroblastoma (Figure 34.3).

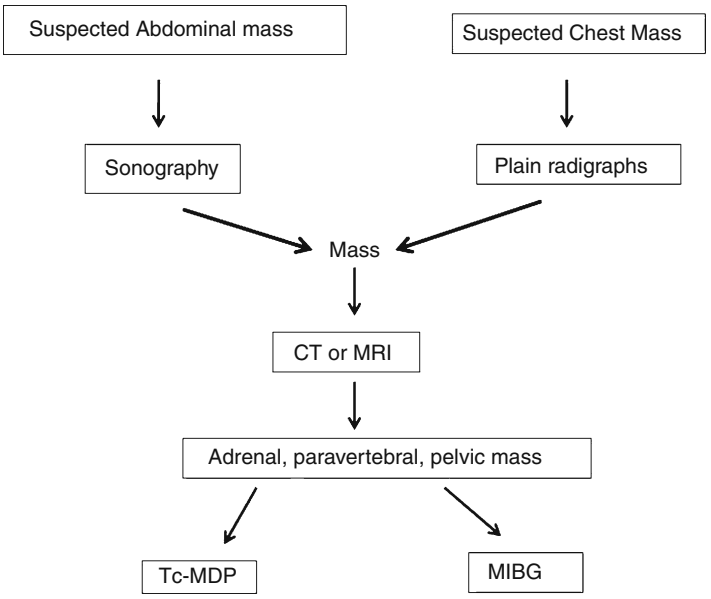

Figure 34.1. Decision tree outlining the role of the different imaging studies in the evaluation of neuroblastoma.

If there is a frank mass on sonography or chest radiography, CT or MRI is the next imaging study, based on their higher resolution and better specificity, to further evaluate the nature and assess the local extent of the mass for operative planning and staging (Figs. 34.4, 34.5, and 34.6)

MIBG scintigraphy, with or without bone scintigraphy, should be performed to evaluate the presence of skeletal and soft tissue metastases (i.e., identify stage 4 disease) (Figs. 34.7 and 34.8).

Table 34.1 presents a stage system for neuroblastoma, and Table 34.2 summarizes the performance characteristics of imaging studies for detection of distant tumor spread.

Table 34.1. INSS staging system for neuroblastoma

Stage	Definition
1	Localized tumor with complete resection, with or without microscopic residual disease; representative ipsilateral lymph nodes negative for tumor microscopically
2A	Localized tumor with incomplete gross excision; representative ipsilateral nonadherent lymph nodes negative for tumor microscopically
2B	Localized tumor with or without complete gross excision, with representative ipsilateral nonadherent lymph nodes positive for tumor. Enlarged contralateral lymph nodes must be negative microscopically
3	Unresectable unilateral tumor infiltrating across the midline, with or without regional lymph node involvement; or localized unilateral tumor with contralateral regional lymph node involvement; or midline tumor with bilateral extension by infiltration (unresectable) or by lymph node involvement
4	Any primary tumor with dissemination to distant lymph nodes, bone, bone marrow, liver, skin, and/or other organs (except as defined for stage 4S)
4S	Localized primary tumor (as defined for stages 1, 2A, or 2B), with dissemination limited to skin, liver, and/or bone marrow. Bone marrow involvement should be minimal (<10% of total nucleated cells identified as malignant on bone marrow biopsy or on marrow aspirate). Limited to infants <1 year of age

Reprinted with permission from Brodeur and Maris (1).

Table 34.2. Performance characteristics of imaging studies for detection of distant tumor spread

Modality	Sensitivity (%)
CT	Not known
Bone scintigraphy(40–42)	90
MRI(32)	85–100
MIBG(48, 49, 51)	90–95
Pentetreotide(57)	57
FDG-PET	Not known

References are in parentheses

Imaging Case Studies

Case 1

Figure 34.2 presents a case of neuroblastoma using sonography.

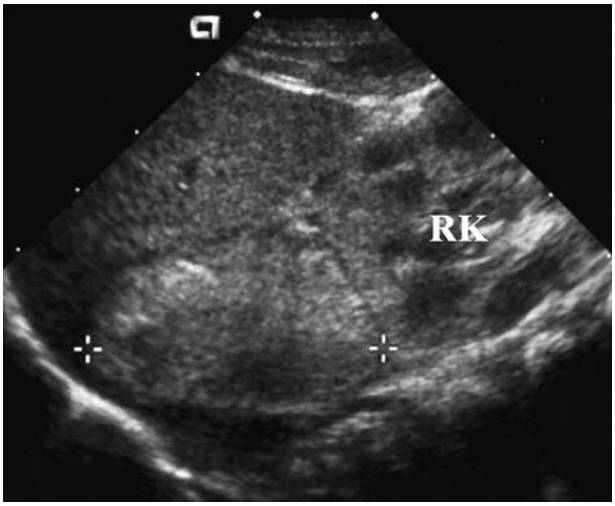

Figure 34.2. Neuroblastoma, sonography. Longitudinal sonogram in a 15-month-old girl shows a right suprarenal mass (calipers). RK = right kidney.

Case 2

Figure 34.3 presents a case of thoracic neuroblastoma using chest radiography.

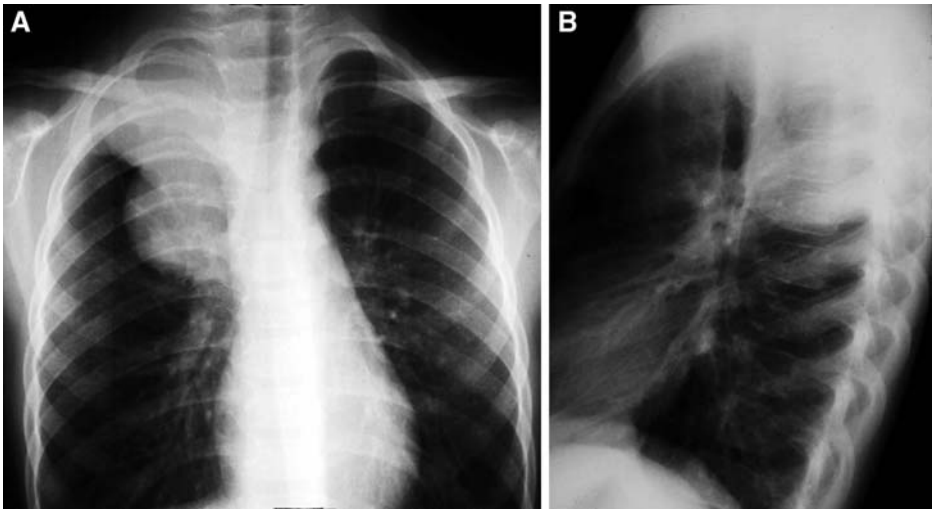

Figure 34.3. Thoracic neuroblastoma, chest radiography. Posteroanterior (**A**) and lateral (**B**) radiographs in a 5- year-old boy with Horner syndrome show a right paravertebral mass.

Case 3

Figure 34.4 presents a case of adrenal neuroblastoma using CT.

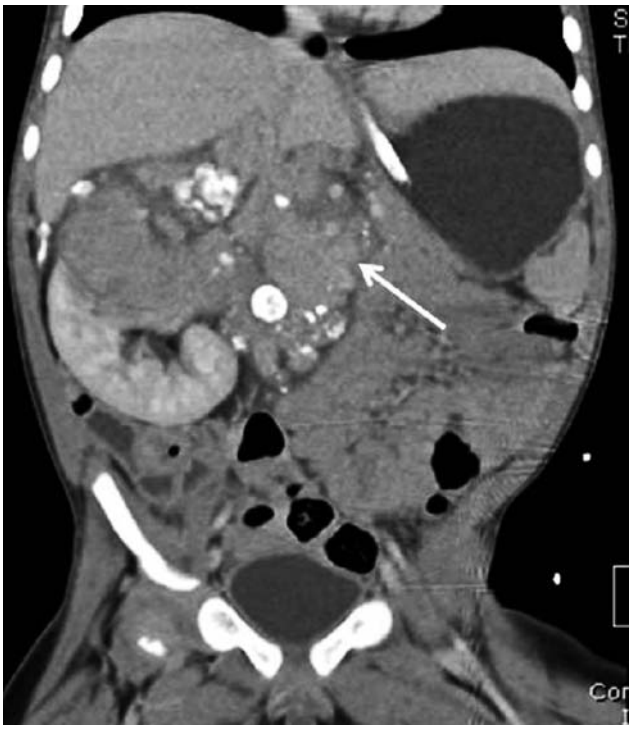

Figure 34.4. Adrenal neuroblastoma, CT. Coronal CT scan (same patient as in Fig. 34.2) shows a large, partially calcified soft tissue mass in the right suprarenal just crossing the midline (*arrow*).

Case 4

Figure 34.5 presents a case of thoracic neuroblastoma using CT and MRI.

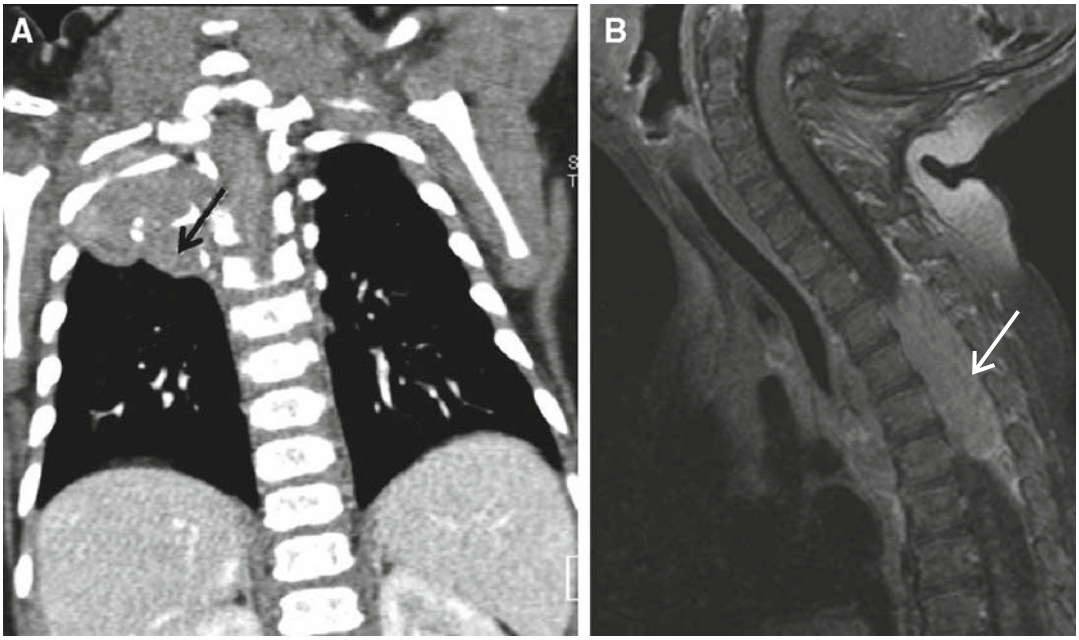

Figure 34.5. Thoracic neuroblastoma, CT and MRI. **A**: Coronal CT reconstruction shows a right paravertebral mass with intraspinal extension (same patient as in Fig. 34.3). **B**: Sagittal T1-weighted image confirms intraspinal extension. *Arrow*=tumor in the spinal canal.

Case 5

Figure 34.6 presents a case of pelvic neuroblastoma using MRI.

Figure 34.6. Pelvic neuroblastoma, MRI. Sonography had shown a pelvic mass in this 2-year-old boy with constipation. Sagittal T2-weighted fat-suppressed MRI shows a large prevertebral mass (M) with intraspinal extension (*arrow*).

Case 6

Figure 34.7 presents a case of metastatic neuroblastoma using bone scintigraphy.

Figure 34.7. Metastatic neuroblastoma, bone scintigraphy. Anterior bone scintigram in a 3-year-old boy shows abnormal areas of increased osseous uptake throughout the skeleton, including the spine, flat bones, and metadiaphyseal parts of long bones, resulting from metastases from neuroblastoma.

Case 7

Figure 34.8 presents a case of metastatic neuroblastoma using MIBG.

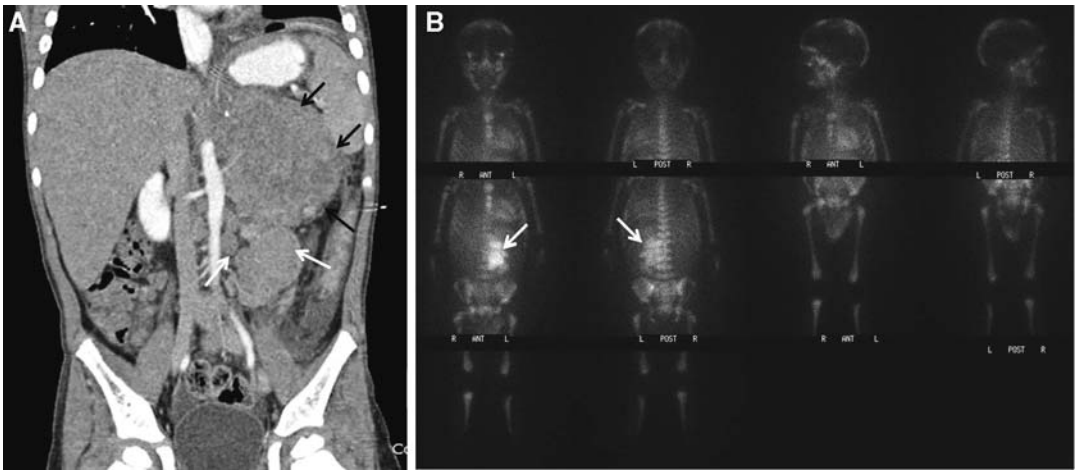

Figure 34.8. Metastatic neuroblastoma, MIBG. **A**: Coronal CT reconstruction shows a large left neuroblastoma (*black arrows*) encasing the left renal vein. Note also enlarged ipsilateral lymph node (*white arrows*). B: Anterior and posterior scintigrams obtained 24 hours after injection of ^{123}I-MIBG demonstrate large primary left adrenal neuroblastoma (*arrows*) as well as increased diffuse skeletal activity consistent with bone and bone marrow metastases. Bone scintigraphy was normal.

Suggested Imaging Protocols for Pediatric Neuroblastoma

Ultrasound

Use a linear or curvilinear transducer (5–7.5 MHz). Acquire gray scale images of the adrenal gland, inferior vena cava, paraaortic and paracaval areas, ipsilateral kidney and liver, and color Doppler images of the inferior vena cava and renal artery and veins.

Sonography should be used both to document the presence of an abdominal or pelvic mass that is suspected or evident clinically and to assess vascular involvement.

Chest Radiography

Acquire at least two orthogonal views.

Chest radiographs should be used to confirm the presence of a thoracic mass that is suspected based on clinical findings or physical examination.

CT

Use the lowest milliamperage and kilovoltage settings. For a 16-row detector, uses 1.25–1.5 mm collimation with a pitch of 1.0–1.5. For a 64-row detector, use 0.6–1.25 mm collimation and a pitch of 1.0–1.5. Begin scanning within 5–10 s after the end of the contrast administration.

CT should be performed to assess the local extent of the primary tumor, including midline extension, vascular encasement, nodal enlargement, and metastases to liver.

MRI

Acquire axial and coronal T1 spin-echo, axial and sagittal T2 fast spin-echo with fat saturation, coronal short tau inversions recovery (STIR), and axial and coronal fat-suppressed T1-weighted images before and after administration of intravenous gadolinium chelate agents.

MRI should be performed to assess local tumor extent, including midline extension,

vascular encasement, nodal enlargement, and metastases to liver.

99mTc Bone Scintigraphy

Inject, wait for 2 hours, and acquire multiple whole-body images.

Bone scintigraphy should be performed to assess skeletal metastases.

^{123}I-MIBG Scintigraphy

Acquire anterior and posterior planar images with a large field of view gamma camera and medium energy collimation from the skull vertex to the proximal lower extremities 24 hours and occasionally 48 hours following injection. Anterior views of the lower extremities usually suffice. SPECT imaging is occasionally performed at 24 hours.

MRI should be performed to assess distant metastases to liver, lymph nodes, and skeleton. Because of its high specificity and ability to detect extraosseous as well as skeletal lesions, MIBG scintigraphy is preferred over bone scintigraphy by the Children's Oncology Group for staging patients with newly diagnosed neuroblastoma.

Future Research

- Comparison study of whole-body MRI and PET/CT imaging to assess total tumor burden. If either whole-body MRI or FDG-PET/CT imaging can accurately detect distant metastases, these techniques may substitute for the combination of CT or conventional MRI and MIBG and may provide a "one-stop shop" for the staging of neuroblastoma.
- Comparison study of whole-body diffusion-weighted MRI and PET-CT imaging to predict likelihood of tumor response to treatment. If biomarkers that are significant early predictors of treatment response can be identified, then unsuccessful treatment approaches can be identified early and alternative regimens employed in the management of individual patients.

References

1. Brodeur GM, Maris JM. In Pizzo PA, Poplack DG (eds.). Principles and Practice of Pediatric Oncology, 5th ed. Philadelphia: Lippincott Williams & Wilkins, 2006: 933–970.
2. Lonergan GJ, Schwab CM, Suarez ES et al. Radiographic 1992; 22: 911–934.
3. Shimada H, Ambros IM, Dehner LP et al. Cancer 1999; 86: 364–372.
4. Bordow SB, Norris MD, Haber PS et al. J Clin Oncol 1998; 16: 3286–3294.
5. Brodeur G M, Seeger R C, Schwab M, Varmus HE, Bishop JM. Science 1984; 224: 1121–1124.
6. Brodeur GM. Nat Rev Cancer 2003; 3: 203–216.
7. Look AT, Hayes A, Shuster J et al. J Clin Oncol 1991; 9: 581–591.
8. Attiyeh EF, London WB, Mosse YP et al. N Engl J Med 2005; 353: 2243–2253.
9. Caron H, van Sluis P, de Kraker J et al. N Engl J Med 1996; 334: 225–230.
10. Maris JM, White PS, Beltinger CP et al. Cancer Res 1995; 55: 4664–4669.
11. Berthold F, Trechow R, Utsch S, Zieschang J. Am J Pediatr Hematol Oncol 1992; 4: 207–215.
12. Zeltzer PM, Marangos PJ, Evans AE, Schneider SL. Cancer 1986; 57: 1230–1234.
13. Gurney JG, Davis S, Severson RK et al. Cancer 1996; 78: 532–541.
14. Maris JM, Weiss MJ, Mosse Y et al. Cancer Res 2002; 6651–6658.
15. Maris JM, Matthay KK. J Clin Oncol 1999; 17: 2264–2279.
16. Evans A, D'Angio G. J Clin Oncol 2005; 27: 6443–6444.
17. London WR, Castleberry RP, Matthay KK et al. J Clin Oncol 2005; 23: 6459–6465.
18. Brodeur G M, Seeger RC, Barrett A et al. J Clin Oncol 1988; 6: 1874–1881.
19. Brodeur G M, Pritchard J, Berthold F et al. J Clin Oncol 1993; 11: 1466–1477.
20. Acharya S, Jayabose S, Kogan SJ et al. Cancer 1997; 80: 304–310.
21. Ho PTC, Estroff JA, Kozakewich H et al. Pediatrics 1993; 92: 358–364.
22. Saylors RLI, Cohn SL, Morgan ER, Brodeur GM. Am J Pediatr Hematol Oncol 1994; 16: 356–360.
23. Schilling FH, Spix C, Berthold F et al. N Engl J Med 2002; 346: 1047–1053.
24. Woods WG, Gao RN, Shuster JJ et al. N Engl J Med 2002; 346: 1041–1046.
25. Yamamoto K, Ohta S, Ito E et al. J Clin Oncol 2002; 20: 1209–1214.
26. Abramson SJ, Berdon WE, Ruzal-Shapiro C, Stolar C, Garvi J. Pediatr Radiol 1993; 23: 253–257.

27. Mitchell WG, Davalos-Gonzalez Y, Brumm V et al. Pediatrics 2002; 109: 86–98.
28. Rudnick E, Khakoo Y, Antunes NL et al. Med Pediatr Oncol 2001: 36: 612–622.
29. Parisi MT, Hattner RS, Matthay KK et al. J Nucl Med 1993; 34: 1922–1926.
30. Abramson, SJ. Radiol Clin North Am 1997; 35: 1415–1453.
31. Berdon W, Ruzal-Shapiro C, Abramson S. Urol Radiol 1992; 14: 252–262.
32. Pfluger T, Czekalla R, Hundt C et al. AJR 1999; 173: 103–108.
33. Siegel MJ, Ishwaran H, Fletcher B et al. Radiology 2002; 223: 168–175.
34. Nitschke R, Smith EI, Shochat S et al. J Clin Oncol 1988; 6: 1271–1279.
35. Hugosson C, Nyman R, Jorulf H et al. Acta Radiol 1999; 40: 534–542.
36. Slovis TL, Meza MP, Cushing B et al. Pediatr Radiol 1997; 27: 273–275.
37. Sofka CM, Semelka RC, Kelekis NL et al. Magn Reson Imaging 1999; 17: 193–198.
38. Dubois SG, Kalika Y, Lukens JN et al. J Pediatr Hematol Oncol 1999; 21: 181–189.
39. Dessner DA, DiPietro MA, Shulkin BL. Pediatr Radiol 1993; 23: 276–280.
40. Heisel MA, Miller JH, Reid BS, Siegel SE. Pediatrics 1983; 71: 206–209.
41. Howman-Giles RB, Gilday DL, Ash J M. Radiology 1979; 131: 497–502.
42. Sty J R, Kun LE, Casper JT. Am J Pediatr Hematol Oncol 1980; 2: 115–118.
43. Goo HW, Choi SH, Ghim T, Moon HN, Seo JJ. Pediatr Radiol 2005; 35: 766–773.
44. Mazumdar O, Siegel MJ, Narra V, Luchtman-Jones L. AJR 2002; 179: 1261–1266.
45. Tanabe T, Ohnuma N, Iwai J et al. Med Pediatr Oncol 1995; 24: 292–299.
46. Andrich MP, Shalaby-Rana E, Movassaghi N, Majd M. Pediatrics 1996; 97: 246–250.
47. Corbett R, Olliff J, Rairley N et al. Eur J Cancer 1991; 27: 1560–1564.
48. Hadj-Dijilani HL, Lebtahi N-E, Delaloye S, Laurin R, Beck D. Eur J Nucl Med 1995; 22: 322–329.
49. Howman Giles R, Shaw PJ, Uren RF, Chung DKV. Semin Nucl Med 2007; 37: 286–302.
50. Parisi MT, Greene MK, Dykes TM et al. Invest Radiol 1992; 27: 768–773.
51. Paltiel HJ, Gelfand MJ, Elgazzar AH et al. Pediatr Radiol 1994; 117–121.
52. Pfluger T. Schmied C, Porn U et al. AJR 2003; 181: 1115–1124.
53. Leung A, Shapiro B, Hattner R et al. J Nucl Med 1997; 38: 1352–1357.
54. Maggi M, Baldi E, Finetti G et al. Cancer Res 1994; 54: 124–133.
55. Manil L, Edeline V, Lumbroso J, Lequen H, Zucker J-M. Nucl Med 1996; 37: 893–896.
56. Shalaby-Rana E, Majd M, Andrich MPL. Clin Nucl Med 1997; 22: 315–319.
57. Schilling FH, Bihl H, Jacobsson H et al. Med Pediatr Oncol 2000; 35: 688–691.
58. Kushner BH, Yeung HWD, Larson SM et al. J Clin Oncol 2001; 19: 3397–3405.
59. Rigo P, Paulus P, Kaschten BJ et al. Eur J Nucl Med 1996; 23: 1641–1674.
60. Shulkin BL, Hutchinson RJ, Castle VP et al. Radiology 1996; 99: 743–750.
61. Koh PS, Raffensperger JG, Berry S et al. J Pediatr 1994; 125: 712–716.
62. Mitchell WG, Snodgrass SR. J Child Neurol 1990; 5: 153
63. Tiedeman K, Pritchard J, Long R et al. Eur J Pediatr 1981; 137: 217–219.
64. Mendelsohn G, Eggleston JC, Olson JL et al. Cancer 1976; 37: 846.

35

Pediatric Abdominal Tumors: Wilms Tumor

Marilyn J. Siegel

Issues

I. What are the clinical findings that raise the suspicion for Wilms tumor?
II. What is the diagnostic performance of the different imaging studies in the detection of the primary tumor mass in patients with Wilms tumor?
III. What are the essential features that need to be assessed on imaging studies in patients with Wilms tumor for surgical planning or staging?
IV. What is the diagnostic performance of the different imaging studies in the detection of regional disease in patients with Wilms tumor?
V. What is the diagnostic performance of the different imaging studies in the detection of distant disease in patients with Wilms tumor?
VI. Is screening indicated in children at higher risk of Wilms tumor?
VII. What is the role of imaging for follow-up of Wilms tumor at the end of treatment?

Key Points

- The clinical presentation of Wilms tumor is usually by palpation of a non-tender abdominal mass but can be nonspecific and sometimes confusing (strong evidence).
- Features that need to be evaluated on imaging studies for surgical planning or staging in patients with Wilms tumor are the presence of vascular invasion, regional lymph node enlargement, contralateral tumors, and lung or liver metastases (strong evidence).
- Ultrasonography, computed tomography (CT), and magnetic resonance imaging (MRI) have high sensitivity for tumor detection and moderate specificity (limited evidence).

M.J. Siegel (✉)
Mallinckrodt Institute of Radiology, Washington University Medical School, St. Louis, MO 63110, USA
e-mail: siegelm@mir.wustl.edu

L.S. Medina et al. (eds.), *Evidence-Based Imaging in Pediatrics*,
DOI 10.1007/978-1-4419-0922-0_35, © Springer Science+Business Media, LLC 2010

- CT and MRI are superior to ultrasonography for detection of regional lymph node involvement and bilateral tumors (limited to moderate evidence).
- CT is superior to chest radiography for detecting pulmonary metastases (moderate evidence).
- Screening children with risk factors for development of Wilms tumor results in detection of early-stage tumors and is cost-effective (moderate to strong evidence).

Definition and Pathophysiology

Wilms tumor, or nephroblastoma, is the most common primary malignant renal tumor in children (1–3). Wilms tumors are derived from primitive metanephric blastema (4). The classic Wilms tumor has "favorable" triphasic histology containing blastemal, stromal tissue, and epithelial elements and is associated with a good clinical outcome (1–4). Rarely (10%), the tumor has "unfavorable" histology characterized by anaplastic nuclear change. Anaplasia is primarily a marker of resistance to adjuvant therapy, and when diffuse it confers a poorer survival rate (4). Wilms tumors are typically large masses (mean diameter 12 cm) that often contain areas of hemorrhage, necrosis, and cyst formation. Most tumors are solitary. The tumor is multicentric in 12–15% of cases and bilateral in 4–7% of cases (3). The tumor can extend into blood vessels or through the renal capsule into the perirenal fat and other surrounding tissues. From the renal vein, Wilms tumor may propagate into the inferior vena cava with occasional extension into the right atrium. Metastases are seen in about 15–20% of children at diagnosis and most often involve the lungs, liver, and regional lymph nodes and less commonly bone and brain (1–4). Precursors of Wilms tumor, known as nephrogenic rests, are found in 25–40% of patients with sporadic Wilms tumor (5–8). Nephrogenic rests are small foci of persistent primitive blastemic cells that can be found in fetal kidneys. They may occur within a renal lobe (intralobar rest) or at the periphery of a renal lobe (perilobar rest) (8). There is a 1–2% risk of Wilms tumor associated with perilobar rests and a 4–5% risk associated with intralobar rests (9). The 2-year relapse-free survival rate for all stages of Wilms tumor combined is 90% (strong evidence).

Epidemiology

Wilms tumor accounts for 7% of all childhood cancers (1–3, 10, 11). The annual incidence is 1 in 10,000 children younger than 15 years of age worldwide (1–3). About 450–500 new cases are diagnosed each year (1, 2, 10). Wilms tumor is more common in African Americans than in Caucasians and is rare in Asians (3, 4, 10, 11). The tumor is equally common in girls and boys (11). The mean age at diagnosis is 3.5 years (2, 3). Most children present with early-stage disease (stage I, 43%; stage II, 23%; stage III, 23%; stage IV, 10%; and stage V, 5%).

Bilateral Wilms tumors (stage V) represent only 5% of cases and are more common in children with predisposing syndromes or family history of Wilms. A positive family history is found in approximately 1.5% of patients with Wilms tumor (12). In a study of 6,209 patients with Wilms tumor entered on the National Wilms Tumor Study, 93 patients (1.5%) from 63 families had a positive family history (12). Certain congenital defects and genetic conditions increase the likelihood for Wilms tumor. These congenital defects include congenital abnormalities (hemihypertrophy and sporadic aniridia) and syndromes, including Beckwith–Wiedemann (hemihypertrophy, omphalocele, macroglossia, and visceromegaly), WAGR (Wilms tumor, aniridia, genitourinary malformation, mental retardation), and Denys–Drash (aniridia and ambiguous genitalia) (13). Several genetic loci are implicated in the pathogenesis of this tumor. One Wilms tumor gene (WT1) located at chromosome 11p13 has been identified in patients with WAGR syndrome. A second genetic locus (WT2), located at chromosome 11p15, has been linked to the Beckwith–Wiedemann syndrome (14). There is also evidence suggesting the

existence of a tumor-suppressor gene located in the short arm of chromosome 7 (4, 14) (strong evidence).

Overall Cost to Society

Although there are several analyses evaluating the cost-effectiveness of chemotherapy in the treatment of Wilms tumor, no cost-effectiveness data were found in the literature specifically incorporating imaging strategies in the management of Wilms tumor.

There is, however, a study evaluating the role of sonography screening for Wilms tumor in high-risk children (15). Using data on stage II–IV cases from the National Wilms Tumor Study (NWTS), a group at the National Cancer Institute performed cost-effectiveness analysis of periodic screening ultrasound in high-risk children (those with Beckwith–Wiedemann syndrome). They modeled a theoretical program of abdominal ultrasound screening of three times per year from birth to age 4, or alternatively to 7 years of age, to detect both Wilms tumor and hepatoblastoma. The costs were less than $15,000 per life year saved for the longer screening length, well below the $50,000 considered cost-effective for other cancer-screening programs (15).

Goals

The goals of imaging in a patient with suspected Wilms tumor are determination of the site of origin of the primary tumor and the extent of regional and distant tumor spread. The current imaging evaluation of patients with Wilms tumor includes abdominal sonography, computed tomography (CT), and/or magnetic resonance imaging (MRI) for detection and local staging of the primary tumor and chest CT with or without chest radiography for detection of pulmonary metastases. The criteria of The National Wilms Tumor Society (NWTS) are used for staging (Table 35.1). Staging of Wilms tumor is primarily based on findings at the time of surgical exploration and tumor histology. Preoperative imaging has a role in identifying distant disease (16, 17). In the National Wilms Tumor Study-4, the 2-year relapse-free survival rates for favorable histology tumors were approximately 93% for stage I, 90% for stage II, 95% for stage III, and 81% for stage IV (18). The 2-year relapse-free survival for all stages combined was 90%, and the overall survival was 96% (3, 18). In another study of patients with anaplastic or unfavorable histology, the 4-year relapse survival rates were approximately 71% for stage II, 59% for stage III, and 17% for stage IV (3, 19).

The second goal of imaging is early identification of tumors in patients who have anomalies known to be associated with Wilms tumor. Finally, the third goal of imaging is to monitor cases for tumor recurrence.

Methodology

The author performed a MEDLINE search using PubMed (National Library of Medicine, Bethesda, MD) for data relevant to the diagnostic performance and accuracy of both clinical and imaging examination of patients with Wilms tumor. The diagnostic performance of the clinical and imaging examinations was based on a systematic literature review performed in MEDLINE (National Library of Medicine, Bethesda, MD) during the years 1975–2007. The clinical examination search strategy used the following key words: (1) *Wilms tumor*; (2) *clinical physical examination*; (3) *epidemiology*; (4) *treatment* or *chemotherapy* or *surgery*. The review of the current diagnostic imaging literature was performed using the following words: (1) *Wilms tumor*; (2) *ultrasound*; (3) *computed tomography* or *CT*; (4) *MRI Magnetic Resonance Imaging* or *MRI*, as well as combinations of these search strings. Animal studies and non-English articles were excluded.

Discussion of Issues

I. What Are the Clinical Findings That Raise the Suspicion for Wilms Tumor?

Summary of Evidence: No single clinical finding leads to the diagnosis of a Wilms tumor

in the pediatric population. Children usually present with an abdominal mass but occasionally have symptoms related to the primary tumor (20, 21). Imaging and surgical biopsy are needed for diagnosis (strong evidence).

All patients with a suspected abdominal mass should undergo imaging to confirm the presence of a mass and its location and extent. In most children, sonography is the initial imaging test of choice for identification of a pediatric abdominal mass. If the sonogram is normal, additional imaging evaluation generally is not required. If sonography cannot provide adequate information or if more information is needed about the character or extent of a neoplasm, CT or MRI can be performed. In general, CT, because of its ready availability, lack of sedation, and established accuracy, is more widely used than MRI. However, MRI is a reliable alternative to CT. MRI can provide important diagnostic information about location and tumor extent.

Supporting Evidence: The most common manifestation of Wilms tumor is an asymptomatic abdominal mass discovered by a parent or physician especially in children aged 2–5 years (peak incidence) (2–4). These tumors grow rapidly, explaining why 70–95% of Wilms tumors in children present as an asymptomatic mass. Abdominal pain, fever, and hematuria (microscopic hematuria seen in up to 25% cases) are less frequent findings at diagnosis (2, 3, 21). Hypertension occurs in 25% of cases and is attributed to an increase in renin production. Rare patients with advanced disease may present with respiratory symptoms related to lung metastases. Physical examination usually reveals a palpable abdominal mass (strong evidence).

The clinical presentation is nonspecific. The differential diagnosis for renal masses includes both benign and malignant renal lesions as well as adrenal and hepatic tumors. In one international study of Wilms tumor, 28 of 511 patients in whom preoperative chemotherapy for Wilms tumor was started prior to diagnosis were found to have either malignant tumors other than Wilms tumor (n=20) or benign conditions (n=8) at time of nephrectomy (22) (strong evidence).

II. What Is the Diagnostic Performance of the Different Imaging Studies in the Detection of the Primary Tumor Mass in Patients with Wilms Tumor?

Summary of Evidence: Imaging is performed to confirm the presence of a mass and its location in the kidney and to identify local invasion, vascular extension, and bilateral or metastatic disease for treatment planning. Ultrasonography, computed tomography (CT), and magnetic resonance imaging (MRI) have equal sensitivity for the detection of the primary tumor (23, 24) (limited to moderate evidence). Specificity of imaging renal masses in children is only moderate. Cross-sectional imaging characteristics do not definitively identify a renal tumor as Wilms tumor and rely on the child's age, clinical presentation, and the pathologic confirmation of the imaging findings.

Supporting Evidence: While variable, the appearance of Wilms tumor on cross-sectional imaging is typically heterogenous, containing both solid and cystic components. Only 15% of cases have calcification. The sensitivity of sonography is estimated at 95% and specificity at 97%, whereas sensitivity of CT and MRI for detection of Wilms tumor is 100%, which is not surprising given the large mean diameter of the tumor (5–10 cm) (23–25) (limited evidence). In a retrospective study of 13 children with pathologically proven Wilms tumor by Reiman et al., the sensitivity of sonography and CT was 100% (23). In another prospective study of 14 patients with Wilms tumors by Belt et al., MRI correctly identified the primary tumor and its site of origin from the kidney (24) (limited to moderate evidence).

III. What Are the Essential Features That Need to be Assessed on Imaging Studies in Patients with Wilms Tumor for Surgical Planning or Staging?

Summary of Evidence: Surgery plays a crucial role in the management of Wilms. The goals of surgical intervention in initial patient management are to establish the diagnosis and the extent of regional tumor. Imaging alone is not

used for tumor staging. The role of preoperative imaging is to serve as a "roadmap" for the surgeon and to identify stage IV disease (e.g., lung metastases) (26–28) (strong evidence).

Supporting Evidence: For planning surgical resection, imaging should evaluate both renal vein and inferior vena caval patency, regional lymph node involvement, and bilateral renal disease. For staging, the role of imaging is identification of pulmonary metastases and bilateral Wilms tumors.

Knowledge of vascular invasion is critical in planning total tumor resection. Renal vein extension occurs in approximately 15–20% of patients, vena caval involvement in 5–10% of patients, and intracardiac extension in 0.5–1% of patients (28). Involvement of the renal vein or inferior vena cava does not adversely affect stage or prognosis if appropriate treatment is given (27, 29) (strong evidence). However, accurate preoperative assessment of renal vein, vena caval, or intracardiac thrombus is important for preoperative planning and the need for intraoperative cardiac bypass or venous reconstruction as well as to allow assessment of benefits of preoperative chemotherapy. Tumor thrombus extending to or above the confluence of the hepatic veins may require a thoracoabdominal approach to prevent tumor embolization to the pulmonary arteries (3). An abdominal approach alone is satisfactory for intravascular thrombus below the hepatic veins.

Spread to regional lymph nodes occurs in about 20% of patients (3). Regional lymph node involvement is associated with a poorer prognosis. In the second and third National Wilms Tumor Study, regional lymph node involvement was associated closely with increased frequency of pulmonary metastasis and mortality (27, 29) (strong evidence).

The incidence of bilateral synchronous tumors ranges from 4.4 to 7.0% (3). The impetus for recognizing contralateral tumors is that this alters patient management. The treatment for patients with bilateral tumors is open biopsy followed by chemotherapy for reducing the tumor burden. The goal of chemotherapy is to facilitate parenchymal-sparing surgery and to avoid nephrectomy. Another reason for recognizing synchronous bilateral tumors at diagnosis is that it indicates stage V disease and a poorer outcome (strong evidence).

The incidence of pulmonary metastases is approximately 15–20% (30, 31). The liver is involved in 15% of cases and bone and brain in the remaining cases (15). Distant metastases indicate stage IV disease and, if favorable histology has a survival of 81%, but if unfavorable histology has a survival of only 17%. In a retrospective study of 31 patients by Owens et al., pulmonary nodules were identified in 31 patients (22%). Those patients in whom nodules were detected only on chest CT were at increased risk of pulmonary relapse (30) (moderate evidence). However, controversy exists about CT-detected pulmonary nodules. A report from the National Wilms Tumor Study Group (NWTSG) reveals that children with Wilms tumor and CT-only pulmonary nodules who receive whole lung irradiation have fewer pulmonary relapses, but a greater number of deaths due to treatment toxicity (32). Further studies are needed to evaluate this issue.

IV. What Is the Diagnostic Performance of the Different Imaging Studies in the Detection of Regional Disease in Patients with Wilms Tumor?

Summary of Evidence: Ultrasonography and MRI can accurately detect gross tumor extension into the renal vein, inferior vena cava, and right atrium (23, 28, 33, 34) (limited to moderate evidence). CT and MRI are superior to sonography for assessment of nephrogenic rests, regional adenopathy, and bilateral tumors, although their relative merits have not been analyzed (23, 33, 34) (limited to moderate evidence). MRI may be better than CT for identification of vascular involvement, although there are no large studies comparing CT with MRI (28) (limited evidence).

Supporting Evidence: Ultrasonography and MRI are sensitive for detecting vascular extension of tumor (23, 28) (limited evidence). In one small series of four patients by Weese et al., ultrasonography and MRI had 100% sensitivity for detecting both renal vein and inferior venal

caval thrombus (28). The sensitivity of CT was 50% (2 of 4 patients) for renal vein thrombus and 30% (1 of 3) for caval thrombus (28) (limited evidence).

Owing to their superior resolution, CT and MRI have advantages compared with ultrasonography in evaluating lymph node involvement (23, 33–35). In a retrospective study by Reiman et al. of 13 patients with Wilms tumors, the total tumor extent was determined correctly by CT scanning in 77% of patients and by sonography in 23% of patients (23) (limited evidence). Specifically, the sensitivity of sonography and CT was 20% (1 of 5 patients) and 40% (2 of 5), respectively, for lymph node detection. In another series by Hugosson et al., CT and MR had equal sensitivity (67%) and specificity (100%) for determination of lymph node involvement when the nodes were larger than 1 cm in diameter (35) (limited evidence). PET has been reported to identify metastatic Wilms tumor in case reports but no large prospective study has been done with FDG-PET to determine the diagnostic performance of this test in Wilm's tumor staging.

CT and MRI are superior to ultrasonography for detection of bilateral tumors. In a retrospective review by Ritchey et al. of 122 children with synchronous bilateral Wilms tumor in NWTS-4, sonography detected 23 of 44 (52%) lesions 3 cm or less in size and CT detected 41 of 49 lesions 3 cm or less in size (87%) (36). None of the bilateral tumors 3 cm were missed with MRI, although the small numbers of subjects imaged with MRI (5 of 122) precluded rigorous comparison of accuracy (36) (moderate evidence). The sensitivity of US to detect renal lesions may also be estimated by extrapolation of adult studies of lesions between 3 and 140 mm in size. For current US technology (phase inversion harmonic US), the estimated sensitivity is 82–95% and the specificity is 82–97% (26).

V. What Is the Diagnostic Performance of the Different Imaging Studies in the Detection of Distant Disease in Patients with Wilms Tumor?

Summary of Evidence: About 15–20% of patients with Wilms tumor have distant metastases, usually to lung, at diagnosis (30, 31). CT is superior to plain chest radiography for detection of pulmonary metastases (moderate evidence).

Supporting Evidence: Chest CT is the study of choice to detect pulmonary metastases in patients with Wilms tumor. In one study by Owens et al., of 141 patients with normal chest radiographs, one or more pulmonary nodules were detected in 31 (22%) of the patients on chest CT (30). In another study by Wilimas et al., of 202 children with normal chest radiographs, preoperative chest CT scans were reviewed blindly by three observers for pulmonary nodules (37). Of these 202 CT scans, the proportions of patients rated as having pulmonary nodules on CT were 12.9, 18, 35.8% for the three reviewers (37). The variability in interpretation of the CT scans limited the value of this study. In both studies, confirmation of the findings was based on clinical follow-up, not biopsy, limiting the utility of the data (30, 37) (moderate evidence). Although chest CT scans are more sensitive than chest radiographs in detecting pulmonary nodules, they are not specific for tumor (38) (strong evidence).

VI. Is Screening Indicated in Children at Higher Risk of Wilms Tumor?

Summary of Evidence: Children with risk factors for Wilms tumor should undergo serial imaging (usually by sonography) to detect tumors while they are small and localized. Screening with ultrasonography in intervals of 3–4 months results in detecting earlier stage Wilms tumors and is cost-effective (15, 35–39) (moderate to strong evidence).

Supportive Evidence: It is recognized that children with family history or anomalies, such as hemihypertrophy, aniridia, and Beckwith–Wiedemann syndrome, have an increased risk of developing Wilms tumor (2–4, 39–43). It is therefore recommended that they be screened (i.e., examined frequently) so that Wilms tumor can be detected at an early stage. In 2001, McNeil and colleagues performed cost-effectiveness analysis of ultrasound screening

every 4 months until 7 years of age in high-risk children that showed a cost of $14,740 per life year saved (15). This is well below the suggested funding level of other cancer-screening programs set at $50,000 per life year saved.

In a review of screened (n=15) and unscreened (n=59) children with Beckwith–Wiedemann syndrome or idiopathic hemihypertrophy who developed Wilms tumors, Choyke et al. found that all children who were screened for tumor had stage I or II disease, while 42% of the unscreened children had stage III or IV disease (41) (moderate evidence). The authors suggested that screening children at intervals of 4 months or less results in earlier diagnosis of Wilms tumor. Based on the finding that 90% of Wilms tumors present by 7 years of age in children with Beckwith–Wiedemann or hemihypertrophy, serial ultrasonography has been recommended every 3 months until age 6, then every 6 months until 8 years of age. In another retrospective review of 4,669 patients treated on two consecutive NWTSG protocols (NWTS 3 and NWTS 4), 53 patients with Wilms tumors and Beckwith–Wiedemann syndrome were compared with patients with patients who had Wilms tumor without Beckwith–Wiedemann syndrome (43). Beckwith–Wiedemann syndrome patients were more likely to present with lower stage tumors (p=0.0001), with more than half (27 of 53) presenting with stage I disease (strong evidence). Another series of 24 patients with aniridia and Wilms tumor has shown that screening increased the detection of low-stage tumors (42) (moderate evidence).

VII. What Is the Role of Imaging for Follow-Up of Wilms Tumor at the End of Treatment?

Wilms tumor recurrence risk is mostly due to unfavorable histology. Recurrences most likely will occur within 4 years from diagnosis and usually occur in the lung or abdomen. The Children's Oncology Group (COG) has recommended chest and abdominal imaging based on the risk of recurrence (Table 35.2) (44).

Take Home Figures and Tables

What Are the Roles of the Imaging Modalities in the Evaluation of Wilms Tumor?

The decision tree in Fig. 35.1 outlines the role of each imaging modality in the evaluation of suspected Wilms tumor. Ultrasonography is the initial imaging study to confirm the presence of a renal mass and evaluate vessel patency (Figs. 35.2 and 35.3) due to its relative low cost, lack of ionizing radiation, and ready availability. Doppler US is used to confirm presence or absence of tumor spread into the renal vein, inferior vena cava, and heart.

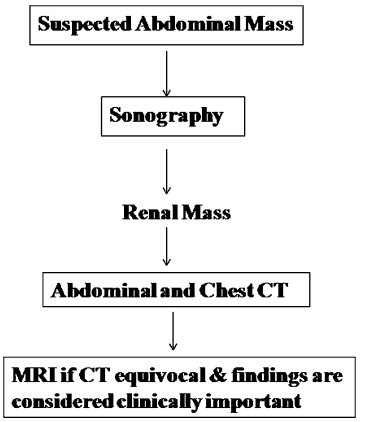

Figure 35.1. Decision tree outlining role of various imaging studies in the evaluation of Wilms tumor.

If sonography confirms a mass, CT is the next imaging study of choice based on its superior ability to examine the whole abdomen as well as the chest. CT is better than sonography for identifying lymph node involvement (Fig. 35.4), although it will miss tumor burden in normal-sized lymph nodes. CT can also demonstrate small lesions in the opposite kidney (Fig. 35.5) and liver metastases that may be missed by sonography as well as pulmonary metastases (Fig. 35.6)

MRI can play a role in evaluating problematic cases. MR is particularly useful for evaluating children with allergy to iodinated contrast material and for confirming presence or absence of vascular extension when sonography or CT is equivocal (Fig. 35.7). In actual practice, most centers in North America use

MDCT scans, rather than MRI, to stage patients with Wilms tumor, because they are more readily available, faster than MRI (no sedation needed), and they evaluate the lungs for metastases.

Imaging of the brain and skeleton do not need to be routinely performed, since metastases to these areas are rare.

Table 35.1 presents the staging criteria for Wilms tumor. Table 35.2 summarizes the imaging recommendations for Wilms tumor reoccurrence.

Table 35.3 summarizes the sensitivity of imaging studies for Wilms tumor.

Table 35.1. National Wilms tumor study group staging system

I. Tumor limited to kidney and completely excised
II. Tumor extends beyond the kidney but is completely removed
III. Residual nonhematogenous tumor confined to abdomen, including:
A. Lymph nodes in the hilus, the periaortic chains, or beyond
B. Implants on the peritoneal surfaces
C. Tumor beyond the surgical margins either microscopically or grossly
IV. Hematogenous metastases to lung, liver, bone, and brain
V. Bilateral renal involvement at diagnosis

Adapted with permission from Dome et al. (3).

Table 35.2. Imaging recommendations for Wilms tumor reoccurrence based on risk stage

Disease group	Region	Imaging modality	Frequency
Very low risk stage I	Chest		End of therapy and then every 2 months ×3, then every 3 months ×4.
	Chest	CXR	Beginning at 21 months from completion of therapy: every 3 months ×4, then every 6 months ×5
	Abdomen/ pelvis	CT or MRI (use same modality each time)	End of therapy then every 2 months ×3, then every 3 months ×4; then change to abdominal US
	Abdomen	US	Beginning at 18 months from completion of therapy: every 3 months ×5, then every 6 months ×5
Low and standard risk stages I–III	Chest	CT	End of therapy and then every 6 months to 3 years (alternating with CXR)
	Chest	CXR	Beginning at 3 months from completion of therapy: every 6 months to 3 years (alternating with CT), then every 6 months to 5 years off therapy
	Abdomen/ pelvis	CT or MRI (use same modality each time)	End of therapy and then every 6 months for 3 years
	Abdomen	US	Beginning 3 months from completion of therapy: every 6 months ×6 (alternating with CT or MRI), then every 6 months to 3 years off therapy, then every 6 months to 5 years off therapy
Higher risk favorable histology	Chest	CT	End of therapy and then every 3 months ×8
	Chest	CXR	Beginning at 24 months from completion of therapy: every 6 months ×4, then every 12 months ×1, then as indicated
	Abdomen/ pelvis	CT or MRI (use same modality each time)	End of therapy and every 3 months ×8; then change to US
	Abdomen	US	Beginning at 24 months from completion of therapy: every 6 months ×4, then every 12 months ×1, then as indicated

With the kind permission of Springer Science+Business Media from Brisse et al. (44).

Table 35.3. Performance characteristics (sensitivity) of imaging studies for Wilms tumor

	Primary tumor (detection) (22)	Vascular invasion (26)	Nodal involvement (22, 33)	Bilateral tumors (34)	Pulmonary nodules (28, 35)
Ultrasound	95%; specificity 97% (26)	100%	20%	52%	N/A
CT	100%	50%	67%	87%	100%
MRI	100%	100%	67%	100%	N/A

Imaging Case Studies

Case 1

Figure 35.2 presents Wilms tumor using a sonogram.

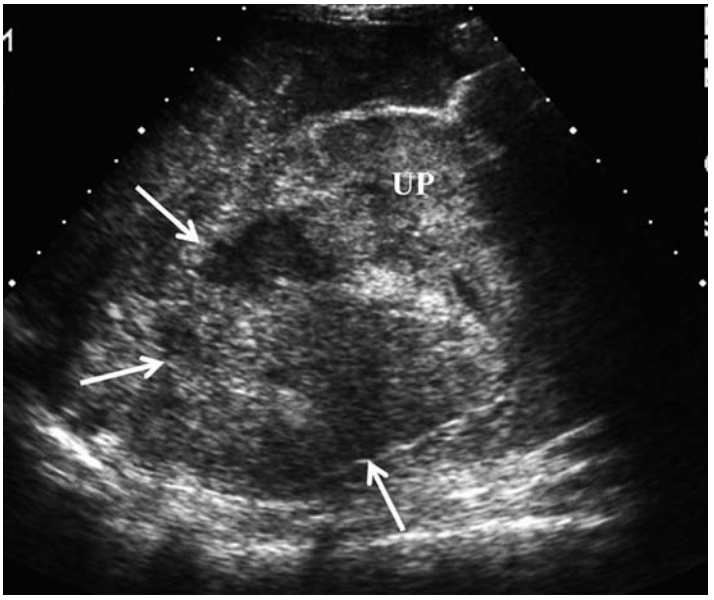

Figure 35.2. Wilms tumor, sonogram. Coronal image of the right flank shows a large, heterogenous echogenic mass (*arrows*) arising from the upper pole (UP) of the right kidney.

Case 2

Figure 35.3 presents Wilms tumor, sonogram, vena caval thrombus.

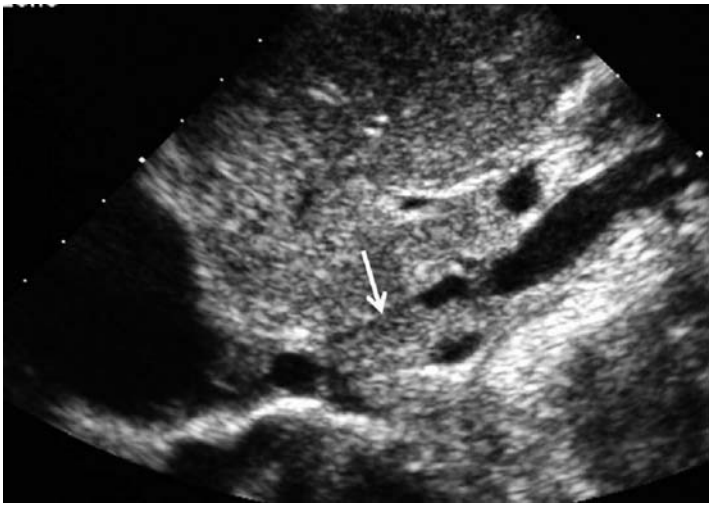

Figure 35.3. Wilms tumor, sonogram, vena caval thrombus. Longitudinal scan of the inferior vena cava in a patient with a right Wilms tumor shows intraluminal thrombus (*arrow*).

Case 3

Figure 35.4 presents Wilms tumor with CT.

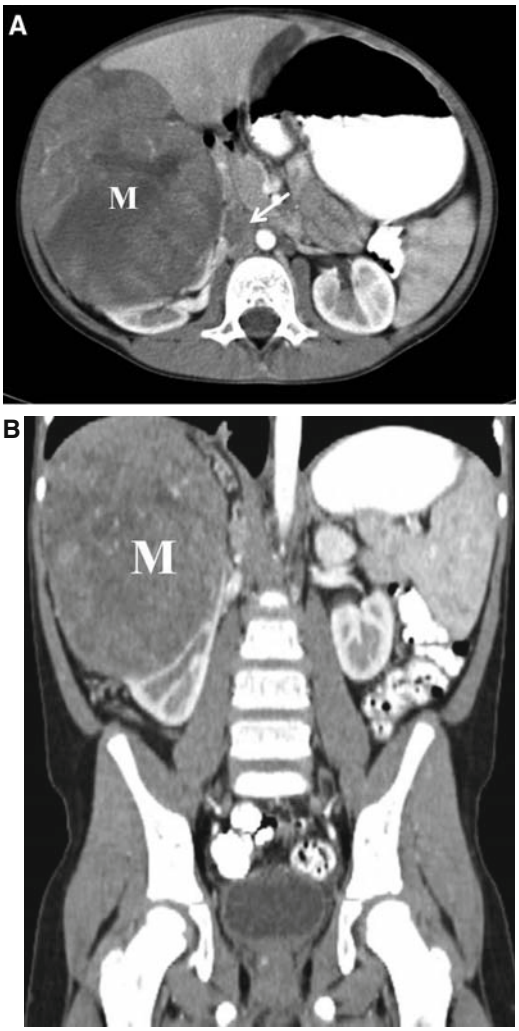

Figure 35.4. Wilms tumor. Axial (**A**) and coronal (**B**) volume rendered contrast-enhanced CT scans demonstrate a large, partially necrotic soft tissue mass (M) distorting and displacing the enhancing parenchyma (*arrow*) in the upper pole of the right kidney (same patient as in Fig. 35.2). Note also hilar lymph node enlargement (*arrow*), which was not identified on sonography.

Case 4

Figure 35.5 presents bilateral Wilms tumor with CT.

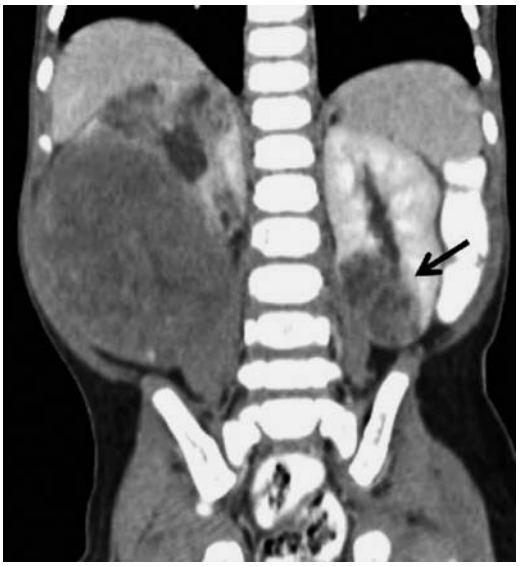

Figure 35.5. Bilateral Wilms tumors. Coronal CT multiplanar reformation shows a large Wilms tumor in the lower pole of the right kidney. A smaller tumor (*arrow*) is present in the lower pole of the left kidney.

Case 5

Figure 35.6 presents metatasis of Wilms tumor.

Figure 35.6. Wilms tumor, pulmonary metastasis. A 5 mm nodule (*arrow*), due to metastatic Wilms tumor, is seen in the periphery of the right upper lobe.

Case 6

Figure 35.7 presents Wilms tumor with MRI.

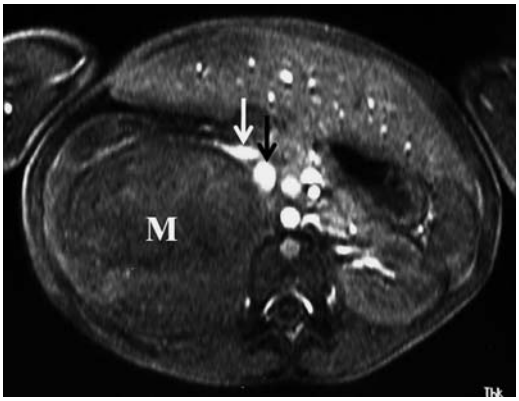

Figure 35.7. Wilms tumor, MRI. Axial gradient echo image shows a large mass (M) in the right kidney and patent renal vein (*white arrow*) and inferior vena cava (*black arrow*).

Suggested Imaging Protocols for Wilms Tumor

Ultrasound

Use a linear or curvilinear transducer (5–7.5 MHz). Acquire gray scale images of the affected kidney, ipsilateral renal vein and inferior vena cava, paraaortic and paracaval areas, liver, and opposite kidney. Doppler imaging should be performed in all patients to assess vascular integrity.

Sonography should be used both to document the presence of a renal mass and to assess the renal vessels and inferior vena cava.

CT

Use the lowest milliamperage and kilovoltage settings. For a 16-row detector, use 1.25–1.5 mm collimation with a pitch of 1.0–1.5. For a 64-row detector, use 0.6–1.25 mm collimation and a pitch of 1.0–1.5. Begin scanning within 5–10 s after the end of the contrast administration. Axial images usually suffice for tumor detection and regional spread. Coronal and sagittal reformations are used to assess total craniocaudal tumor extent.

CT should be performed to assess the local extent of tumor and distant metastases to lung and liver.

MRI

Acquire axial and coronal T1 spin-echo, axial and sagittal T2 fast spin-echo with fat saturation, coronal STIR, and axial and coronal fat-suppressed T1-weighted images before and after administration of intravenous gadolinium chelate agents.

MRI should be performed to assess local tumor extent if there is a contraindication to the use of iodinated contrast material or equivocal CT findings.

Future Research

Future research is limited since Wilms tumor has a generally good prognosis and the role of imaging is primarily to act as a guide for the surgeon, rather than to stage the tumor. One potential research area is the length and interval follow-up of imaging in children undergoing treatment for Wilms tumor. How frequently and for how long should these children have follow-up imaging after treatment is complete? These efforts might decrease the cost in money, radiation exposure, and anxiety to the family of these children.

References

1. Bernstein L, Linet M, Smith MA, Olshan AF. In Ries LAG, Smith MA, Gurney JG (eds.). Cancer Incidence and Survival among Children and Adolescents: United States SEER Program, 1975–1995, National Cancer Institute, SEER Program. Bethesda, MD: NIH Publ. No. 99–4649, 1999; 99:79–90.
2. 2.Brodeur AE, Brodeur GM. Pediatr Rev 1991; 12:196–206.
3. Dome JS, Perlman EJ, Ritchey ML et al. In Pizzo PA, Poplack DG (eds.). Principles and Practice of Pediatric Oncology, 5th ed. Philadelphia: Lippincott Williams & Wilkins, 2006; 905–932.
4. Husain AN, Pysher TJ, Dehner LP. In Stocker JT, Dehner LP (eds.). Pediatric Pathology, 2nd ed. Philadelphia: Lippincott Williams & Wilkins, 2001; 835–903.
5. Bove K, McAdams A. Prespect Pediatr Pathol 1976; 3:185–223.
6. Beckwith JB. Med Pediatr Oncol 1993; 21: 158–168.
7. Beckwith JB, Kiviat NB, Bonadio JF. Pediatr Pathol 1990; 10:1–36.

8. Beckwith JB. Am J Med Genet 1998; 79:268–273.
9. Gylys-Morin V, Hoffer FA, Kozakewich H et al.: Radiology 1993; 188:517–521.
10. Breslow N, Olshan A, Beckwith JB, Green DM. Med Pediatr Oncol 1993; 21:172–181.
11. Stiller CA, Parkin DM. Br J Cancer 1990; 62: 1026–1030.
12. Breslow NE, Olson J, Moksness J, Beckwith JB, Grundy P. Med Pediatr Oncol 1996; 27:398–403.
13. Wiener JS, Coppes MJ, Ritchey ML. J Urol 1988; 159:1316–1325.
14. Coppes MJ, Haber DA, Grundy PE. N Engl J Med 1994; 331:586–590.
15. McNeil DE, Brown M, Ching A, DeBaun MR. Med Pediatr Oncol 2001 Oct; 37(4):349–356
16. Beckwith JB. Pediatr Dev Pathol 1998; 1:79–84.
17. Green DM. Eur J Cancer 1997; 33(3): 409–418.
18. Green DM, Breslow NE, Beckwith JB et al. J Clin Oncol 1998; 16:237–245.
19. Green DM, Beckwith JB, Breslow NE et al. J Clin Oncol 1994; 12:2126–2131.
20. Navoy JE, Royal SA, Vaid YN, Mroczek-Musulman EC. Pediatr Radiol 1995; 25: S76–S86.
21. Andresen J, Steenskov V. Acta Radiol Diag 1981; 22:353–358
22. Tournade MF, Com-Nougue C, de Kraker J et al. J Clin Oncol 2001; 19:488–500.
23. Reiman TA, Siegel MJ, Shackelford GD. Radiology 1986; 160:501–505.
24. Belt TG, Cohen BD, Smith JA, Cory DA, McKenna S et al. 1986; 146:955–961.
25. Breslow NE, Palmer NF, Hill LR, Buring J, D'Angio GJ. Cancer 1978; 41:1577–1589.
26. Schmidt TY, Hohl C, Haage P et al. AJR 2003; 180:1639–1647
27. Breslow N, Churchill G, Beckwith JB et al. J Clin Oncol 1985; 3:521–531.
28. Weese DL, Applebaum H, Taber P. J Pediatr Surg 1991; 26:64–67.
29. Breslow N, Sharples K, Beckwith JB et al. Cancer 1991; 68:2345–2353.
30. Owens CM, Veys PA, Pritchard J, Levitt G et al. J Clin Oncol 2002; 20:2768–2773.
31. Wootton-Gorges AL, Albano EA, Riggs JM et al. Pediatr Radiol 2000; 30:533–539.
32. Meisel JA, Guthrie KA, Breslow NE, Donaldson SS, Green DM. Int J Radiat Oncol Biol Phys 1999 Jun 1; 44(3):579–585.
33. Cohen MD. Clin Radiol 1993; 47:77–81.
34. Ditchfield MR, DeCampo JF, Waters KD, Nolan TM. Med Pediatr Oncol 1995; 24: 93–96.
35. Hugosson C, Nyman R, Jacobsson B et al. Acta Radiol 36: Fasc 3, 1995; 254–260.
36. Ritchey ML, Green DM, Breslow NB, Moksness J, Norkool P. Cancer 1995; 75:600–604.
37. Wilimas JA, Kaste SC, Kauffman WM et al. J Clin Oncol 1997; 15:2631–2635.
38. McCarville MB, Lederman HM, Santana VM et al. Radiology 2006; 239:514–520.
39. Beckwith JB. AJR 1995; 164: 1294–1295.
40. Weng EY, Moeschler JB, Graham JM. AM J Med Genet 1995; 56:366–373.
41. Choyke PL, Siegel MJ, Craft AW et al. Med Ped Oncol 1999;32: 196–200.
42. Green D, Breslow N, Beckwith J et al. Med Pediatr Oncol 1993; 21:188–192.
43. Porteus MH, Narkool P, Neuberg D et al. J Clin Oncol 2000; 18: 2026–2031.
44. Brisse HJ, Smets AM, Kaste SC, Owens CM. Pediatr Radiol 2008; 38:18–29.

36

Imaging of Blunt Trauma to the Pediatric Torso

F.A. Mann, Joel A. Gross, and C. Craig Blackmore

Issues

I. What are the priorities in caring for pediatric victims of trauma? What are the goals for diagnostic testing relative to these priorities?
II. Among pediatric victims of trauma, who needs to be imaged? What are the clinical indications warranting diagnostic imaging?
III. Which pediatric victims of trauma should undergo multiphase CT and follow-up imaging?
IV. How should children with trauma be imaged? What are the performance characteristics of available imaging modalities?
V. Special situation: What are the "blind spots" in imaging? How can these "blind spots" be addressed?

Key Points

- Normal CT of head, chest, abdomen, and pelvis effectively excludes need for emergent or urgent "surgical" intervention (limited to moderate evidence).
- Emergent MR is usually reserved for patients with evolving or unexplained neurological deficits (moderate evidence).
- The diagnostic imaging test of choice for blunt trauma to the abdomen and pelvis is CT (moderate evidence). Sonography should be reserved for subjects too hemodynamically unstable to tolerate CT.
- The chest radiograph is an excellent screening test for mediastinal vascular injury that may require CT angiography or urgent surgery (limited to moderate evidence).
- CT represents a significant radiation burden to young patients. All practitioners should adhere to ALARA (as low as reasonably achievable) principles in minimizing radiation dose to patients. However, when appropriately indicated, CT should be performed because short-term benefits in the acute trauma setting far outweigh long-term risk of radiation.

F.A. Mann (✉)
Department of Medical Imaging, Seattle Radiologists, Swedish Medical Center, Seattle, WA 98104, USA
e-mail: famann@u.washington.edu

L.S. Medina et al. (eds.), *Evidence-Based Imaging in Pediatrics*,
DOI 10.1007/978-1-4419-0922-0_36, © Springer Science+Business Media, LLC 2010

Definition and Pathophysiology

Blunt trauma represents the consequences of the disruption of structural or physiologic integrity of one or more body parts due to external agents (1). Primary injurious events impart disruptive energy through mechanical effects (e.g., pedestrian–vehicle accidents, falls from heights, crush injuries, assaults) and lead to loss of structural and/or functional integrity when deposited energy exceeds viscoelastic limits of the specific tissues absorbing the traumatic energies (e.g., lower deposited energies are required to disrupt the brain than the liver or mature skeleton). Allowing for differences in organ-specific viscoelastic properties, disruption of normal structure and function is typically proportionate to the amount of energy deposited within tissues.

Secondary injuries are due to the host response to primary injuries (e.g., hypotension due to ongoing hemorrhage, ischemia due to compression of attenuated blood vessels by edema) and may lead to further tissue damage and worsening of physiologic function. Most emergent interventions are directed at avoiding or minimizing the cascade of deleterious events due to these secondary injuries.

Epidemiology

Trauma is the leading cause of morbidity and mortality in children (2) in the USA, with a peak mortality rate of 52/100,000 in the 15–19-year-old age groups. Overall, injury accounts for 40–50% of deaths in all pediatric age groups [CDC]. The causes of blunt trauma in pediatric patients are diverse and vary with the source of cases (e.g., single institution trauma registry versus national database [National Pediatric Trauma Registry]), type of institution (e.g., level 1 trauma hospital versus community hospital), major anatomic focus (e.g., chest versus abdomen and pelvis), population and/or nationality studied, ages and sexes included in reports (3–5): motorized vehicles in 30–85% (pedestrians 75–85%, the balance as passengers); falls from height greater than 3 m (10 feet) in 8–35%, bicycle crashes (including handlebar goring) in 5–15%, non-motorized sports in 5–10%, and assaults (including nonaccidental trauma) in 5–10%.

Overall Cost to Society

Trauma to children 0–14 years old accounted for about 15% of total trauma-related costs in 2002 or about US $51 billions (6).

Goals

Facilitate appropriate and timely interventions through the detection and/or characterization of traumatic injuries.

Methodology

MEDLINE searches were performed using PubMed (National Library of Medicine; Bethesda, MD) for the years 1985–2008 using MeSH keywords: *wounds, children, radiology, English, January 1, 1985 to June 30, 2008*. Of the 3,832 references recovered, we excluded animal studies, small case series and case reports, and studies focusing on treatment in which too few imaging details were provided to assess examination performance and findings.

Discussion of Issues

I. What Are the Priorities in Caring for Pediatric Victims of Trauma? What Are the Goals for Diagnostic Testing Relative to These Priorities?

Summary of Evidence: Early diagnosis and definitive treatment of life- and limb-threatening injuries improve outcomes for pediatric victims of blunt trauma (strong evidence) (7–12). Appropriate use of imaging supports non-operative management of most victims of blunt torso trauma and is an adjunct to the recognition of and surgical planning for patients that will not be successfully managed non-operatively.

Supporting Evidence: Coordinated and integrated trauma systems that rapidly provide field response, transport, resuscitation, comprehensive diagnosis, and definitive treatment reduce trauma-related individual morbidity and mortality and societal costs (7–12). For many victims of severe trauma, time to definitive treatment matters critically, which is captured in the intuitive concept of a so-called golden hour (1). During the moments to hours following major injuries, cardiopulmonary stabilization and avoidance of further injuries are done simultaneously with assessments of nature and severity of injuries (primary, secondary, tertiary surveys).

The "ABCDEs" of resuscitation constitute the core priorities performed during the primary survey. The secondary survey, performed after correction of life-threatening injuries identified during the primary survey, is more detailed and seeks to better characterize abnormalities detected during the primary survey and to uncover surgically important injuries whose delayed treatments may be associated with avoidable morbidity and mortality.

Hemodynamic status is the strongest predictor of need for emergent or urgent surgical or endovascular interventions (9, 13–16). Imaging typically occurs as part of the secondary and subsequent patient surveys in victims of blunt-force trauma. Contrast-enhanced CT of the thorax, abdomen, and pelvis helps predict failure of non-operative management by depicting vascular injuries (e.g., aorta, vena cava, mesenteric, and retroperitoneal arteries), solid organ injuries with active extravasation (13–20), hollow viscus injuries (e.g., stomach, duodenum, small and large bowel, gallbladder) (21–28), and patterns of injuries associated with complicated clinical courses, such as injuries to multiple organs or the pancreas (5, 9, 29–37).

As noted above, pediatric patients receive great benefits from imaging. However, currently CT represents the greatest source of ionizing radiation in children despite modality-dependent radiation dose-management tools. Nonetheless, children are far more radiosensitive than adults, and avoidance of unnecessary imaging is the most effective strategy to reduce possible untoward consequences of medical radiation (e.g., solid and hematogenous cancers). (See Chapter 3 on radiation risk.)

Cost-Effectiveness Analysis

Few studies address cost-effectiveness of imaging in pediatric trauma; however, limited evidence exists for the role of CT in managing high-energy blunt torso trauma (38–40).

II. Among Pediatric Victims of Trauma, Who Needs to Be Imaged? What Are the Clinical Indications Warranting Diagnostic Imaging?

Summary of Evidence: Historical (high-energy mechanisms) and initial physical examination findings (abnormal inspections of the head, neck, chest, abdomen, pelvis, and extremities) inform treatment providers of likelihood that blunt trauma victims harbor surgically important injuries (moderate evidence). Among patients with multiple injuries, imaging shortens the time to definitive diagnoses, guides therapy, and reduces the number of non-therapeutic surgical interventions.

Supporting Evidence: Victims of high-energy injury mechanisms are more likely to have sustained multiple significant torso injuries and warrant a high index of suspicion for internal injuries as well as a low threshold for imaging. High-energy mechanisms in which children are commonly injured include pedestrian–vehicle accidents and as passengers in high-speed motor vehicle crashes (41–48); falls from heights greater than 3 m (39, 49–57), and bicycle handle "goring" (49, 58–64).

Some clinical findings associated with torso injuries also warrant imaging or other evaluation incompletely compensated hemodynamic status (hypovolemic shock) (65, 66); closed head injury (e.g., sustained loss of consciousness, depressed Glasgow coma score) (23, 44, 50, 67–69); asymmetric extremity pulses or blood pressures (70); elevated respiratory rate

or abnormal auscultatory examination of the chest (71); abdominal tenderness or pain, or abrasions in patients who cannot be clinically evaluated (40, 72, 73); vertebral pain or tenderness (27); distracting extremity injuries (especially of the upper extremities) (Table 36.1). Comprehensive clinical evaluation is limited in children emergently undergoing endotracheal intubation. Nonetheless, the combination of abnormal findings at abdominal examination (ecchymosis, rigidity, organomegaly, apparent tenderness, etc.) and abnormal liver function (serum transaminases) tests in such pediatric patients predict intra-abdominal injury depiction by contrast-enhanced CT (sensitivity 70–100%, specificity ~90%) (8, 74). Finally, neither trauma scores nor initial clinical evaluation detect clinically important injuries in up to 15% of blunt trauma victims, especially solid organ injuries among pediatric victims of trauma (16).

Few validated clinical prediction rules to guide use of imaging have been published (38, 40, 71, 75, 76). In the detection of clinically important blunt thoracic injuries, any of the following justifies use of advanced imaging: low systolic blood pressure, elevated age-adjusted respiratory rate, abnormal results on inspection of the thorax, abnormal findings at chest auscultation, femur fracture, or Glasgow Coma Scale (GCS) score of less than 15 (71). In the detection of surgically important intra-abdominal injuries in alert (even if intoxicated) patients, spontaneous complaints of abdominal pain or abdominal tenderness at physical examination (72, 77), and in the obtunded patient any of the following justifies adjunctive imaging: antecedent hypotension (78), abdominal wall ecchymosis (e.g., lap belt sign), abnormal liver function tests (8, 79) or serum amylase (75), pelvic ring fractures (80, 81), or hematuria (although isolated microscopic hematuria without other clinical or laboratory findings suggesting thoracic or abdominal injuries does not require adjunctive imaging) (82, 83) (Table 36.2). Macroscopic or microscopic hematuria, as described above, is essentially always present when clinically relevant renal parenchymal disruptions (cortex, cortex and medulla with or without collecting system involvement) are present; however, hematuria may be absent in ureteropelvic junction avulsions and disruptions of the main renal artery or vein (40, 84–86).

Cost-Effectiveness Analysis

Although limited literature directly addresses impact of imaging on costs associated with blunt trauma to the pediatric torso, variation in utilization of adjunctive imaging within and across practices is recognized in assessment of thoracic and abdominal injuries (38, 71, 87). Nonetheless, clinical prediction rules have been available for some time, if not routinely used, to manage imaging costs in blunt torso trauma.

III. Which Pediatric Victims of Trauma Should Undergo Multiphase CT and Follow-Up Imaging?

Summary of Evidence: No evidence supports routine use of multiphase CT examinations for evaluation of pediatric victims of blunt-force trauma. Limited evidence supports the use of additional CT sequences delayed by a few (5–15) minutes to better characterize active parenchymal hemorrhage, parenchymal "blushes," and renal lacerations that may involve the collecting systems or ureters. Limited data also support repeated imaging for ongoing or worsening clinical signs or symptoms (including ongoing fluid requirements, sepsis, and persistently abnormal laboratory tests such as elevated serum amylase and abdominal pain) and to document early response to non-operative/medical management of renal injuries involving the collecting systems or ureters and intimal injuries of the descending aorta or peripheral arteries.

Supporting Evidence: Current generation multidetector CT (MDCT) scanners allow depiction of the hemokinetic course (e.g., arterial, capillary/parenchymal, venous, washout phases) of intravenous contrast by rapidly repeating scanning through the same anatomic region over time, and thereby can provide temporal physiologic data—albeit at a cost of increased radiation (17, 20, 88–93). However, although arterial injuries are particularly well shown on arterial phase images, such injuries are generally also well demonstrated at portal venous and parenchymal phase scanning (38, 94–97). Thus, routine use of arterial phase imaging is not an established practice for pediatric victims of blunt trauma.

Nonetheless, delayed imaging may be warranted when initial imaging is abnormal: vascular "blush" within a parenchyma of a solid organ (90, 98); retroperitoneal hematoma (96); renal lacerations (99); bowel wall thickening (100). Differentiation of intraparenchymal hematomas from arteriovenous fistulae or pseudoaneurysms may require repeated scanning after a short delay (e.g., 5–10 minutes: hemorrhage/hematoma shows persistence or accumulation of extravasated contrast; AV fistulae and pseudoaneurysms show contrast density dilution or washout) (90). Characterization of renal parenchymal (e.g., does laceration extend into collecting system) or ureteral injuries (e.g., are both ureters visible distally) warrants delayed sequences to detect extravasation of urine and should be performed with substantial dose reduction techniques (99, 101).

In contrast to an additional sequence delayed by a few minutes, a very finite set of indications justify repeat CT examinations: (1) within 4–24 hours for persistent or increasing abdominal pain, especially with abnormal clinical examination or laboratory tests (21, 102–105); (2) within 24 hours for medical management of intimal injuries to peripheral great vessels (e.g., descending aorta, iliac and femoral arteries) (69); (3) within 24–48 hours for renal lacerations involving collecting system (106–110); and (4) at anytime for ongoing fluid/blood replacement requirements or sepsis (111). In general, the risk of ionizing radiation and nephrotoxicity from multiple CT scans with contrast is considered to be overbalanced by the benefit from imaging information in these selected patients (insufficient evidence).

Post-discharge imaging of uncomplicated and clinically stable patients that have sustained spleen and/or liver injuries is not necessary (112). If documentation is required to return to specific activity (e.g., sports), US is adequate to demonstrate healing (113, 114).

Cost-Effectiveness Analysis

Almost no data address the cost-effectiveness of differing imaging protocols; however, some reports suggest that clinical decision rules and modality substitution can minimize costs associated with blunt-force pediatric trauma (87, 113, 115, 116).

IV. How Should Children with Trauma Be Imaged? What Are the Performance Characteristics of Available Imaging Modalities?

Summary of Evidence: Moderate evidence supports use of radiography as the most appropriate initial imaging evaluation for blunt trauma to the chest in pediatric patients. Radiography has high sensitivity (92%) for clinically important disease. CECT is most commonly used when further imaging is required.

Moderate evidence also supports use of CT as useful survey adjuncts to clinical examinations in blunt injuries of the abdomen and pelvis. CECT is the imaging modality of choice for characterization of the abdomen in trauma patients. However, clinical status is a more reliable predictor of requirement for operative intervention than imaging (moderate evidence). Ultrasonography is of insufficient sensitivity to allow exclusion of intra-abdominal and retroperitoneal organ injuries (moderate evidence).

Supporting Evidence: In pediatric trauma populations, conventional radiography remains the primary survey for mediastinal, pleural, and lung abnormalities in blunt polytrauma of the chest. Contrast-enhanced CT is the imaging modality of choice when conventional radiography or other imaging increases suspicion for thoracic injury.

Thorax

Aorta and Great Vessels

Where the cardiomediastinal silhouette is normal for a patient's age and sex, acute traumatic aortic injuries can be reasonably excluded by conventional chest radiography (sensitivity ~94%). However, a large minority of patients who are subsequently shown to have normal aortic and great vessels have abnormal cardiothymic silhouettes by chest radiography. In this setting, clinical judgment regarding magnitude of force involved in trauma, direct evidence of other thoracic injuries (such as multiple rib or spine fractures), or a mediastinal hematoma shown on CECT of the abdomen will necessarily guide further imaging evaluations (117–121) (moderate evidence).

Contrast-enhanced CT has a diagnostic accuracy in detecting any acute traumatic cardiovascular abnormality approaching or exceeding that of catheter angiography (sensitivity 95%, specificity 40%) (38). Although the role of CECT in diagnosis of thoracic aortic injuries is evolving in children, especially toddlers and infants, catheter angiography remains the reference standard for diagnosis and guiding therapy in the younger pediatric populations (119).

Chest Wall

With the exception of medicolegal documentation purposes necessary for non-accidental trauma (122), information necessary for recognition and treatment planning for important chest wall injuries may be achieved with conventional radiography (123).

Pleura and Lung

Conventional radiography generally provides sufficient information for the diagnosis of pulmonary contusions and lacerations and their therapy (124). CT is more sensitive in the detection of pneumothoraces than conventional radiography (125, 126). However, the consequences of pneumothoraces that are occult to conventional radiography are generally benign, except when positive pressure ventilation is part of the management of the patient's pulmonary injury (including patients going emergently to the operating theater) (127). As seen in adult trauma populations, CT is more sensitive at the detection of lung hernias through muscular or osseous chest wall disruptions (particularly anteriorly) and better characterizes their need for surgical treatment (lung hernias with narrow necks are more likely to experience pulmonary infarctions than those with broad-based necks) (128). Among pediatric patients, CT is also far more sensitive to the detection of pulmonary lacerations (129). However, there is no current evidence that earlier or more thorough detection of pulmonary laceration effects patient outcome. Certain CT findings, such as sub-pleural lucencies associated with peripheral pulmonary opacity, allow confident diagnosis of contusion, versus the more common causes of pulmonary opacity in trauma (including aspiration and passive atelectasis) (130).

Aerodigestive Tract

Disruption of the aerodigestive tract in children is very rare (131), often leads to pneumomediastinum and may be associated with mediastinal hematoma. Tracheal bronchial injuries may be suggested by massive pneumomediastinum and persistent air leak associated with pneumothorax and may be directly imaged by CT (71, 129). However, bronchoscopy remains the principal diagnostic tool in the acute and emergent setting.

Diaphragm

Children sustain diaphragmatic injuries at a frequency comparable to adult blunt trauma victims (~0.5%), and a high index of suspicion for diaphragmatic ruptures is warranted in appropriate clinical circumstances (lateral impact crashes, especially when left sided); Conventional radiography (chest radiographs with enteral tube placement; fluoroscopy) is abnormal in 60–90% of individuals with acute traumatic diaphragmatic rupture, but most findings are non-specific (hemothorax, atelectasis, etc.) (132). At CECT, the so-called dependent viscera sign (intra-abdominal contents abutting the posterior thoracic wall where the scan level is in the upper-third of the liver or spleen) and collar sign (narrowed waist of an herniated intra-abdominal organ at the site of diaphragm rupture) are nearly 100% specific (133, 134). Other findings, such as the "discontinuous" and thickened diaphragm signs show intermediate sensitivity and specificity (40–75%) (133, 134). MRI has diagnostic performance equivalent to that of CT, albeit difficult to perform in the seriously injured pediatric patient (135). Further, among reported series in which MRI depicted no diaphragmatic disruptions, no delayed diagnoses have been reported (136).

Abdomen and Pelvis (Table 36.3)

Imaging Modalities

- CT: Contrast-enhanced CT is the appropriate initial imaging for pediatric blunt trauma victims who are at risk of abdominopelvic injury. However, there are no large pediatric trials to reliably document the overall sensitivity and specificity of CT for significant intra-abdominal injury (insufficient evidence). Available evidence on individual organs listed below is limited.

- Focused Abdominal Ultrasound in Trauma (FAST): Despite its very high specificity (approaching 100%), low sensitivity (~30–78%) for detection of surgically important internal organ injuries limits the utility of FAST in evaluation of blunt-force torso trauma to detection of large hemoperitoneum in hemodynamically unstable patients (31, 137, 138). A meta-analysis by the Cochrane Collaboration demonstrated the superiority of CT in blunt trauma in both adults and children (138). Children imaged with ultrasound require either serial clinical exams or follow-up imaging to exclude intra-abdominal injury (112). Although not widely available or clinically used, contrast-enhanced ultrasound (CT as reference standard) had sensitivity of 92%, specificity of 100% (139) for liver and spleen injury and 80–90% for renal injury in small experimental studies and may prove useful in the future (limited evidence) (139).
- Radiography: Supine radiography has no role in the evaluation of pediatric blunt trauma victims.

Liver

CT remains the standard approach to imaging children at risk for liver injury. However, supporting pediatric data are limited. Although descriptively useful and commonly expected in radiology reports, CT estimates of the AAST grade of liver injuries is not reliable in guiding therapy on a per patient basis (140) (limited evidence).

Spleen

CT remains the standard approach to imaging children in whom splenic injury is suspected. However, supporting pediatric data are limited. Compared to contrast-enhanced CT, ultrasound has relatively low sensitivity (~60–80%) to depict blunt spleen injuries. Contrast-enhanced CT can be used to reliably classify the AAST injury grade and increasing grades predict longer time to healing (114); however, injury grade does not correlate well with the need for subsequent surgery (114). Intraparenchymal "blush" (arteriovenous fistula or pseudoaneurysm) may be shown at CECT in 10–15% of patients sustaining blunt-force spleen lacerations (15). Different from adult trauma victims in whom detecting an intraparenchymal "blush" predicts subsequent surgical or endovascular intervention, the large majority (~80 versus 96% of spleen injuries without a "blush") of pediatric victims of blunt trauma shown to have intraparenchymal "blush" at contrast-enhanced CT are successfully treated with non-operative management (15, 141) (limited evidence).

Pancreas

The sensitivity of CECT in detection of findings characteristic or strongly suggestive of pancreatic injuries (e.g., linear lucency traversing pancreas, typically in neck or body; peripancreatic hemorrhage; pancreatic "swelling" depicted as loss of lobulated contours and/or decreased density) is relatively low in the first few hours after injury (60–85%) (34, 36, 37, 142) and increases with time elapsed from injury up to approximately 72 hours. CECT, however, is almost 100% sensitive in recognizing, just not classifying, pancreatic injury when major duct injury is subsequently proven to be present (102) (limited evidence).

Kidneys and Ureters

CECT supplemented when abnormal by delayed pyelographic phase acquisitions approach sensitivity and specificity of 100% in detection of clinically important blunt-force renal injuries (143). Complete or high-grade renal artery occlusions may be suggested by retrograde filling of the renal veins from contrast in the inferior vena cava (144). CECT may be less sensitive (90%) at detection of grade I injuries (145). Short-term renal function appears well served by non-operative management, which is supported and guided by dynamic CECT, and open surgical interventions warranted in <15% of all renal injuries. However, based on technetium dimercaptosuccinic acid (Tc99m-DMSA) scintigraphy studies showing potentially clinically important decreases in renal function of injured kidneys' long-term renal function may be compromised among young children and follow-up of renal function warranted (146, 147) (limited evidence).

Hollow Viscus

Stomach

As most gastric perforations present with an acute chemical peritonitis, it is not surprising

that the literature presenting imaging findings related to blunt gastric injuries is relatively silent (except for pneumoperitoneum classically seen with gastric rupture) (26) (limited evidence).

Duodenum

No large or recent studies exist. However, in the limited evidence available, CECT shows an approximate 80% sensitivity in diagnosis of duodenal hematoma (asymmetric wall thickening), a 60–100% sensitivity at depicting rupture (discontinuity of the duodenal wall or extraalimentary gas or oral contrast; with or without asymmetric wall thickening), and a nearly 100% sensitivity at detecting clinically significant injury (hemorrhage or edema in the right anterior pararenal space; although not necessarily correctly grading—especially those including complex pancreatic head injuries) (24, 26, 148) (limited evidence).

Small Bowel, Colon, and Mesentery

Among more than 5,000 consecutive pediatric victims of blunt-force abdominal trauma, no patient required therapeutic laparotomy when contrast-enhanced CT of the abdomen was normal (149). Observing pneumoperitoneum (absent prior diagnostic peritoneal lavage), retroperitoneal air adjacent to retroperitoneal segments of colon, bowel wall defects, thickened bowel walls, mesenteric vessel beading, abrupt termination of mesenteric vessels, or mesenteric vessel extravasation on contrast-enhanced CT depicted surgically important bowel or mesentery injuries with sensitivities of 87–95% and specificities of 48–96% (surgery and clinical outcome as reference standard) (26, 149–152). Interloop fluid, especially adjacent to abnormal appearing bowel (thickened wall, excessive or asymmetric mural enhancement) or mesenteric active extravasation or "blush" correlate well with both mesenteric and surgically important bowel injuries (98). As a note of caution, isolated bowel injuries are uncommon (~1% of therapeutic laparotomies), small bowel injuries are seen approximately twice as frequently as colonic injuries, and only 20% of colon injuries are isolated (23, 26, 153) (limited evidence).

Urinary Bladder and Urethra

CECT has relatively poor sensitivities (<50%) for detection of bladder and urethral lacerations (154). When correctly performed, positive-contrast cystography (either CT cystography or conventional cystography) has sensitivity to detect and correctly classify (intra- or extraperitoneal or combined) native bladder lacerations approaching 100% (155). In depiction of urethral lacerations in boys, urethrography shows sensitivities 85–80% (156), with posterior urethra contributing the vast majority of missed injuries. In girls, physical inspection, especially under general anesthesia, may be necessary to correctly assess perineal and urethral injuries (157, 158). Compared to adults, bladder and urethral injuries are less common in pediatric patients sustaining blunt-force pelvic ring fractures (159, 160); however, anterior ring disruption were more likely to be associated with injuries to the posterior urethra (161) (limited evidence).

Vascular

Contrast-enhanced CT performed during parenchymal or venous phase (i.e., not dedicated CT arteriography) showed a sensitivity of 94.1% to detect active extravasation and a negative-predictive value for the need to intervene of 91.2% (reference standard: catheter angiography or surgery) (95). Catheter angiography is still indicated for endovascular intervention and in selected cases where diagnosis is in doubt (limited evidence).

Cost-Effectiveness Analysis

Cost-effectiveness studies addressing use of adjunctive tests, including imaging, in evaluation of victims of blunt-force torso trauma are lacking (75). However, cost-reduction strategies have been advocated through use of clinical prediction rules (injury severity assessment (87), image only those with abdominal signs or symptoms plus hematuria (40, 83)), image only at site of definitive care to reduce or eliminate redundant imaging studies from which patients have very little chance of benefit (39), and technology substitution for abdominal surveys in hemodynamically stable victims of blunt-force trauma (CECT chest in lieu of catheter aortography (38), abdominal ultrasound in lieu of CECT abdomen and pelvis for initial

diagnosis (112), and follow-up of solid organ injuries (116, 162)).

V. Special Issue: What Are the "Blind Spots" in Imaging? How Can These "Blind Spots" Be Addressed?

Summary of Evidence: The role of adjunctive tests in the evaluation of blunt trauma patients has traditionally been to "stay the surgeon's hands." Appropriately used, survey imaging should distinguish those patients requiring laparotomy from those that do not, and guide non-operative or minimally invasive treatments. In adults, poorer outcomes have been attributed to delays in diagnosis (especially of bowel injuries). Although delays in diagnosis of bowel injuries may not be as catastrophic as in adults, the risk of "missed" bowel injuries can be mitigated by use of excellent imaging performance and interpretation. Finally, radiologists must also be vigilant of masquerading clinical entities such as abdominal compartment syndrome, as failure to diagnose in a timely manner is associated with poor outcomes (limited evidence).

Supporting Evidence

Isolated Free Intraperitoneal Fluid (e.g., Missed Hollow Viscus Injury)

When faced with the finding of isolated free intra-abdominal fluid at CT without an obvious source during the first few hours after injury it is appropriate to worry about "missed" injuries, especially to a hollow viscus (bowel, bladder) (163, 164). A few practical approaches can guide judicious use of non-operative management:

(1) Re-survey the CT and re-inspect the bowel, with particular attention for interloop fluid or abnormal appearing bowel walls. Interloop fluid, especially when adjacent bowel wall shows thickening or abnormal enhancement, strongly suggests bowel injury (149).

(2) Estimate the volume of free fluid. Although not invariate, the larger the volume of free fluid, the more likely the presence of a surgically important injury (165, 166).

(3) Measure the density of the free fluid. Density <20 HU is suggestive of hollow viscus (bowel, bladder, gallbladder) injury (167).

(4) Serial physical examinations or sonography that find increasing abdominal symptoms or free fluid volumes are indicators of clinically active and, therefore, probable surgically important injuries (149, 163, 166, 168).

Abdominal Compartment Syndrome (ACS)

ACS presents, by definition, an end organ dysfunction due to increased intra-abdominal pressure, in which the degree of end organ failure initially parallels the magnitude of intra-abdominal pressure; treatment is emergent decompressive laparotomy (169). Diagnostic difficulties may arise due to the similarities shared with blunt-force bowel injuries: peritoneal fluid, bowel wall hyper-enhancement, bowel wall thickening, and bowel dilatation may be seen with both conditions (152). Findings more specific to ACS at CECT include elevated diaphragm, collapsed/narrowed "slit-like" infrahepatic inferior vena cava, rounded appearance of the abdomen (AP diameter nearly equal to transverse diameter), and direct renal compression or displacement (170–172).

Take Home Tables

Table 36.1 covers predictors of clinically important blunt thoracic injuries. Table 36.2 covers predictors of clinically important intra-abdominal injuries. Table 36.3 covers estimated sensitivities and specificities for CT in abdominal trauma.

Table 36.1. Predictors* of clinically important blunt thoracic injuries

Low systolic blood pressure
Elevated respiratory rate
Abnormal findings on chest inspection
Abnormal chest auscultation
Femur fracture
Glascow Coma Score less than 15

* These predictors have not been validated as a clinical decision rule.

Table 36.2. Predictors* of clinically important intra-abdominal injuries

Abdominal pain or tenderness
Hypotension
Abdominal wall ecchymosis
Abnormal liver function tests
Abnormal serum amylase
Pelvic ring fracture
Hematuria

*These predictors have not been validated as a clinical decision rule.

Table 36.3. Estimated sensitivities and specificities for CT in abdominal trauma

Region	Sensitivity (%)	Specificity (%)	Strength of evidence*	References
Diaphragm	>75	>95	Limited	(133, 134)
Spleen	>95	>95	Limited	(114)
Liver	>95	>95	Limited	(140)
Pancreas	60–85	Unknown	Limited	(34, 36, 37, 142)
Duodenum	60–100	Unknown	Limited	(24, 26, 148)
Bowel	87–95	48–96	Limited	(26, 150–152)
Kidney	>95	>95	Limited	(143)
Bladder#	>95	>95	Limited	(155)

* Limited evidence: none of these values are supported by recent, large pediatric study data.
# Numbers are for CT cystography.

Imaging Case Studies

Case 1

Figure 36.1 is a case of polytrauma in which a 12-year-old male skateboarder is hit by an automobile at highway speed and presented with hemodynamic instability and many obvious skeletal and visceral injuries.

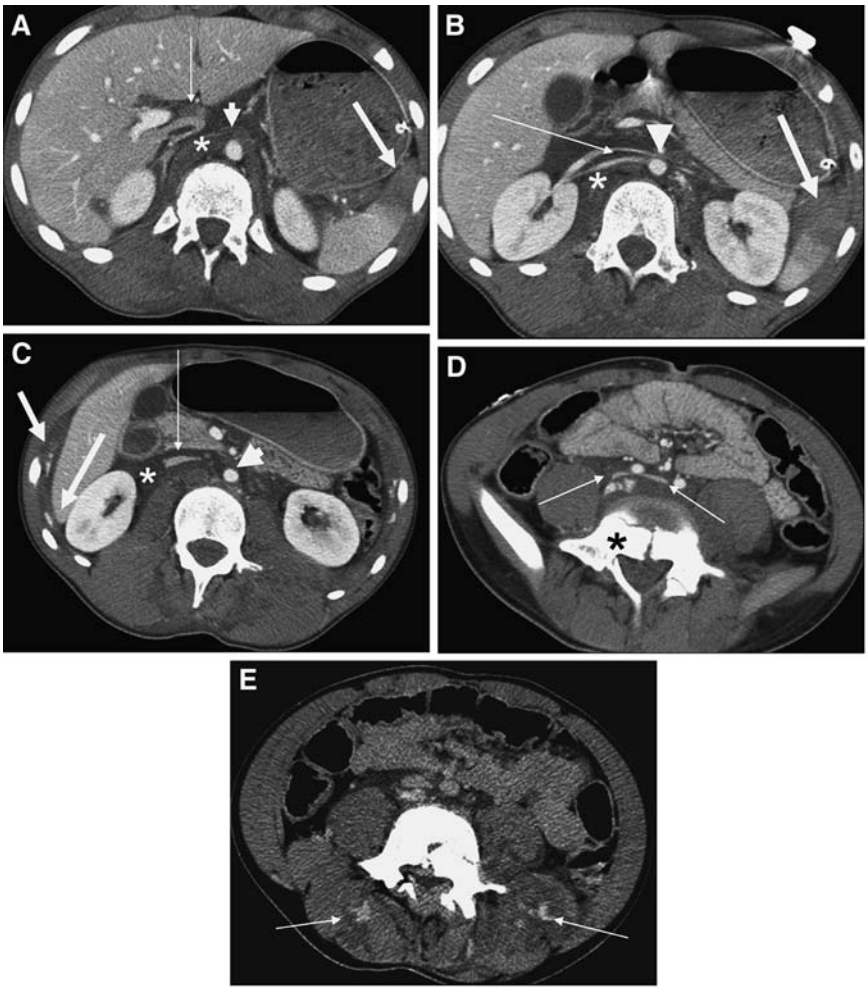

Figure 36.1. Polytrauma: A 12-year-old male skateboarder hit by an automobile at highway speed presented with hemodynamic instability and many obvious skeletal and visceral injuries. Despite very aggressive volume resuscitation and transient hemodynamic improvement, patient expired shortly after imaging. **A**: Axial CECT at level of adrenal glands shows small aorta (*arrowhead*), small IVC (*small arrow*), and hypo-enhancing contracted spleen with laceration of anterior pole (*large arrow*). Shallow (Grade I) laceration of liver is shown adjacent to the right kidney. Retrocrural hematoma (*asterix*) is worrisome for intrathoracic great vessel injury and warrants further evaluation. **B**: Axial CT at level of left renal vein shows small aorta (*arrowhead*), "slit-like IVC" (*small arrow*), and water-density retroperitoneal suffusion consistent with incompletely compensated hemorrhagic shock and retroperitoneal capillary leak due to large volume crystalloid resuscitation (*asterix*). Perisplenic hematoma and laceration of anterior pole of spleen shown (*large arrow*). **C**: Axial CECT through the interpole regions of the kidneys shows active intraperitoneal extravasation of contrast adjacent to lateral aspects of right ninth and tenth ribs, and left tenth rib (*large arrows*); "slit-like" IVC (*small arrow*), and small aorta (*arrowhead*). Water-density retroperitoneal suffusion is present (*asterix*). **D**: Axial CECT at the level of L5 shows 3-column burst fracture with surrounding hemorrhage (*asterix*). Note "slit-like" common iliac veins (*small arrows*) and hyper-enhancing ileum, consistent with hypoperfusion syndrome. **E**: Axial CT slightly cephalad to **D** obtained 5 minutes later shows active venous extravasation (*small arrows*) in the perispinal muscles and adjacent to anterior margin of comminuted L5 vertebra 3-column burst fracture.

Case 2

Figure 36.2 is a case of duodenal laceration in which a 7-year-old male bicyclist without helmet sustained handlebar injury in downhill crash striking some rocks.

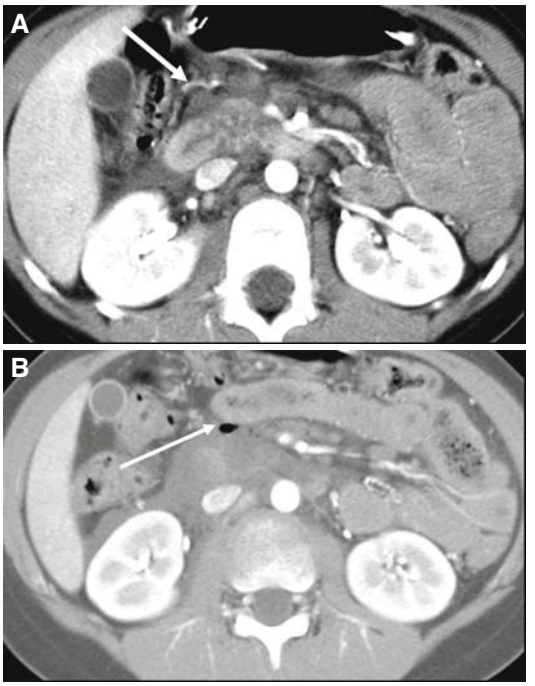

Figure 36.2. Duodenal laceration: A 7-year-old male bicyclist without helmet sustained handlebar injury in downhill crash striking some rocks. At surgery, large volume of bilious fluid was present throughout abdomen. The duodenum showed approximately 50% circumferential laceration at junction of third and fourth portions of duodenum ("blow-out" injury). Contusion with very superficial laceration to pancreatic head was present without other pancreatic parenchyma or duct damage. **A**: Axial CECT at level of horizontal segment of the duodenum shows fluid within the anterior pararenal space (specifically surrounding the duodenum) with mural irregularity and indistinctness strongly suggestive of duodenal wall injury. **B**: Axial CECT just caudal to **A** and portrayed using lung windows shows extra-alimentary gas in the anterior pararenal space (*arrow*) diagnostic of duodenal perforation.

Case 3

Figure 36.3 is a case of pancreatic laceration in which a 9-year-old boy presented with abdominal pain 16 hours after his brother jumped from a bunk bed onto his abdomen.

Figure 36.3. Pancreatic laceration: A 9-year-old male presenting with abdominal pain 16 hours after brother jumped from bunk bed onto abdomen. Surgery found near-complete transection through the pancreatic body with only the inferiormost portion of the pancreas intact. Patient was treated with spleen preserving distal pancreatectomy and discharged 10 days later following an uneventful recovery. Axial CECT at level of left renal vein shows transection of pancreas (*arrow*) to left of SMA with thin strand of parenchyma intact. Large amount of surrounding fluid and hematoma.

Suggested Imaging Protocols for Blunt Trauma to the Pediatric Torso

Abdominal and Pelvic CT

IV contrast is required. Oral contrast is generally not used in the acute initial evaluation, but may be useful for problem solving in selected cases (i.e., duodenal hematoma versus perforation). CT should be performed as a single phase with contrast in the late portal venous phase. The kVp and mA should be weight dependent and the lowest allowable. Coronal reformations should be performed.

FAST

The highest possible transducer frequency should be used (5.0–7.5 MHz). Adequate visualization must be made of the right and left upper quadrants, the right and left paracolic gutters, and the low pelvis (through the bladder acoustic window if possible). Additional subxiphoid scanning of the pericardium may also be useful.

Future Research

- Use the existing national and regional childhood trauma databases, describe the role of CT in pediatric trauma.
- Development and validation of cost-effective clinical prediction rules to guide the use of imaging in pediatric victims of blunt trauma.
- Develop and validate imaging-based criteria in children that enable identification of subjects who require surgical rather than nonsurgical treatment for their injuries.
- Incorporation of imaging, particularly ultrasound, into first responders triage to enable appropriate direction of patients within the trauma system.

References

1. Feliciano DV, Moore EE eds. Trauma, 6th ed. New York: McGraw-Hill Companies: 2008; 1430.
2. Alterman DM. Considerations in Pediatric Trauma. e-Medicine: Pregnancy and Pediatric Trauma Management 2008 8/19/08 [cited 2008 9/25/08]; Available from: http://www.emedicine.com/med/TOPIC3223.HTM.
3. Ciftci AO et al. J Pediatr Surg 1997; 32(12): 1732–1734.
4. Gerstenbluth RE, Spirnak JP, Elder JS. J Urol; 2002; 168(6):2575–2578.
5. Nance ML, Keller MS, Stafford PW. J Pediatr Surg 2000; 35(9):1300–1303.
6. Arias, I. Preventing Childhood Injuries 2008 5/1/08 [cited 2008 9/25]; Available from: http://www.hhs.gov/asl/testify/2008/05/t20080501d.html.
7. Davis DH et al. Pediatrics 2005; 115(1):89–94.
8. Flood RG, Mooney DP. J Trauma 2006; 61(2):340–345.
9. Holmes JH et al. J Trauma 2005; 59(6): 1309–1313.
10. Potoka DA et al. J Trauma 2000; 49(2):237–245.
11. Sherman HF Landry VL, Jones LM. J Trauma 2001; 50(5):784–791.
12. Tataria M et al. J Trauma 2007; 63(3):608–614.
13. Cloutier DR et al. J Pediatr Surg 2004; 39(6): 969–971.
14. Galvan DA, Peitzman AB. Curr Opin Crit Care 2006; 12(6):590–594.
15. Nwomeh BC et al. J Trauma 2004; 56(3):537–541.
16. Saladino R, Lund D, Fleisher G. Ann Emerg Med 1991; 20(6):636–640.
17. Henderson CG et al. J Urol 2007; 178(1):246–250; discussion 250.
18. Ohtsuka Y et al. Pediatr Surg Int 2003; 19 (1–2):29–34.
19. Rogers CG et al. Urology 2004; 64(3): 574–579.
20. Russell RS et al. J Urol 2001; 166(3):1049–1050.
21. Bensard DD et al. J Trauma 1996; 41(3): 476–483.
22. Campbell DJ et al. Am Surg 2003; 69(12): 1095–1099.
23. Canty TG, Sr, Canty TG Jr et al. Trauma 1999; 46(2):234–240.
24. Desai KM et al. J Trauma 2003; 54(4):640–645; discussion 645–646.
25. Jones VS et al. J Pediatr Surg 2007; 42(8): 1386–1388.
26. Mirvis SE, Gens DR, Shanmuganathan K. Am J Roentgenol 1992; 159(6):1217–1221.
27. Santschi M et al. Can J Surg 2005; 48(5):373–376.
28. Winthrop AL, Wesson DE, Filler RM. J Pediatr Surg 1986; 21(9):757–760.
29. Mattix KD et al. J Pediatr Surg 2007; 42(2): 340–344.
30. Meier DE. et al. J Pediatr Surg 2001; 36(2): 341–344.
31. Roche BG, Bugmann P, Le Coultre C. Eur J Pediatr Surg 1992; 2(3):154–156.
32. Takishima T et al. J Pediatr Surg 1996; 31(7): 896–900.
33. Tso EL, Beaver BL, Haller JA, Jr J Pediatr Surg 1993; 28(7):915–919.
34. Arkovitz MS, Johnson N, Garcia VF . J Trauma 1997; 42(1):49–53.
35. Deluca JA et al. Am Surg 2007; 73(1):37–41.
36. Firstenberg MS et al. J Pediatr Surg 1999; 34(7):1142–1147.
37. Jobst MA, Canty TG, Sr., Lynch FP J Pediatr Surg 1999; 34(5):818–823; discussion 823–824.
38. Bruckner BA et al. Ann Thorac Surg 2006; 81(4):1339–1346.
39. Pillai SB et al. J Trauma 2000; 48(6):1048–1050; discussion 1050–1051.
40. Richards JR, Derlet RW. Injury 1997; 28(3): 181–185.
41. Chakravarthy B et al. Pediatr Emerg Care 2007; 23(10):738–744.
42. DiMaggio C, Durkin M. Acad Emerg Med 2002; 9(1):54–62.
43. Ivarsson BJ, Crandall JR, Okamoto M, Traffic Inj Prev 2006; 7(3):290–298.
44. Orsborn R et al. Air Med J 1999; 18(3): 107–110.
45. Peng RY, Bongard FS. J Am Coll Surg 1999; 189(4):343–348.
46. Sala D et al. J Pediatr Surg 2000; 35(10): 1478–1481.

47. Spiguel L et al. Am Surg 2006; 72(6):481–484.
48. Yamamoto LG, Wiebe RA, Matthews WJ, Jr Pediatr Emerg Care 1991; 7(5):267–274.
49. Britton JW. WMJ 2005; 104(1):33–36.
50. Demetriades D et al. J Trauma 2005; 58(2): 342–345.
51. Durkin M.S et al. Neurosurgery 1998; 42(2): 300–310.
52. Hall JR et al. J Trauma 1989; 29(9):1273–1275.
53. Lallier M et al. J Pediatr Surg 1999; 34(7): 1060–1063.
54. Murray JA et al. Am Surg 2000; 66(9):863–865.
55. Peclet MH et al. J Pediatr Surg 1990; 25(1):85–90; discussion 90–91.
56. Scheidler MG et al. J Pediatr Surg 2000; 35(9):1317–1319.
57. Wang MY. et al. J Pediatr Surg 2001; 36(10):1528–1534.
58. Ashbaugh SJ, Macknin ML, VanderBrug Medendorp S. Clin Pediatr (Phila) 1995; 34(5):256–260.
59. Brown RL et al. J Pediatr Surg 2002; 37(3): 375–380.
60. Cushman R et al. CMAJ 1990; 143(2):108–112.
61. Powell EC, Tanz RR. Arch Pediatr Adolesc Med 2000; 154(11):1096–1100.
62. Powell EC, Tanz RR, DiScala C. Ann Emerg Med 1997; 30(3):260–265.
63. Spence LJ et al. J Pediatr Surg 1993; 28(2): 214–216.
64. Winston FK et al. Arch Pediatr Adolesc Med 2002; 156(9):922–928.
65. Unal VS et al. J Trauma 2006; 60(1):224–226; discussion 226.
66. Sanchez JI, Paidas CN. Surg Clin North Am 1999; 79(6):1503–1535.
67. Demetriades D et al. J Am Coll Surg 2004; 199(3):382–387.
68. Taylor GA, Eich MR. Ann Surg 1989; 210(2): 229–233.
69. Karmy-Jones R et al. Ann Thorac Surg 2003; 75(5):1513–1517.
70. Kram HB et al. Ann Thorac Surg 1989; 47(2):282–286.
71. Holmes JF et al. Ann Emerg Med 2002; 39(5):492–499.
72. Perez FG, O'Malley KF, Ross SE. Ann Emerg Med 1991; 20(5):500–502.
73. Moss RL, Musemeche CA. J Pediatr Surg 1996; 31(8):1178–1181; discussion 1181–1182.
74. Hennes HM et al. Pediatrics 1990; 86(1):87–90.
75. Adamson WT et al. J Pediatr Surg 2003; 38(3):354–357; discussion 354–357.
76. Bass DH, Semple PL, Cywes S. J Pediatr Surg 1991; 26(2):196–200.
77. Grosfeld JL, Cooney DR. Pediatr Clin North Am 1975; 22(2):365–377.
78. Mehall JR et al. J Am Coll Surg 2001; 193(4): 347–353.
79. Puranik SR et al. South Med J 2002; 95(2): 203–206.
80. Tepas JJ 3rd et al. Ann Surg 2003; 237(6): 775–780; discussion 780–781.
81. Silber JS et al. J Pediatr Orthop 2001; 21(4): 446–450.
82. Abou-Jaoude WA et al. J Pediatr Surg 1996; 31(1):86–89; discussion 90.
83. Brown SL et al. World J Surg 2001; 25(12): 1557–1560.
84. Perez-Brayfield MR et al. J Urol 2002; 167(6):2543–2546; discussion 2546–2547.
85. Lieu T et al. Pediatrics 1988; 82(2):216–222.
86. Taylor GA, Eichelberger MR, Potter BM. Ann Surg 1988; 208(6):688–693.
87. Stylianos S. J Pediatr Surg 2000; 35(2):164–167; discussion 167–169.
88. Anderson SW et al. Radiology 2008; 246(2): 410–419.
89. Anderson SW et al. Emerg Radiol 2007; 14(3):151–159.
90. Anderson SW et al. Radiology 2007; 243(1): 88–95.
91. Wessel LM et al. J Pediatr Surg 2000; 35(9): 1326–1330.
92. Brody AS et al. Pediatrics 2007; 120(3):677–682.
93. Hall EJ, Brenner DJ. Br J Radiol 2008; 81(965):362–378.
94. Sivit CJ et al. Radiology 1992; 182(3):723–726.
95. Maturen KE et al. J Trauma 2007; 62(3): 740–745.
96. Puapong D et al. J Pediatr Surg 2006; 41(11):1859–1863.
97. Rozycki GS et al. J Trauma 2002; 52(4):618–623; discussion 623–624.
98. Strouse PJ et al. Radiographics 1999; 19(5): 1237–1250.
99. Kawashima A et al. Abdom Imaging 2002; 27(2):199–213.
100. Sivit CJ. Pediatr Radiol 2000; 30(2):99–100.
101. Brown SL, Hoffman DM, Spirnak JP. J Urol 1998; 160(6 Pt 1):1979–1981.
102. Snajdauf J et al. Eur J Pediatr Surg 2007; 17(5):317–321.
103. Allen GS et al. J Trauma 1998; 45(1):69–75; discussion 75–78.
104. Ulman I et al. J Trauma 1996; 41(1):110–113.
105. Ozturk H et al. Surg Today 2003; 33(3):178–182.
106. Ghali AM et al. J Trauma 1999; 46(1):150–158.
107. Yale-Loehr AJ et al. Am J Roentgenol 1989; 152(1):109–113.
108. Santucci RA, Langenburg SE, Zachareas MJ. J Urol 2004; 171(2 Pt 1):822–825.
109. Nance M. et al. J Trauma 2004; 57(3): 474–478; discussion 478.

110. Abdalati H et al. Pediatr Radiol 1994; 24(8): 573–576.
111. Gross M et al. J Pediatr Surg 1999; 34(5):811–816; discussion 816–817.
112. Rovin JD et al. Am Surg 2001; 67(2):127–130.
113. Katz S et al. J Pediatr Surg 1996; 31(5): 649–651.
114. Lynch J. et al. J Pediatr Surg 1997; 32(7): 1093–1095; discussion 1095–1096.
115. Cochran A et al. Am J Surg 2004; 187(6):713–719.
116. Minarik L et al. Pediatr Surg Int 2002; 18 (5–6):429–431.
117. Milas ZL, Dodson TF, Ricketts RR. Am Surg 2004; 70(5):443–447.
118. Rozycki GS et al. J Trauma 2002; 52(4):618–623; discussion 623–624.
119. Spouge AR et al. Pediatr Radiol 1991; 21(5): 324–328.
120. Tiao GM et al. J Pediatr Surg 2000; 35(11): 1656–1660.
121. Eddy AC et al. J Trauma 1990; 30(8):989–991; discussion 991–992.
122. Bulloch B et al. Pediatrics 2000; 105(4):E48.
123. Stafford PW, Harmon CM. Curr Opin Pediatr 1993; 5(3):325–332.
124. Sartorelli KH, Vane DW. Semin Pediatr Surg 2004; 13(2):98–105.
125. Holmes JF et al. J Trauma 2001; 50(3):516–520.
126. Karaaslan T et al. J Trauma 1995; 39(6): 1081–1086.
127. Ball C.G et al. J Trauma 2006; 60(2):294–298; discussion 298–299.
128. Masmoudi S et al. Arch Pediatr 2003; 10(5): 436–438.
129. Manson D et al. Pediatr Radiol 1993; 23(1):1–5.
130. Donnelly LF, Klosterman LA. Radiology 1997; 204(2):385–387.
131. Sartorelli KH, McBride WJ, Vane DW. J Pediatr Surg 1999; 34(3):495–497.
132. Shehata SM, Shabaan BS. J Pediatr Surg 2006; 41(10):1727–1731.
133. Rees O, Mirvis SE, Shanmuganathan K. Clin Radiol 2005; 60(12):1280–1289.
134. Bergin D et al. Am J Roentgenol 2001; 177(5):1137–1140.
135. Koplewitz BZ et al. Pediatr Radiol 2000; 30(7):471–479.
136. Shanmuganathan K et al. Am J Roentgenol 1996; 167(2):397–402.
137. Mutabagani KH et al. J Pediatr Surg 1999; 34(1):48–52; discussion 52–54.
138. Stengel D, Bauwens K, Sehouli J, Rademacher G, Mutze S et al. Cochrane Database Syst Rev 2008; 4:1–25.
139. Valentino M. et al. Radiology, 2008.
140. Hackam D et al. J Pediatr Surg 2002; 37(3): 386–389.
141. Lutz N et al. J Pediatr Surg 2004; 39(3): 491–494.
142. Canty TG Sr, Weinman D. J Trauma 2001; 50(6):1001–1007.
143. Karp MP et al. J Pediatr Surg 1986; 21(7): 617–623.
144. Balkan E, Kilic N, Dogruyol H. Int J Urol 2005; 12(3):311–312.
145. Ku JH et al. Int J Urol 2001; 8(6):261–267.
146. Moog R et al. J Urol 2003; 169(2):641–644.
147. Keller M et al. J Trauma 2004; 57(1):108–110; discussion 110.
148. Shilyansky J et al. J Pediatr Surg 1997; 32(6): 880–886.
149. Albanese CT et al. J Trauma 1996; 40(3):417–421.
150. Atri M et al. Radiology 2008; 249(2):524–533.
151. Stuhlfaut JW et al. Radiology 2004; 233(3): 689–694.
152. Sivit CJ, Eichelberger MR, Taylor JA. Am J Roentgenol 1994; 163(5):1195–1198.
153. Dokucu A et al. J Pediatr Surg 2000; 35(12):1799–1804.
154. McAleer IM, Kaplan GW. Urol Clin North Am 1995; 22(1):177–188.
155. Rehm CG et al. Ann Emerg Med 1991; 20(8):845–847.
156. Reinberg O, Yazbeck S. J Pediatr Surg 1989; 24(10):982–984.
157. Podesta ML, Jordan GH. J Urol 2001; 165(5):1660–1665.
158. Lynch JM, Gardner MJ, Albanese CT. Pediatr Emerg Care 1995; 11(6):372–375.
159. Tarman GJ et al. Urology 2002; 59(1):123–126; discussion 126.
160. Silber JS et al. J Pediatr Orthop 2001; 21(4): 446–450.
161. Batislam E et al. J Trauma 1997; 42(2):285–287.
162. Emery KH et al. Radiology 1999; 212(2): 515–518.
163. Eanniello VC 2nd et al. Conn Med 1994; 58(12):707–710.
164. Drasin TE, Anderson SW, Asandra A, Rhea JT, Soto JA. Am J Roentgenol 2008; 191:1821–1826.
165. Nance ML et al. J Trauma 2002; 52(1):85–87.
166. Venkatesh KR, McQuay N Jr J Trauma 2007; 62(1):216–220.
167. Levine CD et al. Am J Roentgenol 1996; 166(5):1089–1093.
168. Pershad J, Gilmore B. Pediatr Emerg Care 2000; 16(5):375–376.
169. Saggi BH et al. J Trauma 1998; 45(3):597–609.
170. Patel A et al. Am J Roentgenol 2007; 189(5):1037–1043.
171. Epelman M et al. Pediatr Radiol 2002; 32(5): 319–322.
172. Al-Bahrani AZ et al. Clin Radiol 2007; 62(7):676–682.

37

Imaging of Nephrolithiasis and Urinary Tract Calculi in Children

Lynn Ansley Fordham, Richard W. Sutherland, and Debbie S. Gipson

Issues

I. What are the clinical findings that raise the suspicion for urolithiasis?
II. What is the diagnostic performance of the different imaging studies in nephrolithiasis and urinary tract calculi in the pediatric population?
III. What is the natural history of nephrolithiasis and urinary tract calculi and what are the roles of medical therapy versus extracorporeal shock–wave lithotripsy (ESWL) or surgical management?
IV. Special Case: Will the stone pass on its own?
V. What is the role of repeat imaging in children with known stone and in children with recurrent symptoms (suggesting obstructing stone)?

Key Points

- The clinical presentation of pediatric nephrolithiasis and urinary tract calculi can be non-specific (moderate evidence).
- A single abdominal radiograph ("KUB") is recommended as the initial screening test (moderate evidence).
- The Intravenous Pyelogram (IVP) is no longer used for evaluating children for renal stones but has a limited role after ureteral surgery (moderate evidence).
- Ultrasound is the most frequently used imaging test for young children with suspected stones but has a wide range of sensitivity and specificity because of limitations inherent in the modality and because it is user dependent (moderate evidence).

L.A. Fordham (✉)
Department of Radiology, University of North Carolina School of Medicine, North Carolina Children's Hospital, Chapel Hill, NC 27599, USA
e-mail: fdh@med.unc.edu

L.S. Medina et al. (eds.), *Evidence-Based Imaging in Pediatrics*,
DOI 10.1007/978-1-4419-0922-0_37,

- CT is highly sensitive for the detection of nephrolithiasis and urinary tract calculi but incurs added cost and ionizing radiation (moderate evidence).
- In older and/or larger children, CT is the imaging modality of choice to evaluate for nephrolithiasis and urinary tract calculi. The ability to localize renal, ureteral, and bladder calculi and the inherent high spatial resolution allows exact anatomic detail that may be helpful for surgical planning (moderate evidence).
- MR is not currently recommended for evaluation of renal stones but shows promise for imaging in obstruction (limited evidence).

Definition, Pathophysiology, and Epidemiology

Urolithiasis is the presence of stones anywhere in the collecting system within the urinary tract. Nephrolithiasis is defined as calculi within the collecting system in the kidney. Nephrocalcinosis is defined as calcification within the renal parenchyma. Nephrocalcinosis can be further subdivided into cortical and medullary. Patients with nephrocalcinosis can also have nephrolithiasis or urolithiasis (1). Urolithiasis is an increasingly common problem in the pediatric population (2). The increasing incidence of urinary system calculi in American children may be due to higher salt intake and inadequate oral hydration in children today. It can be an incidental finding in children imaged for other reasons or can present with acute symptoms. It accounts for between 1 in 1,000 and 1 in 7,600 pediatric inpatient admissions in North America (3).

The most common stones in the United States are calcium based (3, 4). They form at the tip of the renal papilla when excess calcium is excreted into the urine (5). Calculi with calcium are radiopaque. Uric acid stones are the most common cause of radiolucent kidney stones in children.

Medical therapy can be effective and includes encouraging the child in adequate oral hydration as well as therapy targeted to the type of stones formed (3, 6). Surgical intervention is utilized for large or symptomatic stones. With advances in miniaturization of instrument technology in the last two decades, pediatric stone management has changed from an open surgical approach to less invasive surgical procedures such as extracorporeal shock-wave lithotripsy and endoscopic techniques (6–10).

Overall Cost to Society

The economic impact on urolithiasis is difficult to assess. Cost analyses generally evaluate one modality versus another (11–15) rather than overall costs. One recent meta-analysis in adults compared costs in medical management of stone disease (16). No data were found in the medical literature on the overall cost to society from the diagnosis, treatment, and complications of nephrolithiasis and urinary tract calculi in children.

Goals

The goals of imaging are to identify and localize urinary tract calcification and to differentiate obstructing from non-obstructing stones. Non-obstructive stones which are asymptomatic can in some situations be monitored and treated medically to attempt chemolysis. Stones associated with obstruction can result in renal damage (17, 18). Stones associated with obstruction and infection or pyonephrosis require urgent intervention to prevent bacteremia, sepsis, and renal damage.

Methodology

The authors performed a MEDLINE search using PubMed (National Library of Medicine,

Bethesda, MD) for data relevant to the diagnostic performance and accuracy of both clinical and radiographic examination of patients with nephrolithiasis and urinary tract calculi. The diagnostic performance of the clinical examination (history and physical exam) and surgical outcome was based on a systematic literature review performed in MEDLINE (National Library of Medicine, Bethesda, MD) during the years 1966–November 2008. The clinical examination search strategy used the following statements (1): *nephrolithiasis* (2); *urolithiasis* (3); *renal or kidney* (4); *ureter* or *bladder* (5); *calcul(us)(i)* or *stone* (6); *pediatric* or *child* (7); *clinical examination* (8); *epidemiology* or *physical examination* or *surgery* (7); *treatment* or *surgery.* The review of the current diagnostic imaging literature was done with MEDLINE covering the years 1966–2008. The search strategy used the following key statements and words (1): *MESH heading kidney calculi* (2); *nephrolithiasis* (3); *urolithiasis* (4); *urinary calculi* or *stone* (5); *radiography* (6); *ultrasound* (7); *CT* (8); *MRI* or *Magnetic Resonance Imaging*; as well as combinations of these search strings. Related articles were searched from the initial results. We excluded animal studies and non-English articles.

Discussion of Issues

I. What Are the Clinical Findings That Raise the Suspicion for Urolithiasis?

Summary of Evidence: Children with urolithiasis can present with a wide range of signs and symptoms. Presentations vary depending on whether there is a urinary tract infection or urinary tract obstruction. Children with urolithiasis can present with specific signs and symptoms of flank pain and hematuria or non-specific symptoms such as irritability and nausea. Many children have an identifiable etiology to their stone disease. Therefore, every child with a urinary stone should have a metabolic evaluation (2, 4, 6, 19, 20). The younger child may present with non-specific symptoms such as irritability, vomiting, fever, and hematuria. In the older, verbal child symptoms include flank or abdominal pain and dysuria. Nephrocalcinosis is generally asymptomatic and identified incidentally on evaluation for some other abnormality or identified in the investigation of persistent microhematuria.

Supporting Evidence: VanDervort et al. (2) retrospectively identified 61 patients from 2003 to 2005 with urolithiasis as their primary diagnosis for their hospital/clinic visit. Patients presented with one or more of the following symptoms: abdominal pain (75%), dysuria (13%), gross hematuria (32%), and urinary tract infection (15%). In a recent study of 123 children who presented between 1991 and 2003, 76% presented with pain, 15% hematuria, and 10% urinary tract infection (21). Nephrolithiasis can also be asymptomatic in both pediatric and adult populations (22).

Urolithiasis can be related to underlying structural urological abnormalities (11%) and neurogenic bladder (6%). Most commonly, they are related to metabolic abnormalities which include hypercalciuria in 12–50%, hyperoxaluria in 2–20%, hyperuricosuria in 2–10%, and cystinuria in 2–6% (3, 21, 23, 24). Metabolic causes are increasingly common etiologies of stone disease in children with neurogenic bladder due to improvements in management of urinary tract infection (25). Nephrolithiasis is relatively common in preterm infants, affecting 30% of children with chronic lung disease (26–29). Nephrolithiasis has been associated with short-term furosemide administration (30). Nephrolithiasis is seen in approximately 1–8% of children on ceftriaxone, and nearly all of these will resolve spontaneously (31, 32). Urolithiasis developed in approximately 5% of the pediatric renal transplant recipients at a single center (33). Additives in infant formula such as silicate mild thickeners (34) and melamine (35, 36) have also been linked to the formation of renal calculi and renal failure.

II. What Is the Diagnostic Performance of the Different Imaging Studies in Nephrolithiasis and Urinary Tract Calculi in the Pediatric Population?

Summary of Evidence: Non-contrast spiral CT is the gold standard for imaging the urinary

tract for the presence of calculi (37, 38) (moderate evidence). CT allows precise measurements, localization of stone(s), characterization of stone density, stone morphology, and body habitus that can predict the likelihood of successful stone passage or fragmentation with treatment (39–44) (moderate evidence). However, CT utilizes moderately high doses of ionizing radiation and can be expensive. A variety of approaches have been utilized to decrease the dose in CT. In addition, protocols using US (45) or a combination of US with CT in selected cases may yield relatively high sensitivity and specificity at lower radiation doses (moderate evidence) (46, 47). Plain films can have an important role as well.

Supporting Evidence

Abdominal Radiographs

Plain films (KUB) are somewhat useful for the detection, localization, and measurement of radiopaque calculi (48–54) performing best for calcium-containing stones greater than 3 mm located over the kidneys or bladder. Scout images from the CT, also known as CT KUB or Scout KUB exams, are less sensitive and specific for stone detection than conventional KUB (37, 50, 55) (moderate evidence). In a study with stones ranging from 1 to 10 mm on CT, CT scout radiography detected 40% of the renal calculi compared with 52% seen on KUB (56).

CT

CT has very high sensitivity and specificity for detection of nephrolithiasis and urinary tract calculi. It is estimated to be 91–98% sensitive and 91–100% specific in children (15, 52, 57–63) (moderate evidence). Limitations of CT include the cost, the occasional need for sedation, and the radiation dose.

CT can identify the stone directly, identify secondary findings of obstruction, or identify signs of renal stone passage including periureteral inflammatory changes, ureteral dilatation, and decreased renal attenuation (38, 64). Stone measurements are approximately 12% smaller by CT compared to measurements on KUB. Objects are magnified on plain films and so CT measurements are more accurate (65). CT can evaluate stone density to predict the stone composition (38, 40, 42, 66–75) (moderate evidence) and treatment response including stone passage and fragmentation with lithotripsy (76, 77) (moderate evidence). In one recent study, CT was effective in identifying both dense and lucent residual stone, with 65% more stones detected at CT than antegrade pyelogram (78) (moderate evidence). CT can also be used to differentiate an obstructive stone from a non-obstructive stone (38). It correctly identifies obstructed from non-obstructed systems compared with diuretic renography (79) (moderate evidence). CT can also identify other causes of abdominal pain (80, 81) (moderate evidence).

Radiation dose is a significant issue particularly in the pediatric population, and decreasing the dose is a priority. CT dose is typically tenfold or more higher than a KUB though they can be equivalent (82) if using very low-dose CT techniques (82–90).

Different approaches to dose reduction have been studied (82–84, 86). Reduction in mAs reduces radiation dose with an effective dose calculated at 1.40 mSv for males and 1.97 mSv for females in an adult group scanned at a pitch of 1.5 and 50 mA (86). In a recent study on adults using simulated added noise, 35 mAs was effective at detecting renal calculi but less so with ureteral calculi (89). Tube current modulation has also been effective in detecting stones while decreasing dose in the adult population (88). In an adult population, increasing the pitch to 2.5 or 3 decreases the dose with little diminution in image quality or accuracy (90, 91) (moderate evidence). CT in adults utilizing low-dose techinique of 120 kV, 6.9 effective mAs with a mean effective whole-body dose was 0.5 mSv in men and 0.7 mSv in women, and a sensitivity and specificity in detecting patients with calculi was 97 and 95% for CT compared with 67 and 90% for ultrasound in the same group (82) (moderate evidence).

Intravenous Pyelogram (IVP)

IVP is rarely utilized in the evaluation of the child with urolithiasis. It is occasionally used to evaluate the position of the ureters prior to surgery. CT is more effective than IVU both in stone detection (59, 92) and in identifying obstruction (93, 94). CT and IVP are equivalent in detecting obstruction (92). There is a moderate radiation dose with IVP calculated to be

approximately 2.97–3.63 mSv in adults (92, 95, 96). In a recent prospective randomized study of 200 patients presenting to the emergency room, CT was more sensitive and specific, but there was no difference in outcomes between the IVP and the CT groups (96) (moderate evidence).

Ultrasound

Ultrasound has many advantages including low cost, lack of ionizing radiation, and portability. Limitations of ultrasound include potential incomplete visualization of the entire urinary tract due to body habitus or overlying bowel gas (53, 63, 93, 97–99) and variable skill levels among imagers as ultrasound is operator dependent. The range of reported sensitivities and specificities is broad. Improvements in technique, transducer design, and image processing continue to lead to improved image quality. Fluid ingestion has been shown to decrease visualization of the ureter in adults (100). In a prospective study of fasting adult patients with a full urinary bladder, urolithiasis was identified by US in 291 of 296 patients with urolithiasis. The five cases not identified by US were seen by CT (3), IVP (1), or by passing a stone(1, 45) (moderate evidence). US detection of hydronephrosis in the ER setting in adults with flank pain and hematuria is 83% sensitive and 92% specific for the diagnosis of renal colic (101).

In one small retrospective study in children, all renal tract calculi seen on plain film were also identified on sonography (47) (moderate evidence). In a prospective study in 62 adults with proven ureterolithiasis, US was 93% sensitive and 95% specific compared with CT, which was 91 and 95%, respectively (99). In adults, ultrasound demonstrates 67–77% of renal calculi in the right kidney and 53–54% of the calculi in the left kidney compared with CT (62). CT and US yield similar results in the detection of non-urinary tract etiology of symptoms (102).

The renal artery resistive index has been shown to be useful in some studies for acute obstruction (103–106) but less so in others (107). The difference may be due to the timing or whether there is complete obstruction (108). Asymmetric ureteral jets can also help to identify obstruction (104, 106, 109–111) (moderate evidence). Three-dimensional reconstruction is another US technique which may prove helpful though the data are limited to date (112).

KUB Plus US

A combination of US and plain film can improve the diagnostic performance of US while keeping the radiation dose relatively low (46, 53, 98, 113, 114) (53). In a prospective study of 66 adults, CT had a higher sensitivity and negative predictive value than the combination of KUB and ultrasound for the detection of urolithiasis. When stone visualization and signs of obstruction were combined the sensitivity and specificity of CT was 100% compared with 100% sensitivity and 90% specificity for KUB with US. All stones missed by the combination of KUB with US passed spontaneously (113) (moderate evidence). KUB with US using tissue harmonic imaging had a sensitivity of 96% and specificity of 91% compared with CT (114) (moderate evidence).

Ultrasound Followed by CT for Equivocal Cases

In a small retrospective study in 20 children, US was an effective screening tool with CT helpful in equivocal cases (115) (limited evidence). In a prospective study of 560 patients with unilateral flank pain, urolithiasis was identified by KUB and US in approximately 60% of the patients. CT was obtained in the remaining 40%; 60% of that group were found to have urolithiasis, 6% other diagnoses, and no etiology was identified for flank pain in the remainder (53) (moderate evidence).

Magnetic Resonance Imaging

MR has also been studied in adults. In a study of 51 adults, an MR urogram was used to select a level for targeted CT which led to a fivefold decrease in radiation dose and was 98% specific compared with CT of the entire urinary tract (116) (moderate evidence). In another study in 64 adults, the combination of MR (HASTE sequence) and KUB was compared with non-contrasted CT. CT revealed more ureteral calculi than the combination of plain film and MR while ureteral dilatation of perinephric stranding were more reliably detected with MR (117) (moderate evidence). MR urography compares favorably with conventional urography and

non-contrast CT (118). MR is less sensitive than CT in the detection on obstructing renal calculi, but it is better than CT in identifying the non-calculus etiologies of urinary obstruction in patients with diminished renal function (119) (moderate evidence).

Special Case: Bladder Calculi

Bladder calculi are seen in children with dysfunctional bladder, prior bladder surgery such as bladder augmentation (120–123), and from other infectious and metabolic causes (124, 125). These stones may be much larger and therefore easier to detect with a simple radiograph. Imaging strategies are similar to stone disease in the upper urinary tract (60).

III. What Is the Natural History of Nephrolithiasis and Urinary Tract Calculi and What Are the Roles of Medical Therapy Versus Extracorporeal Shock Wave Lithotripsy (ESWL) or Surgical Management?

Summary of Evidence: The prevalence and incidence of urolithiasis in children is unknown. The natural history of urolithiasis is dependent on the chemical composition of the stone and on the size. Many stones of size <2–4 mm will pass on their own. Larger stones generally require either medical chemolysis or surgical intervention. Recurrent stones are common.

Supporting Evidence: In the United States, nephrolithiasis is identified in 1 in 1,000 to 1 in 7,600 hospital admissions. Stones are found most commonly in Caucasian children and rarely in African-American children. The prevalence of urinary stones varies by region, being more common in the southeastern United States (126). Most children with urolithiasis (75-85%) will be found to have an underlying cause for stone formation, including metabolic abnormalities (52%), urinary tract infection (19%), and structural abnormality in the remainder (23, 126–132). The recurrence risk for stones is estimated to be approximately 5% per year in adults or 50% over a 10-year period (133). For children, conservative estimates are similar with an approximate 6% annual recurrence risk (134). Given this recurrence risk, targeted intervention to reduce or eliminate the underlying stone risk is coupled with routine monitoring for stone recurrence and adjustment of therapeutic interventions (135).

Asymptomatic nephrolithiasis can be due to uric acid or, much less commonly, ephedrine. Medical chemolysis with oral potassium citrate is possible, particularly for uric acid stones. It may take several weeks and only 50% of the stones resolve completely (135–137). Medical chemolysis is possible, particularly for uric acid stones, but will take several weeks with a 50% complete resolution rate. Medical therapy can also be utilized to facilitate stone passage (138). The other types of stones pass spontaneously if size permits. If they do not, they will require ESWL or surgical management. All symptomatic stones will require intervention for early resolution of symptoms. The initial treatment of the stones is dependent on the severity of the signs and symptoms. Infected stones associated with obstruction require immediate treatment with decompression of the infected system. Percutaneous nephrostomy tube placement or ureteral stenting is performed until the infection is cleared. Subsequent treatment can be accomplished electively.

Non-urgent treatment of symptomatic stones in the pediatric population can be performed utilizing extracorporeal shock wave lithotripsy (ESWL), percutaneous nephrolithotripsy (PCNL), ureteroscopy with laser lithotripsy, or open surgical removal. ESWL has become the primary treatment for almost all renal stones in the pediatric population regardless of size (7–9, 139–141). ESWL is less morbid than other surgical techniques with almost the same success rate. ESWL is less successful in mid-ureteral stones and distal ureteral stones secondary to bowel interference, cystine stones secondary to poor fragmentation, lower pole stones that are dependent in the kidney and do not fall down the ureter once fragmented, and staghorn calculus with a large stone burden (142). Treatment options for these include either PCNL, particularly for lower pole stones, or ureteroscopy with laser lithotripsy for ureteral stones (143, 144). Treatment with ESWL or PCNL has been shown to lead to an improvement in glomerular filtration rate (GFR) in children treated for stone disease (145).

IV. Special Case: Will the Stone Pass on Its Own?

Summary of Evidence: Stone passage is difficult to predict accurately. Smaller stones are more likely to pass than larger stones as are more distal compared with more proximal ureteral stones (41, 146).

Supporting Evidence: The spontaneous passage rate for stones 1 mm in diameter was 87%; for stones 2–4 mm, 76%; for stones 5–7 mm, 60%; for stones 7–9 mm, 48%; and for stones larger than 9 mm, 25%. Spontaneous passage rate as a function of stone location was 48% for stones in the proximal ureter, 60% for mid-ureteral stones, 75% for distal stones, and 79% for ureterovesical junction stones (41). CT can be used in computer models which predict stone passage better than size criteria alone (147). The majority of stones 5 mm or less are likely to pass on their own (148).

V. What Is the Role of Repeat Imaging in Children with Known Stone? In Children with Recurrent Symptoms (Suggesting Obstructing Stone)?

Summary of Evidence: After initial treatment, small residual stones may be asymptomatic and either remain in the kidney or pass on their own. Unfortunately, initial "clinically insignificant residual fragments" (CIRF) can become clinically symptomatic (149–151). Residual fragments can act as a nidus for new stone growth and subsequent symptoms (151). Secondary surgical procedures or medical treatment for residual stones requires accurate location of the remaining stones and the stone size and volume. Non-contrasted helical CT scan is the most sensitive radiologic procedure to identify residual stones. Repeat imaging is also utilized as a monitoring tool to assess the adequacy of preventative measures. Asymptomatic patients are monitored using ultrasound to avoid additional radiation exposure.

Supporting Evidence: During the era of open surgery for urolithiasis, the goal of treatment was to render the patient completely free of stones. With less morbid procedures that can be easily repeated, such as ESWL and endoscopy, success has been redefined as rendering the patient free of symptomatic stones but with small clinically insignificant residual stones (CIRF) (152). Future less invasive procedures can be performed if the fragments become symptomatic. Patients with small (<4 mm) residual stone fragments that are asymptomatic have a higher rate of future symptomatic stones presenting with fever, pain, obstruction, and infection as well as renal damage compared to patients that are rendered completely stone free: 6–15% versus 17–80% (149, 150, 153, 154). Stone position and the amount of residual stones will determine which technique will be most effective. Lower pole stones are poorly treated with ESWL and are best treated with ureteroscopy or PCNL (155). Upper pole, middle portion, and renal pelvis stones can be treated with subsequent ESWL, endoscopy, or PCNL. Abdominal radiography is effective in detecting dense calculi larger than 5 mm in size (50) (moderate evidence). CT is more sensitive for small fragments (156). Follow-up imaging is helpful as silent obstruction can occur in up to 23% of patients in the first 5 months after their procedure (17). Follow-up may not be required in patients who do not have residual fragments (157) (moderate evidence).

Take Home Tables and Figures

What Are the Roles of the Imaging Modalities in the Evaluation of Urolithiasis?

The decision tree in Fig. 37.1 outlines the role of each imaging modality in the evaluation of suspected urolithiasis. In the acutely symptomatic child, the plain radiograph is the initial imaging evaluation due to its relative low cost, rapid acquisition, and ready availability. When the clinical suspicion remains high, further imaging with US and/or CT is warranted.

Table 37.1 discusses the performance imaging studies of urolithiasis in children and adults.

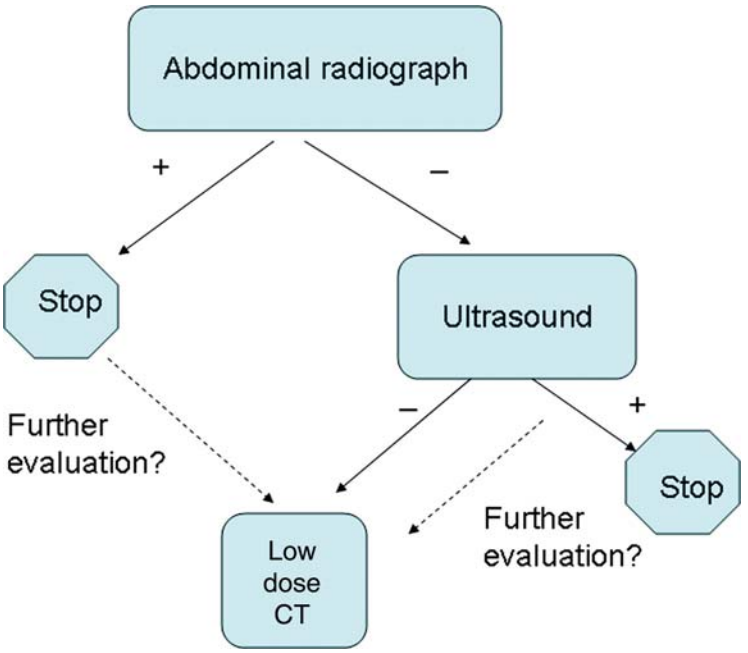

Figure 37.1. Algorithm for imaging suspected urolithiasis in the pediatric population. The algorithm will be affected by the pretest probability and level of clinical suspicion.

Table 37.1. Performance characteristics of imaging studies of urolithiasis in children and adults

	Sensitivity (%)	Specificity (%)
Plain radiograph (49, 50, 52, 56, 114)	52–69	82
IVU (59, 92, 158, 159) (93)	52–87	92–100
US (45, 47, 63, 98, 99, 101, 104, 106, 114, 160) (61)	24–100	82–100
US with KUB (11, 46, 98, 113)	77–100	90–100
CT (15, 52, 57–59)	91–98	91–100
CT low dose* (161) (82–90)	93–99	86–97
MRI (116–119)	69–93	95–100

*Low-dose MDCT defined as =50 mAs technique.
References in parentheses

Imaging Case Studies

Case 1

Figure 37.2 shows nephrocalcinosis in a 45-day-old preterm infant treated with repeated doses of Lasix.

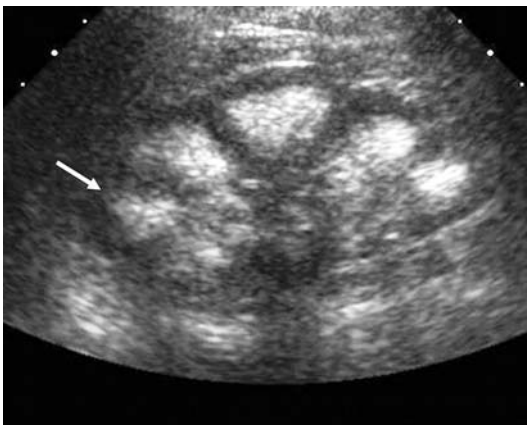

Figure 37.2. Nephrocalcinosis in a 45-day-old preterm infant treated with repeated doses of Lasix. The US image of the right kidney shows echogenic renal pyramids indicating nephrocalcinosis.

Case 2

Figure 37.3 shows staghorn calculus identified by plain film and ultrasound.

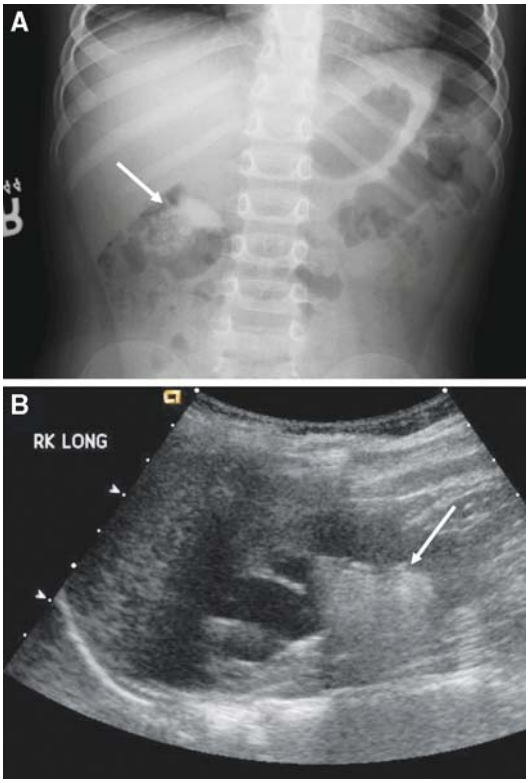

Figure 37.3. **A**: Right-sided staghorn calculus identified on an abdominal plain film. **B**: Ultrasound demonstrated the lower pole staghorn calculus with upper pole hydronephrosis.

Case 3

Figure 37.4 shows ureteral stones with ureteral dilatation identified by ultrasound.

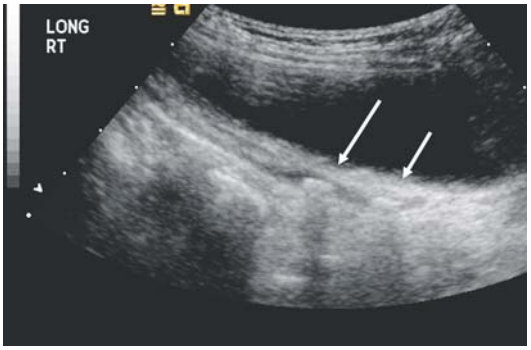

Figure 37.4. Two ureteral stones with ureteral dilatation visualized by sonography through a moderately full urinary bladder which were not identified on plain film.

Case 4

Figure 37.5 presents a patient with myelomeningocele and a negative renal ultrasound exam.

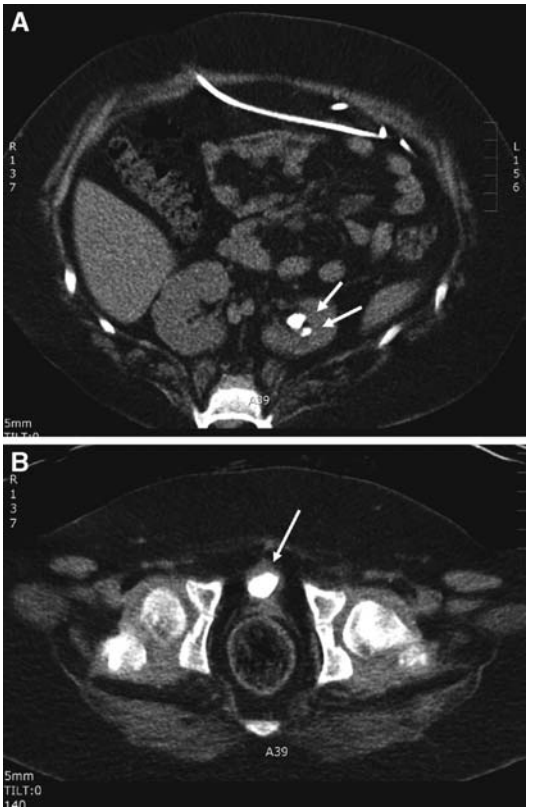

Figure 37.5. Patient with myelomeningocele and a negative renal ultrasound exam. CT clearly demonstrates (**A**) two left renal and (**B**) one bladder stone not seen on US.

Suggested Imaging Protocols Nephrolithiasis and Urinary Tract Calculi in Children

Plain Radiograph

Collimated abdominal radiograph to include the kidneys and the symphysis pubis.

Ultrasound

High-frequency probe (in younger children) 7–12 MHz with evaluation to include the kidneys, proximal and distal ureters, and urinary bladder. Color Doppler to assess for calcifications.

MDCT

Thin section (=3 mm) non-contrast CT. Low-dose technique. Recommend low-dose technique of = 50 mAs.

MRI

Axial and coronal T1 spin echo, axial and sagittal T2 FSE with fat saturation, coronal STIR or HASTE, axial and coronal T1 2D SPGR with fat saturation before and after intravenous gadolinium (in patients with acceptable renal function). Alternative to imaging with CT. Not as sensitive for calcification but can provide functional data.

Future Research

- Can MRI replace MDCT in the evaluation of urolithiasis in children (to avoid ionizing radiation)?
- Can findings on imaging (KUB, CT, MR, and ultrasound) predict the likelihood of success of medical therapy alone and provide early triage to surgical therapy?

References

1. Cheidde L, Ajzen SA, Tamer Langen CH, Christophalo D, Heilberg IP. Nephron Clin Pract 2007; 106(3):c119–c124.
2. VanDervoort K, Wiesen J, Frank R et al. J Urol 2007 Jun; 177(6):2300–2305.
3. Bartosh SM. Urol Clin North Am 2004 Aug; 31(3):575–587, x–xi.
4. Srivastava T, Alon US. Adolesc Med Clin 2005 Feb; 16(1):87–109.
5. Costa-Bauza A, Ramis M, Montesinos V et al. World J Urol 2007 Aug; 25(4):415–421.
6. Dogan HS, Tekgul S. Curr Urol Rep 2007 Mar; 8(2):163–173.
7. Delakas D, Daskalopoulos G, Metaxari M, Triantafyllou T, Cranidis A. J Endourol 2001 Sep; 15(7):675–680.
8. Smaldone MC, Corcoran AT, Docimo SG, Ost MC. J Urol 2008 Nov 12.
9. D'Addessi A, Bongiovanni L, Sasso F, Gulino G, Falabella R et al. J Endourol 2008 Jan 4.
10. D'Addessi A, Bongiovanni L, Racioppi M, Sacco E, Bassi P. J Pediatr Surg 2008 Apr; 43(4):591–596.

11. Ghali AM, Elmalik EM, Ibrahim AI, Abdulhameed E el Tahir MI. Eur Urol 1998; 33(6): 529–537.
12. Grisi G, Stacul F, Cuttin R, Rimondini A, Meduri S et al. Eur Radiol 2000; 10(10): 1620–1627.
13. Homer JA, Davies-Payne DL, Peddinti BS. Australas Radiol 2001 Aug; 45(3):285–290.
14. Pfister SA, Deckart A, Laschke S et al. Eur Radiol 2003 Nov; 13(11):2513–2520.
15. Wang LJ, Ng CJ, Chen JC, Chiu TF, Wong YC. Eur Radiol 2004 Sep; 14(9):1634–1640.
16. Lotan Y, Cadeddu JA, Pearle MS. Urol Res 2005 Jun; 33(3):223–230.
17. Weizer AZ, Auge BK, Silverstein AD et al. J Urol 2002 Jul; 168(1):46–50.
18. Parvex P, Pippi-Salle JL, Goodyer PR. Pediatr Nephrol 2001 Dec; 16(12):1076–1079.
19. Erbagci A, Erbagci AB, Yilmaz M et al. Scand J Urol Nephrol 2003; 37(2):129–133.
20. Spivacow FR, Negri AL, del Valle EE, Calvino I, Fradinger E et al. Pediatr Nephrol 2008 Jul; 23(7):1129–1133.
21. Sternberg K, Greenfield SP, Williot P, Wan J. J Urol 2005 Oct; 174(4 Pt 2):1711–1714; discussion 4.
22. Wimpissinger F, Turk C, Kheyfets O, Stackl W. J Urol 2007 Oct; 178(4 Pt 1):1341–1344; discussion 4.
23. Coward RJ, Peters CJ, Duffy PG et al. Arch Dis Child 2003 Nov; 88(11):962–965.
24. Acar B, Inci Arikan F, Emeksiz S, Dallar Y. World J Urol 2008 Dec; 26(6):627–630.
25. Matlaga BR, Kim SC, Watkins SL, Kuo RL, Munch LC et al. J Urol 2006 May; 175(5): 1716–1719; discussion 9.
26. Cranefield DJ, Odd DE, Harding JE, Teele RL. Pediatr Radiol 2004 Feb; 34(2):138–142.
27. Hein G, Richter D, Manz F, Weitzel D, Kalhoff H. Pediatr Nephrol 2004 Jun; 19(6): 616–620.
28. Hoppe B, Duran I, Martin A et al. Pediatr Nephrol 2002 Apr; 17(4):264–268.
29. Schell-Feith EA, Holscher HC, Zonderland HM et al. Br J Radiol 2000 Nov; 73(875):1185–1191.
30. Ali SK. Congenit Heart Dis 2006 Sep; 1(5): 251–253.
31. Avci Z, Koktener A, Uras N et al. Arch Dis Child 2004 Nov; 89(11):1069–1072.
32. Mohkam M, Karimi A, Gharib A et al. Pediatr Nephrol 2007 May; 22(5):690–694.
33. Khositseth S, Gillingham KJ, Cook ME, Chavers BM. Transplantation 2004 Nov 15; 78(9): 1319–1323.
34. Ulinski T, Sabot JF, Bourlon I, Cochat P. Eur J Pediatr2004 Apr; 163(4–5):239–240.
35. Parry J. BMJ 2008; 337:a1738.
36. Xin H, Stone R. Science 2008 Nov 28; 322(5906):1310–1311.
37. Chowdhury FU, Kotwal S, Raghunathan G, Wah TM, Joyce A et al. Clin Radiol 2007 Oct; 62(10):970–977.
38. Akay H, Akpinar E, Ergun O, Ozmen CA, Haliloglu M. Diagn Interv Radiol 2006 Sep; 12(3):147–150.
39. Ege G, Akman H, Kuzucu K, Yildiz S. Clin Radiol 2003 Dec; 58(12):990–994.
40. El-Nahas AR, El-Assmy AM, Mansour O, Sheir KZ. Eur Urol 2007 Jun; 51(6):1688–1693; discussion 93–94.
41. Coll DM, Varanelli MJ, Smith RC. Am J Roentgenol 2002 Jan; 178(1):101–103.
42. Ketelslegers E, Van Beers BE. Eur Radiol 2006 Jan; 16(1):161–165.
43. Olcott EW, Sommer FG, Napel S. Radiology 1997 Jul; 204(1):19–25.
44. Zarse CA, Hameed TA, Jackson ME et al. Urol Res 2007 Aug; 35(4):201–206.
45. Park SJ, Yi BH, Lee HK, Kim YH, Kim GJ et al. J Ultrasound Med 2008 Oct; 27(10):1441–1450.
46. Catalano O, Nunziata A, Altei F, Siani A. S Am J Roentgenol 2002 Feb; 178(2):379–387.
47. Smith SL, Somers JM, Broderick N, Halliday K. Clin Radiol 2000 Sep; 55(9):708–710.
48. Tisdale BE, Siemens DR, Lysack J, Nolan RL, Wilson JW. Can J Urol 2007 Apr; 14(2): 3489–3492.
49. Katz D, McGahan JP, Gerscovich EO, Troxel SA, Low RK. J Endourol 2003 Dec; 17(10):847–850.
50. Zagoria RJ, Khatod EG, Chen MY. Am J Roentgenol 2001 May; 176(5):1117–1122.
51. Jackman SV, Potter SR, Regan F, Jarrett TW. J Urol 2000 Aug; 164(2):308–310.
52. Eray O, Cubuk MS, Oktay C, Yilmaz S, Cete Y et al. Am J Emerg Med 2003 Mar; 21(2): 152–154.
53. Kobayashi T, Nishizawa K, Watanabe J, Ogura K. J Urol 2003 Sep; 170(3):799–802.
54. Narepalem N, Sundaram CP, Boridy IC, Yan Y, Heiken JP et al. J Urol 2002 Mar; 167(3): 1235–1238.
55. Assi Z, Platt JF, Francis IR, Cohan RH, Korobkin M. Am J Roentgenol 2000 Aug; 175(2): 333–337.
56. Ege G, Akman H, Kuzucu K, Yildiz S. Acta Radiol 2004 Jul; 45(4):469–473.
57. Fielding JR, Steele G, Fox LA, Heller H, Loughlin KR. J Urol 1997 Jun; 157(6):2071–2073.
58. Nachmann MM, Harkaway RC, Summerton SL et al. Am J Emerg Med 2000 Oct; 18(6):649–652.
59. Miller OF, Rineer SK, Reichard SR et al. Urology 1998 Dec; 52(6):982–987.

60. Myers MT, Elder JS, Sivit CJ, Applegate KE. Pediatr Radiol 2001 Mar; 31(3):135–139.
61. Oner S, Oto A, Tekgul S et al. JBR-BTR 2004 Sep–Oct; 87(5):219–223.
62. Ulusan S, Koc Z, Tokmak N. J Clin Ultrasound 2007 Jun; 35(5):256–261.
63. Palmer JS, Donaher ER, O'Riordan MA, Dell KM. J Urol 2005 Oct; 174(4 Pt 1):1413–1416.
64. Goldman SM, Faintuch S, Ajzen SA et al. Am J Roentgenol 2004 May; 182(5):1251–1254.
65. Dundee P, Bouchier-Hayes D, Haxhimolla H, Dowling R, Costello A. J Endourol 2006 Dec; 20(12):1005–1009.
66. Deveci S, Coskun M, Tekin MI, Peskircioglu L, Tarhan NC et al. Urology 2004 Aug; 64(2): 237–240.
67. Gupta NP, Ansari MS, Kesarvani P, Kapoor A, Mukhopadhyay S. BJU Int 2005 Jun; 95(9): 1285–1288.
68. Motley G, Dalrymple N, Keesling C, Fischer J, Harmon W. Urology 2001 Aug; 58(2):170–173.
69. Perks AE, Schuler TD, Lee J et al. Urology 2008 Oct; 72(4):765–769.
70. Sheir KZ, Mansour O, Madbouly K, Elsobky E, Abdel-Khalek M. Urol Res 2005 May; 33(2): 99–104.
71. Wang LJ, Wong YC, Chuang CK et al. Eur Radiol 2005 Nov; 15(11):2238–2243.
72. Weld KJ, Montiglio C, Morris MS, Bush AC, Cespedes RD. Urology 2007 Dec; 70(6): 1043–1046; discussion 6–7.
73. Williams JC, Jr, Kim SC, Zarse CA, McAteer JA, Lingeman JE. J Endourol 2004 Dec; 18(10):937–941.
74. Nakada SY, Hoff DG, Attai S, Heisey D, Blankenbaker D et al. Urology 2000 Jun; 55(6):816–819.
75. Stolzmann P, Scheffel H, Rentsch K et al. Urol Res 2008 Aug; 36(3–4):133–138.
76. Kosar A, Sarica K, Aydos K, Kupeli S, Turkolmez K et al. Int J Urol 1999 Mar; 6(3):125–129.
77. Osman Y, El-Tabey N, Refai H et al. J Urol 2008 Jan; 179(1):198–200; discussion
78. Halachmi S, Ghersin E, Ginesin Y, Meretyk S. J Endourol 2007 May; 21(5):473–477.
79. Bird VG, Gomez-Marin O, Leveillee RJ, Sfakianakis GN, Rivas LA et al. J Urol 2002 Apr; 167(4):1597–1603.
80. Eshed I, Kornecki A, Rabin A, Elias S, Katz R. Eur J Radiol 2002 Jan; 41(1):60–64.
81. Hoppe H, Studer R, Kessler TM, Vock P, Studer UE et al. J Urol 2006 May; 175(5):1725–1730; discussion 30.
82. Kluner C, Hein PA, Gralla O et al. J Comput Assist Tomogr 2006 Jan–Feb; 30(1):44–50.
83. Heneghan JP, McGuire KA, Leder RA, DeLong DM, Yoshizumi T et al. Radiology 2003 Nov; 229(2):575–580.
84. Kalra MK, Maher MM, D'Souza RV et al. Radiology 2005 May; 235(2):523–529.
85. Karmazyn B, Frush D, Applegate KE, Maxfield C, Cohen M et al. Am J Roentgenol. In Press.
86. Kim BS, Hwang IK, Choi YW et al. Acta Radiol 2005 Nov; 46(7):756–763.
87. Liu W, Esler SJ, Kenny BJ, Goh RH, Rainbow AJ et al. Radiology 2000 Apr; 215(1):51–54.
88. Mulkens TH, Daineffe S, De Wijngaert R et al. Am J Roentgenol 2007 Feb; 188(2):553–562.
89. Paulson EK, Weaver C, Ho LM et al. Am J Roentgenol 2008 Jan; 190(1):151–157.
90. Poletti PA, Platon A, Rutschmann OT, Schmidlin FR, Iselin CE et al. Am J Roentgenol 2007 Apr; 188(4):927–933.
91. Diel J, Perlmutter S, Venkataramanan N, Mueller R, Lane MJ et al. J Comput Assist Tomogr 2000 Sep–Oct; 24(5):795–801.
92. Niall O, Russell J, MacGregor R, Duncan H, Mullins J. J Urol 1999 Feb; 161(2): 534–537.
93. Yilmaz S, Sindel T, Arslan G et al. Eur Radiol 1998; 8(2):212–217.
94. Wong SK, Ng LG, Tan BS et al. Ann Acad Med Singapore 2001 Nov; 30(6):568–572.
95. Eikefjord EN, Thorsen F, Rorvik J. Am J Roentgenol 2007 Apr; 188(4):934–939.
96. Mendelson RM, Arnold-Reed DE, Kuan M et al. Australas Radiol 2003 Mar; 47(1):22–28.
97. Diament MJ, Malekzadeh M. J Pediatr 1986 Dec; 109(6):980–983.
98. Ather MH, Jafri AH, Sulaiman MN. BMC Med Imaging 2004 Jul 29; 4(1):2.
99. Patlas M, Farkas A, Fisher D, Zaghal I, Hadas-Halpern I. Br J Radiol 2001 Oct; 74(886):901–904.
100. Ozden E, Gogus C, Turkolmez K, Yagci C. J Ultrasound Med 2005 Dec; 24(12):1651–1657.
101. Gaspari RJ, Horst K. Acad Emerg Med 2005 Dec; 12(12):1180–1184.
102. Catalano O, Nunziata A, Sandomenico F, Siani A. Emerg Radiol 2002 Sep; 9(3):146–154.
103. Onur MR, Cubuk M, Andic C, Kartal M, Arslan G. Urol Res 2007 Dec; 35(6):307–312.
104. Pepe P, Motta L, Pennisi M, Aragona F. Eur J Radiol 2005 Jan; 53(1):131–135.
105. Brkljacic B, Kuzmic AC, Dmitrovic R, Rados M, Vidjak V. Eur Radiol 2002 Nov; 12(11): 2747–2751.
106. Geavlete P, Georgescu D, Cauni V, Nita G. Eur Urol 2002 Jan; 41(1):71–78.
107. Gurel S, Akata D, Gurel K, Ozmen MN, Akhan O. J Ultrasound Med 2006 Sep; 25(9):1113–1120; quiz 21–23.

108. Coley BD, Arellano RS, Talner LB, Baker KG, Peterson T et al. Acad Radiol 1995 May; 2(5):373–378.
109. Burge HJ, Middleton WD, McClennan BL, Hildebolt CF. Radiology 1991 Aug; 180(2): 437–442.
110. Cvitkovic Kuzmic A, Brkljacic B, Rados M, Galesic K. Eur J Radiol 2001 Sep; 39(3):209–214.
111. Leung VY, Chu WC, Yeung CK, Metreweli C. Pediatr Radiol 2007 May; 37(5):417–425.
112. Volkmer BG, Nesslauer T, Kuefer R, Engel O, Kraemer SC et al. Ultrasound Med Biol 2002 Feb; 28(2):143–147.
113. Ripolles T, Agramunt M, Errando J, Martinez MJ, Coronel B, Morales M. Eur Radiol 2004 Jan; 14(1):129–136.
114. Mitterberger M, Pinggera GM, Pallwein L et al. BJU Int 2007 Oct; 100(4):887–890.
115. Eshed I, Witzling M. Pediatr Radiol 2002 Mar; 32(3):205–208.
116. Blandino A, Minutoli F, Scribano E et al. J Magn Reson Imaging 2004 Aug; 20(2):264–271.
117. Regan F, Kuszyk B, Bohlman ME, Jackman S. Br J Radiol 2005 Jun; 78(930):506–511.
118. Sudah M, Vanninen RL, Partanen K et al. Radiology 2002 Apr; 223(1):98–105.
119. Shokeir AA, El-Diasty T, Eassa W et al. J Urol 2004 Jun; 171(6 Pt 1):2303–2306.
120. DeFoor W, Minevich E, Reddy P et al. J Urol 2004 Nov; 172(5 Pt 1):1964–1966.
121. Hernandez DJ, Purves T, Gearhart JP. J Pediatr Urol 2008 Dec; 4(6):460–466.
122. Merenda LA, Duffy T, Betz RR, Mulcahey MJ, Dean G et al. J Spinal Cord Med 2007; 30(Suppl 1):S41–S47.
123. Roberts WW, Gearhart JP, Mathews RI. J Urol 2004 Oct; 172(4 Pt 2):1706–1708; discussion 9.
124. Salah MA, Holman E, Khan AM, Toth C. J Pediatr Surg 2005 Oct; 40(10):1628–1631.
125. Sayasone S, Odermatt P, Khammanivong K et al. Southeast Asian J Trop Med Public Health 2004; 35(Suppl 2):50–52.
126. Gillespie RS, Stapleton FB. Pediatr Rev 2004 Apr; 25(4):131–139.
127. Milliner DS, Murphy ME. Mayo Clin Proc 1993 Mar; 68(3):241–248.
128. Stapleton FB, McKay CP, Noe HN. Pediatr Ann 1987 Dec; 16(12):980–1, 4–92.
129. Diamond DA. Br J Urol 1991 Aug; 68(2): 195–198.
130. Perrone HC, dos Santos DR, Santos MV et al. Pediatr Nephrol 1992 Jan; 6(1):54–56.
131. Escribano J, Balaguer A, Martin R, Feliu A, Espax R. Scand J Urol Nephrol 2004; 38(5):422–426.
132. Nicoletta JA, Lande MB. Pediatr Clin North Am 2006 Jun; 53(3):479–491, vii.
133. Menon M, Resnick MI. In Walsh PC, Retik AB, Vaughan ED Jr et al. (eds.). Campbell's Urology, 8th ed. Philadelphia: WB Saunders, 2002; 3276.
134. Diamond DA, Menon M, Lee PH, Rickwood AM, Johnston JH. J Urol 1989 Aug; 142(2 Pt 2):606–608; discussion 19.
135. Dello Strologo L, Laurenzi C, Legato A, Pastore A. Pediatr Nephrol 2007 Nov; 22(11): 1869–1873.
136. Hoffman N, McGee SM, Hulbert JC. Urology 2003 May; 61(5):1035.
137. Sarica K, Erturhan S, Yurtseven C, Yagci F. J Endourol 2006 Nov; 20(11):875–879.
138. Hollingsworth JM, Rogers MA, Kaufman SR et al. Lancet 2006 Sep 30; 368(9542):1171–1179.
139. Wadhwa P, Aron M, Seth A, Dogra PN, Hemal AK et al. J Endourol 2007 Feb; 21(2): 141–144.
140. Brinkmann OA, Griehl A, Kuwertz-Broking E, Bulla M, Hertle L. Eur Urol 2001 May; 39(5):591–597.
141. Tanaka ST, Makari JH, Pope JC, Adams MC, Brock JW, 3rd, Thomas JC. J Urol 2008 Nov; 180(5):2150–2153; discussion 3–4.
142. Tan MO, Kirac M, Onaran M, Karaoglan U, Deniz N et al. Urol Res 2006 Jun; 34(3): 215–221.
143. El-Assmy A, Hafez AT, Eraky I, El-Nahas AR, El-Kappany HA. J Endourol 2006 Apr; 20(4):252–255.
144. Erturhan S, Yagci F, Sarica K. J Endourol 2007 Apr; 21(4):397–400.
145. Wadhwa P, Aron M, Bal CS, Dhanpatty B, Gupta NP. J Endourol 2007 Sep; 21(9):961–966.
146. Erdodru T, Aker O, Kaplancan T, Erodlu E. Int Braz J Urol 2002 Nov–Dec; 28(6): 516–521.
147. Parekattil SJ, Kumar U, Hegarty NJ et al. J Urol 2006 Feb; 175(2):575–579.
148. Pietrow PK, Karellas ME. Am Fam Physician 2006 Jul 1; 74(1):86–94.
149. Candau C, Saussine C, Lang H, Roy C, Faure F et al. Eur Urol 2000 Jan; 37(1):18–22.
150. Streem SB, Yost A, Mascha E. J Urol 1996 Apr; 155(4):1186–1190.
151. Zanetti G, Seveso M, Montanari E et al. J Urol 1997 Aug; 158(2):352–355.
152. Miles SG, Kaude JV, Newman RC, Thomas WC, Williams CM. Am J Roentgenol 1988 Feb; 150(2):307–309.
153. Afshar K, McLorie G, Papanikolaou F et al. J Urol 2004 Oct; 172(4 Pt 2):1600–1603.
154. Osman MM, Alfano Y, Kamp S et al. Eur Urol 2005 Jun; 47(6):860–864.
155. Cannon GM, Smaldone MC, Wu HY et al. J Endourol 2007 Oct; 21(10):1179–1182.

156. Kupeli B, Gurocak S, Tunc L, Senocak C, Karaoglan U et al. Int Urol Nephrol 2005; 37(2):225–230.
157. Karadag MA, Tefekli A, Altunrende F, Tepeler A, Baykal M et al. J Endourol 2008 Feb; 22(2):261–266.
158. El-Ghar ME, Shokeir AA, El-Diasty TA, Refaie HF, Gad HM et al. J Urol 2004 Sep; 172(3): 985–988.
159. Sourtzis S, Thibeau JF, Damry N, Raslan A, Vandendris M et al. Am J Roentgenol 1999 Jun; 172(6):1491–1494.
160. Fowler KA, Locken JA, Duchesne JH, Williamson MR. Radiology 2002 Jan; 222(1):109–113.
161. Hamm M, Knopfle E, Wartenberg S, Wawroschek F, Weckermann D et al. J Urol 2002 Apr; 167(4):1687–1691.

38

Urinary Tract Infection in Infants and Children

Carol E. Barnewolt, Leonard P. Connolly, Carlos R. Estrada, and Kimberly E. Applegate

Issues

I. What is known about the natural history of urinary tract infections in infants and children?
II. What can imaging reveal in the setting of UTI?
III. What are reasonable imaging strategies when caring for a male infant or child with a history of a febrile urinary tract infection?
IV. What are reasonable imaging strategies when caring for a female infant or child with a history of a febrile urinary tract infection?
V. Special case: postnatal management of fetal hydronephrosis

Key Points

- The presence of fever, in the setting of an appropriately collected urine specimen and positive urine culture, reasonably distinguishes between cystitis (lower tract) and pyelonephritis (upper tract) infections (moderate evidence).
- Pyelonephritis, and hence renal scarring, can occur with or without the existence of vesicoureteric reflux (VUR) (strong evidence).
- Infants and children with their first febrile UTI should undergo imaging workup to detect congenital anomalies or high-grade VUR (with US and VCUG) that increase the risk of renal scar and later dysfunction (limited evidence).
- Higher grades of upper urinary tract obstruction alone, without complicating factors such as stones or infection, may lead to progressive, focal renal damage and progressive loss of renal function (moderate evidence).
- Unrelieved bladder outlet obstruction, caused by posterior urethral valves or neurogenic bladder, predisposes to infection and may result in progressive voiding dysfunction, vesicoureteric reflux, renal scarring, and dysplasia (strong evidence).

C.E. Barnewolt (✉)
Department of Radiology, Children's Hospital Boston, Boston, MA 02115, USA
e-mail: carol.barnewolt@childrens.harvard.edu

L.S. Medina et al. (eds.), *Evidence-Based Imaging in Pediatrics*,
DOI 10.1007/978-1-4419-0922-0_38,

- Low-grade VUR (grades I–III), in the absence of infection, is unlikely to result in progression of renal scarring (moderate evidence).
- High-grade VUR (grades IV–V) is more likely than low-grade VUR to be associated with renal cortical scarring and with recurrent UTI (moderate evidence).
- There is insufficient evidence that early detection of urinary tract obstruction, vesicoureteric reflux (VUR), and/or renal scarring after urinary tract infection (UTI) in infants and children and instigation of therapy, either medical or surgical, minimizes or prevents further scarring (insufficient evidence).
- There is insufficient evidence that instigation of low-dose prophylactic antibiotic therapy, after identification of urinary tract obstruction, lower grades of vesicoureteric reflux (VUR), and/or renal scarring prevents development of recurrent infection and further scars (insufficient evidence). In addition, antibiotic prophylaxis leads to higher rates of resistant infections (limited to moderate evidence).
- There is insufficient evidence that elimination of vesicoureteric reflux with surgical reimplantation or endoscopic introduction of antireflux agents prevents development of recurrent infection and further scars (insufficient evidence).

Definitions and Pathophysiology

Cystitis is defined as inflammation or infection of the bladder and most commonly occurs from retrograde ascent of perineal bacteria up the urethra into the bladder. After infancy, girls, with much shorter urethras than boys, have an eightfold higher incidence.

The diagnosis of a febrile urinary tract infection is made when a urine culture produces growth of greater than 100,000 colony forming units per cubic centimeter of a single pathogen, from an adequately obtained urine specimen (a catheterized or suprapubic specimen in infants), in the setting of a fever of $\geq$38°C. Fever is evidence for the presence of pyelonephritis (an upper tract infection), without the need for direct imaging evidence. The vast majority of infections in infants and children are caused by *Escherichia coli*. Non-*E. coli* infections tend to occur with greater frequency in boys and in association with underlying genitourinary abnormalities such as urinary tract obstruction or vesicoureteric reflux. Infections with Enterobacteria and *Enterococci* also occur in young girls, *Staphylococcus aureus* in adolescent girls, and Proteus in young boys (1–3).

Pyelonephritis can result from blood-borne infection, particularly in the newborn period. However, some infants and children with pyelonephritis acquire the renal infection by ascent of bacteria from the bladder (4–6), perhaps as a result of reflux of infected urine from the bladder. Some data indicate that higher grades of VUR, in combination with high fever and elevated C-reactive protein, have a tenfold increase in risk of persistent scars (7). Animal studies suggest that certain bacterial properties, such as those of the P-fimbriated *E. coli*, allow bacterial ascent without the presence of VUR (8, 9).

Finally, histologic examination of scarred kidneys that were surgically removed, in particular from young, refluxing males, shows focal renal dysplasia along side of segmental scarring. This raises the question that some observed renal abnormalities may be congenital in nature, rather than acquired from infection (10).

Vesicoureteral reflux (VUR) is a congenital condition that most often resolves spontaneously in infancy or early childhood. In infants and children diagnosed with UTI, one-third will have VUR (11). VUR is more common in girls and has a peak age of detection before age 2 years. Family history and Caucasian race are risk factors for VUR. It is graded on a one to five scale: grade I is reflux from the bladder into the distal ureter but not into the renal

collecting system; grade II reflux extends into the renal collecting system; grade III reflux causes distention of the ureter and renal collecting system; grade IV reflux results in tortuosity of the dilated ureter; and grade V shows marked dilation and tortuosity of the ureter and renal collecting system with marked calyceal blunting.

Epidemiology

Urinary tract infection is one of the most common infections in children with approximately 19 episodes per 1,000 children annually. During the first 6 years of life, 8% of all girls and 2% of all boys will have a symptomatic urinary tract infection (12). In *febrile* infants and children, somewhere between 1 and 17% will prove to have a urinary tract infection (1, 12, 13). Results of DMSA scans performed soon after a first UTI in children 2 years of age and younger suggest that 75% of these children with coexisting fever and bacteriuria will prove to have pyelonephritis (14). Caucasian girls with fever are more likely to have a UTI than African American girls or boys of any ethnicity (15, 16). Uncircumcised male infants also have an increased risk of UTI in the first few months of life (17–20).

Even in children with no identifiable urinary tract abnormality, recurrent febrile UTIs cause significant morbidity. In a study of 850 children, 45% of girls and 14% of boys had recurrent UTI. In those with a negative imaging workup (renal US and VCUG) after febrile UTI, 28% of girls and 4% of boys developed a recurrent febrile UTI (21). UTI recurrence rates were greater in young uncircumcised boys than in circumcised boys and in children older than 5 years with dysfunctional voiding patterns.

The incidence of vesicoureteric reflux (VUR) in healthy infants and children is estimated at 17–33% (22–27) and decreases with increasing age (Table 38.1) (1–6, 16, 28–39). During the first year of life, boys may have a higher rate and grade of VUR than girls (40–42). The overall incidence of VUR in siblings of infants and children with VUR was found to be about 37% in one study of 482 siblings, with decreasing incidence in older siblings as follows: 46% for siblings under 2 years, 33% for 2–6 years, and only 7% when older than 6 years of age (43). There is no known correlation between index patient reflux grade, sex, or cortical scars with the likelihood of sibling reflux (44).

Overall Cost to Society

In the United States, urinary tract infections account for more than 1 million outpatient visits among children younger than 18 years, and about 25,000 visits to urologists for evaluation and treatment of VUR annually (45). There were just under 0.1% children hospitalized annually in Australia for UTI (46).

Monetary costs of hospitalization, antibiotic therapy, loss of work for caregivers, imaging evaluation, and complications of infections and therapy have not been scientifically studied in the United States, though there has been some attempt to do so in other countries such as Britain, Australia, and Israel (46–48). It is clear that the approach to treatment and subsequent imaging, despite professional society guidelines, varies greatly from region to region throughout the United States (49–52). The reason for this discrepancy may reflect a lack of evidence to support current recommendations or a lack of awareness or consensus within the medical community (53–56). In fact, a recent review of the clinical effectiveness and cost-effectiveness of tests for the diagnosis and investigation of UTI in children stated that there were insufficient data to support an imaging workup after first UTI in children under 5 years (57).

Goals

There are two immediate goals of imaging in the setting of urinary tract infection (1): to identify urinary tract obstruction and resultant urinary stasis that may warrant surgical intervention to lessen the risk of sepsis, recurrent infection, and preserve renal function; and (2) to prevent the formation and/or minimize the progression of renal scars by identifying patients at increased risk of progressive scar formation. The long-term goal is to prevent the complications of chronic renal scars, namely hypertension, chronic renal failure (CRF), and complications of pregnancy in women. Renal scars may form as a result of pyelonephritis

both with and without accompanying vesicoureteric reflux (10) (Table 38.1).

Methodology

A Medline search was performed by an experienced, trained medical librarian using PubMed (National Library of Medicine, Bethesda, Maryland) for original research and review articles, including clinical trials and meta-analyses, targeted at discussing the diagnosis, treatment, and imaging of urinary tract infection in infants and children. Both English language and non-English language searches were performed, though the non-English literature was only included if an English translation of the abstract was available and the content deemed vital and worthy of further investigation. Animal studies were included as well. The search covered the years 1966 through October 2008. After review of available abstracts, the entire text of relevant articles were obtained and read in detail by the first author.

Discussion of Issues

I. What Is Known About the Natural History of Urinary Tract Infections in Infants and Children?

Summary of Evidence: It is clear that the approach to treatment and subsequent imaging, despite professional society guidelines, varies greatly from region to region throughout the United States (47–50). The reason for this discrepancy may reflect a perceived and real lack of evidence to support current recommendations (51–54).

Few studies provide us with the long-term outcomes of children with UTI (58), despite the large amount of literature since the earliest UTI study in children and young adults by Bright in the early 19th century (59). The modern study of urinary tract infections began in earnest in the mid-20th century when children were evaluated with the evolving radiologic tools of voiding cystourethrography (VCUG) and intravenous urography (IVU), a test only rarely used today (60).

Supporting Evidence: Table 38.1 summarizes the complex and at times conflicting literature that addresses the relationship between urinary tract infection, VUR, and renal cortical scarring in various cohorts, beginning in 1964. There is a lack of standardization of diagnostic criteria, imaging techniques, treatment regimes, or patient follow-up.

By following 389 patients with a first UTI, Oh et al. showed that higher grades of VUR (grades IV and V) are associated with the diagnosis of pyelonephritis on Tc-99m DMSA scans, but that later scars are independent of grade of VUR (61). More recent large studies suggest that prophylactic antibiotic therapy does not prevent recurrent UTI and therefore may not prevent progression of renal compromise. Further, surgical or endoscopic correction of VUR may not improve long-term outcome in these children. Wheeler and colleagues performed a meta-analysis of randomized controlled trials to evaluate the benefits and harms of treatments for vesicoureteric reflux in children. They identified eight trials involving 859 evaluable children comparing long-term antibiotics with surgical correction of reflux (VUR) and antibiotics (seven trials), and antibiotics compared with no treatment (one trial). They concluded that there is no clear clinical benefit from identification and treatment of children with VUR. Further, they state "the additional benefit of surgery over antibiotics alone is small at best. Assuming a UTI rate of 20% for children with VUR on antibiotics for 5 years, nine reimplantations would be required to prevent one febrile UTI, with no reduction in the number of children developing any UTI or renal damage" (62).

The incidence of new cases of end-stage renal disease (ESRD) in Australia and New Zealand did not diminish with the use of prophylactic antibiotics and surgical treatment of VUR (63). Craig and colleagues concluded that "Treatment of children with vesicoureteric reflux has not been accompanied by the hoped-for reduction in the incidence of ESRD attributable to reflux nephropathy."

Acute pyelonephritis is not always associated with VUR (2, 5, 6, 16, 28–35, 37–39); renal cortical scars occur in children with a history of UTI but no VUR (5, 6, 34, 35, 37, 38);

and one can observe cortical defects, perhaps representing cortical dysplasia, without convincing evidence for antecedent urinary tract infection (64).

The prevalence of VUR markedly and spontaneously diminishes in the first few years of life. The likelihood of resolution of VUR increases with decreased grade and with unilateral VUR. Some data suggest that neither gender nor the presence or absence of renal cortical scars effect the rate of VUR resolution (36), while others suggest that resolution of VUR occurs more quickly in boys and in the absence of renal cortical scars (35, 65, 66). For asymptomatic children with low-grade VUR detected in a sibling-screening program, the likelihood of resolution did not vary with age at diagnosis, gender, and whether VUR was unilateral or bilateral (67).

An epidemiologic study from Sweden reports no case of non-obstructive pyelonephritis as a cause of chronic renal failure in a review of patients from a period of 1986–1994, perhaps reflecting the success of a screening program (68). On the other hand, a Chilean review of children with chronic renal failure reports that 17% of 227 patients resulted from reflux nephropathy (69). The very different economic and medical structures of each country make it impossible to know whether this apparent difference reflects a Chilean weakness in treatment of UTI or screening after UTI.

In 1812, Bell described the anatomy of the ureterovesical junction, explaining the configuration that prevents regurgitation of the urine into the ducts of the kidney, emphasizing the importance of the ureteral obliquity (70). Assuming that reflux of infected urine leads to a high incidence of pyelonephritis and resultant scars, prevention of such reflux should decrease the incidence of scarring, thus improving long-term outcomes. However, studies comparing outcomes of patients treated with prophylactic antibiotic (medical treatment) and antireflux procedures (surgical treatment) have not shown a distinct difference between the two groups (39, 62, 71–87). One paper suggests that males with higher grades of reflux have fewer UTIs with antibiotic prophylaxis therapy than without (88).

II. What Can Imaging Reveal in the Setting of UTI?

Summary of Evidence: Routine imaging during an acute episode of UTI is not necessary to make the diagnosis (moderate evidence). In non-routine cases that require imaging, the gold standard imaging test to diagnose pyelonephritis is technetium-99m dimercaptosuccinic acid (Tc-99m DMSA) (moderate evidence), although ultrasound (particularly with the use of Doppler) (89), computed tomography (CT), and magnetic resonance imaging (MRI) are used with lower sensitivity and specificity.

After the first episode of UTI in infants and children, most will receive both a renal US and a VCUG in the United States. However, while common and recommended practice, a systematic review of the literature does not support imaging children under 5 years (90) (moderate evidence).

Table 38.2 provides information about the diagnostic performance of tests for UTI, pyelonephritis, VUR, and renal scarring. Currently, only the DMSA test can adequately predict the later development of renal scar (moderate evidence).

If the patient is not responding to usual medical therapy, a complication, such as abscess formation, may be suspected. Renal abscesses can be detected with cross-sectional imaging; the choice of US versus CT or MR depends on the size of the child and the availability and experience of the imager. The American College of Radiology has developed appropriateness criteria and provided the estimated radiation exposures for imaging subgroups of children after first urinary tract infection (91).

Supporting Evidence

Abdominal Radiographs

Plain radiographs have essentially no role in the evaluation of suspected UTI in infants and children, unless other diagnoses are under consideration. Radiographs can suggest the alternate diagnoses of the gastrointestinal tract, large abdominal masses, and abnormal abdominal/retroperitoneal calcifications.

Sonography

Ultrasound evaluation of the kidneys and bladder is a readily available, safe modality, but is insensitive for the diagnosis of acute pyelonephritis (moderate evidence) and even for the diagnosis of renal abscess. Acute pyelonephritis is suspected with focal swelling, loss of corticomedullary differentiation, and/or a decrease in relative vascularity. Doppler US only marginally improves sensitivity and specificity. It is a useful modality for the qualitative evaluation of urinary tract obstruction at the level of the ureteropelvic junction, ureterovesicular junction, and sometimes for bladder outlet obstruction with the observation of bladder wall thickening. Quantitative grading systems exist for the systematic description of hydronephrosis, though they are not universally adopted (92). Ultrasound provides no direct, quantifiable measure of renal function.

Ultrasound has poor sensitivity and specificity for the identification of vesicoureteric reflux (93–101) (moderate evidence). Specifically, the observation of hydronephrosis does not indicate the presence of VUR, and the absence of hydronephrosis does not exclude the diagnosis of VUR. These limitations may be improved with documentation of changes in collecting system caliber (102).

Intravenous Pyelogram (IVP)

Prior to the era of cross-sectional imaging, IVP was the mainstay of urologic imaging. It has the advantages of availability and assessment of renal function, obstruction, and overall anatomy. It has the disadvantages of venipuncture, risk of iodinated contrast reaction, and exposure to ionizing radiation. It is insensitive, when compared to Tc-99m DMSA, for detection of both acute infection and cortical scars. It has no role in the diagnosis or exclusion of VUR. Therefore, its role is limited to patients with complex ureteral anatomy or postoperative ureteral obstructions.

CT and MRI/MR Urography

Contrast-enhanced CT and MR do not play a role in routine UTI, although they may detect pyelonephritis during emergent imaging of a child with abdominal pain. CT and MR have lower sensitivity and specificity, on average, compared to DMSA for the detection of pyelonephritis and renal scar. Both provide moderate sensitivity and specificity for pyelonephritis, cortical scarring, abscess formation, urinary tract obstruction, and anatomic variants such as subtle duplex systems (103–107). In the case of CT and MR contrast agents, adverse reactions have been reported. Gadolinium administration with MRU is accompanied by risk of nephrogenic systemic fibrosis if the child has renal dysfunction (108).

Nuclear Medicine

Tc-99m DMSA is the gold standard for detection of both acute pyelonephritis, with the observation of flare-shaped regions of decreased radioactivity, and renal scars, as indicated by focal loss of cortical bulk (109). It is far more sensitive and specific in general than is ultrasound and CT/MR. It has the disadvantages of the need for venipuncture to administer the radiopharmaceutical and exposure to radiation.

Tc-99m MAG3 and Tc-99m DTPA each provide quantifiable data to diagnose and exclude urinary tract obstruction, often using intravenous furosemide challenge. Tc-99m MAG3 provides little other anatomic detail. Tc-99m DTPA can be used to assess physiologic parameters such as differential renal function, renal plasma flow, and glomerular filtration. Both also require venipuncture to administer the radiopharmaceutical and exposure to radiation.

Evaluation for Vesicoureteric Reflux

The only reliable way to diagnose or exclude VUR is with a voiding cystogram, either voiding cystourethrography (VCUG) using iodinated contrast agents and fluoroscopy or radionuclide cystogram (RNC) using the radiotracer Tc-99m pertechnetate, instilled along with saline into the urinary bladder, with continuous observation with a gamma camera during the filling and voiding phases. Both require placement of a urethral catheter, which can be an uncomfortable procedure, particularly in inexperienced hands. While briefly uncomfortable, the examination is generally not associated with complications (110). Both tests use small amounts of ionizing radiation. Though the development of pulsed fluoroscopy equipment has lessened the discrepancy in dose between the two studies, RNC continues to

have lower exposures than does VCUG (103–105, 111). However, RNC is less available in general and community hospitals and, therefore, fluoroscopic VCUG is more commonly performed. Contrast-enhanced ultrasound for VCUG is used in Europe to avoid ionizing radiation, but the contrast agents are not approved for use in the United States.

III. What Are Reasonable Imaging Strategies When Caring for a Male Infant or Child with a History of a Febrile Urinary Tract Infection?

Summary of Evidence: In boys, the incidence of infection, beyond the newborn period, is lower than in girls, and the grade of VUR tends to be higher in neonatal boys than in girls (42, 112). Some boys that present with first UTI will have posterior urethral valves, a correctable, mechanical obstruction to urinary flow. Therefore, most current guidelines state that renal US and fluoroscopic VCUG are recommended to identify upper urinary obstruction and/or posterior urethral valves (limited evidence). Renal US alone is inadequate for the evaluation of VUR and renal scar (96) (moderate evidence). These recommendations are emphasized in children under 5 years when detection of urinary system obstructive lesions, the presence of VUR, and the risk of renal scar are higher (limited evidence).

Figures 38.1A and 38.2A provide an imaging strategy for boys, depending on local confidence and use of antibiotic prophylaxis. Evidence is building that the use of antibiotic prophylaxis is not associated with improved outcomes, though data are lacking for higher grades of VUR. Additionally, surgical correction of higher grades of VUR may provide improved outcomes. This strategy, therefore, allows identification of obstruction and VUR, but incorporates evolving data, supporting a watch and wait approach to lower grades of VUR (113).

Supporting Evidence: Ultrasound is readily available, requires no sedation, does not use ionizing radiation, and can identify higher grades of obstruction, but does not identify VUR reliably (114). Widespread prenatal ultrasound has decreased the incidence of obstruction presenting as UTI, not all fetuses are screened, the quality of screening varies widely between geographic areas, and variation in maternal body habitus can effect the sensitivity of this tool (115, 116). Therefore, ultrasound is included as a first-line screen.

VCUG, rather than RNC, is employed to allow the diagnosis or exclusion of posterior urethral valves and to identify VUR. The incidence of PUV is 1 in 5,000–8,000 live male births (117). Modern equipment, and in particular pulsed fluoroscopic techniques, keeps radiation exposure low (118–120). The goal is to identify higher grades of VUR that warrant either antibiotic prophylaxis, periodic reassessment, or surgical reimplantation, depending on evolving data, local culture, and family preference. The goal of these tests and treatment is to prevent cortical scarring (Figs. 38.3 and 38.4). High-grade VUR, age of diagnosis of VUR greater than 5 years, and male gender were the most significant risk factors for renal scarring in a study of 98 infants and children (121).

Renal cortical scintigraphy with technetium-99m dimercaptosuccinic acid (Tc-99m DMSA) is more sensitive for scars than ultrasound, but is reserved for patients found to have high-grade reflux (89, 109, 122–125). The intention is to use the presence of absence of scars, reliably identified, as a guide to clinical management (126). Magnetic resonance imaging (MRI) is an appealing alternative because of its lack of use of ionizing radiation, but it tends to be less widely available and may require sedation of the infant or child (106, 107). Since only a minority of infants and children with proven pyelonephritis will develop scars, DMSA is not recommended for all cases (7, 14, 127, 128).

Finally, a quantitative assessment of obstruction is introduced if ultrasound reveals the presence of moderate to severe hydronephrosis. By definition, this includes kidneys shown to have gross calyceal dilatation, not just pelviectasis, in the absence of VUR. This can be performed with either Tc-99m mercaptoacetyltriglycine (Tc-99m MAG3), Tc-99m diethylene triamine pentaacetic acid (Tc-99m DTPA), or magnetic resonance urography (MRU). MRU has the advantage of lack of use of ionizing radiation, but tends to be less widely available and may require sedation of the infant or child.

IV. What Are Reasonable Imaging Strategies When Caring for a Female Infant or Child with a History of a Febrile Urinary Tract Infection?

Summary of Evidence: Girls have a much higher incidence of UTI than boys. Similar to recommendations for boys, most current guidelines state that renal US and VCUG are recommended to identify upper urinary obstruction and VUR after first UTI (limited evidence). However, radionuclide cystography (RNC) may be used instead of fluoroscopic VCUG since the urethral anatomy is almost invariably normal. Renal US alone is inadequate for the evaluation of VUR and renal scar (moderate evidence). These recommendations are emphasized in children under 5 years when detection of urinary system obstructive lesions, the presence of VUR, and the risk of renal scar are higher (limited evidence).

The imaging strategy for female infants and children with UTI is provided in Figs. 38.1B and 38.2B, depending on local confidence and use of antibiotic prophylaxis.

Supporting Evidence: Ultrasound evaluation of both kidneys and the bladder is used to detect congenital anomalies and obstruction. The reasoning is similar to the situation for boys, with one additional motive: the possible identification of an obstructing ureterocele, usually as part of the upper moiety of a duplex collecting system. While ureteroceles can occur in boys, the incidence is far less in girls (129, 130) (Fig. 38.5). The approach in girls is modified to the use of radionuclide cystography (RNC), a still lower radiation dose technique, rather than VCUG to evaluate for the possibility of VUR (131). If one subscribes to the belief that prophylactic antibiotic use may improve outcomes in the setting of high-grade VUR, the remainder of the scenario is the same for girls as for boys. The use of RNC may be limited to those radiology practices that are experienced and comfortable with children's imaging. Therefore, its use is less common than the fluoroscopic VCUG.

However, should the evidence for the use of prophylactic antibiotic be considered insufficient, the use of RNC is replaced with Tc-99m DMSA. Data suggest that this exam can be used as a surrogate for RNC as a way to eliminate the likelihood of lower grades of VUR, thus eliminating the need for urethral catheterization. This avoids the low, but potential risks and stress that catheterization can cause, even in expert hands (132). If scars are identified, RNC is warranted as a higher grade of VUR may be present, perhaps warranting surgical reimplantation or periodic reassessment for evidence of progression of renal cortical scarring (Fig. 38.6).

V. Special Case: Postnatal Management of Fetal Hydronephrosis

Summary of Evidence: Fetal sonography detects hydronephrosis in 1–5% of all pregnancies (133). Currently, there has been limited standardization of fetal genitourinary system ultrasound technique and subsequent postnatal evaluation. The postnatal imaging with (a) resolution of hydronephrosis and (b) persistent hydronephrosis varies widely based on a lack of consensus. The most common current recommendation is to perform renal and bladder US in neonates that had moderate to severe prenatal hydronephrosis (insufficient evidence). Some centers also recommend VCUG (or RNC for girls).

Supporting Evidence: A meta-analysis was recently performed to determine whether the degree of antenatal hydronephrosis and related antenatal ultrasound findings are associated with postnatal outcome. Although the risk of VUR was similar for all degrees of fetal hydronephrosis, the risk of any postnatal pathology versus the degree of antenatal hydronephrosis was 12% for mild, 45% for moderate, and 88% for severe fetal hydronephrosis. Overall, children with any degree of antenatal hydronephrosis were at greater risk of postnatal pathology as compared with the normal population. Moderate and severe antenatal hydronephrosis has a significant risk of postnatal pathology, indicating that comprehensive postnatal diagnostic management should be performed. Mild antenatal hydronephrosis may carry a risk for postnatal pathology, but additional prospective studies are needed to determine the optimal management of these children (133).

Infants with a history of mild hydronephrosis may not require postnatal evaluation. Distinction between these two groups assumes that the fetal ultrasound examination attempts to characterize the degree of dilatation, does so correctly, and consistently and accurately conveys this information to the postnatal caregivers. This may not be the case (116).

A recent systematic study, evaluating a group of nearly 500 newborns with thorough prenatal and postnatal evaluation, found a VUR incidence of 9%. This study reports that approximately 75% of those with VUR have low-grade reflux that resolves rapidly (grades I–III), but about one-quarters have a high-grade reflux. In the group with high-grade VUR, spontaneous resolution by 2 years of age was rare. Encouragingly, persistent reflux was rarely associated with impaired renal function (134–136). A recent study of over 1,500 infants with persistent postnatal grade II hydronephrosis (Society for Fetal Urography grading system) showed that screening for VUR and treatment with prophylactic antibiotic decreased the risk of febrile UTI when compared with the group who were not screened (137). An increasingly popular approach to the postnatal evaluation of infants with fetal hydronephrosis is to use postnatal ultrasound as a tool to determine whether or not further imaging is recommended (134). If hydronephrosis, scarring, or renal dysplasia is discovered by careful postnatal ultrasound, further evaluation with a reflux study, either RNC or VCUG, is suggested. However, some infants with high-grade vesicoureteric reflux will not be discovered by this technique. The challenge is to determine how much pelviectasis/hydronephrosis is required to warrant VCUG (Figs. 38.7 and 38.8).

It is important to realize that, throughout this analysis of imaging of UTI, we have been operating under the assumption that sterile VUR does not cause impairment in renal function. Some evidence shows that renal cortical defects are related to the presence of high-grade, sterile VUR (138–140).

Take Home Tables and Figures

Table 38.1 summarizes the literature on the role imaging of UTI in children. Table 38.2 provides information about the diagnostic performance of tests for UTI, pyelonephritis, VUR, and renal scarring.

Table 38.1. Summary data on the role of imaging in children with UTI. Summary of investigations to identify the frequency with which urinary tract infections (UTI), vesicoureteric reflux (VUR), and renal cortical scars coexist. In the early years, the presence of scars tended to be evaluated with intravenous urography (IVU), the best available tool at the time. More recently, scars have been more sensitively identified with 99mTc-labeled dimercaptosuccinic acid (DMSA), enhanced further with the use of single photon emission computed tomography (SPECT). Each requires an intravenous puncture and ionizing radiation, but placement of a bladder catheter is rarely required

First Author	Specialty of first author	Prospective versus retrospective	Year of publication	Number of patients	Number of kidneys	Population studied	Overall with reflux (%)	Overall with scars (%)	Scars in the population with VUR (%)	Scars in the population without VUR (%)	Period of follow-up
Kunin (1)	Preventive medicine	R	1964	107	NA	School age children with UTI	19%	13% (IVU)	NA	NA	NA
Smellie (16)	Pediatrics	R	1964	200	NA	3 days–12 years	34%	17% (IVU)	NA	NA	NA
Rolleston (30)	Radiology	P	1970	175	350	3 days–12 months UTI without obstruction	49%	NA	22% (IVU)	NA	5 years
Pylkkanon (31)	NA	P	1981	252	NA	Infants and children with UTI	8%	3% (IVU)	40%	0%	2 years
Bourchier (32)	NA	R	1984	100	NA	Infants with UTI	36%	10% (IVU)	NA	NA	NA
Jakobsson (34)	Pediatrics	P	1992	106	NA	0–15.9 years with symptomatic UTI	25%	52% (DMSA)	88%	40%	2 months
Ditchfield (33)	Radiology	P	1994	150	300	>5 years	33%	NA	NA	NA	NA
Benador (6)	Pediatrics	P	1997	107	NA	0–16 years	36%	60%	63%	63%	2+ months
Jakobsson (33)	Pediatrics	P	1997	185	NA	UTI in child <10 years	37%	36%	51%	27%	2 years
Wennerstrom (35)	Pediatrics	P	1998	688	NA	0–15 years with first symptomatic UTI	33%	11% (IVU)	26%	3%	NA
Gelfand (28)	Radiology	P	2000	919	NA	birth–>10 years UTI, separated by age 0–1 year $ 10 years	29% 46% 18%	NA	NA	NA	NA

Table 38.1. *Continued*

First Author	Specialty of first author	Prospective versus retrospective	Year of publication	Number of patients	Number of kidneys	Population studied	Overall with reflux (%)	Overall with scars (%)	Scars in the population with VUR (%)	Scars in the population without VUR (%)	Period of follow-up
Honkinen (2)	Pediatrics	R	2000	134	NA	UTI with bacteriuria (from birth to 15 years) 1 week–3 months 3–11 months $ 12 months	33% 41% 56%	NA	NA	NA	NA
Smellie (36)	Pediatrics	P	2001	228 149	NA	Infants and children with UTI who were found to have reflux with follow-up at 5 and 10 years			43% 42% (DMSA)		5 years 10 years
Ilyas (29)	Nephrology	R	2002	208	NA	>2 years 2–8 years >8 years	51% 47% 28%	NA	NA	NA	NA
Moorthy (37)	Radiology	R	2005	108	216	<1 year with UTI	12% of kidneys	4% (DMSA)	16%	2%	NA
Gonzalez (38)	Pediatrics	P	2005	161	322	0–11.2 years with defects on DMSA during UTI	28%	32%	(varies with> 60% reflux grade)	47%	
Garin (39)	Pediatrics	P	2006	218	NA	3 months–18 years with defects on DMSA during UTI (excludes reflux $ gr. IV)	52%	24%	NA	NA	1 year

Abbreviations: R=retrospective; P=prospective; IVU=intravenous urogram or pyelogram.

Table 38.2. Reference standard test and diagnostic test performance for the detection of UTI, pyelonephritis, renal scar, and VUR in infants and children

Test	Sensitivity (%)	Specificity (%)	Reference standard	References
UTI			Urine culture	
Cloudy appearing urine	90	72–82		
Urine dip stick*	96	99		
Urine culture (clean catch)	75–100	57–100		
Pyelonephritis			DMSA	
Fever >38.1°C	47	56		
Fever ≥39°C for 2 days (age <2 years)	95	31		
Ultrasound (with Power Doppler)	57	82		(107)
DMSA	50–91	–		(4)
CT or MRI	87–92	88–94		(107)
Renal or bladder congenital anomalies, obstruction			US	
VUR			VCUG	
RNC (radionuclide cystogram)	50–87	88		(141)
US	18	88		(142)
	50	77		(143)
Renal scarring			DMSA	
DMSA nuclear scintigraphy	94	100		(144)
Ultrasound				(145)
Diffuse scarring	47	92		
Focal scarring	5	98		
MRI^	77	87		(146)

*Positive for protein, leukocyte esterase, and nitrate
^MRI without gadolinium compared to DMSA as the gold standard (146)
Data from Whiting et al. (57) unless otherwise stated.

Figures 38.1 and 38.2 show flowcharts that provide a strategy for the imaging evaluation of male and female infants and children; Fig. 38.1 assumes the use of prophylactic antibiotics, and Fig. 38.2 assumes that prophylactic antibiotics will not be used.

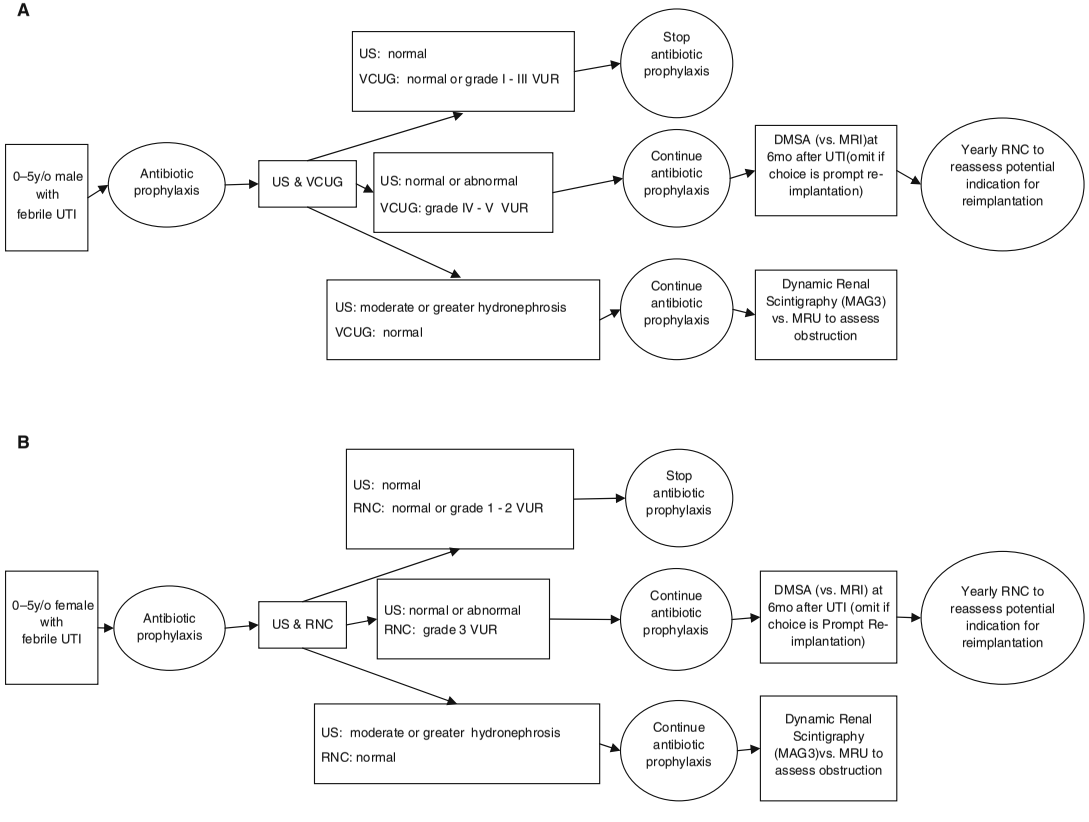

Figure 38.1. These flowcharts provide a strategy for the imaging evaluation of male (**A**) and female (**B**) infants and children. These flowcharts assume that the use of prophylactic antibiotic is of no demonstrable benefit in improving overall outcomes but remains commonly used. (US = ultrasound, VCUG = voiding cystourethrogram, DMSA = 99mTc-labeled dimercaptosuccinic acid, MRI = magnetic resonance imaging, MAG3 = 99mTc-labeled mercaptoacetyltriglycine, MRU = magnetic resonance urography, RNC = radionuclide cystogram).

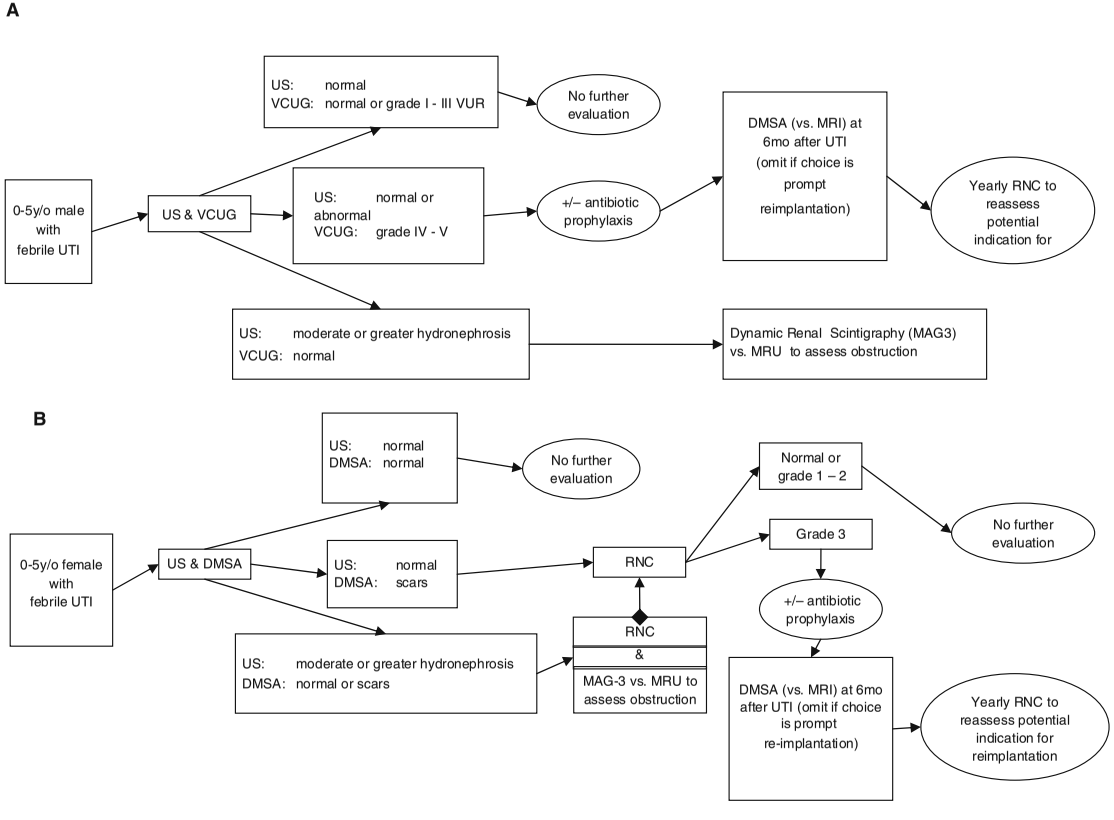

Figure 38.2. These flowcharts are a modified version of those in Fig. 38.1 and do not use prophylactic antibiotics. (US = ultrasound, VCUG = voiding cystourethrogram, DMSA = 99mTc-labeled dimercaptosuccinic acid, MRI = magnetic resonance imaging, MAG3 = 99mTc-labeled mercaptoacetyltriglycine, MRU = magnetic resonance urography, RNC = radionuclide cystogram).

Imaging Case Studies

Case 1

Figure 38.3 shows the case of an adolescent boy who first presented at 14 years of age with a UTI and hematuria.

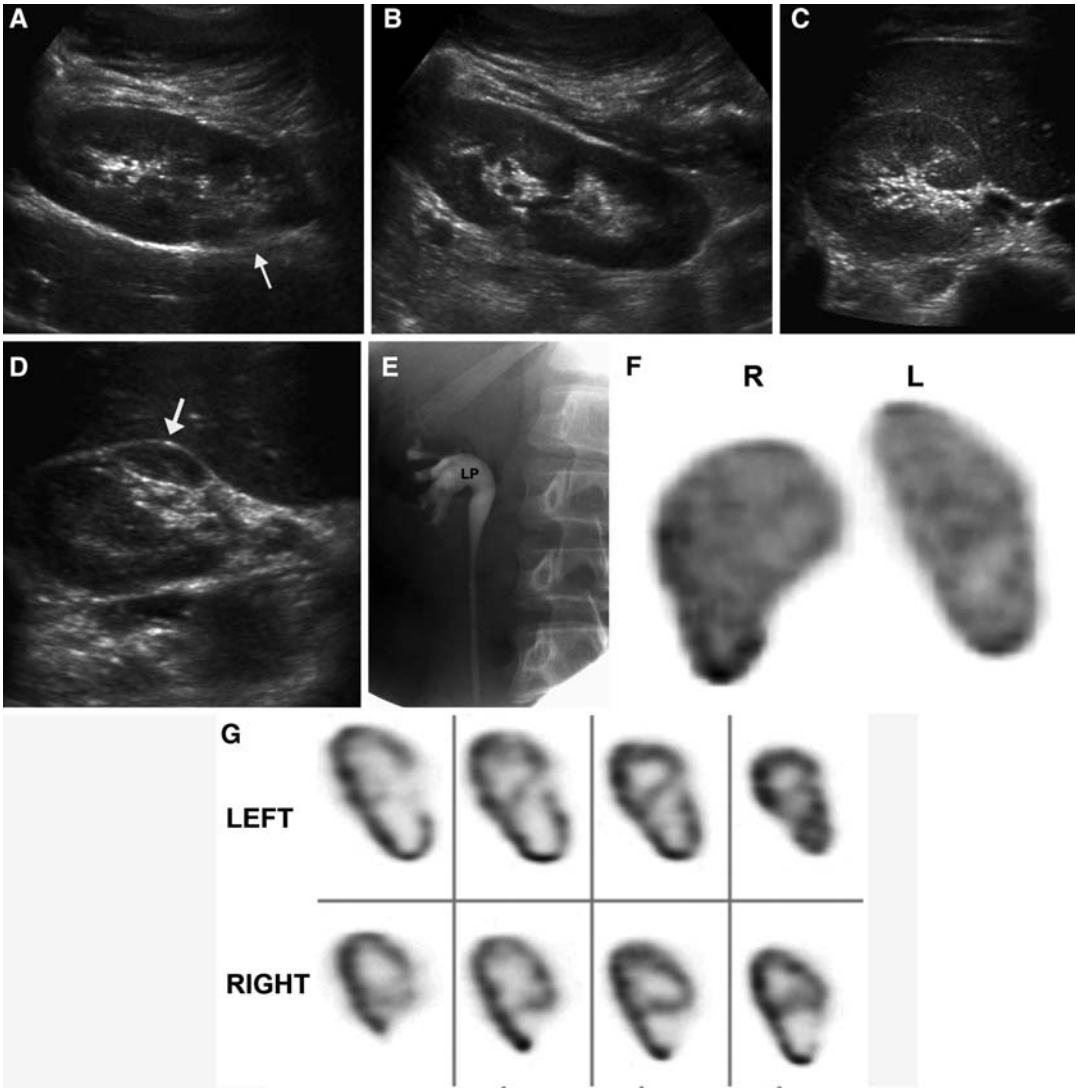

Figure 38.3. These series of images were performed over a period of 3 months for evaluation of an adolescent boy who first presented at 14 years of age with a UTI and hematuria. Evaluation began with ultrasound, where it was suspected that the right kidney contained a duplex collecting system and there was evidence for associated right lower pole scarring (**A**, prone sagittal view of the right kidney, *arrow* indicates site of focal cortical thinning; **B**, prone sagittal view of normal appearing left kidney; **C**, normal transverse view if the upper pole of the right kidney; **D** transverse view of the scarred right lower pole, *arrow* indicates site of anterior cortical thinning), raising the question of VUR into the lower moiety, which was subsequently proved by VCUG (**E**, LP = lower pole). Tc-99m DMSA confirmed the suspicion of right lower pole scarring on reconstructed (**F**) and source SPECT views (**G**).

Case 2

Figure 38.4 shows the case of a boy who first presented at 4 years of age for evaluation after a sibling was found to have VUR.

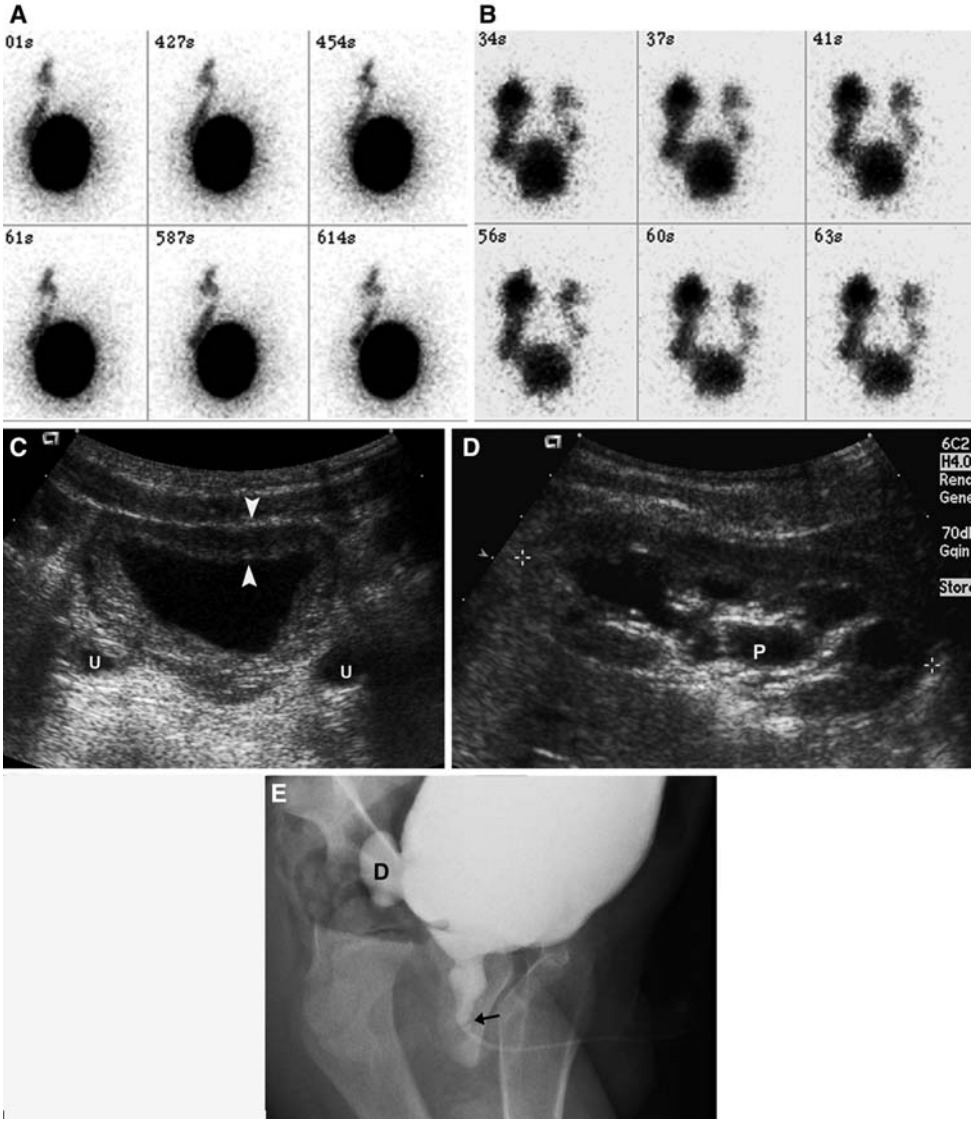

Figure 38.4. This example is a lesson in the importance of careful evaluation of urethral anatomy in boys. Interestingly, this little boy first presented at 4 years of age for evaluation after a sibling was found to have VUR. Radionuclide cystogram demonstrated left grade 2 VUR on prone views (**A**), which had become bilateral and increased in grade 1 year later (**B**). Subsequent reimplantation was performed and a postoperative ultrasound revealed bilateral, distal hydroureter, bladder wall thickening, and persistent hydronephrosis (**C**) transverse view of the urinary bladder, u = distal hydroureter, *arrowheads* indicate a thickened bladder wall; **D**, prone, sagittal view of the moderately hydronephrotic right kidney, p = dilated renal pelvis. Subsequent VCUG (**E**) revealed the presence of previously unrecognized posterior urethral valves (*arrow*) and a moderate-sized bladder diverticulum (D = diverticulum). Theoretically, progression of VUR and subsequent ureteral reimplantation may have been avoided had the presence of posterior urethral valves been recognized and addressed.

Case 3

Figure 38.5 shows a case of a 2-month-old female infant who presented with a febrile UTI.

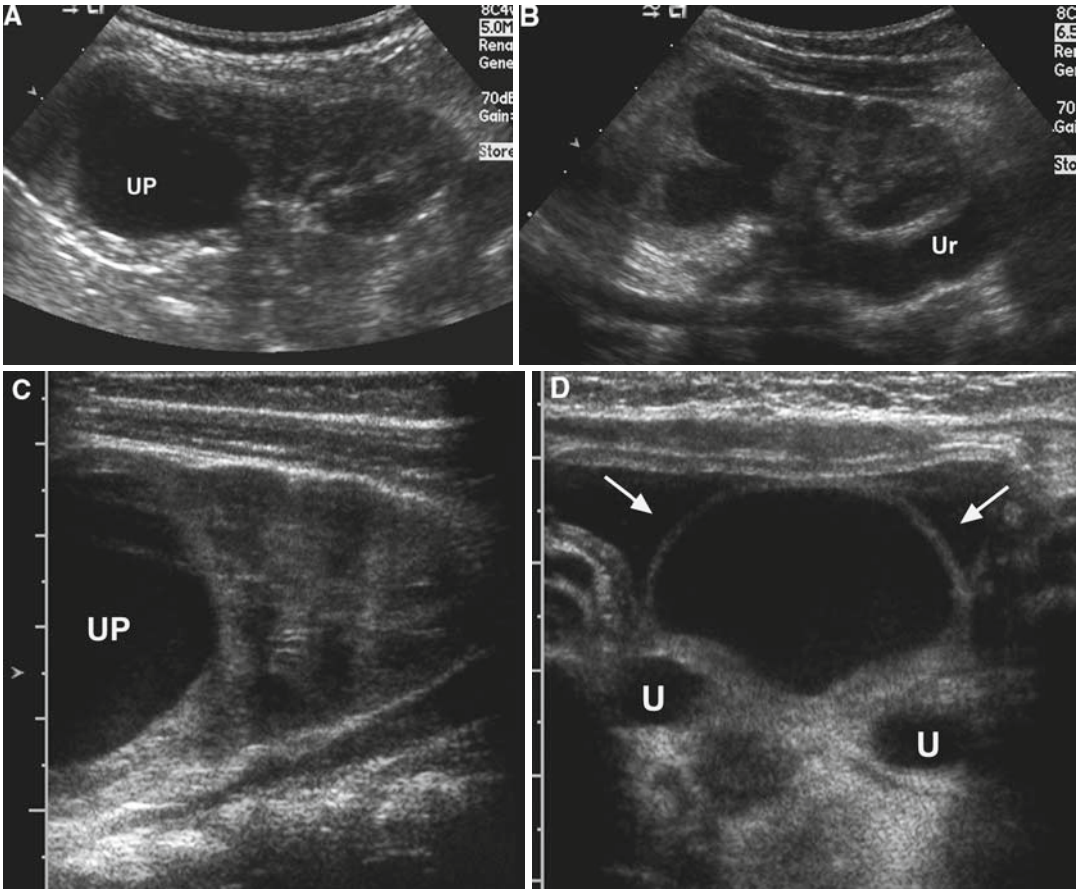

Figure 38.5. This 2-month-old female infant presented with a febrile UTI, where her initial ultrasound demonstrated the presence of a duplex left kidney, with upper pole hydroureteronephrosis (**A–C**, sagittal views of the left kidney demonstrating a dilated upper pole pelvis (UP) and dilated upper pole ureter (Ur)), associated with a moderately large ureterocele and bilateral, distal hydroureter (**D**, transverse view of the bladder demonstrating dilated distal ureters (u) and a ureterocele (*arrows*)). VCUG performed on the same day reveals a filling defect within the urinary bladder on early-fill views of the bladder (**E**, arrowheads outline left ureterocele) and on an oblique view of the right side (**F**, arrowhead = left ureterocele, arrow = refluxing right ureter), with the additional observation of high-grade VUR on the right (**G**, B = bladder, RU = dilated, refluxing right ureter). With voiding, the ureterocele prolapsed into the urethra (**H**, arrowheads = ureterocele prolapsing into the urethra). Subsequent Tc-99m DMSA, both routine (**I**) and pinhole views (**J**), revealed a photopenic defect in the left upper pole. Without the ultrasound and VCUG findings, this may have been difficult to differentiate from a large focal scar. With the identification of a complex anatomic anomaly by ultrasound, it was important to redirect from RNC to VCUG to demonstrate the finer points of urinary tract anatomy that could not have been fully discerned by RNC. This is one of only a few situations where VCUG, rather than RNC, is preferable in girls and can be determined based on information provided by ultrasound.

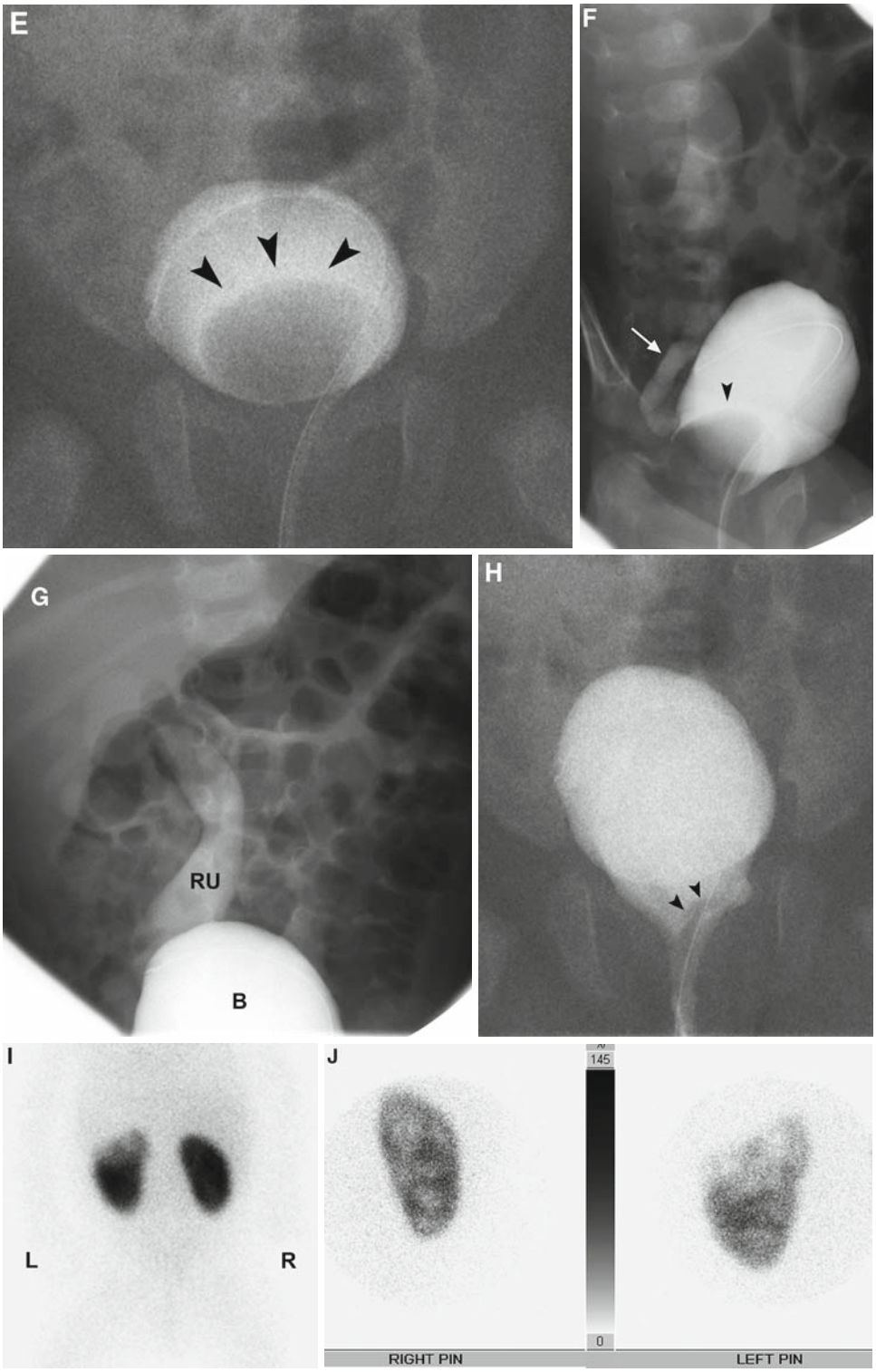

Figure 38.5. *Continued*

Case 4

Figure 38.6 shows a case of a 4-year-old little girl who presented with a febrile UTI and was found to have VUR.

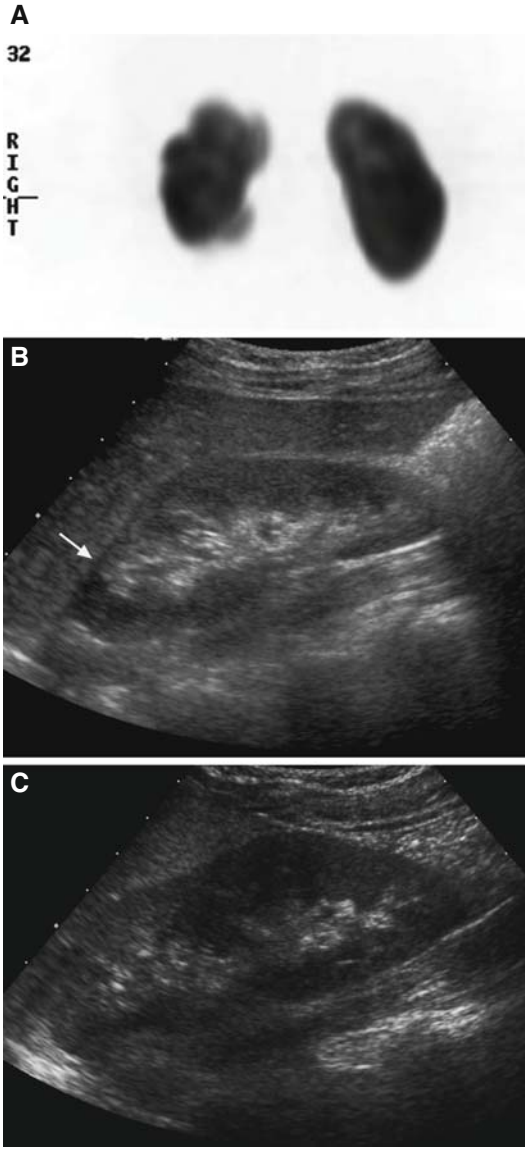

Figure 38.6. This 4-year-old little girl presented with a febrile UTI and was found to have VUR. Tc-99m DMSA revealed evidence of scarring of both the upper and lower poles of the right kidney, but no scars on the left (**A**). These scars were only faintly discernible on ultrasound, and perhaps only with knowledge of the Tc-99m DMSA findings (**B**, sagittal view of the right kidney, *arrow* = subtle, focal area of cortical thinning; **C**, sagittal view of the normal left kidney).

Case 5

Figure 38.7 shows the case of a male fetus who was revealed to have bilateral hydronephrosis that was followed periodically throughout pregnancy and was last imaged prior to delivery at 35 weeks gestation. Figure 38.8 shows postnatal ultrasound views of the kidney obtained at 2 weeks of age, after the fetal diagnosis of hydronephrosis.

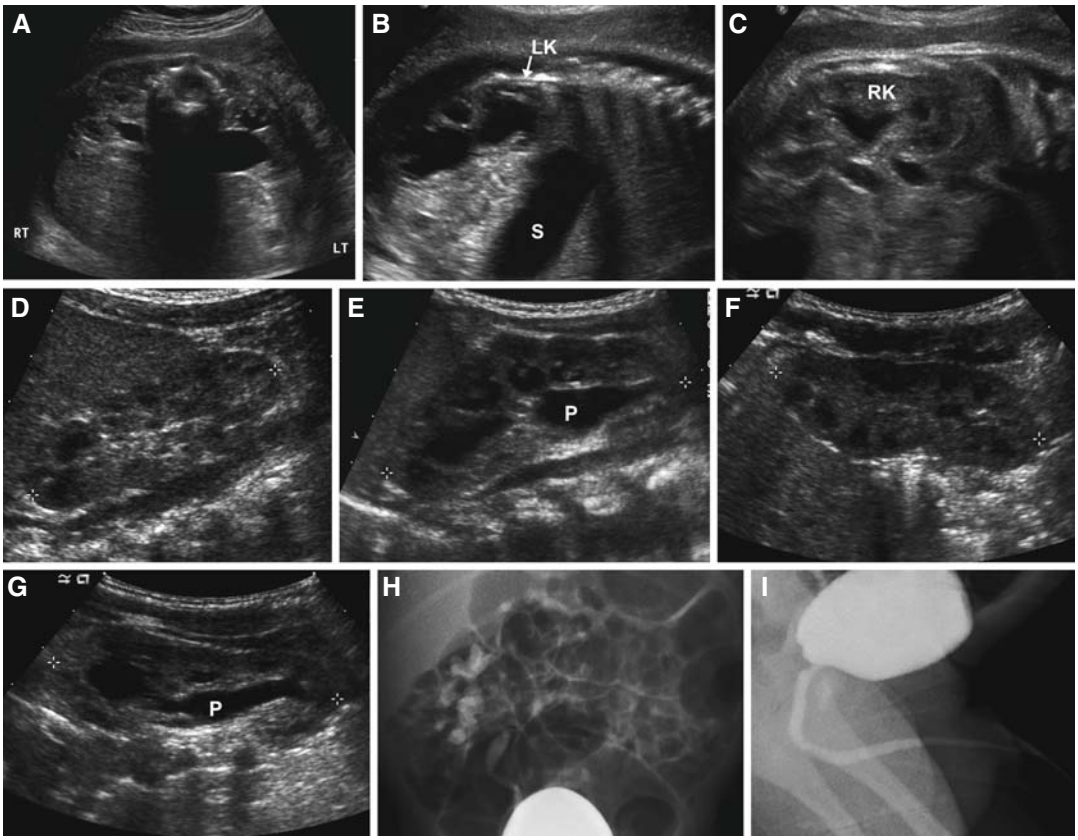

Figure 38.7. Routine prenatal ultrasound screening of this male fetus revealed bilateral hydronephrosis that was followed periodically throughout pregnancy and was last imaged prior to delivery at 35 weeks gestation (**A**, transverse view showing mild right and moderate left hydronephrosis; **B**, sagittal view of the moderately hydronephrotic left fetal kidney, S = stomach, LK = left kidney; **C**, sagittal view of the mildly hydronephrotic right fetal kidney, RK = right kidney). After delivery, at 3 weeks of life, postnatal renal ultrasound revealed a normal appearing right kidney and mild to moderate left hydronephrosis (**D**, supine view of normal right kidney; **E**, supine view of moderately hydronephrotic left kidney; **F**, prone view of normal right kidney; **G**, prone view of moderately hydronephrotic left kidney). VCUG on the same day as the ultrasound revealed grade III VUR on the right (the side where the postnatal ultrasound had been normal) (**H**) and no VUR on the left (implying the presence of some degree of obstruction at the level of the left ureteropelvic junction). The urethra was normal (**I**). This example illustrates the great challenge in predicting or excluding the presence of VUR on ultrasound alone.

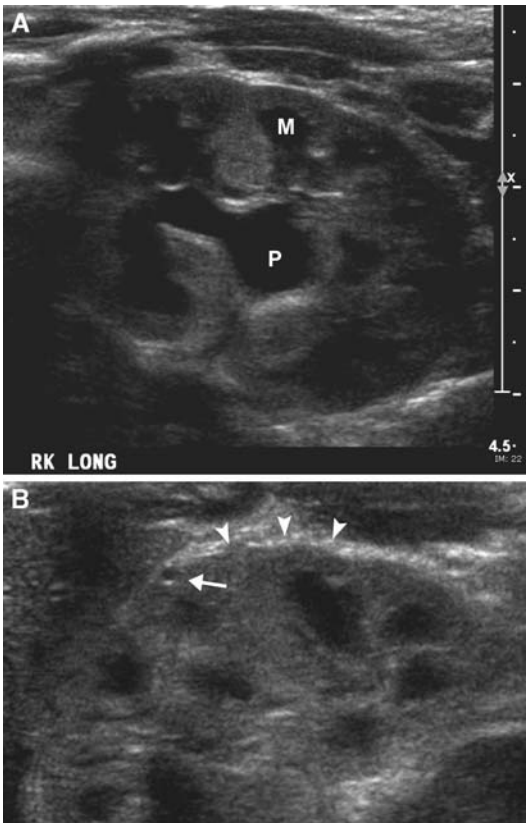

Figure 38.8. These postnatal ultrasound views of the kidney were obtained at 2 weeks of age, after the fetal diagnosis of hydronephrosis. At worst, one might describe this as mild to moderate hydronephrosis (**A**, p = renal pelvis, m = medullary pyramid). Nonetheless, high detail views reveal several very tiny cortical cysts along the renal cortical surface (**B**, arrow = tiny cyst, arrowheads = cortical surface of kidney). These subtle findings suggest the possibility of renal dysplasia and probably warrant formal evaluation for VUR, with VCUG in males, to exclude the possibility of posterior urethral valves, and RNC in girls, minimizing radiation exposure.

Suggested Imaging Protocols for Urinary Tract Infections in Infants and Children

See Figs. 38.1 and 38.2.

Future Research

- Large, multi-center, prospective, controlled studies of infants and children with carefully diagnosed UTI, assessing the controversies of (a) prophylactic antibiotic use, and (b) whether surgical or endoscopic management of VUR provides improved renal function and decreased recurrent UTI.
- Development of non-imaging predictors of risk of UTI and/or progression of renal impairment after UTI.
- Standardization of prenatal evaluation of fetal and postnatal hydronephrosis, to predict outcome.
- Development of a standardized, automated protocol for MRU in infants and children.

References

1. Kunin CM, Deutscher R, Paquin A, Jr. Medicine 1964; 43:91–130.
2. Honkinen O, Jahnukainen T, Mertsola J, Eskola J, Ruuskanen O. Pediatr Infect Dis J 2000; 19:630–634.
3. Marcus N, Ashkenazi S, Yaari A, Samra Z, Livni G. Pediatr Infect Dis J 2005; 24:581–585.
4. Rushton HG, Majd M. J Urol 1992; 148: 1726–1732.
5. Jakobsson B, Soderlundh S, Berg U. Arch Dis Child 1992; 67:1338–1342.
6. Benador D, Benador N, Slosman D, Mermillod B, Girardin E. Lancet 1997; 349:17–19.
7. Stokland E, Hellstrom M, Jacobsson B, Jodal U, Sixt R. J Pediatr 1996; 129:815–820.
8. Roberts JA. J Urol 1983; 129:1102–1106.
9. Roberts JA, Suarez GM, Kaack B, Kallenius G, Svenson SB. J Urol 1985; 133:1068–1075.
10. Risdon RA, Yeung CK, Ransley PG. Clin Nephrol 1993; 40:308–314.
11. http://kidney.niddk.nih.gov/Kudiseases/pubs/vesicoureteralreflux/
12. Marild S, Jodal U. Acta Paediatr 1998; 87: 549–552.
13. Hoberman A, Wald ER. Pediatr Infect Dis J 1997; 16:11–17.
14. Hoberman A, Charron M, Hickey RW, Baskin M, Kearney DH et al. NE J Med 2003; 348: 195–202.
15. Chen L, Baker MD. Pediatr Emerg Care 2006; 22:485–487.
16. Smellie JM, Hodson CJ, Edwards D, Normand IC. Br Med J 1964; 2:1222–1226.
17. Wiswell TE, Roscelli JD. Pediatrics 1986; 78: 96–99.
18. Herzog LW. Am J Dis Child 1989; 143:348–350.
19. Schoen EJ, Colby CJ, Ray GT. Pediatrics 2000; 105:789–793.

20. Zorc JJ, Levine DA, Platt SL et al. Pediatrics 2005; 116:644–648.
21. Mingin GC, Hinds A, Nguyen HT, Baskin LS. Urology 2004; 63:562–565; discussion 565.
22. Sargent MA. Pediatr Radiol 2000; 30:587–593.
23. Peters PC, Johnson DE, Jackson JH, Jr. J Urol 1967; 97:259–260.
24. Iannaccone G, Panzironi PE. Acta Radiologica 1955; 44:451–456.
25. Gibson HM. J Urol 1949; 62:40–43.
26. Forsythe WI, Whelan RF. Br J Urol 1958; 30: 189–197.
27. Krepler P. Zeitschrift fur Kinderheilkunde 1968; 104:103–114.
28. Gelfand MJ, Koch BL, Cordero GG, Salmanzadeh A, Gartside PS. Pediatr Radiol 2000; 30:121–124.
29. Ilyas M, Mastin ST, Richard GA. Pediatr Nephrol 2002; 17:30–34.
30. Rolleston GL, Shannon FT, Utley WL. Br Med J 1970; 1:460–463.
31. Pylkkanen J, Vilska J, Koskimies O. Acta Paediatrica Scandinavica 1981; 70:879–883.
32. Bourchier D, Abbott GD, Maling TM. Arch Dis Child 1984; 59:620–624.
33. Ditchfield MR, De Campo JF, Cook DJ et al. Radiology 1994; 190:413–415.
34. Jakobsson B, Svensson L. Acta Paediatrica 1997; 86:803–807.
35. Wennerstrom M, Hansson S, Jodal U, Stokland E. Arch Pediatr Adolesc Med 1998; 152: 879–883.
36. Smellie JM, Jodal U, Lax H, Mobius TT, Hirche H et al. J Pediatr 2001; 139:656–663.
37. Moorthy I, Easty M, McHugh K, Ridout D, Biassoni L et al. Arch Dis Child 2005; 90:733–736.
38. Gonzalez E, Papazyan JP, Girardin E. J Urol 2005; 173:571–574; discussion 574–575.
39. Garin EH, Olavarria F, Garcia Nieto V, Valenciano B, Campos A et al. Pediatrics 2006; 117:626–632.
40. Chandra M, Maddix H, McVicar M. J Urol 1996; 155:673–677.
41. Sillen U. Pediatr Nephrol 1999; 13:355–361.
42. Silva JM, Oliveira EA, Diniz JS et al. Pediatr Nephrol 2006; 21:510–516.
43. Connolly LP, Treves ST, Connolly SA et al. J Urol 1997; 157:2287–2290.
44. Noe HN. J Urol 1992; 148:1739–1742.
45. http://emedicine.medscape.com/article/439403-overview
46. Craig JC, Irwig LM, Knight JF, Roy LP. J Paediatr Child Health 1997; 33:434–438.
47. Stark H. Pediatr Nephrol 1997; 11:174–177; discussion 180–171.
48. Cohen AL, Rivara FP, Davis R, Christakis DA. Pediatrics 2005; 115:1474–1478.
49. Practice parameter: the diagnosis, treatment, and evaluation of the initial urinary tract infection in febrile infants and young children. American Academy of Pediatrics. Committee on Quality Improvement. Subcommittee on Urinary Tract Infection. Pediatrics 1999; 103: 843–852.
50. Armstrong EP. Am J Manag Care 2001; 7: 269–280.
51. Conway PH, Edwards S, Stucky ER, Chiang VW, Ottolini MC et al. Pediatrics 2006; 118: 441–447.
52. Altemeier WA, 3rd. Pediatr Ann 1999; 28: 663–664.
53. Dick PT, Feldman W. J Pediatr 1996; 128:15–22.
54. Newman TB. Pediatrics 2005; 116:1613–1614.
55. Garin EH, Young L. Pediatrics 2007; 120: 249–250.
56. Greenfield SP, Chesney RW, Carpenter M et al. J Urol 2008; 179:405–407.
57. Whiting P, Westwood M, Bojke L et al. Health Technology Assessment 2006; 10: iii–iv, xi–xiii, 1–154.
58. Verrier Jones K. Arch Dis Child 2005; 90: 663–664.
59. Rosenheim ML. In The Richard Bright Memorial Lecture, delivered on the occasion of the Bright Centenary Celebrations at Guy's Hospital Medical School, 1958; 403–423.
60. Bailey RR. Clin Nephrol 1973; 1:132–141.
61. Oh MM, Jin MH, Bae JH, Park HS, Lee JG, Moon du G. J Urol 2008; 180:2167–2170.
62. Wheeler D, Vimalachandra D, Hodson EM, Roy LP, Smith G et al. Arch Dis Child 2003; 88: 688–694.
63. Craig JC, Irwig LM, Knight JF, Roy LP. Pediatrics 2000; 105:1236–1241.
64. Nguyen HT, Bauer SB, Peters CA et al. J Urol 2000; 164:1674–1678; discussion 1678–1679.
65. Schwab CW, Jr., Wu HY, Selman H, Smith GH, Snyder HM, 3rd et al. J Urol 2002; 168: 2594–2599.
66. Silva JM, Diniz JS, Lima EM, Vergara RM, Oliveira EA. BJU Int 2006; 97:1063–1068.
67. Connolly LP, Treves ST, Zurakowski D, Bauer SB. J Urol 1996; 156:1805–1807.
68. Esbjorner E, Berg U, Hansson S. Pediatr Nephrol 1997; 11:438–442.
69. Lagomarsimo E, Valenzuela A, Cavagnaro F, Solar E. Pediatr Nephrol 1999; 13:288–291.
70. Bell C. Account of the muscles of the ureters; and their effects in the irritable states of the bladder, 1812.
71. Olbing H, Claesson I, Ebel KD et al. Renal scars and parenchymal thinning in children with vesicoureteral reflux: a 5-year report of the International Reflux 72.

69. Piepsz A, Tamminen-Mobius T, Reiners C, et al. Eur J Pediatr 1998; 157:753–758.
73. Smellie JM, Barratt TM, Chantler C et al. Lancet 2001; 357:1329–1333.
74. Jodal U, Smellie JM, Lax H, Hoyer PF. Pediatr Nephrol 2006; 21:785–792.
75. Prospective trial of operative versus non-operative treatment of severe vesicoureteric reflux: 2 years' observation in 96 children. British Medical Journal (Clinical Research Ed.) 1983; 287: 171–174.
76. Prospective trial of operative versus non-operative treatment of severe vesicoureteric reflux in children: 5 years' observation. Birmingham Reflux Study Group. British Medical Journal (Clinical Research Ed.) 1987; 295: 237–241.
77. Le Saux N, Pham B, Moher D. CMAJ 2000; 163:523–529.
78. Thompson RH, Chen JJ, Pugach J, Naseer S, Steinhardt GF. Urology 2001; 166:1465–1469.
79. Williams G, Lee A, Craig J. J Pediatr 2001; 138:868–874.
80. Hellerstein S, Nickell E. Pediatr Nephrol 2002; 17:506–510.
81. Wald ER. Pediatrics 2006; 117:919–922.
82. Georgaki-Angelaki H, Kostaridou S, Daikos GL et al. Scand J Infect Dis 2005; 37:842–845.
83. Faust WC, Pohl HG. Curr Opin Urol 2007; 17:252–256.
84. Conway PH, Cnaan A, Zaoutis T, Henry BV, Grundmeier RW et al. JAMA 2007; 298: 179–186.
85. Lee SJ, Shim YH, Cho SJ, Lee JW. Pediatr Nephrol 2007; 22:1315–1320.
86. Larcombe J. Clin Evid 2005:444–457.
87. Al-Sayyad AJ, Pike JG, Leonard MP. J Urol 2005; 174:1587–1589; discussion 1589.
88. Roussey-Kesler G, Gadjos V, Idres N et al. J Urol 2008; 179:674–679; discussion 679.
89. Hitzel A, Liard A, Vera P, Manrique A, Menard JF et al. J Nucl Med 2002; 43:27–32.
90. Westwood ME, Whiting PF, Cooper J, Watt IS, Kleijnen J. BMC Pediatr 2005;15:2
91. Podberesky DJ, Unsell BJ, Gunderman R et al. Urinary tract infection – child. [online publication]. Reston (VA): American College of Radiology (ACR) 7 p. [70 references]. In Imaging EPoP, ed., 2006.
92. Fernbach SK, Maizels M, Conway JJ. Pediatr Radiol 1993; 23:478–480.
93. Blane CE, DiPietro MA, Zerin JM, Sedman AB, Bloom DA. J Urol 1993; 150:752–755.
94. DiPietro MA, Blane CE, Zerin JM. Radiology 1997; 205:821–822.
95. Davey MS, Zerin JM, Reilly C, Ambrosius WT. Pediatr Radiol 1997; 27:908–911.
96. Rickwood AM, Carty HM, McKendrick T et al. BMJ 1992; 304:663–665.
97. Tibballs JM, De Bruyn R. Arch Dis Child 1996; 75:444–447.
98. Yerkes EB, Adams MC, Pope JCT, Brock JW, 3rd. J Urol 1999; 162:1218–1220.
99. Jaswon MS, Dibble L, Puri S et al. Fetal Neonatal Edn 1999; 80:F135–F138.
100. Brophy MM, Austin PF, Yan Y, Coplen DE. J Urol 2002; 168:1716–1719; discussion 1719.
101. Phan V, Traubici J, Hershenfield B, Stephens D, Rosenblum ND et al. Pediatr Nephrol 2003; 18:1224–1228.
102. Anderson NG, Allan RB, Abbott GD. Pediatr Nephrol 2004; 19:749–753.
103. Grattan-Smith JD. Pediatr Radiol 2008; 38(Suppl 2):S275–S280.
104. Jones RA, Schmotzer B, Little SB, Grattan-Smith JD. Pediatr Radiol 2008; 38(Suppl 1):S18–S27.
105. Kirsch AJ, Grattan-Smith JD, Molitierno JA, Jr. Curr Opin Urol 2006; 16:283–290.
106. Lonergan GJ, Pennington DJ, Morrison JC, Haws RM, Grimley MS et al. Radiology 1998; 207:377–384.
107. Majd M, Nussbaum Blask AR, Markle BM, et al. Radiology 2001; 218:101–108.
108. Agarwal R, Brunelli SM, Williams K, Mitchell MD, Feldman HI et al. Nephrol Dial Transplant, 2008.
109. Lavocat MP, Granjon D, Allard D, Gay C, Freycon MT et al. Pediatr Radiol 1997; 27: 159–165.
110. Vates TS, Shull MJ, Underberg-Davis SJ, Fleisher MH. J Urol 1999; 162:1221–1223.
111. Barnewolt CE, Paltiel HJ, Lebowitz RL, Kirks DR. In Kirks DR (ed.). Practical Pediatric Imaging – Diagnostic Radiology of Infants and Children, 3rd ed. Philadelphia: Lippincott Raven, 1998; 1010–1019.
112. Goldraich NP, Goldraich IH. J Urol 1992; 148:1688–1692.
113. NICE Clinical Guideline 54. Urinary tract infection in children: diagnosis, treatment and long-term management. National Institute for Health and Clinical Excellence, developed by the National Collaborating Centre for Women's and Children's Health, August 2007. [online publication]. London, UK.
114. Smellie JM, Rigden SP, Prescod NP. Arch Dis Child 1995; 72:247–250.
115. Gelfand MJ, Barr LL, Abunku O. Pediatr Radiol 2000; 30:665–670.
116. Hohenfellner K, Seemayer S, Stolz G et al. Klin Padiatr 2000; 212:320–325.
117. http://rad.usuhs.edu/medpix/medpix_home.html?mode=display_factoid&recnun=2800 .
118. Ward VL. Pediatr Radiol 2006; 36:168–172.

119. Ward VL, Barnewolt CE, Strauss KJ et al. Radiology 2006; 238:96–106.
120. Ward VL, Strauss KJ, Barnewolt CE et al. Radiology 2008; 249:1002–1009.
121. Vachvanichsanong P, Dissaneewate P, Thongmak S, Lim A. Nephrology (Carlton) 2008; 13:38–42.
122. Christian MT, McColl JH, MacKenzie JR, Beattie TJ. Arch Dis Child 2000; 82:376–380.
123. Bjorgvinsson E, Majd M, Eggli KD. Am J Roentgenol 1991; 157:539–543.
124. Benador D, Benador N, Slosman DO, Nussle D, Mermillod B et al. J Pediatr 1994; 124:17–20.
125. Preda I, Jodal U, Sixt R, Stokland E, Hansson S. J Pediatr 2007; 151:581-584, 584 e581.
126. Cascio S, Chertin B, Colhoun E, Puri P. J Urol 2002; 168:1708–1710; discussion 1710.
127. Jakobsson B, Berg U, Svensson L. Arch Dis Child 1994; 70:111–115.
128. Rushton HG, Majd M, Jantausch B, Wiedermann BL, Belman AB. J Urol 1992; 147: 1327–1332.
129. Friedland GW, Cunningham J. Am J Roentgenol Radium Ther Nucl Med 1972; 116: 792–811.
130. Husmann D. In Gonzalez E, Bauer S (eds.). Pediatric Urology Practice. Philadelphia: Lippincott Williams & Wilkins, 1999; 295–311.
131. Treves ST, Gelfand MJ, Willi UV. In Treves ST (ed.). Pediatric Nuclear Medicine, 2nd ed. New York, NY: Springer-Verlag, 1995; 411–429.
132. Rachmiel M, Aladjem M, Starinsky R, Strauss S, Villa Y et al. Pediatr Nephrol 2005; 20: 1449–1452.
133. Lee RS, Cendron M, Kinnamon DD, Nguyen HT. Pediatrics 2006; 118:586–593.
134. Ismaili K, Hall M, Piepsz A et al. J Pediatr 2006; 148:222–227.
135. Coelho GM, Bouzada MC, Lemos GS, Pereira AK, Lima BP et al. J Urol 2008; 179:284–289.
136. Walsh TJ, Hsieh S, Grady R, Mueller BA. Urology 2007; 69:970–974.
137. Estrada CR, Peters CA, Retik AB, Nguyen HT. J Urol 2009; 181:801–806; discussion 806–807.
138. Yeung CK, Godley ML, Dhillon HK, Gordon I, Duffy PG et al. Br J Urol 1997; 80:319–327.
139. Stock JA, Wilson D, Hanna MK. J Urol 1998; 160:1017–1018.
140. Hellerstein S. Curr Opin Pediatr 2000; 12: 125–128.
141. De Sadeleer, De Boe V, Keuppens F, Desprechins B, Verboven M et al. Eur J Nucl Med 1994;21;223–227.
142. Zamir G, Sakran W, Horowitz Y, Koren A, Miron D. Arch Dis Child 2004;89:466–468.
143. Alshamsam L, Harbi AA, Fakeeh K, Al Banyan E. Ann Saudi Med 2009;29:46–49.
144. Shanon A, Feldman W, McDonald P, Martin DJ, Matzinger MA et al. J Pediatr 1992;120:399–403.
145. Moorthy I, Wheat D, Gordon I. Pediatr Nephrol 2004;19:153–156.
146. Kavanagh EC, Ryan S, Awan A, McCourbrey S, O'Connor R et al. Pediatr Radiol 2005;35: 275–281.

39

Imaging of Female Children and Adolescents with Abdominopelvic Pain Caused by Gynecological Pathologies

Stefan Puig

Issues

I. What is the diagnostic performance of the different imaging studies for the diagnosis or exclusion of ovarian torsion?
II. What is the best imaging technique for the diagnosis of pelvic inflammatory disease (PID)?
III. What is the best imaging technique for the diagnosis of endometriosis?
IV. What is the best technique for the diagnosis of an ectopic pregnancy?

Key Points

- The clinical presentation of abdominopelvic pain and gonadal pathologies is often nonspecific and therefore difficult to diagnose (limited evidence).
- Surgical emergencies such as ovarian torsion should be considered when a girl presents with acute abdominopelvic pain (limited to moderate evidence).
- In menstruating girls and adolescents, pregnancy (orthotopic or ectopic) should be considered as a cause of abdominopelvic discomfort/pain (limited evidence).
- The initial imaging modality of choice for evaluating the uterus and adnexa is ultrasound (US) (limited to moderate evidence). If US is nondiagnostic and the clinical picture remains uncertain, MRI is the preferred next imaging test. CT may also be considered in patients with acute symptoms (limited evidence).

S. Puig (✉)
Research Programm on Evidence-Based Diagnostics, Institute of Public Health, Paracelsus Private Medical University, Salzburg A-500, Austria
e-mail: stefan.puig@pmu.ac.at

L.S. Medina et al. (eds.), *Evidence-Based Imaging in Pediatrics*,
DOI 10.1007/978-1-4419-0922-0_39,

- Other gynecological causes of abdominopelvic pain such as endometriosis and pelvic inflammatory disease have a significant impact on societal health care costs (limited to moderate evidence).
- Various complications associated with tumors may lead to acute abdominopelvic pain (limited evidence).

Definition

In general, acute pelvic or lower abdominal pain in girls (as in boys) is mainly associated with gastrointestinal disorders (1). However, it may be secondary to a wide range of gynecological disorders in girls and female adolescents (2). Therefore, a gynecological etiology should always be considered in young female patients with lower abdominal and/or pelvic discomfort or pain. In adolescents, a gynecological process is more commonly the cause for acute pain than appendicitis. Klein et al. found in 20% of girls older than 12 years of age a pelvic inflammation or gynecological process (including pregnancy) as a cause for pain, whereas appendicitis was only found in 4% (3). A gynecological problem (adnexitis or ovarian cysts) was identified in 12% of the populations studied by Puig et al., including children, adolescents, and young adults who received preoperative misdiagnosis of appendicitis and underwent a negative appendectomy (4). Specifically, in younger patients it is difficult to localize the pain during physical examination, making it a diagnostic challenge.

The presentation and types of pain from gynecologic infectious and inflammatory conditions are variable. It may be intermittent and localized to one quadrant; severe, acute, and generalized; crampy; chronic and cyclical; chronic and non-cyclical; or present as an acute abdomen. Nausea, vomiting, or bleeding may accompany the pain. In ovarian neoplasms, clinical presentation includes abdominal distension, a palpable abdominal mass, genitourinary symptoms, or constipation.

Gynecological conditions that should be considered and will be discussed in this chapter include congenital Müllerian anomalies, pelvic inflammatory disease, ovarian tumors, ovarian cysts, ovarian torsion, trauma, and pregnancy (2, 5).

Pathology and Epidemiology

Congenital Anomalies

Congenital anomalies of the Müllerian system are estimated to occur in approximately 0.1–1.5% of women in the general population and approximately 90% of these anomalies involve the uterus (6, 7). Girls with uterovaginal anomalies may present with pain and occasionally with an abdominal/pelvic mass due to vaginal obstruction. Because of the complexity of the embryology, obstruction may occur at different levels and in various degrees, including imperforate hymen, complete vaginal membrane, or atresia of the vagina and/or uterus (2, 5, 6). These conditions are usually encountered either in the neonatal period or in adolescence at the time of menarche (2). Hydrometrocolpos, backflow of uterine blood products into the fallopian tubes and adnexa, is associated with the development of endometriosis.

Endometriosis

Endometriosis is defined as the presence of endometrium-like tissue (endometrial glands) outside of the normal location in the uterus (8, 9). It is a relatively common disease affecting 0.5–15% of women, in general, and 25–80% of all women with pelvic pain and/or infertility (9–15). Endometriosis is the most common cause of pelvic pain, which may be non-cyclical (15). The true prevalence of endometriosis remains unclear (16). Estimates of prevalence range up to 10% in the general population. Large-scale studies suggest a prevalence of 0.5–5% in fertile and 25–40% in infertile women (17, 18). For adolescents, a prevalence of 25–38% of patients with pelvic pain has been reported. If the pain is persistent, the prevalence increases to 70–79% (19–23) (limited evidence). Although endometriosis is generally accepted to be associated with infertility, its actual impact on fecundity and the mechanisms underlying

this effect are less clear. Unfortunately, well-designed scientific studies are lacking on this issue (16, 24).

Pelvic Inflammatory Disease

Pelvic inflammatory disease (PID) is associated with *Chlamydia trachomatis* and *Neisseria gonorrhoeae* infections, and therefore the incidence increases with sexual activity (25–27). *Mycoplasma genitalium* and microorganisms of the vaginal flora including anaerobes, streptococci, staphylococci, *Escherichia coli*, and *Haemophilus influenzae* might also be implicated in the etiology of the disease. However, the importance of the different pathogens varies in different countries and regions (27). The infection spreads from the vagina to the fallopian tubes and leads to pelvic pain, vaginal discharge or dyspareunia, endometritis, salpingitis, parametritis, oophoritis, tubo-ovarian abscess, and/or pelvic peritonitis (27). In a large British screening study, the prevalence of Chlamydia was 6.2% (95% CI, 4.9–7.8%) in 16–24-year-old women and 5.3% (95% CI, 4.4–6.3%) in men (28). Factors associated with PID are related to sexual behavior (young age, multiple partners, recent new partners in the previous 3 months, past history of sexually transmitted disease) and interruption of the cervical barrier (e.g., termination of pregnancy, insertion of an intrauterine device within the past 6 weeks, hysterosalpingography, in vitro fertilization, and intrauterine insemination) (27).

When present, clinical symptoms and signs in PID lack sensitivity. Compared to laparoscopic diagnosis, the positive predictive value of a clinical diagnosis of PID is 65–90% (27, 29–31). The clinical diagnosis includes a broad range of differential diagnoses: ectopic pregnancy, acute appendicitis, endometriosis, irritable bowel syndrome, complications of an ovarian cyst (e.g., rupture, torsion), or functional pain (pain of unknown physical origin) (27).

Adnexal Torsion

Adnexal torsion is defined as a complete or partial rotation of the ovary and/or fallopian tube including the vascular pedicle (32). While ovarian torsion is the twisting of an ovary on its ligamentous supports, which might result in a compromised blood supply, the term adnexal torsion describes a twisting of either the ovary or fallopian tube, or both. Concomitant torsion of an ovary and the ipsilateral fallopian tube occurs in up to 67% of patients with adnexal torsion (32–34). It is an important cause of abdominal pain, which may lead to initial compromise of the lymphatic and venous drainage, later to arterial occlusion and thrombosis, resulting in a hemorrhagic infarction (2, 25, 35). It may occur at any age, most commonly in the first two decades of life (2). Some authors reported a peak incidence after menarche (25) and others reported the highest prevalence in pregnant women with a peak of 17–20% (32, 36–39). Adnexal torsion is supposed to account for up to 2.7% of all cases with acute abdominal pain in children, and is the fifth most common gynecologic emergency with a reported incidence of 3% in one series of acute gynecologic complaints (34, 40, 41). Despite the relatively uncommon nature of this condition, most reviews report three to five cases per year at large institutions (34, 42, 43). In any case, it is a medical/surgical emergency (25). Ovaries with any type of mass are predisposed to torsion (32, 33, 44). Torsion of normal ovaries is more common in adolescents. Postulated causes of normal adnexal torsion include mobile fallopian tubes or mesosalpinx, elongated pelvic ligaments, fallopian tube spasm, strenuous exercise, or abrupt changes in intra-abdominal pressure (32, 34, 43, 45). A limited number of studies have shown that the right ovary is more likely to twist, because the space in the lesser pelvis occupied by the sigmoid colon may protect the left ovary (32, 33, 46, 47). Adnexal torsion is often misdiagnosed as appendicitis. In a retrospective study, Pomeranz and Sabnis found 38% of children with adnexal torsion and abdominal pain, who had the preliminary diagnosis of appendicitis (48).

Abdominopelvic Mass

Functional cysts, ovarian torsion, and benign neoplasms are the most common ovarian masses among young adolescents. In pubescent girls and adult women, ovarian follicle size is up to 2.5 cm; cysts larger than 4 cm generally require a follow-up sonogram at 2 or 6 weeks to ensure resolution (during a different point in the girl's menstrual cycle).

In younger children, the ovaries are a solid and homogenous structure, which may contain primordial follicles. These follicles measure up to 9 mm in diameter in most children and usually regress spontaneously (25). Neonatal ovarian cysts develop under the influence of maternal, placental, and fetal hormones during the third trimester. The majority resolve spontaneously after birth. The prevalence of ovarian cysts in children is unclear. A small number of studies reported frequencies between 33 and 84% (49, 50) (limited evidence). Cohen et al. found macrocysts larger than 9 mm in diameter in 18% of children of up to 2 years of age (49). Uncomplicated cysts may present as palpable abdominopelvic mass lesions (25). Cysts may be complicated by torsion, hemorrhage, or rupture. Torsion is more common in cysts which have a diameter over 5 cm or a long pedicle. Differential diagnosis of neonatal ovarian cysts includes hydronephrosis, hydrocolpos, enteric duplication cyst, choledochal cyst, urachal cyst, bowel atresia, or obstruction (25) (limited evidence). Older children and adolescents with ovarian cysts may present with acute abdominal pain due to hemorrhage or cyst rupture (25, 51).

Girls with an ovarian neoplasm may present with abdominal distension and a palpable abdominal mass. The tumors may be complicated by torsion and/or rupture (25). Ovarian dermoid/teratoma is the most common tumor of the ovaries, accounting for 50% of pediatric and 20% of adult ovarian tumors (52). Ovarian teratomas may be associated with various complications, leading to acute lower abdominal pain, such as adnexal torsion (16% of ovarian teratomas), rupture (1–4%), and infection (1%) (52–55). Epithelial tumors account for about 17% and sex cord-stromal tumors for about 13% of pediatric ovarian tumors (25).

Pregnancy

Pregnancy is not uncommon and should always be considered in adolescents who present with acute pelvic pain (2). The incidence of ectopic pregnancies is unclear. Zane et al. estimated a total number of 10,221–77,129 ectopic pregnancy cases per year in the USA (56). In the UK, nearly 32,000 ectopic pregnancies are diagnosed every year, resulting in an incidence of about 11 per 1,000 pregnancies (57). It is the second leading cause of maternal mortality and accounts for 80% of first trimester maternal deaths (25, 57). In younger women ectopic pregnancy accounts for 0.5% of pregnancies (25). Menon et al. compared the incidence of ectopic pregnancies in symptomatic women, which was significantly lower in women under 20 years of age (9.7%) compared to those of 20 years of age and older (21.7%) (58) (limited evidence).

Overall Cost to Society

Pelvic Inflammatory Disease

There are numerous cost analyses on PID. Yeh et al. calculated the costs of major complications of PID based on a cohort of 100,000 women aged 20–24 years, in which 8,550 ectopic pregnancies, 16,800 cases of infertility, and 18,600 cases of chronic pelvic pain were projected to occur (59). They found an average per-person lifetime cost of US $2,150. Average lifetime costs for women who developed major complications were US $6,350 for chronic pelvic pain, US $6,840 for ectopic pregnancy, and US $1,270 for infertility. The majority of costs (79%) were due to upper genital tract infection (59) (moderate evidence).

Endometriosis

In 2006, Gao et al. published a systematic review on economic consequences of endometrioses and related symptoms (60). They included 13 relevant studies evaluating treatment costs, time lost from work, employment status, and other parameters. Only 1 of these 13 studies presented data of the entire hospitalization process (61), being based on data from the "Healthcare Cost and Utilization Project" (HCUP). The mean inpatient charges per admission for endometriosis were US $6,597 in 1991 and US $7,449 in 1992 (61). Based on the publication of Zhao and colleagues, the HCUP data were reevaluated by Gao et al. for the year 2002, calculating an increase of 61% or a mean per-patient charge of US $12,644 (60). Simoens et al. published a systematic review of estimates and methodology of studies quantifying the costs of endometriosis (62). They found one study indicating that annual health care costs of endometriosis are substantial, amounting to

direct costs of US $2,801 per patient in 2002 and annual indirect costs of US $1,023 per patient. The direct costs were broken down into hospitalization costs of US $2,518 (90%) and outpatient costs of US $283 (10%) (63). Delayed correct diagnosis of endometriosis is a major reason for costs in these patients. About 3–12 years may pass between symptom onset and definitive diagnosis (62, 64). In this period of time, unnecessary investigations and treatments are likely to be initiated.

For other specific diagnoses of pelvic pain, accurate cost analyses are not available. However, the economic and psychosocial impacts are important (65–68) and may be reduced due to earlier diagnosis (69, 70).

Goals

In cases of abdominopelvic pain, identification or exclusion of gonadal causes in girls and adolescents is mandatory, since it may be a surgical emergency. Clinical presentation is often nonspecific and may overlap with clinical presentation of other abdominal pathologies such as appendicitis.

In patients with chronic pelvic pain, early correct diagnosis of the underlying cause is desirable to avoid unnecessary treatments and costs as well as compromised quality of life.

Methodology

The diagnostic performance of the clinical examination (history and physical exam) and the accuracy of both clinical and radiographic examinations in young patients with abdominopelvic pain caused by gonadal pathologies was evaluated based on a systematic literature review using PubMed (Medline, National Library of Medicine, Bethesda, MD), Cochrane library, and the National Guideline Clearinghouse. All searches were performed in July 2008 without any time restrictions. The clinical examination search strategy used the following statements: (1) *abdominal* or *abdominopelvic* or *pelvic* and *pain*; (2) *clinical examination*; (3) *epidemiology*; (4) *physical examination*; (5) *imaging* (including *MRI, ultrasound, scintigraphy*, and acronyms of these terms); (6) *diagnosis*; as well as combinations of these search strings. Animal studies and non-English and non-German studies were excluded.

Discussion of Issues

I. What Is the Diagnostic Performance of the Different Imaging Studies for the Diagnosis or Exclusion of Ovarian Torsion?

Summary of Evidence: Sonography is the first-line modality in children and adolescents with abdominal and/or pelvic pain suspected to be of gynecological origin (limited evidence).

The most common finding in ovarian torsion is an enlarged heterogenous ovary (limited evidence).

Presence or absence of arterial or venous flow is neither sensitive nor specific for the diagnosis of ovarian/adnexal torsion (limited evidence). Therefore, close clinical correlation is mandatory and if suspected, laparoscopy confirmation and treatment are required.

Supporting Evidence: Chiou et al. reviewed surgically proven cases of adnexal torsion between 1990 and 2006 (71). A correct preoperative diagnosis was made in 15 (71%) of 21 with initial sonography versus 5 (38%) of 13 cases with initial CT. A correct imaging diagnosis was made more frequently in premenopausal than in menopausal patients ($p = 0.02$) (Table 39.1). Common imaging findings were an adnexal mass (65% on sonography, 87% on CT, and 75% on MRI), a displaced adnexal mass/enlarged ovary (53% on sonography, 87% on CT, and 75% on MRI), and ascites (53% on sonography, 73% on CT, and 50% on MRI) (71).

A retrospective study with surgically and pathologically proven ovarian torsions found in 100% of the patients an enlarged torsed ovary, with the median volume 12 times (range 4.4–27.3) that of the normal contralateral side (72). In 62%, venous or arterial flow was present in the torsed ovary (72). A twisted vascular pedicle (whirpool sign) was found in up to 88% of twisted ovaries (44, 73).

The sensitivity of sonography was 100% and specificity was 93% in a small study of 28 girls, using an enlarged ovary as the criterion for abnormal (limited evidence). The volume of the

enlarged ovaries ranged from 34 to 365 cm^3 (mean 130 ± 99 cm^3) (37).

The classical description of a torsed ovary on sonography is enlargement with peripheral small cysts (follicles) and a small amount of pelvic free fluid. However, this finding is not common.

II. What Is the Best Imaging Technique for the Diagnosis of PID?

Summary of Evidence: Transvaginal ultrasound is superior to transabdominal ultrasound in the diagnosis of PID (limited evidence). For the depiction and management planning of pelvic abscesses, cross-sectional imaging with US, CT, or MRI is often required. Comparisons between US, CT, and MRI are not available (limited evidence).

Supporting Evidence: Studies evaluating the value of imaging techniques in young patients with PID are very limited. Bulas et al. studied the diagnostic performance of transabdominal and transvaginal sonography in 84 patients aged 12–21 years with the clinical diagnosis of acute PID (74). Transvaginal sonography demonstrated superior resolution of 25 dilated fallopian tubes. Heterogeneous pelvic masses, described as tubo-ovarian abscesses on transabdominal sonograms, could be separated on transvaginal sonograms into various stages of PID including pyosalpinx, hydrosalpinx, tubo-ovarian complex, and tubo-ovarian abscess. Thirty-one transabdominal and transvaginal studies were normal despite patients fulfilling strict clinical criteria for PID. The level of severity of PID, as determined at transabdominal sonography, was altered in 28 cases, with medical therapy changed in 23 cases because of additional transvaginal sonographic findings. Transvaginal sonography provided superior anatomic details in the evaluation of patients with PID, demonstrating abnormalities that were not seen at transabdominal sonography in 71% of patients.

CT (and MRI) findings in early PID include obscuration of the normal pelvic floor fascial planes, thickening of the uterosacral ligaments, cervicitis, oophoritis, salpingitis, and accumulation of simple fluid in the endometrial canal, fallopian tubes, and pelvis. As the disease progresses, the simple fluid may become complex and the inflammatory changes may progress to frank tubo-ovarian or pelvic abscesses (75).

III. What Is the Best Imaging Technique for the Diagnosis of Endometriosis?

Summary of Evidence: Transvaginal sonography is the imaging test of choice for the evaluation of endometriosis. MRI is more expensive but performs similarly to transvaginal sonography for the diagnosis of intestinal endometriosis. For some less common imaging findings, MRI has higher sensitivity and diagnostic likelihood ratios for uterosacral ligament and vaginal endometriosis (limited evidence). Transrectal sonography is also a sensitive test but is less well tolerated by patients and less widely used for this diagnosis.

Supporting Evidence: Bazot and colleagues compared physical examination, transvaginal sonography, rectal endoscopic sonography, and magnetic resonance imaging for the diagnosis of endometriosis in 92 adult patients prior to surgery in a retrospective study (76). MRI performed similarly to ultrasound for the diagnosis of intestinal endometriosis but had higher sensitivity and likelihood ratios for uterosacral ligament and vaginal endometriosis. This study has limited value for the diagnosis of endometriosis in children, because transvaginal and rectal endoscopic sonography are not the imaging techniques of choice in this age group (Table 39.1). However, since MRI was the superior technique compared to ultrasound and physical examination, the results are also valuable for a younger age group.

IV. What Is the Best Technique for the Diagnosis of an Ectopic Pregnancy?

Summary of Evidence: Pregnancy and ectopic pregnancy are both best imaged by sonography. Initially, abdominal sonography is performed and when there are unclear findings that suggest pregnancy or ectopic pregnancy,

transvaginal sonography improves diagnostic accuracy (moderate evidence).

Supporting Evidence: Beta-hCG levels assist in interpreting sonographic findings. Ectopic pregnancy is suspected if transabdominal sonography does not show an intrauterine gestational sac and the patient's β-hCG level is greater than 6,500 IU/L or if transvaginal sonography does not show an intrauterine gestational sac and the patient's β-hCG is 1,500 IU/L or greater. Combined transvaginal sonography and serial quantitative β-hCG measurements are approximately 96% sensitive and 97% specific for diagnosing ectopic pregnancy (77–79) (moderate evidence) (Table 39.1).

Take Home Tables

Table 39.1 discusses the diagnostic performance of ultrasound in pediatric female pelvic conditions.

Table 39.1. Diagnostic performance of ultrasound in pediatric female pelvic conditions

	Ovarian torsion	Pelvic inflammatory disease	Endometriosis	Ectopic pregnancy
Sensitivity	**1.00**	**0.72**	**0.75–0.95***	**0.96***
Specificity	**0.93**	**N/A**	**0.83–1.00***	**0.97***
Accuracy	**0.71**	**N/A**	**0.83***	**N/A**

N/A: Not available

*Using endovaginal ultrasound (adolescents and adults).

Data from references (37, 44, 72, 73, 76–79) (limited evidence).

Imaging Case Studies

Case 1

Figure 39.1 illustrates a very large ovarian cyst in a 10-year-old girl who presented with acute abdominal pain and urinary retention.

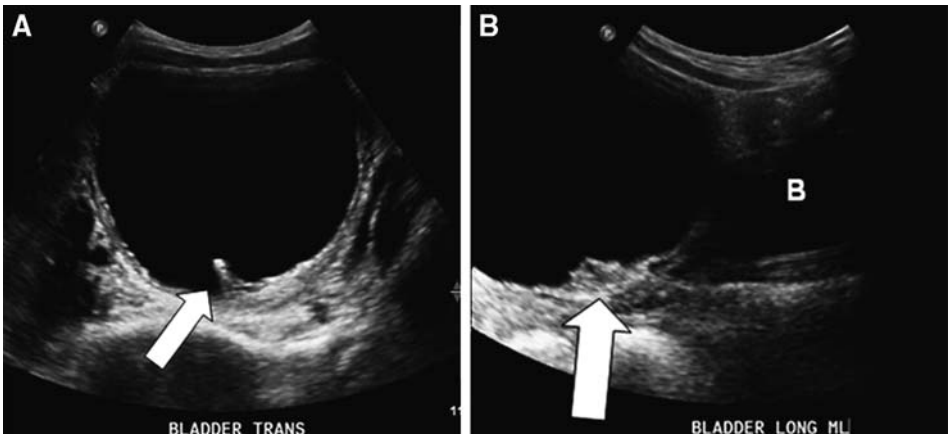

Figure 39.1. Very large ovarian cyst. A 10-year-old girl presented with acute abdominal pain and urinary retention. At sonography, she had a very large simple cyst measuring up to 11 cm (**a:** in trans, **b:** in long**).** Note the wall of the cyst had a few focal thickened strands (*whitearrows*). The bladder is visualized inferior to the cyst in **b** (labeled B). At surgery, the ovary had torsed and was removed.

Case 2

Figure 39.2 illustrates a hemorrhagic ovarian cyst in an 11-year-old girl who presented with severe left lower quadrant abdominal pain.

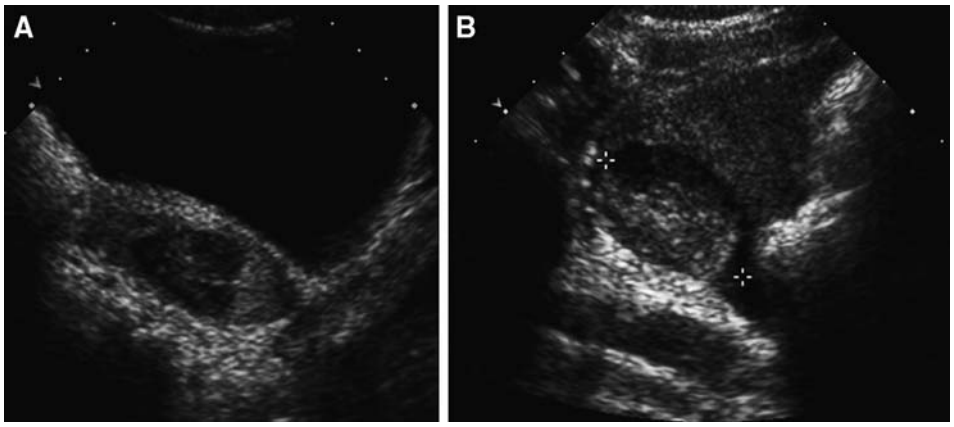

Figure 39.2. Hemorrhagic ovarian cyst. An 11-year-old girl presented with severe left lower quadrant abdominal pain. Her ultrasound revealed a debris-fluid level (**a**, *arrow*) within her left ovary which represents acute hemorrhage into an ovarian cyst. **b** shows the left ovary with the echogenic blood and faintly seen in the periphery are some normal follicles. Both her pain and the fluid resolved without the need for surgery.

Suggested Imaging Protocols

Plain Radiographs

Plain radiographs are not recommended.

Ultrasound

Ultrasound is the key screening tool and often the only examination indicated. Ultrasound with a 7 MHz probe is ideal for children (5 MHz for older children). For obese children or adolescents, 3 MHz may be required. To evaluate the female reproductive tract, a full urinary bladder is essential. If the bladder is not adequately full, it might be useful to repeat the examination every 15 minutes. Further evaluation with CT or MRI may depend on the results of the sonograms, the clinical examination, and acuity of the problem.

MDCT

Intravenous contrast is essential to visualize infection or inflammation and abscess. Oral or rectal contrast may help to distinguish fluid-filled bowel loops in the pelvis.

MRI

Axial and coronal T1 spin echo, axial and sagittal T2 FSE with fat saturation, coronal STIR or HASTE, and axial and coronal T1 2D SPGR with fat saturation before and after intravenous gadolinium (in patients with acceptable renal function). Alternative to imaging with CT. Not as sensitive for calcification but can provide functional data.

Future Research

- What are the clinical predictors for ovarian pathology that leads to appropriate use of sonography?
- What is the appropriate use of MR imaging in girls with gynecologic disorders?

References

1. Carrico CW, Fenton LZ, Taylor GA, DiFiore JW, Soprano JV. Am J Roentgenol 1999; 172: 513–516.
2. Hollmann AS, Macdonald S. In Carty H (ed.). Emergency Pediatric Radiology. Berlin: Springer, 1999; 217–232.
3. Klein MD, Rabbani AB, Rood KD et al. J Pediatr Surg 2001; 36:1375–1380.
4. Puig S, Hörmann M, Rebhandl W, Felder-Puig R, Prokop M et al. Radiology 2003; 226:101–104.
5. Strouse PJ. Singapore Med J 2003; 44:312–322.
6. Bailez MM. Semin Pediatr Surg 2007; 16:278–287.
7. Rock JA, Schlaff WD. Fertil Steril 1985; 43:681–692.
8. Bhatt S, Kocakoc E, Dogra VS. Ultrasound Q 2006; 22:273–280.
9. Woodward PJ, Sohaey R, Mezzetti TP, Jr. Radiographics 2001; 21:193–216; questionnaire 288–194.
10. Chatman DL, Ward AB. J Reprod Med 1982; 27:156–160.
11. Guo SW, Wang Y. Gynecol Obstet Invest 2006; 62:121–130.
12. Guo SW, Wang Y. Fertil Steril 2006; 86:1584–1595.
13. Black AY, Jamieson MA. Curr Opin Obstet Gynecol 2002;14:467–474.
14. Vinatier D, Orazi G, Cosson M, Dufour P. Eur J Obstet Gynecol Reprod Biol 2001; 96: 21–34.
15. Laufer MR, Sanfilippo J, Rose G. J Pediatr Adolesc Gynecol 2003; 16:S3–S11.
16. Ozkan S, Murk W, Arici A. Ann N Y Acad Sci 2008; 1127:92–100.
17. Eskenazi B, Warner ML. Obstet Gynecol Clin North Am 1997; 24:235–258.
18. Houston DE, Noller KL, Melton LJ 3rd, Selwyn BJ, Hardy RJ. Am J Epidemiol 1987; 125:959–969.
19. Matalliotakis IM, Cakmak H, Fragouli YG, Goumenou AG, Mahutte NG et al. Arch Gynecol Obstet 2008; 277:389–393.
20. Kontoravdis A, Hassan E, Hassiakos D, Botsis D, Kontoravdis N et al. Clin Exp Obstet Gynecol 1999; 26:76–77.
21. Laufer MR, Goitein L, Bush M, Cramer DW, Emans SJ. J Pediatr Adolesc Gynecol 1997; 10:199–202.
22. Reese KA, Reddy S, Rock JA. J Pediatr Adolesc Gynecol 1996; 9:125–128.
23. Vercellini P, Fedele L, Arcaini L, Bianchi S, Rognoni MT et al. J Reprod Med 1989; 34:827–830.
24. Osuga Y, Koga K, Tsutsumi O et al. Gynecol Obstet Invest 2002; 53(Suppl 1):33–39,
25. Paterson A. In Carty H (ed.). Imaging Children. Edinburgh, New York: Elsevier Churchill Livingstone, 2005;915–941.
26. Gray-Swain MR, Peipert JF. Curr Opin Obstet Gynecol 2006; 18:503–510.
27. Ross J, Judlin P, Nilas L. European guideline for the management of pelvic inflammatory disease – Minor update August 2008.

28. Low N, McCarthy A, Macleod J et al. Health Technol Assess 2007; 11:iii–iv, ix–xii, 1–165.
29. Bevan CD, Johal BJ, Mumtaz G, Ridgway GL, Siddle NC. Br J Obstet Gynaecol 1995; 102:407–414.
30. CDC. Sexually transmitted diseases treatment guidelines 2002. Centers for Disease Control and Prevention. MMWR Recomm Rep 2002; 51:1–78.
31. Morcos R, Frost N, Hnat M, Petrunak A, Caldito G. J Reprod Med 1993; 38:53–56.
32. Chang HC, Bhatt S, Dogra VS. Radiographics 2008; 28:1355–1368.
33. Albayram F, Hamper UM. J Ultrasound Med 2001; 20:1083–1089.
34. Breech LL, Hillard PJ. Curr Opin Obstet Gynecol 2005; 17:483–489.
35. Quillin SP, Siegel MJ. Radiographics 1993; 13:1281–1293; discussion 1294.
36. Bouguizane S, Bibi H, Farhat Y et al. J Gynecol Obstet Biol Reprod (Paris) 2003; 32:535–540.
37. Graif M, Itzchak Y. Am J Roentgenol 1988; 150:647–649.
38. Hata K, Hata T, Senoh D et al. Br J Obstet Gynaecol 1990; 97:163–166.
39. Stark JE, Siegel MJ. Am J Roentgenol 1994; 163:1479–1482.
40. Burnett LS. Surg Clin North Am 1988; 68:385–398.
41. Hibbard LT. Am J Obstet Gynecol 1985; 152:456–461.
42. Houry D, Abbott JT. Ann Emerg Med 2001; 38:156–159.
43. Mordehai J, Mares AJ, Barki Y, Finaly R, Meizner I. J Pediatr Surg 1991; 26:1195–1199.
44. Lee EJ, Kwon HC, Joo HJ, Suh JH, Fleischer AC. J Ultrasound Med 1998; 17:83–89.
45. Littman ED, Rydfors J, Milki AA. Hum Reprod 2003; 18:1641–1642.
46. Beaunoyer M, Chapdelaine J, Bouchard S, Ouimet A. J Pediatr Surg 2004; 39:746–749.
47. Warner MA, Fleischer AC, Edell SL et al. Radiology 1985; 154:773–775.
48. Pomeranz AJ, Sabnis S. Pediatr Emerg Care 2004; 20:172–174.
49. Cohen HL, Shapiro MA, Mandel FS, Shapiro ML. Am J Roentgenol 1993; 160:583–586.
50. Orbak Z, Kantarci M, Yildirim ZK, Karaca L, Doneray H. J Pediatr Endocrinol Metab 2007; 20:397–403.
51. Webb EM, Green GE, Scoutt LM. Radiol Clin North Am 2004; 42:329–348.
52. Park SB, Kim JK, Kim KR, Cho KS. Radiographics 2008; 28:969–983.
53. Comerci JT, Jr., Licciardi F, Bergh PA, Gregori C, Breen JL. Obstet Gynecol 1994; 84:22–28.
54. Kido A, Togashi K, Konishi I et al. Am J Roentgenol 1999; 172:445–449.
55. Outwater EK, Siegelman ES, Hunt JL. Radiographics 2001; 21:475–490.
56. Zane SB, Kieke BA, Jr., Kendrick JS, Bruce C. Matern Child Health J 2002; 6:227–236.
57. RCOG. Why Mothers Die 1997–1999. The fifth report of the Confidential Enquiries into Maternal Deaths in the United Kingdom. London: RCOG Press, 2001.
58. Menon S, Sammel MD, Vichnin M, Barnhart KT. J Pediatr Adolesc Gynecol 2007; 20:181–185.
59. Yeh JM, Hook EW, 3rd, Goldie SJ. Sex Transm Dis 2003; 30:369–378.
60. Gao X, Outley J, Botteman M, Spalding J, Simon JA et al. Fertil Steril 2006; 86:1561–1572.
61. Zhao SZ, Wong JM, Davis MB, Gersh GE, Johnson KE. Am J Manag Care 1998; 4: 1127–1134.
62. Simoens S, Hummelshoj L, D'Hooghe T. Hum Reprod Update 2007; 13:395–404.
63. Kunz K, Kuppermann M, Moynihan C, Williamson A, Mazonson PT. Am J Managed Care 1995; 1:25–29.
64. Husby GK, Haugen RS, Moen MH. Acta Obstet Gynecol Scand 2003; 82:649–653.
65. Pandian Z, Bhattacharya S, Vale L, Templeton A. Cochrane Database Syst Rev 2005:CD003357.
66. Pashayan N, Lyratzopoulos G, Mathur R. BMC Health Serv Res 2006; 6:80.
67. Philips Z, Barraza-Llorens M, Posnett J. Hum Reprod 2000; 15:95–106.
68. Stones RW, Selfe SA, Fransman S, Horn SA. Baillieres Best Pract Res Clin Obstet Gynaecol 2000; 14:415–431.
69. Ballard K, Lowton K, Wright J. Fertil Steril 2006; 86:1296–1301.
70. Schenken RS. Fertil Steril 2006; 86:1305–1306; discussion 1317.
71. Chiou SY, Lev-Toaff AS, Masuda E, Feld RI, Bergin D. J Ultrasound Med 2007; 26: 1289–1301.
72. Servaes S, Zurakowski D, Laufer MR, Feins N, Chow JS. Pediatr Radiol 2007; 37:446–451.
73. Vijayaraghavan SB. J Ultrasound Med 2004; 23:1643–1649; quiz 1650–1641.
74. Bulas DI, Ahlstrom PA, Sivit CJ, Blask AR, O'Donnell RM. Radiology 1992; 183:435–439.
75. Sam JW, Jacobs JE, Birnbaum BA. Radiographics 2002; 22:1327–1334.
76. Bazot M, Lafont C, Rouzier R, Roseau G, Thomassin-Naggara I et al. Fertil Steril 2008; Epub ahead of print.
77. Mol BW, van der Veen F, Bossuyt PM. Hum Reprod 1999; 14:2855–2862.
78. Gracia CR, Barnhart KT. Obstet Gynecol 2002; 97:464–470.
79. Buckley RG, King KJ, Disney JD, Ambroz PK, Gorman JD et al. Acad Emerg Med 1998; 5:951–960.

40

Imaging of Boys with an Acute Scrotum: Differentiation of Testicular Torsion from Other Causes

Stefan Puig

Issues

I. What are the clinical findings that raise the suspicion of testicular torsion in children with acute scrotal pain?
II. What is the diagnostic performance of the different imaging studies in children with acute scrotal pain?
III. In cases of testicular torsion, is manual reduction required?

Key Points

- Testicular torsion is a clinical emergency. Time is the major factor responsible for salvage of testes (moderate evidence).
- The first-line imaging of patients with suspected testicular torsion is Doppler sonography, which is highly sensitive and specific (moderate evidence).
- Scintigraphy using technetium 99m to assess blood flow to the testes is no longer a common imaging tool due to the more available, less expensive, and rapid test with Doppler sonography (limited to moderate evidence).
- If imaging cannot exclude testicular torsion, surgical exploration is recommended (moderate evidence).
- Successful manual detorsion of testicular torsion leads to reperfusion, which is immediately visible with Doppler sonography. In cases of successful manual detorsion, surgical exploration with orchiopexy is still necessary (limited evidence).
- Absolute dependence on clinical features can lead to a misdiagnosis of testicular torsion. Therefore, US examination should be part of the presurgical evaluation, if promptly available (limited evidence).

S. Puig (✉)
Research Programm on Evidence-Based Diagnostics, Institute of Public Health, Paracelsus Private Medical University, Salzburg A-5020, Austria
e-mail: stefan.puig@pmu.ac.at

L.S. Medina et al. (eds.), *Evidence-Based Imaging in Pediatrics*,
DOI 10.1007/978-1-4419-0922-0_40,

Definition and Pathophysiology

A testicular torsion is a clinical emergency (1, 2). It occurs when the testicle is abnormally mobile and twists on its vascular pedicle and may result in testicular infarction (2). According to the mechanism, torsion of a testis can be divided into extravaginal (prenatal or neonatal) and the more common intravaginal torsion (3, 4). The exact cause for extravaginal or neonatal torsion is unknown and usually no anatomic defect can be identified to explain the torsion (5). It is a rare event and accounts for approximately 10% of all testicular torsions (6). In patients with an intravaginal torsion, the most common anatomical anomaly identified is a narrow attachment of the tunica vaginalis from the spermatic cord to the testes secondary to high insertion of the tunica on the spermatic cord. This results in the "Bell-Clapper" deformity characterized by increased testicular mobility (5). In an autopsy series of 51 males, the Bell-Clapper deformity was found in 12%. Since this is a much higher prevalence than the incidence of testicular torsion, factors other than this anatomical predisposition may be involved (7) (limited evidence).

Testicular torsion should be differentiated from other acute scrotal diseases, such as acute epididymo-orchitis, torsion of appendage of testis, or acute idiopathic scrotal edema (8, 9) (Table 40.1). The cause for the torsion might be several minor traumas, as they occur during sport activities (8). Of the etiologies for acute scrotal pain, testicular torsion is the only real emergency (10–12). Immediate detorsion within a very narrow time window is necessary to provide a high testicle salvage rate, since irreversible ischemia may start after 6 hours (3) (moderate evidence). Dunne and O'Loughlin reported a series of 56 patients between 13 and 36 years of age, in which the average duration of pain in patients with viable testes was 9 hours compared to 56 hours of average duration of pain in those patients with non-viable testes (1). Previous reports found 80% infarcted testes 10 hours after pain onset, and after 24 hours all testes were lost (1, 13). Nearly 75% of patients need an orchiectomy if detorsion is delayed for more than 12 hours (14) (limited evidence).

Sessions et al. reported a median duration of torsion of 5 hours (0.5 hours to 6 days) in patients (116 testes) undergoing orchiopexy and 2.2 days (2.5 hours to 2 weeks) in those (70 testes) undergoing orchiectomy, which reveals the weakness of time as an accurate predictor for salvageable testes. The same group noted a median of 540° (range: 180°–1,080°) in patients with orchiectomy compared to a median of 360° (range: 180°–1,080°) in those with orchiopexy (15).

Epidemiology

The incidence of spermatic cord torsion in patients presenting with an acute scrotum varies between 18 and 45%, depending on the age of patients (15–17). The overall incidence is 1 in 4,000 in young males under the age of 25, with a peak age of 12–18 years. Cummings et al. reported that nearly 61% of patients were under 21 years of age (18). In children and adolescents under 17 years of age, the incidence of spermatic cord torsion in patients with an acute scrotum is about 26%. There is a peak in the first year of life with 39% and a second peak in young adolescents with 30% during puberty when the testes grow (19, 20).

The most common cause of acute scrotal pain in patients younger than age 18 is epididymitis (21). In prepubertal boys, acute scrotal pain occurs most frequently from torsion of the testicular appendages (21, 22).

Overall Cost to Society

No data were found on the overall cost to society from the diagnosis, treatment, and complications of testicular torsion. However, in cases of testicular torsion, imaging of the scrotum will increase the costs, since surgery is required in those patients anyway. But, this is counterbalanced by imaging eliminating unnecessary surgery in subjects found not to have torsion. Günther et al. calculated in 2006 (according to the German diagnosis-related group's catalog) a cost reduction of €1,000 (€2,300 versus €1,300) per patient if torsion can be ruled out and unnecessary surgical exploration is avoided (8, 9). Furthermore, orchiectomy will result in the implantation of testicular prostheses which might reduce the psychological impact of a testicle loss, but has some complication rates

and will lead to further costs (23) (limited evidence).

Goals

In cases of acute scrotal pain, the main goal is the differentiation of testicular torsion, which requires emergency surgery, from non-surgical causes of acute scrotal pain, such as epididymitis (epididymo-orchitis) and torsion of the testicular appendix, because clinical presentation may overlap (24–27). In testicular torsion, manual detorsion may reduce time of ischemia before surgical evaluation is possible (3).

Methodology

The diagnostic performance of the clinical examination (history and physical exam) and surgical outcome was based on a systematic literature review using PubMed (National Library of Medicine, Bethesda, MD), Cochrane library, and the National Guideline Clearinghouse for data relevant to the diagnostic performance and accuracy of both clinical and radiographic examinations in patients with testicular torsion performed between January 1967 and July 2008. The clinical examination search strategy used the following statements: (1) *testicular torsion or acute scrotum*; (2) *clinical examination*; (3) *epidemiology*; (4) *physical examination*; (5) *imaging* (including *MRI, ultrasound, scintigraphy*, as well as acronyms of these terms); (6) *diagnosis*; (7) *detorsion*; as well as combinations of these search strings. Animal studies and non-English and non-German studies were excluded.

Discussion of Issues

I. What Are the Clinical Findings That Raise the Suspicion of Testicular Torsion in Children with Acute Scrotal Pain?

Summary of Evidence: Clinical presentation and physical examination are nonspecific and include previous trauma, pain attacks, nausea, vomiting, elevation and transverse position of the testis, anterior rotation of epididymidis, and absence of the cremaster reflex. These findings have the highest sensitivity, specificity, positive and negative predictive values for testicular torsion, and the lowest for epididymitis (moderate evidence). Karmazyn et al. scored the following three key historical elements as predictors for testicular torsion: onset of pain less than 6 hours, absence of cremasteric reflex, and diffuse testicular tenderness (25). Out of 141 subjects, in the absence of any of these elements, none of the subjects had testicular torsion. When these three clinical findings were present, 87% were diagnosed with testicular torsion.

Supporting Evidence: Clinical presentation and physical examination do not differ significantly in children and adolescents with testicular torsion, torsion of testicular appendage, or epididymitis. However, children with testicular appendage torsion are typically younger with a peak age of 7–14 years. Previous history of trauma and pain attacks, presence of nausea and vomiting, and absence of urinary complaints are the main predictors of testicular torsion (11) (limited evidence). A so-called pathognomonic finding, the blue dot sign (tender nodule with blue discoloration on the upper pole of the testis), is only infrequently encountered (11, 21, 28). Physical findings consisting of elevation and transverse location of testis, anterior rotation of epididymis, and absence of cremaster reflex are highly suggestive for testicular torsion (3, 11, 24, 25, 29) (limited to moderate evidence). A Finnish study published in 2007 analyzed the clinical findings in 388 boys under 17 years of age with acute scrotum, in which the "blue dot sign" was only found in 10% (17/174) with torsion of the testicular appendage (20). Boys with acute scrotal pain of uncertain etiology based on clinical exam should undergo sonography to exclude the diagnosis of torsion as well as identify other reasons for the pain.

II. What Is the Diagnostic Performance of the Different Imaging Studies in Children with Acute Scrotal Pain?

Summary of Evidence: Ultrasound with power Doppler has become the imaging modality of choice to diagnose or exclude torsion (moderate evidence). It is a useful addition to the clinical examination, specifically to avoid unnecessary

surgery (moderate evidence). Other imaging tools, such as the near-obsolete nuclear medicine test, are not superior to ultrasound (27) (limited evidence). If Doppler sonography is equivocal, MRI or scintigraphy can add diagnostic information but due to both higher costs and the relative delay to obtain these studies, particularly after hours, the clinical value is limited (limited evidence).

Supporting Evidence

Doppler Ultrasound

In clinical practice, ultrasound is preferred over other imaging tools (30–32). Several cohort studies reported a sensitivity of at least 90% and a specificity of more than 95% (33–42) (moderate evidence). In combination with certain clinical conditions such as blunt trauma, specificity may reach 100% (40). Ideally, both pulsed and color Doppler ultrasound should be used. The real-time whirlpool sign on gray scale sonography in combination with the absence of flow in the distal spermatic cord, testis, and epididymitis were found to be the most specific and sensitive signs of torsion. However, published data on these findings are limited to a few studies (43–45). In general, the first ultrasound sign in patients with testicular torsion is hypo- or avascularity of the testicle with preserved homogeneous echotexture in the acute phase (Figs. 40.1, 40.2) (27). A false-negative finding might be due to flow in the capsule that is from a different arterial supply than the twisted spermatic cord (46).

Data on contrast-enhanced Doppler ultrasound are limited as well, and these contrast agents are not available for clinical use in the United States. In 1996, Coley et al. published their results of an animal study including 40 testes of 20 rabbits (47). They compared unenhanced and contrast-enhanced power Doppler sonography, color Doppler sonography, and radionuclide scintigraphy. The best results were achieved with color Doppler sonography (Figs. 40.1, 40.2). Contrast-enhanced power Doppler sonography, using Levovist® (Schering, Germany), did not improve the diagnostic accuracy of power Doppler, which was below color Doppler and equal to scintigraphy. However, due to several technical developments, these data from 1996 have limited value today, and power Doppler has the ability to show slower flow than color Doppler (47–49). Therefore, power Doppler can be especially useful in prepubertal boys who have lower blood flow (21, 50, 51) (limited to moderate evidence). Gray scale ultrasound of the scrotum without color or power Doppler is relatively insensitive and therefore not recommended in the evaluation of boys with acute scrotum (21).

MRI

Several experimental studies showed the value of MRI in detecting hypoperfused testes. After torsion of testes, the gadolinium enhancement and apparent diffusion coefficient (ADC) values in diffusion-weighted images are decreased (52, 53). In case of inconclusive ultrasound and physical examination, MRI might be helpful (54). Watanabe et al. calculated a sensitivity of 93% and a specificity of 100% in 39 patients with inconclusive previous clinical examinations (55) (limited evidence). MRI can also visualize hemorrhagic necrosis in testicular torsion using contrast-enhanced and blood-sensitive sequences (56) (limited evidence).

However, due to the relatively expensive, less available, and time-consuming examination, including anesthesia in some children, MRI has no value in a potential emergency setting (8).

Radionuclide Imaging

Color Doppler sonography and technitium 99 m scintigraphy show similar sensitivities in the diagnosis of testicular torsion in boys (57). Nussbaum-Blask and colleagues prospectively compared color Doppler sonography and scintigraphy in 46 children, age 1 day to 18 years, reported in 2002 (57). Sonography correctly diagnosed 11 of 14 surgical conditions and 31 of 32 nonsurgical conditions. There was one indeterminate sonogram, no false-positive examinations, and three false-negative examinations (sensitivity = 79% [95% CI, 67–91%], specificity = 97% [95% CI, 94–99%], accuracy = 91%). Color flow was demonstrated in the asymptomatic testis in 34 of 44 boys. Scintigraphy correctly diagnosed 11 of 14 surgical conditions and 29 of 32 nonsurgical conditions. There were two indeterminate scintigrams, two false-positive and two false-negative examinations (sensitivity = 79% [95% CI, 67–91%], specificity

= 91% [95% CI, 82–99%], accuracy = 87%) (57). However, the reported sensitivity in this study is lower than in other cohort studies. Technical advancements in Doppler make these results lower than current practice.

Scintigraphy has a high potential in differentiating ischemic from infectious disease (36). The specificity in the diagnosis of ischemia versus other photon-deficient lesions is slightly lower (21, 58) (limited to moderate evidence). Photon-deficient areas secondary to hydrocele, spermatocele, edematous appendix testis, and inguinal hernia can be mistaken for an avascular testis and therefore produce false positives (58). Also, the size of testes in infants and small children increases the risk of both false positives and false negatives (21). For these reasons, and because of the longer preparation and exam performance time, lower availability, and higher costs relative to Doppler sonography, scintigraphy is no longer favored. Radionuclide scintigraphy also uses ionizing radiation and requires intravenous access while Doppler does not (3, 57).

III. In Cases of Testicular Torsion, Is Manual Reduction Required?

Summary of Evidence: Manual detorsion of the testicle leads to immediate reperfusion of the affected testis and might be helpful to salvage the organ (limited evidence). If the ultrasound examination is performed by a physician with such experience, this procedure can be performed during the examination (Figs. 40.1, 40.2). However, it is successful in only 30–70% of patients. This procedure must be followed by bilateral orchiopexy to prevent future repeat testicular torsion (strong evidence).

Supporting Evidence

Detorsion

Successful manual detorsion can lessen the surgical urgency of a twisted spermatic cord (3, 15, 59–61). Most testes are torsed in the medial direction. Therefore, experienced clinicians such as the urologist can detorse these testes from the medial to the lateral side (3). The subjective endpoint is the dramatic resolution of scrotal pain (3). One has to consider that the testis can be torsed up to 1,080° (15). A detorsed testis shows blood flow at ultrasound or scintigraphy immediately after the maneuver (Figs. 40.1, 40.2) (15, 60, 61). Adequate sedation and/or spermatic cord anesthesia should be administered, since this procedure is painful (3). Surgical exploration and orchiopexy remain necessary despite symptomatic improvement with manual detorsion (3, 15, 60).

The number of reports in the literature is small, with reported success rates varying from 30 to nearly 100%. Garel et al. reported successful six out of seven patients in which manual detorsion led to immediate reperfusion of the organ at Doppler interrogation. The failed attempt in the seventh patient was due to a failure to manipulate beyond an initial 1 1/2 rotations (540°) (60). Cattolica manually detorsed 34 out of 35 testes successfully in 104 patients during a 10-year period (59).

Take Home Figures and Tables

Figure 40.1 is an algorithm showing the workup for a patient suspected of acute scrotum.

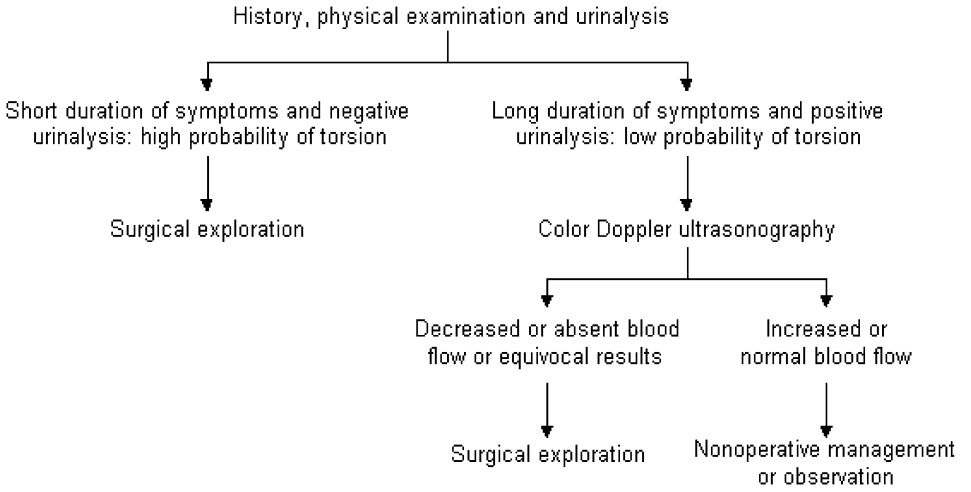

Figure 40.1. Flowchart for patient workup. Note that if the clinician (i.e., an urologist) is experienced in making the diagnosis of acute torsion, they may skip the ultrasound. However, in most situations, the ultrasound is recommended prior to surgery. The age of the patient is important. Testicular torsion is most common in neonates and postpubertal boys, although it can occur in males of any age. Schönlein–Henoch purpura and torsion of a testicular appendage typically occur in prepubertal boys, whereas epididymitis most often develops in postpubertal boys. (Adapted with permission from Galejs LE, Kass EJ. Diagnosis and Treatment of the Acute Scrotum. American Family Physician Feb 15, 1999; 817, 59; 4. Copyright © 1999 American Academy of Family Physicians. All Rights Reserved.).

Tables 40.1 and 40.2 discuss causes of acute scrotum in a child and a summary of the diagnostic performance of clinical examination versus imaging for the diagnosis of acute testicular torsion, respectively.

Table 40.1. Causes for an acute scrotum in childhood

Torsion	Inflammation	Trauma	Generalized illness	Other causes
Torsion of the testicular appendages	Epididymitis	Hematoma Hematocele	Schoenlein–Henoch purpura	Inguinal hernia Perforated appendicitis
Testicular torsion	Orchitis	Testicle rupture	Leukemia Lymphoma	Emphysema, edema of the scrotum, testicular tumor, meconium orchitis

Adapted with kind permission of Springer Science+Business Media from Günther and Schenk (8).

Table 40.2 Summary of diagnostic performance of clinical examination versus imaging for the diagnosis of acute testicular torsion

Test for torsion	Sensitivity (%)	Specificity (%)	References
Clinical exam*	87	100	(24)
Technitium scintigraphy	79	>90	(24, 29, 62, 63)
Doppler sonography	>90	>95	(33–40, 42, 62, 63)

*Onset of pain less than 6 hours, absence of cremasteric reflex, and diffuse testicular tenderness.

Imaging Case Studies

Case 1

Figure 40.2 presents color Doppler sonography of an 18-year-old patient with acute scrotum.

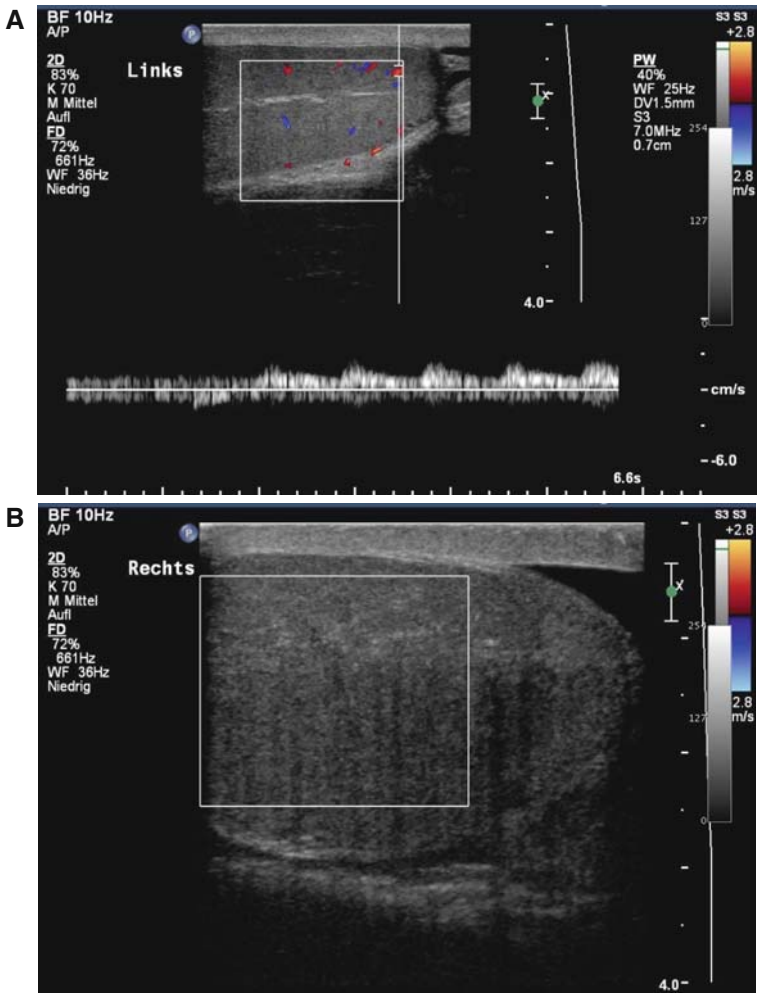

Figure 40.2. Color Doppler sonography of an 18-year-old patient with acute scrotum. (**A)** shows the unaffected left side with regular arterial and venous bloodflow. In comparison, there is no blood flow on the right side (**B**). The parenchyma of the twisted testis is normal, and symmetric to the unaffected left testes, a small hydrocele can be seen. After manual detorsion, reperfusion (hyperperfusion) of the right testis is visible (**C**). After this maneuver, the patient underwent orchiopexy.

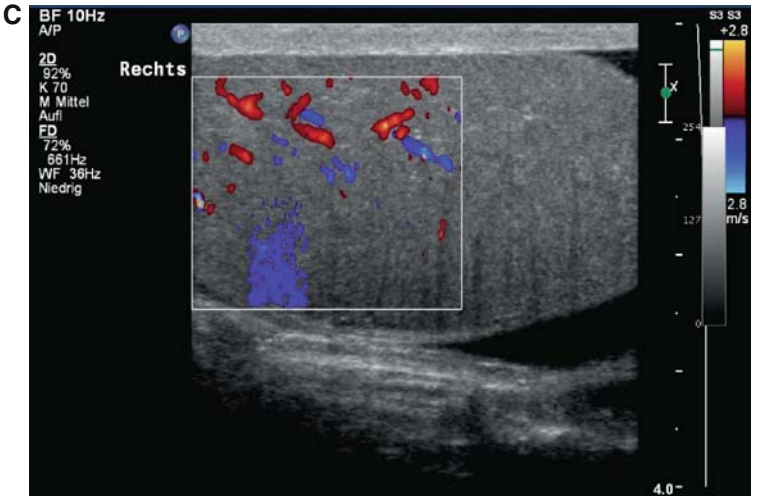

Figure 40.2. *Continued*

Suggested Imaging Protocols for Acute Scrotum

Timely diagnosis and intervention is critical to decrease the chances of testicular loss (3, 15).

Ultrasound

Linear transducer high-frequency transducer (7–12 MHz). Compare with opposite testis for blood flow and parenchymal homogeneity (Figs. 40.1, 40.2). If possible, try to visualize the twisted spermatic cord "whirlpool sign." Spectral, color, and power Doppler should be used to evaluate the lack of blood flow within the testicular parenchyma. Doppler frequencies range from 3.5 to 10 MHz. Standoff pads can be used, if necessary, to improve imaging (64).

Manual Detorsion

Successful manual detorsion leads to immediate reperfusion of the testis. Since in most torsions the spermatic cord is twisted from lateral to medial, detorsion has to be performed from medial to lateral (the right testis counterclockwise, the left testis clockwise). Doppler is used both during this procedure and immediately afterward to assess testicular blood flow.

Future Research

- Accuracy of second-generation contrast media (e.g., SonoVue®, Bracco, Milan, Italy) that might improve diagnosis, specifically in combination with modern ultrasound scanners with harmonic imaging (65, 66).
- Prospective comparison of Doppler sonography with near-infrared spectroscopy, which is capable of noninvasively measuring a mixed venous and arterial hemoglobin tissue saturation of hemoglobin, that might allow noninvasive, bedside emergency diagnosis of testicular torsion (67).

References

1. Dunne PJ, O'Loughlin BS. Aust N Z J Surg 2000; 70:441–442.
2. Hollmann AS, Macdonald S. In Carty H (ed.). Emergency Pediatric Radiology. Berlin: Springer, 1999; 217–232.
3. Kapoor S. Int J Clin Pract 2008; 62:821–827.
4. Samnakay N, Tudehope D, Walker R. J Paediatr Child Health 2006; 42:734–736.
5. Favorito LA, Cavalcante AG, Costa WS. Int Braz J Urol 2004; 30:420–424.
6. Kaye JD, Levitt SB, Friedman SC, Franco I, Gitlin J et al. J Urol 2008; 179:2377–2383.
7. Caesar RE, Kaplan GW. Urology 1994; 44: 114–116.

8. Günther P, Schenk JP. Radiologe 2006; 46: 590–595.
9. Günther P, Schenk JP, Wunsch R et al. Eur Radiol 2006; 16:2527–2532.
10. Ben-Sira L, Laor T. Pediatr Radiol 2000; 30: 125–128.
11. Ciftci AO, Senocak ME, Tanyel FC, Buyukpamukcu N. Eur J Pediatr Surg 2004; 14:333–338.
12. Somekh E, Gorenstein A, Serour F. J Urol 2004; 171:391–394; discussion 394.
13. Munro I. Lancet 1981; 2:76–77.
14. Anderson JB, Williamson RC. Br J Surg 1988; 75:988–992.
15. Sessions AE, Rabinowitz R, Hulbert WC, Goldstein MM, Mevorach RA. J Urol 2003; 169: 663–665.
16. Caldamone AA, Valvo JR, Altebarmakian VK, Rabinowitz R. J Pediatr Surg 1984; 19:581–584.
17. Clift VL, Hutson JM. Pediatr Surg Int 1989; 4:185–188.
18. Cummings JM, Boullier JA, Sekhon D, Bose K. J Urol 2002; 167:2109–2110.
19. Lewis AG, Bukowski TP, Jarvis PD, Wacksman J, Sheldon CA. J Pediatr Surg 1995; 30:277–281; discussion 281-272.
20. Mäkelä E, Lahdes-Vasama T, Rajakorpi H, Wikström S. Scand J Surg 2007; 96:62–66.
21. Remer EM, Francis IR, Baumgarten DA et al. Acute Onset of Scrotal Pain-Without Trauma, Without Antecedent Mass. Reston (VA): American College of Radiology (ACR), 2007:5.
22. Karmazyn B, Steinberg R, Livne P et al. J Pediatr Surg 2006; 41:500–504.
23. Bodiwala D, Summerton DJ, Terry TR. Ann R Coll Surg Engl 2007; 89:349–353.
24. Kadish HA, Bolte RG. Pediatrics 1998; 102:73–76.
25. Karmazyn B, Steinberg R, Kornreich L et al. Pediatr Radiol 2005; 35:302–310.
26. Kass EJ, Lundak B. Pediatr Clin North Am 1997; 44:1251–1266.
27. Nussbaum Blask AR, Rushton HG. Am J Roentgenol 2006; 187:1627–1635.
28. Ringdahl E, Teague L. Am Fam Physician 2006; 74:1739–1743.
29. Rabinowitz R. J Urol 1984; 132:89–90.
30. Sparano A, Acampora C, Scaglione M, Romano L. Emerg Radiol 2008.
31. Kapasi Z, Halliday S. Emerg Med J 2005; 22: 559–560.
32. Varga J, Zivkovic D, Grebeldinger S, Somer D. Urol Int 2007; 78:73–77.
33. Baker LA, Sigman D, Mathews RI, Benson J, Docimo SG. Pediatrics 2000; 105:604–607.
34. Dewire DM, Begun FP, Lawson RK, Fitzgerald S, Foley WD. J Urol 1992; 147:89–91.
35. Hendrikx AJ, Dang CL, Vroegindeweij D, Korte JH. Br J Urol 1997; 79:58–65.
36. Kravchick S, Cytron S, Leibovici O et al. Eur Radiol 2001; 11:1000–1005.
37. Schwaibold H, Fobbe F, Klan R, Dieckmann KP. Urol Int 1996; 56:96–99.
38. Stehr M, Boehm R. Eur J Pediatr Surg 2003; 13:386–392.
39. Yuan Z, Luo Q, Chen L, Zhu J, Zhu R. Ann Nucl Med 2001; 15:225–229.
40. Pepe P, Panella P, Pennisi M, Aragona F. Eur J Radiol 2006; 60:120–124.
41. Hod N, Maizlin Z, Strauss S, Horne T. Isr Med Assoc J 2004; 6:13–15.
42. Patriquin HB, Yazbeck S, Trinh B et al. Radiology 1993; 188:781–785.
43. Arce JD, Cortes M, Vargas JC. Pediatr Radiol 2002; 32:485–491.
44. Baud C, Veyrac C, Couture A, Ferran JL. Pediatr Radiol 1998; 28:950–954.
45. Vijayaraghavan SB. J Ultrasound Med 2006; 25:563–574.
46. Atkinson GO, Jr., Patrick LE, Ball TI, Jr., Stephenson CA, Broecker BH et al. Am J Roentgenol 1992; 158:613–617.
47. Coley BD, Frush DP, Babcock DS et al. Radiology 1996; 199:441–446.
48. Sidhu PS. Clin Radiol 1999; 54:343–352.
49. Zinn HL, Cohen HL, Horowitz M. J Ultrasound Med 1998; 17:385–388.
50. Bader TR, Kammerhuber F, Herneth AM. Radiology 1997; 202:559–564.
51. Luker GD, Siegel MJ. Radiology 1996;198: 381–385.
52. Cheng HC, Khan MA, Bogdanov A, Jr., Kwong K, Weissleder R. Invest Radiol 1997; 32: 763–769.
53. Kaipia A, Ryymin P, Makela E, Aaltonen M, Kahara V et al. Int J Androl 2005; 28:355–359.
54. Fernandez-Perez GC, Tardaguila FM, Velasco M et al. Am J Roentgenol 2005; 184:1587–1593.
55. Watanabe Y, Dohke M, Ohkubo K et al. Radiology 2000; 217:219–227.
56. Watanabe Y, Nagayama M, Okumura A et al. J Magn Reson Imaging 2007; 26:100–108.
57. Nussbaum Blask AR, Bulas D, Shalaby-Rana E, Rushton G, Shao C et al. Pediatr Emerg Care 2002; 18:67–71.
58. Lutzker LG, Zuckier LS. Semin Nucl Med 1990; 20:159–188.
59. Cattolica EV. J Urol 1985; 133:803–805.
60. Garel L, Dubois J, Azzie G, Filiatrault D, Grignon A et al. Pediatr Radiol 2000; 30:41–44.
61. Sparks JP. Ann R Coll Surg Engl 1971; 49:77–91.
62. Middleton WD, Siegel BA, Melson GL, Yates CK, Andriole GL. Radiology 1990; 177:177–181.
63. Paltiel HJ, Connolly LP, Atala A, Paltiel AD, Zurakowski D et al. Radiology 1998; 207: 223–231.

64. ACR Guidelines and Standards Committee. ACR Practice Guideline for the performance of scrotal ultrasound examinations. American College of Radiology, 2006.
65. Kollmann C. Eur J Radiol 2007; 64:164–172.
66. Krestan C. Radiologe 2005; 45:513–519.
67. Capraro GA, Mader TJ, Coughlin BF et al. Ann Emerg Med 2007; 49:520–525.

Part VI

Prenatal Imaging

41

Imaging of Fetal Anomalies

Dorothy I. Bulas

Issues

I. Does early fetal imaging (before 24 weeks gestation) improve maternal or fetal outcome?
II. Does third trimester fetal imaging improve maternal or fetal outcome?
III. Is ultrasound (US) safe for imaging the fetus?
IV. Is MRI safe for imaging the fetus?
V. What is the diagnostic performance of US and MRI in the assessment of fetal anomalies?
VI. What is the role of MR imaging in the evaluation of the fetus?

Key Points

- Routine ultrasound in early pregnancy (before 24 weeks gestation) is useful for gestational age assessment, identification of multiple pregnancies, and identification of unsuspected fetal anomalies (strong evidence).
- Routine ultrasound in late pregnancy (after 24 weeks gestation) may not be associated with improvements in overall perinatal mortality though there is a lack of data with regard to long-term neurodevelopmental outcome (moderate evidence).
- High-risk pregnancies benefit from ultrasound assessment including Doppler ultrasound of umbilical and fetal vessels in late pregnancy with a trend in reduction of perinatal deaths (moderate to strong evidence).
- The accuracy of ultrasound in the evaluation of fetal anomalies is influenced by the skill of the sonographer, quality of equipment, prevalence of a defect, gestational age of the fetus, maternal body habitus, oligohydramnios, and examination protocol (moderate evidence).

D.I. Bulas (✉)
Department of Diagnostic Imaging and Radiology, George Washington University School of Medicine and Health Sciences, Children's National Medical Center, Washington DC 20010, USA
e-mail: dbulas@cnmc.org

L.S. Medina et al. (eds.), *Evidence-Based Imaging in Pediatrics*,
DOI 10.1007/978-1-4419-0922-0_41,

- MRI evaluation of fetal abnormalities is not limited by fetal lie, oligohydramnios, overlying fat, bone, or air (moderate evidence).
- MRI can be a useful adjunct in the evaluation of certain fetal anomalies particularly within the brain and chest (limited evidence).
- No data were found in the medical literature that evaluated the cost-effectiveness of US versus MR in the evaluation of fetal anomalies (limited evidence).
- MRI using higher strength magnets (≥3 T) and Doppler ultrasound in the first trimester should be minimized due to theoretical risks (US moderate evidence, MRI limited evidence).

Definition and Pathophysiology

The ability to directly visualize the fetus and its environment noninvasively has changed the practice of obstetrics and neonatology. The usefulness of ultrasound (US) in the assessment of gestational age, detection of multiple pregnancies, evaluation of fetal growth, and identification of fetal anomalies has resulted in an unprecedented expansion in its application in obstetrics. Nearly every pregnant woman in the USA today is offered a fetal screening US during the second trimester that is used to decide if further imaging or other testing is needed.

The incidence of major congenital anomalies at birth is 2–3% but is responsible for up to 25% of perinatal deaths and an even larger percentage of perinatal morbidity (1). Detecting anomalies prenatally increases the option for pregnancy management and treatment.

As the diagnosis of fetal anomalies becomes a major goal in the evaluation of the fetus and as complex perinatal therapies advance, MRI has become a complementary tool in the assessment of fetal anomalies.

Epidemiology

Congenital malformations, including chromosomal abnormalities, are present in 3–6% of newborns and account for 20–30% of perinatal deaths (1). These conditions are associated with higher rates of intrauterine death, preterm birth, and intrauterine growth restriction. Prenatal diagnosis can reduce mortality from congenital anomalies by guiding interventions during pregnancy and optimizing preparation for delivery, as well as planning neonatal management options. Termination of pregnancies affected by anomalies also has impacted the decrease in the neonatal mortality rate (2). The impact of prenatal diagnosis on fetal and infant outcomes is dependent on gestational age at time of diagnosis, effect on maternal outcome, and neonatal prognosis with or without therapy.

Regional differences in the availability of prenatal diagnosis can influence mortality rates. In a birth cohort study of live births, stillbirths, and infant deaths in Canada for the years 1991–1998, the infant mortality rate was between 6.1 and 6.4 per 1,000 live births from 1991 to 1995, then dropped to 5.4 and 5.5 per 1,000 in 1996 and 1997, respectively. Infant deaths from congenital anomalies declined 21% from 1.86 to 1.47 per 1,000 over the same period while fetal deaths caused by pregnancy termination increased (2). Prenatal diagnoses and pregnancy terminations for congenital anomalies were associated with decreased overall infant mortality.

In the United States, the infant mortality rate has consistently declined with an overall decrease of 10% from 1990 to 2003. In 2003, the infant mortality rate reached 6.74 deaths per 1,000 live births attributable to a drop in late fetal deaths (3).

Overall Cost to Society

Serious congenital anomalies account for 25% of neonatal deaths and can lead to debilitating long-term disabilities at considerable societal cost (1). Complicating the issue is the factor of whether a family will elect to terminate

if a fetal anomaly is identified with ultrasound or MR imaging. Societal views with regard to when and how a termination may proceed also impacts the cost-effectiveness of fetal imaging (4–8). Thus, the use of imaging in pregnancy has important health and economic outcomes for both families and the health-care system.

In one American study, cost savings from early detection and therapeutic abortion were considered for fetal conditions for which lifetime cost estimates were available (such as spina bifida, major cardiac disease, cleft palate, and diaphragmatic hernia) (9). Potential cost savings from averting treatment for preterm labor and postdate gestations were also considered. Fetal anomaly detection by US before 24 weeks was calculated using RADIUS trial data from tertiary and nontertiary centers (10–12). The ratio of overall savings to cost of the exam was between 1.35 and 1.70 (savings of $1.35–$1.70 per $1 spent) if US was performed in tertiary care centers. However, if a nontertiary care center performed the study (in which the identification of anomalies was documented to be much lower), the ratio of savings to cost was between 0.40 and 0.74 (loss of $0.26–$0.60 per $1 spent). Their conclusion was that routine second trimester US screening could be associated with net benefits with the caveat that the US was performed by experienced sonographers (9). In a smaller series of 2,031 patients, sensitivity in identifying major anomalies was documented to be 90% in the high-risk group and 48% in the low-risk screening group. Projected newborn cost savings offset the cost of routine midtrimester screening in this cost analysis (13).

Randomized controlled trials (RCT) and cost-effectiveness data have been analyzed in the literature incorporating imaging strategies of the fetus (14–16). Despite these evidence-based recommendations, prenatal US has become a social experience and expectation and has resulted in discordance of evidence and the clinical use of US imaging particularly in late pregnancy in low-risk pregnancies (17).

Goals

In fetal imaging, the goals are early assessment of gestational age, detection of multiple pregnancies, evaluation of fetal growth, fetal well-being, and identification of fetal anomalies. There are various imaging techniques and tools that are available. First trimester scans, including the use of transvaginal transducers can supply information on gestation age, multiplicity, and identification of some anomalies. Second and third trimester US and MR imaging can identify anomalies that were too subtle or not yet developed during the first trimester. Assessment of growth and well-being can be sequentially followed as needed by US and Doppler of the umbilical, uterine, and fetal vessels in high-risk cases. MRI can confirm US findings and identify additional anomalies that may impact counseling, the planning and execution of perinatal intervention, delivery preparation, and neonatal therapy.

Methodology

The author performed a MEDLINE search using PubMed (National Library of Medicine, Bethesda MD) for data relevant to the diagnostic performance and accuracy of both ultrasound and MR imaging of fetuses at risk for anomalies. The Cochrane library was also searched. The review of current diagnostic fetal imaging literature was based on a systematic literature review performed in MEDLINE covering the years 1980–February 2008. The search strategy used the following key statements and words: (1) *Fetus,* (2) *Fetal imaging,* (3) *Ultrasound,* (4) *Magnetic Resonance Imaging,* (5) *Prenatal Imaging,* (6) *Fetal anomalies,* (7) *Doppler*; as well as combinations of these search strings. Non-English articles were excluded.

Discussion of Issues

I. Does Early Fetal Imaging (Before 24 Weeks Gestation) Improve Maternal or Fetal Outcome?

Summary of Evidence: Advantages of early pregnancy US screening include more accurate calculation of gestational age, earlier identification of multiple pregnancies, and the diagnosis of non viable pregnancies (strong evidence).

Whether all obstetrical patients should undergo US screening and whether such screening improves pregnancy outcome remains controversial. Currently, the American College of Obstetricians and Gynecologists (ACOG) supports the use of US when there is a specific medical indication and advises against casual use of US during pregnancy (strong evidence) (18).

The introduction of faster MR sequences with high contrast, large field of view, and multiplanar imaging without limitations from overlying gas, bone, or fat has led to its increased use as a complementary tool in the further assessment of fetal anomalies initially identified by US (limited evidence).

Supporting Evidence: The question as to whether prenatal exams should be performed routinely in the first or second trimester or reserved for specific indications has been investigated by numerous large studies as well as the Cochrane Pregnancy and Childbirth Group trials register and Cochrane controlled trials register (15, 16).

In the early 1980s, four trials showed there was more accurate pregnancy dating and a higher rate of detection of twins in US-screened groups (19–22). However, an improvement in overall pregnancy outcome was not documented. Five randomized trials in the 1990s showed that routine US was associated with a decrease in labor inductions and earlier twin detection. No difference in birth weight or NICU admission rates, however, was noted (23–25). In the Cochrane review of nine trials in 2001, routine US was found to be useful in the calculation of gestational age and was associated with reduced rates of induction of labor for post-term pregnancy (odds ratio 0.61, 95% confidence interval 0.52–0.72). Routine US was also found to be useful in the early identification of multiple pregnancies, important in management, and delivery planning (twins undiagnosed at 26 weeks odds ratio 0.08; 95% confidence interval 0.04–0.16) (15). However, in their analysis, routine US in low-risk pregnant women did not appear to decrease perinatal morbidity and mortality (odds ratio 0.86; 95% CI 0.67–1.12) (strong evidence) unless the detection of a fetal abnormality was a specific aim of the exam (moderate to strong evidence). The 1993 Routine Antenatal Diagnostic Imaging with US (RADIUS) trial was a multicenter randomized study of 15,000 low-risk women who were randomized to either routine US exams in the second and third trimester or only when specific clinical concern occurred (10). US was useful in the detection of unsuspected twins, placenta previa, and assignation of gestational age (strong evidence). The US exam in this series, however, was not comprehensive with regard to evaluating fetal anomalies and thus did not take into account pregnancies that might have been terminated if an anomaly was detected. Because of this, the RADIUS evidence failed to disclose a benefit in either perinatal morbidity or mortality. Detection rate for anomalies for this series was low (16.6%) as compared to European studies (51%) during the same time period. If the detection rate had been as good as the European studies, a demonstrable benefit to screening would have been shown (12).

In a similar randomized trial of 9,310 pregnant women in Helsinki by Saari-Kemppainen et al. a decrease in perinatal mortality was reported among the US-screened group (9 per 1,000 to 4.6 per 1,000) (7). This was felt to be due to the high rate of detection of fetal anomalies in this European series (58% of major malformations identified before 24 weeks) with subsequent termination of these fetuses (7).

As the focus of routine US shifts to optimizing the rate of fetal anomaly detection, routine sonography is cost-effective and has the potential to decrease neonatal mortality if rate of anomaly detection exceeds 35% (provided parents elect pregnancy termination). If the detection rate of anomalies by US is less than 35% (due to inexperienced sonographers/ incomplete surveys) or the family does not elect to terminate, the neonatal mortality rate may not decrease despite routine screening. A meta-analysis by Bucher et al. based on four randomized clinical trials found the perinatal mortality rate lower in patients with routine scanning due to early detection of fetal anomalies leading to terminations (odds ratio 0.64; 95% confidence interval 0.43–0.97) (26). Some anomalies are best visualized near the end of 24 weeks while others can be identified much earlier (27). Pregnant women requesting US to assess fetal normalcy

should have a midtrimester exam by a highly experience sonographer with a comprehensive detailed assessment of fetal heart, extremities, and face.

Numerous reports have described improved resolution and identification of additional fetal anomalies by MR. In these small series, the impact of parental counseling and perinatal management has been described.

II. Does Third Trimester Fetal Imaging Improve Maternal or Fetal Outcome?

Summary of Evidence: Routine third trimester US and Doppler studies in low-risk populations have so far not been shown to benefit the mother or fetus (moderate evidence). Thus, US and Doppler studies currently are used selectively when specific clinical indications are present (moderate to strong evidence) (16). The lack of data on maternal psychologic effects and effects on both short and long-term neonatal childhood outcome, however, limits the current evidence.

When a fetal anomaly is detected after 24 weeks gestation, MR may provide additional information as studies are not limited by fetal position, overlying fat or bone, oligohydramnios and provide a large field with multiplanar images. These additional findings may affect counseling, direct prenatal intervention, influence delivery planning, and neonatal management (limited evidence).

Supporting Evidence

Ultrasound

In a meta-analysis of seven trials recruiting 25,000 women, no difference in antenatal obstetric and neonatal intervention or morbidity was identified in those screened routinely in late pregnancy versus those imaged only for specific indications (16). There was no associated improvement in overall perinatal mortality. In one trial, placental grading as an adjunct to the third trimester scan was associated with a reduction in the stillbirth rate. Limitations of this review include lack of data with regard to both maternal psychological effects and long-term pediatric outcomes such as neurodevelopment (16).

Doppler US Velocimetry

Doppler US velocimetry (the blood flow rate) of the uterine, umbilical, and fetal vessels has been shown to provide the clinician with important information on hemodynamics in the third trimester, particularly those at *high risk* (i.e., *intrauterine growth retardation, congenital heart disease).* Gestational age-related reference values have been established for maternal uterine artery, arcuate artery, umbilical artery, as well as fetal cerebral, aortic, renal, and femoral arteries. Uterine arterial remodeling occurs following successful placentation with decrease in intimal muscle resulting in increasing diastolic flow and loss of elasticity (28). Diastolic velocities increase with advancing gestation. Intrauterine growth retardation (IUGR) has been reported when pulsitility or resistance indices increase or notching in the waveform at end-systole develops at 22–24 weeks gestation (28, 29). Uterine flow velocity waveforms are useful in predicting the frequency and severity of preeclampsia and IUGR (28, 30, 31). Umbilical arterial flow using the systolic/diastolic (S/D) ratio is also useful to assess decline in placental resistance with advancing gestational age. The umbilical artery peak systolic flow velocity gradually decreases while diastolic flow velocity increases. In growth-retarded fetuses and fetuses developing intrauterine distress, the umbilical artery waveform changes as placental vascular resistance increases.

Applied as a screening test in an unselected pregnant population, umbilical velocimetry has not been found to be cost-effective (16, 32) as a significant change in indices does not develop until more than 60% of the terminal placental arteries are obliterated (Strong Evidence) (31). On the other hand, in preselected populations of high-risk pregnancies, Doppler of the umbilical artery has a high predictive value with regard to diagnosing fetal compromise (33). The fetus with an abnormal umbilical artery velocimetry will redistribute blood flow to the heart and brain (34). Fetal brain sparing during hypoxia is characterized by an increase in diastolic and mean blood flow velocity in the middle cerebral artery and helps identify fetal

distress in high-risk populations (41, 42). Abnormal intrauterine umbilical and fetal blood flow Doppler velocities are associated with higher mortality and morbidity in the neonatal period. Long-term follow-up studies have showed an association between the abnormal intrauterine umbilical and fetal blood flow and subsequent postnatal neurodevelopmental impairment including mental retardation and severe motor impairment (34–36).

MRI

Magnetic Resonance Imaging (MRI) is a more expensive modality that uses no ionizing radiation, has excellent tissue contrast, and can provide a large field of view. Limitations of sonography resulting from decreased amniotic fluid volume, fetal positioning, and acoustic shadowing from the ossifying skull, and maternal body habitus can be overcome by fetal MR imaging.

As the identification of fetal anomalies influences the perinatal mortality and morbidity rate, MRI can play a role in perinatal management after 24 weeks gestation. Numerous series have demonstrated improved resolution of fetal anomalies in cases initially identified by US (37–49). While these series are small, the confirmation of US findings and the demonstration of additional anomalies have been shown to affect counseling, delivery planning, and immediate postnatal care. MRI evaluation of specific anomalies such as airway masses, sacrococcygeal teratomas, and meningomyeloceles have allowed for the planning and execution of in utero surgery. When fetal surgery is not an option, the fetal MRI has been used for postnatal surgical planning (30, 38). No large randomized prospective studies, however, are currently available concerning the use of fetal MR for a specific indication.

III. Is US Safe for Imaging the Fetus?

Summary of Evidence: Diagnostic ultrasound is based on the detection and display of acoustic energy that is reflected from various tissue interfaces. Sound frequencies used for diagnostic applications typically range from 2 to 15 MHz. After three decades of extensive human use, there are no known reports of harm (strong evidence). In vitro and animal experiments, however, have shown that prolonged insonation can produce bioeffects by thermal, cavitational, or other mechanisms (50–53). Epidemiological data are reassuring, but are based on early US devices that had substantially lower energy output than current machines. Thus, there remains some concern that the potential for tissue heating could exceed safety limits if pulsed and color Doppler, particularly in the first trimester, are used for prolonged periods of dwell time.

Supporting Evidence: The Food and Drug Administration (FDA) allows current instruments to have higher acoustic energy output than in the past as long as they display energy output as thermal index (TI) and mechanical index (MI) as guides for heat- and cavitation-induced bioeffects. No independently confirmed experimental evidence has demonstrated damage in animal models below a thermal index (TI) of 2 and a mechanical index (MI) of less than 0.3. The American Institute of Ultrasound in Medicine (AIUM) Bioeffects Committee states that "no confirmed biological effects on patients or instrument operators caused by exposure at intensities typical of present diagnostic US instruments have ever been reported. Although the possibility exists that such biological effects may be identified in the future, current data indicate that the benefits to patients with the prudent use of diagnostic US outweigh the risks, if any, that may be present" (54).

Recommendations for obstetric US exposure suggest that the principles of ALARA (as low as reasonably achievable) should be followed because of the potential for tissue heating. Operators can minimize risk by limiting dwell time, limiting exposure to critical structures, and following equipment-generated exposure information.

A high degree of safety has been established for exposures to spatial peak temporal average intensities of <100 mW/cm^2. Several epidemiologic studies have reported no increase in the incidence of fetal death, abnormality, intrauterine growth retardation, or malignancy with up to 12-year follow-up (50–53) (moderate to strong evidence). One large randomized control study compared neonatal and pediatric outcomes in fetuses who underwent repeated

prenatal US from those given one routine US and demonstrated smaller average birth weights in those with repeated exposure to prenatal US. However, long-term follow-up of these children showed normal catch-up growth and normal behavioral and cognitive function (55). Another study also demonstrated no behavioral or neurologic effects on reading, dyslexia, writing, math, or overall school performances at age 8–9 (56). An association with non-right handedness and prenatal US exposure has been reported in two randomized studies (57). Associated left handedness in males was shown in a cohort study (58). These studies require further investigation as these were statistical associations with no definite neurologic deficits noted.

Higher acoustic output and energy deposition in tissues is of concern as more imaging is performed in the first trimester with longer exposure times particularly with the use of Doppler. Acoustic outputs from modern devices have increased 10–15 fold and epidemiologic evidence is from B-mode scanners used 20 years ago (59, 60). Potential for tissue heating when the thermal index exceeds 1 has been evaluated in fetal sheep (33). Exposure can be reduced through the use of output control and by reducing the amount of time the beam is focused on one place. All diagnostic US devices should also comply with FDA output display standards—MI and TI < 1 (53).

IV. Is MRI Safe for Imaging the Fetus?

Summary of Evidence: Currently, there is no definite evidence that MR imaging using clinical parameters produces harmful effects on human embryos or fetuses. However, the long-term safety of MRI exposure to the fetus has not been definitively demonstrated.

There are two potential safety issues for fetal MR imaging—teratogenic effects and acoustic damage. Reassuring evidence in both animals and humans suggests that the acoustic noise does not damage fetal hearing. There has been concern that prolonged exposure to high-field magnetic resonance imaging could potentially affect embryogenesis, chromosomal structure, or fetal development. Compliance with U.S. Food and Drug Administration (FDA) and International Commission on Non-Ionizing Radiation Protection (ICNIRP) guidelines requires control of specific absorption rate (SAR) values. The UK's Medical Device Agency (MDA) guidelines require control of the maximum SAR (10 W/kg) within the fetus. Single-shot fast spin echo (ssFSE/HASTE) sequences on 1.5 T magnets often require operation at the SAR limits imposed by safety guidelines. With higher field strength magnets (e.g., 3 T), these limits may be even more significant for fetal imaging (61, 62).

Because of the potential risk of MR imaging to the developing fetus and the current limitations of resolution due to small size and fetal motion artifact in the first trimester, imaging after 18 weeks gestation is suggested.

Supporting Evidence: Many studies have been performed to assess the safety of MR imaging in pregnant animals and animal embryos. However, there is a lack of consensus as to whether there is an actual risk to the fetus (63–66). These studies used MR scanners of differing field strengths and differing scanning conditions, including a range of radio-frequencies, scan times, and gradient magnetic fields. Thus, it is difficult to directly extrapolate these animal studies to clinical human fetal MR examinations.

Studies on the safety of MR imaging in pregnant women are limited as well. Several series have shown no adverse long-term effects of fetal MR in children who were imaged as fetuses, though sample sizes were small (67–72). There is concern that with higher strength units and prolonged times, biological effects may be noted if applied at sensitive stages of fetal development. Potential side effects of the echo planar technique on the fetal ear have been suggested but have not been documented on follow-up studies (68). The American College of Radiology white paper on MR safety published in 2002 states that "Pregnant patients can be accepted to undergo MR images at any stage of pregnancy if, in the determination of an attending radiologist, the risk–benefit ratio to the patient warrants that the study be performed" (73).

Gadolinium contrast material crosses the placenta, fetal urine excretion then occurs with

a cycle of swallowing and excreting the contrast. Elimination time is unknown but prolonged. Fetal animal studies have demonstrated growth retardation, visual problems, and bone and visceral anomalies after administration of high doses of the drug (Magnevist® product information, Bayer HealthCare). Thus, the use of gadolinium is not recommended for fetal MRI.

V. What Is the Diagnostic Performance of US and MRI in the Assessment of Fetal Anomalies?

Summary of Evidence: There is a wide range in reported sensitivities (14–85%) of US in identifying specific anomalies that is dependant on the type of anomaly, gestational age at time of the study, the skill of the sonographer, and whether the population is at high or low risk for anomalies (74–78). The greatest accuracies are reported in renal and cranial anomalies. Pregnant women requesting fetal US should have a midtrimester exam by an experienced sonographer with a comprehensive, detailed assessment that includes the fetal heart, spine, extremities, and face. Structural abnormalities that can be most reliably diagnosed by US include hydrocephalus, anencephaly, myelomeningocele, skeletal dysplasias, omphalocele, gastroschisis, duodenal atresia, cleft lip, renal abnormalities, and a variety of congenital cardiac abnormalities. MRI detects 5–50% of anomalies missed by US with the lower number reflecting US performed by more experienced users.

Supporting Evidence

Ultrasound

US is the initial imaging modality of choice for the assessment of the fetus. Yet, it is operator dependent, and factors such as fetal position, maternal obesity, overlying bone, gas, and oligohydramnios can limit the examination. Factors influencing accuracy include skill of sonographer, equipment quality, number of studies done, gestational age at time of exam, type of defect, maternal body habitus, and exam protocol. Structural abnormalities such as cerebral malformations lesions can be sonographically occult.

The US accuracy in detecting abnormalities in the low-risk population has been variable in numerous series. Sensitivities for identification of an anomaly have ranged from as low as 14% to as high as 85% while specificities have ranged from 93 to 99% (74–78) One of the largest studies of fetal anomaly detection with US screening was the Eurofetus study which included 200,000 women from 14 European countries. US exams performed between 18 and 22 weeks identified 56% of anomalies (73% of major anomalies) (79). The anomalies best detected in this study were renal (89%) and CNS (88%). Less successful were the identification of cardiac (major 39%, minor 21%), and musculoskeletal (73% major, 18% minor) anomalies. There was an 84% true-positive rate and 10% false-positive rate (79).

Centers that had the best sensitivities were using the most recent equipment on populations at high risk for anomalies. Other studies have also demonstrated that targeted exams on high-risk patients have a higher accuracy (sensitivity 86–99%, specificity 91–100%) (80–82).

In the Eurofetus study, Levi and Montenagro demonstrated that detection rates were higher when performed in hospitals by certified technicians (60–80%) versus those performed in a doctor's office (25–30%) (79). The RADIUS trial also showed that operator experience was a critical factor in assessing efficacy of US screening. Experience of the sonographers had a measurable impact on anomaly detection. Highly experienced sonographers detected 35% of anomalies compared with only 13% by less experienced sonographers (10).

The number of exams and gestational age at the time the exam is performed influence detection rate as well. Thirty-eight percent of anomalies diagnosed in the Eurofetus study were identified after 29 weeks (83). This may be due to the fact that some anomalies become apparent or developed later in pregnancy (84). In a review of 17 registries, the overall prenatal detection rate was 64% (25–88% across regions). In this series gestational age at time of diagnosis was less than 24 weeks for 68% of cases ($p<0.0001$) (82).

When comparing US findings to postnatal MRI, the MRI demonstrated additional anomalies in 56% of patients (40). Similarly, when comparing US findings to autopsy results, US

often does not identify all anomalies. Kaiser et al. noted additional findings were identified at autopsy in 51% of fetuses aborted because of an abnormality noted on prenatal sonography. There was a 3% false-positive rate (failure to confirm anomaly for which the termination was carried out) (85).

MRI

Magnetic Resonance Imaging (MRI) is a more expensive modality that uses no ionizing radiation, has excellent tissue contrast, and can provide a large field of view. Limitations of sonography resulting from decreased amniotic fluid volume, fetal positioning, and acoustic shadowing from the ossifying skull, and maternal body habitus can be overcome by fetal MR imaging. Fetal MR imaging allows direct visualization of both sides of the fetal brain in any plane, detailed evaluation of the developing brain, including direct visualization and assessment of the developing cortex, sulci, and olfactory bulbs which are extremely difficult to visualize with sonography (40, 44, 86, 87). Structural abnormalities such as heterotopias, cerebellar dysplasia, encephalomalacia, and cervical masses can be sonographically occult yet identified by fetal MRI (41, 88–92).

Interpreting fetal MRI can be challenging as structures are small and change with fetal maturation. Fetal motion particularly in early gestation or in the presence of polyhydramnios limits resolution. While obesity is not as limiting with MR compared to US, table limits (usually 350 pounds or less) and type of coil used may limit image quality.

Limitations in fetal MR accuracy include short pulse sequence options to decrease fetal movement artifact, with resultant low signal-to-noise ratio. Currently no coils are dedicated to in utero imaging. Available phased array coils and parallel acquisition can help improve the signal. Fetal motion artifact may affect image quality particularly in earlier gestation limiting the ability to obtain true sagittal images. Studies performed in the second trimester may be too early to identify developmental anomalies yet to occur. No high-resolution T1w imaging is currently available, so small foci of cortical malformation may be missed.

The lack of understanding of normal temporal and structural fetal development may compromise interpretations. For example, inferior vermian hypoplasia has been overdiagnosed by fetal MRI (93, 94). Delay between known anatomic stages of development and those detected by fetal MRI has been noted to lag up to 5 weeks (95).

The rate of detection of fetal-associated abnormalities missed by US varies from 5 to 50% in large part due to inexperience of the sonographer. MRI is not as operator dependent and does not face the same limitations as US with regard to overlying bone, fat, oligohydramnios, and fetal lie. Many studies have shown that fetal MR imaging can detect sonographically occult abnormalities in up to 50% of cases studied for a variety of indications (39–43, 48, 95, 96).

Some studies have disputed the superiority of MR. One study noted that US by experienced sonographers was as good or even better than MR in the detection of fetal CNS anomalies (37). In their series of 42 cases, they concluded the major role of MRI was reassuring parents concerning the presence or absence of brain anomalies.

Inexperience in fetal MR interpretation with lack of long-term follow-up data limits the assessment of current MR sensitivity and specificity. While MR has added diagnostic specificity for the diagnosis of posterior fossa anomalies, posterior fossa dysgenesis remains challenging due to both false-positive and false-negative diagnosis (83, 97–99).

Comparing US to MR in the assessment of ventriculomegaly, Benacerraf et al. noted that MRI provided additional information in only 2/14 cases with isolated ventriculomegaly (46). However, of 12 cases with ventriculomegaly and other CNS anomalies, MRI identified additional anomalies which influenced outcome in 10 cases (migrational abnormalities ($n = 4$), porencephaly ($n = 4$), one diagnosis each of abnormal myelination, hypoplasia of the corpus callosum, microcephaly, a kinked brain stem, and cerebellar hypoplasia). They concluded that while US was an accurate diagnostic modality for the evaluation of fetuses, MRI added important additional information in fetuses with ventriculomegaly.

The variability of US performance makes comparison of MR and US accuracy problematic. It is best to view MR as a complementary tool to problem solve in special cases of US abnormal findings. The results of fetal MR imaging, whether verifying absence of abnormality, confirming sonographically detected abnormalities, or discovering additional abnormalities that were not apparent by sonography, have been shown to affect clinical decision-making during pregnancy by both physicians and parents. Fetal MR results affect patient counseling and result in changes in pregnancy management in nearly half of cases (40, 100).

VI. What Is the Role of MR Imaging in the Evaluation of the Fetus?

Summary of Evidence: Over 1,000 articles have been published on fetal MRI since 1983. Fetal MRI has been particularly helpful with the diagnosis and management of suspected fetal CNS abnormalities on US (37–40). Fetal MRI can aid in the diagnosis of ventriculomegaly, agenesis of the corpus callosum, posterior fossa abnormalities, cortical gyral malformation, hemorrhages, holoprosencephaly, and vascular malformations. MRI has changed the diagnosis and aided in the management of many cases of suspected CNS abnormalities on US (44, 101–104).

Fetal MRI is performed to assess central nervous system abnormalities and cases in which fetal surgery is being considered (neural tube defects, congenital diaphragmatic hernia, and masses that obstruct the airway). Complex anomalies including sacrococcygeal teratomas and conjoined twins benefit from the large field of view (75, 105). When oligohydramnios is present, MR may better demonstrate anatomy (48). The American College of Radiology Guidelines for MRI of the female pelvis has amended its indication for pelvic MRI to include the identification of congenital fetal anomalies (106).

Supporting Evidence: MRI can clarify the diagnosis and help patients make decisions such as whether to continue with the pregnancy (95). Limitations of MRI include expense, lack of availability, maternal claustrophobia and anxiety, maternal obesity (table weight limit), fetal motion particularly in the presence of polyhydramnios, and chemical shift artifacts. Vascular hemodynamics, cardiac assessment and limb evaluation are limited. There continues to be a lack of normal values particularly volumetric data. Limitations in accurate interpretation of images exist. Greater understanding of temporal and structural variations in fetal development is still required. Large prospective studies using serial and quantitative MR in both normal and abnormal fetuses with long-term outcome is critical for true determination of MR accuracy in counseling

Levine et al. compared 242 US studies and 242 MRI studies in 214 fetuses with suspected CNS anomalies. At confirmatory level 2 US, 69 fetuses had normal CNS imaging. Eighty percent of the fetuses had postnatal follow-up. Fetal MRI provided additional information in 50% of cases, revealing new major CNS findings in 32%. In patients with previable fetuses, the information was used to help decide whether to continue the pregnancy. In patients with viable fetuses the information was used to help determine the mode and location of delivery (107).

In monochorionic twin pregnancies complicated by intrauterine fetal demise or twin to twin transfusion syndrome, fetal MRI has been useful in the diagnosis of multicystic encephalomalacia (108, 109). MRI has also been shown to be useful in the assessment of conjoined twin anatomy due to its large field of view (110).

MRI has been useful in the assessment of fetal airway compression by neck masses so that in utero surgery and/or ex utero intrapartum treatment procedure (EXIT) deliveries can be planned (41, 111). Fetal lung volume measurements may be helpful when assessing outcome for congenital diaphragmatic hernias and congenital lung masses (112, 113).

Numerous series have attempted to compare MR findings to US results and postnatal findings. These series, however, remain small in number with long-term outcome data not yet available on a large scale.

Fetal MR imaging has become an increasingly important tool in evaluating fetuses that have abnormalities suspected on the basis of family history or fetal sonography. While fetal MRI is not recommended as a primary imaging method, with continuing improvements in technology, MR will continue to be a rapidly growing field in future years.

Take Home Tables

Tables 41.1 and 41.2 discuss the performance characteristics of imaging studies for detection of fetal anomalies and present algorithms for imaging fetal anomalies, respectively.

Table 41.1. Performance characteristics of imaging studies for detection of fetal anomalies (references in parentheses)

Modality	Sensitivity (%)	Specificity (%)
US*	14–99 (9–13, 74–82)	93–99 (9–13, 74–82)
Low-risk population	14–74 (10, 13, 74–79)	98–99 (74–79)
High-risk population	86–9 (13, 79–82)	95–99 (79–82)
Inexperienced operator	14–35 (9, 10, 12, 13, 79)	
Experienced operator	51–99 (7, 12, 13, 79–82)	91–100 (80–82)
Major anomalies (79)	73 (79)	
Renal anomalies	89	
CNS anomalies	88	
Cardiac anomalies – major	39	
Cardiac anomalies – minor	21	
Musculoskeletal – major	73	
Musculoskeletal – minor	18	
MRI**	Not available	Not available
Inexperienced US operators	50–56% additional detection rates of fetal anomalies over US (40)	
Experienced US operators	5–50% additional detection rates of fetal anomalies over US (37, 40, 46, 107)	

*18–22-week gestation screening US.
**MRI at third trimester or late second trimester.

Table 41.2. Algorithm for fetal imaging

<24 weeks gestation	>24 weeks gestation
Routine US if indication is present or if mother requests it	US if indication is present
Doppler velocimetry screening for high-risk pregnancy	Doppler velocimetry screening for high-risk pregnancy
MR after 18 weeks gestation if US identifies an abnormality that could be better delineated by MR (i.e., CNS, chest)	MR if US identifies an abnormality that may be better delineated by MR (i.e., CNS, chest)

Imaging Case Studies

Case 1

Figure 41.1 presents a case of osteogenesis imperfecta.

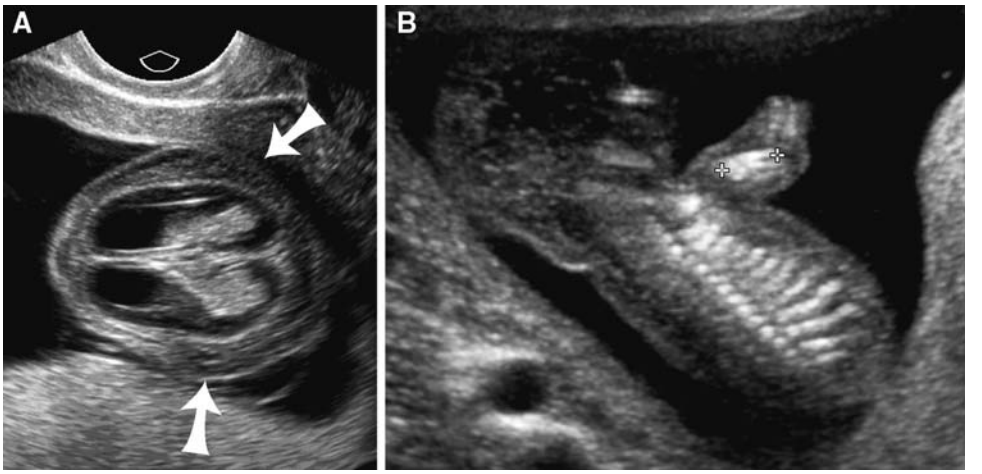

Figure 41.1. A: 13-week gestation transvaginal ultrasound demonstrates edema surrounding the skull (*arrows*) consistent with a large cystic hygroma. The skull appears poorly mineralized in this transverse view. **B**: Coronal image of the fetal chest at 13 weeks gestation demonstrates a short humerus (*cursers*) and irregular ribs. Autopsy confirmed the diagnosis of osteogenesis imperfecta.

Case 2

Figure 41.2 presents a case of agenesis of the corpus callosum which is associated with colpocephaly.

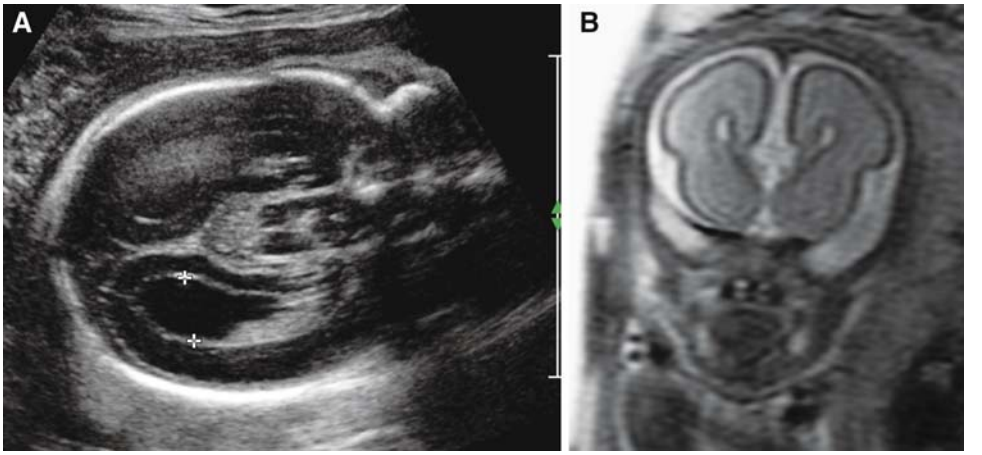

Figure 41.2. A: Transverse US image of a 23-week fetal brain. There is mild ventriculomegaly measuring 11 mm with a tear drop configuration of the lateral ventricle suggestive of colpocephaly. **B**: Coronal MRI performed on the same day confirmed the presence of agenesis of the corpus callosum which is associated with colpocephaly.

Case 3

Figure 41.3 presents a case of mild ventriculomegaly, absent septum pellucidum, suggesting a diagnosis of septo-optic dysplasia. Additional cranial anomalies including bilateral open lip schizencephaly are found.

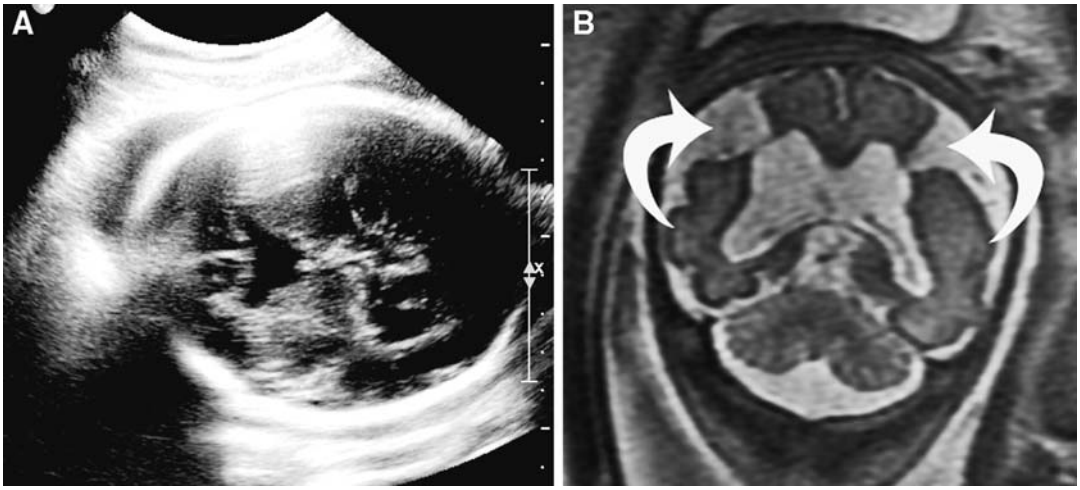

Figure 41.3. **A**: Transverse sonogram of the fetal brain at 33 weeks gestation demonstrates mild ventriculomegaly and absent septum pellucidum, suggesting a diagnosis of septo-optic dysplasia. **B**: Fetal MRI performed on the same day confirmed US findings and demonstrates additional cranial anomalies including bilateral open lip schizencephaly (*arrows*).

Case 4

Figure 41.4 presents a case of sacrococcygeal teratoma

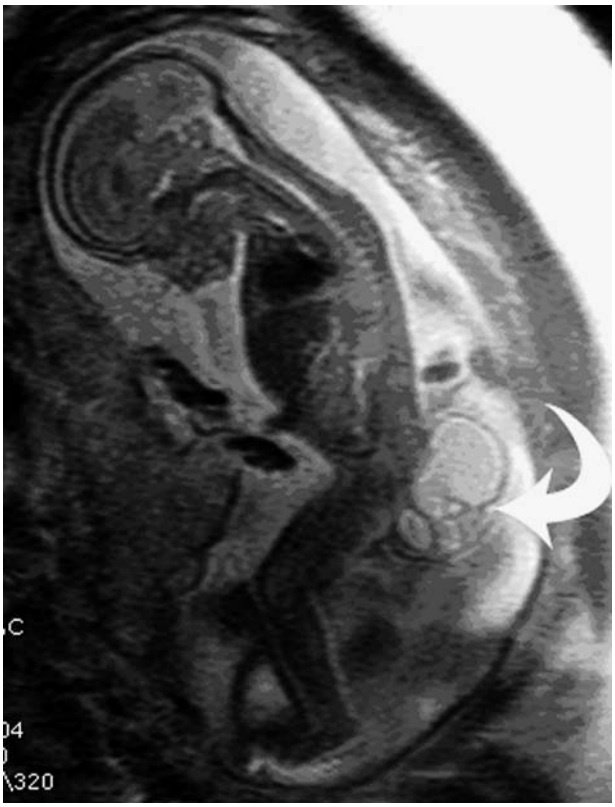

Figure 41.4. Longitudinal MR image of a 20-week fetus demonstrates a large cystic mass in the buttocks region consistent with a sacrococcygeal teratoma (*arrow*). There was no intra-abdominal extension.

Suggested Imaging Protocols for Fetal Anomalies

Ultrasound

Standard fetal anatomic survey:

- transverse and longitudinal scan of uterus, 3 VC, amniotic fluid
- BPD, HC, Skull shape, cavum septum pellucidum, thalami, ventricles, cerebellum, nuchal skin fold, profile, nose/lips, orbits, palate, spine – cor, sag, transverse planes
- Cardiac – 4CV, RVOT, LVOT, aortic arch, ductal arch
- AC, kidneys, cord insertion, bladder, FL, four extremities.
- Curved array C3-9 mHz transducers
- Linear transducer L8–12 mHz for spine and renal anomalies.
- 3D/4D transducers for facial, extremity, cardiac anomalies.
- Transvaginal probes for early gestation, cranial anomalies.

MRI

Exams are performed without sedation or contrast:

- Body coil or body torso phased array surface coil
- Quiet maternal breathing in supine or decubitus position (for maternal comfort)

- Coronal or Sagittal Scout with respect to mother—large field of view T2w Single Shot FSE-TSE/ SSFSE/HASTE
- Three planes with respect to fetal head—small field of view 3–5 mm T2w Single Shot FSE-TSE/SSFSE/HASTE
- Three planes with respect to fetal body—small field of view 3–5 mm T2w Single Shot FSE-TSE /SSFSE/HASTE
- Small field of view—3–5 mm balanced FFE/FIESTA/2DtruFISP/heavy T2w hydrography through areas of interest
- Coronal and/or Sag T1w GRE/MPGR T1/FLASH T1
- Coronal/Axial and/or EPI as needed

Future Research

- Should fetal MRI be used routinely as an adjunct when US identifies a fetal anomaly?
- Which fetal anomalies benefit most from further evaluation by MRI?
- Standard fetal MRI measurement methods and normal measurements (included volumes) need to be established.
- Do higher strength magnets (≥3 T) provide improved fetal resolution?
- Are these higher strength magnets safe for fetal use?
- Can diffusion-weighted, diffusion tensor imaging, proton magnetic resonance spectroscopy (H-MRS) and functional MRI contribute to our understanding of normal as well as abnormal fetal brain development?.
- Can faster fetal MRI techniques be developed to evaluate the fetal heart?

References

1. Morrison I. Semin Perinatol 1985; 9:144.
2. Liu S, Joseph KS, Kramer MS et al. JAMA 2002; 287(12): 1561–1567.
3. Hamilton BE, Minino AM, Martin JA et al. 2007; 119(2):345–360.
4. Waitzman NJ, Romano PS, Scheffler RM. Inquiry 1994; 31:188–205.
5. Waitzman NJ, Romano PS, Scheffler RM et al. MMWR Morb Mortal Wkly Rep 1995; 44: 694–699.
6. Pryde PG, Isada NB, Hallak M et al. Obstet Gynecol 1992; 80:52–59.
7. Saari-Kemppainen A, Karjalainen O, Ylostalo P et al. Lancet 1990; 336:387–391.
8. Beazoglou T, Heffley D, Kyriopoulos J et al. Prenat Diagn 1998; 18:1241–1252.
9. Vintzileos AM, Ananth CV, Smulian JC et al. Am J Obstet Gynecol 2000; 182(3):655–660.
10. Ewigman BG, Crane JP, Frigoletto FD et al. N Engl J Med 1993; 329:821–827.
11. LeFevre ML, Bain RP, Ewigman BG et al. Am J Obstet Gynecol 1993; 169:483–489.
12. Crane JP, LeFevre ML, Winborn RC et al. Am J Obstet Gynecol 1994; 171:392–399.
13. Van Dorsten JP, Hulsey TC, Newman RB et al. Am J Obstet Gynecol 1998; 178(4):742–749.
14. Leivo T, Tuominen R, Saari-Kemppainen A et al. Ultrasound Obstet Gynecol 1996; 7:309–314.
15. Neilson JP. Cochrane Database of Systematic Review 1995, Issue 2, Art No: CD000182DOI:10.1002/14651858.
16. Bricker L, Neilson JP. Cochrane Database of Systematic Review 2007, 18(2): nCD001451.
17. Parer J. Am J Obstet Gynecol 2003; 188;6–12.
18. ACOG Committee Opinion. Number 297. Obstet Gynecol 2004 Aug; 104(2):423–424.
19. Bakketeig LS, Jacobson G, Brodtkorb CJ et al. Lancet 1984; 2:207–211.
20. Eik-Nes SH, Okland O, Aure JC et al. Lancet 1984:11:347.
21. Bennett MJ, Little GH, Dewhurst J et al. Br J Obstet Gynaecol 1988; 89:338–341.
22. Neilson JP, Munjanja SP, Whitfield Cr. BMJ 1984:289;1179–1182.
23. Secher NJ, Hansen PK, Lenstrup C et al. Br J Obstet Gynaecol 1987; 94:105–109.
24. Waldenstrom U, Nilsson S, Fall O et al. Lancet 1988:2;585–588.
25. Ewigman B, LeFebre M, Hesser J. Obstet Gynecol 1990; 76:189–194.
26. Bucher H, Schmidt JG. BMJ 1993 Jul 3; 307(6895):13–17.
27. Thomas DF. Prenat Diagn 2001; 21:1001–1004.
28. Harman C, Baschet A. Curr Opin Obstet Gynecol 2003; 15:147.
29. Detti L, Akiyama M, Mari G. Curr Opin Obstet Gynecol 2002; 14:587.
30. Fleischer A, Schumlman H, Farmakides G. Am J Obstet Gynecol 1986; 154:806.
31. Thompson RS, Trudinger BJ. Ultrasound Med Biol 1990; 16:449.
32. Neilson JP, Alfirevic Z. Cochrane Database Syst Rev 2000; (2):CD000073.
33. Westergaard HB, Langhoff-Roos J, Lingman G et al. Ultrasound Obstet Gynecol 2001; 17:46.
34. Wladimiroff JW, Wijingaard JAGW, Degani S. Obstet Gynecol 1987; 69:705.

35. Wienerroither H, Steiner H, Tomaselli J et al. Obstet Gynecol 2001 97:449.
36. Kurschera J, Tomaselli J, Urlesberger B et al. Early Human Development 2002; 29:47.
37. Quinn T, Hubbard A, Adzick NS. J Pediatr Surg 1998; 33:553–558.
38. Breysem L, Bosmans H, Dymarkowski S et al. Eur Radiol 2003; 13:1538–1548.
39. Frates MC, Kumar AJ, Benson CB et al. Radiology 2004; 232:398–404.
40. Levine D, Barnes PD, Madsen JR et al. Radiology 1997; 204:635–642.
41. Poatamo J, Vanninen R, Partanen K et al. Ultrasound Obstet Genocol 1999; 13(5):327–349.
42. Malinger G, Ben Sira L, Lev D et al. Ultrasound Obstet Gynecol 2004; 23:333–340.
43. Whitby E, Paley Davie, MN, Spigg A et al. Br J Obstet Gynecol 2001; 106:519–526.
44. Glenn O, Goldstein R, Li K et al. J Ultrasound Med 2005; 24:791–804.
45. Patel TR, Bannister CM, Thome J. Eur J Pediatr Surg 2003 Dec ;13(Suppl 1):S18–S22.
46. Benacerraf B, Shipp TD, Bromle B et al. J Ultrasound Med 2007; 26:1513–1522.
47. Matsuoka S, Takeuchi K, Yamanaka Y et al. Fetal Diagn Ther 2003; 18:447–453.
48. Poutamo J, Vanninen R, Partanen K et al. Acta Obstet Gynecol Scand 2000; 79:65–71.
49. Cassart M, Massez A, Metens T et al. Am J Roentgenol 2004; 182:689–695.
50. Kremkau WF. In Laurence JH, Tobias CA (eds.). Advances in Biology and Physics, Vol. 3:191. New York: Academic Press, 1984.
51. Stark C, Orleans M, Haverkamp AD et al. Obstetr Gynecol 1984; 63:194–200.
52. Lyons EA, Dyke C, Toms M et al. Radiology 1988; 166:687–690.
53. Bly S, VandenHof MC et al. J Obstet Gynecol Can 2005; 7(6):572–580.
54. AIUM official statements. AIUM reporter November 1993, p. 6.
55. Newnham JP, Doherty DA, Kendall GE, et al. Lancet 2004 Dec 4–10; 364(9450): 2038–2044.
56. Salveen KA, Vakketig LS, EikNes SH et al. Lancet 1992:339;85–89.
57. Sulvesen K, Eik-Nes SH. Ultrasound Obstet Gynecol 1999 13:241–246.
58. Kieler H, Knattingius S, Haglund B et al. Epidemiology 2001:12:618–621.
59. Duck FA, Martin K. Phys Med Biol 1991; 36:1423–1432.
60. Henderson J Whittingham TA, Dunn T. BMUS Bulletin Nov 1997:10–14.
61. Hand JW, Li Y, Thomas EL et al. Magn Reson Med 2006; 55:883–893.
62. Shellock FG, Kanal E. JMRI 1991; 1:97–101.
63. Yip YP, Capriotti C, Tlagala SL et al. J Magn Reson Imaging 1994; 4:742–748.
64. Yip YP, Capriotti C, Yip JW. J Magn Reson Imaging 1995; 5:457–462.
65. Mevissen M, Buntenkotter S, Loscher W. Teratology 1994; 50:229–237.
66. Magin RL, Lee JK, Klintsova A et al. J Magn Reson Imaging 2000; 12:140–149.
67. Myers C, Duncan KR, Gowland PA et al. Br J Radiol 1998; 71:549–551.
68. Glover P, J Hykin, Gowland PA et al. Br J Radiol 1995; 68:1090–1094.
69. Baker P, Johnson I, Harvey R et al. Am J Obstet Gynecol 1994; 170:32–33.
70. Clements H, Duncan KR, Fielding K et al. Br J Radiol 2000; 73:190–194
71. Kok RD, de Vries MM, Heerschap A et al. Magn Reson Imaging 2004; 22:851–854.
72. De Wilde JP, Rivers AW, Price DU et al. Prog Biophys Mol Biol 2005; 87:335–353.
73. Kanal E, Borgstede JP, Barkovich AJ et al. Am J Roentgenol 2002; 178:1335–1347.
74. Lys S, DeWals P, Grimee P et al. Eur J Obstet Gynecol Reprod Biol 1989 30:101–109.
75. Li TM, Greenes RA, Weisbjurg M et al. Med Decis Making 1988 8 48–54.
76. Levi S, Crouzeere P Schapps FP et al. US screening for fetal malformations Lancet 1989; 1:679.
77. Shirley IM, Bottomley F, Robindson VP. Br J Radiol 1992; 65:564–569.
78. Chitty LS Hung AGGH, Moore J et al. BMJ 1992; 303:1165–1169.
79. Levi S, Montenagro N. Ann NY Acad Sci 1998; 847:103–117.
80. Sabbagha RE Sheikh Z, Tamura RK. AM J OBstet Gynecol 1985; 152:822–827.
81. Crane JP Lefevre ML, Winborn RC et al. AM J Obsete gyncol 1994:171;392–399.
82. Garne E, Loane M, Dolk H et al. Ultrasound Obstet Gynecol 2005 Jan ; 25(1):6–11.
83. Tilea B, Delezoide A, Khung-Savatovski S et al. US OB Gyn 2007; 29:651–659.
84. Van Dorsten JP, Hulsey TC, Newman RB, Menard MK. Am J Obstet Gynecol 1998 Apr ; 178(4):742–749.
85. Kaiser L et al. Prenatal Diagn 2000; 20: 970–975.
86. Azoulay R, Fallet Bianco C, Garel C et al. Pedatr Radiol 2006 36:97–107.
87. Simon EM, Goldstein RB. Am J Neuroradiol. 2000; 21:1688–1698.
88. de Laveaucoupet J, Audibert F, Guis F et al. Prenat Diagn 2001; 21:729–736.
89. Whitby EH, Paley MNJ, Sprigg A et al. BJOG 2004; 111:784–792.

90. Kirkinen P, Partnaen K, Merikanto J et al. Acta Obstetricia et Gynecologic Scandinavia 1997; 76:917–922.
91. Glenn OA, Barkovich J. Am J Neuroradiol 2006; 27:1807–1814.
92. Levine D, Trop I, Mehta TS, Barnes PD. Radiology 2002; 223:652–660.
93. Leitner Y, Goez H, Gull I et al. J Child Neurol 2004:19:435–438.
94. Patel TR, Bannister CM, Thorne J. Eur J Pedatir Surg 2003; 13(Suppl 1):S18–S22.
95. Chong BW, Babcook CJ, Pang D et al. Neurosurgery 1997; 41:924–928.
96. Coakley FV, Hricak H, Filly RA et al. Radiology 1999; 213:691–696.
97. Ouahba J, Luton D, Vuillard E et al. BJOG 2006; 113:1072–1079.
98. Triulzi F, Parazzini C, Righini A. Semin Fetal Neonatal Med 2005; 10:411–420.
99. Blaicher W, Bernaschek G, Deutinger J et al. J Perinat Med 2004;3253–3257.
100. Seibert JR. Birth Defects Res A Clin Mol Teratol 2006; 76:674–684.
101. Bekker MN, van Vugt JMG. Eur J Obstet Gynecol Reprod Biol 2001; 96:173–178.
102. Ghai S, Fong KW, Toi A et al. RadioGraphics 2006 26:389–405.
103. Girard N, Chaumoitre K, Confort-Gouny S et al. Curr Opin Obstet Gynecol 2006; 18:164–176.
104. Garel C. Pediatr Radiol 2004; 34:694–699.
105. Valsky DV, Ben-Sira L, Porat S et al. J Ultrasound Med 2004; 23:519–523.
106. Hedrick HL, Flake AW, Crombleholme TM et al. J Pediatr Surg 2004 Mar ; 39(3):430–438.
107. ACR Practice Guideline for the Performance of MRI of the Soft Tissue Components of the Pelvis. Reston, VA: ACR Amended 2006.
108. Levine D, Barnes PD, Robertson RR et al. Radiology 2003; 229:51–61.
109. Kline-Fath BM, Calvo-Garcia MA, O'Hara SM et al. Pediatr Radiol 2007 Jan ; 37(1):47–56.
110. Weiss JL, Cleary-Goldman J, Tanji K et al. Am J Obstet Gynecol 2004 Feb ; 190(2):563–565.
111. Hu LS,Caire J, Twickler DH et al. Pediatr Radiol 2006 Jan ; 36(1):76–81.
112. Mota R, Ramalho C, Monteiro J et al. Fetal Diagn Ther 2007; 22(2):107–111.
113. Bouvenot GG, Mourot MG, Sonigo P et al. Ultrasound Obstet Gynecol 2005; 26(7): 738–744.

Index

L.S. Medina et al. (eds.), *Evidence-Based Imaging in Pediatrics*,
DOI 10.1007/978-1-4419-0922-0, © Springer Science+Business Media, LLC 2010